# British Journal of Pharmacology

July 1993

Volume 109 Number 3 pages 601–892

*Br. J. Pharmacol.* (1993), **109**, 603–605

**SPECIAL REPORT**

© Macmillan Press Ltd, 1993

# Prevention of nitric oxide synthase induction in vascular smooth muscle cells by microtubule depolymerizing agents

Nándor Marczin, Andreas Papapetropoulos, *Tamás Jilling & [1]John D. Catravas

Department of Pharmacology and Toxicology, Medical College of Georgia, Augusta, GA 30912-2300 and *Department of Physiology and Biophysics, University of Alabama at Birmingham, Birmingham, AL35294, U.S.A.

We investigated the role of microtubules in the induction of nitric oxide synthase in cultured vascular smooth muscle cells. We found that like interleukin-1α, lipopolysaccharide elicited a time and concentration-dependent accumulation of cyclic GMP via induction of nitric oxide synthase. Nocodazole and colchicine, two chemically distinct microtubule depolymerizing agents, completely prevented lipopolysaccharide- and interleukin-induced (and nitric oxide-mediated) cyclic GMP generation. In contrast to lipopolysaccharide and interleukin-1α, cyclic GMP accumulation in response to sodium nitroprusside, an exogenous nitrovasodilator, was not altered by either nocodazole or colchicine. Our findings demonstrate that microtubule depolymerizing agents inhibit nitric oxide synthase induction and suggest a prominent role for microtubules in mediating the activation of the inducible nitric oxide pathway in smooth muscle cells.

**Keywords:** Colchicine: nocodazole; cytoskeleton; guanylate cyclase; cyclic GMP; sodium nitroprusside; endotoxin; interleukin-1α

**Introduction** Vascular smooth muscle cells are not only targets of endothelium-derived nitric oxide, but may also be the source of nitric oxide in pathological conditions. An endotoxin and cytokine-inducible pathway synthesizing large amounts of nitric oxide and increasing guanosine 3′:5′-cyclic monophosphate (cyclic GMP) in the vasculature, appears to be responsible for the hypotension, reduced responsiveness to vasoconstrictors and cardiovascular collapse associated with septic shock (Fleming *et al.*, 1990; Busse & Mülsch, 1990; Kilbourne *et al.*, 1990; Beasley *et al.*, 1991). The mechanisms underlying the induction of nitric oxide synthase in the smooth muscle cells are not fully understood.

The cytoskeleton has been implicated in the regulation of cell shape, intracellular transport, secretion, signal transduction and gene activation (Penman *et al.*, 1983). Microtubules are involved in certain actions of endotoxin in macrophages, such as in the release of tumour necrosis factor α (TNF α) and in the inhibition of TNF α binding (Ding *et al.*, 1990). In light of this relationship between cytoskeleton and gene activation, we investigated the effects of microtubule depolymerizing agents on the induction of nitric oxide synthase in vascular smooth muscle cells.

**Methods** Rat aortic smooth muscle cells from Wistar rats were isolated by enzymatic dissociation and were identified by standard methods. Smooth muscle cells were subcultured at a seeding density of 5,000 $cm^{-2}$, were maintained in 50% F12 nutrient medium and 50% Dulbecco's Modified Eagle Medium (GIBCO Laboratories), supplemented with 10% foetal bovine serum, L-glutamine (200 mg $l^{-1}$), penicillin (Sigma, 10,000 u $l^{-1}$) and streptomycin (Sigma, 10,000 u $l^{-1}$) and reached confluence after 5–7 days.

Nitric oxide synthase activity was detected as L-arginine-sensitive intracellular accumulation of cyclic GMP. To monitor activation of the inducible pathway, smooth muscle cells were exposed to *E. coli* lipopolysaccharide (LPS, Sigma) in the presence or absence of the transcription inhibitor actinomycin D, the protein synthesis inhibitor cycloheximide, or various inhibitors of nitric oxide action. To depolymerize microtubules, smooth muscle cells were chilled to 4°C and incubated with dimethylsulphoxide (DMSO) as vehicle or were exposed to various concentrations of nocodazole (Calbiochem) or colchicine (Sigma) for 90 min at 4°C. Cells were then rewarmed to 37°C in the continued presence or absence of the agents for 30 min. LPS- or interleukin-1α (Boehringer Mannheim)-stimulation was then performed in the continued presence or absence of nocodazole or colchicine. After 3 h of exposure, generation of cyclic GMP was assessed by incubating the cells for 15 min in the presence of 3-isobutyl-1-methylxanthine (IBMX; 1 mM) to prevent the breakdown of cyclic GMP. Intracellularly accumulated cyclic GMP was then extracted into HCl and measured by radioimmunoassay (Marczin *et al.*, 1992).

Data are expressed as mean ± s.e.mean. Comparisons were performed by the one-way analysis of variance, followed by Dunnett's *t* test. Differences among means were considered significant when $P < 0.05$.

**Results** Preliminary experiments suggested that nitric oxide formation occurred with a delay of 2 h after LPS exposure, was maximal at 3 h (24 fold increase in cyclic GMP levels from baseline), and was maintained at least for 24 h. Polymyxin B, an antibiotic with antiendotoxin activity, completely prevented the stimulation of cyclic GMP generation by LPS (Figure 1a, PMB). Accumulation of cyclic GMP was also significantly reduced by inclusion, during the final 30 min of LPS incubation, of an inhibitor of nitric oxide synthase, $N^G$-monomethyl-L-arginine (Figure 1a, L-NMMA), whereas L-NMMA had no modulatory effects on baseline cyclic GMP levels in the absence of LPS (116 ± 11%). Methylene blue, an inhibitor of nitric-oxide-mediated guanylate cyclase activation, completely abolished the effect of LPS (Figure 1a, MB). The cyclic GMP increase elicited by LPS was also prevented by actinomycin D, an RNA transcription inhibitor, or cycloheximide, a protein synthesis inhibitor (Figure 1a). Similar results were obtained with dexamethasone, an inhibitor of nitric oxide synthase induction (Figure 1a, DM; Radomski *et al.*, 1990).

Although nocodazole treatment had no effect on basal cyclic GMP levels, it prevented LPS-induced cyclic GMP accumulation in a concentration-dependent manner (Figure 1b). Colchicine (10 μM) also inhibited LPS-stimulated cyclic GMP levels by 87%. Exposure of smooth muscle cells to interleukin-1α produced a 31 ± 3 fold increase in cyclic GMP levels. This effect of interleukin-1α was inhibited by both nocodazole (data not shown) and colchicine (Figure 1c).

[1] Author for correspondence.

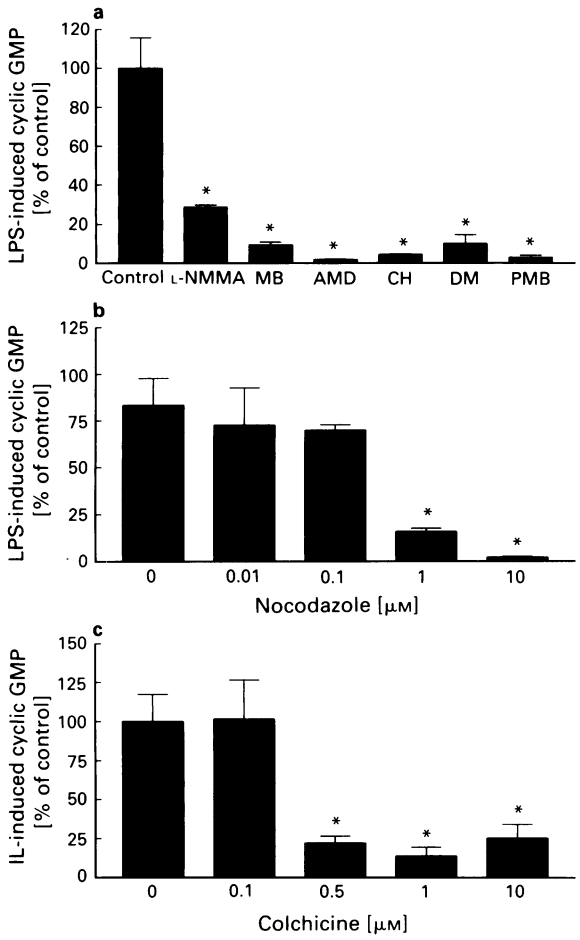



**Figure 1** Modulation of lipopolysaccharide (LPS)- and interleukin-1α-induced cyclic GMP formation in cultured aortic smooth muscle cells of rat. (a) Effects of $N^G$-methyl-L-arginine (L-NMMA, 1 mM), methylene blue (MB, 20 μM), actinomycin D (AMD, 5 μg ml$^{-1}$), cycloheximide (CH, 20 μM), dexamethasone (DM, 10 μM) and polymyxin B (PMB, 2 μg ml$^{-1}$) on LPS (1 μg ml$^{-1}$)-induced cyclic GMP levels. *$P<0.05$ from cyclic GMP levels in Control cultures. (b) Concentration effects of nocodazole on LPS (1 μg ml$^{-1}$)-induced cyclic GMP levels. (c) Concentration effects of colchicine on interleukin-1α (10 u ml$^{-1}$)-induced cyclic GMP levels. *$P<0.05$ from cyclic GMP levels in the absence of nocodazole or colchicine. Data shown are means ± s.e.mean in 4 cultures.

To investigate whether nocodazole and colchicine interfered with the activation of the endogenous nitric oxide generation pathway or inhibited guanylate cyclase activation, cyclic GMP formation in response to exogenous nitrovasodilator, or to co-culture of smooth muscle cells and bovine aortic endothelial cells (BAE), was determined. Sodium nitroprusside at 1 μM produced cyclic GMP levels comparable to those seen with LPS or interleukin (41 ± 5 fold increases). Microtubule depolymerization with either nocodazole or colchicine (10 μM) had virtually no effect on sodium nitroprusside-stimulated cyclic GMP formation in smooth muscle cells (89 ± 14% and 101 ± 9%, respectively) or on bradykinin-stimulated cyclic GMP formation in co-cultures of BAE and smooth muscle cells.

**Discussion** The major novel finding of our study is that microtubule depolymerizing agents prevented LPS- and cytokine-induced cyclic GMP formation in vascular smooth muscle cells, a proposed pathophysiological mechanism underlying septic shock and side-effects of antitumour therapy with cytokines.

Our characterization of LPS-induced cyclic GMP formation suggests the induction of a transcriptionally-regulated nitric oxide synthase as an underlying mechanism for guanylate cyclase stimulation. The slow onset, time-dependence and sensitivity of cyclic GMP responses to actinomycin D, cycloheximide and dexamethasone are all consistent with this assumption and with previous reports on cytokine-induced cyclic GMP formation in cultured vascular cells (Beasley *et al.*, 1991). Nocodazole and colchicine, two chemically distinct microtubule depolymerizing agents, prevented the stimulation of cyclic GMP generation by both LPS and interleukin-1α. This effect of nocodazole and colchicine is unlikely to involve a direct action on soluble guanylate cyclase, since cyclic GMP formation of comparable magnitude in response to sodium nitroprusside remained unaltered by these agents. Thus, we suggest that microtubule depolymerizing agents interfere with the induction of nitric oxide synthase, and furthermore, that the activation of this pathway depends on intact microtubule assembly.

There are other examples for similar involvement of microtubules in mediating expression of certain genes by immunomodulators. Disruption of microtubules reduces the expression of positive acute phase proteins in hepatocytes and tissue plasminogen activator in endothelial cells (Carter *et al.*, 1989; Santell *et al.*, 1992). Depolymerization of these filaments, on the other hand, stimulates expression of plasminogen activator inhibitor in endothelial cells (Santell *et al.*, 1992). The precise means by which cytoplasmic microtubules influence the activation of the inducible nitric oxide pathway remains to be determined. It may play a role in the interaction between the activators and the cell surface, in the internalization process, signal transduction leading to activation of the gene, transcription of mRNA and protein synthesis.

In conclusion, we have identified a new class of inhibitors of the activation of the nitric oxide pathway in vascular smooth muscle cells with therapeutic potential in immunologically based pathological conditions. We have also suggested a new mechanism potentially underlying some antiinflammatory properties of microtubule depolymerizing agents.

## References

BEASLEY, D., SCHWARTZ, J.H. & BRENNER, B.M. (1991). Interleukin 1 induces prolonged L-arginine-dependent cyclic guanosine monophosphate and nitrite production in rat vascular smooth muscle cells. *J. Clin. Invest.*, **87**, 602–608.

BUSSE, R. & MÜLSCH, A. (1990). Induction of nitric oxide synthase by cytokines in vascular smooth muscle cells. *FEBS Letters*, **275**, 87–90.

CARTER, K.C., COOPER, R., PAPACONSTANTINOU, J. & RITCHIE, D.G. (1989). Microtubule depolymerization inhibits the regulation of $\alpha_1$-acid glycoprotein mRNA by hepatocyte stimulating factor. *J. Biol. Chem.*, **264**, 515–519.

DING, A.H., PORTEU, F., SANCHEZ, E. & NATHAN, C.F. (1990). Downregulation of tumor necrosis factor receptors on macrophages and endothelial cells by microtubule depolymerizing agents. *J. Exp. Med.*, **171**, 715–727.

FLEMING, I., GRAY, G.A., JULOU-SCHAEFFER, G., PARRATT, J.R. & STOCLET, J.C. (1990). Incubation with endotoxin activates the L-arginine pathway in vascular tissue. *Biochem. Biophys. Res. Commun.*, **171**, 562–568.

KILBOURNE, R.G., JUBRAN, A., GROSS, S.S., GRIFFITH, O.W., LEVI, R., ADAMS, J. & LODATO, R.F. (1990). Reversal of endotoxin-mediated shock by $N^G$-methyl-L-arginine, an inhibitor of nitric oxide synthesis. *Biochem. Biophys. Res. Commun.*, **172**, 1132–1138.

MARCZIN, N., RYAN, U.S. & CATRAVAS, J.D. (1992). Effects of oxidant stress on endothelium-derived relaxing factor-induced and nitrovasodilator-induced cGMP accumulation in vascular cells, in culture. *Circ. Res.*, **70**, 326–340.

PENMAN, S., CAPCO, D.G., FEY, E.G., CHATTERJEE, P., REITER, T., ERMISH, S. & WAN, K. (1983). The three-dimensional structural networks of cytoplasm and nucleus: functions in cells and tissue. *Modern Cell Biol.*, **2,** 385–415.

RADOMSKI, M.W., PALMER, R.M.J. & MONCADA, S. (1990). Glucocorticoids inhibit the expression of an inducible, but not the constitutive nitric oxide synthase in vascular smooth muscle cells. *Proc. Natl. Acad. Sci. U.S.A.*, **87,** 10043–10047.

SANTELL, L., MAROTTI, K., BARTFIELD, N.S., BAYNHAM, P. & LEVIN, E.G. (1992). Disruption of microtubules inhibits the stimulation of tissue plasminogen activator expression and promotes plasminogen activator inhibitor type 1 expression in human endothelial cells. *Exp. Cell. Res.*, **201,** 358–365.

*(Received March 4, 1993*
*Accepted March 23, 1993)*

*Br. J. Pharmacol.* (1993), **109**, 606–608

**SPECIAL REPORT**

© Macmillan Press Ltd, 1993

# Evidence for the involvement of both ATP and nitric oxide in non-adrenergic, non-cholinergic inhibitory neurotransmission in the rabbit portal vein

Antonia L. Brizzolara, Rahima Crowe & [1]Geoffrey Burnstock

Department of Anatomy and Developmental Biology and Centre for Neuroscience, University College London, Gower Street, London WC1E 6BT

The NANC inhibitory innervation of the longitudinal muscle of the rabbit portal vein has been examined. Neurogenic relaxations were partially inhibited by the $P_2$-purinoceptor antagonist, suramin. Addition of the NO-synthase inhibitor $N^G$-nitro-L-arginine methyl ester (L-NAME) also significantly reduced responses to electrical stimulation and the addition of L-arginine reversed this effect. A combination of both suramin and L-NAME abolished the neurogenic relaxation. A maximum relaxation of the vein was evoked by sodium nitroprusside which was not affected by L-NAME or suramin. Histochemical staining demonstrated the presence of NADPH-diaphorase containing nerves between the longitudinal and circular muscle coats of the media and also in the adventitia. It is concluded that both ATP and NO are inhibitory neurotransmitters in the NANC nerves of the rabbit portal vein.

**Keywords:** ATP; nitric oxide; cotransmission; NANC nerves

**Introduction** The longitudinal muscle of the rabbit portal vein has a non-adrenergic, non-cholinergic (NANC) innervation (Hughes & Vane, 1967) that mediates a relaxation which is independent of the endothelium (Kennedy & Burnstock, 1985). However, the neurotransmitter(s) in these NANC fibres has not been clearly identified. Previous results of pharmacological and histochemical studies suggest that ATP is involved, producing a relaxation via an action on $P_{2y}$-purinoceptors located on the smooth muscle of this vessel (Hughes & Vane, 1967; Burnstock *et al.*, 1979; Kennedy & Burnstock, 1985). There is now a growing body of evidence for the presence of nitric oxide (NO) in NANC inhibitory nerves innervating vascular tissues including penile, cerebral, mesenteric, coronary and pulmonary vessels (see Rand, 1992, for review; Klimaschewski *et al.*; 1992).

In this study, the effects of suramin, a $P_2$-purinoceptor antagonist and $N^G$-nitro-L-arginine methyl ester (L-NAME), a NO-synthase inhibitor, have been examined on the neurogenic inhibitory relaxations of the rabbit hepatic portal vein. Evidence is presented to suggest that ATP and NO are both transmitters in NANC nerves innervating this tissue.

**Methods** Experiments were performed on isolated portal veins from male, 3 month old New Zealand White rabbits. The vessel was suspended vertically between two platinum electrodes in 10 ml organ baths and bathed in Krebs solution containing (mM): NaCl 133, KCl 4.7, $NaHPO_4$ 1.35, $NaHCO_3$ 16.3, $MgSO_4$ 0.61, glucose 7.8 and $CaCl_2$ 2.52, pH 7.2, at 37°C and oxygenated with 95% $O_2$ and 5% $CO_2$. Adrenergic and cholinergic neurotransmission were blocked by guanethidine (3.4 μM) and atropine (0.114 μM), respectively. Tone was raised by the addition of ergotamine (8.6 μM). Intramural nerves were stimulated with trains of biphasic pulses of supramaximal voltage, 0.7 ms duration, 2–64 Hz for 10 s at 5 min intervals from a Grass S88 stimulator. The neurogenic origin of the response was confirmed by the abolition of all responses by tetrodotoxin (3 μM). At the end of each experiment, sodium nitroprusside (SNP; 10 μM) was added to produce maximal relaxation of the preparation. The rabbit portal vein was studied histochemically for the presence of reduced nicotinamide adenine dinucleotide phosphate (NADPH)-diaphorase, a marker for NO-containing nerves (Hope *et al.*, 1991).

$N^G$-nitro-L-arginine methyl ester (hydrochloride), ergotamine, sodium nitroprusside and NADPH-diaphorase were supplied by Sigma Chemical Company. Suramin was a gift from Bayer.

**Results** Suramin (30 μM and 100 μM) partially inhibited the response of the rabbit portal vein to NANC nerve stimulation (Figure 1a). The degree of inhibition by suramin 0.1 mM was no greater than that produced by 30 μM. L-NAME (30 μM and 100 μM) produced a small increase in tone and also partially inhibited the NANC relaxations (Figure 1b). The inhibitory effect of 100 μM L-NAME was greater than that of 30 μM L-NAME. L-Arginine (10 mM) alone had no effect on the response to nerve stimulation but was able to reverse the inhibition produced by L-NAME (Figure 1c). The inhibitory effect of suramin was unaffected by L-arginine. When neurogenic relaxations had been partially inhibited by suramin (30 μM), subsequent addition of L-NAME (100 μM) abolished the remaining responses (Figure 1a). Similarly, in vessels initially treated with L-NAME (100 μM), the response to NANC nerve stimulation was reduced and subsequent addition of suramin (30 μM) abolished the residual responses (Figure 1b). SNP (0.01–10 μM) caused a dose-dependent relaxation of the rabbit portal vein that was unaffected by suramin or L-NAME.

The NADPH-diaphorase reaction stained nerves at the border between the longitudinal and circular muscle coats of the media (Figure 1d) and also in the adventitia. Some nerves showing positive staining were present in the outer longitudinal muscle coat, perhaps representing nerves passing from the adventitia to the interface between the two muscle coats.

**Discussion** The present results suggest that both ATP and NO are inhibitory neurotransmitters in the NANC nerves of the rabbit portal vein. The $P_2$-purinoceptor antagonist, suramin, was employed to show that the neurogenic NANC relaxant response of this preparation is partially mediated by ATP. This result supports the proposal that NANC inhibitory neurotransmission in the rabbit portal vein is partially mediated by ATP via receptors that are located on the smooth muscle rather than on the endothelium (Kennedy & Burnstock, 1985).

[1] Author for correspondence.

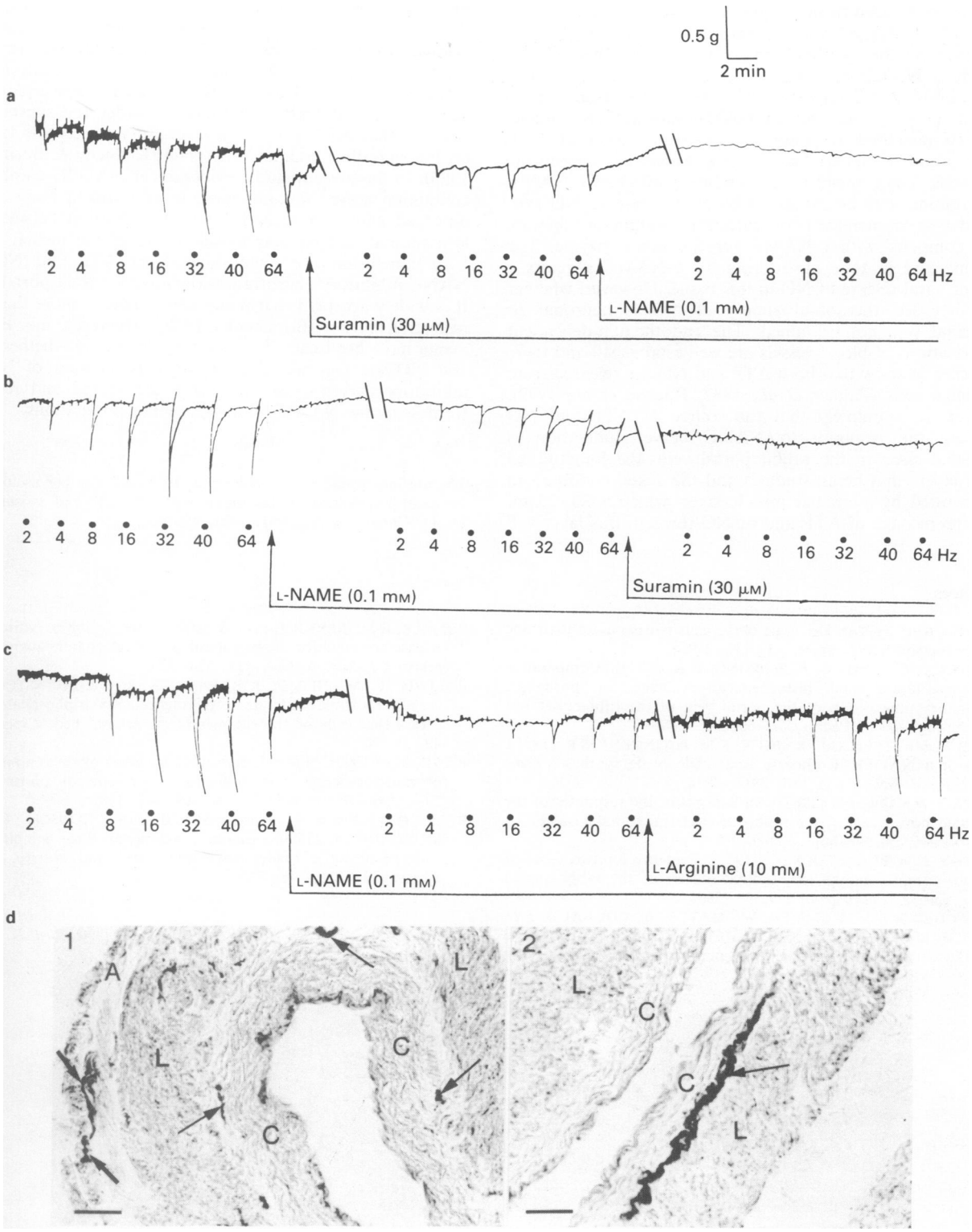



**Figure 1** Relaxations of the rabbit portal vein to neurogenic transmural stimulation for 10 s (2–64 Hz, 0.7 ms, 100 v) at 5 min intervals. Guanethidine (3.4 μM) and atropine (0.114 μM) were present throughout to block adrenergic and cholinergic neurotransmission respectively. Tone was induced with ergotamine (8.6 μM). Panel (a) shows that pre-incubation with suramin (30 μM) for 20 min reduced the nerve-mediated relaxations compared with controls and that suramin-resistant neurogenic relaxations were abolished 20 min after the addition of $N^G$-nitro-L-arginine methyl ester (L-NAME, 0.1 mM). Panel (b) shows that neurogenic relaxations remaining after 20 min pretreatment of the tissue with L-NAME (0.1 mM) were abolished 20 min after the addition of suramin (30 μM). In (c), the effect of adding L-NAME (0.1 mM) to the tissue is shown; there was an additional rise in tone and inhibition of the response to nerve stimulation after a 20 min incubation period. The subsequent treatment of tissues with L-arginine (10 mM) for 20 min reversed this effect. Panel (d) shows the histochemical localization of reduced nicotinamide adenine dinucleotide phosphate (NADPH)-diaphorase in the rabbit portal vein. (d1) NADPH-diaphorase reaction seen in nerve fibres between the inner circular (C) and the outer longitudinal muscle coats (thin black arrows). Note also the NADPH-diaphorase positive nerves in adventitia (A) (thick black arrows). Tangentional section. (d2) NADPH-diaphorase reaction seen in a dense nerve plexus between the inner circular (C) and outer longitudinal muscle coats of the portal vein (thin black arrow). Tranverse section. Calibration bar for d1 and d2 is 30 μm. Each of the traces in (a), (b) and (c) is representative of similar results in 6 separate experiments.

NO is synthesized from L-arginine by NO synthase (Palmer *et al.*, 1987). Part of the evidence for the involvement of L-arginine in the synthesis of NO is the ability of the analogue L-NAME and other arginine analogues to inhibit the synthesis of NO (Rees *et al.*, 1990). In this study, treatment of the portal vein with L-NAME substantially reduced the nerve-mediated response and a combination of both suramin and L-NAME completely abolished neurogenic relaxations. The reversal of the inhibitory effect of L-NAME by L-arginine may be explained by an increase in NO synthesis due to an increased concentration of arginine substrate which competes with L-NAME for the same enzyme. The small increase in tone on addition of L-NAME suggests a constant basal release of NO in this tissue. However, whether the source for this basal supply of NO is neuronal or endothelial was not examined. The endothelium-dependent vasodilatations of blood vessels are well-established and there is evidence to show that both ATP and NO are released from endothelial cells (Palmer *et al.*, 1987; Ralevic *et al.*, 1992). However, it is unlikely that the source of ATP and NO mediating the response to NANC nerve stimulation is endothelial since in the rabbit portal vein, the longitudinal muscle layer (that being studied) and the vessel endothelium are separated by a circular muscle layer, which is 20–25 $\mu$m thick; the passage of ATP and/or NO through this layer will probably lead to their degradation before they reach their site of action on the longitudinal muscle. Histochemical evidence for the presence of purinergic perivascular nerves in the rabbit portal vein has been presented previously (Burnstock *et al.*, 1979). These studies revealed a dense plexus of nerve fibres in the adventitial-medial border and substantiate the idea that ATP mediates a response via receptors located on the smooth muscle of this vessel (Kennedy & Burnstock, 1985). In the present study, evidence for NADPH-diaphorase containing nerves was obtained. In addition to fibres in the outer adventitia, a second plexus was located between the longitudinal and circular muscle coats of the media.

In conclusion, we have shown that ATP and NO are NANC inhibitory neurotransmitters in the rabbit portal vein. It is widely accepted that many nerves release more than one neurotransmitter (Burnstock, 1976). However, no experiments have been carried out yet to determine whether ATP and NO are colocalized in a single population of NANC inhibitory nerves or whether they are stored and released from separate NANC inhibitory nerve populations.

The authors would like to thank Dr B. Pittam for her useful comments and criticisms of this manuscript. The editorial assistance of Dr D. Christie is gratefully acknowledged.

## References

BURNSTOCK, G. (1976). Do some nerve cells release more than one neurotransmitter? *Neurosci.*, **1**, 239–249.

BURNSTOCK, G., CROWE, R. & WONG, H.K. (1979). Comparative pharmacological and histochemical evidence for purinergic inhibitory innervation of the portal vein of the rabbit, but not guinea-pig. *Br. J. Pharmacol.*, **65**, 377–388.

HOPE, B.T., MICHAEL, G.J., KNIGGE, K.M. & VINCENT, S.R. (1991). Neuronal NADPH-diaphorase is a nitric oxide synthase. *Proc. Natl. Acad. Sci. U.S.A.*, **88**, 2811–2814.

HUGHES, J. & VANE, J.R. (1967). An analysis of the responses of the isolated portal vein of the rabbit to electrical stimulation. *Br. J. Pharmacol.*, **30**, 40–66.

KENNEDY, C. & BURNSTOCK, G. (1985). Evidence for two types of $P_2$-purinoceptor in the longitudinal muscle of the rabbit portal vein. *Eur. J. Pharmacol.*, **111**, 49–56.

KLIMASCHEWSKI, L., KUMMER, W., MAYER, B., COURAUD, J.Y., PRIESSLER, U., PHILIPPIN, B. & HEYM, C. (1992). Nitric oxide synthase in cardiac nerve fibers and neurons of rat and guinea pig heart. *Circ. Res.*, **71**, 1533–1537.

PALMER, R.M., FERRIGE, A.G. & MONCADA, S. (1987). Nitric oxide release accounts for the biological activity of endothelium-derived relaxing factor. *Nature*, **327**, 524–526.

RALEVIC, V., MILNER, P., KIRKPATRICK, K.A. & BURNSTOCK, G. (1992). Flow-induced release of adenosine 5'-triphosphate from endothelial cells of the rat mesenteric arterial bed. *Experientia*, **48**, 31–34.

RAND, M.J. (1992). Nitrergic transmission: nitric oxide as a mediator of non-adrenergic, non-cholinergic neuro-effector transmission. *Clin. Exp. Pharmacol. Physiol.*, **19**, 147–169.

REES, D.D., PALMER, R.M.J., SCHULZ, R., HODSON, H.F. & MONCADA, S. (1990). Characterisation of three inhibitors of endothelial nitric oxide synthase *in vitro* and *in vivo*. *Br. J. Pharmacol.*, **101**, 746–752.

*(Received April 1, 1993*
*Accepted April 22, 1993)*

*Br. J. Pharmacol.* (1993), **109**, 609–611

**SPECIAL REPORT**

© Macmillan Press Ltd, 1993

# 5-$HT_{1B}$ receptors mediate potent contractile responses to 5-HT in rat caudal artery

[1]Douglas A. Craig & Graeme R. Martin

Analytical Pharmacology Group, Biochemical Sciences, Wellcome Research Laboratories, Beckenham, Kent BR3 3BS

5-Hydroxytryptamine (5-HT) evoked potent contractile responses in phenoxybenzamine-treated ring segments of rat caudal artery, partially contracted with U46619. Responses were mimicked by 5-$HT_1$-selective agonists with the potency order: RU24969 > 5-carboxamidotryptamine > 5-HT = CP-93,129 >> sumatriptan. 8-Hydroxy-*N*,*N*-dipropylaminotetralin was virtually inactive. Responses were unaffected by spiperone (0.1 μM) and mesulergine (1.0 μM), but were antagonized competitively by (±)-cyanopindolol affording agonist-independent $pK_B$ estimates of 8.4 to 8.9. The pharmacological profile of this receptor is consistent with that of the 5-$HT_{1B}$ subtype. Since the 5-$HT_{1B}$ receptor is the rodent homologue of the 5-$HT_{1D\beta}$ subtype, it might be anticipated that 5-$HT_{1D\beta}$ receptors will be found to mediate vasoconstrictor responses in non-rodent species.

**Keywords:** Rat caudal artery; vasoconstriction; 5-$HT_{1B}$ receptor; 5-$HT_{1D}$; 5-$HT_{1D\beta}$; CP-93,129; RU24969; sumatriptan

## Introduction

In a variety of species the vasoconstrictor action of 5-hydroxytryptamine (5-HT) has been shown to involve 5-$HT_1$-like as well as 5-$HT_2$ receptors (see Feniuk & Humphrey, 1989). Classification of the 5-$HT_2$ receptor is unambiguous but the precise identity of the 5-$HT_1$-like receptor remains uncertain. Several studies have suggested that it is a 5-$HT_{1D}$ receptor (e.g. Martin *et al.*, 1991), although this remains a contentious issue (Perren *et al.*, 1991). The problem has been confounded further by the recent disclosure that there exist pharmacologically similar 5-$HT_{1D\alpha}$ and 5-$HT_{1D\beta}$ receptor subtypes (Weinshank *et al.*, 1992) and that the 5-$HT_{1D\beta}$ subtype is the species homologue of the pharmacologically distinct 5-$HT_{1B}$ receptor in rodents (Adham *et al.*, 1992). Interestingly, a 5-$HT_1$-like receptor mediating vascular contraction in rodents has hitherto not been reported. Here we describe such a receptor mediating contraction of rat caudal artery and show that it exhibits the pharmacology of a 5-$HT_{1B}$ receptor.

## Methods

Male Wistar rats (250–350 g) were killed by asphyxiation with $CO_2$. The proximal 8 cm of the caudal artery were carefully removed and cleaned of adhering tissue. Arterial rings (3 mm long) were suspended between wire hooks (150 μm diameter) for measurement of isometric tension and placed in Krebs solution (pH 7.4, 37°C), the composition of which has been detailed by Martin *et al.* (1991).

After 30 min, a force of 1 g was applied to each ring and reinstated until a resting tone of approximately 0.5 g was maintained. Tissues were treated with pargyline (500 μM, 30 min) to inhibit monoamine oxidases and, except in preliminary experiments, with phenoxybenzamine (PBZ, 3 μM for 1 h, 5 washes) to eliminate 5-$HT_2$- and α-adrenoceptor-mediated effects of 5-HT, as well as agonist uptake. To study the effect of agonists at the 5-$HT_1$-like receptor, tissues were first contracted with the stable thromboxane analogue, U46619 (10–30 nM, approximate $EC_{20}$ concentration). When this contraction had stabilized, concentration-effect curves were constructed by the cumulative addition of agonists in 0.5 log M increments. The relative efficacies of agonists at the 5-$HT_1$-like receptor were estimated by the response to 10 μM 5-HT applied at the end of the concentration-effect curve. To study the effects of antagonists two concentration-effect curves were constructed in each tissue, the first serving as the control and the second constructed after 1 h incubation with antagonist. Concentration ratios (CR) for the two curves were determined for the agonist concentrations producing half-maximal effects ($EC_{50}$), and estimates of the apparent antagonist $pK_B$ were calculated according to the relationship: $pK_B = \log (CR - 1/ [\text{antagonist}])$.

### *Drugs*

5-HT creatinine sulphate, spiperone, prazosin hydrochloride, idazoxan hydrochloride, 8-OH-DPAT (8-hydroxy-N,N-dipropylaminotetralin hydrobromide) (Sigma Chemical Co., St. Louis, MO, U.S.A.); 5-carboxamidotryptamine maleate, mesulergine maleate (RBI, Natick, Mass, U.S.A.); CP-93,129 (3-(1,2,5,6-tetrahydropyrid-4-yl)pyrrolo[3,2-b]pyrid-5-one) (Pfizer Inc., Groton, CT, U.S.A.); RU24969 (5-methoxy-3-[1,2,3,6-tetrahydropyridin-4-yl]-1H-indole) (Roussell-Uclaf, Romaineville, France); (±)-cyanopindolol (Dr Daniel Hoyer, Sandoz Pharmaceuticals, Basel, Switzerland). Cyanopindolol was dissolved at 10 mM in ethanol and diluted in water. The remaining drugs were dissolved in distilled water.

## Results

In naive arterial rings, 5-HT (0.03 to 10 μM) evoked concentration-related contractions (Figure 1a). The presence of a small sustained contraction to U46619 revealed an additional, higher potency phase of the 5-HT concentration-effect curve (not shown). The lower, but not the higher potency phase could be blocked partially by the combination of prazosin (0.1 μM) and idazoxan (1.0 μM) and totally by the further addition of spiperone (0.1 μM) or mesulergine (1.0 μM), indicating that this phase involved α-adrenoceptors as well as 5-$HT_2$ receptors. To isolate more effectively the receptor mediating the high potency phase, tissues were exposed to PBZ (see methods). After PBZ treatment, 5-HT failed to elicit a contraction when applied on its own (Figure 1b). In contrast, when PBZ-treated rings were first contracted with U46619, 5-HT produced a monophasic concentration-effect curve ($pEC_{50} = 7.65$; Figure 1c, Table 1). This curve

[1] Author for correspondence.

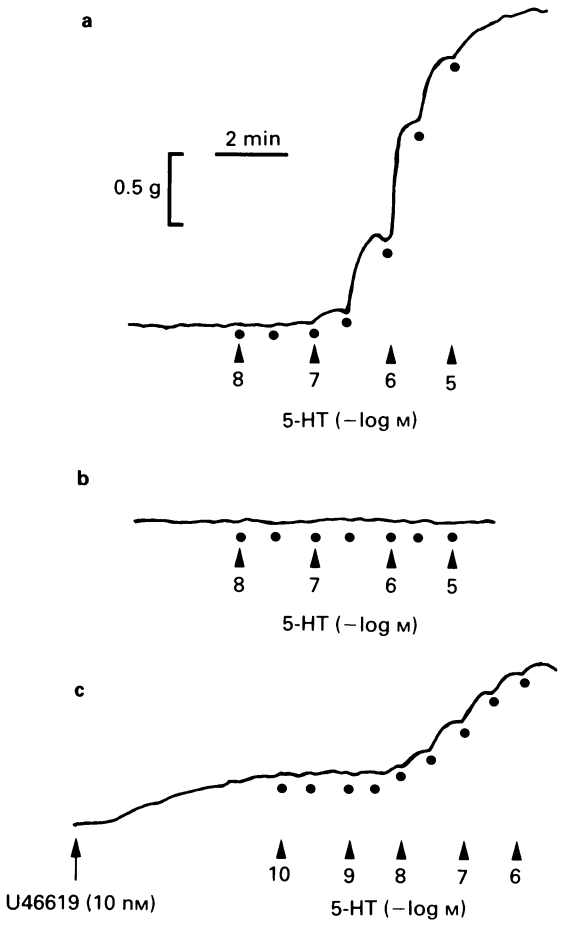



**Figure 1** Contractile responses to 5-hydroxytryptamine (5-HT) in a single ring of rat caudal artery under different experimental conditions. (a) Responses to 5-HT alone, applied in 0.5 log M increments to the untreated tissue. (b) Failure of 5-HT alone to elicit contractions after phenoxybenzamine (PBZ) treatment (3 μM, 1 h). (c) High potency responses to 5-HT revealed subsequent to elevating muscle tone with U46619 after PBZ-treatment.

corresponded in location to that of the high potency 5-HT response revealed by U46619 before PBZ treatment.

In PBZ-treated rings exposed to U46619, the effect of 5-HT was mimicked by the agonists 5-CT (5-$HT_1$-like-selective), RU24969 and CP-93,129 (5-$HT_{1B}$-selective), and sumatriptan (5-$HT_{1D}$-selective), whereas 8-OH-DPAT (5-$HT_{1A}$-selective; 10 μM) evoked less than 10% of the maximum response to 5-HT (Table 1). (±)-Cyanopindolol (0.1 μM) produced parallel dextral shifts of the concentration-effect curves to 5-HT, 5-CT, RU24969, and CP-93,129 with no depression of the maximum response, affording apparent $pK_B$ estimates of 8.4 to 8.9 (Table 1).

## Discussion

In various blood vessels from the rat, including the caudal artery (Feniuk & Humphrey, 1989), 5-HT-induced contraction has been shown to be mediated by 5-$HT_2$ receptors. This study presents the first evidence for the presence of contractile 5-$HT_1$-like receptors in rodent vasculature. Although 5-$HT_1$-like mediated responses were not detected in tissues exposed to 5-HT alone, they could be revealed by prior contraction with a low concentration of the thromboxane analogue, U46619.

Tissues were treated with PBZ to preclude complications arising from agonist actions at 5-$HT_2$ receptors, α-adrenoceptors and uptake sites. Under these conditions all agonists evoked monophasic cumulative concentration-effect curves, characteristic of an interaction with a homogeneous receptor population. The pharmacology of the receptor is inconsistent with a 5-$HT_2$, 5-$HT_3$, or 5-$HT_4$ classification on the basis of: (1) the high potency of 5-CT relative to 5-HT (an order which is reversed for the aforementioned subtypes; (2) insensitivity to antagonism by spiperone and mesulergine at concentrations 60 to 250 fold greater than their affinities at 5-$HT_2$ receptors; and (3) sensitivity to antagonism by (±)-cyanopindolol, which exhibits negligible affinity at 5-$HT_2$, 5-$HT_3$ and 5-$HT_4$ sites.

Within the 5-$HT_1$-like subgroup, only 5-$HT_{1A}$ and 5-$HT_{1B}$ receptors exhibit affinities for (±)-cyanopindolol in the order of those obtained in the present study ($pK_B$ range = 8.4 to 8.9). The failure of 8-OH-DPAT, a potent and selective 5-$HT_{1A}$ agonist, to evoke significant contractions at 10 μM argues against the involvement of 5-$HT_{1A}$ receptors. Positive identification of the present site as 5-$HT_{1B}$ is supported by (1) potent agonism by CP-93,129 (150–650 fold selective for 5-$HT_{1B}$ over other 5-$HT_1$-like receptors, Macor *et al.*, 1990). (2) the absolute and relative agonist potencies: RU24969 > 5-CT > 5-HT = CP-93,129 >> sumatriptan, and (3) the agonist-independence of antagonist $pK_B$ estimates for (±)-cyanopindolol. Similar results have been reported elsewhere for 5-$HT_{1B}$ receptors (Schoeffter & Hoyer, 1989; Macor *et al.*, 1990; O'Connor & Kruk, 1992).

Since 5-$HT_{1D}$ and 5-$HT_{1B}$ receptors evidently share similar anatomical distributions and functional roles, the demonstration that 5-$HT_{1B}$ receptors mediate vasoconstriction is intriguing. In light of recent evidence that the 5-$HT_{1B}$ receptor is the rodent homologue of the 5-$HT_{1D\beta}$ receptor subtype (Adham *et al.*, 1992), this novel observation suggests that 5-$HT_{1D\beta}$ receptors may subserve vasoconstriction in non-rodent species.

**Table 1** Potencies and relative intrinsic activities for agonists and $pK_B$ estimates for (±)-cyanopindolol versus various agonists in rat caudal artery

| *Agonist* | $pEC_{50}$[a] | | *i.a.*[b] | n[c] | $pK_B$[a] | | n |
|---|---|---|---|---|---|---|---|
| 5-HT | 7.65 | (0.04) | 1.00 | 12 | 8.90 | (0.05) | 4 |
| 5-CT | 8.14 | (0.06) | 1.00 | 17 | 8.45 | (0.04) | 4 |
| RU24969 | 8.72 | (0.21) | 0.83 | 6 | 8.46 | (0.15) | 3 |
| CP-93,129 | 7.37 | (0.13) | 1.00 | 8 | 8.38 | (0.7) | 3 |
| Sumatriptan | 5.64 | (0.02) | 1.00 | 5 | ND | – | – |
| 8-OH-DPAT | <5.0 | – | 0.07 | 3 | ND | – | – |

[a]Mean ± s.e.mean in parentheses. [b]Intrinsic activity relative to 5-HT. [c]Determinations made in tissues from *n* different animals. ND (not determined).

## References

ADHAM, N., ROMANIENKO, P., HARTIG, P., WEINSHANK, R. & BRANCHEK, T. (1992). The rat 5-hydroxytryptamine$_{1B}$ receptor is the species homologue of the human 5-hydroxytryptamine$_{1D\beta}$ receptor. *Mol. Pharmacol.*, **41,** 1–7.

FENIUK, W. & HUMPHREY, P. (1989). Mechanisms of 5-hydroxytryptamine-induced vasoconstriction. In *The Peripheral Actions of 5-Hydroxytryptamine*. ed. Fozard, J.R. pp. 110–122. New York: Oxford University Press.

MACOR, J., BURKHART, C., HEYM, J., IVES, J., LEBEL, L., NEWMAN, M., NIELSEN, J., RYAN, K., SCHULZ, D., TORGERSEN, L. & KOE, B. (1990). 3-(1,2,5,6-Tetrahydropyrid-4-yl)pyrrolo-3,2-b]pyrid-5-one: a potent and selective serotonin (5-HT$_{1B}$) agonist and rotationally restricted phenolic analogue of 5-methoxy-3-(1,2,5,6-tetrahydropyrid-4-yl)indole. *J. Med. Chem.*, **33,** 2087–2093.

MARTIN, G.R., PRENTICE, D.J. & MACLENNAN, S.J. (1991). The 5-HT receptor in rabbit saphenous vein. Pharmacological identity with the 5-HT$_{1D}$ recognition site? *Fund. Clin. Pharmacol.*, **5,** (5), 417.

O'CONNOR, J. & KRUK, Z. (1992). Pharmacological characteristics of 5-hydroxytryptamine autoreceptors in rat brain slices incorporating the dorsal raphe of the suprachiasmatic nucleus. *Br. J. Pharmacol.*, **106,** 524–532.

PERREN, M., FENIUK, W. & HUMPHREY, P. (1991). Vascular 5-HT$_1$-like receptors that mediate contraction of the dog isolated saphenous vein and carotid arterial vasoconstriction in anaesthetized dogs are not of the 5-HT$_{1A}$ or 5-HT$_{1D}$ subtype. *Br. J. Pharmacol.*, **102,** 191–197.

SCHOEFFTER, P. & HOYER, D. (1989). 5-Hydroxytryptamine 5-HT$_{1B}$ and 5-HT$_{1D}$ receptors mediating inhibition of adenylate cyclase activity. *Naunyn Schmied. Arch. Pharmacol.*, **340,** 285–292.

WEINSHANK, R., ZGOMBICK, J., MACCHI, M., BRANCHEK, T. & HARTIG, P. (1992). Human serotonin ID receptor is encoded by a subfamily of two distinct genes: 5-HT$_{1D\alpha}$ and 5-HT$_{1D\beta}$. *Proc. Natl. Acad. Sci. U.S.A.*, **89,** 3630–3634.

*(Received March 30, 1993*
*Accepted April 26, 1993)*

*Br. J. Pharmacol.* (1993), **109**, 612–617 © Macmillan Press Ltd, 1993

# Oestradiol inhibits smooth muscle cell proliferation of pig coronary artery

Roberto Vargas, Barbara Wroblewska, Alfredo Rego, Joshua Hatch & [1]Peter W. Ramwell

Department of Physiology & Biophysics, Georgetown University Medical Center, Washington, District of Columbia, U.S.A.

**1** The effect of oestradiol 17β on vascular smooth muscle proliferation was examined in segments of the pig left anterior descending coronary artery (LAD). It was established by cytochemical techniques that out-growth from the segments was composed of vascular smooth muscle cells.

**2** [$^3$H]-thymidine uptake by pig LAD segments was used as an index of vascular smooth muscle cell proliferation. Nitroprusside and forskolin significantly inhibited [$^3$H]-thymidine uptake and were used as positive controls.

**3** Oestradiol 17β (180–360 nM) inhibited thymidine uptake by pig LAD segments ($P<0.05$). The inhibition was observed only in the absence of phenol red, which is a weak oestrogen receptor agonist. The anti-oestrogens tamoxifen and its more potent metabolite 4-hydroxytamoxifen, both of which are partial oestrogen receptor agonists, also significantly inhibited thymidine uptake. However, pretreatment with either tamoxifen or 4-hydroxytamoxifen did not signficantly block oestradiol 17β-induced inhibition of thymidine uptake.

**4** The LAD segments bound [$^3$H]-oestradiol 17β in a time-dependent manner and about 20 to 30% was displaced by an excess of unlabelled oestradiol 17β. Autoradiography showed [$^3$H]-oestradiol 17β was evenly distributed in the cytosol and nuclei of cells in the three layers of the vessel wall.

**5** The data suggest that oestradiol 17β inhibits smooth muscle cell proliferation in porcine LAD segments, possibly through an oestrogen receptor mechanism. This *in vitro* effect suggests an *in vivo* role for oestradiol 17β in directly protecting coronary arteries against myointimal proliferation in premenopausal women.

**Keywords:** Proliferation; oestradiol 17β; tamoxifen; coronary artery

## Introduction

The physiological and therapeutic role of oestrogen in coronary heart disease (CHD) is of considerable interest to the large number of premenopausal women taking oral contraceptives and postmenopausal women taking oestrogen.

Atherosclerosis as well as other vascular responses to injury have a proliferative component (Ross & Glomset, 1973) which includes smooth muscle cell migration and proliferation (Clowes *et al.*, 1983; Walker *et al.*, 1986). We have shown oestradiol 17β to prevent myointimal proliferation in rabbit cardiac and aortic allografts (Foegh *et al.*, 1987; Cheng *et al.*, 1991). Oestrogen has been reported to suppress surgically induced vascular intimal hyperplasia in rabbits (Rhee *et al.*, 1977).

Oestradiol also inhibits diet-induced atherosclerosis in rat and rabbit (Moskowitz *et al.*, 1956; Constantinides *et al.*, 1962; Renaud, 1970). Ethinyl oestradiol has been reported to reduce plaque area in the aorta of cholesterol-fed female *Macaca fascicularis* (Clarkson *et al.*, 1987; 1990). This effect of ethinyl oestradiol was attributed to the increased HDL-cholesterol induced by the drug. However, ethinyl oestradiol diminished the plaque area in the aorta even when its anti-atherogenic effect on the plasma pattern of lipoproteins was counteracted with progestins. The lack of correlation between the pattern of plasma lipoproteins and the effect on the degree of atherosclerosis suggests a direct effect of ethinyl oestradiol on cellular events occurring in the vessel wall. In this context it is noteworthy that Fischer-Dzoga *et al.* (1983) found oestradiol 17β to inhibit the proliferation induced by hyperlipemic serum in cell cultures of rabbit aorta smooth muscle cells.

The obvious question arises as to the presence and localization of oestrogen receptors in vascular tissue. Oestrogen receptors have been identified in endothelium and vascular smooth muscle cells of several mammalian species (Stumpf *et al.*, 1977; Lin *et al.*, 1982; Lin & Shain, 1986). Oestradiol treatment of oophorectomized baboons (*Papio* sp.) caused the redistribution of oestrogen receptors from cytoplasmic to the nuclear fraction in vascular smooth muscle cells (Lin *et al.*, 1986). These findings imply a role for oestrogen in the regulation of vascular cell function but whether or not oestrogen receptors are implicated in the control of vascular smooth muscle cell proliferation is not established.

At this time there is no evidence that oestradiol 17β inhibits smooth muscle proliferation in the coronary vasculature except in rabbit cardiac allografts (Foegh *et al.*, 1987). The purpose of this study was to evaluate the effect of oestradiol 17β on coronary artery smooth muscle cell proliferation *in vitro* using the uptake of radioactive thymidine into isolated segments of the left anterior descending branch of porcine coronary artery tree. The porcine coronary artery was chosen because of its similarity to that of man. A preliminary account of this work was presented at the 63rd Scientific Session of the American Heart Association in Dallas, Texas, November 12–15, 1990 (Vargas *et al.*, 1990).

## Methods

### *Vessel preparation*

Hearts were obtained from pigs slaughtered at Horst Co. (Hagerstown, MD, U.S.A.). The hearts (10) were harvested and transported to our laboratory in ice-cold Ringer-lactate. Hearts were obtained from male pigs castrated before sexual maturity and from sexually mature female pigs. Segments were prepared from the left anterior descending coronary artery 5 to 10 mm from the origin. Adherent tissue and fat

[1] Author for correspondence at: Georgetown University, Department of Physiology & Biophysics, 3900 Reservoir Rd. N.W., Washington, D.C. 20007, U.S.A.

were removed from the vessels. Segments of 3 to 5 mm were prepared (5 to 7 for each heart) under sterile conditions and placed in ice-cold minimum essential medium, Eagle's Dulbecco's modification (DMEM) containing gentamicin (50 $\mu g\ ml^{-1}$).

*Time course of [$^3$H]-thymidine uptake*

LAD segments were incubated overnight in DMEM culture medium containing gentamicin (25 $\mu g\ ml^{-1}$) and supplemented with L-glutamine (2 mM) in a humidified 5% $CO_2$ atmosphere at 37°C. After this incubation period, the test drugs and [$^3$H]-thymidine (sp. activity 2.6–3.1 TBq $mmol^{-1}$) were added to the medium and the segments were incubated for an additional 24 to 96 h, depending on the experimental protocol. The experiments were performed in serum-free DMEM without phenol red. The experiments in which the effect of serum was evaluated were performed in the same way as described above, but different concentrations of foetal calf serum (1, 5 and 10%) were added to the culture medium. The tissues were incubated with [$^3$H]-thymidine for 24 h. All concentrations of serum were tested with each experiment. Medium without serum was used as a control. The exposure to [$^3$H]-thymidine was terminated by washing the tissue, replacing the medium with ice-cold phosphate buffer saline (PBS, pH 7.2 without $Ca^{2+}$ and $Mg^{2+}$) and further incubating the segments with PBS containing unlabelled thymidine (1 mM) for 20 to 30 min at 4°C. The tissues were then digested in NaOH (0.5 N) for 18–24 h at 60°C. Aliquots were taken for measurement of radioactivity (Beckman, LS-3150 T scintillation counter). Protein content was determined by the method of Lowry *et al.* (1951).

*Immunofluorescent staining for α-actin and desmin of smooth muscle cells*

LAD explants were placed upright and incubated in 300 µl of serum-free DMEM for up to one week. The segments were removed after three days incubation or when cell out-growth was observed under the inverted microscope. Fresh medium was added every day. The cells growing from the explants were allowed to attach to cover slips. The cover slips were washed with PBS and the cell permeability was increased with lysophosphatidyl choline for 15 min at 37°C. The permeabilized cells were treated for 10 to 20 min with rhodamine labelled phalloidin and washed with PBS. The cover slips were mounted on slides for fluorescence microscopy to observe actin staining.

Cells were also stained for desmin. The cover slips were incubated with 1:30 dilution of a polyclonal antibody for desmin (Sigma Chemicals Co., St. Louis, MO, U.S.A.) for 15 min at room temperature. After washing with PBS, the cells were incubated with a 1:100 dilution of fluorescein isocyanate-labelled goat anti-rabbit IgG (Sigma Chemicals Co., St. Louis, MO, U.S.A.) for 30 min. After additional washing with PBS, the slides were mounted for fluorescence microscopy.

*Uptake of [$^3$H]-oestradiol 17β into vascular segments*

Segments from porcine LAD were isolated as described above. They were exposed to [$^3$H]-oestradiol 17β (sp. activity 5.2 to 6.3 TBq $mmol^{-1}$) for varying time periods (0.5 to 60 min) in Krebs-Ringers bicarbonate buffer at 37°C. For each time point a control with unlabelled oestradiol 17β (100 µM) was used. After the incubation period the rings were frozen in liquid nitrogen and later digested in NaOH (0.5 N) overnight at 60°C. Aliquots were taken for scintillation counting and for determination of protein content.

*Autoradiography*

In another series of experiments, vascular rings were incubated with [$^3$H]-oestradiol 17β for periods ranging from 10 to 20 min. The rings were fixed overnight in 10% formalin and then placed in fresh formalin for two additional days. Progressive dehydration of the tissues was accomplished with increasing concentrations of ethanol. The tissues were then embedded in paraffin and cross sections of 4 to 6 µm were prepared. The sections were stained with Mayer's haematoxylin. Stained sections were rehydrated overnight and coated with photographic emulsion $NTB_2$ (the emulsion was warmed at 40°C for 12 h prior to application to the slides). After a two weeks exposure the sections were developed with Dektol for 45 s and fixed with GBX for 5 min.

*Drugs and materials*

Gentamicin, L-glutamine, PBS and DMEM were purchased from Biofluids (Rockville, MD, U.S.A.). [$^3$H]-thymidine and [$^3$H]-oestradiol 17β were obtained from Amersham (Arlington Heights, IL, U.S.A.). Thymidine, oestradiol 17β, tamoxifen, phalloidin, lysophosphatidyl choline and anti-desmin polyclonal antibody were obtained from Sigma Chemicals Co. (St. Louis, MO, U.S.A.). Rhodamine labelled phalloidin was obtained from Molecular Probes Inc. (Eugene, OR, U.S.A.). Phosphate buffered formalin 10% was purchased from Fischer Scientific (Fair Lawn, NJ, U.S.A.). $NTB_2$, Dektol and GBX were obtained from Eastman Kodak Co. (Rochester, NY, U.S.A.). 4-Hydroxytamoxifen was kindly donated by Dr Robert Clarke. [$^3$H]-thymidine was prediluted with sterile PBS (500 µCi $ml^{-1}$) and was kept refrigerated. Oestradiol, tamoxifen and 4-hydroxytamoxifen were prepared in ethanol in a stock solution (1 mg $ml^{-1}$) and further diluted in the same solvent to keep the volume of administration constant.

*Statistics*

The data calculated as absolute values in c.p.m. $mg^{-1}$ of protein. The [$^3$H]-oestradiol 17β uptake experiments are expressed as individual points. Each point is the mean of duplicated measurements. The [$^3$H]-thymidine uptake experiments are presented as mean ± s.e.mean of the percentage of uptake in the control group. The means are compared by analysis of variance (ANOVA), using a Newman-Keuls test for post-hoc comparisons. $P<0.05$ is accepted as statistical significance.

## Results

The cells migrating from porcine LAD explants after 1 to 2 weeks incubation in medium without serum, stained pos-

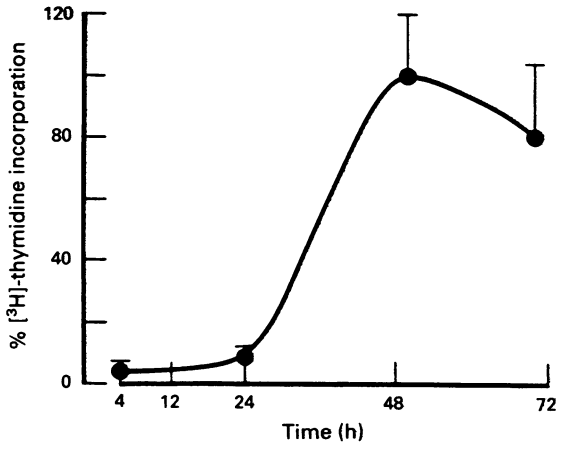



**Figure 1** Time course of [$^3$H]-thymidine uptake into segments of porcine left anterior descending coronary artery (LAD). Each point is a mean ± s.e.mean ($n = 4$ or 6 segments) of the total uptake at each time point, expressed as a percentage of the maximum uptake at 48 h (195,234 ± 70,779 c.p.m. $mg^{-1}$ of protein).

**Table 1** Effect of forskolin and sodium nitroprusside (SNP) on the uptake of [$^3$H]-thymidine into rings of pig LAD

| *Agent* | μM | *[$^3$H]-thymidine uptake* (c.p.m. mg$^{-1}$ protein) | % |
|---|---|---|---|
| Control | | 234,771 ± 40,018 | 100 |
| Forskolin | 100 | 147,641 ± 25,373[a] | 63 |
| Control | | 151,035 ± 25,103 | 100 |
| SNP | 10 | 137,232 ± 18,123 | 91 |
| SNP | 50 | 78,389 ± 14,782[b] | 52 |
| SNP | 75 | 45,932 ± 6,172[b] | 30 |
| SNP | 100 | 3,498 ± 419[b] | 2 |

[a]$P<0.05$; [b]$P<0.01$.
The segments were incubated overnight in DMEM with glutamine and gentamicin. The drugs were added at the indicated final concentration together with [$^3$H]-thymidine (2.5 μCi ml$^{-1}$) and incubated for 24 h. The incubation was ended by washing the segments with ice-cold buffer. The results are mean ± s.e.mean of the absolute values (c.p.m. mg$^{-1}$ protein). The experiment was performed three times. Six segments were used for each concentration.

itively for α-actin and desmin. The stain identified >90% of the cells as vascular smooth muscle.

### *[$^3$H]-thymidine uptake*

Vascular segments of pig LAD incorporated radioactive thymidine in a time-dependent manner. Significant uptake of [$^3$H]-thymidine occurred after 24 h exposure and reached a plateau at 48 h (Figure 1).

In Table 1 the uptake of thymidine into LAD segments is shown to be inhibited by approximately 40% by forskolin (100 μM). Sodium nitroprusside (10 to 1000 μM) nearly abolished [$^3$H]-thymidine uptake with an approximate $IC_{50}$ of 50 μM.

Uptake of [$^3$H]-thymidine was also affected by experimental conditions other than time and antiproliferative drugs. For example, when the concentration of foetal bovine serum in the medium was 5 or 10% the [$^3$H]-thymidine uptake was significantly reduced to about 50% of that incorporated into LAD segments when serum was absent (Figure 2).

### *[$^3$H]-oestradiol 17β uptake and autoradiographic studies*

[$^3$H]-oestradiol 17β was taken up by pig LAD segments in a time-dependent manner (Figure 3a). Equilibrium was achieved between 30 to 45 min of incubation. The total uptake of [$^3$H]-oestradiol 17β was higher in segments from sexually mature female pigs than in tissues from castrated males. [$^3$H]-oestradiol was partially displaced (30%) by an excess of unlabelled oestradiol 17β (Figure 3b).

The [$^3$H]-oestradiol 17β taken up by the tissues was localized by autoradiography. The silver grains were distributed evenly between the different cells within the vessel wall, and as expected, between both cytoplasmic and nuclear compartments (Figure 4).

### *Effect of oestradiol 17β on [$^3$H]-thymidine uptake*

Oestradiol 17β inhibited [$^3$H]-thymidine uptake into pig LAD segments. Oestradiol 17β, at concentrations of 180, 360 and 720 nM, significantly reduced the uptake to 45 ± 16, 48 ± 12 and 25 ± 10% of the controls (Figure 5). This inhibitory effect of oestradiol 17β was concentration-dependent and was significantly expressed only when the weak oestrogen receptor agonist, phenol red, was absent from the culture medium.

The oestrogen receptor partial agonists, tamoxifen and 4-hydroxytamoxifen, at concentrations of 0.1 and 1 μM, significantly inhibited [$^3$H]-thymidine uptake. Equimolar con-

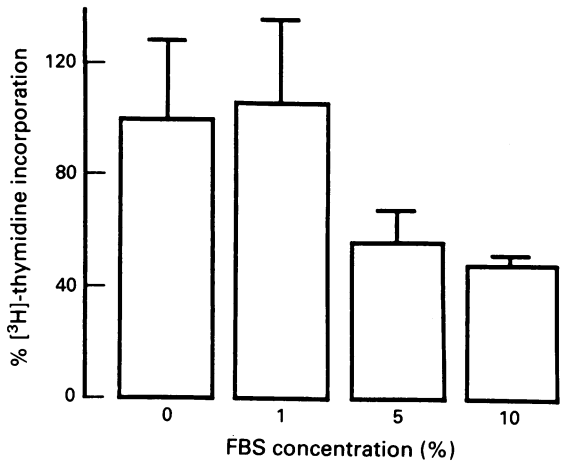



**Figure 2** Effect of three different concentrations of foetal bovine serum (FBS) on [$^3$H]-thymidine uptake (24 h incubation) into segments of porcine LAD. Each column represents the mean ± s.e.mean ($n = 5$ or 6 segments) of the uptake expressed as a percentage of the total uptake into segments when foetal bovine serum was absent from medium (3,824 ± 890 c.p.m. mg$^{-1}$ of protein).

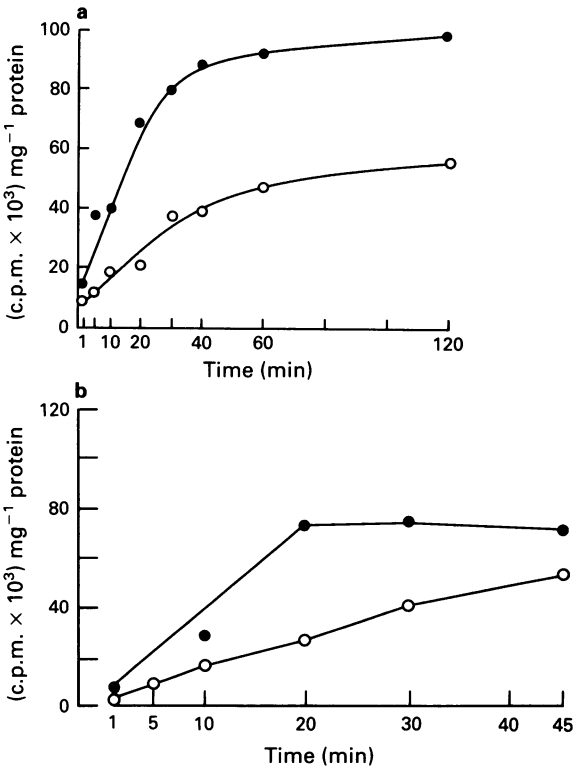



**Figure 3** (a) Time course of [$^3$H]-oestradiol 17β uptake by segments of porcine LAD from castrated male (○) and intact female (●) pigs. Each point is a duplicate measurement of the total uptake expressed as c.p.m. mg$^{-1}$ protein. The experiment was replicated three times. In all three experiments the total uptake of [$^3$H]-oestradiol 17β by vessels from intact females was higher than in vessels from castrated males. The total uptake, at 60 min, in vessels from males expressed as a percentage of the uptake in those from females was: 51, 62 and 64% in each experiment. The final concentration of [$^3$H]-oestradiol 17β in the incubation medium was 400 ng ml$^{-1}$. The maximum oestradiol uptake at 120 min in each experiment was: females, 96,223, 266,585 and 186,000 c.p.m. mg$^{-1}$ protein; males, 54,067, 97,247 and 120,000 c.p.m. mg$^{-1}$ protein. (b) Time course of [$^3$H]-oestradiol 17β uptake by segments of LAD from male (○) and female pigs (●). The two lines represent the total uptake in the presence of an excess of unlabelled oestradiol 17β (100 μM) in the incubation medium.

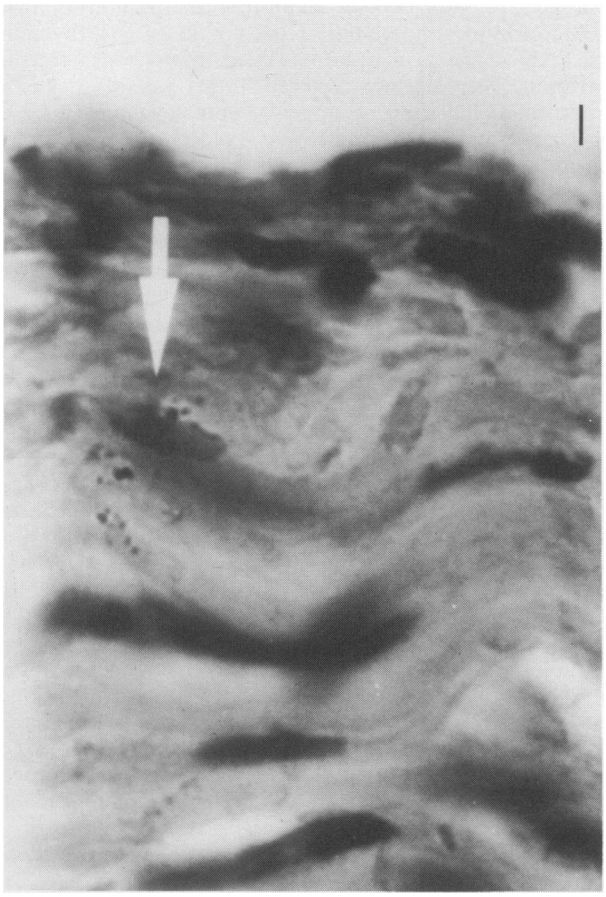


**Figure 4** Autoradiograph of an LAD explant incubated with [$^3$H]-oestradiol 17$\beta$ for 60 min. The photograph shows the silver grains over the nucleus and in the cytoplasm of the smooth muscle cells. $NTB_2$ emulsion. Staining with Mayer's haemotoxylin. The bar represents 10 $\mu$m.

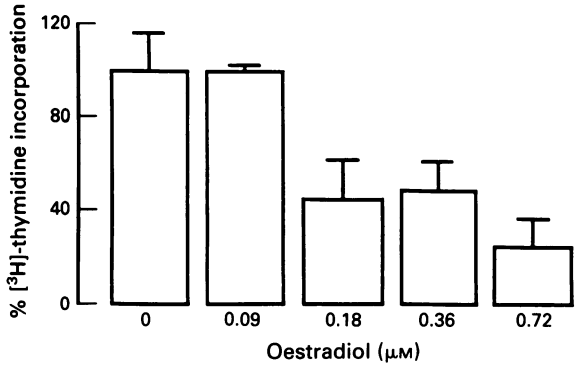



**Figure 5** Oestradiol 17$\beta$ inhibition of [$^3$H]-thymidine uptake into segments of porcine LAD. Vascular segments were exposed to oestradiol 17$\beta$ and radioactive thymidine for 48 h. The results are mean ± s.e.mean ($n = 4$) of [$^3$H]-thymidine uptake into the control tissues treated with the vehicle (152,876 ± 31,694 c.p.m. mg$^{-1}$ protein).

centrations (1 $\mu$M) of tamoxifen and its active metabolite 4-hydroxytamoxifen had oestrogen-like effects in reducing [$^3$H]-thymidine uptake to 28 and 16%, of the control respectively (Figure 6). In the same experiment oestradiol 17$\beta$ (360 nM) was more active and reduced thymidine uptake to 41 ± 5% of the control.

However, pretreatment of the segments with either of the two partial agonists, tamoxifen or 4-hydroxytamoxifen, failed to antagonize the inhibitory effect of oestradiol 17$\beta$.

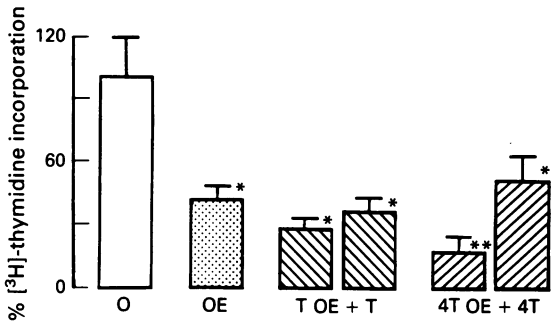



**Figure 6** Effects of 1 $\mu$M of either tamoxifen (T) or 4-hydroxytamoxifen (4T) on oestradiol 17$\beta$ (OE) inhibition of [$^3$H]-thymidine uptake into segments of porcine LAD (48 h incubation). The antioestrogens were added to the medium 3 h before oestradiol 17$\beta$ (360 nM). The columns represent mean ± s.e.mean ($n = 4$) of the percentage of the total uptake into segments treated only with the vehicle (301,999 ± 60,236 c.p.m. mg$^{-1}$ protein).

## Discussion

The purpose of these studies was to determine the effect of nanomolar concentrations of oestradiol 17$\beta$ on the proliferation of coronary artery smooth muscle cell *in vitro*. Oestradiol 17$\beta$ (180–720 nM) significantly inhibited [$^3$H]-thymidine uptake into porcine LAD segments. This suggests that in our experimental conditions, oestradiol 17$\beta$ inhibits smooth muscle cell proliferation in the pig (LAD) coronary artery.

The LAD coronary artery preparation used in this study was evaluated with several compounds known to affect cellular proliferation. Firstly, treatment with either forskolin or sodium nitroprusside is reported to inhibit cellular replication, probably by increasing basal levels of cyclic AMP and cyclic GMP, respectively, as described by Friedman (1976); Kempski *et al.* (1987) and by Garg & Hassid (1989). In our studies, both forskolin (100 $\mu$M) and sodium nitroprusside (50, 75 and 100 $\mu$M) significantly inhibited [$^3$H]-thymidine uptake in a concentration-dependent manner.

Serum is expected to increase cell proliferation due to the presence of growth factors. However, serum can also inhibit thymidine uptake into cells in culture medium (Berthois *et al.*, 1986) depending on concentration, pretreatment with activated charcoal, and cell types. In the LAD segments, a concentration of 1% had no effect, but a significant decrease of [$^3$H]-thymidine uptake was observed after incubation with 5 and 10 fold higher concentrations of foetal bovine serum. Serum is reported to increase prostacyclin production which acts in an autocrine fashion (McIntyre *et al.*, 1978) to inhibit cell proliferation indirectly by increasing basal levels of cyclic AMP. In addition, serum is also required for endothelial growth and preservation (Diglio *et al.*, 1988). Thus, the inhibition of [$^3$H]-thymidine uptake by 5 to 10% which we observed may relate to preservation of the endothelium resulting in inhibition of SMC growth.

The cells (>90%) growing out from the LAD segments were identified by specific immunofluorescence staining of the cytoskeleton proteins $\alpha$-actin and desmin (Skaill *et al.*, 1986; Kocher & Gabbiani, 1986) as smooth muscle cells. It remains to be determined to what extent [$^3$H]-thymidine was incorporated into the proliferating smooth muscle cells.

Oestradiol 17$\beta$ is reported to inhibit proliferation in primary cultures of smooth muscle cells from rabbit aorta (Fischer-Dzoga *et al.*, 1983). This effect of oestradiol 17$\beta$ on vascular SMC proliferation may be mediated directly by activation of oestrogen receptors and/or indirectly by releasing other hormones and growth factors (Sutherland *et al.*, 1983; Davidson & Lippman, 1989). Support for a direct effect of oestrogens on the vessel wall stems from the finding of high affinity oestrogen binding sites in extracts prepared from rabbit aorta ($K_d$ $2.8 \times 10^{-10}$ M) by Colburn & Buon-

assisi (1978), from rat aorta smooth muscle cell ($K_d$ $5.0 \times 10^{-8}$ M) by Nakao *et al.* (1981) and from dog coronary artery ($K_d$ $3.6 \times 10^{-9}$ M) by Harder & Coulson (1979).

Oestrogen appears to activate vascular oestrogen receptors as suggested by its ability to increase progesterone binding sites in baboon (*Papio* sp.) aortic SMC (Lin *et al.*, 1986) which is similar to its effects in uterus, ovary and breast where the response is widely believed to be receptor-mediated. Other effects of oestradiol 17β on SMC which may also involve oestrogen receptor activation include: augmented prostacyclin production by smooth muscle cells obtained from rat aorta (Chang *et al.*, 1980) as well as inhibition of collagen synthesis and hydroxy proline incorporation into rabbit aorta (Fischer & Swain, 1985).

We found radiolabelled oestradiol 17β to be incorporated into the porcine LAD segments in a time-dependent manner. The autoradiographs demonstrated that the tracer was present in the cytoplasm as well as in the nucleus of the different cells. Previous studies by Stumpf *et al.* (1977) have shown that nuclear localization of radioactive oestradiol 17β occurs in vascular tissues as well as in other target tissues for the hormone (Stumpf *et al.*, 1977; Haras *et al.*, 1989). Our finding of nuclear localization of oestradiol as well as in the cytoplasm indicates that the porcine LAD may indeed be a target for oestradiol 17β. Thus, the inhibition by oestradiol 17β of [$^3$H]-thymidine uptake into pig LAD segments may relate to oestrogen receptors. The distribution of [$^3$H]-oestradiol 17β in the segments further suggests that oestradiol may act directly on the smooth muscle cells and/or indirectly by affecting paracrine mechanisms involving other cells within the vessel wall.

The presence of phenol red, a weak oestrogen agonist, completely prevented the inhibitory effect of oestradiol 17β on [$^3$H]-thymidine uptake into LAD segments. In this context it is relevant to recall that oestrogen increases proliferation of MCF 7 cells and that this effect is also prevented by the presence of phenol red in the medium (Berthois *et al.*, 1986; Welshons *et al.*, 1988); this effect of phenol red was attributed to its weak oestrogen activity and its occupation of oestrogen receptor, which reinforces the notion that the inhibition by oestradiol 17β of the uptake of [$^3$H]-thymidine into LAD segments may be mediated by oestrogen receptor activation. Therefore, we explored further whether this effect of oestradiol 17β is an oestrogen-receptor-mediated response by using classical anti-oestrogens, which are used in the treatment of human breast cancer.

Tamoxifen and its active metabolite, 4-hydroxytamoxifen, are both non-steroidal anti-oestrogens but they are also partial agonists (Jordan, 1984). The side effects of tamoxifen treatment in women are typical of those resulting from administration of oestrogen. We found these two anti-oestrogens, in the absence of oestradiol 17β, significantly to inhibit [$^3$H]-thymidine uptake into the pig LAD. This inhibition may be an oestrogen-like effect of these partial agonists. These findings suggest that there may be at least two different oestrogen receptors. One is the classical uterine oestrogen receptor antagonized by tamoxifen. Conversely, tamoxifen is an oestrogen agonist for the other oestrogen receptor at least at the μM concentration used. These concentrations are those normally used of tamoxifen known to antagonize oestrogen in breast cancer cell lines. Our data cannot exclude completely the possibility of non-receptor-mediated actions of oestradiol participating in the described inhibitory effect. However, they reinforce the notion that oestradiol-induced inhibition of [$^3$H]-thymidine incorporation may be mediated through oestrogen receptors.

In summary, we describe for the first time an inhibitory effect of oestradiol 17β on thymidine uptake into segments of pig LAD. This effect seems to be mediated through oestrogen receptors. We suggest that oestradiol inhibition of smooth muscle cell proliferation may be one of the factors involved in the decreased incidence of coronary artery disease in young women.

This work was supported by Grants HL40069, HL32319 and HL36802 from the Heart, Lung and Blood Institute of the National Institute of Health.

## References

BERTHOIS, Y., KATZENELLENBOGEN, J.A. & KATZENELLENBOGEN, B.S. (1986). Phenol red in tissue culture media is a weak estrogen: implications concerning the study of estrogen-responsive cells in culture. *Proc. Natl. Acad. Sci. U.S.A.*, **83**, 2496–2500.

CHANG, W.C., NAKAO, J., ORIMO, H. & MUROTA, S.I. (1980). Stimulation of prostacyclin biosynthetic activity by estradiol in rat aortic smooth muscle cells in culture. *Biochem. Biophys. Acta*, **619**, 107–118.

CHENG, L.P., KUWAHARA, M., JACOBSSON, J. & FOEGH, M.M. (1991). Inhibition of myointimal hyperplasia and macrophage infiltration by estradiol in aorta allografts. *Transplantation*, **52**, 967–972.

CLARKSON, T.B., ADAMS, M.R., KAPLAN, J.R. & KORITNIK, D.R. (1987). Gonadal steroids in cardiac atherosclerosis in primates. *Transplant. Proc.*, **19** (Suppl. 5), 85–89.

CLARKSON, T.B., SHIVELY, C.A., MORGAN, T.M., KORITNIK, D.R., ADAMS, M.R. & KAPLAN, J.R. (1990). Oral contraceptives and coronary artery atherosclerosis of cynomolgus monkeys. *Obstet. Gynecol.*, **75**, 217–222.

CLOWES, A.W., REIDY, M.A. & CLOWES, M.M. (1983). Kinetics of cellular proliferation after arterial injury: I. Smooth muscle growth in the absence of endothelium. *Lab. Invest.*, **49**, 327–333.

COLBURN, P. & BUONASSISI, V. (1978). Estrogen-binding sites in endothelial cell cultures. *Science*, **201**, 817–819.

CONSTANTINIDES, P., GUTMANN-AUERSPERG, N., HOSPES, D. & WILLIAMS, K. (1962). Estradiol and prednisolone in rabbit atherosclerosis. *Arch. Pathol.*, **73**, 277–280.

DAVIDSON, N.E. & LIPPMAN, M.E. (1989). The role of estrogens in growth regulation of breast cancer. *Oncogenesis*, **1**, 89–111.

DIGLIO, C.A., GRAMMAS, P., GIACOMELLI, F. & WIENER, J. (1988). Rat heart-derived endothelial cell cultures: isolation, cloning and characterization. *Tissue and Cell*, **20**, 477–492.

FISCHER, G. & SWAIN, M.L. (1985). Effects of estradiol and progesterone on the increased synthesis of collagen in atherosclerotic rabbit aortas. *Atherosclerosis*, **54**, 177–185I.

FISCHER-DZOGA, K., WISSLER, R.W. & VESSELINOVITCH, D. (1983). The effect of estradiol on the proliferation of rabbit aortic medial tissue culture cells induced by hyperlipidemic serum. *Exp. Mol. Pathol.*, **39**, 355–363.

FOEGH, M.L., KHIRABADI, B.S., NAKANISHI, T., VARGAS, R. & RAMWELL, P.W. (1987). Estradiol protects against experimental cardiac transplant atherosclerosis. *Transplant. Proc.*, **19** (Suppl. 5) 90–95.

FRIEDMAN, D.L. (1976). Role of cyclic nucleotides in cell growth and differentiation. *Physiol. Rev.*, **56**, 652–708.

GARG, U.C. & HASSID, A. (1989). Nitric oxide-generating vasodilators and 8-bromo-cyclic guanosine monophosphate inhibit mitogenesis and proliferation of cultured rat vascular smooth muscle cells. *J. Clin. Invest.*, **83**, 1774–1777.

HARAS, D., SAMPEREZ, S. & JOUAN, P. (1989). Positive and negative effects of estradiol-17β in the rat uterus. *J. Steroids Biochem.*, **33**, 1073–1080.

HARDER, D.R. & COULSON, P.B. (1979). Estrogen receptors and effects of estrogen on membrane electrical properties of coronary vascular smooth muscle. *J. Cell Physiol.*, **100**, 375–382.

JORDAN, V.C. (1984). Biochemical pharmacology of antiestrogen action. *Pharmacol. Rev.*, **36**, 245–257.

KEMPSKI, O., WROBLEWSKA, B. & SPATZ, M. (1987). Effects of forskolin on growth and morphology of cultured glial and cerebrovascular endothelial and smooth muscle cells. *Int. J. Devl. Neuroscience*, **5**, 435–445.

KOCHER, O. & GABBIANI, G. (1986). Cytoskeletal features of normal and atheromatous human arterial smooth muscle cells. *Human Pathol.*, **17**, 875–880.

LIN, L.A., MCGILL, H.C. & SHAIN, S.A. (1982). Hormone receptors of the baboon cardiovascular system. Biochemical characterization of aortic and myocardial cytoplasmic progesterone receptors. *Circ. Res.*, **50**, 610–616.

LIN, A.L. & SHAIN, S.A. (1986). Sexual dimorphism characterizes steroid hormone modulation of rat aortic hormone receptors. *Endocrinol.*, **119**, 296–302.

LIN, A.L., GONZALEZ, R., CAREY, K.D. & SHAIN, S.A. (1986). Estradiol-17β affects estrogen receptor distribution and elevates progesterone receptor content in baboon aorta. *Arteriosclerosis*, **6**, 495–504.

LOWRY, O.H., ROSEBROUGH, N.J., FARR, A.L. & RANDALL, R.J. (1951). Protein measurement with folin phenol reagent. *J. Biol. Chem.*, **193**, 265–275.

MCINTYRE, D.E., PEARSON, J.D. & GORDON, J.L. (1978). Localization and stimulation of prostacyclin production in vascular cells. *Nature*, **271**, 549–551.

MOSKOWITZ, M.S., MOSKOWITZ, A.A., BRADFORD, W.L. & WISSLER, R.W. (1956). Changes in serum lipids and coronary arteries of the rat in response to estrogens. *Arch. Pathol.*, **61**, 245–263.

NAKAO, J., CHANG, W.C., MUROTA, S.I. & ORIMO, H. (1981). Estradiol-binding sites in rat aortic smooth muscle cells in culture. *Atherosclerosis*, **38**, 75–80.

RENAUD, S. (1970). Thrombosis and atherosclerosis prevention by estrogens in hyperlipemic rats. *Atherosclerosis*, **12**, 467–473.

RHEE, C.Y., SPAET, T.H., STEMERMAN, M.B., LAJAM, F. & SHIANG, H.H. (1977). Estrogen suppression of surgically induced vascular intimal hyperplasia in rabbits. *J. Lab. Clin. Med.*, **90**, 77–84.

ROSS, R. & GLOMSET, J.A. (1973). Atherosclerosis and arterial smooth muscle cell: proliferation of smooth muscle is a key event in the genesis of the lesion of atherosclerosis. *Science*, **180**, 1332–1339.

SKAILL, O., ROPRAZ, P., TRZECLAK, A., BENZONANA, G., GILLESSEN, D. & GABBIANI, G. (1986). A monoclonal antibody against α-actin: a new probe for smooth muscle differentiation. *J. Cell. Biol.*, **103**, 2787–2796.

STUMPF, W.E., SAR, M. & AUMULLER, G. (1977). The heart: a target organ for estradiol. *Science*, **196**, 319–321.

SUTHERLAND, R.L., REDDEL, D.F. & GREEN, M.D. (1983). Effect of oestrogens on cell proliferation and cell kinetics. A hypothesis on the cell cycle effects of antioestrogens. *Eur. J. Cancer Clin. Oncol.*, **19**, 307–318.

VARGAS, R., WROBLEWSKA, B., HATCH, J., GROJEC, M., FOEGH, M. & RAMWELL, P.W. (1990). Estradiol inhibition of thymidine uptake in explants of porcine left anterior descending coronary artery. *Circulation*, **82**, 2273.

WALKER, L.N., BOWEN-POPE, D.F., ROSS, R. & REIDY, M.A. (1986). Production of platelet-derived growth factor-like molecules by cultured arterial smooth muscle cells accompanies proliferation after arterial injury. *Proc. Natl. Acad. Sci. U.S.A.*, **83**, 7311–7315.

WELSHONS, W.V., WOLF, M.F., MURPHY, C.S. & JORDAN, V.C. (1988). Estrogenic activity of phenol red. *Mol. Cell. Endocrinol.*, **57**, 169–178.

*(Received January 20, 1993*
*Accepted February 24, 1993)*

*Br. J. Pharmacol.* (1993), **109**, 618–624 © Macmillan Press Ltd, 1993

# Development of a radioligand binding assay for 5-$HT_4$ receptors in guinea-pig and rat brain

[1]C.J. Grossman, G.J. Kilpatrick & K.T. Bunce

Pharmacology Division, Glaxo Group Research Ltd., Park Road, Ware, Herts SG12 0DP

**1** The 5-$HT_4$ receptor antagonist, GR113808, has been radiolabelled to a high specific activity with tritium.

**2** Characterization of specific [$^3$H]-GR113808 binding in homogenates of guinea-pig striatum and hippocampus revealed a single site of high affinity ($K_d$ values 0.20 and 0.13 nM respectively).

**3** [$^3$H]-GR113808 binding was reversible and displayed rapid kinetics such that association and dissociation were complete within 3 min.

**4** Specific [$^3$H]-GR113808 binding was potently and stereoselectively inhibited by agonists and antagonists acting at the 5-$HT_4$ receptor but not by compounds selective for other 5-HT receptors or other neurotransmitter receptors.

**5** Autoradiographic analysis revealed a discrete localization in both guinea-pig and rat brain with high concentrations of binding in brain areas such as the striatum, substantia nigra and olfactory tubercle.

**6** [$^3$H]-GR113808 binding to homogenates of guinea-pig striatum meets the criteria for labelling of the 5-$HT_4$ receptor and, as such, represents the first characterization of this receptor in a radioligand binding assay.

**Keywords:** 5-$HT_4$ receptors; GR113808; radioligand binding; guinea-pig hippocampus; guinea-pig striatum; autoradiography

## Introduction

Receptors for 5-hydroxytryptamine (5-HT) of the 5-$HT_4$ type have been identified in a variety of functional preparations both centrally and peripherally (Bockaert *et al.*, 1992). In the central nervous system 5-$HT_4$ receptors have been shown to mediate an activation of adenylate cyclase (Dumuis *et al.*, 1988; Bockaert *et al.*, 1990). In the periphery, 5-$HT_4$ receptors produce a variety of responses including relaxation of smooth muscle (Reeves *et al.*, 1991), neuronal cholinergically mediated contraction of guinea-pig ileum and proximal colon (Eglen *et al.*, 1990; Elswood *et al.*, 1991), enhancement of the 'twitch' response in electrically field stimulated guinea-pig ileum (Craig & Clarke, 1990) and induction of chloride secretion in rat distal colon (Bunce *et al.*, 1991). 5-$HT_4$ receptors have also been implicated in cardiovascular effects in both pig and man (Bom *et al.*, 1988; Villalon *et al.*, 1990: Kaumann *et al.*, 1990).

GR113808 ([1-[2-methylsulphonyl)amino]ethyl]-4-piperidinyl]methyl 1-methyl-1H-indole-3-carboxylate) (Figure 1, Grossman *et al.*, 1993) is a highly potent and competitive antagonist of 5-$HT_4$ receptor-mediated effects in guinea-pig proximal colon and rat oesophagus ($pA_2$ 9.2; Schild slope 1.1 and $pA_2$ 9.5 Schild slope 0.7 respectively). GR113808 is also highly selective with only weak affinity at 5-$HT_3$ receptors ($pK_i$ 6.0) and no activity at other 5-HT receptors (up to 10 μM). GR113808 has been radiolabelled to a specific activity of 83.4 Ci mmol$^{-1}$ with tritium and we now report on the binding characteristics of this compound.

## Methods

### *Tissue preparation*

Dunkin Hartley guinea-pigs (~400 g) were killed by cervical dislocation and the brain removed and dissected. Tissue was used immediately.

For binding, pooled striatal or hippocampal brain tissue was placed in 15 volumes of HEPES buffer (50 mM pH 7.4, 4°C). This was homogenized in an Ultra-Turrax homogenizer for 12 s and subsequently centrifuged at 48,000 *g* and 4°C in a Sorvall RC5C centrifuge. The resulting pellet was resuspended in HEPES buffer to make a homogenate at 30 mg ml$^{-1}$ for striatum and 50 mg ml$^{-1}$ for hippocampus.

### *Homogenate binding*

All determinations were performed in triplicate. Assay tubes contained: 300 μl HEPES buffer at pH 7.4, 200 μl of a solution of either a competing agent (for drug competition studies), 5-HT to give a final concentration of 30 μM (to determine non-specific binding) or buffer (for determination of total binding), 400 μl of [$^3$H]-GR113808 in HEPES buffer

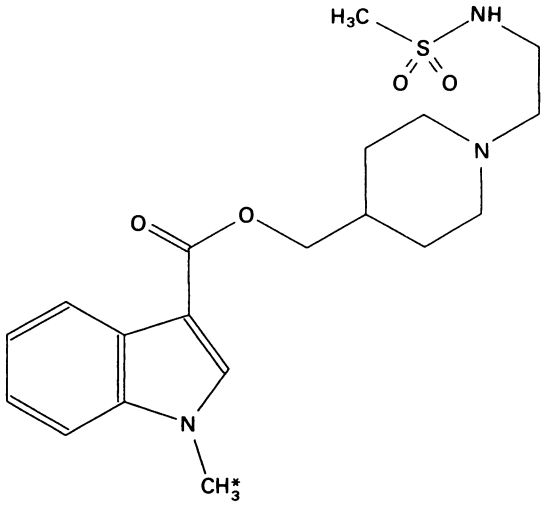



**Figure 1** Structure of GR113808. *Indicates the site at which the compound has been radiolabelled with tritium.

[1] Author for correspondence.

to give a final concentration of 0.1 nM and 100 µl of tissue preparation. Assay tubes were incubated at 37°C.

To determine the rate of association, reactions were stopped 0, 0.5, 1, 2, 3, 4, 5, 10, 15, 20 min after addition of the tissue and specific binding was determined. For dissociation, 5-HT (30 µM) was added to the assay tube for the same time periods after the reaction had proceeded for 30 min. The reaction was terminated by rapid vacuum filtration and washing (1 × 4 ml; see Results) with ice-cold buffer through Whatman GF/B filter paper using a Brandel Cell Harvester. Filters were presoaked in a solution of polyethylenimine (~0.1%) to reduce filter binding. For saturation analysis assay tubes were set up as above with the exception that 15 concentrations of [$^3$H]-GR113808 in HEPES buffer were used to give final concentrations of 0.004–2 nM. For both saturation analysis and drug competition studies, assay tubes were incubated at 37°C for 30 min and the reaction terminated as above. Filters were placed in 8 ml of Packard Emulsifier Safe scintillation cocktail overnight before scintillation counting.

### *Protein assays*

Tissue protein was asssayed by the Bio-Rad Protein Assay (Bradford, 1976). Bovine serum albumin was used as the standard.

### *Data calculation*

Equilibrium saturation parameters and p$K_i$ values were calculated by use of the computer programme 'Ligand' (Munson & Rodbard, 1980). Hill coefficients were obtained with the computer programme 'Allfit' (DeLean *et al.*, 1977). Significance testing was carried out with an unpaired Student's *t* test. Values were considered significantly different when $P<0.05$.

### *Autoradiography*

Lister hooded rats or Dunkin Hartley guinea-pigs were killed and the brain removed. Slide mounted sections of the brain were prepared as described by Kilpatrick *et al.* (1988). Briefly, rat and guinea-pig brains were mounted in O.C.T. embedding compound, frozen in liquid nitrogen and 20 µm sections cut using a cryostat. Sections were taken alternately onto separate slides for determination of total and non-specific binding. The slide-mounted sections were incubated in HEPES buffer containing 0.1 nM [$^3$H]-GR113808 at 37°C for 30 min. Non-specific binding was determined by the addition of 5-HT to the HEPES buffer to give a final concentration of 30 µM. At the end of the 30 min incubation period slides were washed in ice-cold buffer for 2 × 5 s, dipped in ice-cold water to remove the buffer and then allowed to dry in a stream of air. Slides were exposed to autoradiographic film (Hyperfilm – $^3$H; Amersham International) for 6 weeks prior to development. Quantitative measurements of specific binding were made with a Cambridge Instruments Quantimet 970.

### *Drugs and solutions*

[$^3$H]-GR113808 had a specific activity of 83.4 Ci mmol$^{-1}$ and was synthesized by Amersham International. The following compounds (source) were used: 5-hydroxytryptamine creatinine sulphate (Sigma), 5-methoxytryptamine hydrochloride (Sigma), metoclopramide hydrochloride (Sigma), dopamine (Sigma), γ-aminobutyric acid (Sigma), atropine sulphate (Sigma), tropisetron (Research Biochemicals Inc), ketanserin tartrate (Janssen), spiperone (Janssen) methysergide maleate (Sandoz), histamine phosphate (BDH), granisetron hydrochloride (Glaxo), ondansetron hydrochloride (Glaxo), α-methyl-5-hydroxytryptamine maleate (α-Me-5-HT; Glaxo), 2-methyl-5-hydroxytryptamine HCl.$H_2$0 (2-Me-5-HT; Glaxo), 5-carboxamidotryptamine maleate (5-CT; Glaxo), 8-hydroxy-2-(di-n-propylamino)tetralin (8-OH-DPAT, Glaxo), 5-OH-indalpine maleate (Glaxo), cisapride (Janssen; made into tartrate at Glaxo), renzapride (Glaxo), **R,S**-zacopride, **R**-zacopride, **S**-zacopride hydrochloride (Glaxo), SDZ205-557 (2-methoxy-4-amino-5-chloro-benzoic acid 2-(diethylamino) ethyl ester; Glaxo), BIMU1 (endo-N-(8-methyl-8-azabicyclo-[3.2.1] oct-3-yl)-2,3-dihydro-3-ethyl-2-oxo-1H-benzimidazole-1-carboxamide; Glaxo), BIMU8 (endo-N-(8-methyl-8-azabicyclo-[3.2.1] oct-3-yl)-2,3-dihydro-(1-methyl) ethyl-2-oxo-1H-benzimidazole-1-carboxamide; Glaxo), GR113808 maleate (Glaxo).

## Results

### *Establishment of suitable preparation*

In washed crude homogenates of guinea-pig striatum 5-HT (30 µM) inhibited 70–80% of total [$^3$H]-GR113808 (0.1 nM) binding. In guinea-pig hippocampus specific binding was slightly lower (50–70%) (specific binding = total binding minus binding in the presence of 5-HT (30 µM)). The specific binding in both tissues was linear over a wide range of tissue concentration (1–10 mg, per assay tube; data not shown).

### *Association and dissociation of specific [$^3$H]-GR113808 binding*

The rates of association and dissociation of specific [$^3$H]-GR113808 binding were investigated. Results indicate that, in

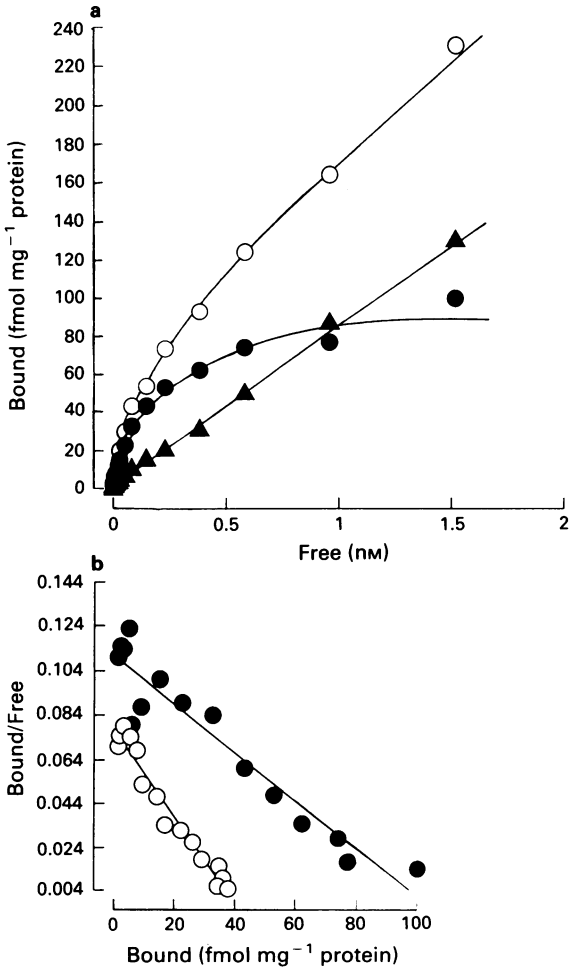



**Figure 2** (a) Saturation analysis of [$^3$H]-GR113808 (0.004–2 nM) binding in guinea-pig striatum where (○) is total binding; (●) is specific binding; and (▲) is non-specific binding determined by the addition of 30 µM 5-HT. (b) Scatchard transformation of specific [$^3$H]-GR113808 (0.004–2 nM) binding to homogenates of guinea-pig striatum (●) and guinea-pig hippocampus (○). Results are from a single experiment but are representative of three such experiments.

both hippocampus and striatum, association and dissociation occur very rapidly such that the ligand is either fully associated or dissociated within 3 min. From a number of studies using longer association periods it was found a steady-state of specific binding existed for at least 1 h (data not shown). As the ligand was half saturated at time 0 min it was not possible to calculate rate constants accurately for association and dissociation. Because of this fast dissociation rate, samples were only washed once during the filtration stage of the assay to minimize dissociation of ligand from the receptor.

### *Saturation analysis*

Equilibration saturation studies of specific binding of [$^3$H]-GR113808 (0.004–2 nM) revealed a single saturable site of high affinity in both tissues (striatum; $K_d = 0.20 \pm 0.02$ nM, $B_{max} = 92.7 \pm 7.1$ fmol mg$^{-1}$ protein; hippocampus: $K_d = 0.13 \pm 0.01$ nM, $B_{max} = 40.0 \pm 1.1$ fmol mg$^{-1}$ protein; values are ± s.e.mean, $n = 3$) (Figure 2). Non-specific binding increased linearly with increasing ligand concentration in both tissues.

### *Drug competition studies*

A range of 5-HT$_4$ receptor agonists and antagonists completely inhibited the specific binding of [$^3$H]-GR113808. Inhibition curves were apparently monophasic (Figure 3). Affinity values and Hill slopes derived from these curves using computer analysis are presented in Table 1. Of the agonists tested, only those active in 5-HT$_4$ receptor containing preparations (5-HT, 5-methoxytryptamine, 5-CT, αMe-5-HT, BIMU1, BIMU8) potently inhibited [$^3$H]-GR113808 binding. By contrast, agonists for other 5-HT receptors, for example the 5-HT$_{1A}$ agonist, 8-OH-DPAT, the so called 5-HT$_{1P}$ receptor agonist, 5-OH-indalpine, the 5-HT$_{1D}$ receptor agonist, sumatriptan and the 5-HT$_3$ receptor agonist, 2-Me-5-HT, had no effect on [$^3$H]-GR113808 binding at concentrations up to 10 μM. The substituted benzamides, metoclopramide, cisapride, renzapride and zacopride, partial agonists at the 5-HT$_4$ receptor all potently inhibited [$^3$H]-GR113808 binding. Specific [$^3$H]-GR113808 binding was also inhibited by the 5-HT$_4$ receptor antagonists, tropisetron, SDZ205-557 and unlabelled GR113808. Hill slopes for the inhibition of [$^3$H]-GR113808 binding by 5-HT$_4$ receptor agonists and antagonists were not significantly different from unity (95% confidence limits overlapped unity), with the exception of 5-methoxytryptamine, 5-CT, α-Me-5-HT, renzapride and tropisetron in guinea-pig striatum and BIMU1 in guinea-pig hippocampus.

Several antagonists at other 5-HT receptors and ligands for other neurotransmitters were also tested. The 5-HT$_1$-like receptor antagonists, spiperone and methysergide, the 5-HT$_2$ receptor antagonist, ketanserin, and the 5-HT$_3$ receptor antagonists, ondansetron and granisetron had no effect on the binding of [$^3$H]-GR113808 up to 10 μM. Similarly atropine, histamine, dopamine and GABA had no effect on [$^3$H]-GR113808 binding when tested at 10 μM.

The effect of GTP and the non hydrolysable analogue GppNHp on 5-HT affinity was determined in both the hippocampus and the striatum. In guinea-pig hippocampus the addition of GppNHp (100 μM) and $Mg^{2+}$ (100 μM) had little effect on the ability of 5-HT to displace [$^3$H]-GR113808 binding lowering the p$K_i$ value from 7.1 to 6.9 ($n = 2$). However, in guinea-pig striatum, GTP (100 μM) reduced the affinity of 5-HT from p$K_i = 7.3 \pm 0.1$ to $6.7 \pm 0.2$ ($n = 4$). The Hill coefficient was slightly increased from 0.77 to 0.83. Similarly, GppNHp also reduced the affinity of 5-HT from p$K_i = 7.3 \pm 0.1$ to $6.6 \pm 0.1$ ($n = 3$). In binding studies using homogenates of striatum it was found that the addition of $Mg^{2+}$ (100 μM) completely inhibited specific binding of [$^3$H]-GR113808 and therefore this was omitted from the assay.

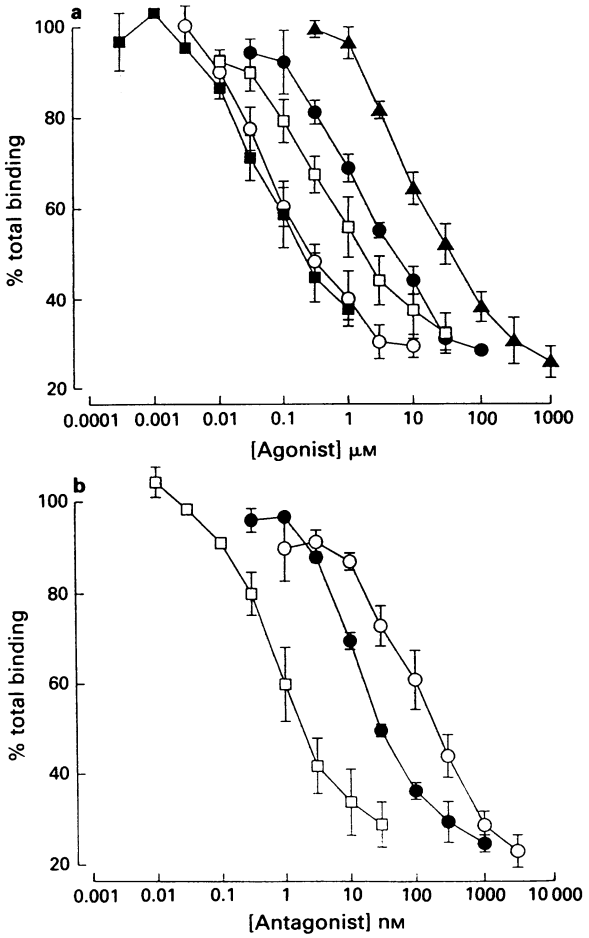



**Figure 3** Inhibition of 0.1 nM [$^3$H]-GR113808 binding in homogenates of guinea-pig striatum by 5-HT$_4$ receptor agonists and antagonists. (a) Agonists: (■) BIMU1; (○) 5-HT; (□) 5-methoxytryptamine; (●) α-Me-5-HT; (▲) 5-carboxamidotryptamine. (b) Antagonists: (□) GR113808; (●) SDZ205-557; (○) tropisetron. Results are presented as a percentage of the total binding in the absence of a competing agent and are the means ± s.e.mean of 3 separate observations. For abbreviations, see text.

### *Autoradiographic analysis of 5-HT$_4$ receptor distribution in guinea-pig and rat brain*

Autoradiographic analysis of specific [$^3$H]-GR113808 binding indicated that it was differentially localized throughout the guinea-pig and rat brain ($n = 4$; Table 2, Figure 4). The areas showing the highest levels of specific binding included the striatum, olfactory tubercle, globus pallidus, nucleus accumbens and substantia nigra in both species. The interpeduncular nucleus (IPN) had the highest levels of binding in the rat (Table 2). In both the guinea-pig and the rat, neither the frontal cortex nor the cerebellum showed measurable specific binding of [$^3$H]-GR113808. Non-specific binding of the [$^3$H]-GR113808 was uniform throughout the brain of both guinea-pig and rat.

## Discussion

Specific [$^3$H]-GR113808 binding was detected in homogenates of guinea-pig striatum and hippocampus. Because functional responses are not measured in a binding assay, it is important that certain criteria are met before concluding that this represents the 5-HT$_4$ receptor rather than a non-receptor site (Burt, 1978). The characteristics of specific [$^3$H]-GR113808 binding in relation to these criteria are discussed below.

**Table 1** The affinities of various compounds that compete for 0.1 nM [$^3$H]-GR113808 binding in homogenates of guinea-pig striatum and hippocampus.

| Compound | *Guinea-pig striatum* p$K_i$† | Hill coefficient†† | *Guinea-pig hippocampus* p$K_i$† | Hill coefficient†† |
|---|---|---|---|---|
| Agonist‡ | | | | |
| 5-HT | 7.3 | 0.77 | 7.1 | 0.82 |
| 5-methoxytryptamine | 6.5 | 0.65 | 6.2 | 0.90 |
| α-Me-5-HT | 5.8 | 0.58 | 5.8 | 0.90 |
| 5-carboxamidotryptamine | 5.2 | 0.71 | 4.9 | 0.76 |
| BIMU8 | 7.9* | 0.84* | 7.6* | 0.87* |
| Partial agonists** | | | | |
| BIMU1 | 7.8 | 0.89 | 7.8 | 0.84 |
| Metoclopramide | 6.3 | 1.00 | 6.2 | 0.90 |
| Cisapride | 7.5 | 0.93 | 7.2 | 0.80 |
| Renzapride | 7.0 | 0.84 | 6.9 | 0.75 |
| **R,S**-zacopride | 6.8 | 0.77 | 6.7 | 0.83 |
| **S**-zacopride | 6.7 | 0.87 | 6.6 | 0.80 |
| **R**-zacopride | 6.3 | 0.62 | 6.0 | 0.75 |
| Antagonists*** | | | | |
| Tropisetron | 7.2 | 0.81 | 7.2 | 0.88 |
| SDZ205-557 | 8.2 | 1.01 | 8.1 | 0.69 |
| GR113808 | 9.5 | 0.94 | 9.6 | 0.89 |

Affinity estimates are given as p$K_i$ values determined using the computer programme 'Ligand'. Values are the mean of three determinations except * where only one value was obtained. Hill coefficents are obtained from the curve fitting programme 'Allfit'.
†s.e.mean $\leq 0.2$.
††s.e.mean $\leq 0.23$.
‡Elswood *et al.*, 1991; Turconi *et al.*, 1991.
**Eglen *et al.*, 1990; Turconi *et al.*, 1991.
***Dumuis *et al.*, 1988; Buchheit *et al.*, 1992; Grossman *et al.*, 1993.

**Table 2** Distribution of 0.1 nM [$^3$H]-GR113808 binding assessed by autoradiographic analysis of sections of guinea-pig and rat brain

| *Brain area* | *Specific binding* (nCi mg$^{-1}$ tissue) *Guinea-pig* | *Rat* |
|---|---|---|
| Olfactory tubercle | 1.14 ± 0.19 | 0.81 ± 0.11 |
| N. accumbens | 0.89 ± 0.12 | 0.28 ± 0.03 |
| Striatum | 1.02 ± 0.09 | 0.37 ± 0.03 |
| Frontal cortex | 0.02 ± 0.05 | 0.04 ± 0.03 |
| Globus pallidus | 1.08 ± 0.15 | 0.56 ± 0.08 |
| Septum | 0.22 ± 0.04 | 0.07 ± 0.07 |
| Substantia nigra | 0.99 ± 0.13 | 0.36 ± 0.08 |
| S. colliculus | 0.18 ± 0.06 | 0.27 ± 0.09 |
| Hippocampus (dorsal) | 0.31 ± 0.09 | 0.09 ± 0.11 |
| Hippocampus (medial) | 0.26 ± 0.05 | 0.18 ± 0.03 |
| Hippocampus (ventral) | 0.29 ± 0.08 | 0.14 ± 0.11 |
| Cerebellum | 0.04 ± 0.02 | − 0.05 ± 0.03 |
| IPN | − | 0.93 ± 0.14 |

Values are presented as the mean and s.e.mean of measurements from four animals.

In functional studies in the rat oesophagus, GR113808 elicits surmountable antagonism at the 5-HT$_4$ receptor (Grossman *et al.*, 1993). Consistent with this, specific [$^3$H]-GR113808 binding was also reversible. Indeed specific [$^3$H]-GR113808 binding displayed very rapid kinetics such that the association and dissociation of the ligand was complete within 3 min. Due to this very rapid rate it was not possible to determine accurately association and dissociation rate constants.

Functional receptors exist in finite numbers and so it is important to show that specific binding is saturable. Specific [$^3$H]-GR113808 binding readily saturated (Figure 2). Scatchard transformation of specific binding in both the guinea-pig striatum and the hippocampus revealed the involvement of a single site. Curve fitting analysis revealed an equilibrium dissociation constant for [$^3$H]-GR113808 (0.20 nM and 0.13 nM for striatum and hippocampus respectively) very close to the affinity estimates derived from functional receptor assays in guinea-pig proximal colon and rat oesophagus (p$A_2$ 9.2–9.5).

The most important evidence that a binding site represents a functional receptor is that agonists and antagonists which are active at the receptor inhibit binding with the expected activity. Of the indole agonists tested, all those that are active in functional studies, 5-methoxytryptamine, α-Me-5-HT and 5-CT, potently inhibited [$^3$H]-GR113808 binding whilst agonists that are inactive in functional studies, 2-Me-5-HT, 8-OH-DPAT, 5-OH-indalpine and sumatriptan, had no effect on [$^3$H]-GR113808 binding. The benzimidazolone compounds, BIMU1 and BIMU8 have been shown to be partial agonists in 5-HT$_4$ receptor containing preparations, including the mouse colliculi and guinea-pig ileum (both contractions of unstimulated preparations and enhancement of twitch in field stimulated preparations) (Turconi *et al.*, 1991) as well as rat oesophageal tunica muscularis mucosae (Baxter & Clarke, 1992). Both compounds potently inhibited [$^3$H]-GR113808 binding with p$K_i$ values of 7.3 and 7.9 in the striatum for BIMU1 and BIMU8 respectively.

Similarly, benzamides which are partial agonists in a wide range of 5-HT$_4$ receptor containing preparations, including the guinea-pig proximal colon (Elswood *et al.*, 1991), electrical field stimulated guinea-pig ileum (Craig & Clarke, 1990) and guinea-pig hippocampus (Bockaert *et al.*, 1990), also potently inhibited specific [$^3$H]-GR113808 binding. In functional studies in rat oesophagus and guinea-pig colon, renzapride and **R,S**-zacopride have very similar acitivity with renzapride being fractionally more potent (Reeves *et al.*, 1991; Elswood *et al.*, 1991). In the present binding study, renzapride also revealed a slightly higher affinity than **R,S**-zacopride (p$K_i$ = 7.0 and 6.8 respectively in the striatum and 6.9 and 6.7 in the hippocampus). In guinea-pig colon, cisapride and metoclopramide have been tested as antagonists, with cisapride some 10 fold more potent than metoclopramide. This result was mirrored in the present binding study where p$K_i$ estimates for cisapride and metoclopramide

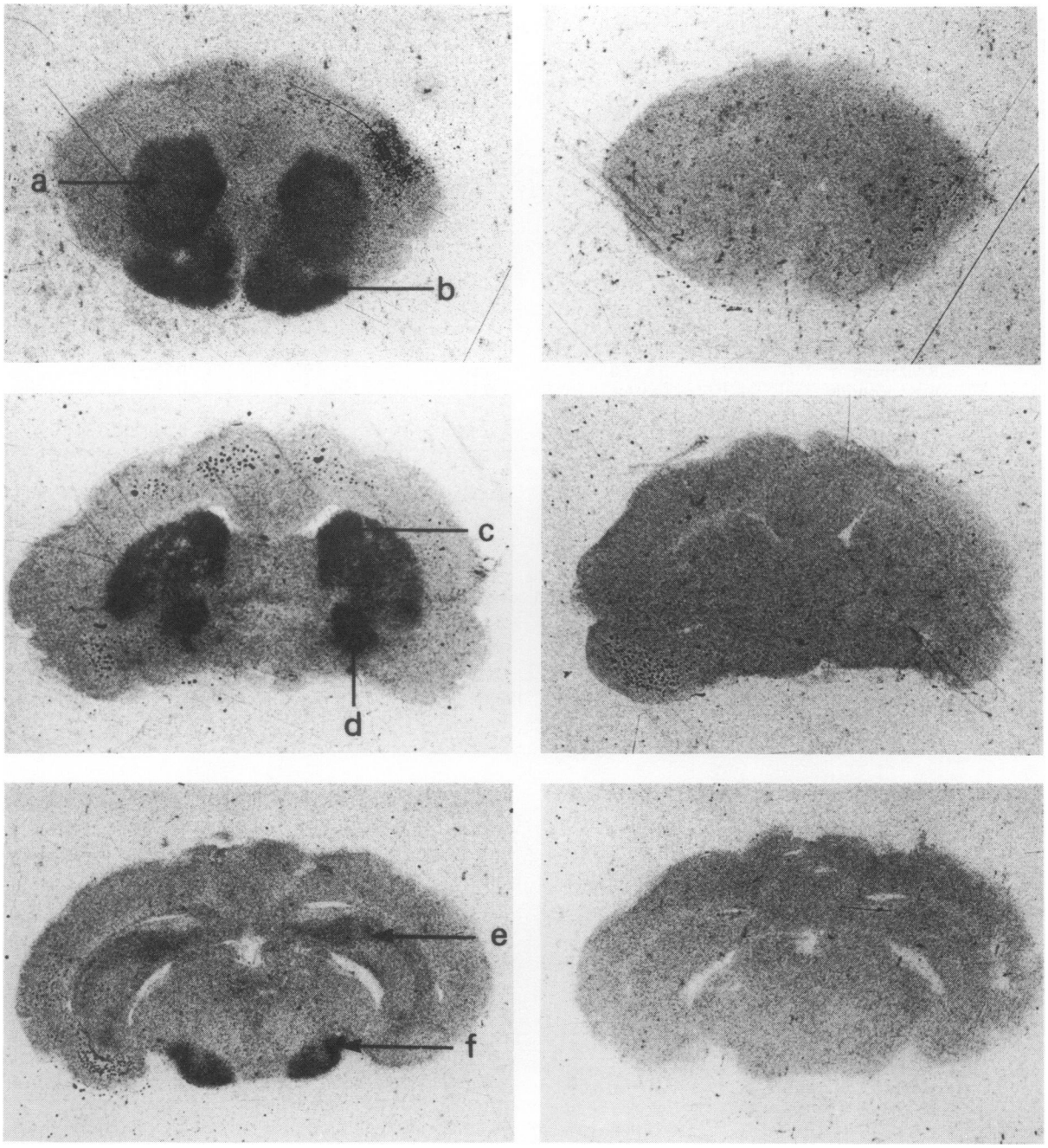



**Figure 4** Autoradiographs of 0.1 nM [$^3$H]-GR113808 binding in sections of guinea-pig brain. Sections in the left hand column show total binding and sections in the right hand column show non-specific binding defined by the inclusion of 5-HT (30 μM). Regions of high levels of binding are indicated; a, striatum; b, olfactory tubercle; c, striatum; d, globus pallidus; e, hippocampus; f, substantia nigra.

were 7.5 and 6.3 respectively in the striatum and 7.2 and 6.2 in the hippocampus. The use of the enantiomers of zacopride has indicated small but significant differences in the affinities of **R**- and **S**-zacopride for the [$^3$H]-GR113808 binding site in homogenates of both guinea-pig hippocampus and striatum ($P = 0.01$ and 0.04 respectively). This compares well with functional data in guinea-pig ileum where **S**-zacopride has been shown to be a full agonist and **R**-zacopride a weak partial agonist (Eglen *et al.*, 1990). This indicates a stereoselectivity for the [$^3$H]-GR113808 binding site.

The affinity of 5-HT$_4$ receptor antagonists in the present binding study compares well with functional data for these compounds. Tropisetron, the first 5-HT$_4$ receptor antagonist identified, has affinity values in functional studies ranging from 6.0–6.7 (Dumuis *et al.*, 1988; Craig & Clarke, 1990; Eglen *et al.*, 1990; Elswood *et al.*, 1991; Reeves *et al.*, 1991) in both the guinea-pig hippocampus and the striatum p$K_i$ values of 7.2 were obtained. Thus, in binding studies, tropisetron seems to have between 3 and 10 fold higher affinity than in functional studies. The more recently identified 5-HT$_4$ receptor antagonist, SDZ205-557 (Buchheit *et al.*, 1992) inhibited [$^3$H]-GR113808 binding with p$K_i$ values of 8.0 and 8.2 in guinea-pig hippocampus and striatum respectively. As with tropisetron, the affinity estimate obtained in the binding assay is higher than that obtained in functional studies. Unlabelled GR113808 also inhibited [$^3$H]-GR113808 binding with a p$K_i$ value of 9.5 in guinea-pig striatum and 9.6 in guinea-pig hippocampus. Again this value compares closely with affinity estimates from functional assays in guinea-pig colon and rat oesophagus where

GR113808 has $pA_2$ values of 9.2 and 9.5 respectively (Grossman *et al.*, 1993).

Hill coefficients for 5-HT are slightly increased by the addition of GTP, however, values obtained both in the presence and absence of GTP are not significantly different from unity. In guinea-pig striatum some agonists had Hill coefficients significantly lower than unity although this did not appear to be the case in the hippocampus. In future experiments it would be interesting to determine the effect of GTP on agonist Hill coefficients in guinea-pig striatum. The Hill coefficient for inhibition of [$^3$H]-GR113808 binding by tropisetron is also lower than unity and thus contrasts with that observed for the other antagonists tested. The reason for this is, however, now known.

5-HT$_4$ receptors are thought to be coupled to adenylate cyclase as 5-HT$_4$ receptor stimulation leads to an increase in cyclic AMP levels in a number of preparations both centrally (Dumuis *et al.*, 1988; Bockaert *et al.*, 1990) and peripherally (Kaumann *et al.*, 1990; Ford *et al.*, 1992). However, the addition of the nonhydrolysable analogue of GTP, GppNHp, to homogenates of guinea-pig hippocampus had little effect on the binding of 5-HT, which may suggest little coupling of the 5-HT$_4$ receptor to a G-protein. By contrast, in guinea-pig striatum, the addition of GTP or GppNHp lowered the affinity of 5-HT by approximately 3 fold. This difference suggests that the addition of GTP results in the conversion of the 5-HT$_4$ receptor to a lower affinity state which is indicative of a G-protein coupled receptor (Houslay, 1990). The variation in the effects of the addition of GTP to hippocampus and striatum may suggest tissue-specific differences in the coupling of the receptor with a G-protein such that coupling efficiency is higher in the striatum.

It is unlikely that a functional receptor would be uniformly distributed throughout the brain. Autoradiographic analysis of 5-HT$_4$ receptor distribution in both the guinea-pig and the rat indicated that 5-HT$_4$ receptor distribution is primarily localized to two anatomically and functionally distinct systems both of which employ dopamine as a neurotransmitter. Firstly the extrapyramidal motor system (striatum, globus pallidus and substantia nigra) and secondly the mesolimbic system (nucleus accumbens and olfactory tubercle). Although the distribution of 5-HT$_4$ receptors appears to be essentially the same in both the rat and the guinea-pig, the density of 5-HT$_4$ receptors appears to be considerably higher in the guinea-pig. Also, in the rat, the highest level of binding is in the interpeduncular nucleus which is unlabelled in the guinea-pig.

In conclusion, the specific binding of [$^3$H]-GR113808 meets the criteria for the identification of the 5-HT$_4$ receptor. As such, the binding is reversible, saturable, of high affinity, discretely localized and inhibited by 5-HT$_4$ receptor agonists and antagonists with affinities close to those expected from functional assays.

The development of a radioligand for the 5-HT$_4$ receptor provides an opportunity to determine the distribution of this receptor in human brain and peripheral tisues. Such a compound will also allow more detailed studies of the receptor including investigation of regulation mechanisms, its ontogeny and may also ultimately aid receptor purification.

We thank Katie Evans for her expert technical assistance.

## References


BAXTER, G.S. & CLARKE, D.E. (1992). Benzimidazolone derivatives act as 5-HT$_4$ receptor ligands in rat oesophagus. *Eur. J. Pharmacol.*, **212**, 225–229.

BOCKAERT, J., FOZARD, J.R., DUMUIS, A. & CLARKE, D.E. (1992). The 5-HT$_4$ receptor: a place in the sun. *Trends Pharmacol. Sci.*, **13**, 141–145.

BOCKAERT, J., SEBBEN, M. & DUMUIS, A. (1990). Pharmacological characterisation of 5-hydroxytryptamine$_4$ (5-HT$_4$) receptors positively coupled to adenylate cyclase in adult guinea-pig hippocampal membranes: effect of substituted benzamide derivatives. *Mol. Pharmacol.*, **37**, 408–411.

BOM, A.H., DUNCKER, D.J., SAXENA, P.R. & VERDOUW, P.D. (1988). 5-Hydroxytryptamine-induced tachycardia in the pig: possible involvement of a new type of 5-hydroxytryptamine receptor. *Br. J. Pharmacol.*, **93**, 663–671.

BRADFORD, M.M. (1976). A rapid and sensitive method for the quantitation of microgram quantities of protein utilising the principle of protein-dye binding. *Anal. Biochem.*, **72**, 248–254.

BUCHHEIT, K.-H., GAMSE, R. & PFANNKUCHE, H.-J. (1992). SDZ205-557, a selective, surmountable antagonist for 5-HT$_4$ receptors in the isolated guinea-pig ileum. *Naunyn-Schmied. Arch. Pharmacol.*, **345**, 387–393.

BUNCE, K.T., ELSWOOD, C.J. & BALL, M.T. (1991). Investigation of the 5-hydroxytryptamine receptor mechanism mediating the short circuit current response in rat colon. *Br. J. Pharmacol.*, **102**, 811–816.

BURT, D.R. (1978). Criteria for receptor identification. In *Neurotransmitter Receptor Binding* ed. Yammamura, Hi, Enna, S.J. & Kuhar, M.J. pp. 41–45. New York: Raven Press.

CRAIG, D.A. & CLARKE, D.E. (1990). Pharmacological characterisation of a neuronal receptor for 5-hydroxytryptamine in guinea-pig ileum with properties similar to the 5-hydroxytryptamine$_4$ receptor. *J. Pharmacol. Exp. Ther.*, **252**, 1378–1386.

DELEAN, A., MUNSON, P.J. & RODBARD, D. (1977). Simultaneous analysis of families of sigmoidal curves: application to bioassay, radioligand assay and physiological dose-response curves. *Am. J. Physiol.*, **235**, E97–E102.

DUMUIS, A., BOUHELAL, R., SEBBEN, M., CORY, R. & BOCKAERT, J. (1988). A nonclassical 5-hydroxytryptamine receptor positively coupled with adenylate cyclase in the central nervous system. *Mol. Pharmacol.*, **34**, 880–887.

EGLEN, R.M., SWANK, S.R., WALSH, L.K.M. & WHITING, R.L. (1990). Characterisation of 5-HT$_3$ and 'atypical' 5-HT receptors mediating guinea-pig ileal contractions *in vitro*. *Br. J. Pharmacol.*, **101**, 513–520.

ELSWOOD, C.J., BUNCE, K.T. & HUMPHREY, P.P.A. (1991). Identification of putative 5-HT$_4$ receptors in guinea-pig ascending colon. *Eur. J. Pharmacol.*, **196**, 149–155.

FORD, A.P.D.W., BAXTER, G.S., EGLEN, R.M. & CLARKE, D.E. (1992). 5-Hydroxytryptamine stimulates cyclic AMP formation in the tunica muscularis mucosae of the rat oesophagus via 5-HT$_4$ receptors. *Eur. J. Pharmacol.*, **211**, 117–120.

GROSSMAN, C.J., GALE, J.D., BUNCE, K.T., KILPATRICK, G.J., WHITEHEAD, J.W.F., OXFORD, A.W. & HUMPHREY, P.P.A. (1993). Development of a radioligand binding assay for the 5-HT$_4$ receptor: use of a novel antagonist. Cambridge Meeting of the B.P.S. *Br. J. Pharmacol.*, (in press).

HOUSLAY, M.D. (1990). Altered expression and functioning of guanine nucleotide binding (regulatory) proteins during growth, transformation, differentiation and in pathological states. In *G-Proteins as Mediators of Cellular Signalling Processes* ed. Houslay, M.D. & Milligan, G., pp. 197–227. New York: Wiley.

KAUMANN, A.J., SANDERS, L., BROWN, A.M., MURRAY, K.J. & BROWN, N.J. (1990). A 5-hydroxytryptamine receptor in human atrium. *Br. J. Pharmacol.*, **100**, 879–885.

KILPATRICK, G.J., JONES, B.J. & TYERS, M.B. (1988). The distribution of specific binding of the 5-HT$_3$ receptor ligand [$^3$H]-GR65630 in rat brain using quantitative autoradiography. *Neurosci. Lett.*, **94**, 156–160.

MUNSON, P.J. & RODBARD, D. (1980). Ligand: a versatile computerised approach for characterisation of ligand-binding systems. *Anal. Biochem.*, **107**, 220–239.

REEVES, J.J., BUNCE, K.T. & HUMPHREY, P.P.A. (1991). Investigation into the 5-hydroxytryptamine receptor mediating smooth muscle relaxation in the rat oesophagus. *Br. J. Pharmacol.*, **103,** 1067–1072.

TURCONI, M., SCHIANTARELLI, P., BORSINI, F., RIZZI, C.A., LADINSKY, H. & DONETTI, A. (1991). Azabicycloalkyl benzimidazolones: interaction with serotonergic 5-$HT_3$ and 5-$HT_4$ receptors and potential therapeutic implications. *Drugs of the Future*, **16,** 1011–1026.

VILLALON, C.M., DENBOER, M.O., HEILIGERS, J.P.C. & SAXENA, P.R. (1990). Mediation of 5-hydroxytryptamine-induced tachycardia in the pig by the putative 5-$HT_4$ receptor. *Br. J. Pharmacol.*, **100,** 665–667.

*(Received January 25, 1993*
*Revised February 24, 1993*
*Accepted March 2, 1993)*

*Br. J. Pharmacol.* (1993), **109**, 625–631 © Macmillan Press Ltd, 1993

# [$^3$H]-idazoxan binding to rabbit cerebral cortex recognises multiple imidazoline $I_2$-type receptors: pharmacological characterization and relationship to monoamine oxidase

[1]Anne Renouard, Peter S. Widdowson & Alex Cordi

Institut de Recherches Servier, 11 rue des Moulineaux, 92150 Suresnes, France

**1** In rabbit cerebral cortical homogenates, saturation analysis of [$^3$H]-idazoxan, an $\alpha_2$-adrenoceptor antagonist, revealed high affinity binding to a single site with high density. Competition experiments demonstrated that the [$^3$H]-idazoxan recognition site was insensitive to the catecholamines, adrenaline and noradrenaline and possessed a low affinity for the $\alpha_2$- and $\alpha_1$-adrenoceptor antagonists, rauwolscine, yohimbine and prazosin, suggesting that the site was not an adrenoceptor. Mapping [$^3$H]-idazoxan binding sites in the forebrain of rabbits by autoradiography, showed high densities of $I_2$ sites in the medial preoptic area and in the stria terminalis. Moderate binding was found in caudate nucleus, putamen, cerebral cortex and hippocampus.

**2** The imidazolines cirazoline, naphazoline, guanabenz and BRL44408 along with amiloride, which is structurally related to the imidazolines, all had high affinity for the [$^3$H]-idazoxan site, suggesting that the site was related to the $I_2$ imidazoline-recognition site described by other groups. However, the imidazolines, clonidine and UK-14,304 and the structurally related rilmenidine all had a low affinity for the binding site, showing that [$^3$H]-idazoxan was not binding to the $I_1$ imidazoline-recognition site found in rat, bovine and human medulla oblongata.

**3** Naphazoline, guanabenz, clonidine and amiloride competition studies had Hill slopes which were significantly different from unity ($P<0.01$) and computer analysis showed that the [$^3$H]-idazoxan binding data could be best fitted to a model which considers binding to two sites ($P<0.01$). One site has a high affinity for idazoxan, cirazoline, naphazoline, guanabenz and amiloride and a moderate affinity for BRL44408 and clonidine (70% of binding) and the second site (30% of binding) has a high affinity for idazoxan and cirazoline, but a lower affinity for naphazoline, guanabenz, amiloride, BRL44408 and clonidine.

**4** Experiments using [$^3$H]-RX821002, in contrast to [$^3$H]-idazoxan, clearly demonstrated the presence of a single type of $\alpha_2$-adrenoceptor in rabbit cortex with a pharmacological profile which is similar to the $\alpha_{2A}$-adrenoceptor possessing a high affinity for yohimbine, rauwolscine, BRL44408 and oxymetazoline, but a lower affinity for prazosin.

**5** The monoamine oxidase inhibitors, clorgyline, pargyline and deprenyl had at least a ten fold lower affinity at the rabbirt cortex $I_2$ site as compared to their known affinity at monoamine oxidase suggesting that the $I_2$ site is not related to the active site of the enzyme, monoamine oxidase. In addition, the peripheral benzodiazepine ligands, PK-11195 or Ro 5-4864 both had very low affinities at the $I_2$ site in rabbit cortex suggesting that the [$^3$H]-idazoxan binding was not to the peripheral benzodiazepine binding site.

**Keywords:** [$^3$H]-idazoxan; rabbit cortex; imidazolines; $\alpha_2$-adrenoceptors; monoamine oxidase; [$^3$H]-RX821002

## Introduction

It is now widely recognised that the radiolabelled imidazoline, [$^3$H]-idazoxan, in addition to possessing a high affinity for $\alpha_2$-adrenoceptors, also recognises a second non-adrenoceptor site, with equal affinity in tissues of rat, guinea-pig and man (Brown *et al.*, 1990; Wikberg & Uhlén, 1990; De Vos *et al.*, 1991). In contrast to [$^3$H]-idazoxan binding to rat, guinea-pig and human tissues, [$^3$H]-idazoxan does not label $\alpha_2$-adrenoceptors in rabbit tissues, such as urethral smooth muscle (Yablonski *et al.*, 1988; 1991), adipocytes (Lagin & Lafontan, 1989), kidney (Coupry *et al.*, 1987) or brain (Renouard *et al.*, 1992). Although earlier investigators had suggested that the non-adrenoceptor site may represent a novel subtype of $\alpha$-adrenoceptor, it is now generally accepted that it is not related to adrenoceptors (Michel & Insel, 1989; Parini *et al.*, 1989). The non-adrenoceptor 'imidazoline-prefering site' has been classified as the $I_2$ site by Ernsberger (1991) and is pharmacologically distinct from the $I_1$ 'imidazoline-preferring site', another non-adrenoceptor site, which is recognised by clonidine and related structures (rilmenidine and moxonidine) (Michel & Insel 1989; Ernsberger *et al.*, 1990; Ernsberger, 1991; Michel & Ernsberger, 1992).

Purification studies of subcellular fractions from human and rabbit liver have demonstrated that [$^3$H]-idazoxan binding to $I_2$ sites was localized to mitochondrial fractions (Tesson *et al.*, 1991). Further purification of mitochondria of rabbit liver demonstrated that [$^3$H]-idazoxan binding was positively correlated with monoamine oxidase (MAO) activity in the outer mitochondrial membranes, but negatively correlated with cytochrome oxidase activity in the inner mitochondrial membrane (Tesson *et al.*, 1991). Thus, in contrast to $\alpha_2$-adrenoceptor binding, which is localized to the plasma membranes, [$^3$H]-idazoxan binding to $I_2$ sites appears to be located intracellularly on the outer membrane of mitochondria.

Due to the apparent specificity of [$^3$H]-idazoxan for the labelling of $I_2$ sites in rabbit tissues and its relative abundance, the rabbit has been used extensively to characterize pharmacologically $I_2$ sites (Langin & Lafontan, 1989; Coupry *et al.*, 1987; Renouard *et al.*, 1992). There is now emerging pharmacological evidence that $I_2$ sites in certain species, in-

[1] Author for correspondence.

cluding rabbits, may constitute a heterogeneous population of sites (Michel & Insel, 1989; Wikberg *et al.*, 1991; Diamant *et al.*, 1992; Stewart *et al.*, 1992). [$^3$H]-idazoxan binding to $I_2$ sites can be divided into two subtypes, based on their affinity for amiloride (Michel & Insel 1989; Diamant *et al.*, 1992). Rabbit kidney, adipocytes and liver and human placenta all show a high affinity for amiloride whilst human kidney, guinea-pig ileum and rat liver have lower affinities for amiloride (Michel & Insel, 1989; Diamant *et al.*, 1992). Many of the pharmacological differences in amiloride affinity can be attributed to species differences, for example, rabbit tissues generally show a higher affinity for amiloride than do tissues from rats, guinea-pigs and man (Michel & Insel, 1989; Diamant *et al.*, 1992). However, recent evidence is emerging for two types of $I_2$ sites in the same species, for example human liver, kidney and adipocytes show an approximately 50 fold lower affinity for amiloride than does the human placenta (Daimant *et al.*, 1992). Also clonidine and the stereoisomers of medetomidine can differentiate two $I_2$ subtypes in guinea-pig tissues (Wikberg *et al.*, 1991). In addition, naphazoline distinguishes two $I_2$ sites in rat, rabbit and dog kidney (Stewart *et al.*, 1992).

Although a physiological role for $I_2$ sites has not yet been identified, [$^3$H]-idazoxan binding has been demonstrated to be sensitive to pH and potassium ions but not to sodium ions, thus raising the possibility that $I_2$ sites are structurally related to the $H^+/Na^+$ antiporter (Bidet *et al.*, 1990).

Recently, the MAO inhibitor, clorgyline, was shown to possess a high affinity for $I_2$ sites in the rat parieto-occipital cortex (Olmos *et al.*, 1992). In addition, chronic clorgyline treatment of rats was observed to reduce [$^3$H]-idazoxan binding to brain $I_2$ sites, suggesting a down-regulation effect (Olmos *et al.*, 1992).

The demonstration of $I_2$ sites on the outer membrane of mitochondria of rabbit and human liver homogenates, coupled with the high positive correlation of [$^3$H]-idazoxan binding with MAO activity suggests that $I_2$ sites may be related to a type of MAO. This suggestion is strengthened by the report of a high affinity of clorgyline for rat brain $I_2$ sites and the relative abundance of $I_2$ sites in tissues rich in MAO activity, such as placenta, brain, liver and kidney (Weyler & Salach, 1985; Perry *et al.*, 1988; Tesson *et al.*, 1991; Diamant *et al.*, 1992).

We investigated the pharmacology of $I_2$ sites in rabbit cerebral cortex, to discover whether there was evidence for multiple subtypes of $I_2$ sites and to discover whether there was any relationship between $I_2$ sites and MAO.

## Methods

### *Membrane preparation*

Male albino, New Zealand rabbits (Charles River, France) were killed by either a blow to the neck or by pentobarbitone overdose (40 mg kg$^{-1}$ i.v.) administered by the ear vein. The administration of pentobarbitone was not found to affect [$^3$H]-idazoxan binding. The brains were removed and the cerebral cortex dissected free of white matter on a cooled surface. The tissue was homogenized in buffer (50 mM Tris-HCl, 1 mM EDTA, pH 7.5; 4°C) with a polytron for 1 min and then centrifuged for 10 min (1,000 *g*; 4°C) to pellet cellular debris. The supernatent was centrifuged for 30 min (20,000 *g*; 4°C) and the $P_2$ pellet resuspended in fresh buffer. The tissue homogenates (10 mg protein ml$^{-1}$) were divided into 1 ml aliquots and frozen. The tissue was stored at −80°C until use.

### *Receptor binding*

[$^3$H]-idazoxan (0.1–12.0 nM) and [$^3$H]-RX821002 (0.1–20.0 nM) binding were performed in 50 mM Tris-HCl, 2 mM $MgCl_2$, 1 mM EDTA buffer (pH 7.5, 22°C) in a total volume of 0.5 ml. Binding was initiated by the addition of 0.4 ml protein suspension (0.1 mg ml$^{-1}$) and the incubation continued for 30 min at 22°C. Non-specific binding was estimated with 10 μM (+)-idazoxan for [$^3$H]-idazoxan binding or 10 μM adrenaline for [$^3$H]-RX821002 binding. Bound radioligand was separated from free by rapid filtration over Whatman GF/B filters and the membranes washed (3 × 3 ml) with ice-cold 50 mM Tris-HCl (pH 7.5) buffer. Binding was estimated by liquid scintillation counting in a Packard 1500 Tri-Carb counter (counting efficiency = 47%). The protein was dissolved in 1 M NaOH and the concentration estimated by the method of Lowry *et al.* (1951) with bovine serum albumin as a standard.

### *Autoradiography*

Brains from male New Zealand albino rabbits were carefully removed following pentobarbitone overdose. The brains were placed immediately in ice-cold saline (0.9% w/v) to firm the tissue and then snap frozen in isopentane cooled on dry ice (−20°C). The frozen brains were stored in an air tight container at −80°C until used, which did not exceed one week: 20 μm sections of rabbit forebrain, at the level of the caudate nucleus, were made with a cryostat, and the sections thaw mounted onto gelatin-subbed glass slides. The sections were dried overnight at 4°C and then stored frozen at −80°C until use.

Sections were briefly brought to room temperature and then preincubated for 30 min in a Tris buffer at room temperature (50 mM Tris-HCl, 2 mM $MgCl_2$, 1 mM EDTA, pH 7.5; 22°C) as described previously (Hudson *et al.*, 1991). The sections were incubated with either 7 nM [$^3$H]-idazoxan or 3 nM [$^3$H]-RX821002 for 30 min and then washed twice in ice-cold incubation buffer (pH 7.5) for 20 s each and finally dipped in ice-cold deionized water to remove salts. Non-specific binding was estimated with 10 μM (+)-idazoxan or 10 μM (−)-adrenaline for [$^3$H]-idazoxan binding or with 10 μM (−)-adrenaline for [$^3$H]-RX821002 binding. The sections were rapidly dried under a stream of warm day air and then placed in X-ray cassettes. Tritium-sensitive film (Hyperfilm, Amersham France) was juxtaposed against the slides with autoradiography standards (Microscales, Amersham France) and the film exposed for between 3 to 5 weeks. The film was then developed with Kodak LX24 (Kodak-Pathé, Paris, France). The sections were stained with cresyl violet to aid anatomical characterization.

### *Data analysis*

Equilibrium binding parameters ($K_d$ and $B_{max}$) and binding isotherms from competition studies were obtained by the iterative non-linear least square curve fitting programme, 'LUNDON' (Lundon Software, Cleveland, Ohio, U.S.A.). The inhibitory constant ($K_i$) was calculated from the $IC_{50}$ using the equation of Cheng & Prusoff (1973). The single site and two site models for each isotherm were compared using the differential $F$ value as described previously (McKinnon *et al.*, 1992).

### *Chemicals and drugs*

[$^3$H]-idazoxan (42 Ci mmol$^{-1}$) and [$^3$H]-RX821002 (1,4-6,7(n)-benzodioxan-2-methoxy-2-yl)-2-imidazole) (55 Ci mmol$^{-1}$) were both obtained from Amersham France. Naphazoline HCl, clorgyline HCl, pargyline HCl, (−)-noradrenaline, (−)-adrenaline, prazosin HCL, yohimbine HCl and guanabenz were purchased from Sigma, La Vallpierre, France. Amiloride HCl, deprenyl HCl, PK 11195 (1-(2-chlorophenyl)-N-methyl-N-(1-methylpropyl)-3-isoquinolinecarboxamide), Ro 5-4864 (*p*-chloro-1,3 dihydro-1-methyl-5-phenyl-2H-1,4-benzodiazepin-2-one) and rauwolscine HCl were from Research Biochemicals Inc. (RBI), Wayland, MA, USA. UK-14304 tartrate (5-bromo-6-[2-imidazolin-2-ylamino] quinox-

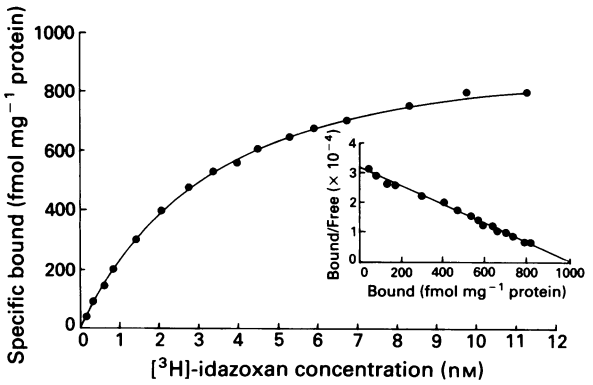



**Figure 1** Representative saturation experiment using [$^3$H]-idazoxan in rabbit cerebral cortex: specific binding with 10 μM (+)-idazoxan used to define non-specific binding. Inset shows Scatchard transformation of the data.

**Table 1** Competition of 2 nM [$^3$H]-idazoxan binding in rabbit cerebral cortex membranes

| | $K_i$ (nM) | nH |
|---|---|---|
| (+)-Idazoxan | 1.4 ± 0.1 | 0.86 ± 0.06 |
| Cirazoline | 1.4 ± 0.1 | 0.88 ± 0.07 |
| Naphazoline | 21.2 ± 5.5 | 0.48 ± 0.05* |
| Amiloride | 23.4 ± 8.1 | 0.54 ± 0.07* |
| Guanabenz | 29.1 ± 5.6 | 0.52 ± 0.06* |
| BRL44408 | 654 ± 184 | 0.91 ± 0.03 |
| UK 14,304 | 1018 ± 56 | 0.86 ± 0.05 |
| Deprenyl | 1995 ± 110 | 0.79 ± 0.03 |
| Rilmenidine | 2523 ± 488 | 0.81 ± 0.06 |
| Clonidine | 2803 ± 648 | 0.76 ± 0.01* |
| Prazosin | 5211 ± 76 | 0.87 ± 0.05 |
| Clorgyline | 5930 ± 1825 | 0.88 ± 0.07 |
| Yohimbine | 11,900 ± 173 | 0.95 ± 0.07 |
| RX821002 | 20,858 ± 4149 | 0.96 ± 0.05 |
| Rauwolscine | 26,877 ± 5288 | 1.16 ± 0.09 |
| Pargyline | 29,063 ± 7852 | 0.90 ± 0.04 |
| PK-11195 | 36,562 ± 6488 | 0.92 ± 0.19 |
| Ro 5-4864 | 42,813 ± 5150 | 1.16 ± 0.09 |
| (−)-Adrenaline | > 100,000 | ND |
| (−)-Noradrenaline | > 100,000 | ND |

Affinity values and Hill slopes (nH) obtained from the displacement of specific binding of [$^3$H]-idazoxan from rabbit cerebral cortex membranes. *denotes a Hill slope which is significantly different from unity with the respective $K_i$ values assuming binding to one site. Each value represents the mean ± s.e.mean of at least three separate experiments. ND = not determined.

aline) was from Pfizer, Orsay, France. (+)-Idazoxan, RX821002, BRL44408 (2-[2H-(1-methyl-1,3-dihydroisoindole)methyl]-4,5 dihydroimidazole) and cirazoline were synthesized in the laboratory of A. Cordi, Servier, Suresnes. All other chemicals were of the highest purity commercially available.

## Results

[$^3$H]-idazoxan was demonstrated to bind with high affinity to a single, large population of sites in rabbit cerebral cortex membranes ($K_d$ = 3.5 ± 0.2 nM, $B_{max}$ = 880 ± 80 fmol mg$^{-1}$ protein, $n$ = 6 animals) (Figure 1). At the $K_d$ value of 3.5 nM, the specific binding of [$^3$H]-idazoxan is approximately 95% using 10 μM (+)-idazoxan to measure non-specific binding. The addition of 10 μM (−)-adrenaline to the binding buffer did not alter [$^3$H]-idazoxan binding, even at the highest concentration of radioligand. Typical results of 6 nM [$^3$H]-idazoxan are, total binding = 13,046 d.p.m., binding with 10 μM (−)-adrenaline 12,859 d.p.m. and binding with 10 μM (+)-idazoxan 828 d.p.m.

Competition experiments at 2 nM [$^3$H]-idazoxan showed

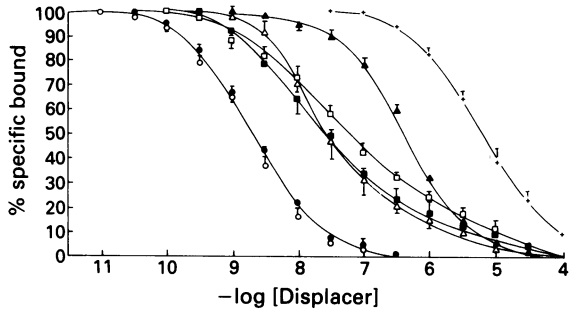



**Figure 2** Competition experiments using 2 nM [$^3$H]-idazoxan. Data shown as mean ± s.e.mean for 3–4 experiments: (○) (+)-idazoxan; (●) cirazoline; (■) naphazoline; (□) amiloride; (△) guanabenz; (▲) BRL44408; (+) clonidine.

**Table 2** Analysis of competition curves of naphazoline, amiloride, guanabenz and clonidine which have been modelled to a two site fit ($P < 0.01$)

| | $K_i$ (High) | $K_i$ (Low) | % high |
|---|---|---|---|
| Naphazoline | 3.2 ± 0.9 | 900 ± 144 | 65 ± 8 |
| Amiloride | 10.8 ± 3.7 | 3847 ± 2529 | 74 ± 3 |
| Guanabenz | 12.9 ± 4.7 | 1863 ± 660 | 73 ± 4 |
| Clonidine | 1737 ± 376 | 27400 ± 5800 | 68 ± 4 |

Data shown as $K_i$ values at sites which have a high and low affinity for the compounds and also the percentage of high affinity sites (% high) as compared to the specific binding at 2 nM [$^3$H]-idazoxan. Data represented as mean ± s.e.mean for 4 experiments carried out in duplicate.

that the catecholamines (−)-adrenaline and (−)-noradrenaline were not able to displace radioligand binding, even at 100 μM (Table 1). The adrenoceptor-antagonists, yohimbine, rauwolscine and RX821002 had a low affinity at the [$^3$H]-idazoxan site, as did the MAO inhibitor pargyline. The selective MAO type-A inhibitor, clorgyline and the selective MAO type-B inhibitor, deprenyl both had moderate affinities at the [$^3$H]-idazoxan binding site (Table 1). The peripheral benzodiazepine drugs, Ro 5-4864 and PK-11195 were also inactive at the [$^3$H]-idazoxan site. In contrast, the imidazolines (+)-idazoxan, cirazoline, guanabenz, naphazoline and BRL44408, as well as amiloride, which is structurally related to the imidazolines, showed a high affinity for the [$^3$H]-idazoxan binding site (Table 1, Figure 2). However, the imidazolines, clonidine UK-14,304 and rilmenidine, an oxazoline (Laubie *et al.*, 1985) all had low affinities for the [$^3$H]-idazoxan binding site (Table 1).

Hill coefficients for naphazoline, amiloride, guanabenz and clonidine were significantly less than unity suggesting that [$^3$H]-idazoxan bound to multiple binding sites, whilst all the other compounds produced Hill coefficients which were not significantly different for unity (Table 1). Computer analysis of the competition curves for naphazoline, amiloride, guanabenz and clonidine could resolve the binding into two components ($F$-test, $P < 0.01$). One component represents binding to a site which constitutes approximately 70% of [$^3$H]-idazoxan binding at 2 nM and has a high affinity for naphazoline, guanabenz and amiloride and a moderate affinity for clonidine (Table 2). The second component represent [$^3$H]-idazoxan binding to a second site (40% of total binding at 2 nM) and displays an approximately 300 fold lower affinity for amiloride and naphazoline, a 140 fold lower affinity for guanabenz and a 10 fold lower affinity for clonidine (Table 2).

Binding of [$^3$H]-RX821002 to rabbit cerebral cortex was used to identify $\alpha_2$-adrenoceptors. Saturation experiments with [$^3$H]-RX821002 detected a single population of sites in rabbit cerebral cortex with high affinity ($K_d$ = 1.6 ± 0.2 nM, $B_{max}$ = 88 ± 22 fmol mg$^{-1}$ protein, $n$ = 6 animals) but with a

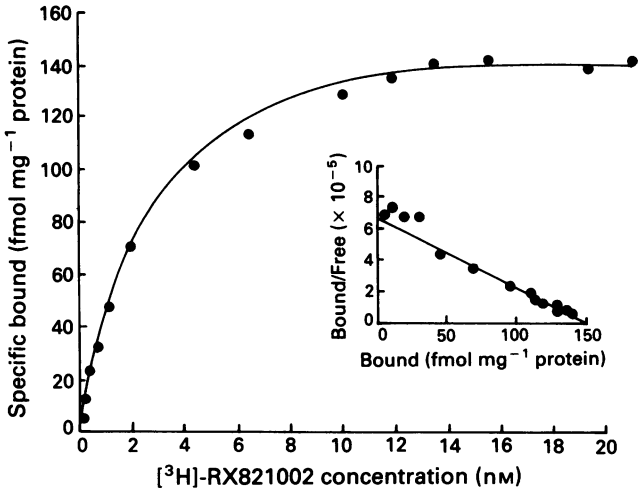



**Figure 3** Representative saturation experiment using [$^3$H]-RX821002: specific binding with 10 μM (−)-adrenaline used to define non-specific binding. Inset shows Scatchard transformation of the data.

**Table 3** Competition experiments using [$^3$H]-RX821002

| | $K_I$ (nM) | nH |
|---|---|---|
| Oxymetazoline | 1.95 ± 0.75 | 0.98 ± 0.04 |
| Yohimbine | 2.09 ± 0.54 | 1.05 ± 0.06 |
| BRL44408 | 3.97 ± 0.75 | 0.79 ± 0.06 |
| RX821002 | 7.00 ± 0.80 | 0.85 ± 0.10 |
| Rauwoscine | 8.24 ± 0.50 | 0.89 ± 0.07 |
| (−)-Adrenaline | 12.35 ± 2.65 | 0.70 ± 0.03* |
| (−)-Noradrenaline | 18.00 ± 5.00 | 0.52 ± 0.05* |
| (+)-Idazoxan | 19.8 ± 3.6 | 1.06 ± 0.04 |
| Clonidine | 26.8 ± 1.3 | 0.74 ± 0.09 |
| Cirazoline | 127 ± 15 | 1.11 ± 0.06 |
| Prazosin | 2427 ± 581 | 0.88 ± 0.08 |

Data shown as mean ± s.e.mean for experiments carried out at least three times.
*Hill coefficients which are significantly less than unity ($P<0.05$, Student's $t$ test).

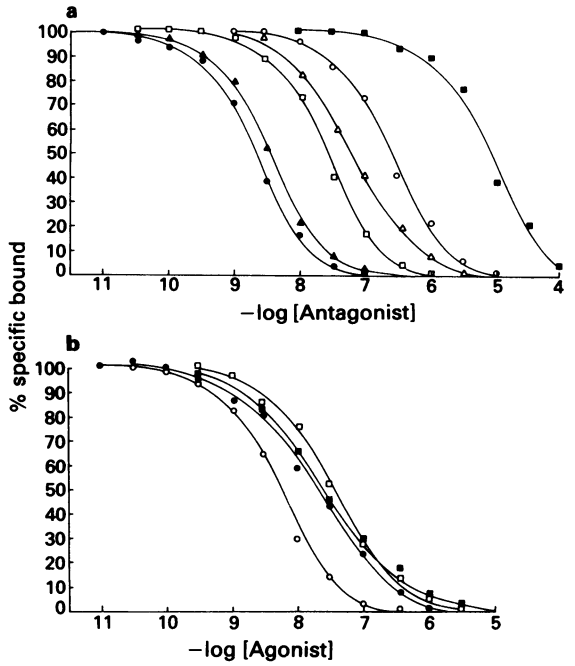



**Figure 4** Competition of 0.3 nM [$^3$H]-RX821002 binding in rabbit cerebral cortex. (a) Antagonists: (●) yohimbine; (▲) RX821002; (□) (+)-idazoxan; (△) BRL44408; (○) cirazoline; (■) prazosin. (b) Agonists: (●); (−)-adrenaline; (○) oxymetazoline; (■) (−)-noradrenaline; (□) clonidine.

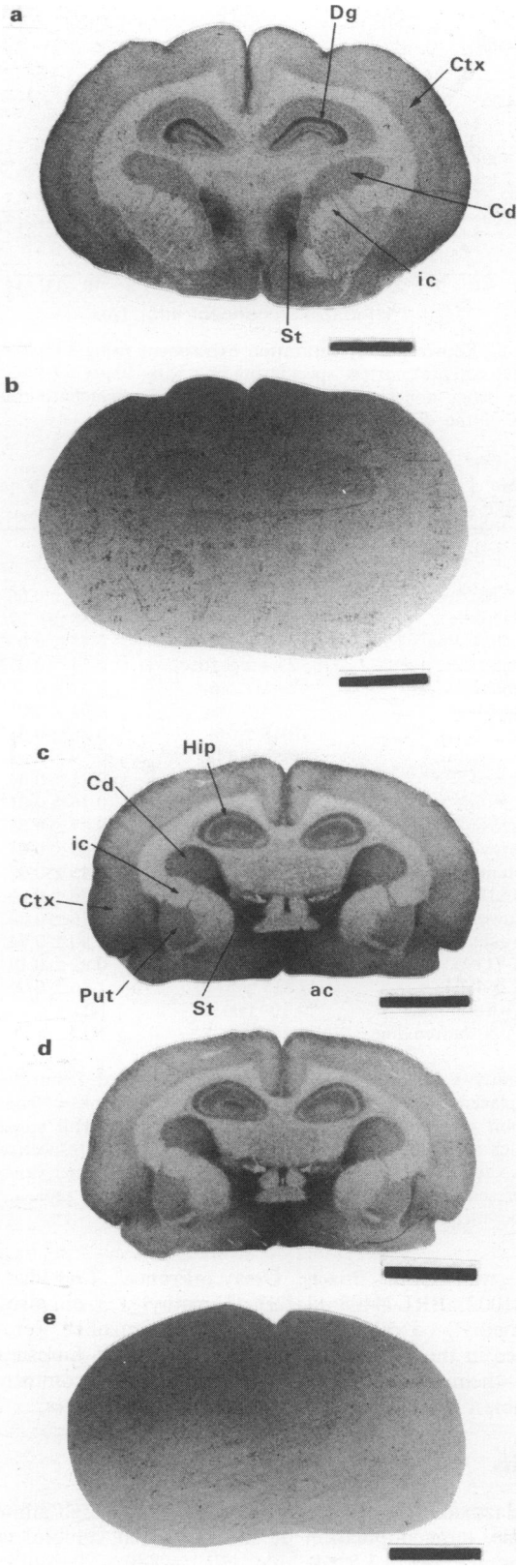



**Figure 5** Binding of 7 nM [$^3$H]-idazoxan (c–e) and 3 nM [$^3$H]-RX821102 (a–b) to forebrain sections of rabbit brain as revealed by autoradiography. (c) Total binding; (d) binding with 10 μM (−)-adrenaline; (e) non-specific binding in the presence of 10 μM (+)-idazoxan; (a) total binding; (b) non-specific binding in the presence of 10 μM (−)-adrenaline. Hip = hippocampus, Caud = caudate nucleus, Put = putamen, ic = internal capsule, st = stria terminalis, MPO = medial preoptic area, Ctx = cerebral cortex, ac = anterior commisure. Calibration bars = 5 mm.

10 fold lower density as compared to the [$^3$H]-idazoxan recognition sites (Figure 3). Competition experiments with [$^3$H]-RX821002 demonstrated a potency ratio table that was indicative of binding to $\alpha_2$-adrenoceptors and was clearly different from the pharmacology of the site labelled by [$^3$H]-idazoxan (Table 3). All the $\alpha_2$-adrenoceptor antagonists, rauwolscine, yohimbine, BRL44408 and RX821002 had high affinities for the [$^3$H]-RX821002 binding site with Hill slopes close to unity as did the $\alpha_2$-adrenoceptor agonists, clonidine and oxymetazoline (Table 3, Figure 4). The catacholamines (−)-adrenaline and (−)-noradrenaline had high affinities for the [$^3$H]-RX821002 binding site with Hill slopes that were less than unity (Table 3). The $\alpha_1$-adrenoceptor ligands, prazosin and cirazoline both had low affinities at the [$^3$H]-RX821002 binding site.

Autoradiography using both [$^3$H]-idazoxan and [$^3$H]-RX821002 demonstrated a differential distribution of $I_2$ sites and $\alpha_2$-adrenoceptors in rabbit forebrain (Figure 5). High densities of $I_2$ sites were observed in the stria terminalis, medial preoptic area and medial portion of the caudate nucleus. Moderate densities of $I_2$ sites were observed in the cerebral cortex, the density being the highest in the superficial layer I. Moderate densities of $I_2$ sites were also observed in the lateral caudate nucleus, putamen and hippocampus. Binding was lowest in the anterior commisure, internal capsule, and thalamic structures. The addition of 10 μM (−)-adrenaline to the incubation buffer did not alter the [$^3$H]-idazoxan binding in any region (Figure 5). In contrast, [$^3$H]-RX821002 binding was highest in the pyramidal layer of the hippocampus, the superficial layer I of the cerebral cortex and the stria terminalis (Figure 5). Moderate binding of [$^3$H]-RX821002 was observed throughout the cerebral cortex and in the caudate nucleus and putamen. Lowest binding was to white matter.

## Discussion

We have demonstrated that [$^3$H]-idazoxan binding to rabbit cerebral cortical membranes recognises a large population of sites which are not recognised by either (−)-adrenaline or (−)-noradrenaline. These data are in agreement with previous reports of [$^3$H]-idazoxan binding in rabbit tissues, including brain (Coupry *et al.*, 1987; Langin & Lafontan, 1989; Tesson *et al.*, 1991; Renouard *et al.*, 1992). The failure of the $\alpha_1$-adrenoceptor antagonists, rauwolscine or yohimbine, or the $\alpha_2$-adrenoceptor antagonist, prazosin to compete for the [$^3$H]-idazoxan binding site with high affinity also confirms that this is not an $\alpha_2$-adrenoceptor. However, the $\alpha_2$-adrenoceptor antagonists, idazoxan and BRL44408 and the $\alpha_2$-adrenoceptor agonist, cirazoline, all had a high affinity for the [$^3$H]-idazoxan site. Since idazoxan, cirazoline and BRL44408 all contain imidazoline moities in their structure, we propose that the [$^3$H]-idazoxan is binding to the proposed imidazoline sites described by a number of groups (Coupry *et al.*, 1987; Langin & Lafontan, 1989; Michel & Insel, 1989; Wikberg *et al.*, 1991; Tesson *et al.*, 1991; Stewart *et al.*, 1992). This proposal is further confirmed by the demonstration of high affinities of other imidazoline-containing compounds such as naphazoline and guanabenz and the structurally related amiloride. The low affinities of clonidine and rilmenidine for the site suggests that the [$^3$H]-idazoxan is binding to the $I_2$ site, proposed by Ernsberger (1991). This $I_2$ site in rabbit cortex is clearly distinct from the $I_1$-imidazoline site which is located in bovine and rat medulla oblongata and shows a nanomolar affinity for clonidine, UK-14,304 and rilmenidine (Ernsberger *et al.*, 1990; Ernsberger, 1991; Michel & Ernsberger, 1992).

Using receptor autoradiography, we were able to demonstrate high levels of $I_2$ binding sites in the dopamine-rich caudate nucleus and putamen and also in the frontal cortical areas. The highest densities of $I_2$ sites were found in the medial preoptic area and in the bed nucleus of the stria terminalis. The observation that 10 μM adrenaline failed to reduce the binding in any of the brain regions demonstrates that [$^3$H]-idazoxan does not label $\alpha_2$-adrenoceptors in rabbit forebrain. $\alpha_2$-Adrenoceptors, labelled with [$^3$H]-RX821002 were also found to be concentrated in the superficial layer of the cerebral cortex, stria terminalis but were found in much lower densities in the medial preoptic area and medial caudate nucleus as compared to $I_2$ sites.

Our failure to displace any of the [$^3$H]-idazoxan binding with either adrenaline or noradrenaline and our demonstration of low potencies of $\alpha_2$-adrenoceptor antagonists may suggest that rabbit brain does not possess $\alpha_2$-adrenoceptors since [$^3$H]-idazoxan has been reported to label $\alpha_2$-adrenoceptors in human, rat and guinea-pig brain (Brown *et al.*, 1990; Wikberg & Uhlén 1990; De Vos *et al.*, 1991). However, using a radiolabelled methoxy-analogue of idazoxan, [$^3$H]-RX821002, a selective $\alpha_2$-adrenoceptor antagonist having a low affinity at $I_2$ sites (Langin *et al.*, 1989; Hudson *et al.*, 1991; Mallard *et al.*, 1992), we were able to observe a second population of binding sites with a pharmacology similar to that expected of an $\alpha_2$-adrenoceptor. The failure of [$^3$H]-idazoxan to recognise $\alpha_2$-adrenoceptors in rabbit brain may be related to its lower affinity in rabbit tissues as compared to guinea-pig, human and rat brain, possibly reflecting a species difference in the $\alpha_2$-adrenoceptor. In addition, the much larger population of $I_2$ sites labelled with [$^3$H]-idazoxan would make it difficult to observe and characterize the much smaller population of $\alpha_2$-adrenoceptors in rabbit tissues. A pharmacological analysis of the $\alpha_2$-adrenoceptor in rabbit cortex suggests that it may be related to the $\alpha_{2A}$ subtype found in human platelets which has a high affinity for oxymetazoline, rauwolscine and yohimbine and a lower affinity for prazosin (Kobilka *et al.*, 1987). Thus in the rabbit cerebral cortex, $I_2$ sites outnumber $\alpha_2$-adrenoceptors by ten-to-one.

Competitive studies with three imidazoline-containing compounds, plus amiloride, show that [$^3$H]-idazoxan binding in rabbit cortex can be resolved into two components, suggesting two binding sites. One site which constitutes between 60–70% of [$^3$H]-idazoxan binding at 2 nM, has a high affinity for (+)-idazoxan, cirazoline, amiloride, guanabenz, naphazoline and a moderate affinity for clonidine and BRL44408. The remaining [$^3$H]-idazoxan binding is to a site with a high affinity for (+)-idazoxan, cirazoline, a moderate affinity for BRL44408 but a 100 fold lower affinity for naphazoline, guanabenz and amiloride. The second site also has an approximately 10 fold lower affinity for clonidine. Therefore, in addition to other groups, we have provided further evidence that [$^3$H]-idazoxan binding in certain species recognises multiple $I_2$-type imidazoline sites (Wikberg *et al.*, 1991; Stewart *et al.*, 1992). Stewart *et al.* (1992) recently found that naphazoline can discriminate two [$^3$H]-idazoxan binding sites in rat, rabbit and dog kidney with an approximately 100 fold difference in affinity, neither site was sensitive to GTP and therefore these are not affinity states of the same receptor. These data agree with our demonstration that in rabbit cerebral cortex, naphazoline is able to discriminate two sites with an approximately 100 fold difference in potency and it is therefore plausible that the two sites observed in rat, rabbit and dog kidney are analogous to our two sites in rabbit cerebral cortex.

The demonstration that [$^3$H]-idazoxan binding to purified mitochondria from rabbit liver is highly correlated with MAO activity (Tesson *et al.*, 1991), coupled with the reported high affinity of the MAO type-A inhibitor, clorgyline at [$^3$H]-idazoxan sites (Olmos *et al.*, 1992) suggests a possible relationship between $I_2$ sites and MAO. A comparison of the distribution of MAO type B in rat brain (Willoughby *et al.*, 1988) with the density of [$^3$H]-idazoxan binding to $I_2$ sites (Mallard *et al.*, 1992) demonstrates a correlation between the two. High levels of both $I_2$ density and MAO type B were found in the interpeduncular nuclei, arcuate hypothalamus, linings of the aquaduct and ventricles

with moderate levels in the ventromedial and lateral hypothalamus and habenular nuclei and low levels in the caudate putamen and cerebral cortex (Willoughby *et al.*, 1988; Mallard *et al.*, 1992). In addition, high levels of [$^3$H]-idazoxan binding are found in dopamine-rich areas of human brain such as substantia nigra and caudate nucleus (DeVos *et al.*, 1991), regions which are rich in MAO type B actvity. These data suggest that $I_2$ sites may be associated with the enzyme, MAO type B. However, the relatively low affinity of deprenyl, a selective inhibitor of MAO type B and clorgyline, an MAO type A inhibitor and the very low potency of the non-selective MAO inhibitor, pargyline at $I_2$ sites suggests that [$^3$H]-idazoxan is not binding to the active site of MAO. However, it is quite plausible that [$^3$H]-idazoxan binds to another site on the MAO protein. In our experiments, competition studies with clorgyline were best fitted to a model in which binding is to only one site. We failed to demonstrate that clorgyline is able to discriminate between the two binding sites as shown by Olmos *et al.* (1992). However, the affinity of clorgyline at $I_2$ sites in rabbit cerebral cortex (6 $\mu$M) is similar to the lower affinity site in rat cerebral cortex (10 $\mu$M) described by Olmos *et al.* (1992) suggesting that these sites may be related. We suggest therefore that the [$^3$H]-idazoxan binding site which has a high affinity for clorgyline is absent from rabbit cerebral cortex. Also the human placenta, which contains only MAO type A (Weyler & Salach, 1985) has a high density of $I_2$ sites (Diamant *et al.*, 1992). Therefore [$^3$H]-idazoxan cannot be considered to bind selectively to a site on the enzyme MAO type B.

Mallard *et al.* (1992) have recently suggested that $I_2$ sites in rat brain may be associated with the peripheral type benzodiazepine sites since there is considerable overlap in their anatomical distribution (Benavides *et al.*, 1983; Mallard *et al.*, 1992). However, we failed to demonstrate a high affinity of two drugs with high affinity at peripheral benzodiazepine sites, PK11195 and Ro5-4864, for [$^3$H]-idazoxan binding, suggesting that $I_2$ sites are not directly associated with the [$^3$H]-PK11195 binding sites (Benavides *et al.*, 1983).

## References


BENAVIDES, J., QUARTERONET, D., IMBAULT, F., MALGOURIS, C., UZAN, A., RENAULT, C., DUBROEUCQ, M.C., GUEREMY, C. & LE FUR, G. (1983). Labelling of 'peripheral-type' benzodiazepine binding sites in the rat brain using [$^3$H]-PK11195, an isoquinoline carboxamide derivative: kinetic studies and autoradiographic localization. *J. Neurochem.*, **41**, 1744–1750.

BIDET, M., POUJEOL, P. & PARINI, A. (1990). Effect of imidazolines on $Na^+$ transport and intracellular pH in renal proximal tubule cells. *Biochem. Biophys. Acta*, **1024**, 173–178.

BROWN, C.M., MACKINNON, A.C., MCGRATH, J.C., SPEDDING, M. & KILPATRICK, A.T. (1990). Alpha$_2$-adrenoceptor subtypes and imidazoline-like binding in the rat brain. *Br. J. Pharmacol.*, **99**, 803–809.

CHENG, Y.C. & PRUSOFF, W.H. (1973). Relationship between the inhibitory constant (Ki) and the concentration of inhibitor which caused 50 per cent inhibition ($pIC_{50}$) of an enzymatic reaction. *Biochem. Pharmacol.*, **22**, 3099–3108.

COUPRY, I., PODEVIN, R.A., DAUSSE, J.-P. & PARINI, A. (1987). Evidence for imidazoline binding sites in basolateral membranes from rabbit kidney. *Biochem. Biophys. Res. Commun.*, **147**, 1055–1060.

DE VOS, H., CONVENTS, A. DE KEYSER, J. DE BACKER, J.-P., VAN MEGAN, I.J.B., EBINGER, G. & VAUQUELIN, G. (1991). Autoradiographic distribution of alpha$_2$-adrenoceptors, NAIBS and 5-$HT_{1A}$ receptors in human brain using [$^3$H]idazoxan and [$^3$H]rauwolscine. *Brain Res.*, **566**, 13–20.

DIAMANT, S., ELDAR-GEVA, T. & ATLAS, D. (1992). Imidazoline binding sites in human placenta: evidence for heterogeneity and a search for physiological function. *Br. J. Pharmacol.*, **106**, 101–108.

ERNSBERGER, P. (1991). Heterogeneity of imidazoline binding in brain: proposed $I_1$ and $I_2$ subtypes. *Third IBRO World Congress Neuroscience*, Abstract P41.8.

ERNSBERGER, P., GIULIANO, R., WILLETTE, R.N. & REISS, D.J. (1990). Role of imidazole receptors in the vasodepressor response to clonidine analogs in the rostral ventrolateral medulla. *J. Pharmacol. Exp. Ther.*, **253**, 408–418.

HUDSON, A.L., MALLARD, N.J., TYACKE, R. & NUTT, D.J. (1991). [$^3$H]RX821002: a highly selective ligand for the identification of alpha$_2$-adrenoceptors in the rat brain. *Mol. Pharmacol.*, **2**, 219–229.

KOBILKA, B.K., MATSUI, H., KOBILKA, T.S., YANG-FENG, T.L., FRANCKE, U., CARON, M.G., LEFKOWITZ, R.J. & REGAN, J.W. (1987). Cloning, sequencing and expression of the gene coding for the human platelet alpha$_2$-adrenergic receptor. *Science*, **238**, 650–658.

LANGIN, D. & LAFONTAN, M. (1989). [$^3$H]idazoxan binding at non-alpha$_2$-adrenoceptors in rabbit adipocyte membranes. *Eur. J. Pharmacol.*, **159**, 199–203.

LANGIN, D., LAFONTAN, M., STILLINGS, M.R. & PARIS, H. (1989) [$^3$H]RX821002: a new tool for the identification of alpha$_{2A}$-adrenoceptors. *Eur. J. Pharmacol.*, **167**, 95–104.

LAUBIE, M., POIGNANT, J.C., SCUVEE-MOREAU, J., DRESSE, A. & SCHMITT, H. (1985). Pharmacological properties of (N-dicyclopropyl-methylamino-2-oxazoline) (S3341), an alpha$_2$ adrenoceptor agonist. *J. Pharmacol. (Paris)*, **16**, 259–265.

LOWRY, O.H., ROSEBROUGH, N.J., FARR, A.C. & RANDALL, R.J. (1951). Protein measurement with the Folin phenol reagent. *J. Biol. Chem.*, **193**, 265–275.

MACKINNON, A.C. KILPATRICK, A.T., KENNY, B.A., SPEDDING, M. & BROWN, C.M. (1992). [$^3$H]-RS-15385-197, a selective and high affinity radioligand for alpha$_2$ adrenoceptors; implications for receptor classification. *Br. J. Pharmacol.*, **106**, 1011–1018.

MALLARD, N.J., HUDSON, A.L. & NUTT, D.J. (1992). Characterization and autoradiographical localization of non-adrenoceptor idazoxan binding sites in the rat brain. *Br. J. Pharmacol.*, **106**, 1019–1027.

MICHEL, M.C. & ERNSBERGER, P. (1992). Keeping an eye on the I site: imidazoline preferring receptors. *Trends Pharmacol. Sci.*, **13**, 369–370.

MICHEL, M.C. & INSEL, P.A. (1989). Are there multiple imidazoline binding sites? *Trends Pharmacol. Sci.*, **10**, 342–344.

OLMOS, G., GABILONDO, A.M. MIRALLES, A. & GARCIA-SEVILLA, J.A. (1992). Long-term treatment with clorgyline down-regulates the density of imidazoline receptors in the rat brain. *Fund. Clin. Pharmacol.*, **6**, (Suppl 1), Abstract III 18.

PARINI, A., COUPRY, I., GRAHAM, R.M., UZIELLI, I., ATLAS, D. & LANIER, S.M. (1989). Characterization of an imidazoline/guanidinium receptive site distinct from alpha$_2$-adrenergic receptor. *J. Biol. Chem.*, **264**, 11874–11878.

PERRY, D.C., GRIMM, L.J., KETTLER, K.G. & KELLAR, K.J. (1988). [$^3$H]tryptamine binding sites are not identical to monoamine oxidase in rat brain. *J. Neurochem.*, **51**, 1535–1540.

RENOUARD, A., WIDDOWSON, P.S. & GIESEN-CROUSE, E. (1989). [$^3$H]idazoxan recognizes only imidazoline (IGRS) sites in rabbit brain: species differences for alpha$_2$-adrenergic recognition. *Fund. Clin. Pharmacol.*, **6** (Suppl 1), Abstract P6.

STEWART, M., MACKINNON, A.C., HUSSAIN, J.F., SPEDDING, M. & BROWN, C.M. (1992). Naphazoline distinguishes two non-adrenergic sites for [$^3$H]idazoxan in kidney membranes. *Fund Clin. Pharmacol.*, **6** (Suppl 1), Abstract P12.

TESSON, F., PRIP-BUUS, C., LEMOINE, A., PEGORIER, J.P. & PARINI, A. (1991). Subcellular distribution of imidazoline-guanidinium receptive sites in human and rabbit liver. *J. Biol. Chem.*, **266**, 155–160.

WEYLER, W. & SALACH, J.I. (1985). Purification and properties of mitochondrial monoamine oxidase type A from human placenta. *J. Biol. Chem.*, **260**, 13199–13207.

WIKBERG, J.E.S. & UHLEN, S. (1990). Further characterisation of the guinea pig cerebral cortex idazoxan receptor: solubilization, distinction from the imidazole site and demonstration of cirazoline as an idazoxan receptor-selective drug. *J. Neurochem.*, **55**, 192–203.

WIKBERG, J.E.S., UHLEN, S. & CHHAJLANI, V. (1991). Medetomidine stereoisomers delineate two closely related subtypes of idazoxan (imidazoline) I-receptors in the guinea pig. *Eur. J. Pharmacol.*, **193**, 335–340.

WILLOUGHBY, J., GLOVER, V. & SANDLER, M. (1988). Histochemical localisation of monoamine oxidase A and B in rat brain. *J. Neural. Transm.*, **74**, 29–42.

YABLONSKI, F., RIFFAUD, J.P., LACOLLE, J.Y. & DAUSSE, J.P. (1988). Evidence for non-adrenergic binding sites for [$^3$H]idazoxan in the smooth muscle of rabbit urethra. *Eur. J. Pharmacol.*, **154**, 209–212.

YABLONSKI, I.F., LACOLLE, J.Y. & DAUSSE, J.P. (1991). Non-adrenergic binding sites for the 'alpha$_2$-antagonist [$^3$H]idazoxan in rabbit urethral smooth muscle. *J. Rec. Res.*, **11**, 153–162.

*(Received November 9, 1992*
*Revised February 6, 1993*
*Accepted February 11, 1993)*

*Br. J. Pharmacol.* (1993), **109**, 632–636 © Macmillan Press Ltd, 1993

# Vasorelaxant mechanism of KRN2391 and nicorandil in porcine coronary arteries of different sizes

Atsushi Miwa, Soichiro Kaneta, Kazuhiro Motoki, Yasuhiro Jinno, Hideo Kasai, Yuji Okada, Hideaki Fukushima & [1]Nobuyuki Ogawa

Pharmaceutical Research Laboratory, Kirin Brewery Co. Ltd., Miyahara-cho 3, Takasaki, Gunma 370-12, Japan

**1** The relaxant mechanisms of action of KRN2391, a novel vasodilator, and nicorandil on epi-myocardial coronary artery (2.5– 3.0 mm outer diameter) and mid-myocardial coronary artery (0.8–1.0 mm outer diameter) were investigated in porcine isolated coronary arteries. In addition, the vasorelaxant responses of KRN2391 and nicorandil were compared with those of nitroglycerin and cromakalim, a $K^+$ channel opener, in epi- and mid-myocardial coronary arteries.

**2** Nitroglycerin showed a more potent relaxant effect on epi-myocardial coronary arteries than on mid-myocardial coronary arteries, whereas cromakalim produced greater relaxation responses in mid-myocardial coronary arteries. There was no difference between epi- and mid-myocardial coronary arteries in terms of the relaxant effect of KRN2391 and nicorandil.

**3** Relaxation induced by KRN2391 in epi- and mid-myocardial coronary arteries was inhibited by oxyhaemoglobin, a pharmacological antagonist of nitrovasodilators, and glibenclamide, a pharmacological antagonist of $K^+$ channel opening drugs. However, the inhibitory effect of glibenclamide on KRN2391-induced relaxation was greater in mid-myocardial coronary artery than in epi-myocardial coronary artery.

**4** Relaxation induced by nicorandil was inhibited by oxyhaemoglobin alone in epi-myocardial coronary arteries and by both oxyhaemoglobin and glibenclamide in mid-myocardial coronary arteries.

**5** In epi- and mid-myocardial coronary arteries, relaxation induced by cromakalim was inhibited by glibenclamide but not by oxyhaemoglobin, whereas relaxation induced by nitroglycerin was inhibited by oxyhaemoglobin but not by glibenclamide.

**6** These results suggest that KRN2391 and nicorandil exhibit a dual mechanism of action acting partly as a nitrate and partly as a $K^+$ channel opener. The mechanism of action of these drugs depend on the segment of coronary artery studied. Furthermore, the dual mechanism of action of KRN2391 and nicorandil seems to contribute to the equipotent relaxant effect between epi- and mid-myocardial coronary arteries.

**Keywords:** KRN2391; nicorandil; nitroglycerin; cromakalim; coronary artery

## Introduction

KRN2391, N-cyano-*N'*-(2-nitroxyethyl)-3-pyridinecarboximidamide monomethanesulphonate (Figure 1), is a novel vasodilator possessing a dual mechanism of action as a nitrate and as a $K^+$ channel opener (Kashiwabara *et al.*, 1991). This conclusion is based on the ability of KRN2391 to enhance $^{86}Rb$ efflux from pre-loaded vascular smooth muscle and to increase vascular guanosine 3':5'-cyclic monophosphate (cyclic GMP) formation (Kashiwabara *et al.*, 1991; Jinno *et al.*, 1992). In addition, the dual mechanism of KRN2391 is supported by the finding that KRN2391-induced blood vessel relaxation is inhibited by both $K^+$ channel blockers and methylene blue, an inhibitor of soluble guanylate cyclase (Kashiwabara *et al.*, 1991). However, the mechanism of action of KRN2391 appears to depend on the segment of coronary arteries investigated. Fukata *et al.* (1991) report that KRN2391 acts as a nitrate in canine large coronary arteries. In contrast, Kingsbury *et al.* (1991) show that KRN2391 acts as a $K^+$ channel opener in coronary resistive arterioles of dogs. Nicorandil in addition to KRN2391, is also known to exhibit both a nitrate action and a $K^+$ channel opening action (Taira, 1987; Kukovetz *et al.*, 1991). Both drugs also show a selective increase in coronary blood flow as their haemodynamic profiles (Uchida *et al.*, 1978; Sakai *et al.*, 1981; Ogawa *et al.*, 1990). As a consequence of such pharmacological characteristics, nicorandil has been used clinically as an antianginal drug. Therefore, KRN2391 may also be expected to be of use in ischaemic heart diseases such as angina pectoris.

When using a coronary vasodilator in ischaemic heart disease, the redistribution of coronary blood flow from normal areas to ischaemic areas is an important factor, i.e. coronary steal is a problem (Winbury *et al.*, 1969). In particular, a coronary vasodilator with high selectivity for small coronary arteries may well cause inappropriate distribution of blood flow within the myocardium (Winbury *et al.*, 1969). Accordingly, we examined the relaxant activity of KRN2391 and nicorandil in large and small sizes of porcine coronary arteries. In addition, the mechanism of action of KRN2391 and nicorandil was further investigated in these arteries.

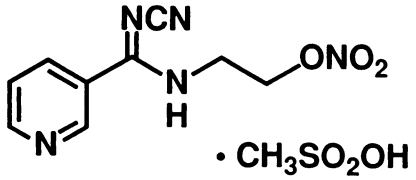



**Figure 1** Chemical structure of KRN2391.

[1] Author for correspondence.

## Methods

Fresh porcine hearts were obtained from a local abattoir. Hearts were excised within 10 min after death and immediately immersed in ice-cold Krebs-Henseleit solution of the following composition (mM: NaCl 118.0, KCl 4.7, $MgSO_4$ 1.2, $CaCl_2$ 2.5, $KH_2PO_4$ 1.2, $NaHCO_3$ 25.0, glucose 10.0). The anterior descending branch (epi-myocardial location, 2.5–3.0 mm, outer diameter) and mid-myocardial location (0.8–1.0 mm, outer diameter) of the left coronary arteries were isolated as large and small vessels, respectively. The interval between cardiac excision and coronary dissection was about 60 min. Arteries were cut into 2 mm rings which were mounted between two stainless steel triangular hooks and suspended in a 10 ml organ bath filled with Krebs-Henseleit solution which was maintained at 37°C and gassed with 95% $O_2$:5% $CO_2$. The tension was adjusted to 2.0 g for epi-myocardial vessels and 0.5 g for mid-myocardial vessels. After an equilibration period of 120 min, preparations were contracted by changing the bath solution to one containing 25 mM KCl. This potassium-depolarizing solution was prepared by replacing 20.3 mM NaCl with 20.3 mM KCl in the control bathing solution. After the arteries reached a stable tension, each vasodilator was administered in a cumulative manner. Oxyhaemoglobin ($10^{-5}$ M) and glibenclamide ($10^{-6}$ M) were added 20 min before the arteries were contracted with 25 mM KCl. The tension of each vessel was measured isometrically with a force-displacement transducer (Nihon Kohden, TB-611T).

### *Drugs*

KRN2391, nicorandil and cromakalim were synthesized in our laboratory. Haemoglobin and glibenclamide were purchased from Sigma Chemical Co. (St Louis, MO, U.S.A.), nitroglycerin from Nippon Kayaku Co. Ltd. (Tokyo, Japan) and papaverine hydrochloride from Wako (Osaka, Japan). Nicorandil ($5 \times 10^{-2}$ M) was dissolved in 0.1 N HCl. Cromakalim ($10^{-2}$ M) and glibenclamide ($10^{-3}$ M) were dissolved in dimethyl sulphoxide. These solutions were diluted in Krebs-Henseleit solution when necessary. Oxyhaemoglobin was prepared as described previously (Martin *et al.*, 1985). KRN2391 was dissolved in Krebs-Henseleit solution.

### *Statistical analysis*

Relaxations caused by the test drugs were expressed as a percentage of the maximum relaxation attainable which was assessed at the end of each experiment by addition to the bath of $10^{-4}$ M papaverine. The mean $EC_{50}$ was determined from the concentration-relaxation curves which were fitted by linear regression. Differences were evaluated for significance ($P < 0.05$), using Student's $t$ test for unpaired data for single comparisons and analysis of variance for multiple comparisons. When multiple comparisons were made with a single control, Dunnet's test was used to determine the significance level. Data are presented as mean ± standard error of mean (s.e.mean).

## Results

### *Relaxant response to KRN2391, nicorandil, nitroglycerin and cromakalim in epi- and mid-myocardial coronary arteries*

KRN2391, nicorandil, nitroglycerin and cromakalim produced concentration-dependent relaxations in epi- and mid-myocardial coronary arteries (Figure 2). There was no regional difference in the coronary artery relaxation induced by KRN2391 and nicorandil. Greater relaxation induced by nitroglycerin was seen in epi-myocardial coronary arteries than in mid-myocardial coronary arteries. In contrast, cromakalim induced greater relaxation in mid-myocardial coronary arteries than in epi-myocardial coronary arteries.

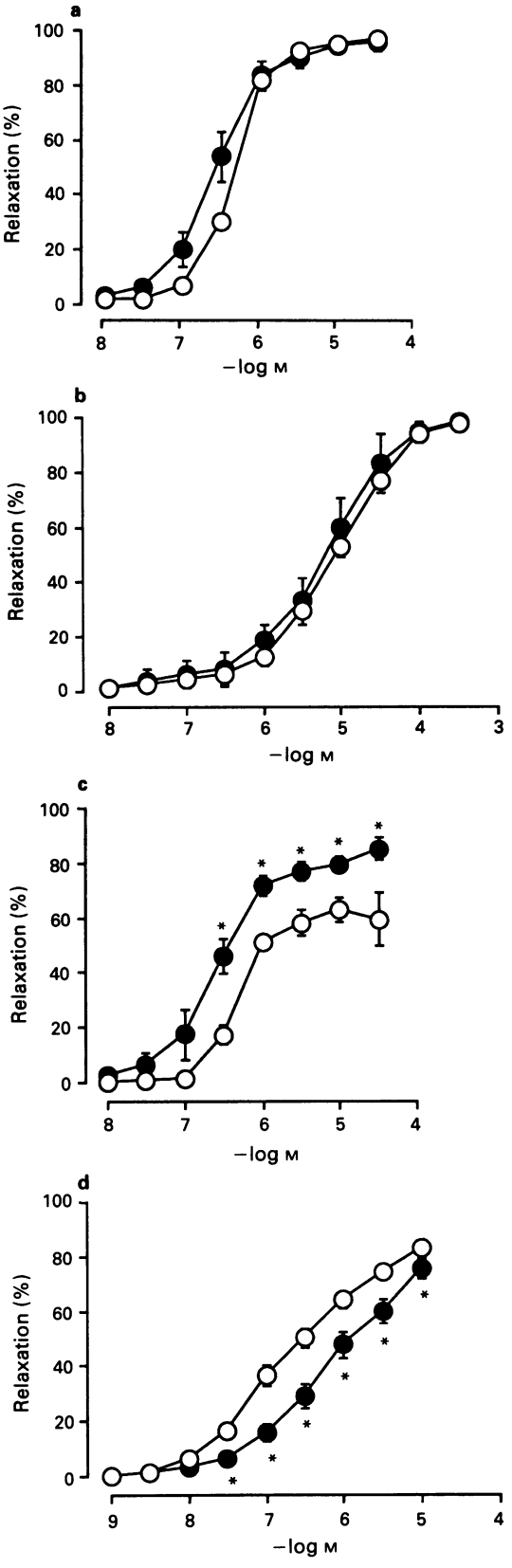



**Figure 2** Concentration-relaxation curves for (a) KRN2391, (b) nicorandil, (c) cromakalim and (d) nitroglycerin in epi- (○) and mid- (●) myocardial coronary arteries contracted by 25 mM KCl. Each point represents the mean ± s.e.mean ($n = 5-7$). *$P < 0.05$ compared with corresponding value of large coronary artery.

The $EC_{50}$ values for nitroglycerin were in the order of epi- < mid-myocardial coronary arteries, and the values for cromakalim were in the order of epi- > mid-myocardial coronary arteries (Table 1). There was no significant differences between epi- and mid-myocardial coronary arteries with respect to $EC_{50}$ values for KRN2391 and nicorandil (Table 1). The potency of KRN 2391 was greater than that of nicorandil or of cromakalim in epi-myocardial coronary arteries and than that of nicorandil in mid-myocardial coronary arteries (Table 1).

### *Effects of oxyhaemoglobin and glibenclamide on relaxations produced by KRN2391, nicorandil, nitroglycerin and cromakalim in epi-myocardial coronary arteries*

The concentration-relaxation curve for KRN2391 was shifted to the right by $10^{-5}$ M oxyhaemoglobin. Glibenclamide ($10^{-6}$ M) inhibited the relaxation induced by high concentrations ($10^{-6}$ and $3 \times 10^{-6}$ M) of KRN2391 but not that by low concentrations of KRN2391 ($10^{-8}$–$3 \times 10^{-7}$ M) (Figure 3). The concentration-relaxation curves for nicorandil and nitroglycerin were shifted to the right by oxyhaemoglobin but not affected by glibenclamide (Figure 3). The concentration-relaxation curve from cromakalim was shifted to the right by glibenclamide ($10^{-6}$ M) but was not affected by oxyhaemoglobin ($10^{-5}$ M) (Figure 3).

### *Effects of oxyhaemoglobin and glibenclamide on relaxations produced by KRN2391, nicorandil, cromakalim and nitroglycerin in mid-myocardial coronary artery*

The concentration-relaxation curves for KRN2391 and nicorandil were shifted by both oxyhaemoglobin and glibenclamide to the right (Figure 4). The relaxations induced by cromakalim and nitroglycerin were inhibited by glibenclamide ($10^{-6}$ M) and oxyhaemoglobin ($10^{-5}$ M), respectively (Figure 4). Glibenclamide ($10^{-6}$ M) and oxyhaemoglobin ($10^{-5}$ M) had no effect on the relaxations induced by nitroglycerin and cromakalim, respectively (Figure 4).

## Discussion

In the present study, nitroglycerin and cromakalim produced different magnitudes of relaxation in epi-myocardial coronary arteries compared to mid-myocardial coronary arteries. In contrast, KRN2391 and nicorandil failed to show a similar selective relaxant effect on epi- and mid-myocardial coronary arteries, but the potency of KRN2391 was greater than that of nicorandil in both coronary arteries. Nitroglycerin exhibited a more potent relaxant effect in epi-myocardial coronary arteries than in mid-myocardial coronary arteries whereas cromakalim produced greater relaxation in mid-myocardial coronary arteries. The present results with nitroglycerin are in agreement with those of Schnaar & Sparks, (1972) and Sellke *et al.* (1990). The non-selective vasodilator actions of KRN2391 and nicorandil between epi- and mid-myocardial coronary arteries appear to be associated with

**Table 1** The $EC_{50}$ values for the relaxant effects of KRN2391, nicorandil, cromakalim and nitroglycerin in epi- and mid-myocardial coronary arteries of pigs

| | *log $EC_{50}$* | |
|---|---|---|
| *Drugs* | *Epi-myocardial* | *Mid-myocardial* |
| KRN2391 | − 6.29 ± 0.02 | − 6.47 ± 0.15 |
| Nicorandil | − 5.11 ± 0.08[b] | − 5.28 ± 0.22[b] |
| Cromakalim | − 5.45 ± 0.16[b] | − 6.23 ± 0.11[a] |
| Nitroglycerin | − 6.38 ± 0.09 | − 6.00 ± 0.11[a] |

Values represent the mean ± s.e.mean ($n = 5$–7). [a]$P < 0.05$ compared with corresponding value for epi-myocardial coronary artery, [b]$P < 0.05$ compared with value for KRN2391.

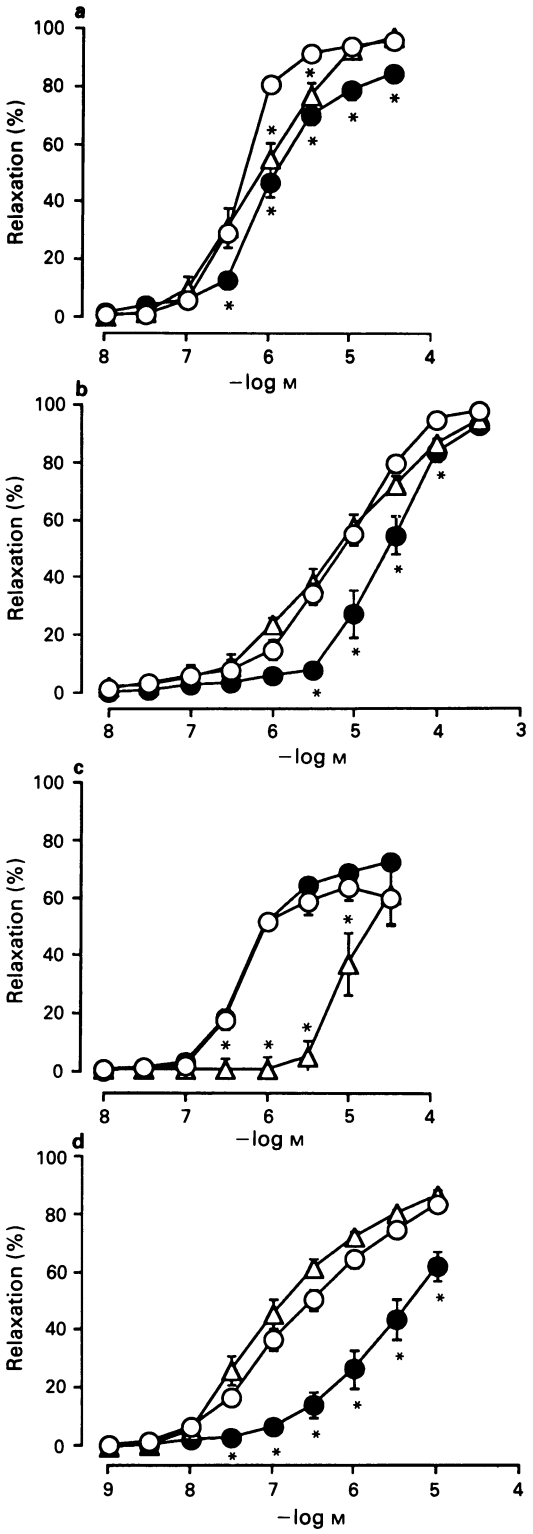



**Figure 3** Concentration-relaxation curves for (a) KRN2391, (b) nicorandil, (c) cromakalim and (d) nitroglycerin in epi-myocardial coronary arteries contracted by 25 mM KCl in the absence (○) and the presence of $10^{-5}$ M oxyhaemoglobin (●) and $10^{-6}$ M glibenclamide (△). Curves for epi-myocardial coronary arteries in Figure 2 are used as control curves for each drug in this figure. Each point represents the mean ± s.e.mean ($n = 5$–7). *$P < 0.05$ compared with corresponding control value.

their mechanism of action as both a nitrate and a $K^+$ channel opener. In contrast, the selective vasodilator actions of nitroglycerin and cromakalim between epi- and mid-myocardial coronary arteries are thought to be based on a nitrate action and a $K^+$ channel opening action, respectively, because oxyhaemoglobin, a pharmacological antagonist of nitrovasodilators (Martin *et al.*, 1985), and glibenclamide, a pharmacological antagonist of $K^+$ channel openers (Cavero *et al.*, 1989; Eltze 1989), had no effect on cromakalim- and nitroglycerin-induced responses, respectively. The difference in the relaxation response between epi- and mid-myocardial coronary arteries is likely to be important in the redistribution of coronary blood flow. Under ischaemic conditions of the heart, coronary vasodilators which are selective for small resistance arteries increase coronary blood flow in non-ischaemic areas, resulting in a decrease in coronary blood flow within ischaemic areas (Cohen *et al.*, 1976; Gallagher *et al.* 1980). Such a phenomenon has been called 'coronary steal'. Clinically, dipyridamole, an adenosine potentiator, has been reported to induce coronary steal (Wilcken *et al.*, 1971). In addition, the preferential action of adenosine on small coronary arteries has been observed *in vitro* (Miwa & Toda 1985). Therefore, cromakalim, as well as dipyridamole, may cause coronary steal. Nitroglycerin is reported to dilate large coronary arteries *in vivo* as well as *in vitro* and to show beneficial effects on the redistribution of coronary blood flow (Sakamoto *et al.*, 1987). Since we cannot find any report showing that nicorandil induces coronary steal in clinical therapy, the non-selective vasodilator actions of KRN2391 and nicorandil between epi- and mid-myocardial coronary arteries are not thought to be a disadvantage in the redistribution of coronary blood flow.

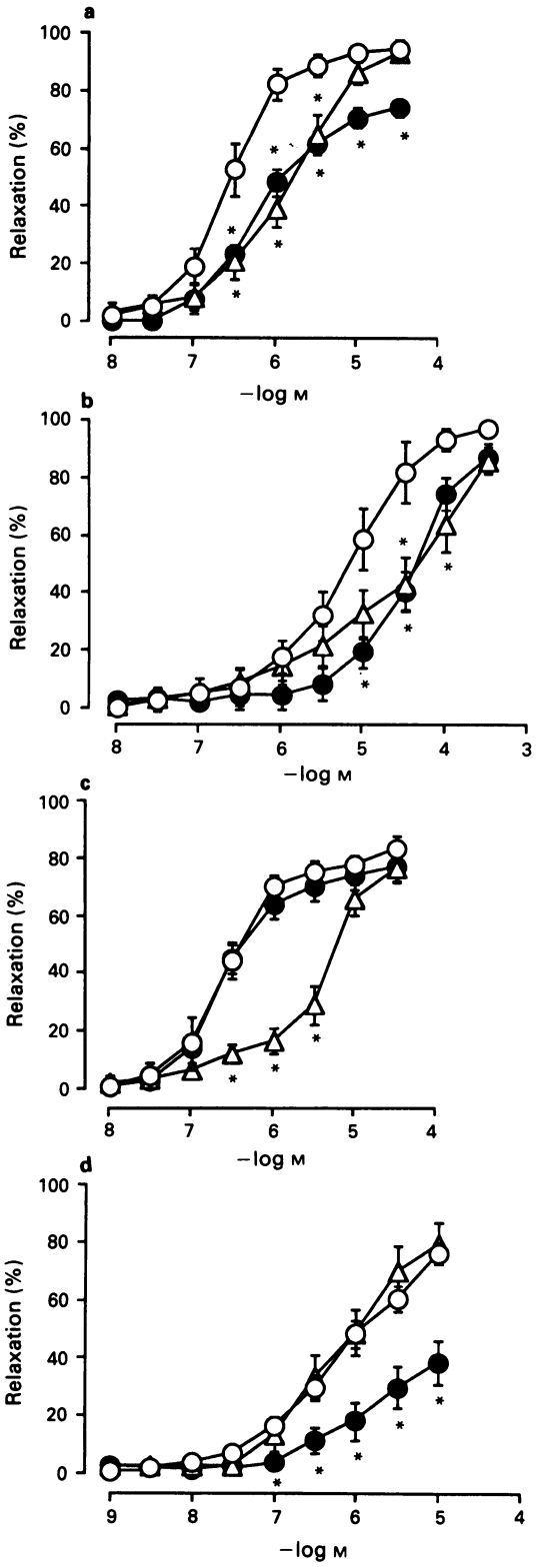



**Figure 4** Concentration-relaxation curves for (a) KRN2391, (b) nicorandil, (c) cromakalim and (d) nitroglycerin in mid-myocardial coronary arteries contracted by 25 mM KCl in the absence (○) and the presences of $10^{-5}$ M oxyhaemoglobin (●) and $10^{-6}$ M glibenclamide (△). Curves for mid-myocardial coronary arteries in Figure 2 are used as control curves for each drug in this figure. Each point represents the mean ± s.e.mean ($n = 5$–8). *$P < 0.05$ compared with corresponding control value.

The present data also demonstrate that KRN2391 acts as both a nitrate and as a $K^+$ channel opener in epi- and mid-myocardial coronary arteries since relaxations of epi- and mid-myocardial coronary arteries induced by KRN2391 were inhibited by oxyhaemoglobin and glibenclamide. Nicorandil-induced relaxation was inhibited by oxyhaemoglobin alone in epi-myocardial coronary arteries, but by oxyhaemoglobin and glibenclamide in mid-myocardial coronary arteries, suggesting that nicorandil behaves predominantly as a nitrate in epi-myocardial coronary arteries and as both a nitrate and a $K^+$ channel opener in mid-myocardial coronary arteries. Satoh *et al.* (1991) also reported that nicorandil-induced relaxation of canine large coronary arteries was inhibited by methylene blue, an inhibitor of soluble guanylate cyclase (Gruetter *et al.*, 1981) but not by glibenclamide, supporting the present results with nicorandil. In addition, Imagawa *et al.* (1992) observed that the increase in coronary blood flow induced by nicorandil was inhibited by glibenclamide in anaesthesized dogs, but the magnitude of shift of the dose-response curve in increasing coronary blood flow by glibenclamide was greater for cromakalim than for nicorandil. Therefore, these authors suggested that the glibenclamide-insensitive component in the increase in coronary blood flow produced by nicorandil might be a nitrate-like action. Since relaxation of coronary resistance arterioles largely contributes to the increase in coronary blood flow *in vivo*, the result from Imagawa *et al.* (1992) appears to reflect the present result using nicorandil in mid-myocardial coronary arteries. It has also been reported that the relaxation of canine large coronary arteries induced by KRN2391 may be inhibited by methylene blue but not by glibenclamide, suggesting that KRN2391, as well as nicorandil, behaves as a nitrate in canine large coronary arteries (Fukata *et al.*, 1991). The effect of KRN2391 in canine large coronary arteries was different from the present study in porcine large (epi-myocardial) coronary arteries. This may be due to species differences. Recently, we observed that KRN2391 increased cyclic GMP formation in porcine large coronary arteries, but the increase with KRN2391 was lower than that observed with nicorandil and nitroglycerin, despite showing the same degree of blood vessel relaxation (Jinno *et al.*, 1992). This result suggests that KRN2391 possesses an additional relaxant mechanism which does not depend on cyclic GMP formation. The present data appear to provide evidence that such a vasorelaxant mechanism does not

depend on cyclic GMP formation by KRN2391 and may well be based on its $K^+$ channel opening action. Furthermore, the present study, using porcine coronary arteries, showed that KRN2391 acts as both a nitrate and a $K^+$ channel opener in mid-myocardial coronary arteries as well as in epi-myocardial coronary arteries. However, the inhibitory effect of glibenclamide on KRN2391-induced relaxation was greater in mid-myocardial coronary arteries than in epi-myocardial coronary arteries. Therefore, the precise mechanism of action of KRN2391 and nicorandil are likely to depend on the segment of coronary artery employed.

The mechanism of actions of KRN2391 and nicorandil seems to contribute to their relative selectivity of effect. Thus, in epi- and mid-myocardial coronary arteries, cromakalim-induced relaxation was inhibited by glibenclamide but not by oxyhaemoglobin, whereas nitroglycerin-induced relaxation was inhibited by oxyhaemoglobin but not by glibenclamide. Therefore, it is considered that the additional $K^+$ channel opening actions of KRN2391 and nicorandil in mid-myocardial coronary arteries in which nitroglycerin-induced relaxation is weaker than in epi-myocardial coronary arteries, contribute to equipotent relaxant effects between epi- and mid-coronary arteries.

In conclusion, it is considered that KRN2391 and nicorandil produce equipotent relaxant effects in epi- and mid-myocardial coronary arteries. These results with KRN2391 and nicorandil are thought to be based on the dual mechanism of action as a nitrate and as a $K^+$ channel opener. In addition, the action of KRN2391 is more potent than that of nicorandil in epi- and mid-myocardial coronary arteries.

## References


CAVERO, I., MONDOT, S. & MESTRE, M. (1989). Vasorelaxant effects of cromakalim in rats are mediated by glibenclamide-sensitive potassium channels. *J. Pharmacol. Exp. Ther.*, **248**, 1261–1268.

COHEN, M.V., SONNENBLICK, E.H. & KIRK, E.S. (1976). Coronary steal: its role in detrimental effect of isoproterenol after acute coronary occlusion in dogs. *Am. J. Cardiol.*, **38**, 880–888.

ELTZE, M. (1989). Glibenclamide is a competitive antagonist of cromakalim, pinacidil, and RP 49356 in guinea-pig pulmonary artery. *Eur. J. Pharmacol.*, **165**, 231–239.

FUKATA, Y., HARADA, K., KASHIWABARA, T., OGAWA, N., FUKUSHIMA, H. & NISHIKORI, K. (1991). Different vasodilating mechanism of KRN2391 on isolated canine large coronary and cranial mesenteric arteries. *Jpn. J. Pharmacol.*, **55**, (Suppl. I), 253P.

GALLAGHER, K.P., FOLTS, J.D., SHEBUSKI, R.J., RANKIN, J.H.G. & ROWE, G.G. (1980). Subepicardial vasodilator reserve in the presence of critical coronary stenosis in dogs. *Am. J. Cardiol.*, **46**, 67–73.

GRUETTER, C.A., KADOWITZ, P.J. & IGNARRO, L.J. (1981). Methylene blue inhibits coronary arterial relaxation and guanylate cyclase activation by nitroglycerin, sodium nitrite, and amyl nitrite. *Can. J. Physiol. Pharmacol.*, **59**, 150–156.

IMAGAWA, J., AKIMA, M., NABATA, H. & TAIRA, N. (1992). Spasmolytic action of nicorandil in canine conductive coronary arteries *in vivo* is not modified by glibenclamide. *J. Cardiovasc. Pharmacol.*, **19**, 108–114.

JINNO, Y., KASAI, H., OHTA, H., NISHIKORI, K., FUKUSHIMA, H. & OGAWA, N. (1992). Contribution of cyclic GMP formation to KRN2391-induced relaxation in coronary artery of the pig. *Br. J. Pharmacol.*, **106**, 906–909.

KASHIWABARA, T., NAKAJIMA, S., IZAWA, T., FUKUSHIMA, H. & NISHIKORI, K. (1991). Characteristics of KRN2391, a novel vasodilator, compared with those of cromakalim, pinacidil and nifedipine in rat aorta. *Eur. J. Pharmacol.*, **196**, 1–7.

KINGSBURY, M., SATOH, K. & TAIRA, N. (1991). The cardiovascular profile of KRN2391 and its congener, in which the nitroxy group is replaced by a hydroxy group. *Jpn. J. Pharmacol.*, **55** (Suppl. I), 255P.

KUKOVETZ, W.R., HOLZMANN, S., BRAIDA, C. & PÖCH, G. (1991). Dual mechanism of the relaxing effect of nicorandil by stimulation of cyclic GMP formation and hyperpolarization. *J. Cardiovasc. Pharmacol.*, **17**, 627–633.

MARTIN, W., VILLANI, G.M., JOTHINANDAN, D. & FURCHGOTT, R.F. (1985). Selective blockade of endothelium-dependent and glyceryl trinitrate-induced relaxation by hemoglobin and by methylene blue in the rabbit aorta. *J. Pharmacol. Exp. Ther.*, **232**, 708–716.

MIWA, K. & TODA, N. (1985). The regional difference of relaxations induced by various vasodilators in isolated dog coronary and mesenteric arteries. *Jpn. J. Pharmacol.*, **38**, 313–320.

OGAWA, N., KANETA, S., JINNO, Y., HARADA, K., OHTA, H., FUKUSHIMA, H. & NISHIKORI, K. (1990). Pharmacological profile of KRN2391, a novel vasodilator. *Eur. J. Pharmacol.*, **183**, 1266–1267.

SAKAI, K., SHIRAKI, Y. & NABATA, H. (1981). Cardiovascular effects of a new coronary vasodilator N-(2-hydroxyethyl) nicotinamide nitrate (SG-75): comparison with nitroglycerin and diltiazem. *J. Cardiovasc. Pharmacol.*, **3**, 139–150.

SAKAMOTO, S., YOKOYAMA, M., KASHIKI, M. & FUKUZAKI, H. (1987). Comparative effects of intracoronary vasodilators on restoring coronary perfusion during flow-reducing coronary stenosis in the dog. *J. Am. Coll. Cardiol.*, **9**, 119–126.

SATOH, K., YAMADA, H. & TAIRA, N. (1991). Differential antagonism by glibenclamide of the relaxant effects of cromakalim, pinacidil and nicorandil on canine large coronary arteries. *Naunyn-Schmiedebergs Arch. Pharmacol.*, **343**, 76–82.

SCHNAAR, R.L. & SPARKS, H.V. (1972). Response of large and small coronary arteries to nitroglycerin, $NaNO_2$, and adenosine. *Am. J. Physiol.*, **223**, 223–228.

SELLKE, F.W., MYERS, P.R., BATES, J.N. & HARRISON, D.G. (1990). Influence of vessel size on the sensitivity of porcine coronary microvessels to nitroglycerin. *Am. J. Physiol.*, **258**, H515–H520.

TAIRA, N. (1987). Similarity and dissimilarity in the mode and mechanism of action between nicorandil and classical nitrates: an overview. *J. Cardiovasc. Pharmacol.*, **10** (Suppl. 8), S1–S9.

UCHIDA, Y., YOSHIMOTO, N. & MURAO, S. (1978). Effect of 2-nicotinamidethyl nitrate (SG-75) on coronary circulation. *Jpn. Heart J.*, **19**, 112–124.

WILCKEN, D.E.L., PAOLONI, H.J. & EIKENS, E. (1971). Evidence for intravenous dipyridamole (persantin) producing a 'coronary steal' effect in the ischaemic myocardium. *Aust. N.Z. J. Med.*, **1**, 8–14.

WINBURY, M.M., HOWE, B.B. & HEFNER, M.A. (1969). Effect of nitrates and other coronary dilators on large and small coronary vessels: a hypothesis for the mechanism of action of nitrates. *J. Pharmacol. Exp. Ther.*, **168**, 70–95.


*(Received November 24, 1992*
*Revised February 18, 1993*
*Accepted February 22, 1993)*

*Br. J. Pharmacol.* (1993), **109**, 637–644 © Macmillan Press Ltd, 1993

# Induction by endothelin-1 of epithelium-dependent relaxation of guinea-pig trachea *in vitro*: role for nitric oxide

[1]János G. Filep, Bruno Battistini & Pierre Sirois

Department of Pharmacology, Faculty of Medicine, University of Sherbrooke, Sherbrooke, P.Q., Canada J1H 5N4

**1** The purpose of the present experiments was to study the underlying mechanisms responsible for the relaxant action of endothelin-1 (ET-1) in the guinea-pig trachea *in vitro*.

**2** In tracheal strips precontracted (60–70% of the maximum) with carbachol, ET-1 (1–100 nM) evoked slowly developing concentration-dependent relaxations. Preincubation of the tissues with the thromboxane $A_2$/prostaglandin $H_2$ receptor antagonist, BM 13505 (5 μM) significantly potentiated the relaxant response to ET-1.

**3** Removal of the epithelium changed the response of precontracted tracheal preparations to ET-1 from a relaxation to a sustained contraction.

**4** ET-1-induced relaxations were abolished by methylene blue (10 μM) and were almost completely attenuated by oxyhaemoglobin (5 μM) and $N^G$-monomethyl-L-arginine (L-NMMA, 100 μM), an inhibitor of nitric oxide synthesis, but were not altered by indomethacin (10 μM).

**5** In tracheal strips under passive tension, ET-1 (1–100 nM) elicited dose-dependent contractions. The sensitivity of tissues to ET-1 was significantly enhanced by removal of the epithelium (apparent $EC_{50}$ values were 28.1 ± 4.1 and 12.5 ± 0.8 nM in intact and rubbed trachea, respectively, $n = 7$, $P < 0.01$).

**6** Preincubation of intact tracheal strips with methylene blue, oxyhaemoglobin or L-NMMA did not mimic the effect of epithelium removal on ET-1-induced contractions.

**7** There was a concentration-dependent increase in thromboxane $A_2$ but not in $PGE_2$ and prostacyclin release from intact tracheal strips following stimulation with ET-1 (5–100 nM).

**8** These results show that ET-1 exerts a dual action on guinea-pig isolated trachea: it evokes contractions at low resting tone, whereas it induces relaxations at higher resting tone. The relaxant action of ET-1 may be mediated by nitric oxide released from epithelial cells and resultant activation of smooth muscle guanylate cyclase.

**Keywords:** Endothelin-1; epithelium-derived relaxing factor; nitric oxide; guanylate cyclase; isolated trachea (guinea-pig)

## Introduction

Recent evidence suggests an important role for the airway epithelium in modulating the responsiveness of the underlying smooth muscle. Hyperreactivity of the airways is associated with damage or loss of the airway epithelium in bronchial asthma (Laitinen *et al.*, 1985). Removal of the epithelial layer from isolated airways of several mammalian species has been shown to enhance the contractile response to various bronchoconstrictor agents, including histamine, acetylcholine, 5-hydroxytryptamine and leukotrienes $C_4$ and $D_4$ (Barnes *et al.*, 1985; Holroyde, 1986; Goldie *et al.*, 1986; Hay *et al.*, 1987). These findings led to the concepts that intact epithelium may either act as a protective barrier between constrictors and airway smooth muscle (Holroyde, 1986; Undem *et al.*, 1988) or it may modulate the airway tone through release of relaxant substances, which may include prostanoids (Raeburn, 1990) and epithelium-derived relaxing factor(s) (Vanhoutte, 1988).

Endothelin-1 (ET-1), a 21-amino-acid peptide has been identified in the supernatant of cultured endothelial cells (Yanagisawa *et al.*, 1988) and tracheal epithelial cells (Black *et al.*, 1989). Specific binding of ET-1 to airway smooth muscle cells (Turner *et al.*, 1989b; Rozengurt *et al.*, 1990) as well as to epithelial cells has also been detected by immunohistochemistry (Rozengurt *et al.*, 1990). Thus, being produced and released locally, ET-1 is well situated to modulate airway tone either through acting on epithelial and/or smooth muscle cells. Indeed, numerous studies have shown that ET-1 exerts an airway constrictor action both *in vitro* and *in vivo*. On a molar basis, it is one of the most potent bronchoconstrictor agents yet described (Uchida *et al.*, 1988; Maggi *et al.*, 1989; Battistini *et al.*, 1990). ET-1 has also been reported to induce relaxation in precontracted rabbit tracheal segments (Grunstein *et al.*, 1991) and in tracheal strips isolated from guinea-pigs following an anaphylactic reaction (Saotome *et al.*, 1991). Furthermore, transient relaxation preceding the contractile response to ET-1 has been reported in some *in vitro* preparations of guinea-pig trachea (Turner *et al.*, 1989a), and in guinea-pig airway smooth muscle *in situ* (White *et al.*, 1991). These findings indicate that ET-1 is capable of releasing a relaxant factor from the trachea under certain circumstances. Bronchodilator prostaglandins (Grunstein *et al.*, 1991), lipoxygenase products derived from non-epithelial tissues (Saotome *et al.*, 1991) as well as an epithelium-derived relaxing factor of unknown nature (Grunstein *et al.*, 1991) have been implicated in mediating the relaxant action of ET-1. Recently, nitric oxide (NO) has been suggested as a mediator of the non-adrenergic, non-cholinergic relaxant response of guinea-pig trachea (Li & Rand, 1991; Kannan & Johnson, 1992). Furthermore, inhalation of NO gas induces rapid and potent bronchodilatation in the methacholine bronchoconstricted guinea-pig (Dupuy *et al.*, 1992). These findings led us to hypothesize that NO might mediate the relaxant action of ET-1 in guinea-pig airways.

The present experiments were designed to characterize further the relaxant action of ET-1 in the guinea-pig trachea *in vitro* and to identify the underlying mechanisms. The present data provide evidence that ET-1 elicits a concentration-dependent relaxation of isolated precontracted trachea,

[1] Author for correspondence at present address: Research Center, Maisonneuve-Rosemont Hospital, University of Montreal, 5415 boul. de l' Assomption, Montreal, P.Q., Canada H1T 2M4.

which may be mediated by NO released from epithelial cells and resultant activation of smooth muscle guanylate cyclase.

## Methods

### *Tissue preparation*

Male Dunkin-Hartley guinea-pigs (420–540 g) were killed by cervical dislocation followed by exsanguination. The trachea was then rapidly removed and placed in oxygenated (95% $O_2$ and 5% $CO_2$) Krebs-Henseleit solution (composition in mM: NaCl 118, KCl 4.7, $CaCl_2$ 2.5, $KH_2PO_4$ 1.18, $NaHCO_3$ 25, $MgSO_4.7H_2O$ 1.18 and glucose 11.1) at 37°C, pH 7.0. Following removal of adherent fat and connective tissue the trachea was cut in half. One half was left intact, while in some experiments the other half was stripped of epithelium by gently rubbing the lumen with a cotton-tipped applicator. Proximal and distal halves were randomly selected for removal of the epithelium. Then tracheal segments were cut in spirals (approximately 2.8 mm width by 30 mm long). Tissues were mounted separately in 5 ml organ baths and were connected to isometric force-displacement transducers (Grass model FTO3C) under an initial tension of 1.0 g. Tissues were equilibrated for 60 min in oxygenated Krebs-Henseleit solution. Organ baths were flushed with fresh solution every 15 min. Changes in tension were recorded continuously on a Grass 7D polygraph. In all tissues contractile responses to a single concentration of histamine (4.5 μM) was established before examination of the effects of ET-1 and complete recovery to resting tension was allowed following addition of histamine.

### *Experimental protocols*

*Endothelin-1-induced relaxation* To study the relaxant effect of ET-1, submaximal tone (usually 60–70% of the maximum) was first induced with carbachol (0.1 μM). Previously we have found that ET-1-induced contraction of guinea-pig isolated airways was, in part, mediated by thromboxane $A_2$ (Filep *et al.*, 1990; 1991). Therefore, the relaxation experiments were performed either in the absence or in the presence of BM 13505 (5 μM), a specific thromboxane $A_2$/prostaglandin $H_2$ receptor antagonist (Patscheke *et al.*, 1987). At the concentration employed, BM 13505 neither affects prostanoid formation (Patscheke *et al.*, 1987; Filep *et al.*, 1991) nor interferes with the biological responses to other bronchoactive agents, including platelet-activating factor, 5-hydroxytryptamine and histamine (Patscheke *et al.*, 1987; Battistini *et al.*, 1990). Cumulative concentrations of ET-1 (1–100 nM) were added to intact and rubbed tracheal strips, the next concentration being added when the preceding one had reached a steady-state effect. In another set of experiments, tracheal strips with intact epithelium were preincubated with methylene blue (10 μM), an inhibitor of soluble guanylate cyclase (Martin *et al.*, 1985), oxyhaemoglobin (5 μM), which binds NO (Hille *et al.*, 1977), $N^G$-monomethyl-L-arginine (L-NMMA, 100 μM), an inhibitor of NO synthesis (Rees *et al.*, 1989; 1990) or their vehicle for 10 min in the presence of BM 13505 (5 μM) before addition of the first concentration of ET-1. Some tracheal strips were preincubated with indomethacin (10 μM) for 20 min before addition of ET-1. In additional experiments, the reversibility of the action of L-NMMA was studied by use of L-arginine (1 mM) and D-arginine (1 mM).

*Endothelin-1-induced contraction* Concentration-response curves for ET-1 (1–100 nM) were obtained by its cumulative addition to intact and rubbed tracheal strips. Each ET-1 concentration was left in contact with the preparations until the response reached a steady-state level.

In another set of experiments, tracheal strips with or without intact epithelium were preincubated with methylene blue (10 μM), oxyhaemoglobin (5 μM), L-NMMA (100 μM) or their vehicle at 37°C for 10 min before cumulative addition of ET-1 to give final concentrations of 1–100 nM. Since methylene blue by itself slightly increased the tone in tracheal strips (3–8% of the contraction evoked by 4.5 μM histamine), tone was reduced, after treatment with this agent, to levels of untreated strips by adjusting the mechanical stretching force.

Only one concentration-response curve for ET-1 was obtained from each preparation. To minimize variation between tissues, ET-1-induced responses are expressed as the percentage of the contraction evoked by 4.5 μM of histamine.

*Endothelin-1-induced prostanoid release* In another set of experiments the effects of ET-1 on prostaglandin release were also studied. Tracheal strips with intact epithelium were prepared and incubated under the same experimental conditions as described above. Following a control incubation period of 4 min, three consecutive concentrations of ET-1 (5, 10 and 100 nM) were added to the organ baths. In additional experiments the effects of ET-1 were studied in tracheal strips preincubated with indomethacin (10 μM) for 20 min before addition of ET-1 (100 nM). Following an incubation period of 4 min, an aliquot of the incubation medium was removed and stored at −20°C until analysis of immunoreactive prostaglandin $E_2$ ($PGE_2$), 6-keto-$PGF_{1\alpha}$, the stable metabolite of prostacyclin and thromboxane $B_2$ ($TXB_2$), the stable metabolite of $TXA_2$. Each tissue was weighed at the end of the experiment. Prostanoid release is expressed as pg released per 4 min per 100 mg tissue wet weight.

### *Measurements of prostanoids*

Concentrations of immunoreactive $PGE_2$, 6-keto-$PGF_{1\alpha}$ and $TXB_2$ in the incubation medium were measured directly by enzyme immunoassays (Cayman Labs, Ann Arbor, MI, U.S.A.). The detection limit of the $PGE_2$, 6-keto-$PGF_{1\alpha}$ and $TXB_2$ assays were 1.5, 0.3 and 0.5 pg/tube, respectively. Intraassay coefficients of variation were 4.1% ($n = 6$), 5.8% ($n = 5$) and 4.2% ($n = 5$), respectively. The $PGE_2$ antiserum cross reacted with $TXB_2$ 4.0%, $PGF_{2\alpha}$ 2.5% and 6-keto-$PGF_{1\alpha}$ 1.4%. The 6-keto-$PGF_{1\alpha}$ antiserum cross-reacted with $PGF_{2\alpha}$ 12%, 6,15-diketo-$PGF_{1\alpha}$ 8% and $TXB_2$ 0.2%. The $TXB_2$ antiserum had 11% cross-reactivity with 2,3-dinor-$TXB_2$, whereas it had less than 0.7% cross reactivity with other prostanoids.

### *Histology*

After completion of concentration-response studies, tissues were removed from the organ baths and were cut into approximately 3 × 4 mm pieces. Pieces were taken randomly and prepared for light and scanning electron microscopy. For light microscopical examinations, samples were fixed in Bouin fixative, then 5 μm thick sections were prepared and stained with haematoxylin and eosin. For scanning electron-microscopical examinations, samples were prepared according to the method of Postek *et al.* (1980) using critical point drying. Tissues were examined in a Cambridge stereoscan 120 electron-microscope.

### *Drugs*

Endothelin-1 (Peninsula Labs, Belmont, CA, U.S.A.) was dissolved in distilled water and stored in aliquots at −20°C under $N_2$ for up to 3 weeks. BM 13505 (4-[2-(4-chlorobenzene sulphonyl-amino)ethyl] benzene acetic acid, Boehringer-Mannheim GmbH, Mannheim, Germany) and indomethacin (Merck, Sharp & Dohme, Canada) were dissolved in ethanol and were diluted further with Krebs-Henseleit solution as appropriate. The final concentration of ethanol in the organ bath never exceeded 0.1%. Methylene blue (Fischer Scientific, Fair Lawn, NJ, U.S.A.), L-arginine, D-arginine (free base), carbachol (carbamylcholine chloride, Sigma Chemical

Co., St. Louis, MO, U.S.A.) and $N^G$-monomethyl-L-arginine (Research Biochemicals Inc., Natick, MA, U.S.A.) were dissolved in Krebs-Henseleit solution. Oxyhaemoglobin was prepared from commercial bovine haemoglobin (Sigma) as described previously (Miller & Vanhoutte, 1989). The purity and concentration of oxyhaemoglobin in the final solution was determined spectrophotometrically. The solution was frozen in aliquots and stored at −20°C up to 10 days.

### *Statistical analysis*

Values are reported as means ± s.e.mean. Statistical evaluation of the data was performed by (1) two-way analysis of variance using ranks (Friedman test) for repeated measures with a subsequent Wilcoxon-Wilcox test (Wilcoxon & Wilcox, 1964) to identify differences between measurements taken during the control period and measurements taken following various concentrations of ET-1; (2) by Dunn multiple contract hypothesis test (Dunn, 1964) when different treatments were compared to the same control or (3) by Wilcoxon signed rank test and by Mann-Whitney U test for paired and unpaired observations, respectively. A $P<0.05$ level was considered significant for all tests.

## Results

### *Endothelin-1-induced epithelium-dependent relaxation*

Addition of cumulative concentrations of ET-1 (1–100 nM) to intact tracheal strips precontracted with carbachol resulted in a dose-dependent relaxation both in the absence and presence of BM 13505 (5 μM) (Figures 1, 2). However, the relaxant action of ET-1 was about two fold higher in the presence of BM 13505 (Figure 1). The threshold concentration of ET-1 to evoke relaxation was about 5 nM, whereas statistically significant relaxations were observed at concentrations higher than 10 nM (Figure 1). The relaxation developed following a lag time of 1–2.5 min and reached a plateau within 4–8 min (Figure 2). At higher concentrations (50–100 nM), ET-1-induced relaxations were preceded by small, transitory contractions (Figure 2). After induction of contraction in rubbed tracheal strips with carbachol, the relaxations elicited by 5 and 10 nM ET-1 were nearly abolished, whereas the relaxations evoked by higher concentrations of ET-1 (50–100 nM) were changed to sustained contractions (Figure 1).

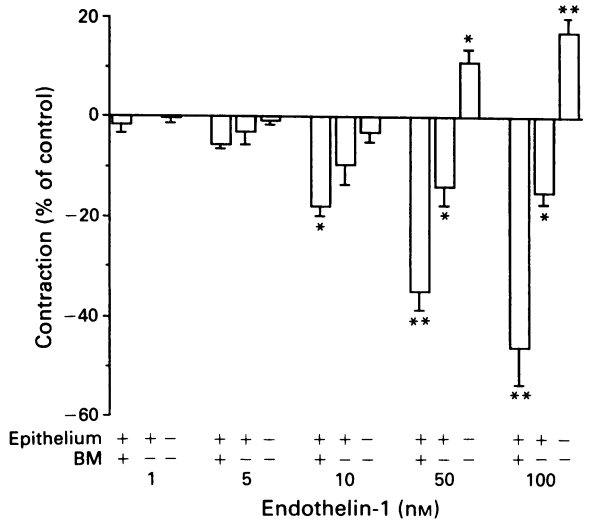
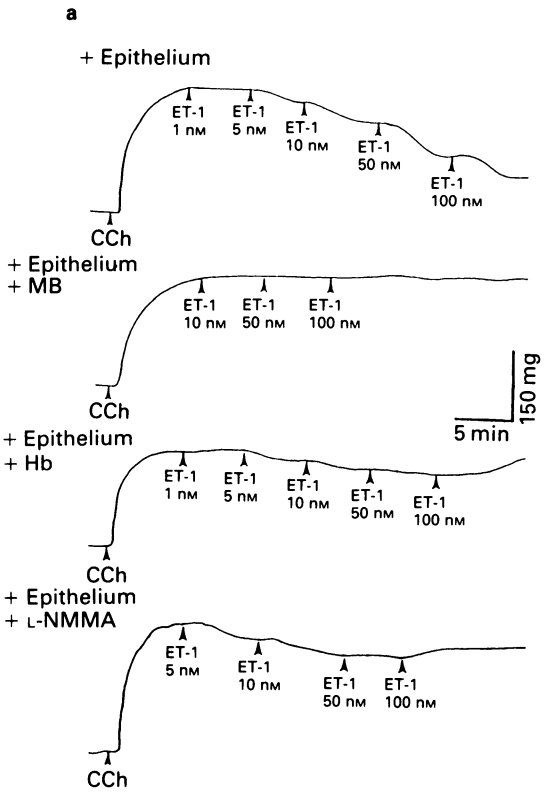



**Figure 1** Endothelin-1 (ET-1)-induced epithelium-dependent relaxations of the guinea-pig trachea *in vitro*. Tissues were precontracted with 0.1 μM carbachol, then cumulative concentrations of ET-1 were added in the absence (−BM) and presence (+BM) of the specific thromboxane $A_2$/prostaglandin $H_2$ receptor antagonist, BM 13505 (5 μM). Epithelium +, intact epithelium; epithelium −, epithelium was removed. Values are means with s.e.mean of 8–10 experiments. $*P<0.05$; $**P<0.01$ (compared to control by Wilcoxon-Wilcox test).



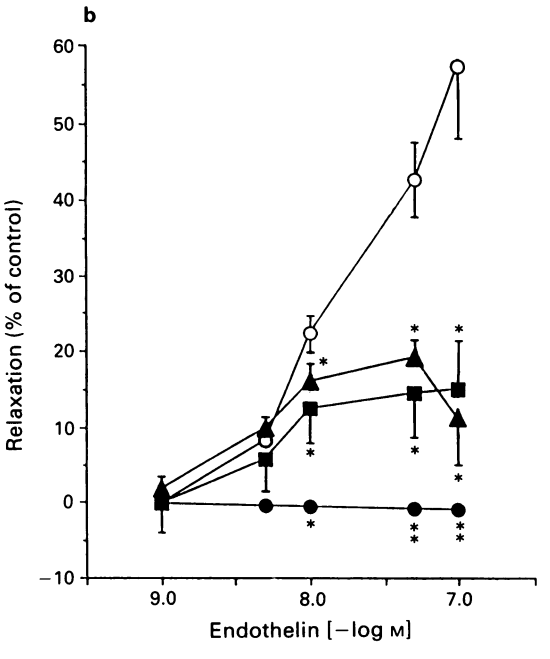




**Figure 2** Effects of methylene blue, oxyhaemoglobin and $N^G$-monomethyl-L-arginine on endothelin-1 (ET-1)-induced relaxation of guinea-pig isolated trachea. Tracheal strips were preincubated with methylene blue (MB, 10 μM) (●), oxyhaemoglobin (Hb, 5 μM) (■), $N^G$-monomethyl-L-arginine (L-NMMA, 100 μM) (▲) or vehicle (○) for 10 min, then contractions were evoked by carbachol (CCh, 0.1 μM) in the presence of BM 13505 (5 μM) before addition of cumulative concentrations of ET-1 (1–100 nM). (a) Representative tracings; (b) Values are means with s.e.mean. Control $n=12$, MB $n=7$, Hb and L-NMMA $n=5$. $*P<0.05$; $**P<0.01$ compared to control by Dunn multiple contrast test.

### *Effects of methylene blue, oxyhaemoglobin, L-NMMA and indomethacin on ET-1-induced relaxation*

Incubation of intact precontracted tracheal strips for 10 min with methylene blue (10 μM) abolished the relaxation induced by ET-1 (Figure 2). When intact tracheal strips were preincubated with oxyhaemoglobin (5 μM) for 10 min before inducing contractions with carbachol, ET-1-induced relaxation was markedly attenuated (Figure 2). Oxyhaemoglobin treatment did not affect significantly the lag time of ET-1 (Figure 2). Prolongation of the incubation time did not result in an increase in the inhibitory potency of oxyhaemoglobin (data not shown). Preincubation of the tissues with L-NMMA (100 μM) for 10 min resulted in similar inhibition of ET-1-induced relaxations as those observed with oxyhaemoglobin (Figure 2). A higher concentration of L-NMMA (1 mM) did not produce additional inhibitory effects. As shown in Table 1, the inhibitory action of L-NMMA was reversed by L-arginine (1 mM), but not by D-arginine (1 mM). The cyclo-oxygenase blocker, indomethacin (10 μM) failed to alter significantly ET-1-induced relaxations (Table 1).

### *Effect of epithelium removal on ET-1-induced contraction*

In the intact guinea-pig trachea, ET-1 (1–100 nM) evoked tonic, concentration-dependent contractions. The contractions developed slowly, reaching a steady-state level within 3–5 min. In these experiments, we did not observe relaxation following addition of ET-1 to the organ bath. Removal of the epithelium markedly enhanced the responsiveness of guinea-pig trachea to ET-1 as reflected by a 2.3 fold decrease in the apparent $EC_{50}$ values (28.1 ± 4.1 nM in the intact trachea, $n = 7$ versus 12.5 ± 0.8 nM in the trachea without epithelium, $n = 7$, $P < 0.01$) and an increase in the contractile response evoked by 100 nM ET-1 (131 ± 42 and 254 ± 53 mg in the intact and denuded trachea, respectively, $n = 7$, $P < 0.01$).

### *Effects of methylene blue, oxyhaemoglobin and L-NMMA on ET-1-induced contraction*

Addition of methylene blue (10 μM) to the organ bath resulted in a slowly developing, slight increase in tone (3–8% of the contraction evoked by 4.5 μM histamine). Consequently, care was taken to match tone with that of control preparations. The contractile response of intact tracheal strips to ET-1 tended to be somewhat higher in the presence of methylene blue than in control tissues. However, these changes did not reach statistical significance (Figure 3). Neither oxyhaemoglobin (5 μM) nor L-NMMA (100 μM) affected significantly ET-1-induced contractions (Figure 3). Similarly, methylene blue, oxyhaemoglobin and L-NMMA failed to alter significantly the contractile responses of denuded tracheal strips to ET-1 (data not shown).

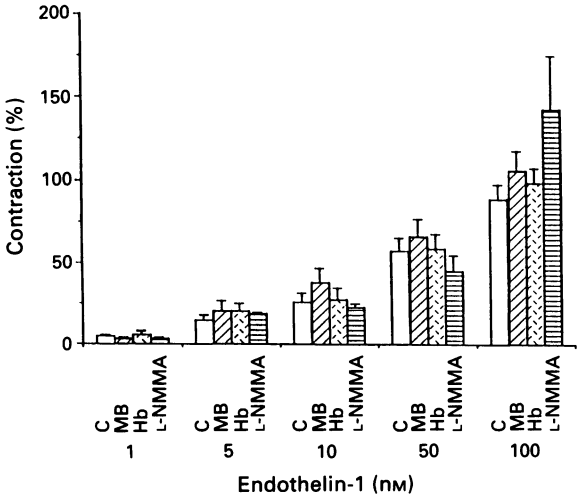



**Figure 3** Effects of methylene blue, oxyhaemoglobin and $N^G$-monomethyl-L-arginine on endothelin-1 (ET-1)-induced contraction in guinea-pig tracheal strips *in vitro*. Tissues were preincubated with methylene blue (MB, 10 μM), oxyhaemoglobin (Hb, 5 μM), $N^G$-monomethyl-L-arginine (L-NMMA, 100 μM) or vehicle (control, C) for 10 min at 37°C before addition of cumulative concentrations of ET-1. Maximum contractions observed after each concentration of ET-1 are expressed as % of the contraction evoked by 4.5 μM histamine. Values are means with s.e.mean. Control $n = 9$, MB $n = 5$, HB $n = 9$, L-NMMA $n = 4$.

### *ET-1-induced prostanoid release*

In another set of experiments the effects of ET-1 on $PGE_2$, prostacyclin and thromboxane $A_2$ production by intact tracheal strips were studied. Analysis of the incubation medium showed that the basal release of $PGE_2$, 6-keto-$PGF_{1\alpha}$ and $TXB_2$ were 40–70, 120–200 and 80–140 pg per 4 min per 100 mg tissue wet weight, respectively. Cumulative addition of 5, 10 and 100 nM of ET-1 did not induce significant changes in $PGE_2$ and 6-keto-$PGF_{1\alpha}$ levels in the medium (Table 2). On the other hand, 10 and 100 nM ET-1 caused about 62 and 190% increases in thromboxane release, respectively (Table 2). Preincubation of the tissues with indomethacin (10 μM) reduced basal prostanoid production by more than 75% and prevented ET-1 (100 nM)-induced $TXA_2$ release (Table 2).

### *Histology*

Light microscopical examinations revealed that rubbing the trachea removed the epithelium without producing obvious damage to the underlying submucosa and smooth muscle layers. Examination of randomly selected tissue pieces by scanning electron microscopy revealed that more than 96% of epithelial cells were removed by rubbing the tracheae,

**Table 1** Effect of various agents on relaxant responses to endothelin-1 in guinea-pig tracheal strips with intact epithelium

| | | *Endothelin-1* (50 nM) | | |
|---|---|---|---|---|
| | n | *Control* | *+Agent* | P |
| L-NMMA, 100 μM | 5 | 40 ± 4 | 17 ± 3 | <0.05 |
| L-NMMA, 100 μM + L-arginine, 1 mM | 4 | 44 ± 4 | 40 ± 2 | >0.05 |
| L-NMMA, 100 μM + D-arginine, 1 mM | 3 | 47 ± 5 | 18 ± 3 | <0.05 |
| Indomethacin, 10 μM | 5 | 45 ± 4 | 40 ± 5 | >0.05 |

Data are expressed as means (± s.e.mean) % reductions in the level of carbachol (0.1 μM)-induced tone. The experiments were performed in the presence of BM 13505 (5 μM). $n$ = the number of paired observations. $P$ values were obtained by the Wilcoxon signed ranked test. L-NMMA, $N^G$-monomethyl-L-arginine.

**Table 2** Effects of endothelin-1 (ET-1) and indomethacin on prostanoid release from the guinea-pig trachea *in vitro*

| | $TXB_2$ | 6-keto $PGF_{1\alpha}$ | $PGE_2$ |
|---|---|---|---|
| | (pg released $4\ min^{-1}$ $100\ mg^{-1}$ tissue wet wt) | | |
| Vehicle | 99 ± 10 | 157 ± 17 | 56 ± 8 |
| ET-1, 5 nM | 108 ± 9 | 139 ± 19 | 54 ± 10 |
| ET-1, 10 nM | 160 ± 15* | 182 ± 25 | 69 ± 12 |
| ET-1, 100 nM | 289 ± 32** | 193 ± 15 | 77 ± 20 |
| *P* | 0.001 | NS | NS |
| Indomethacin, 10 μM | 13 ± 1 | 23 ± 5 | 12 ± 1 |
| Indomethacin, 10 μM plus ET-1, 100 nM | 14 ± 1 NS[a] | 25 ± 3 NS[a] | 14 ± 2 NS[a] |

Epithelium-intact tracheal strips were challenged consecutively with saline (vehicle for ET-1) and increasing concentrations of endothelin-1 (ET-1). Following an incubation period of 4 min, an aliquot was removed for determination of prostanoid concentrations. Values are means ± s.e.mean of duplicate measurements for 5 separate experiments. *P* values are the probability levels of two-way analysis of variance using ranks (Friedman test). $*P<0.05$; $**P<0.001$ values were obtained by Wilcoxon-Wilcox test for multiple comparisons of vehicle versus various concentrations of ET-1. NS, not significant.
[a]Compared to indomethacin, 10 μM (Mann-Whitney U test).

whereas amongst control tissues 80–90% of the epithelium remained intact following the experiments. Removal of the epithelium potentiated by 2.4 fold the contractions elicited by 0.1–1.0 μM histamine, whereas it did not affect the maximum contractile response to 4.5 μM histamine (235 ± 11 and 225 ± 14 mg contraction in intact and rubbed tracheal strips, respectively, $n = 6$, $P > 0.05$). These findings confirm that the technique used to remove epithelial cells had not damaged the underlying smooth muscle.

## Discussion

The present experiments provide further evidence that ET-1 can elicit a dual action in the guinea-pig isolated trachea depending on the basal tone of smooth muscle. ET-1 causes relaxations when basal tone is high and evokes constrictions at lower basal tone. Both the relaxant and constrictor actions of ET-1 depend upon the presence of an intact epithelium, as removal of the epithelial cells abolishes the relaxant effect and potentiates the constrictor action of ET-1.

Our data show that ET-1 produces dose-dependent relaxation of epithelium-intact guinea-pig tracheal strips precontracted with carbachol to 60–80% of the maximum. The relaxations appeared to be slower in onset than those reported for other bronchoconstrictors (Vanhoutte, 1988; Bramley *et al.*, 1990). Threshold concentrations of ET-1 to induce relaxation in precontracted tissues were similar to those required to evoke contractions (Maggi *et al.*, 1989; Filep *et al.*, 1990; 1991). The relaxant effect of ET-1 was augmented by more than twofold in the presence of BM 13505, a thromboxane $A_2$/prostaglandin $H_2$ receptor antagonist. We have reported previously that ET-1 induces release of $TXA_2$ from the guinea-pig trachea *in vitro*, which may, in part, mediate its airway constrictor action in the guinea-pig (Filep *et al.*, 1990; 1991). Since $TXA_2$ is a very potent constrictor in the guinea-pig airways (Svensson *et al.*, 1977), one may expect that $TXA_2$ receptor blockade would lead to potentiation of ET-1-induced relaxations.

The present study confirms that ET-1 is a potent constrictor of guinea-pig isolated trachea when the resting tone is low (Uchida *et al.*, 1988; Maggi *et al.*, 1989; Hay, 1990; Filep *et al.*, 1990; 1991; Henry *et al.*, 1990). However, ET-1 was approximately 50 fold less potent in this series of experiments (apparent $EC_{50} = 28.1$ nM) than was previously reported by Uchida *et al.* (1988) ($EC_{50} = 0.53$ nM), but it was more potent than in the studies of Hay (1990) and Henry *et al.* (1990) (estimated $EC_{50} = 50–60$ nM). The reasons for this discrepancy are not clear but might be attributed to differences in tissue preparations (tracheal rings in the earlier experiments versus tracheal strips in the present experiments), differences in the integrity of the airway epithelium, in addition to different strains of guinea-pig used. In these, as well as in the present experimental conditions, the response to ET-1 was monophasic, i.e. the contractions were not preceded by a transient relaxation as has been observed by using an *in situ* guinea-pig tracheal preparation (White *et al.*, 1991) and tracheal strips (Turner *et al.*, 1989a). However, these latter and the present experimental conditions are not easily comparable. In the *in situ* preparation, resting tension was relatively high compared with active tension (White *et al.*, 1991), whereas in the living system, active tension is relatively low compared with resting tension. Thus, it is possible that the *in situ* preparation used by White *et al.* (1991) may resemble precontracted tracheal strips *in vitro*. On the other hand, tissue damage is reduced and hypoxia is avoided in the *in situ* preparation as arterial circulation of the airways is preserved. These may result in enhanced sensitivity of the tracheal preparations to bronchoactive agents.

Removal of the epithelium from the guinea-pig trachea has pronounced effects on the responses to ET-1. Thus, removal of the epithelium changed the response to ET-1 from a relaxation to a sustained contraction in tissues precontracted with carbachol and markedly enhanced the contractile response to ET-1 under resting conditions (i.e. in the absence of carbachol). In order to study whether or not the epithelium influences the reactivity of the underlying smooth muscle through release of NO, the responses to ET-1 were compared in the absence and presence of chemical agents that are known to interfere with the synthesis or actions of NO.

The relaxant action of ET-1 in precontracted tracheal strips was markedly attenuated by L-NMMA and oxyhaemoglobin, whereas methylene blue mimicked the effect of epithelium removal (i.e. slight contractions rather than relaxations were observed following addition of 50–100 nM ET-1 to the organ bath). L-NMMA has been shown to inhibit formation of endothelium-derived NO from endogenous L-arginine (Rees *et al.*, 1989; 1990), resulting in diminished activation of smooth muscle guanylate cyclase and decreased levels of guanosine 3′:5′-cyclic monophosphate (cyclic GMP) in the smooth muscle (Gold *et al.*, 1990). Oxyhaemoglobin generally abolishes NO-induced vascular relaxations because of its high binding affinity for NO (Ignarro *et al.*, 1984). Methylene blue inhibits cytosolic guanylate cyclase (Martin *et al.*, 1985) and accumulation of cyclic GMP by NO (Ignarro *et al.*, 1984; Ignarro, 1989; Gold *et al.*, 1990). Furthermore, methylene blue has been shown to produce free radicals (McCord & Fridovich, 1970) that can destroy relaxing factor(s) (Rubanyi *et al.*, 1986; Gryglewski *et al.*, 1986). The effects of L-NMMA, methylene blue and oxyhaemoglobin in the guinea-pig trachea closely resemble their actions on endothelium-derived relaxing factor/NO in vascular tissues (Palmer *et al.*, 1987; Ignarro, 1989). The inhibitory action of L-NMMA was readily reversible by L-arginine but not by D-arginine, indicating specific inhibition of NO synthase by L-NMMA. It seems unlikely that the inhibitory action of methylene blue or

oxyhaemoglobin was due to a non-specific interaction with ET-1, as neither methylene blue nor oxyhaemoglobin affected significantly ET-1-induced contractions in epithelium-intact and denuded tracheal strips. Since L-NMMA, methylene blue and oxyhaemoglobin are structurally unrelated compounds, it is also unlikely that their inhibitory effect can be attributed to a common non-specific action.

In contrast to the present findings, methylene blue (10–50 μM) either failed to inhibit relaxation responses to histamine and muscarinic agonists (Güc *et al.*, 1988; Fernandes *et al.*, 1989; Hay *et al.*, 1992) or at a concentration of 50 μM, it potentiated the maximal relaxant effects of histamine and methacholine in co-axial assemblies (Fernandes & Goldie, 1990). This potentiating action of methylene blue cannot be accounted for by inhibition of soluble guanylate cyclase, but rather it may have been non-specific and might be the consequence of alteration of basal smooth muscle tone. The increased basal tone can lead to an apparent increase in maximal relaxant response to the agonists (Raeburn, 1990). Since methylene blue appears to exert actions other than inhibition of soluble guanylate cyclase, its sole use may not provide a sufficient means to characterize epithelium-derived relaxing factor(s). Furthermore, according to our best knowledge, no information is available on the effects of oxyhaemoglobin and L-NMMA on epithelium-dependent relaxations in co-axial bioassays. Based on the differential effect of methylene blue on tracheal strips and co-axial assemblies, it is possible that the guinea-pig trachea may secrete different relaxant factors (Vanhoutte, 1988) that may be selective for some agonists. Detection of these relaxant factors is further complicated by the type of the assays used. For example, carbachol-induced relaxant factor release can only be detected by a co-axial bioassay system (Fernandes & Goldie, 1990), whereas platelet-activating factor-induced relaxations were observed by using tracheal strips (Brunelleschi *et al.*, 1987) but not by a co-axial bioassay (Fernandes & Goldie, 1990). In addition, it is unclear at present whether or not the epithelium-dependent relaxant responses observed in co-axial bioassay are attributable to hypoxia (Gunn & Piper, 1989; Hay *et al.*, 1992).

Taken together, the present findings suggest that ET-1-induced relaxations can be attributed, in part, to NO release from guinea-pig tracheal strips precontracted with carbachol. The recent observations that NO gas and the relatively stable NO adducts, S-nitrosothiols are potent bronchodilators in the guinea-pig both *in vivo* (Dupey *et al.*, 1992) and *in vitro* (Jansen *et al.*, 1992) give further support to this notion. Since epithelium removal abolished the relaxant effect of ET-1, one possibility is that that the synthesis of NO occurs in the epithelial and not in the smooth muscle cells. Alternatively, ET-1 may induce the release of a substance from the epithelium which then releases NO from another source(s). Whether ET-1 could directly stimulate NO release from epithelial cells remains to be investigated. These observations provide strong evidence against the possibility that the epithelium can be considered as a diffusion and/or metabolic barrier, preventing ET-1 from reaching tracheal smooth muscle in precontracted tracheal strips. One should keep in mind that unlike methylene blue, neither L-NMMA nor oxyhaemoglobin inhibited completely the relaxant action of ET-1. Higher concentrations of L-NMMA (1 mM) or oxyhaemoglobin (20 μM) did not produce significantly more antagonism. The reason for this is not known, but may be attributed to the release of other relaxing factor(s). Several metabolites of arachidonic acid, in particular $PGE_2$ and prostacyclin, are bronchodilators (for recent review see Raeburn, 1990). However, it seems unlikely that prostanoids mediate ET-1-induced relaxations since ET-1 did not induce significant $PGE_2$ and prostacyclin release from guinea-pig tracheal strips and indomethacin failed to inhibit the relaxations elicited by ET-1. Previous studies using co-axial bioassays have also demonstrated that histamine and methacholine-induced relaxations were not affected by cyclo-oxygenase inhibition (Ilhan & Sahin, 1986; Güc *et al.*, 1988; Fernandes *et al.*, 1989; Fernandes & Goldie, 1990). Furthermore, the findings that inhibition of cyclo-oxygenase does not prevent the potentiating effect of epithelium removal on bronchoconstrictor responses (Flavahan *et al.*, 1985; Farmer *et al.*, 1987; Undem *et al.*, 1988) give further support to this notion.

Based on the above conclusion, it might be expected that inhibition of NO synthesis and/or action of NO could potentiate the contractile response to ET-1. However, preincubation of tracheal strips with L-NMMA, methylene blue or oxyhaemoglobin under resting conditions (i.e. in the absence of carbachol) did not potentiate the contractile action of ET-1. On the other hand, removal of the epithelium potentiates ET-1-induced contractions (Maggi *et al.*, 1989; Hay, 1989; 1990, and the present study). One interpretation of these observations is that the NO formation by ET-1 is tone-dependent in the guinea-pig trachea as has been reported for blood vessels (Vargas *et al.*, 1990; Mehta *et al.*, 1992). Thus, like intense vasoconstriction, constriction of airway smooth muscle might lead to increased NO production in response to ET-1. A tone-dependent change in sensitivity of the trachea to NO cannot be ruled out at present. The possibility that epithelium removal led to decreased formation of bronchorelaxant prostanoids seems unlikely as under the same experimental conditions, indomethacin significantly attenuated the contractile action of ET-1 (Filep *et al.*, 1991). Another explanation might be that under resting conditions the epithelium may function primarily as a protective (diffusion and/or metabolic) barrier, reducing the contact between agonists and airway smooth muscle. Indeed, inhibition of neutral endopeptidase has been reported to enhance the contractile response to ET-1 in guinea-pig isolated airways (Maggi *et al.*, 1989; Hay, 1989). Furthermore, ET-1 could have reached smooth muscle cells from the luminal surface in the absence of epithelium.

In summary, the present results indicate that ET-1 can elicit contractions and epithelium-dependent relaxations of the guinea-pig isolated trachea depending on the tone of the tissue. The epithelium may function as a protective barrier under resting conditions. The relaxant action of ET-1 in precontracted tracheal strips is likely to be mediated by NO released from epithelial cells and subsequent activation of guanylate cyclase in smooth muscle cells.

BM 13505 was a generous gift from Dr K. Stegmeier (Boehringer-Mannheim GmbH, Mannheim, Germany). We thank the Medical Research Council of Canada for financial support and Ms Solange Cloutier for technical assistance. J.G.F. and P.S. are in receipt of a Medical Research Council Fellowship and a Scientist Award, respectively.

## References

BARNES, P.J., CUSS, F.M. & PALMER, J.B. (1985). The effect of airway epithelium on smooth muscle contraction in bovine trachea. *Br. J. Pharmacol.*, **86**, 685–692.

BATTISTINI, B., FILEP, J. & SIROIS, P. (1990). Potent thromboxane-mediated in vitro bronchoconstrictor effect of endothelin in the guinea-pig. *Eur. J. Pharmacol.*, **178**, 141–142.

BLACK, P.N., GHATEI, M.A., TAKAHASHI, K., BRETHERTON-WATT, D., KRAUSZ, T., DOLLERY, C.T. & BLOOM, S.R. (1989). Formation of endothelin by cultured airway epithelial cells. *FEBS Lett.*, **255**, 129–132.

BRAMLEY, A.M., SAMHOUN, M.N. & PIPER, P.J. (1990). The role of the epithelium in modulating the responses to guinea-pig trachea induced by bradykinin *in vitro*. *Br. J. Pharmacol.*, **99**, 762–766.

BRUNELLESCHI, S., HAYE-LEGRAND, I., LABAT, C., NOREL, X., BENVENISTE, J. & BRINK, C. (1987). Platelet-activating factor-acether-induced relaxation of guinea pig airway muscle: role of prostaglandin $E_2$ and the epithelium. *J. Pharmacol. Exp. Ther.*, **243**, 356–363.

DUNN, O.J. (1964). Multiple comparisons using rank sums. *Technometrics*, **6**, 241–252.

DUPUY, P.M., SHORE, S.A., DRAZEN, J.M., FROSTELL, C., HILL, W.A. & ZAPOL, W.M. (1992). Bronchodilator action of inhaled nitric oxide in guinea pigs. *J. Clin. Invest.*, **90**, 421–428.

FARMER, S.G., HAY, D.W.P., RAEBURN, D. & FEDAN, J.J. (1987). Relaxation of guinea-pig tracheal smooth muscle to arachidonate is converted to contraction following epithelium removal. *Br. J. Pharmacol.*, **92**, 231–236.

FERNANDES, L.B. & GOLDIE, R.G. (1990). Pharmacological evaluation of a guinea-pig tracheal epithelium-derived inhibiting factor (EpDIF). *Br. J. Pharmacol.*, **100**, 614–618.

FERNANDES, L.B., PATERSON, J.W. & GOLDIE, R.G. (1989). Co-axial bioassay of a smooth muscle relaxant factor released from guinea-pig tracheal epithelium. *Br. J. Pharmacol.*, **96**, 117–124.

FILEP, J.G., BATTISTINI, B. & SIROIS, P. (1990). Endothelin induces thromboxane release and contraction of isolated guinea-pig airways. *Life Sci.*, **47**, 1845–1850.

FILEP, J.G., BATTISTINI, B. & SIROIS, P. (1991). Pharmacological modulation of endothelin-induced contractions of guinea-pig isolated airways and thromboxane release. *Br. J. Pharmacol.*, **103**, 1633–1640.

FLAVAHAN, N.A., AARHUS, L.L., RIMELE, T.J. & VANHOUTTE, P.M. (1985). Respiratory epithelium inhibits bronchial smooth muscle tone. *J. Appl. Physiol.*, **58**, 834–838.

GOLD, M.E., WOOD, K.S., BYRNS, R.E., FUKUTO, J. & IGNARRO, L.J. (1990). $N^G$-methyl-L-arginine causes endothelium-dependent contraction and inhibition of cyclic GMP formation in artery and vein. *Proc. Natl. Acad. Sci. U.S.A.*, **87**, 4430–4434.

GOLDIE, R.G., PAPADIMITRIOU, J.M., PATERSON, J.W., RIGBY, P.J., SELF, H.M. & SPINA, D. (1986). Influence of the epithelium on responsiveness of guinea-pig isolated trachea to contractile and relaxant agonists. *Br. J. Pharmacol.*, **87**, 5–14.

GRUNSTEIN, M.M., CHUANG, S.T., SCHRAMM, C.M. & PAWLOWSKI, N.A. (1991). Role of endothelin-1 in regulating rabbit airway contractility. *Am. J. Physiol.*, **260**, L75–L82.

GRYGLEWSKI, R.J., PALMER, R.M.J. & MONCADA, S. (1986). Superoxide anion is involved in the breakdown of endothelium-derived relaxing factor. *Nature*, **320**, 454–456.

GÜC, M.O., ILHAN, M. & KAYAALP, S.O. (1988). The rat anococcygeus muscle is a convenient bioassay organ for the airway epithelium-derived relaxant factor. *Eur. J. Pharmacol.*, **148**, 405–409.

GUNN, L.K. & PIPER, P.J. (1989). Limitations of the co-axial bioassay. *Br. J. Pharmacol.*, **100**, 371P.

HAY, D.W.P. (1989). Guinea-pig tracheal epithelium and endothelin. *Eur. J. Pharmacol.*, **171**, 241–245.

HAY, D.W.P. (1990). Mechanism of endothelin-induced contraction in guinea-pig trachea: comparison with rat aorta. *Br. J. Pharmacol.*, **100**, 383–392.

HAY, D.W.P., FARMER, S.G., RAEBURN, D., MUCCITELLI, R.M., WILSON, K.A. & FEDAN, J.S. (1987). Differential effects of epithelium removal on the responsiveness of guinea-pig tracheal smooth muscle to bronchoconstrictors. *Br. J. Pharmacol.*, **92**, 381–388.

HAY, D.W.P., MUCCITELLI, R.M., PAGE, C.P. & SPINA, D. (1992). Correlation between airway epithelium-induced relaxation of rat aorta in the co-axial bioassay and cyclic nucleotide levels. *Br. J. Pharmacol.*, **105**, 954–958.

HENRY, P.J., RIGBY, P.J., SELF, G.J., PREUSS, J.M. & GOLDIE, R.G. (1990). Relationship between endothelin-1 binding sites densities and constrictor activities in human and animal airway smooth muscle. *Br. J. Pharmacol.*, **100**, 786–792.

HILLE, R., PALMER, G. & OLSON, J.S. (1977). Chain equivalence in reaction of nitric oxide with hemoglobin. *J. Biol. Chem.*, **252**, 403–405.

HOLROYDE, M.C. (1986). The influence of epithelium on the responsiveness of guinea-pig isolated trachea. *Br. J. Pharmacol.*, **87**, 501–507.

IGNARRO, L.J. (1989). Biological actions and properties of endothelium-derived nitric oxide formed and released from artery and vein. *Circ. Res.*, **65**, 1–21.

IGNARRO, L.J., BURKE, T.M., WOOD, K.S., WOLIN, M.S. & KADOWITZ, P.J. (1984). Association between cyclic GMP accumulation and acetylcholine-elicited relaxation of bovine intrapulmonary artery. *J. Pharmacol. Exp. Ther.*, **228**, 682–690.

ILHAN, M. & SAHIN, I. (1986). Tracheal epithelium releases a vascular smooth muscle relaxant factor: demonstration by bioassay. *Eur. J. Pharmacol.*, **131**, 293–296.

JANSEN, A., DRAZEN, J., OSBORNE, J.A., BROWN, R., LOSCALZO, J. & STAMLER, J.S. (1992). The relaxant properties in guinea-pig airways of S-nitrosothiols. *J. Pharmacol. Exp. Ther.*, **261**, 154–160.

KANNAN, M.S. & JOHNSON, D.E. (1992). Nitric oxide mediates the neural nonadrenergic, noncholinergic relaxation of pig tracheal smooth muscle. *Am. J. Physiol.*, **262**, L511–L514.

LAITINEN, L.A., HEINO, M., LAITINEN, A., KAVA, T. & HAAHTELA, T. (1985). Damage of the airway epithelium and bronchial reactivity in patients with asthma. *Am. Rev. Respir. Dis.*, **131**, 599–606.

LI, C.G. & RAND, N.J. (1991). Evidence that part of the NANC relaxant response of guinea-pig trachea to electrical field stimulation is mediated by nitric oxide. *Br. J. Pharmacol.*, **102**, 91–94.

MAGGI, C.A., PATACCHINI, R., GIULIANI, S. & MELI, A. (1989). Potent contractile effect of endothelin on isolated guinea-pig airways. *Eur. J. Pharmacol.*, **160**, 179–182.

MARTIN, W., VILLANI, G.M., JOTHIANANDAN, D. & FURCHGOTT, R.F. (1985). Selective blockade of endothelium-dependent and glyceryl trinitrate-induced relaxation by hemoglobin and methylene blue in the rabbit aorta. *J. Pharmacol. Exp. Ther.*, **232**, 708–716.

MCCORD, J.M. & FRIDOVICH, I. (1970). The utility of superoxide dismutase in studying free radical reactions. *J. Biol. Chem.*, **215**, 1374–1377.

MEHTA, J.L., LAWSON, D.L., YANG, B.C., MEHTA, P. & NICHOLS, W.W. (1992). Modulation of vascular tone by endothelin-1: role of preload, endothelial integrity and concentration of endothelin-1. *Br. J. Pharmacol.*, **106**, 127–132.

MILLER, V.M. & VANHOUTTE, P.M. (1989). Is nitric oxide the only endothelium-derived relaxing factor in canine femoral veins? *Am. J. Physiol.*, **257**, H1910–H1916.

PALMER, R.M.J., FERRIGE, A.G. & MONCADA, S. (1987). Nitric oxide release accounts for the biological activity of endothelium-derived relaxing factor. *Nature*, **327**, 524–526.

PATSCHEKE, H., STEGMEIER, K., HORNBERGER, W., STAIGER, C.H. & NEUGEBAUER, G. (1987). Inhibition of platelet activation by the novel thromboxane receptor antagonist BM 13505 (abstract). *Thromb. Haemostasis.*, **58**, 182.

POSTEK, M., HOWARD, K., JOHNSON, A. & MCMICHAEL, K. (1980). Specimen preparation. In *Scanning Electron Microscopy: a Student Handbook*. pp. 115–240. Burlington, V.T.: Ladd.

RAEBURN, D. (1990). Eicosanoids, epithelium and airway reactivity. *Gen. Pharmacol.*, **21**, 11–16.

REES, D.D., PALMER, R.M.J., HODSON, H.F. & MONCADA, S. (1989). A specific inhibitor of nitric oxide formation from L-arginine attenuates endothelium-dependent relaxation. *Br. J. Pharmacol.*, **96**, 418–424.

REES, D.D., PALMER, R.M.J., SCHULZ, R., HODSON, H.F. & MONCADA, S. (1990). Characterization of three inhibitors of endothelial nitric oxide synthase *in vitro* and *in vivo*. *Br. J. Pharmacol.*, **101**, 746–752.

ROZENGURT, N., SPRINGALL, D.R. & POLAK, J.M. (1990). Localization of endothelin-like immunoreactivity in airway epithelium of rats and mice. *J. Pathol.*, **160**, 5–8.

RUBANYI, G.M. & VANHOUTTE, P.M. (1986). Superoxide anions and hyperoxia inactivate endothelium-derived relaxing factor. *Am. J. Physiol.*, **250**, H822–H827.

SAOTOME, M., NOMURA, A., OHSE, H., ENDOH, T., KAMEYAMA, M., NINOMIYA, H., OHTSUKA, M., ISHII, Y., HAMADA, M., WATANABE, A., UCHIDA, Y. & HASEGAWA, S. (1991). Tracheal smooth muscle relaxation, induced by endothelin-1, is due to a lipoxygenase product derived from non-epithelial tissue (abstract). *Am. Rev. Respir. Dis.*, **143**, A159.

SVENSSON, J., STRANDBERG, K., TUVEMO, T. & HAMBERG, M. (1977). Thromboxane $A_2$: effects on airway and vascular smooth muscle. *Prostaglandins*, **14**, 425–436.

TURNER, N.C., DOLLERY, C.T. & WILLIAMS, A.J. (1989a). Endothelin-1-induced contractions of vascular and tracheal smooth muscle. Effects of nicardipine and BRL 34915. *J. Cardiovasc. Pharmacol.*, **13**, S180–S182.

TURNER, N.C., POWER, R.F., POLAK, J.M., BLOOM, S.R. & DOLLERY, C.T. (1989b). Endothelin-induced contraction of tracheal smooth muscle and identification of specific endothelin binding sites in the trachea of the rat. *Br. J. Pharmacol.*, **98,** 361–366.

UCHIDA, Y., NINOMIYA, H., SAOTOME, M., NOMURA, A., OHTSUKA, M., YANAGISAWA, M., GOTO, K., MASAKI, T. & HASEGAWA, S. (1988). Endothelin, a novel vasoconstrictor peptide, as a potent bronchoconstrictor. *Eur. J. Pharmacol.*, **154,** 227–228.

UNDEM, B.J., RAIBLE, D.G., ADKINSON, N.F. Jr & ADAMS III, G.K. (1988). Effect of removal of the epithelium on antigen-induced smooth muscle contraction and mediator release from guinea-pig isolated trachea. *J. Pharmacol. Exp. Ther.*, **244,** 653–665.

VANHOUTTE, P.M. (1988). Epithelium-derived relaxing factor(s) and bronchial reactivity. *Am. Rev. Resp. Dis.*, **138,** S24–S30.

VARGAS, H.M., INGARRO, L.J. & CHAUDHURI, G. (1990). Physiological release of nitric oxide is dependent on the level of vascular tone. *Eur. J. Pharmacol.*, **190,** 393–397.

WHITE, S.R., HATHAWAY, D.P., UMANS, J.G., TALLET, J., ABRAHAMS, C. & LEFF, A.R. (1991). Epithelial modulation of airway smooth muscle response to endothelin-1. *Am. Rev. Respir. Dis.*, **144,** 373–378.

WILCOXON, F. & WILCOX, R.A. (1964). *Some Rapid Approximate Statistical Procedures.* pp. 36–38. Pearl River, N.Y.: Lederle Laboratories.

YANAGISAWA, M., KURIHARA, M., KIMURA, S., TOMOBE, Y., KOBAYASHI, M., MITSUI, Y., YAZAKI, Y., GOTO, T. & MASAKI, T. (1988). A novel potent vasoconstrictor peptide produced by vascular endothelial cells. *Nature*, **332,** 411–415.

*(Received September 21, 1992*
*Revised February 17, 1993*
*Accepted February 18, 1993)*

*Br. J. Pharmacol.* (1993), **109**, 645–650 © Macmillan Press Ltd, 1993

# Role of neuronal and vascular $Ca^{2+}$-channels in the ACTH-induced reversal of haemorrhagic shock

[1]Salvatore Guarini, Carla Bazzani & Alfio Bertolini

Institute of Pharmacology, University of Modena, via G. Campi 287, 41100 Modena, Italy

**1** In a rat model of volume-controlled haemorrhagic shock causing the death of all control (saline-treated) animals within 30 min, the intravenous (i.v.) bolus injection of ACTH-(1-24) at a dose of 160 $\mu g\,kg^{-1}$ produced an impressive and sustained restoration of arterial pressure, pulse pressure and respiratory function, with 100% survival at the end of the observation period (2 h).

**2** Both intracerebroventricular (i.c.v., 0.015–0.06 $\mu g\,kg^{-1}$) and i.v. (5 $\mu g\,kg^{-1}$) pretreatment with the N-calcium channel blocker, ω-conotoxin GVIA, and i.v. (but not i.c.v.) pretreatment with the L-calcium channel blocker, nicardipine (125–500 $\mu g\,kg^{-1}$) dose-dependently prevented the ACTH-induced shock reversal.

**3** These results further indicate that the effect of ACTH in haemorrhagic shock may involve a neuronal link and the eventual restoration of vascular tone mediated by N- and L-type calcium channels, respectively.

**Keywords:** Shock; haemorrhagic shock; haemorrhage; ACTH; $Ca^{2+}$-channels; nicardipine; ω-conotoxin; $Ca^{2+}$-channel blockers

## Introduction

The neuropeptides of the ACTH-MSH family (melanocortins), while having negligible influence on cardiovascular and respiratory functions under normal conditions (Iyoda *et al.*, 1986; Bertolini *et al.*, 1986c), have an impressive effect in shock conditions. Indeed, the intravenous (i.v.) bolus injection of melanocortins into animals (rats, dogs) bled to an otherwise invariably and rapidly fatal condition of haemorrhagic shock induces, within a few minutes, a dose-dependent and sustained restoration of cardiovascular and respiratory functions and an impressive increase in the survival time without the need for other supportive treatments or fluid infusion (Bertolini *et al.*, 1986a,b,c; 1989). The minimum active dose is 20 $\mu g\,kg^{-1}$, and with the maximum effective dose (160 $\mu g\,kg^{-1}$, i.e. 54 $nmol\,kg^{-1}$) of the most potent melanocortin [the tetracosactide, ACTH-(1-24)] (Bertolini *et al.*, 1986c) the mean survival time is extended to 44 ± 18 h (range 15 to 312 h) (Guarini *et al.*, 1990b), while all control (saline-treated) animals die within 30 min. Some anecdotal reports seem to indicate that ACTH-(1-24) also has similar effects in man in conditions of haemorrhagic or cardiogenic shock (Bertolini *et al.*, 1987; Noera *et al.*, 1989; 1991; Pinelli *et al.*, 1989).

The mechanism of action does not involve the adrenal glands, for shock reversal is obtained with melanocortins practically devoid of corticotropic activity [α-MSH, ACTH-(4-10), ACTH-(1-16)], as well as in adrenalectomized animals (Bertolini *et al.*, 1986a,c). Rather, it seems that melanocortins activate (or restore) a complex vasomotor reflex that eventually leads to the mobilization of the peripherally-pooled residual blood and which is seemingly obtunded, in conditions of failure of the circulatory homeostasis, by the massive release of endogenous opioids (Lang *et al.*, 1982; Farrell *et al.*, 1983; Holaday, 1983; Elam *et al.*, 1984; Bernton *et al.*, 1985; Schadt & Gaddis, 1985; Szabo *et al.*, 1989; Bertolini *et al.*, 1989). Available data indicate that this vasomotor reflex involves afferent sensory fibres originating from vascular chemo- and baro-receptors, and efferent postganglionic sympathetic fibres. Indeed, the effect of ACTH is prevented by bilateral cervical vagotomy (Guarini *et al.*, 1986), is mimicked by protoveratrines (Bertolini *et al.*, 1990), and is not observed in rats pretreated with ganglion-blocking drugs (unpublished data), guanethidine or dibenamine (Guarini *et al.*, 1988). The final step seemingly consists in the restoration of vascular tone, at least in certain vascular beds (for reviews see: Bertolini *et al.*, 1989; Guarini *et al.*, 1991). An essential role seems to be played by brain cholinergic neurones, since melanocortin-induced shock reversal is prevented by the intracerebroventricular (i.c.v.) injection of hemicholinium-3 (Guarini *et al.*, 1990a) and by the blockade of brain $M_3$ muscarinic receptors (Guarini *et al.*, 1990c), while it is mimicked by the administration of centrally-acting cholinomimetic drugs (Guarini *et al.*, 1989). There is strong evidence that acetylcholine plays an important role in cardiovascular regulation (Brezenoff & Giuliano, 1982), and pharmacological activation of brain cholinoceptors results in marked pressor responses in several species, including man (Dirnhuber & Cullumbine, 1955; Varagić, 1955; Medacović & Varagić, 1957; Brezenoff & Jenden, 1969; Brezenoff, 1972; Janowsky *et al.*, 1986).

The mechanism of action of melanocortin peptides involves the increase of intracellular $Ca^{2+}$ concentration in target neurones (for reviews see: Jolles *et al.*, 1980; O'Donohue & Dorsa, 1982; De Wied & Jolles, 1982; Wiegant *et al.*, 1986; Eberle, 1988). It is now clear that at least four general categories (types) of $Ca^{2+}$-channels exist in neurones (for reviews see: Snutch *et al.*, 1990; Mogul & Fox, 1991; Starr *et al.*, 1991; Mintz *et al.*, 1992; Llinás *et al.*, 1992): L-type (high activation voltages, blockade by dihydropyridines; typically expressed by arterial smooth muscle), N-type (intermediate activation voltage, blockade by ω-conotoxin; typically expressed by neuronal cells), T-type (more negative activation voltage, partial blockade by medium-chain alcohols and by amiloride; carry a small proportion of the total $Ca^{2+}$ current), P-type (activation voltage intermediate between those of N- and T-type, blockade by ω-Aga-IVA and by the polyamines FTX and sFTX; involved in synaptic transmission throughout the brain).

It has been shown that blockade of N-type $Ca^{2+}$-channels by means of ω-conotoxin prevents the behavioural effects of ACTH (Argiolas *et al.*, 1990). Accordingly, we set out to gain further insight into the mechanism(s) of melanocortin-induced shock reversal by studying the influence of neuronal N-type and vascular L-type $Ca^{2+}$-channel blockade on the effect of ACTH-(1-24) in our model of volume-controlled haemorrhagic shock in rats.

[1] Author for correspondence.

## Methods

### Animals and surgery

A total of 88 adult Wistar rats of either sex (Morini, S. Polo d'Enza, Reggio nell'Emilia, Italy), weighing 280–300 g, were used. They were caged in groups of 5 (males and females separately) and maintained in conditioned colony-rooms (temperature 22 ± 1°C, 60% humidity), on a natural light-dark cycle, with food and water continuously available. They were acclimatized for at least one week before being used. Some of them were prepared for i.c.v. treatment by stereotaxically implanting under ketamine plus xylazine anaesthesia (115 mg $kg^{-1}$ plus 2 mg $kg^{-1}$ intraperitoneally (i.p.)) stainless-steel cannulae (23 gauge; Plastic Products Co., Roanoke, Va, U.S.A.) aimed at one brain lateral ventricle (Paxinos & Watson, 1982). Rats so prepared were kept in individual cages and only those that showed liquor efflux were used for shock experiments, 5–7 days later.

The experiments were performed under ethylurethane anaesthesia (1.25 g $kg^{-1}$, i.p.). Urethane was chosen because it provides long-lasting and stable general anaesthesia with minimal interference with cardiovascular regulatory functions (Maggi & Meli, 1986a,b).

After heparinization (heparin sodium 600 iu $kg^{-1}$, i.v.), and clean dissection, polyethylene catheters were inserted into a common carotid artery and into an iliac vein. Systemic arterial pressure and pulse pressure (PP) were continuously recorded by means of a pressure transducer (P23 Db, Statham, Oxnard, CA, U.S.A.) connected to a polygraph (Battaglia-Rangoni, Bologna, Italy). Respiratory rate (RR) was recorded by means of three electrodes subcutaneously implanted in the chest and connected through a preamplifier (ARI A380, Battaglia-Rangoni, Bologna, Italy) to the polygraph. A severe volume-controlled haemorrhagic shock was produced by intermittent blood withdrawal from the venous catheter over a period of 25–30 min until mean arterial pressure (MAP), automatically calculated and continuously digitally displayed by the polygraph, decreased to and stabilized at 20 to 25 mmHg. The total bleeding volume was 2.22 ± 0.16 ml 100 $g^{-1}$ body wt ($n = 88$; mean ± s.e.mean).

### Drugs

ACTH-(1-24) and nicardipine hydrochloride were purchased from Sigma Chemical Co. (St. Louis, MO, U.S.A.); synthetic ω-conotoxin GVIA was obtained from Research Biomedicals Incorporated, (Natick, MA, U.S.A.), ketamine hydrochloride from Farmaceutici Gellini (Aprilia, Italy), xylazine hydrochloride from Bayer Italia (Milano, Italy), ethylurethane from Fluka AG (Buchs, Switzerland), and heparin sodium from Prodotti Gianni (Milano, Italy). The i.v. and i.p. injections were made in a volume of 0.1 ml 100 $g^{-1}$ body wt; those performed i.c.v. were in a volume of 5 μl/rat at the infusion rate of 1 μl 20 $s^{-1}$. Control animals received equal volumes of saline. Dosage rates refer to the salt. Animals were continuously monitored for 120 min after treatment, or until death.

### Experimental protocol

Animals were randomly assigned to one of the following treatments: (1) pretreatment with nicardipine i.v. (125–500 μg $kg^{-1}$); (2) pretreatment with nicardipine i.c.v. (3–12 μg $kg^{-1}$); (3) pretreatment with ω-conotoxin GVIA i.v. (5–10 μg $kg^{-1}$); (4) pretreatment with ω-conotoxin GVIA i.c.v. (0.015–0.06 μg $kg^{-1}$). The animals of all groups, after shock induction, were treated with ACTH-(1-24) at the dose of 160 μg $kg^{-1}$, i.v., chosen on the basis of previous dose-effect studies (Bertolini *et al.*, 1986a; 1989), or with saline.

### Statistics

MAP, PP and RR values of all groups were compared by 2-way ANOVA, separate comparisons being made for data obtained before bleeding, after bleeding and at intervals after treatment; in the case of after-treatment data, ANOVA was followed by Student-Newman-Keuls test. When appropriate, Student's *t* test for paired data was also used. Survival rates were analysed by Fisher's exact probability test.

## Results

Under our experimental conditions, the pretreatment baseline values of the recorded parameters (Figures 1–3) were similar (i.e. not significantly different) in all experimental groups. As previously described (Bertolini *et al.*, 1986a,b,c; 1989; Guarini *et al.*, 1989; 1990b), the acute hypovolaemia induced in our model of volume-controlled haemorrhagic shock in anaethetized rats was incompatible with survival, all saline-treated animals dying within 26 ± 3 min after treatment. On the other hand, and again in agreement with previous results (Bertolini *et al.*, 1986a,b,c; 1989; Guarini *et al.*, 1990a,b,c), the timely i.v. bolus injection of ACTH-(1-24) at a dose of 160 μg $kg^{-1}$ produced, within a few minutes, an impressive restoration of cardiovascular and respiratory functions (Figures 1–3). Although no other supportive treatment (blood, plasma, or other fluids infusion) was given, all ACTH-treated rats were still surviving at the end of the observation period (2 h after treatment), with MAP, PP and RR values (76 ± 5 mmHg, 41 ± 3 mmHg and 102 ± 9 breaths $min^{-1}$ respectively) not significantly different from basal, pre-bleeding values ($P > 0.05$, Student's *t* test for paired data).

As shown in Figures 1, 2 and 3, i.c.v. pretreatment with ω-conotoxin dose-dependently antagonized the effect of ACTH-(1-24) on MAP, PP, RR and survival of haemorrhage-shocked rats: 50% of the animals pretreated with 0.03 μg $kg^{-1}$ of ω-conotoxin and 75% of those pretreated with 0.06 μg $kg^{-1}$ died within the 2 h of observation (mean survival times: 38 ± 8 and 48 ± 7 min, respectively). In non-bled animals, the i.c.v. injection of the highest dose of ω-conotoxin (0.06 μg $kg^{-1}$, $n = 4$) produced a slight increase of MAP (+21 ± 3 mmHg), lasting about 30 min. Again in non-bled animals, the i.v. injection of ω-conotoxin at a dose of 5 μg $kg^{-1}$ ($n = 4$) produced a slight, not significant hypotension (MAP = − 10 ± 3 mmHg) ($n = 4$) lasting for the observation period (90 min).

In haemorrhage-shocked rats, the i.v. pretreatment with ω-conotoxin at a dose of 5 μg $kg^{-1}$ completely antagonized the effect of ACTH-(1-24), all rats dying within 60 min (rats pretreated with 10 μg $kg^{-1}$ i.v., died shortly after ACTH injection).

Neither i.c.v. nor i.v. pretreatment with ω-conotoxin significantly modified *per se* the outcome of shock in saline-treated animals (data not shown).

Figures 1, 2 and 3 also show that while the effect of ACTH-(1-24) in haemorrhagic shock was not influenced by i.c.v. pretreatment with nicardipine up to a dose of 12 μg $kg^{-1}$ (dose range: 3–12 μg $kg^{-1}$), it was antagonized by i.v. pretreatment with this drug, starting from a dose of 125 μg $kg^{-1}$; after a dose of 500 μg $kg^{-1}$, 75% of the animals died within the 2 h of observation (mean survival time: 43 ± 2 min).

None of the pretreatments with nicardipine significantly modified *per se* the outcome of shock in saline-treated animals (data not shown).

## Discussion

The present results show that the effect of ACTH-(1-24) on haemorrhagic shock is prevented by either the i.c.v. or i.v.

injection of ω-conotoxin, as well as by the i.v. (but not i.c.v.) injection of nicardipine.

ω-Conotoxin potently and persistently blocks the high voltage-operated neuronal calcium channels of the N-type (McCleskey *et al.*, 1987; Olivera *et al.*, 1987). On the other hand, nicardipine, like all calcium channel blockers of the dihydropyridine group, selectively blocks high voltage-operated calcium channels of the L-type (Godfraind *et al.*, 1986; Vanhoutte & Paoletti, 1987) and primarily causes direct arterial vasodilatation.

Several lines of evidence would now indicate that the most abundant $Ca^{2+}$ channels related to synaptic transmission in the mammalian brain are of the P-type (Mintz *et al.*, 1992; Llinás *et al.*, 1992); these channels are not blocked by ω-conotoxin, but by ω-Aga IVA. However, although ω-conotoxin appears to cause only a small reduction in the total amount of $Ca^{2+}$ influx in the CNS (Suskiw *et al.*, 1987; Lundy *et al.*, 1991), it potently inhibits the release of a number of neurotransmitters in the mammalian brain (Reynolds *et al.*, 1986; Dooley *et al.*, 1987; 1988; Lundy *et*

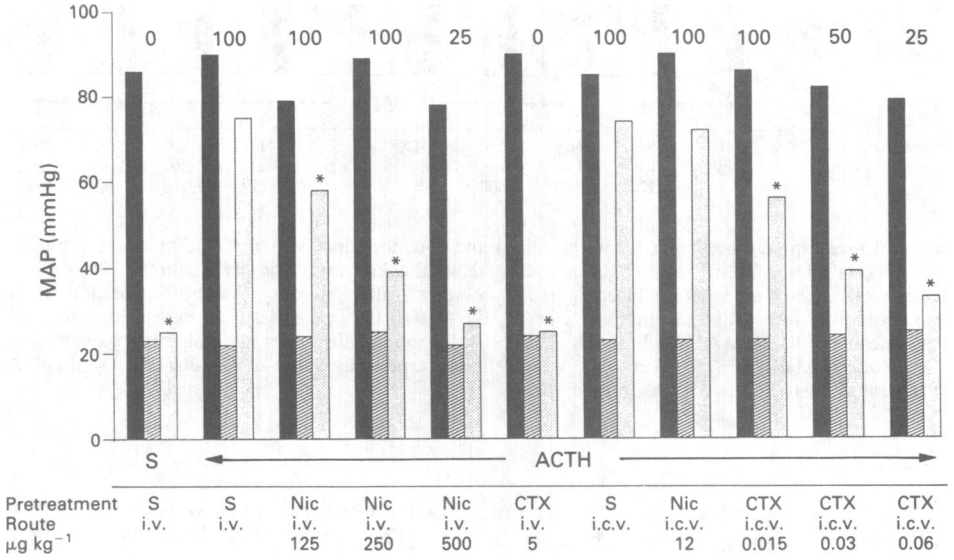



**Figure 1** Influence of nicardipine (Nic, 2 min before bleeding) and ω-conotoxin GVIA (CTX, 2 min before bleeding) on the effect of ACTH-(1-24) (ACTH) on mean arterial pressure (MAP) and survival rate in haemorrhage-shocked rats. Eight animals per group. Histogram heights indicate the MAP mean value before bleeding (solid columns), after bleeding (hatched columns) and 15–20 min after treatment (stippled columns) with saline (S, 1 ml $kg^{-1}$) or ACTH (160 μg $kg^{-1}$); s.e.mean not represented for the sake of clarity, was $<10\%$ of the mean in all cases. The figures above the histograms indicate the percentage survival 2 h after treatment. ANOVA of MAP values of all groups before and after bleeding gave $P$ values $>0.05$; after treatment gave $P$ values $<0.001$. $*P<0.05$, at least, versus the corresponding value of S-pretreated (1 ml $kg^{-1}$ i.v. or 5 μl/rat i.c.v.) and ACTH-treated rats (Student-Newman-Keuls test); comparisons between survival rates gave $P$ values $<0.05$ (50% survival), $<0.01$ (25% survival) and $<0.005$ (0% survival) (Fisher's test).

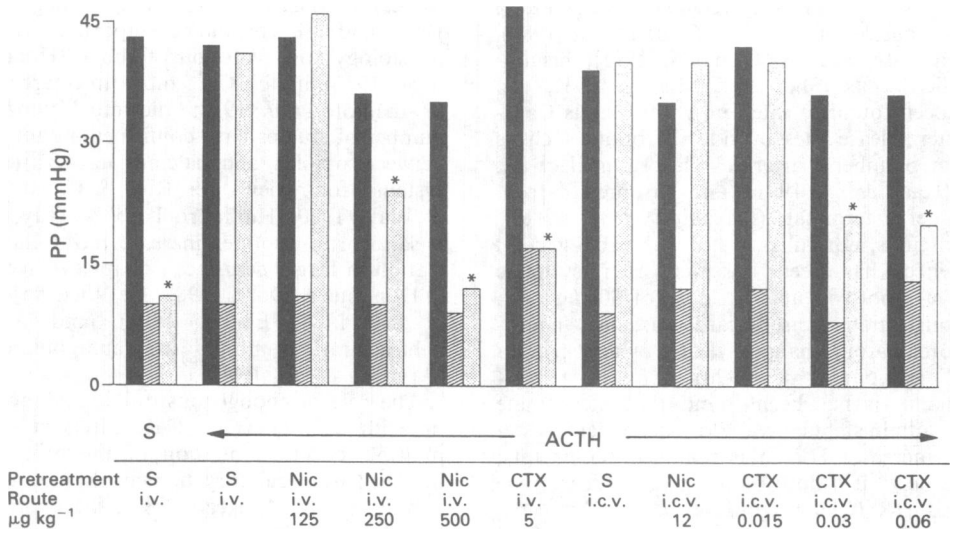



**Figure 2** Influence of nicardipine (Nic, 2 min before bleeding) and ω-conotoxin GVIA (CTX, 2 min before bleeding) on the effect of ACTH-(1-24) (ACTH) on pulse pressure (PP) in haemorrhage-shocked rats. The same animals as in Figure 1. Histogram heights indicate the PP mean value before bleeding (solid columns), after bleeding (hatched columns) and 15–20 min after treatment (stippled columns) with saline (S, 1 ml $kg^{-1}$) or ACTH (160 μg $kg^{-1}$); s.e.mean not represented for the sake of clarity, was $<10\%$ of the mean in all cases. ANOVA of PP values of all groups before and after bleeding gave $P$ values $>0.05$; after treatment gave $P$ values $<0.001$. $*P<0.001$ versus the corresponding value of S-pretreated (1 ml $kg^{-1}$, i.v. or 5 μl/rat, i.c.v.) and ACTH-treated rats (Student-Newman-Keuls test).

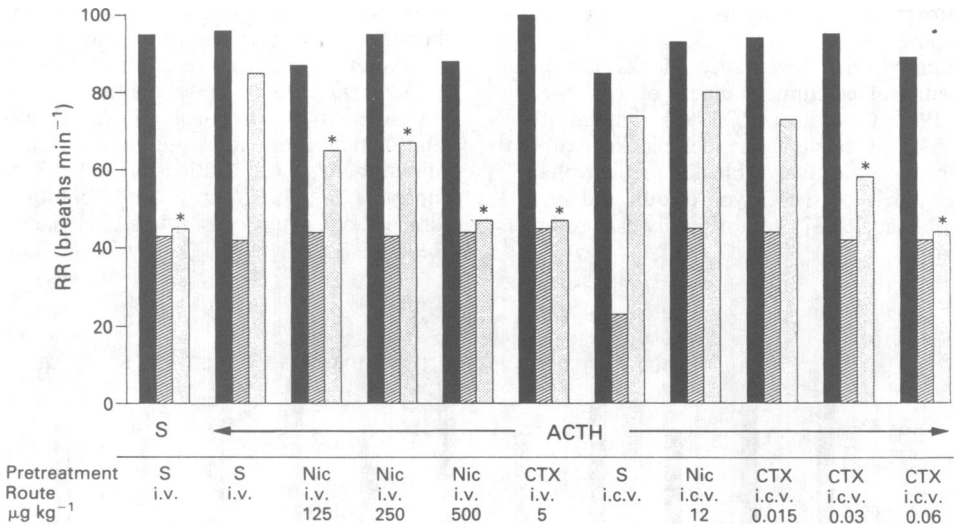



**Figure 3** Influence of nicardipine (Nic, 2 min before bleeding) and ω-conotoxin GVIA (CTX, 2 min before bleeding) on the effect of ACTH-(1-24) (ACTH) on respiratory rate (RR) in haemorrhage-shocked rats. The same animals as in Figure 1. Histogram heights indicate the RR mean value before bleeding (solid columns), after bleeding (hatched columns) and 15–20 min after treatment (stippled columns) with saline (S, 1 ml $kg^{-1}$) or ACTH (160 μg $kg^{-1}$); s.e.mean not represented for the sake of clarity, was $<10\%$ of the mean in all cases. ANOVA of RR values of all groups before and after bleeding gave $P$ values $>0.05$; after treatment gave $P$ values $<0.001$. $^*P<0.05$, at least, versus the corresponding value of S-pretreated (1 ml $kg^{-1}$, i.v., or 5 μl/rat, i.c.v.) and ACTH-treated rats (Student-Newman-Keuls test).

*al.*, 1991). Hence, it has been suggested that, particularly for brain acetylcholine, the release is mainly governed by a small proportion of strategically located N-type, ω-conotoxin-sensitive, calcium channels: the $N_B$ channels (Lundy *et al.*, 1991).

L-type $Ca^{2+}$ channels are found both in non-neuronal tissue (typically in arterial smooth muscle) and in the nervous system. Both neuronal and non-neuronal L-type channels are all sensitive to dihydropyridines, although the $\alpha_1$ subunit to which these drugs bind is somewhat different in the different tissues (for a review see: Sher *et al.*, 1991).

N-type $Ca^{2+}$ channels are highly expressed in the brain, but have also been found outside the central nervous system: mammalian peripheral nerve terminals (Lundy & Frew, 1988), frog neuromuscular junction (Koyano *et al.*, 1987), heart and skeletal muscle of chicken (Cruz *et al.*, 1987), adrenal chromaffin cells (Sher & Clementi, 1991), insulin-secreting pancreatic β-cells (Sher & Clementi, 1991), etc. ω-Conotoxin has been found to interfere with various $Ca^{2+}$-mediated transmitter release sites outside the brain, such as noradrenaline from peripheral arteries (Clasbrummel *et al.*, 1989) and heart (Haas *et al.*, 1991), and vasopressin from neurohypophysial nerve terminals (Dayanithi *et al.*, 1988).

However, in conscious, normal rats, no observable general or neurological effect has been observed after systemic administration of ω-conotoxin up to a dose of 300 μg $kg^{-1}$, while i.c.v. administration caused cardiovascular, neurological and thermoregulatory changes, clearly evident from a dose of 90 μg $kg^{-1}$ (Shapira *et al.*, 1990).

On the other hand, it has been found that nicardipine (10–300 μg $kg^{-1}$), administered i.v., dose-dependently decreases MAP and increases HR in normal, conscious rats; when administered i.c.v. at a dose of 10 μg $kg^{-1}$, nicardipine increases MAP and HR (Champerouz *et al.*, 1991).

Our present data, showing that the i.c.v. injection of ω-conotoxin dose-dependently prevents the ACTH-induced shock reversal, suggest that brain $Ca^{2+}$ channels of the N-type are importantly involved and strengthen the hypothesis that the mechanism of the ACTH-induced shock reversal may involve a neuronal link and, as the final step, the restoration of vascular tone, at least in certain vascular beds (Bertolini *et al.*, 1989). In fact, both the blockade of N-type calcium channels in or outside the CNS and the blockade of L-type calcium channels at the peripheral level largely prevent the effect of ACTH in haemorrhagic shock. The blockade of peripheral N-type calcium channels probably acts indirectly, possibly through the inhibition of noradrenaline release at the arteriolar level (Clasbrummel *et al.*, 1989), and the blockade of peripheral L-type calcium channels acts directly, preventing the contraction of arteriolar smooth muscle.

Our original idea (Bertolini *et al.*, 1986a,b,c) that the anti-shock effect of melanocortin peptides is a consequence of their being functional antagonists of opioids, is further supported by the present results. Indeed, opioid neuropeptides, which are massively released in shock conditions (Lang *et al.*, 1982; Farrell *et al.*, 1983; Elam *et al.*, 1984; Bernton *et al.*, 1985) and are considered important factors in the pathophysiology and evolution of shock (Holaday, 1983; Bernton *et al.*, 1985), inhibit $Ca^{2+}$ influx into target neurones and cells (Yamamoto *et al.*, 1978; Guerrero-Munoz *et al.*, 1979), and a number of studies have confirmed an antagonistic interaction between opioids and calcium in a variety of experimental systems (for reviews, see Ross & Cardenas, 1979; Chapman & Way, 1980; Huidobro-Toro & Way, 1983). Conversely, melanocortin peptides increase intracellular calcium concentration in target neurones (for reviews see: Jolles *et al.*, 1980; O'Donohue & Dorsa, 1982; De Wied & Jolles, 1982; Wiegant *et al.*, 1986; Eberle, 1988), and melanocortin-induced behavioural symptoms are antagonized by ω-conotoxin (Argiolas *et al.*, 1990).

The role of endogenous opioids in shock might be bound up with their effect on $Ca^{2+}$ fluxes at multiple levels, with multiple effects: inhibition of the firing of brain neurones involved in circulatory homeostasis (Korf *et al.*, 1974; Punnen *et al.*, 1984; Reis, 1987), inhibition of the release of noradrenaline from peripheral sympathetic terminals (Schadt & Gaddis, 1985; Morita *et al.*, 1988; Schadt, 1989) and of acetylcholine in the CNS (Duggan & North, 1983) and inhibition of excitation-contraction coupling in the arterioral muscle cells. The shock reversal induced by the administration of pharmacological amounts of melanocortin peptides might depend on their opposite effects on $Ca^{2+}$ fluxes, with consequently increased acetylcholine release in the CNS

(Versteeg, 1980; Botticelli & Wurtman, 1991), increased noradrenaline release both from central (Endröczi, 1976) and peripheral (Szabo *et al.*, 1987; 1989) sympathetic terminals, and with eventual restoration of vascular tone.

This work was supported in part by grants from Ministero dell'Università e della Ricerca Scientifica e Tecnologica and Consiglio Nazionale delle Ricerche, Roma.

## References


ARGIOLAS, A., MELIS, M.R., STANCAMPIANO, R. & GESSA, G.L. (1990). Role of calcium in the expression of ACTH-induced stretching, yawning and penile erection. *Brain Res. Bull.*, **24**, 853–856.

BERNTON, E.W., LONG, J.B. & HOLADAY, J.W. (1985). Opioids and neuropeptides: mechanisms in circulatory shock. *Fed. Proc.*, **44**, 290–299.

BERTOLINI, A., FERRARI, W. & GUARINI, S. (1989). The adrenocorticotropic hormone (ACTH)-induced reversal of hemorrhagic shock. *Resuscitation*, **18**, 253–267.

BERTOLINI, A., FERRARI, W., GUARINI, S. & TAGLIAVINI, S. (1990). Circulatory and respiratory consequences of massive hemorrhage are reversed by protoveratrines. *Experientia*, **46**, 704–708.

BERTOLINI, A., GUARINI, S. & FERRARI, W. (1986a). Adrenal-independent, anti-shock effect of ACTH-(1-24) in rats. *Eur. J. Pharmacol.*, **122**, 387–388.

BERTOLINI, A., GUARINI, S., FERRARI, W. & ROMPIANESI, E. (1986b). Adrenocorticotropin reversal of experimental hemorrhagic shock is antagonized by morphine. *Life Sci.*, **39**, 1271–1280.

BERTOLINI, A., GUARINI, S., FERRARI, W., NOERA, G., MASSINI, C. & DI TIZIO, S. (1987). ACTH-(1-24) restores blood pressure in acute hypovolaemia and haemorrhagic shock in humans. *Eur. J. Clin. Pharmacol.*, **32**, 537–538.

BERTOLINI, A., GUARINI, S., ROMPIANESI, E. & FERRARI, W. (1986c). α-MSH and other ACTH fragments improve cardiovascular function and survival in experimental hemorrhagic shock. *Eur. J. Pharmacol.*, **130**, 19–26.

BOTTICELLI, L.J. & WURTMAN, R.J. (1981). Corticotropin regulates transsynaptically the activity of septo-hippocampal cholinergic neurons. *Nature*, **289**, 75–76.

BREZENOFF, H.E. (1972). Cardiovascular responses to intrahypothalamic injections of carbachol and certain cholinesterase inhibitors. *Neuropharmacology*, **11**, 637–644.

BREZENOFF, H.E. & GIULIANO, R. (1982). Cardiovascular control by cholinergic mechanisms in the central nervous system. *Ann. Rev. Pharmacol. Toxicol.*, **22**, 341–381.

BREZENOFF, H.E. & JENDEN, D.J. (1969). Modification of arterial blood pressure in rats following microinjection of drugs into the posterior hypothalamus. *Neuropharmacology*, **8**, 593–600.

CHAMPEROUX, P., LACOLLEY, P., LAURENT, S., BRISAC, A.M. & SAFAR, M. (1991). Central hypotensive effects of nicardipine in conscious freely moving spontaneously hypertensive rats. *Clin. Exp. Hyp.*, **13**, 669–676.

CHAPMAN, D.B. & WAY, E.L. (1980). Metal ion interactions with opiates. *Annu. Rev. Pharmacol. Toxicol.*, **20**, 553–579.

CLASBRUMMEL, B., OSSWALD, H. & ILLES, P. (1989). Inhibition of noradrenaline release by ω-conotoxin GVIA in the rat tail artery. *Br. J. Pharmacol.*, **96**, 101–110.

CRUZ, L.J., JOHNSON, D.S. & OLIVERA, B.M. (1987). Characterization of the ω-conotoxin target. Evidence for tissue-specific heterogeneity in calcium channel types. *Biochemistry*, **26**, 820–824.

DAYANITHI, G., MARTIN-MOUTOT, N., BARLIER, S., COLIN, D.A., KRETZ-ZAEPFEL, M., COURAUD, F. & NORDMANN, J.J. (1988). The calcium channel antagonist ω-conotoxin inhibits secretion from peptidergic nerve terminals. *Biochem. Biophys. Res. Commun.*, **156**, 255–262.

DE WIED, D. & JOLLES, J. (1982). Neuropeptides derived from pro-opiocortin: behavioral, physiological and neurochemical effects. *Physiol. Rev.*, **62**, 976–1059.

DIRNHUBER, P. & CULLUMBINE, H. (1955). The effect of anticholinesterase agents on the rat's blood pressure. *Br. J. Pharmacol. Chemother.*, **10**, 12–15.

DOOLEY, D.J., LUPP, A. & HERTTING, G. (1987). Inhibition of central neurotransmitter release by ω-conotoxin GVIA, a peptide modulator of the N-type voltage-sensitive calcium channel. *Naunyn-Schmiedebergs Arch. Pharmacol.*, **336**, 467–470.

DOOLEY, D.J., LUPP, A., HERTTING, G. & OSSWALD, H. (1988). ω-Conotoxin GVIA and pharmacological modulation of hippocampal noradrenaline release. *Eur. J. Pharmacol.*, **148**, 261–267.

DUGGAN, A.W. & NORTH, R.A. (1983). Electrophysiology of opioids. *Pharmacol. Rev.*, **35**, 219–281.

EBERLE, A.N. (1988). *The Melanotropins*. Basel: Karger.

ELAM, R., BERGMANN, F. & FEUERSTEIN, G. (1984). Simultaneous changes of catecholamines and Leu-enkephalin-like immunoreactivity in plasma and cerebrospinal fluid of cats undergoing acute hemorrhage. *Brain. Res.*, **303**, 313–317.

ENDRÖCZI, E. (1976). Effect of $ACTH_{1-24}$ and $ACTH_{4-10}$ on the distribution of $^3$H-noradrenaline in the brain of adrenalectomized rats. *Acta Physiol. Acad. Sci. Hung.*, **48**, 59–64.

FARRELL, L.D., HARRISON, T.S. & DEMERS, L.M. (1983). Immunoreactive metenkephalin in the canine adrenal: response to acute hypovolemic stress. *Proc. Soc. Exp. Biol. Med.*, **173**, 515–518.

GODFRAIND, T., MILLER, R. & WIBO, M. (1986). Calcium antagonism and calcium entry blockade. *Pharmacol. Rev.*, **38**, 321–416.

GUARINI, S., BAZZANI, C., TAGLIAVINI, S. & BERTOLINI, A. (1991). Nuovi aspetti del trattamento farmacologico dello shock: evidenze sperimentali. In *Atti del Convegno Nazionale Monitoraggio in Anestesia e in Terapia Intensiva*. ed. Grana, G., Stacca, R. & Barbieri, A. pp. 603–608. Modena: Mucchi.

GUARINI, S., FERRARI, W. & BERTOLINI, A. (1988). Involvement of the sympathetic nervous system in the cardiovascular effects of ACTH-(1-24) during hemorrhagic shock in rats. *Naunyn-Schmiedebergs Arch. Pharmacol.*, **337**, 556–560.

GUARINI, S., ROMPIANESI, E., FERRARI, W. & BERTOLINI, A. (1986). Influence of vagotomy and of atropine on the anti-shock effect of adrenocorticotropin. *Neuropeptides*, **8**, 19–24.

GUARINI, S., TAGLIAVINI, S., BAZZANI, C., FERRANTE, F. & BERTOLINI, A. (1990a). Intracerebroventricular injection of hemicholinium-3 prevents the ACTH-induced, but not the physostigmine-induced, reversal of hemorrhagic shock in rats. *Pharmacology*, **40**, 85–89.

GUARINI, S., TAGLIAVINI, S., BAZZANI, C., FERRARI, W. & BERTOLINI, A. (1990b). Early treatment with ACTH-(1-24) in a rat model of hemorrhagic shock prolongs survival and extends the time-limit for blood reinfusion to be effective. *Crit. Care Med.*, **18**, 862–865.

GUARINI, S., TAGLIAVINI, S., BAZZANI, C., PASINI, M. & BERTOLINI, A. (1990c). Brain $M_3$ muscarinic receptors are involved in the ACTH-induced reversal of hemorrhagic shock. *Naunyn-Schmiedebergs Arch. Pharmacol.*, **342**, 36–39.

GUARINI, S., TAGLIAVINI, S., FERRARI, W. & BERTOLINI, A. (1989). Reversal of haemorrhagic shock in rats by cholinomimetic drugs. *Br. J. Pharmacol.*, **98**, 218–224.

GUERRERO-MUNOZ, F., GUERRERO, M.L., WAY, E.L. & LI, C.H. (1979). Effect of β-endorphin on calcium uptake in the brain. *Science*, **206**, 89–91.

HAASS, M., RICHARDT, G., BRENN, T., SCHÖMIG, E. & SCHÖMIG, A. (1991). Nicotine-induced release of noradrenaline and neuropeptide Y in guinea-pig heart: role of calcium channels and protein kinase C. *Naunyn-Schmiedebergs Arch. Pharmacol.*, **344**, 527–531.

HOLADAY, J.W. (1983). Cardiovascular effects of endogenous opiate systems. *Annu. Rev. Pharmacol. Toxicol.*, **23**, 541–594.

HUIDOBRO-TORO, J.P. & WAY, E.L. (1983). Opiates. In *Psychopharmacology*. Part 1: *Preclinical Psychopharmacology*, ed. Grahame-Smith, D.G. & Cowen, P.J. pp. 300–343. Amsterdam, Oxford, Princeton: Excerpta Medica.

IYODA, I., TAKAHASHI, H., LEE, L.C., KAMBARA, S., OKAJIMA, H., SASAKI, S., TAKEDA, K., YOSHIMURA, M. & IJICHI, H. (1986). Centrally induced cardiovascular and sympathetic responses to adrenocorticotrophic hormone. *Cardiovasc. Res.*, **20**, 778–782.

JANOWSKY, D.S., RISCH, S.C., KENNEDY, B., ZIEGLER, M. & HUEY, L. (1986). Central muscarinic effects of physostigmine on mood, cardiovascular function, pituitary and adrenal neuroendocrine release. *Psychopharmacology*, **89**, 150–154.

JOLLES, J., ZWIERS, H., VAN DONGEN, C.J., SCHOTMAN, P., WIRTZ, K.W.A. & GISPEN, W.H. (1980). Modulation of polyphosphoinositide metabolism by ACTH-sensitive protein phosphorylation. *Nature*, **286**, 623–625.

KORF, J., BUNNEY, B.S. & AGHAJANIAN, G.K. (1974). Noradrenergic neurons: morphine inhibition of spontaneous activity. *Eur. J. Pharmacol.*, **25**, 165–169.

KOYANO, K., ABE, T., NISHIUCHI, Y. & SAKAKIBARA, S. (1987). Effects of synthetic ω-conotoxin on synaptic transmission. *Eur. J. Pharmacol.*, **135**, 337–343.

LANG, R.E., BRUCKNER, U.B., HERMANN, K., KEMPF, B., RASCHER, W., STURM, V., UNGER, TH. & GANTEN, D. (1982). Effect of hemorrhagic shock on the concomitant release of endorphin and enkephalin-like peptides from the pituitary and adrenal glands in the dog. *Adv. Biochem. Psychopharmacol.*, **33**, 363–368.

LLINÁS, R., SUGIMORI, M., HILLMAN, D.E. & CHERKSEY, B. (1992). Distribution and functional significance of the P-type, voltage-dependent $Ca^{2+}$ channels in the mammalian central nervous system. *Trends Neurosci.*, **15**, 351–355.

LUNDY, P.M. & FREW, R. (1988). Evidence of ω-conotoxin GVIA sensitive $Ca^{2+}$ channels in mammalian peripheral nerve terminals. *Eur. J. Pharmacol.*, **156**, 325–330.

LUNDY, P.M., FREW, R., FULLER, T.W. & HAMILTON, M.G. (1991). Pharmacological evidence for an ω-conotoxin, dihydropyridine-insensitive neuronal $Ca^{++}$ channel. *Eur. J. Pharmacol. Mol. Pharmacol.*, **206**, 61–68.

MAGGI, C.A. & MELI, A. (1986a). Suitability of urethane anesthesia for physiopharmacological investigations in various systems. Part 1: General considerations. *Experienta*, **42**, 109–114.

MAGGI, C.A. & MELI, A. (1986b). Suitability of urethane anesthesia for physiopharmacological investigations in various systems. Part 2: Cardiovascular system. *Experienta*, **42**, 292–297.

MCCLESKEY, E.W., FOX, A.P., FELDMAN, D.H., CRUZ, L.J., OLIVERA, B.M., TSIEN, R.W. & YOSHIKAMI, D. (1987). ω-Conotoxin: direct and persistent blockade of specific types of calcium channels in neurons but not muscle. *Proc. Natl. Acad. Sci. U.S.A.*, **84**, 4327–4331.

MEDACOVIĆ, M. & VARAGIĆ, V. (1957). The effect of eserine and neostigmine on the blood pressure of conscious rats. *Br. J. Pharmacol. Chemother.*, **12**, 24–27.

MINTZ, I.M., VENEMA, V.J., SWIDEREK, K.M., LEE, T.D., BEAN, B.P. & ADAMS, M.E. (1992). P-type calcium channels blocked by the spider toxin ω-AGA-IVA. *Nature*, **355**, 827–829.

MOGUL, D.J. & FOX, A.P. (1991). Evidence for multiple types of $Ca^{2+}$ channels in acutely isolated hippocampal Ca3 neurones of the guinea-pig. *J. Physiol.*, **433**, 259–281.

MORITA, H., NISHIDA, Y., MOTOCHIGAWA, H., UEMURA, N., HOSOMI, H. & VATNER, S.F. (1988). Opiate receptor-mediated decrease in renal nerve activity during hypotensive hemorrhage in conscious rabbits. *Circ. Res.*, **63**, 165–172.

NOERA, G., ANGIELLO, L., BIAGI, B. & PENSA, P. (1991). Haemorrhagic shock in cardiac surgery. Pharmacological treatment with ACTH (1-24). *Resuscitation*, **22**, 123–127.

NOERA, G., PENSA, P., GUELFI, P., BIAGI, B., CURCIO, C. & BENTINI, B. (1989). ACTH-(1-24) and hemorrhagic shock: preliminary clinical results. *Resuscitation*, **18**, 145–147.

O'DONOHUE, T.L. & DORSA, D.M. (1982). The opiomelanotropinergic neuronal and endocrine systems. *Peptides*, **3**, 353–395.

OLIVERA, B.M., CRUZ, L.J., DE SANTOS, V., LECHEMINANT, G.W., GRIFFIN, D., ZEIKUS, R., MCINTOSH, J.M., GALYEAN, R., VARGA, J., GRAY, W.R. & RIVIER, J. (1987). Neuronal calcium channel antagonists. Discrimination between calcium channel subtypes using ω-conotoxin from *Conus magus* venom. *Biochemistry*, **26**, 2086–2090.

PAXINOS, G. & WATSON, C. (1982). *The Rat Brain in Stereotaxic Coordinates*. New York: Academic Press.

PINELLI, G., CHESI, G., DI DONATO, C., REVERZANI, A. & MARANI, L. (1989). Preliminary data on the use of ACTH-(1-24) in human shock conditions. *Resuscitation*, **18**, 149–150.

PUNNEN, S., WILLETTE, R.N., KRIEGER, A.J. & SAPRU, H.N. (1984). Cardiovascular response to injections of enkephalin in the pressor area of the ventrolateral medulla. *Neuropharmacology*, **23**, 939–946.

REIS, D.J. (1987). Neurotransmitters acting in the C1 area in the tonic and reflex control of blood pressure. *J. Cardiovasc. Pharmacol.*, **10**, suppl. 12, S22–S25.

REYNOLDS, I.J., WAGNER, J.A., SNYDER, S.H., THAYER, S.A., OLIVERA, B.M. & MILLER, R.J. (1986). Brain voltage-sensitive calcium channel subtypes differentiated by ω-conotoxin GVIA. *Proc. Natl. Acad. Sci. U.S.A.*, **83**, 8804–8807.

ROSS, D.H. & CARDENAS, H.L. (1979). Nerve cell calcium as a messenger for opiate and endorphin actions. *Adv. Biochem. Psychopharmacol.*, **20**, 301–336.

SCHADT, J.C. (1989). Sympathetic and hemodynamic adjustments to hemorrhage: a possible role for endogenous opioid peptides. *Resuscitation*, **18**, 219–228.

SCHADT, J.C. & GADDIS, R.R. (1985). Endogenous opiate peptides may limit norepinephrine release during hemorrhage. *J. Pharmacol. Exp. Ther.*, **232**, 656–660.

SHAPIRA, S., ADEYEMO, O.M. & FEUERSTEIN, G. (1990). Integrated autonomic and behavioral responses to L/N $Ca^{2+}$-channel blocker ω-conotoxin in conscious rats. *Am. J. Physiol.*, **259**, R427–R438.

SHER, E., BIANCARDI, E., PASSAFARO, M. & CLEMENTI, F. (1991). Physiopathology of neuronal voltage-operated calcium channels. *FASEB J.*, **5**, 2677–2683.

SHER, E. & CLEMENTI, F. (1991). ω-Conotoxin-sensitive voltage-operated calcium channels in vertebrate cells. *Neuroscience*, **42**, 301–307.

SNUTCH, T.P., LEONARD, J.P., GILBERT, M.M., LESTER, H.A. & DAVIDSON, N. (1990). Rat brain expresses a heterogeneous family of calcium channels. *Proc. Natl. Acad. Sci. U.S.A.*, **87**, 3391–3395.

STARR, T.V.B., PRYSTAY, W. & SNUTCH, T.P. (1991). Primary structure of a calcium channel that is highly expressed in the rat cerebellum. *Proc. Natl. Acad. Sci. U.S.A.*, **88**, 5621–5625.

SUSZKIW, J.B., MURAWSKY, M.M. & FORTNER, R.C. (1987). Heterogeneity of presynaptic calcium channels revealed by species differences in the sensitivity of synaptosomal $^{45}Ca$ entry to omega conotoxin. *Biochem. Biophys. Res. Commun.*, **145**, 1283–1286.

SZABO, B., HEDLER, L. & STARKE, K. (1989). Facilitation of the release of noradrenaline: an extra-adrenal effect of adrenocorticotropic hormone. *Resuscitation*, **18**, 229–242.

SZABO, B., HEDLER, L., LICHTWALD, K. & STARKE, K. (1987). ACTH increases noradrenaline release in pithed rabbits with electrically stimulated sympathetic outflow. *Eur. J. Pharmacol.*, **136**, 391–399.

VANHOUTTE, P.M. & PAOLETTI, R. (1987). The WHO classification of calcium antagonists. *Trends Pharmacol. Sci.*, **8**, 4–5.

VARAGIĆ, V. (1955). The action of eserine on the blood pressure of the rat. *Br. J. Pharmacol. Chemother.*, **10**, 349–353.

VERSTEEG, D.H.G. (1980). Interaction of peptides related to ACTH, MSH and β-LPH with neurotransmitters in the brain. *Pharmacol. Ther.*, **11**, 535–557.

WIEGANT, V.M., VERHAAGEN, J., ALOYO, V. & GISPEN, W.H. (1986). ACTH and signal transduction in the neuronal membrane. In *Central Actions of ACTH and Related Peptides*. Symposia in neuroscience. ed. De Wied, D. & Ferrari, W. vol. 4, pp. 79–92. Padova-Berlin: Liviana Press-Springer Verlag.

YAMAMOTO, H., HARRIS, R.A., LOH, H.H. & WAY, E.L. (1978). Effects of acute and chronic morphine treatments on calcium localization and binding in brain. *J. Pharmacol. Exp. Ther.*, **205**, 255–264.

*(Received May 21, 1992*
*Revised December 24, 1992*
*Accepted February 22, 1993)*

*Br. J. Pharmacol.* (1993), **109**, 651–654 © Macmillan Press Ltd, 1993

# Effect of delayed weaning on opioid receptor control of swim stress-induced antinociception in the developing rat

Bala Y. Muhammad & [1]Ian Kitchen

Receptors and Cellular Regulation Research Group, School of Biological Sciences, University of Surrey, Guildford, Surrey GU2 5XH

**1** The opioid type of swim-stress induced antinociception (SIA) is mediated via μ-sites in preweanling rats and predominantly by δ-sites in postweanling animals. We have studied the effect of delay of weaning on the receptor transition of this behaviour in the developing rat.

**2** Litters were weaned normally at day 21 or allowed to remain with their mothers until assessment of swim SIA. Animals were stressed by warm water (20°C) swimming for 3 min periods and antinociception assessed by the tail immersion test (50°C).

**3** Naloxone (10 mg $kg^{-1}$) partially reversed swim SIA in both 25 day old weaned and non-weaned rats.

**4** Naltrindole (1 mg $kg^{-1}$) partially reversed swim SIA in 25 day old weaned rats but had no effect in non-weaned animals. Naltrindole (5 mg $kg^{-1}$) completely abolished swim SIA in weaned rats but was without effect in non-weaned groups. Antinociceptive responses to the μ-agonist, alfentanil (60 μg $kg^{-1}$) were unaffected by naltrindole at 1 mg $kg^{-1}$ but were partially reversed at 5 mg $kg^{-1}$.

**5** In 30 day old non-weaned rats, naltrindole (5 mg $kg^{-1}$) abolished the swim SIA.

**6** In conclusion, transition from μ- to δ-receptor control of swim SIA in rat pups can be delayed by between 5 and 10 days by delay of weaning. The environmental stimulus of weaning can activate opioid receptor subtype operation of biological responses in the developing animal.

**Keywords:** Stress-induced antinociception; weaning; opioid receptors; naltrindole; naloxone; ontogeny; development; neonate

## Introduction

Stress-induced analgesia in man and its experimental animal counterpart, stress-induced antinociception (SIA), are adaptive physiological responses that have been well characterized in the adult. Dependent on the environmental stimulus it can be divided into opioid and non-opioid types (on the basis of reversal with naloxone or naloxone insensitivity respectively) and further subclassified as neural (and independent of the hypothalamic-pituitary-adrenal (HPA) axis) or hormonal, dependent on HPA functioning (see Watkins & Meyer, 1982; Bodnar, 1990). Recently, we reported that SIA can also be observed in young rats in response to warm water (20°C) swimming (Jackson & Kitchen, 1989). Long periods of swimming (10 min) produce a naloxone-insensitive, non-opioid form of SIA which is not evident until postnatal day 25 and independent of the HPA axis (Jackson & Kitchen, 1989). Shorter swims (3 min) produced an opioid type of SIA which is dependent on the HPA axis (Jackson & Kitchen, 1989) and with the use of swimming aids can be observed as early as postnatal day 10 (Muhammad & Kitchen, 1992).

We have shown previously that the opioid receptor subtype which operates the opioid form of SIA differs in the neonate in comparison with the adult. Evidence from studies with naloxone and the δ-selective antagonists ICI,17864 and naltrindole show that up to postnatal day 20, swim SIA is mediated by μ-receptors but by day 25, it is predominantly δ-sites which operate this behaviour (Jackson & Kitchen, 1989; Kitchen & Pinker, 1990). The mechanisms underlying this receptor transition remain to be elucidated and we have now considered the possibility that the behavioural stimulus of weaning (at day 21) might be an important factor in the change. We report here, that weaning is a critical element in initiating the transition from μ- to δ- opioid receptor operation of swim SIA and that delay of weaning can temporarily delay this event.

[1] Author for correspondence.

## Methods

### *Animal and experimental conditions*

Wistar albino rats (University of Surrey strain) of either sex were used and maintained in litters of eight pups (where possible cross-fostered at birth) and allowed free access to water and rat chow. In groups where animals were weaned this was carried out at day 21 and the young rats continued to be housed in groups of eight without their mother. In groups where animals were not weaned, the mother remained with the litter at all times except during drug administration, swimming and nociceptive testing. Weaned and non-weaned animals of 25 and 30 days of age were studied. All rats were maintained at 21 ± 1°C in a constant 12 h light dark cycle (lights on at 07 h 00 min) and experimental procedures were carried out in a quiet, windowless, air-controlled laboratory. All procedures were carried out between 11 h 00 min and 16 h 00 min to minimize diurnal variation in nociceptive responses.

### *Swim stress procedures and nociceptive testing*

Animals were divided into treatment groups so that nociceptive testing took place for saline and drug-treated rats on two or three separate days to minimize interday and interlitter variation. Nociceptive responses were recorded immediately before drug administration by use of the tail immersion test at 50°C as previously described (Janssen *et al.*, 1963; Kitchen *et al.*, 1984). Opioid receptor antagonists (naloxone or naltrindole) were administered in 0.9% saline i.p. in dose volumes no greater than 0.2 ml, 10 min before swimming stress. Animals were stressed by placing them individually in a plastic water tank (29 × 22 × 28 cm deep) containing water at 20 ± 1°C for a period of 3 min as previously described for young rats (Jackson & Kitchen, 1989). At the end of the swimming period, rats were removed from the water, dried and returned to the home cage before subsequent nociceptive testing. Tail immersion responses were measured at 1, 5, 10, 15 and 30 min following swimming stress. In some studies the μ-receptor agonist, alfentanil, was administered 10 min after

administration of naltrindole and nociceptive responses assessed (without swim stress) at 2, 5, 10 and 15 min after alfentanil.

### *Drugs and statistical procedures*

Alfentanil and naloxone were gifts from Janssen Pharmaceuticals and Du Pont respectively. Naltrindole was purchased from Research Biochemicals Incorporated. Nociceptive treatment groups were compared using repeated measures ANOVA and *post hoc* comparisons made by Duncans Multiple Range Test using the SUPERANOVA software package for the Macintosh.

## Results

Naloxone (10 mg $kg^{-1}$) and naltrindole (1 or 5 mg $kg^{-1}$) had no significant effect on nociceptive latencies in unstressed 25 day old animals from either weaned or non-weaned groups (Figures 1–3).

The magnitude of SIA in response to swimming was similar in both weaned and non-weaned groups (latency 5–7 s; Figures 1–3). Naloxone at a dose of 1 mg $kg^{-1}$ did not significantly alter swim SIA in 25 day old weaned or non-weaned animals (data not shown). In 25 day old rats naloxone at 10 mg $kg^{-1}$ significantly attenuated swim SIA in weaned and non-weaned animals (Figure 1). In contrast, naltrindole (1 mg $kg^{-1}$) had no effect on swim SIA in 25 day old non-weaned groups (Figure 2) but in weaned animals naltrindole partially and significantly attenuated SIA. In 25 day old rats treated with 5 mg $kg^{-1}$ naltrindole, swim SIA was totally abolished in weaned animals but unaffected in non-weaned rats. In 30 day old non-weaned rats, naltrindole (5 mg $kg^{-1}$) abolished the swim SIA (Figure 4).

Antinociceptive responses to the $\mu$-agonist, alfentanil, in 25 day old rats were unaffected by naltrindole at 1 mg $kg^{-1}$ (data not shown) but were partially and significantly antagonized by naltrindole at 5 mg $kg^{-1}$ (Figure 5).

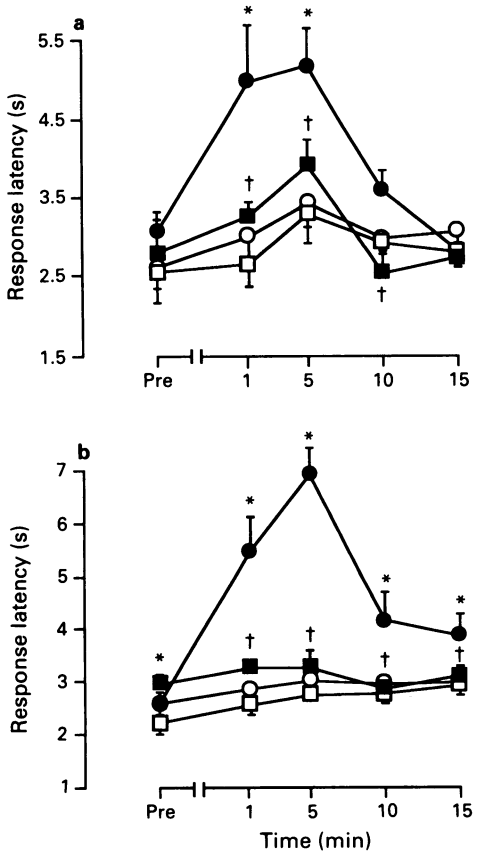



**Figure 1** Effect of naloxone (10 mg $kg^{-1}$) on antinociception induced by a 3 min swim in (a) 25 day old weaned and (b) 25 day old non-weaned rats. Values represent means with s.e.mean for groups of 6–8 animals. (○) Saline-injected, unstressed; (●) saline-injected, swim-stressed; (□) naloxone 10 mg $kg^{-1}$, unstressed; (■) naloxone 10 mg $kg^{-1}$ stressed. Pre = pretest responses 10 min before swim stress. Responses at 30 min were equivalent to those at 15 min and are omitted for clarity of presentation. $*P < 0.05$ swim stressed vs appropriate unstressed control; $\dagger P < 0.05$ saline-treated, swim-stressed vs naloxone-treated swim-stressed.

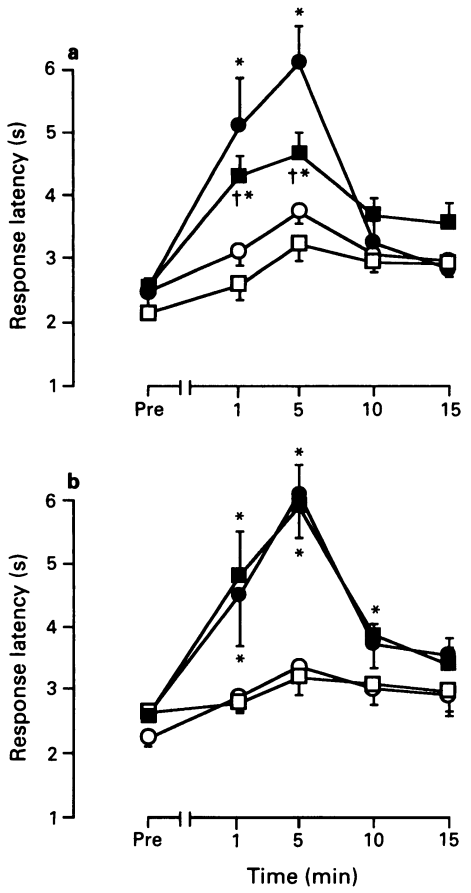



**Figure 2** Effect of naltrindole (1 mg $kg^{-1}$) on antinociception induced by a 3 min swim in (a) 25 day old weaned and (b) 25 day old non-weaned rats. Values represent means with s.e.mean for groups of 6–8 animals. (○) Saline-injected, unstressed; (●) saline-injected swim-stressed; (□) naltrindole 1 mg $kg^{-1}$, unstressed; (■) naltrindole 1 mg $kg^{-1}$ stressed. Pre = pretest responses 10 min before swim stress. Responses at 30 min were equivalent to those at 15 min and are omitted for clarity of presentation. $*P < 0.05$ swim stressed vs appropriate unstressed control; $\dagger P < 0.05$ saline-treated, swim-stressed vs naloxone-treated swim-stressed.

## Discussion

In common with our previous findings in weaned animals, swim SIA in 25 day old rats is partially reversed by both naltrindole (1 mg $kg^{-1}$) and by naloxone (10 mg $kg^{-1}$) (Jackson & Kitchen, 1989; Kitchen & Pinker, 1990). This dose of naltrindole is selective for antagonism of $\delta$-sites at this age (Kitchen & Pinker, 1990; Crook *et al.*, 1992) and naloxone at this dose has blocking activity at both $\mu$- and $\delta$-opioid receptors (Paterson *et al.*, 1983; James & Goldstein, 1984). Antagonism of SIA by naloxone could therefore be ascribed to $\mu$- or $\delta$-receptor blockade or to a mixture of antagonism at

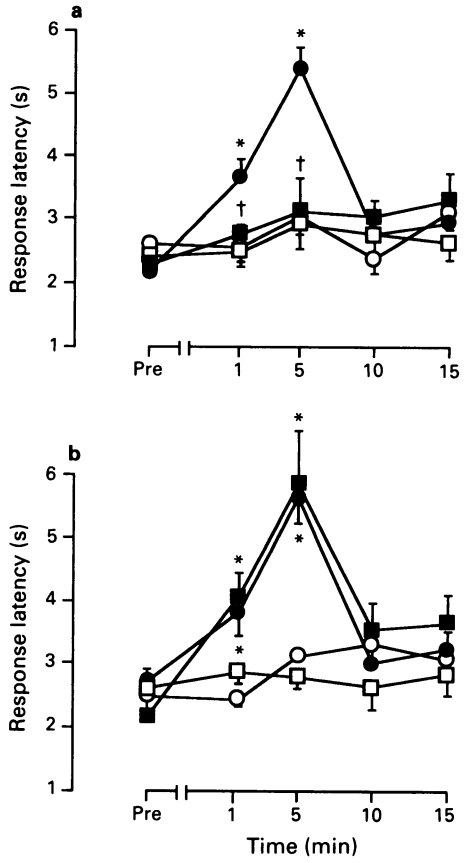



**Figure 3** Effect of naltrindole (5 mg kg$^{-1}$) on antinociception induced by a 3 min swim in (a) 25 day old weaned and (b) 25 day old non-weaned rats. Values represent means with s.e.mean for groups of 6–8 animals. (○) Saline-injected, unstressed; (●) saline-injected swim-stressed; (□) naltrindole 5 mg kg$^{-1}$, unstressed; (■) naltrindole 5 mg kg$^{-1}$ stressed. Pre = pretest responses 10 min before swim stress. Responses at 30 min were equivalent to those at 15 min and are omitted for clarity of presentation. *$P < 0.05$ swim-stressed vs appropriate unstressed control; †$P < 0.05$ saline-treated, swim-stressed vs naloxone-treated swim-stressed.

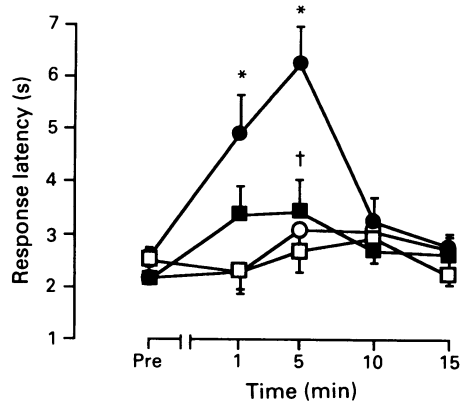



**Figure 4** Effect of naltrindole (5 mg kg$^{-1}$) on antinociception induced by a 3 min swim in 30 day old non-weaned rats. Values represent means with s.e.mean for groups of 6–8 animals. (○) Saline-injected, unstressed; (●) saline-injected swim-stressed; (□) naltrindole 5 mg kg$^{-1}$, unstressed; (■) naltrindole 5 mg kg$^{-1}$ stressed. Pre = pretest responses 10 min before swim stress. Responses at 30 min were equivalent to those at 15 min and are omitted for clarity of presentation. *$P < 0.05$ swim-stressed vs appropriate unstressed control; †$P < 0.05$ saline-treated, swim-stressed vs naloxone-treated swim-stressed.

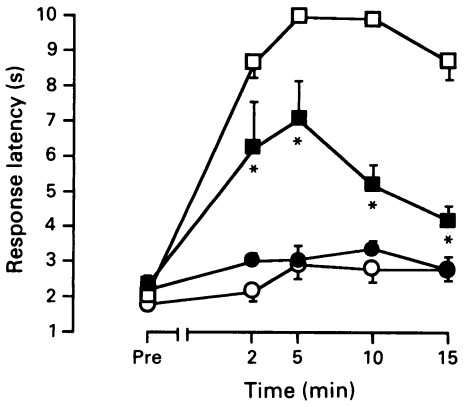



**Figure 5** Effect of naltrindole (5 mg kg$^{-1}$) on antinociception induced by alfentanil (60 μg kg$^{-1}$). Values represent means with s.e.mean of 6 animals. (○) Saline-injected; (●) naltrindole alone (5 mg kg$^{-1}$); (□) alfentanil alone (60 μg kg$^{-1}$); (■) alfentanil (60 μg kg$^{-1}$) + naltrindole (5 mg kg$^{-1}$). Pre = pretest responses 10 min before alfentanil administration. *$P < 0.05$ alfentanil vs alfentanil + naltrindole.

both sites. The complete reversal of swim SIA by naltrindole at 5 mg kg$^{-1}$ in weaned animals might suggest that δ-sites exclusively mediate this response but at this dose naltrindole may have some μ-antagonist activity (Figure 5) and it is therefore consistent with our previous proposal that both δ- and to some degree μ-sites are involved in swim SIA at day 25 (Jackson & Kitchen, 1989; Kitchen & Pinker, 1990).

The complete reversal of swim SIA by naloxone (10 mg kg$^{-1}$) in non-weaned animals points to opioid receptor mediation but it is clearly not δ-receptors that are operative, as naltrindole is without effect at either 1 or 5 mg kg$^{-1}$. The profile of sensitivity to these antagonists is consistent with the profile observed in 20 day old preweanling animals where the evidence points to the μ-receptor mediating swim SIA (Jackson & Kitchen, 1989). It therefore seems probable that delaying weaning delays the transition from μ- to δ-receptor operation of this behaviour. It is not possible to discount totally a contribution from κ-sites to warm-water swim SIA in non-weaned animals but as previous studies have failed to show κ-receptor involvement in this behaviour in both mice and rats (Hart *et al.*, 1983; Jackson & Kitchen, 1989) this seems unlikely. It should be noted however that levels of dynorphin in the CNS are not affected by restraint stress (Morley *et al.*, 1982) but can be shown to be decreased in response to cold water swim stress (Vaswani *et al.*, 1988). As dynorphin is recognized as an endogenous ligand for the κ-receptor (Chavkin *et al.*, 1982) a contribution of κ-sites to some types of SIA remains a possibility (Panerai *et al.*, 1984).

At the normal age of weaning (21 days) around 75% of the total adult complement of δ-sites are developed in the brain whilst μ- and κ-sites are fully mature (Spain *et al.*, 1985; McDowell & Kitchen, 1986; Kitchen *et al.*, 1990; 1992). This raises the possibility that a subpopulation of δ-opioid receptors might develop in the fourth postnatal week and that ordinarily weaning is the stimulus for this development. Evidence for δ-receptor heterogeneity is increasing (Sofuoglu *et al.*, 1991; 1992; Jiang *et al.*, 1991; Mattia *et al.*, 1991; 1992) and the sensitivity of putative $\delta_1$ and $\delta_2$ sites to antagonism by naloxone and naltrindole show differences in 25 day old rats (Crook *et al.*, 1992). Further, it has recently been reported that in mice, swim SIA is mediated by the $\delta_2$ subtype (Vanderah *et al.*, 1992) and it may be that weaning influences the development of a δ-receptor subtype. At a biochemical level, weaning has been shown to activate enzyme systems at the mRNA transcription level (Coupe *et al.*, 1990; Girard *et al.*, 1991) and a similar effect at the genetic level for neurotransmitter receptors is thus feasible. An alternative possibility is that weaning is instrumental in

coupling δ-sites to second messengers and that this phenomenon normally accounts for the receptor transition. In support of this possibility although adrenergic and cholinergic stimulation of cyclic nucleotides is fully developed at birth and two weeks respectively, morphine stimulated changes in cyclic AMP and cyclic GMP do not peak until day 21 (Muraki *et al.*, 1983). Further, studies with selective opioid receptor agonists reveal that δ-mediated inhibition of dopamine sensitive adenylate cyclase does not begin to be effective until day 14, whereas μ effects are evident during gestation (De Vries *et al.*, 1990). The effect of delayed weaning is temporary, as naltrindole is able to block swim SIA at day 30 and presumably other influences eventually precipitate the change in receptor operation in the absence of the weaning process.

In conclusion, weaning can delay the transition from μ- to δ-receptor control of swim SIA by between 5 to 10 days in the rat. This is the first report that weaning can influence CNS opioid receptor operation of biological responses and the molecular mechanisms underlying these *in vivo* effects remain to be elucidated. The possibility that weaning delays the development of a subtype of the δ-receptor is currently being addressed.

We are grateful to Janssen and Du Pont for the gifts of drugs. B.Y.M. is supported by a Kebbi State Scholarship, Nigeria.

## References


BODNAR, R.J. (1990). Effects of opioid peptides on peripheral stimulation and stress-induced analgesia in animals. *Crit. Rev. Neurobiol.*, **6**, 39–49.

CHAVKIN, C., JAMES, I. & GOLDSTEIN, A. (1982). Dynorphin is the specific endogenous ligand for the κ-opioid receptor. *Science*, **215**, 413–415.

COUPE, C., PERDEREAU, D., FERRÉ, P., HITIER, Y., NARKEWICZ, M. & GIRARD, J. (1990). Lipogenic enzyme activities and mRNA in rat adipose tissue at weaning. *Am. J. Physiol.*, **258**, E126–E133.

CROOK, T.J., KITCHEN, I. & HILL, R.G. (1992). Effects of the δ opioid receptor antagonist naltrindole on antinociceptive response to selective δ agonists in post-weanling rats. *Br. J. Pharmacol.*, **107**, 573–576.

DE VRIES, T.J., HOGENBOOM, F., MULLDER, A.H. & SCHEFFELMEER, A.N.M. (1990). Ontogeny of μ-opioid, δ-opioid and κ-opioid receptors mediating inhibition of neurotransmitter release and adenylate cyclase activity in rat brain. *Dev. Brain Res.*, **54**, 63–69.

GIRARD, J., PERDEREAU, D., NARKEWICZ, M., COUPE, C., FERRÉ, P., DECAUX, J.F. & BOSSARD, P. (1971). Hormonal regulation of liver phosphoenolpyruvate carboxykinase and glucokinase gene expression at weaning in the rat. *Biochimie*, **73**, 71–76.

HART, S.L., SLUSARCZYK, H. & SMITH, T.W. (1983). The involvement of opioid δ-receptors in stress induced antinociception in mice. *Eur. J. Pharmacol.*, **95**, 283–285.

JACKSON, H.C. & KITCHEN, I. (1989). Swim-stress induced antinociception in young rats. *Br. J. Pharmacol.*, **96**, 617–622.

JAMES, I.F. & GOLDSTEIN, A. (1984). Site directed alkylation of multiple opioid receptors. I. Binding selectivities. *Mol. Pharmacol.*, **25**, 337–342.

JANSSEN, P.A.J., NEIMEGGERS, C.J.E. & DONY, J.G.H. (1963). The inhibitory effect of fentanyl and other morphine-like analgesics on the warm water induced tail withdrawal reflex. *Arzneim. Forsch.*, **13**, 502–504.

JIANG, Q., TAKEMORI, A.E., SULTANA, M., PORTOGHESE, P.S. & PORRECA, F. (1991). Differential antagonism of opioid delta antinociception by [D-Ala$^2$,Leu$^5$,Cy$^6$] enkephalin and naltrindole 5′-isothiocynate: evidence for delta receptor subtypes. *J. Pharmacol. Exp. Ther.*, **257**, 1069–1075.

KITCHEN, I., KELLY, M. & HUNTER, J.C. (1992). Ontogenetic studies with ($^3$H) CI-977 reveal early development of κ-opioid sites in rat brain. *Mol. Neuropharmacol.*, **2**, 269–272.

KITCHEN, I., KELLY, M. & VIVEROS, M.P. (1990). Ontogenesis of κ-opioid receptors in rat brain using [$^3$H] U69593 as a binding ligand. *Eur. J. Pharmacol.*, **175**, 93–96.

KITCHEN, I., MCDOWELL, J., WINDER, C. & WILSON, J.M. (1984). Low level lead exposure alters morphine antinociception in neonatal rats. *Toxicol. Lett.*, **22**, 119–123.

KITCHEN, I. & PINKER, S.R. (1990). Antagonism of swim-stress induced antinociception by the δ-opioid receptor antagonist naltrindole in neonatal and adult rats. *Br. J. Pharmacol.*, **100**, 685–688.

MCDOWELL, J. & KITCHEN, I. (1986). Ontogenesis of δ-opioid receptors in rat brain using $^3$H [D-Pen$^2$,D-Pen$^5$] enkephalin as a binding ligand. *Eur. J. Pharmacol.*, **128**, 287–289.

MATTIA, A., VANDERAH, T., MOSBERG, H.I. & PORRECA, F. (1991). Lack of antinociceptive cross-tolerance between [D-Pen$^2$, D-Pen$^5$] enkephalin and [D-Ala$^2$] deltorphin II in mice: evidence for delta receptor subtypes. *J. Pharmacol. Exp. Ther.*, **258**, 583–587.

MATTIA, A., FARMER, S.C., TAKEMORI, A.E., SULTANA, M., PORTOGHESE, P.S., MOSBERG, H.I., BOWEN, W.D. & PORRECA, F. (1992). Spinal opioid delta antinociception in the mouse: mediation by a 5′-NTII-sensitive delta receptor subtype. *J. Pharmacol. Exp. Ther.*, **260**, 518–525.

MORLEY, J.E., ELSON, M.K., LEVINE, A.S. & SHAFER, R.B. (1982). The effect of stress on central nervous system. Concentrations of the opioid peptide, dynorphin. *Peptides*, **3**, 901–906.

MUHAMMAD, B.Y. & KITCHEN, I. (1992). A method for the study of swimming stress and stress-induced antinociception in neonatal rats. *J. Pharmacol. Toxicol. Meth.* (in press).

MURAKI, T., NAKADATE. T. & KATA, R. (1983). Developmental changes in the effect of morphine eniephrine and carbachol on plasma cyclic nucleotide levels in rats. *Eur. J. Pharmacol.*, **94**, 203–209.

PANERAI, A.E., MARTINI, A., SACERDOTE, P. & MANTEGAZZA, P. (1984). κ-receptor antagonist reverse 'non opioid' stress-induced analgesia. *Brain Res.*, **304**, 153–156.

PATERSON, S.J., ROBSON, L.E. & KOSTERLITZ, H.W. (1983). Classification of opioid receptors. *Br. Med. Bull.*, **39**, 31–36.

SOFUOGLU, M., PORTOGHESE, P.S. & TAKEMORI, A.E. (1991). Differential antagonism of delta opioid agonists by naltrindole and its benzofuran analogue (NTB) in mice: evidence for delta opioid receptor subtypes. *J. Pharmacol. Exp. Ther.*, **257**, 676–680.

SOFUOGLU, M., PORTOGHESE, P.S. & TAKEMORI, A.E. (1992). δ-Opioid receptor binding in mouse brain: evidence for heterogenous binding sites. *Eur. J. Pharmacol.*, **216**, 273–277.

SPAIN, J.W., ROTH, B.L. & COSCIA, G.J. (1985). Differential ontogeny of multiple opioid receptors (μ, δ and κ). *J. Neurosci.*, **5**, 584–588.

VANDERAH, T.W., WILD, K.D., TAKEMORI, A.E., SULTANA, M., PORTOGHESE, P.S., BOWEN, W.D., MOSBERG, H.I. & PORRECA, F. (1992). Mediation of swim-stress antinociception by the opioid delta$_2$ receptor in the mouse. *J. Pharmacol. Exp. Ther.*, **262**, 190–198.

VASWANI, K.K., RICHARD, C.W. & TEJWANI, G.A. (1988). Cold water swim stress-induced changes in the levels of opioid peptides in the rat CNS and peripheral tissues. *Pharmacol. Biochem. Behav.*, **29**, 163–168.

WATKINS, L.R. & MEYER, D.J. (1982). Organisaton of endogenous opiate and non-opiate pain control systems. *Science*, **216**, 1185–1192.


*(Received October 21, 1992*
*Revised February 12, 1993*
*Accepted February 22, 1993)*

*Br. J. Pharmacol.* (1993), **109**, 655–660 © Macmillan Press Ltd, 1993

# *In vivo* microdialysis of noradrenaline overflow: effects of α-adrenoceptor agonists and antagonists measured by cumulative concentration-response curves

[1]M.J.A. van Veldhuizen, Matthijs G.P. Feenstra, Rob P.W. Heinsbroek & Gerard J. Boer

Graduate School Neurosciences Amsterdam, Netherlands Institute for Brain Research, Meibergdreef 33, 1105 AZ Amsterdam-ZO, The Netherlands

**1** The purpose of the present study was to compare the effects of several α-adrenoceptor agonists and antagonists on cerebral cortical overflow of endogenous noradrenaline (NA) in freely moving rats. One or two days after the implantation of transcerebral dialysis tubes in the frontoparietal cortex, extracellular NA levels were monitored on-line with high performance liquid chromatography and electrochemical detection. The drugs were applied locally via the dialysis membrane, and effects on NA overflow were determined in cumulative concentration-response curves.

**2** The average basal cortical NA overflow of all experiments was 0.25 pg $min^{-1}$. The $\alpha_2$-adrenoceptor agonists caused a concentration-dependent decrease in NA levels. UK-14,304 was the most potent and B-HT 933 the least potent agonist. The maximal decrease in NA overflow was to 10–15% of control levels after UK-14,304 or moxonidine, to 30% after clonidine and to 50% after B-HT 933 administration. Continuous activation of the presynaptic $\alpha_2$-adrenoceptor with $10^{-6}$ M UK-14,304 caused a decrease in NA levels to 40–50% of basal levels. This decrease was reached within 1 h and remained stable for the entire 3 h measurement period. The $\alpha_1$-adrenoceptor agonists, phenylephrine and methoxamine, induced an increase in NA levels to 225% and 300%, respectively, at a concentration of $10^{-3}$ M.

**3** Local application of $\alpha_2$-adrenoceptor antagonists caused an increase in NA levels, with idazoxan being more potent than piperoxan. Yohimbine did not cause any significant change.

**4** All drugs used in these *in vivo* experiments had *in vitro* recoveries across the dialysis membrane between 10 and 20%.

**5** We conclude that microdialysis with local drug application is suitable for the comparison of the pharmacological effects of drugs with affinity for α-adrenoceptors on cortical NA overflow *in vivo*, provided that the passage across the membrane is equal for the different drugs.

**Keywords:** Microdialysis; noradrenaline overflow; $\alpha_2$-autoreceptor; clonidine; B-HT 933; moxonidine; UK-14,304; idazoxan; piperoxan; yohimbine

## Introduction

Several neurotransmitters can modulate their own release via a negative feedback mechanism mediated by presynaptic autoreceptors (Starke *et al.*, 1989). Receptor-mediated modulation of peripheral noradrenaline (NA) release in various *in vitro* and *in vivo* preparations has been described extensively (reviews by Gillespie, 1980; Langer, 1981; Starke, 1981; 1987). Evidence that NA overflow is modulated by presynaptic $\alpha_2$-autoreceptors in the brain comes primarily from *in vitro* studies with brain tissue slices or synaptosomal preparations (Farnebo & Hamberger, 1971; Starke & Montel, 1973; Mulder *et al.*, 1978). Confirmation and expansion of *in vitro* results can now be obtained through *in vivo* microdialysis. The extracellular concentration of neurotransmitters, measured *in vivo* with brain microdialysis, often reflects active neuronal release (Ungerstedt, 1984; Westerink *et al.*, 1987). The extracellular NA measured in the cerebral cortex of the freely moving rat reflects calcium-dependent and tetrodotoxin-sensitive release (l'Heureux *et al.*, 1986; Van Veldhuizen *et al.*, 1990). *In vivo* it has been confirmed that $\alpha_2$-adrenoceptors control cerebral NA release (Dennis *et al.*, 1987; Abercrombie *et al.*, 1988; Itoh *et al.*, 1990). However, in these studies drugs were predominantly applied systemically.

In the present microdialysis study we used local drug administration, combining the advantages of *in vitro* studies, the possibility of comparing drug effects in cumulative dose-response studies (Frankhuyzen & Mulder, 1982), with the advantage of *in vivo* studies, the possibility of measuring effects in an intact system. This method has some advantages over peripheral administration: (1) for each rat a cumulative concentration-response curve can be determined (viz. by successive addition to the perfusion fluid of increasing drug concentrations); (2) drugs can easily reach the target tissue (no blood brain barrier to pass); (3) effects of drugs are restricted to the area of application. We compared the effects of several locally applied $\alpha_2$- and $\alpha_1$-adrenoceptor agonists and antagonists on cortical NA overflow. In addition, we examined the effect of continuous activation of the $\alpha_2$-adrenoceptor. To investigate possible differences in passage of the drugs across the dialysis membrane, *in vitro* recovery of the drugs was also measured.

## Methods

### *Animals*

Male Wistar rats (180–250 g) were obtained from Harlan (Zeist, The Netherlands). Rats were housed individually in perspex cages (25 × 25 × 32 cm) during the microdialysis experiment. They had free access to food and water, and were subjected to a light/dark schedule of 12 h (lights on at 7 h 00 min). Testing took place during the light period.

### *Surgical procedure*

Transcortical cannulae were made according to Imperato & Di Chiara (1984). The semipermeable membrane, with a dialysis zone of 9 mm, was of cellulose ester (i.d. 0.22 mm,

[1] Author for correspondence.

o.d. 0.27 mm, mol wt. cut-off 10 kD; Cordis Dow Medical International). Under chloralhydrate anaesthesia (400 mg $kg^{-1}$, i.p.) a rat was mounted on a Kopf stereotaxic frame with the incisor bar set at − 2.5 mm. The skull was exposed and holes were drilled on each side of the temporal bone. The cannula was inserted horizontally in the cortex (A 0, V − 2.0 mm vs bregma). Both cannulae ends were bent upwards and cemented on the skull.

After the experiments the location of the cannula was verified. For this purpose the rats were decapitated, and brains were frozen for cryostat sectioning. Subsequently, sections were stained with thionine for histological evaluation.

### *Dialysis procedure*

Experiments were carried out in freely moving rats the day after surgery. The transcortical cannula was perfused with Ringer solution (NaCl 154 mM, KCl 4 mM, $CaCl_2$ 2.2 mM, pH 6.2) at a flow rate of 3 μl $min^{-1}$. Cortical dialysate was collected in a 50 μl sample loop and injected automatically (Rheodyne 5701) on-line once every 20 min into a high performance liquid chromatography (h.p.l.c.) system.

### *Analysis of NA in dialysates*

Dialysates were analysed for NA by reversed phase liquid chromatography at room temperature on a Supelcosil column (LC-18-DB, 250 × 4.6 mm, 5 μm) protected by a Supelguard column (LC-18-DB, 20 × 4.6 mm, 5 μm). The mobile phase was a citric acid (10.4 mM)/sodium acetate (61 mM) buffer (pH 5.1) with 7% methanol, 0.3 mM EDTA and varying concentrations (0.52–0.93 mM) of heptane sulphonic acid; the latter was used to move the NA peak to empty places in the chromatogram. The flow rate through the system was 0.8 ml $min^{-1}$ (Waters 510 or 590).

For electrochemical detection of NA we used an ESA Coulochem 5100A or 5200 dual electrode, cell model 5011, in a differential mode. At the first detector cell an oxidising potential between + 350 and + 400 mV was applied, while the second detector was set at a reducing potential between − 250 and − 400 mV. *In vivo* NA levels were compared with a standard NA solution in Ringer. The detection limit of NA was between 0.17 and 0.6 pg.

### *Drug treatment*

Drug solutions were perfused after 5 steady basal NA samples (100 min) had been obtained. Each drug was administered in increasing concentrations and each concentration was perfused for 4 sampling periods of 20 min. The experiment was ended with 4 sampling periods under basal conditions (i.e. Ringer perfusion). For continuous activation of the $\alpha_2$-adrenoceptor, the agonist UK-14,304 was perfused for about 3 h at a concentration of $10^{-6}$ M. For each drug, as well as for the continuous activation experiment, a group of 3 to 5 rats was used (in the case of clonidine $10^{-4}$ M, piperoxan and yohimbine $10^{-3}$ M only 2 measurements were available).

The following drugs were used: clonidine hydrochloride, (±)-piperoxan hydrochloride, (±)-methoxamine hydrochloride, (−)-phenylephrine hydrochloride (Sigma, St. Louis, U.S.A.), moxonidine base (BDF Beiersdorf, Hamburg, Germany), UK-14,304 tartrate (bromoxidine; Pfizer, Sandwich, UK), B-HT 933 dihydrochloride (azepexole; Boehringer, Ingelheim, Germany), (±)-idazoxan hydrochloride (Reckitt & Colman, Kingston upon Hull, UK), yohimbine hydrochloride (Janssen Chimica, Beerse, Belgium).

### *Data analysis*

NA overflow was expressed as pg $min^{-1}$ ± s.e.mean without correction for recovery. Basal NA overflow for each animal was defined as the average of the 5 samples taken immediately before drug application. In the illustrations drug-induced changes of NA overflow are expressed as percentages of this average basal level obtained in each individual rat. Statistical evaluation was done with absolute values. The first sampling period after each change in drug concentration was excluded from the analysis, since these results were likely to reflect the effects of a mixture of two concentrations. To compare differences among averages (basal versus drug-modulated overflow) the last three sampling periods of each drug concentration were averaged and compared by one-way analysis of variance (ANOVA) with repeated measures (level of significance $\alpha = 0.05$; if $n \geqslant 3$). Where appropriate, a *post-hoc* comparison of the means was made with the Newman-Keuls test. To compare the various drugs, the results were analysed with ANOVA (repeated measures) with Drug and Dose as the main factors.

### In vitro *recovery of drugs and NA*

The recovery of drugs across the membrane was tested *in vitro* at room temperature by submersion of the cannula in a bath (10 ml) containing Ringer solution. The passage of drugs from the perfusion fluid to the bath was determined by perfusing Ringer solution containing drugs in known concentrations at 3 μl $min^{-1}$. After 20 min of equilibration, a 40 min sample of perfusate was collected for analysis of the drug. The cannula was perfused for 20 min with Ringer solution before another drug was tested.

The reverse situation, passage of drugs from the bath to the perfusion fluid, was also tested: Ringer solution was used as perfusion fluid and the membrane was now immersed in a 10 ml Ringer bath containing the drug (all drugs $10^{-4}$ M). As the cannulae were immersed in different drug solutions, the membranes were rinsed with Ringer solution before application of a new drug.

The recovery of NA was also determined as passage from the bath to the perfusion fluid, both in the absence and in the presence of drugs. The membrane was submerged in a NA solution (1 ng $ml^{-1}$) and Ringer or a $10^{-5}$ M drug solution was perfused. NA concentrations were determined as described above for the *in vivo* experiments.

Analysis of drugs was carried out on the same day by reversed-phase h.p.l.c. with u.v. detection (230 nm). The mobile phase was a sodium-phosphate buffer, containing 0.1% tri-ethylamine and adjusted to pH 3.0 with phosphoric acid. The concentration of acetonitril differed for the various drugs: for B-HT 933 (azepexole) and phenylephrine 0%; for clonidine, moxonidine and UK-14,304 (bromoxidine) 10%; for methoxamine 15%; for idazoxan, piperoxan and yohimbine 25%; for prazosin 35% (Sigma, St. Louis, U.S.A.). The column was a Supelcosil column LC-18-DB (250 × 4.6 mm, 5 μm), the flow rate was 1.0 ml $min^{-1}$ (HP pump 1090) and the injection volume was 50 μl.

Recovery was expressed as a percentage and was calculated for passage across the membranes from the formula $[(c_i\text{-}c_d)/c_i] \times 100\%$ when the drug was present in the perfusion medium, and $(c_d/c_i) \times 100\%$ when the drug was present in the bath, with $c_i$ being the initial drug concentration (in perfusion medium and bath, respectively) and $c_d$ the drug concentration measured in perfusate or dialysate, respectively.

For each drug both directions of membrane passage were measured in triplicate in 3 membranes. A paired two-tailed Student's *t* test was used for each drug to test whether differences in recovery depend on the direction of membrane passage. Analysis of variance was applied to compare different drugs. The level of significance was $\alpha = 0.05$.

## Results

During the initial phase, basal NA overflow (5 steady basal levels) in cortical dialysates of freely moving rats was 0.250 ± 0.021 pg $min^{-1}$ ($n = 42$ rats). The basal levels in con-

trol rats may fluctuate during the measurement period (8–9 h), but no overall decrease or increase was seen ($n = 3$).

### $\alpha_2$-*Adrenoceptor agonists*

Figure 1 exemplifies the concentration-dependent decrease in cortical NA overflow induced by $\alpha_2$-adrenoceptor agonists. The results with UK-14,304 clearly show that a new steady state NA level is achieved within one or two sampling periods after changing the perfusion medium. This new level remained constant in the following sampling periods apparently independent of the duration of the application, as shown in Figure 2 where one concentration of UK-14,304 was present for about 3 h. If after UK-14,304 Ringer solution was perfused again, NA levels did not recover to the pre-drug level within 80 min but returned to baseline gradually after 2–3 h ($n = 3$; data not shown).

The effects of UK-14,304 as well as of other $\alpha_2$-adrenoceptor agonists on cortical NA overflow are summarized in Figure 3. UK-14,304, clonidine, moxonidine and B-HT 933 all led to concentration-dependent reductions in NA overflow. UK-14,304 was the most potent $\alpha_2$-adrenoceptor agonist, with a half-maximal effect at $10^{-7}$ M. Whereas moxonidine and UK-14,304 reduced NA overflow to 10 to

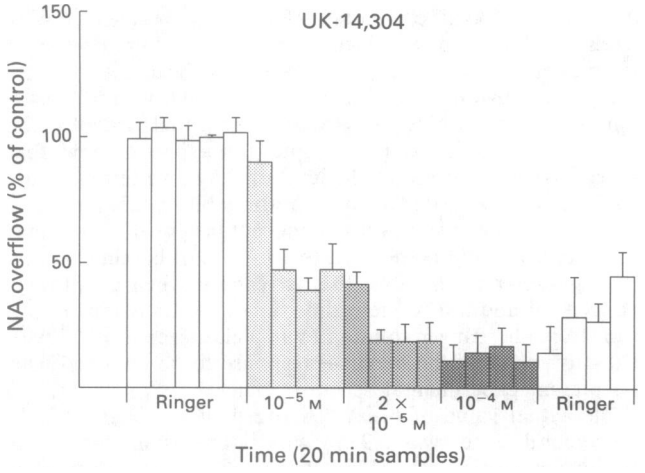



**Figure 1** Effect of UK-14,304 on cortical noradrenaline (NA) overflow. UK-14,304 was dissolved in Ringer solution and each concentration was applied for 80 min. Columns represent means ± s.e.mean expressed as a percentage of basal overflow (Ringer perfusion). Basal NA overflow was 0.143 ± 0.020 pg min$^{-1}$ ($n = 5$ rats).

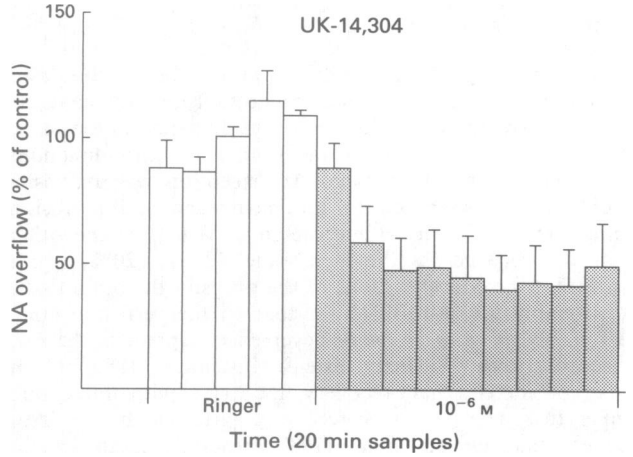



**Figure 2** Effect of continuous perfusion with UK-14,304 on cortical noradrenaline (NA) overflow. The drug was dissolved in Ringer solution and a concentration of $10^{-6}$ M UK-14,304 was applied for 3 h. Columns represent means ± s.e.mean expressed as a percentage of basal overflow. Basal NA overflow was 0.381 ± 0.094 pg min$^{-1}$ ($n = 3$).

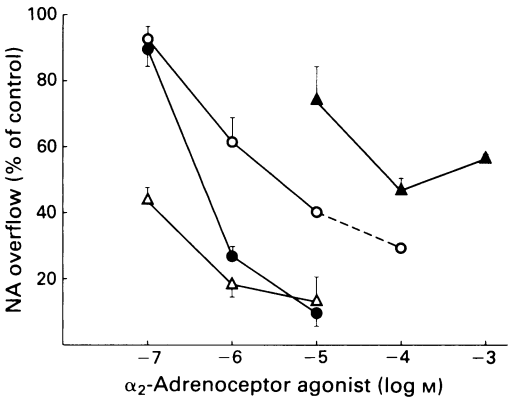



**Figure 3** Effect of $\alpha_2$-adrenoceptor agonists on cortical noradrenaline (NA) overflow. The drugs were dissolved in Ringer solution and each concentration was applied for 80 min. The points represent means ± s.e.mean of the last 60 min of infusion obtained in 3 to 5 rats per drug. Basal NA overflow was 0.276 ± 0.074 pg min$^{-1}$, ($n = 3$) (○) ($n = 2$ at $10^{-4}$ M (dotted line)); for moxonidine 0.232 ± 0.020 pg min$^{-1}$, $n = 3$ (●); for UK-14,304 0.143 ± 0.020 pg min$^{-1}$, $n = 5$ (△); for B-HT 933 0.216 ± 0.037 pg min$^{-1}$, $n = 3$ (▲). Drug-evoked differences from basal level are statistically significant for UK-14,304 from $10^{-7}$ M onwards, for clonidine and moxonidine from $10^{-6}$ M onwards and for B-HT 933 from $10^{-4}$ M onwards (ANOVA followed by post-hoc Newman-Keuls).

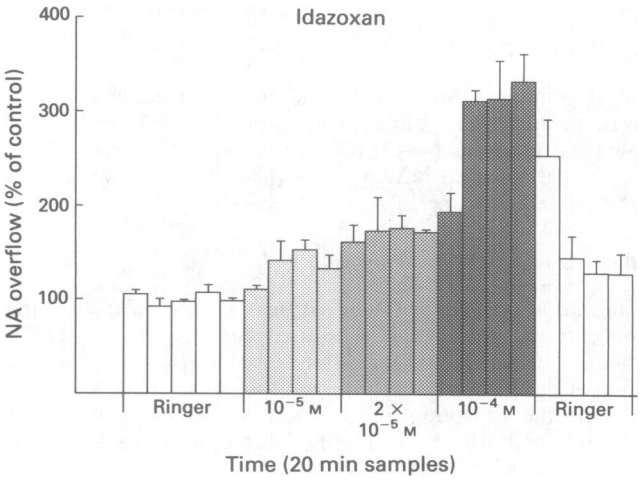



**Figure 4** Effect of idazoxan on cortical noradrenaline (NA) overflow. Idazoxan was dissolved in Ringer solution and each concentration was applied for 80 min. Columns represent means ± s.e.mean expressed as a percentage of basal overflow. Basal NA overflow was 0.212 ± 0.050 pg min$^{-1}$ ($n = 3$).

15%, both at $10^{-5}$ M, the effect of $10^{-4}$ M clonidine or B-HT 933 was a reduction to no more than 30% and 47%, respectively. Moxonidine and clonidine were about equipotent but had different maximal effects, while B-HT 933 was the least potent and least effective agonist.

### $\alpha_2$-*Adrenoceptor antagonists*

Local administration of the $\alpha_2$-adrenoceptor antagonist, idazoxan, caused a concentration-dependent increase in extracellular NA (Figure 4). Again, a new equilibrium was reached after one or two sampling periods for each concentration. Ringer perfusion after drug treatment led to a rapid return of NA concentrations to basal levels.

The effects of the $\alpha_2$-adrenoceptor antagonists on NA overflow are depicted in Figure 5. A concentration-dependent significant increase in NA overflow also occurred during perfusion with piperoxan, but this response was less marked than the response to idazoxan. In contrast, yohimbine failed to have an effect.

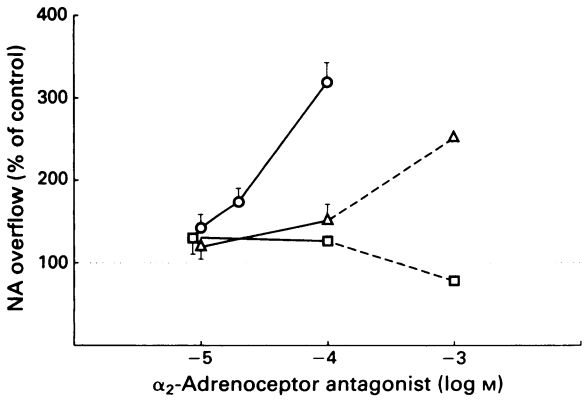



**Figure 5** Effect of $\alpha_2$-adrenoceptor antagonists on cortical noradrenaline (NA) overflow. The drugs were dissolved in Ringer solution and each concentration was applied for 80 min. The points represent means ± s.e.mean of the last 60 min of infusion obtained in 3 rats per drug (for piperoxan and yohimbine $n = 2$ at $10^{-3}$ M (dotted line)). Basal NA overflow was for idazoxan 0.212 ± 0.050 pg min$^{-1}$ (○); for piperoxan 0.389 ± 0.053 pg min$^{-1}$ (△) and for yohimbine 0.227 ± 0.074 pg min$^{-1}$ (□). Drug-evoked differences from basal level are statistically significant for idazoxan from $2 \times 10^{-5}$ M onwards and for piperoxan from $10^{-4}$ M onwards; for yohimbine no effect was found (ANOVA followed by post-hoc Newman-Keuls).

### $\alpha_1$-Adrenoceptor ligands

Local administration of the $\alpha_1$-adrenoceptor agonists, methoxamine and phenylephrine, had no effect on NA overflow at low concentrations ($n = 3$, results not shown); concentrations of $10^{-3}$ M increased NA to 225% (phenylephrine; $n = 1$) and 300% (methoxamine; $n = 2$), respectively.

### In vitro *recovery of drugs and NA*

Calibration curves of the drugs were linear in the concentration-range that was used for the *in vivo* experiments: $10^{-6}$–$10^{-3}$ M for agonists and $10^{-6}$–$10^{-4}$ M for antagonists.

With the exception of prazosin, *in vitro* recovery was similar, about 10–20%, in either direction across the membrane and showed no significant differences between drugs (Table 1). The $\alpha_1$-adrenoceptor antagonist prazosin adhered so much to the membrane and the perfusion tubing that only 30% of the initial perfusion concentration ($10^{-4}$ M) was detected in the perfusate. In the reverse situation, when the membrane was placed in $10^{-4}$ M prazosin, the dialysate contained only 2%.

**Table 1** *In vitro* recovery of drugs

| | *Drug in perfusion fluid* $[(c_i-c_d)/c_i] \times 100\%$ | *Drug in bath* $(c_d/c_i) \times 100\%$ |
|---|---|---|
| *$\alpha_2$-Adrenoceptor agonists* | $10^{-5}$ M | $10^{-4}$ M |
| Clonidine | 15.7 ± 2.2 | 16.0 ± 1.3 |
| Moxonidine | 11.0 ± 0.5 | 10.3 ± 1.3 |
| UK-14,304 | 19.5 ± 2.5 | 13.6 ± 1.3 |
| B-HT 933 | 13.5 ± 1.9[b] | 12.0 ± 0.9 |
| *$\alpha_2$-Adrenoceptor antagonists* | $10^{-5}$ M | $10^{-4}$ M |
| Idazoxan | 12.7 ± 0.7 | 12.0/15.2[a] |
| Piperoxan | ND | 9.3/14.7[a] |
| Yohimbine | 13.2 ± 1.5 | 9.4/11.2[a] |
| *$\alpha_1$-Adrenoceptor ligands* | $10^{-4}$ M | $10^{-4}$ M |
| Phenylephrine | 11.0 ± 1.9 | ND |
| Methoxamine | 11.0 ± 1.5 | ND |
| Prazosin | 70.6 ± 0.5* | 2.4 ± 0.3 |

Recovery of drugs was determined in 3 membranes. Means ± s.e.mean are given in percentages. Drugs were measured in the initial standard solution (perfusion fluid or bath), resulting in $c_i$, and in the perfusate or dialysate, resulting in $c_d$.
[a]$n = 2$ measurements; [b]$10^{-4}$ M; ND, not determined.
*$P < 0.05$, paired Student's $t$ test compared to drug in bath.

The passage of NA from the bath through the dialysis membrane into the Ringer solution (recovery) was 17.4 ± 0.3% ($n = 3$ membranes in duplicate). The recovery of NA was not influenced by the presence of any of the drugs ($10^{-5}$ M) in the perfusion fluid.

## Discussion

The present study shows that it is possible to determine cumulative concentration-response curves and, hence, potencies of drugs *in vivo* by using brain microdialysis combined with local administration of drugs via the perfusion fluid. This is the first comparison of the effects of several locally applied drugs selective for the $\alpha_2$-adrenoceptor on central NA overflow *in vivo*. The experimental set-up proved to be satisfactory. Within 20 to 40 min after the start of drug perfusion, the overflow of NA reached a new steady state and always returned to baseline values after drug treatment. Why baseline values were obtained more rapidly after the testing of antagonists than after agonists is not clear.

The NA overflow which we determined in the cortex represents a release related to basal neuronal activity. The local effects of the $\alpha_2$-adrenoceptor antagonists show that under basal conditions, at the level of the nerve terminal, the NA overflow was under tonic autoinhibitory control. The local effects of exogenous $\alpha_2$-adrenoceptor agonists show that NA overflow could be reduced to 10–15% of baseline values. This is similar to the level that is reached when overflow is reduced by addition of tetrodotoxin or by omission of calcium from the Ringer solution (Van Veldhuizen *et al.*, 1990), and it is probably the maximal response to be obtained with the present experimental set-up.

The actual value of basal NA overflow we determined in the cerebral cortex was 0.25 pg min$^{-1}$. This is similar to our previous measurements (Van Veldhuizen *et al.*, 1990), but lower than the levels reported by Dennis *et al.* (1987) and l'Heureux *et al.* (1986), who used a similar set-up. These differences are still common in microdialysis literature and are likely to be caused by differences in experimental conditions.

### In vitro *recovery*

To compare drug effects one has to know whether the drugs pass the membrane to a similar extent. Our measurements on *in vitro* recovery show that all drugs had about the same recovery and that recovery was similar in both directions across the dialysis membrane. An exception was prazosin, which adhered so much to the membrane and perfusion tubing that it was not administered *in vivo*. For the other drugs recovery across the membrane was 10–20%, which means that the concentrations of the drugs in the brain tissue are probably 5 to 10 fold lower than in the perfusion fluid. Regrettably, *in vitro* recovery never exactly predicts the real concentration *in vivo* (Benveniste & Hüttemeier, 1989). When it is considered that recovery increases with increasing temperature, the 10–20% recovery agrees with the 25% recovery that Dennis *et al.* (1987) reported in an *in vivo* experiment with radiolabelled [$^3$H]-idazoxan. From the similar recovery of the drugs, and the fact that the recovery of NA was not influenced by any of the drugs, we conclude that observed differences in drug effects on NA overflow solely reflect differences in interaction between drugs and brain tissue.

*Effects of locally applied drugs*

In the present study both moxonidine and UK-14,304 (bromoxidine) were more effective in reducing NA overflow than clonidine or B-HT 933 (azepexole). These *in vivo* results confirm earlier *in vitro* findings that UK-14,304 and moxonidine are full $\alpha_2$-adrenoceptor agonists (Grant & Scrutton, 1980; Armah, 1988), in contrast to the partial agonism which has been described for clonidine (Medgett *et al.*, 1978). A previous *in vitro* study with B-HT 933, however, did not predict the restricted effectiveness of this compound (Cichini & Singer, 1987).

The $\alpha_2$-adrenoceptor antagonists caused a concentration-dependent increase in NA overflow, with idazoxan being more potent than piperoxan. The absence of an effect on NA overflow by yohimbine is discussed below.

The effect of the $\alpha_1$-adrenoceptor agonists, an increase in NA overflow, suggests that NA overflow is also modulated by the $\alpha_1$-adrenoceptor. However, this effect was only found at high concentrations. In some tissues activation of presynaptic $\alpha_1$-adrenoceptors is thought to result in an inhibition of NA release (Murphy & Majewski, 1989). On the other hand, some $\alpha_1$-adrenoceptor agonists may release NA by a tyramine-like mechanism (Vizi *et al.*, 1986).

While the difference in potency between idazoxan and piperoxan is in agreement with literature data (Doxey *et al.*, 1983; Baron & Siegel, 1990; Mermet *et al.*, 1990) and our own data on [$^3$H]-RX821002 binding to central $\alpha_2$-adrenoceptors (Boer *et al.*, 1993), the comparison of the results obtained with agonists with literature data presents some problems. The evoked *in vitro* release of [$^3$H]-NA from rat cortical slices was reduced less potently by moxonidine than by clonidine ($pIC_{35}$ 6.9 vs 7.7; Schlicker *et al.*, 1990), and UK-14,304 and clonidine were about equipotent (Ong *et al.*, 1991), in contrast to our results. This order in *in vitro* potency was confirmed by binding studies (clonidine$\approx$UK-14,304$>$moxonidine$>$B-HT 933; Boer *et al.*, 1993), whereas *in vivo* UK,14,304$>$moxonidine$\approx$clonidine$>$B-HT 933 was found. Thus, in relation to the other drugs, clonidine appeared to be more potent *in vitro* than *in vivo*. Part of these discrepancies may be due to the fact that the experimental design in *in vitro* release studies is basically different from that *in vivo*; high potassium concentrations or repetitive electric pulses are used in a standardized way to stimulate NA release, and measurements are made in a damaged biological system. In contrast, *in vivo* non-stimulated NA overflow can be measured in an intact biological system.

*Local versus systemic administration*

The concentration profile of the locally administered compound in the surrounding tissue is usually unknown. However, continuous application of UK-14,304 resulted in a stable level of NA within 20–40 min, suggesting that there is no accumulation of drug in the tissue surrounding the membrane. Therefore the effect of the previous drug concentration will be negligible in cumulative concentration-response curves (Frankhuyzen & Mulder, 1982).

Systemically injected $\alpha_2$-adrenoceptor drugs can affect transmitter overflow by actions on receptors located on the nerve terminal and on somatodendritic autoreceptors located in the cell body region. Through local perfusion of drugs the contribution of somatodendritic receptors can be excluded. Comparison of the effects of drugs administered in one of both ways on the overflow at the level of the nerve terminal can reveal the contribution of each receptor population (Westerink *et al.*, 1990).

Local administration of $10^{-5}$ M clonidine caused a 60% reduction in cortical NA overflow, similar to the 50–60% reduction after systemic administration of 0.3 mg kg$^{-1}$, i.p., reported in the cortex by l'Heureux *et al.* (1986) and in the hippocampus by Abercrombie *et al.* (1988). The clonidine concentration in brain tissue after the systemic administration of 0.4 mg kg$^{-1}$ clonidine (Nazarali *et al.*, 1986) was $2 \times 10^{-6}$ M, which is in the same range as that around our membranes when corrected for recovery. Thus, in the cortex the effect of 0.3 mg kg$^{-1}$, i.p. clonidine seems comparable with the effect of $10^{-5}$ M perfused locally. This might indicate that activation of somatodendritic $\alpha_2$-autoreceptors on NA cell bodies does not add to the local effect of clonidine.

Locally perfused $10^{-4}$ M idazoxan caused an increase in cortical NA overflow to 300%, which is comparable to the 250% increase after local perfusion of $10^{-4}$ M idazoxan reported by Dennis *et al.* (1987) and to the 250–300% increase after systemic administration of 20 mg kg$^{-1}$, i.p., idazoxan (l'Heureux *et al.*, 1986; Dennis *et al.*, 1987). Again, both central and peripheral drug administration resulted in comparable effects on cortical NA overflow.

However, for yohimbine the difference between local infusion and systemic administration is quite profound. Yohimbine has been shown to produce increases in NA release in most *in vitro* and *in vivo* studies (e.g. Taube *et al.*, 1977; Szemeredi *et al.*, 1991; reviews by Langer, 1981; Goldberg & Robertson, 1983; Starke *et al.*, 1989), but had no significant effect in the present *in vivo* dialysis study. This lack of effect must be the result of the local administration, since systemic administration (5.0 mg kg$^{-1}$, i.p.) increased NA overflow to 200–230% in the cortex (own unpublished data) and hippocampus (Abercrombie *et al.*, 1988). This discrepancy is not due to a hampered passage across the dialysis membrane or to interference with the passage of NA. Nor is it due to the non-imidazoline character of yohimbine as compared to idazoxan (Bousquet *et al.*, 1984; Tibiriça *et al.*, 1991). Drugs with an imidazoline structure and affinity for the $\alpha_2$-adrenoceptor (such as clonidine, UK-14,304, moxonidine and idazoxan) can influence NA overflow via an imidazoline receptor. Two findings suggest that $\alpha_2$-adrenoceptors but not imidazoline receptors are involved in the response measured. First, we showed that the non-imidazolines B-HT 933 and piperoxan affected NA overflow in concentrations relevant for interaction with $\alpha_2$-adrenoceptors. Second, idazoxan increased NA overflow, whereas it has been shown to inhibit [$^3$H]-NA release via an imidazoline receptor after $\alpha_2$-adrenoceptor blockade with rauwolscine (Göthert & Molderings, 1991). Apparently, inhibition of somatodendritic autoreceptors on NA neurones by yohimbine *in vivo* results in increased NA overflow in terminal regions, whereas local administration does not. However, there may be alternative explanations since yohimbine has, besides its well documented and unequivocal $\alpha_2$-adrenoceptor antagonistic properties (see above), a variety of other effects (Goldberg & Robertson, 1983). For instance, local anaesthetic actions in central neurones have been reported to result in an inhibitory effect on NA release (Hagan & Hughes, 1986). It is not clear, however, why these effects would be apparent only after local administration, even of low concentrations. Another explanation could be that upon local administration the inhibitory effects of yohimbine on the $\alpha_2$-adrenoceptor are balanced by an action on other receptors, e.g. 5-hydroxytryptamine receptors for which yohimbine has significant affinity (Goldberg & Robertson, 1983; Winter & Rabin, 1992).

We want to thank H. Stoffels for drawing the illustrations, Prof. Dr D.F. Swaab for critically reading the manuscript and A. Janssen for his linguistic comments. The work was supported by the Van den Houten Foundation.

Moxonidine, UK-14,304, B-HT 933 and idazoxan were generous gifts of BDF Beiersdorf, Pfizer, Boehringer and Reckitt & Colman, respectively.

## References


ABERCROMBIE, E.D., KELLER, R.W. & ZIGMOND, M.J. (1988). Characterization of hippocampal norepinephrine release as measured by microdialysis perfusion: pharmacological and behavioural studies. *Neurosci.*, **27**, 897–904.

ARMAH, B.I. (1988). Unique presynaptic $\alpha_2$-receptor selectivity and specificity of the antihypertensive agent moxonidine. *Arzneimittel Forschung, Drug Res.*, **38**, 1435–1442.

BARON, B.M. & SIEGEL, W. (1990). p-$^{125}$I-Iodoclonidine, a novel radiolabeled agonist for studying central $\alpha_2$-adrenergic receptors. *Mol. Pharmacol.*, **38**, 348–356.

BENVENISTE, H. & HÜTTEMEIER, P.C. (1989). Microdialysis – theory and application. *Prog. Neurobiol.*, **35**, 195–215.

BOER, G.J., VAN DER HEE, R. & FEENSTRA, M.G.P. (1993). Alpha-2 adrenoceptor assayed in rat brain by the new ligand [$^3$H]-RX821002. *Biogenic Amines*, (in press).

BOUSQUET, P., FELDMAN, J. & SCHWARTZ, J. (1984). Central cardiovascular effects of alpha adrenergic drugs: differences between catecholamines and imidazolines. *J. Pharmacol. Exp. Ther.*, **230**, 232–236.

CICHINI, G. & SINGER, E.A. (1987). B-HT 920, B-HT 933, and B-HT 958: presynaptic effects on electrically evoked $^3$H-noradrenaline release from slices of rat brain cortex and hypothalamus. *Naunyn-Schmiedebergs Arch. Pharmacol.*, **335**, 613–617.

DENNIS, T., L'HEUREUX, R., CARTER, C. & SCATTON, B. (1987). Presynaptic alpha-2 adrenoceptors play a major role in the effects of idazoxan on cortical noradrenaline release (as measured by in vivo dialysis) in the rat. *J. Pharmacol. Exp. Ther.*, **241**, 642–649.

DOXEY, J.C., ROACH, A.G. & SMITH, C.F.C. (1983). Studies on RX 781094: a selective, potent and specific antagonist of $\alpha_2$-adrenoceptors. *Br. J. Pharmacol.*, **78**, 489–505.

FARNEBO, L.-O. & HAMBERGER, B. (1971). Drug-induced changes in the release of $^3$H-monoamines from field stimulated rat brain slices. *Acta Physiol. Scand.*, Suppl. **371**, 35–44.

FRANKHUYZEN, A.L. & MULDER, A.H. (1982). A cumulative dose-response technique for the characterization of presynaptic receptors modulating [$^3$H]noradrenaline release from rat brain slices. *Eur. J. Pharmacol.*, **78**, 91–97.

GILLESPIE, J.S. (1980). Presynaptic receptors in the autonomic nervous system. In *Handbook of Experimental Pharmacology. Adrenergic Activators and Inhibitors*. ed. Szekeres, L. pp. 353–425. Berlin: Springer-Verlag.

GOLDBERG, M.R. & ROBERTSON, D. (1983). Yohimbine: a pharmacological probe for study of the $\alpha_2$-adrenoceptor. *Pharmacol. Rev.*, **35**, 143–180.

GÖTHERT, M. & MOLDERINGS, G.J. (1991). Involvement of presynaptic imidazoline receptors in the $\alpha_2$-adrenoceptor-independent inhibition of noradrenaline release by imidazoline derivatives. *Naunyn-Schmiedebergs Arch. Pharmacol.*, **343**, 271–282.

GRANT, J.A. & SCRUTTON, M.C. (1980). Interaction of selective α-adrenoceptor agonists and antagonists with human and rabbit blood platelets. *Br. J. Pharmacol.*, **71**, 121–134.

HAGAN, R.M. & HUGHES, I.E. (1986). Yohimbine affects the evoked overflow of neurotransmitters from rat brain slices by more than one mechanism. *J. Pharm. Pharmacol.*, **38**, 195–200.

IMPERATO, A. & DI CHIARA, G. (1984). Trans-striatal dialysis coupled to reverse phase high performance liquid chromatography with electrochemical detection: a new method for the study of the in vivo release of endogenous dopamine and metabolites. *J. Neurosci.*, **4**, 966–977.

ITOH, Y., OISHI, R., NISHIBORI, M. & SAEKI, K. (1990). In vivo measurement of noradrenaline and 3,4-dihydroxyphenylethyleneglycol in the rat hypothalamus by microdialysis: effects of various drugs affecting noradrenaline metabolism. *J. Pharmacol. Exp. Ther.*, **255**, 1090–1097.

LANGER, S.Z. (1981). Presynaptic regulation of the release of catecholamines. *Pharmacol. Rev.*, **32**, 337–362.

L'HEUREUX, R., DENNIS, T., CURET, O. & SCATTON, B. (1986). Measurement of endogenous noradrenaline release in the rat cerebral cortex in vivo by transcortical dialysis: effects of drugs affecting noradrenergic transmission. *J. Neurochem.*, **46**, 1794–1801.

MEDGETT, I.C., MCCULLOCH, M.W. & RAND, M.J. (1978). Partial agonist action of clonidine on prejunctional and postjunctional α-adrenoceptors. *Naunyn-Schmiedebergs Arch. Pharmacol.*, **304**, 215–221.

MERMET, C., SUAUD-CHAGNY, M.F. & GONON, F. (1990). Electrically evoked noradrenaline release in the rat hypothalamic paraventricular nucleus studied by in vivo electrochemistry: autoregulation by alpha-2 receptors. *Neurosci.*, **34**, 423–432.

MULDER, A.H., DE LANGEN, C.D.J., DE REGT, V. & HOGENBOOM, F. (1978). Alpha-receptor mediated modulation of $^3$H-noradrenaline release from rat brain cortex synaptosomes. *Naunyn-Schmiedebergs Arch. Pharmacol.*, **303**, 193–196.

MURPHY, T.V. & MAJEWSKI, H. (1989). Modulation of noradrenaline release in slices of rat kidney cortex through $\alpha_1$- and $\alpha_2$-adrenoceptors. *Eur. J. Pharmacol.*, **169**, 285–295.

NAZARALI, A.J., BAKER, G.B. & BOISVERT, D.P. (1986). Analysis of clonidine in biological tissues and body fluids by gas chromatography with electron-capture detection. *J. Chromatogr.*, **380**, 393–400.

ONG, M.L., BALL, S.G. & VAUGHAN, P.F.T. (1991). Regulation of noradrenaline release from rat occipital cortex tissue chops by $\alpha_2$-adrenergic agonists. *J. Neurochem.*, **56**, 1387–1393.

SCHLICKER, E., ARMAH, B.I. & GÖTHERT, M. (1990). Central presynaptic α2-autoreceptors are involved in the blood pressure-lowering effect of moxonidine. *J. Cardiovasc. Pharmacol.*, **16**, 15–22.

STARKE, K. (1981). Presynaptic receptors. *Annu. Rev. Pharmacol. Toxicol.*, **21**, 7–30.

STARKE, K. (1987). Presynaptic α-autoreceptors. *Rev. Physiol. Biochem. Pharmacol.*, **107**, 73–146.

STARKE, K., GÖTHERT, M. & KILBINGER, H. (1989). Modulation of neurotransmitter release by presynaptic autoreceptors. *Physiol. Rev.*, **69**, 864–989.

STARKE, K. & MONTEL, H. (1973). Alpha-receptor-mediated modulation of transmitter release from central noradrenergic neurones. *Naunyn-Schmiedebergs Arch. Pharmacol.*, **279**, 53–60.

SZEMEREDI, K., KOMOLY, S., KOPIN, I.J., BAGDY, G., KEISER, H.R. & GOLDSTEIN, D.S. (1991). Simultaneous measurement of plasma and brain extracellular fluid concentrations of catechols after yohimbine administration in rats. *Brain Res.*, **542**, 8–14.

TAUBE, H.D., STARKE, K. & BOROWSKI, E. (1977). Presynaptic receptor systems on the noradrenergic neurones of rat brain. *Naunyn-Schmiedebergs Arch. Pharmacol.*, **299**, 123–141.

TIBIRIÇA, E., FELDMAN, J., MERMET, C., GONON, F. & BOUSQUET, P. (1991). An imidazoline-specific mechanism for the hypotensive effect of clonidine: a study with yohimbine and idazoxan. *J. Pharmacol. Exp. Ther.*, **256**, 606–613.

UNGERSTEDT, U. (1984). Measurement of neurotransmitter release by intracranial dialysis. In *Measurement of Neurotransmitter Release in vivo*. ed. Marsden, C.A. pp. 81–105. New York: Wiley.

VAN VELDHUIZEN, M.J.A., FEENSTRA, M.G.P., BOER, G.J. & WESTERINK, B.H.C. (1990). Microdialysis studies on cortical noradrenaline release: basic characteristics, significance of extracellular calcium and massive post-mortem increase. *Neurosci. Lett.*, **119**, 233–236.

VIZI, E.S., SOMOGYI, G.T., HARSING, L.G. & ZIMANYI, I. (1986). Release of [$^3$H]noradrenaline by $\alpha_1$-adrenoceptor agonists. *Neurochem. Res.*, **11**, 71–84.

WESTERINK, B.H.C., DAMSMA, G., ROLLEMA, H., DE VRIES, J.B. & HORN, A.S. (1987). Scope and limitations of in vivo brain dialysis: a comparison of its application to various neurotransmitter systems. *Life Sci.*, **41**, 1763–1776.

WESTERINK, B.H.C., DE BOER, P., TIMMERMAN, W. & DE VRIES, J.B. (1990). In vivo evidence for the existence of autoreceptors on dopaminergic, serotonergic, and cholinergic neurons in the brain. In *Annals New York Acad. Sci.*, Vol. 604. *Presynaptic Receptors and the Question of Autoregulation of Neurotransmitter Release*. ed. Kalsner, S. & Westfall, Th.C. pp. 492–504. New York: New York Acad. Sci.

WINTER, J.C. & RABIN, R.A. (1992). Yohimbine as a serotonergic agent: evidence from receptor binding and drug discrimination. *J. Pharmacol. Exp. Ther.*, **263**, 682–689.


*(Received January 14, 1993*
*Revised February 15, 1993*
*Accepted February 23, 1993)*

*Br. J. Pharmacol.* (1993), **109**, 661–666 © Macmillan Press Ltd, 1993

# Modification by charybdotoxin and apamin of spontaneous electrical and mechanical activity of the circular smooth muscle of the guinea-pig stomach

Keiko Suzuki, Kaoru M. Ito, Yukie Minayoshi, *Hikaru Suzuki, *Masahisa Asano & [1]Katsuaki Ito.

Department of Veterinary Pharmacology, Faculty of Agriculture, Miyazaki University, Miyazaki 889-21 and *Department of Physiology and Pharmacology, Nagoya City University Medical School, Nagoya 467, Japan

**1** The effects of charybdotoxin and apamin, putative blockers of $Ca^{2+}$-activated $K^+$ channels, on spontaneous electrical and mechanical activity of circular smooth muscle of the guinea-pig stomach antrum were examined in the presence of 1 μM tetrodotoxin and 1 μM atropine.

**2** Both charybdotoxin (> 3 nM) and apamin (> 3 nM) dose-dependently increased the amplitude of spontaneous contractions without altering their frequency. The maximum effect of charybdotoxin was much greater than that of apamin. Both toxins increased the amplitude of intracellular $Ca^{2+}$ oscillations measured with fura-2.

**3** When the extracellular $Ca^{2+}$ concentration was lowered to 1.5 mM or less, apamin did not significantly potentiate the contractions whereas charybdotoxin still potentiated them but with less potency.

**4** Charybdotoxin (30 nM) increased the amplitude of spikes and slow waves, and slightly decreased the resting membrane potential. On the other hand, apamin (100 nM) preferentially increased the slow wave amplitude with no effect on the resting membrane potential.

**5** These results suggest that both toxins affect the spontaneous contraction by modifying the electrical activity and that charybdotoxin-sensitive $K^+$ channels and apamin-sensitive ones are differently involved in the spontaneous electrical activity.

**Keywords:** Charybdotoxin; apamin; guinea-pig stomach; membrane potential; contraction; K channel; slow wave

## Introduction

Charybdotoxin (CTX), a component of the venom of the scorpion *Leiurus quinquestriatus*, is a 37 amino acid peptide with three disulphide bridges (Sugg *et al.*, 1990). It was first introduced as a selective blocker of large conductance $Ca^{2+}$-activated $K^+$ channels (BK channels) in skeletal muscle (Miller *et al.*, 1985). The blocking action of CTX on $Ca^{2+}$-activated $K^+$ channels in smooth muscles has been demonstrated in myocytes from the rabbit aorta (Talvenheimo *et al.*, 1988) and from the canine colon and stomach (Carl *et al.*, 1990a). CTX caused or potentiated contractions in many types of smooth muscles (Murray *et al.*, 1991; Suarez-Kurtz *et al.*, 1991; Ito *et al.*, 1992). Apamin is a bee venom polypeptide of 18 amino acids with two disulphide bridges (Romey *et al.*, 1984), which has been shown to block a $Ca^{2+}$-activated $K^+$ channel of small conductance (SK channel) in skeletal muscle (Blatz & Magleby, 1986). This channel may be responsible for the generation of after-hyperpolarization in some nerves (Romey *et al.*, 1984). In some types of visceral smooth muscle this toxin reversed the ATP-induced hyperpolarization to depolarization or blocked inhibitory junction potentials (Vladimirova & Shuba, 1978; Banks *et al.*, 1979; Maas & Den Hertog, 1979; Komori & Suzuki, 1986), whereas such effects were not found in other muscles (Nakao *et al.*, 1986; Lydrup, 1991). The lack of a direct contractile action of apamin has been observed in many kinds of smooth muscles (Allen *et al.*, 1986; Winquist *et al.*, 1989; Fujii *et al.*, 1990), although contraction is initiated in a few tissues (e.g. the guinea-pig taenia coli, Maas & Den Hertog, 1979). These two toxins are becoming specific tools for the study of the role of $Ca^{2+}$-activated $K^+$ channels in excitable and non-excitable cells.

Circular smooth muscle of the smooth antrum exhibits spontaneous electrical changes, which are composed of slow waves and superimposed spikes (Tomita, 1981). The involvement of $Ca^{2+}$-activated $K^+$ channels in such spontaneous activity has been suggested (Mitra & Morad, 1985; Carl *et al.*, 1990b). In this study we examined the effects of apamin and CTX on the spontaneous electrical and mechanical activity of the guinea-pig stomach antrum in order to ascertain whether some kinds of $Ca^{2+}$-activated $K^+$ channels are involved.

## Methods

The methods were those described in a previous paper (Ito *et al.*, 1992) except for the measurement of $Ca^{2+}$ transients with fura-2. The stomach antra were isolated from male guinea-pigs (200–250 g). After removing the mucosal layer, small strips of circular muscle with the longitudinal layer attached were cut to 2 mm wide and 10 mm long for tension or fura-2 experiments, or 2 mm wide and 4 mm long for microelectrode experiments. For tension experiments the muscle was suspended along the direction of the circular muscle with a basal tension of 1 g in a Magnus bath containing 5 ml Krebs solution (37°C) gassed with 95% $O_2$ and 5% $CO_2$. Isometric tension was recorded with a force-displacement transducer (Nihon-Kohden SB-1T).

Cytosolic $Ca^{2+}$ was measured with fura-2 simultaneously with tension as described by Sato *et al.* (1988). Briefly, the muscle was loaded with 5 μM fura-2/AM that had been sonicated together with 0.02% cremophore EL to increase the solubility of fura-2/AM. After loading for 4–5 h at room temperature, the preparation was placed horizontally in an organ bath constructed in a fluorimeter (JASCO CAF-100).

[1] Author for correspondence.

One end of the muscle was connected to a force-displacement transducer. A part of the muscle was excited by light through rotating filters (48 Hz) of 340 nm and 380 nm. The emitted light from the muscle was collected by a photomultiplier, and the ratio of fluorescence at 500 nm due to excitation at 340 nm and 380 nm was calculated. The time constant for the signal was set at 0.25 s.

Preparations used for microelectrode studies were mounted in a superfusion chamber (fluid volume 2 ml) and superfused with the Krebs solution (35°C) gassed with 95% $O_2$ and 5% $CO_2$. A cell was impaled from the mucosal side by a glass microelectrode filled with 3 M KCl (tip resistance 50–80 MΩ). The signal was amplified by a microelectrode amplifier (Nihon-Kohden MEZ-8101) and recorded on a pen-writing oscillograph (NEC-Sa'nei Recti-Horiz) and video cassette tape using a PCM processor (Sony PCM-501 ES). The effects of apamin and CTX were observed in the presence of 1 μM tetrodotoxin and 1 μM atropine.

The Krebs solution had the following composition (mM): NaCl 137.4, KCl 5.9, $CaCl_2$ 2.5, $MgCl_2$ 1.2, $NaHCO_3$ 15.5, $NaH_2PO_4$ 1.2 and glucose 11.5 (pH 7.4 when gassed with 5% $CO_2$). Drugs used were apamin (Sigma), charybdotoxin (CTX, Peptide Institute), cromakalim (Beecham), atropine (Tokyo Kasei) tetrodotoxin (Sankyo), acetylcholine (Tokyo Kasei), fura-2/AM (dissolved in dimethyl sulphoxide, Dojin Laboratories) and cremophore EL (Nacalai Tesque). Cromakalim was dissolved in ethanol as described elsewhere (Ito *et al.*, 1992). Other drugs were dissolved in distilled water.

Data are expressed as mean ± s.e.mean. The $pD_2$ value was calculated as described by Ito *et al.* (1992). The statistical significance was tested by Student's *t* test for paired or unpaired observations at the level of $P<0.05$.

## Results

### *Effects of charybdotoxin and apamin on the spontaneous contraction*

Figure 1 shows examples of the effects of CTX (10 nM and 30 nM) and apamin (10 nM and 100 nM) on spontaneous contractions of circular smooth muscle of the guinea-pig stomach antrum. Both toxins increased the amplitude of the spontaneous contractions without affecting their frequency. With high concentrations of CTX (100 nM or more) a slight elevation of the resting tension was observed in some muscles (e.g., in 3 of 9 preparations at 100 nM), while such an effect was rarely observed in the case of apamin. The presence of tetrodotoxin (1 μM) and atropine (1 μM) did not affect the actions of CTX and apamin, suggesting that the potentiation was not mediated by neural factors. The enhancement of contraction by CTX and apamin was dependent on the concentration (Figure 2), and also on the spontaneous contraction itself to some extent, in that, when the spontaneous contraction was small, the potentiation tended to be relatively small. Although the effect of apamin was the same at more than 10 nM, the time to peak effect was shorter with a higher concentration. The effects of both toxins were reversible if more than 1 h washing was given. The maximal potentiation of spontaneous contraction by CTX (486 ± 131% of control contraction, at 100 nM, $n=9$) was much greater ($P<0.05$, unpaired *t* test) than that by apamin (246 ± 18% at 10 nM, $n=37$).

When cromakalim was cumulatively added during the sustained enhancement due to 30 nM CTX or 100 nM apamin, it inhibited the contraction with a $pD_2$ of 6.57 ± 0.05 ($n=7$) or 6.57 ± 0.09 ($n=10$), respectively (data not shown). Cromakalim inhibited the spontaneous contraction in the absence of either toxin with a $pD_2$ of 6.65 ± 0.06 ($n=9$, Ito *et al.*, 1992).

### *Relations of mechanical effects of charybdotoxin and apamin to $Ca^{2+}$*

Cytosolic $Ca^{2+}$ in gastric smooth muscles was measured with the $Ca^{2+}$ indicator fura-2 simultaneously with the tension. As shown in Figure 3, cytosolic $Ca^{2+}$ oscillated spontaneously, accompanied by spontaneous contractions. Acetylcholine (1 μM) elevated the basal level of $Ca^{2+}$ with superimposing oscillations, resulting in development of basal tension. CTX (30 nM) increased the amplitude of $Ca^{2+}$ oscillation and contraction to 151.4 ± 10.4% and 321.7 ± 30.1% ($n=23$), re-

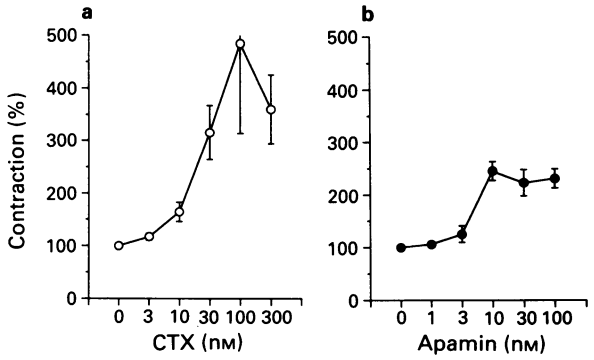



**Figure 2** Dose-response relationship for charybdotoxin (CTX)- and apamin-induced potentiations of spontaneous contraction of the guinea-pig stomach. On the ordinate scale the amplitude of spontaneous contraction just prior to application of CTX or apamin is expressed as 100%. The points are means with the s.e.mean of 7–22 preparations for CTX and 13–57 preparations for apamin.

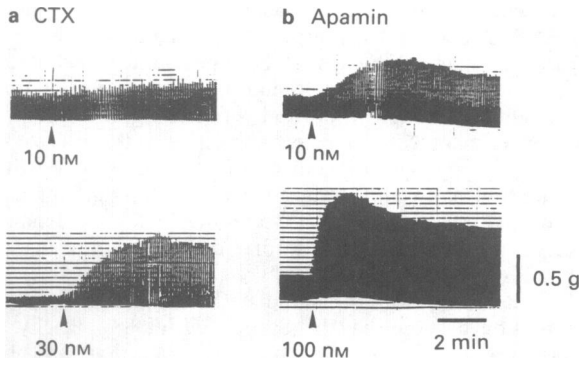



**Figure 1** Examples of the potentiating effects of charybdotoxin (CTX, 10 nM and 30 nM) and apamin (10 nM and 100 nM) on spontaneous contractions in circular smooth muscles of the guinea-pig stomach.

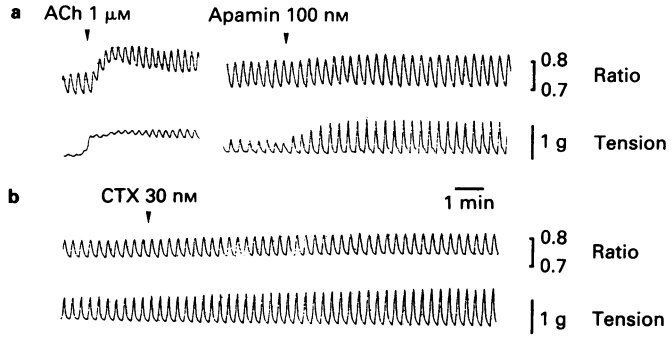



**Figure 3** Examples of the effects of acetylcholine (ACh), apamin and charybdotoxin (CTX) on cytosolic $Ca^{2+}$ levels and tension in the guinea-pig stomach loaded with fura-2. (a) Effects of acetylcholine (1 μM) and apamin (100 nM). The data were obtained from the same preparation. (b) Effects of CTX (30 nM). In (a) and (b), upper trace: fluorescence ratio, lower trace: tension.

spectively, of the control level. In some muscles, CTX slightly elevated the basal level of $Ca^{2+}$, but the elevation was much smaller than that due to acetylcholine. Apamin (100 nM) also increased the parameters to 134.9 ± 4.9% and 196.7 ± 18.5% ($n = 14$), respectively.

The spontaneous contraction of the guinea-pig stomach depended on the concentration of external $Ca^{2+}$. With decreased $Ca^{2+}$ concentrations the amplitude of spontaneous contractions decreased. The frequency of spontaneous contraction did not change until $Ca^{2+}$ was reduced to 0.5 mM when it decreased. Figure 4 shows the potentiating effects of 30 nM CTX and 100 nM apamin at various concentrations of external $Ca^{2+}$. When external $Ca^{2+}$ was 1.5 mM or less, apamin did not significantly potentiate the contraction. With lower $Ca^{2+}$ concentrations the potentiating effect of CTX decreased but was still significant.

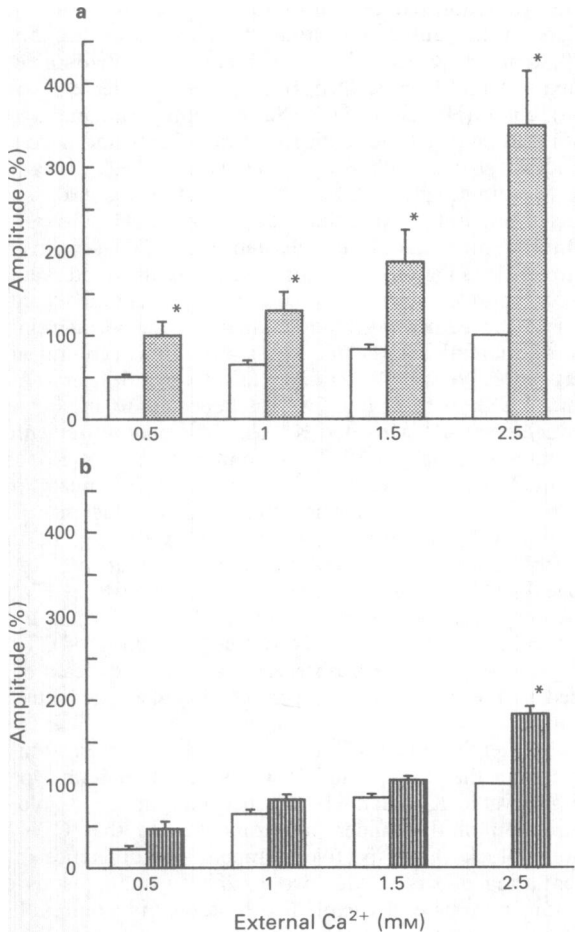



**Figure 4** Dependence of potentiation by charybdotoxin (CTX, 30 nM) and apamin (100 nM) of spontaneous contraction on external $Ca^{2+}$ concentration. The amplitude of control spontaneous contraction at 2.5 mM $[Ca^{2+}]_o$ is expressed as 100%. In (a) open columns: control; shaded columns CTX. In (b) open columns: control; shaded columns apamin. *Significantly different ($P < 0.05$) from control at the respective $[Ca^{2+}]_o$ (paired $t$ test). Data represent the mean with the s.e.mean of 8–10 preparations for CTX or 10–20 preparations for apamin.

### *Effects of charybdotoxin and apamin on the membrane potential*

Every cell in the antrum region impaled with a microelectrode exhibited slow waves with a frequency of 4–8 cycles $min^{-1}$. However, not every cell showed spike activity on the slow waves. Figures 5 and 6 show examples of the effects of 30 nM CTX and 100 nM apamin, respectively, on the membrane potential of circular smooth muscles with or without spontaneously generated spikes, and Table 1 summarizes the resulting changes in membrane potential parameters. When

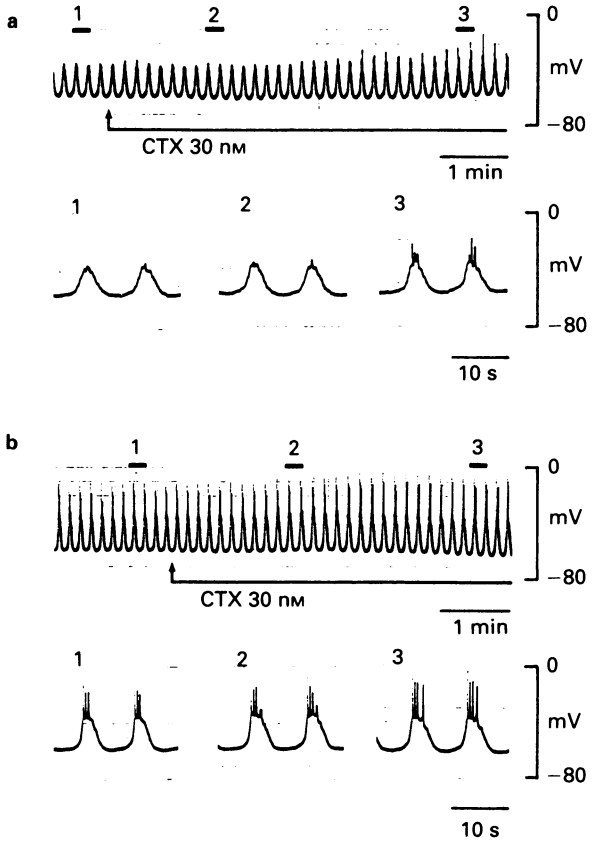



**Figure 5** Effect of 30 nM charybdotoxin (CTX) on the membrane potential of guinea-pig stomach. (a) Effects of CTX in a preparation which did not exhibit spikes on the slow waves. (b) Effects in a preparation exhibiting spikes on the slow waves. In (a) and (b) the lower panels show the recordings of the sections labelled 1, 2 and 3 in the upper panel at a faster time base.

**Table 1** Changes in electrical properties of guinea-pig stomach caused by charybdotoxin (CTX) and apamin

| *Treatment* | *Resting membrane potential* (mV) | *Slow wave amplitude* (mV) | *Slow wave frequency* ($min^{-1}$) | *Spike amplitude* (mV) |
|---|---|---|---|---|
| Control | − 68.3 ± 2.3 | 20.3 ± 3.4 | 5.7 ± 0.5 | 5.0 ± 2.4 |
| + CTX 10 nM | − 63.4 ± 3.8* | 20.8 ± 2.8 | 6.1 ± 0.3 | 8.1 ± 2.5* |
| Control | − 61.0 ± 4.3 | 20.2 ± 2.7 | 6.2 ± 0.5 | 3.6 ± 1.4 |
| + CTX 30 nM | − 56.6 ± 4.6* | 22.7 ± 3.2* | 6.2 ± 0.5 | 5.9 ± 0.5* |
| Control | − 59.8 ± 1.4 | 21.0 ± 1.5 | 6.2 ± 0.4 | 4.2 ± 1.8 |
| + Apamin 100 nM | − 58.9 ± 1.6 | 25.2 ± 1.2* | 6.2 ± 0.4 | 6.3 ± 0.4 |

*$P < 0.05$ (vs control, paired $t$ test), $n = 6$ for each group. Data are collected from the preparations which exhibited spike activity on slow waves.

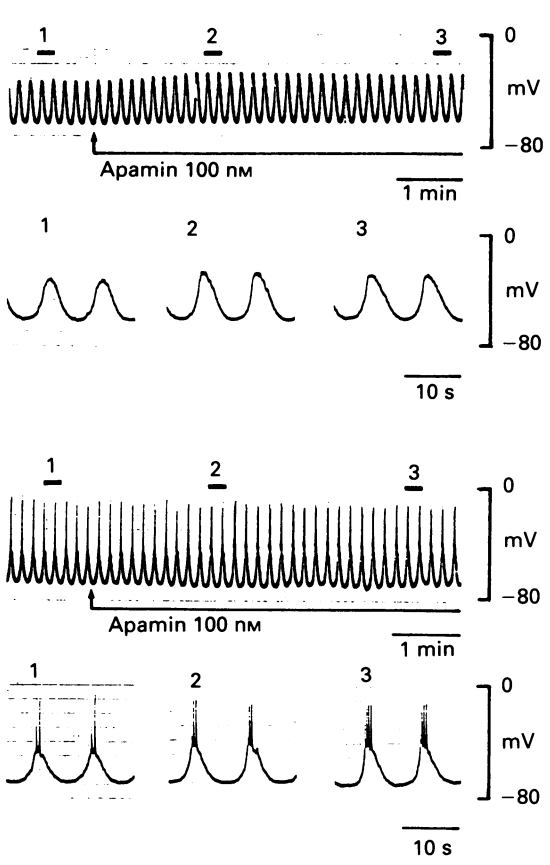



**Figure 6** Effect of 100 nM apamin on the membrane potential of guinea-pig stomach. (a) Effects of apamin in a preparation which did not exhibit spikes on the slow waves. (b) Effects in a preparation exhibiting spikes on the slow waves. In (a) and (b) the lower panels show the recordings of the sections labelled 1, 2 and 3 in the upper panel at a faster time base.

CTX was applied to cells not showing spikes, it often induced spike activity, concomitant with a slight increase in slow wave amplitude (Figure 5a). In cells showing spikes, CTX increased the amplitude and/or the number of spikes (Figure 5b). In many cells CTX decreased the resting membrane potential (maximum diastolic potential) by 3–5 mV. Lower concentration of CTX (10 nM) increased the amplitude of spikes with no effect on slow waves (Table 1).

On the other hand, apamin increased the amplitude of slow waves in either spike-generating or non-generating cells (Figure 6). No special effects on the spikes were observed (Table 1). Apamin did not alter the resting membrane potential. When a 10 times higher concentration of apamin (1 μM) was used, the effects were the same as with the 100 nM apamin (3 observations, data not shown).

## Discussion

In this study CTX and apamin enhanced the spontaneous contractions of the circular smooth muscle of the guinea-pig stomach. This enhancement resulted from an increase in the amplitude of intracellular $Ca^{2+}$ oscillations. Observations showing that apamin did cause or potentiate contraction in smooth muscles under physiological conditions are very rare (Maas & Den Hertog, 1979). This indicates that apamin-sensitive $K^+$ channels are not functional in most types of smooth muscle and the guinea-pig stomach is a rare example of a tissue in which these channels are involved in spontaneous activity. The fact that apamin inhibited ATP-induced hyperpolarization and the inhibitory junction potential in the guinea-pig stomach (Vladimirova & Shuba, 1978; Komori & Suzuki, 1986) supports the view that apamin-sensitive $K^+$ channels exist in this tissue.

Although small conductance $Ca^{2+}$-activated $K^+$ channels have been found in the rabbit portal vein (Inoue *et al.*, 1985), taenia coli (Hu *et al.*, 1989) and jejunum, and the guinea-pig mesenteric artery (Benham *et al.*, 1986), the channel conductance (63–92 pS) is still larger than that of the apamin-sensitive SK channel found in skeletal muscle (10–14 pS, Blatz & Magleby, 1986), and the sensitivity to apamin was not tested in smooth muscles. Therefore, the existence of $Ca^{2+}$-activated $K^+$ channels which are sensitive to apamin should be demonstrated by a patch clamp study. Since apamin antagonized responses to putative inhibitory transmitters in the guinea-pig stomach (Vladimirova & Shuba, 1978; Komori & Suzuki, 1986), taenia coli (Vladimirova & Shuba, 1978; Maas & Den Hertog, 1979; Wier & Weston, 1986), colon (Hugues *et al.*, 1982) or ileum (Yamanaka *et al.*, 1985) but showed no action in vascular smooth muscles (Winquist *et al.*, 1989; Brayden & Nelson, 1992), it is likely that apamin-sensitive $K^+$ channels exist in visceral smooth muscles but not in vascular smooth muscles.

On the other hand, the existence of CTX-sensitive $K^+$ channels is suggested in both non-vascular and vascular smooth muscles since CTX caused or potentiated contractions of the guinea-pig bladder, taenia coli, portal vein and uterus (Suarez-Kurtz *et al.*, 1991), the rabbit cerebral artery (Brayden & Nelson, 1992) and the rat carotid artery (Asano *et al.*, 1992). Although CTX was reported to inhibit small conductance $Ca^{2+}$-activated $K^+$ channels in *Aplysia* neurones (Herman & Erxleben, 1987) or voltage-dependent $K^+$ channels in T-lymphocytes (Deutsch *et al.*, 1991), many patch clamp studies have confirmed that large conductance $Ca^{2+}$-activated $K^+$ channels are sensitive to CTX e.g. in single smooth muscle cells from stomach (Carl *et al.*, 1990a), trachealis (Murray *et al.*, 1991) and vascular tissues (Talvenheimo *et al.*, 1988; Pavenstadt *et al.*, 1991; Brayden & Nelson, 1992). Therefore, it is likely that the effects of CTX on the guinea-pig stomach observed in this study can be ascribed to the block of large conductance $Ca^{2+}$-activated $K^+$ channels.

The potentiation by CTX of spontaneous contraction was larger than that by apamin. If we assume that both types of $Ca^{2+}$-activated $K^+$ channel are functioning in a physiological contraction of the guinea-pig stomach, and that CTX and apamin block the respective channels, the difference in the potentiating effects of the two toxins on spontaneous contractions may be easily explained by the conductances. If the $Ca^{2+}$ concentration of the external medium ($[Ca^{2+}]_o$) was lowered, the cytoplasmic $Ca^{2+}$ concentration would be expected to decrease, and the activity of $Ca^{2+}$-activated $K^+$ channels will be reduced. The reduced potentiation by CTX and apamin at low $[Ca^{2+}]_o$ indicates that the action of these toxins is associated with $Ca^{2+}$-activated $K^+$ channels. Apamin did not significantly increase the contraction at 1.5 mM $Ca^{2+}$ or less, whereas, CTX significantly potentiated it even at 0.5 mM $Ca^{2+}$. The small conductance $Ca^{2+}$-activated $K^+$ channel in skeletal muscles is more sensitive to $Ca^{2+}$ than the large conductance channel (Blatz & Magleby, 1986). If the apamin-sensitive $K^+$ channel in the guinea-pig stomach is also more sensitive to $Ca^{2+}$ than the CTX-sensitive one, the apamin-induced potentiation of contractions should have been observed at lower $Ca^{2+}$ concentrations than for the CTX-effect. The significant potentiation by CTX but not by apamin at low $Ca^{2+}$ concentrations appears contradictory. However, the conductance of BK channels is 5–10 times larger than that of SK channels (Cook, 1988). Therefore, an alternative explanation for the lack of potentiation at low $Ca^{2+}$ concentration by apamin could be because of the small conductance of the channel.

The effects of CTX and apamin on the membrane potential were tested at 30 nM and 100 nM which enhanced spontaneous contractions by 316 ± 52% ($n = 22$) and 231 ± 18%

($n = 57$), respectively. CTX and apamin had different effects on the electrical activity of guinea-pig stomach. The predominant effect of apamin was an increase in the slow wave amplitude, while CTX increased the amplitudes of both spikes and slow waves. At a lower concentration (10 nM) CTX affected the amplitude of the spikes but not the slow waves. The increase in slow wave amplitude by apamin was greater than that by CTX. Some studies suggest that large conductance $Ca^{2+}$-activated $K^+$ channels show voltage-dependency, such that the open probability of the channel increases at a less negative voltage (Benham *et al.*, 1986; Singer & Walsh, 1987; Toro *et al.*, 1991). Therefore, it is possible that large conductance $Ca^{2+}$-activated $K^+$ channels play a more significant role in the spike phase than the slow wave phase, which would account for the fact that the CTX-effect appears more noticeably on spikes. On the assumption that the CTX-sensitive $K^+$ channel has a large conductance, the blockade by CTX of such a channel would remove the large offsetting effect of $Ca^{2+}$-activated $K^+$ channels on $Ca^{2+}$ channels, thus permitting greater $Ca^{2+}$ entry and resulting in a considerable potentiation of contraction.

## References


ALLEN, S.L., BOYLE, J.P., CORTIJO, J., FOSTER, R.W., MORGAN, G.P. & SMALL, R.C. (1986). Electrical and mechanical effects of BRL34915 in guinea-pig isolated trachealis. *Br. J. Pharmacol.*, **89,** 395–405.

ASANO, M., MASUZAWA, K., MATSUDA, T. & ITO, K. (1992). Increased function of $Ca^{2+}$-activated $K^+$ channels in the resting state of carotid arteries from spontaneously hypertensive rats. *Jpn. J. Pharmacol.*, **58,** Suppl. II, 396P.

BANKS, B.E.C., BROWN, C., BURGESS, G.M., BURNSTOCK, G., CLARET, M., COCKS, T.M. & JENKINSON, D.H. (1979). Apamin blocks certain neurotransmitter-induced increases in potassium permeability. *Nature*, **282,** 415–417.

BENHAM, C.D., BOLTON, T.B., LANG, R.J. & TAKEWAKI, T. (1986). Calcium-activated potassium channels in single smooth muscle cells of rabbit jejunum and guinea-pig mesenteric artery. *J. Physiol.*, **371,** 45–67.

BLATZ, A.L. & MAGLEBY, K.L. (1986). Single apamin-blocked Ca-activated $K^+$ channels of small conductance in cultured rat skeletal muscle. *Nature*, **323,** 718–720.

BRAYDEN, J.E. & NELSON, M.T. (1992) Regulation of arterial tone by activation of calcium-dependent potassium channels. *Science*, **256,** 532–535.

CARL, A., GARCIA, M.L., KENYON, J.L. & SANDERS, K.M. (1990a). Block of $Ca^{2+}$-activated K channels in smooth muscle from canine GI-tract by charybdotoxin. *Biophys. J.*, **57,** 507a.

CARL, A., MCHALE, N.G., PUBLICOVER, N.G. & SANDERS, K.M. (1990b). Participation of $Ca^{2+}$-activated $K^+$ channels in electrical activity of canine gastric smooth muscle. *J. Physiol.*, **429,** 205–221.

COOK, N.S. (1988). The pharmacology of potassium channels and their therapeutic potential. *Trends Pharmacol. Sci.*, **9,** 21–28.

DEUTSCH, C., PRICE, M., LEE, S., KING, V.F. & GARCIA, M.L. (1991). Characterization of high affinity binding sites for charybdotoxin in human T lymphocytes. Evidence for association with the voltage-gated $K^+$ channel. *J. Biol. Chem.*, **266,** 3668–3674.

FUJII, K., FOSTER, C.D., BRADING, A.F. & PAREKH, A.B. (1990). Potassium channel blockers and the effects of cromakalim on the smooth muscle of the guinea-pig bladder. *Br. J. Pharmacol.*, **99,** 779–785.

HERMANN, A. & ERXLEBEN, C. (1987). Charybdotoxin selectively blocks small Ca-activated K channels in *Aplysia* neurons. *J. Gen. Physiol.*, **90,** 27–47.

HU, S.L., YAMAMOTO, Y. & KAO, C.Y. (1989). The $Ca^{2+}$-activated $K^+$ channel and its functional roles in smooth muscle cells of guinea pig taenia coli. *J. Gen. Physiol.*, **94,** 833–847.

HUGUES, M., DUVAL, D., SCHMID, H., KITABGI, P., LAZDUNSKI, M. & VINCENT, J.-P. (1982). Specific binding and pharmacological interactions of apamin, the neurotoxin from bee venom, with guinea pig colon. *Life Sciences*, **31,** 437–443.

INOUE, R., KITAMURA, K. & KURIYAMA, H. (1985). Two Ca-dependent K-channels classified by the application of tetraethylammonium distribute to smooth muscle membranes of the rabbit portal vein. *Pflügers Arch.*, **405,** 173–179.

ITO, K., KANNO, T., SUZUKI, K., MASUZAWA-ITO, K., TAKEWAKI, T., OHASHI, H., ASANO, M. & SUZUKI, H. (1992). Effects of cromakalim on the contraction and the membrane potential of the circular smooth muscle of guinea-pig stomach. *Br. J. Pharmacol.*, **105,** 335–340.

KOMORI, K. & SUZUKI, H. (1986). Distribution and properties of excitatory and inhibitory junction potentials in circular muscle of the guinea-pig stomach. *J. Physiol.*, **370,** 339–355.

LYDRUP, M.-L. (1991). Role of $K^+$ channels in spontaneous electrical and mechanical activity of smooth muscle in the guinea-pig mesotubarium. *J. Physiol.*, **433,** 327–340.

MAAS, A.J.J. & DEN HERTOG, A. (1979). The effect of apamin on the smooth muscle cells of the guinea-pig taenia coli. *Eur. J. Pharmacol.*, **58,** 151–156.

MILLER, C., MOCZDLOWSKI, E., LATTORE, R. & PHILLIPS, M. (1985). Charybdotoxin, a protein inhibitor of single $Ca^{2+}$-activated $K^+$ channels from mammalian skeletal muscle. *Nature*, **313,** 316–318.

MITRA, R. & MORAD, M. (1985). $Ca^{2+}$ and $Ca^{2+}$-activated $K^+$ channels from mammalian gastric smooth muscles. *Science*, **229,** 269–272.

MURRAY, M.A., BERRY, J.L., COOK, R.W., FOSTER, R.W., GREEN, K.A. & SMALL, R.C. (1991). Guinea-pig isolated trachealis: the effects of charybdotoxin on mechanical activity, membrane potential changes and the activity of plasmmalemmal $K^+$-channels. *Br. J. Pharmacol.*, **103,** 1814–1818.

NAKAO, K., INOUE, R., YAMANAKA, K. & KITAMURA, K. (1986). Actions of quinidine and apamin on after-hyperpolarization of the spike in circular muscle cells of the guinea-pig ileum. *Naunyn-Schmied. Arch. Pharmacol.*, **334,** 508–513.

PAVENSTADT, H., LINDEMAN, S., LINDEMAN, V., SPATH, M., KUNZELMANN, K. & GREGER, R. (1991). Potassium conductance of smooth muscle cells from rabbit aorta in primary culture. *Pflügers Arch.*, **419,** 57–68.

ROMEY, G., HUGUES, M., SCHMID-ANTOMARCHI, H. & LAZDUNSKI, M. (1984). Apamin: a specific toxin to study a class of $Ca^{2+}$-dependent $K^+$ channels. *J. Physiol. Paris*, **79,** 259–264.

SATO, K., OZAKI, H. & KARAKI, H. (1988). Changes in cytosolic calcium level in vascular smooth muscle strip measured simultaneously with contraction using fluorescent calcium indicator fura 2. *J. Pharmacol. Exp. Ther.*, **246,** 294–300.

SINGER, J.J. & WALSH, J.V.Jr. (1987). Characterization of calcium-activated potassium channels in single smooth muscle cells using the patch-clamp technique. *Pflügers Arch.*, **408,** 98–101.

SUAREZ-KURTZ, G., GARCIA, M.L. & KACZOROWSKI, G.J. (1991). Effects of charybdotoxin and iberiotoxin on the spontaneous motility and tonus of different guinea pig smooth muscle tissues. *J. Pharmacol. Exp. Ther.*, **269,** 439–443.

SUGG, E.E., GARCIA, M.L., REUBEN, J.P., PATCHETT, A.A. & KACZOROWSKI, G.J. (1990). Synthesis and structural characterization of charybdotoxin, a potent peptidyl inhibitor of the high conductance $Ca^{2+}$-activated $K^+$ channel. *J. Biol. Chem.*, **265,** 18745–18746.

TALVENHEIMO, J.A., LAM, G. & GELBAND, C. (1988). Charybdotoxin inhibits the 250pS $Ca^{2+}$-activated $K^+$ channel in aorta and contracts aorta smooth muscle. *Biophys. J.*, **53,** 258a.

TOMITA, T. (1981). Electrical activity (spikes and slow waves) in gastrointestinal smooth muscles. In *Smooth Muscle: an Assessment of Current Knowledge.* ed. Bülbring, E., Brading, A., Jones, A.W. & Tomita, T. pp. 127–156. London: E. Arnold.

TORO, L., VACA, L. & STEFANI, E. (1991). Calcium-activated potassium channels from coronary smooth muscle reconstituted in lipid bilayers. *Am. J. Physiol.*, **260,** H1779–H1789.

VLADIMIROVA, I.A. & SHUBA, M.F. (1978). Effect of strychnine, hydrastine, and apamin on synaptic transmission in smooth muscle cells. *Neurofiziologia*, **10,** 295–299.

WIER, S.W. & WESTON, A.H. (1986). Effect of apamin on responses to BRL 34915, nicorandil and other relaxants in the guinea-pig taenia caeci. *Br. J. Pharmacol.*, **88,** 113–120.

WINQUIST, R.J., HEANEY, L.A., WALLACE, A.A., BASKIN, E.P., STEIN, R.B., GARCIA, M.L. & KACZOROWSKI, G.J. (1989). Glyburine blocks the relaxation responses to BRL 34915 (cromakalim), minoxidil sulfate and diazoxide in vascular smooth muscle. *J. Pharmacol. Exp. Ther.*, **248,** 149–156.

YAMANAKA, K., FURUKAWA, K. & KITAMURA, K. (1985). The different mechanisms of action of nicorandil and adenosine triphosphate on potassium channels of circular smooth muscle of the guinea-pig small intestine. *Br. J. Pharmacol.*, **331,** 96–103.

*(Received February 1, 1993*
*Accepted February 25, 1993)*

*Br. J. Pharmacol.* (1993), **109**, 667–672 © Macmillan Press Ltd, 1993

# Cellular mechanism of the positive inotropic effect of hydralazine in mammalian myocardium

David G. Hurrell, Cynthia L. Perreault, Lin Miao, Bernard J. Ransil & [1]James P. Morgan

The Charles A. Dana Research Institute and the Harvard-Thorndike Laboratories of the Beth Israel Hospital and the Department of Medicine (Cardiovascular Division), Harvard Medical School, Boston, MA, U.S.A.

**1** The purpose of this study was to elucidate the cellular mechanism of the positive inotropic effect of hydralazine, a vasodilator widely used for afterload reduction in patients with heart failure that has also been reported to have positive inotropic effects on the heart. After isolation, right ventricular papillary muscles from the ferret were maintained in bicarbonate-buffered salt solution (30°C). A concentration-response relationship was obtained for hydralazine ($10^{-6}$ to $10^{-3}$ M). In order to mimic different levels of catecholamine release found in heart failure, we utilized two methods of stimulation: (a) threshold punctate pulses and (b) suprathreshold punctate stimulation with voltage approximately 10% above threshold.

**2** In a first group of muscles ($n = 16$), a maximally effective concentration of hydralazine ($10^{-3}$ M) increased peak isometric tension by $39 \pm 9\%$ ($P<0.05$). Doses lower than $10^{-5}$ M had no significant effect. The bioluminescent $Ca^{2+}$ indicator, aequorin, was loaded into a subset of these muscles ($n = 7$). A significant increase in peak light (i.e., intracellular $Ca^{2+}$) developed, concurrently with an increase in peak tension ($38 \pm 5\%$ to $66 \pm 8\%$). This inotropic response was associated with a decrease in time to peak tension (ms), $221 \pm 7$ to $186 \pm 5$ ($P<0.05$), and time to peak light, $65 \pm 4$ to $52 \pm 2$ ($P<0.05$). These effects were markedly attenuated by pretreatment with autonomic blocking agents.

**3** In a second group of muscles ($n = 12$), histamine was used to stimulate cyclic AMP production in the presence of propranolol. Hydralazine ($3 \times 10^{-4}$ M) led to a shift in the $pD_2$ (i.e. the negative log of the concentration of histamine producing 50% of the maximal response) from $6.1 \pm 0.1$ to $5.9 \pm 0.1$ ($P<0.05$), thus increasing the sensitivity of the muscles to histamine. Hydralazine also increased maximum tension from $160 \pm 77\%$ to $195 \pm 57\%$ ($P<0.05$) above baseline. Thus, hydralazine altered the potency and efficacy of histamine despite the presence of β-adrenoceptor blockade.

**4** A third group of muscles were chemically skinned to examine the effects of hydralazine on myofilament $Ca^{2+}$ responsiveness. Pretreatment of ferret papillary muscles with hydralazine ($10^{-3}$ M) before skinning did not shift the force-pCa curve after skinning ($n = 16$). However, hydralazine added to previously skinned fibres desensitized the myofilaments, as indicated by a rightward shift of the force-pCa curve ($n = 12$). Maximum tension development was not changed.

**5** The pharmacological effects of hydralazine are characteristic of inotropic drugs that act mainly via cyclic AMP; however, the increase in peak tension demonstrated with histamine in the presence of hydralazine also suggests an effect on cyclic AMP-independent second messenger pathways. These data are consistent with reports that large doses of hydralazine may increase cellular levels of cyclic AMP, as well as other second messengers, by direct cardiac and indirect neuronal mechanisms.

**Keywords:** Aequorin; calcium indicators; hydralazine; heart failure; calcium activation; histamine; inotropic agents

## Introduction

Congestive heart failure is a disease that affects millions of people worldwide, and its associated mortality has gone nearly unabated despite modern therapy (Smith, 1985). Encouraging results have been reported in clinical trials using hydralazine and isosorbide dinitrate to prolong survival in patients with mild-to-moderate heart failure (V-Heft I and V-Heft II; Cohn *et al.*, 1986; 1991). While the major benefit of hydralazine is generally believed to be mediated through its vasodilator action, the drug may also elicit positive inotropic and chronotropic responses in both animal models and man (Gershwin *et al.*, 1967; Khatri *et al.*, 1977; Leier *et al.*, 1980). Moreover, a positive inotropic response to hydralazine can be demonstrated under conditions in which the rate of myocardial contraction is held constant (Rabinowitz, 1986; Azuma *et al.*, 1987). The mechanism of the inotropic effect of hydralazine remains incompletely defined, as does the role inotropy may play in the improved survival demonstrated in these trials. Unfortunately, the PROMISE trial, a large clinical study of 1088 patients, has demonstrated that the inotropic agent milrinone, a phosphodiesterase inhibitor, leads to increased mortality in patients with moderate-to-severe congestive heart failure (Packer *et al.*, 1991). Therefore, the mechanism by which an inotropic agent mediates its effect may be important in establishing its clinical utility.

Studies have suggested the positive inotropic effect of hydralazine is dependent upon the β-adrenoceptor and is completely abolished by propranolol and reserpine (Rabinowitz *et al.*, 1986; Rendig *et al.*, 1988). Specifically, Rabinowitz *et al.* (1986) and Saegusa *et al.* (1986) proposed that hydralazine stimulates release of catecholamines from the adrenergic nerve endings. Hydralazine may also inhibit phosphodiesterase activity in some concentrations (Ishii *et al.*, 1979). In total, this research suggests that hydralazine may exert its positive inotropic effect via an adenosine 3′:5′-cyclic monophosphate (cyclic AMP)-dependent mechanism. Additionally, cyclic AMP-independent mechanisms have also been suggested. Azuma *et al.* (1987) found the inotropic response was only partially inhibited by propranolol and concluded that hy-

[1] Author for correspondence at: Cardiovascular Division, Beth Israel Hospital, 330 Brookline Ave., Boston, MA 02215, U.S.A.

dralazine may act on the slow $Ca^{2+}$ channels to stimulate $Ca^{2+}$ influx.

The purpose of the present study was to define the mechanism of the positive inotropic response to hydralazine by elucidating its effect on intracellular calcium ($Ca^{2+}$) regulation, its interaction with both intrinsic catecholamines and histamine, and its direct effects on the myofilaments. Our results provide new information about the actions of hydralazine on intracellular $Ca^{2+}$ modulation and myofilament $Ca^{2+}$ responsiveness.

## Methods

### *Muscle preparation*

Papillary muscles of $< 1.0$ mm in diameter were excised from the right ventricle of adult male ferrets, 12–14 weeks old, under chloroform anaesthesia. The methods have been described in detail by Gwathmey & Morgan (1985); Mackinnon *et al.* (1988) and Kihara *et al.* (1989). The muscles were removed from the hearts and then placed in a physiological salt solution bubbled with a gaseous mixture of 95% $O_2$ and 5% $CO_2$ to pH 7.4. The experiments were performed at 30°C. The muscles were stimulated to contract at 0.33 Hz with pulses of 5 ms duration and threshold voltage applied via punctate electrodes at the base. An equilibrium period was allowed during which time the muscles were stretched until maximal isometric force developed ($L_{max}$). We used two stimulation protocols: (1) threshold punctate stimulation; and (2) suprathreshold punctate stimulation with voltage approximately 10% above threshold (Blinks, 1966). This level of voltage produces significant catecholamine release in the ferret papillary muscle preparation (Perreault *et al.*, 1990b) as a means to mimic the elevated catecholamine states found in heart failure. Since it was possible to obtain up to four papillary muscles per ferret, our $n$ reflects the number of muscles, not the number of ferrets.

### *Intact muscle studies*

Sixteen intact ferret papillary muscles were studied. As defined above, suprathreshold punctate stimulation was performed. Cumulative concentration-response relationships were obtained for hydralazine ($10^{-6}$ to $10^{-3}$ M). The β-adrenoceptor antagonist, propranolol ($6 \times 10^{-7}$ M) was added to the organ bath and allowed to equilibrate. Of particular importance to the present study is the effect of this dose of propranolol on the release of catecholamines from sympathetic nerve endings in the papillary muscles used in our experiments. Blinks (1966) and Perreault *et al.* (1990) have demonstrated that the response to maximal sympathetic nerve stimulation via field pulses can produce the same maximal response as exogenously applied catecholamines. We have performed six additional experiments in which field pulses were applied at increasing voltage (2–12 V) until a maximal response was obtained. Propranolol ($6 \times 10^{-7}$ M) decreased the response to field stimulation at all voltages and depressed the maximal response by 5%. In the 2–4 V stimulation range (similar to the punctate voltage levels used to stimulate the muscles) no significant response to field pulses was observed with propranolol present in the bath. These data indicate that the dose of propranolol used in these experiments was adequate to minimize catecholamine release as a confounding variable with regard to interpreting our results. Hydralazine concentration-response relationships were then repeated. All measurements of peak tension were taken under steady-state conditions.

In a second set of fibres ($n = 7$) the bioluminescent $Ca^{2+}$ indicator, aequorin, was loaded by macroinjection, as described in detail elsewhere (Kihara & Morgan, 1989). Light signals were recorded with a photomultiplier by means of a light collecting apparatus designed by Blinks (1982). Once steady state was obtained, it was necessary to average successive signals in order to obtain a satisfactory signal-to-noise ratio. The light signal was measured in nanoamperes of anode current and passed through a filter with a 10 ms time constant. Tension, light, and the stimulus artefact were recorded simultaneously on strip chart paper and magnetic tape. A concentration-response relationship was obtained for hydralazine in the absence and presence of propranolol ($6 \times 10^{-7}$ M), atropine ($2 \times 10^{-6}$ M), and phentolamine ($1 \times 10^{-6}$ M). Measurements were obtained for peak light and peak tension and time to peak light and tension.

In a third set of fibres ($n = 12$), we tested whether the inotropic response to hydralazine was independent of catecholamine release. We used histamine to stimulate cyclic AMP production via the $H_2$ receptor (Johnson, 1980), thus independently of catecholamine receptors. Muscles were allowed to reach baseline in the presence of propranolol ($6 \times 10^{-7}$ M) and a concentration-response relationship was obtained to histamine ($10^{-8}$ to $10^{-5}$ M). This was repeated in the presence of hydralazine ($3 \times 10^{-4}$ M) plus propranolol ($6 \times 10^{-7}$ M).

Data analysis of intact muscles was conducted using the Wilcoxon Signed Rank Test to determine paired significance. Statistical significance was set at $P < 0.05$.

### *Skinned muscle studies*

Muscles were chemically skinned by a 30 min exposure to a solution of the following composition (mM): imidazole 60, KCl 60, EGTA 5, $MgCl_2$ 7, $K_2ATP$ 5, saponin 250 μg $ml^{-1}$, pH 7.1 at 21°C. Saponin in this concentration has been shown to remove both the sarcolemma and sarcoplasmic reticulum (Endo & Iino, 1980). The relaxing and activating solutions contained 10 mM EGTA and had a pMgATP of 2.5, pMg of 2.5, and a pH adjusted to 7.1 with KOH in the presence of 30 mM TES. The skinning, relaxing and activating solutions all contained creatine phosphokinase, 15 u $ml^{-1}$, and creatine phosphate, 12 mM, as an ATP regenerating system. The total salt concentrations necessary for obtaining the desired pCa, pMg, and pMgATP at a constant ionic strength of 0.16 M were calculated according to a programme developed by Fabiato & Fabiato (1979). The absolute stability constants used were as reported by Fabiato (1981). In order to study any sustained effect of hydralazine treatment, a group of muscles ($n = 16$) was pretreated with hydralazine ($10^{-3}$ M) and allowed to reach baseline. Equilibrium was attained and these muscles were exposed to increasing calcium in a stepwise fashion, but without the further addition of hydralazine. In a second group of muscles ($n = 12$), skinning was performed first, followed by relaxation-activation cycles obtained by increasing the calcium in a stepwise fashion, with and without hydralazine ($10^{-3}$ M). In half of these muscles a relaxation-activation cycle was performed first, followed by control. There were no significant differences noted in the $pCa_{50}$, $F_{max}$, or $n$ obtained by this method.

Data analysis was performed by the Hill equation for the dependency of force on free calcium:

$$F = F_{max}\ ([Ca^{2+}]^n/Q + [Ca^{2+}]^n) \times 100\%$$

where Q is an effective dissociation constant (Segel, 1975), F if the developed force (i.e., isometric force), $F_{max}$ is the maximal force developed (100%), and $n$ is proportional to the slope of the force versus $\log[Ca^{2+}]$ curve when $F = 1/2F_{max}$, the calcium concentration required for 50% maximal force development ($pCa_{50}$) is given by: $pCa_{50} = -(\log Q)/n$ (Segel, 1975; Perreault *et al.*, 1990a).

The data were fitted to a modified Hill equation of the form:

$$F = F_{max}/1 + 10^{\log Q - n\log[Ca^{2+}]}$$

This calculation was performed using MLAB, a general non-linear regression package available in the NIH-sponsored PROPHET data analysis system. The curve fit parameters n and $pCa_{50}$ were calculated for each individual curve from the above modified Hill equation and their means were compared by paired and unpaired $t$ test where appropriate. Statistical significance was set at $P < 0.05$.

### *Drugs*

Hydralazine, histamine, atropine, and propranolol were obtained from Sigma Chemical Company, St. Louis, Missouri, U.S.A. and dissolved in water. Phentolamine was purchased from Ciba-Geigy Corp., Summit, N.J., U.S.A. Aequorin was purchased from Dr J.R. Blinks of Friday Harbor, Washington, U.S.A.

## Results

### *Effects of hydralazine on the amplitude and time course of the contraction and $Ca^{2+}$ transient*

Table 1 presents the effects of increasing concentrations of hydralazine on the tension response and the $[Ca^{2+}]_i$ transient recorded with aequorin. In these experiments, the muscles were stimulated to contract at suprathreshold voltage to stimulate catecholamine release from the sympathetic nerve endings, which produced approximately a 10% increase in peak tension above levels produced by threshold punctate stimulation. Concentration-response relationships are presented for both peak tension and peak light in Table 1. Hydralazine ($10^{-3}$ M) caused a $39 \pm 9\%$ increase in peak tension from baseline ($2.5 \pm 0.4$ g to $3.5 \pm 0.5$ g; $P < 0.05$). This change in tension was associated with a significant increase in peak light. This increase in peak light is reflective of an increase in $[Ca^{2+}]_i$ transients in parallel with peak tension. A similar trend was present at lower concentrations, as well (Table 1), but did not reach statistical significance. Table 1 also provides data on the time courses for both peak tension and peak light. Both time to peak tension and time to peak light were signficantly abbreviated at maximally effective inotropic concentrations of hydralazine. Figure 1 displays an experimental recording of both the light and tension responses for control and hydralazine-treated muscles over several concentrations ($10^{-5}$ to $10^{-3}$ M) and the paired response in the presence of autonomic blockers. With the addition of propranolol, phentolamine, and atropine as well as hydralazine, over several concentrations, produced no significant increase in peak tension or peak light and the time courses of tension and light were not altered.

### *Histamine stimulated inotropic effects of hydralazine*

Following the observation that hydralazine increases the maximum isometric tension produced by suprathreshold stimulation, we explored whether this response was dependent upon catecholamine release. Propranolol alone has been shown to attenuate markedly the positive inotropic effects of hydralazine. Therefore, after β-adrenoceptor blockade with propranolol ($6 \times 10^{-7}$ M), histamine was added in increasing concentrations ($10^{-8}$ to $10^{-5}$ M). Histamine stimulation in the presence of hydralazine ($3 \times 10^{-4}$ M) shifted the $pD_2$ (i.e. the negative log of the concentration of histamine producing 50% of the maximal response) from $5.9 \pm 0.1$ to $6.1 \pm 0.1$ ($P < 0.05$). It was also noted that the maximum response to histamine in control fibres was $160 \pm 23\%$ above baseline stimulation while hydralazine treatment ($3 \times 10^{-4}$ M) produced an additional increase to $195 \pm 17\%$ in the same muscles ($P < 0.05$). As shown in Table 1, the dose of hydralazine would not be expected to increase tension development of propranolol-blocked muscles in the absence of histamine stimulation.

### *Effects of hydralazine on myofilament $Ca^{2+}$ responsiveness*

To determine what effect, if any, hydralazine has on myofilament $Ca^{2+}$ responsiveness, which includes calcium sensitivity, maximal calcium-activated force, and the slope of the calcium-force relationship, we examined the effects of the drug in skinned muscle preparations.

An experimental tracing is presented in Figure 2. Pretreatment with hydralazine did not shift the force-pCa relationship at the calcium concentration required for 50% maximal force development ($pCa_{50}$), nor did it significantly alter the maximal amount of force that a muscle could generate in the presence of calcium, $F_{max}$ (Table 2). The Hill coefficient (n), which reflects the slope of the fit at $pCa_{50}$, was not altered by pretreatment with hydralazine. However, hydralazine ($10^{-3}$ M) added after skinning had been performed, decreased the sensitivity of the myofilaments to calcium. The force-pCa curve was shifted to the right at the $pCa_{50}$ ($P < 0.05$). While there was a similar trend in the $pCa_{50}$ with $3 \times 10^{-6}$ M hydralazine, it was not statistically significant (data not shown). The Hill coefficient (n) was not altered by hydralazine. Maximal calcium-activated force, $F_{max}$, also was not significantly altered in the presence of hydralazine. Figure 3 depicts curves obtained from the $pCa_{50}$ and n as calculated from the modified Hill equation for all three sets of data.

## Discussion

The most important findings of our study include: (1) the mechanism of the positive inotropic effect of hydralazine is

**Table 1** Effects of hydralazine on aequorin-loaded ferret papillary muscles stimulated with suprathreshold punctate voltage

| | | *Hydralazine* (M) | | | |
|---|---|---|---|---|---|
| | | 0 | $10^{-5}$ | $10^{-4}$ | $10^{-3}$ |
| PT (%; $n = 16$) | Pre | $59 \pm 4$ | $60 \pm 4$ | $68 \pm 3$ | $78 \pm 3$* |
| | Post | $47 \pm 3$ | $44 \pm 3$ | $48 \pm 3$ | $52 \pm 2$ |
| PL (%; $n = 7$) | Pre | $38 \pm 5$ | $44 \pm 8$ | $45 \pm 7$ | $66 \pm 8$* |
| | Post | $26 \pm 4$ | $24 \pm 3$ | $22 \pm 4$ | $25 \pm 3$ |
| tPt (ms; $n = 7$) | Pre | $221 \pm 7$ | $208 \pm 10$ | $208 \pm 9$* | $186 \pm 5$* |
| | Post | $196 \pm 4$ | $203 \pm 6$ | $204 \pm 4$ | $208 \pm 5$ |
| tPL (ms; $n = 7$) | Pre | $65 \pm 4$ | $60 \pm 5$ | $56 \pm 3$ | $52 \pm 2$* |
| | Post | $56 \pm 5$ | $57 \pm 5$ | $57 \pm 2$ | $56 \pm 3$ |

Data shown are mean ± s.e.mean. % = % of maximal response to $Ca^{2+}$; absolute maximal response to hydralazine in the absence of adrenoceptor blockers was from $2.5 \pm 0.4$ g to $3.5 \pm 0.5$ g. PT = peak tension; PL = peak light; tPt = time to peak tension; tPL = time to peak light. Muscles were stimulated without (pre) and with (post) autonomic blocking agents.
*$P < 0.05$ compared to control. All muscles were stimulated with suprathreshold voltage via punctate electrodes at 0.33 Hz and bathed in 1 mM $Ca^{2+}$ at 30°C.

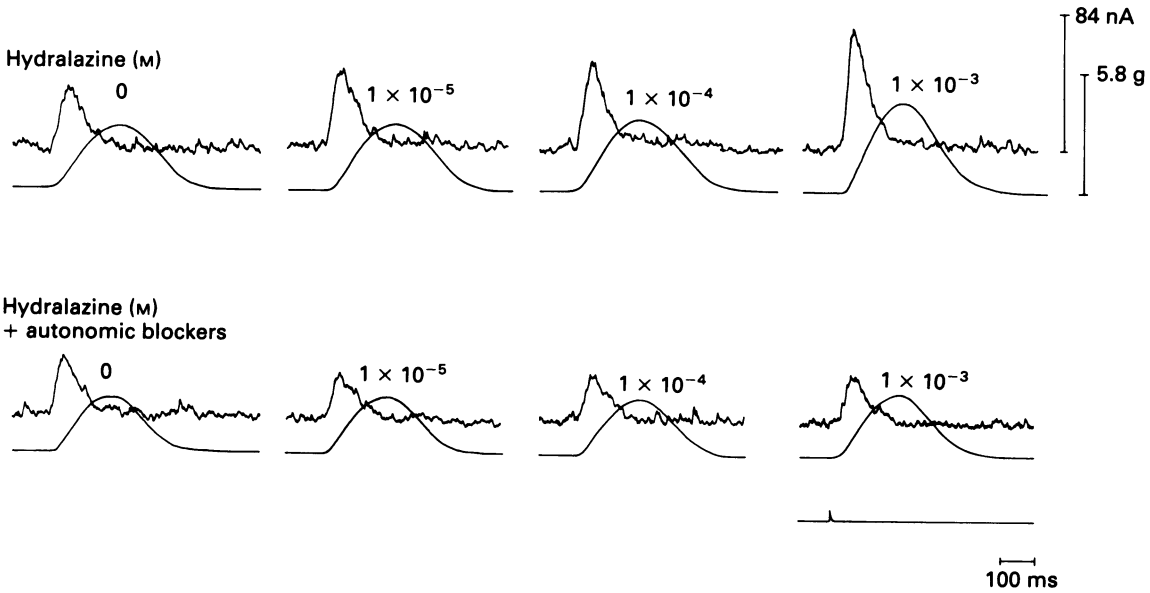



**Figure 1** The effects of hydralazine alone and in the presence of autonomic blockers in an aequorin-loaded ferret papillary muscle. Muscle in the upper panels was treated with hydralazine alone, while that in the lower panels was treated with propranolol ($6 \times 10^{-7}$ M), atropine ($2 \times 10^{-6}$ M), and phentolamine ($10^{-6}$ M), as well as hydralazine. The aequorin signal amplitude (i.e., light) is expressed as nA of current recorded from a photomultiplier; tension is expressed in grams (g). Each tracing represents the average of 30 responses obtained at steady state.

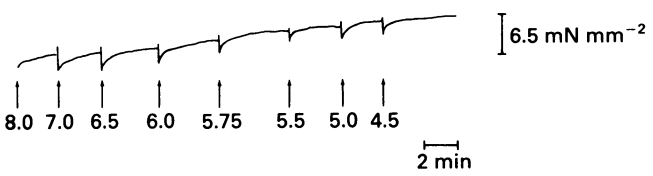



**Figure 2** Representative experimental recording obtained from a saponin-skinned ferret right ventricular papillary muscle. Bottom arrows indicate pCa(− log[$Ca^{2+}$]) of buffer solution.

dependent on a concurrent rise in $[Ca^{2+}]_i$; (2) the positive inotropic effect of hydralazine is consistent with both cyclic AMP-dependent and independent mechanisms; (3) hydralazine has direct negative inotropic effects on the myofilaments.

### *Peak tension and peak light in ferret myocardium*

Contraction-relaxation cycles in the heart are governed by cytosolic $Ca^{2+}$ fluxes that are modulated by the sarcolemma and sarcoplasmic reticulum (Ruegg, 1988). Interventions that alter the strength of cardiac contraction produce changes in either the $[Ca^{2+}]_i$ concentration and/or in the $Ca^{2+}$ requirements of the contractile apparatus. Cyclic AMP is a second messenger that regulates both effects through activation of a variety of cyclic AMP-dependent protein kinases (Opie, 1982). These kinases phosphorylate the sarcolemma and sarcoplasmic reticulum, as well as the contractile elements, which results in (1) increased transsarcolemmal influx of $Ca^{2+}$, (2) decreased $Ca^{2+}$ responsiveness of the contractile elements, and (3) increased re-uptake of $Ca^{2+}$ by the sarcoplasmic reticulum. Most inotropic agents used in clinical medicine produce an inotropic effect by increasing cellular levels of cyclic AMP. Since catecholamine levels are elevated in heart failure (Chidsey *et al.*, 1965), we used two stimulation protocols to study the effects of altered catecholamine levels on the inotropic response. Hydralazine demonstrated a positive inotropic response in intact fibres, which is similar to previous reports in both dogs and cats (Rabinowitz *et al.*, 1986). In our experiments, and in previous studies (Rabinowitz *et al.*, 1986), this effect was abolished by propranolol, suggesting that the mechanism may be related to noradrenaline release from the adrenergic nerve endings.

We studied the effects of hydralazine on cellular $Ca^{2+}$ modulation with the bioluminescent $Ca^{2+}$ indicator, aequorin, that emits light when it combines with free, ionized calcium. In mammalian myocardium, the aequorin light signal apears to reflect predominantly the release and re-uptake of $Ca^{2+}$ by the sarcoplasmic reticulum (Morgan *et al.*, 1984;

**Table 2** Effects of hydralazine on $Ca^{2+}$ sensitivity ($pCa_{50}$), maximum force development ($F_{max}$), and Hill coefficient (n) in saponin-skinned ferret papillary muscles

| | | *Hydralazine* ($10^{-3}$ M) | |
|---|---|---|---|
| | *Control* | *After skinning* | *Before skinning* |
| $pCa_{50}$ | 6.08 ± 0.06[1] | 5.86 ± 0.06[1,2] | 6.02 ± 0.04[2] |
| n | 1.54 ± 0.27 | 1.23 ± 0.06 | 3.81 ± 1.58 |
| $F_{max}$ | 3.47 ± 0.57 | 3.84 ± 0.53 | 4.22 ± 0.28 |
| *n* | 12 | 12 | 16 |

Data shown are mean ± s.e.mean. $[Ca^{2+}]_0 = 1.0$ mM.
[1]Control vs. After skinning $P < 0.05$; [2]After skinning vs. Before skinning $P < 0.05$.

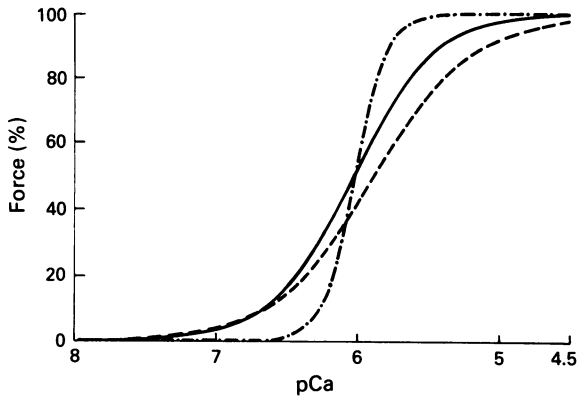



**Figure 3** The effect of hydralazine on the force vs. calcium relation of skinned ferret right ventricular papillary muscles. The curves represent control fibres (—), hydralazine ($10^{-3}$ M) treatment after skinning (– – –), and hydralazine ($10^{-3}$ M) treatment before skinning (–·–·–). Force is plotted on the vertical axis as a percentage of maximal response to calcium. The horizontal axis denotes the pCa ($-\log[Ca^{2+}]$) of buffer solution. The curve parameters n and $pCa_{50}$ were fitted to a modified Hill equation.

Morgan & Morgan, 1984; 1989). Moreover, the relative ratio of the amplitude of the light signal to a given increase in tension can be used as an index of myofilament $Ca^{2+}$ responsiveness (Gwathmey & Morgan, 1985; Morgan & Morgan, 1984; 1989). Our data demonstrate the following: (1) hydralazine causes a simultaneous increase in peak light and peak tension indicating the mechanism of action depends upon a concurrent increase in $[Ca^{2+}]_i$; (2) the positive inotropic effect is associated with an abbreviated time to peak light and time to peak tension; (3) the positive inotropic response is associated with an increase in the ratio of the peak light to peak tension consistent with $Ca^{2+}$ desensitization of the myofilaments. This combination of effects is characteristic of agents that act by increasing intracellular cyclic AMP concentrations (Morgan & Morgan, 1989). On the other hand, our data demonstrate no significant effect of hydralazine on peak light or peak tension in the presence of autonomic blockers. This blunted effect suggests that the inotropic response of hydralazine is either secondary to catecholamine release, and/or the response is facilitated by stimulation of the β-adrenoceptor-mediated production of cyclic AMP.

### *Effects of autonomic agents and varying stimulation protocols*

To study further the possibility of an inotropic mechanism independent of catecholamine release and dependent upon cyclic AMP, muscles were stimulated with histamine in the presence of β-adrenoceptor blockade with propranolol to stimulate adenylate cyclase activity independent of the adrenoceptors. Without histamine stimulation, such β-blocked muscles would be expected to show little in the way of an inotropic response to hydralazine (see Table 1). However, in the presence of hydralazine, our data demonstrated a potentiation of the positive inotropic response to histamine with a leftward shift in the $pD_2$, again consistent with phosphodiesterase inhibition. Therefore, the positive inotropic effect of hydralazine may not be solely mediated by catecholamine release from the adrenergic nerve endings, but may occur in response to any manoeuvre that increases intracellular cyclic AMP levels. A second mechanism of positive inotropy is suggested by the increase in maximal tension found with hydralazine in histamine-stimulated muscles. Morad *et al.* (1978) have demonstrated that agents which are cyclic AMP-dependent decrease peak tension in maximally activated muscles, probably through desensitization of the myofilaments via phosphorylation of troponin I (Opie, 1983). Therefore, the observed increase in peak tension with histamine supports an additional mechanism of positive inotropy for hydralazine which is cyclic AMP-independent. However, it is important to note that these effects occurred in a dosage range generally considered to be above concentrations generally reached in the clinical setting and their relevance to man remains to be established.

### *Direct effects of hydralazine on the myofilaments*

Inotropic agents that increase contractile force and act independently of changes in cyclic AMP have been demonstrated to act directly on the myofilaments, operating as sensitizing or desensitizing agents (Ruegg *et al.*, 1984; Perreault *et al.*, 1990a,b). In the present studies, pretreatment of intact fibres with hydralazine prior to skinning did not elicit an effect, indicating that hydralazine does not have a sustained effect on the contractile elements. This may be because hydralazine does not achieve high enough concentrations in the sarcoplasm of intact myocytes to exert a direct myocardial effect or because any such action is reversed by subsequent detergent treatment. However, hydralazine treatment of previously skinned fibres shifted the force-$pCa_{50}$ curve to the right, consistent with a desensitizing effect on the cardiac myofilaments, without altering the force of maximal contraction ($F_{max}$). The cellular mechanism of this effect on skinned fibres is probably different from that observed in aequorin-loaded muscles since the sarcolemmal mechanisms required for cyclic AMP generation are removed by detergent skinning. In addition, the increased peak tension of histamine stimulated intact fibres in the presence of hydralazine is not due to changes of calcium binding mediated directly by myofilaments; rather, the increased calcium responsiveness is probably due to cytoplasmic or membrane alterations mediated by a second messenger system such as through activation of diacylglycerol (DAG) or phosphatidyl-inositol trisphosphate ($IP_3$), which have been removed by the skinning process. The precise mechanism responsible for the desensitizing, direct effects of hydralazine on the myofilaments remains speculative, but may involve an alteration in thin filament force regulation, such as a change in the affinity of troponin-C for $Ca^{2+}$ as previously proposed for cocaine, a drug also known to act as a desensitizer (Perreault *et al.*, 1990b). Of interest is the fact that the direct and cyclic AMP-independent desensitizing effects of hydralazine on the myofilaments did not appear to be functionally important in ferret papillary muscles at any concentration of hydralazine we studied, since a negative inotropic effect was not observed. However, the significance of these effects may vary with species, the degree of activation of the muscle, or in the presence of disease states.

In summary, our findings suggest that hydralazine can produce a positive inotropic effect in mammalian myocardium. This response, measured as peak tension, is concentration-dependent and attenuated by β-adrenoceptor blockade. The increase in tension with hydralazine is mediated via an increase in $[Ca^{2+}]_i$, and both time to peak light and time to peak tension are abbreviated, consistent with a cyclic AMP-mediated effect. Further support to a cyclic AMP-dependent mechanism of hydralazine is demonstrated by a shift in the concentration-response curve for histamine in the presence of propranolol. An additional mechanism of positive inotropy which is cyclic AMP-independent is supported by an increase in peak tension in these same muscles. This effect is most probably mediated by a yet unidentified second messenger. In contrast, hydralazine acts as a direct desensitizer of myofilaments in skinned fibres in which the sarcolemma has been removed as a diffusion barrier to the drug, but this effect does not appear to be significant under the conditions of our intact muscle experiments. While recent clinical studies, such as the PROMISE

trial, suggest that increased cellular levels of cyclic AMP negatively impact survival, hydralazine appears to possess similar properties and yet has proven utility in mild-to-moderate heart failure. This may be explained by the lower potency of hydralazine compared to drugs like milrinone for producing a rise in cellular cyclic AMP, and/or by the potential importance of other cyclic AMP-independent mechanisms identified solely with hydralazine. Alternatively, the results of the PROMISE trial may not apply to all cyclic AMP-dependent inodilator agents.

The authors gratefully acknowledge Mr Jason Kravitz and Patricia Roche for their expert assistance in the preparation of this manuscript. This work was supported in part by a grant from the NIH (HL31117) and a Grant-in-Aid from the American Heart Association.

## References

AZUMA, J., SAWAMURA, A., HARADA, H., AWATA, N., KISHIMOTO, S. & SPERELAKIS, N. (1987). Mechanism of direct cardiostimulating actions of hydralazine. *Eur. J. Pharmacol.*, **135**, 137–144.

BLINKS, J.R. (1966). Field stimulation as a means of effecting the graded release of autonomic transmitter in isolated heart muscle. *J. Pharmacol. Exp. Ther.*, **151**, 221–235.

BLINKS, J.R. (1982). The use of photoproteins as calcium indicators in cellular physiology. In *Techniques in Cellular Physiology, Part III.* ed. Baker, P.F. pp. 126/1–126/38. Ireland: Elsevier/North-Holland Scientific Publisher Ltd.

CHIDSEY, C.A., BRAUNWALD, E. & MORROW, A.G. (1965). Catecholamine excretion and cardiac stores of norepinephrine in congestive heart failure. *Am. J. Med.*, **39**, 442–451.

COHN, J.N., ARCHIBALD, D.G. & ZIESCHE, S. (1986). Effect of vasodilator therapy on mortality in chronic congestive heart failure: results of a Veterans Administration Cooperative Study. *N. Engl. J. Med.*, **314**, 1547–1552.

COHN, J.N., JOHNSON, M.S. & ZIESCHE, S. (1991). A comparison of enalapril with hydralazine-isosorbide dinitrate in the treatment of chronic congestive heart failure. *N. Engl. J. Med.*, **325**, 303–310.

ENDO, M. & IINO, M. (1980). Specific perforation of muscle cell membranes with preserved sarcoplasmic reticulum functions by saponin treatment. *J. Muscle. Res. Cell. Motil.*, **1**, 89–100.

FABIATO, A. (1981). Myoplasmic free calcium concentration reached during the twitch of an intact isolated cardiac cell and during calcium-induced release of calcium from the sarcoplasmic reticulum of a skinned cardiac cell from the adult rat or rabbit ventricle. *J. Gen. Physiol.*, **78**, 457–497.

FABIATO, A. & FABIATO, F. (1979). Calculator programs for computing the compositions of solutions containing multiple metals and ligands used for experiments in skinned muscle cells. *J. Physiol. (Paris)*, **75**, 463–505.

GERSHWIN, M.E. & SMITH, N.T. (1967). Mode of action of hydralazzine in guinea pig atria. *Arch. Int. Pharmacodyn.*, **170**, 108–116.

GWATHMEY, J.K. & MORGAN, J.P. (1985). The effects of milrinone and piroximone on intracellular calcium handling in working myocardium from the ferret. *Br. J. Pharmacol.*, **85**, 97–108.

ISHII, A., KUBO, K., DEGUCHI, T. & TANAKA, M. (1979). Inhibition of cyclic AMP phosphodiesterase activity by ecarazine, hydrochloride, hydralazine and their metabolites. *Yakagaku Zasshi*, **99**, 533.

JOHNSON, C.L. (1980). In *Pharmacology of Histamine Receptors.* ed. Ganellin, R. & Parsons, M. pp. 146–216. London: J. Wright & Sons.

KHATRI, I., USMURA, N., NOTARGIACOMO, A. & FREIS, E.D. (1977). Direct and reflex cardiostimulatory effects of hydralazine. *Am. J. Cardiol.*, **40**, 38–42.

KIHARA, Y. & MORGAN, J.P. (1989). A comparative study of three methods for intracellular loading of the calcium indicator aequorin in ferret papillary muscles. *Biochem. Biophys. Res. Commun.*, **162**, 402–407.

KIHARA, Y., GWATHMEY, J.K., GROSSMAN, W. & MORGAN, J.P. (1989). Mechanisms of positive inotropic effects and delayed relaxation produced by DPI 201-106 in mammalian working myocardium: effects on intracellular calcium handling. *Br. J. Pharmacol.*, **96**, 927–939.

LEIER, C.V., DESCH, C.E., MAGORIEN, R.D., TRIFFON, D.W., UNVERFERTH, D.V., BOUDOULAS, H. & LEWIS, R.P. (1980). Positive inotropic effects of hydralazine in human subjects: comparison with prazosin in the setting of congestive heart failure. *Am. J. Cardiol.*, **46**, 1039–1044.

MACKINNON, R., GWATHMEY, J.K., ALLEN, P.D., BRIGGS, B.M. & MORGAN, J.P. (1988). Modulation by the thyroid state of intracellular calcium and contractility in ferret ventricular muscle. *Circ. Res.*, **63**, 1080–1089.

MORAD, M., WEISS, J. & CLEEMAN, L. (1978). The inotropic action of adrenaline on cardiac muscle: does it relax or potentiate tension? *Eur. J. Cardiol.*, **7**, suppl., 53–62.

MORGAN, J.P., CHESEBRO, J.H., PLUTH, J.R., PUGA, F.J. & SCHAFF, H.V. (1984). Intracellular calcium transients in human working myocardium as detected with aequorin. *J. Am. Coll. Cardiol.*, **3**, 410–418.

MORGAN, J.P. & MORGAN, K.G. (1984). Calcium and cardiovascular function: intracellular calcium levels during contraction and relaxation of mammalian cardiac and vascular smooth muscle as detected with aequorin. *Am. J. Med.*, **77** (Suppl. 5A), 33–46.

MORGAN, J.P. & MORGAN, K.G. (1989). Intracellular calcium and cardiovascular function in heart failure: effects of pharmacologic agents. *Cardiovasc. Drugs Ther.*, **3** (Suppl. C), 959–970.

OPIE, L.H. (1983). Role of cyclic nucleotides in heart metabolism. *Cardiovasc. Res.*, **16**, 483.

PACKER, M., CARVER, J.R. & RODEHEFFER, R.J. (1991). Effect of oral milrinone on mortality in severe chronic heart failure. *N. Engl. J. Med.*, **325**, 1468–1475.

PERREAULT, C.L., BING, O.H.L., BROOKS, W.W., RANSIL, B.J. & MORGAN, J.P. (1990a). Differential effects of hypertrophy and failure on right versus left ventricular calcium activation. *Circ. Res.*, **67**, 707–712.

PERREAULT, C.L., HAGUE, N.L., RANSIL, B.J. & MORGAN, J.P. (1990b). The effects of cocaine on intracellular $Ca^{2+}$ handling and myofilament $Ca^{2+}$ responsiveness of ferret ventricular myocardium. *Br. J. Pharmacol.*, **101**, 679–685.

RABINOWITZ, B., PARMLEY, W.W., HAR-ZAHAV, Y., ELAZAR, E., BLUMLEIN, S., NERINSKY, R. & NEUFELD, H.N. (1986). Correlation between effects of hydralazine on force and on the adenyl cyclase system of ventricular myocardium in dogs and cats. *Cardiovasc. Res.*, **20**, 215–220.

RENDIG, S.V., SEGEL, L.D. & AMSTERDAM, E.A. (1988). Direct effects of hydralazine on cardiac contractile function, haemodynamics, and myocardial energetics in isolated myocardium. *Cardiovasc. Res.*, **22**, 322–328.

RUEGG, J.C. (1988). *Calcium in Muscle Activation*, pp. 1–285. New York: Springer-Verlag.

RUEGG, J.C., PFITZER, G., EUBLER, D. & ZEUGNER, C. (1984). Effect on contractility of skinned fibers from mammalian heart and smooth muscle by a new benzimidazole derivative, 4,5-dihydro-6[(2-4-methoxyphenyl)-1H-benzimidazole-5-yl]-5-methyl-3(2H)-pyridazinone. *Arzneim. Forsch. Drug Res.*, **34**, 1736.

SAEGUSA, K., FURUKAWA, Y. & CHIBA, S. (1986). Pharmacological analyses of hydralazine-induced cardiac action in intact dogs and isolated, blood-perfused canine atria. *J. Cardiovasc. Pharmacol.*, **8**, 614–620.

SEGEL, I.H. (1975). *Enzyme kinetics: Behavior and Analysis of Rapid Equilibrium and Steady State Enzyme Systems.* pp. 360–361. New York: John Wiley and Sons, Inc.

SMITH, W.M. (1985). Epidemiology of congestive heart failure. *Am. J. Cardiol.*, **55**, 3A.

*(Received June 11, 1992*
*Revised February 16, 1993*
*Accepted February 25, 1993)*

*Br. J. Pharmacol.* (1993), **109**, 673–678 © Macmillan Press Ltd, 1993

# Effect of nafamostat mesilate on $Na^+$ and $K^+$ transport properties in the rabbit cortical collecting duct

[1]Shigeaki Muto, Masashi Imai & Yasushi Asano

Departments of Nephrology and Pharmacology, Jichi Medical School, 3311-1 Minamikawachi, Tochigi 329-04 Japan

**1** To determine the mechanism(s) of hyperkalemia caused by nafamostat mesilate (NM), a serine-protease inhibitor, we investigated the effects of the drug on $Na^+$ and $K^+$ transport properties of the collecting duct (CD) cell in the isolated and perfused cortical collecting duct from rabbit kidneys.

**2** NM at $10^{-4}$ M in the lumen, hyperpolarized the apical membrane in parallel with increases in transepithelial resistance ($R_T$) and fractional apical membrane resistance ($fR_A$).

**3** These effects were completely inhibited by pretreatment with 50 μM luminal amiloride, whereas they were not affected by luminal addition of 2 mM $Ba^{2+}$.

**4** NM at $10^{-4}$ M in the bath slightly but significantly depolarized the basolateral membrane without any changes in $R_T$ or $fR_A$, although NM at $10^{-5}$ M in the bath had no effect on the electrical parameters.

**5** It is concluded that NM mainly acts on the apical membrane of the CD cell and inhibits the amiloride-sensitive $Na^+$ conductance in the apical membrane.

**Keywords:** Nafamostat mesilate; electrophysiology; collecting duct cell; $Na^+$ conductance; $K^+$ conductance; $Na^+$-$K^+$-ATPase pump

## Introduction

Nafamostat mesilate (6-amidino-2-naphthyl *p*-guanidinobenzoate dimethanesulphonate, NM, Torii Pharmaceutical Co., Japan), is a serine-protease inhibitor (Aoyama *et al.*, 1984) used for treatment of pancreatitis (Iwaki *et al.*, 1986) and disseminated intravascular coagulation (DIC) (Yoshikawa *et al.*, 1983; Hitomi *et al.*, 1985; Takahashi *et al.*, 1989). It has also been widely used in haemodialysis as an anticoagulant in patients with bleeding tendencies (Akizawa *et al.*, 1985; Yamazaki *et al.*, 1989; Ohtake *et al.*, 1991).

Recently, it has been reported that continuous intravenous infusion of NM to the patients with pancreatitis or DIC causes hyperkalemia due to reduced urinary excretion of $K^+$ (Okamoto *et al.*, 1992). However, the exact mechanism(s) underlying this disorder have not yet been evaluated.

It has been well established that the cortical collecting duct (CCD) from mammalian kidneys is a key nephron site of $K^+$ transport (Stanton *et al.*, 1981; Stokes, 1981; Kaissling & LeHir, 1982; Stanton & Giebisch, 1982; Koeppen *et al.*, 1983; Muto *et al.*, 1987a,b; 1988). This segment is composed of at least two cell types (Kaissling & Kriz, 1979), the collecting duct (CD) cell and the intercalated (IC) cell. The CD cell is responsible for $Na^+$ and $K^+$ transport (Koeppen *et al.*, 1983; Muto *et al.*, 1987a,b; 1988), whereas the IC cell transports $H^+$, $HCO_3^-$ and $Cl^-$ (Madsen & Tisher, 1986; Muto *et al.*, 1987a; Ridderstrale *et al.*, 1988; Muto *et al.*, 1990). Therefore, the present study was conducted to determine whether or not NM directly acts on the CD cell and modulates $Na^+$ and $K^+$ transports in the isolated perfused CCD from rabbit kidneys.

## Methods

### *Isolation and perfusion of tubules*

Japanese female white rabbits weighing 1.5 to 2.5 kg were fed a standard laboratory chow and had free access to tap water. They were anaesthetized with intravenous administration of pentobarbitone (35 mg $kg^{-1}$). Both kidneys were removed and placed in a dish containing a cold intracellular-fluid-like solution of the following composition (mM): KCl 14, $K_2HPO_4$ 44, $KH_2PO_4$ 14, $NaHCO_3$ 9 and sucrose 160.

Segments of the CCD were dissected from the cortex, and transferred to a bath fixed on an inverted microscope (Diaphot; Nikon, Tokyo, Japan). Each tubule was perfused *in vitro* according to the techniques developed by Burg *et al.* (1966) as modified in this laboratory for the use of intracellular microelectrodes (Muto *et al.*, 1990; 1991). Since the details of the technique have been published previously (Muto *et al.*, 1990; 1991), they will be presented here briefly. Tubules were suspended between two pipettes. The perfusion rate exceeded 20 nl $min^{-1}$ in all tubules. The distal end of the tubule was held in the collecting pipette with unpolymerized Sylgard 184 (Dow Corning, Midland, MI, U.S.A.). The tubule was perfused in the bathing chamber of ~100 μl which permits rapid exchange of the bathing solution within 5 s. The bathing solution flowed at 5–15 ml $min^{-1}$ from the reservoirs by gravity through a water jacket to permit the bath temperature to be regulated at 37°C.

### *Microelectrode studies*

The transepithelial and cellular electrical properties of the tubule were measured by techniques described previously in this laboratory (Muto *et al.*, 1990; 1991). The transepithelial voltage ($V_T$) was measured through the perfusion pipette, which was connected to one channel of a dual electrometer (Duo 733; W-P Instruments, Inc., New Haven, CT, U.S.A.) with a 3 M KCl-3% agar bridge and a calomel half-cell electrode. The basolateral membrane voltage ($V_B$) was measured with 0.5 M KCl-filled microelectrodes, which were made from borosilicate glass capillaries (GD-1.5; 1.5 mm o.d., 1.0 mm i.d.; Narishige Scientific Laboratory, Tokyo, Japan) by using a vertical puller (PE-2, Narishige Scientific Laboratory). Both voltages were referenced to the bath and were recorded on a four-pen chart recorder (R64; Rikadenki, Tokyo, Japan). The electrical potential difference across the apical membrane ($V_A$) was calculated by the following equation: $V_A = V_T - V_B$.

[1] Author for correspondence.

As previously described (Muto *et al.*, 1990; 1991), cable analysis was used to calculate the transepithelial resistance ($R_T$), and the fractional apical membrane resistance ($fR_A$) [$= R_A/(R_A + R_B)$], where $R_A$ and $R_B$ are the resistances of the apical and basolateral membranes, respectively.

### *Identification of the CD cell*

Electrical Identification of the CD cell was performed according to the criteria described previously by Muto *et al.* (1987a; 1990; 1991). The CD cell has a relatively low $fR_A$; high $V_B$; apical $Na^+$ and $K^+$ conductances; and basolateral $K^+$ and $Cl^-$ conductances.

### *Solutions and materials*

The control bathing and perfusing solution contained (mM): NaCl 110, KCl 5, $MgCl_2$ 1, $CaCl_2$ 1.8, $NaHCO_3$ 25, Na acetate 10, $Na_2HPO_4$ 0.8, $NaH_2PO_4$ 0.2, L-alanine 5, and D-glucose 8.3. This control solution had an osmolality between 285 and 295 mOsm $kg^{-1}$ $H_2O$, and was equilibrated with 95% $O_2$/5% $O_2$ and adjusted to pH 7.4 at 37°C.

Amiloride (Sigma Chemical Co., St. Louis, MO, U.S.A.) was added to the luminal perfusate to achieve a final concentration of 50 μM. $BaCl_2$ was used at a final concentration of 2 mM. NM was supplied by Torii & Co., Ltd. (Tokyo, Japan).

### *Statistics*

All values are presented as means ± s.e.mean. Differences between two groups were evaluated with the paired *t* test. *P* value less than 0.05 was considered to be significant.

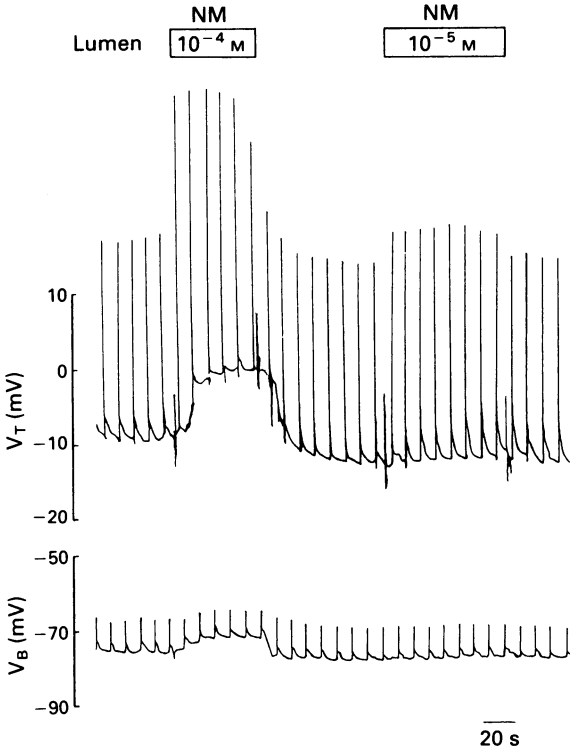



**Figure 1** Typical tracings showing effects of nafamostat mesilate (NM) in the lumen on $V_T$ and $V_B$ of the collecting duct cell. Voltage spikes are due to 50 nA constant-current pulses at 10 s intervals.

## Results

### *Effect of nafamostat mesilate in the lumen on electrical properties of the CD cell*

To examine whether or not NM acts on the apical membrane of the CD cell, we added NM at $10^{-5}$ or $10^{-4}$ M to the luminal perfusate while monitoring the electrical parameters. Figure 1 shows a typical tracing of the changes in $V_T$ and $V_B$ of the CD cell before and after addition of the drug. Table 1 summarizes the effects of NM in the lumen on barrier voltages and resistances. NM at $10^{-5}$ M in the lumen had no effect on the electrical parameters. Upon addition of luminal NM at $10^{-4}$ M, the lumen-negative $V_T$ was rapidly decreased, and the $-V_B$ was also slightly decreased. Thus, the major effect of NM was to cause the apical membrane to hyperpolarize by 4 mV. Simultaneously, the $R_T$ and the $fR_A$ were increased by 16 Ω·cm² and 0.06, respectively. These results suggest that NM at $10^{-4}$ M in the lumen may inhibit the $Na^+$ conductance at the apical membrane of the CD cell.

To examine whether NM in the lumen inhibits the amiloride-sensitive $Na^+$ conductance in the apical membrane of the CD cell, we added a $Na^+$ channel inhibitor, amiloride, to the luminal perfusate, and examined the effect of NM on the CD cell. Figure 2 shows a typical tracing of the changes in $V_T$ and $V_B$ of the CD cell before and after addition of luminal NM ($10^{-4}$ M) in the presence of luminal amiloride (50 μM). Table 2 summarizes the effects of NM in the lumen on the electrical properties of the CD cell in the presence of luminal amiloride. After addition of 50 μM amiloride to the perfusate, the lumen-negative $V_T$ was decreased by 14.3 mV, and the $V_B$ was also significantly depolarized by 7.0 mV, resulting in a hyperpolarization of $V_A$ by 7.5 mV. The $R_T$ and the $fR_A$ were also elevated by 28.5 Ω·cm² and 0.18, respectively. However, luminal NM at $10^{-4}$ M in the presence of luminal amiloride had no effect on either $V_T$, $V_B$, $V_A$, $R_T$ or $fR_A$. These results indicate that NM inhibits mainly the amiloride-sensitive $Na^+$ conductance at the apical membrane of the CD cell.

**Table 1** Effects of nafamostat mesilate (NM) in the lumen on the electrical properties of the collecting duct (CD) cell in the rabbit cortical collecting duct

| *Condition* | $V_T$ (mV) | $V_B$ (mV) | $V_A$ (mV) | $R_T$ (Ω·cm²) | $fR_A$ |
|---|---|---|---|---|---|
| Control | −10.8 ± 1.9 (9) | −76.0 ± 1.9 (9) | 65.1 ± 1.5 (9) | 119.1 ± 8.9 (9) | 0.39 ± 0.08 (9) |
| NM $10^{-4}$ M (lumen) | −5.0 ± 2.1** (9) | −73.4 ± 2.6† (9) | 69.1 ± 1.4†† (9) | 135.4 ± 9.6†† (9) | 0.45 ± 0.08** (9) |
| Control | −9.7 ± 2.4 (8) | −76.7 ± 2.4 (8) | 67.0 ± 2.2 (8) | 110.2 ± 4.4 (5) | 0.44 ± 0.10 (5) |
| NM $10^{-5}$ M (lumen) | −9.7 ± 2.3 (8) | −76.7 ± 2.4 (8) | 67.2 ± 2.1 (8) | 111.6 ± 4.6 (5) | 0.44 ± 0.10 (5) |

Values are mean ± s.e.mean; no. of experiments is in parentheses.
**$P < 0.001$; ††$P < 0.01$; †$P < 0.05$ compared with preceding period.

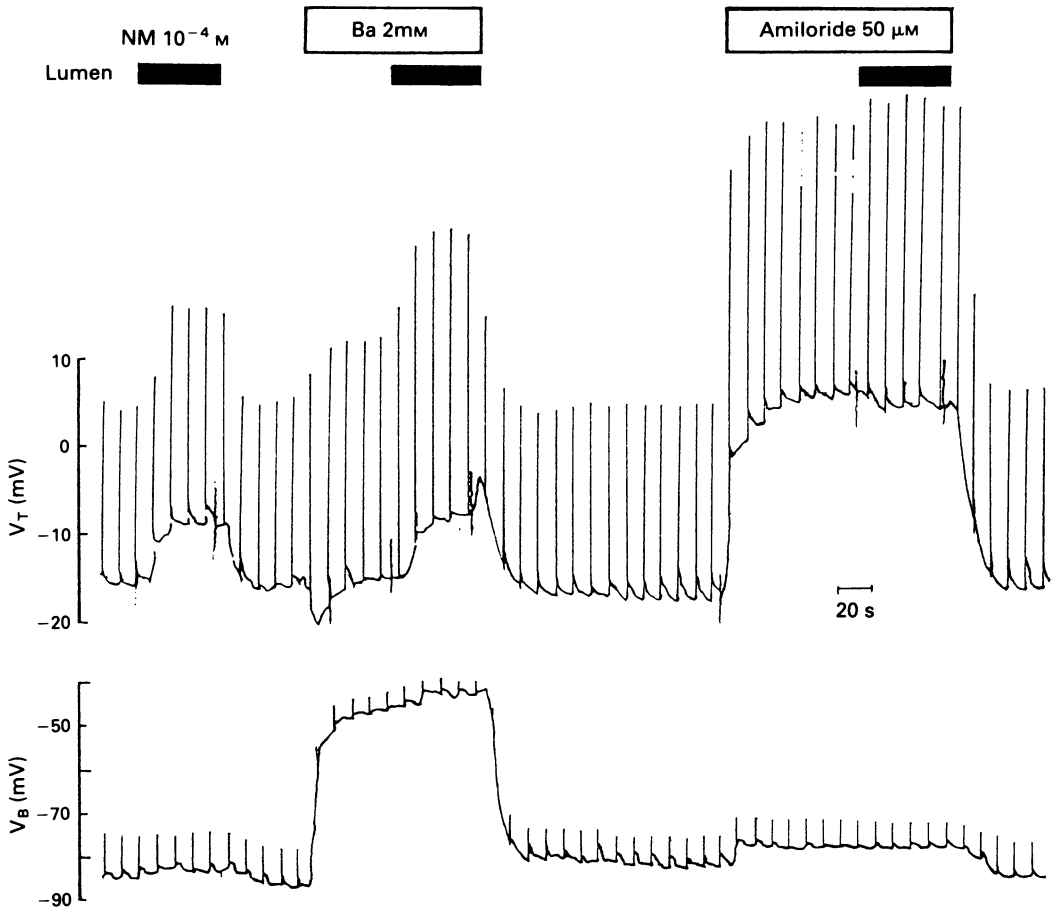



**Figure 2** Typical tracings showing effects of nafamostat mesilate (NM) in the lumen on $V_T$ and $V_B$ of the collecting duct cell in the presence of luminal $Ba^{2+}$ or amiloride. Voltage spikes are due to 50 nA constant-current pulses at 10 s intervals.

**Table 2** Effects of nafamostat mesilate (NM) in the lumen on the electrical properties of the collecting duct (CD) cell in the presence of luminal amiloride

| *Condition* | $V_T$ (mV) | $V_B$ (mV) | $V_A$ (mV) | $R_T$ ($\Omega \cdot cm^2$) | $fR_A$ |
|---|---|---|---|---|---|
| Control | $-9.7 \pm 2.4$ (8) | $-80.2 \pm 2.8$ (8) | $70.3 \pm 3.4$ (8) | $116.8 \pm 8.1$ (6) | $0.31 \pm 0.08$ (6) |
| Amiloride 50 μM (lumen) | $4.6 \pm 1.3$* (8) | $-73.2 \pm 3.7$† (8) | $77.8 \pm 2.9$* (8) | $145.3 \pm 11.3$†† (6) | $0.49 \pm 0.08$† (6) |
| Amiloride 50 μM (lumen) + NM $10^{-4}$ M (lumen) | $4.3 \pm 1.2$ (8) | $-72.6 \pm 3.9$ (8) | $77.0 \pm 3.2$ (8) | $144.3 \pm 11.1$ (6) | $0.51 \pm 0.09$ (6) |

Values are mean ± s.e.mean; no. of experiments is in parentheses.
*$P<0.005$; ††$P<0.01$; †$P<0.05$ compared with preceding period.

To exclude the possibility that NM may inhibit the $K^+$ conductance at the apical membrane of the CD cell, we added a $K^+$ channel inhibitor, $Ba^{2+}$, to the luminal perfusate, and examined the action of NM on the CD cell. Figure 2 also shows a typical tracing of the changes in $V_T$ and $V_B$ of the CD cell before and after addition of luminal NM ($10^{-4}$ M) in the presence of luminal $Ba^{2+}$ (2 mM). Table 3 summarizes the effects of NM in the lumen on the electrical properties of the CD cell in the presence of luminal $Ba^{2+}$. When 2 mM $Ba^{2+}$ was added to the luminal perfusate, the lumen-negative $V_T$ rapidly increased, and then slowly decreased to reach a new steady state level. The $V_B$ was rapidly depolarized within several seconds, and was then slowly depolarized further to a new steady state level. Thus, the $V_A$ was rapidly depolarized during this fast phase, and was then slowly depolarized to a new steady state level. At that time, both $R_T$ and $fR_A$ were significantly increased. When NM at $10^{-4}$ M was added to the luminal perfusate in the presence of luminal $Ba^{2+}$, the lumen-negative $V_T$ was further decreased by 10 mV, and the $V_B$ was also further depolarized by 5.4 mV. The calculated $V_A$ was hyperpolarized by 3.7 mV. Simultaneously, both $R_T$ and $fR_A$ were further increased by 19.8 $\Omega \cdot cm^2$ and 0.04, respectively. These results indicate that NM in the lumen does not primarily affect the $Ba^{2+}$-sensitive $K^+$ conductance in the apical membrane of the CD cell.

### *Effect of NM in the bath on electrical properties of the CD cell*

To examine whether or not NM acts on the basolateral membrane of the CD cell, we added NM at $10^{-5}$ or $10^{-4}$ M

**Table 3** Effects of nafamostat mesilate (NM) in the lumen on the electrical properties of the collecting duct (CD) cell in the presence of lumina $Ba^{2+}$

| *Condition* | $V_T$ (mV) | $V_B$ (mV) | $V_A$ (mV) | $R_T$ ($\Omega \cdot cm^2$) | $fR_A$ |
|---|---|---|---|---|---|
| Control | $-8.5 \pm 1.3$ (7) | $-80.8 \pm 1.9$ (7) | $72.3 \pm 2.8$ (7) | $110.0 \pm 9.8$ (5) | $0.35 \pm 0.10$ (5) |
| $Ba^{2+}$ 2 mM (lumen) initial | $-11.8 \pm 1.7$** (7) | $-52.8 \pm 2.2$** (7) | $41.0 \pm 2.5$** (7) | $197.8 \pm 15.0$† (5) | $0.83 \pm 0.03$* (5) |
| $Ba^{2+}$ 2 mM (lumen) steady state | $-8.6 \pm 1.6$* (7) | $-47.1 \pm 2.0$* (7) | $38.4 \pm 2.7$† (7) | $208.2 \pm 13.3$ (5) | $0.84 \pm 0.03$ (5) |
| $Ba^{2+}$ 2 mM (lumen) + NM $10^{-4}$ M (lumen) | $0.4 \pm 1.0$** (7) | $-41.7 \pm 2.3$†† (7) | $42.1 \pm 3.1$†† (7) | $228.0 \pm 17.6$† (5) | $0.88 \pm 0.02$†† (5) |

Values are mean ± s.e.mean; no. of experiments is in parentheses.
**$P<0.001$; *$P<0.005$; †$P<0.05$; ††$P<0.01$ compared with preceding period.

to the bathing solution and monitored the barrier voltages and resistances. Figure 3 shows a typical tracing of the changes in $V_T$ and $V_B$ of the CD cell before and after addition of the drug. Table 4 summarizes the effects of NM in the bath on barrier voltages and resistances. NM at $10^{-5}$ M in the bath had no effect on the electrical parameters. When NM at $10^{-4}$ M was added in the bath, the lumen-negative $V_T$ was slightly but significantly decreased by 1.3 mV, and the $V_B$ was also depolarized by 3.8 mV. At that time, neither $R_T$ nor $fR_A$ was significantly changed.

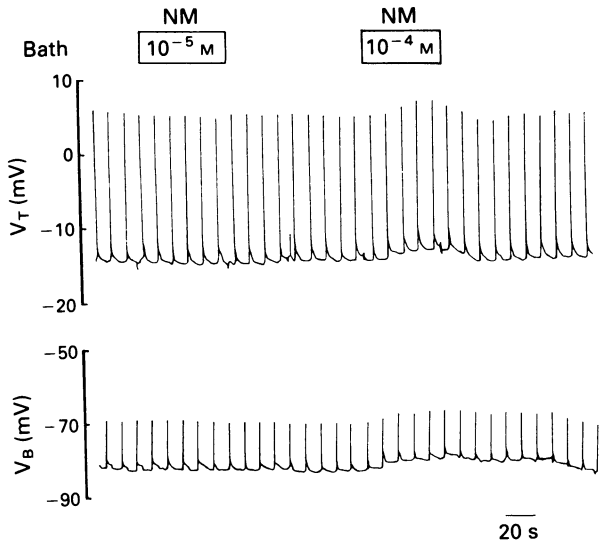



**Figure 3** Typical tracings showing effects of nafamostat mesilate (NM) in the bath on $V_T$ and $V_B$ of the collecting duct cell. Voltage spikes are due to 50 nA constant-current pulses at 10 s intervals.

## Discussion

This study was designed to determine the mechanisms of NM-induced hyperkalemia, and particularly the direct action of NM on the CCD perfused *in vitro*. In the present study, we demonstrate that NM acts on mainly the apical membrane of the CD cell to inhibit the amiloride-sensitive $Na^+$ conductance. In addition, NM also has a depolarizing effect on the basolateral membrane of the CD cell.

$K^+$ transport by the distal tubule, including the CCD, has been studied extensively by micropuncture and microperfusion techniques (Stanton *et al.*, 1981; Stokes, 1981; Stanton & Giebisch, 1982; Muto *et al.*, 1988). A number of factors affect $K^+$ secretion in the distal tubule, including the $V_T$, the state of $K^+$ metabolism, tubular load of $Na^+$, tubular fluid flow, and plasma aldosterone concentration (Wright & Giebisch, 1992). $K^+$ is secreted in the CD cell by a two-step process that involves uptake from the blood into the cell via the basolateral membrane $Na^+$-$K^+$ pump and passive diffusion from the cell to the lumen through a large apical membrane conductive pathway (Koeppen *et al.*, 1983; O'Neil & Sansom, 1984; Sansom & O'Neil, 1985; 1986; Muto *et al.*, 1987a,b; Sansom *et al.*, 1989). On the other hand, in the apical membrane of the CD cell, $Na^+$ is reabsorbed passively from lumen to cell along a favourable electrochemical gradient through a $Na^+$ conductance and is actively transported from cell to blood, also via the $Na^+$-$K^+$ pump in the basolateral membrane (Koeppen *et al.*, 1983; O'Neil & Sansom 1984; Muto *et al.*, 1987a,b).

In the present study, we found that NM acts on the CD cell and inhibits the $Na^+$ conductance in the apical membrane. This notion is directly supported by the hyperpolarization of the apical membrane and increased $R_T$ and $fR_A$ of the CD cell observed with addition of NM in the lumen. Furthermore, in the presence of luminal amiloride, NM did not

**Table 4** Effects of nafamostat mesilate (NM) in the bath on the electrical properties of the collecting duct (CD) cell in the rabbit cortical collecting duct

| *Condition* | $V_T$ (mV) | $V_B$ (mV) | $R_T$ ($\Omega \cdot cm^2$) | $fR_A$ |
|---|---|---|---|---|
| Control | $-8.1 \pm 2.3$ (7) | $-78.1 \pm 2.6$ (7) | $104.0 \pm 2.9$ (7) | $0.40 \pm 0.06$ (7) |
| NM $10^{-4}$ M (bath) | $-6.8 \pm 1.9$† (7) | $-74.3 \pm 2.4$* (7) | $103.7 \pm 2.6$ (7) | $0.41 \pm 0.06$ (7) |
| Control | $-6.2 \pm 1.8$ (7) | $-74.8 \pm 2.1$ (7) | $100.0 \pm 5.7$ (6) | $0.50 \pm 0.08$ (6) |
| NM $10^{-5}$ M (bath) | $-6.0 \pm 1.8$ (7) | $-72.8 \pm 1.6$ (7) | $101.8 \pm 5.1$ (6) | $0.51 \pm 0.09$ (6) |

Values are mean ± s.e.mean; no. of experiments is in parentheses.
*$P<0.005$; †$P<0.05$ compared with preceding period.

affect transepithelial or transmembrane voltages or resistances. In addition, pretreatment of luminal $Ba^{2+}$ did not alter the effect of luminal NM on the barrier voltages and resistances. Taken together, these results indicate that NM in the lumen inhibits the amiloride-sensitive $Na^+$ conductance in the apical membrane of the CD cell. Therefore, the change in $V_A$ upon addition of luminal NM decreases the electrochemical potential for $K^+$ and thus reduces the driving force for diffusion of $K^+$ from cell to lumen, resulting in an inhibition of $K^+$ secretion.

In contrast to the action of NM on the apical membrane, NM in the bath caused both the lumen-negative $V_T$ and $V_B$ to decrease significantly without any changes in $R_T$ or $fR_A$. These results suggest that NM may act on the basolateral membrane of the CD cell and inhibit an electrogenic $Na^+$ transport system, possibly the $Na^+$-$K^+$-ATPase pump.

Although we demonstrated that NM at $10^{-4}$ M acts on both apical and basolateral membranes by different mechanisms, it is pertinent to discuss which action might contribute to the NM-induced hyperkalemia. Iwaki *et al.* (1986) examined the effects of NM on the pancreatic enzymes in the enterokinase-induced experimental acute pancreatitis in rats, and reported that NM inhibited the enterokinase with an $IC_{50}$ value of $1.5 \times 10^{-6}$ M. According to Takahashi *et al.* (1989), the concentration of NM required for $IC_{50}$ of the enzyme activities of thrombin and plasmin were $6.0 \times 10^{-6}$ and $1.0 \times 10^{-6}$ M, respectively. In addition, when infused continuously into patients with DIC at a dose of 0.1 or 0.2 mg $kg^{-1}$ $h^{-1}$, the concentration of NM in blood were in the range of $3.0 \times 10^{-8}$–$3.0 \times 10^{-7}$ M (Takahashi *et al.*, 1989). Hitomi *et al.* (1985) also reported that $IC_{50}$ of NM for plasma kallikrein was $3.0 \times 10^{-9}$ M. Therefore, the effects of NM on the CD cell observed in this study may not be related to a specific effect on serine-protease but rather they may be non-specific side effects. Since it is impossible for NM to reach plasma concentration as high as $10^{-4}$ M, it is unlikely that the basolateral action contributes to the hyperkalemic action of NM. On the other hand, it is possible that the concentration of NM in the tubular lumen, especially in the CCD, might become higher than in the plasma due to water absorption along the nephron. Diuretics, such as trichlormethiazide (Shimizu *et al.*, 1988) and frusemide (Greger *et al.*, 1983), are known to inhibit the $Na^+$-$Cl^-$ cotransport in the apical membrane of the rabbit connecting tubule and the $Na^+$-$K^+$-$2Cl^-$ cotransport in the rabbit cortical thick ascending limb of Henle's loop, respectively. These diuretics are secreted from the proximal tubule into the lumen and act on the apical membrane of the more distal nephron segments in the range of $10^{-4}$–$10^{-5}$ M. Although the exact renal handling of NM is unknown, it is not unreasonable to assume that under some circumstances, the concentration of the drug or its active metabolite in the CCD might reach the level of $10^{-4}$ M, exerting natriuretic and antikaliuretic actions.

In conclusion, NM at $10^{-4}$ M mainly acts on the apical membrane of the CD cell and inhibits the amiloride-sensitive $Na^+$ conductance in the apical membrane, resulting in an inhibition of $K^+$ secretion. This would indicate that the direct action of this drug on the CD cell contributes, at least in part, to its hyperkalemic effect.

We would like to thank Ms H. Kasakura for expert secretarial assistance in preparing the manuscript.

## References


AKIZAWA, T., SATO, M., KITAOKA, T., KOSHIKAWA, S., ASANO, Y., HIRASAWA, Y. IIDA, K., MIURA, N., NAKAMURA, K., KAZAMA, M. & OTA, K. (1985). The usefulness of the multi-enzyme inhibitor, nafamostat mesilate, in high bleeding risk haemodialysis. *Proc. Eur. Dial. Transplant Assoc.*, **22**, 336–338.

AOYAMA, T., INO, Y., OZEKI, M., ODA, M., SATO, T., KOSHIYAMA, Y., SUZUKI, S. & FUJITA, M. (1984). Pharmacological studies of FUT-175, nafamostat mesilate. I. Inhibition of protease activity in in vivo and in vitro experiments. *Jpn. J. Pharmacol.*, **35**, 203–227.

BURG, M.B., GRANTHAM, M., ABRAMOV, S. & ORLOFF, J. (1966). Preparation and study of fragments of single rabbit nephrons. *Am. J. Physiol.*, **210**, 1293–1298.

GREGER, R., SCHLATTER, E. & LANG, F. (1983). Evidence for electroneutral sodium chloride cotransport in the cortical thick ascending limb of Henle's loop of rabbit kidneys. *Pflügers Arch.*, **396**, 308–314.

HITOMI, Y., IKARI, N. & FUJII, S. (1985). Inhibitory effect of a new synthetic protease inhibitor (FUT-175) on the coagulation system. *Haemostasis*, **15**, 164–168.

IWAKI, M., INO, Y., MOTOYOSHI, A., OZEKI, M., SATO, T., KURUMI, M. & AOYAMA, T. (1986). Pharmacological studies of FUT-175, nafamostat mesilate. V. Effects on the pancreatic enzymes and experimental acute pancreatitis in rats. *Jpn. J. Pharmacol.*, **41**, 155–162.

KAISSLING, B. & KRIZ, W. (1979). Structural analysis of the rabbit kidney. *Adv. Anat. Embryol. Cell Biol.*, **56**, 1–123.

KAISSLING, B. & LEHIR, M. (1982). Distal tubular segments of the rabbit kidney after adaptation to altered Na- and K-intake. *Cell Tissue Res.*, **224**, 469–492.

KOEPPEN, B.M., BAIGI, B.A. & GIEBISCH, G.H. (1983). Intracellular microelectrode characterization of the rabbit cortical collecting duct. *Am. J. Physiol.*, **244**, F35–F47.

MADSEN, K.M. & TISHER, C.C. (1986). Structural-functional relationships along the distal nephron. *Am. J. Physiol.*, **250**, F1–F15.

MUTO, S., FURUYA, H., TABEI, K. & ASANO, Y. (1991). Site and mechanism of action of epidermal growth factor in rabbit cortical collecting duct. *Am. J. Physiol.*, **260**, F163–F169.

MUTO, S., GIEBISCH, G. & SANSOM, S. (1987a). Effects of adrenalectomy on CCD: evidence for differential response of two cell types. *Am. J. Physiol.*, **253**, F742–F752.

MUTO, S., GIEBISCH, G. & SANSOM, S. (1988). An acute increase of peritubular K stimulates K transport through cell pathways of CCT. *Am. J. Physiol.*, **255**, F104–F114.

MUTO, S., SANSOM, S. & GIEBISCH, G. (1987b). Effects of high K diet on electrical properties of cortical collecting duct from adrenalectomized rabbit. *J. Clin. Invest.*, **81**, 376–380.

MUTO, S., YASOSHIMA, K., YOSHITOMI, K., IMAI, M. & ASANO, Y. (1990). Electrophysiological identification of α- and β-intercalated cells and their distribution along the rabbit distal nephron segments. *J. Clin. Invest.*, **86**, 1829–1839.

OHTAKE, Y., HIRASAWA, H., SUGAI, T., ODA, S., SHIGA, H., MATSUDA, K. & KITAMURA, N. (1991). Nafamostat mesilate as anticoagulant in continuous hemofiltration and continuous hemodiafiltration. *Contr. Nephrol.*, **93**, 215–217.

OKAMOTO, T., MARUKAWA, S., HAYAMI, H., OZAKI, K., ISHIDA, H. & KONO, K. (1992). Effect of nafamostat mesilate on renin-aldosterone system. *Masui*, **41**, 329–330. (Abs in English).

O'NEIL, R.G. & SANSOM, S.C. (1984). Electrophysiological properties of cellular and paracellular conductive pathways of the rabbit cortical collecting duct. *J. Membr. Biol.*, **82**, 281–295.

RIDDERSTRALE, Y., KASHGARIAN, M., KOEPPEN, B., GIEBISCH, G., STETSON, D., ARDITO, T. & STANTON, B. (1988). Morphological heterogeneity of the rabbit collecting duct. *Kidney Int.*, **34**, 655–670.

SANSOM, S.C. & O'NEIL, R.G. (1985). Mineralocorticoid regulation of apical cell membrane $Na^+$ and $K^+$ transport of the cortical collecting duct. *Am. J. Physiol.*, **248**, F858–F868.

SANSOM, S.C. & O'NEIL, R.G. (1986). Effects of mineralocorticoids on transport properties of cortical collecting duct basolateral membrane. *Am. J. Physiol.*, **251**, F743–F757.

SANSOM, S.C., AGULIAN, S., MUTO, S., ILLIG, V. & GIEBISCH, G. (1989). K activity of CCD principal cells from normal and DOCA-treated rabbits. *Am. J. Physiol.*, **256**, F136–F142.

SHIMIZU, T., YOSHITOMI, K., NAKAMURA, M. & IMAI, M. (1988). Site and mechanism of action of trichlormethiazide in rabbit distal nephron segments perfused in vitro. *J. Clin. Invest.*, **82,** 721–730.

STANTON, B.A., BIEMESDERFER, D., WADE, J.B. & GIEBISCH, G. (1981). Structural and functional study of rat distal nephron: effects of potassium adaptation and potassium depletion. *Kidney Int.*, **19,** 36–48.

STANTON, B.A. & GIEBISCH, G.H. (1982). Potassium transport by the renal distal tubule: effects of potassium loading. *Am. J. Physiol.*, **243,** F487–F493.

STOKES, J.B. (1981). Potassium secretion by the cortical collecting tubule: relation to sodium absorption, luminal sodium concentration, and transepithelial voltage. *Am. J. Physiol.*, **241,** F395–F402.

TAKAHASHI, H., TAKIZAWA, S., TATEWAKI, W., NAGAI, K., WADA, K., HANANO, M. & SHIBATA, A. (1989). Nafamostat mesilate (FUT-175) in the treatment of patients with disseminated intravascular coagulation. *Thomb. Haemost.*, **62,** 372.

YAMAZAKI, Z., HIRAISHI, M., KANAI, F., TAKAHAMA, T., IDEZUKI, Y. & INOUE, N. (1989). Pharmacodynamics of FUT-175 anticoagulant in adsorbent plasma perfusion. *Trans. Am. Artif. Intern. Organs*, **35,** 567–569.

YOSHIKAWA, T., MURAKAMI, M., FURUKAWA, Y., KATO, H., TAKEMURA, S. & KONDO, M. (1983). Effects of FUT-175, a new systhetic protease inhibitor on endotoxin-induced disseminated intravascular coagulation in rats. *Haemostasis*, **13,** 374–378.

WRIGHT, F.S. & GIEBISCH, G. (1992). Regulation of potassium excretion. In *The Kidney: Physiology and Pathophysiology. 2nd ed.*, ed. Seldin, D.W. & Giebisch, G. pp. 2209–2278. New York: Raven Press.

*(Received January 4, 1993*
*Revised February 26, 1993*
*Accepted March 1, 1993)*

*Br. J. Pharmacol.* (1993), **109**, 679–684 © Macmillan Press Ltd, 1993

# Effects of KRN2391, nicorandil and diltiazem on the changes in the electrocardiogram caused by endothelin-1 in anaesthetized rats

[1]Katsuhiko Harada, Atsushi Miwa, Soichiro Kaneta, Toshio Izawa, Hideaki Fukushima & Nobuyuki Ogawa

Pharmaceutical Research Laboratory, Kirin Brewery Co. Ltd., Miyahara-cho 3, Takasaki, Gunma 370-12 Japan

**1** The effect of KRN2391, a novel vasodilator, on the changes of electrocardiogram caused by endothelin-1 (ET-1) was studied in anaesthetized rats and compared with the effects of nicorandil and diltiazem. In addition, the effect of KRN2391 on the action potential of guinea-pig papillary muscle was studied.

**2** The intracoronary administration (i.c.) of ET-1 (5 μg) induced not only ST segment elevation of the electrocardiogram due to contraction of the coronary artery, but also arrhythmias involving atrio-ventricular block (A-V block), ventricular premature contraction (VPC) and ventricular fibrillation (VF), and resulted in death in most animals. However, the administration of methacholine (3 μg, i.c.) produced ST segment elevation alone without developing arrhythmias.

**3** Pretreatment with intravenous administration of KRN2391 (30 μg kg$^{-1}$) inhibited the ST segment elevation and the development of arrhythmias induced by ET-1, and decreased the incidence of death.

**4** Nicorandil (1000 μg kg$^{-1}$) prevented the ST segment elevation without suppression of the occurrence of VF. Diltiazem (100 μg kg$^{-1}$) suppressed both the ST segment elevation and the occurrence of VF but not other arrhythmias. Nicorandil at 3000 μg kg$^{-1}$ and diltiazem at 300 μg kg$^{-1}$ produced not only a suppression of ST segment elevation and VF incidence but also a decrease in the occurrence of arrhythmias. These doses of nicorandil and diltiazem produced a decrease in death in a dose-dependent manner.

**5** KRN2391 (10 and 30 μg kg$^{-1}$), nicorandil (1000 and 3000 μg kg$^{-1}$) and diltiazem (100 and 300 μg kg$^{-1}$) significantly decreased mean blood pressure in a dose-dependent manner. Heart rate was decreased by nicorandil (3000 μg kg$^{-1}$) and diltiazem (100 and 300 μg kg$^{-1}$) but was not affected by KRN2391 (10 and 30 μg kg$^{-1}$).

**6** KRN2391 (30 μM) significantly shortened the action potential duration of guinea-pig ventricle at 50% and 90% repolarization ($APD_{50}$ and $APD_{90}$). The effect of KRN2391 was inhibited by a $K^+$ channel blocker, glibenclamide (30 μM).

**7** These results suggest that the occurrence of ST segment elevation and arrhythmias induced by ET-1 are due to a dual direct action on both coronary vascular smooth muscle and myocardium. Therefore, the protective effects of KRN2391, nicorandil and diltiazem on ET-1-induced heart disorders appear to be due to their direct actions on coronary vascular smooth muscle and the myocardium.

**Keywords:** Endothelin; KRN2391; nicorandil; diltiazem; ST segment elevation; arrhythmia

## Introduction

At present, coronary spasm is thought to be a cause of variant angina. Although many factors, such as endogenous vasoconstrictors derived from endothelial cells and platelets, have been demonstrated, the precise mechanism of coronary vasospasm remains unclear. Endothelin is now considered to play an important role in the development of hypertension and variant angina since endothelin was discovered as a novel potent vasoconstrictor released from endothelial cells (Yanagisawa *et al.*, 1988). Toyo-oka *et al.* (1991) observed clinically that the coronary sinus blood concentrations of endothelin increased in patients with variant angina and probable coronary vasospasm. In addition, when endothelin was administered into the coronary artery of dogs or rats, coronary constriction and ST segment elevation of the electrocardiogram similar to the clinical phenomenon of variant angina were observed (Nichols *et al.*, 1990; Yorikane & Koike, 1990).

Recently, we identified a novel vasodilator, KRN2391 (Figure 1), possessing both a $K^+$ channel opening action and a nitrate action (Kashiwabara *et al.*, 1991). KRN2391 may be useful in ischaemic heart disease because it shows selectivity for the coronary vascular beds in dogs (Ogawa *et al.*, 1990) and protective effects in vasopressin- (Harada *et al.*, 1990), isoprenaline- and methacholine-induced anginal models in rats (Harada *et al.*, 1991). In the present study, we have examined the effect of KRN2391 on the anginal characteristics induced by the intracoronary administration of endothelin-1 (ET-1) and compared it with those of other antianginal drugs, nicorandil and diltiazem, in anaesthetized rats.

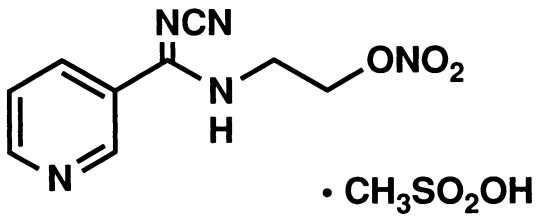



**Figure 1** Chemical structure of KRN2391.

[1] Author for correspondence.

## Methods

### *Electrocardiogram measurements*

Male Wistar rats weighing 250–310 g were anaesthetized with urethane and α-chloralose (1 g $kg^{-1}$, i.p. and 25 mg $kg^{-1}$, i.p., respectively). The change in the ST-segment of the Lead II electrocardiogram (ECG) was used to monitor ischaemia. A polyethylene cannula was introduced from the right carotid artery to inject ET-1 and its tip was positioned at the coronary ostia. The position of the tip of the cannula was confirmed by the elevation in ST segment induced by methacholine (3 μg, i.c.). It is well known that the intracoronary administration of methacholine causes an elevation of ST segment of the ECG by myocardial ischaemia related to coronary spasm (Aono *et al.*, 1981; Sakai *et al.*, 1981). ET-1 was injected over 5 s in a volume of 20 μl. KRN2391, nicorandil and diltiazem were administered intravenously through the femoral vein, 2 min before the injection of ET-1. A Lead II ECG was recorded using an electrocardiograph (AP-621G, Nihon Kohden, Tokyo, Japan). The effects of KRN2391, nicorandil and diltiazem on ET-1-induced ECG changes were examined in different animals.

### *Blood pressure and heart rate measurements*

In a separate group of animals (male Wistar rats weighing 270–310 g) blood pressure was measured via a cannula in the carotid artery using a pressure transducer (TP-200T, Nihon Kohden, Tokyo, Japan) through a carrier amplifier (AP-647G, Nihon Kohden, Tokyo, Japan). Mean blood pressure (MBP) was calculated as follows: MBP (mmHg) = (systolic blood pressure − diastolic blood pressure) × 1/3 + diastolic blood pressure. Heart rate (HR) was measured by a heart rate counter (AT-601G, Nihon Kohden, Tokyo, Japan) triggered by the pulses. Drugs were administered into the femoral vein.

### *Action potential recording*

Male guinea-pigs weighing 500–550 g were anaesthetized with sodium pentobarbitone (40 mg $kg^{-1}$, i.p.). The hearts were rapidly excised and placed in Tyrode solution equilibrated with 95% $O_2$ and 5% $CO_2$. Papillary muscles less than 1 mm in diameter and 2–3 mm in length were separated and mounted in a tissue chamber (3 ml volume). The preparation was superfused at a rate of 6 ml $min^{-1}$ with Tyrode solution equilibrated with 95% $O_2$ and 5% $CO_2$. The temperature of the tissue bath was maintained at 35 ± 0.5°C. The preparations were stimulated electrically at a rate of 0.5 Hz with rectangular pulses of 1 ms duration and twice threshold voltage through bipolar platinum electrodes, and equilibrated for at least 60 min after excision. Membrane potentials were recorded via glass microelectrodes filled with 3 M KCl (resistances of 15–25 MΩ) using a d.c. preamplifier (MEZ-8300, Nihon Kohden, Tokyo, Japan) and were displayed using a

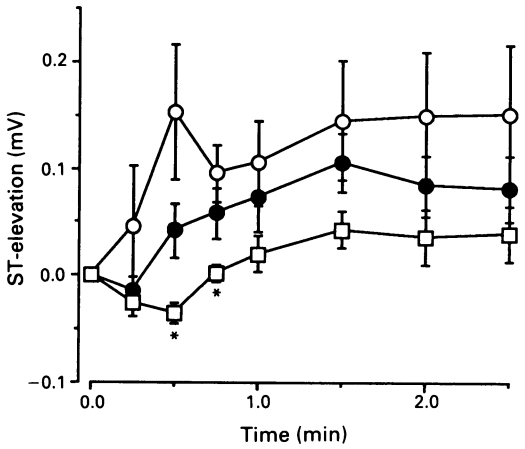



**Figure 3** The effect of KRN2391 on ST segment elevation induced by the intracoronary administration of endothelin-1 (ET-1) in anaesthetized rats. (○) Responses in vehicle-treated animals ($n = 6$); (●) responses in KRN2391 (10 μg $kg^{-1}$)-treated animals ($n = 5$); (□) responses in KRN2391 (30 μg $kg^{-1}$)-treated animals ($n = 5$). Each point represents the mean ± s.e.mean. *Significant difference from the corresponding value in the vehicle-treated group ($P < 0.05$).

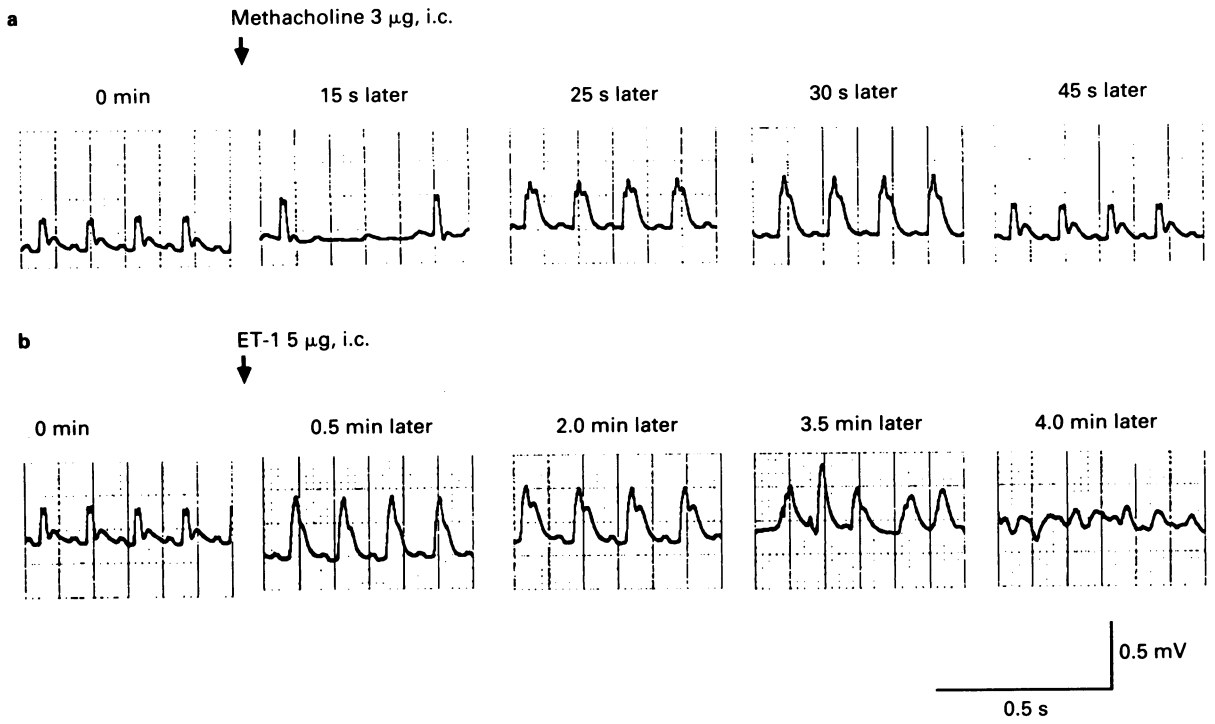



**Figure 2** Typical recording of the changes of electrocardiogram induced by intracoronary administration of methacholine (a) and endothelin-1 (ET-1) (b) in anaesthetized rats.

memory oscilloscope (VC-11, Nihon Kohden, Tokyo, Japan). Membrane potentials were recorded onto an electric recorder (WT-647G, Nihon Kohden, Tokyo, Japan). Action potentials were recorded with single cell impalements before and 15 min after exposure to each concentration of the drug applied cumulatively into the superfusate. Action potential parameters measured were the resting membrane potential (RP), the action potential amplitude (APA), and the action potential duration at the levels of 20, 50 and 90% repolarization ($APD_{20}$, $APD_{50}$, $APD_{90}$). The maximum rate of rise of the action potential ($V_{max}$) was obtained with an electronic differentiator (EQ-601G, Nihon Kohden, Tokyo, Japan).

### *Drugs and solutions*

Tyrode solution for microelectrode studies contained (in mM): NaCl 137, KCl 2.7, $MgCl_2$ 1.0, $CaCl_2$ 1.8, $NaH_2PO_4$ 11.9, glucose 5.5. KRN2391 and nicorandil were synthesized in our laboratory. Diltiazem hydrochloride, methacholine chloride and glibenclamide were purchased from Sigma Chemical Company (St. Louis, MO, U.S.A.) and ET-1 from the Peptide Institute (Osaka, Japan). KRN2391, diltiazem hydrochloride, nicorandil and methacholine chloride were dissolved in saline for intravenous administration. For action potential measurements, KRN2391 was dissolved in distilled water. Glibenclamide (10 mM) was dissolved in dimethylsulphoxide. ET-1 was dissolved in saline and stored in a polyethylene vial at − 20°C until used.

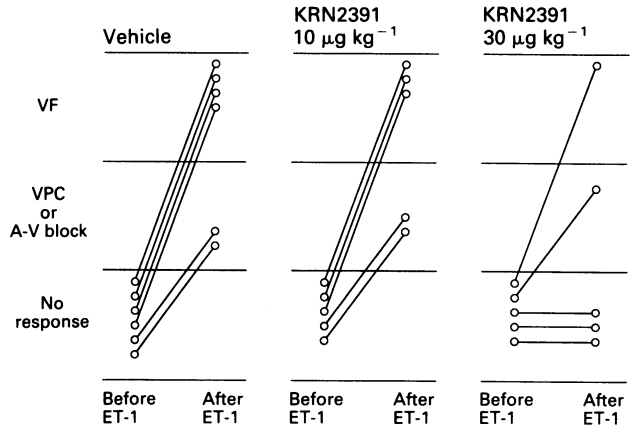



**Figure 4** The effect of KRN2391 on arrhythmias induced by the intracoronary administration of endothelin-1 (ET-1) in anaesthetized rats. VF: ventricular fibrillation; VPC: ventricular premature contraction: A-V block: atrio-ventricular block.

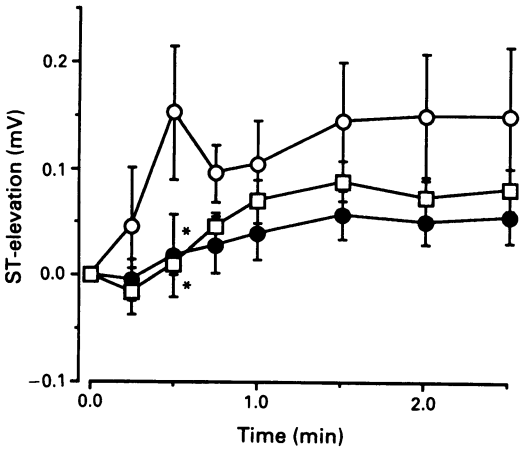



**Figure 5** The effect of nicorandil on ST segment elevation induced by intracoronary administration of endothelin-1 (ET-1) in anaesthetized rats. (○) Responses in vehicle-treated animals ($n = 7$); (●) responses in nicorandil (1000 μg kg$^{-1}$)-treated animals ($n = 7$); (□) responses in nicorandil (3000 μg kg$^{-1}$)-treated animals ($n = 7$).Each point represents the mean ± s.e.mean. *Significant difference from the corresponding value in the vehicle-treated group ($P < 0.05$).

### *Statistical analysis*

Differences were considered at a level of significance of $P < 0.05$, using Student's $t$ test for paired data for single comparisons and analysis of variance for multiple comparisons. When multiple comparisons were made with a single control, Dunnett's test was used to determine levels of significance. Data are presented as the mean ± s.e.mean.

## Results

### *Effects of intracoronary administration of methacholine and endothelin-1 on ECG*

A typical record of the ECG observed following the administration of methacholine (3 μg, i.c.) or ET-1 (5 μg, i.c.) is shown in Figure 2. Methacholine induced transient cardiac arrest followed by ST segment elevation of the ECG. The duration of ST segment elevation by methacholine was less than 10 s. ET-1 also produced ST segment elevation and the duration of ST segment elevation by ET-1 was longer than that produced by methacholine. In addition, arrhythmias involving atrio-ventricular block (A-V block), ventricular premature contraction (VPC) and ventricular fibrillation (VF) were present 2.6 to 5.0 min after administratin of ET-1. These arrhythmias resulted in death of four out of six rats in the control observations. However, methacholine did not induce arrhythmias and death, in spite of showing ST segment elevation.

### *Effects of KRN2391, nicorandil and diltiazem on endothelin-1 (5 μg, i.c.)-induced heart disorders*

Pretreatment with KRN2391, 30 μg kg$^{-1}$, i.v., significantly inhibited ST segment elevation induced by ET-1 (5 μg, i.c.) (Figure 3). A dose of 10 μg kg$^{-1}$ KRN2391 also tended to attenuate ET-1-induced ST segment elevation but this effect was not significant. Although ET-1 caused arrhythmias in all rats and death in four out of six rats in the control group, arrhythmias and death in rats given KRN2391 at 30 μg kg$^{-1}$ occurred in two out of five rats and one out of five rats, respectively. That is, the occurrences of A-V block, VPC and VF were decreased by 30 μg kg$^{-1}$ KRN2391 (Figure 4).

Nicorandil at 1000 and 3000 μg kg$^{-1}$ significantly suppressed the ST segment elevation induced by ET-1 to almost the same level as KRN2391 (Figure 5). Nicorandil at 1000 μg kg$^{-1}$ did not decrease the occurrence of arrhythmias by ET-1, but decreased the incidence of death to two out of seven rats (Figure 6). Nicorandil at 3000 μg kg$^{-1}$ diminished the occurrence of VF and death to one out of seven rats compared with four out of six rats given vehicle.

Diltiazem, at 100 and 300 μg kg$^{-1}$, significantly inhibited ET-1-induced ST segment elevation to almost the same level (Figure 7). Diltiazem at 100 μg kg$^{-1}$ decreased the occurrences of VF and death, i.e. these were observed in four out of six rats given vehicle but in two out of seven rats given 100 μg kg$^{-1}$ (Figure 8). However, diltiazem (100 μg kg$^{-1}$) did not suppress arrhythmias with the exception of VF. A dose of 300 μg kg$^{-1}$ diltiazem decreased the occurrence of arrhythmias involving VF.

### *Effects of KRN2391, nicorandil and diltiazem on haemodynamics*

Table 1 shows the effects of KRN2391, nicorandil and diltiazem at the doses which were used to examine their effects

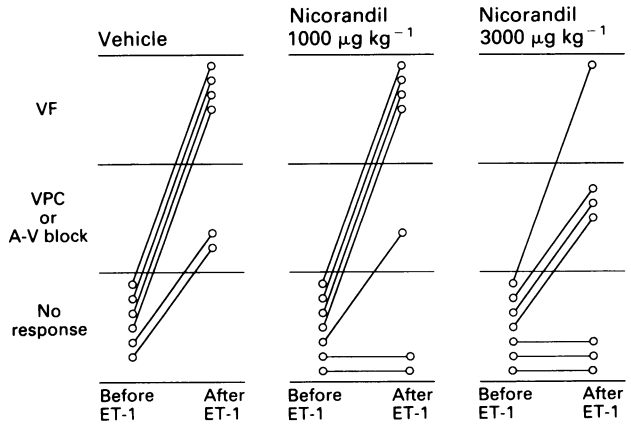



**Figure 6** The effect of nicorandil on arrhythmias induced by intracoronary administration of endothelin-1 (ET-1) in anaesthetized rats. VF: ventricular fibrillation; VPC: ventricular premature contraction; A-V block: atrio-ventricular block.

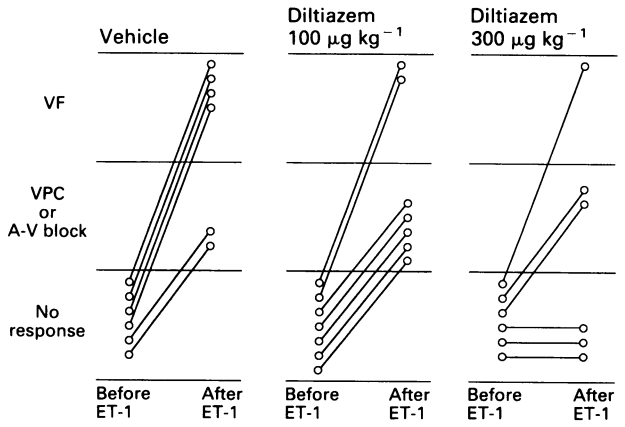



**Figure 8** The effect of diltiazem on arrhythmias induced by intracoronary administration of endothelin-1 (ET-1) in anaesthetized rats. VF: ventricular fibrillation; VPC: ventricular premature contraction; A-V block: atrio-ventricular block.

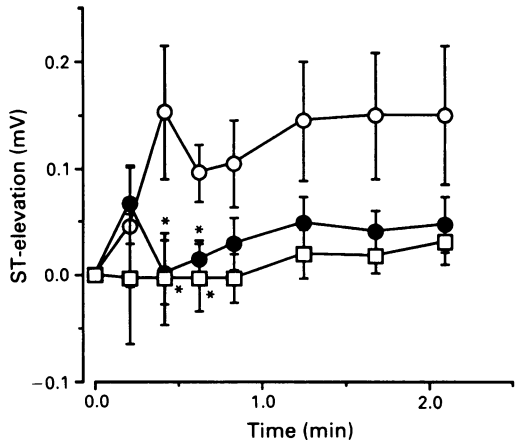



**Figure 7** The effect of diltiazem on ST segment elevation induced by intracoronary administration of endothelin-1 (ET-1) in anaesthetized rats. (○) Responses in vehicle-treated animals ($n = 6$); (●) responses in diltiazem (100 μg kg$^{-1}$)-treated animals ($n = 7$); (□) responses in diltiazem (300 μg kg$^{-1}$)-treated animals ($n = 6$). Each point represents the mean ± s.e.mean. *Significant difference from the corresponding value in the vehicle-treated group ($P < 0.05$).

**Table 1** Effects of KRN2391, nicorandil and diltiazem on mean blood pressure and heart rate in anaesthetized rats

| *Drug* (μg kg$^{-1}$) | | *MBP* (Δ%) | *HR* (Δ%) |
|---|---|---|---|
| KRN2391 | 10 | − 7.0 ± 1.7* | 1.9 ± 1.6 |
| | | (115 ± 5) | (450 ± 20) |
| | 30 | − 22.9 ± 3.3* | 3.5 ± 2.8 |
| | | (111 ± 4) | (454 ± 14) |
| Nicorandil | 1000 | − 34.9 ± 3.9* | 0.9 ± 1.0 |
| | | (113 ± 6) | (441 ± 14) |
| | 3000 | − 52.4 ± 2.8* | − 22.7 ± 1.9* |
| | | (117 ± 1) | (468 ± 8) |
| Diltiazem | 100 | − 12.5 ± 1.8* | − 9.0 ± 1.0* |
| | | (112 ± 8) | (425 ± 9) |
| | 300 | − 26.0 ± 2.4* | − 21.8 ± 1.7* |
| | | (112 ± 6) | (428 ± 18) |

MBP: mean blood pressure, HR: heart rate. The changes in MBP and HR are presented as the percent changes from the basal MBP (mmHg) and HR (beats min$^{-1}$) values (parentheses). Values are mean ± s.e.mean. ($n = 4$).
*Significantly different from the basal values $P < 0.05$.

on ET-1-induced heart disorders, on MBP and HR. KRN2391 (10 and 30 μg kg$^{-1}$), nicorandil (1000 and 3000 μg kg$^{-1}$) and diltiazem (100 and 300 μg kg$^{-1}$) all produced decreases in MBP in a dose-dependent manner. A decrease in HR was induced by nicorandil at 3000 μg kg$^{-1}$ and diltiazem at 100 and 300 μg kg$^{-1}$. KRN2391 at 10 and 30 μg kg$^{-1}$ and nicorandil at 1000 μg kg$^{-1}$ had no effect on HR. The effects of these drugs on MBP reached a peak 1–2 min after administration. Hypotensive effects of nicorandil lasted more than 60 min at both doses, those of KRN2391 at 10 and 30 μg kg$^{-1}$ lasted for about 10 and 20 min, respectively, and those of diltiazem at 100 and 300 μg kg$^{-1}$ lasted for about 15 and 40 min, respectively.

### *Electrophysiological effects of KRN2391*

KRN2391 (30 μM) significantly shortened $APD_{50}$ and $APD_{90}$ of guinea-pig papillary muscles, but had no effect on other parameters (Table 2). The effect of KRN2391 (30 μM) on action potential duration was inhibited by glibenclamide (30 μM) (Table 2).

## Discussion

The present results showed that ET-1 induced not only ST segment elevation due to myocardial ischaemia but also produced arrhythmias. In contrast, methacholine produced ST segment elevation without associated arrhythmias and death. The results with ET-1 and methacholine in the present studies were similar to those obtained in previous reports (Aono *et al.*, 1981; Sakai *et al.*, 1981; Yorikane & Koike, 1990). The effects of ET-1 and methacholine are thought to be due to myocardial ischaemia related to the contraction of coronary arteries. It has been observed that ET-1 and methacholine produce coronary vasoconstriction in isolated perfused hearts of rats (Aono *et al.*, 1981; Sakai *et al.*, 1981; Neubauer *et al.*, 1990). However, arrhythmias induced by ET-1 were not solely due to myocardial ischaemia, because methacholine did not produce arrhythmias in spite of ST segment elevation. Therefore, ET-1 may produce an increase in intracellular $Ca^{2+}$ in the myocardium in addition to vasoconstriction, because increase in $Ca^{2+}$ appears to play an important role in the development of ventricular arrhythmias (Billman, 1989). Lauer *et al.* (1989) reported that ET-1 increased intracellular $Ca^{2+}$ in ventricular myocytes. Yorikane *et al.* (1991) also observed that ET-1 induced early afterdepolarizations contributing to the development of

**Table 2** Effects of KRN2391 and glibenclamide (Glib) on action potential of guinea-pig papillary muscles

| | *APA* (mV) | *RP* (mV) | $APD_{20}$ (ms) | $APD_{50}$ (ms) | $APD_{90}$ (ms) | $V_{max}$ ($V\,s^{-1}$) |
|---|---|---|---|---|---|---|
| Control | 139 ± 1 | − 96 ± 2 | 150 ± 17 | 241 ± 14 | 297 ± 11 | 141 ± 8 |
| KRN2391 10 μM | 138 ± 2 | − 99 ± 2 | 130 ± 16 | 214 ± 17 | 271 ± 15 | 142 ± 8 |
| KRN2391 30 μM | 130 ± 6 | − 98 ± 2 | 89 ± 19 | 140 ± 26* | 181 ± 29* | 128 ± 8 |
| KRN2391 30 μM + Glib 30 μM | 138 ± 2 | − 100 ± 3 | 141 ± 29 | 244 ± 21 | 299 ± 19 | 130 ± 8 |

APA: action potential amplitude, RP: resting membrane potential, $APD_{20}$, $APD_{50}$ and $APD_{90}$: action potential duration of 20, 50 and 90% repolarization, $V_{max}$: the maximum rate of rise of action potential. Values are mean ± s.e.mean. ($n = 4$).
*Significantly different from the values of control $P < 0.05$.

some types of arrhythmias. Thus, it is considered that the direct combined effects of ET-1 on coronary arteries and the myocardium contribute to the development of ST segment elevation and arrhythmias.

The present study showed that KRN2391 protected the heart from ST segment elevation and arrhythmias induced by ET-1. Nicorandil and diltiazem also suppressed ST segment elevation and arrhythmias induced by ET-1. However, the doses of nicorandil and diltiazem for the suppression of arrhythmia by ET-1 were higher than those required for suppression of ST segment elevation, because 1000 $\mu g\,kg^{-1}$ nicorandil and 100 $\mu g\,kg^{-1}$ diltiazem did not produce an obvious suppression of arrhythmia in spite of reducing ST segment elevation. The doses of KRN2391, nicorandil and diltiazem which produced suppression of the occurrence of arrhythmia were 30, 3000 and 300 $\mu g\,kg^{-1}$, respectively.

KRN2391 30 $\mu g\,kg^{-1}$ was the dose which produced a 22.9% decrease in MBP without affecting HR; 300 $\mu g\,kg^{-1}$ of diltiazem produced not only a 26.0% decrease in MBP but also a 21.8% decrease in HR. Nicorandil at 3000 $\mu g\,kg^{-1}$ also produced 52.4% and 22.7% reductions in MBP and HR, respectively. Thus, these results suggest that KRN2391 can suppress ET-1-induced arrhythmias at a dose which induced weak hypotension in comparison with nicorandil and diltiazem and did not affect HR.

The protective effects of KRN2391, nicorandil and diltiazem on ST segment elevation appear to be due to the inhibitory action on the contraction of coronary arteries induced by ET-1. Earlier studies suggested that ET-1-induced vasoconstriction was caused by the activation of voltage-dependent $Ca^{2+}$ channels (Yanagisawa *et al.*, 1988) and the hydrolysis of phosphatidyl inositol which leads to $Ca^{2+}$ release from the intracellular $Ca^{2+}$ store (Van Renterghem *et al.*, 1988). Recently, Miyoshi *et al.* (1992) reported that ET-1 blocked ATP-sensitive $K^+$ channels in the porcine coronary artery. In addition, ET-1-induced contraction of coronary arteries has been shown to be attenuated by $Ca^{2+}$ channel blockers and $K^+$ channel openers (Kim *et al.*, 1989; Turner *et al.*, 1989). Concerning the mechanism of vasodilatation induced by $K^+$ channel openers, hyperpolarization caused by the increase in outward $K^+$ current is thought to inhibit voltage-dependent $Ca^{2+}$ channels (Cook *et al.*, 1988). Therefore, ET-1-induced vasoconstriction may be attenuated by both $Ca^{2+}$ channel blockers and $K^+$ channel openers. Nicorandil, like KRN2391, show a dual mechanism of action as a nitrate and a $K^+$ channel opener (Taira, 1987). Although nicorandil, like KRN2391, suppressed the ST segment elevation induced by ET-1, the antiarrhythmic effect of nicorandil was weaker than that of KRN2391. The mechanism for the effect of nicorandil on the coronary vascular beds and the myocardium may be different from that of KRN2391.

Recently, Yorikane *et al.* (1991) observed that ET-1 produced prolongation of action potential duration followed by the development of early afterdepolarizations in canine myocardial preparations, and suggested that the electrophysiological change in the myocardium caused by ET-1 was associated with the occurrence of arrhythmias. Furthermore, they reported that nicardipine, a $Ca^{2+}$ channel blocker, inhibited the development of early afterdepolarizations caused by ET-1. This effect of nicardipine was thought to be based on a shortening of action potential duration, i.e. the prolongation of action potential duration by ET-1 was antagonized by nicardipine. In the myocardium, $K^+$ channel openers, such as pinacidil and cromakalim, are also known to produce a shortening of action potential through an increase in $K^+$ conductance (Osterrieder, 1988; Martin & Chinn, 1990). In addition, the shortening of action potential duration was also observed with nicorandil (Kojima & Ban, 1988). In the present study, KRN2391 produced a shortening of action potential duration through its $K^+$ channel opening action. Therefore, it is considered that the effects of KRN2391, nicorandil and diltiazem on action potential contribute to the reduction of appearance of VF and death induced by ET-1.

In summary, we have shown that ET-1 induces arrhythmias in addition to ST segment elevation of the ECG and methacholine produces only ST segment elevation. The protective effects of KRN2391, nicorandil and diltiazem on ET-1-induced heart disorders are considered to be due to their direct actions on coronary vascular smooth muscle and on the myocardium. Although KRN2391 inhibited the occurrence of arrhythmia concomitantly with the suppression of ST segment elevation, the inhibitory effects of nicorandil and diltiazem on arrhythmias required higher doses than those needed to suppress ST segment elevation.

## References


AONO, J., AKIMA, M. & SAKAI, K. (1981). Effects of N-(2-hydroxyethyl)nicotinamide nitrate (SG-75) on methacholine-induced ECG changes in intact anesthetized rats. *Jpn. J. Pharmacol.*, **31**, 823–830.

BILLMAN, G.E. (1991). The antiarrhythmic and antifibrillatory effects of calcium antagonists. *J. Cardiovasc. Pharmacol.*, **18** (Suppl. 10), S107–S117.

COOK, N.S., WEIR, S.W. & DANZEISEN, M.C. (1988). Anti-vasoconstrictor effects of the $K^+$ channel opener cromakalim on the rabbit aorta – comparison with the calcium antagonist isradipine. *Br. J. Pharmacol.*, **95**, 741–752.

HARADA, K., FUKATA, Y., OGAWA, N. & NISHIKORI, K. (1990). Antianginal effect of KRN2391, a novel vasodilator, on the experimental model of angina pectoris induced by vasopressin treatment in anesthetized rats. *Jpn. J. Pharmacol.*, **52** (suppl. I), 216P.

HARADA, K., FUKATA, Y., OHTA, H., OGAWA, N., FUKUSHIMA, H. & NISHIKORI, K. (1991). Antianginal effect of KRN2391 on the experimental models of anesthetized rats. *Jpn. J. Pharmacol.*, **55** (Suppl. I), 330P.

KASHIWABARA, T., NAKAJIMA, S., IZAWA, T., FUKUSHIMA, H. & NISHIKORI, K. (1991). Characteristics of KRN2391, a novel vasodilator, compared with those of cromakalim, pinacidil and nifedipine in rat aorta. *Eur. J. Pharmacol.*, **196,** 1–7.

KOJIMA, M. & BAN, T. (1988). Nicorandil shortens action potential duration and antagonises the reduction of $V_{max}$ by lidocaine but not by disopyramide in guinea-pig papillary muscles. *Naunyn-Schmied. Arch. Pharmacol.*, **337,** 203–212.

KIM, S., MORIMOTO, S., KOH, E., MIYASHITA, Y. & OGIHARA, T. (1989). Comparison of effects of a potassium channel opener BRL34915, a specific potassium ionophore valinomycin and calcium channel blockers on endothelin-induced vascular contraction. *Biochem. Biophys. Res. Commun.*, **164,** 1003–1008.

LAUER, M.R., GUNN, M.D. & CIUSIN, W. (1989). Effect of endothelin on cytosolic calcium and membrane current in single ventricular myocytes. *Circulation*, **80** (Suppl. II), II–194.

MARTIN, C.L. & CHINN, K. (1990). Pinacidil opens ATP-dependent $K^+$ channels in cardiac myocytes in an ATP- and temperature-dependent manner. *J. Cardiovasc. Pharmacol.*, **15,** 510–514.

MIYOSHI, Y., NAKAYA, Y., WAKATSUKI, T., NAKAYA, S., FUJINO, K., SAITO, K. & INOUE, I. (1992). Endothelin blocks ATP-sensitive $K^+$ channels and depolarizes smooth muscle cells of porcine coronary artery. *Circ. Res.*, **70,** 612–616.

NEUBAUER, S., ERTL, G., HAAS, U., PULZER, F. & KOCHSIEK, K. (1990). Effects of endothelin-1 in isolated perfused rat heart. *J. Cardiovasc. Pharmacol.*, **16,** 1–8.

NICHOLS, A.J., KOSTER, P.F. & OHLSTEIN, E.H. (1990). The effect of diltiazem on the coronary haemodynamic and cardiac functional effects produced by intracoronary administration of endothelin-1 in the anaesthetized dog. *Br. J. Pharmacol.*, **99,** 597–601.

OGAWA, N., KANETA, S., JINNO, Y., HARADA, K., OHTA, H., FUKUSHIMA, H. & NISHIKORI, K. (1990). Pharmacological profile of KRN2391, a novel vasodilator. *Eur. J. Pharmacol.*, **183,** 1266 (abstr.).

OSTERRIEDER, W. (1988). Modification of $K^+$ conductance of heart cell membrane by BRL34915. *Naunyn-Schmied. Arch. Pharmacol.*, **337,** 93–97.

SAKAI, K., AKIMA, M. & AONO, J. (1981). Evaluation of drug effects in a new experimental model of angina pectoris in the intact anesthetized rat. *J. Pharmacol. Methods*, **5,** 325–336.

TAIRA, N. (1987). Similarity and dissimilarity in the mode and mechanism of action between nicorandil and classical nitrates: an overview. *J. Cardiovasc. Pharmacol.*, **10** (Suppl. 8), S1–S9.

TOYO-OKA, T., AIZAWA, T., SUZUKI, N., HIRATA, Y., MIYAUCHI, T., SOO SHINN, W., YANAGISAWA, M., MASAKI, T & SUGIMITO, T. (1991). Increased plasma level of endothelin-1 and coronary spasm induction in patients with vasospastic angina pectoris. *Circulation*, **83,** 476–483.

TURNER, N.C., DOLLERY, C.T. & WILLIAMS, A.J. (1989). Endothelin-1-induced contractions of vascular and tracheal smooth muscle: effects of nicardipine and BRL 34915. *J. Cardiovasc. Pharmacol.*, **13** (Suppl. 5), S180–S182.

VAN RENTERGHEM, C., VIGNE, P., BARHANIN, J., SCHMID-ALLIANA, A., FRELIN, C. & LAZDUNSKI, M. (1988). Molecular mechanism of action of the vasoconstrictor peptide endothelin. *Biochem. Biophys. Res. Commun.*, **157,** 977–985.

YANAGISAWA, M., KURIHARA, H., KIMURA, S., TOMOBE, Y., KOBAYASHI, M., MITSUI, Y., YAZAKI, Y., GOTO, K. & MASAKI, T. (1988). A novel potent vasoconstrictor peptide produced by vascular endothelial cells. *Nature*, **332,** 411–415.

YORIKANE, R. & KOIKE, H. (1990). The arrhythmogenic action of endothelin in rats. *Jpn. J. Pharmacol.*, **53,** 259–263.

YORIKANE, R., KOIKE, H. & MIYAKE, S. (1991). Electrophysiological effects of endothelin-1 on canine myocardial cells. *J. Cardiovasc. Pharmacol.*, **17** (Suppl. 7), S159–S162.

*(Received November 24, 1992*
*Revised March 3, 1993*
*Accepted March 4, 1993)*

*Br. J. Pharmacol.* (1993), **109**, 685–692 © Macmillan Press Ltd, 1993

# Dual effects of chlorobutanol on secretory response and intracellular $Ca^{2+}$ dynamics in isolated pancreatic acini of the rat

[1]*Y. Habara & *†T. Kanno

*Laboratory of Cellular Metabolism, Department of Molecular Physiology, National Institute for Physiological Sciences, Okazaki 444, Japan and †Department of Physiology, Faculty of Veterinary Medicine, Hokkaido University, Sapporo 060, Japan

**1** The effects of chlorobutanol, a widely used drug preservative, on exocrine response and intracellular $Ca^{2+}$ dynamics were examined in isolated pancreatic acini of the rat.

**2** Chlorobutanol (1 mg $ml^{-1}$) markedly inhibited the secretory response to cholecystokinin octapeptide (CCK-8), carbamylcholine chloride (carbachol), or sodium fluoride, a direct G-protein activator. However, chlorobutanol itself induced a maximal release of amylase when the dose was increased to 4 mg $ml^{-1}$.

**3** An oscillatory fluctuation of cytoplasmic $Ca^{2+}$ concentration, $[Ca^{2+}]_c$, induced by 5 pM CCK-8 or 0.3 μM carbachol was totally abolished in the presence of 1 mg $ml^{-1}$ chlorobutanol.

**4** A biphasic change in $[Ca^{2+}]_c$ induced by 100 pM CCK-8, a rapid rise followed by a gradual decay, was transformed to an oscillatory fluctuation by the preservative.

**5** Chlorobutanol inhibited 13 pM [$^{125}$I]-CCK-8 or 0.5 nM [$^{3}$H]-methylscopolamine chloride binding to the acinar cells in a dose-dependent manner.

**6** These results indicate that chlorobutanol produces discernible pharmacological effects on the secretory response in rat pancreatic acinar cells through changes in the $Ca^{2+}$ dynamics. Possible sites of action could be at a binding process of secretagogues to their receptors, at an activation process of a G-protein located in the plasma membrane, or at the processes following G-protein activation. However, the possibility that the preservative may distort the $Ca^{2+}$-transport function of the plasma membrane or the membrane of intracellular organella, especially $Ca^{2+}$-sequestering pools, cannot be excluded.

**Keywords:** Exocrine pancreas; $Ca^{2+}$; chlorobutanol; signal transduction

## Introduction

Chlorobutanol coexists as a preservative in various therapeutic drugs. This chemical shows a weak anaesthetic effect and is structurally related to volatile anaesthetics such as chloroform, ethyl chloride, or halothane. During the course of experiments using isolated rat adrenal chromaffin cells in which a spontaneous fluctuation of the cytoplasmic calcium concentration, $[Ca^{2+}]_c$, has been recorded, we observed that commercially available catecholamine solutions which contain chlorobutanol could attenuate these spontaneous changes in $[Ca^{2+}]_c$ (Warashina *et al.*, unpublished observations). After observing this unexpected but explicit effect of the preservative, we surveyed previous reports and found that several workers have demonstrated an inhibitory effect of chlorobutanol on physiological functions in various types of cells. Myocardial excitation (Hermsmeyer & Aprigliano, 1976), contractile responses of aorta (Barrigon *et al.*, 1984), blood pressure (Bowler *et al.*, 1985), and skeletal muscle contraction (Sim *et al.*, 1987) have all been shown to be distorted or inhibited by chlorobutanol. Most of these reports have proposed that the inhibitory action of the preservative may be due to perturbation of intracellular $Ca^{2+}$ mobilization, a key signal for excitation-contraction coupling. As described above, we also found a similar inhibitory action of chlorobutanol on the rat adrenal chromaffin cell which is one of the typical endocrine cells that utilize $Ca^{2+}$ as an intracellular messenger for signal transduction.

This investigation was thus carried out to examine further the effect of chlorobutanol and to identify possible sites of action using rat pancreatic acinar cells, which we have long utilized to investigate cellular mechanism(s) of stimulus-secretion coupling. In the current study, we attempted to determine (1) whether the secretory response to different stimuli can be influenced by chlorobutanol, (2) whether intracellular $Ca^{2+}$ dynamics during secretion can be affected by chlorobutanol, and (3) whether secretagogues binding to the receptors can be affected by the preservative.

The results confirmed that the preservative possesses a distinct action on $Ca^{2+}$ dynamics and secretory responses, and suggest that care should be taken when therapeutic drugs containing chlorobutanol are chosen for clinical or experimental purposes. On the other hand, the preservative can be a useful tool for investigation of cellular signal transduction processes.

## Methods

Male SPF rats of Sprague-Dawley strain weighing 200–250 g b.w. were fasted overnight and used for the experiments.

### *Isolation of pancreatic acini*

Pancreatic acini were isolated by collagenase digestion as described previously (Hootman *et al.*, 1986; Habara & Kanno, 1991). Briefly, the tail portion of the pancreas was excised, injected with collagenase 65 u $ml^{-1}$ in HEPES-buffered Ringer solution (2.5 ml) containing 0.1 mg $ml^{-1}$ of soybean trypsin inhibitor and incubated for a total of 60 min with vigorous shaking at 37°C. The tissue was then

[1] Author for correspondence.

mechanically disrupted with a pipette, filtered through 150 μm nylon mesh, rinsed three times, pelleted, and resuspended in a suitable amount of the Ringer solution. The composition of the Ringer solution was as follows (mM): NaCl 118, KCl 4.7, $CaCl_2$ 2.5, $MgCl_2$ 1.13, $NaH_2PO_4$ 1.0, D-glucose 5.5 and HEPES 10. The solution was supplemented with bovine serum albumin (2 mg $ml^{-1}$), Eagle's minimal essential amino acids, and L-glutamine (2.0 mM). The pH of the solution was adjusted to 7.4 with NaOH and gassed with 100% $O_2$. Isolated acini were usually preincubated for 30 min or preperifused for 60 min at 37°C before the experiments.

### *Incubation experiments and perifusion experiments*

The effects of chlorobutanol on the secretory responses were examined in two different experimental systems, namely incubation experiments (Hootman *et al.*, 1986) and perifusion experiments (Kanno *et al.*, 1989). In the incubation experiments, the secretory response was assessed by measuring amylase activity released into the media over the 30 min stimulation period with various concentrations of CCK-8 or carbachol in the presence or the absence of different concentrations of chlorobutanol. The effect of the preservative was also examined by using 10 mM sodium fluoride (NaF), a direct activator of guanine nucleotide binding proteins (G-proteins), which is known to induce $Ca^{2+}$-dependent secretory responses in rat pancreatic acini (Habara *et al.*, 1990). Amylase activities were expressed as a percentage of the total activity initially present in the acini. The perifusion experiments were also carried out to investigate the effect of chlorobutanol on the time course of the secretory response that was induced by continuous stimulation with the secretagogues and the effect was later compared with that on the $[Ca^{2+}]_c$ dynamics. An aliquot of acini suspension was loaded onto a Millipore filter (5 μm pore size) held in a plastic holder, and perifused with the Ringer solution at a rate of 1 ml $min^{-1}$ using a Perista Minipump. The perifusates were collected into glass tubes at 2 min intervals. To assess the effect of chlorobutanol, acini were first perifused with the Ringer solution containing 1 mg $ml^{-1}$ of chlorobutanol for 10 min followed by a continuous stimulation with various concentrations of CCK-8 or carbachol in the presence of the same dosage of chlorobutanol. Control experiments were done with the same protocol in the absence of the preservative. Amylase activities were determined by the modified method of Bernfeld (Kanno, 1975). Chlorobutanol itself did not interfere with the amylase measurement.

### *Measurement of cytoplasmic calcium concentration*

Temporal and spatial dynamics of $[Ca^{2+}]_c$ were monitored by a digital image analysing technique (Argus-50/Ca, Hamamatsu Photonics, Hamamatsu, Japan) using a silicon intensified target camera as reported previously (Kanno *et al.*, 1989; 1991; Habara & Kanno, 1991). Acini were incubated with a final concentration of 10 μM Fura-2-AM for 40 min with gentle shaking at 37°C. After rinsing, Fura-2-loaded acini were transferred onto a Cell-Tak-coated non-fluorescent cover glass which was mounted in a Sykus-Moore chamber. The chamber was then set on a stage of an inverted microscope (TMD-2, Nikon, Tokyo, Japan) equipped with a Nomarsky type differential interference contrast (DIC) device. Fura-2 fluorescence images (at 510 nm) were formed by a pair of excitation wavelengths (340 nm and 380 nm) via a × 40 objective (Fluor 40, NA 0.85, Nikon, Tokyo, Japan). The ratio of the fluorescence intensities formed by each excitation wavelength was calculated pixel by pixel after background subtraction and converted to a calcium concentration. Temporal analyses of $[Ca^{2+}]_c$ were carried out by selecting four different areas (4 $\mu m^2$ each) from separate cells of acinus. The continuous stimulation of acini with secretagogues was made by perifusing acini with the Ringer solution containing a given concentration of CCK-8 or carbachol in the absence or the presence of chlorobutanol (1 mg $ml^{-1}$). The effect of the preservative alone on $[Ca^{2+}]_c$ was also investigated.

### *Receptor binding*

Receptor binding experiments were carried out with [$^{125}$I]-CCK-8 and [$^3$H]-NMS to examine possible antagonism by chlorobutanol. The [$^3$H]-NMS binding experiments were performed by a method described previously (Hootman *et al.*, 1986; Habara *et al.*, 1986). Briefly, acini were incubated with 0.5 nM [$^3$H]-NMS in the absence or the presence of various concentrations of chlorobutanol for 60 min at 37°C with gentle shaking. After the incubation was terminated, the cell suspensions were poured onto Whatman GF/A filters that were placed on grids of a vacuum filtering apparatus (Millipore, Tokyo branch, Tokyo, Japan). Acini on the filters were rinsed three times with 5 ml of ice cold 0.9% saline, and the filters were transferred into plastic scintillation vials. One millilitre of Solvable and 10 ml of liquid scintillator (Atomlight) were added to the vials, mixed vigorously, and the radioactivities were determined with an Aloka liquid scintillation spectrophotometer.

The effect of chlorobutanol on CCK-8 binding was assessed by incubating acini with 13 pM [$^{125}$I]-CCK-8 for 30 min at 37°C with shaking, in the presence of various

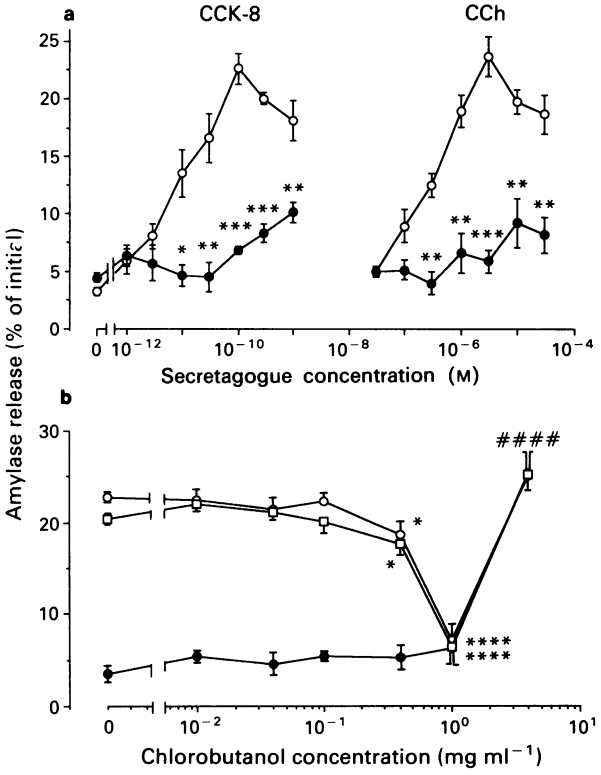



**Figure 1** Effect of chlorobutanol on cholecystokinin octapeptide (CCK-8)- or carbachol (CCh)-induced amylase release in rat pancreatic acini. (a) Acini were stimulated with increasing concentrations of secretagogues for 30 min in the presence (●, 1 mg $ml^{-1}$) or absence (○) of chlorobutanol. Amylase release was expressed as a percentage of the total activity initially present in the acini. (b) Acini were stimulated with 100 pM CCK-8 (○) or 3 μM carbachol (□) for 30 min in the presence of various concentrations of chlorobutanol. Effect of the preservative on basal release (●) is also shown. Each symbol represents mean ± s.e.mean obtained from 3 experiments. $*P<0.05$, $**P<0.02$, $***P<0.01$, $****P<0.001$ (in (b), maximal response in absence of chlorobutanol vs. responses in presence of the preservative). $\#\#\#\#P<0.001$ (basal release without chlorobutanol vs. release induced by 4 mg $ml^{-1}$ preservative).

concentrations of the preservative. After vacuum filtration and rinsing with 0.9% saline containing 0.2% BSA, the filters were transferred into plastic tubes and the radioactivities were determined with an Aloka gamma counter. The ability of chlorobutanol to block agonist or antagonist binding was expressed as percentage binding compared with the maximal binding capacity which was obtained in the absence of the preservative. The inhibitory capacities of atropine, carbachol, and CCK-8 were also determined as standard inhibitions.

### *Materials*

The following drugs and materials were purchased. Bovine serum albumin (Fraction V), carbamylcholine chloride (carbachol), atropine sulphate, and soybean trypsin inhibitor (Type 1-S) were from Sigma Chemical Co. (St. Louis, MO, U.S.A.); highly purified collagenase (CLSPA) from Worthington Biochemical (Freehold, NJ, U.S.A.); cholecystokinin octapeptide (CCK-8) from Peptide Institute (Minoh, Japan); Eagle's minimal essential amino acids medium from Flow Laboratories (Irvine, Scotland); Cell-Tak from Collaborative Research (Bedford, MA, U.S.A.); soluble Zulkowsky starch from Merck (Darmstadt, Germany); Fura-2-AM and Fura-2 from Dojindo (Kumamoto, Japan). Other drugs, including chlorobutanol (1,1,1-trichloro-2-methyl-2-propanol), acetone, chloroform, chlorbutol, chloretone, Methaform, and Sedaform were from Nacalai Tesque (Kyoto, Japan). Bolton-Hunter labelled [$^{125}$I]-CCK-8 (81.4 TBq mmol$^{-1}$), [N-methyl-$^3$H]-scopolamine chloride ([$^3$H]-NMS, 2.94 TBq mmol$^{-1}$), Atomlight as a scintillator, and Solvable were from Du Pont/New England Nuclear (Boston, MA, U.S.A.).

### *Statistical analysis*

Statistical analyses were carried out by the unpaired Student's *t* test.

## Results

### *Inhibitory effect of chlorobutanol on secretory responses to CCK-8 or carbachol in incubated acini*

Figure 1a shows an inhibitory effect of 1 mg ml$^{-1}$ chlorobutanol on the secretagogue-induced amylase release examined in the incubation experiments. Acini were incubated in the Ringer solution containing increasing concentrations of CCK-8 (1 pM–1 nM) or carbachol (30 nM–30 μM) for 30 min in the presence or the absence of chlorobutanol (1 mg ml$^{-1}$). In the absence of chlorobutanol, a bell-shaped dose-response relationship was obtained by stimulation with CCK-8 or carbachol. Chlorobutanol (1 mg ml$^{-1}$) markedly inhibited the amylase release induced by CCK-8 at all concentrations tested. The maximal response induced by 100 pM CCK-8 (22.6 ± 1.32%) was reduced to 6.8 ± 0.36% ($P<0.01$). The secretory response to carbachol was also evenly inhibited. The response evoked by 3 μM carbachol (23.7 ± 1.78%) was reduced to 5.9 ± 1.00% ($P<0.01$). However, when the concentration of the secretagogues increased, chlorobutanol did not completely inhibit the amylase release. The inhibitory effect of the preservative on the maximally induced responses was also examined with various concentrations of chlorobutanol (Figure 1b). The inhibitory effect was negligible within a concentration range 0.01–0.1 mg ml$^{-1}$ and a minimal inhibition was observed at a concentration of 0.4 mg ml$^{-1}$ ($P<0.05$). A higher concentration of chlorobutanol (1 mg ml$^{-1}$) completely inhibited the amylase release induced by 100 pM CCK-8 ($P<0.001$) or 3 μM carbachol ($P<0.001$). Following this considerable inhibition in the secretagogue-induced secretory response, an increased dosage of chlorobutanol itself (4 mg ml$^{-1}$ but not 2.5 mg ml$^{-1}$) evoked near maximal amylase release ($P<0.001$).

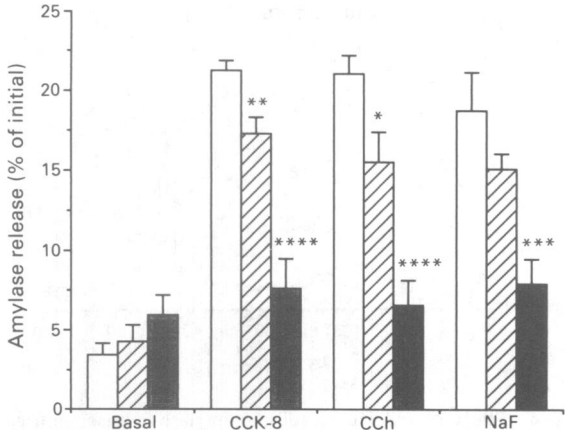



**Figure 2** Effect of chlorobutanol on NaF-induced amylase release. Acini were incubated with Ringer solution containing 10 mM NaF and 10 μM $AlCl_3$ for 30 min at 37°C in the presence (0.5 mg ml$^{-1}$; hatched column or 1 mg ml$^{-1}$; solid column) or absence (open column) of chlorobutanol. Each column denotes mean ± s.e.mean obtained from 3 experiments. Symbols denoting significance as in Figure 1.

### *Inhibitory effect of chlorobutanol on secretory response to NaF in incubated acini*

The inhibitory effect of chlorobutanol was further examined in the NaF-induced secretory response to elucidate whether chlorobutanol acts on receptor sites of the secretagogues, G-proteins, or post G-protein processes. NaF/$AlCl_3$ (10 mM/10 μM) stimulated amylase release (18.8 ± 2.36%) which was comparable to the responses induced by other secretagogues (Figure 2). Chlorobutanol (0.5 mg ml$^{-1}$) caused a small but significant inhibition of the 100 pM CCK-8- or 3 μM carbachol-induced amylase release ($P<0.02$ and 0.05). Because of variations in the results obtained, this dose of the preservative did not show significant inhibitory effect on the 10 mM NaF-induced amylase release. When the chlorobutanol concentration was increased to 1 mg ml$^{-1}$, the NaF-induced amylase release ($P<0.01$) as well as the CCK-8- or the carbachol-induced secretory responses ($P<0.001$) were significantly inhibited. The magnitude of the inhibition by chlorobutanol of the secretory response to NaF was comparable to that to the CCK-8 or to the carbachol.

### *Effect of chlorobutanol on secretory response and $[Ca^{2+}]_c$ dynamics induced by continuous stimulation with CCK-8 or carbachol in perifused acini*

The effect of chlorobutanol was further examined in the perifusion system, in which acini were continuously stimulated with secretagogues in the presence or the absence of the preservative. As shown in Figures 3 and 4, the secretory response to 5 pM CCK-8 (Figure 3a) or to 0.3 μM carbachol (Figure 4a) was almost completely inhibited when 1 mg ml$^{-1}$ chlorobutanol was present 10 min before and during the stimulation ($P<0.01$ and 0.001; Figure 3b and 4b). When the concentration of the secretagogues was increased to 100 pM (Figure 3c) or 3 μM (Figure 4c), a biphasic secretory pattern, the first transient peak followed by a sustained release, was obtained. At these concentrations of the secretagogues, chlorobutanol (1 mg ml$^{-1}$) did not completely inhibit the first transient release but the sustained release was found to be diminished ($P<0.001$; Figure 3d and 4d). Withdrawal of chlorobutanol from the perifusing solution evoked a significant and prolonged rebound of amylase release when acini were previously exposed to 100 pM CCK-8 (Figure 3d). Significant but transient amylase release occurred in all other cases after the cessation of the stimulation (Figure 3b and 4b,d).

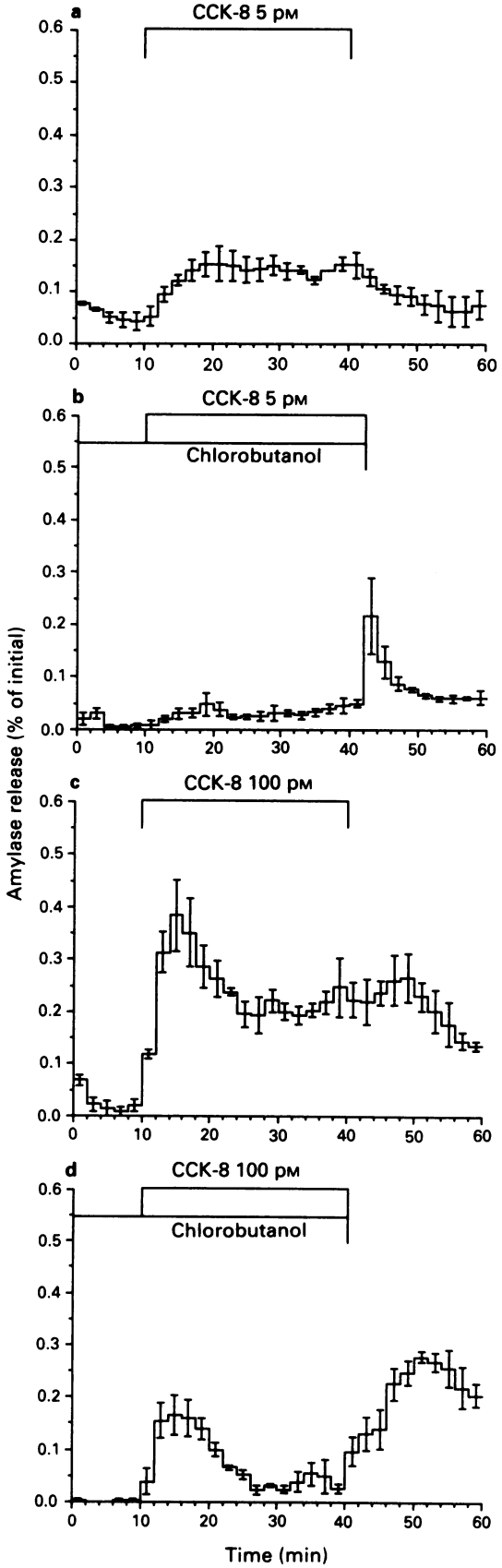



**Figure 3** Effect of chlorobutanol on amylase release induced by continuous stimulation with cholecystokinin octapeptide (CCK-8). Acini were continuously perifused with Ringer solution containing 5 pM (a,b) or 100 pM (c,d) CCK-8 for 30 min in the presence (b,d) or absence (a,c) of chlorobutanol (1 mg $ml^{-1}$). Perifusates were collected at 2 min intervals before, during, and after stimulation. Results are means ± s.e.mean obtained from 3 experiments. Statistical analyses were performed by comparing the amount of amylase released over a 30 min period of stimulation in the presence or absence of chlorobutanol. For further details, see text.

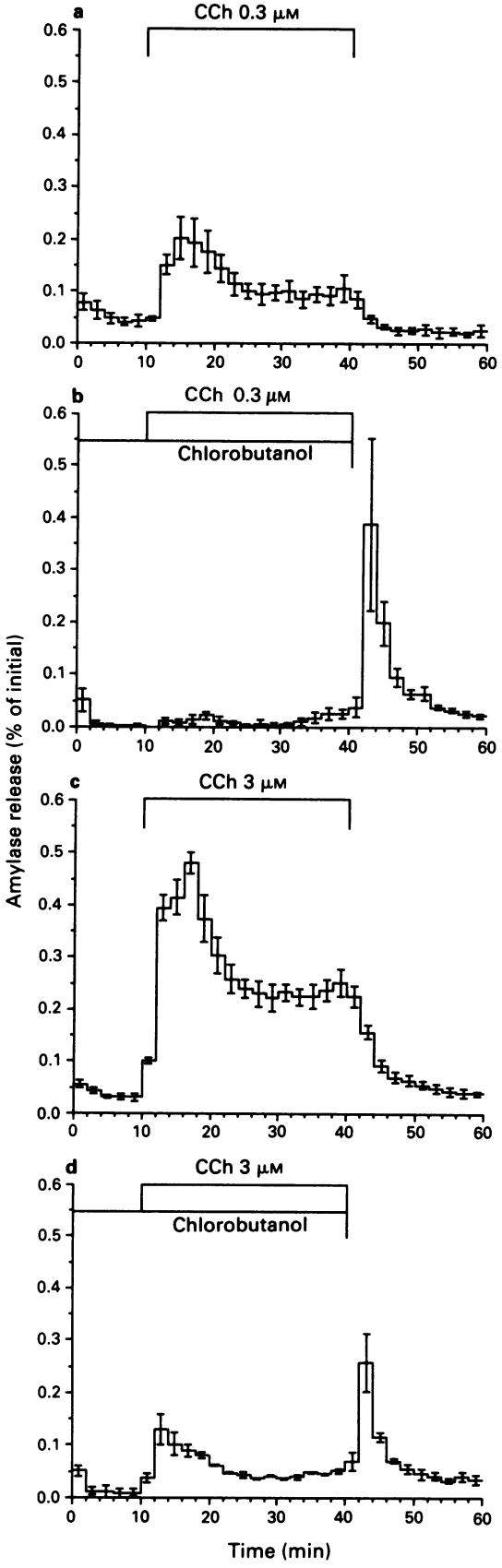



**Figure 4** Effect of chlorobutanol on amylase release induced by continuous stimulation with carbachol. Acini were continuously perifused with Ringer solution containing 0.3 μM (a,b) or 3 μM (c,d) carbachol for 30 min in the presence (b,d) or absence (a,c) of chlorobutanol (1 mg $ml^{-1}$). Perifusates were collected at 2 min intervals before, during, and after stimulation. Results are means ± s.e.mean obtained from 3 experiments.

The effect of chlorobutanol on the $[Ca^{2+}]_c$ dynamics was examined under similar conditions. Continuous stimulation with 5 pM CCK-8 produced an oscillatory fluctuation of $[Ca^{2+}]_c$ (Figure 5a), a peak value of which was usually within a range of several hundreds of nM. When 1 mg ml$^{-1}$ chlorobutanol was simultaneously perifused before and during the stimulation, the 5 pM CCK-8-induced oscillatory spikes of $[Ca^{2+}]_c$ were transformed to a slow and continual elevation, on which miniature fluctuations were superimposed (Figure 5b). A large biphasic change in $[Ca^{2+}]_c$, a rapid rise to several μM followed by a gradual decay, was observed when an acinus was stimulated with 100 pM CCK-8 (Figure 5c). Chlorobutanol (1 mg ml$^{-1}$) markedly altered this biphasic pattern to an oscillatory fluctuation (Figure 5d) that has usually been recorded when an acinus was stimulated with low concentrations of CCK-8. A similar inhibition by chlorobutanol of $[Ca^{2+}]_c$ fluctuation was also observed in the 0.3 μM carbachol-induced response (Figure 6a,b). The inhibitory effect of chlorobutanol on the $[Ca^{2+}]_c$ dynamics elicited by a high concentration of carbachol (3 μM) seemed to be much more potent than that by 100 pM CCK-8 (Figure 6c,d). A similar inhibition was also found in the NaF-induced $[Ca^{2+}]_c$ dynamics (data not shown). When acini were perifused with the buffer containing chlorobutanol alone, a gradual increase in $[Ca^{2+}]_c$ was found (Figure 7a–d) in a dose-dependent manner. Chlorobutanol, 4 mg ml$^{-1}$, which itself caused near maximal amylase release, gradually increased $[Ca^{2+}]_c$ to a final value in excess of 2 μM.

### *Effect of chlorobutanol on [$^{125}$I]-CCK-8 or [$^{3}$H]-NMS binding*

As illustrated in Figure 8a, chlorobutanol inhibited 0.5 nM [$^{3}$H]-NMS binding to the acinar cells in a dose-dependent manner. When compared with the inhibitory effect of carbachol, chlorobutanol inhibited the binding more sharply, indicating that the blockade is not due to simple competitive inhibition. The application of CCK-8 inhibited 13 nM [$^{125}$I]-CCK-8 binding and, analogous to the inhibitory effect on [$^{3}$H]-NMS binding, chlorobutanol also inhibited [$^{125}$I]-CCK-8 binding in a dose-dependent manner.

Based upon these results, we conducted several further experiments to elucidate possible underlying mechanisms of the stimulatory effect of 4 mg ml$^{-1}$ chlorobutanol (data not shown). Additional results we obtained were: (1) the $[Ca^{2+}]_c$ increase induced by 4 mg ml$^{-1}$ chlorobutanol was not modified when $CaCl_2$ was eliminated from the buffer either in the presence or the absence of 0.5 mM EGTA, and (2) the secretory response induced by 4 mg ml$^{-1}$ chlorobutanol was not abolished with 30 μM atropine or in a $Ca^{2+}$-deficient environment.

## Discussion

The present experiments demonstrated that chlorobutanol inhibits both the secretory response and the $[Ca^{2+}]_c$ dynamics induced by CCK-8 or carbachol in rat pancreatic acinar cells. This inhibitory effect may simply be explained by a primary blockade of secretagogue binding to its receptors as demonstrated in the binding experiment. Analyses of Figure 8 gave us the following figures: chlorobutanol (1 mg ml$^{-1}$, 5.36 mM) inhibits approximately 15% of 0.5 nM [$^{3}$H]-NMS binding and the effectiveness of the preservative is equivalent to that of 1 nM atropine or 10 μM carbachol; chlorobutanol (1 mg ml$^{-1}$) inhibits approximately 40% of 13 pM [$^{125}$I]-CCK-8 binding and is equivalent to 1 nM cold CCK-8. Therefore, the inhibitory action of the preservative can partly be explained by interaction between chlorobutanol and CCK-8, or carbachol, at each receptor site.

However, the interpretation seems to be more complex since the inhibitory effect was also found in the NaF-induced secretory response, indicating that the preservative may also

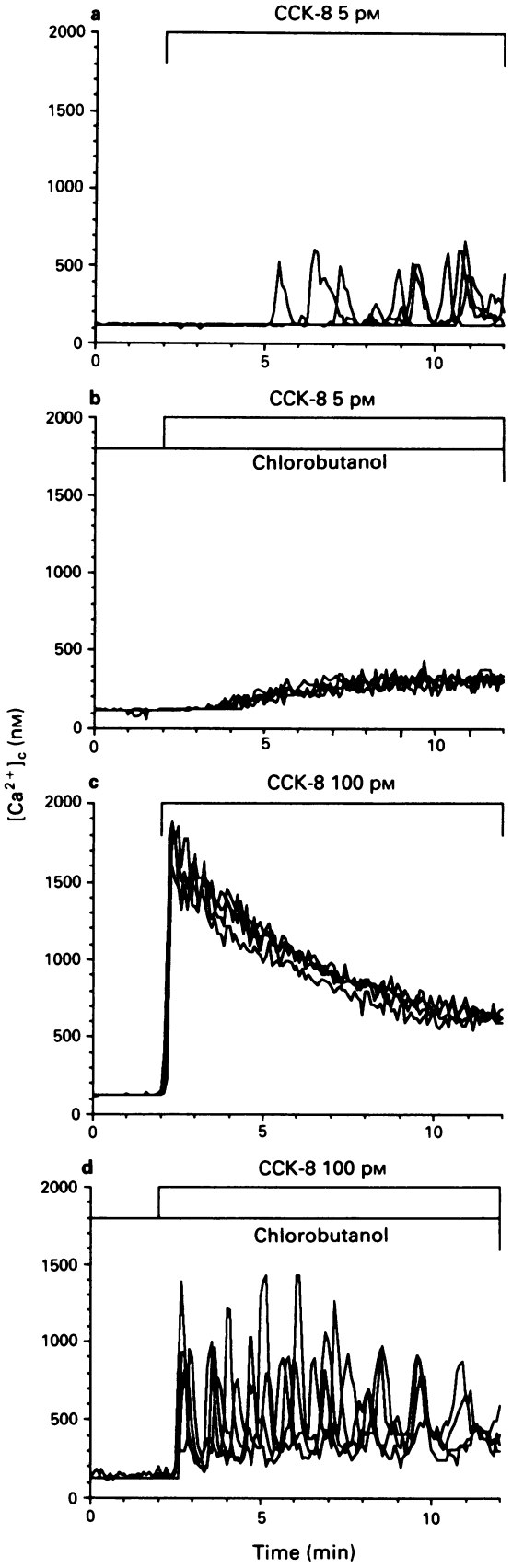



**Figure 5** Effect of chlorobutanol on cholecystokinin octapeptide (CCK-8)-induced $[Ca^{2+}]_c$ dynamics. Acini loaded with Fura-2 were stimulated with 5 pM (a,b) or 100 pM (c,d) CCK-8 for 10 min in the presence (b,d) or absence (a,c) of 1 mg ml$^{-1}$ chlorobutanol. Fluorescence ratios were calculated pixel by pixel and temporal dynamics of average $[Ca^{2+}]_c$ calculated from 4 μm$^2$ in 4 different areas of acinus are shown. Each recording represents a typical example obtained from several experiments.

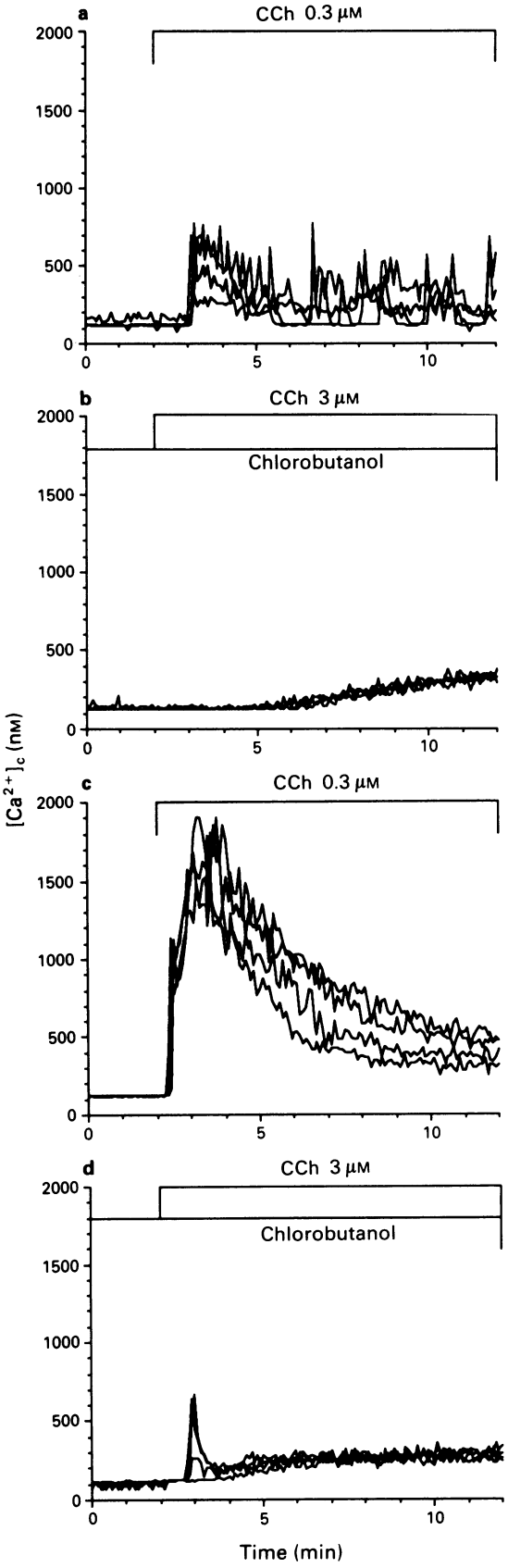



**Figure 6** Effect of chlorobutanol on carbachol (CCh)-induced $[Ca^{2+}]_c$ dynamics. Acini loaded with Fura-2 were stimulated with 0.3 μM (a,b) or 3 μM (c,d) carbachol for 10 min in the presence (b,d) or absence (a,c) of 1 mg $ml^{-1}$ chlorobutanol. Fluorescence ratios averaged from 4 $\mu m^2$ in four different areas were converted to $[Ca^{2+}]_c$. Each recording represents a typical example obtained from several experiments.

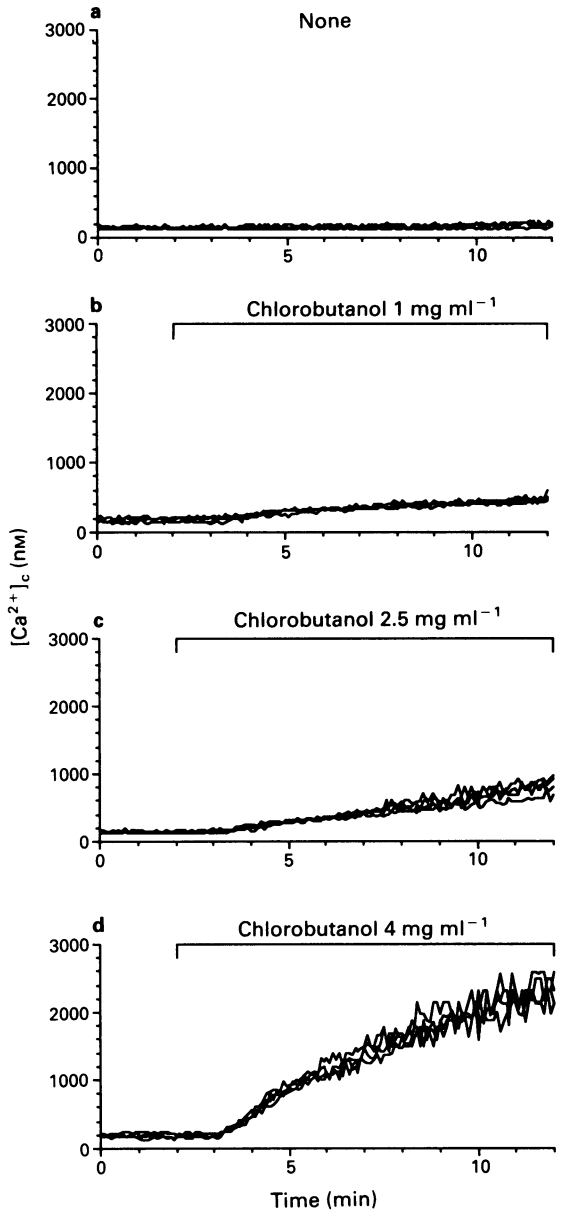



**Figure 7** Effect of chlorobutanol on $[Ca^{2+}]_c$ dynamics. Fura-2-loaded acini were perifused with HEPES-buffered Ringer solution containing (a) 0, (b) 1, (c) 2.5, or (d) 4 mg $ml^{-1}$ chlorobutanol and temporal changes in $[Ca^{2+}]_c$ in four different regions were plotted. Each result shows a typical example obtained from at least 3 different experiments.

act on post receptor processes such as G-protein activation, or the processes activated by G-proteins, or both. This view is compatible with our recent finding in rat isolated adrenal chromaffin cells, in which, independently of muscarinic receptor activation, chlorobutanol abolished the $Ca^{2+}$-reintroduction-induced or the high $K^+$-induced $[Ca^{2+}]_c$ rise (Warashina *et al.*, unpublished observations). Therefore, there is a possibility that chlorobutanol directly affects plasma membrane properties such as ionic channels or carriers.

Hermsmeyer & Aprigliano (1976) demonstrated that chlorobutanol caused conduction disruption and desynchronization in myocardial muscle cells, suggesting that the effect is not directly on the $Ca^{2+}$ mobilization process of excitation-contraction coupling but on the plasma membrane. Bowler *et al.* (1985) pointed out that chlorobutanol caused a rapid fall in arterial blood pressure by depression of myocar-

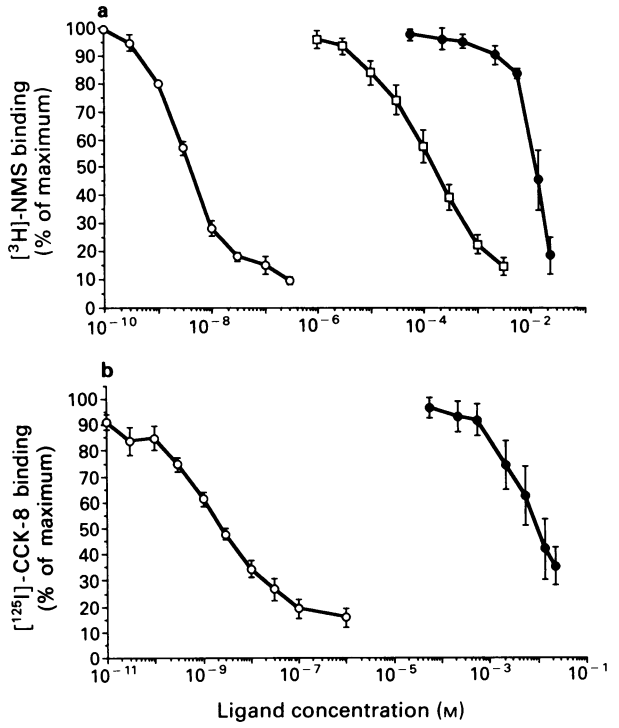



**Figure 8** Effect of chlorobutanol on [$^3$H]-N-methyl-scopolamine (NMS) or [$^{125}$I]-cholecystokinin octapeptide (CCK-8) binding. (a) Acini were incubated with 0.5 nM [$^3$H]-NMS for 60 min at 37°C in the presence of various concentrations of atropine (○), carbachol (□), or chlorobutanol (●). (b) Acini were incubated with 13 pM [$^{125}$I]-CCK-8 for 30 min at 37°C in the presence of various concentrations of CCK-8 (○) or chlorobutanol (●). Binding capacity of the ligands was expressed as a percentage of maximal binding obtained in the absence of any inhibitory ligands. Each value represents mean ± s.e.mean obtained from 3 separate experiments.

dial contractility and systemic vascular resistance. Barrigon *et al.* (1984) showed that the KCl- or noradrenaline-induced contractions in the rat isolated thoracic aorta were decreased by chlorobutanol and $Ca^{2+}$-reintroduction-induced contraction was also inhibited, suggesting that the preservative reduces the availability of intracellular $Ca^{2+}$ to the contractile machinery. They also noted that below 1.4 mM, chlorobutanol inhibited $Ca^{2+}$ influx, especially voltage-dependent $Ca^{2+}$ entry, and at high concentrations the preservative also exerted an intracellular effect possibly involving antagonism between $Ca^{2+}$ influx and the contractile elements or inhibition of $Ca^{2+}$ release from intracellular stores. However, Sim *et al.* (1987) failed to show any effect of chlorobutanol on functions of the sarcoplasmic reticulum in skeletal muscle such as $Ca^{2+}$-ATPase activity and the $Ca^{2+}$ uptake process in malignant hyperpyrexia but the preservative did antagonize contraction. Based upon these findings, it is conceivable that chlorobutanol reduces various types of $Ca^{2+}$ entry processes including receptor-operated $Ca^{2+}$ entry, voltage-dependent $Ca^{2+}$ entry, and even $Ca^{2+}$-reintroduction-induced $Ca^{2+}$ entry. A possible action on the $Ca^{2+}$ entry process at low concentration of chlorobutanol may well explain the incomplete inhibition of amylase release when higher concentrations of secretagogues were used (Figures 1a, 3d and 4d). There is evidence that the secretory response induced by secretagogues at concentrations greater than the physiological range is mainly caused by $Ca^{2+}$ released from intracellular stores (Kanno & Habara, 1992). Thus, we presumed that amylase release which was not abolished by 1 mg ml$^{-1}$ chlorobutanol may be triggered by $Ca^{2+}$ release from such stores. The transient response found in the presence of chlorobutanol in perifusion experiments (Figures 3d and 4d) may also be attributable to $Ca^{2+}$ release, which cannot be inhibited by low concentrations of chlorobutanol.

The stimulatory effect of 4 mg ml$^{-1}$ but not 2.5 mg ml$^{-1}$ chlorobutanol *per se* seems to paradoxical (Figure 1b). No apparent morphological change was observed in the structure of the acini under the DIC microscope after treatment with this dosage of the preservative. The plateau level of $[Ca^{2+}]_c$ reached approximately 2.2 μM, which is similar to that found when acini were stimulated with 100 pM CCK-8 or 3 μM carbachol, both of which induced maximal secretory responses. Possible mechanism(s) underlying both inhibition and stimulation cannot simply be deduced from the present results but the biochemical studies of Campello *et al.* (1964) may provide some clues as to the site(s) of action of chlorobutanol. Several possibilities were discussed by these authors and they suggested that chlorobutanol may act as an inhibitor of the respiratory chain between pyridine nucleotide and flavoprotein. Further, they also stated that increasing concentrations of the preservative are able to act more drastically on the mitochondrial structure or even on other sites of the respiratory chain. The conclusion was that chlorobutanol might have more than one effect on the properties of isolated mitochondria. Although, as stated by Kanno (1990), the metabolic relevance to the secretory process has not been fully established, it is conceivable that low concentrations of chlorobutanol perturb the mitochondrial respiratory chain to cause a direct or indirect inhibition of exocytosis through a deterioration in the $[Ca^{2+}]_c$ dynamics, while high concentrations stimulate exocytosis in pancreatic acinar cells through a resulting increase in $[Ca^{2+}]_c$. This process cannot be blocked by muscarinic antagonists or $Ca^{2+}$-deficient conditions.

Finally, it should be noted that chlorobutanol has been widely used as a preservative for various therapeutic drugs, including synthetic oxytocin (Syntocinon) (Barrigon *et al.*, 1984), bradykinin (Hermsmeyer & Aprigliano, 1976), heparin (Bowler *et al.*, 1986), adrenaline (Bosmin, Daiichi Pharmaceutical), and noradrenaline (Arterenol, Hoechst). It has been claimed that some of the observed effects of these agents may be due to the preservative. Thus, Barrigon *et al.* (1984) pointed out that chlorobutanol reduced systemic vascular resistance, produced local anaesthesia, and inhibited $^{45}Ca$ entry and enhanced $^{45}Ca$ efflux in rat aortic strips. Sim *et al.* (1987) reported that chlorobutanol, a smooth muscle relaxant, also acted as a skeletal muscle relaxant. Moreover, Bowler *et al.* (1986) pointed out that chlorobutanol is potentially harmful and suggested that the data sheet should warn of its hypotensive, sedative, and cumulative effects. We have now provided evidence that chlorobutanol does have substantial modulatory effects not only on excitation-contraction coupling but also on stimulus-secretion coupling. A very high concentration (4 mg ml$^{-1}$) cannot be achieved *in vivo* by systemic administration of the drugs containing the preservative but when local injection is performed, it is possible that tissues such as the skeletal muscle, vascular smooth muscle, or even nerve fibres near the injection site could be exposed to such concentrations. Therefore, it should again be emphasized that while chlorobutanol can be a useful drug preservative and antagonist for $Ca^{2+}$ dynamics, serious care should be taken when preparations containing chlorobutanol are adopted for therapeutic and experimental use.

We thank Dr A. Warashina, Department of Physiology School of Medicine, Niigata University, Niigata 951, for his suggestions and discussions and Ms Y. Abe for her technical assistance.

## References

BARRIGON, S., TEJERINA, T., DELGADO, C. & TAMARGO, J. (1984). Effects of chlorbutol on $^{45}Ca$ movements and contractile responses of rat aorta and its relevance to the actions of Syntocinon. *J. Pharm. Pharmacol.*, **36**, 521–526.

BOWLER, G.M.R., GALLOWAY, D.W., MEIKLEJOHN, B.H. & MACINTYRE, C.C.A. (1986). Sharp fall in blood pressure after injection of heparin containing chlorbutol. *Lancet*, **i**, 848–849.

CAMPELLO, A.P., VIANNA, C.H.M., BRANDAO, D., VOSS, D.O. & BACILA, M. (1964). The effect of chlorobutanol on the respiratory metabolism and on the normal properties of isolated mitochondria. *Biochem. Pharmacol.*, **13**, 211–223.

HABARA, Y. & KANNO, T. (1991). Dose-dependency in spatial dynamics of $[Ca^{2+}]_c$ in pancreatic acinar cells. *Cell Calcium*, **12**, 533–542.

HABARA, Y., SATOH, Y., SAITO, T. & KANNO, T. (1990). A G-protein activator, NaF, induces $[Ca^{2+}]_o$-dependent $[Ca^{2+}]_c$ oscillation and secretory response in rat pancreatic acini. *Biomed. Res.*, **11**, 389–398.

HABARA, Y., WILLIAMS, J.A. & HOOTMAN, S.R. (1986). Antimuscarinic effects of chloroquine in rat pancreatic acini. *Biochem. Biophys. Res. Commun.*, **137**, 664–669.

HERMSMEYER, K. & APRIGLIANO, O. (1976). Effects of chlorobutanol and bradykinin on myocardial excitation. *Am. J. Physiol.*, **230**, 306–310.

HOOTMAN, S.R., BROWN, M.E., WILLIAMS, J.A. & LOGSDON, C.D. (1986). Regulation of muscarinic acetylcholine receptors in cultured guinea pig pancreatic acini. *Am. J. Physiol.*, **251**, G75–G83.

KANNO, T. (1975). The electrogenic sodium pump in the hyperpolarizing and secretory effects of pancreozymin in the pancreatic acinar cell. *J. Physiol.*, **245**, 599–616.

KANNO, T. (1990). The metabolic basis of secretion by the exocrine pancreas. In *Epithelial Secretion of Water and Electrolytes*. ed. Young, J.A. & Wong, P.Y.D. pp. 267–275. Berlin: Springer-Verlag.

KANNO, T. & HABARA, Y. (1992). Intra- and inter-cellular propagation of recurring $Ca^{2+}$ tide in pancreatic acinus. *Biomed. Res.* (in press).

KANNO, T., HABARA, Y. & SATOH, Y. (1991). $Ca^{2+}$ wave propagation in cells of pancreatic acinus reverses after cell dispersion. *Biomed. Res.*, **12**, 429–434.

KANNO, T., SAITO, T. & YAMASHITA, T. (1989). Spatial and temporal oscillation of $[Ca^{2+}]_i$ during continuous stimulation with CCK-8 in isolated rat pancreatic acini. *Biomed. Res.*, **10**, 475–484.

SIM, A.T.R., WHITE, M.D. & DENBOROUGH, M.A. (1987). The effects of chlorbutol on skeletal muscle sarcoplasmic reticulum function in porcine malignant hyperpyrexia. *Int. J. Biochem.*, **19**, 827–830.

*(Received September 21, 1992*
*Revised February 22, 1993*
*Accepted March 8, 1993)*

*Br. J. Pharmacol.* (1993), **109**, 693–698 © Macmillan Press Ltd, 1993

# Functional characterization of three adenosine receptor types

M.F. Gurden, J. Coates, F. Ellis, B. Evans, M. Foster, [1]E. Hornby, [2]I. Kennedy, D.P. Martin, [3]P. Strong, C.J. Vardey & A. Wheeldon

Pharmacology and Chemistry Divisions, Glaxo Group Research, Ware, Hertfordshire, SG12 0DP

**1** The purpose of the present study was to classify adenosine receptors into $A_1$ and $A_2$ subtypes in a wide range of isolated tissues and cell types (rat adipocytes and atria, guinea-pig ileum and atria ($A_1$); guinea-pig aorta, dog coronary artery and human platelets and neutrophils ($A_2$)) using the **R**- and **S**-diastereoisomers of N-phenylisopropyladenosine (PIA), N-cyclopentyladenosine (CPA), the novel compound, N-[(1S,*trans*)-2-hydroxycyclopentyl]adenosine (GR79236), N-[(2-methylphenyl)methyl]adenosine (metrifudil), 2-(phenylamino)adenosine (CV1808), and 2-[[2-[4-(2-carboxyethyl)phenyl]ethyl]amino]-*N*-ethylcarboxamidoadenosine (CGS21680); N-ethylcarboxamidoadenosine (NECA) was used as a standard.

**2** Results obtained in all tissue preparations previously reported to contain $A_1$-receptors could be described by a single rank order of agonist potency: CPA $\geqslant$ GR79236, **R**-PIA $\geqslant$ NECA $>>$ **S**-PIA $\geqslant$ metrifudil $\geqslant$ CV1808, CGS21680.

**3** In contrast, two distinct rank orders of agonist potency were observed in preparations previously reported to contain $A_2$-receptors. In dog coronary artery, human neutrophils and platelets the rank order of potency was: CV1808, CGS21680 $\geqslant$ NECA $>$ **R**-PIA $\geqslant$ metrifudil $\geqslant$ CPA $>$ GR79236, **S**-PIA. However, in guinea-pig aorta the rank order was: NECA $>$ metrifudil $>$ **R**-PIA, CPA $>$ CV1808, GR79236 $\geqslant$ **S**-PIA, CGS21680.

**4** The results of this study are consistent with the existence of three types of adenosine receptor: $A_1$- and two subtypes of $A_2$-receptor. The receptor present in dog coronary artery, human platelets and neutrophils, probably corresponds to the $A_{2a}$ subtype, whilst that present in the guinea-pig aorta may be of the $A_{2b}$ subtype.

**Keywords:** Adenosine receptors; $A_1$, $A_2$; GR79236; metrifudil; $P_1$-purinoceptors

## Introduction

It is now generally accepted that adenosine receptors can be divided into two types, termed $A_1$ and $A_2$. This classification was first proposed by Van Calker *et al.* (1979), based on the relative potencies of adenosine and some of its derivatives as stimulants or inhibitors of adenosine 3':5'-cyclic monophosphate (cyclic AMP) formation in cultured brain cells. Although antagonists selective for adenosine $A_1$- or $A_2$-receptors have been described (Trevidi *et al.*, 1990), to date pharmacological classification of these receptors has usually depended on the use of selective agonists.

Studies investigating the structure-activity relationships for adenosine derivatives at $A_1$- and $A_2$-receptors have led to a number of key conclusions. Firstly, certain $N^6$-substituted compounds, such as cyclopentyladenosine (CPA) and **R**-phenylisopropyladenosine (**R**-PIA), show selectivity for $A_1$- versus $A_2$-receptors (Londos *et al.*, 1980; Bruns *et al.*, 1986). Furthermore, the work of Smellie *et al.* (1979) suggested that the relative potency of the **R**- and **S**-isomers of PIA is higher at $A_1$- than $A_2$-receptors. Secondly, certain 2-substitituted derivatives, such as CV1808 (2-(phenylamino)adenosine) and CGS21680 (2-[[2-[4-[-(2-carboxyethyl)phenyl]ethyl]amino]-N-ethylcarboxamidoadenosine) show selectivity for $A_2$- versus $A_1$-receptors (Bruns *et al.*, 1986; Jarvis *et al.*, 1989). Finally, although N-ethylcarboxamidoadenosine (NECA) is sometimes considered to be selective for $A_2$-receptors, it is, in fact, a potent, non-selective agonist (Bruns *et al.*, 1986). This profile makes NECA a useful standard with which other agonists may be compared in receptor classification studies.

Although these conclusions are generally accepted, anomalies have been reported. Thus, variations in the relative potencies of NECA and $N^6$-substituted derivatives such as PIA and CPA led Ribeiro & Sebastiao (1986) to suggest the existence of a sub-type of the adenosine $A_1$-receptor, which they termed $A_3$. However, our own work (Kennedy *et al.*, 1992a) failed to confirm any key differences, leading us to conclude that comparisons of the relative potencies of these agonists provides no evidence to support a sub-classification of adenosine $A_1$-receptors.

The classification of receptors as being of the $A_2$-type originally depended upon the low potency, relative to NECA, of agonists such as **R**-PIA and CPA. However, in some tissues generally considered to contain $A_2$-receptors, the differences in potency between NECA and the $N^6$-substituted derivatives were small. Thus, we have reported that the adenosine receptors mediating inhibition of U-46619-stimulated platelet aggregation (Foster *et al.*, 1987) and relaxation of dog coronary artery (Bhalla *et al.*, 1985) could not be classified as being either of the $A_1$- or $A_2$-type according to these criteria. Similar results obtained in the dog coronary circulation *in vivo* led Kusachi *et al.* (1983) to propose the existence of a 'hybrid' receptor, having characteristics of both adenosine $A_1$- and $A_2$-receptors.

Alternatively, these anomalies may be explained by a proposal advanced by Bruns and co-workers (1986). These authors compared the binding affinities of a range of compounds for the rat striatal $A_2$-receptor with their known potencies as stimulants of cyclic AMP formation in the human fibroblast and concluded that the preparations contained different receptors. Those present in the striatum were termed $A_{2a}$- and those in the fibroblast $A_{2b}$-receptors. The compounds showing the greatest apparent degree of selectivity (for the putative $A_{2a}$- versus $A_{2b}$-sub-type) were 2-substituted analogues such as CV1808. More recently, 2-substituted derivatives of NECA, such as CGS21680, have been reported

[1] Present address: Department of Vascular Biology, Fidia Research, Abano Terme, Italy.
[2] Present address: Glaxo Institute of Applied Pharmacology, Department of Pharmacology, University of Cambridge, Tennis Court Road, Cambridge, CB2 1QJ.
[3] Author for correspondence: Cardiovascular and Respiratory Pharmacology, Glaxo Group Research, Ware, Hertfordshire, SG12 0DP.

to be potent ligands at the rat striatal $A_2$-receptor (Jarvis *et al.*, 1989).

The purpose of the present study was two fold. Firstly, to extend our previous observations on the relative potencies of agonists in preparations containing adenosine $A_1$ receptors (Kennedy *et al.*, 1992a) to include a wider range of tissues and compounds, and secondly to determine the relative potencies of agonists in a range of preparations usually considered to contain adenosine $A_2$-receptors (guinea-pig aorta, Collis & Brown, 1983; human neutrophil, Cronstein *et al.*, 1988; human platelet, Haslam & Cusack, 1981; dog coronary artery, Kusachi *et al.*, 1983), and so investigate the utility of the $A_{2a}$-/$A_{2b}$-receptor classification scheme. The compounds used here include a novel adenosine $A_1$-receptor agonist, N-[(1S, *trans*)-2-hydroxycyclopentyl]adenosine (GR 79236) and N-[(2-methylphenyl)methyl]adenosine (metrifudil) which was selected since its reported cardiovascular profile in man suggests that it may be a vasodilator (Schaumann & Kutscha, 1972). A preliminary account of part of this work has been published in abstract form (Gurden & Kennedy, 1992; Kennedy *et al.*, 1992b).

## Methods

Tissues were obtained from male Dunkin Hartley guinea-pigs (250–300 g), male AH/A rats (Glaxo Group Research, 200–300 g; 100–120 g for adipocyte experiments), pure-bred (Glaxo Group Research) beagle dogs of either sex and blood from healthy human volunteers.

### *Isolated smooth and cardiac muscle preparations*

Rings of isolated thoracic aorta (guinea-pig), left anterior descending coronary arteries (beagle dogs) and left and right atria (rat and guinea-pig) were bathed in a modified Krebs solution of the following composition (mM): NaCl 118, $NaHCO_3$ 25, KCl 4.7, $MgSO_4$ 0.6, $KH_2PO_4$ 1.2, D-glucose 11.2, $CaCl_2$ 1.3. Indomethacin ($2.8 \times 10^{-6}$ M) was included for experiments with guinea-pig aorta and dog coronary artery.

Rings of guinea-pig aorta were suspended (resting tension 0.5–0.75 g) on parallel steel wires (one fixed and one attached to the tension transducer) in organ baths. Following equilibration for 1 h, during which time preparations were washed regularly, phenylephrine ($1 \times 10^{-4}$ M) was added to the organ baths to induce a maximal level of tone. The tissues were then washed repeatedly to reverse the effect of the phenylephrine. The procedure was then repeated with a concentration of phenylephrine (usually $3 \times 10^{-6}$ M) which produced approximately 50% of the maximum tone, and was repeated until constant responses were obtained. The effects of adenosine derivatives were then studied, and responses expressed as the percentage reversal of the phenylephrine-induced tone.

Rings of dog coronary artery were suspended on parallel steel wires (resting tension 0.4 g) in organ baths. Following equilibration for 2 h, during which preparations were washed regularly, the stable thromboxane-mimetic, U-46619, was added to the baths at a concentration (usually $1 \times 10^{-7}$ M) sufficient to produce a maximal contraction of the tissues. The preparations were then washed repeatedly to reverse the effect of U-46619. A concentration of U-46619 ($1 \times 10^{-8}$–$3 \times 10^{-8}$ M) producing approximately 50% of the maximum response was then added and repeated, following washing, until constant responses were obtained. Preliminary experiments indicated that U-46619-induced tone was not well maintained in some preparations. The fade seen, however, could be reduced by inclusion of adenosine deaminase (5 u $ml^{-1}$) in the bathing fluid. The effects of adenosine derivatives on U-46619-induced tone were therefore assessed in the presence of the enzyme.

Methods and experimental protocols for the other preparations used have been described in detail previously (Kennedy *et al.*, 1992a). In brief, strips of guinea-pig ileum longitudinal muscle were stimulated electrically at 0.2 Hz (1 ms pulse width; supra-maximal voltage), and the ability of adenosine derivatives to inhibit the electrically-evoked twitch response was measured. Left atrial preparations were paced electrically at a frequency of 1 (rat) or 3 (guinea-pig) Hz (1 ms pulse width; twice threshold voltage), and the ability of adenosine derivatives to inhibit orciprenaline-induced postive inotropic responses was measured. The negative chronotropic effects of adenosine derivatives were determined in spontaneously-beating right atria.

### *Isolated cell preparations*

Rat adipocytes were obtained from epididymal fat pads using the methods described by Stratton *et al.* (1985), and the ability of adenosine derivatives to inhibit noradrenaline-induced lipolysis was assessed as described previously (Kennedy *et al.*, 1992a).

Neutrophils were prepared from venous blood drawn from the forearm of healthy human volunteers. The anticoagulated blood (10 units heparin $ml^{-1}$ blood) was mixed with plasmagel (2/3 the volume of blood) and left to sediment at 37°C for 35–40 min. The supernatant buffy-coat was removed by aspiration and Ficoll-paque (1/5 volume of buffy coat) underlaid. A granulocyte pellet was prepared by centrifugation, and then washed twice in calcium-free, Tris buffer (mM: NaCl 122, KCl 2.7, Tris 25, glucose 5.6, $MgCl_2$ 1.0, bovine serum albumin 0.1% (w/v); pH 7.4), washed again in buffer containing calcium chloride ($1 \times 10^{-3}$ M) and then finally suspended in this buffer. Aliquots of the suspensions were taken to determine total white blood cell numbers. Granulocyte suspensions were normally found to comprise >95% neutrophils. Cells were resuspended to a concentration of $1-2 \times 10^6$ cells $ml^{-1}$, and indomethacin ($3 \times 10^{-6}$ M), adenosine deaminase (1 u $ml^{-1}$), cytochalasin B (5 $\mu g\ ml^{-1}$) and cytochrome C ($1 \times 10^{-4}$ M) were added. Concentration-inhibition curves for adenosine derivatives were then constructed (10 min pre-incubation, 37°C) versus N-formyl-methionyl-leucyl-phenylalanine (fMLP)-stimulated ($2 \times 10^{-7}$ M) release of $O_2^-$ by monitoring the reduction of cytochrome C at 550 nm. The effects of each concentration of agonist were assessed in triplicate.

Platelet rich plasma (PRP) was prepared by centrifugation (2500 *g* for 2 min) of human venous blood, collected into 1/10 volume of 0.13 M trisodium citrate containing $1 \times 10^{-4}$ M aspirin. Gel-filtered platelets (GFP) were prepared by the application of PRP to a column of Sephadex CL2B (Hornby *et al.*, 1989). The platelets were eluted with a modified HEPES buffered Tyrode solution. The GFP suspension was reconstituted with fibrinogen (3 mg $ml^{-1}$, $CaCl_2$ ($2 \times 10^{-3}$ M) and $MgCl_2$ ($1 \times 10^{-3}$ M)). Concentration-effect curves for the aggregatory response to U-46619, assessed with an optical aggregometer (Born, 1962), were carried out and the just-maximal concentration of U-46619 selected. Concentration-inhibition curves to adenosine derivatives were then constructed, following a 5 min pre-incubation at 37°C using the selected U-46619 concentration to stimulate aggregation.

### *Analysis of results*

The responses obtained to NECA in each preparation were measured and a log concentration-effect curve constructed. From this, the agonist concentration producing 50% of its own maximum response ($EC_{50}$), was estimated. In the guinea-pig ileum and all four atrial preparations, the effects of NECA were rapidly reversed by washing. Consequently, the concentration-effect relationships for other compounds were determined from a second curve constructed 30–60 min after the NECA curve had been completed. However, NECA responses were not readily reversible in dog coronary artery and the guinea-pig aorta. In these preparations, therefore, and in

rat isolated adipocytes and human isolated neutrophils and platelets, concentration-effect curves to NECA and test agonists were constructed in parallel. Where the maximum response to a test agonist was equivalent to that of NECA, the equipotent molar concentration ratio (EMCR) was then calculated by dividing the $EC_{50}$ value for the test compound (calculated as above) by the appropriate value for NECA. However, where a full concentration-effect curve could not be obtained, the EMCR was calculated using a lower equieffective concentration (greater than 20% and from the parallel portion of the concentration-effect curves).

### *Experiments using adenosine receptor antagonists*

The sensitivity of agonist responses to either 8-phenyltheophylline (8-PT) or 1,3-diethyl-8-phenylxanthine (DPX) has been investigated in a range of tissues. In the guinea-pig ileum and all atrial preparations, 8-PT was added to the bathing fluid and kept in contact with the tissue 45 min before, and during, the construction of the second agonist concentration-effect curve. However, in the dog coronary artery and guinea-pig aorta preparations, only one agonist concentration-effect curve could be obtained in each tissue. Here, 8-PT was added to the bathing fluid 60 min before the agonist concentration-effect curve was constructed.

In rat adipocyte experiments, cells were incubated with 8-PT for 30 min prior to addition of the agonist, and throughout the subsequent incubation with noradrenaline. Thus, cells were in contact with the antagonist for 45 min before the lipolytic stimulant was added. In human neutrophil experiments, cells were incubated with the antagonist for 10 min before addition of the agonist, and throughout the subsequent stimulation with fMLP. Thus, cells were in contact with 8-PT for 20 min before the stimulant of $O_2^-$ formation was added. However, our preliminary experiments with human platelets demonstrated that adenosine-receptor blocking concentrations of 8-PT potentiated the anti-aggregatory effects of NECA. Accordingly, DPX, but not 8-PT was used as an antagonist in these studies. The suspension of GFP was prepared as described previously. Concentration-effect curves for the aggregatory response to U-46619 were constructed in an optical aggregometer and the concentration causing 90–100% aggregation calculated and used as a standard stimulus throughout the experiment. GFP was incubated in the presence or absence of DPX ($1 \times 10^{-7}$–$3 \times 10^{-6}$ M) for 5 min at 37°C, before the addition of NECA.

Antagonist potency was expressed as a concentration ratio (CR), determined by dividing the $EC_{50}$ of the agonist in the absence of the antagonist by that obtained in its presence. If only one antagonist concentration, [B], was used, an estimate of the affinity of the antagonist for the receptor being studied was then calculated as an apparent $pK_b$ (see Gaddum, 1957) using:

$$pK_b = \log (CR-1) - \log [B]$$

Where CRs had been determined from 3 (or more) antagonist concentrations, a $pA_2$ value was calculated by the method of Arunlakshana & Schild (1959).

### *Drugs*

The following compounds were used: **R**-PIA and **S**-PIA (Boehringer Mannheim), CV1808 (2-(phenylamino)adenosine) and CGS21680 (2-[[2-[4-(2-carboxyethyl)phenyl]ethyl] amino]-N-ethylcarboxamidoadenosine) and 8-phenyltheophylline and 1,3-diethyl-8-phenylxanthine (batches from both Research Biochemicals Inc and Chemistry Division, Glaxo Group Research, Ware), indomethacin, L-phenylephrine, noradrenaline ((−)-arterenol) and orciprenaline (metaproterenol hemisulphate; Sigma Chemical Co), and U-46619 (11α,9α-epoxymethanoprostaglandin $H_2$; Cayman Chemicals). NECA, CPA, metrifudil (N-[2-(methylphenyl)methyl]adenosine) and GR79236 (N-[(1S,*trans*)-2-hydroxycyclopentyl]adenosine) were synthesized in the Chemistry Division (Glaxo Group Research, Ware). All other chemicals were standard laboratory reagents of analytical grade where possible.

GR79236, CPA, **R**- and **S**-PIA, NECA, metrifudil, CV 1808 and CGS21680 were prepared as stock solutions in HCl (0.01–0.1 M) or in 10% dimethylsulphoxide (DMSO) for experiments with GFP. A stock solution of 8-phenyltheophylline ($1 \times 10^{-2}$ M) was prepared in 0.1 M NaOH. Indomethacin and U-46619 were dissolved in 1% (w/v) $NaHCO_3$. L-Phenylephrine and orciprenaline were dissolved in distilled water. Further dilutions of all solutions were prepared in distilled water or Krebs buffer.

## Results

### *Preparations reported to contain $A_1$ receptors*

NECA produced a concentration-dependent inhibition of lipolysis by rat isolated adipocytes, an inhibition of the electrically-evoked twitch response in the guinea-pig ileum,

**Table 1** Relative potencies of adenosine analogues in tissues containing $A_1$-receptors

| *Preparation* | *NECA $EC_{50}$* (nM) | *EMCR* (NECA = 1) *R-PIA* | *CPA* | *GR79236* | *S-PIA* | *Metrifudil* | *CV1808* | *CGS21680* |
|---|---|---|---|---|---|---|---|---|
| Rat adipocyte | 20 (17–24) $n=20$ | 0.54 (0.34–0.86) $n=6$ | 0.21 (0.10–0.43) $n=4$ | 0.34 (0.16–0.65) $n=6$ | 32 (18–58) $n=6$ | 56 (17–188) $n=4$ | 114 (32–408) $n=4$ | 253 (79–808) $n=6$ |
| Guinea-pig ileum | 52 (44–61) $n=20$ | 1.15 (0.81–1.64) $n=7$ | 0.37 (0.30–0.50) $n=8$ | 1.33 (0.80–2.21) $n=5$ | 56 (41–75) $n=15$ | 51 (37–71) $n=8$ | 101 (59–175) $n=6$ | 299 (161–553) $n=5$ |
| Rat left atrium | 46 (28–76) $n=16$ | 0.50 (0.31–0.82) $n=6$ | 0.24 (0.14–0.40) $n=6$ | 0.45 (0.22–0.95) $n=6$ | 18 (11–28) $n=6$ | 149 (52–431) $n=6$ | 1128 (738–1724) $n=6$ | 419 (301–583) $n=6$ |
| Guinea-pig left atrium | 30 (24–37) $n=22$ | 1.74 (1.07–2.81) $n=6$ | 0.57 (0.52–0.62) $n=6$ | 1.62 (0.71–3.69) $n=6$ | 32 (24–43) $n=7$ | 115 (81–162) $n=7$ | 257 (166–399) $n=6$ | 386 (209–713) $n=5$ |
| Rat right atrium | 93 (72–119) $n=20$ | 0.70 (0.31–1.57) $n=6$ | 0.21 (0.17–0.26) $n=6$ | 0.77 (0.45–1.32) $n=6$ | 25 (12–52) $n=7$ | 59 (24–149) $n=4$ | 1041 (736–1473) $n=4$ | 382 (326–447) $n=3$ |
| Guinea-pig right atrium | 148 (115–189) $n=23$ | 1.66 (0.99–2.78) $n=6$ | 0.45 (0.23–0.88) $n=6$ | 1.71 (0.3–8.7) $n=3$ | 49 (22–107) $n=5$ | 139 (109–176) $n=3$ | 1322 (494–3536) $n=3$ | 430 (141–1306) $n=3$ |

Equipotent molar concentration ratios (EMCR), together with the $EC_{50}$ of NECA, are presented as geometric mean values, with 95% confidence limits shown in parentheses and where $n$ = the number of observations.

and negative inotropic or chronotropic responses in both guinea-pig and rat left and right atria, respectively. Geometric mean $EC_{50}$ values for NECA ranged from $2.0 \times 10^{-8}$ M for inhibition of lipolysis by rat adipocytes, to $14.8 \times 10^{-8}$ M for negative chronotropic activity in guinea-pig right atria. The other agonists evaluated produced responses which were qualitatively similar to those of NECA. In addition, where full concentration-effect curves could be constructed, the maximal responses which were elicited were not different from that of NECA. Comparison of the relative potencies of the compounds evaluated here in these six preparations (Table 1) shows a common rank order of agonist potency: CPA $\geqslant$ GR79236, **R-PIA** $\geqslant$ NECA $>>$ **S-PIA** $\geqslant$ metrifudil $\geqslant$ CV18-08, CGS21680.

It is noteworthy, however, that whilst CPA was consistently the most potent agonist in the 6 preparations, it was at the most, only 5 times more potent than NECA.

The agonist effects of NECA in all six tissues were antagonized by 8-PT (Figure 1, Table 2). In those tissues examined (rat adipocyte, guinea-pig ileum, rat left atrium and guinea-pig right atrium), the agonist effects of GR79236 were similarly antagonized by 8-PT. Furthermore, the $pA_2/pK_b$ values obtained in this series of experiments appeared to be agonist-independent. However, there was a trend for affinity estimates for 8-PT to be higher in tissue preparations from the rat than those from the guinea-pig.

**Table 2** Antagonist potency of 8-phenyltheophylline in tissues containing $A_1$-receptors

| *Preparation* | *$pA_2$ (Slope)/$pK_b$ vs NECA* | *GR79236* |
|---|---|---|
| Rat adipocyte | 7.0 (0.73)* $n=4$ | 6.6 (0.85) $n=3$ |
| Guinea-pig ileum | 6.36 (0.95) $n=13$ | 6.14 $n=4$ |
| Rat left atrium | 7.32 (1.09) $n=7$ | 7.10 $n=3$ |
| Guinea-pig left atrium | 6.49 (0.93) $n=6$ | NT |
| Rat right atrium | 7.81 (0.83) $n=5$ | NT |
| Guinea-pig right atrium | 6.25 (1.11) $n=3$ | NT |

Results are presented as the mean of either $pA_2$ values (slopes shown in brackets) or $pK_b$ values, where $n$ = the number of observations. NT = not tested.
*Slope significantly ($P<0.05$, $t$ test) less than unity.

### *Preparations reported to contain $A_2$-receptors*

NECA produced concentration-dependent relaxations of the guinea-pig aorta and coronary artery preparations, inhibition of U-46619-induced human platelet aggregation and inhibition of fMLP-induced $O_2^-$ production by human neutrophils. The other agonists evaluated produced qualitatively similar responses. Furthermore, where full concentration-effect curves could be constructed, the maximal responses obtained were not different from those to NECA. Comparison of the relative potencies of the eight compounds used in this study, however, show that the rank order of agonist potency characteristic of preparations containing adenosine $A_1$-receptors did not apply to these tissues and secondly, rank order of agonist potency did not apply to all of these preparations (Table 3). In the case of dog coronary artery, human neutrophils and platelets, the rank order of agonist potency was: CV1808, CGS21680 $\geqslant$ NECA $>$ **R-PIA** $\geqslant$ metrifudil $\geqslant$ CPA $>$ GR79236, S-PIA. However, for guinea-pig aorta, the rank order of agonist potency was: NECA $>$ metrifudil $>$ **R-PIA**, CPA $>$ CV1808, GR79236 $\geqslant$ S-PIA, CGS21680.

The agonist effects of NECA in dog coronary artery, guinea-pig aorta and human neutrophils were antagonized by 8-PT (Figure 2, Table 4). The agonist effects of metrifudil in guinea-pig aorta, and of CGS21680 in dog coronary artery, were found to be antagonized similarly. Here, the affinity estimates for 8-PT were apparently both agonist- and tissue-independent (Table 4). In the human platelet the inhibitory effects of NECA on U-46619-induced aggregation were antagonized by DPX. Schild analysis of these data resulted in a $pA_2$ value ($\pm$ s.e.mean) for DPX of 7.31 ($\pm$ 0.14) with a slope of 0.85 ($\pm$ 0.1), a value similar to the compound's reported affinity for adenosine receptors (Bruns *et al.*, 1986).

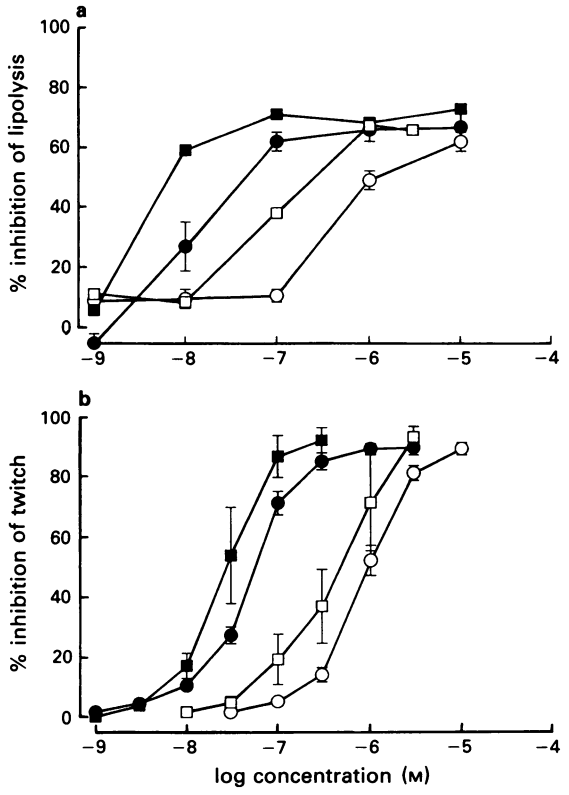



**Figure 1** Antagonism of the effects of NECA and GR79236 on rat adipocytes and guinea-pig ileum by 8-phenyltheophylline (8-PT). Mean concentration-effect curves to NECA (● and ○) and GR 79236 (■ and □) in the absence (filled symbols) and presence (open symbols) of 8-PT ($1 \times 10^{-5}$ M) on rat adipocytes (a) and guinea-pig ileum (b). Results are shown as mean ($\pm$ s.e.mean, where $n>3$) values from 4 (NECA) or 3 (GR79236) observations for rat adipocytes and 13 (NECA) and 4 (GR79236) observations for guinea-pig ileum. For abbreviations, see text.

## Discussion

In the present study, the effects of the adenosine analogues tested appear to be mediated via activation of adenosine receptors. Although responses have not been shown to be blocked by adenosine receptor antagonists (8-PT or DPX) in every tissue, we have shown that the effects of GR79236, metrifudil and CGS21680 are antagonized in preparations containing receptors for which the agonists show selectivity. In addition, the effects of the non-selective agonist, NECA, are sensitive to antagonists in all preparations.

The rank order of agonist potency obtained in guinea-pig ileum, rat adipocytes and the atrial preparations is consistent with the reported presence of adenosine $A_1$-receptors in these

**Table 3** Relative potencies of adenosine analogues in tissues containing $A_2$-receptors

| Preparation | *NECA* $EC_{50}$ (nM) | *EMCR* (NECA = 1) *Metrifudil* | *CV1808* | *CGS21680* | *R-PIA* | *CPA* | *GR79236* | *S-PIA* |
|---|---|---|---|---|---|---|---|---|
| Dog coronary artery | 44 (29–67) $n = 30$ | 16.5 (8–33) $n = 6$ | 0.75 (0.37–1.52) $n = 5$ | 1.23 (0.4–3.5) $n = 6$ | 10.5 (5.7–19.3) $n = 10$ | 20.8 (8–51) $n = 6$ | 131 (90–190) $n = 6$ | 80 (52–123) $n = 7$ |
| Guinea-pig aorta | 250 (222–281) $n = 42$ | 4.6 (2.7–7.5) $n = 8$ | 102 (52–199) $n = 7$ | 626 (430–912) $n = 6$ | 31 (16–63) $n = 8$ | 29 (21–41) $n = 8$ | 145 (93–227) $n = 6$ | 304 (136–684) $n = 6$ |
| Human platelet | 54 (34–84) $n = 19$ | 6.0 (2.41–14.9) $n = 4$ | 1.14 (0.61–2.13) $n = 6$ | 0.88 (0.18–4.24) $n = 4$ | 2.74 (1.73–4.3) $n = 19$ | 14.3 (5.3–38.3) $n = 7$ | 156 (50–494) $n = 4$ | 50.9 (34–75.5) $n = 19$ |
| Human neutrophil | 5.0 (4.1–6.1) $n = 46$ | 21.1 (13.3–33.4) $n = 4$ | 0.57 (0.21–1.60) $n = 6$ | 1.10 (0.22–5.6) $n = 4$ | 9.0 (3.5–23) $n = 4$ | 72 (38–137) $n = 4$ | 494 (266–917) $n = 5$ | 204 (134–310) $n = 4$ |

Equipotent molar concentration ratios (EMCR), together with the $EC_{50}$ of NECA, are presented as geometric mean values, with 95% confidence limits shown in parentheses and where $n$ = the number of observations.

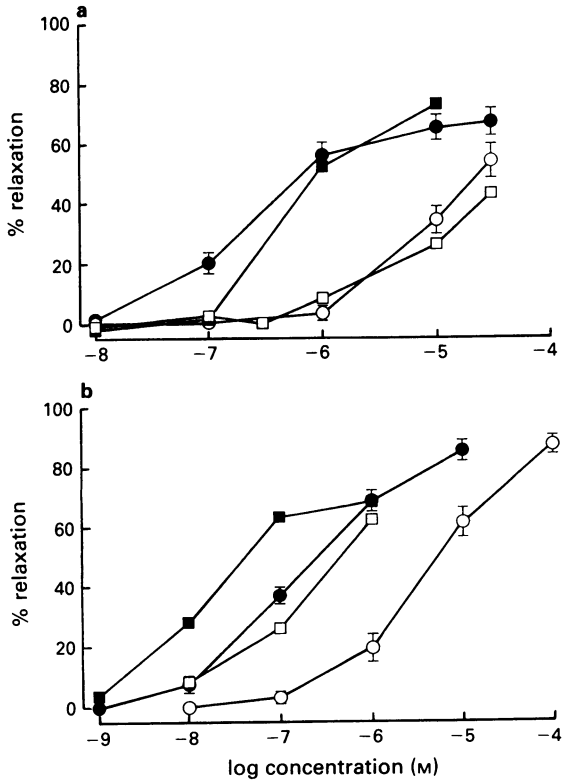



**Figure 2** Antagonism of the effects of NECA and metrifudil on guinea-pig aorta and of NECA and CGS21680 on dog coronary artery by 8-phenyltheophylline (8-PT). Mean concentration-effect curves to NECA (● and ○; $n = 13$) and metrifudil (■ and □; $n = 2$) on the guinea-pig aorta (a) and NECA (● and ○; $n = 6$) and CGS21680 (■ and □; $n = 6$) on the dog coronary artery (b) in the absence and presence of 8-PT ($1 \times 10^{-5}$ M). Results are shown as mean values (± s.e.mean where $n > 3$).

**Table 4** Antagonist potency of 8-phenyltheophylline in tissues containing $A_2$-receptors

| Preparation | $pA_2$ (Slope)/$pK_b$ vs *NECA* | *Metrifudil* | *CGS21680* |
|---|---|---|---|
| Guinea-pig aorta | 6.78 (0.90) $n = 13$ | 6.5 $n = 2$ | NT |
| Dog coronary artery | 6.5 $n = 6$ | NT | 6.28 $n = 3$ |
| Human neutrophil | 7.1 (0.89) $n = 6$ | NT | NT |

Results are presented as the mean of either $pA_2$ values (slopes shown in brackets) or $pK_b$ values, where $n$ = the number of observations. NT = not tested.

tissues (see Kennedy *et al.*, 1992a,b for relevant literature). In particular the potency of $N^6$-substituted compounds, such as GR79236, **R**-PIA and CPA, was similar to or greater than that of NECA. In addition, in this study, we have found that CV1808 and CGS21680 were substantially weaker than NECA in these tissues, consistent with data from ligand binding studies (Bruns *et al.*, 1986; Jarvis *et al.*, 1989). However, the results obtained in this study and those from our previous work (Kennedy *et al.*, 1992a), do not provide any evidence for the existence of sub-types of the $A_1$-receptor. It is possible that there are receptor sub-types, but the compounds and preparations used in the present study do not allow them to be detected. In marked contrast, however, two distinct rank orders of agonist potency have been obtained from tissues previously characterized as containing adenosine $A_2$-receptors (Collis & Brown, 1983; Cronstein *et al.*, 1988; Haslam & Cusack, 1981; Kusachi *et al.*, 1983). Thus, in dog coronary artery, human neutrophils and human platelets, CV1808 and CGS21680 were similar in potency to NECA, whilst in guinea-pig aorta, both compounds were substantially less active than NECA.

Ligand binding studies have shown that CGS21680 and CV1808 have high affinity for the adenosine $A_{2a}$-receptor in rat striatum, and in the case of CV1808, selectivity for this receptor versus the adenosine $A_{2b}$-receptor in human fibroblasts (Bruns *et al.*, 1986; Jarvis *et al.*, 1989). It is, therefore, likely that the receptors which we have studied in dog coronary artery, human platelets and human neutrophils are similar to, if not identical with, the striatal adenosine $A_{2a}$-receptor. Furthermore, it is possible that the guinea-pig aorta contains an adenosine receptor similar to that in human fibroblasts (see Hargreaves *et al.*, 1991, Martin, 1992). However, since no ligands which are selective for this receptor have yet been described, no firm conclusions may be drawn at present. Although the guinea-pig aorta appears to be the only example of this receptor type studied here, it should be noted that receptors which show similar characteristics with respect to CGS21680 and CV1808 mediate relaxation of dog saphenous vein, guinea-pig fundus and rat bladder and duodenum (Hargreaves *et al.*, 1991; Gurden & Kennedy, 1992; Nicholls *et al.*, 1992).

Although **R**-PIA, CPA and GR79236 showed selectivity for adenosine $A_1$- over $A_2$-receptors, the degree of selectivity was variable. The three compounds have similar potencies in tissues containing $A_1$ receptors, so their selectivity is dependent upon their abilities to stimulate $A_2$ receptors. **R**-PIA was the least selective of the three, whilst GR79236 appeared to

be the most selective, showing up to 1453 fold (rat adipocytes versus human neutrophils) selectivity for $A_1$ versus $A_2$ receptors.

Smellie *et al.* (1979) have suggested that the ratio of the potencies of the **R**- and **S**-isomers of PIA could be used to differentiate between adenosine $A_1$- and $A_2$-receptors. We have found that although this ratio does tend to be higher in the tissues containing $A_1$-receptors, the difference can be modest. Thus, the highest value was 59 for rat adipocyte ($A_1$), and the lowest value was 7.6 for dog coronary artery ($A_{2a}$). However, the lowest value obtained for the guinea-pig left atrium in which the receptor is characterized as being of the $A_1$-sub-type, was 18.4. This overlaps with the highest value obtained for a tissue containing adenosine $A_2$-receptors, namely 22.7 for human neutrophils ($A_{2a}$). Our findings therefore support the proposal of Bruns *et al.* (1986) that the potency ratio is of strictly limited value in the classification of adenosine receptors.

The 2-substituted compounds CV1808 and CGS21680 showed a high degree of selectivity for adenosine $A_{2a}$- over either $A_1$- or the putative $A_{2b}$-receptor (guinea-pig aorta). Thus, comparing EMCR values, CGS21680 showed a minimum of 206 fold selectivity for adenosine $A_{2a}$- versus $A_1$-receptors (dog coronary artery versus rat adipocyte) and 509 fold selectivity for $A_{2a}$- versus the putative $A_{2b}$-receptor (dog coronary artery versus guinea-pig aorta). Our inability to distinguish between the selectivity profiles of CV1808 and CGS 21680 was suprising, since previous binding and functional studies have reported that CGS21680 is the more selective compound (Jarvis *et al.*, 1989; Hutchison *et al.*, 1989). We have no explanation for this difference at present. In contrast, metrifudil did not differentiate between adenosine $A_{2a}$- and the putative $A_{2b}$-receptor, but did display modest selectivity for $A_2$- versus $A_1$-receptors.

In conclusion, the results of the present study provide further evidence for the existence of three types of adenosine receptor, corresponding to the $A_1$-, $A_{2a}$- and, possibly, $A_{2b}$-subtypes. Key compounds for distinguishing these sub-types are the $N^6$-substituted compounds, CPA and GR79236 and the 2-substituted compounds, CV1808 and CGS21680. Using these compounds, together with the reference agonist NECA, adenosine $A_1$-receptors can be defined by the rank order of agonist potency: CPA $\geqslant$ GR79236 $\geqslant$ NECA $>>$ CV1808, CGS21680, whilst the adenosine $A_{2a}$-receptor can be defined as: CV1808, CGS21680 $\geqslant$ NECA $>>$ CPA $>$ GR79236. The putative adenosine $A_{2b}$-receptor may be defined by a rank order of agonist potency of: NECA $>$ CPA $>$ CV1808, GR 79236 $\geqslant$ CGS21680. However, although a more satisfactory definition in these terms must await the discovery of selective agonists or antagonists for this receptor site, receptors reported to correspond to the $A_1$, $A_{2a}$ and $A_{2b}$ subtypes have apparently been cloned and expressed (see Pierce *et al.*, 1992 for references).

The authors gratefully acknowledge the technical assistance of Ms L.S. Davies, Mrs C. Southgate and Mr D. Gallagher. We are also grateful to Miss T. Chapple for her assistance with the preparation of the manuscript.

## References


ARUNLAKSHANA, O. & SCHILD, H.O. (1959). Some quantitative uses of drug antagonists. *Br. J. Pharmacol. Chemother.*, **14**, 48–58.

BHALLA, P., GURDEN, M.F. & KENNEDY, I. (1985). Studies on the adenosine receptors in dog coronary artery. *Br. J. Pharmacol.*, **86**, 438P.

BORN, G.V.R. (1962). Quantitative investigations into the aggregation of blood platelets. *J. Physiol.*, **162**, 67P.

BRUNS, R.F., LU, G.H. & PUGSLEY, G.H. (1986). Characterisation of the $A_2$ adenosine receptor labelled by [$^3$H]NECA in rat striatal membranes. *Mol. Pharmacol.*, **29**, 331–346.

COLLIS, M.G. & BROWN, C.M. (1983). Adenosine relaxes the aorta by interacting with an $A_2$ receptor and an intracellular site. *Eur. J. Pharmacol.*, **96**, 61–69.

CRONSTEIN, B.N., KRAMER, S.B., ROSENSTEIN, E.B., KORCHAK, H.M., WEISSMANN, G. & HIRSCHHORN, R. (1988). Occupancy of adenosine receptors raises cyclic AMP alone and in synergy with occupancy of chemoattractant receptors and inhibits membrane depolarization. *Biochem. J.*, **252**, 709–715.

FOSTER, M., HORNBY, E.J. & PERRY, C. (1987). Adenosine analogues as inhibitors of human platelet aggregation. *Br. J. Pharmacol.*, **92**, 736P.

GADDUM, J.H. (1957). Theories of drug antagonism. *Pharmacol. Rev.*, **9**, 211–218.

GURDEN, M.F. & KENNEDY, I. (1992). Characterisation of the adenosine receptors in dog coronary artery, guinea-pig aorta and guinea-pig fundus. *Br. J. Pharmacol.*, **105**, 115P.

HARGREAVES, M.B., STOGGALL, S.M. & COLLIS, M.G. (1991). Evidence that the adenosine receptor mediating relaxation in dog lateral saphenous vein and guinea-pig aorta is of the $A_{2b}$ subtype. *Br. J. Pharmacol.*, **102**, 198P.

HASLAM, R.J. & CUSACK, N.J. (1981). Blood platelet receptor for ADP and for adenosine. In *Purinergic receptors*, ed. Burnstock, G. London: Chapman & Hall.

HORNBY, E.J., FOSTER, M.F., McCABE, P.J. & STRATTON, L.E. (1989). The inhibitory effect of GR32191, a thromboxane receptor blocking drug, on human platelet aggregation, adhesion and secretion. *Thromb. Haemostatis.*, **61**, 429–436.

HUTCHISON, A.J., WEBB, R.L., OEI, H.H., GHAI, G.R., ZIMMERMAN, M.B. & WILLIAMS, M. (1989). CGS 21680C, an $A_2$ selective adenosine receptor agonist with preferential hypotensive activity. *J. Pharmacol. Exp. Ther.*, **251**, 47–55.

JARVIS, M.F., SCHULZ, R., HUTCHISON, A.J., DO, U.H., SILLS, M.A. & WILLIAMS, M. (1989). [$^3$H]CGS21680, a selective $A_2$ adenosine receptor agonist directly labels $A_2$ receptors in rat brain. *J. Pharmacol. Exp. Ther.*, **251**, 888–893.

KENNEDY, I., GURDEN, M.F. & STRONG, P. (1992a). Do adenosine $A_3$-receptors exist? *Gen. Pharmacol.*, **23**, 303–307.

KENNEDY, I., GURDEN, M.F., STRONG, P., HORNBY, E., FOSTER, M. & VARDEY, C.J. (1992b). Pharmacological classification of adenosine receptors in isolated tissues. *Int. J. Pur. Pyr. Res.*, **3**, 83.

KUSACHI, S., THOMPSON, R.D. & OLSSON, R.A. (1983). Ligand selectivity of dog coronary artery adenosine receptor resembles that of adenylate cyclase stimulatory ($R_a$) receptors. *J. Pharmacol. Exp. Ther.*, **227**, 316–321.

LONDOS, C., COOPER, D.M.F. & WOLFF, J. (1980). Subclasses of external adenosine receptors. *Proc. Natl. Acad. Sci. U.S.A.*, **77**, 2551–2554.

MARTIN, P.L. (1992). Relative agonist potencies of $C^2$-substituted analogues of adenosine: evidence for adenosine $A_{2b}$ receptors in guinea-pig aorta. *Eur. J. Pharmacol.*, **216**, 235–242.

NICHOLLS, J., HOURANI, S.M.O. & KITCHEN, I. (1992). Characterisation of P1-purinoceptors on rat duodenum and urinary bladder. *Br. J. Pharmacol.*, **105**, 639–642.

PIERCE, K.D., FURLONG, T.J., SELBIE, L.A. & SHINE, J. (1992). Molecular cloning and expression of an adenosine $A_{2b}$ receptor from human brain. *Biochem. Biophys. Res. Commun.*, **187**, 86–93.

RIBEIRO, J.A. & SEBASTIAO, A.M. (1986). Adenosine receptors and calcium: basis for proposing a third ($A_3$) adenosine receptor. *Prog. Neurobiol.*, **26**, 179–209.

SCHAUMANN, E. & KUTSCHA, W. (1972). Klinisch-pharmakologische untersuchungen mit einem neuen peroral wirksamen adenosinderivat. *Arzneim. Forsch. Drug Res.*, **22**, 783–790.

SMELLIE, F.W., DALY, J.W., DUNWIDDIE, T.V. & HOFFER, B.J. (1979). The dextro and levorotatory isomers of N-phenylisopropyl adenosine: stereospecific effects on cyclic AMP formation and evoked synaptic responses in brain slices. *Life Sci.*, **25**, 1739–1748.

STRATTON, G.D., MYLES, D.D., STRONG, P. & SKIDMORE, I.F. (1985). The development of tolerance to antilipolytic agents by isolated rat adipocytes. *Biochem. Pharmacol.*, **34**, 275–279.

TREVIDI, B.K., BRIDGES, A.J. & BRUNS, R.F. (1990). Structure-activity relationships of adenosine $A_1$ and $A_2$ receptors. In *Adenosine and Adenosine Receptors*. ed. Williams, M. pp. 57–103. Clifton: Humana Press.

VAN CALKER, D., MULLER, M. & HAMPRECHT, B. (1979). Adenosine regulates via two different types of receptors the accumulation of cyclic AMP in cultured brain cells. *J. Neurochem.*, **33**, 999–1005.


*(Received January 13, 1993*
*Revised March 3, 1993*
*Accepted March 8, 1993)*

*Br. J. Pharmacol.* (1993), **109**, 699–702 © Macmillan Press Ltd, 1993

# The novel 5-$HT_{1A}$ receptor antagonist, SDZ 216-525, decreases 5-HT release in rat hippocampus *in vivo*

[1]T. Sharp, R. McQuade, *J.R. Fozard & *D. Hoyer

MRC Unit and University Department of Clinical Pharmacology, Radcliffe Infirmary, Woodstock Road, Oxford OX2 6HE, UK and *Preclinical Research, 360/604, SANDOZ Pharma, CH 4002 Basel, Switzerland

**1** Recent evidence suggests that the novel compound SDZ 216-525 is a selective and possibly silent 5-$HT_{1A}$ receptor antagonist. Here we have examined the action of SDZ 216-525 on central 5-$HT_{1A}$ autoreceptor function. The experiments involved measurement of drug effects on extracellular 5-HT in the ventral hippocampus of the chloral hydrate anaesthetized rat by use of microdialysis.

**2** Acute injection of SDZ 216-525 (0.1, 0.3, 1.0 and 3 mg $kg^{-1}$, s.c.) caused a dose-related decrease in 5-HT output with an estimated $ED_{50}$ of at least 0.3 mg $kg^{-1}$. This $ED_{50}$ value is 20–30 times greater than $ED_{50}$ values previously obtained for 8-hydroxy-2-(di-n-propylamino) tetralin (8-OH-DPAT) and NAN-190. In comparison, SDZ 216-525 is reported to have slightly higher affinity for the 5-$HT_{1A}$ site than 8-OH-DPAT and NAN-190.

**3** The inhibitory effect of SDZ 216-525 (1 mg $kg^{-1}$, s.c.) on 5-HT was blocked by the 5-$HT_1$/$\beta$-adrenoceptor antagonist, (−)-pindolol (8 mg $kg^{-1}$, s.c.) but not by a combination of the $\beta_1$- and $\beta_2$-selective adrenoceptor antagonists metoprolol and ICI 118,551 (4 mg $kg^{-1}$, each).

**4** Although in several experimental models SDZ 216-525 has high affinity, selectivity and lacks intrinsic activity at the 5-$HT_{1A}$ receptor, our experiments show that the drug decreases extracellular 5-HT in ventral hippocampus of the chloral hydrate anaesthetized rat via a pindolol-sensitive mechanism. We conclude that either SDZ 216-525 promotes (with low potency *in vivo*) 5-$HT_{1A}$ receptor/G-protein interactions, or that the 5-$HT_{1A}$ autoreceptor is a 5-$HT_{1A}$ receptor subtype different from the postsynaptic 5-$HT_{1A}$ receptor.

**Keywords:** SDZ 216-525; 5-$HT_{1A}$ receptor; microdialysis; 8-hydroxy-2-(di-n-propylamino)tetralin (8-OH-DPAT); NAN-190

## Introduction

Currently studies on the pharmacology of the 5-$HT_{1A}$ receptor are hampered by the lack of suitable drug tools. Thus, whilst there are available a number of high affinity 5-$HT_{1A}$ receptor ligands, most either lack selectivity and/or display mixed agonist/antagonist properties.

Recently, the pharmacological properties of the 5-$HT_{1A}$ receptor ligand, SDZ 216-525, (methyl-4{4-[4-(1,1,3-trioxo-2H-1,2- benziosothiazol-2-yl) butyl]-1-piperazinyl} 1H-indole-2-carboxylate; Compound 24, Seiler *et al.*, 1992) were described (Hoyer *et al.*, 1992; Boddeke *et al.*, 1992; Schoeffter *et al.*, 1993). This compound displays high affinity and selectivity for brain 5-$HT_{1A}$ binding sites versus other binding sites for 5-hydroxytryptamine (5-HT) (5-$HT_{1B}$, 5-$HT_{1C}$, 5-$HT_{1D}$, 5-$HT_2$, 5-$HT_3$) and other neurotransmitters ($\alpha_1$, $\alpha_2$, $\beta_1$, $\beta_2$ and $D_2$). In biochemical studies using receptor-linked effector systems, SDZ 216-525 potently antagonizes the effects of the selective agonist 8-hydroxy-2-(di-n-propylamino)tetralin (8-OH-DPAT) on 5-$HT_{1A}$ receptors ($pK_B = 10$) but displays no intrinsic activity. In comparison, SDZ 216-525 has little affinity or activity in biochemical models of 5-$HT_{1B}$, 5-$HT_{1C}$ or 5-$HT_{1D}$ receptor function. Evidence from *in vivo* experiments also suggests that SDZ 216-525 is a potent and possibly silent 5-$HT_{1A}$ receptor antagonist. Thus, in the rat the drug does not induce forepaw treading, flat-body posture and hypothermia but inhibits these responses when induced by 8-OH-DPAT (Hoyer *et al.*, 1992; Schoeffter *et al.*, 1993).

A number of high affinity 5-$HT_{1A}$ receptor ligands, including NAN-190 and BMY 7378, which display low intrinsic activity at the 5-$HT_{1A}$ receptor in many models of 5-$HT_{1A}$ receptor function, seemingly have agonist activity at the somatodendritic 5-$HT_{1A}$ autoreceptor. This activity is apparent in both electrophysiological studies which show that NAN-190 and BMY 7378 inhibit the firing of raphé 5-HT neurones (VanderMaelen *et al.*, 1986; Greuel & Glaser, 1992; Hodgkiss *et al.*, 1992) and neurochemical studies which show that these drugs decrease 5-HT release *in vivo* (Sharp *et al.*, 1990; Sharp & Hjorth, 1990; Hjorth & Sharp, 1990). Here we have tested the effect of SDZ 216-525 on 5-$HT_{1A}$ autoreceptor function using the latter approach.

## Methods

### In vivo *measurement of 5-HT release using microdialysis*

The microdialysis procedure used is described in detail elsewhere (Sharp *et al.*, 1989). In brief, male Sprague Dawley rats (260–360 g, Harlan-Olac, Bicester, U.K.) were anaesthetized with chloral hydrate and a microdialysis probe (short-loop type, Cordis Dow cellulose membrane) was stereotaxically implanted into the ventral hippocampus (stereotaxic co-ordinates: anterior-posterior − 4.0 mm, lateral − 4.6 mm, dorsal-ventral − 8.5 mm, relative to bregma and dura surface with a head-flat position). The microdialysis probe was perfused continuously (1 $\mu$l $min^{-1}$) with artifical CSF containing 1 $\mu$M citalopram, a selective 5-HT reuptake inhibitor. Perfusates were collected every 20 min and analysed immediately for 5-HT by high performance liquid chromatography with electrochemical detection.

### *Experimental protocol*

After probe implantation, there followed a control period of about 3 h to allow the level of 5-HT in the perfusates to stabilize. Drugs were then injected subcutaneously over the next 30 min and 5-HT measurements were continued for a further 2 h.

SDZ 216-525 was tested in two groups of experiments; (i)

[1] Author for correspondence.

SDZ 216-525 was administered alone to naive rats, and (ii) SDZ 216-525 was administered to rats pretreated 30 min previously with either the 5-$HT_1$/β-adrenoceptor antagonist (−)-pindolol or the β-adrenoceptor antagonists, metoprolol ($\beta_1$) and ICI 118,551 ($\beta_2$), in combination.

### *Drugs*

SDZ 216-525 (methyl 4-{4-[4-(1,1,3-trioxo-2H-1,2-benziosothiazol-2-yl)butyl]-1-piperazinyl}1H-indole-2-carboxylate, synthesized at SANDOZ Pharma, Basel, Switzerland) was dissolved in malonic acid (5 mg compound mixed with 5 mg malonic acid in 1 ml water). Metoprolol tartrate (Hassle, Mölndal, Sweden) and ICI 118,551 ((±)-erythro-(±)-1-(7-methylindan-4-yloxy)-3-isopropylamino-butan-2-ol HCl; ICI, Macclesfield, U.K.) were dissolved in saline. (−)-Pindolol (SANDOZ Pharma, Basel, Switzerland) was dissolved in a few drops of glacial acetic acid and made up to volume in 5% (w/v) glucose solution. Drugs were injected subcutaneously in a volume of 1 ml $kg^{-1}$.

### *Data presentation and analysis*

5-HT in the perfusates over time is expressed as a percentage of the absolute amount of 5-HT in the sample obtained immediately before drug administration. This method of presentation allows direct comparison of the present data with those of our earlier studies. Using percentage data, areas under the curve for the 0–120 min period postdrug were calculated and used to construct a dose-response curve. $ED_{50}$ values were estimated graphically.

Treatment effects were analysed statistically (using raw data) either by within group comparisons (pre versus post-treatment) using 1-way ANOVA with repeated measures (followed by Dunnett's test) or by between group comparisons using 2-way ANOVA with repeated measures. Probability values of 0.05 or less were considered to be statistically significant.

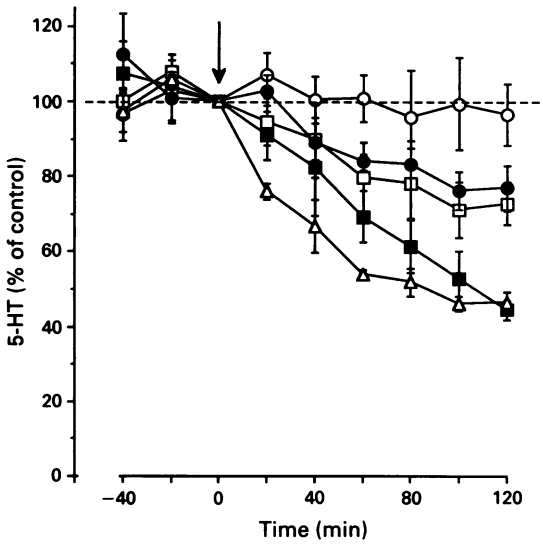



**Figure 1** Effect of different doses of SDZ 216-525 and malonic acid vehicle on 5-hydroxytryptamine (5-HT) in microdialysates from ventral hippocampus of the chloral hydrate anaesthetized rat. Treatment groups are identified as follows: malonic acid vehicle (○, $n = 6$); 0.1 mg $kg^{-1}$ (●, $n = 4$); 0.3 mg $kg^{-1}$ (□, $n = 6$); 1 mg $kg^{-1}$ (■, $n = 7$); 3 mg $kg^{-1}$ (△, $n = 3$). 5-HT in the microdialysates is expressed as a % (mean ± s.e.mean) of the absolute amount of 5-HT in the sample collected immediately before drug injection ($t = 0$). Absolute amounts of 5-HT (pmol/sample, mean ± s.e.mean) at $t = 0$ were as follows: controls: 0.061 ± 0.006; 0.1 mg $kg^{-1}$: 0.056 ± 0.004; 0.3 mg $kg^{-1}$: 0.069 ± 0.010; 1 mg $kg^{-1}$: 0.060 ± 0.006; 3 mg $kg^{-1}$: 0.066 ± 0.004. See results for details of statistical analysis.

## Results

### *Effect of administration of SDZ 216-525 on 5-HT release in hippocampus of naive rats*

In chloral hydrate anaesthetized, treatment-naive rats injection of SDZ 216-525 induced a clear-cut and dose-related (0.1, 0.3, 1 and 3 mg $kg^{-1}$, s.c.) decrease in 5-HT levels in hippocampal microdialysates (Figure 1). 5-HT levels decreased to about 50% of pre-drug values by 120 min following injection of 1 mg $kg^{-1}$ SDZ 216-525. The highest dose tested (3 mg $kg^{-1}$, s.c.) also reduced 5-HT levels to about 50% of pre-drug values but within 60 min of injection. A higher dose was not tested due to poor drug solubility at high concentrations.

In comparison to SDZ 216-525, injection of malonic acid vehicle did not alter 5-HT output over the 2 h post drug period compared to pre-injection control values (Figure 1).

Statistical analysis (1 way ANOVA followed by Dunnett's test) of the data revealed significant effects of SDZ 216-525 at all doses tested but no effect of vehicle injection when compared to pretreatment values.

Figure 2 compares the dose-response curve for SDZ 216-525 with curves previously published for 8-OH-DPAT and NAN-190. The latter data were obtained in experiments carried out under identical conditions to those described in the present paper. From these curves it is estimated that the $ED_{50}$ for SDZ 216-525 is at least 0.3 mg $kg^{-1}$, s.c. which is 20–30 times greater than corresponding $ED_{50}$ values for 8-OH-DPAT (0.015 mg $kg^{-1}$, s.c.) and NAN-190 (0.009 mg $kg^{-1}$, s.c.). Note that the maximum suppression of 5-HT release detected following both NAN-190 and SDZ 216-525 was less than that following 8-OH-DPAT (Figure 2).

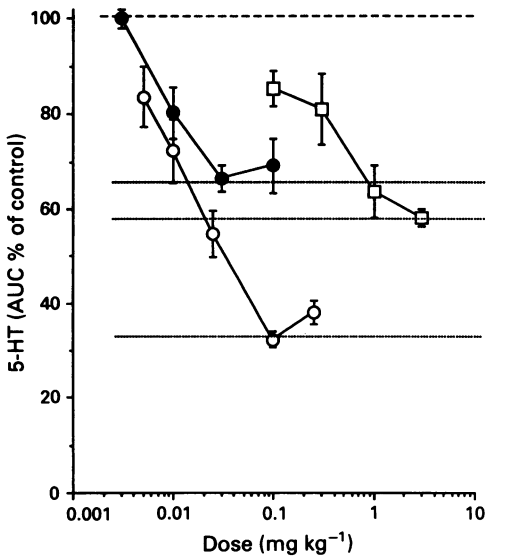



**Figure 2** Log-dose response curves for the inhibitory effect of SDZ 216-525 (□), 8-hydroxy-2-(di-n-propylamino)tetralin (8-OH-DPAT) (○) and NAN-190 (●) on 5-hydroxytryptamine (5-HT) output in ventral hippocampus of the chloral hydrate anaesthetized rat. The values for 5-HT are calculated from the areas under the curve (AUC) for the 0–120 min period post drug injection and are expressed as a % of control (the dotted line at 100% represents no change). The time course data for SDZ 216-525 are shown in Figure 1. The data for 8-OH-DPAT and NAN-190 are taken in part from Sharp *et al.* (1989) and Hjorth & Sharp (1990). Each point is a mean ± s.e.mean value.

*Effect of pretreatment with (−)-pindolol, metropolol and ICI 118,551 on the 5-HT response to SDZ 216-525*

The 5-HT response to 1 mg kg$^{-1}$, s.c., SDZ 216-525 was blocked in rats pretreated with 8 mg kg$^{-1}$, s.c. of the 5-HT$_1$/β-antagonist (−)-pindolol (Figure 3). In contrast, the 5-HT response to SDZ 216-525 persisted in rats pretreated with a combination of 4 mg kg$^{-1}$, s.c. of each of the β-blockers metoprolol and ICI 118,551 (Figure 3). Neither (−)-pindolol nor metoprolol and ICI 118,551 altered basal 5-HT output when injected alone in these experiments (Hjorth & Sharp, 1993).

Statistical analysis of the data using 1-way ANOVA (followed by Dunnett's test) revealed significant changes in 5-HT ($P<0.05$) following 1 mg kg$^{-1}$ SDZ 216-525 alone or in combination with metoprolol and ICI 118,551 but no significant changes ($P>0.05$) after 1 mg kg$^{-1}$ SDZ 216-525 in combination with (−)-pindolol. Statistical analysis of the data by 2-way ANOVA revealed a significant interaction between the SDZ 216-525 alone versus SDZ 216-525 plus (−)-pindolol ($F=4.172$, d.f. 8, 88; $P<0.001$) but no interaction between SDZ 216-525 alone versus SDZ 216-525 plus β-blockers ($F=0.702$, d.f. 8, 72; $P=0.689$).

## Discussion

Here we show that the novel and putative silent 5-HT$_{1A}$ receptor antagonist, SDZ 216-525, induces a clear-cut and dose-related decrease in extracellular 5-HT in the ventral hippocampus of anaesthetized rats. This response is blocked by pretreatment with the 5-HT$_1$/β-adrenoceptor-antagonist (−)-pindolol but not the control β-adrenoceptor antagonists, metoprolol and ICI 118,551. This implicates the involvement of receptors of the 5-HT$_1$ subtype rather than other receptors of 5-HT or indeed receptors of other neurotransmitters. Given the high affinity and selectivity of SDZ 216-525 for the 5-HT$_{1A}$ binding sites versus other binding sites for 5-HT (5-HT$_{1B}$, 5-HT$_{1C}$, 5-HT$_{1D}$, 5-HT$_2$, 5-HT$_3$) and other neurotransmitters

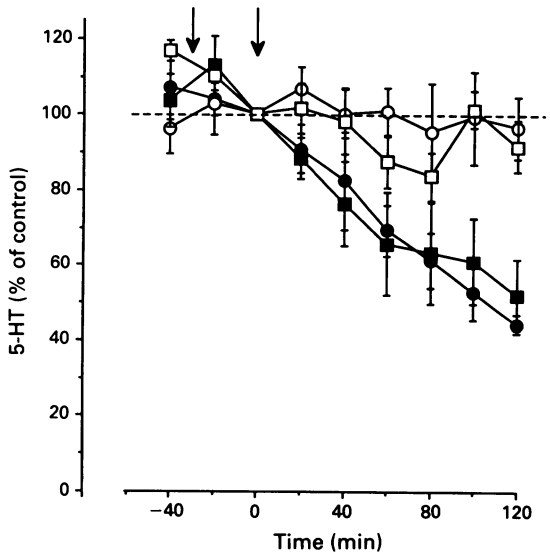



**Figure 3** Effect of pretreatment with the 5-HT$_1$/β-adrenoceptor antagonist (−)-pindolol (8 mg kg$^{-1}$, s.c.) and a combination of the $\beta_1$- and $\beta_2$-selective adrenoceptor antagonists, metoprolol and ICI 118,551 (each at 4 mg kg$^{-1}$, s.c.) on the inhibitory effect of SDZ 216-525 (1 mg kg$^{-1}$, s.c.) on 5-hydroxytryptamine (5-HT) output in the ventral hippocampus. Treatment groups are identified as follows: controls (○, $n=6$); SDZ 216-525 alone (●, $n=7$); SDZ 216-525 plus (−)-pindolol (□, $n=6$); SDZ 216-525 plus metoprolol and ICI 118,551 (■, $n=4$). Absolute amounts of 5-HT (pmol/sample, mean ± s.e.mean) at $t=0$ were as follows: controls: 0.061 ± 0.006; SDZ 216-525: 0.060 ± 0.006; SDZ 216-525 plus (−)-pindolol: 0.048 ± 0.003; SDZ 216-525 plus metoprolol and ICI 118,551: 0.048 ± 0.005. See results for details of statistical analysis.

($\alpha_1$, $\alpha_2$, $\beta_1$, $\beta_2$ and $D_2$: Hoyer *et al.*, 1992; Schoeffter *et al.*, 1993), a strong candidate for the mechanism underlying the inhibition of 5-HT release by SDZ 216-525 is activation of 5-HT$_{1A}$ autoreceptors, probably those located on the soma and dendrites of 5-HT neurones in the midbrain raphé.

In conflict with the present findings, biochemical studies to date indicate that SDZ 216-525 lacks intrinsic activity at the 5-HT$_{1A}$ receptor. Thus, the drug does not inhibit forskolin-stimulated adenylate cyclase in calf hippocampal membranes but antagonizes potently the inhibition induced by 8-OH-DPAT (Hoyer *et al.*, 1992; Schoeffter *et al.*, 1993). Furthermore, in another biochemical model of 5-HT$_{1A}$ receptor function, 5-HT$_{1A}$-mediated calcium mobilization in Hela cells, SDZ 216-525 displays the property of a potent and silent 5-HT$_{1A}$ receptor antagonist even under conditions of high receptor reserve which favours the expression of intrinsic activity (Boddeke *et al.*, 1992). Findings from studies using *in vivo* models of 5-HT$_{1A}$ receptor function also support the idea that SDZ 216-525 is a 5-HT$_{1A}$ receptor antagonist lacking intrinsic activity. Specifically, in the rat SDZ 216-525 (0.03–1 mg kg$^{-1}$, s.c.) blocks 8-OH-DPAT-induced forepaw treading, flat-body posture and hypothermia without inducing these effects itself (Hoyer *et al.*, 1992; Schoeffter *et al.*, 1993).

Previously we have reported that a number of 5-HT$_{1A}$ receptor ligands with apparently low intrinsic activity at the 5-HT$_{1A}$ receptor, including NAN-190 and BMY 7378, also decrease 5-HT release in hippocampus via a pindolol-sensitive mechanism (Sharp *et al.*, 1990; Hjorth & Sharp, 1990). Furthermore, both NAN-190 and BMY 7378 inhibit the firing of 5-HT neurones when applied locally to the raphé (VanderMaelen *et al.*, 1986; Hodgkiss *et al.*, 1992), the latter effect being antagonized by high concentrations of the 5-HT$_1$/β-adrenoceptor-antagonist, (−)-propranolol (Greuel & Glaser, 1992). These findings have led to the idea that NAN-190 and BMY 7378 are weak partial 5-HT$_{1A}$ receptor agonists and not silent 5-HT$_{1A}$ receptor antagonists.

It seems reasonable to assume that SDZ 216-525 is also a partial 5-HT$_{1A}$ agonist on the basis of the present findings that first, SDZ 216-525 decreased 5-HT release when injected alone but with an efficacy likely to be less than that of 8-OH-DPAT (cf. Figure 2) and secondly, the inhibitory effect of SDZ 216-525 on 5-HT was blocked by (−)-pindolol. The present data do not exclude the possibility that blockade of $\alpha_1$-adrenoceptors has a part to play in the 5-HT response to SDZ 216-525, a mechanism which may contribute to the decrease in 5-HT release induced by NAN-190 (Hjorth & Sharp, 1990; Claustre *et al.*, 1991). However, it should be pointed out that data from binding studies show that the affinity of SDZ 216-525 for $\alpha_1$-adrenoceptors is about 70 times lower than that for 5-HT$_{1A}$ receptors (Schoeffter *et al.*, 1993).

It remains to be determined why 5-HT$_{1A}$ ligands with low intrinsic activity at the 5-HT$_{1A}$ receptor, apparently express agonist activity at the 5-HT$_{1A}$ autoreceptor. Plausible explanations include high 5-HT$_{1A}$ receptor reserve in the raphé (Meller *et al.*, 1990), high efficiency coupling between this receptor and its effector mechanisms and even differences in 5-HT$_{1A}$ receptor subtype in the raphé compared to other brain regions (Radja *et al.*, 1992).

The results of biochemical studies showing that SDZ 216-525 does not display 5-HT$_{1A}$ receptor agonist activity under conditions where receptor reserve is high (Boddeke *et al.*, 1992), suggests that the coupling between the 5-HT$_{1A}$ autoreceptor and its effector mechanisms may be a more important factor. If 5-HT$_{1A}$ autoreceptors are extremely well coupled to their effector system as suggested (Meller *et al.*, 1990; Sharp *et al.*, 1990), compounds with very low or no intrinsic activity at postsynaptic 5-HT$_{1A}$ receptors may display agonism at autoreceptors. However, some of these compounds act as agonists at concentrations significantly higher than those expected from radioligand binding studies (also see below).

Support for the view that there are 5-$HT_{1A}$ receptor subtypes comes from the present observation that the potency of SDZ 216-525 at inhibiting 5-HT release ($ED_{50}$ = 0.3 mg $kg^{-1}$, s.c.) is some 20–30 times less than that of 8-OH-DPAT (0.015 mg $kg^{-1}$, s.c.) and NAN-190 (0.009 mg $kg^{-1}$, s.c.) whereas the affinity of SDZ 216-525 for the 5-$HT_{1A}$ binding site ($pK_D$ = 9.2) is slightly greater than that of 8-OH-DPAT (8.7) and NAN-190 (8.9). Clearly, differences between potency *in vivo* and binding affinity *in vitro* could be explained by poor entry of SDZ 216-525 into the brain; the action of an active metabolite cannot be excluded. It ought to be added, however, that it was reported very recently that SDZ 216-525 (1 mg $kg^{-1}$, s.c.) decreased hippocampal 5-HT release (as measured by microdialysis) but that this effect was not blocked by the putative silent 5-$HT_{1A}$ receptor antagonist, (±)-WAY 100135 (Gurling *et al.*, 1993). The interesting possibility that SDZ 216-525 is differentially sensitive to (−)-pindolol and (±)-WAY 100135 deserves further investigation.

In conclusion, the present study shows that the novel compound SDZ 216-525 decreases 5-HT release in rat hippocampus *in vivo* via a pindolol-sensitive mechanism. It is possible that this compound is a weak partial 5-$HT_{1A}$ receptor agonist rather than a silent 5-$HT_{1A}$ receptor antagonist as recent biochemical studies suggest. This matter, however, warrants further study given the continuing speculation concerning 5-$HT_{1A}$ receptor subtypes.

We thank Drs A. Stoll and M.P. Seiler for synthesizing SDZ 216-525.

## References

BODDEKE, H.W.G.M., FARGIN, A., RAYMOND, J.R., SCHOEFFTER, P. & HOYER, D. (1992). Agonist/antagonist interactions with cloned human 5-$HT_{1A}$ receptors: variations in intrinsic activity studied in transfected HeLa cells. *Naunyn Schmeid Arch. Pharmacol.*, **345**, 257–263.

CLAUSTRE, Y., ROUQUIER, L., SERRANO, A., BENAVIDES, J. & SCATTON, B. (1991). Effect of the putative 5-$HT_{1A}$ receptor antagonist NAN-190 on rat brain serotonergic transmission. *Eur. J. Pharmacol.*, **203**, 71–77.

GREUEL, J.M. & GLASER, T. (1992). The putative 5-$HT_{1A}$ receptor antagonists NAN-190 and BMY 7378 are partial agonists in the rat dorsal raphé nucleus in vitro. *Eur. J. Pharmacol.*, **211**, 211–219.

GURLING, J., ASHWORTH-PREECE, M.A., HARTLEY, J.E., FLETCHER, A., DOURISH, C.T. & ROUTLEDGE, C. (1993). Effects of the putative 5-$HT_{1A}$ receptor antagonist SDZ 216-525 in two models of somatodendritic 5-$HT_{1A}$ autoreceptor function. Proceedings of the British Pharmacological Society, Cambridge Meeting, 5th–7th January, p. 147. *Br. J. Pharmacol.*, (in press).

HJORTH, S. & SHARP, T. (1990). Mixed agonist/antagonist properties of NAN-190 at 5-$HT_{1A}$ receptors: behavioural and in vivo brain microdialysis studies. *Life Sci.*, **46**, 955–963.

HJORTH, S. & SHARP, T. (1993). *In vivo* microdialysis evidence for central 5-$HT_{1A}$ and 5-$HT_{1B}$ autoreceptor-blocking properties of the β-adrenoceptor antagonist (−) penbutolol. *J. Pharmacol. Exp. Ther.*, (in press).

HODGKISS, J.P., DAWSON, I.M. & KELLY, J.S. (1992). An intracellular study of the action of NAN-190 on neurons in the dorsal raphe nucleus of the rat. *Brain Res.*, **576**, 157–161.

HOYER, D., SCHOEFFTER, P., PALACIOS, J.M., KALKMAN, H.O., BRUINVELS, A.T., FOZARD, J.R., SIEGL, H. & STOLL, A. (1992). SDZ 216-525: a selective, potent and silent 5-$HT_{1A}$ receptor antagonist. *Br. J. Pharmacol.*, **105**, 29P.

MELLER, E., GOLDSTEIN, M. & BOHMAKER, K. (1990). Receptor reserve for 5-hydroxytryptamine$_{1A}$-mediated inhibition of serotonin synthesis: possible relationship to anxiolytic properties of 5-hydroxytryptamine$_{1A}$ agonists. *Mol. Pharmacol.*, **37**, 231–237.

RADJA, F., DAVAL, G., HAMON, M. & VERGÉ, D. (1992). Pharmacological and physiological properties of pre- versus postsynaptic 5-hydroxytryptamine$_{1A}$ receptor binding sites in the rat brain: a quantitative autoradiographic study. *J. Neurochem.*, **58**, 1338–1346.

SCHOEFFTER, P., FOZARD, J.R., STOLL, A., SEILER, M.P. & HOYER, D. (1993). SDZ 216-525, a selective and potent 5-$HT_{1A}$ receptor antagonist. *Eur. J. Pharmacol.*, (Mol. Pharmacol. section), (in press).

SEILER, M.P., STOLL, A., HAGENBACH, A., FLOERSHEIM, P., FOZARD, J.R., KALKMAN, H.O., KIR, A.K., SIEGL, H., SCHOEFFTER, P. & HOYER, D. (1992). Novel approaches to drugs acting on '5-$HT_1$like' receptors. In *Trends in Medicinal Chemistry '90'*. ed. Sarel, S., Mechoulam, R. & Agranat, I. pp. 90–105. Oxford: Blackwell Scientific Publications.

SHARP, T., BACKUS, L.I., HJORTH, S., BRAMWELL, S.R. & GRAHAME-SMITH, D.G. (1990). Further investigation of the in vivo pharmacological properties of the putative 5-$HT_{1A}$ antagonist, BMY 7378. *Eur. J. Pharmacol.*, **176**, 331–340.

SHARP, T., BRAMWELL, S.R. & GRAHAME-SMITH, D.G. (1989). 5-$HT_1$ agonists reduce 5-hydroxytryptamine release in rat hippocampus *in vivo* as determined by brain microdialysis. *Br. J. Pharmacol.*, **96**, 283–290.

SHARP, T. & HJORTH, S. (1990). Application of brain microdialysis to study the pharmacology of the 5-$HT_{1A}$ autoreceptor. *J. Neurosci. Methods*, **34**, 83–90.

VANDERMAELEN, C.P., BRASELTON, J.P. & GELLBACH, G. (1987). In vivo and in vitro electrophysiological studies indicate that BMY 7378 is a partial agonist at 5-$HT_{1A}$ receptors in the rat dorsal raphé nucleus. *Soc. Neurosci. Abstr.*, **13**, 459.5

*(Received January 15, 1993*
*Revised March 8, 1993*
*Accepted March 9, 1993)*

*Br. J. Pharmacol.* (1993), **109**, 703–712 © Macmillan Press Ltd, 1993

# Effects of calyculin A on tension and myosin phosphorylation in skinned smooth muscle of the rabbit mesenteric artery

Akito Suzuki & Takeo Itoh

Department of Pharmacology, Faculty of Medicine, Kyushu University, Fukuoka 812, Japan

**1** Using β-escin and ionomycin-treated skinned smooth muscle strips of the rabbit mesenteric artery, the effects of calyculin A (CL-A, an inhibitor of type 1 and 2A phosphatases) on mechanical activities, phosphorylation of myosin light chain (MLC) and the relationship between the two were studied in $Ca^{2+}$-free solution containing 4 mM EGTA and these effects were compared with those evoked by $Ca^{2+}$.

**2** The threshold concentration of $Ca^{2+}$ required to increase either tension or MLC-phosphorylation was 0.1 μM and maximum effects were obtained at 10 μM. MLC was mainly monophosphorylated, rather than diphosphorylated, in the presence of $Ca^{2+}$. $ED_{50}$ value for $Ca^{2+}$ was 0.54 μM for either tension or MLC-phosphorylation. The relationship between tension and MLC-phosphorylation is linear in the pCa range 7–5.5.

**3** In $Ca^{2+}$-free solution (containing either 20 mM EGTA or 4 mM EGTA with or without 4 mM BAPTA), 3 μM CL-A produced a contraction, the maximum amplitude of which was similar to that evoked by 10 μM $Ca^{2+}$. CL-A (0.03–3 μM) concentration-dependently increased both tension and MLC-phosphorylation in $Ca^{2+}$-free solution containing 4 mM EGTA. The threshold concentration of CL-A required for the increase in either tension or MLC-phosphorylation was 0.03 μM and maximum effects were obtained at 3 μM. In the presence of CL-A, MLC was not only monophosphorylated but also diphosphorylated. $ED_{50}$ values for CL-A were 0.39 μM for tension, 0.44 μM for the monophosphorylated form of MLC and 0.54 μM for all phosphorylated (mono + di) forms. The relationship between tension and the monophosphorylated form of MLC was linear over the concentration range studied and was similar to that for $Ca^{2+}$.

**4** H-7 (3 μM, an inhibitor of protein kinase C) inhibited neither the tension nor phosphorylation of MLC induced by 10 μM $Ca^{2+}$ or 3 μM CL-A. At a high concentration (30 μM), H-7 slightly inhibited both the tension and phosphorylation of MLC induced by either stimulant without a change in the tension-MLC-phosphorylation relationship. KN-62, an inhibitor of $Ca^{2+}$-calmodulin-dependent protein kinase II, did not modify either the tension or the phosphorylation of MLC induced by 10 μM $Ca^{2+}$ or 3 μM CL-A. CK-II, another inhibitor of $Ca^{2+}$-calmodulin-dependent protein kinase II, did not inhibit the contraction induced by 3 μM CL-A.

**5** SM-1 (0.03–0.3 mM) and ML-9 (0.1 and 0.3 mM), inhibitors of MLC-kinase, each lowered the resting level of MLC-phosphorylation in $Ca^{2+}$-free solution and also inhibited both the tension and MLC-phosphorylation induced by 10 μM $Ca^{2+}$ or 3 μM CL-A, in a concentration-dependent manner. Neither SM-1 nor ML-9 modified the relationship between tension and either monophosphorylated or all phosphorylated (mono + di) forms of MLC in the presence of $Ca^{2+}$ or CL-A.

**6** In a solution containing MgITP (the substrate for myosin ATPase but not for MLC-kinase) with no MgATP, 10 μM $Ca^{2+}$ failed to produce contraction. Under these conditions, the amplitude of the contraction induced by 3 μM CL-A was greatly diminished in comparison with that induced in the presence of MgATP.

**7** The present results suggest that in smooth muscle cells of the rabbit mesenteric artery, CL-A in $Ca^{2+}$-free solution, produces a maximum contraction through an indirect activation of $Ca^{2+}$-calmodulin-independent (constitutively active) MLC-kinase via its inhibitory action on MLC-phosphatases. Based on this evidence, it is hypothesized that, in these cells, a constitutively active MLC-kinase may be present, though its action may be concealed by that of endogenous MLC-phosphatase.

**Keywords:** Calyculin A; myosin phosphatase; myosin phosphorylation; protein kinase C; $Ca^{2+}$-calmodulin-dependent protein kinase II; myosin light chain kinase; vascular smooth muscle

## Introduction

Contraction-relaxation in smooth muscle is believed to be regulated by the $Ca^{2+}$-surrounding the myofilaments in the cell. Phosphorylation of 20 k-dalton myosin light chain (MLC) by $Ca^{2+}$-calmodulin-dependent MLC-kinase is considered to be responsible for the coupling between an increased cellular concentration of $Ca^{2+}$ and contraction in the smooth muscle cell (Stull *et al.*, 1991). However, there is some evidence that the phosphorylation of MLC does not entirely depend on the cellular concentration of $Ca^{2+}$. For example, in skinned vascular smooth muscle, noradrenaline and guanosine 5'-O-(γ-thiotriphosphate) (GTPγS) each enhance both MLC-phosphorylation and tension at a given $Ca^{2+}$-concentration, possibly through an inhibition of MLC-phosphatase via the mediation of unidentified guanosine 5'-triphosphate (GTP)-binding proteins (Fujiwara *et al.*, 1989; Kitazawa *et al.*, 1991; Kubota *et al.*, 1992). Thus, the sensitivity of the contractile proteins to $Ca^{2+}$ may depend on the balance between the activities of MLC-kinase and MLC-phosphatase in smooth muscle cells.

It was recently found that okadaic acid or calyculin A (CL-A), each isolated from a marine sponge, is a specific inhibitor of protein phosphatases 1 and 2A which dephosphorylate serine and threonine residues and has been used to characterize the role of MLC-phosphatase in smooth muscle contraction (Kato *et al.*, 1986; Takai *et al.*, 1987; Cohen *et al.*, 1990). CL-A has a potency similar to that of okadaic acid as an inhibitor of type 2A phosphatase but is 10–100 times more effective as an inhibitor of type 1 phosphatase (Ishihara

*et al.*, 1989a). Thus, this toxin is thought to be a more selective inhibitor of MLC-phosphatase in smooth muscle.

CL-A enhances the tension induced by low concentrations of $Ca^{2+}$ and also produces contraction itself in $Ca^{2+}$-free solution containing 2 mM EGTA in Triton X-100-treated skinned smooth muscle of the guinea-pig taenia coli (Ishihara *et al.*, 1989b). Since this toxin increased the phosphorylation of MLC in a Myosin B preparation purified from chicken gizzard in $Ca^{2+}$-free solution containing 2 mM EGTA (Ishihara *et al.*, 1989b), these results may suggest that MLC-phosphorylation is a mechanism responsible for the CL-A-induced contraction in $Ca^{2+}$-free solution in skinned taenia coli. However, it was recently reported that okadaic acid stimulates the adenosine 5'-triphosphate (ATP)-dependent interaction between the actin and myosin of smooth muscle via a direct effect on myosin (Hayakawa *et al.*, 1991). So far, there is no available evidence about the relationship between tension and MLC-phosphorylation induced by CL-A in $Ca^{2+}$-free solution in skinned smooth muscle where the intracellular environment is well controlled. Further, the characterization of the kinases responsible for this $Ca^{2+}$-independent MLC-phosphorylation has not been well studied. Thus, the mechanisms of CL-A-induced contraction in $Ca^{2+}$-free solution require further clarification.

To investigate the mechanism of CL-A-induced contraction in $Ca^{2+}$-free solution, we studied the temporal and steady state relationships between tension and MLC-phosphorylation in the presence of CL-A in β-escin-treated skinned smooth muscle strips of the rabbit mesenteric artery and compared these effects with those induced by $Ca^{2+}$. To help characterize the kinases which are supposed to be responsible for the CL-A-induced contraction in $Ca^{2+}$-free solution, the effects were examined of inhibitors of MLC-kinase, $Ca^{2+}$-calmodulin-dependent protein kinase II and protein kinase C on the relationship between the tension and MLC-phosphorylation induced by $Ca^{2+}$ or CL-A. The effect of cyclic AMP was also observed on the contraction induced by $Ca^{2+}$ or CL-A. Finally, to study the role of MLC-phosphorylation on the CL-A-induced contraction, the effect of CL-A on mechanical activities was observed in a solution containing inosine-5'-triphosphate, which is a substrate for myosin ATPase but not for MLC-kinase (Cassidy & Kerrick, 1982).

## Methods

Male albino rabbits, weighing 1.9–2.5 kg, were anaesthetized with pentobarbitone sodium (40 mg $kg^{-1}$, i.v.) and then exsanguinated. The third branch of the mesenteric artery (diameter around 0.1 mm) in the ileum region was excised immediately and opened longitudinally under a binocular microscope, after connective tissue had been removed, in a dissecting chamber filled with Krebs solution.

### *Tension measurements*

Fine circularly-cut muscle strips (0.3–0.5 mm length, 0.04–0.05 mm width, 0.02–0.03 mm thickness) were prepared with small knives, the bundles being cut transversely. The length, width, thickness and cross-sectional area of the preparation were measured with the inverted-microscope as described previously (Itoh *et al.*, 1986). Endothelial cells were removed by gentle rubbing of the internal surface of the vessels with small knives. Mechanical responses were measured with a circular strip attached to a strain gauge horizontally (UL-2, Shinko Co., Tokyo, Japan). The resonant frequency of the strain gauge was 60 Hz. The transducer was connected to a carrier amplifier (AP-620G, Nihon Kohden Co., Ltd., and 6M91, San-ei Co., Ltd., Tokyo, Japan) and the output signal was connected to a Macintosh computer (SE/30, Apple Co. Ltd.) through an analog-digital converter (Mac Lab, Analog Digital Instruments Pty Ltd. Australia). Drift was less than 3 μN $h^{-1}$. The strip was superfused in a chamber with a capacity of 0.3 ml filled with Krebs solution. The perfusate was changed rapidly from one end, while the solution already present was simultaneously aspirated off by a water pump from the other end. The resting tension was adjusted to obtain maximum contraction in 128 mM $K^+$ and was not greater than 15 μN.

Chemically skinned smooth muscle strips were prepared by use of β-escin (Itoh *et al.*, 1991). In preliminary experiments, 25 μM β-escin was applied in an activating solution containing 10 μM $Ca^{2+}$. A relaxing solution was first applied and 10 μM $Ca^{2+}$ then applied in the presence or absence of β-escin. $Ca^{2+}$ itself did not induce any tension in the absence of β-escin, but tension slowly developed after application of 10 μM $Ca^{2+}$ with 25 μM β-escin, and maximum tension was obtained within 25–40 min. Thus, in the present experiments, 25 μM β-escin was applied for 45 min in the relaxing solution. To prevent deterioration of the $Ca^{2+}$-induced contraction, 0.1 μM calmodulin was applied throughout the experiments, as described previously (Itoh *et al.*, 1986). In order to avoid spurious effects due to $Ca^{2+}$-release from intracellular storage sites in the skinned muscle strips, the experiments were carried out in the presence of 1 μM ionomycin and a high concentration of EGTA (4 mM or 20 mM) with or without 4 mM BAPTA. All experiments were done at room temperature (20–23°C).

For each skinned strip, 10 μM $Ca^{2+}$ was first applied to enable recording of the maximum contraction and the $Ca^{2+}$ then washed out with a relaxing solution to relax the tissue. $Ca^{2+}$ (10 μM) or CL-A (3 μM) were subsequently applied in the presence or absence of various kinase inhibitors. The amplitude of contraction induced by the second application of 10 μM $Ca^{2+}$ or 3 μM CL-A was normalized with respect to the first $Ca^{2+}$-induced one. In some experiments, strips were pretreated with SM-1, H-7, ML-9, CK-II, KN-62 or adenosine 3':5'-cyclic monophosphate (cyclic AMP) for 5 min in the relaxing solution and these substances were present during the subsequent application of 10 μM $Ca^{2+}$ or 3 μM CL-A. To obtain the $Ca^{2+}$-tension relationship, various concentrations of $Ca^{2+}$ were cumulatively applied at 10 min intervals from low to high concentration. To obtain the dose-response relationship for the effect of CL-A on tension, a given concentration of this agent was first applied for 20 min, followed by a subsequent application of 3 μM CL-A for 20 min (i.e. two concentrations for each strip) since CL-A induced a very slow development of tension at any given concentration. The amplitudes of contraction induced by various concentrations of CL-A were normalized with respect to that induced by 10 μM $Ca^{2+}$ in the same strip.

### *Measurements of myosin light chain phosphorylation*

Muscle strips (0.3–0.5 mm length, 1.3–1.5 mm width, 0.02–0.03 mm thickness) were suspended in a relaxing solution for over 10 min. Then, the tissues were skinned using relaxing solution containing 25 μM β-escin with 1 μM ionomycin for 45 min and washed again with the relaxing solution (containing no β-escin). Each skinned muscle strip was then suspended in a solution containing $Ca^{2+}$ for 10 min or CL-A for 20 min. The strips were quick-frozen with 10% trichloroacetic acid (TCA) in acetone-dry ice containing 10 mM dithiothreitol and allowed to reach room temperature. The strips were then washed three times with diethyl ether to remove residual TCA. Protein, including MLC, was extracted in a lysing solution containing 8 M urea, 20 mM Tris, 23 mM glycine, 10 mM dithiothreitol, 0.004% bromophenol blue and saturated sucrose (pH 8.6) (Persechini *et al.*, 1986; Kubota *et al.*, 1992).

Nonphosphorylated, monophosphorylated and diphosphorylated forms of MLC were separated by urea/glycerol-polyacrylamide gel electrophoresis followed by electrophoretic transfer of the proteins to nitrocellulose paper and quantitation of the relative amounts of each form by an immunoblot procedure, as reported previously (Persechini *et al.*, 1986).

Polyacrylamide gels containing 10% acrylamide, 0.5% *bis* acrylamide, 20 mM Tris and 23 mM glycine at pH 8.6 were pre-electrophoresed for 1 h at 400 V at room temperature, the lower reservoir containing 20 mM Tris and 23 mM glycine (pH 8.6) and the upper reservoir 20 mM Tris, 23 mM glycine, 2.3 mM thioglycolate and 2.3 mM dithiothreitol. Protein extracted from the skinned muscle strips was then electrophoresed for 50 min at 400 V. Subsequently, the proteins were transferred from the gel by electroblotting to a nitrocellulose paper (moistened by 20% methanol, 48 mM Tris and 39 mM glycine) for 25 min at 15 V, with a Bio-rad transblot apparatus (Trans-Blot SD, semi-dry transfer cell, Bio-rad, CA, U.S.A.). Then the nitrocellulose paper was incubated overnight with antibodies against bovine tracheal MLC (Persechini *et al.*, 1986) in a solution containing 137 mM NaCl, 9.5 mM $Na_2HPO_4$, 2.7 mM KCl and 1.3 mM $KH_2PO_4$ (PBS) with 0.1% Tween 20 after incubation in PBS containing 5% skim milk for 1 h (for blocking).

Finally, the nitrocellulose paper was incubated for 15 min with biotin-labelled goat anti-rabbit IgG (Histofine, Seikagaku Kogyo, Japan) in a solution containing 132.6 mM NaCl, 8.6 mM $K_2HPO_4$ and 1.5 mM $KH_2PO_4$ (PBS-SAB, pH 7.6) and then with alkaline phosphatase-labelled streptavidin in PBS-SAB for 15 min at room temperature. Regions containing MLC were visualized as dark blue bands after incubation with the colour development reagents, 5-bromo-4-chloro-3-indolyl phosphate toluidine and *p*-nitroblue tetrazolium chloride (Alkaline phosphatase substrate kit, Vector Laboratories, CA, U.S.A.) in 100 mM Tris-HCl (pH 9.5). Relative amounts of nonphosphorylated, monophosphorylated and diphosphorylated MLC were quantified densitometrically by scanning the blot with a chromatoscanner (CS-930, Shimadzu, Japan). The phosphorylation of MLC was expressed in mol $PO_4$/mol MLC.

### *Solutions*

*(a) Krebs solution* This contained (mM): $Na^+$ 137.4, $K^+$ 5.9, $Mg^{2+}$ 1.2, $Ca^{2+}$ 2.6, $HCO_3^-$ 15.5, $H_2PO_4^-$ 1.2, $Cl^-$ 134; glucose 11.5. A high $K^+$ solution was prepared by replacing all NaCl with KCl, isosmotically. The solutions were bubbled with 95% $O_2$ and 5% $CO_2$ and their pH maintained at 7.3–7.4.

*(b) Relaxing and activating solutions* The usual relaxing solution contained: 87 mM potassium methanesulphonate (KMS), 20 mM piperazine-N-N'-*bis*-(2-ethanesulphonic acid) (PIPES), 5.1 mM $Mg(MS)_2$, 5.2 mM ATP, 5 mM phosphocreatine, 1 μM ionomycin and 4 mM ethylene glycol-*bis*-(β-aminoethyl)-*N,N,N',N'*-tetraacetic acid (EGTA). In some experiments, the relaxing solution contained 20 mM EGTA or 4 mM EGTA with 4 mM 1,2-*bis*(2-aminophenoxy)ethane-*N,N,N',N'*-tetraacetic acid (BAPTA) and the free Mg concentration was adjusted to 1 mM. Various $Ca^{2+}$ concentrations were prepared by adding appropriate amounts of $Ca(MS)_2$ to 4 mM EGTA, based on the calculation given previously (Itoh *et al.*, 1986). In the present experiments, the apparent association constants for MgITP and CaITP were assumed to be the same as for MgATP and CaATP, respectively. Thus, in a solution containing inosine 5'-triphosphate (ITP), ATP was just replaced with an equimolar concentration of ITP in the presence or absence of $Ca^{2+}$ and phosphocreatine was removed from the solution. The pH of the solution was adjusted to 7.1 at 25°C with KOH and the ionic strength standardized at 0.2 M by changing the amount of KMS added.

### *Calculation of Hill coefficient*

The slope of the concentration-response relationship for the effect of $Ca^{2+}$ or CL-A on tension and MLC-phosphorylation is shown as the Hill coefficient (N) and mid-point position ($pK = (-\log K)$, where $K$ is the $ED_{50}$ concentration). These were obtained by fitting the data points for each curve to equation (1) by a non-linear least-squares method using commercially available software (Kaleida graph, Abelbeck Software, PA, U.S.A.) for Macintosh Computer (Apple Co. Ltd.):

$$F/F_0 = (C/K)^N/[1 + (C/K)^N] \quad (1)$$

Where C represents the concentration of $Ca^{2+}$ or CL-A, F is the amplitude of the contraction at any given concentration of either stimulant, and $F_0$ is the maximum response evoked by 10 μM $Ca^{2+}$ or 3 μM CL-A expressed as a relative response of 1.0.

### *Drugs*

Drugs used were calyculin A (CL-A, Wako Pure Chemical Industries, Japan), EGTA, BAPTA and PIPES (Dojin, Japan), calmodulin, inosine 5'-triphosphate (ITP), cyclic AMP and β-escin (Sigma), ATP (Na salt; Kojin, Japan), 1-(5-chloronaphthalene-1-sulphonyl)-1H-hexahydro-1,4-diazepine hydrochloride (ML-9), 1-(5-isoquinolinesulphonyl)-2-methylpiperazine dihydrochloride (H-7) and 1-[N,O-*bis*(1,5-isoquinolinesulphonyl)-N-methyl-L-tyrosyl]-4-phenylpiperazine (KN-62) (Seikagaku Kogyo, Japan) and ionomycin (free acid; Calbiochem). SM-1 and CK-II were provided by Dr T. Watanabe (Department of Pharmacology, Peptide Institute Inc., Japan) and the antibody against bovine tracheal myosin light chain was provided by Dr J.T. Stull (Department of Physiology and Pharmacology, University of Texas Southwestern Medical Centre, TX, U.S.A.). All other chemicals were of the highest reagent grade.

### *Statistics*

The values recorded were expressed as mean ± standard deviation (s.d.) and the number of observations indicated. Statistical significance was assessed with Student's *t* test for paired and unpaired values. Probabilities less than 5% ($P < 0.05$) were considered significant.

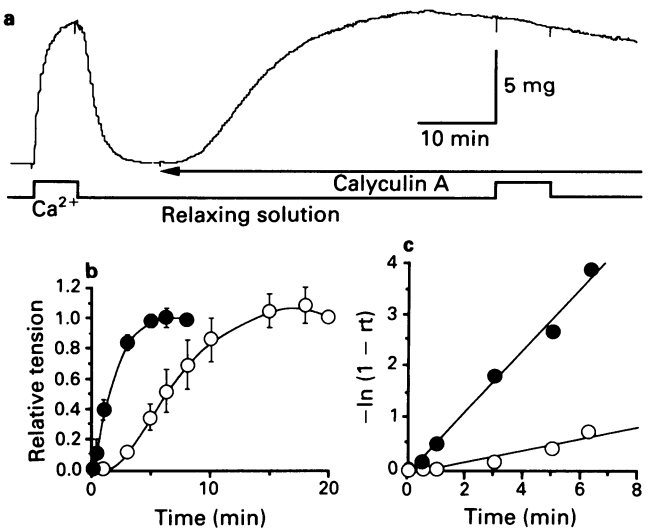



**Figure 1** Effects of $Ca^{2+}$ (10 μM) and calyculin A (3 μM) on mechanical activities in β-escin-treated skinned smooth muscle strips of the rabbit mesenteric artery. (a) An actual trace: $Ca^{2+}$ (10 μM) was first applied, followed by a washout with a $Ca^{2+}$-free solution containing 4 mM EGTA (relaxing solution) to relax the tissue. Calyculin A (3 μM) was then applied in the relaxing solution and $Ca^{2+}$ (10 μM) again applied at the peak of the calyculin A-induced contraction. For analysis, the maximum amplitude of contraction induced by 10 μM $Ca^{2+}$ was normalized as a relative tension of 1.0 for each strip. (b and c) Time course of tension development after application of 10 μM $Ca^{2+}$ (●) or 3 μM calyculin A (○). In (c), the ordinate shows the negative logarithm of (1 – rt), where rt is the amplitude of the induced tension expressed relative to the maximum amplitude of contraction evoked by 10 μM $Ca^{2+}$. Results shown are each the mean of 5 observations ± s.d.

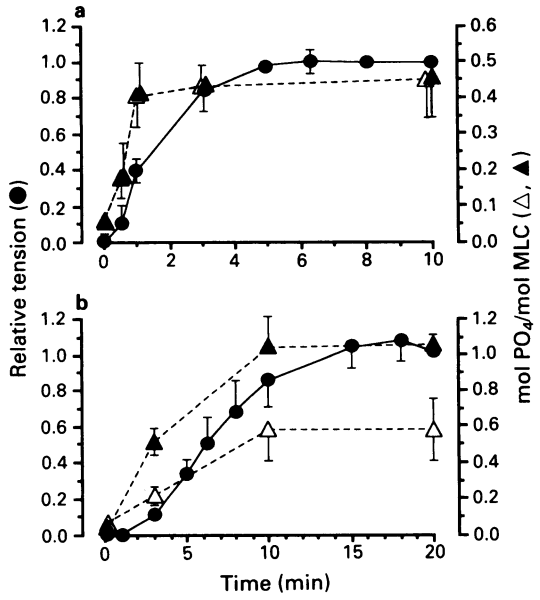



**Figure 2** Time-dependent changes in tension (●) and monophosphorylated (△) or all phosphorylated (mono + di, ▲) forms of myosin light chain (MLC) induced by 10 μM $Ca^{2+}$ (a) or 3 μM calyculin A (b) in β-escin-treated skinned smooth muscle strips. The maximum amplitude of contraction induced by 10 μM $Ca^{2+}$ was normalized as a relative tension of 1.0 for each strip. $Ca^{2+}$ (10 μM) or calyculin A (3 μM) was applied at time 0 in a relaxing solution containing 4 mM EGTA. Results shown are each the mean of 5 observations ± s.d.

## Results

### *Calyculin A increases tension and phosphorylation of myosin light chain in $Ca^{2+}$-free solution*

With 10 μM $Ca^{2+}$, the isometric tension of skinned smooth muscle made with β-escin reached a maximum value of 48.9 ± 15.2 kN $m^{-2}$ ($n = 35$); this was 1.78 ± 0.52 times larger than the 128 mM $K^+$-induced contraction in unskinned muscle strips ($n = 35$). These values are very similar to those reported previously for saponin-skinned muscle from the same artery (Itoh *et al.*, 1986).

Figure 1a shows an actual trace of the effects of 3 μM calyculin A (CL-A) and 10 μM $Ca^{2+}$ on mechanical activities in a β-escin-treated skinned smooth muscle strip. After the tissue was skinned with β-escin, 10 μM $Ca^{2+}$ was first applied and then washed out by $Ca^{2+}$-free solution containing 4 mM EGTA (usual relaxing solution). Subsequently, 3 μM CL-A was applied, also in the relaxing solution (Figure 1a). $Ca^{2+}$ (10 μM) caused no further increase in the amplitude of contraction induced by 3 μM CL-A when applied at the peak (Figure 1a). The effect of 3 μM CL-A was irreversible, i.e. after washout of 3 μM CL-A, the tension remained the same for over 10 min.

With CL-A (3 μM), there was a slow development of tension to a peak, followed by a gradual decay. The maximum amplitude of contraction induced by 3 μM CL-A was similar to that induced by 10 μM $Ca^{2+}$ (1.06 ± 0.11 times, $n = 16$). The times required to reach half and maximum amplitude of contraction following application of 10 μM $Ca^{2+}$ were 1.25 ± 0.15 min and 7.40 ± 0.72 min, respectively ($n = 5$) and those for 3 μM CL-A were respectively 6.45 ± 0.97 min and 18.46 ± 0.98 min. The maximum rate of rise of tension induced by 3 μM CL-A was one fifth that induced by 10 μM $Ca^{2+}$, the maximum rate induced by 10 μM $Ca^{2+}$ being 0.81 ± 0.17 relative tension $min^{-1}$ and that by 3 μM CL-A 0.16 ± 0.05 relative tension $min^{-1}$ (Figure 1c), where the maximum tension induced by 10 μM $Ca^{2+}$ was normalized as a relative tension of 1.0 for each preparation. The time required to reach the maximum rate of rise of tension was 0.72 ± 0.20 min ($n = 5$) for 10 μM $Ca^{2+}$ and 4.81 ± 1.23 min ($n = 5$) for 3 μM CL-A. Both $Ca^{2+}$ (10 μM) and CL-A (3 μM) developed tension with a single exponential time course within 7 min (Figure 1c). The slope of the line for 10 μM $Ca^{2+}$ was 0.63 ($r^2 = 0.991$) and that for 3 μM CL-A was 0.112 ($r^2 = 0.924$). Thus, the ratio of these slopes (10 μM $Ca^{2+}$/3 μM CL-A) was 5.4.

To test the effect of increased buffering capacity for any contaminating $Ca^{2+}$ over and above that in the usual relaxing solution (containing 4 mM EGTA), the effects of 3 μM CL-A on mechanical activities were also observed in a $Ca^{2+}$-free solution containing 20 mM EGTA or 4 mM EGTA with 4 mM BAPTA. In the latter $Ca^{2+}$-free solution, CL-A (3 μM) again developed tension and the maximum amplitude of contraction was similar to that induced by 10 μM $Ca^{2+}$ (0.94 ± 0.05 times in 20 mM EGTA and 0.93 ± 0.02 times in 4 mM EGTA with 4 mM BAPTA, $n = 4$). These values were almost the same as that obtained in the usual relaxing solution containing 4 mM EGTA.

Figure 2 shows the effects of 10 μM $Ca^{2+}$ (a) and 3 μM CL-A (b) on tension (●) and the monophosphorylated (△) or all phosphorylated (▲, mono + di) forms of the 20-k dalton myosin light chain (MLC) as a function of time. $Ca^{2+}$ (10 μM) or CL-A (3 μM) was applied in $Ca^{2+}$-free solution containing 4 mM EGTA. $Ca^{2+}$ (10 μM) and CL-A (3 μM) each increased the phosphorylation of MLC and this preceded the development of tension (Figure 2a and b). The peak for either form of phosphorylated MLC was obtained within 3 min of the application of 10 μM $Ca^{2+}$ (Figure 2a). $Ca^{2+}$ (10 μM) mainly increased the monophosphorylated form of MLC (over 95%, Figure 2a). By contrast, CL-A (3 μM) increased both monophosphorylated and diphosphorylated forms of MLC (Figure 2b). The peak for either

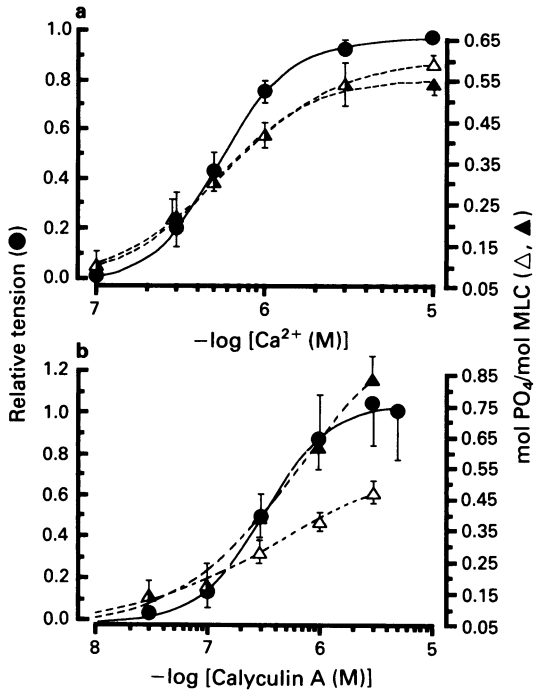



**Figure 3** Concentration-dependent effects of $Ca^{2+}$ (a) or calyculin A (b) on increase in tension (●) and monophosphorylated (△) or all phosphorylated (mono + di, ▲) forms of myosin light chain (MLC) in β-escin-treated skinned smooth muscle strips. $Ca^{2+}$ and calyculin A at any given concentration were applied for 10 min and 20 min, respectively in a relaxing solution containing 4 mM EGTA. The maximum amplitude of contraction induced by 10 μM $Ca^{2+}$ was normalized as a relative tension of 1.0 for each strip. The curves for the effects of $Ca^{2+}$ and calyculin A on tension and MLC-phosphorylation were obtained by fitting the data points to equation (1) by a non-linear least-squares method (see Methods). Results shown are each the mean of 4–8 observations ± s.d.

the monophosphorylated (△) or all phosphorylated (▲, mono + di) forms of MLC was obtained 10 min after application of 3 μM CL-A in $Ca^{2+}$-free solution containing 4 mM EGTA. Thus, the time-dependent changes in MLC-phosphorylation following application of 3 μM CL-A were much slower than those induced by 10 μM $Ca^{2+}$. However, the maximum amount of the monophosphorylated form of MLC measured on application of 3 μM CL-A was similar to that seen with 10 μM $Ca^{2+}$ and the amount of all phosphorylated (mono + di) forms of MLC was twice that seen with 10 μM $Ca^{2+}$.

We studied the concentration-dependent effects of $Ca^{2+}$ and of CL-A on tension and on the monophosphorylated and all phosphorylated (mono + di) forms of MLC (Figure 3). The threshold concentration of $Ca^{2+}$ required to produce contraction was 0.1 μM and the maximum contraction was obtained with 10 μM (Figure 3a). The $ED_{50}$ values of $Ca^{2+}$ for contraction, the monophosphorylated form of MLC and all phosphorylated (mono + di) forms of MLC were 0.54 ± 0.07 μM ($n = 5$), 0.54 ± 0.08 and 0.55 ± 0.08 ($n = 5$), respectively, and their Hill coefficients were respectively 2.2 ± 0.2, 1.5 ± 0.2 and 1.5 ± 0.2. The threshold concentration of CL-A for contraction in $Ca^{2+}$-free solution was 0.03 μM and the maximum effect was obtained at 3 μM (Figure 3b). The $ED_{50}$ values of CL-A for contraction, the monophosphorylated form of MLC and all phosphorylated (mono + di) forms of MLC were 0.30 ± 0.11 μM ($n = 8$), 0.67 ± 0.45 and 0.75 ± 0.32 ($n = 4$), respectively and their Hill coefficients were respectively 1.3 ± 0.5, 0.67 ± 0.45 and 0.74 ± 0.69. The relationship between tension and the monophosphorylated form of MLC in the presence of various concentrations of CL-A was similar to that for $Ca^{2+}$ ($r^2 = 0.999$, Figure 4). The relationship between tension and all phosphorylated (mono + di) forms of MLC in the presence of CL-A was shifted to the right with respect to the relationship between tension and the monophosphorylated form of MLC in the presence of either CL-A or $Ca^{2+}$ (Figure 4).

### *Effects of SM-1 and ML-9 on the tension and MLC-phosphorylation effects induced by $Ca^{2+}$ or calyculin A*

SM-1 is a synthetic peptide which selectively inhibits native and constitutively active MLC-kinases, both *in vitro* and *in vivo* (Ikebe *et al.*, 1987b; Itoh *et al.*, 1989), ML-9 is a isoquinolinesulphonyl derivative which also selectively inhibits MLC-kinase, at its ATP-binding site (Saitoh *et al.*, 1987). To elucidate the roles of MLC-kinase in the contraction induced by 3 μM CL-A or 10 μM $Ca^{2+}$ in β-escin-treated skinned smooth muscle strips, we studied the effects of SM-1 and ML-9. In these experiments, 10 μM $Ca^{2+}$ was always first applied to get the normalized tension for each strip. Following the removal of $Ca^{2+}$ by $Ca^{2+}$-free solution containing 4 mM EGTA (relaxing solution), 10 μM $Ca^{2+}$ or 3 μM CL-A was then applied in the presence of one of the two inhibitors of MLC-kinase. Under similar conditions, when 10 μM $Ca^{2+}$ was applied alone three times, reproducible responses were recorded (the amplitude of the third $Ca^{2+}$-induced contraction was 0.95 ± 0.03 times the first, $n = 4$). Pretreatment with each inhibitor was for 5 min and the inhibitor was present throughout the subsequent application of 10 μM $Ca^{2+}$ or 3 μM CL-A.

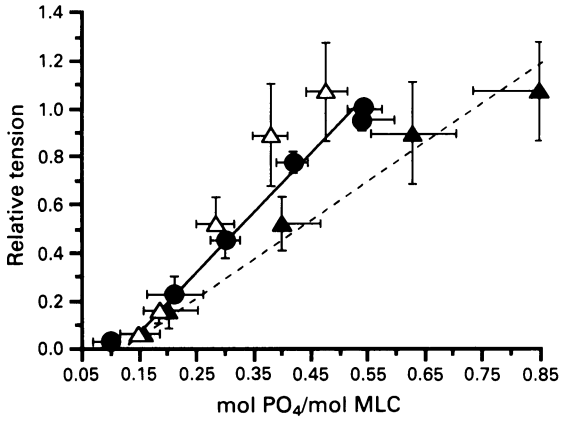



**Figure 4** Relationship between tension and monophosphorylated or all phosphorylated (mono + di) forms of myosin light chain (MLC) in the presence of various concentrations of $Ca^{2+}$ or calyculin A in β-escin-treated skinned smooth muscle strips: (●), monophosphorylated form of MLC in the presence of $Ca^{2+}$; (△), monophosphorylated form of MLC in the presence of calyculin A; (▲), all phosphorylated (mono + di) forms of MLC in calyculin A. The line was fitted by linear regression analysis. The slope of the line for the relationship between tension and the monophosphorylated form of MLC in the presence of $Ca^{2+}$ or calyculin A was 2.35 ($r^2 = 1$) and that for the relationship between tension and all phosphorylated forms of MLC in the presence of calyculin A was 1.53 ($r^2 = 0.999$). The data shown in Figure 3 were used for this analysis. Results shown are each the mean of 4–8 experiments with s.d.

Figure 5a shows actual traces of the effect of 0.1 mM SM-1 on the contraction induced by 10 μM $Ca^{2+}$ (a(i)) or 3 μM CL-A (a(iii)). SM-1 (0.1 mM) greatly inhibited the amplitude of contraction induced by either 10 μM $Ca^{2+}$ or 3 μM CL-A. The action of 0.1 mM SM-1 was partially reversible: following a 20 min washout, the $Ca^{2+}$-induced contraction partly recovered (to over 70% of the control). In $Ca^{2+}$-free solution containing 4 mM EGTA, the level of MLC-phosphorylation was 0.05 ± 0.03 mol $PO_4$/mol MLC ($n = 13$). SM-1 (0.03–0.3 mM) concentration-dependently lowered the resting level of MLC-phosphorylation (0.03 ± 0.01 mol $PO_4$/mol MLC in the presence of 0.03 mM SM-1; 0.02 ± 0.01 mol $PO_4$/mol MLC in 0.1 mM SM-1 and 0.01 ± 0.01 mol $PO_4$/mol MLC in 0.3 mM SM-1, $n = 5$). SM-1 (0.03–0.3 mM) also concentration-dependently inhibited the increase in both tension and all phosphorylated (mono and di) forms of MLC induced by 10 μM $Ca^{2+}$ or 3 μM CL-A (Figure 5b and c).

Figure 6 shows the concentration-dependent effects of ML-9 on the increase in tension (a) and phosphorylation of MLC (b) induced by 10 μM $Ca^{2+}$ and 3 μM CL-A. The level of MLC-phosphorylation under resting conditions was 0.05 ± 0.02 mol $PO_4$/mol MLC ($n = 6$) and this was lowered by 0.3 mM ML-9 to 0.02 ± 0.02 mol $PO_4$/mol MLC ($n = 6$). ML-9 (0.1 and 0.3 mM) concentration-dependently inhibited the increase in both tension and the monophosphorylated or diphosphorylated forms of MLC induced by 10 μM $Ca^{2+}$ or 3 μM CL-A. Neither SM-1 nor ML-9 modified the relationship between tension and the monophosphorylated or all phosphorylated (mono + di) forms of MLC in the presence of 10 μM $Ca^{2+}$ or 3 μM CL-A (Figure 7).

### *Effect of inhibitors of protein kinase C or $Ca^{2+}$-calmodulin-dependent protein kinase II on contraction and MLC-phosphorylation induced by $Ca^{2+}$ or calyculin A*

Activators of protein kinase C enhance the amplitude of contraction induced by low concentrations of $Ca^{2+}$ with or without a corresponding increase in the phosphorylation of MLC (Fujiwara *et al.*, 1988; Singer, 1990; Sato *et al.*, 1992). To clarify the role of protein kinase C in the contraction and MLC-phosphorylation induced by $Ca^{2+}$ and by CL-A, we studied the effects of H-7 (an inhibitor of protein kinase C with a $K_i$ value of 6.0 μM, Hidaka *et al.*, 1984). H-7 (3 μM) did not modify either the tension or the MLC-phosphorylation induced by 10 μM $Ca^{2+}$ or 3 μM CL-A (Figure 8). In a higher concentration (30 μM), H-7 marginally lowered the resting level of MLC-phosphorylation (0.05 ± 0.02 mol $PO_4$/mol MLC in control and 0.03 ± 0.02 mol $PO_4$/mol MLC in the presence of 30 μM H-7, $n = 4$) and inhibited the increase in tension and in both the monophosphorylated and all phosphorylated (mono + di) forms of MLC induced by 10 μM $Ca^{2+}$ or 3 μM CL-A (Figure 8). Under these conditions, 30 μM H-7 seems to inhibit non-selectively the increase in the monophosphorylated and diphosphorylated forms of

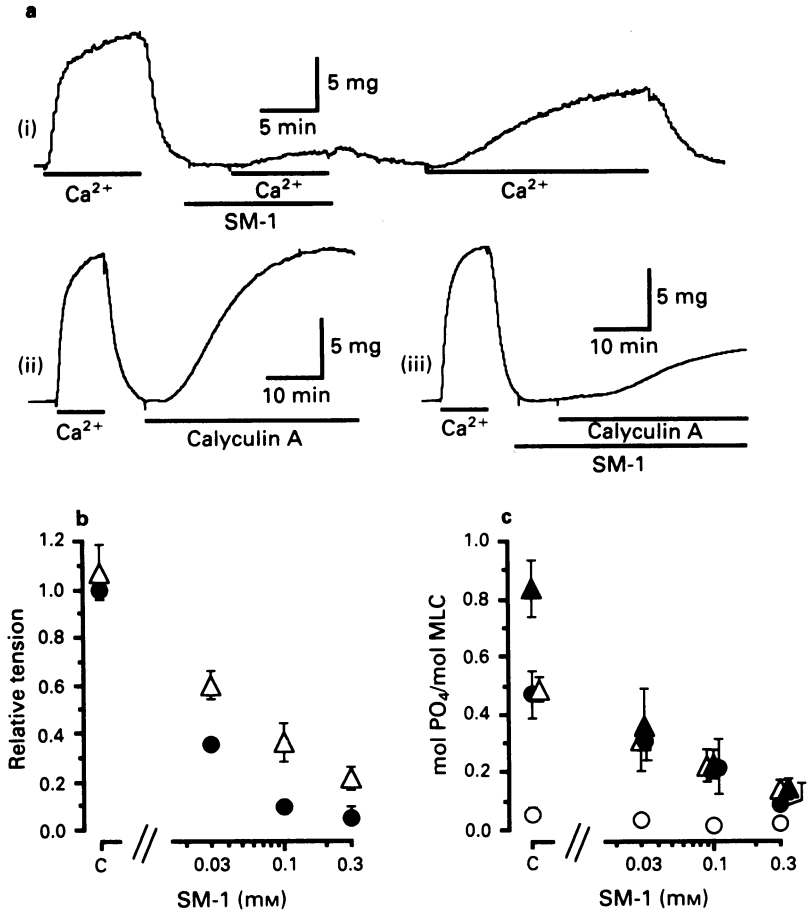



**Figure 5** Effects of a peptide inhibitor of myosin light chain kinase, SM-1, on increase in tension and phosphorylation of myosin light chain (MLC) induced by 10 μM $Ca^{2+}$ or 3 μM calyculin A in β-escin-treated skinned muscle strips. (a) $Ca^{2+}$ (10 μM) was first applied to each strip (control response). (a(i)) After a recording of the control response, 10 μM $Ca^{2+}$ was again applied in the presence of 0.1 mM SM-1. The amplitude of the $Ca^{2+}$-induced contraction partly recovered following washout of SM-1. a(ii) and (iii) Calyculin A (3 μM) was applied in $Ca^{2+}$-free solution containing 4 mM EGTA in the absence (a(ii)) or presence (a(iii)) of 0.1 mM SM-1: a(ii) and a(iii) were obtained from different strips. As shown by the bars, SM-1 (0.1 mM) was present for 5 min in $Ca^{2+}$-free solution and was present during the subsequent application of either $Ca^{2+}$ or calyculin A. (b) and (c) Concentration-dependent effects of SM-1 on increase in tension (b) and monophosphorylated or all phosphorylated (mono + di) forms of MLC (c) induced by 10 μM $Ca^{2+}$ or 3 μM calyculin A. (b) (●) In the presence of 10 μM $Ca^{2+}$; (△) in 3 μM calyculin A. The maximum amplitude of contraction induced by 10 μM $Ca^{2+}$ was normalized as a relative tension of 1.0 for each strip. (c) (○) Monophosphorylated form of MLC under resting conditions; (●) monophosphorylated form of MLC in the presence of 10 μM $Ca^{2+}$; (△) monophosphorylated form of MLC in 3 μM calyculin A; (▲) all phosphorylated (mono + di) forms of MLC in 3 μM calyculin A. Results shown are each the mean of 5 observations ± s.d.

MLC induced by 3 μM CL-A. H-7 (3 μM and 30 μM) did not modify the relationship between tension and the monophosphorylated or all phosphorylated (mono + di) forms of MLC observed in the presence of 10 μM $Ca^{2+}$ or 3 μM CL-A (Figure 7).

It was recently found that $Ca^{2+}$-calmodulin-dependent protein kinase II ($Ca^{2+}$/CaM-kinase II) phosphorylates smooth muscle myosin and enhances actin-activated myosin ATPase activity, *in vitro* (Edelman *et al.*, 1990). It has also been reported that $Ca^{2+}$/CaM-kinase II phosphorylates MLC-kinase and thus lowers the affinity of MLC-kinase for the $Ca^{2+}$-calmodulin complex (Ikebe & Reardon, 1990; Tansey *et al.*, 1992). KN-62 competitively inhibits the calmodulin binding of $Ca^{2+}$/CaM-kinase II with a $K_i$ value of 0.9 μM (Tokumitsu *et al.*, 1990; Tansey *et al.*, 1992). In addition, CK-II, which is a synthetic peptide corresponding to the auto-inhibitory domain of $Ca^{2+}$/CaM-kinase II from brain, has been reported to inhibit $Ca^{2+}$/CaM-kinase II directly (residues 281–309, Payne *et al.*, 1988; McCarron *et al.*, 1992).

To clarify the role of $Ca^{2+}$/CaM-kinase II in the contraction induced by $Ca^{2+}$ and CL-A, the effects of KN-62 and CK-II were observed on the contractions induced by 10 μM $Ca^{2+}$ and 3 μM CL-A. CK-II (30 μM) inhibited the contraction induced by 10 μM $Ca^{2+}$ (0.51 ± 0.06 times control) but had almost no effect on the contraction induced by 3 μM CL-A (0.88 ± 0.04 times control $Ca^{2+}$-response, $n = 4$). CK-II has a weak calmodulin antagonist activity (McCarron *et al.*, 1992) and this action might be responsible for the CK-II-induced inhibition of the $Ca^{2+}$-induced contraction. Although CK-II (30 μM) had no effect on the maximum amplitude of contraction induced by 3 μM CL-A, this peptide prevented the gradual decay in tension after the peak until 60 min following application of 3 μM CL-A (not shown).

KN-62 (3 μM) did not modify either the tension or the MLC-phosphorylation induced by 10 μM $Ca^{2+}$ or 3 μM CL-A (Figure 8). Since KN-62 (3 mM) is dissolved in dimethylsulphoxide which at concentrations over 0.1% slightly inhibited the amplitude of contraction induced by 10 μM $Ca^{2+}$, the effect of higher concentrations of KN-62 (> 3 μM) was not examined to avoid the solvent's effects in the present experiments.

### *Effects of cyclic AMP on contraction induced by $Ca^{2+}$ or calyculin A*

It has been hypothesized that cyclic AMP activates its dependent protein kinase and decreases the affinity of MLC-kinase

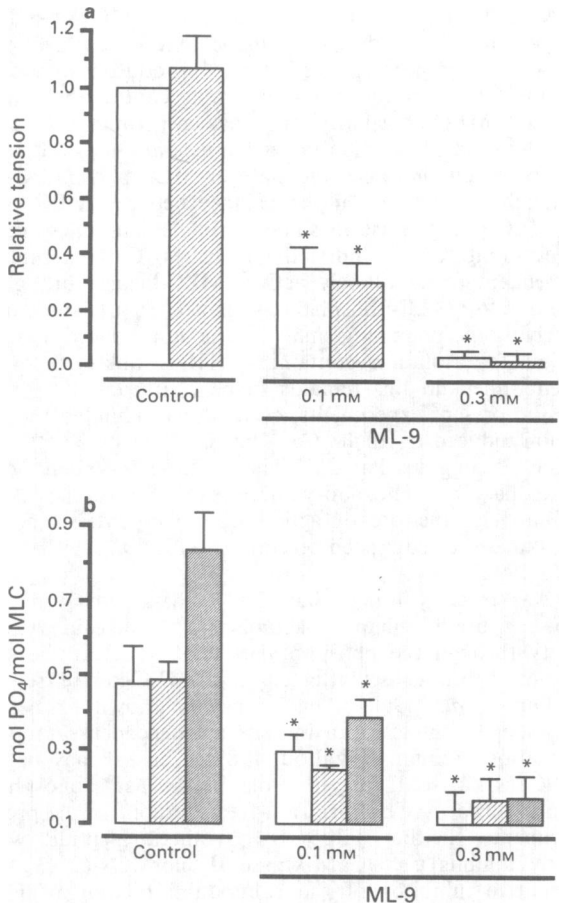



**Figure 6** Effects of ML-9 on increase in tension (a) and phosphorylation of myosin light chain (MLC) (b) induced by 10 μM $Ca^{2+}$ or 3 μM calyculin A in β-escin-treated skinned smooth muscle strips. (a) Open columns, in the presence of 10 μM $Ca^{2+}$; hatched columns, with 3 μM calyculin A. The maximum amplitude of contraction induced by 10 μM $Ca^{2+}$ was normalized as a relative tension of 1.0 for each strip. (b) Open columns, monophosphorylated form of MLC in the presence of 10 μM $Ca^{2+}$; hatched columns, monophosphorylated form of MLC in 3 μM calyculin A; closer hatched columns, all phosphorylated (mono + di) forms of MLC in 3 μM calyculin A. Pretreatment with ML-9 (0.1 or 0.3 mM) was for 5 min and it was present during the subsequent application of $Ca^{2+}$ or calyculin A. *Significant difference from the corresponding control. Results shown are each the mean of 5 observations with s.d.

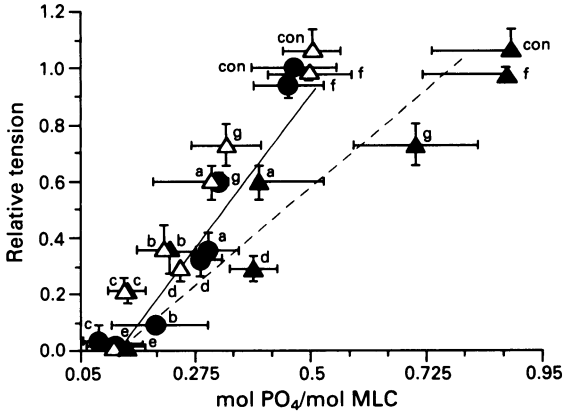



**Figure 7** Relationships between tension and monophosphorylated or all phosphorylated (mono + di) forms of myosin light chain (MLC) in the presence of 10 μM $Ca^{2+}$ or 3 μM calyculin A with or without various types of kinase inhibitors in β-escin-treated skinned smooth muscle strips: (●) monophosphorylated form of MLC in the presence of 10 μM $Ca^{2+}$; (△) monophosphorylated form of MLC in the presence of 3 μM calyculin A; (▲) all phosphorylated (mono + di) forms of MLC in 3 μM calyculin A. For data fitting, the parameters used in Figure 4 were adopted and calculated correlation coefficients were 0.93 for the relationship between tension and the monophosphorylated form of MLC and 0.94 for the relationship between tension and all phosphorylated forms of MLC. Con, corresponding control; (a) in the presence of 0.03 mM SM-1; (b) 0.1 mM SM-1; (c) 0.3 mM SM-1; (d) 0.1 mM ML-9; (e) 0.3 mM ML-9; (f) 3 μM H-7; (g) 30 μM H-7. The maximum amplitude of contraction induced by 10 μM $Ca^{2+}$ was normalized as a relative tension of 1.0 for each strip. Results shown are each the mean of 4–5 observations with s.d.

for a $Ca^{2+}$-calmodulin complex through the phosphorylation of MLC-kinase and, as a result, inhibits $Ca^{2+}$-induced contractions (Conti & Adelstein, 1981). To characterize further the CL-A-induced contraction, the effect was observed of cyclic AMP on contraction induced by CL-A. After recording a 10 μM $Ca^{2+}$-induced contraction as a control, 0.1 mM cyclic AMP was applied in a relaxing solution (containing 4 mM EGTA) and either 10 μM $Ca^{2+}$ or 3 μM CL-A then applied in the presence of 0.1 mM cyclic AMP. Cyclic AMP (0.1 mM) inhibited the contraction induced by 10 μM $Ca^{2+}$ (0.68 ± 0.06 times control, $n = 4$) but not that induced by 3 μM CL-A (0.94 ± 0.02 times control $Ca^{2+}$-response, $n = 4$).

### *Effects of inosine 5'-triphosphate (ITP) on contraction induced by $Ca^{2+}$ or calyculin A*

MgITP is a substrate for myosin ATPase, but not for MLC-kinase (Cassidy & Kerrick, 1982). To study the role of MLC-kinase in the contraction induced by CL-A, the effects of 10 μM $Ca^{2+}$ or 3 μM CL-A were observed in a solution containing MgITP with no MgATP.

$Ca^{2+}$ (10 μM) was first applied in the presence of 5 mM MgATP to record a control response and the strip was relaxed by application of a relaxing solution. Following an application of rigor solution ($Ca^{2+}$ and ATP-free solution containing 4 mM EGTA), a $Ca^{2+}$-free solution containing 4 mM EGTA and 5 mM MgITP, but no MgATP, was then applied. Finally, either 10 μM $Ca^{2+}$ or 3 μM CL-A was applied in the presence of 5 mM MgITP. In the presence of MgITP, 10 μM $Ca^{2+}$ failed to produce contraction (0.03 ± 0.03 times the control $Ca^{2+}$-response, $n = 4$). When 3 μM CL-A was applied in the $Ca^{2+}$-free solution containing 5 mM MgITP, this agent very slowly produced a minute contraction (0.16 ± 0.05 times the control $Ca^{2+}$-response at 45 min after application of 3 μM CL-A, $n = 4$).

## Discussion

Calyculin A (CL-A), like okadaic acid, is a potent inhibitor of type 1 and 2A phosphatases which are possible candidates for myosin phosphatase in smooth muscle (Takai *et al.*, 1987; Ishihara *et al.*, 1989a). These MLC-phosphatase inhibitors have no effect on the activity of MLC-kinase, $Ca^{2+}$/CaM-dependent phosphodiesterase, $Ca^{2+}$/CaM-kinase II or protein kinase C (Takai *et al.*, 1987; Suganuma *et al.*, 1988; Ishihara *et al.*, 1989a). In the present experiments using β-escin-treated skinned smooth muscle of the rabbit mesenteric artery CL-A produced a contraction with a corresponding increase in the phosphorylation of MLC in $Ca^{2+}$-free solution containing 4 mM EGTA. The increase in phosphorylation of MLC always preceded the development in tension following application of either 10 μM $Ca^{2+}$ or 3 μM CL-A. Both the amplitude of contraction and the amount of the monophosphorylated form of MLC induced by 3 μM CL-A were similar to the maximum induced by $Ca^{2+}$. Under the conditions in which CL-A was applied the concentration of $Ca^{2+}$ is quite low (calculated $Ca^{2+}$ is less than 10 nM) and the release of $Ca^{2+}$ from the intracellular stores in the strip was minimized by the application of 1 μM ionomycin (Fujiwara *et al.*, 1989). Further, an increase in the concentration of EGTA to 20 mM or addition of 4 mM BAPTA had no effects on the CL-A-induced contraction in $Ca^{2+}$-free solution. These results sug-

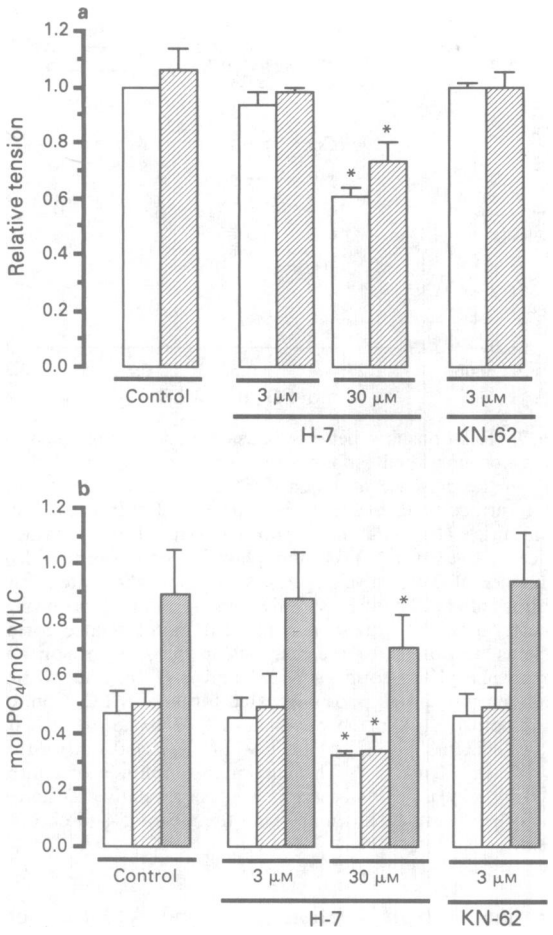



**Figure 8** Effects of H-7 (3 or 30 μM) or KN-62 (3 μM) on increase in tension (a) and phosphorylation of myosin light chain (b) induced by 10 μM $Ca^{2+}$ or 3 μM calyculin A in β-escin-treated skinned smooth muscle strips. (a) Open columns, in the presence of 10 μM $Ca^{2+}$; hatched columns, in 3 μM calyculin A. The maximum amplitude of contraction induced by 10 μM $Ca^{2+}$ was normalized as a relative tension of 1.0 for each strip. (b) Open columns, monophosphorylated form of myosin light chain (MLC) in the presence of 10 μM $Ca^{2+}$; hatched columns, monophosphorylated form of MLC in 3 μM calyculin A; closer hatched columns, all phosphorylated (mono + di) forms of MLC in 3 μM calyculin A. H-7 (3 or 30 μM) or KN-62 (3 μM) were each present for 5 min in $Ca^{2+}$-free solution and were also present during the subsequent application of $Ca^{2+}$ or calyculin A. *Significant difference from the corresponding control. Results shown are each the mean of 4 observations with s.d.

gest that CL-A produces a maximum contraction and MLC-phosphorylation possibly through the mediation of $Ca^{2+}$-calmodulin-independent kinases which phosphorylate MLC.

It is well known that in smooth muscle cells, MLC-kinase plays a major role in the phosphorylation of MLC following an increase in the cellular concentration of $Ca^{2+}$. SM-1 is a synthetic peptide which corresponds to amino acid residues 480-501 of the smooth muscle MLC-kinase and selectively inhibits MLC-kinase (Ikebe *et al.*, 1987b; Itoh *et al.*, 1989). In the present experiments, SM-1 (0.1 and 0.3 mM) concentration-dependently lowered the resting level of MLC-phosphorylation in $Ca^{2+}$-free solution containing 4 mM EGTA and inhibited the increase in both tension and the phosphorylation of MLC induced by 10 μM $Ca^{2+}$ or 3 μM CL-A. ML-9 (0.3 mM), another type of MLC-kinase inhibitor (Saitoh *et al.*, 1987), also lowered the resting level of MLC-phosphorylation and inhibited the increase in both tension and the phosphorylation of MLC induced by 10 μM $Ca^{2+}$ or 3 μM CL-A. The relationship between tension and the monophosphorylated form of MLC in the presence of CL-A was similar to that with $Ca^{2+}$. Neither SM-1 nor ML-9 modified this relationship in the presence of either $Ca^{2+}$ or CL-A, indicating that the mechanism of the CL-A-induced contraction is likely to be the same as that for $Ca^{2+}$. Further, in a solution containing MgITP, $Ca^{2+}$ produced no contraction and CL-A produced only a minute contraction, suggesting that MLC-phosphorylation has a pivotal role in the CL-A-induced contraction in $Ca^{2+}$-free solution as it does for $Ca^{2+}$ contractions. Since the state of MLC-phosphorylation is thought to depend on the balance between MLC-kinase and MLC-phosphatase in smooth muscle cells, these results suggest that CL-A indirectly activates $Ca^{2+}$-calmodulin-independent (constitutively active) MLC-kinase through an inhibition of MLC-phosphatases. However, the mechanism underlying the remaining small contraction induced by CL-A in $Ca^{2+}$-free solution containing ITP is unknown at the present time and this remains to be clarified.

In the present experiments, cyclic AMP inhibited the contraction induced by 10 μM $Ca^{2+}$ but not that by 3 μM CL-A. This result suggests that $Ca^{2+}$-calmodulin-independent MLC-kinase has no phosphorylation sites for cyclic AMP. Alternatively, the site of action of cyclic AMP is not on MLC-kinase, as suggested recently (Stull *et al.*, 1991; Shafiq *et al.*, 1992).

It was recently found that $Ca^{2+}$/CaM-kinase II purified from rat brain enhances actin-activated myosin ATPase activity through the phosphorylation of MLC at the same amino acid residue as that acted on by MLC-kinase (serine[19], Edelman *et al.*, 1990). This kinase is known to become $Ca^{2+}$-independent after an initial $Ca^{2+}$-dependent autophosphorylation (Schulman & Lou, 1989). Thus, it may be that $Ca^{2+}$/CaM-kinase II plays a role in the MLC-phosphorylation induced by CL-A in $Ca^{2+}$-free solution. In the present experiments, neither CK-II (a synthetic peptide which directly inhibits $Ca^{2+}$/CaM-kinase II) nor KN-62 (3 μM, a competitive inhibitor of the calmodulin binding of $Ca^{2+}$/CaM-kinase II) inhibited the contraction induced by 3 μM CL-A in $Ca^{2+}$-free solution. Further, KN-62 (3 μM) had no effect on either the resting or CL-A-activated level of MLC-phosphorylation. These results suggest that, in skinned smooth muscle of the rabbit mesenteric artery, $Ca^{2+}$/CaM-kinase II may not play a major role in the initiation of the phosphorylation of MLC induced by CL-A. The observation that CK-II inhibited the tension decay after the peak following application of CL-A, might suggest that this kinase plays some role in the tension maintaining mechanisms in the presence of CL-A.

In the present experiments, $Ca^{2+}$ mainly increased the monophosphorylated form of MLC, while CL-A increased both the monophosphorylated and diphosphorylated forms of MLC in $Ca^{2+}$-free solution. It is known that in addition to MLC-kinase, protein kinase C also catalyses the phosphorylation of MLC at distinct serine[1,2] and threonine[9] residues (Ikebe *et al.*, 1987a). In an aortic smooth muscle homogenate of the hog, the phosphorylation of MLC is predominantly due to MLC-kinase in the presence of $Ca^{2+}$ alone, whereas in the presence of $Ca^{2+}$ with okadaic acid, MLC-kinase and protein kinase C are involved in the phosphorylation (Erdödi *et al.*, 1988). Protein kinase C has seven isoenzymes and some of them (δ, ε, ζ) lack a $Ca^{2+}$-binding region (Housey *et al.*, 1987), indicating that the δ, ε and ζ types of protein kinase C do not require $Ca^{2+}$ for their full activation. These results suggest that the $Ca^{2+}$-independent forms of protein kinase C may be involved in the CL-A-induced MLC-phosphorylation in $Ca^{2+}$-free solution.

In the present experiments, H-7 (an inhibitor of protein kinase C) at a concentration of 30 μM inhibited the increase in tension and MLC-phosphorylation induced by 10 μM $Ca^{2+}$ or 3 μM CL-A. However, it is known that protein kinase C inhibits actin-activated myosin ATPase activity through the phosphorylation of MLC in purified contractile proteins of smooth muscle (Ikebe *et al.*, 1987a). Further, in skinned carotid arterial smooth muscle, the protein kinase C mediated phosphorylation of MLC on serine[1,2] was neither associated with a mechanical response by itself nor did it

have an effect on the $Ca^{2+}$-calmodulin-stimulated force or shortening velocity (Sutton & Haeberle, 1990). Furthermore, an activation of protein kinase C by phorbol ester produces a contraction independent of MLC-phosphorylation in swine carotid artery (Singer, 1990). In the present experiments, H-7 (30 $\mu$M) did not modify the relationship between tension and MLC-phosphorylation in the presence of $Ca^{2+}$ or CL-A, nor did MLC-kinase inhibitors (SM-1 and ML-9). Since there is a region with a high degree of sequence homology in most kinases (Edelman *et al.*, 1987) and H-7 inhibits protein kinase C at the ATP-binding site (Hidaka *et al.*, 1984), a part of this drug's action might be due to an inhibition of MLC-kinase. Thus, a role for protein kinase C in the CL-A-induced increase in tension and MLC-phosphorylation seems unlikely.

It was recently reported that okadaic acid uncouples MLC-phosphorylation and tension in the presence of carbachol in un-skinned bovine tracheal strips (Tansey *et al.*, 1990). The authors suggested that phosphoprotein(s) other than phosphorylated MLC might be involved in the regulation of tension maintenance in un-skinned bovine tracheal smooth muscle. However, in the present experiment, we observed almost the same relationship between tension and MLC-phosphorylation in the presence of $Ca^{2+}$ as in the presence of CL-A. At the present time, we do not know the reason for this discrepancy. It may result from the use of different phosphatase inhibitors (okadaic acid and CL-A) or different types of smooth muscle. Alternatively, the different conditions of the smooth muscle (un-skinned or skinned) may have caused the different results. This remains to be clarified.

In conclusion, CL-A produced a maximum contraction with a corresponding increase in phosphorylation of myosin light chain in $Ca^{2+}$-free solution. It is suggested that a $Ca^{2+}$-calmodulin-independent form (constitutively active) of myosin light chain kinase plays a pivotal role in CL-A-induced responses in skinned smooth muscle of the rabbit mesenteric artery.

We thank Professor H. Kuriyama for his advice on this work and Dr R.J. Timms for the language editing. We gratefully acknowledge Dr J.T. Stull (Univ. of Texas, Dallas, TX, U.S.A.) for providing an antibody against bovine tracheal myosin light chain and Dr T. Watanabe for SM-1 and CK-II (Peptide Institute Inc., Osaka, Japan). This work was partly supported by a Grant-in-Aid from the Ministry of Education of Japan.

## References

CASSIDY, P. & KERRICK, W.G.L. (1982). Superprecipitation of gizzard actomyosin, and tension in gizzard muscle skinned fibers in the presence of nucleotides other than ATP. *Biochim. Biophys. Acta*, **705**, 63–69.

COHEN, P., HOLMES, C.F.B. & TSUKITANI, Y. (1990). Okadaic acid: a new probe for the study of cellular regulation. *Trends Biochem. Sci.*, **15**, 98–102.

CONTI, M.A. & ADELSTEIN, R.S. (1981). The relationship between calmodulin binding and phosphorylation of smooth muscle myosin kinase by the catalytic subunit of 3':5' cAMP-dependent protein kinase. *J. Biol. Chem.*, **256**, 3178–3181.

EDELMAN, A.M., BLUMENTHAL, D.K. & KREBS, E.G. (1987). Protein serine/threonine kinases. *Annu. Rev. Biochem.*, **56**, 567–613.

EDELMAN, A.M., LIN, W.H., OSTERHOUT, D.J., BENNETT, M.K., KENNEDY, M.B. & KREBS, E.G. (1990). Phosphorylation of smooth muscle myosin by type II $Ca^{2+}$/calmodulin-dependent protein kinase. *Mol. Cell. Biochem.*, **97**, 87–98.

ERDÖDI, F., ROKOLYA, A., SALVO, J.D., BARANY, M. & BARANY, K. (1988). Effect of okadaic acid on phosphorylation-dephosphorylation of myosin light chain in aortic smooth muscle homogenate. *Biochem. Biophys. Res. Commun.*, **153**, 156–161.

FUJIWARA, T., ITOH, T., KUBOTA, Y. & KURIYAMA, H. (1988). Actions of a phorbol ester on factors regulating contraction in rabbit mesenteric artery. *Circ. Res.*, **63**, 893–902.

FUJIWARA, T., ITOH, T., KUBOTA, Y. & KURIYAMA, H. (1989). Effects of guanosine nucleotides on skinned smooth muscle tissue of the rabbit mesenteric artery. *J. Physiol.*, **408**, 535–547.

HAYAKAWA, K., OKAGAKI, T., DOBASHI, T., SAKANISHI, A., KANEKO, K. & KOHAMA, K. (1991). Okadaic acid stimulates the ATP-dependent interaction between actin and myosin of smooth muscle via a direct effect on myosin. *Biochem. Biophys. Res. Commun.*, **177**, 1155–1160.

HIDAKA, H., INAGAKI, M., KAWAMOTO, S. & SASAKI, Y. (1984). Isoquinolinesulfonamides, novel and potent inhibitors of cyclic nucleotide dependent protein kinase and protein kinase C. *Biochemistry*, **23**, 5036–5041.

HOUSEY, G.M., O'BRIAN, C.A., JOHNSON, M.D., KIRSCHMEIER, P. & WEINSTEIN, I.B. (1987). Isolation of cDNA clones encoding protein kinase C: evidence for a protein kinase C-related gene family. *Proc. Natl. Acad. Sci. U.S.A.*, **84**, 1065–1069.

IKEBE, M., HARTSHORNE, D.J. & ELZINGA, M. (1987a). Phosphorylation of the 20,000-dalton light chain of smooth muscle myosin by the calcium-activated, phospholipid-dependent protein kinase. *J. Biol. Chem.*, **262**, 9569–9573.

IKEBE, M. & REARDON, S. (1990). Phosphorylation of smooth myosin light chain kinase by smooth muscle $Ca^{2+}$/calmodulin-dependent multifunctional protein kinase. *J. Biol. Chem.*, **265**, 8975–8978.

IKEBE, M., STEPINSKA, M., KEMP, B.E., MEANS, A.R. & HARTSHORNE, D.J. (1987b). Proteolysis of smooth muscle myosin light chain kinase. *J. Biol. Chem.*, **260**, 13828–13834.

ISHIHARA, H., MARTIN, B.L., BRAUTIGAN, D.L., KARAKI, H., OZAKI, H., KATO, Y., FUSETANI, N., WATABE, S., HASHIMOTO, K., UEMURA, D. & HARTSHORNE, D.J. (1989a). Calyculin A and okadaic acid: inhibitors of protein phosphatase activity. *Biochem. Biophys. Res. Commun.*, **159**, 871–877.

ISHIHARA, H., OZAKI, H., SATO, K., HORI, M., KARAKI, H., WATABE, S., KATO, Y., FUSETANI, N., HASHIMOTO, K., UEMURA, D. & HARTSHORNE, D.J. (1989b). Calcium-independent activation of contractile apparatus in smooth muscle by calyculin-A. *J. Pharmacol. Exp. Ther.*, **250**, 388–396.

ITOH, T., IKEBE, M., KARGACIN, G.J., HARTSHORNE, D.J., KEMP, B.E. & FAY, F.S. (1989). Effects of modulators of myosin light-chain kinase activity in single smooth muscle cells. *Nature*, **338**, 164–167.

ITOH, T., KANMURA, Y. & KURIYAMA, H. (1986). Inorganic phosphate regulates the contraction-relaxation cycle in skinned muscles of the rabbit mesenteric artery. *J. Physiol.*, **376**, 231–252.

ITOH, T., SUZUKI, S. & KURIYAMA, H. (1991). Effects of pinacidil on contractile proteins in high $K^+$-treated intact, and in $\beta$-escin-treated skinned smooth muscle of the rabbit mesenteric artery. *Br. J. Pharmacol.*, **103**, 1697–1702.

KATO, Y., FUSETANI, N., MATSUNAGA, S. & HASHIMOTO, K. (1986). Calyculin A, a novel antitumour metabolite from the marine sponge *Discodermia* calyx. *J. Am. Chem. Soc.*, **108**, 2780–2781.

KITAZAWA, T., GAYLINN, B.D., DENNEY, G.H. & SOMLYO, A.P. (1991). G-protein-mediated $Ca^{2+}$ sensitization of smooth muscle contraction through myosin light chain phosphorylation. *J. Biol. Chem.*, **266**, 1708–1715.

KUBOTA, Y., NOMURA, M., KAMM, K.E., MUMBY, M.C. & STULL, J.T. (1992). GTP$\gamma$S-dependent regulation of smooth muscle contractile elements. *Am. J. Physiol.*, **262**, C405–C410.

MCCARRON, J.G., MCGEOWN, J.G., REARDON, S., IKEBE, M., FAY, F.S. & WALSH, J.V.Jr. (1992). Calcium-dependent enhancement of calcium current in smooth muscle by calmodulin-dependent protein kinase II. *Nature*, **357**, 74–77.

PAYNE, M.E., FONG, Y.L., ONO, T., COLBRAN, R.J., KEMP, B.E., SODERLING, T.R. & MEANS, A.R. (1988). Calcium/calmodulin-dependent protein kinase II. *J. Biol. Chem.*, **263**, 7190–7195.

PERSECHINI, A., KAMM, K.E. & STULL, J.T. (1986). Different phosphorylated forms of myosin in contracting tracheal smooth muscle. *J. Biol. Chem.*, **261**, 6293–6299.

SAITOH, M., ISHIKAWA, T., MATSUSHIMA, S., NAKA, M. & HIDAKA, H. (1987). Selective inhibition of catalytic activity of smooth muscle myosin light chain kinase. *J. Biol. Chem.*, **262**, 7796–7801.

SATO, K., HORI, M., OZAKI, H., TAKANO-OHMURO, H., TSUCHIYA, T., SUGI, H. & KARAKI, H. (1992). Myosin phosphorylation-independent contraction induced by phorbol ester in vascular smooth muscle. *J. Pharmacol. Exp. Ther.*, **261**, 497–505.

SCHULMAN, H. & LOU, L.L. (1989). Multifunctional $Ca^{2+}$/calmodulin-dependent protein kinase: domain structure and regulation. *Trends Biochem. Sci.*, **14,** 62–66.

SHAFIQ, J., SUZUKI, S., ITOH, T. & KURIYAMA, H. (1992). Mechanisms of vasodilation induced by NKH477, a water-soluble forskolin derivative, in smooth muscle of the porcine coronary artery. *Circ. Res.*, **71,** 70–81.

SINGER, H.A. (1990). Phorbol ester-induced stress and myosin light chain phosphorylation in swine carotid medial smooth muscle. *J. Pharmacol. Exp. Ther.*, **252,** 1068–1074.

STULL, J.T., GALLAGHER, P.J., HERRING, B.P. & KAMM, K.E. (1991). Vascular smooth muscle contractile elements. Cellular regulation. *Hypertension*, **17,** 723–732.

SUGANUMA, M., FUJIKI, H., SUGURI, H., YOSHIZAWA, S., HIROTA, M., NAKAYASU, M., OJIKA, M., WAKAMATSU, K., YAMADA, K. & SUGIMURA, T. (1988). Okadaic acid: an additional non-phorbol-12-tetradecanoate-13-acetate-type tumor promoter. *Proc. Natl. Acad. Sci. U.S.A.*, **85,** 1768–1771.

SUTTON, T.A. & HAEBERLE, J.R. (1990). Phosphorylation by protein kinase C of the 20,000-dalton light chain of myosin in intact and chemically skinned vascular smooth muscle. *J. Biol. Chem.*, **265,** 2749–2754.

TAKAI, A., BIALOJAN, C., TROSCHKA, M. & RÜEGG, J.C. (1987). Smooth muscle myosin phosphatase inhibition and force enhancement by black sponge toxin. *FEBS Lett.*, **217,** 81–84.

TANSEY, M.G., HORI, M., KARAKI, H., KAMM, K.E. & STULL, J.T. (1990). Okadaic acid uncouples myosin light chain phosphorylation and tension in smooth muscle. *FEBS Lett.*, **270,** 219–221.

TANSEY, M.G., WORD, R.A., HIDAKA, H., SINGER, H.A., SCHWORER, C.M., KAMM, K.E. & STULL, J.T. (1992). Phosphorylation of myosin light chain kinase by the multifunctional calmodulin-dependent protein kinase II in smooth muscle cells. *J. Biol. Chem.*, **267,** 12511–12516.

TOKUMITSU, H., CHIJIWA, T., HAGIWARA, M., MIZUTANI, A., TERASAWA, M. & HIDAKA, H. (1990). KN-62, 1-[N,O-bis(5-isoquinolinesulfonyl)-N-methyl-L-tyrosyl]-4-phenylpiperazine, a specific inhibitor of $Ca^{2+}$/calmodulin-dependent protein kinase II. *J. Biol. Chem.*, **265,** 4315–4320.

*(Received December 14, 1992*
*Accepted March 10, 1993)*

*Br. J. Pharmacol.* (1993), **109**, 713–718 © Macmillan Press Ltd, 1993

# Effect of RP 67580, a non-peptide neurokinin$_1$ receptor antagonist, on facilitation of a nociceptive spinal flexion reflex in the rat

[1]J.M.A. Laird, R.J. Hargreaves & R.G. Hill

Department of Pharmacology, Merck, Sharp and Dohme Research Laboratories, Neuroscience Research Centre, Terlings Park, Harlow, Essex

**1** In order to examine the contribution of neurokinin$_1$ (NK$_1$) receptors to facilitation of a spinal nociceptive reflex in the rat, we have investigated the effects of RP 67580 ((3a**R**,7a**R**)-7,7-diphenyl-2(1-imino-2-(2-methoxyphenyl/ethyl)perhydroisoindole)), a non-peptide neurokinin$_1$ (NK$_1$) receptor antagonist, selective for the rodent receptor sub-type, on the activity of individual motorunits. These results were compared with the effects of RP 68651, the inactive 3a**S**, 7a**S** enantiomer of RP 67580, as a control for non-specific activity.

**2** Experiments were performed on 15 rats anaesthetized with a continuous i.v. infusion of alphaxalone/alphadalone and spinalized at T9-10. Single unit recordings of motorunit activity from biceps femoris/semitendinosus were made with a concentric needle electrode. In each experiment, a vehicle dose followed by 4 sequential rising doses of either RP 67580 or RP 68651 were given at 15 min intervals. High intensity electrical stimuli were applied to the hindlimb receptive field of the motorunit at a rate of 1 per 60 s throughout the experiment to establish a baseline. A conditioning stimulus (20 of these stimuli at 1 Hz) was delivered 5 min after each dose and the effect of the size of the baseline response examined.

**3** The conditioning stimulus evoked a facilitation of the baseline at the start of all experiments (mean increase ± s.e.mean = 151 ± 20%). RP 67580 attenuated this facilitation, with an $ID_{50}$ (± s.e.mean) of 2.5 ± 4.2 μg kg$^{-1}$, i.v., whereas RP 68651 at doses of up to 3 mg kg$^{-1}$, i.v. did not. There was no statistically significant effect of drug on the baseline reflex, nor on the response to the conditioning stimulus. Doses of 300 and 3000 μg kg$^{-1}$ of both RP 67580 and RP 68651 evoked small depressor effects on systemic arterial blood pressure.

**4** We conclude that the facilitation of a spinal flexor reflex by noxious conditioning stimuli in the rat is mediated by NK$_1$ receptors whereas the baseline reflex is not. The results suggest that brain penetrant NK$_1$ receptor antagonists may have central anti-nociceptive effects.

**Keywords:** Tachykinins; nociception; spinal cord; flexion reflex; pain; substance P

## Introduction

The excitability of spinal flexor reflexes in experimental animals has been shown to be increased by injury or inflammation of the periphery (Woolf, 1983; Ferrell *et al.*, 1988). Similar though more transient increases in flexor reflex excitability can be induced by high intensity electrical conditioning stimuli, and also by the intrathecal administration of tachykinins (Woolf & Wiesenfeld-Hallin, 1986). Experiments measuring the release of tachykinins in the spinal cord of experimental animals have shown that intense or prolonged noxious stimuli are required to evoke detectable release of substance P (Duggan *et al.*, 1988). It is possible that release of substance P in the spinal cord by injury and inflammation of peripheral tissues may contribute to the increased central excitability seen after such insults (Cervero & Laird, 1991). This increased central excitability may be responsible for some of the changes in pain sensation characteristic of injury and inflammation (Treede *et al.*, 1992).

It has been reported that the non-peptide NK$_1$ receptor antagonist, racemic (2**S**,3**S**/2**R**,3**R**) CP-96,345 (*cis*-2-)diphenylmethyl)-N-((2-methoxyphenyl)methyl)-1-azabicyclo(2.2.2)octan-3-amine) attenuates spinal reflex facilitation in the rat (Xu *et al.*, 1991a,b). However, CP-96,345 is active at calcium channels, an effect which is neither stereoselective nor species-dependent (Schmidt *et al.*, 1992), and since 2**S**,3**S** CP-96,345 is selective for the human rather than the rodent NK$_1$ receptor subtype (Beresford *et al.*, 1991), it is likely that in rodents the potency difference between effects on calcium channels and NK$_1$ receptors is minimal (Schmidt *et al.*, 1992). It has been demonstrated that the antinociceptive effects of 2**S**,3**S** CP-96,345 in carrageenin-induced hyperalgesia and the formalin paw test in rats are not stereospecific (equivalent effects being produced by CP-96,344, the 2**R**,3**R** enantiomer of CP-96,345), and thus are probably due to activity at ion channels (Nagahisa *et al.*, 1992b). Therefore, activity at ion channels rather than at NK$_1$ receptors may account for the attenuation of spinal reflex facilitation in the rat by racemic (2**S**,3**S**/2**R**,3**R**) CP-96,345 (Xu *et al.*, 1992a,b).

Another non-peptide NK$_1$ receptor antagonist which is selective for the rodent receptor sub-type ($IC_{50}$ = 4.2 nM), RP 67580 ((3a**R**,7a**R**)-7,7-diphenyl-2(1-imino-2-(2-methoxyphenyl/ethyl)perhydroisoindole)), has recently been described by Garret *et al.* (1991). The 3a**S**,7a**S** enantiomer of this compound, RP 68651, is essentially inactive ($IC_{50}$ > 10000 nM). In order to determine the contribution of NK$_1$ receptors to facilitation of a spinal nociceptive reflex in the rat, we have examined the effects of RP 67580, and compared these with the effects of the inactive enantiomer RP 68651 as a control for non-specific activity.

## Methods

### *Electrophysiological experiments*

Experiments were conducted on 15 male Sprague-Dawley rats (250 to 370 g). Anaesthesia was induced with isofluorane

[1] Author for correspondence.

(4% in $O_2$). The left jugular vein was cannulated and anaesthesia maintained for the remainder of the experiment with i.v. infusion of alphaxalone/alphadolone (Saffan; 6–12 mg $kg^{-1} h^{-1}$). The level of anaesthesia was adjusted such that areflexia was maintained throughout surgery, and thereafter, such that no precipitate changes in blood pressure were observed in the application of noxious stimuli. The left carotid artery, trachea and right femoral vein were cannulated to allow recording of systemic arterial blood pressure, artificial ventilation and administration of drugs respectively. A small laminectomy was performed at $T_9-T_{10}$, the dura removed and the animal spinalized. Body temperature was monitored with a rectal probe and maintained within normal physiological limits by a feedback-controlled heating blanket. At least 1 h was allowed for recovery from spinal shock before recordings were made.

Single unit recordings of motorunit activity were made from the biceps femoris/semitendinosus muscle with a bipolar concentric needle electrode. High intensity electrical stimuli were applied to the receptive field of the motor unit in the area of skin innervated by the sural nerve with needle electrodes. Single shocks (1 ms square pulses, 2 × T) were applied at a rate of 1 per 60 s throughout the experiment to establish a baseline. The conditioning stimulus was 20 of these stimuli delivered at 1 Hz.

In each experiment, vehicle (distilled water) was administered followed by four sequential rising doses of the drug given i.v. at 15 min intervals at a dose volume of 1 ml $kg^{-1}$. In the first series of experiments, doses of 3, 30, 300 and 3000 $\mu g\ kg^{-1}$ (base weight) of either RP 67580 or RP 68651 were given, $n = 5$ per group. In a further series of experiments, performed to establish the $ID_{50}$ of RP 67580, doses of 0.03, 0.3, 3 and 30 $\mu g\ kg^{-1}$ of RP 67580 were given ($n = 5$).

Five minutes after each dose a conditioning stimulus was applied. The next baseline test stimulus was applied 30 s after the end of the conditioning stimulus. The response to this stimulus was taken as the conditioned response. The magnitude of the conditioned response was expressed as percentage change from the mean of baseline responses over the preceding 5 min.

The recorded action potentials were digitised using a spike processor and collected using a CED 1401 interface and microcomputer. Only the component of the response occurring at least 100 ms after the stimulus (presumably the C-fibre evoked component) was considered, in order to avoid the inclusion of movement artifacts. Statistical analysis was performed with analysis of variance (ANOVA) repeated measures tests, with subsequent contrast analysis where significant main effects or interactions were seen.

### *Determination of plasma elimination profile of RP 67580*

The plasma elimination profile for RP 67580 was determined in a separate group of 24 rats by dosing i.v. at 3 mg $kg^{-1}$ (free base weight) made up in distilled water and taking a terminal blood sample under general anaesthesia (isofluorane 4% in 100% $O_2$) at 1, 3, 5, 15, 30, 60, 240 and 360 min after dosing ($n = 3$ per time point). A plasma fraction was obtained for each blood sample by centrifugation. Samples were stored at −18°C before analysis. The concentration of RP 67580 in each plasma sample was determined by high performance liquid chromatography (h.p.l.c.) u.v. detection (210 nm) following liquid-liquid extraction.

### *Materials*

RP 67580 and RP 68651 were synthesized at Merck Research Laboratories, Rahway, U.S.A. Alphaxalone/alphadolone (Saffan) was obtained from Pitman-Moore, U.K.

## Results

### *Facilitation of the spinal reflex*

Application of the conditioning stimulus at the start of the experiment, before any drugs had been administered evoked facilitation of the flexor reflex in every case ($n = 15$; Figure 1). The percentage increase over the baseline immediately prior to the conditioning stimulus was 151 ± 20% (mean ± s.e.mean). An illustration of the effects of RP 67580 and of RP 68651 in 2 individual experiments is shown in Figure 1. In the first series of experiments, RP 67580 was found to attenuate this facilitation of the flexor reflex in a dose-dependent manner (Figure 2a), whereas the less active (3aS,7aS) enantiomer, RP 68651 did not attenuate facilitation over the same dose range (Figure 2b). A two way ANOVA test showed a statistically significant difference between the effect of the 2 enantiomers ($P < 0.05$) and also a significant effect of dose ($P < 0.05$). Subsequent contrast analysis showed that the facilitation evoked after doses of 3 to 3000 $\mu g\ kg^{-1}$ of RP 67580 was significantly different from that seen after vehicle administration ($P < 0.05$). None of the doses of RP 68651 had a statistically significant effect on facilitation of the reflex, compared to the effect of the vehicle dose. There was a greater variation in the facilitation produced by the conditioning stimulus in the experiments in which RP 68651 was administered. This was largely due to a gradual increase in the degree of facilitation over time in 2 of the 5 experiments.

In the first series of experiments all doses of RP 67580 tested produced an effect on reflex facilitation that was significantly different from that seen after vehicle administration. Thus, in order to enable the calculation of $ID_{50}$ for the effect of RP 67580 on reflex facilitation (dose of RP 67580 giving half maximal inhibition of reflex facilitation), a second series of 5 experiments was performed in which a vehicle dose and sequential doses of 0.03 to 30 $\mu g\ kg^{-1}$ of RP 67580 were given. In this second series of experiments, RP 67580 also attenuated reflex facilitation in a dose-dependent manner. An $ID_{50}$ (± s.e.mean) was then calculated from the combined data from the 2 series of experiments (Figure 2a). An inhibition curve was fitted to the raw data by non-linear least squares regression analysis and an iterative procedure (RS1 software) and gave an $ID_{50}$ of 2.5 ± 4.2 $\mu g\ kg^{-1}$.

### *Response to the conditioning stimulus*

The conditioning stimulus (20 stimuli at 1 Hz) evoked a response that showed 'windup' (a progressive increase in the response to successive stimuli during the first 16 stimuli; Mendell, 1966) in all cases after vehicle administration and, in almost all experiments (14/15), after administration of each dose of RP 67580 and RP 68571. No windup was seen after doses of 30, 300 and 3000 $\mu g\ kg^{-1}$ RP 67580 in one experiment.

The response evoked by the conditioning stimulus was analysed by considering the total number of spikes evoked by the train of 20 stimuli, and also by considering the total number of spikes evoked by each group of 5 stimuli, that is, stimuli number 1–5, 6–10, 11–15 and 16–20, to examine the effect of the drugs on the process of windup (Table 1). A two way ANOVA test for drug and dose showed no statistically significant effect on the response to the whole train of 20 stimuli. Similarly, separate two way ANOVA tests for each of the blocks of 5 stimuli showed no statistically significant effect of drug or of dose on the response.

### *Baseline reflex*

The mean size (± s.e.mean) of the baseline reflex after vehicle administration was 6.0 ± 1.7 spikes ($n = 15$). The baseline

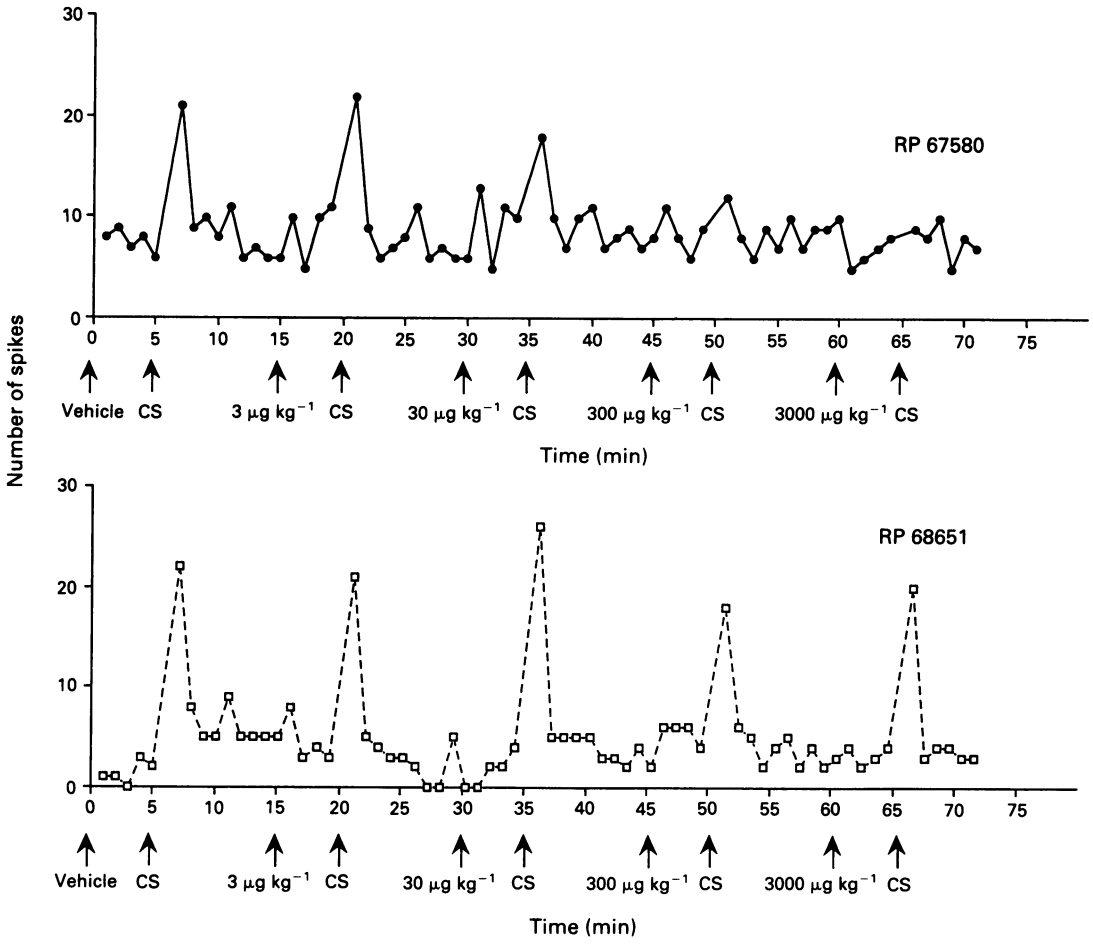



**Figure 1** Illustration of the effect of RP 67580 and of RP 68651 on a spinal flexor reflex in two individual experiments. Single shock stimuli were applied at a rate of 1 per 60 s throughout the experiment, and the number of spikes evoked by each stimulus is plotted. Sequential rising doses of drug were administered at the times indicated by the arrows. Conditioning stimuli were applied at the times marked CS.

reflex increased gradually over the course of each experiment, as can be seen in the individual examples shown in Figure 1. The mean increase in the number of spikes ( ± s.e.mean) over the course of the experiments (baseline after last dose compared to baseline at the start of the experiment) was 3.0 ± 4.0 spikes ($n = 15$). However, this gradual increase did not appear to be a drug effect since it was seen in all experiments regardless of drug or dose. The mean increase after 4 sequential doses (3–3000 μg $kg^{-1}$) of RP 67580 was 3.5 ± 3.0 ($n = 5$). The mean increase after 4 sequential doses of RP 68651 was 1.8 ± 1.1 ($n = 5$).

The possibility of an effect of drug on the baseline reflex was examined by analysing the effects on a single response 5 min after each dose (the time at which the reflex facilitation was tested), and also by analysing the effects on the mean of the 4 baseline responses recorded in the 5 min between the dose and the application of the conditioning stimulus. Separate two way ANOVA tests (on the raw data) showed no statistically significant effect of drug or of dose on the single response, nor on the mean of the 4 baseline responses.

### *Effects on systemic blood pressure*

The mean systemic arterial blood pressure was measured 5 min after each dose (the time at which the reflex facilitation was tested). Vehicle doses produced a mild pressor response (< 10 mmHg) compared to the mean blood pressure immediately before the dose (Figure 3). Administration of doses of 300 and 3000 μg $kg^{-1}$ of both RP 67580 and RP 68651 produced mild depressor responses (< 10 mmHg; Figure 3). These differences from the effect produced by vehicle administration were statistically significant ($P < 0.05$).

### *Pharmacokinetics*

The plasma elimination profile of RP 67580 dosed at 3 mg $kg^{-1}$ i.v. is shown in Figure 4. A biexponential model was fitted to the individual data points to describe the decay profile. The solution (y (nM) = $50542\ e^{(-0.65)*t} + 1363\ *e^{(-0.04)*t}$ where $t$ = time (min)) was then used to estimate the plasma concentrations at each time point when reflex facilitation was tested (with the assumption that the plasma concentration was linearly related to the dose given but that the profile of the decay was unaltered). The calculated plasma concentrations after each dose, taking into account the preceding sequential doses are shown in Table 2.

The minimum effective dose for attentuation of reflex facilitation by RP 67580 was 3 μg $kg^{-1}$. From the observed plasma clearance rate (assuming a linear relationship between dose and clearance rate), the plasma concentration would have fallen to 3.1 nM at the time the conditioning stimulus was applied, 5 min after the i.v. dose, from a peak of at least 21.8 nM. This is consistent with the binding data, which gives an $IC_{50}$ ( ± s.e.mean) in rat brain membranes of 4.2 ± 0.6 nM (Garret *et al.*, 1991). The separation in affinity for the rodent $NK_1$ receptor between RP 67580 and the less active enantiomer, RP 68651, is approximately 2000 fold, which corresponds with the lack of activity of RP 68651 at doses up to 3000 μg $kg^{-1}$ in the present study.

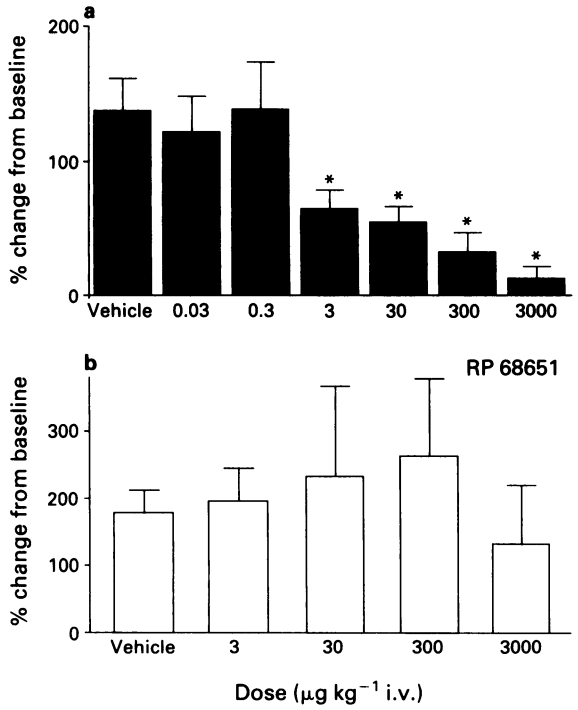



**Figure 2** Histograms showing the effect of RP 67580 and of RP 68651 on facilitation of a spinal flexor reflex by a noxious conditioning stimulus. Facilitation is expressed as mean percentage change from the baseline reflex. Error bars are s.e.mean. (a) The effect of RP 67580; combined data from 2 series of experiments with doses 0.03 to 30 and 3 to 3000 μg kg$^{-1}$ respectively, $n = 5$ in each case. *Indicates doses after which the response was significantly different compared to the response after vehicle treatment ($P < 0.05$). (b) The effect of RP 68651, $n = 5$.

**Table 1** Mean number of spikes (± s.e.mean) evoked by the conditioning stimulus, considered as groups of 5 stimuli

| | *Mean number of spikes evoked after the dose of* | | |
|---|---|---|---|
| *Stimuli number* | *Vehicle* ($n = 15$) | *RP 67580* (3 mg kg$^{-1}$) ($n = 5$) | *RP 68651* (3 mg kg$^{-1}$) ($n = 5$) |
| 1–5 | 127 ± 34 | 137 ± 46 | 64 ± 16 |
| 6–10 | 274 ± 58 | 189 ± 42 | 135 ± 47 |
| 11–15 | 299 ± 61 | 192 ± 47 | 148 ± 41 |
| 16–20 | 278 ± 55 | 170 ± 39 | 122 ± 39 |
| Afterdischarge | 75 ± 28 | 6 ± 3 | 28 ± 16 |
| Total | 1053 ± 221 | 669 ± 157 | 447 ± 150 |

The mean number of spikes (± s.e.mean) evoked by each of the 4 blocks of 5 stimuli making up the conditioning stimulus. The 'vehicle' column shows the mean response evoked by the conditioning stimulus at the start of the experiment. The remaining columns show the response evoked by the conditioning stimulus after 4 sequential doses (3–3000 μg kg$^{-1}$) of RP 67580 and of RP 68651 respectively.

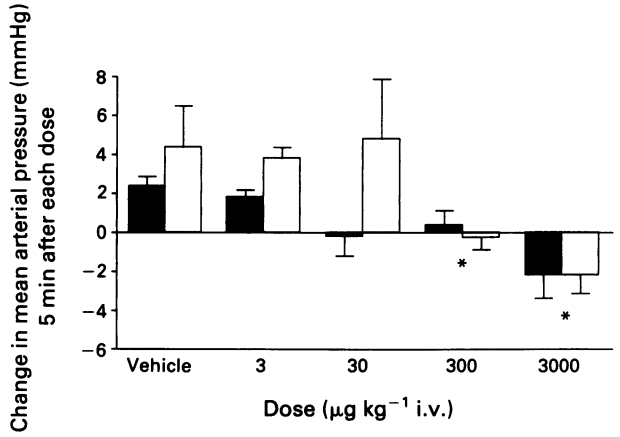



**Figure 3** Histogram showing the effect of RP 67580 and of RP 68651 on the mean systemic arterial blood pressure. The difference in the blood pressure measured 5 min after each dose of drug (the time the conditioning stimulus was applied). compared with the blood pressure immediately before the dose was given is plotted. Error bars are s.e.mean, $n = 5$ per group. Solid columns indicate the response to RP 67580 and open columns the response to RP 68651. *Indicates doses after which the response was significantly different compared to the response after vehicle treatment ($P < 0.05$).

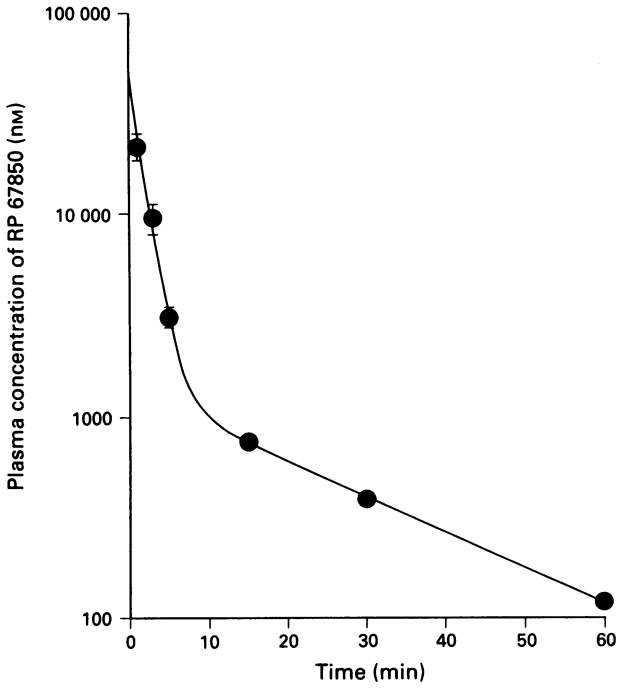



**Figure 4** Plasma elimination profile of RP 67580 determined by dosing rats i.v. with 3 mg kg$^{-1}$ and taking plasma at the time points indicated ($n = 3$ per time point). The concentration of RP 67580 in each sample was determined by h.p.l.c. Error bars are s.e.mean. The curve was fitted using a biexponential model ($y = a^* \exp^{-b^*t} + c^* \exp^{-d^*t}$).

## Discussion

We have shown that the rodent-selective $NK_1$ antagonist RP 67580 dose-dependently attenuated facilitation of a nociceptive spinal reflex in the rat whereas the less active enantiomer, RP 68651, did not. The $ID_{50}$ of the effect of RP 67580 was found to be 2.5 μg kg$^{-1}$. There was no effect of the drug on the size of the baseline reflex, nor on the response to the conditioning stimulus.

The vaso-depressor effects seen with high doses of RP 67580 in the present experiments were not enantioselective, and thus are unlikely to account for the attenuation of reflex facilitation. These effects are similar to those reported for CP-96,345 in dogs (Constantine *et al.*, 1992) and rats (Donnerer *et al.*, 1992; Lembeck *et al.*, 1992). The non-specific cardiovascular effects of CP-96,345 are attributed to its action on ion channels. The depressor effects of RP 67580 seen in the present study were much less marked than those reported for CP-96,345 in the rat (Donnerer *et al.*, 1992), which may be due to the low thoracic spinalization in the present study, or possibly indicate that RP 67580 has a lower

**Table 2** Plasma concentrations of RP 67580 when reflex facilitation was tested

| *Time* (min) | *Contribution from the dose of* 3 μg kg$^{-1}$ | 30 μg kg$^{-1}$ | 300 μg kg$^{-1}$ | 3000 μg kg$^{-1}$ | *Total* (nM) |
|---|---|---|---|---|---|
| 5 | 3.1 | | | | 3.1 |
| 20 | 0.61 | 31.0 | | | 31.61 |
| 35 | 0.34 | 6.1 | 310 | | 316.0 |
| 50 | 0.18 | 3.4 | 61 | 3100 | 3165.0 |

The calculated plasma concentrations of drug at each of the times reflex facilitation was tested. These plasma concentrations were extrapolated from the plasma elimination profile defined with doses of 3 mg kg$^{-1}$ (Figure 4) with the assumption that the plasma concentration was linearly related to the dose given, but that the time-profile of the decay was unaltered.

affinity for ion channels than CP-96,345.

The facilitation of the reflex by the high intensity electrical conditioning stimulus seen in the present study is similar to that previously reported (Woolf & Wiesenfeld-Hallin, 1986; Xu *et al.*, 1992a,b). The facilitation evoked by high intensity electrical conditioning stimuli is short-lived (1 or 2 min in the present study) but is similar to the much more prolonged increase in reflex excitability seen after noxious stimuli which produce a sustained afferent barrage, such as heat-induced injury or inflammation (Woolf, 1983; Ferrell *et al.*, 1988). The increases in reflex excitability evoked by noxious stimuli are generally thought to reflect an increase in central excitability. Such an increase in central excitability is thought to contribute to the characteristic changes in pain sensation seen after noxious stimulation or injury ('Phase 2 pain'; Cervero & Laird, 1991; Treede *et al.*, 1992). The same types of conditioning stimuli have been directly shown to produce increases in excitability in dorsal horn neurones. Thus, high intensity electrical stimuli with stimulus parameters very similar to those used in the present study have been shown to evoke transient increases in the excitability of rat dorsal horn neurones (Cervero *et al.*, 1984; Cook *et al.*, 1989). Several types of 'natural' noxious stimulation of the periphery have been shown to produce increased excitability in dorsal horn neurones (Hoheisel & Mense, 1989; Hylden *et al.*, 1989; Laird & Cervero, 1989; Neugebauer & Schaible, 1990; Woolf & King, 1990) and also in thalamic neurones (Guildbaud *et al.*, 1987).

The present results demonstrate that the non-peptide $NK_1$ antagonist RP 67580 administered i.v. dose-dependently and enantioselectively attenuated facilitation of a nociceptive spinal reflex in the rat. These observations correspond with the previous report (Xu *et al.*, 1992b) that doses of 1 and 3 mg kg$^{-1}$ of racemic **2S,3S/2R,3R** CP-96,345 administered i.v. attenuates reflex facilitation in the rat, although there are some differences in the effects of CP-96,345 (Xu *et al.*, 1992b) compared with those of RP 67580 seen in the present study. Xu *et al.* (1992b) report that CP-96,345 at effective doses not only attenuated facilitation evoked by the electrical conditioning stimulus, but also depressed the reflex response, such that the conditioned response was considerably smaller than the baseline response seen immediately before the conditioning stimulus. Even at the highest doses tried in the present experiments, the effect of RP 67580 was to attenuate facilitation evoked by the electrical conditioning stimulus, such that the conditioned response was equal to the response seen immediately before the conditioning stimulus. Further, Xu *et al.* (1992b) found that high doses of **2S,3S/2R,3R** CP-96,345 significantly inhibited the response to the high intensity electrical conditioning stimulus itself, whereas in the present study, there was no statistically significant effect of RP 67580 or RP 68651 on the response to the conditioning stimulus.

Nonetheless, the present results and those of Xu *et al.* (1992b) suggest that reflex facilitation evoked by the conditioning stimulus in the rat is due to substance P acting at $NK_1$ receptors. Thus it is possible that $NK_1$ receptor activation contributes to the central changes seen in the nociceptive system after noxious stimulation or injury of the periphery. This possibility is further supported by the observation that ventral root potentials recorded from an *in vitro* preparation of neonatal rat spinal cord taken from animals in which a peripheral u.v.-induced inflammatory hyperalgesia was present are reduced to 60% of control by superfusion of CP-96,345 (Thompson *et al.*, 1993). Similarly, CP-96,345 inhibited the prolonged excitatory postsynaptic potential (e.p.s.p) following noxious cutaneous stimulation or a train of intense electrical stimuli in a sample of 5 dorsal horn neurones in the cat (de Konick & Henry, 1991). Significantly, in de Konick & Henry's experiments (1991) there was no effect on the brief response to a single electrical stimulus, nor on the excitation during the train of electrical stimuli. Thompson *et al.* (1993) found that ventral root potentials recorded from *in vitro* preparations taken from control rats are not affected by superfusion of CP-96,345. These observations correspond with the lack of effect of RP 67580 on the baseline and on the response to the conditioning stimulus seen in the present study.

The inhibitory effects of non-peptide $NK_1$ receptor antagonists in electrophysiological preparations including the present study suggest that they have anti-nociceptive actions. The actions of non-peptide $NK_1$ receptor antagonists in behavioural nociceptive tests are less clear cut. Only two published studies to date have shown enantioselective inhibition of nociceptive responses in behavioural tests (Yamamoto & Yaksh, 1991; Nagahisa *et al.*, 1992a). Several other studies have been published showing antinociceptive effects in behavioural tests of CP-96,345 (Birch *et al.*, 1992; Lecci *et al.*, 1992) or RP 67580 (Garret *et al.*, 1991). However, since these latter studies did not include controls for non-specific effects, the reported anti-nociceptive effects may not reflect $NK_1$ receptor antagonism. This is important in light of the recent observation that systemic administration of ion channel blocking agents such as verapamil have anti-nociceptive effects in behavioural tests (Miranda *et al.*, 1992), the detection of non-specific activity of CP-96,345 at ion channels (Schmidt *et al.*, 1992) and the report that the antinociceptive effects of CP-96,345 in several behavioural tests in the rat is not enantioselective (Nagahisa *et al.*, 1992b). Nonetheless, both CP-96,345 and RP 67580 are presumably effective $NK_1$ receptor antagonists in rodents, since they have similar potent and enantioselective effects on neurogenic inflammation (Garret *et al.*, 1991; Nagahisa *et al.*, 1992a; Lembeck *et al.*, 1992; Shepheard *et al.*, 1993). Thus the evidence for anti-nociceptive activity of $NK_1$ receptor antagonists in behavioural tests is equivocal.

The differences between the behavioural data and that from electrophysiological studies may be related to the intensity of stimuli employed. Nociceptive tests in awake animals generally involve responses to stimuli at threshold or near threshold intensities. In the present study, there was no effect of even high doses of RP 67580 on the baseline flexor reflex, which suggests that $NK_1$ receptors are not activated by the stimuli that evoke the simple flexion reflex. This is in line with studies of substance P release in the spinal cord (Duggan *et al.*, 1988), and also with the finding that CP-96,345 did not influence the responses of cat dorsal horn neurones to single high intensity electrical stimuli (de Konick & Henry, 1991). However, prolonged high intensity stimulation does evoke detectable substance P release (Duggan *et al.*, 1988), and responses evoked by such stimuli are blocked by $NK_1$ receptor antagonists, as in the present study.

## *Conclusions*

Our results demonstrate that RP 67580 attenuates reflex facilitation in the rat in a dose-dependent and enantioselective manner, without affecting the baseline reflex, thus

validating the previous report (Xu *et al.*, 1992a,b) that the facilitation of a spinal flexor reflex by noxious conditioning stimuli in the rat can be attenuated by non-peptide $NK_1$ receptor antagonists by demonstrating that this effect is $NK_1$-mediated rather than due to the non-specific effects seen in behavioural nociceptive tests (Nagahisa *et al.*, 1992b). We conclude that the facilitation of a spinal flexor reflex by noxious conditioning stimuli in the rat is mediated by $NK_1$ receptors whereas the baseline flexor reflex is not, and thus propose that substance P acting at $NK_1$ receptors is involved in the increase in excitability that occurs after intense or prolonged noxious stimulation, but not in the processing of brief noxious stimuli. This suggests that brain-penetrant $NK_1$ receptor antagonists may have central antinociceptive effects, with the advantage of inhibiting the response to prolonged and intense inputs, whilst sparing the protective responses to brief, acute noxious stimuli.

We wish to thank our colleagues in Medicinal Chemistry, MRL for the synthesis of RP 67580 and RP 68651, and David Tattersall and Alan Watt for pharmacokinetic data.

## References


BERESFORD, I.L.M., BIRCH, P.J., HAGAN, R.M. & IRELAND, S.J. (1991). Investigation into species variants in tachykinin $NK_1$ receptors by use of the non-peptide antagonist, CP-96,345. *Br. J. Pharmacol.*, **104**, 292–293.

BIRCH, P.J., HARRISON, S.M., HAYES, A.G., ROGERS, H. & TYERS, M.B. (1992). The non-peptide $NK_1$ receptor antagonist (±)-CP-96,345, produces antinociceptive and anti-oedema effects in the rat. *Br. J. Pharmacol.*, **105**, 508–510.

CERVERO, F. & LAIRD, J.M.A. (1991). One pain or many pains? A new look at pain mechanisms. *News Physiol. Sci.*, **6**, 268–273.

CERVERO, F., SCHOUENBERG, J., SJOLUND, B.H. & WADDELL, P.J. (1984). Cutaneous inputs to dorsal horn neurons in adult rats treated at birth with capsaicin. *Brain Res.*, **301**, 47–57.

CONSTANTINE, J.W., LEBEL, W.S. & WOODY, H.A. (1991). Inhibition of tachykinin-induced hypertension in dogs by CP-96,345, a selective blocker of NK-1 receptors. *Naunyn-Schmeid. Arch. Pharmacol.*, **344**, 471–477.

COOK, A.J., WOOLF, C.J., WALL, P.D. & MCMAHON, S.B. (1987). Dynamic receptive field plasticity in rat spinal cord dorsal horn following C-primary afferent input. *Nature*, **325**, 151–153.

DONNERER, J., STARK, U., TRITTHART, H.A. & LEMBECK, F. (1992). CP-96,345, a non-peptide antagonist of substance P. III. Cardiovascular effects in mammals unrelated to actions on substance P receptors. *Naunyn-Schmied. Arch. Pharmacol.*, **346**, 328–332.

DUGGAN, A.W., HENDRY, I.A., MORTON, C.R., HUTCHINSON, W.D. & ZHAO, Z.Q. (1988). Cutaneous stimuli releasing immunoreactive substance P in the dorsal horn of the cat. *Brain Res.*, **451**, 261–273.

FERRELL, W.R., WOOD, L. & BAXENDALE, R.H. (1988). The effect of acute joint inflammation on flexion reflex excitability in the decerebrate, low spinal cat. *Q.J. Exp. Physiol.*, **73**, 95–102.

GARRET, C., CARRUETTE, A., FARDIN, V., MOUSSAOUI, S., PEYRONEL, J.-F., BLANCHARD, J.-C. & LADURON, P.M. (1991). Pharmacological properties of a potent and selective nonpeptide substance P antagonist. *Proc. Natl. Acad. Sci. U.S.A.*, **88**, 10208–10212.

GUILDBAUD, G., BENOIST, J.M., KAYSER, V. & NEIL, A. (1987). Responses of ventrobasal thalamic neurones to carrageenan-induced inflammation in the rat. In *Fine Afferent Fibres and Pain*, ed. Schmidt, R.F., Schaible, H.-G. & Vahle-Hinz, C. Weinheim, pp 412–425. Germany: VCH Verlagsgesellshaft.

HOHEISEL, U. & MENSE, S. (1989). Long-term changes in discharge behaviour of cat dorsal horn neurons following noxious stimulation of deep tissues. *Pain*, **36**, 239–247.

HYLDEN, J.L.K., NAHIN, R.L., TRAUB, R.J. & DUBNER, R. (1989). Expansion of receptive fields of spinal lamina I projection neurons in rats with unilateral adjuvant-induced inflammation: the contribution of central dorsal horn mechanisms. *Pain*, **37**, 229–243.

DE KONICK, Y. & HENRY, J.L. (1991). Substance P-mediated slow excitatory postsynaptic potentials elicited in dorsal horn neurons *in vivo* by noxious stimulation. *Proc. Natl. Acad. Sci. U.S.A.*, **88**, 11344–11348.

LAIRD, J.M.A. & CERVERO, F. (1989). A comparative study of the changes in receptive field properties of multireceptive and nocireceptive rat dorsal horn neurons following noxious mechanical stimulation. *J. Neurophysiol.*, **62**, 854–863.

LECCI, A., GIULIANI, S., PATACCHINI, R., VITI, G. & MAGGI, C.A. (1991). Role of tachykinin receptors in thermonociception: effect of (±)-CP-96,345, a non-peptide substance P antagonist, on the hot-plate test in mice. *Neurosci. Letts.*, **129**, 299–302.

LEMBECK, F., DONNERER, J., TSUCHIYA, M. & NAGAHISA, A. (1992). The non-peptide tachykinin antagonist, CP-96,345, is a potent inhibitor of neurogenic inflammation. *Br. J. Pharmacol.*, **105**, 527–530.

MENDELL, L.M. (1966). Physiological properties of unmyelinated fibre projections to the spinal cord. *Exp. Neurol.*, **16**, 316–332.

MIRANDA, H.F., BUSTAMENTE, D., KRAMER, V., PELISSIER, T., SAAVEDRA, H., PAELIE, C., FERNANDEZ, E. & PINARDI, G. (1992). Antinociceptive effects of $Ca^{2+}$ channel blockers. *Eur. J. Pharmacol.*, **217**, 137–141.

NAGAHISA, A., KANAI, Y., SUGA, O., TANIGUCHI, K., TSUCHIYA, M., LOWE, J.A. & HESS, H.-J. (1992a). Antiinflammatory and analgesic activity of a non-peptide substance P receptor antagonist. *Eur. J. Pharmacol.*, **217**, 191–195.

NAGAHISA, A., ASAI, R., KANAI, Y., MURASE, A., TSUCHIYA-NAKAGAKI, M., NAKAGAKI, T., SHIEH, T.-C. & TANIGUCHI, K. (1992b). Non-specific activity of (±)-CP-96,345 in models of pain and inflammation. *Br. J. Pharmacol.*, **107**, 273–275.

NEUGEBAUER, V. & SCHAIBLE, H.-G. (1990). Evidence for a central component in the sensitization of spinal neurons with joint input during development of acute arthritis in cat's knee. *J. Neurophysiol.*, **64**, 299–311.

SCHMIDT, A.W., MCLEAN, S. & HEYM, J. (1992). The substance P receptor antagonist CP-96,345 interacts with $Ca^{2+}$ channels. *Eur. J. Pharmacol.*, **215**, 351–352.

SHEPHEARD, S.L., WILLIAMSON, D.J., HILL, R.G. & HARGREAVES, R.J. (1993). The non-peptide neurokinin 1 receptor antagonist RP 67580 blocks neurogenic plasma extravasation in the dura mater of rats. *Br. J. Pharmacol.*, **108**, 11–12.

THOMPSON, S.W.N., URBAN, L. & DRAY, A. (1993). NMDA and tachykinin receptor-mediated contributions to the C-fibre evoked response in the neo-natal rat spinal cord *in vitro* are enhanced following peripheral inflammation. *Br. J. Pharmacol.*, (in press).

TREEDE, R.-D., MEYER, R.A., RAJA, S.N. & CAMPBELL, J.N. (1992). Peripheral and central mechanisms of cutaneous hyperalgesia. *Prog. Neurobiol.*, **38**, 397– 421.

WOOLF, C.J. (1983). Evidence for a central component of postinjury pain hypersensitivity. *Nature*, **306**, 686–688.

WOOLF, C.J. & KING, A.E. (1990). Dynamic alterations in the cutaneous mechanoreceptive fields of dorsal horn neurons in the rat spinal cord. *J. Neurosci.*, **10**, 2717–2726.

WOOLF, C.J. & WIESENFELD-HALLIN, Z. (1986). Substance P and calcitonin gene-releated peptide synergistically modulate the gain of the nociceptive flexor reflex in the rat. *Neurosci. Letts.*, **66**, 226–230.

XU, X.-Y., DALSGAARD, C.J. & WIESENFELD-HALLIN, Z. (1992a). Intrathecal CP-96,345 blocks reflex facilitation induced in rats by substance P and C-fiber-conditioning stimulation. *Eur. J. Pharmacol.*, **216**, 337–344.

XU, X.-Y., DALSGAARD, C.J. & WIESENFELD-HALLIN, Z. (1992b). Spinal substance P and N-methyl-D-Aspartate receptors are co-activated in the induction of central sensitization of the nociceptive flexor reflex. *Neurosci.*, **51**, 641–648.

YAMAMOTO, T. & YAKSH, T.L. (1991). Stereospecific effects of a non-peptidic NK-1 selective antagonist, CP-96,345: antinociception in the absence of motor dysfunction. *Life Sci.*, **49**, 1955–1963.


*(Received January 21, 1993*
*Revised March 5, 1993*
*Accepted March 10, 1993)*

*Br. J. Pharmacol.* (1993), **109**, 719–724 © Macmillan Press Ltd, 1993

# Intracellular cross-talk between receptors coupled to phospholipase C via pertussis toxin-sensitive and insensitive G-proteins in $DDT_1MF$-2 cells

[1]John M. Dickenson & Stephen J. Hill

Department of Physiology and Pharmacology, Medical School, Queen's Medical Centre, Nottingham NG7 2UH

**1** The effect on intracellular free calcium concentration ($[Ca^{2+}]_i$) of simultaneous activation of receptors coupled to phospholipase C via pertussis toxin (PTX)-sensitive and -insensitive G-proteins has been investigated in the hamster vas deferens smooth muscle cell line, $DDT_1MF$-2.

**2** In fura-2-loaded $DDT_1MF$-2 cells, activation of adenosine $A_1$-receptors (which are linked to PTX-sensitive G-proteins) with a maximal concentration of $N^6$-cyclopentyladenosine (CPA; 300 nM) increased $[Ca^{2+}]_i$ from 121 ± 5 nM to 254 ± 20 nM ($n = 8$). These experiments were performed in the presence of extracellular $Ca^{2+}$. Stimulation of histamine $H_1$-receptors (which are linked to PTX-insensitive G-proteins) with a low concentration of histamine (1 μM) increased $[Ca^{2+}]_i$ from 128 ± 8 nM to 150 ± 13 nM ($n = 8$). When combined, CPA (300 nM) and histamine (1 μM) synergistically raised $[Ca^{2+}]_i$ from 134 ± 6 nM to 607 ± 61 nM ($n = 8$).

**3** Removal of extracellular $Ca^{2+}$ (experiments performed in $Ca^{2+}$-free buffer containing 0.1 mM EGTA) had no effect on the synergistic interaction between CPA (300 nM) and histamine (1 μM).

**4** The addition of maximal concentrations of CPA (300 nM) and histamine (100 μM) resulted in a rise in $[Ca^{2+}]_i$ which was additive when compared to the $Ca^{2+}$ responses obtained with the two agonists alone. Low (30 nM) and subthreshold (3 nM) concentrations of CPA did not alter the $Ca^{2+}$ response elicited by maximal concentrations of histamine (100 μM).

**5** Subthreshold concentrations of CPA (3 nM) and low concentrations of histamine (1 μM) elicited synergistic rises in $[Ca^{2+}]_i$.

**6** Synergistic $Ca^{2+}$ responses were not observed between histamine $H_1$- and ATP-receptors when cells were simultaneously stimulated with either 1 μM or 10 μM of each agonist.

**7** These data suggest that adenosine $A_1$-receptors linked to PTX-sensitive G-protein(s) and histamine $H_1$-receptors linked to PTX-insensitive G-proteins interact synergistically to raise $[Ca^{2+}]_i$. In contrast, activation of ATP-receptors which are linked to PTX-insensitive G-protein(s) do not interact synergically with histamine $H_1$-receptors.

**Keywords:** Histamine; $H_1$-receptors; adenosine; $A_1$-adenosine receptors; nucleotide receptors; ATP; intracellular calcium; $DDT_1MF$-2 cells; smooth muscle

## Introduction

There are numerous reports in the literature which have documented interactions or 'cross talk' between different intracellular second messenger receptor-effector systems (for reviews see Hill & Kendall, 1989; 1992). For example, stimulation of adenosine $A_1$-receptors can potentiate histamine $H_1$- and $\alpha_1$-adrenoceptor-induced accumulation of inositol phosphates in guinea-pig cerebral cortical slices and FRTL-5 thyroid cells respectively (Hollingsworth *et al.*, 1986; Hill & Kendall, 1987; Okajima *et al.*, 1989). In contrast, adenosine $A_1$-receptor stimulation in the cerebral cortex of mouse (Kendall & Hill, 1988) and man (Kendall & Firth, 1990) attenuates the histamine response. In the above examples, adenosine-receptor activation failed to stimulate inositol phospholipid hydrolysis on its own. The precise mechanisms underlying these interactions remain to be unravelled.

In $DDT_1MF$-2 cells we have previously measured [$^3$H]-inositol phospholipid hydrolysis and $[Ca^{2+}]_i$ changes in response to histamine $H_1$-receptor stimulation (Dickenson & Hill, 1991; 1992; White *et al.*, 1993). Activation of $H_1$-receptors stimulates the release of $Ca^{2+}$ from intracellular stores (inositol 1,4,5-trisphophate-induced, Berridge & Irvine, 1989) and $Ca^{2+}$ entry (influx) across the plasma membrane which requires the continued presence of agonist on the receptor (receptor-mediated $Ca^{2+}$ influx) (Dickenson & Hill, 1991; 1992). Furthermore, Ramkumar *et al.* (1990) have shown that $DDT_1MF$-2 cells express adenosine $A_1$-receptors that are coupled negatively to adenylate cyclase via a pertussis toxin (PTX)-sensitive $G_i$-protein. In addition to the predicted negative coupling of the $A_1$-receptor to adenylate cyclase (Ramkumar *et al.*, 1990) we unexpectedly found that $A_1$-receptor stimulation in $DDT_1MF$-2 cells can elicit inositol phospholipid hydrolysis and $Ca^{2+}$ mobilization (White *et al.*, 1992; Dickenson & Hill, 1993).

In a recent report by Camps *et al.* (1992), it was shown that phospholipase C can be stimulated by βγ subunits of guanine-nucleotide-binding proteins. The $A_1$-receptor-mediated calcium response in $DDT_1MF$-2 cells may thus be a consequence of $G_i$ derived βγ subunits activating phospholipase C rather than a direct coupling of the $A_1$-receptor to phospholipase C (Dickenson & Hill, 1993). Furthermore, this raises the possibility that the augmentation of receptor-mediated inositol phospholipid hydrolysis, by receptors not directly coupled to phospholipase C, may be mediated by βγ subunits released by the simultaneous activation of a second G-protein coupled receptor (which in the case of the $A_1$-receptor would be $G_i$ derived βγ subunits).

The $A_1$-receptor-mediated increase in $[Ca^{2+}]_i$ in $DDT_1MF$-2 cells occurs via a PTX-sensitive G-protein(s), whereas the $H_1$-receptor is coupled to phospholipase C via a PTX-insensitive G-protein (Dickenson & Hill, 1993). Several recent

[1] Author for correspondence.

studies have investigated the intracellular cross-talk between $A_1$-receptors and receptors coupled to phospholipase C in $DDT_1MF$-2 cells. Schachter & Wolfe (1992) reported that $A_1$-receptor activation potentiates noradrenaline stimulated inositol phosphate accumulation. Furthermore, Gerwins & Fredholm (1992a,b) have shown that adenosine $A_1$-receptors can interact synergistically with bradykinin and ATP receptors (both of which are coupled to phospholipase C via PTX-insensitive G-proteins) to raise inositol 1,4,5-trisphosphate and mobilise intracellular calcium. Based on these findings it would be predicted that in $DDT_1MF$-2 cells, adenosine $A_1$-receptors should interact synergistically with histamine $H_1$-receptors (which are linked to PTX-insensitive G-proteins), and that conjoint activation of two PTX-insensitive G-protein linked receptors (e.g. histamine $H_1$- and ATP) should not interact synergistically.

The aim of this investigation was to study the possible intracellular cross-talk between adenosine $A_1$-receptors which can mobilize intracellular calcium through PTX-sensitive G-protein(s) and histamine $H_1$- and ATP-receptors which mobilize intracellular calcium via PTX-insensitive G-protein(s).

## Methods

### *Cell culture*

The hamster vas deferens smooth muscle cell ($DDT_1MF$-2) was obtained from the European Collection of Animal Cell Cultures (Porton Down, Salisbury, U.K.). $DDT_1MF$-2 cells were cultured at 37°C in a humidified air/$CO_2$ (90:10) atmosphere in 75 $cm^2$ flasks (Costar). The growth medium was Dulbecco's modified Eagle's medium supplemented with 2 mM-L-glutamine and 10% (v/v) foetal calf serum (FCS). Cells were passaged twice a week (1/6 split ratio) by vigorous shaking of the flask and placed into 75 $cm^2$ flasks and fed with fresh growth medium every 48 h. Cells for $[Ca^{2+}]_i$ determinations were grown on 24 mm × 10 mm glass coverslips in 90 mm petri dishes. All experiments were performed on confluent monolayers (passages 4–17, numbers assigned after receiving the cell line).

### *Measurement of intracellular free calcium*

Intracellular free calcium was measured by loading confluent cell monolayers with the calcium-sensitive fluorescent dye, fura-2. Individual coverslips were placed in 35 mm petri dishes with 1 ml of physiological buffer (composition, mM; NaCl 145, glucose 10, KCl 5, $MgSO_4$ 1, HEPES 10, $CaCl_2$ 2, pH 7.45) containing 10% FCS (v/v), 3 μM fura-2/AM and incubated for 30 min at 37°C. After this 'loading' period the fura-2 containing buffer was replaced with fresh buffer, that was free of fura-2 and FCS but contained 0.1% bovine serum albumin, and left at 37°C for a further 15 min. Loaded coverslips were then mounted in a specially designed holder which enhabled the coverslip to be positioned across the diagonal of a polymethacrylate cuvette. Each cuvette contained 2.9 ml of physiological buffer (drugs were added to the cuvettes in 100 μl aliquots) and fluorescent measurements were made at 37°C with a Perkin Elmer LS 50 spectrometer. The excitation wavelengths were 340 and 380 nm, with emission at 500 nm. The slit-widths were set at 10 nm for both the excitation and emission wavelengths and the time taken to switch between 340 and 380 nm was 0.8 s. Intracellular free $[Ca^{2+}]$ was calculated every 1.9 s from the equation (Grynkiewicz *et al.*, 1985):

$$[Ca^{2+}]_i = (R - R_{min}) \times (S_{380,min}/S_{380/max}) \times K_d \over (R_{max} - R)$$

where $K_d$ is the affinity of fura-2 for $Ca^{2+}$ (224 nM at 37°C) and $S_{380,min}/S_{380,min}$ is the ratio ($\beta$ value) of the fluorescent values obtained at 380 nm in the absence and presence of saturating $[Ca^{2+}]_i$. The maximum and minimum R values ($R_{max}$ and $R_{min}$) were determined on separate coverslips under saturating $[Ca^{2+}]_i$ (achieved by increasing the extracellular $[Ca^{2+}]$ to 20 mM followed by 10 μM ionomycin, pH 7.45) and calcium-free (achieved by use of 8.3 mM EGTA immediately followed by 25 μl of 1.0 M NaOH to compensate for the decrease in pH, in the presence of 10 μM ionomycin) conditions respectively. Corrections for autofluorescence were made by measuring the fluorescence produced by coverslips that had not been loaded with fura-2. Where $Ca^{2+}$-free conditions were required experiments were performed in nominally $Ca^{2+}$-free buffer containing 0.1 mM EGTA.

### *Data analysis*

Data are shown as means ± s.e.mean. Statistical analysis was performed with Student's unpaired *t* test. A *P* value $<0.05$ was considered as statistically significant. Rises in intracellular free $[Ca^{2+}]$ were evaluated by importing the fluorescence data into the spreadsheet AsEasyAs (TRIUS Inc). Basal $[Ca^{2+}]_i$ levels were determined by calculating the mean of the ten data points (measured every 1.9 s) prior to drug addition, whereas the maximum $Ca^{2+}$ signal was deemed to be the largest $Ca^{2+}$ response obtained immediately after drug addition.

### *Chemicals*

Fura-2/AM and ionomycin were from Calbiochem. Histamine, adenosine-5′-triphosphate, $N^6$-cyclopentyladenosine (CPA), were purchased from Sigma Chemical Company (U.K.). Dulbecco's modified Eagle's medium and foetal calf serum (FCS) were from Northumbria Biologicals (U.K.). All other chemicals were of analytical grade.

## Results

### *Interactions between adenosine $A_1$- and histamine $H_1$-receptors*

Our previous studies have shown that in $DDT_1MF$-2 cells, stimulation of histamine $H_1$- and adenosine $A_1$-receptors results in a rapid and maintained increase in $[Ca^{2+}]_i$ (Dickenson & Hill, 1991; 1992; 1993). Furthermore, the $A_1$-receptor-mediated increase in $[Ca^{2+}]_i$ is sensitive to pertussis toxin (PTX) pretreatment, whereas the response to histamine is insensitive to PTX (Dickenson & Hill, 1993). In this study stimulation of $DDT_1MF$-2 cells with a maximal concentration of the selective $A_1$-receptor agonist $N^6$-cyclopentyladenosine (CPA; 300 nM, Figure 1a) increased $[Ca^{2+}]_i$ from 121 ± 5 nM to 254 ± 20 nM ($n = 8$, $P<0.05$), experiments performed in the presence of extracellular $Ca^{2+}$ (2 mM). Stimulation with a low concentration of histamine (1 μM) increase $[Ca^{2+}]_i$ from 128 ± 8 nM to 150 ± 13 nM ($n = 8$, $P<0.05$, see Figure 1b). This concentration of histamine was chosen to produce a small or subthreshold calcium response and the small mean histamine response is a consequence of combining data from eight experiments, out of which only two responded to 1 μM histamine (in these two experiments $[Ca^{2+}]_i$ increased from 104 nM to 230 nM and from 108 nM to 155 nM). Histamine (1 μM) was therefore subthreshold in the other six experiments. Figure 1c shows a profile obtained by stimulating $DDT_1MF$-2 cells simultaneously with CPA (300 nM) and histamine (1 μM). Clearly, the resulting $Ca^{2+}$ signal is greater than adding together the $Ca^{2+}$ responses of the two agonists alone, with $[Ca^{2+}]_i$ increasing from 134 ± 6 nM to 607 ± 61 nM ($n = 8$). Synergism between histamine and CPA was also evident in batches of cells which did not respond to 1 μM histamine (see Figure 2). These data suggest that adenosine $A_1$- and histamine $H_1$-receptors interact synergistically to increase $[Ca^{2+}]_i$ in $DDT_1MF$-2 cells.

The possible involvement of extracellular $Ca^{2+}$ in the

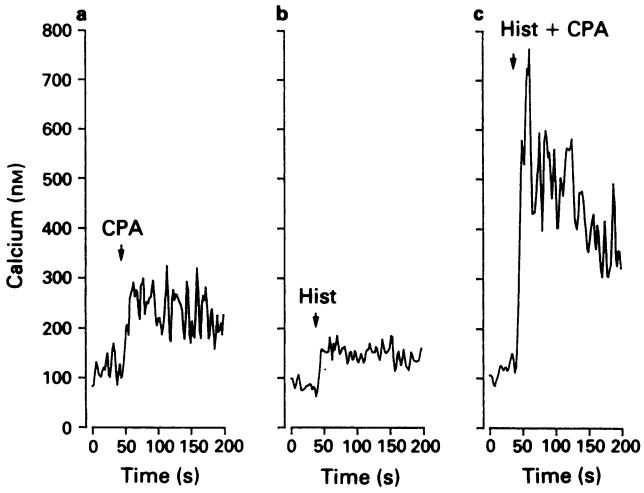



**Figure 1** Interactions between histamine $H_1$- and adenosine $A_1$-receptor mediated increases in $[Ca^{2+}]_i$ in the presence of extracellular $Ca^{2+}$. Cells were stimulated with (a) $N^6$-cyclopentyladenosine (CPA; 300 nM), (b) histamine (Hist; 1 μM), and (c) a combination of histamine and $N^6$-cyclopentyladenosine (1 μM Hist plus 300 nM CPA). Similar results are obtained in two other experiments.

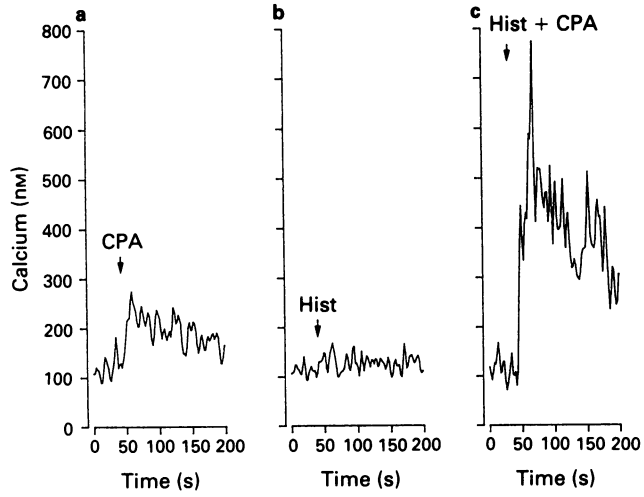



**Figure 2** Interactions between histamine $H_1$- and adenosine $A_1$-receptor mediated increases in $[Ca^{2+}]_i$ in the presence of extracellular $Ca^{2+}$. Cells were stimulated with (a) $N^6$-cyclopentyladenosine (CPA; 300 nM), (b) histamine (His; 1 μM), and (c) a combination of histamine and $N^6$-cyclopentyladenosine (1 μM Hist plus 300 nM CPA). Similar results were obtained in at least five other experiments.

synergistic interaction between adenosine $A_1$- and $H_1$-receptors was examined by performing experiments initiated in nominally $Ca^{2+}$-free buffer containing 0.1 mM EGTA. Figure 3a shows CPA (300 nM)-stimulated increases in $[Ca^{2+}]_i$ measured in the absence of extracellular $Ca^{2+}$. The initial rise in $[Ca^{2+}]_i$ (120 ± 5 nM to 291 ± 29 nM, $n = 10$, $P < 0.05$) is due to release of $Ca^{2+}$ from intracellular stores, whereas the increase in $[Ca^{2+}]_i$ obtained when extracellular $Ca^{2+}$ is re-applied is a consequence of $Ca^{2+}$ influx (120 ± 5 nM to 294 ± 20, $n = 10$, $P < 0.05$). A similar $Ca^{2+}$ profile was obtained with a low concentration of histamine (1 μM, see Figure 3b). Intracellular $Ca^{2+}$ release increased $[Ca^{2+}]_i$ from 98 ± 5 nM to 191 ± 34 ($n = 11$, $P < 0.05$), whereas $Ca^{2+}$ influx (observed after reapplying 2 mM $Ca^{2+}$) increased $[Ca^{2+}]_i$ to 187 ± 25 nM ($n = 11$, $P < 0.05$). The mean histamine $Ca^{2+}$ responses represent the combined data from eleven experiments, out of which five did not respond to

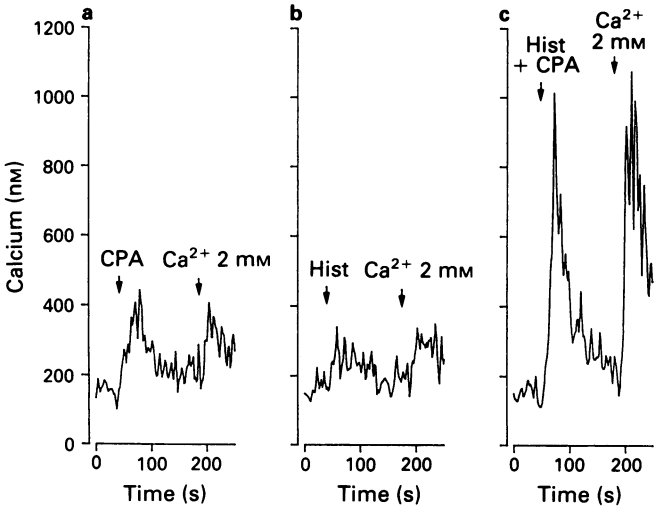



**Figure 3** Interactions between histamine $H_1$- and adenosine $A_1$-receptor mediated increases in $[Ca^{2+}]_i$ in the absence of extracellular $Ca^{2+}$. Cells were stimulated with (a) $N^6$-cyclopentyladenosine, (b) histamine and (c) a combination of $N^6$-cyclopentyladenosine and histamine in nominally $Ca^{2+}$-free buffer containing 0.1 mM EGTA after which exogenous $Ca^{2+}$ (2 mM) was re-applied. $N^6$-cyclopentyladenosine (CPA: 300 nM), histamine (Hist; 1 μM) or $CaCl_2$ (2 mM) were added alone or in combination where indicated. Similar results were obtained in at least nine other experiments.

1 μM histamine. In 'responding' cells, intracellular $Ca^{2+}$ release and $Ca^{2+}$ influx increased $[Ca^{2+}]_i$ to 273 ± 38 nM ($n = 6$) and 235 ± 26 nM ($n = 6$) respectively. Figure 3c shows the effect on intracellular $Ca^{2+}$ release and $Ca^{2+}$ influx of CPA (300 nM) and histamine (1 μM) when added together (experiments initiated in the absence of extracellular $Ca^{2+}$). Synergistic responses were obtained for the release of intracellular $Ca^{2+}$ (113 ± 4 nM to 789 ± 102 nM, $n = 10$, $P < 0.05$) and $Ca^{2+}$ influx (maximum $Ca^{2+}$ response after reapplying 2 mM $Ca^{2+}$ was 763 ± 101 nM, $n = 10$, $P < 0.05$).

The data presented thus far indicate that in DDT$_1$MF-2 cells, maximal concentrations of the $A_1$-receptor agonist, CPA (300 nM) can potentiate responses to low concentrations of histamine (1 μM). We performed experiments to determine whether maximal concentrations of histamine (100 μM) could potentiate responses to low or subthreshold concentrations of CPA. Figure 4 shows the effect of 100 μM histamine on various concentrations of CPA ($3 \times 10^{-7}$–$3 \times 10^{-9}$ M). Combined maximal concentrations of histamine (100 μM) and CPA (300 nM) elicited $Ca^{2+}$ responses which were additive (100 μM histamine increased $[Ca^{2+}]_i$ from 121 ± 5 nM to 337 ± 20 nM; 300 nM CPA increased $[Ca^{2+}]_i$ from 128 ± 4 nM to 253 ± 15 nM; combined histamine and CPA increased $[Ca^{2+}]_i$ from 130 ± 8 nM to 470 ± 37 nM; $n = 7$). Similarly, reduction of the CPA concentration to 30 nM or 3 nM (in the presence of 100 μM histamine) did not produce a synergistic $Ca^{2+}$ response (Figure 4). These data suggest that in contrast to the observed synergy between maximally effective concentrations of CPA and low concentrations of histamine, maximal concentrations of histamine do not appear to potentiate $Ca^{2+}$ responses elicited by low or subthreshold concentrations of CPA (3 nM and 30 nM).

The synergy between histamine and CPA was also evident when a low concentration of histamine (1 μM) was combined with a subthreshold concentration of CPA (3 nM; see Figure 5). Stimulation of cells with 3 nM CPA failed to elicit a $Ca^{2+}$ response (basal $[Ca^{2+}]_i$ 131 ± 9 nM, $n = 9$), whereas 1 μM histamine increased $[Ca^{2+}]_i$ from 140 ± 14 nM to 157 ± 10 nM ($n = 9$). The mean histamine $Ca^{2+}$ response represents the combined data from the nine experiments, out of which five did not respond to 1 μM histamine. In 'responding' cells,

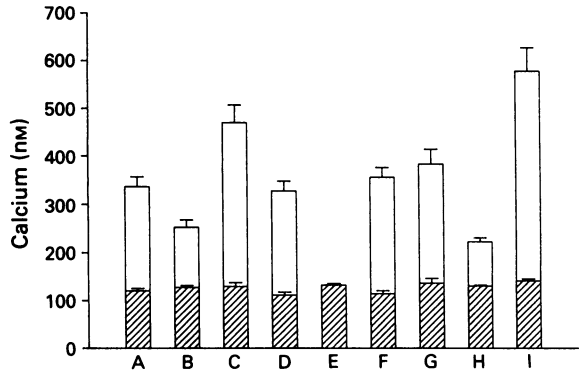



**Figure 4** The effect of a maximal concentration of histamine on $N^6$-cyclopentyladenosine-mediated increases in $[Ca^{2+}]_i$ in the presence of extracellular $Ca^{2+}$. Cells were stimulated with: (A) Histamine (Hist; 100 μM; $n = 7$): (B) $N^6$-cyclopentyladenosine (CPA; 300 nM; $n = 7$): (C) 100 μM Hist + 300 nM CPA ($n = 7$): (D) 100 μM Hist ($n = 10$): (E) 3 nM CPA ($n = 10$): (F) 100 μM Hist + 3 nM CPA ($n = 10$): (G) 100 μM Hist ($n = 6$): (H) 30 nM CPA ($n = 6$): (I) 100 μM Hist + 30 nM CPA ($n = 6$). The basal $[Ca^{2+}]_i$ is represented by the hatched area within each column. Statistical analysis (Student's unpaired $t$ test) comparing the predicted additive $Ca^{2+}$ responses of (A) and (B), (D) and (E), and (G) and (H) (after subtracting basal $[Ca^{2+}]_i$) with the $Ca^{2+}$ responses obtained in columns (C), (F) and (I) (minus basal $[Ca^{2+}]_i$) showed the effects were additive. Data represent mean ± s.e.mean of $n$ experiments.

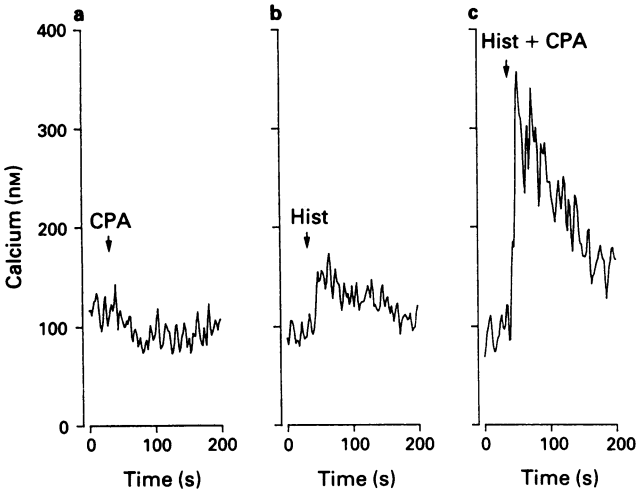



**Figure 5** Interactions between 1 μM histamine and 3 nM $N^6$-cyclopentyladenosone on $[Ca^{2+}]_i$ in the presence of extracellular $Ca^{2+}$. Cells were stimulated with (a) $N^6$-cyclopentyladenosine, (b) histamine and (c) a combination of histamine and $N^6$-cyclopentyladenosine. $N^6$-cyclopentyladenosine (CPA: 3 nM) and histamine (Hist; 1 μM) were added alone or in combination where indicated. Similar results were obtained in at least eight other experiments.

$[Ca^{2+}]_i$ increased from 118 ± 16 nM to 171 ± 17 nM ($n = 4$). When added simultaneously, 1 μM histamine and 3 nM CPA produced a dramatic increase in $[Ca^{2+}]_i$ from 150 ± 15 nM to 506 ± 69 nM ($n = 9$, see Figure 5c).

### *Interactions between histamine $H_1$- and ATP-receptors*

Several studies using $DDT_1MF$-2 cells have shown that ATP increases inositol 1,4,5-trisphosphate ($IP_3$) and intracellular calcium via PTX-insensitive G-protein(s) (Hoiting *et al.*, 1990; Gerwins & Fredholm, 1992b). Furthermore, we have reported that the accumulation of [$^3$H]-inositol phosphates elicited by ATP (100 μM) was insensitive to PTX pretreatment (White *et al.*, 1993). Recently, Gerwins & Fredholm (1992a) showed that ATP can interact synergistically with adenosine $A_1$-receptors to mobilize intracellular calcium. Therefore, we performed experiments to determine whether histamine $H_1$- and ATP-receptors synergistically mobilize intracellular calcium in $DDT_1MF$-2 cells.

Low concentrations of histamine (1 μM; basal $[Ca^{2+}]_i$ 137 ± 7 nM; $n = 9$; Figure 6a) and ATP (1 μM; basal $[Ca^{2+}]_i$ 129 ± 7 nM; $n = 9$; Figure 6b) failed to increase $[Ca^{2+}]_i$ when added alone. Co-addition of histamine (1 μM) and ATP (1 μM) elicited a small rise in $[Ca^{2+}]_i$ from 119 ± 6 nM to 183 ± 8 nM ($n = 9$; Figure 6c). Half maximal concentrations of histamine (10 μM; basal $[Ca^{2+}]_i$ 104 ± 3 nM; $n = 5$) and ATP (10 μM; basal $[Ca^{2+}]_i$ 109 ± 4 nM; $n = 5$) increased $[Ca^{2+}]_i$ to 211 ± 11 nM ($n = 5$; Figure 7a) and 280 ± 18 nM

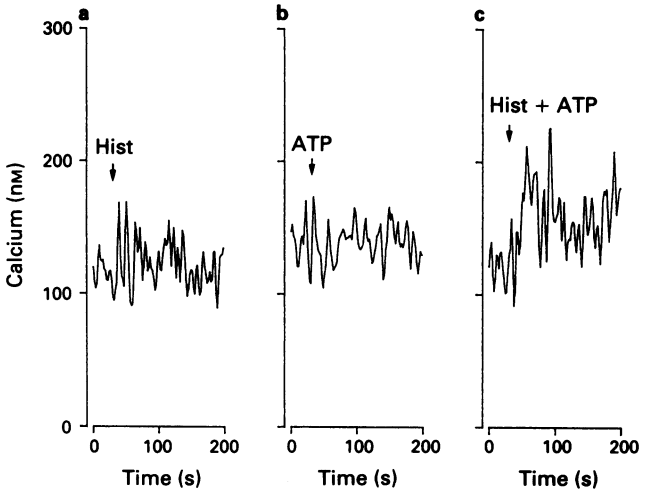



**Figure 6** Interactions between histamine $H_1$- and ATP-receptor-mediated increases in $[Ca^{2+}]_i$ in the presence of extracellular $Ca^{2+}$. Cells were stimulated with (a) histamine, (b) ATP, and (c) a combination of histamine and ATP. Histamine (Hist; 1 μM) and ATP (1 μM) were added alone or in combination where indicated. Similar results were obtained in at least eight other experiments.

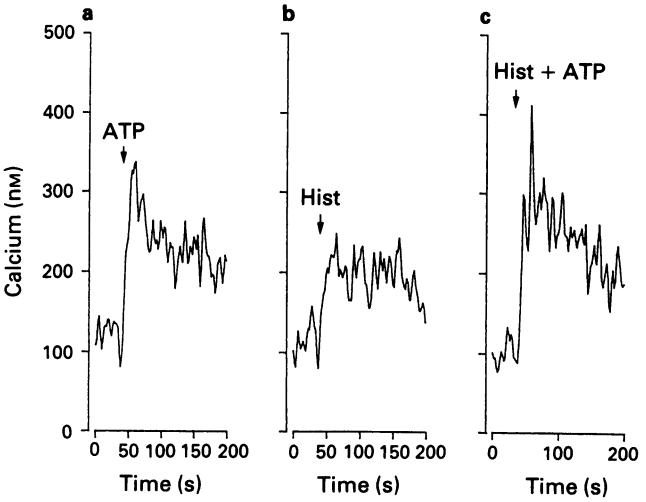



**Figure 7** Interactions between histamine $H_1$- and ATP-receptor-mediated increases in $[Ca^{2+}]_i$ in the presence of extracellular $Ca^{2+}$. Cells were stimulated with (a) histamine, (b) ATP, and (c) a combination of histamine and ATP. Histamine (Hist; 10 μM) and ATP (10 μM) were added alone or in combination where indicated. Similar results were obtained in at least four other experiments.

($n = 3$; Figure 7b) respectively. When combined, $[Ca^{2+}]_i$ increased from $103 \pm 6$ nM to $367 \pm 15$ nM ($n = 5$; Figure 7c) which is indicative of an additive $Ca^{2+}$ response. These data suggest that histamine $H_1$- and ATP-receptors do not produce the same synergistic interaction as that observed with conjoint histamine $H_1$- and adenosine $A_1$-receptor activation.

## Discussion

The present study set out to investigate the intracellular cross-talk between histamine $H_1$- and adenosine $A_1$-receptor-mediated increases in intracellular calcium in DDT$_1$MF-2 cells. The data presented show that histamine $H_1$- and adenosine $A_1$-receptors interact synergistically to mobilize intracellular calcium (see Figures 1 and 2). In contrast, simultaneous activation of histamine $H_1$- and ATP-receptors elicited $Ca^{2+}$ responses which were purely additive (see Figures 6 and 7).

In DDT$_1$MF-2 cells, adenosine $A_1$-receptor stimulation has been shown to attenuate forskolin-induced cyclic AMP accumulation ($A_1$-receptors are negatively coupled via $G_i$ to adenylate cyclase) and mobilize intracellular calcium via PTX-sensitive protein(s) (Ramkumar, 1990; Gerwins & Fredholm, 1992a; Dickenson & Hill, 1993). In contrast, histamine $H_1$-, bradykinin and ATP-receptor-mediated inositol phospholipid hydrolysis and mobilization of intracellular $Ca^{2+}$ occur via PTX insensitive G-protein(s) (White *et al.*, 1993).

Recently, Gerwins & Fredholm (1992a,b) have shown that adenosine $A_1$-receptors can interact synergistically with bradykinin and ATP-receptors to raise inositol 1,4,5-trisphosphate and mobilise intracellular calcium in DDT$_1$MF-2 cells. These results, along with the data presented in this paper, suggest that adenosine $A_1$-receptors (which are coupled to PTX-sensitive G-protein(s)) can interact synergistically with a number of different receptors coupled to phospholipase C via PTX-insensitive G-protein(s), e.g. histamine $H_1$- (this study), bradykinin and ATP-receptors (Gerwins & Fredholm, 1992a,b). In marked contrast, synergism is not observed when histamine $H_1$- and ATP-receptors are activated simultaneously (both coupled to PTX-insensitive G-proteins). The precise mechanism(s) by which synergistic interactions between different receptor-effector systems occur have not been elucidated, although extracellular $Ca^{2+}$, intracellular $Ca^{2+}$, protein kinase A, protein kinase C, and the products of arachidonic acid metabolism have all been implicated (Gerwins & Fredholm, 1992a,b).

However, one possible mechanism may involve intracellular cross-talk at the G-protein level. Recently, Camps *et al.* (1992) have shown that G-protein $\beta\gamma$ subunits can stimulate phospholipase C in cytosolic fractions obtained from HL-60 cells. Therefore, in DDT$_1$MF-2 cells, the $A_1$-receptor mediated calcium response may be a consequence of $G_i$ derived $\beta\gamma$ subunits activating phospholipase C and not due to a direct coupling of the $A_1$-receptor to phospholipase C. This raises the possibility that the augmentation of receptor-mediated inositol phospholipid hydrolysis and calcium mobilization is mediated by $\beta\gamma$ subunits released by the simultaneous activation of a second G-protein coupled receptor (which in the case of the $A_1$-receptor would be $G_i$ derived $\beta\gamma$ subunits). Similarly, $G_i$-protein derived $\beta\gamma$ subunits have recently been shown to augment adenylate cyclase II-mediated cyclic AMP formation (Federman *et al.*, 1992). Interestingly, several recent studies using cloned $G_i$-coupled receptors (e.g. 5-HT$_{1A}$, muscarinic $M_2$ and $M_4$, and $\alpha_2$-receptors) expressed at high concentrations in transfected mammalian cells have revealed that they are able to inhibit adenylate cyclase (the normal effector system for these receptors) and activate phospholipase C (Peralta *et al.*, 1988; Cotecchia *et al.*, 1990; Boddeke *et al.*, 1992). These data suggest the $\alpha_i$ and $\beta\gamma$ subunits released from these $G_i$-coupled receptors may independently inhibit adenylate cyclase and stimulate phospholipase C.

The $Ca^{2+}$ responses obtained with a maximal concentration of histamine (100 $\mu$M) in the presence of low concentrations of CPA (3 nM and 30 nM) were additive (see Figure 4). It would appear that histamine $H_1$-receptor stimulation (using 100 $\mu$M histamine) does not potentiate $Ca^{2+}$ responses to low concentrations of CPA (e.g. 30 nM or 3 nM), whereas both maximal (300 nM) and subthreshold concentrations of CPA (3 nM) interact synergistically with low concentrations of histamine (1 $\mu$M). These results suggest that in DDT$_1$MF-2 cells, it is the $A_1$-receptor that potentiates the calcium responses elicited by low concentrations of histamine (possibly via $G_i$ derived $\beta\gamma$ subunits) and not $H_1$-receptor stimulation augmenting $A_1$-receptor-mediated $Ca^{2+}$ responses.

In summary, the present study has shown that adenosine $A_1$- and $H_1$-receptors, which mobilise intracellular calcium via PTX-sensitive $G_i$ and insensitive $G_q$-protein(s) respectively, interact synergistically to raise $[Ca^{2+}]_i$. In contrast, there is no synergism between $H_1$- or ATP-receptors, which mobilize intracellular $Ca^{2+}$ via PTX-insensitive G-protein(s). The DDT$_1$MF-2 smooth muscle cell appears to provide an ideal system in which to investigate the molecular mechanisms involved in intracellular cross-talk between adenosine $A_1$- and histamine $H_1$-receptors.

The authors thank the Wellcome Trust for financial support.

## References


BERRIDGE, M.J. & IRVINE, R.F. (1989). Inositol phosphates and cell signalling. *Nature*, **341**, 197–205.

BODDEKE, H.W.G.M., FARGIN, A., RAYMOND, J.R., SCHOEFFTER, P. & HOYER, D. (1992). Agonist/antagonist interactions with cloned human 5-HT$_{1A}$ receptors: variations in intrinsic activity studied in transfected HeLa cells. *Naunyn-Schmied Arch. Pharmacol.*, **345**, 257–263.

CAMPS, M., HOU, C., SIDIROPOULOS, D., STOCK, J.B., JAKOBS, K.H. & GIERSCHIK, P. (1992). Stimulation of phospholipase C by guanine-nucleotide-binding protein $\beta\gamma$ subunits. *Eur. J. Biochem.*, **206**, 821–831.

COTECCHIA, S., KOBILKA, B.K., DANIEL, K.W., NOLAN, R.D., LAPETINA, E.Y., CARON, M.G., LEFKOWITZ, R.J. & REGAN, J.W. (1990). Multiple second messenger pathways of $\alpha$-adrenergic receptor subtypes expressed in eukaryotic cells. *J. Biol. Chem.*, **265**, 63–69.

DICKENSON, J.M. & HILL, S.J. (1991). Histamine-stimulated increases in intracellular calcium in the smooth muscle cell line, DDT$_1$MF-2. *Biochem. Pharmacol.*, **42**, 1545–1550.

DICKENSON, J.M. & HILL, S.J. (1992). Histamine $H_1$-receptor-mediated calcium influx in DDT$_1$MF-2 cells. *Biochem. J.*, **284**, 425–431.

DICKENSON, J.M. & HILL, S.J. (1993). Adenosine $A_1$-receptor stimulated increases in intracellular calcium in the smooth muscle cell line, DDT$_1$MF-2. *Br. J. Pharmacol.*, **108**, 85–92.

FEDERMAN, A.D., CONKLIN, B.R., SCHRADER, K.A., REED, R.R. & BOURNE, H.R. (1992). Hormonal stimulation of adenylyl cyclase through $G_i$-protein $\beta\gamma$ subunits. *Nature*, **356**, 159–161.

GERWINS, P. & FREDHOLM, B.B. (1992a). ATP and its metabolite adenosine act synergistically to mobilise intracellular calcium via the formation of inositol 1,4,5-trisphosphate in a smooth muscle cell line. *J. Biol. Chem.*, **267**, 16081–16087.

GERWINS, P. & FREDHOLM, B.B. (1992b). Stimulation of adenosine $A_1$-receptors and bradykinin receptors, which act via different G-proteins, synergistically raises inositol 1,4,5-trisphosphate and intracellular calcium in DDT$_1$MF-2 smooth muscle cells. *Proc. Natl. Acad. Sci. U.S.A.*, **89**, 7330–7334.

GRYNKIEWICZ, G., POENIE, M. & TSIEN, R.Y. (1985). A new generation of $Ca^{2+}$ indicators with greatly improved fluorescence properties. *J. Biol. Chem.*, **260**, 3440–3450.

HILL, S.J. & KENDALL, D.A. (1987). Studies on the adenosine-receptor medating the augmentation of histamine-induced inositol phospholipid hydrolysis in guinea-pig cerebral cortex. *Br. J. Pharmacol.*, **91**, 661–670.

HILL, S.J. & KENDALL, D.A. (1989). Cross-talk between different receptor-effector systems in the mammalian CNS. *Cell. Signalling*, **1**, 135–141.

HILL, S.J. & KENDALL, D.A. (1992). Cross-talk between intracellular second messenger transduction systems. *Drugs News & Perspectives*, **5**, 39–48.

HOITING, B., MOLLEMAN, A., DUIN, M., DEN HERTOG, A. & NELEMANS, A. (1990). $P_2$ purinoceptor-mediated inositol phosphate formation in relation to cytoplasmic calcium in $DDT_1MF$-2 smooth muscle cells. *Eur. J. Pharmacol.*, **189**, 31–39.

HOLLINGSWORTH, E.B., DE LA CRUZ, R.A. & DALY, J.W. (1986). Accumulation of inositol phosphates and cyclic AMP in brain slices: synergistic interactions of histamine and 2-chloroadenosine. *Eur. J. Pharmacol.*, **122**, 45–50.

KENDALL, D.A. & FIRTH, J.L. (1990). Adenosine inhibition of histamine-stimulated inositol phospholipid hydrolysis in human cerebral cortical slices. *Br. J. Pharmacol.*, **100**, 37–40.

KENDALL, D.A. & HILL, S.J. (1988). Adenosine inhibition of histamine stimulated inositol phospholipid hydrolysis in mouse cerebral cortex. *J. Neurochem.*, **50**, 497–502.

OKAJIMA, F., SATO, K., SHO, K. & KONDO, Y. (1989). Stimulation of adenosine receptor enhances $\alpha_1$-adrenergic receptor-mediated activation of phospholipase C and $Ca^{2+}$ mobilisation in a pertussis toxin-sensitive manner in FRTL-5 thyroid cells. *FEBS Letts.*, **248**, 145–149.

PERALTA, E.G., ASHKENAZI, A., WINSLOW, J.W., RAMACHANDRAN, J. & CAPON, D.J. (1988). Differential regulation of PI hydrolysis and adenylyl cyclase by muscarinic receptor subtypes. *Nature*, **334**, 434–437.

RAMKUMAR, V., BARRINGTON, W.W., JACOBSON, K.A. & STILES, G.L. (1990). Demonstration of both $A_1$ and $A_2$ adenosine receptors in $DDT_2MF$-2 smooth muscle cells. *Mol. Pharmacol.*, **37**, 149–156.

SCHACHTER, J.B. & WOLFE, B.B. (1992). Cyclic AMP differentiates two separate but interacting pathways of phosphoinositide hydrolysis in the $DDT_1$-MF-2 smooth muscle cell line. *Mol. Pharmacol.*, **41**, 587–597.

WHITE, T.E., DICKENSON, J.M., ALEXANDER, S.P.H. & HILL, S.J. (1992). Adenosine $A_1$-receptor stimulation of inositol phospholipid hydrolysis and calcium mobilisation in $DDT_1MF$-2 cells. *Br. J. Pharmacol.*, **106**, 215–221.

WHITE, T.E., DICKENSON, J.M. & HILL, S.J. (1993). Histamine $H_1$-receptor-mediated inositol phospholipid hydrolysis in $DDT_1MF$-2 cells: agonist and antagonist properties. *Br. J. Pharmacol.*, **108**, 196–203.

*(Received December 9, 1992*
*Revised March 4, 1993*
*Accepted March 11, 1993)*

*Br. J. Pharmacol.* (1993), **109**, 725–735 © Macmillan Press Ltd, 1993

# Pharmacology of a cloned potassium channel from mouse brain (MK-1) expressed in CHO cells: effects of blockers and an 'inactivation peptide'

[1]Brian Robertson & David G. Owen

Electrophysiology Laboratory, Wyeth Research, Taplow, Maidenhead SL6 0PH

**1** Chinese hamster ovary cells (CHO), maintained in cell culture, were stably transfected with DNA for the MK-1 voltage-activated potassium channel, previously cloned from a mouse brain library.

**2** Voltage-activated currents were recorded by the whole-cell patch clamp method. In CHO cells transfected with the vector only, there were no significant outward voltage activated currents. However, large outward voltage-activated potassium currents were always observed in those cells which had been transfected with the vector containing the DNA encoding for MK-1.

**3** These potassium currents activated from $-40$ mV, and reversed at the potassium equilibrium potential. The half-maximal conductance of MK-1 was at $-10$ mV and had a slope factor of 11 mV when fitted with a Boltzmann function. There was only very slight ($<10\%$) inactivation of MK-1 even at very large positive voltages.

**4** MK-1 was reversibly blocked by: 4-aminopyridine (4-AP, 0.1–4 mM), Toxin I (10–100 nM), mast cell degranulating peptide (1 μM), tetraethylammonium (TEA, 4–10 mM), tedisamil (100 μM), quinine (100 μM) and ciclazindol (100 μM); all applied to the outside of the cell from a 'U tube' rapid perfusion system. 4-AP may block closed as well as open MK-1 potassium channels.

**5** A synthetic 20 amino acid peptide derived from the N-terminus sequence of the *Shaker* B potassium channel (the 'inactivation peptide') produced dramatic inactivation of MK-1 when applied to the inside, but not the outside of the cell. Reducing peptide concentration or 'degrading' the peptide produced less inactivation.

**6** The block of MK-1 by the synthetic inactivation peptide was quite different in time dependence from block by *internal* TEA (0.4–4 mM), which probably blocks much more quickly but less potently than the peptide.

**Keywords:** MK-1; cloned potassium channel; patch clamp; CHO cells; mouse brain; neurones

## Introduction

Voltage-activated potassium channels are important modulators of neuronal excitability in the mammalian CNS. In conjunction with electrophysiological techniques, pharmacological agents which block $K^+$ channels have been vital in isolating major sub-types of $K^+$ channels in the CNS, thus permitting their characterization. However, in many cases blockers are not necessarily specific for sub-types of $K^+$ channels identified electrophysiologically. Naturally-occurring toxins isolated from snakes and scorpions, in particular, have proved amongst the most specific and certainly the most potent blockers (Dreyer, 1990; Strong, 1990), although even here we find apparently selective toxins such as the *B*K blocker, charybdotoxin, blocking voltage-activated $K^+$ currents (Strong, 1990) and the *s*K blocker, quinine, inhibiting delayed rectifier-like $K^+$ channels (McFadzean & England, 1992). The explosion of molecular cloning of $K^+$ channels appears only to confirm the inadequacies of existing pharmacological blockers, since there appear to be more cloned $K^+$ channels than those distinguished pharmacologically. Fortunately however, the cloning and expression of $K^+$ channels offers electrophysiologists for the first time the opportunity to study unequivocally the properties of single populations of sub-types of ion channels (see Stühmer, 1991 for review).

We have taken advantage of cloning and expression techniques and obtained a mouse brain $K^+$ channel, MK1 (Kv1.1, Chandy, 1991), which is stably-expressed in transformed Chinese hamster ovary (CHO) cells. This channel is widely expressed in mouse brain, most notably in the hippocampus (Adams *et al.*, 1991; 1993), and may be an important target for K channel toxins, such as Toxin I, which is known to block homologous channels, RBK-1 and RCK-1 (Stühmer *et al.*, 1988; Wang *et al.*, 1992). The present study describes the actions of a number of important $K^+$ channel blockers commonly used as pharmacological tools, on this single identified $K^+$ channel. We also describe modification of MK-1 by the so-called 'inactivation ball' of the *Shaker* B $K^+$ channel which has been shown to be responsible for N-type inactivation in this archetypal $K^+$ channel (Hoshi *et al.*, 1991), suggesting that the receptor for this peptide is well conserved. Importantly, these experiments have been performed, for the first time, in a mammalian cell system. A preliminary account of some of his work has been previously reported (Robertson & Owen, 1993).

## Methods

### *Transfection and cell culture procedures*

CHO-K1 cell lines were kindly supplied by Dr Bruce Tempel (University of Washington, Seattle, U.S.A.). Two separate lines of CHO cells were used, one containing the control host plasmid (pZMK228R) only, whilst the other cell line contained the plasmid with the cDNA insert for the mouse brain potassium channel gene MK-1 (pZMK6.2SS, Tempel *et al.*, 1988). Cells were grown in tissue culture in 75 ml flasks in a medium containing: 92% RPMI (Sigma); 5% foetal bovine serum (ICN Flow, High Wycombe); 1% L-glutamine (ICN Flow); 1% antibiotic solution (Sigma) and 1% geneticin solution (0.3 mg $ml^{-1}$, geneticin sulphate in 10% HEPES

[1] Author for correspondence.

buffered distilled water solution). Flasks of cells were maintained in an incubator with an atmosphere containing 5% $CO_2$ at 37°C. Cells were subsequently plated onto 35 mm plastic petri dishes (Gibco, Paisley, Strathclyde) at least 2 h before electrophysiological recording.

### *Voltage clamp and electrophysiological recording solutions*

CHO cells were voltage-clamped by use of an Axopatch 1C amplifier (Axon Instruments, U.S.A.) and standard whole-cell patch clamp methods. Patch electrodes were made from aluminosilicate glass (SM150F, Clark Electromedical Instruments, Reading), with a 'bullet' shaped tip to minimize access resistance. Electrodes had a resistance of 1–3 MΩ after heat polishing on a Narashige microforge.

Electrodes were back-filled with an 'intracellular solution' which comprised (in mM): K aspartate 120, KCl 20, $MgCl_2$ 1, MgATP 2, EGTA (ethylene glycol-*bis*(β-aminoethyl ether) *N*,*N*,*N*′,*N*′-tetraacetic acid) 10, HEPES (N-[2-hydroxyethyl]-piperazine-*N*′-[2-ethanesulphonic acid]) 10, adjusted to pH 7.4 with NaOH. The intracellular solution was stored frozen in 1 ml aliquots and defrosted just before use.

Cells were continuously perfused at 3 ml $min^{-1}$ with an 'extracellular solution' which comprised (in mM): NaCl 135, $MgCl_2$ 4, EGTA 1, KCl 5, glucose 25 and HEPES 10; adjusted to pH 7.4 with NaOH. Drugs and other compounds were dissolved in the extracellular solution and applied directly to cells via a 'U-tube' rapid perfusion system. All experiments reported here were conducted at room temperature (21–26°C).

The potassium channel blockers 4-aminopyridine (4-AP), tetraethylammonium chloride (TEA) and quinine HCl were obtained from Sigma Chemical Company. Ciclazindol was from Wyeth-Ayerst; tedisamil was a generous gift from Kali-Chemie Pharma (Hannover, Germany); Toxin I was purified by John Stow of Physical Chemistry at Wyeth Research from crude *Dendroaspis polylepis polylepis* snake venom (obtained from Sigma); mast cell degranulating peptide trifluoroacetate (MCDP) was purchased from Research Biochemicals Incorporated (Natick, MA, U.S.A.); and the *Shaker* B 'inactivation peptide' (of sequence MAAVAGLYGLGEDRQHRK KQ) was synthesized by Peptide Products Ltd (Salisbury, Wiltshire), and was confirmed by n.m.r. as >95% pure. All peptides were kept frozen and added to solutions just before experiments. Voltage-gated currents were elicited and recorded with pClamp software (version 5.5.1, Axon Instruments) running on a Dell 220 PC with an Axolab 1100 interface. Currents were routinely sampled at a rate of 0.6 kHz or faster, and written directly to hard disk for later analysis with either Clampfit software on the PC, or Axograph software (both from Axon Instruments) on a Macintosh IIci. Cells were usually held at − 100 mV, and cell leak and capacity artefacts were removed from current traces on-line with a p-on-4 subtraction procedure. Graphical analysis and current-voltage plots etc. were prepared using Kaleidagraph software. Curves (e.g. exponentials and Boltzmanns) were fitted using algorithms designed to minimize sum of squared errors.

## Results

The results will be presented in three parts. The first section will focus on the physiological properties of MK-1, the second will describe some of the pharmacology of MK-1 and the final section will be concerned with the pharmacology and physiology of MK-1 channels modified with the *Shaker* B 'inactivation' peptide.

### *Electrophysiology of MK-1*

*Currents in untransfected CHO cells* In CHO cells that had been transfected with the vector only, and not the cDNA insert for MK-1, no significant outward currents were observed (see e.g. Figure 1a, $n = 6$ cells). This indicates that unmodified CHO cells have little or no active potassium conductances of their own. However, on a faster time scale, small (<250 pA) voltage-activated inward currents could sometimes be observed (see Figure 1b). These currents were presumably carried by sodium ions through either sodium, or possibly under these recording conditions, calcium channels. No further analysis of these inward currents was undertaken, and it was not necessary to block these since they were not resolved in all CHO cells and because of their small amplitude and duration did not compromise the recording of MK-1 currents.

*Currents in transfected CHO cells* In cells that had been transfected with MK-1 a large 'delayed rectifier' type of

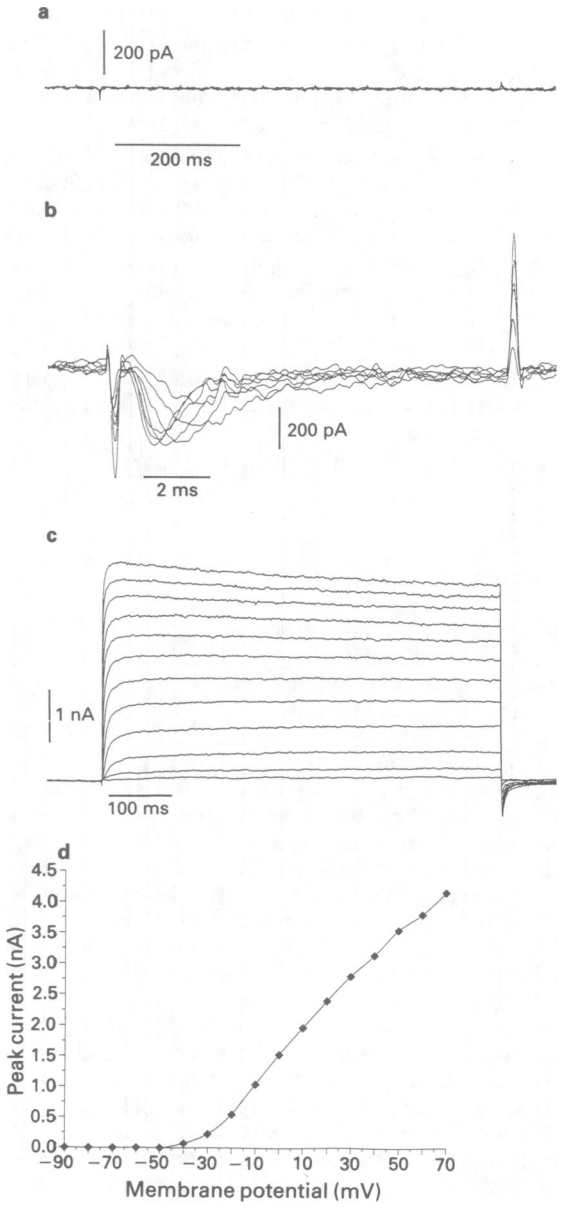



**Figure 1** (a) No outward current in a CHO cell transfected with control vector only. Traces are current resulting from voltage steps from − 30 to + 90 mV from a holding potential of − 100 mV. (b) Some untransfected CHO cells have small voltage-activated inward sodium currents, elicited here on voltage steps from − 5 to + 25 mV from a holding potential of − 90 mV. (c) Activation of potassium current in CHO cells transfected with the cDNA for MK-1. Currents activated on voltage steps from − 40 to + 70 mV. Holding potential − 100 mV. (d) Peak current-voltage relationship for one cell transfected with MK-1.

outward current was always seen. (This current has now been observed in recordings from over 260 transfected CHO cells). A typical example of the MK-1 potassium current in response to incremental voltage steps from − 40 to + 70 mV is seen in Figure 1c. A peak current-voltage relationship for MK-1 is shown in Figure 1d, and reveals a gradual increase in current from a threshold of ~ − 40 mV, which may increase to as much as 10 nA at + 70 mV in some cells.

On a faster time scale (see Figure 2a) we observed that MK-1 rose fairly slowly, over several ms, and followed sigmoid kinetics. For the more negative steps there is a short but obvious delay before activation. Figure 2b shows a plot of rise time (measured as 10–90% of peak) versus step potential; each point is the mean of between 9–18 measurements, and the graph shows approximately an e-fold change for 43 mV change in membrane potential. An activation

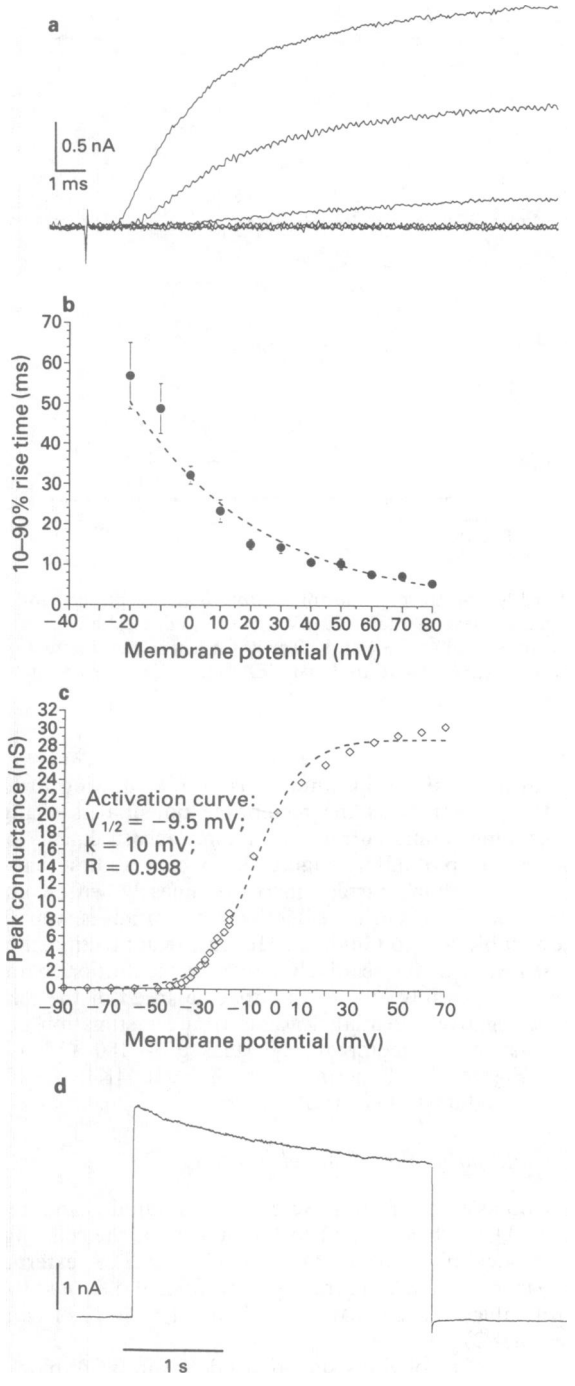



**Figure 2** (a) Activation of MK-1 at a higher resolution. Steps between − 80 and + 20 mV in 20 mV increments. Voltage step begins at the point of the residual capacity artefact. $V_h$ = − 100 mV. (b) 10–90% rise time to peak current versus membrane potential. Data from 9–18 cells. Broken curve represents an exponential fit to this data, showing ~e-fold shift for 43 mV change in $V_m$. R = 0.985. (c) Activation curve for MK-1 from a single cell. Potassium null potential assumed to be − 85 mV, and conductance calculated from peak current. Superimposed is a Boltzmann fit to the data, with R = 0.998. (d) Slow 'inactivation' of MK-1 on a step to + 80 mV from a holding potential of − 100 mV. A single exponential fitted to the decay of this current gives a time constant of 1.8 s.

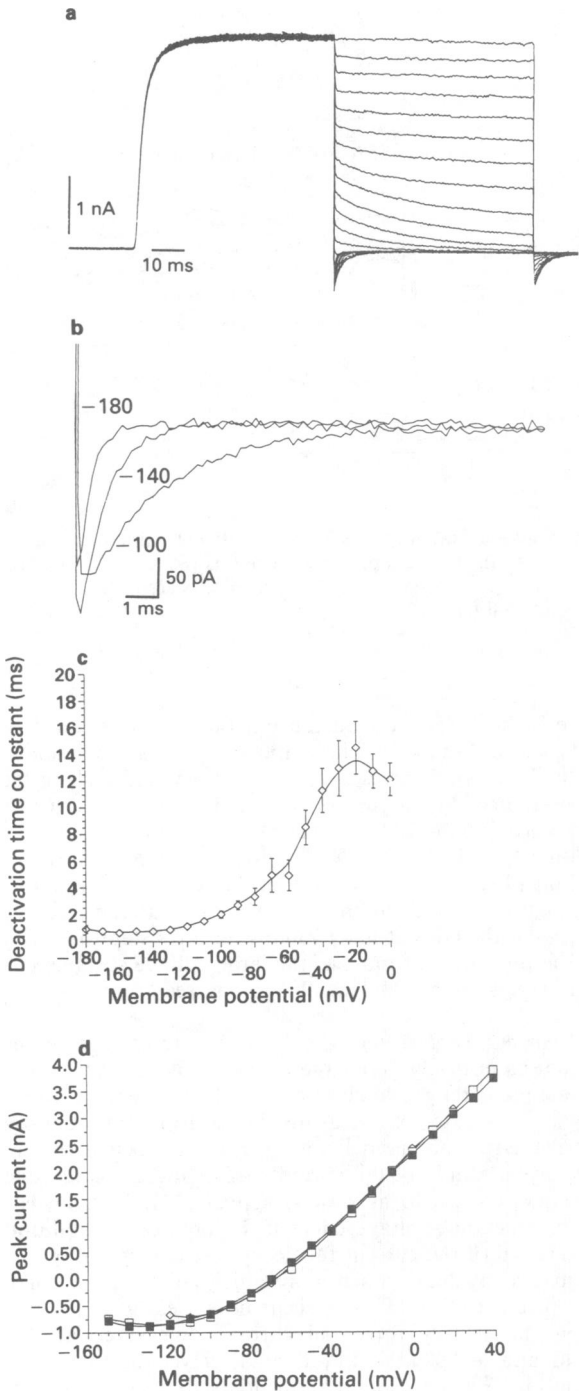



**Figure 3** (a) Tail currents following a conditioning step to + 60 mV. Tail steps from − 180 to + 60 mV in 10 mV increments. $V_h$ = − 100 mV. (b) Three tail currents to − 180, − 140 and − 100 mV following a conditioning step to + 60 mV (not shown). (c) Deactivation time constants derived from single exponential fits to tail currents versus membrane voltage. Mean data ± s.e.mean from 5 cells, smooth curve fit by computer. (d) peak amplitudes of tail current versus step potential. Three separate measurements from a single cell. Same conditions as other cells illustrated.

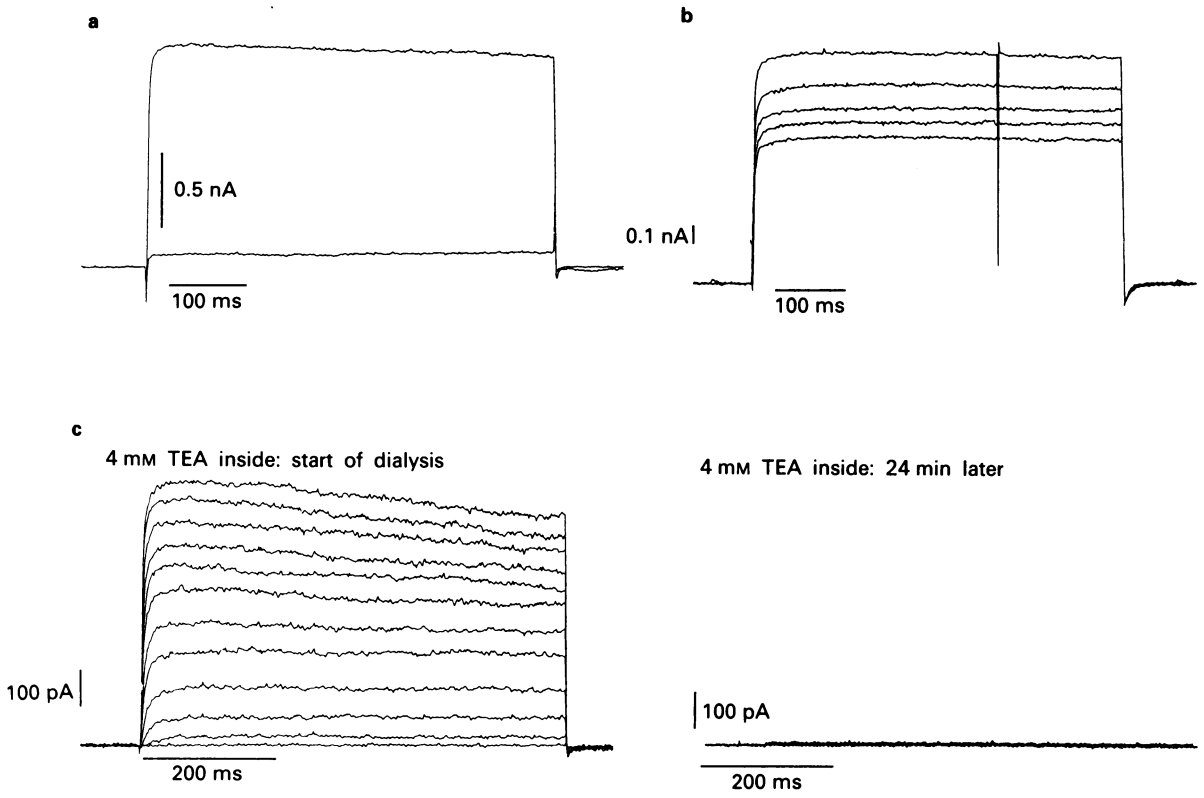



**Figure 4** (a) Block of MK-1 by 10 mM tetraethylammonium (TEA) externally; top trace is control, bottom is in the presence of TEA. In this example peak current is reduced to 5% of control. Voltage steps from − 90 to + 70 mV. (b) First minutes' block by 4 mM TEA inside the cell. Each trace is separated by 10 s intervals. Steps from − 100 to + 60 mV. Top trace has a 'zap' artefact. (c) Full current-voltage responses for MK-1 at the start and after several minutes exposure to 4 mM TEA internally. Steps range from − 40 to + 70 mV. $V_h$ = − 100 mV.

curve for the MK-1 conductance is plotted from data from a single cell in Figure 2c. The graph also shows a Boltzmann fit to the data, which gives a $V_{\frac{1}{2}}$ of − 9.5 mV and a slope factor (k) of 10 mV. Mean data on Boltzmann fits from four other cells gave $V_{\frac{1}{2}}$ = − 10.9 mV and k = 11.1 mV.

Some 'inactivation' of MK-1 does occur, albeit very slowly. This phenomenon is only seen on large positive steps (see e.g. Figure 1c), and Figure 2d shows one extreme case, where ~25% of the current inactivated over a 3 s step to + 80 mV. On the time scale of most of the large voltage steps used here (< 1 s), less than 10% inactivation is seen.

*Tail current analysis of MK-1* Tail current measurements can tell us not only about the reversal potential of a conductance and thereby give clues as to its ionic identity, but they may also be used to measure deactivation time constants, that is the rate of channel closing from the open state. Figure 3a shows a family of tail currents following a voltage step to + 60 mV, chosen to maximally activate MK-1 channels (see e.g. conductance-voltage curve in Figure 2c). In addition to the reversal of the current the decay rate changes: the tails on negative steps decay much more quickly than those obtained with positive steps. This is seen more clearly in Figure 3b, which shows only three tail currents (measured at − 180, − 140 and − 100 mV) but here displayed at much higher resolution. Fitting single exponentials to these traces yields time constants ($\tau_d$s) of 0.5, 0.9 and 2.9 ms respectively. Plotting such time constants derived from tail current measurements on 5 cells shows a bell shaped dependence of deactivation time constant on membrane potential (Figure 3c). In a few cells, a second, much slower exponential component was observed on tail current measurements, however, this was exceptional and is excluded from the present analysis.

Measuring the peak amplitudes of the tail currents gives a direct measure of the instantaneous current flowing through the MK-1 channels as the membrane potential is changed. The resulting ohmic current from three measurements on a single cell is plotted in Figure 3d, which shows that the outward potassium current increases linearly with voltage, but for inward current considerable rectification is seen. This is presumably due to Goldman-Hodgkin-Katz rectification as a consequence of the relatively low K concentration extracellularly, but possibly also to the extreme speed of the relaxations at negative potentials leading to underestimation of the true peak current (compare e.g. steps to − 180 and − 140 mV in Figure 3b). Experiments with higher $[K]_o$ would be needed to address this problem.

### *MK-1 and potassium channel blockers*

MK-1 potassium currents were blocked rapidly and reversibly by TEA when applied to the outside of the cell. Figure 4a illustrates inhibition of MK-1 by 10 mM TEA externally; the mean reduction in current was to 8.3 ± 1.4% ($n$ = 10) of control values. TEA 4 mM reduced MK-1 to 20% of control values ($n$ = 3).

There was no obvious time-dependence in TEA blockade (see below for examples of kinetic changes with other $K^+$ channel blockers): the current was simply scaled downwards throughout the voltage step at all potentials. We were also interested in examining TEA block from the inside of MK-1 channels, especially for comparison to the block induced by the *Shaker* peptide discussed below. TEA was included in the intracellular solution in the recording pipette at either 0.4, 2 or 4 mM. In 4 cells with 0.4 mM TEA added inside, 'normal' MK-1 responses were obtained (data not shown); however currents evoked with large depolarizing steps were much noisier than those observed in control solution. It is assumed that this noisiness is due to a kind of flickery block due to

TEA transiently occluding MK-1 channels (see Spruce *et al.*, 1987).

When 4 mM TEA was applied internally to the CHO cells a fairly rapid and substantial block of MK-1 was obtained. Figure 4b shows five consecutive traces evoked by a voltage step from − 100 to + 60 mV. Each trace is separated by an interval of 10 s, and shows TEA gradually blocking MK-1. Once again, note that there is no overall change in the *kinetics* of MK-1 and the current is simply reduced. Another example is shown in Figure 4c, illustrating that 4 mM TEA eventually blocks MK-1 completely, leaving no outward current at all even on the largest depolarizing steps. Identical results were obtained in all 5 cells tested.

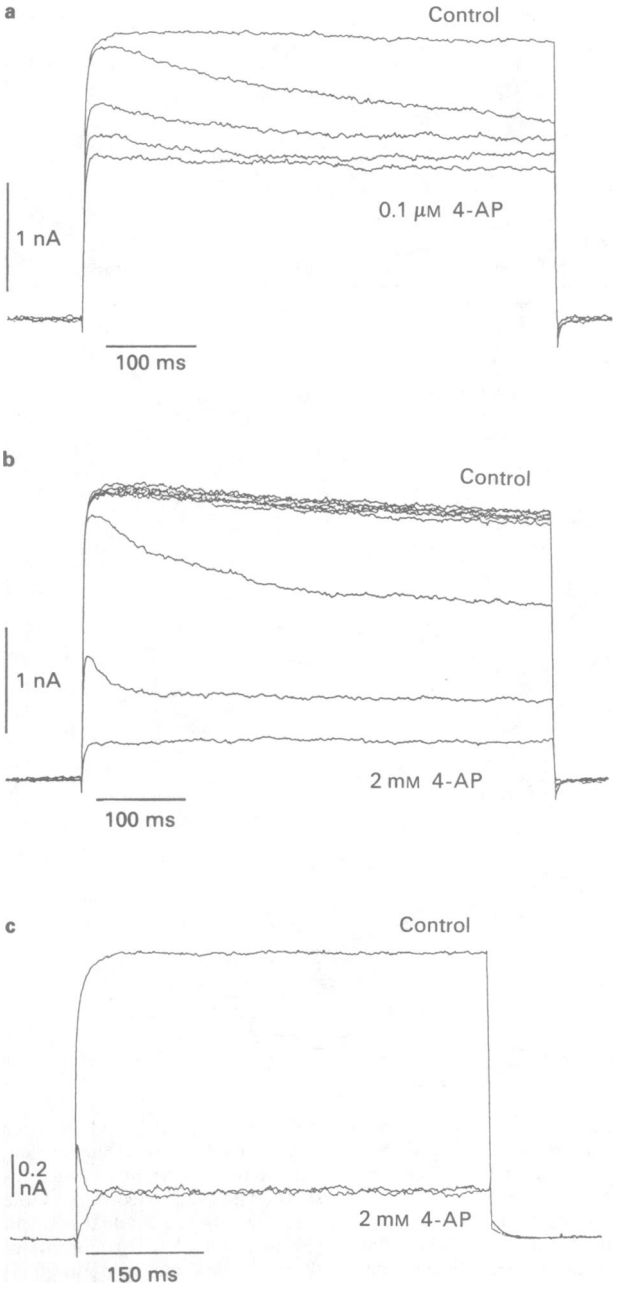



**Figure 5** (a) Inhibition of MK-1 evoked by a voltage step to + 60 mV by 0.1 mM 4-aminopyridine (4-AP) externally. Traces separated by 10 s. Final steady-state inhibition is to 56% of control in this cell. (b) Progressive block by 2 mM 4-AP. Largest traces are several control steps, followed by three identical steps after exposure to 4-AP. Steady-state block is 12% of control in this example. (c) 4-AP inhibits MK-1 in the absence of voltage steps. Top trace is control, middle trace is after 60 s exposure to 2 mM 4-AP (note small decay phase at start of current), followed by equilibrium block 60 s later. Final block is 16% of control.

Although the concentrations of TEA employed here were very limited, it is of interest that 4 mM TEA is slightly more effective in blocking MK-1 from the inside than the outside (i.e. 100% block with 4 $mM_i$, versus ~90% block with 10 $mM_o$).

External 4-aminopyridine (4-AP) blocks MK-1 potassium channels: 0.1 mM reduced peak current at + 60 mV to 63.8 ± 2.4% ($n = 4$) of control values, whilst a higher concentration, 2 mM, reduced peak current to 9.1 ± 2.3% ($n = 5$). Block by 4-AP came on quickly and was fully and rapidly reversible. However some interesting effects were also seen during 4-AP block. For instance in Figure 5a we can see that in addition to the progressive block of MK-1 (step from − 100 to + 60 mV) that during the first few steps in the drug there is more block at the end of the voltage step than at the beginning, until finally a steady-state block is achieved (bottom trace). These changes are much more obvious with 2 mM 4-AP (Figure 5b), where there is a clear decay phase in MK-1 current before the drug block reaches equilibrium (bottom trace). As might be expected the decay induced in MK-1 is faster for the higher concentration of 4-AP. Similar kinetic changes were seen in every cell tested with 4-AP, and these transformations in current decay suggest that 4-AP is blocking *open channels during the voltage step*. We believe that 4-AP may also block MK-1 channels which are in the *closed* state. This is suggested from experiments like those illustrated in Figure 5c where three identical steps to + 60 mV are given at 60 s intervals. These long intervals are spent at a holding potential of − 100 mV, where it is assumed that all or certainly most of the MK-1 potassium channels remain closed. Immediately after the first step, 4-AP was applied, no further steps were made for 60 s, and then the middle trace was recorded. This showed that much, but not all of the current was already blocked. The brief exponential decay of some of

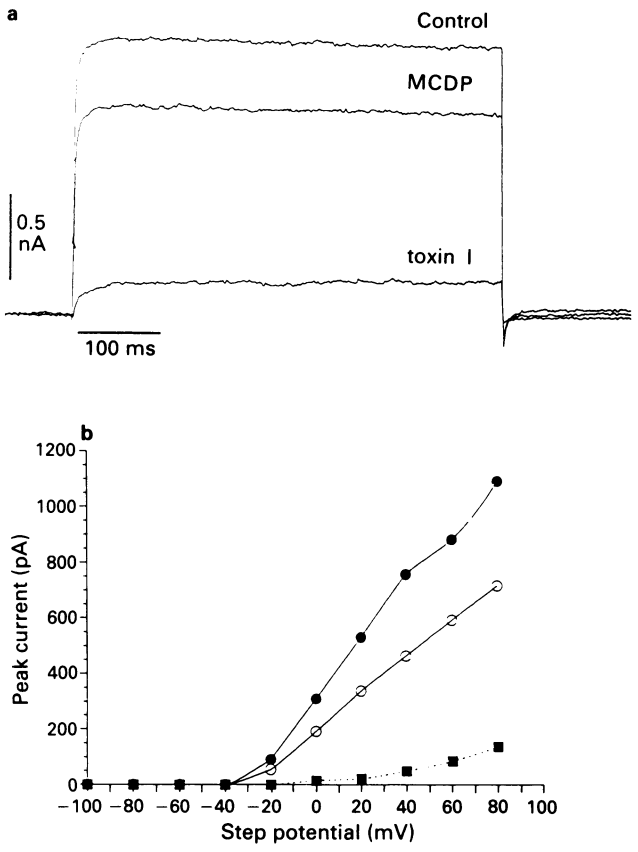



**Figure 6** MK-1 is inhibited by mast cell degranulating protein (MCDP, 1 μM) and toxin I (100 nM). (a) Shows control (top), MCDP (middle) and toxin I (bottom) currents recorded on a voltage step from − 100 to + 60 mV. (b) Current-voltage relation for this same cell: (●) control; (○) 1 μM MDCP; ■ toxin I.

this current is due to 4-AP block of open channels. The final trace (bottom) 60 s later shows the final block achieved with this concentration of 4-AP. Together, these experiments suggest that 4-AP may block MK-1 channels in both closed and open states.

MK-1 is also blocked by two animal-derived toxins, Mast Cell Degranulating Peptide (MCDP), which is a 23 amino acid peptide from bee (*Apis mellifera*) venom; and by the 60 amino acid toxin I isolated from *Dendroaspis polylepis polylepis* snake venom.

MCDP was tested at 1 μM, at which concentration MK-1 is reduced to 77 ± 2.6% ($n = 7$) of control values at + 60 mV. Toxin I is much more potent however, 100 nM reducing MK-1 to 10.6 ± 1.7% ($n = 6$) of control under similar conditions. Toxin I (50 nM) reduced peak current to 63% of control in 2 experiments. Some of these results are illustrated in Figure 6, of which part (a) shows control, MCDP and toxin I traces obtained on voltage jumps from − 100 to + 60 mV in a single cell. No kinetic changes are obvious. Figure 6b illustrates peak current-voltage plots for this same cell in the presence and absence of the toxins. There is no voltage-dependence of block. It is worth noting that although block by these toxins was reversible on washing out, it usually took longer for the current to recover fully than with the other non-peptide inhibitors used. Also, the rising phases of MK-1 currents became much slower after removal of toxin I from the perfusate: we can think of no simple explanation for this. Perhaps the toxins induce extra inactivated or closed states in the $K^+$ channel, resulting in slower opening kinetics. Stühmer *et al.* (1988) have observed a similar phenomenon with MCDP washout on RCK-1 channels.

Tedisamil is a Class III antiarrhythmic which has recently been shown to block certain voltage- and calcium-activated potassium currents in a variety of peripheral and central tissues (see e.g. Dukes *et al.*, 1990). It has been suggested that this drug is a simple 'open channel blocker', and we were interested to see if these $K^+$ channels cloned from mouse brain were similarly affected. At a concentration of 100 μM, tedisamil markedly altered both the peak amplitude and the decay of MK-1; example traces may be seen in Figure 7. The best way of characterizing the effects of such compounds is not through simply measuring inhibition of peak as we have

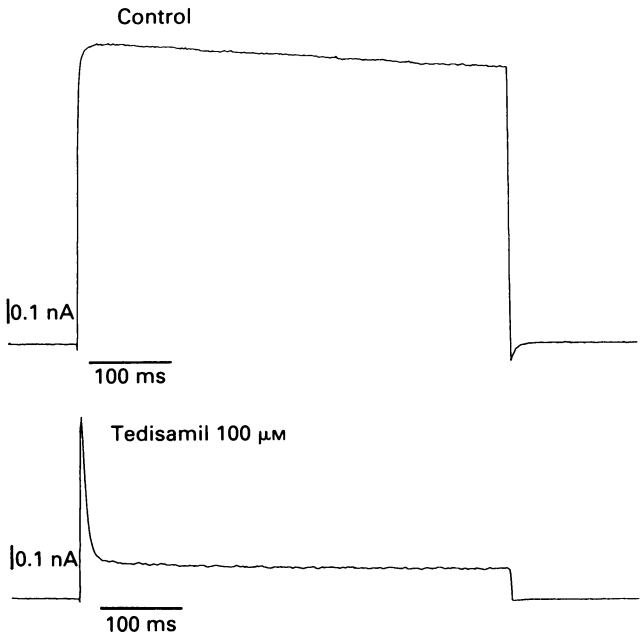



**Figure 7** Block of MK-1 by 100 μM tedisamil. Averaged traces (between 4 and 8 separate records) show control and drug responses. Peak current and charge transfer are reduced to 60% and 11% respectively in this example. $\tau_d$ in control is 5.5 s, decreasing to 5.1 ms and 137 ms in tedisamil. Step to + 60 mV from − 100 mV.

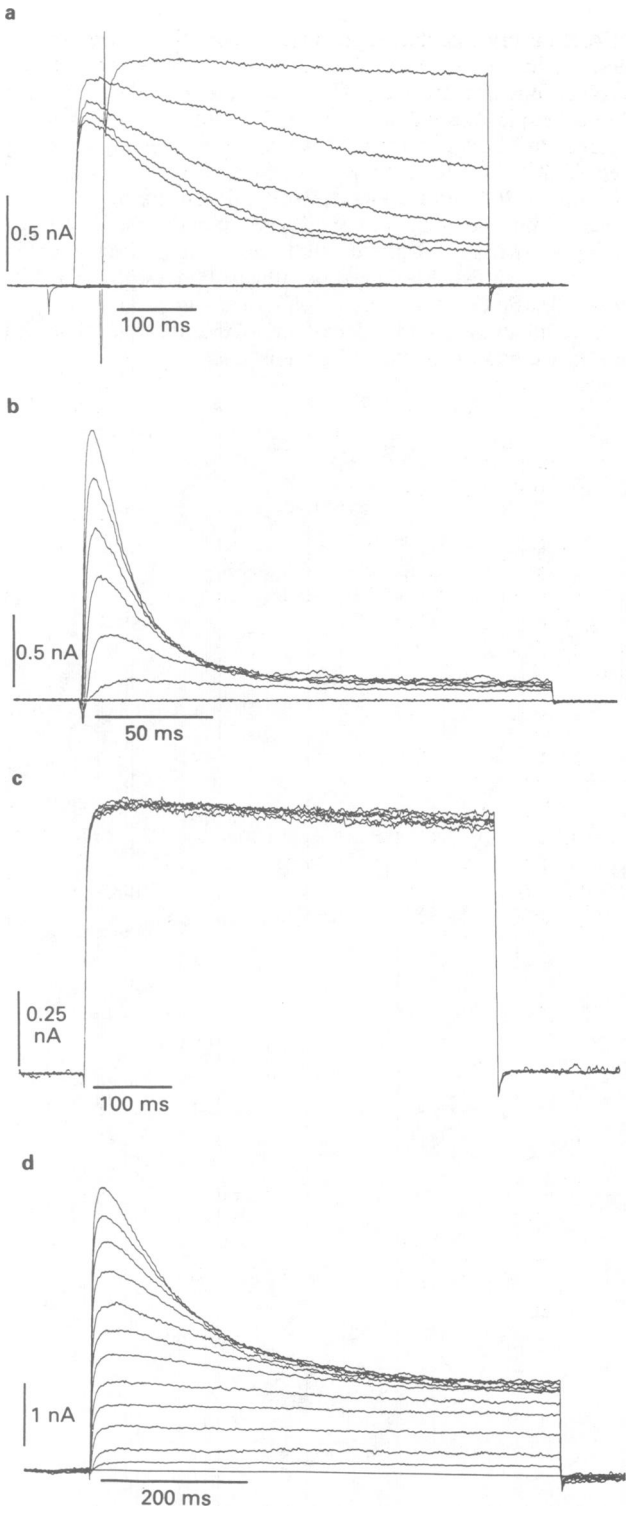



**Figure 8** (a) *Shaker* B peptide rapidly modifies MK-1. The bottom, flat traces were recorded in cell attached mode, before bursting into the cell with a 'zap'. The top trace is the initial current recorded just after (see large artefact) establishing whole-cell recording. Other traces are sequential steps 10 s apart showing the gradual acceleration of current. (Steps from − 100 to + 60 mV). (b) Current responses to voltage steps from − 80 to + 80mV increasing in 20 mV increments after peptide effect has equilibrated. Time constants of decay fitted to these traces are as follows: − 20 mV: 63.8 ms; 0 mV: 37.2 ms; + 20 mV: 27.9 ms; + 40 mV: 22.5 ms; + 60 mV: 18.7 ms; + 80 mV: 16.6 ms. $V_h = -100$ mV. (c) MK-1 is not modified when the *Shaker* B peptide ball is applied *outside* the cell. Traces recorded during a voltage step from − 100 to + 60 mV with 400 μM peptide externally. (d) Current in response to incremental voltage steps from − 40 to + 70 mV, with 'degraded' peptide inside. Time constants of decay are: + 10 mV: 370 ms; + 20 mV: 294 ms; + 30 mV: 218 ms; + 40 mV: 170 ms; + 50 mV: 145 ms; + 60 mV: 125 ms; + 70 mV: 111 ms.

before, but by calculating the more illustrative *charge transfer* during the voltage step (obtained by integrating the total current over the duration of the step). The peak current was reduced to 52.7 ± 6.3% of control ($n = 5$) whilst the overall charge transferred during the voltage step was diminished to only 14.8 ± 2.7% of control ($n = 5$). The average decay phase of MK-1 in the presence of 100 μM tedisamil was 8.9 ± 1.5 ms ($n = 5$). A slower phase was sometimes also measured, being ~100 ms. Moreover tedisamil inhibition was only slowly reversible; this is consistent with the postulated intracellular site of action.

The antimalarial drug, quinine HCl has been reported to possess $K^+$ channel blocking activity (see e.g. McFadzean & England, 1992). At 100 μM quinine reduced MK-1 peak outward current to 25.1 ± 4.6% of control values ($n = 6$), whilst charge transfer was reduced to 16.7 ± 4.1% ($n = 6$). A little time-dependence of quinine block was observed.

The anorectic agent, ciclazindol, has recently been shown to have inhibitory actions at both ATP-dependent and voltage-gated potassium channels. Here we show that at least at the relatively high concentrations used here, ciclazindol (100 μM) reduced peak MK-1 current to 49.2 ± 4.7% of control ($n = 6$), and charge transfer was similarly reduced to 49.1 ± 6.3% of control values ($n = 6$).

### *Modification of MK-1 currents by the* Shaker *B peptide*

The best studied $K^+$ channel at present is the *Shaker* B channel cloned from *Drosophila* muscle. Unlike MK-1 $K^+$ channels these *Shaker* channels close quickly after opening. In a recent series of elegant experiments it has been shown that this inactivation mechanism is due to part of the N-terminal sequence of the channel, some 20 amino acids, acting as a molecular 'ball' entering and occluding the inside mouth of the channel (Zagotta *et al.*, 1990). We were interested to determine if a similar mechanism could be induced in the essentially non-inactivating MK-1 channel. To this end we included a synthetically manufactured copy of the *Shaker* B 20-mer peptide in the patch pipette solution at a concentration of 400 μM. (A total of 53 CHO cells were recorded with the *Shaker* peptide inside – all were modified). Figure 8a shows the typical response obtained during the first minutes' dialysis with the peptide. The bottom (flat) traces are in cell-attached mode before bursting into the CHO cell, then we have burst the patch with a 'zap' during the voltage step, and straightaway get our normal, sustained MK-1 current. However in the following few seconds as the ball dialyses into the cell (there are 10 s intervals between traces) the current was transformed into an inactivating potassium current. The next part of the Figure (8b) shows a current-voltage family of modified MK-1 once the effect has stabilized (steps from − 40 to + 80 mV, compared this with e.g. Figure 1c, noting difference in timescales).

The peptide proved to be ineffective when applied at 400 μM outside the cell (Figure 8c, $n = 5$) since no inactivation was induced. This result suggests that the blocking mechanism may be selective for the intracellular face of the channel. The peptide was also tested at 200 μM intracellularly, but very little inactivation was evident ($n = 6$). Attempts were also made to degrade the peptide to determine if the blocking action was dependent on some native structure in the molecule. Initially the peptide was 'aged' for 24 h in the intracellular solution at room temperature, but MK-1 was still quickly transformed into a rapidly inactivating $K^+$ current ($n = 3$). A further sample of this 'aged peptide' solution was then heated at 60°C for 2 h and vigorously sonicated before testing, and a typical result ($n = 3$) is shown in Figure 8d. It is clear that the current treated with this

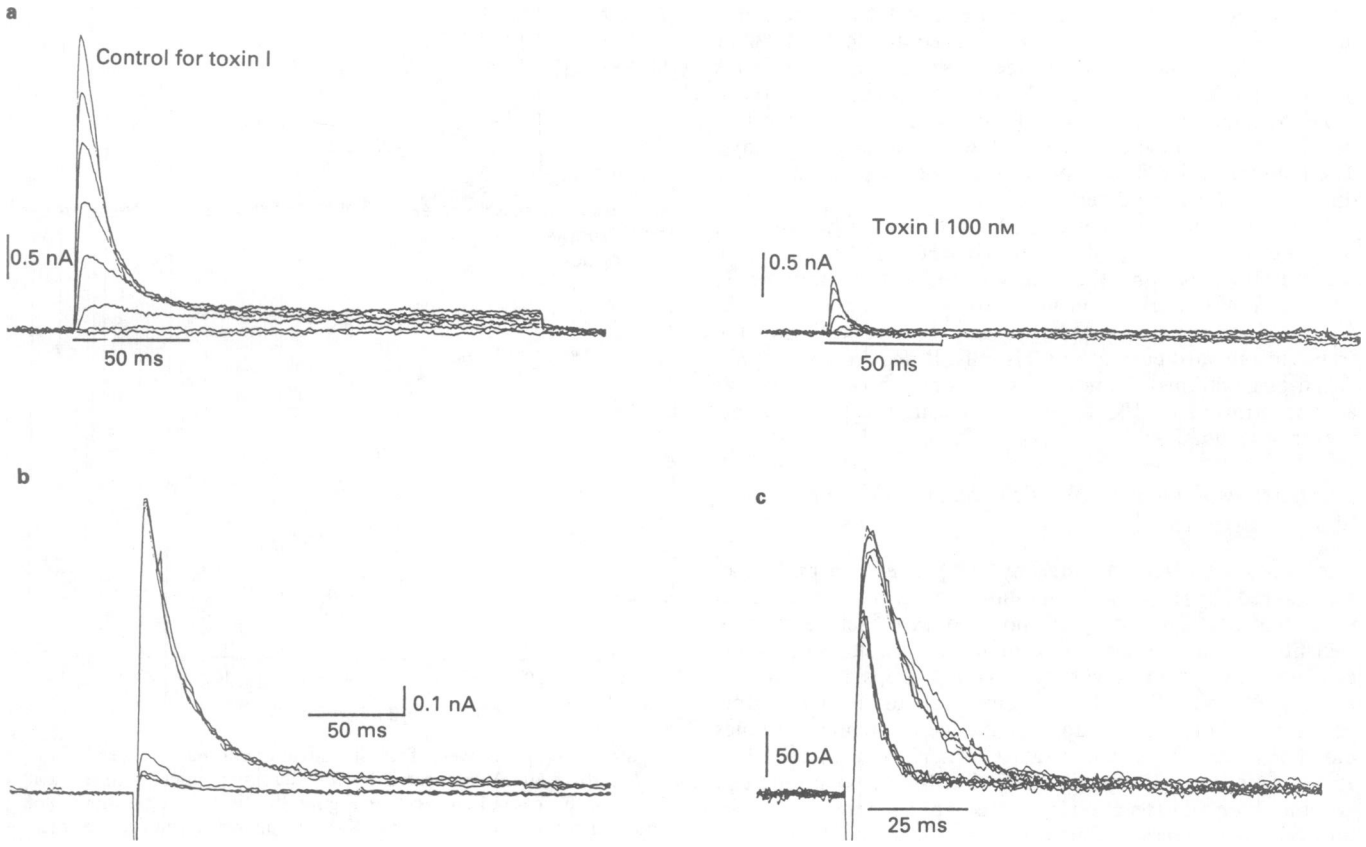



**Figure 9** (a) Block of peptide-modified MK-1 by 100 nM toxin I. Peak current at + 60 mV was reduced to 23% of control in this example. (b) Tetraethylammonium 10 mM also blocks modified MK-1. In this example peak outward current was reduced to 5% of control. (c) Inhibition of peptide-treated MK-1 by 100 μM tedisamil. Top traces control, lower traces in drug. In this cell peak current was reduced to 63% of control; charge transfer to 57% of control, and $\tau_d$ changed from 12.2 in control to 4.6 ms in tedisamil (mean values from 6 separate records).

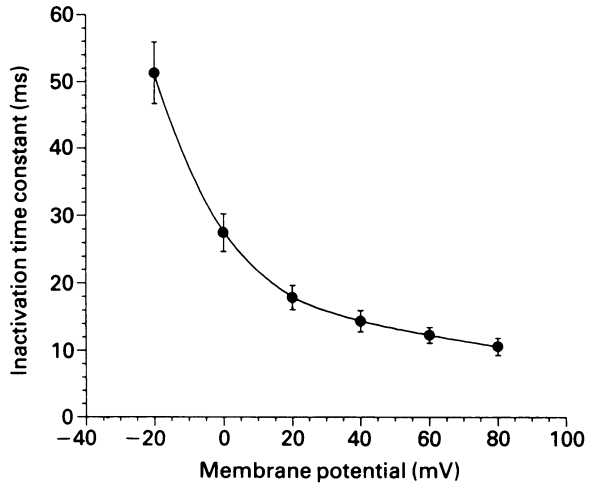



**Figure 10** Time constants of inactivation of peptide-modified MK-1 change with membrane voltage. Data points are mean $\tau_d$s obtained from single exponential fits on currents from 10 cells (± s.e.mean). Smooth curve fitted by computer.

'degraded' peptide inactivates much more slowly; indeed the fitted time constants are of the order of hundreds rather than the tens of milliseconds seen with the normal peptide e.g. $\tau_d$ for the step to + 60 mV is 125 ms in this example, compared to a mean value of 12 ms (see below) for control peptide.

As may be expected, the basic pharmacology of the 'transformed' MK-1 was unaltered. Sensitivity to Toxin I (100 nM, $n = 7$, e.g. Figure 9a) and external TEA (10 mM, $n = 7$, Figure 9b) were unchanged, and the current decay was also accelerated by tedisamil (100 μM, $n = 4$, Figure 9c). Tedisamil (100 μM) suppressed peak current to 64 ± 4.4%; charge transfer during the voltage step was reduced to 44.3 ± 14% of control values; and decay rate decreased from 55.4 ± 28 ms in control solution to 6.8 ± 1.9 ms (all measurements from 4 separate cells, note that control value is larger than normal because one of these cells had a slower than average decay). The final value for decay rate in tedisamil is not substantially different between modified and unmodified MK-1 current.

In three separate cells where MK-1 had been transformed with the *Shaker* B peptide we tested whether the decay rate could be increased by the oxidising reagent, chloramine T, which removes inactivation in a variety of $K^+$ channels. (At 500 μM chloramine T completely removes inactivation of the transient outward current in $GH_3$ cells: B. Robertson, unpublished observations). Somewhat surprisingly however, even at a concentration of 500 μM, no change in decay rate whatsoever was obtained.

### *Electrophysiological assay of the block induced by the* Shaker *B peptide*

The 'block' of MK-1 channels by the *Shaker* B peptide may be assayed by a variety of standard electrophysiological measurements. The decay of modified MK-1 currents were well fitted with a single exponential, and the time constants of inactivation ($\tau_d$) at a variety of voltage steps are plotted in Figure 10. Over the voltage range − 20 to + 80 mV, time constants become more rapid as the step potential becomes more positive. The mean $\tau_d$ at + 60 mV from 12 cells was 12 ± 1.2 ms. It is thought unlikely that the inactivation step, i.e. the blocking reaction itself is voltage-sensitive, since previous single channel studies on *Shaker* channels show no voltage sensitivity for this step (Hoshi *et al.*, 1990). However, the voltage-dependence of the decay rate closely follows the activation curve for unmodified MK-1 (see Figure 2c). The steepest change in $\tau_d$ occurs over the range − 20 to + 20 mV, which corresponds to the steepest part of the conductance/activation curve. From + 20 to + 80 mV both the inactiva-

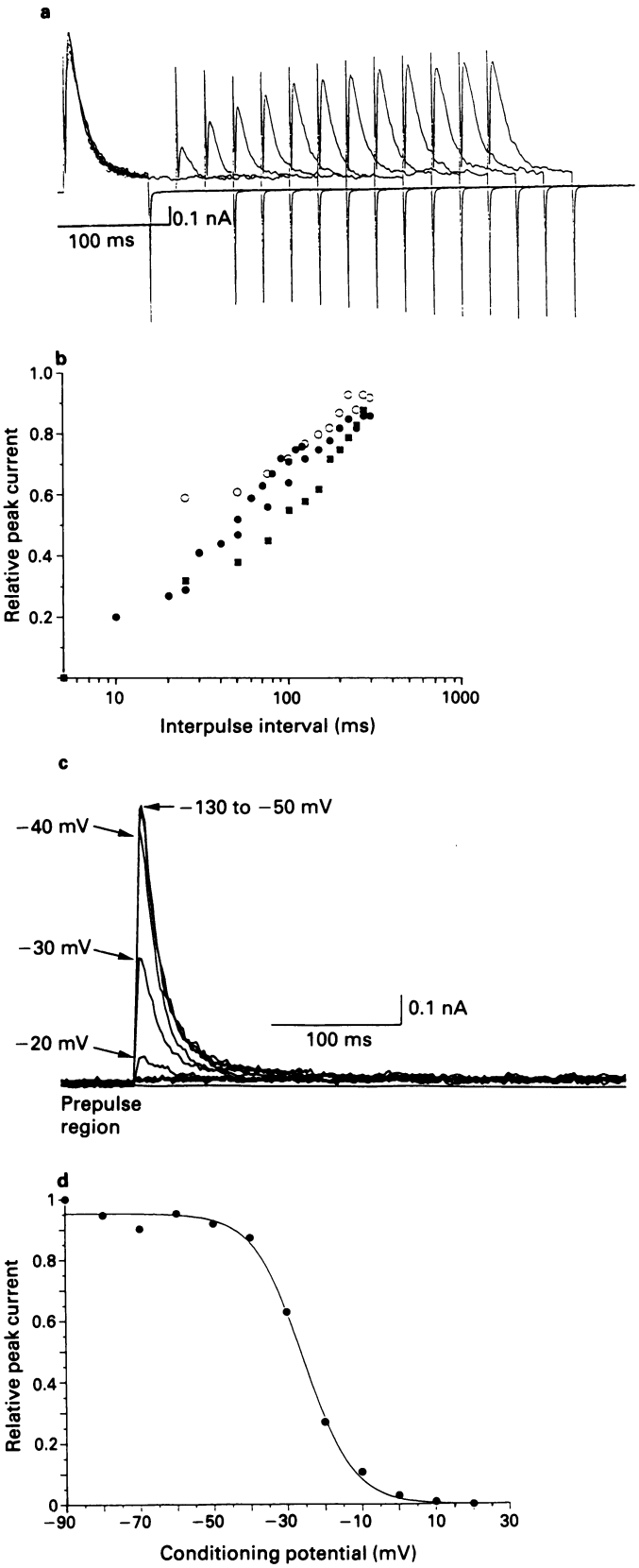



**Figure 11** (a) Recovery from inactivation: a pair of steps from − 100 to + 60 mV separated by an increasing interval (increment 25 ms in this case). [Same cell as Figure 8b]. (b) Semilogarithmic plot showing recovery of modified MK-1 with increasing interpulse interval. Data from three separate cells, denoted by different symbols. (c) Example data used for construction of h-infinity curve. Traces are current obtained on a step top + 60 mV after various conditioning steps from − 130 to − 20 mV, as labelled. Preceding 1 s conditioning step only partly shown. (d) Steady-state inactivation curve for four cells, normalised to peak current value. Boltzmann fit to this data gives a $V_{\frac{1}{2}} = -25$ mV, and a slope factor $k = -7.6$ mV; $R = 0.998$.

tion time constant and the activation curves show a much shallower dependence on voltage. The simplest explanation for the voltage dependence of $\tau_d$ is that inactivation is coupled to activation, and that as the probability and speed of channel opening increase at more positive voltages, then the blocking particle will enter the channel sooner, quickening the decay of the ensemble current.

Two pulse experiments provide a valuable tool for probing the gating kinetics of voltage-activated channels. Experiments of the sort illustrated in Figure 11a can be used to measure the rate of recovery from inactivation: a pair of identical pulses to + 60 mV are separated by a variable time ($t$) at the holding potential (− 100 mV). The first step is long and large enough to inactivate the modified MK-1 channels completely. The cell is then repolarized to − 100 mV to initiate recovery from inactivation and then the second pulse provides a measure of the number of channels back in a conducting state. The traces illustrated show the current recovering gradually as the interpulse interval is lengthened. Results from 3 other cells are plotted semilogarithmically in Figure 11b. Recovery from inactivation is ~90% complete in 300 ms and is full in 1 s. (An interval of 1–10 s between voltage pulses was used for all the standard protocols employed here).

The steady-state voltage-dependence of inactivation for peptide-modified MK-1 was investigated with 1 s prepulses ranging from − 130 to + 30 mV, followed by a test pulse to + 60 mV. The test pulse was used to determine the fraction of channels not inactivated by the prepulse, and some traces are shown in Figure 11c. It is clear from these traces that the prepulses from − 130 to − 50 mV have no effect on the test pulse current; however, the pulses from − 40 to − 20 mV have a profound effect on the amplitude of this current. These and other results are plotted graphically in Figure 11d, and the data from four cells is well fit with a Boltzmann distribution with $V_{\frac{1}{2}}$ = − 25 mV and a slope factor k of − 7.8 mV. As expected, the greatest degree of inactivation occurs over the range where MK-1 activates most steeply.

## Discussion and conclusions

The combination of the techniques of molecular biology and electrophysiology provide unprecedented access to single, identified ion channels from the mammalian brain in a convenient and robust preparation. Here we have studied the properties of the MK-1 potassium channel cloned from mouse brain, which is now known to be located in several significant neuronal structures (Adams *et al.*, 1991; 1993). In addition, because the channel is expressed here in a mammalian cell line, we get closer to the true native environment of MK-1 compared to oocyte expression systems.

The expression of the MK-1 message in CHO cells results in a slowly activating, essentially non-inactivating potassium current much like the classical 'delayed rectifier' first observed by Hodgkin and Huxley in squid axon. Full activation of the MK-1 current takes several milliseconds even at very positive potentials, and is preceded by a short delay (see also Houamed *et al.*, 1989), presumably due to the presence of multiple closed states before channel opening. The activation parameters are similar to those reported for homologous channels RBK-1 and RCK-1 from the rat brain (Stühmer *et al.*, 1988; Christie *et al.*, 1989) but the half maximal conductance value is almost 20 mV more positive. This may be due to the fact that MK-1 is here expressed in a mammalian, as opposed to an amphibian expression system. The slope of the conductance-voltage curve obtained in the present study (11 mV) is about mid-way between values previously reported for homologous channels, i.e. 6–14 mV (Stühmer *et al.*, 1988; Christie *et al.*, 1989; Klumpp *et al.*, 1991). In every case so far reported, MK-1 and its rat homologues have inactivation rates measured in seconds as opposed to the rapid, millisecond inactivation seen for some other members of the *Shaker* potassium channel family. The tail currents measured here predominantly had a single time constant, with a bell-shaped dependence on membrane potential. A single time constant for deactivation, of approximately the same duration, has been observed for RCK-1 channels by Koren *et al.* (1990). The mean values obtained here at very negative potentials appear to saturate at ~0.7 ms, implying an approximate value for the MK-1 channel closing rate of ~1400 $s^{-1}$. However, the true value for channel closing is likely to be faster because of the limited bandwidth available in the present study.

TEA was effective in blocking MK-1 channel from both the inside and the outside, as has been shown previously for RBK-1 and RCK-1. For these two rat channels, the $K_i$ s for internal and external block are roughly similar, being around 0.3 mM (Christie *et al.*, 1989; Taglialatela *et al.*, 1991; Newland *et al.*, 1992). The binding sites for block of several potassium channels by internal and external TEA have been localized to a sequence of only 19 amino acids that lie between the S5 and S6 regions of the channel (the H5 region). Recent work on the *Shaker* K channel has shown that the pore-blocking site for external TEA may be constructed from only four aromatic tyrosine residues, one from each channel subunit, which interact simultaneously with the blocker (Kavanaugh *et al.*, 1991; Heginbotham & MacKinnon, 1992). TEA did not induce any kinetic changes in MK-1; the gradual equivalent shift of peak and final current and the flickery block seen here when TEA was included inside the cell support the conclusion that TEA is a rapid channel blocker (Spruce *et al.*, 1987).

4-AP proved more effective than TEA in blocking MK-1. Published $K_i$ values for RBK-1 and RCK-1 vary between 0.16 and 1 mM (Stuhmer *et al.*, 1988; Christie *et al.*, 1989; Wang *et al.*, 1992), which are in accordance with the inhibition by 4-AP seen here. Klumpp *et al.* (1991) have reported a $K_i$ value of 1.1 mM for 4-AP inhibition of mouse retinal MK-1. 4-AP proved a much more interesting blocker than TEA, since our results suggest that 4-AP is able to block open MK-1 channels during the voltage step, as well as closed channels between voltage steps. Wagoner & Oxford (1990) have also suggested that 4-AP blocks closed and open transient potassium channels in $GH_3$ cells. Unfortunately, there are no details yet from site-directed mutagenesis studies of where 4-AP may bind to cause inhibition of MK-1 or related $K^+$ channels.

The toxins MCDP and toxin I proved to be potent inhibitors of MK-1. Perhaps this channel is one of the CNS targets of these toxins, thereby causing the powerful convulsive effects of these compounds when they are injected intracerebroventricularly (see Harvey & Anderson, 1991 for review). (However, RCK2- and RCK5-subtype potassium channels are also sensitive to these toxins). Recent studies indicate that both toxins induce a long lasting increase in excitability in rat isolated hippocampal slices, reminiscent of long term potentiation (Southan & Owen, 1992). MCDP was much less effective than toxin I in blocking MK-1; previous reports comparing these two toxins on similar, slowly inactivating potassium channels bear this out, with $K_i$ values for the snake toxin being 4 to 18 times greater than the apian inhibitor (e.g. Stansfeld *et al.*, 1987; Stühmer *et al.*, 1988; Wang *et al.*, 1992).

Tedisamil, which is a novel Class III antiarrythmic (see e.g. Beatch *et al.*, 1991), was a dramatic blocker of MK-1, producing a marked inactivation of the current in both peptide-modified and unmodified states. This action is consistent with tedisamil being an open-channel blocker, as previously suggested (Dukes *et al.*, 1990). It was originally believed that tedisamil was selective for rapidly inactivating voltage-gated potassium currents, but has since been shown to be an effective blocker of both non-inactivating and calcium-activated $K^+$ currents in central nervous and peripheral tissues (e.g. McLarnon & Wang, 1991; Pfrunder & Kreye, 1991). The slow washout of the responses observed here are

concordant with an intracellular site of action, but this mechanism appears *independent* of the intracellular block by the inactivation peptide. Since tedisamil also blocks central potassium channels including MK-1, this drug may be useful for the modulation of CNS transmission.

Quinine has been used principally to block large-conductance calcium activated $K^+$ channels, but McFadzean & England (1992) have recently shown that this compound is an extremely effective blocker of the slowly inactivating $K^+$ current in anococcygeal smooth muscle cells. Similar results were reported by Fatherazi & Cook (1991), who found that quinine was more effective against ATP-sensitive $K^+$ channels and a delayed rectifier $K^+$ current than against $Ca^{2+}$-activated $K^+$ currents in pancreatic islet cells. However, Christie *et al.* (1989), who used quinine to exclude the possibility that they were recording $Ca^{2+}$-activated $K^+$ currents, found no inhibition of RBK-1 by 100 μM quinine: this is surprising in view of the close similarity between MK-1 and RBK-1 (only 3 amino acids are different out of 497). The antagonism of slow, voltage-activated $K^+$ channels and $Ca^{2+}$-activated $K^+$ channels by both quinine and tedisamil suggest that many of these different sub-types of potassium channel share some common structural features.

We found that relatively high concentrations of ciclazindol (100 μM) block MK-1, and Noak *et al.* (1992) report that this compound antagonizes both voltage- and ATP-dependent $K^+$ channels. Whether these effects are relevant to the (presumably) centrally-mediated anorectic actions of ciclazindol is not clear.

We have demonstrated that the 'inactivation peptide', from the last 20 amino acids of the N-terminal sequence of *Shaker* B potassium channels, is capable of blocking MK-1 channels from mouse brain. This block is characterized by the transformation of the current from a 'delayed rectifier' type to a rapidly inactivating, 'A-type' outward current. The peptide was ineffective however when added to the outside surface of MK-1 channels, suggesting that the receptor site for the ball is only present on the cytoplasmic surface. Isacoff *et al.* (1991) have recently studied the properties of this putative receptor, and find that mutations of certain highly conserved residues between S4 and S5 segments markedly influence the normal inactivation in *Shaker* B potassium channels and that induced in DRK-1 channels. This region is also conserved in MK-1 channels; it would be of interest to perform similar site-directed mutations to prove that this region also forms part of the ball peptide receptor site on this channel. These studies indicate that the binding site has been conserved through evolution of the *Shaker* potassium channel family.

A fairly high concentration of peptide was required in this study to produce appreciable inactivation, certainly when compared to the original studies on *Shaker* B channels. The $K_d$ for the ball peptide on its 'own' channels is 8 μM, which is identical to the $K_d$ obtained by Foster *et al.* (1992) for the peptide on calcium-activated potassium channels from rat brain and skeletal muscle. However, there are significant differences in $K_d$ even between the 'same' channels, as Toro *et al.* (1992) report a $K_d$ of 95 μM for ball inhibition of $K_{Ca}$ channels from smooth muscle. One reason for this may be that even though the 'receptor site' may be identical in sequence between channels, the electrostatic environment or diffusional approach may be made quite different by changes in remote regions. It is also possible that a greater concentration of peptide was required here because it was applied to the channels via whole-cell dialysis, and we do not know the actual concentration of the molecule at the critical region on the inside membrane surface. All of the other studies of ball-induced inhibition of K channels have been conducted with either inside-out patches or in bilayers, where the concentration of the peptide is known exactly.

Structural work has suggested that the ball peptide may adopt an α-helical conformation (Lee *et al.*, 1992), but it is thought unlikely that there is much tertiary structure associated with the molecule. In contrast, the equivalent inactivation particle from RCK-4 channels (which display rapid inactivation) is possibly more complex, due to the presence of cysteine in the molecule. Removal of these cysteines alters inactivation properties (Ruppersberg *et al.*, 1991). These authors have indeed suggested that the cysteine groups may be an important route for coupling cellular metabolism to potassium channel inactivation.

Several lines of evidence indicate that it is unlikely that the peptide induces inactivation through some 'non-selective' action, since single point modifications to the peptide markedly alter its effectiveness (Hoshi *et al.*, 1990). Firm evidence that the ball peptide actually physically blocks the ion conduction pathway in $K^+$ channels has come from experiments demonstrating competition between internal TEA and the inactivation process (Choi *et al.*, 1991). Additionally, Demo & Yellen (1991) demonstrated that recovery from inactivation may be speeded up by increasing $K^+$ externally (as if K ions entering the pore knock the ball out of its blocking site) and show in single channel experiments that the inactivation ball must leave the channel before it can close.

Further new developments made possible by molecular biology have been in the exploration of transmitter-channel coupling (Hoger *et al.*, 1991), characterization of the action of clinically useful drugs (Snyders *et al.*, 1992) and in the precise mapping of ion channel subtypes on individual neurones (Sheng *et al.*, 1992). In conclusion, it is clear that the marriage of the techniques of molecular biology and electrophysiology now permits unparalled access to the study of ion channels present in the mammalian brain.

It is a pleasure to thank Janette Scott and Fay Heblich for their excellent tissue culture and maintenance of CHO cells. John Stow of Physical Chemistry, Wyeth Research, kindly provided purified toxin I. We value the contributions, both chemical and discoursive, of Albert Opalko, Wyeth Research, and we would also like to thank Bruce Tempel for supplying us with the MK-1 clone and the transfected cells used in this study.

## References

ADAMS, L.A., HOUAMED, K.M., DORSA, D.M. & TEMPEL, B.L. (1993). Glial- and neuronal-specific $K^+$ channel gene expression in the CNS of the mouse. *Proc. Natl. Acad. Sci. U.S.A.*, (in press).

ADAMS, L.A., HOUAMED, K.M. & TEMPEL, B.L. (1991). Glial- and neuronal-specific $K^+$ channel gene expression in the CNS of the mouse. *Soc. Neurosci. Abst.*, **17**, 1279.

BEATCH, G.N., ABRAHAM, S., MACLEOD, B.A., YOSHIDA, N.R. & WALKER, M.J.A. (1991). Antiarrythmic properties of tedisamil (KC8857), a putative transient outward $K^+$ current blocker. *Br. J. Pharmacol.*, **102**, 13–18.

CHANDY, K.G.C. (1991). Simplified gene nomenclature. *Nature*, **352**, 26.

CHOI, K.L., ALDRICH, R.W. & YELLEN, G. (1991). Tetraethylammonium blockade distinguishes two inactivation mechanisms in voltage-activated $K^+$ channels. *Proc. Natl. Acad. Sci. USA.*, **88**, 5092–5095.

CHRISTIE, M.J., ADELMAN, J.P., DOUGLASS, J. & NORTH, R.A. (1989). Expression of a cloned rat brain potassium channel in *Xenopus* oocytes. *Science*, **244**, 221–224.

DEMO, S.D. & YELLEN, G. (1991). The inactivation gate of the *Shaker* $K^+$ channel behaves like an open channel blocker. *Neuron*, **7**, 743–753.

DREYER, F. (1990). Peptide toxins and potassium channels. *Rev. Physiol. Biochem. Pharmacol.*, **115**, 93–136.

DUKES, I.D., CLEEMAN, L. & MORAD, M. (1990). Tedisamil blocks the transient and delayed rectifier $K^+$ currents in mammalian cardiac and glial cells. *J. Pharmacol. Exp. Ther.*, **254,** 560–569.

FATHERAZI, S. & COOK, D.L. (1991). Specificity of Tetraethylammonium and Quinine for three K channels in insulin-secreting cells. *J. Membr. Biol.*, **120,** 105–114.

FOSTER, C.D., CHUNG, S., ZAGOTTA, W.N., ALDRICH, R.W. & LEVITAN, I.B. (1992). A peptide derived from the *Shaker* B $K^+$ channel produces short and long blocks of reconstituted $Ca^{2+}$-dependent $K^+$ channels. *Neuron*, **9,** 229–236.

HARVEY, A.L. & ANDERSON, A.J. (1991). Dendrotoxins: snake toxins that block potassium channels and facilitate transmitter release. In *Snake Toxins*. ed. Harvey, A.L. pp. 131–164. New York, Pergamon Press Inc.

HEGINBOTHAM, L. & MACKINNON, R. (1992). The aromatic binding site for tetraethylammonium ion on potassium channels. *Neuron*, **8,** 483–491.

HOGER, J.H., WALTER, A.E., VANCE, D., YU, L., LESTER, H.A. & DAVIDSON, N. (1991). Modulation of a cloned mouse brain potassium channel. *Neuron*, **6,** 227–236.

HOSHI, T., ZAGOTTA, W.N. & ALDRICH, R.W. (1990). Biophysical and molecular mechanisms of *Shaker* potassium channel inactivation. *Science*, **250,** 533–538.

HOSHI, T., ZAGOTTA, W.N. & ALDRICH, R.W. (1991). Two types of inactivation in *Shaker* $K^+$ channels: effects of alterations in the carboxy-terminal region. *Neuron*, **7,** 547–556.

HOUAMED, K., TEMPEL, B. & ALMERS, W. (1989). Mouse brain gene MBK-1 codes for a voltage-sensitive channel of the delayed rectifier type. *Soc. Neurosci. Abstr.*, **15,** 538.

ISACOFF, E.Y., JAN, Y.N. & JAN, L.Y. (1991). Putative receptor for the cytoplasmic inactivation gate in the *Shaker* $K^+$ channel. *Nature*, **353,** 86–90.

KAVANAUGH, M.P., VARNUM, M.D., OSBORNE, P.B., CHRISTIE, M.J., BUSCH, A.E., ADELMAN, J.P. & NORTH, R.A. (1991). Interaction between tetraethylammonium and amino acid residues in the pore of cloned voltage-dependent potassium channels. *J. Biol. Chem.*, **266,** 7583–7587.

KLUMPP, D.J., FARBER, D.B., BOWES, C., SONG, E.-J. & PINTO, L.H. (1991). The potassium channel MBK1 (Kv1.1) is expressed in the mouse retina. *Cell. Mol. Neurobiol.*, **11,** 611–622.

KOREN, G., LIMAN, E.R., LOGOTHETIS, D.E., NADAL-GINARD, B. & HESS, P. (1990). Gating mechanism of a cloned potassium channel expressed in frog oocytes and mammalian cells. *Neuron*, **2,** 39–51.

LEE, C.W.B., ALDRICH, R.W. & GLERASCH, L.M. (1992). Conformational studies of the N-terminal domain of the *Shaker* B $K^+$ ion channel by CD and NMR. *Biophys. J.*, **61,** A379.

MCFADZEAN, I. & ENGLAND, S. (1992). Properties of the inactivating outward current in single smooth muscle cells isolated from the rat anococcygeus. *Pflügers Arch.*, **421,** 117–124.

MCLARNON, J.G. & WANG, X.-P. (1991). Actions of cardiac drugs on a calcium-dependent potassium channel in hippocampal neurons. *Mol. Pharmacol.*, **39,** 540–546.

NEWLAND, C.F., ADELMAN, J.P., TEMPEL, B.L. & ALMERS, W. (1992). Repulsion between tetraethylammonium ions in cloned voltage-gated potassium channels. *Neuron*, **8,** 975–982.

NOAK, Th., EDWARDS, G., DIETMER, P., GREENGRASS, P., MORITA, T., ANDERSSON, P.-O., CRIDDLE, D., WYLLIE, M.G. & WESTON, A.H. (1992). The involvement of potassium channels in the action of ciclazindol in rat portal vein. *Br. J. Pharmacol.*, **106,** 17–24.

PFRUNDER, D. & KREYE, V.A.W. (1991). Tedisamil blocks single large-conductance $Ca^{2+}$-activated $K^+$ channels in membrane patches from smooth muscle cells of the guinea-pig portal vein. *Pflügers Arch.*, **418,** 308–312.

ROBERTSON, B. & OWEN, D. (1993). Actions of some blockers and the *Shaker* B 'inactivation' peptide on a mouse brain cloned potassium channel (MK-1) expressed in Chinese Hamster ovary (CHO) cells. *J. Physiol.*, **459,** 92P.

RUPPERSBERG, J.P., STOCKER, M., PONGS, O., HEINEMANN, S.H., FRANK, R. & KOENEN, M. (1991). Regulation of fast inactivation of cloned mammalian $I_K(A)$ channels by cysteine oxidation. *Nature*, **352,** 711–714.

SHENG, M., TSAUR, M.-L., JAN, Y.N. & JAN, L.Y. (1992). Subcellular segregation of two A-type $K^+$ channel proteins in rat central neurons. *Neuron*, **9,** 271–284.

SNYDERS, D.J., KNOTH, K.M., ROBERDS, S.L. & TAMKUN, M.M. (1992). Time-, voltage-, and state-dependent block by quinidine of a cloned human cardiac potassium channel. *Mol. Pharmacol.*, **41,** 322–330.

SOUTHAN, A.P. & OWEN, D.G. (1992). Dendrotoxins induce a form of long lasting synaptic potentiation in hippocampal pyramidal neurones. *Soc. Neurosci. Abst.*, **18,** 628.6.

SPRUCE, A.E., STANDEN, N.B. & STANFIELD, P.R. (1987). The action of external tetraethylammonium ions on unitary delayed rectifier potassium channels of frog skeletal muscle. *J. Physiol.*, **393,** 467–478.

STANSFELD, C., MARSH, S., PARCY, D., DOLLY, J.O. & BROWN, D. (1987). Mast cell degranulating peptide and dendrotoxin selectively inhibit a fast activating $K^+$ current and bind to common neuronal proteins. *Neurosci.*, **23,** 893–902.

STRONG, P.N. (1990). Potassium channel toxins. *Pharmacol. Ther.*, **46,** 137–162.

STUHMER, W. (1991). Structure-function studies of voltage-gated ion channels. *Annu. Rev. Biophys. Biochem.*, **20,** 65–78.

STUHMER, W., STOCKER, M., SAKMANN, B., SEEBURG, P., BAUMANN, A., GRUPE, A. & PONGS, O. (1988). Potassium channels expressed from rat brain cDNA have delayed rectifier properties. *FEBS Lett.*, **242,** 199–206.

TAGLIATELA, M., VANDONGEN, A.M.J., DREWE, J.A., JOHO, R.H., BROWN, A.M. & KIRSCH, G.E. (1991). Patterns of internal and external tetraethylammonium block in four homologous $K^+$ channels. *Mol. Pharmacol.*, **40,** 299–307.

TEMPEL, B.L., JAN, Y.N. & JAN, L.Y. (1988). Cloning of a probable potassium channel gene from mouse brain. *Nature*, **332,** 837–839.

TORO, L., STEFANI, E. & LATORRE, R. (1992). Internal blockade of a $Ca^{2+}$-activated $K^+$ channel by *Shaker* B inactivating 'ball' peptide. *Neuron*, **9,** 237–245.

WANG, S.-Y., CASTLE, N.A. & WANG, G.K. (1992). Identification of RBK-1 potassium channels in C6 astrocytoma cells. *Glia*, **5,** 146–153.

WAGONER, P.K. & OXFORD, G.S. (1990). Aminopyridines block an inactivating potassium current having slow recovery kinetics. *Biophys. J.*, **58,** 1481–1489.

ZAGOTTA, W.N., HOSHI, T. & ALDRICH, R.W. (1990). Restoration of inactivation in mutants of *Shaker* potassium channels by a peptide derived from ShB. *Science*, **250,** 568–571.

*(Received January 26, 1993*
*Accepted February 25, 1993)*

*Br. J. Pharmacol.* (1993), **109**, 736–738 © Macmillan Press Ltd, 1993

# Differential effects of BQ-123 against endothelin-1 and endothelin-3 on the rat vas deferens: evidence for an atypical endothelin receptor

Anthony Eglezos, Paola Cucchi, Riccardo Patacchini, **Laura Quartara, *Carlo Alberto Maggi & [1]Jacques Mizrahi

Pharmacology Department, Laboratori Guidotti S.p.A. Via Livornese 402, San Piero a Grado, 56122 Pisa; *Pharmacology Department and **Peptides Synthesis Lab. Chemistry Department, A. Menarini Pharmaceuticals S.r.L. Florence, Italy

**1** Endothelin-1 and endothelin-3 enhanced concentration-dependently the rat vas deferens twitch response to electrical stimulation, endothelin-1 being three times more potent. Sarafotoxin S6c was at least 200 times less active than endothelin-1.

**2** The response to endothelin was antagonized in a competitive manner by the supposedly selective $ET_A$ receptor antagonist, BQ-123 ($pA_2$: 7.0 ± 0.1). In contrast, the endothelin-1 concentration-response curve was only shifted two fold in the presence of 10 μM BQ-123, while no effect was observed at 1 μM.

**3** This evidence suggests the rat vas deferens contains an endothelin receptor not conforming to the $ET_A/ET_B$ receptor subtype classification so far proposed.

**Keywords:** Endothelin-1; endothelin-3; receptor subtypes; BQ-123; sarafotoxin S6c; rat vas deferens

## Introduction

The endothelins have a wide spectrum of biological actions, mediated through the interaction with at least two distinct receptor subtypes: $ET_A$ (Arai *et al.*, 1990) and $ET_B$ (Sakurai *et al.*, 1990). These receptor subtypes have been classified by the rank order of potency of the endogenous endothelins, endothelin-1 being at least ten times more active than endothelin-3 on $ET_A$ receptors, while being equally active on the non-selective $ET_B$ receptor. The existence of an additional subtype ($ET_C$) preferentially binding endothelin-3, has been proposed on bovine endothelial cells (Emori *et al.*, 1990). Recently, new selective ligands have become available for endothelin receptor characterization. Sarafotoxin S6c was described as a selective $ET_B$ receptor agonist (Williams *et al.*, 1991), and BQ-123, as a selective $ET_A$ receptor antagonist with very low affinity for $ET_B$ receptors (Ihara *et al.*, 1992; D'Orléans-Juste *et al.*, 1992). The pharmacological profile of the $ET_C$ receptor obtained with these new tools has not yet been reported.

On the basis of the rank order of agonist potency, facilitation of the rat vas deferens twitch response to endothelins has been attributed to activation of $ET_B$ receptors (Maggi *et al.*, 1989; Telemaque & D'Orléans-Juste, 1991). Because of recent data suggesting further heterogeneity of endothelin receptor subtypes (Harrison *et al.*, 1992), we have used both a selective agonist and antagonist in an attempt to characterize further the endothelin receptor mediating facilitation of the rat vas deferens twitch response.

## Methods

Male Sprague Dawley rats (Charles-River, 250–300 g) were killed by cervical dislocation and the vasa deferentia (pars prostatica) rapidly removed, cleaned and placed in tissue baths containing warm (37°C) oxygenated (95% $O_2$, 5% $CO_2$) Krebs solution. Activity was recorded isotonically (Ugo Basile, Italy) along the longitudinal axis (1.5 cm), under a resting tension of 0.5 g. The tissues were field stimulated sub-maximally (10 V, 0.25 ms pulse width, pulse interval of 200 ms, trains of 5 s every 60 s) by platinium electrodes connected to a Digit 3T stimulator. Under these conditions the twitch response could be abolished by 1 μM tetrodotoxin ($n = 4$; data not shown).

Following a 60–90 min equilibration period, cumulative concentration-response curves to endothelins were constructed (only one concentration-response curve was established per tissue). In studies with BQ-123, tissues were incubated with the antagonist for 30 min prior to initiation of agonist concentration-response curves. At concentrations up to 10 μM, BQ-123 had no effects, *per se*, on the twitch response.

Endothelin-1 and endothelin-3 were purchased from NovaBiochem (Switzerland), sarafotoxin S6c from Peninsula Laboratories (U.K.), and BQ-123, cyclo(D-Trp-D-Asp-Pro-D-Val-Leu) was synthesized by solid-phase methodology.

Results are presented as mean ± s.e.mean of at least three separate experiments. $EC_{50}$ values were calculated by the Macintosh Allfit programme, and $pA_2$ values were calculated by Schild plot analysis.

## Results

Endothelin-1 and endothelin-3 enhanced in a concentration-dependent manner the rat vas deferens twitch response, with a characteristic long lasting effect which was resistant to washing out. Threshold concentrations for both peptides were between 0.1–0.5 nM.

Maximal stimulatory effects (296 and 262% above basal) were obtained with a concentration of 100 nM of either peptide, and the $EC_{50}$ values were 9.0 and 25.0 nM respectively (Figure 1). Sarafotoxin S6c exhibited very weak agonist activity, with a threshold stimulatory effect at 500 nM (Figure 1), and an increase of 60% above basal at the maximum concentration tested (1 μM).

BQ-123 (1 μM), had no significant effects on the endothelin-1-induced stimulation of the vas deferens twitch response (Figure 2a) whereas at 10 μM, the threshold response was shifted from 0.1 to 0.5 nM, the $EC_{50}$ from 8.0 to 18.0 nM and the maximal response appeared to be somewhat decreased.

BQ-123 antagonized in a competitive manner the

[1] Author for correspondence at present address: ITALFARMACO Research Center, Pharmacology Department, Via Dei Lavoratori, 54, Cinisello Balsamo 20092, Milan, Italy.

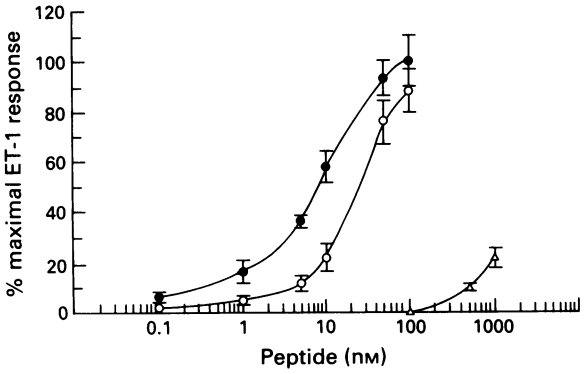



**Figure 1** Concentration-response curves to endothelin-1 (●), endothelin-3 (○) and sarafotoxin S6c (△) for facilitation of the twitch response of rat vas deferens to electrical stimulation. Results are presented as % of the maximal response to endothelin-1. Each point represents the mean ± s.e.mean of at least three determinations.

endothelin-3-mediated twitch enhancement of the rat vas deferens as assessed by Schild plot analysis ($pA_2$:7.0 ± 0.12; slope = 1.09; Figure 2b). Further, the maximal response to endothelin-3 was not affected at any BQ-123 concentrations.

## Discussion

Sarafotoxin S6c, a selective $ET_B$ receptor agonist (Williams *et al.*, 1991) and BQ-123, selective $ET_A$ receptor antagonist (Ihara *et al.*, 1992) were used in an attempt to characterize further the endothelin receptor population present on the rat vas deferens pars prostatica. Endothelin-1 and endothelin-3 induced similar maximal facilitatory effects on the twitch response to field stimulation, with endothelin-1 being almost three times more potent. Under the currently accepted classification scheme (Arai *et al.*, 1990; Sakurai *et al.*, 1990), this would be consistent with the receptor being of the isopeptide-non-selective $ET_B$ type. However, we have found that in the rat vas deferens sarafotoxin S6c induced only weak agonist activity, which would not be consistent with an action on the classical, sarafotoxin S6c-sensitive $ET_B$ receptor (Williams *et al.*, 1991).

In the absence of a selective $ET_B$ receptor antagonist, BQ-123, introduced as a selective antagonist at the $ET_A$ receptor (Ihara *et al.*, 1992), was used. We have shown that BQ-123 antagonizes competitively the endothelin-1-mediated vasoconstriction of the endothelium-denuded rat thoracic aorta to yield a $pA_2$ value of 7.0 ± 0.1, consistent with that described for the porcine aorta ($pA_2$:7.4; Ihara *et al.*, 1992). Remarkably, on the rat vas deferens, BQ-123 was inactive at 1 μM as an antagonist of endothelin-1 and at the higher concentration (10 μM) only a weak antagonism was observed. This antagonism appeared to be non-competitive, as previously observed in neuroblastoma cells (Hiley *et al.*, 1992), since the maximal effect was significantly reduced. Conversely, BQ-123 was a reasonably potent ($pA_2$ = 7.0) competitive antagonist of the endothelin-3 response. Previous studies have shown BQ-123 to be a selective $ET_A$ receptor

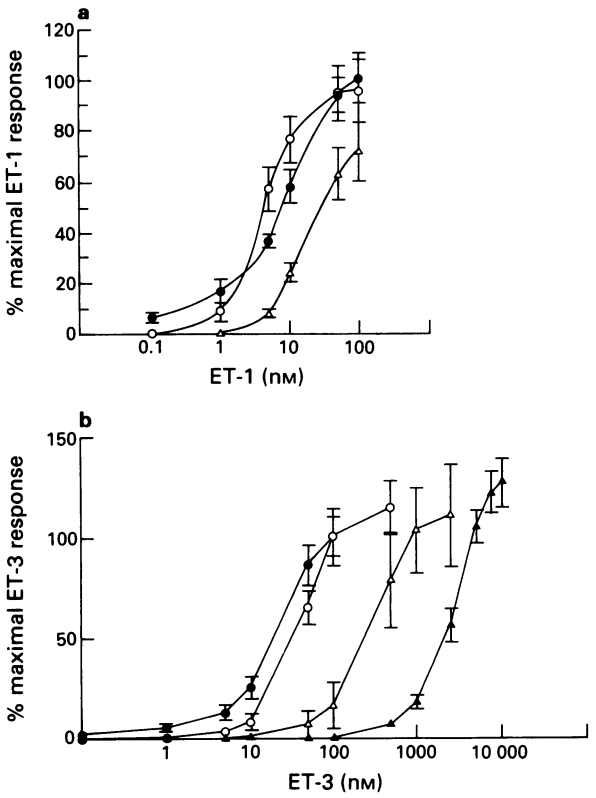



**Figure 2** Concentration-response curves to: (a), endothelin-3 in the absence (●) and presence of BQ-123, 0.1 μM (○) and 10 μM (△) and to: (b) endothelin-3 in the absence (●) and presence of BQ-123, 0.1 μM (○), 1 μM (△) and 10 μM (▲) for facilitation of the twitch response of the rat vas deferens to electrical stimulation. Results are presented as % of the maximal response to endothelin-1 or endothelin-3 in the absence of BQ-123. Each point represents the mean ± s.e.mean of at least three determinations.

antagonist with low affinity for $ET_B$ receptors (D'Orléans-Juste *et al.*, 1992; Ihara *et al.*, 1992). The fact that in the rat vas deferens BQ-123 had a preferential antagonist effect on the endothelin-3 response, suggests that the endothelin-1 and endothelin-3-mediated enhancement of the twitch response to electrical stimulation could be mediated by a receptor population distinct from either $ET_A$ or $ET_B$. Taken together with the weak agonist activity of sarafotoxin S6c, our findings indicate that the pharmacology of endothelin receptor(s) in the rat vas deferens cannot easily be accommodated within the $ET_A/ET_B$ classification. The possibility that the $ET_C$, non $ET_A/ET_B$ receptor, tentatively described in cultured bovine endothelial cells (Emori *et al.*, 1990) or the site mediating contraction of porcine coronary arteries (Harrison *et al.*, 1992), may be similar to that found in the rat vas deferens deserves further consideration.

The technical assistance of Moreno Bachi is acknowledged. This work was supported by grant no. 55202 from IMI.

## References

ARAI, H., ARAMORI, I., OHKUBO, H. & NAKANISHI, S. (1990). Cloning and expression of cDNA encoding an endothelin receptor. *Nature*, **348**, 732–735.

D'ORLEANS-JUSTE, P., TELEMAQUE, S., CLAING, A., IHARA, M. & YANO, M. (1992). Human big-endothelin-1 and endothelin-1 release prostacyclin via the activation of ET1 receptors in the rat perfused lung. *Br. J. Pharmacol.*, **105**, 773–775.

EMORI, T., HIRATA, Y. & MARUMO, F. (1990). Specific receptors for endothelin-3 in cultured bovine endothelial cells and its cellular mechanism of action. *FEBS Lett.*, **263**, 261–264.

HARRISON, V.J., RANDRIANTSOA, A. & SCHOEFFTER, P. (1992). Heterogeneity of endothelin-sarafotoxin receptors mediating contraction of pig artery. *Br. J. Pharmacol.*, **105**, 511–513.

HILEY, C.R., COWLEY, D.J., PELTON, J.T. & HARGREAVES, A.C. (1992). BQ-123, cyclo(D-Trp-D-Asp-Pro-D-Val-Leu), is a non-competitive antagonist of the actions of endothelin-1 in SK-N-MC human neuroblastoma cells. *Biochem. Biophys. Res. Commun.*, **184,** 504–510.

IHARA, M., NOGUCHI, K., SAEKI, T., FUKORODA, T., TSUCHIDA, S., KIMURA, S., FUKAMI, T., ISHIKAWA, K., NISHIKIBE, M. & YANO, M. (1992). Biological profiles of highly potent novel endothelin antagonists selective for the $ET_A$ receptor. *Life Sci.*, **50,** 247–255.

MAGGI, C.A., GIULIANI, S., PATACCHINI, R., ROVERO, P., GIACCHETTI, A. & MELI, A. (1989). The activity of peptides of the endothelin family in various mammalian smooth muscle preparations. *Eur. J. Pharmacol.*, **174,** 23–31.

SAKURAI, T., YANAGISAWA, M., TAUWA, Y., MIYAZAKI, H., KIMURA, S., GOTO, K. & MASAKI, T. (1990). Cloning of a cDNA encoding a non-isopeptide selective sub-type of the endothelin receptor. *Nature*, **348,** 732–735.

TELEMAQUE, S. & D'ORLEANS-JUSTE, P. (1991). Presence of a phosphoramidon-sensitive endothelin-converting enzyme which converts Big-Endothelin-1, but not Big-Endothelin-3 in the rat vas deferens. *Naunyn-Schmiedeb. Arch. Pharmacol.*, **344,** 500–507.

WILLIAMS, D.L. Jr., JONES, K.L., PETTIBONE, D.J., LIS, E.V. & CLINESCHMIDT, B.V. (1991). Sarafotoxin S6c: an agonist which distinguishes between endothelin receptor subtypes. *Biochem. Biophys. Res. Commun.*, **175,** 556–561.

*(Received June 22, 1992*
*Revised February 19, 1993*
*Accepted February 24, 1993)*

*Br. J. Pharmacol.* (1993), **109**, 739–747 © Macmillan Press Ltd, 1993

# Inhibition of nitric oxide synthesis reveals non-cholinergic excitatory neurotransmission in the canine proximal colon

C. William Shuttleworth, Kenton M. Sanders & [1]Kathleen D. Keef

Department of Physiology, University of Nevada School of Medicine, Reno, NV 89557, U.S.A.

**1** Neuromuscular transmission in the circular muscle of the canine proximal colon was examined, in the presence and absence of nitric oxide synthase inhibitors, by use of mechanical and intracellular microelectrode recording techniques.

**2** Electrical field stimulation (EFS; 0.1–20 HZ) produced frequency-dependent contractions of circular muscle strips which reached a maximum at 15 Hz. These reponses were enhanced by $N^G$-monomethyl-L-arginine (L-NMMA; 300 μM) and reduced by atropine (1 μM). The effects of L-NMMA were reversed by L-arginine (3 mM). All responses to EFS were abolished by tetrodotoxin (1 μM).

**3** In the presence of atropine, phentolamine and propranolol (all at 1 μM; 'non-adrenergic, non-cholingergic (NANC) conditions'), EFS evoked frequency-dependent inhibition of phasic contractions which reached a maximum at 5 Hz. At higher frequencies of EFS, inhibition diminished, and these responses were followed by post-stimulus excitation.

**4** Under NANC conditions and in the presence of L-$N^G$-nitroarginine methyl ester (L-NAME; 200 μM), EFS evoked contractions at frequencies of 5 Hz or greater. These contractions were reduced by co-incubation with L-arginine (2 mM) and abolished by tetrodotoxin (1 μM).

**5** In the presence of atropine (1 μM), EFS (5–20 Hz) caused frequency-dependent inhibition of electrical slow waves. In the presence of L-NAME (100 μM) and atropine, the inhibitory response to EFS was abolished and an increase in slow wave duration was seen at stimulation frequencies greater than 5 Hz. The effects of EFS on slow wave duration were abolished by tetrodotoxin (1 μM).

**6** Atropine-resistant contractions to EFS were enhanced by indomethacin (10 μM) and reduced or abolished by the non-selective $NK_1/NK_2$ tachykinin receptor antagonist D-$Pro^2$, D-$Trp^{7,9}$ SP, and by the selective $NK_2$ receptor antagonist MEN 10,376 (10 μM).

**7** Exogenous tachykinins mimicked non-cholinergic excitatory electrical and mechanical responses. The rank order of potency for contraction was neurokinin A > neurokinin B > substance P, suggesting a predominance of the $NK_2$ sub-type of tachykinin receptors on colonic smooth muscle cells. Low concentrations of neurokinin A also increased the amplitude and duration of electrical slow waves.

**8** These results suggest that: (i) in previous studies, non-cholinergic excitatory responses were masked by the simultaneous release of NO; (ii) non-cholinergic excitatory responses occur throughout the period of stimulation and are not manifest only as 'rebound' excitation; (iii) one or more tachykinins, possibly, acting via $NK_2$ receptors, may mediate non-cholinergic excitatory responses.

**Keywords:** Tachykinins; neurokinin A; substance P; arginine analogues; enteric nervous system; gastrointestinal motility, smooth muscle, nitric oxide; colon; neuromuscular transmission

## Introduction

Neurotransmission to gastrointestinal smooth muscle is accomplished by the release of a variety of transmitters from intrinsic neurones. Recently, nitric oxide (NO) has been shown to participate in enteric inhibitory transmission (see Rand 1992; Sanders & Ward 1992 for reviews). Adenosine 5'-triphosphate (ATP) and vasoactive intestinal peptide (VIP) are also candidate transmitters, possibly released by the same population of inhibitory neurones that release NO (see reviews Hoyle & Burnstock, 1989; Furness *et al.*, 1992). Acetylcholine (ACh) has long been known to be a primary excitatory neurotransmitter, but there is also strong evidence that other excitatory transmitters are released from enteric motoneurones. The best candidates for these responses are one or more members of the tachykinin family of peptides. For example, substance P and related tachykinins are contained in cholinergic motoneurones supplying the longitudinal muscle of the guinea-pig ileum (Frano *et al.*, 1979; Brookes *et al.*, 1992), and these peptides can be released and cause depolarization and contraction of ileal smooth muscle (Neil *et al.*, 1983; Donnerer *et al.*, 1984; Costa *et al.*, 1985). Non-cholinergic excitatory transmission is typically more prominent at higher stimulus intensities and this is consistent with reports that higher stimulus frequencies are required to release substance P-like peptides from isolated strips of ileum (Baron *et al.*, 1983; Holzer, 1984).

There is biochemical evidence suggesting that tachykinins are present in canine colonic muscles (Brodin *et al.*, 1981; McDonald *et al.*, 1990) and tachykinin-like immunoreactivity has been localized in enteric neurones that supply the muscularis (Tange, 1983; Furness *et al.*, 1990). There is also autoradiographic evidence that tachykinin binding sites exist on colonic muscle cells (Mantyh *et al.*, 1988) and it is likely that these receptors mediate the electrical and contractile responses to agonists such as substance P in these muscles (Huizinga *et al.*, 1984; Keef *et al.*, 1992). Despite the presence of the neuromuscular apparatus necessary to produce tachykinin-mediated excitation, there are surprisingly few studies describing functional responses of this system (e.g. Gonda *et al.*, 1988).

Non-cholinergic excitatory neurotransmission has been difficult to resolve because these responses are typically obscured by the temporal overlap of enteric inhibitory (i.e. non-cholinergic, non-adrenergic (NANC)) influences. Non-cholinergic excitatory input has usually been observed as a 'rebound' response following cessation of nerve stimulation, yet it is quite possible that the influence of non-cholinergic excitatory neurotransmission occurs throughout the period of

[1] Author for correspondence.

stimulation. Since NO has been shown to mediate enteric inhibitory neurotransmission in the canine colon (Dalziel *et al.*, 1991; Thornbury *et al.*, 1991; Ward *et al.*, 1992b; Huizinga *et al.*, 1992), this influence can be abolished by addition of arginine analogues that inhibit nitric oxide synthase (Dalziel *et al.*, 1991). In the present study we have used a combination of atropine and arginine analogues to unmask and characterize non-cholinergic excitatory neural responses in the circular muscle of the proximal colon. We have also attempted to determine whether tachykinins may be responsible for this non-cholinergic excitatory neurotransmission.

## Methods

Mongrel dogs of either sex were obtained from vendors licensed by the United States Department of Agriculture. The use of dogs for these experiments was approved by the Institutional Animal Care and Use Committee. The animals were killed with pentobarbitone sodium (45 mg $kg^{-1}$). The abdomen was opened and a segment of proximal colon 6–14 cm from the ileocaecal sphincter was removed. Other organs were also removed and used in several other approved investigations. The colon was opened along the mesenteric border, washed of remaining faecal material and pinned out in a dissecting dish containing oxygenated Krebs-Ringer bicarbonate solution.

### *Mechanical experiments*

Strips (approx. 1 mm × 10 mm × 1.3 mm) of muscle were cut parallel to the circular muscle fibres, and the mucosa was removed by sharp dissection. These strips were attached to a Gould strain gauge and maintained in Krebs solution at 37°C. A resting force of 1.0 g was applied to the muscles and the muscles were equilibrated for 2 h. ACh (1 μM) was applied at 15 min intervals until a stable response was observed. Peak contractile amplitude was determined by a brief exposure to ACh (100 μM).

The influences of enteric inhibitory nerves (Sanders & Smith, 1986a,b) were measured on spontaneous contractile activity or on phasic contractions elicited in quiescent preparations by histamine (0.1–3 μM). The mean amplitude of spontaneous contractions or those initiated by histamine was 0.4 ± 0.07 g ($n = 9$), which represented approximately 2.5% of the maximum ACh-induced contraction (15.7 ± 0.9 g, $n = 27$). The ability to elicit either neural inhibition or rebound excitation was not affected by histamine. To quantitate enteric inhibitory neural responses, all contractile peaks during a 3 min period of time before nerve stimulation were averaged and compared to the average amplitude of contractile peaks observed during nerve stimulation.

Responses to nerve stimulation were measured at 10–30 min intervals with longer periods interposed between higher frequencies of nerve stimulation. In some tissues non-cholinergic excitatory responses exhibited tachyphylaxis to repeated stimulation at a constant stimulus frequency. For this reason the effects of indomethacin and tachykinin receptor antagonists were tested only on muscles in which repeated responses were reproducible.

### *Electrophysiological experiments*

Muscle strips were pinned to the floor of an electrophysiological chamber in a manner to expose a view of the entire thickness of the muscularis externa. The muscles were constantly perfused with warmed, oxygenated Krebs solution. Temperature was monitored with a small thermistor probe (YSI 400) and was maintained at 37.5 ± 0.5°C. Muscle strips were allowed to equilibrate for approximately 120 min before experiments were begun.

Muscle cells near the submucosal surface of the circular smooth muscle layer were impaled with glass microelectrodes filled with 3 M KCl solution and having resistances of 30–50 MΩ. Impalements were accepted based on previously discussed criteria (Sanders & Smith, 1986a). Membrane potential was measured with a high input impedance electrometer (WPI S-7100) and outputs were displayed on an oscilloscope (Tektronix 5111A). Analogue electrical signals were recorded on magnetic tape (Hewlett Packard 3964A) and reproduced on chart paper (Gould 2200).

### *Solutions and drugs*

The Krebs solution used in this study contained (in mM): NaCl 118.5, KCl 4.7, $CaCl_2$, 2.5, $MgCl_2$ 1.2, $NaHCO_3$ 23.8, $KH_2PO_4$ 1.2, dextrose 11. This solution had a pH of 7.4 at 37.5°C when bubbled to equilibrium with 95% $O_2$–5% $CO_2$. Drugs used in this study included subtance P, MEN 10,376 ([Tyr$^5$, D-Trp$^{6,8,9}$, Lys$^{10}$]-NKA(4-10)), and D-Pro$^2$, D-Trp$^{7,9}$ SP (all from Peninsula). Neurokinin A, neurokinin B, acetylcholine chloride, tetrodotoxin, atropine sulphate, phentolamine hydrochloride, propranolol hydrochloride, histamine dihydrochloride, L-N$^G$-nitroarginine methyl ester (L-NAME), N$^G$-monomethyl-L-arginine (L-NMMA), L-arginine were all from Sigma.

### *Analysis of data*

All excitatory responses were tabulated as the peak contractile response. The $n$ values given in this study represent the number of animals. Averaged data are expressed as means ± s.e.mean. Differences between data sets were determined by Student's $t$ test.

## Results

### *Mechanical experiments*

*Responses to electrical field stimulation* In the absence of any antagonists, electrical field stimulation (EFS, 2 min trains; 1–20 Hz) results in frequency-dependent contractions of muscle strips. Responses consisted of a series of phasic contractions at approximately the same frequency as the spontaneous contractile activity (Figure 1a). These responses were qualitatively similar to reponses elicited by exogenous ACh (see Keef *et al.*, 1992). At 20 Hz contractions were 81.7 ± 7.2% ($n = 8$) of the response to a maximal concentration of ACh (100 μM). Tetrodotoxin (1 μM) abolished responses to EFS ($n = 4$). L-NMMA (300 μM; 30 min) augmented the amplitude of nerve-stimulated contractions at frequencies of 1 to 15 Hz (Figure 1b). L-NMMA was used as an antagonist of NO synthesis in these experiments because L-NAME has been shown to block muscarinic receptors in this and other smooth muscles (Buxton *et al.*, 1993). Figure 2 summarizes responses before and after L-NMMA. The effects of L-NMMA were reversed by L-arginine (3 mM, 20 min, $n = 3$, see Figure 4a).

When muscles were exposed to a combination of atropine, phentolamine and propranolol (each 1 μM; 'NANC' conditions), EFS (0.1–10 Hz) caused a frequency-dependent reduction in the amplitude of phasic contractions (Figure 3a). The frequency-response relationship was biphasic, with an increase in inhibition observed between 0.1 and 5 Hz, a reduction in inhibition at 10 Hz, and usually excitation above 10 Hz. A frequency-response curve constructed from averaged data is shown in Figure 3b. After cessation of stimulation at 10 and 20 Hz, 'rebound contractions' were observed in 9 of 11 preparations (see Figure 3a). Rebound contractions reached an amplitude of 21.9 ± 2.5% ($n = 5$) of the maximal response to ACh at 20 Hz (Figure 3c). Nerve-mediated inhibition was blocked by L-NAME (200 μM) revealing underlying excitation (see below) and inhibition was restored by L-arginine (2 mM; 20 min, $n = 3$) in the continued presence of L-NAME (Figure 4b).

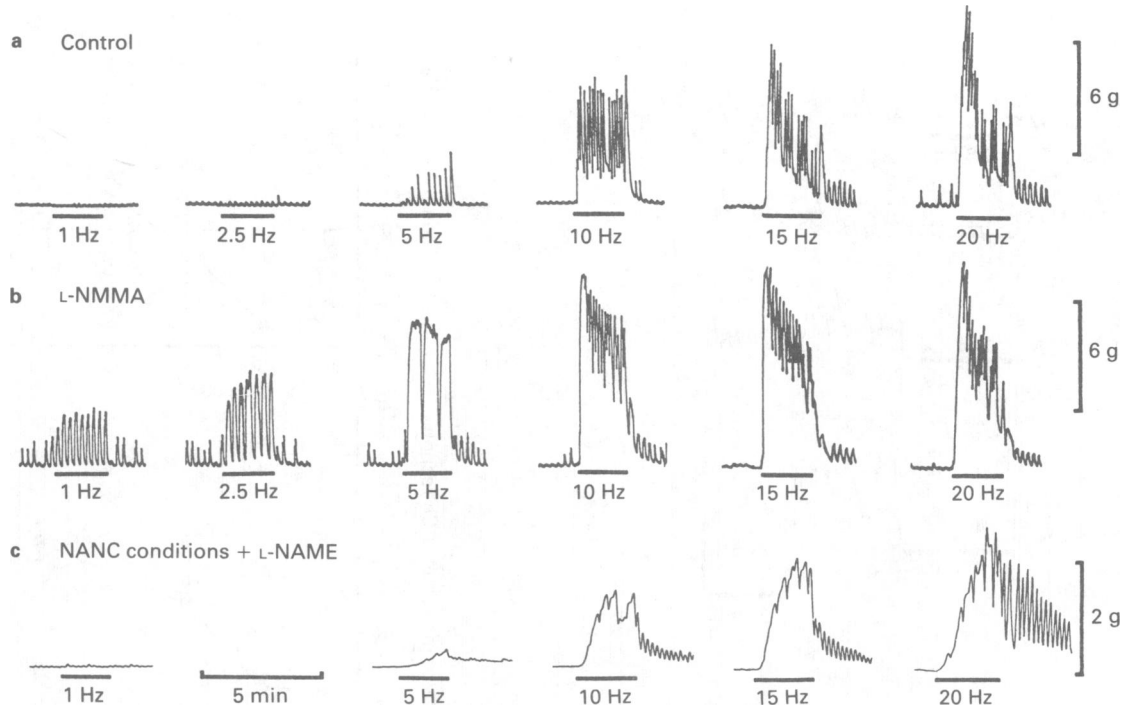



**Figure 1** Contractile responses to electrical field stimulation (1 to 20 Hz): (a) shows control responses in the absence of antagonists. Excitatory responses dominated, and could be elicited at frequencies of 5 Hz and above. (b) Shows responses of the same muscle strip after removing the influence of enteric inhibitory nerves by addition of $N^G$-monomethyl-L-arginine (L-NMMA; 300 μM). As previously reported, arginine analogues that inhibit nitric oxide synthesis caused an enhancement of spontaneous activity (Ward *et al.*, 1992a). Under these conditions, frequency-dependent excitatory responses were noted at all frequencies tested. (c) Shows responses of another muscle strip after addition of 'non-adrenergic, non-cholinergic' solution (containing atropine, phentolamine, and propranolol; all at 1 μM) and L-$N^G$-nitroarginine methyl ester (L-NAME; 200 μM) to unmask the non-cholinergic excitatory component of the response. Note contractile responses were elicited at frequencies of 5 Hz and above.

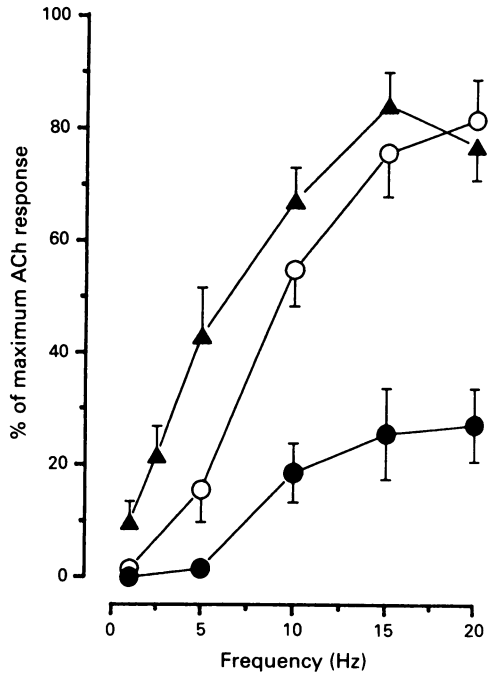



**Figure 2** Frequency-response relationships for excitatory effects of electrical field stimulation: (○) are control responses in the absence of antagonists; (▲) are excitatory responses after removal of the influence of nitric oxide-dependent inhibition by addition of $N^G$-monomethyl-L-arginine (L-NMMA); (●) are responses after adrenergic, cholinergic and NO-dependent responses have been antagonized (see text and Figure 1 for details). Data are means ± s.e.mean; $n = 6-11$.

Following 30 min of exposure to L-NAME (200 μM) under NANC conditions, EFS elicited contractile responses that were characterized by prolonged phasic contractions (Figure 1c). After cessation of the stimulus the contractions declined in amplitude over a period of several minutes. Figure 2 summarizes responses to EFS in preparations treated with antagonists of adrenergic, cholinergic and NO-dependent neurotransmission. The remaining responses are defined as non-cholinergic excitatory responses. The amplitudes of non-cholinergic excitatory responses were significantly less than contractions evoked in the absence of any antagonists (Figure 2). For example, at 20 Hz the non-cholinergic excitatory responses were 27.2 ± 6.5% ($n = 7$) of the maximal ACh contraction; contractions elicited at 20 Hz in the absence of antagonists averaged 81.7 ± 7.2% ($n = 8$) of the maximal ACh contraction.

The contractile effects of substance P (SP), neurokinin B (NKB) and neurokinin A (NKA) were compared in the presence of atropine. Muscles were exposed to concentrations of tachykinins ranging from 0.1 nM to 1.4 μM with 30 min of wash in Krebs solution between exposures. Each muscle was exposed to no more than 3 concentrations of a given tachykinin. These compounds caused contractile responses that consisted of prolonged phasic contractions, similar to non-cholinergic excitatory nerve responses. The order of potency for these compounds was NKA > NKB > SP. Figure 5 shows typical responses to the tachykinins and averaged concentration-response relationships.

The effects of tachykinin receptor antagonists on non-cholinergic excitatory responses and responses to NKA were also studied. The non-selective $NK_1/NK_2$ tachykinin receptor antagonist, D-$Pro^2$, D-$Trp^{7,9}$ SP (Buck & Schatzer 1988; Shuttleworth *et al.*, 1991) reduced non-cholinergic excitatory responses (10–15 Hz) to 25 ± 14% ($n = 3$) of their control amplitude. Addition of a selective $NK_2$ receptor antagonist,

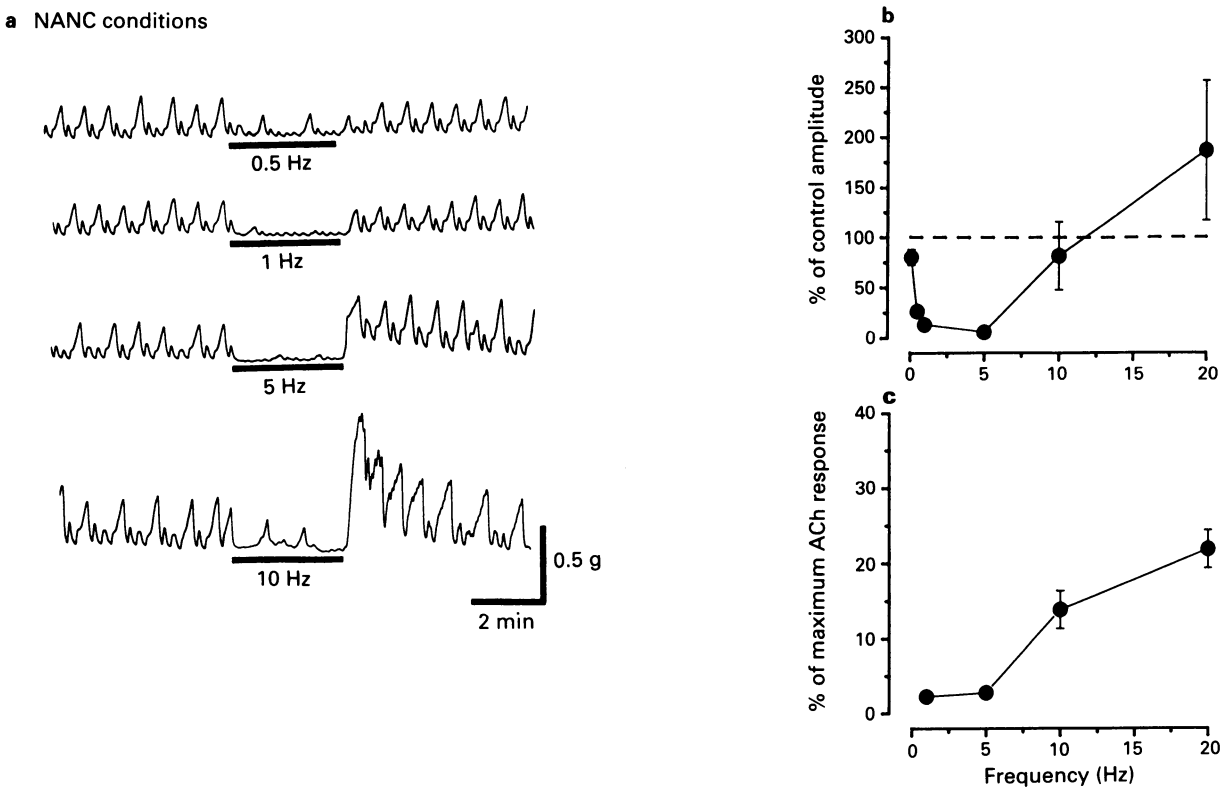



**Figure 3** Effects of electrical field stimulation (EFS) under 'non-adrenergic, non-cholinergic' (NANC) conditions. Phasic contractions in (a) were induced in this muscle strip by the addition of histamine (0.2 μM). EFS elicited frequency-dependent inhibition at frequencies of 0.5 Hz and above. The response was characterized by inhibition during the period of stimulation and a 'rebound' excitation immediately after stimulation at frequencies of 5 Hz and above. (b) Shows a summary of inhibitory responses ($n = 6-10$). Inhibitory responses reached a maximum at 5 Hz. Dotted line denotes level of the control response before EFS. (c) Shows a summary of 'rebound' excitatory responses ($n = 5-9$). Data in (b) and (c) are means ± s.e.mean.

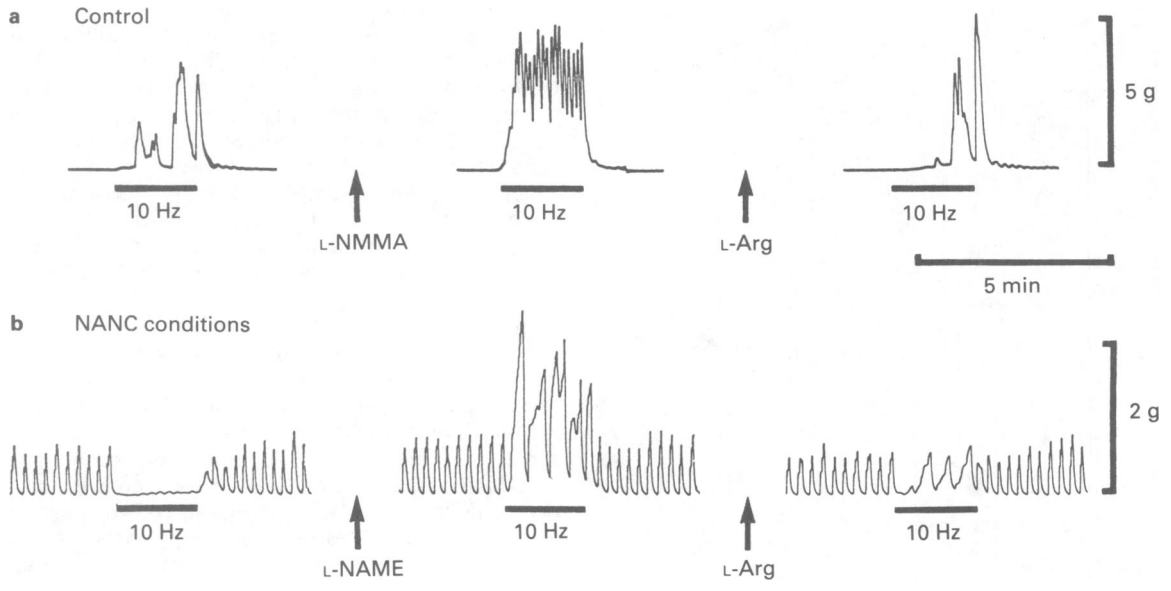



**Figure 4** Effects of L-arginine (L-Arg) on the actions of arginine analogues. (a) Shows representative excitatory responses to electrical field stimulation (EFS; 10 Hz) before addition of antagonists (control) and after $N^G$-monomethyl-L-arginine (L-NMMA; 300 μM). As shown in Figure 1, L-NMMA, enhanced the amplitude of the contractile response to EFS. This enhancement was reversed by subsequent addition of L-Arg (3 mM; in continued presence of L-NMMA), as shown in the third response in (a). (b) Shows inhibitory responses elicited by EFS under 'non-adrenergic, non-cholinergic' conditions. L-$N^G$-nitroarginine methyl ester (L-NAME; 200 μM) blocked the inhibitory response, unmasking a non-cholinergic excitatory response. This effect was reversed by addition of L-Arg (2 mM; in the continued presence of L-NAME).

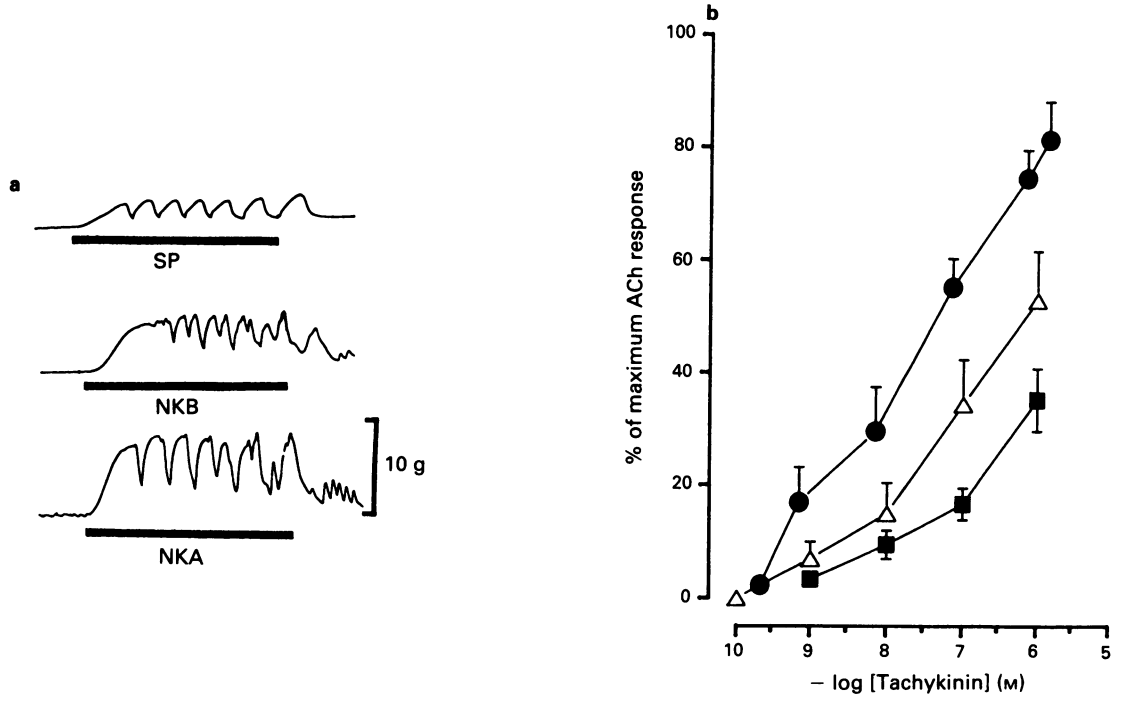



**Figure 5** Contractile effects of tachykinins: (a) shows responses of one muscle strip to a 4 min exposure to substance P (SP), neurokinin B (NKB) and neurokinin A (NKA) (all at 1 μM). Panel (b) Shows concentration-response relationships for SP (■; $n = 9-11$), NKB (△; $n = 3-8$) and NKA (●; $n = 3-10$). These responses were elicited in the presence of atropine (1 μM). Data points are means ± s.e.mean.

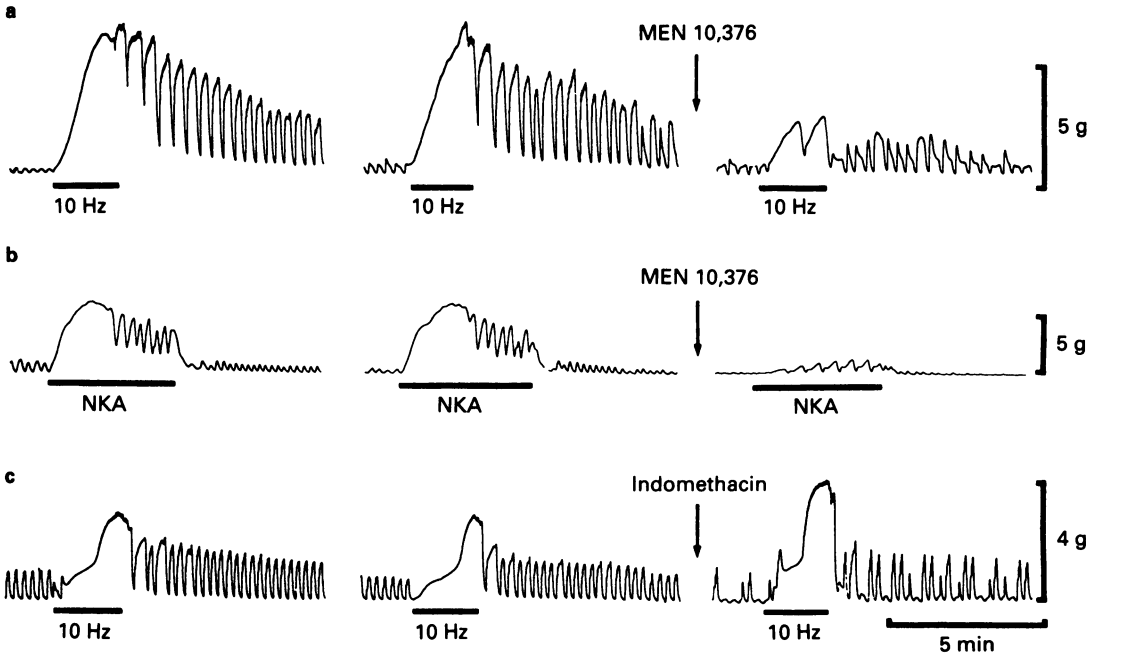



**Figure 6** Effects of tachykinin antagonist MEN 10,376 and indomethacin on non-cholinergic excitatory and neurokinin A (NKA) responses. (a) Shows 2 successive responses to EFS (10 Hz) in the presence of 'non-adrenergic, non-cholinergic' (NANC) conditions and L-$N^G$-nitroarginine methyl ester (L-NAME; 200 μM). Approximately 30 min was allowed between responses to minimize tachyphylaxis. Then MEN 10,376 (10 μM) was added for 20 min. The response to EFS in the presence of MEN 10,376 was greatly attenuated. (b) Shows a similar protocol in another muscle strip that was exposed repeatedly to NKA (0.07 μM). Atropine (1 μM) was present during NKA responses. MEN 10,376 also inhibited NKA responses. (c) Shows 2 successive responses to EFS (10 Hz) in the presence of NANC conditions and L-NAME. After the second response, the muscle was exposed to indomethacin for 30 min. Indomethacin increased the amplitude of the non-cholinergic excitatory response.

MEN 10,376 (Maggi et al., 1991; 10 μM) caused a transient stimulation of phasic contraction, but this response decreased to control levels with continued exposure to the drug. MEN 10,376 (10 μM; 20 min) reduced the amplitude of non-cholinergic excitatory nerve responses (10–15 Hz, 2 min train) to 25 ± 9% ($n = 5$) of their control amplitude. MEN 10,376 also reduced responses to NKA (10 nM and 70 nM) to 9 ± 1% and 39 ± 11% ($n = 3$) of their control amplitude, respectively (Figure 6a,b). To determine whether the non-cholinergic excitatory responses were affected by the synthesis of eicosanoids, we tested the effects of indomethacin (10 μM; 30 min). Indomethacin enhanced the amplitude of the non-cholinergic excitatory responses (10–15 Hz) from 24 ± 3% to 33 ± 3.6% of a maximum ACh contraction ($n = 5$, Figure 6c).

### *Electrophysiological experiments*

The mechanism of non-cholinergic excitatory nerve responses was investigated in a series of intracellular electrophysiological experiments. Cells near the submucosal surface of the circular muscle layer were impaled in muscles from 12 dogs. Resting membrane potential (RMP) averaged −79 ± 0.8 mV. Spontaneous slow waves were recorded in all preparations. The upstroke of depolarization was 51 ± 1.6 mV, plateau amplitude 45 ± 1.4 mV, and duration 4.5 ± 0.4s. These values are consistent with previously reported electrical activity recorded from the canine colon (Smith et al., 1987).

Previous studies have demonstrated cholinergic (Sander & Smith, 1986a) and NANC inhibitory (Ward et al., 1992b) neural responses in canine colonic muscles. In the present study we tested neural effects in the presence of atropine (1 μM), and in the absence and presence of L-NAME (100 μM). Before L-NAME, EFS at 5 and 10 Hz (10 s; 0.3 or 0.5 ms duration pulses) caused inhibition of slow waves during the period of stimulation and a post-stimulus enhancement in slow wave amplitude and duration (Figure 7a). These results are consistent with previous findings (Ward et al., 1992b). At 20 Hz, excitation was observed during EFS, even in the absence of L-NAME (consistent with contractility data). In the presence of L-NAME, EFS did not cause inhibition of slow waves. At 10 Hz or greater, EFS caused prolongation of slow waves during the stimulus (Figure 7b). The excitatory effect persisted after the termination of stimuli. These electrical effects are consistent with the enhancement in amplitude and duration of phasic contractions observed in mechanical studies. Responses to EFS were blocked by TTX (1 μM; $n = 5$). Table 1 summarizes effects of EFS on slow waves.

**Table 1** Effects of electrical field stimulation (EFS) on duration of electrical slow waves

| | *Control slow wave duration* (s) | *Slow wave duration during EFS* (s) | |
|---|---|---|---|
| *Atropine* (1 μM) | | | |
| 5 Hz | 4.0 ± 0.3 | 2.4 ± 0.4 | $P<0.01$ (7) |
| 10 Hz Initial[a] | 3.7 ± 0.3 | 1.7 ± 0.4 | $P<0.05$ (5) |
| | 4.0 ± 0.3 | 9.8 ± 2.2 | $P<0.05$ (7) |
| 20 Hz Initial[a] | 3.7 ± 0.4 | 2.0 ± 0.9 | NS (4) |
| | 3.9 ± 0.3 | 24.9 ± 1.3 | $P<0.001$ (7) |
| *Atropine* + *L-NAME* (100 μM) | | | |
| 5 Hz | 4.4 ± 0.2 | 5.3 ± 0.5 | NS (8) |
| 10 Hz[b] | 3.9 ± 0.2 | 12.6 ± 2.4 | $P<0.01$ (8) |
| 20 Hz[b] | 4.1 ± 0.5 | 28.0 ± 1.3 | $P<0.001$ (8) |
| *Atropine* + *L-NAME* + *TTX* (1 μM) | | | |
| 5 Hz | 4.5 ± 0.3 | 4.2 ± 0.3 | NS (4) |
| 10 Hz | 4.3 ± 0.3 | 4.1 ± 0.4 | NS (5) |
| 20 Hz | 4.0 ± 0.1 | 4.2 ± 0.6 | NS (5) |

[a]In the presence of atropine alone, EFS at 10 and 20 Hz often resulted in a shortened slow wave, followed by a longer slow wave during the period of stimulation (see Figure 7). In preparations where this was seen, values are given for the duration of Initial slow wave seen during the period of EFS. The second value represents mean data for the second slow wave initiated during the period of stimulation, together with results from preparations where only a single broad slow wave was initiated during the period of stimulation. [b] In the presence of L-NAME and atropine, EFS at 10 and 20 Hz never resulted in slow waves of decreased duration. In 3 preparations, EFS at 10 Hz gave two components during stimulus. In 2 preparations, 20 Hz gave two components during stimulation. The total duration of these events initiated during the stimulation period were used to calculate the means given, together with results from preparations where a single slow wave of increased duration was initiated during the period of stimulation.

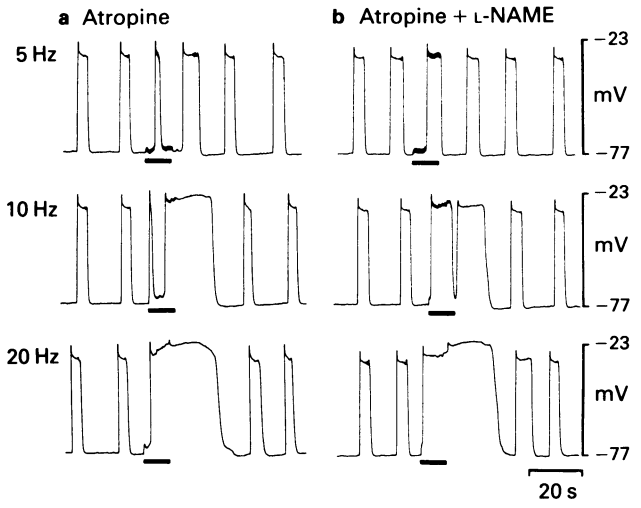



**Figure 7** Intracellular electrical records showing effects of electrical field stimulation (EFS) on slow waves. (a) Shows control responses to EFS (5 to 20 Hz) in the presence of atropine (1 μM). EFS caused a shortening of slow waves during stimulation at 5 to 10 Hz. After the stimulus a post-stimulus ('rebound') excitation was manifest in the form of a slow wave of prolonged duration. At 20 Hz, EFS elicited only an excitatory response. (b) Shows responses of the same cell, in the presence of L-$N^G$-nitroarginine methyl ester (L-NAME; 100 μM). EFS in the presence of atropine and L-NAME caused enhancement of slow waves at frequencies above 5 Hz. The effects of EFS on slow waves are consistent with the contractile responses represented in Figures 1 and 2. Horizontal bars indicate period of EFS.

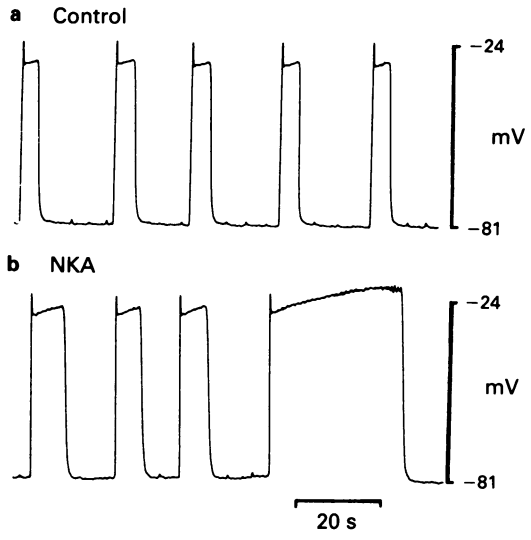



**Figure 8** Effects of neurokinin A (NKA) on electrical slow waves. (a) Shows a series of slow waves recorded in the presence of atropine (1 μM). Addition of NKA (1 nM) increased the amplitude and duration of slow waves. (b) Shows an excerpt from a continuous impalement 5 min after the addition of NKA.

Since the predominant tachykinin receptor subtype in this tissue appears to be $NK_2$ (see Discussion), the most potent endogenous ligand of these receptors (NKA) was tested on slow wave activity. Low concentrations of NKA (0.1–1 nM) caused an increase in the amplitude and duration of slow waves (Figure 8). Impalements were very difficult to maintain in the presence of NKA, and therefore higher concentrations of NKA could not be tested. The effects of NKA (1 nM) were tested in muscles from 5 dogs. In the presence of atropine alone (1 μM), control slow wave duration was 4.5 ± 0.4 s. NKA initiated long duration slow waves in each preparation (22.1 ± 7.4 s duration), and increased the amplitude of the plateau phase of these events (44.8 ± 1.3 mV and 51.4 ± 1.8 mV in control and NKA, respectively). Other parameters of slow waves were unaffected by this concentration of NKA (i.e. RMP averaged −79.0 ± 1.1 mV vs −78.2 ± 1.5 mV in control and NKA, respectively, and initial upstroke amplitude of slow waves averaged 51.8 ± 2.2 mV and 51.0 ± 22 mV in control and NKA, respectively).

## Discussion

The circular muscle of the canine proximal colon is supplied by intrinsic excitatory and inhibitory motoneurones (Sanders & Smith 1986a,b; Furness *et al.*, 1990). EFS is likely to activate these neural inputs simultaneously. The present study shows that EFS in the absence of antagonists results in a predominantly excitatory response due to the dominant action of ACh. Muscarinic antagonism revealed inhibitory responses to EFS at frequencies of 10 Hz or below. This inhibition has commonly been referred to as 'NANC' inhibition and is observed in most, if not all gastrointestinal smooth muscles (see Hoyle & Burnstock, 1989). In the present study we have found that non-cholinergic excitation occurs simultaneously with NANC inhibition at stimulus frequencies of 5 Hz and above. We have characterized non-cholinergic neuronal responses for the first time in the absence of interference from NO, which appears to be the predominant enteric inhibitory transmitter in canine colonic muscles (see Thornbury *et al.*, 1991; Ward *et al.*, 1992b).

The frequency-dependence of cholinergic and non-cholinergic excitatory responses was significantly different. When enteric inhibitory responses were reduced with nitric oxide synthase inhibitors excitatory responses were observed at frequencies of 1 Hz or above. In the same muscles after atropine, excitatory responses were not observed at frequencies below 5 Hz. This suggests that the release of the non-cholinergic excitatory transmitter(s) may have a higher threshold than the release of ACh as suggested by Costa *et al.* (1985) in the guinea-pig intestine. The difference in threshold is an interesting aspect of the regulation of transmitter release in enteric neurones. Brookes *et al.* (1992) have shown that excitatory motoneurones in the guinea-pig intestine co-express choline acetyltransferase and substance P. Therefore, ACh and tachykinins may be released by the same motoneurones. The mechanism for the frequency-dependence of release of these two neurotransmitters is currently unknown.

Another difference between cholinergic and non-cholinergic excitatory responses was the maximum mechanical effects elicited by these neural components. Maximal neural responses in the absence of atropine were about 3 fold greater in amplitude than noncholinergic excitatory responses, suggesting a greater contribution of ACh to the integrated response. This occurred despite the fact that the best candidate for the excitatory transmitter, NKA, produced contractions similar in amplitude to contractions produced by ACh. In fact, on a molar basis, NKA is more potent that ACh ($EC_{50}$ for ACh in this tissue is 1.9 μM; see Keef *et al.*, 1992). The reasons for these differences are not yet understood, but one possibility is that a submaximal concentration of tachykinins is released during maximal stimulation. It is also possible that the release of an as yet unidentified inhibitory transmitter (such as vasoactive intestinal peptide) could produce the difference between cholinergic and non-cholinergic responses under the conditions of our experiments.

The electrical mechanism of the non-cholinergic excitatory responses was investigated in microelectrode studies. EFS enhanced the amplitude and duration of slow waves in the presence of atropine and L-NAME, which is consistent with the increase in force and duration of phasic contractions elicited by EFS. Previous studies have shown that the force of phasic contractions in the proximal colon is related to the amplitude and duration of slow waves (Sanders & Smith, 1986b; Barajas-Lopez & Huizinga, 1989). The relationship between slow waves and phasic contractions appears to be due to the enhancement in $Ca^{2+}$ entry during the sustained plateau phase of the slow wave (Ward & Sanders, 1992).

After cessation of EFS in the presence of atropine, a post-stimulation or 'rebound' excitation was observed. Previous electrophysiological studies have shown that this response is partially blocked by inhibitors of NO responses (i.e. arginine analogues and oxyhaemoglobin) and by indomethacin (Ward *et al.*, 1992b). The latter suggests the involvement of eicosanoids in rebound excitation, but rebound responses were not blocked by indomethacin at higher frequencies of stimulation, suggesting that other substances may participate in these effects. Our data show that removal of NANC inhibitory influences results in excitatory responses (Figure 1c and 6a), and it is the persistence of these effects long after the termination of EFS that appears as 'rebound' excitation when NANC inhibitory effects are present (see Figure 3a). Therefore, the term 'rebound' excitation may be misleading since it implies that the response depends upon a period of inhibition (Wood & Marsh 1973). We would suggest instead that the term '*post-stimulus excitatory persistence*' more accurately describes the 'rebound' phenomenon.

There is considerable evidence from other tissues that tachykinins may serve as transmitters mediating enteric non-cholinergic excitatory neuromuscular transmission (see Introduction). Immunohistochemical studies of the canine colon (Tange, 1983; Furness *et al.*, 1990) have suggested that SP is expressed by nerve fibres within the muscularis. More recent discoveries have shown that expression of several tachykinins could contribute to the immunochemical labelling previously attributed to SP. For example, an antiserum used to localize SP in canine enteric neurones (Furness *et al.*, 1990) has since been shown to recognize both NKA and SP in guinea-pig enteric neurones (Shuttleworth *et al.*, 1991). Therefore, it is possible that NKA is also contained in, and released from, neurones supplying the muscularis of the canine colon. While the relative concentrations of SP/NKA in enteric neurones of the canine colon are currently unknown, approximately equal concentrations of NKA and SP have been reported in canine ileum (McDonald *et al.*, 1990). In the present study tachykinins mimicked non-cholinergic contractions and NKA caused a prolongation of electrical slow waves. Previous studies have shown that SP has similar effects on colonic muscles (Huizinga *et al.*, 1984; Keef *et al.*, 1992).

Distinct binding sites for radiolabelled SP and NKA have been localized on circular muscle cells of the canine colon by quantitative autoradiography (Mantyh *et al.*, 1988). Their results suggest the existence of $NK_1$ and $NK_2$ receptors in this preparation. The natural ligands, SP, NKA and NKB have only limited selectivity for $NK_1$, $NK_2$ and $NK_3$ receptors, respectively (Helke *et al.*, 1990). Thus, the relatively shallow slopes of the concentration-response curves for these peptides found in the present study tend to suggest that responses are mediated by the activation of multiple receptor subtypes. However, the rank order of potency NKA > SP > NKB observed suggests that $NK_2$ receptors may be the dominant receptor-type in the tissue (Helke *et al.*, 1990). The

suggestion that tachykinins are involved in mediating non-cholinergic excitatory responses in the colon is greatly strengthened by the observation that the non-selective $NK_1/NK_2$ receptor antagonist, D-Pro$^2$, D-Trp$^{7,9}$ SP (Buck & Schatzer 1988, Shuttleworth *et al.*, 1991) reduced contractions in response to EFS. Furthermore, the selective $NK_2$ receptor antagonist, MEN 10,376 (Maggi *et al.*, 1991) effectively antagonized non-cholinergic contractions and the responses to NKA, suggesting that $NK_2$ tachykinin receptors mediate a significant portion of these responses.

Non-cholinergic excitatory neural effects would be expected to interfere with studies of the influence of enteric inhibitory nerves. Since responses to both systems overlap, particularly at higher frequencies of stimulation, it is difficult to evaluate exclusively the magnitude of inhibitory responses without blocking non-cholinergic excitation. Therefore, experiments where enteric inhibitory neurotransmission is antagonized could conclude that blockade of inhibitory neurotransmission is total when in fact it is only reduced to a level where it is counterbalanced by the effects of non-cholinergic excitatory neurotransmission. This problem could also be confounded by possible presynaptic effects of NO, as proposed by Knudsen & Tottrup (1992) and Gustaffson *et al.* (1990) in gastrointestinal muscles of the guinea-pig. The availability of more potent and selective antagonists for tachykinins will provide a powerful tool in determining the full extent and transmitters involved in enteric inhibitory, as well as excitatory, responses.

The authors are grateful to Karri Kuenzli and Leah Milton for technical assistance. This work was supported by a Program Project Grant from the National Institutes of Health (DK 41315).

## References


BARAJAS-LOPEZ, C. & HUIZINGA, J.D. (1989). Different mechanisms of contraction generation in circular muscle of canine colon. *Am. J. Physiol.*, **256**, G570–G580.

BARON, S.A., JAFFE, B.M. & GINTZLER, A.R. (1983). Release of substance P from the enteric nervous system: direct quantitation and characterization. *J. Pharmacol. Exp. Ther.*, **227**, 365–368.

BRODIN, E. & NILSSON, G. (1981). Concentration of substance P-like immunoreactivity (SPLI) in tissues of dog, rat and mouse. *Acta Physiol. Scand.*, **112**, 305–312.

BROOKES, S.J.H., SONG, Z.-M., STEELE, P.A. & COSTA, M. (1992). Identification of motor neurons to the longitudinal muscle of the guinea pig ileum. *Gastroenterology*, **103**, 961–973.

BUCK, S.H. & SCHATZER, S.A. (1988). Agonist and antagonist binding to tachykinin peptide NK-2 receptors. *Life Sci.*, **42**, 2701–2708.

BUXTON, I.L.O., CHEEK, D.J., ECKMAN, D.M., WESTFALL, D.P., SANDERS, K.M. & KEEF, K.D. (1993). $N^G$-Nitro L-arginine methyl ester and other alkyl esters of arginine are muscarinic receptor antagonists. *Circ. Res.*, **72**, 387–395.

COSTA, M., FURNESS, J.B., PULLIN, C.O. & BORNSTEIN, J. (1985). Substance P enteric neurons mediate non-cholinergic transmission to the circular muscle of the guinea-pig intestine. *Naunyn-Schmiedebergs Arch Pharmacol.*, **328**, 446–453.

DALZIEL, H.H., THORNBURY, K.D., WARD, S.M. & SANDERS, K.M. (1991). Involvement of nitric oxide synthetic pathway in inhibitory junction potentials in canine proximal colon. *Am. J. Physiol.*, **260**, G789–G792.

DONNERER, J., BARTHO, L., HOLZER, P. & LEMBECK, F. (1984). Intestinal peristalsis associated with release of immunoreactive substance P. *Neuroscience*, **11**, 913–918.

FRANCO, R., COSTA, M. & FURNESS, J.B. (1979). Evidence for the release of endogenous substance P from intestinal nerves. *Naunyn-Schmiedebergs Arch. Pharmacol.*, **308**, 195–201.

FURNESS, J.B., LLOYD, K.C.K., STERNINI, C. & WALSH, J.H. (1990). Projections of substance P vasoactive intestinal peptide and tyrosine hydroxylase immunoreactive nerve fibres in the canine intestine, with special reference to the innervation of the circular muscle. *Arch. Histol. Cytol.*, **53**, 129–140.

FURNESS, J.B., BORNSTEIN, J.C., MURPHY, R. & POMPOLO, S. (1992). Roles of peptides in transmission in the enteric nervous system. *Trends Neurosci.*, **15**, 66–71.

GONDA, T., DANIEL, E.E., KOSTOLANSKA, F., OKI, M. & FOX, J.E.T. (1988). Neural control of canine colon motor function: studies *in vitro*. *Can J. Physiol. Pharmacol.*, **66**, 359–368.

GUSTAFSSON, L.E., WIKLUND, C.U., WIKLUND, N.P., PERSSON, M.G. & MONCADA, S. (1990). Modulation of autonomic neuroeffector transmission by nitric oxide in guinea-pig ileum. *Biochem. Biophys. Res. Commun.*, **173**, 106–110.

HELKE, C.J., KRAUSE, J.E., MANTYH, P.W., COUTURE, R. & BANNON, M.J. (1990). Diversity in mammalian tachykinin peptidergic neurons: multiple peptides, receptors, and regulatory mechanisms. *FASEB J.*, **4**, 1606–1615.

HOLZER, P. (1984). Characterization of the stimulus-induced release of immunoreactive substance P from the myenteric plexus of the guinea-pig small intestine. *Brain Res.*, **297**, 127–136.

HOYLE, C.H.V. & BURNSTOCK, G. (1989). Neuromuscular transmission in the gastrointestinal tract. In *Handbook of Physiology*, Sect 6: *The Gastrointestinal System*. Vol I. ed. Maklouf, G.M. pp. 435–464. Washington D.C: American Physiological Society.

HUIZINGA, J.D., CHANG., G., DIAMANT, N.E. & EL-SHARKAWY, T.Y. (1984). Electrophysiological basis of excitation of canine colonic circular muscle by cholinergic agents and substance P. *J. Pharmacol. Exp. Ther.*, **231**, 692–699.

HUIZINGA, J.D., TOMLINSON, J. & PINTIN-QUEZADA, J. (1992). Involvement of nitric oxide in nerve-mediated inhibition and action of vasoactive intestinal peptide in colonic smooth muscle. *J. Pharmacol. Exp. Ther.*, **260**, 803–808.

KEEF, K.D., WARD, S.M., STEVENS, R.J., FREY, B.W. & SANDERS, K.M. (1992). Electrical and mechanical effects of acetylcholine and substance P in subregions of canine colon. *Am. J. Physiol.*, **262**, G298–G307.

KNUDSEN, M.A. & TOTTRUP, A. (1992). A possible role of the L-arginine-nitric oxide pathway in the modulation of cholinergic transmission in the guinea-pig taenia coli. *Br. J. Pharmacol.*, **107**, 837–841.

MAGGI, C.A., GIULIANI, S., BALLATI, L., LECCI, A., MANZINI, S., PATACCHINI, R., RENZETTI, A.R., ROVERO, P., QUARTARA, L. & GIACHETTI, A. (1991). In vivo evidence for tachykininergic transmission using a new NK-2 receptor selective antagonist, MEN 10,376. *J. Pharmacol. Exp. Ther.*, **257**, 1172–1178.

MANTYH, P.W., MANTYH, C.R., GATES, T., VIGNA, S.R. & MAGGIO, J.E. (1988). Receptor binding sites for substance P and substance K in the canine gastrointestinal tract and their possible role in inflammatory bowel disease. *Neuroscience*, **25**, 817–837.

McDONALD, T.J., AHMAD, S., ALLESCHER, H.-D., KOSTKA, P., DANIEL, E.E., BARNETT, W. & BRODIN, E. (1990). Canine myenteric, deep muscular and submucosal plexus preparations of purified nerve varicosities: contents and chromatographic forms of certain neuropeptides. *Peptides*, **11**, 95–102.

NIEL, J.P., BYWATER, R.A.R. & TAYLOR, G.S. (1983). Effect of substance P on non-cholinergic fast and slow post-stimulus depolarization in the guinea-pig ileum. *J. Auton. Nerv. Syst.*, **9**, 573–584.

RAND, M.J. (1992). Nitrergic transmission: nitric oxide as a mediator of non-adrenergic, non-cholinergic neuroeffector transmission. *Clin. Exp. Pharmacol. Physiol.*, **19**, 147–169.

SANDERS, K.M. & SMITH, T.K. (1986a). Enteric neural regulation of slow waves in circular muscle of the canine proximal colon. *J. Physiol.*, **377**, 297–313.

SANDERS, K.M. & SMITH, T.K. (1986b). Motoneurons of the submucous plexus regulate electrical activity of the circular muscle of canine proximal colon. *J. Physiol.*, **380**, 293–310.

SANDERS, K.M. & WARD, S.M. (1992). Nitric oxide as a mediator of non-adrenergic, non-cholinergic neurotransmission. *Am. J. Physiol.*, **262**, G379–G392.

SHUTTLEWORTH, C.W.R., MURPHY, R., FURNESS, J.B. & POMPOLO, S. (1991). Comparison of the presence and actions of substance P and neurokinin A in guinea-pig taenia coli. *Neuropeptides*, **19**, 23–34.

SMITH, T.K., REED, J.B. & SANDERS, K.M. (1987). Origin and propagation of electrical slow waves in circular muscle of the canine proximal colon. *Am. J. Physiol.*, **252,** C215–C224.

TANGE, A. (1983). Distribution of peptide-containing endocrine cells and neurons in the gastrointestinal tract of the dog: immunohistochemical studies using antisera to somatostatin, substance P, vasoactive intestinal polypeptide, Met-enkephalin and neurotensin. *Biomed. Res.*, **4,** 9–24.

THORNBURY, K.D., WARD, S.M., DALZIEL, H.H., CARL, A., WESTFALL, D.P. & SANDERS, K.M. (1991). Nitric oxide mimics non-adrenergic, non-cholinergic hyperpolarization in gastrointestinal muscles. *Am. J. Physiol.*, **261,** G553–G557.

WARD, S.M., DALZIEL, H.H., BRADLEY, M.E., BUXTON, I.L.O., KEEF, K., WESTFALL, D.P. & SANDERS, K.M. (1992a). Involvement of cyclic GMP in non-adrenergic, non-cholinergic inhibitory neurotransmission in dog proximal colon. *Br. J. Pharmacol.*, **107,** 1075–1082.

WARD, S.M., DALZIEL, H., THORNBURY, K.D., WESTFALL, D.P. & SANDERS, K.M. (1992b). Nonadrenergic, non-cholinergic inhibition and rebound excitation in canine colon depend on nitric oxide. *Am. J. Physiol.*, **262,** G237–G243.

WARD, S.M. & SANDERS, K.M. (1992). Upstroke component of electrical slow waves in canine colonic smooth muscle due to nifedipine-resistant $Ca^{2+}$ current. *J. Physiol.*, **455,** 321–337.

WOOD, J.D. & MARSH, D.R. (1973). Effects of atropine, tetrodotoxin and lidocaine on rebound excitation of guinea-pig small intestine. *J. Pharmacol. Exp. Ther.*, **184,** 590–598.

*(Received December 4, 1992*
*Revised February 17, 1993*
*Accepted February 23, 1993)*

*Br. J. Pharmacol.* (1993), **109**, 748–750 © Macmillan Press Ltd, 1993

# Protective effects of ranolazine in guinea-pig hearts during low-flow ischaemia and their association with increases in active pyruvate dehydrogenase

B. Clarke, M. Spedding, L. Patmore & [1]J.G. McCormack

Department of Pharmacology, Syntex Research Centre, Research Avenue South, Heriot-Watt University Research Park, Riccarton, Edinburgh EH14 4AP

**1** In isolated Langendorff-perfused, electrically-paced, hearts of guinea-pigs, global low-flow-ischaemia (LFI; at 0.7 ml $min^{-1}$) resulted in marked increases in the rates of release of lactate, lactate dehydrogenase (LDH) and creatine kinase (CK) over a 30 min period. At the end of the LFI period, tissue ATP content was significantly reduced from a control value of 11.8 ± 0.8 (5) to 5.6 ± 0.8 (5) μmol $g^{-1}$ dry weight.

**2** The presence of ranolazine [(±)-N-(2,6-dimethyl-phenyl)-4[2-hydroxy-3-(2-methoxy-phenoxyl)-propyl]-1-piperazine acetamide dihydro-chloride; RS-43285-193] at 10 μM, from 20 min prior to and during LFI, resulted in significant reductions in the release of lactate, LDH and CK during the ischaemic period and a significant preservation of tissue ATP (9.0 ± 1.1 (6) μmol $g^{-1}$ dry wt.). Ranolazine did not prevent the reductions in creatine phosphate or glycogen observed in LFI, nor did it have any significant effects on any contractile parameters before or during the LFI period.

**3** Neither ranolazine nor LFI affected the total amounts of tissue pyruvate dehydrogenase (PDH) activity; however, the significant reduction in the amount of active, non-phosphorylated PDH caused by LFI (from 88.2 ± 5.5 to 44.2 ± 3.2% of total activity) was partially but significantly prevented by ranolazine (67.2 ± 6.8%). This effect of ranolazine on PDH may be part of the mechanism whereby the compound reduces lactate release and preserves tissue ATP during ischaemia.

**Keywords:** Ranolazine; ischaemia; pyruvate dehydrogenase; guinea-pig heart

## Introduction

The novel anti-anginal agent, ranolazine [(±)-N-(2,6-dimethyl-phenyl)-4[2-hydroxy-3(2-methoxyphenoxy)propyl]-1-piperazine acetamide di-hydrochloride; RS-43285-193] (Jain *et al.*, 1990; Cocco *et al.*, 1992) has been shown to be effective in inhibiting the biochemical and gross electrocardiographical consequences of transient myocardial ischaemia in the intact dog (Allely *et al.*, 1987; Allely & Alps, 1988) without causing direct haemodynamic effects. Ranolazine has also been shown to be remarkably effective in preventing myocardial enzyme release in an intact primate model of ischaemia with reperfusion (Allely & Alps, 1990). It has been suggested that ranolazine may alleviate the symptoms of transient myocardial ischaemia by altering substrate utilization (Allely *et al.*, 1987). The present study was undertaken to characterize the effects of ranolazine in an *in vitro* model of ischaemia, the guinea-pig isolated heart subjected to low-flow perfusion, in order to obtain direct biochemical evidence of cardioprotection, and also to gain some insights into the mechanism(s) underlying the anti-ischaemic properties of ranolazine. A small part of the present work has been previously reported briefly as a Meeting abstract (Clarke *et al.*, 1992).

## Methods

Hearts from female Dunkin-Hartley guinea-pig (200–400 g) were retrogradely perfused (Langendorff method) at ~9 ml $min^{-1}$ with a modified Krebs/bicarbonate solution containing 11.7 mM glucose and 1.9 mM $CaCl_2$ and gased with $O_2/CO_2$ (19/1) (normoxic control conditions); hearts were electrically-paced throughout at 250–300 beats $min^{-1}$ (~25% above control intrinsic rate in each case). Each preparation was maintained at 37°C within a humidified chamber and allowed to equilibrate for 30 min prior to a pretreatment period of 20 min with or without 10 μM ranolazine. Low-flow-ischaemia (LFI) (± ranolazine) was induced by reducing the perfusion flow rate to 0.7 ml $min^{-1}$ for 30 min; normoxic controls were perfused for 80 min as given above. Perfusate was collected at 2 min intervals for subsequent analysis of lactate, lactate dehydrogenase (LDH) and creatine kinase (CK) release, and then at the end of the perfusions the hearts were freeze-clamped using Wollenberg clamps pre-cooled in liquid $N_2$ before subsequent analysis of adenosine-5'-triphosphate (ATP), creatine phosphate and glycogen contents; all of these assays were performed with standard commercial kits, except for glycogen which was assayed by the method of Good *et al.* (1933). Samples were extracted and analysed for both active, non-phosphorylated, pyruvate dehydrogenase ($PDH_a$) activity and total PDH activity as described in McCormack & Denton (1989). A unit of enzyme activity is defined as that which converts 1 μmol of substrate $min^{-1}$ at 30°C. Statistical analysis was by unpaired Student's *t* test and by analysis of variance and application of Dunnett's *t* test.

## Results

Figure 1 (a–c) shows that LFI caused marked increases in the efflux of lactate, LDH and CK respectively from untreated hearts, and thus clearly shows that the present protocol is suitable for testing cardioprotection to ischaemic insult. We chose to study the effects of a concentration of ranolazine (10 μM) which had previously been shown to give maximal protection against several indices of ischaemic damage in *in vitro* rat heart preparations (Ferrandon *et al.*, 1988; 1990). Ranolazine reduced the magnitude of all of the presently used indices of damage during LFI (Figure 1), and

[1] Author for correspondence.

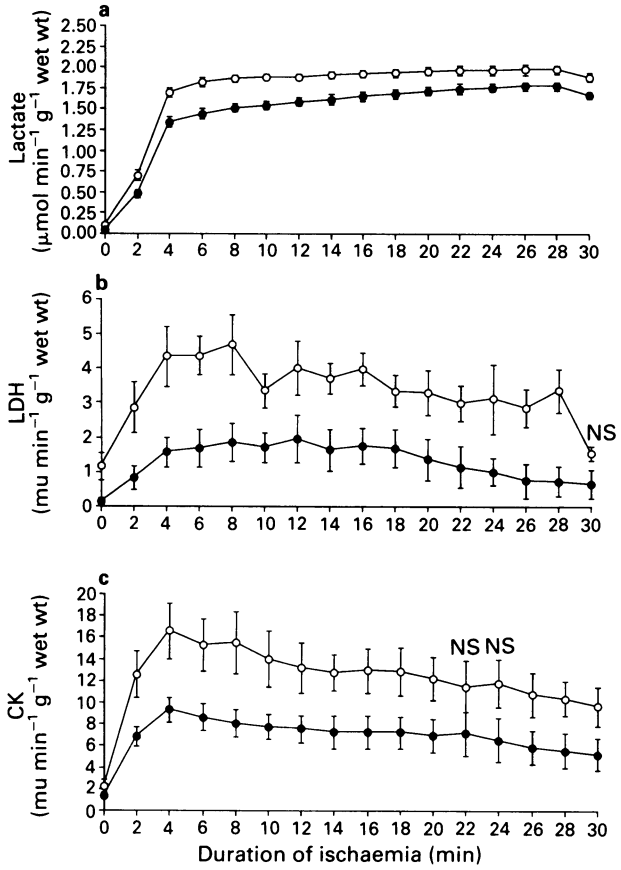



**Figure 1** Effects of ranolazine on (a) lactate efflux and the release of (b) lactate dehydrogenase (LDH) and (c) creatine kinase (CK) from the perfused guinea-pig heart during a period of low-flow ischaemia. Values are means ± s.e.mean for 5 (untreated) or 6 (ranolazine-treated) hearts; g wet wt = g wet weight. The effects of 10 μM ranolazine (●) were significantly different ($P \leq$ at least 0.05) from the untreated controls (○) at all time points other than those (three) marked NS.

in all but 3 out of 45 instances (as indicated) significant differences from untreated control values ($P$ at least $\leq 0.05$) were obtained. Table 1 shows that LFI resulted in a decrease in the tissue contents of ATP, creatine phosphate and glycogen at the end of the perfusions, and also a decrease in the amount of active PDH. Ranolazine also prevented the decrease in tissue ATP but did not affect the creatine phosphate or glycogen contents. Ranolazine largely prevented the LFI-induced decrease in active PDH; neither ranolazine nor LFI affected the total amount of PDH which ranged from 28 to 49 units $g^{-1}$ dry weight. Ranolazine was without effect on contractile function either in normoxia or in LFI (results not shown).

## Discussion

This study shows that ranolazine can prevent some of the deleterious consequences of cardiac ischaemia in an *in vitro* isolated heart model. This is supportive of the reports of its cardioprotective effects seen *in vivo* (see Introduction), and *in vitro* in rat heart preparations where several other different indices of cell damage were measured (Ferrandon *et al.*, 1988; 1990). The present demonstration of the preservation of tissue ATP content is particularly noteworthy, and may offer at least partial explanation for the improvement in functional parameters on reperfusion following ischaemia noted in some earlier studies.

PDH occupies a key site in respiratory fuel selection, effectively dictating the rate of carbohydrate utilization, and is subject to very complex regulation by many different factors (see Randle, 1986). There are not many reports of PDH measurement in guinea-pig heart (compared to rat heart for instance), however, the values obtained for total activity in the present study are similar to those found previously (e.g. Bunger *et al.*, 1983). The control values of $PDH_a$ obtained in the present study appear to be fairly high as a % of total activity (see McCormack & Denton, 1989); however, they are again similar to those found in an earlier study on glucose-perfused guinea-pig hearts electrically paced at the relatively high frequency used (Hansford *et al.*, 1990).

In rat heart, ischaemia or reperfusion have previously been shown to lead to an inactivation of PDH (Kobayashi & Neely, 1983; Patel & Olson, 1984) under conditions similar to those used in the present study, which indicates that a similar situation may occur in the guinea-pig. Ischaemia is likely to give rise to increased intramitochondrial $NADH/NAD^+$ and acetyl CoA/CoA ratios which would lead to complex inactivation; however, the reduced ATP/ADP would balance this to some extent by favouring activation (see Kobayashi & Neely, 1983). In this context it is worth noting that ranolazine preserves tissue ATP in ischaemia yet is associated with PDH activation.

The anti-ischaemic mechanism of ranolazine appears to differ from many commonly prescribed anti-anginal agents (e.g. β-blockers, calcium channel blockers) in that haemodynamics appear to be unaffected (Allely & Alps, 1988; 1989). Although it is not clear whether the activation (or prevention of ischaemic inhibition) of PDH is a part of the cause, or a consequence of the cardioprotective or anti-anginal mechanism, an attractive hypothesis can be built around the former possibility. An activation of PDH could result in a decrease in lactate release by allowing more lactate to be used as a substrate, and could also account at least to some degree for enhanced ATP production per unit of $O_2$ by favouring carbohydrate oxidation compared to fat (see e.g. Hutter *et al.*, 1985). This of course would be most beneficial under times of $O_2$ limitation such as reduced coronary flow and/or increased work demand, and may lower the delivered oxygen content at which biochemical and mechanical evidence of ischaemia develop (Burkhoff *et al.*, 1991). Tissue ATP preservation and perhaps reduced lactic acidosis may

**Table 1** Effects of low-flow ischaemia (LFI) and ranolazine on the ATP, creatine phosphate (CrP), glycogen and active pyruvate dehydrogenase ($PDH_a$) contents of guinea-pig heart

| *Parameter* | *Normoxia* (5) | *LFI* (5) | *LFI + ranolazine* (6) |
|---|---|---|---|
| ATP | 11.8 ± 0.8 | 5.6 ± 0.8** | 9.0 ± 1.1† |
| CrP | 10.4 ± 0.1 | 1.9 ± 0.3** | 2.3 ± 0.3** |
| Glycogen | 92.9 ± 10.9 | 38.9 ± 5.0** | 43.0 ± 3.0** |
| $PDH_a$ | 88.2 ± 5.5 | 44.2 ± 3.2* | 67.2 ± 6.8† |

Ranolazine was present at 10 μM; see methods for experimental conditions. The number of hearts for each condition is given in parentheses. Metabolite values are expressed in μmol $g^{-1}$ dry weight; $PDH_a$ values are expressed as % of total PDH.
Significant effects of LFI compared to the appropriate normoxic controls are indicated by $*P \leq 0.01$, and $**P \leq 0.001$, and significant effects of ranolazine versus the LFI untreated group are indicated by $\dagger P \leq 0.05$.

thus allow more preservation of cellular viability and hence account for the observed effects on LDH and CK release as indicators of ischaemic cell damage.

The present observations offer some insights into potential mechanisms for the cardioprotective and anti-anginal effects of ranolazine. It will be important to see whether the drug has direct effects on PDH or whether the described effects are an indirect consequence of its affecting metabolism elsewhere; e.g. inhibition of fat oxidation would lead to activation of PDH (Randle, 1986).

## References


ALLELY, M.C. & ALPS, B.J. (1988). The effects of the novel antianginal agent ranolazine (i.d.) in a canine model of transient myocardial ischaemia. *Br. J. Pharmacol.*, **93**, 246P.

ALLELY, M.C. & ALPS, B.J. (1989). A comparison of the effects of a series of anti-anginal agents in a novel canine model of transient myocardial ischaemia. *Br. J. Pharmacol.*, **96**, 977–985.

ALLELY, M.C. & ALPS, B.J. (1990). Prevention of myocardial enzyme release by ranolazine in a primate model of ischaemia with reperfusion. *Br. J. Pharmacol.*, **99**, 5–6.

ALLELY, M.C., ALPS, B.J. & KILPATRICK, A.T. (1987). The effects of the novel anti-anginal compound RS 43285 on [lactic acid], [$K^+$] and pH in a canine model of transient myocardial ischaemia. *Biochem. Soc. Trans.*, **15**, 1057–1058.

BUNGER, R., PERMANETTER, B. & YAFFE, S. (1983). Energy utilisation and pyruvate as determinants of pyruvate dehydrogenase in norepinephrine-stimulated heart. *Pflügers Arch.*, **397**, 214–219.

BURKHOFF, D., WEISS, R.G., SCHULMAN, S.P., KALIL-FILHO, R., WANNENBURG, T. & GERSTENBLITH, G. (1991). Influence of metabolic substrate on rat heart function and metabolism at different coronary flows. *Am. J. Physiol.*, **261**, H741–H750.

CLARKE, B., MCCORMACK, J.G. & SPEDDING, M. (1992). The anti-ischaemic effects of ranolazine in guinea pig heart are associated with increases in active pyruvate dehydrogenase. *J. Mol. Cell. Cardiol.*, **24** (Suppl. IV), S52.

COCCO, G., ROUSSEAU, M.F., BOUVY, T., CHERON, P., WILLIAMS, G., DETRY, J.M. & POULEUR, H. (1992). Effects of a new metabolic modulator, Ranolazine, on exercise tolerance in Angina Pectoris patients treated with beta-blocker or diltiazem. *J. Cardiovasc. Pharmacol.*, **20**, 131–138.

FERRANDON, P., CHAYLAT, C., FLIGIEL, E. & ARMSTRONG, J.M. (1990). Ranolazine but not allopurinol or dipyridamole reduces the ventricular acidosis and lactate production produced by low perfusion flow in isolated rat hearts. *Fund. Clin. Pharmacol.*, **4**, 426.

FERRANDON, P., PASCAL, J.-C. & ARMSTRONG, J.M. (1988). Protective effects of the novel anti-ischaemic agent ranolazine (RS-43285) in the reperfused rat heart. *Br. J. Pharmacol.*, **93**, 247P.

GOOD, C.A., KRAMER, H. & SOMOGYI, M. (1933). The determination of glycogen. *J. Biol. Chem.*, **100**, 485–491.

HANSFORD, R.G., HOGUE, B., PROKOPCZUK, A., WASILEWSKA, E. & LEWARTOWSKI, B. (1990). Activation of pyruvate dehydrogenase by electrical stimulation, and low-$Na^+$ perfusion of guinea pig heart. *Biochim. Biophys. Acta*, **1018**, 282–286.

HUTTER, J.F., PIPER, H.M. & SPIECKERMANN, P.G. (1985). Effects of fatty acid oxidation on efficiency of energy production in rat heart. *Am. J. Physiol.*, **249**, H723–H728.

JAIN, D., DASGUPTA, P., HUGHES, L.O., LAHIRI, A. & RAFTERY, E.B. (1990). Ranolazine (RS-43285): a preliminary study of a new anti-anginal agent with a selective effect on ischaemic myocardium. *Eur. J. Clin. Pharmacol.*, **38**, 111–114.

KOBAYASHI, K. & NEELY, J.R. (1983). Effects of ischaemia and reperfusion on pyruvate dehydrogenase activity in isolated rat hearts. *J. Mol. Cell. Cardiol.*, **15**, 359–367.

MCCORMACK, J.G. & DENTON, R.M. (1989). Influence of calcium ions on mammalian intramitochondrial dehydrogenases. *Methods Enzymol.*, **174**, 95–118.

PATEL, T.B. & OLSON, M.S. (1984). Regulation of pyruvate dehydrogenase complex in ischemic rat heart. *Am. J. Physiol.*, **246**, H858–H864.

RANDLE, P.J. (1986). Fuel selection in animals. *Biochem. Soc. Trans.*, **14**, 799–806.


*(Received February 11, 1993*
*Revised March 8, 1993*
*Accepted March 9, 1993)*

*Br. J. Pharmacol.* (1993), **109**, 751-759 © Macmillan Press Ltd, 1993

# Endogenous tachykinins facilitate transmission through parasympathetic ganglia in guinea-pig trachea

[1]N. Watson, *J. Maclagan & P.J. Barnes

Department of Thoracic Medicine, National Heart and Lung Institute, Dovehouse Street, London, SW3 and *Department of Academic Pharmacology, Royal Free Hospital School of Medicine, Rowland Hill Street, London NW3

**1** Exogenous and endogenous tachykinins facilitate cholinergic nerve-induced bronchoconstriction in guinea-pig. Using a vagally innervated guinea-pig tracheal tube preparation we have investigated the involvement of endogenous capsaicin-sensitive neuropeptides in both pre- and postganglionic cholinergic neurotransmission. The effects of the neutral endopeptidase inhibitor (NEP), phosphoramidon, were investigated in this preparation either alone or in conjunction with sensory neuropeptide depletion by capsaicin pretreatment. The subtype of neurokinin receptor mediating this facilitatory effect of tachykinins has also been examined, by the use of selective tachykinin receptor agonists and a selective $NK_1$ receptor antagonist.

**2** Cholinergic contractions of the sealed Krebs filled tracheal tube preparation were recorded as increases in intraluminal pressure and were induced either by (i) pre-ganglionic vagus nerve stimulation (PGS), (ii) stimulation of postganglionic intramural nerves via transmural stimulating electrodes (TMS) in the presence of ganglion-blocking concentrations of hexamethonium and (iii) application of exogenous acetylcholine (ACh).

**3** The effect of phosphoramidon, which inhibits the breakdown of tachykinins, was investigated on ACh-, PGS- and TMS-induced contractions. Phosphoramidon (1-10 $\mu$M) facilitated contractions of the trachea induced by PGS, in a concentration-dependent manner, but had no effect on contractions of the trachea induced either by TMS or exogenous ACh.

**4** The facilitatory effect of phosphoramidon (10 $\mu$M) on PGS-induced contractions was abolished by pretreating guinea-pigs with capsaicin $7 \pm 2$ days before the *in vitro* experiments. Capsaicin pretreatment did not significantly alter responses to the spasmogens, ACh or substance P. Depletion of sensory neuropeptides, by capsaicin pretreatment was confirmed by the lack of response to capsaicin (1 $\mu$M) *in vitro*.

**5** The facilitatory effect of phosphoramidon (10 $\mu$M) on PGS-induced contractions was inhibited by the selective $NK_1$ receptor antagonist, GR71251 (1 $\mu$M). When applied to the tissues during nerve stimulation, GR71251 caused a small, but significant, inhibition of PGS-induced contractions during low frequency stimulation. No significant effect of GR71251 on TMS-induced contractions was seen at any frequency. There was no significant effect of the $NK_1$ receptor antagonist on contractions of the trachea induced by exogenous ACh.

**6** The selective $NK_1$ receptor agonist, GR73632 facilitated contractions of the trachea induced by stimulation of both pre- and postganglionic cholinergic nerves, in a concentration-dependent manner, at concentrations that had no significant effect on basal tone (0.01-0.3 nM). The facilitatory effect of GR73632 on both PGS- and TMS-induced contractions was antagonized by GR71251 (1 $\mu$M). In contrast, neurokinin A (1-10 nM), which preferentially stimulates $NK_2$ receptors, facilitated contractions induced by both PGS and TMS, and caused a significant increase in basal tone of the trachea. The selective $NK_3$ receptor agonist, senktide (30-300 mM), had no significant effect on nerve-induced contractions or basal tone of the trachea.

**7** These results suggest that there is release of endogenous tachykinins during vagus nerve stimulation, which can be depleted by capsaicin pretreatment and, which facilitate cholinergic nerve-induced contractions at the level of the parasympathetic ganglia. Facilitatory tachykinin receptors on the postganglionic nerve terminals can be demonstrated by exogenous agonists but do not appear to be activated by endogenous tachykinins under the stimulation conditions of these studies. These data suggest that $NK_1$ receptors may be involved in mediating this facilitatory response to tachykinins but do not exclude an involvement of $NK_2$ receptors. It appears unlikely, however, that $NK_3$ receptors are involved.

**Keywords:** Tachykinin neuropeptides; cholinergic transmission; pulmonary parasympathetic ganglia; tracheal smooth muscle

## Introduction

Exogenous tachykinins have been shown to facilitate cholinergic neurotransmission in guinea-pig airways via $NK_2$ receptors (Hall *et al.*, 1989). A component of the bronchoconstrictor response to vagus nerve stimulation is inhibited by sensory neuropeptide depletion with capsaicin (Martling *et al.*, 1984) indicating a facilitatory role of endogenous capsaicin-sensitive tachykinins *in vivo* (Stretton *et al.*, 1992; Martling *et al.*, 1984). Immunohistochemical studies have demonstrated a rich innervation of substance P-immunoreactive nerves in guinea-pig airways, innervating airway smooth muscle, blood vessels, glands and epithelium (Sheppard *et al.*, 1983). Substance P-immunoreactive nerves have also been localized in close association with airway ganglia with their cell bodies being located within the airways (Dey *et al.*, 1991). Elec-

[1] Author for correspondence at present address: Institute of Pharmacology R2-101, Syntex Discovery Research, 3401 Hillview Ave., Palo Alto, CA 94303, U.S.A.

trophysiological studies have demonstrated slow excitatory postsynaptic potentials (e.p.s.ps) within airway ganglia (Cameron & Coburn, 1984; Coburn, 1984; Coburn & Kalia, 1986; Burnstock *et al.*, 1987). Similar postsynaptic events in sympathetic ganglia have been shown to be mediated by the neuropeptide luteinizing hormone releasing hormone (Jan *et al.*, 1980; Kuffler, 1980; Jan & Jan, 1981). Airway ganglia are located within a plexus which overlies the airway smooth muscle. The plexus is a complex nerve network containing both myelinated and unmyelinated nerve fibres and nerve cell bodies, and provides a means for communication along the length of the airway and between it and the central nervous system (Baluk & Gabella, 1989). Therefore, functional, immunohistochemical and electrophysiological studies suggest a role for endogenous tachykinins in transmission within airway ganglia.

The aim of the present study was to determine whether (i) a facilitatory role of endogenous tachykinins could be demonstrated during stimulation of pre- and/or postganglionic cholinergic nerves, (ii) whether the source of these endogenous tachykinins is sensitive to depletion by capsaicin pretreatment, and (iii) what subtype of tachykinin receptor may be mediating these effects. In order to do this we have used the vagally-innervated tracheal tube preparation of the guinea-pig (Blackman & McCaig, 1983) which enables the stimulation of both pre- and postganglionic cholinergic fibres to the airways *in vitro*. This preparation therefore provides a means of assessing transmission through the parasympathetic airway ganglia, which are embedded within the neuronal plexus and run along the length of the trachea (Baker *et al.*, 1986; Baluk & Gabella, 1989).

Preliminary reports of this work have been made to the British Association for Lung Research (Watson *et al.*, 1992a), the British Pharmacological Society (Watson *et al.*, 1992b) and the American Thoracic Society (Watson *et al.*, 1992c,d).

## Methods

Male Dunkin Hartley guinea-pigs (250–350 g) were killed by cervical dislocation, the trachea was cannulated and removed with vagi and recurrent laryngeal nerves intact (Blackman & McCaig, 1983). Indomethacin (5 μM) and propranolol (1 μM) were present in the Krebs buffer solution (composition: NaCl 118.4, KCl 4.9, $NaHCO_3$ 25.0, $KH_2PO_4$ 1.2, $MgSO_4.7H_2O$ 1.2, $CaCl.6H_2O$ 2.5, glucose 11.1 mM) to eliminate prostaglandin-induced tone and the complication of stimulating sympathetic nerves respectively. Hexamethonium (75 μM) was present during transmural stimulation to ensure that the responses recorded were the result of stimulation of postganglionic nerves. Contractions of the trachealis muscle were recorded as increases in intraluminal pressure (ILP), induced by either (i) preganglionic vagus nerve stimulation (PGS), (ii) stimulation of postganglionic intramural nerves via transmural stimulation (TMS) in the presence of hexamethonium, or (iii) application of exogenous spasmogens, ACh or substance P.

### *Inhibition of endogenous tachykinin breakdown with phosphoramidon*

The effects of the neutral endopeptidase inhibitor, phosphoramidon (1–10 μM) were investigated on contractions of the trachea induced by stimulation of either pre- or postganglionic cholinergic nerves over a range of stimulation frequencies (4–50 Hz). Post-junctional effects of the highest concentration of phosphoramidon (10 μM) were assessed in a separate set of experiments by performing cumulative concentration-effect curves to ACh in the absence and the presence of phosphoramidon.

### *Sensory neuropeptide depletion and its effect on responses to phosphoramidon*

*Capsaicin pretreatment protocol* Guinea-pigs (200–300 g) were divided into three groups: no pretreatment, vehicle pretreatment and capsaicin pretreatment. All animals were given terbutaline sulphate (0.1 mg $kg^{-1}$) subcutaneously and aminophylline (25 mg $kg^{-1}$) intraperitoneally at time zero and time = 25 min. Shortly after, at time = 27 min, all animals received ketamine (50 mg $kg^{-1}$) and xylazine (0.1 mg $kg^{-1}$) both intramuscularly. At time = 30 min animals in the no pretreatment group received nothing, capsaicin pretreatment animals received capsaicin (50 mg $kg^{-1}$) in a Tween 80/ethanol/saline vehicle (10:10:80% mixture by vol.) and animals in the vehicle pretreatment group received the vehicle for capsaicin (Belvisi *et al.*, 1990). Tracheae were removed and prepared for *in vitro* experiments as described above, on day 7 ± 2 days after the capsaicin pretreatment procedure.

The effect of phosphoramidon (10 μM) on PGS- and TMS-induced contractions was investigated over a range of stimulation frequencies (4–50 Hz), in tracheae from each of the three groups. Assessment of the post-junctional responsiveness to exogenous ACh (0.3 mM) and substance P (0.3 μM) was also determined. Sensitivity to capsaicin (1 μM) was examined in all tissues at the end of the *in vitro* experiments in order to determine the intactness of capsaicin-sensitive sensory neuropeptide stores and therefore the effectiveness of capsaicin pretreatment.

### *The effect of a selective $NK_1$ receptor antagonist*

The effects of the peptidase-sensitive, $NK_1$ receptor antagonist, GR71251 (1 μM) (Hagan *et al.*, 1990) were investigated on PGS- and TMS-induced contractions over a range of stimulation frequencies (4–50 Hz). Tissues pre-incubated with GR71251 for 15 min were then exposed to phosphoramidon (10 μM) and the effect of phosphoramidon investigated over the same range of stimulation frequencies in the presence of GR71251. Although GR71251 is sensitive to degradation by peptidases, we chose to investigate the effects of GR71251 on nerve-induced contractions in the absence of phosphoramidon because phosphoramidon facilitated PGS-induced contractions in its own right, which would have complicated the interpretation. This protocol also enabled an assessment of the effects of $NK_1$ receptor blockade on the response to phosphoramidon.

### *The effect of NK receptor agonists*

The effects of the selective, peptidase resistant $NK_1$ receptor agonist, GR73632 (0.01–1 nM) (Hagan *et al.*, 1989), were investigated on basal tone, PGS- and TMS-induced contractions. Post-junctional effects of GR73632 were assessed by performing cumulative concentration-effect curves to ACh alone and then in the presence of GR73632 (0.3 nM). The effect of GR73632 on PGS- (0.3 nM) and TMS- (0.1 mM) induced contractions was re-examined over a range of stimulation frequencies, after a 15 min incubation with the $NK_1$ receptor antagonist GR71251 (1 μM) and phosphoramidon (10 μM).

The effects of neurokinin A (1–10 nM) and senktide (30–300 nM) were also investigated on basal tone and PGS- and TMS-induced contractions of tracheae in separate sets of experiments.

### *Statistical analysis*

A Wilcoxon signed ranks test was used to determine the significance of differences between control responses and those in the presence of drug, within the same preparation. A Mann-Whitney U test was used to determine the significance of differences arising between preparations. All results are

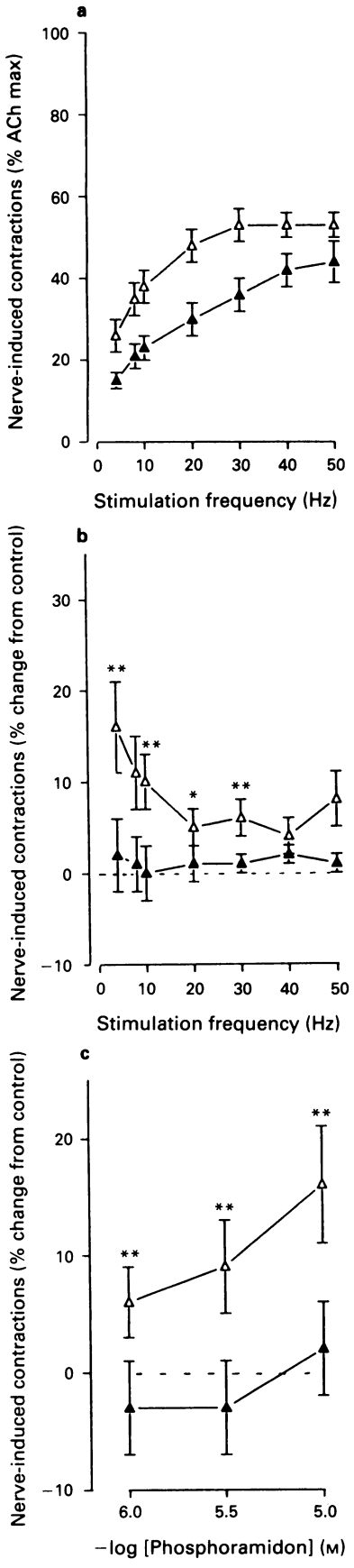



**Figure 1** (a) Control responses to preganglionic stimulation (PGS, Δ, 0.2 ms, 30 V) and transmural stimulation (TMS, ▲, 0.2 ms, 60 V) over a range of stimulation frequencies, expressed as a % of the maximum increase in intraluminal pressure induced by acetylcholine (ACh, 0.3 nM). (b) Effect of phosphoramidon (10 μM) on PGS- (Δ) and TMS- (▲) induced contractions over a range of stimulation frequencies. (c) Effect of different concentrations of phosphoramidon (1–10 μM) on PGS- (Δ) and TMS- (▲) induced contractions at 4 Hz stimulation frequency. Nerve-induced contractions in (b) and (c) are expresses as the % change from control responses before addition of phosphoramidon, shown in (a) and are the mean ± s.e.mean where $n = 10$. $^*P<0.05$; $^{**}P<0.02$ change from control.

expressed as the mean ± s.e.mean of 6–10 experiments; $P<0.05$ was considered significant.

### *Materials*

Indomethacin (1 mg $ml^{-1}$) was dissolved in a buffer of composition $KH_2PO_4$ 19.77 and $NaHPO_4$ 118.34 mM, adjusted to a pH of 7.8 with NaOH and sonicated for 2–4 min. The following drugs were used: atropine sulphate and acetylcholine bromide (BDH Ltd., Dagenham, Essex), indomethacin, hexamethonium bromide, capsaicin (8-methyl-N-vanillyl-6-nonenamide), Tween 80, phosphoramidon (N-(α-rhamnopyranosyloxyhydroxy-phosphinyl)-Leu-Trp) and tetrodotoxin (Sigma Chemical Co. Ltd., Poole, Dorset), propranolol hydrochloride (Imperial Chemical Industries Ltd., Andover, Hants) and senktide (succinyl-[$Asp^6$,$MePhe^8$] SP (6-11)) (Cambridge Research Biochemicals). GR73632 (δ-aminovaleryl [$Pro^9$, N-$MeLeu^{10}$] SP (7-11)) and GR71251 (D-$Pro^9$ [Spiro-γ-lactam] $Leu^{10}$-$Trp^{11}$] SP (1-11)) were generously provided by Glaxo Research (Ware, Herts). A 1 mM stock solution of both the GR compounds was made up in 0.01 M acetic acid and vehicle/time controls were run in parallel tracheae for both these compounds. Aminophylline was obtained from Antigen (Roscrea, Ireland), ketamine hydrochloride from Park-Davis (Pontypool, Gwent), terbutaline sulphate from Astra Pharmaceuticals (Kings Langley, Herts) and xylazine from Bayer (Bury St. Edmunds, Suffolk).

## Results

The tracheal tube preparation had a low constant intraluminal pressure (ILP) in the absence of prostaglandin-induced tone. Contractions of the trachea induced by preganglionic vagus nerve stimulation (PGS, 4–50 Hz, 0.2 ms, 30 V at source), transmural nerve stimulation (TMS 4–50 Hz, 0.2 ms, 60 V at source) and exogenous ACh (0.1 μM–0.3 mM) were recorded as increases in ILP and were abolished by atropine (1 μM). PGS-induced contractions were also abolished by hexamethonium (75 μM) and tetrodotoxin (1 μM). TMS was always performed in the presence of hexamethonium (75 μM) and contractions induced by TMS were abolished by tetrodotoxin (1 μM). Contractions of the trachea induced by PGS were consistently larger than those induced by TMS, but under no circumstance did the size of the contractions induced by either form of stimulation exceed 80% of the maximum response to ACh (0.3 mM) (Figure 1a).

### *Inhibition of endogenous tachykinin breakdown using phosphoramidon*

Phosphoramidon facilitated PGS-induced contractions in a concentration-dependent manner, while having no significant effect on TMS-induced contractions (Figure 1b and c). The facilitation of PGS-induced contractions, by phosphoramidon (1–10 μM), was consistently observed at stimulation frequencies of 30 Hz and less (Figure 1b and c). There was no significant difference between the contractions induced by ACh in the absence or presence of 10 μM phosphoramidon (data not shown).

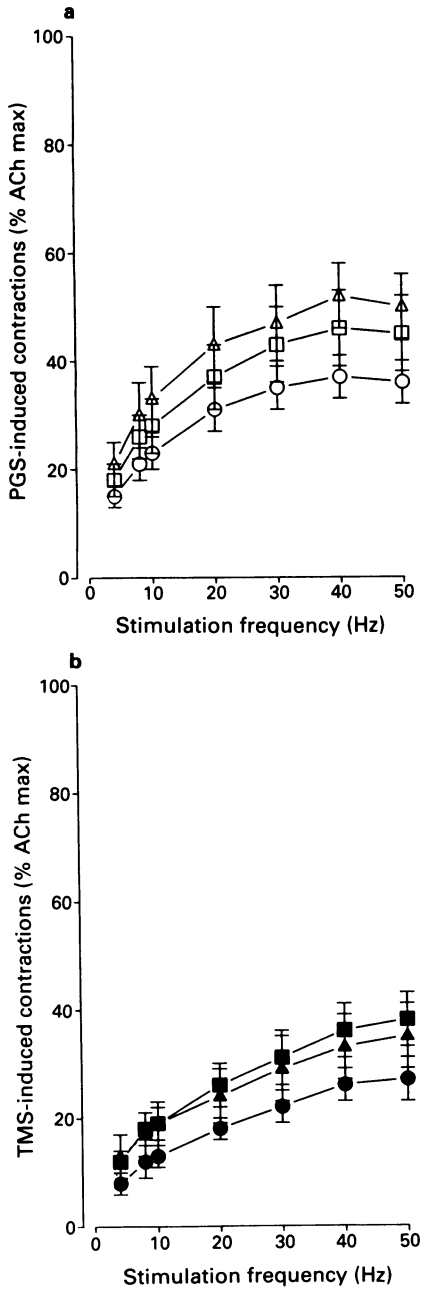



**Figure 2** Contractions of the trachea induced by (a) preganglionic stimulation (PGS, 0.2 ms, 30 V) and (b) transmural stimulation (TMS, 0.2 ms, 60 V) over a range of stimulation frequencies in tracheae from the three treatment groups: no pretreatment (□, ■), vehicle-pretreated (△, ▲) and capsaicin-pretreated (○, ●). Contractions are expressed as a % of the maximum increase in intraluminal pressure induced by acetylcholine (ACh, 0.3 mM) and are the mean ± s.e.mean, where $n = 8$.

### *Sensory neuropeptide depletion and its effect on responses to phosphoramidon*

There was no significant difference in the size of contractions induced by PGS in tracheae from any of the groups at any of the stimulation frequencies tested (Figure 2a), nor was there any difference in the size of contractions induced by TMS in tracheae from the three groups (Figure 2b). Phosphoramidon (10 μM) significantly facilitated PGS-induced contractions at all frequencies in tracheae from the two control groups (no pretreatment and vehicle pretreated), with the exception of 40 Hz in the no pretreatment group. However, there was no significant effect of phosphoramidon, on PGS-induced contractions in tracheae from capsaicin pretreated animals, at any of the frequencies tested (Figure 3, top panel). TMS-induced contractions were not significantly affected by phosphoramidon in any of the three groups at any of the frequencies tested (Figure 3, bottom panel). Contractions induced by exogenous ACh were not significantly different in tracheae from any of the three groups, nor were the contractions induced by a single concentration of exogenous substance P (Figure 4). All tissues were exposed to a single concentration of capsaicin at the end of the *in vitro* experiments and all tissues in the two control groups contracted, while none of the tracheae from the capsaicin pretreated group responded (Figure 4). There was no significant difference in the size of the response to capsaicin in the two control groups.

### *The effect of a selective $NK_1$ receptor antagonist*

The selective $NK_1$ receptor antagonist, GR71251, significantly inhibited PGS-induced contractions at 4, 8, 10 and 20 Hz when compared to control responses, before addition of GR71251, and at 4, 8 and 10 Hz when compared to vehicle/time controls (Figure 5a). TMS-induced contractions were not significantly different at any stimulation frequency either from control responses or vehicle/time controls (Figure 5b). Contractions induced by exogenous ACh were not significantly altered by the presence of GR71251 (1 μM) or vehicle (data not shown).

Incubation with GR71251 (1 μM) 15 min before the addition of phosphoramidon (10 μM), completely blocked the facilitatory effect of phosphoramidon on PGS-induced contractions (Figure 6a), while having no effect on contractions induced by TMS (Figure 6b).

### *The effect of NK receptor agonists*

The $NK_1$ receptor agonist, GR73632, significantly facilitated contractions of the trachea induced by both PGS and TMS at concentrations that did not significantly alter basal tone (0.01–0.3 nM) (Figure 7 and Table 1). The facilitatory effect of GR73632 on PGS- and TMS-induced contractions was significantly antagonized by a 15 min pre-incubation with the $NK_1$ receptor antagonist, GR71251 (1 μM) in the presence of phosphoramidon (10 μM) (Figure 7).

Neurokinin A significantly (1–10 nM) facilitated contractions of the trachea induced by stimulation of both pre- and postganglionic cholinergic nerves while at the same time causing a significant increase in basal tone of the tracheal tube preparation (Table 1). The selective $NK_3$ receptor agonist, senktide (30–300 nM), had no significant effect on basal tone or nerve-induced contractions (Table 1).

## Discussion

The present study has shown that the release of endogenous tachykinins, which can be depleted by capsaicin pretreatment, facilitates contractile responses induced by preganglionic cholinergic nerve stimulation and has identified the tachykinin receptors involved in this facilitatory effect as $NK_1$ receptors, by use of a selective agonist and antagonist for this receptor subtype. These data support the growing evidence from immunohistochemical (Sheppard *et al.*, 1983; Dey *et al.*, 1991), electrophysiological (Cameron & Coburn, 1984; Baker *et al.*, 1986; Myers *et al.*, 1990) and functional (Martling *et al.*, 1984; Hall *et al.*, 1989; Stretton *et al.*, 1992) studies, which suggest that tachykinins may play a facilitatory role in cholinergic control of airway smooth muscle tone.

In the presence of indomethacin, the tracheal tube preparation had a low constant intraluminal pressure upon which rapid spike contractions could be induced by either preganglionic vagus nerve stimulation (PGS) or stimulation of postganglionic intramural nerves via transmural stimulation

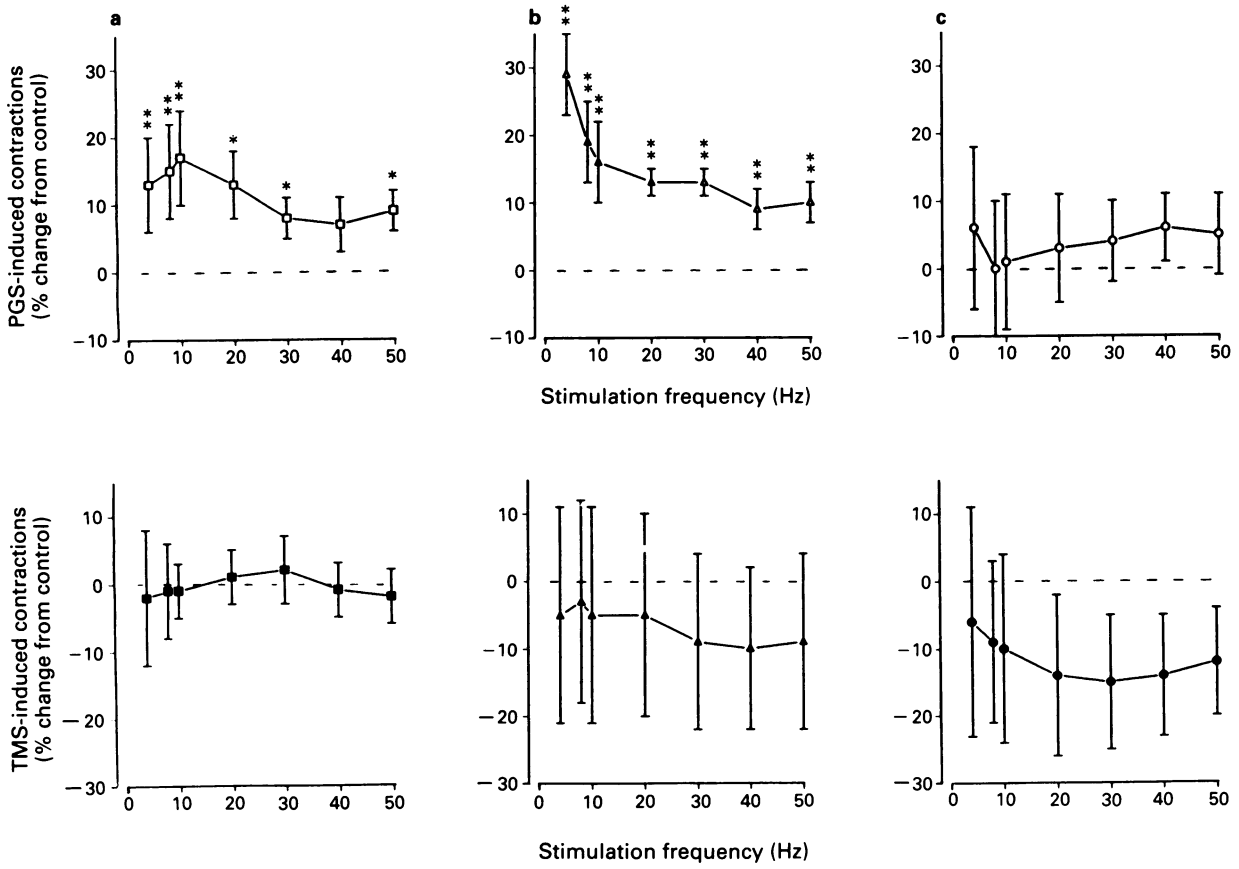



**Figure 3** Effect of phosphoramidon (10 $\mu$M) on contractions of the trachea induced by preganglionic stimulation (PGS, upper panel) and transmural stimulation (TMS, lower panel) in tracheae from the three treatment groups (a) no pretreatment (b) vehicle pretreated and (c) capsaicin pretreated. Results are expressed as the % change from control responses before addition of phosphoramidon and are the mean ± s.e.mean, where $n = 8$. $^{*}P < 0.05$; $^{**}P < 0.02$, compared to control responses.

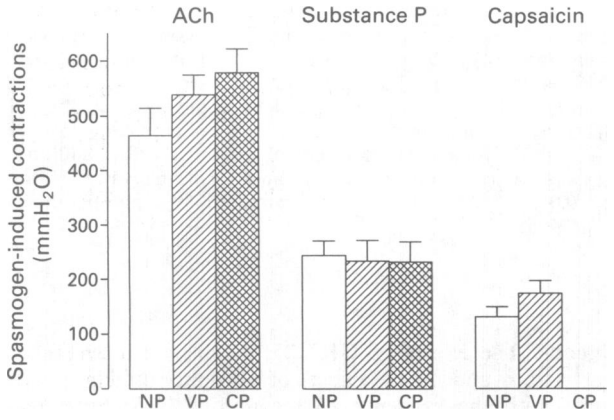



**Figure 4** Effect of the spasmogens acetylcholine (ACh), substance P and capsaicin on intraluminal pressure of tracheae from each of the three treatment groups: no pretreatment (NP), vehicle pretreated (VP) and capsaicin pretreated (CP). Contractions are expressed as the increase in intraluminal pressure in $mmH_2O$.

(TMS). These stimulation-induced contractions were abolished by atropine (1 $\mu$M) and tetrodotoxin (1 $\mu$M) indicating the cholinergic, neuronal nature of these responses and lack of an excitatory non-adrenergic, non-cholinergic (e-NANC) contractile component. If the tone of this preparation is raised with histamine, there does not appear to be any inhibitory non-adrenergic, non-cholinergic (i-NANC) response to preganglionic vagus nerve stimulation, however, there is an i-NANC relaxation response associated with TMS (Blackman & McCaig, 1983). The presence of an i-NANC response during TMS, but not during PGS, may account for the smaller responses associated with TMS when compared to PGS, since both the putative i-NANC neurotransmitters, vasoactive intestinal peptide (VIP) and nitric oxide (NO), have been shown to inhibit cholinergic nerve-induced contractions (Ellis & Farmer, 1989; Brave *et al.*, 1991). Therefore, while an i-NANC response cannot be detected in this preparation in the absence of inherent tone, its presence cannot be ignored in experiments where no attempt has been made to block its effects.

The major enzyme responsible for the breakdown of tachykinin neuropeptides is the metallopeptidase, neutral endopeptidase 24.11 (Erdos & Skidgel, 1989). Inhibition of this enzyme by phosphoramidon would be expected to exaggerate and prolong the actions of both endogenously released and exogenously applied tachykinins. Phosphoramidon facilitated PGS-induced contractions in a concentration-dependent manner, but had no significant effect on TMS- or ACh-induced contractions. This suggests that there is release of tachykinin neuropeptides during preganglionic cholinergic nerve stimulation but not during postganglionic cholinergic nerve stimulation. By inference, these findings indicate that there are facilitatory neurokinin receptors in parasympathetic ganglia.

Our findings with phosphoramidon on TMS-induced contractions are not consistent with those of Sekizawa and colleagues (1984), who showed facilitation of contractions of the ferret trachea induced by electrical field stimulation (EFS). These conflicting results may relate to species differences, but it is also possible that the facilitation ob-

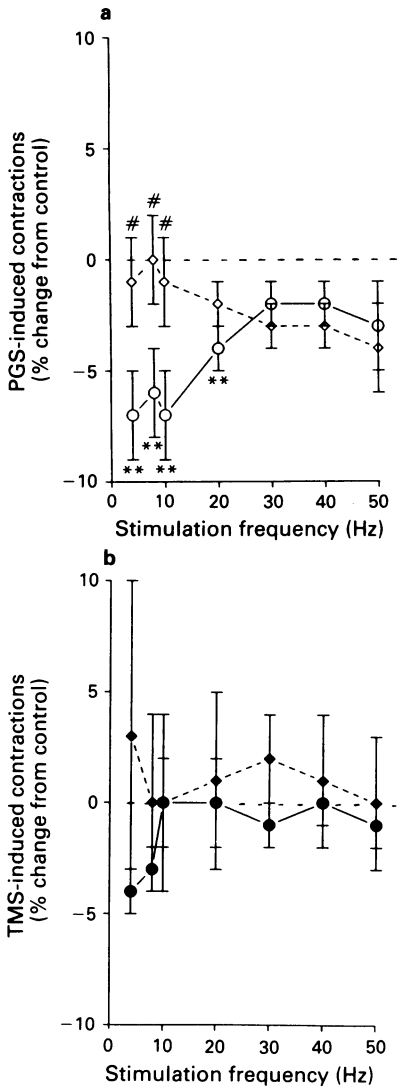



**Figure 5** Effect of the $NK_1$ receptor antagonist, GR71251, (○, ●) or vehicle (◇, ◆) on contractions of the trachea induced by (a) preganglionic stimulation (PGS, 0.2 ms, 30 V) and (b) transmural stimulation (TMS, 0.2 ms, 60 V) over a range of stimulation frequencies. Contractions are expressed as the % change from control responses at each frequency, before addition of GR71251 or vehicle. Results are the mean ± s.e.mean, where $n = 6$. $^*P < 0.02$, change from control before GR71251, $\#P < 0.05$, compared to vehicle/time control.

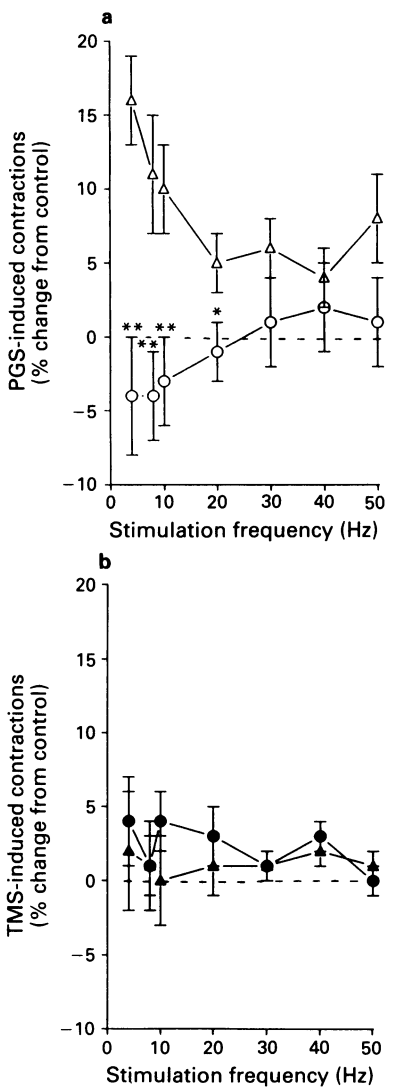



**Figure 6** Effect of phosphoramidon (10 μM) on (a) preganglionic stimulation (PGS, 0.2 ms, 30 V) and (b) transmural stimulation (TMS, 0.2 ms, 60 V)-induced contractions over a range of stimulation frequencies in the absence (△, ▲) and presence (○, ●) of the $NK_1$ receptor antagonist GR71251 (1 μM). Contractions are expressed as the % change from control responses before addition of phosphoramidon and are the mean ± s.e.mean where $n = 6$–8. $^*P < 0.05$; $^{**}P < 0.02$ phosphoramidon v phosphoramidon + GR71251.

served by Sekizawa and colleagues (1984) was due to an effect at the ganglia, since it is unclear whether EFS was performed in the presence of ganglionic nicotinic receptor blockade. In the absence of such blockade, EFS is likely to result in stimulation of all fibres embedded in the tissue, both pre- and postganglionic.

These data, therefore, suggest that there is release of facilitatory tachykinin neuropeptides during PGS but not during TMS. This is further supported by the findings with the $NK_1$ receptor antagonist, GR71251, which significantly inhibited PGS-induced contractions, while having no effect on TMS-induced contractions. Facilitation by phosphoramidon was consistently observed at low stimulation frequencies which accord with the effect of GR71251 at low stimulation frequencies (<20 Hz). The effect of GR71251 on PGS-induced contractions was small, but this may relate to the low concentration used and the fact that this compound is sensitive to degradation by peptidases. The reasons for this choice of protocol have already been discussed in the methods. The effects of GR71251 (1 μM) on nerve-induced contractions and on the effects of phosphoramidon are consistent with the existence of facilitatory $NK_1$ receptors in parasympathetic ganglia, activated by endogenously released tachykinins.

Phosphoramidon is a selective inhibitor of NEP, however, the tachykinin neuropeptides are not the only substrates for this enzyme. For example, the putative i-NANC neurotransmitter, VIP may also be inactivated by NEP (Rhoden & Barnes, 1989; Liu *et al.*, 1991). While it is not possible to detect an i-NANC response during TMS in tracheae lacking basal tone, its presence and inhibitory influence on cholinergic responses needs to be considered. Therefore, it is possible that the lack of effect of phosphoramidon on TMS-induced contractions, is not due to the fact that tachykinin neuropeptides are not released during TMS, but rather, that the inhibition of facilitatory tachykinin breakdown is opposed by the inhibition of inhibitory VIP breakdown, the net effect being no change.

This explanation for the lack of effect of phosphoramidon on TMS-induced contractions seems unlikely. First, when GR71251 was applied alone during nerve stimulation, PGS-induced contractions were significantly inhibited at low stimulation frequencies, while TMS-induced contractions were unaltered. If tachykinins were released by both forms of cholinergic nerve stimulation, one might have expected GR 71251 to exert the same effect regardless of the form of stimulation, however, this was not the case. Second, if facilitatory tachykinins were released during both forms of cholinergic nerve stimulation then, in the presence of GR 71251, the inhibitory VIP component should have remain unopposed and, therefore, TMS-induced contractions would have been inhibited in the presence of both GR71251 and phosphoramidon; however, this was not the case either.

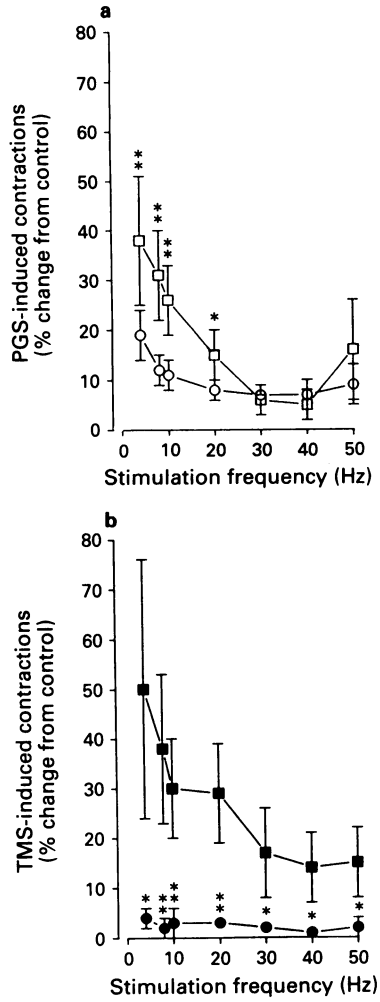



**Figure 7** Effect of the $NK_1$ receptor agonist, GR73632 on (a) preganglionic stimulation (PGS, 0.3 nM) and (b) transmural stimulation (TMS, 0.1 nM)-induced contractions of the trachea in the absence (□, ■) and the presence (○, ●) of the $NK_1$ receptor antagonist, GR71251 (1 μM), over a range of stimulation frequencies. Contractions are expressed as the % change from control responses before addition of the agonist and are the mean ± s.e.mean, where $n = 6-8$. $^*P<0.05$; $^{**}P<0.02$, GR73632 v GR73632 + GR71251.

Tachykinin neuropeptides are often associated with unmyelinated sensory C-fibres and require either chemical (capsaicin) or high intensity (antidromic) electrical stimulation to release them (Holzer, 1991). In the present study modest intensity electrical stimulation (0.2 ms) was used to induce contractions which could be blocked entirely by atropine. Therefore, the source of the facilitatory neuropeptides is unlikely to be the excitatory non-adrenergic, non-cholinergic afferent nerves. Previous studies (Martling *et al.*, 1984; Stretton *et al.*, 1992) have demonstrated that depletion of sensory neuropeptides by capsaicin pretreatment, not only abolished contractions induced by antidromic stimulation of pulmonary peptidergic afferent fibres running in the vagus nerves, but also inhibited contractions induced by stimulation of pulmonary cholinergic efferent fibres running in the vagus nerves.

In order to determine whether a capsaicin-sensitive store of tachykinins might be responsible for the facilitatory effect of phosphoramidon observed in our studies, the effects of capsaicin pretreatment were investigated on the response of PGS- and TMS-induced contractions to phosphoramidon and on nerve- ACh- and substance P-induced contractions. No significant difference in the size of nerve-induced contractions in tracheae from any of the three groups was detectable. This was unexpected based on our findings with phosphoramidon and those of others using capsaicin pretreatment (Martling *et al.*, 1984; Stretton *et al.*, 1992). This difference may be due to the fact that the effect, in trachea alone, is small and may require the presence of the smaller resistance airways in order to amplify it to a point where it can be detected. The data obtained with phosphoramidon, in capsaicin pretreated animals, suggests that modest electrical stimulation (0.2 ms pulse duration) of cervical vagal efferent fibres results in the activation of a population of capsaicin-sensitive tachykinin-containing neurones. This population of neurones may be one of a number of groups of unmyelinated nerves which run the length of the ganglionated tracheal plexus and appear to provide a communication network between glanglia within this plexus (Baluk & Gabella, 1989; Dey *et al.*, 1991).

The data obtained with the neurokinin receptor agonists and $NK_1$ receptor antagonist, further support the conclusion that there are facilitatory neurokinin receptors at the level of the parasympathetic ganglia and suggests that these receptors are of the $NK_1$ subtype. The data obtained with the agonists

**Table 1** The effect of tachykinin receptor agonists on basal tone and nerve-induced contractions of the guinea-pig trachea

| *Tachykinin receptor agonist* | *Increase in basal tone* ($mmH_2O$) | *Nerve-induced contractions* | | | |
|---|---|---|---|---|---|
| | | *PGS* | | *TMS* | |
| | | $B_1$ ($mmH_2O$) | *facilitation* (%) | $B_1$ ($mmH_2O$) | *facilitation* (%) |
| GR73632 (0.1 nM) | 1 ± 0 | 324 ± 21 | 7 ± 3* | 178 ± 26 | 17 ± 9 |
| Neurokinin A (5 nM) | 19 ± 5* | 147 ± 16 | 27 ± 6* | 112 ± 15 | 38 ± 7* |
| Senktide (30 nM) | 0 ± 0 | 240 ± 32 | 1 ± 1 | 170 ± 19 | 0 ± 1 |

The effect of neurokinin receptor agonists on basal tone and nerve-induced contractions of the trachea (preganglionic stimulation, PGS 0.2 ms, 30 Hz, 30 V at source and transmural stimulation, TMS 0.2 ms, 30 Hz, 60 V at source). The maximum responses to ACh in GR73632, neurokinin A and senktide-treated tracheae were 502 ± 44, 489 ± 44 and 505 ± 40 $mmH_2O$ respectively. The control responses before addition of agonist ($B_1$) are given in absolute values ($mmH_2O$) and were less than 80% of the maximum response to ACh in all three cases. The facilitation by tachykinin agonists of nerve-induced contraction is expressed as the % change from control response ($B_1$). Values are the mean ± s.e.mean where $n = 6-8$.
$^*P<0.05$, compared to control.

suggests that there are also facilitatory $NK_2$ receptors present on the postganglionic nerve. However, since a range of selective agonists for these receptor subtypes were not investigated this classification is not conclusive. Nevertheless, these findings are consistent with those of Hall and colleagues (1989), who showed that the neurokinin receptor-mediating the facilitation of cholinergic nerve-induced contractions by exogenous agonist was an $NK_2$ receptor. The ganglionic $NK_1$ receptors were not detected in the study by Hall and colleagues (1989) presumably because of the effect of activating the postjunctional $NK_2$ receptors and absence of a suitably selective agonist in that study. More detailed studies with a selective $NK_2$ receptor agonist were precluded in our study by the fact that large increases in basal tone are associated with these compounds and this complicates the interpretation of such data. The data obtained with senktide, suggest that it is unlikely that neurokinin $NK_3$ receptors are involved in these responses.

The effects of phosphoramidon and GR73632 on PGS-induced contractions are small, suggesting that the physiological relevance of this facilitatory mechanism in proximal airways may be minimal. However, as has already been discussed, with an intact system of smaller resistance airways and a higher concentration of antagonist, these effects may be considerably greater. Another important consideration is that while this facilitatory mechanism may be small under normal conditions where an active breakdown mechanism exists, in circumstances where this enzyme is inactivated, this facilitatory mechanism may become important. There is evidence that NEP is inactivated by viral infection (Jacoby *et al.*, 1988) and also by exposure to high concentrations of the industrial chemical, toluene diisocyanate (TDI), which causes asthma (Shepperd *et al.*, 1988). This mechanism might therefore explain in part the hyper-responsiveness to vagus nerve stimulation observed under these conditions (Buckner *et al.*, 1985).

The mechanism by which tachykinins facilitate ganglionic cholinergic neurotransmission in the airways are unknown, but may be similar to those described for luteinizing hormone releasing hormone (LHRH) in sympathetic ganglia (Jan *et al.*, 1980; Kuffler, 1980; Jan & Jan, 1981). Airway parasympathetic ganglion cells, like sympathetic ganglion cells, exhibit slow excitatory postsynaptic potentials (e.p.s.ps) when the interganglionic nerve trunk of the trachea is stimulated (Cameron & Coburn, 1984). Slow e.p.s.ps are often associated with peptidergic neurotransmission (Kuffler, 1980; Hartzel, 1981) and in sympathetic ganglia these slow e.p.s.ps can be evoked by an LHRH-like peptide (Jan *et al.*, 1980; Jan & Jan, 1981). Tachykinins may be the neurotransmitters responsible for these slow e.p.s.ps, since they facilitate parasympathetic neurotransmission as do slow e.p.s.ps (Martling *et al.*, 1984; Sekizawa *et al.*, 1987; Hall *et al.*, 1989; Stretton *et al.*, 1992) and have been identified in nerves closely association with airway ganglia (Dey *et al.*, 1991). Preliminary electrophysiological studies of guinea-pig bronchial ganglia indicate that tachykinins mimic the depolarization induced by capsaicin in these nerve cell bodies (Myers & Undem, 1992). Such a facilitatory mechanism may provide a fine control for neurotransmission through airway ganglia.

We are very grateful to Dr R.M. Hagan (Glaxo Research, Ware, UK) for providing GR71251 and GR73632 and to Dr Duncan Rogers (Dept. Thoracic Medicine, National Heart and Lung Institute, London) for his help with the capsaicin pretreatment procedure. This work was funded by the National Asthma Campaign of Great Britain.

## References

BAKER, D.G., McDONALD, D.M., BASBAUM, C.B. & MITCHELL, R.A. (1986). The architecture of nerves and ganglia of the ferret trachea as revealed by acetylcholinesterase histochemistry. *J. Comp. Neurol.*, **246**, 513–526.

BALUK, P. & GABELLA, G. (1989). Innervation of the guinea-pig trachea: a quantitative morphological study of intrinsic neurons and extrinsic nerves. *J. Comp. Neurol.*, **235**, 117–132.

BELVISI, M.G., BARNES, P.J. & ROGERS, D.F. (1990). Neurogenic inflammation in the airways: characterisation of electrical parameters for vagus nerve stimulation in the guinea-pig. *J. Neurosci. Methods*, **32**, 159–167.

BLACKMAN, J.G. & McCAIG, D. (1983). Studies on the isolated innervated preparation of guinea-pig trachea. *Br. J. Pharmacol.*, **80**, 703–710.

BRAVE, S.R., HOBBS, A.J., GIBSON, A. & TUCKER, J.F. (1991). The influence of L-$N^G$-nitro arginine on field stimulation induced contractions and ACh release in guinea-pig tracheal smooth muscle. *Biochem. Biophys. Res. Commun.*, **179**, 1017–1022.

BUCKNER, C.K., SONGSIRIDES, V., DICK, E.C. & BUSS, W.W. (1985). *In vivo* and *in vitro* studies on the use of the guinea-pig as a model of virus-provoked airway hyper-reactivity. *Am. Rev. Respir. Dis.*, **132**, 305–310.

BURNSTOCK, G., ALLEN, G.J. & HASSALL, J.S. (1987). The electrophysiologic and neurochemical properties of paratracheal neurones *in situ* and in dissociated cell culture. *Am. Rev. Respir. Dis.*, **136**, S23–26.

CAMERON, A.R. & COBURN, R.F. (1984). Electrical and anatomical characteristics of cells of ferret paratracheal ganglion. *Am. J. Physiol.*, **246**, C450–458.

COBURN, R.F. (1984). Neural coordination of excitation of ferret trachealis muscle. *Am. J. Physiol.*, **246**, C459–466.

COBURN, R.F. & KALIA, M.P. (1986). Morphological features of spiking and nonspiking cells in the paratracheal ganglion of the ferret. *J. Comp. Neurol.*, **254**, 341–351.

DEY, R.D., ALTEMUS, J.B. & MICHALKIEWICZ, M. (1991). Distribution of vasoactive intestinal peptide- and substance P-containing nerves originating from neurons of airway ganglia in cat bronchi. *J. Comp. Neurol.*, **304**, 330–340.

ELLIS, J.L. & FARMER, S.G. (1989). Modulation of cholinergic neurotransmission by vasoactive intestinal peptide and peptide histidine isoleucine in guinea-pig tracheal smooth muscle. *Pulm. Pharmacol.*, **2**, 107–112.

ERDOS, E.G. & SKIDGEL, R.A. (1989). Neutral endopeptidase 24.11 (enkephalinase) and related regulatory peptide hormones. *FASEB J.*, **3**, 145–151.

HAGAN, R.M., IRELAND, S.J., JORDAN, C.C., BAILEY, F., STEPHENS-SMITH, M.L., DEAL, M. & WARD, P. (1989). Novel, potent and selective agonists at NK-1 and NK-2 receptors. *Br. J. Pharmacol.*, **98**, 717P.

HAGAN, R.M., IRELAND, S.J., JORDAN, C.C., BERRESFORD, J.M., STEPHENS-SMITH, M.L., EVANS, G. & WARD, P. (1990). GR 71251, a novel potent and highly selective antagonist at neurokinin NK1 receptors. *Br. J. Pharmacol.*, **99**, 62P.

HALL, A.K., BARNES, P.J., MELDRUM, L.A. & MacLAGAN, J. (1989). Facilitation by tachykinins of neurotransmission in guinea-pig pulmonary parasympathetic nerves. *Br. J. Pharmacol.*, **97**, 274–280.

HARTZELL, H.C. (1981). Mechanisms of slow postsynaptic potentials. *Nature*, **291**, 539–544.

JACOBY, D.B., TAMAOKI, J., BORSON, D.B. & NADEL, J.A. (1988). Influenza infection causes airway hyper-responsiveness by decreasing enkephalinase. *J. Appl. Physiol.*, **64**, 2653–2658.

HOLZER, P. (1991). Capsaicin: Cellular targets, mechanisms of action, and selectivity for thin sensory neurons. *Pharmacol. Rev.*, **43**, 143–191.

JAN, L.Y. & JAN, Y.N. (1981). Role of an LHRL-like peptide as a neurotransmitter in sympathetic ganglia of the frog. *Fed. Proc.*, **40**, 2560–2564.

JAN, Y.N., JAN, L.Y. & KUFFLER, S.W. (1980). Further evidence for peptidergic transmission in sympathetic ganglia. *Proc. Natl. Acad. Sci. U.S.A.*, **77**, 5008–5012.

KUFFLER, S.W. (1980). Slow synaptic responses in autonomic ganglia and the pursuit of a peptidergic transmitter. *J. Exp. Biol.*, **89**, 257–286.

LIU, L.-W., TORTZ, M., ERDOS, E.G. & SAID, S.I. (1991). Vasoactive intestinal peptide (VIP) and helodermin degredation by airway enzymes. *Am. Rev. Respir. Dis.*, **143,** (abstract) A86.

MARTLING, C.-R., SARIA, A., ANDERSSON, P. & LUNDBERG, J.M. (1984). Capsaicin pretreatment inhibits vagal cholinergic and non-cholinergic control of pulmonary mechanics in the guinea-pig. *Naunyn Schmeid. Arch Pharmacol.*, **325,** 343–348.

MYERS, A. & UNDEM, B. (1992). Tachykinin-mediated stimulation of bronchial parasympathetic ganglion neurons. (Abstract). *Am. Rev. Respir. Dis.*, **145,** A261.

MYERS, J.A., UNDEM, B.J. & WEINREICH, D. (1990). Electrophysiological properties of neurons in guinea-pig bronchial parasympathetic ganglia. *Am. J. Physiol.*, **259,** L403–409.

RHODEN, K.J. & BARNES, P.J. (1989). Epithelial modulation of NANC and VIP-induced responses: role of neutralendopeptidase. *Eur. J. Pharmacol.*, **171,** 247–250.

SEKIZAWA, K., TAMAOKI, J., NADEL, J.A. & BORSON, D.B. (1987). Enkephalinase inhibitor potentiates substance P and electrically induced contractions of ferret trachea. *J. Appl. Physiol.*, **63,** 1401–1405.

SHEPPARD, D., THOMPSON, J.E., SCYPINSKI, L., DUSSER, D., NADEL, J.A. & BORSON, D.B. (1988). Toluene diisocyanate increases airway responsiveness to substance P and decreases airway neutral endopeptidase. *J. Clin. Invest.*, **81,** 1111–1115.

SHEPPARD, M.N., KURIAN, S.S., HENZEN-LOGMANS, S.C., MICHETTI, F., COCCHIA, D., COLE, P., RUSH, R.A., MARANGOS, P.J., BLOOM, S.R. & POLAK, J.M. (1983). Neurone-specific enolase and S-100: New markers for delineating the innervation of the respiratory tract in man and other mammals. *Thorax*, **38,** 333–340.

STRETTON, C.D., BELVISI, M.G. & BARNES, P.J. (1992). The effect of sensory nerve depletion on cholinergic neurotransmission in guinea-pig airways. *J. Pharmacol. Exp. Ther.*, **260,** 1073–1080.

WATSON, N., MACLAGAN, J. & BARNES, P.J. (1992a). Evidence for an involvement of tachykinins in cholinergic neurotransmission in guinea-pig airways. (Abstract). *Respir. Med.*, **86,** 77.

WATSON, N., MACLAGAN, J. & BARNES, P.J. (1992b). Demonstration of a facilitatory role of endogenous tachykinins in cholinergic neurotransmission in guinea-pig trachea. *Br. J. Pharmacol.*, **105,** 78P.

WATSON, N., MACLAGAN, J. & BARNES, P.J. (1992c). Endogenous tachykinins facilitate ganglionic cholinergic neurotransmission, via $NK_1$ receptors. *Am. Rev. Respir. Dis.*, **145,** (4) A261.

WATSON, N., MACLAGAN, J. & BARNES, P.J. (1992d). Involvement of endogenous tachykinins in ganglionic cholinergic neurotransmission in guinea-pig airways. *Am. Rev. Respir. Dis.*, **145,** A261.

*(Received September 4, 1992*
*Revised January 13, 1993*
*Accepted March 1, 1993)*

*Br. J. Pharmacol.* (1993), **109**, 760–764 © Macmillan Press Ltd, 1993

# Binding of angiotensin antagonists to rat liver and brain membranes measured *ex vivo*

[1]Fiona H. Marshall, Samantha A. Clark, [2]Anton D. Michel & Julie C. Barnes

Department of Neuropharmacology, Glaxo Group Research Ltd, Park Road, Ware, Hertfordshire, SG12 0DP

**1** The effects of the angiotensin antagonists GR117289, losartan and Sar$^1$Ala$^8$-angiotensin II on the *ex vivo* binding of [$^{125}$I]-Sar$^1$Ile$^8$-angiotensin II to rat liver and cortex/hippocampus (Cx/H) membranes have been investigated.

**2** GR117289 (0.1–30 mg kg$^{-1}$, s.c., 2 h pretreatment) caused a dose-dependent reduction in [$^{125}$I]-Sar$^1$Ile$^8$-angiotensin II binding to both liver and cortex/hippocampus membranes.

**3** Administration of a submaximal dose of GR117289 (1 mg kg$^{-1}$, s.c.) indicated that the peak inhibition of binding in the liver occurred within 0.5 h, whereas the peak inhibition of binding in the Cx/H occurred 2 h after drug treatment.

**4** The effect of GR117289 was long lasting. Binding was still reduced in the Cx/H 48 h after drug treatment (10 mg kg$^{-1}$, s.c.) but had returned to normal 72 h after drug treatment. In the liver binding was still reduced 72 h after treatment with the same dose.

**5** Losartan (1–30 mg kg$^{-1}$, s.c.) was equipotent with GR117289 in its ability to reduce liver binding, but was less effective at inhibiting binding to central receptors.

**6** The non-peptide antagonist Sar$^1$Ala$^8$-angiotensin II (3 and 10 mg kg$^{-1}$) reduced binding in the liver but not in the Cx/H membranes.

**7** These results suggest that, unlike the peptide antagonist Sar$^1$Ala$^8$-angiotensin II, the non-peptide angiotensin antagonists, GR117289 and losartan, are able to cross the blood brain barrier and occupy central angiotensin II receptors.

**Keywords:** Angiotensin antagonists; *ex vivo* binding; cortex; hippocampus; liver; losartan; Sar$^1$Ala$^8$-angiotensin II; GR117289

## Introduction

Angiotensin II (AII) is an important hormone, responsible for the maintenance of fluid and electrolyte homeostasis. As well as being present in the periphery all the components of the renin-angiotensin system are now known to occur in the brain (Hirose *et al.*, 1978). AII binding sites are also found widely distributed within the brain (Bennet & Snyder, 1976; Mendelsohn *et al.*, 1984) and the concept of an endogenous brain angiotensin system is now well established (Phillips, 1987).

So far, the exact roles of AII in the CNS have yet to be determined. However AII does appear to be involved in the central regulation of body fluid volume and control of reproductive hormone levels (Phillips, 1987). In addition, a neurotransmitter-like action has been described for AII and numerous interactions between AII and other transmitters have been reported. These include enhancement of noradrenaline release (Garcia-Sevilla *et al.*, 1979; Meldrum *et al.*, 1984), inhibition of acetylcholine release (Barnes *et al.*, 1989) and regulation of 5-hydroxytryptamine (5-HT) synthesis and release (Nahmod *et al.*, 1978).

AII receptors can be divided into two subtypes, $AT_1$ and $AT_2$ (Bumpus *et al.*, 1991), based on the selectivity of a number of recently described non-peptide antagonists. Losartan (DuP 753, Chiu *et al.*, 1989) and GR117289 (Robertson *et al.*, 1992) are selective for the $AT_1$ subtype, whilst PD 123177 (Chiu *et al.*, 1989) is selective for the $AT_2$ subtype. So far, almost all the actions of AII have been found to be mediated by $AT_1$ receptors, the function of the $AT_2$ receptors having yet to be established (see Zahran *et al.*, 1992). Both $AT_1$ and $AT_2$ subtypes have been shown to be present in the brain (Gehlert *et al.*, 1991).

In order to study further the function of brain AII and its receptors it is important to determine the ability of the recently described antagonists to penetrate the blood brain barrier. Song *et al.* (1991) have reported that losartan administered intravenously will block binding of [$^{125}$I]-Sar$^1$Ile$^8$-AII ([$^{125}$I]-Sarile) to areas within the blood brain barrier, such as the median preoptic nucleus and paraventricular hypothalamic nucleus. In this study, we provide further evidence for the brain penetration of losartan and have examined in detail the ability of GR117289 to cross the blood brain barrier. We have compared the central penetration of the non-peptide $AT_1$ receptor selective antagonists with that of the non-selective peptide antagonist Sar$^1$Ala$^8$-AII (saralasin). We have used the technique of *ex vivo* binding to investigate the effects of the angiotensin antagonists administered *in vivo* on the binding of [$^{125}$I]-Sarile to both brain membranes and to membranes from a peripheral tissue, the liver.

## Methods

### Ex vivo *binding*

GR117289 (0.1–30 mg kg$^{-1}$), losartan (0.1–10 mg kg$^{-1}$) or saralasin (3, 10 mg kg$^{-1}$) were administered s.c. to male Lister-Hooded rats (Glaxo bred) (200–250 g). At various times later (0.5–72 h) the rats were anaesthetized with a lethal dose of pentobarbitone (Expiral, 200 mg kg$^{-1}$, i.p.) and perfused transcardially with 50 ml of ice cold saline to remove any blood from the brain and liver. The liver and brain from individual animals were removed. The cortex and underlying hippocampus (Cx/H) was then dissected from the brain and the remaining tissue was discarded. The tissue was weighed, placed in a volume of Tris buffer (50 mM Tris, 100 mM NaCl, 10 mM $MgCl_2$, 1 mM EDTA, pH 7.4) to give a concentration of 12 mg ml$^{-1}$ (liver) or 200 mg ml$^{-1}$ (Cx/H), and homogenized with a Polytron PT10 homogenizer using

[1] Author for correspondence.
[2] Present address: Glaxo Institute of Applied Pharmacology, Department of Pharmacology, University of Cambridge, Tennis Court Road, Cambridge, CB2 1QJ.

three 5 s bursts at the maximum setting. Aliquots (50 µl) of the membranes were incubated in Tris buffer, containing 0.1% bovine serum albumin (BSA) and 1 mM bacitracin, with approximately 0.05 nM [$^{125}$I]-Sarile in a total assay volume of 150 µl. Total and nonspecific binding were determined by the absence or presence of AII (1 µM) respectively. Assay tubes were incubated for 90 min at 20°C. Bound and free radioactivity were separated by rapid filtration, using a Brandel cell harvester, through Whatman GF/B filters, which were pretreated for at least 2 h with 0.1% polyethyleneimine. The filters were washed with ice cold wash buffer (100 mM NaCl, 5 mM $MgCl_2$) and trapped radioactivity was determined in an LKB gamma counter.

### In vitro *competition binding studies*

In order to determine the affinity of GR117289, saralasin and losartan for AII receptors in the liver and Cx/H membranes, radioligand competition binding studies were conducted *in vitro* on membranes prepared as described for the *ex vivo* binding experiments. In addition, in order to determine the proportion of $AT_2$ receptors in the tissue, competition studies were also performed using the $AT_2$ antagonist, PD123177. The assay was conducted as described for the *ex vivo* binding experiments except that membranes from vehicle-treated control rats were incubated with the radioligand in the presence or absence of varying concentrations of the competing drugs.

### *Chemicals*

Human angiotensin II was obtained from Peninsula Laboratories. Saralasin was obtained from Sigma. Losartan potassium was obtained from DuPont Merck Pharmaceutical Company. GR117289 (1-[[3-bromo-2-[2-(1H-tetrazol-5-yl) phenyl]5-benzofuranyl]methyl]-2-butyl-4-chloro-1H-imidazole-5-carboxylic acid) and PD123177 (1-(4-amino-3-methylphenyl)methyl-5-(diphenyl-acetyl-4,5,6,7-tetrahydro-1H-imidazol [4.5-C]pyridine-6-carboxylic acid) were synthesized by Medicinal Chemistry, Glaxo Group Research. [$^{125}$I]-Sar$^1$Ile$^8$-angiotensin II was obtained from NEN, Dupont (specific activity 81.4 TBq mmol$^{-1}$). All other chemicals were obtained from Sigma.

### *Data analysis*

Data are expressed as a percentage of specific (total minus nonspecific) binding of vehicle-treated control rat. Statistical analysis was conducted on the raw data (d.p.m.), by a one-way analysis of variance (ANOVA) followed by a Dunnett's *t* test. Competition studies were analysed with iterative curve fitting techniques (Michel & Whiting, 1984) and data are expressed as $pIC_{50}$ values.

## Results

### In vitro *competition binding studies*

Specific binding in the liver and Cx/H membranes was 12765 ± 316 and 1823 ± 108 d.p.m. respectively ($n = 20$). In

**Table 1** Affinity estimates for GR117289, losartan, saralasin and PD123177 measured in competition binding studies with [$^{125}$I]-Sar$^1$Ile$^8$-angiotensin II

| | *Liver* | | *Cortex/Hippocampus* | |
|---|---|---|---|---|
| | $pIC_{50}$ | *Hill slope* | $pIC_{50}$ | *Hill slope* |
| GR117289 | 8.2 ± 0.1 | 0.9 ± 0.2 | 7.8 ± 0.2 | 0.9 ± 0.1 |
| Losartan | 7.6 ± 0.1 | 0.9 ± 0.1 | 7.5 ± 0.5 | 1.1 ± 0.1 |
| Saralasin | 7.8 ± 0.4 | 1.1 ± 0.1 | 7.2 ± 0.8 | 0.8 ± 0.1 |
| PD123177 | < 5 | | < 5 | |

Data are expressed as $pIC_{50}$ values with Hill slopes (mean ± s.e.mean, $n = 3$).

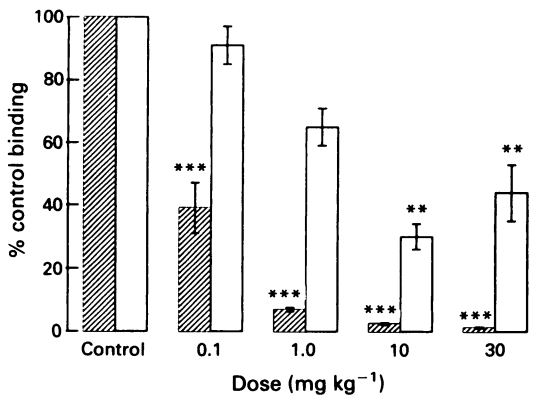



**Figure 1** Effect of a 2 h pretreatment of GR117289 (0.1–30 mg kg$^{-1}$, s.c.) on the *ex vivo* binding of [$^{125}$I]-Sar$^1$Ile$^8$-angiotensin II in liver (hatched columns) and cortex/hippocampus (open columns) membranes. Data are expressed as percentages of binding in vehicle-treated control rats. Statistical analysis was performed on raw data (d.p.m.) using a one-way ANOVA followed by a Dunnett's *t* test: ***$P < 0.001$, **$P < 0.01$.

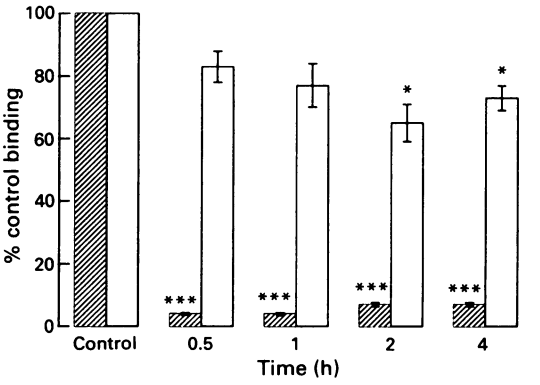



**Figure 2** Onset of action of the effect of GR117289 (1 mg kg$^{-1}$) on the *ex vivo* binding of [$^{125}$I]-Sar$^1$Ile$^8$-angiotensin II in liver (hatched columns) and cortex/hippocampus (open columns) membranes. Data are expressed as percentages of binding in vehicle-treated control rats. Statistical analysis was performed on raw data (d.p.m.) using a one-way ANOVA followed by a Dunnett's *t* test: ***$P < 0.001$, *$P < 0.05$.

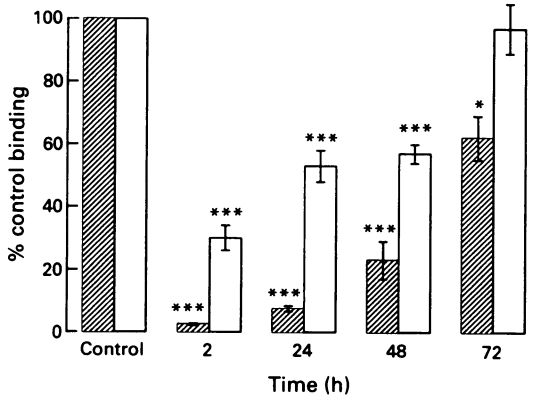



**Figure 3** Duration of action of GR117289 (10 mg kg$^{-1}$, s.c.) on the *ex vivo* binding of [$^{125}$I]-Sar$^1$Ile$^8$-angiotensin II in liver (hatched columns) and cortex/hippocampus (open columns) membranes. Data are expressed as percentages of binding in vehicle-treated control rats. Statistical analysis was performed on raw data (d.p.m.) using a one-way ANOVA followed by a Dunnett's *t* test: ***$P < 0.001$, *$P < 0.05$.

the liver and Cx/H membranes, losartan, GR117289 and saralasin completely displaced [$^{125}$I]-Sarile binding, the $pIC_{50}$ values are shown in Table 1. In all cases the Hill slopes (nH) were not significantly different from unity ($P<0.05$, using a Student's $t$ test) suggesting that binding was to a single type of receptor. In contrast, PD123177 failed to displace the binding except at high concentrations ($pIC_{50}<5$). These data are consistent with binding to $AT_1$ receptors and do not provide evidence for binding to $AT_2$ receptors.

### Ex vivo *binding*

GR117289 (0.1–30 mg kg$^{-1}$) administered s.c. 2 h before the rats were killed caused a dose-dependent inhibition of [$^{125}$I]-Sarile binding in the liver and Cx/H. GR117289 (10 and 30 mg kg$^{-1}$) caused an almost complete inhibition of liver binding; however in the Cx/H 10 mg kg$^{-1}$ caused maximal reduction in binding to only 30 ± 5% of control values with 30 mg kg$^{-1}$ causing no further reduction (Figure 1).

In order to investigate the time course for GR117289 to penetrate the brain, a submaximal dose (1 mg kg$^{-1}$, s.c.) was administered 0.5, 1, 2 and 4 h before the rats were killed. In the liver, a maximal reduction in binding at this dose was observed within 0.5 h. In contrast, in the Cx/H membranes, there was an increasing reduction in the levels of binding over the first three time points (0.5, 1 and 2 h), after which no further reduction was observed (Figure 2).

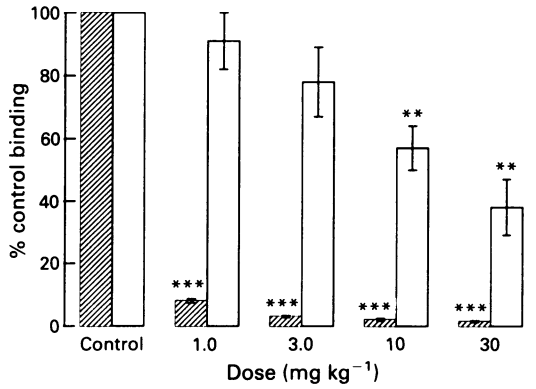



**Figure 4** Effect of a 2 h pretreatment of losartan (1–30 mg kg$^{-1}$, s.c.) on the *ex vivo* binding of [$^{125}$I]-Sar$^1$Ile$^8$-angiotensin II in liver (hatched columns) and cortex/hippocampus (open columns) membranes. Data are expressed as percentages of binding in vehicle-treated control rats. Statistical analysis was performed on raw data (d.p.m.) using a one-way ANOVA followed by a Dunnett's $t$ test: ***$P<0.001$, **$P<0.01$.

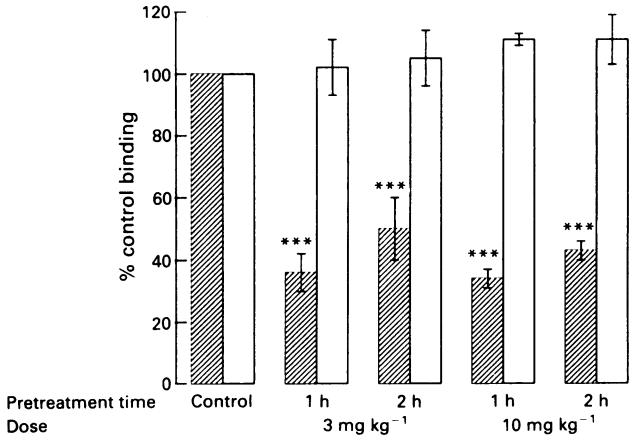



**Figure 5** Effect of a 1 or 2 h pretreatment of Sar$^1$Ala$^8$-angiotensin II (3 and 10 mg kg$^{-1}$, s.c.) on the *ex vivo* binding of [$^{125}$I]-Sar$^1$Ile$^8$-angiotensin II in liver (hatched columns) and cortex/hippocampus (open columns) membranes. Data are expressed as percentages of binding in vehicle-treated control rats. Statistical analysis was performed on raw data (d.p.m.) using a one-way ANOVA followed by a Dunnett's $t$ test: ***$P<0.001$.

To investigate the duration of action of GR117289, animals were killed 2, 24, 48 and 72 h after administration of GR 117289 (10 mg kg$^{-1}$, s.c.). A long lasting reduction in [$^{125}$I]-Sarile binding to Cx/H and liver membranes was observed following drug treatment. In the Cx/H, [$^{125}$I]-Sarile binding increased gradually over the time course of the experiment, but did not return to control levels until 72 h after drug administration. In the liver membranes, the reduction in binding also decreased gradually over the 24, 48 and 72 h time course, although in this case, the levels were still reduced 72 h after treatment with GR117289 (Figure 3).

Losartan (0.1–30 mg kg$^{-1}$, s.c.; 2 h pretreatment) caused a dose-dependent reduction in binding to liver and Cx/H membranes. In both the liver and Cx/H, losartan produced a similar reduction in binding to GR117289 (Figure 4).

A 1 or 2 h pretreatment with saralasin (3 or 10 mg kg$^{-1}$, s.c.) reduced binding in the liver membranes. A similar magnitude of effect was observed with both 3 and 10 mg kg$^{-1}$, and there was no difference between the 1 and 2 h pretreatment times. In contrast to the effect in the liver, saralasin failed to inhibit [$^{125}$I]-Sarile binding to Cx/H membranes (Figure 5).

## Discussion

This paper describes the use of an *ex vivo* binding technique to examine the penetration into the brain of the angiotensin antagonists, GR117289, losartan and saralasin. This technique has been used previously to demonstrate the brain penetration of a range of drugs including neuroleptics (Burki, 1986), opioids (Richards & Sadee, 1985) and adenosine antagonists (Baumgold *et al.*, 1992).

*In vitro* competition studies in the liver and cortex/hippocampus membranes, demonstrated that GR117289 and losartan were able to displace completely the binding of [$^{125}$I]-Sarile. The Hill slopes of the displacement curves were close to unity suggesting that binding was to a single population of receptors. Furthermore, the $AT_2$ antagonist, PD 123177, failed to displace any binding. Taken together these results suggest that in both types of tissues, binding was solely to the $AT_1$ type of AII receptor. This agrees with previous reports showing that the liver contains exclusively $AT_1$ receptors (Dudley *et al.*, 1990) and autoradiographic studies which have shown that [$^{125}$I]-Sarile binding in the cortical and hippocampal areas is displaced by losartan but not by WL 19, an $AT_2$ receptor antagonist (Gehlert *et al.*, 1991). The affinities of GR117289 and losartan are similar to those previously described for $AT_1$ receptors measured in binding studies (Chiu *et al.*, 1989; Marshall *et al.*, 1991). In these binding studies the affinity value for GR117289 is actually an underestimate due to the presence of high concentrations of BSA in the assay buffer (Marshall *et al.*, 1991). In the rabbit aorta, for example, the $pK_B$ of GR117289 for inhibition of AII-induced contractions is 9.8 (Robertson *et al.*, 1992). A 'high' concentration of BSA (0.1%) was used in the current study as this is necessary when using [$^{125}$I]-Sarile in order to achieve a reasonable level of specific binding. The affinity of saralasin obtained in these studies is slightly lower than has previously been described in conventional binding experiments, where membranes were prepared with a number of washing steps (Dudley *et al.*, 1990). This may be due to additional metabolism of saralasin in membranes prepared by homogenization only.

The use of *ex vivo* binding is limited by the potential redistribution of the *in vivo* administered drug between the bound and free form during membrane preparation and *in vitro* incubation. As it is not possible to determine the extent of the dissociation of drug during these *ex vivo* experiments; no calculations have been made to take into account the dilution of the tissue in the binding assay. However, evidence from functional experiments in the rabbit aorta suggests that the binding of GR117289 to $AT_1$ receptors is only 'slowly

reversible' (Robertson *et al.*, 1992) and thus, it is likely that dissociation of GR117289 from the receptors in these experiments will be minimal. Another limitation of the *ex vivo* technique is the possibility that drug administration could alter the density of $AT_1$ receptors and that the changes in binding levels observed are due to changes in receptor number rather than an actual blockade of receptors by the antagonist. However, we feel that with the short pretreatment times used in this study it is unlikely that changes in receptor levels will occur to any significant extent and would therefore prefer to conclude that the reduction in specific binding reflects receptor blockade.

The presence of $AT_1$ receptors in the liver has enabled the binding in the brain following drug treatment to be compared to binding in the periphery. In this study, GR117289 was found to be very potent in inhibiting binding to liver membranes, with a significant reduction in binding being observed with 0.1 mg $kg^{-1}$. These doses correlate well with those required to reduce blood pressure in the renal hypertensive rat (Hilditch *et al.*, 1992). GR117289 also caused a significant and dose-dependent reduction in brain binding, though the magnitude of reduction was less than observed in the liver. This suggests that GR117289 can penetrate the blood brain barrier, though higher doses will probably be needed to block the central effects of AII than are needed to block peripheral AII actions such as those on blood pressure.

It is interesting that in Cx/H membranes, while GR117289 at 10 mg $kg^{-1}$ was able to inhibit binding to 30% controls, no further inhibition was seen with 30 mg $kg^{-1}$. It is unclear why the remaining population of receptors cannot be blocked by GR117289. *In vitro* all the [$^{125}$I]-Sarile binding can be displaced by GR117289 indicating that the remaining 30% is not due to a subpopulation of receptors that are insensitive to GR117289. Dissociation of the drug from the receptors during the membrane preparation and *in vitro* incubation seems unlikely as the *ex vivo* binding of [$^{125}$I]-Sarile to liver membranes can be completely blocked by treatment with GR117289. One other explanation is that a small population of the receptors in this region are not accessible to peripherally administered GR117289. However, further studies need to be conducted, including the administration of even higher doses to investigate this further.

Time course experiments with GR117289 showed that the drug has a very rapid onset of action in the liver, with maximal reduction at 1 mg $kg^{-1}$ already seen 30 min after drug administration. However, in the brain, the maximal reduction in binding with 1 mg $kg^{-1}$ was not observed until 2 h after treatment, indicating a relatively slow penetration of the blood brain barrier. GR117289 (10 mg $kg^{-1}$) caused a long lasting reduction in the binding to both liver and cortex/hippocampal membranes. This duration of action correlates well with that on blood pressure in the renal hypertensive rat where blood pressure was still reduced 48 h after a 3 mg $kg^{-1}$ (i.a.) dose of GR117289 (Hilditch *et al.*, 1992). This long lasting effect may be due to the slowly reversible nature of the binding, or may indicate that the levels of GR117289 in the extracellular space remain high for some time.

Losartan also caused a dose-dependent reduction in liver and brain binding, with a similar magnitude to GR117289. Song *et al.* (1991) have used *ex vivo* autoradiography to demonstrate that peripherally administered losartan (10 mg $kg^{-1}$, i.v.) can reduce binding to regions in the brain such as the hypothalamus. We have confirmed the ability of losartan to penetrate the blood brain barrier and have shown that peripherally administered losartan will block $AT_1$ receptors in the forebrain. The doses used in this study correlate well with doses that have been shown to antagonize central actions of AII. Dennes *et al.* (1992) demonstrated that losartan (3, 10 and 30 mg $kg^{-1}$) dose-dependently reduced drinking in rats induced by intraventricular administration of AII. In addition, 10 mg $kg^{-1}$ losartan improved cognitive performance in a delayed non-matching to position task in the rat and partially reversed a scopolamine-induced spatial memory deficit in the radial maze, effects which may be mediated by forebrain $AT_1$ receptors (Dennes *et al.*, 1992). Wong *et al.* (1990) have reported that losartan is metabolized *in vivo* to a related compound EXP3174, which has a similar affinity to losartan for $AT_1$ receptors. It is possible that the action of losartan described here and indeed in other behavioural studies may be a result of receptor blockade by EXP3174 rather than losartan itself.

Saralasin, a peptide antagonist of angiotensin receptors, has similar affinity for $AT_1$ receptors to the non-peptide antagonists, losartan and GR117289. In this study, saralasin (10 mg $kg^{-1}$) was able to reduce liver binding to a maximum of 64% of controls, 1 h after drug treatment. This is significantly less than the reduction in binding caused by similar doses of the non-peptide antagonists, despite their similar affinity for $AT_1$ receptors. This difference may be due to a more rapid metabolism of the peptide *in vivo*. Although saralasin was able to reduce binding to peripheral angiotensin receptors it caused no reduction in binding to central angiotensin receptors, suggesting that saralasin does not penetrate the blood brain barrier.

In conclusion, the technique of *ex vivo* binding can be used to investigate the central penetration of angiotensin antagonists. We have demonstrated that, unlike the peptide antagonist saralasin, GR117289 and losartan can penetrate the blood brain barrier and bind to central $AT_1$ receptors. These drugs will therefore be useful to investigate further the role of the renin-angiotensin system in the brain. Furthermore the technique of *ex vivo* binding will be useful in predicting the doses and duration of action of these and other $AT_1$ antagonists prior to their use in behavioural studies.

## References


BARNES, J.M., BARNES, N.M., COSTALL, B., HOROVITZ, Z.P. & NAYLOR, R.J. (1989). Angiotensin II inhibits the release of [$^3$H]-acetylcholine from rat entorhinal cortex *in vitro*. *Brain Res.*, **491**, 136–143.

BAUMGOLD, J., NIKODIJEVIC, O. & JACOBSEN, K.A. (1992). Penetration of adenosine antagonists into mouse brain as determined by *ex vivo* binding. *Biochem. Pharmacol.*, **43**, 889–894.

BENNET, J.P. & SNYDER, S.H. (1976). Angiotensin II binding to mammalian brain membranes. *J. Biol. Chem.*, **23**, 7423–7430.

BUMPUS, F.M., CATT, K.J., CHIU, A.T., DEGASPARO, M., GOODFRIEND, T., HUSAIN, A., PEACH, M.J., TAYLOR, D.G. & TIMMERMANS, P.B.M.W.M. (1991). Nomenclature for angiotensin receptors. *Hypertension*, **17** (S), 720–721.

BURKI, H.R. (1986). Binding of psychoactive drugs to rat brain amine receptors, measured *ex vivo*, and their effect on the metabolism of biogenic amines. *Naunyn-Schmieds Arch. Pharmacol.*, **322**, 258–266.

CHIU, A.T., HERBIN, W.F., MACALL, D.E., ARDECKY, R.J., CARINI, D.J., DUNCIA, R., PEASE, L.J., WONG, P.C., WEXLER, R.R., JOHNSON, A.I. & TIMMERMANS, P.B.M.W.M. (1989). Identification of angiotensin II receptor subtypes. *Biochem. Biophys. Res. Commun.*, **165**, 196–203.

DENNES, R.P., BARNES, J.C., MICHEL, A.D. & TYERS, M.B. (1992). The effect of the $AT_1$ receptor antagonist, losartan (DuP 753) on cognitive performance in the radial maze and in a delayed non-matching to position task in the rat. *Br. J. Pharmacol.*, **105**, 88P.

DUDLEY, T.D., PANEK, R.L., MAJOR, T.C., LU, G.H., BRUNS, R.F., KLINEFUS, B.A., HODGES, J.C. & WEISHARR, R.E. (1990). Subclasses of angiotensin II binding sites and their functional significance. *Mol. Pharmacol.*, **38**, 370–377.

GARCIA-SEVILLA, J.A., DUBOCOVICH, M.L. & LANGE, S.Z. (1979). Angiotensin II facilitates the potassium-evoked release of [$^3$H]-noradrenaline from the rabbit hypothalamus. *Eur. J. Pharmacol.*, **56**, 173–176.

GEHLERT, D.R., GACKENHEIMER, S.L. & SCHOBER, D.A. (1991). Autoradiographic localization of subtypes of angiotensin II antagonist binding in the rat brain. *Neuroscience*, **44**, 501–514.

HILDITCH, A., AKERS, J.S., TRAVERS, A., HUNT, A.A., ROBERTSON, M.J., DREW, G.M., MIDDLEMISS, D. & ROSS, B.C. (1991). Cardiovascular effects of the angiotensin receptor antagonist, GR 117289, in conscious renal hypertensive and normotensive rats. *Br. J. Pharmacol.*, **104**, 423P.

HIROSE, S., YOKOSAWA, H. & INGAMI, T. (1978). Immunological identification of renin in rat brain and distinction from acid protease. *Nature*, **274**, 392–393.

MARSHALL, F.H., BARNES, J.C., BROWN, J.D., MICHEL, A.D. & TYERS, M.B. (1991). The interaction of GR117289 with the angiotensin $AT_1$ and $AT_2$ binding sites. *Br. J. Pharmacol.*, **104**, 425P.

MELDRUM, M.J., XNE, C.S., BADINO, L. & WESTFALL, T.C. (1984). Angiotensin facilitation of noradrenergic neurotransmission in central tissues of the rat: effects of sodium restriction. *J. Cardiovasc. Pharmacol.*, **6**, 989–995.

MENDELSOHN, F.A.O., QUIRION, R., SAAVEDRA, J.M., AGUITERA, G. & CATT, K.J. (1984). Autoradiographic localization of angiotensin II receptors in the rat brain. *Proc. Natl. Acad. Sci. U.S.A.*, **81**, 1575–1579.

MICHEL, A.D. & WHITING, R.L. (1984). Analysis of ligand binding data using a microcomputer. *Br. J. Pharmacol.*, **83**, 406P.

NAHMOD, V.E., FINKELMAN, S., BENARROCH, E.E. & PIROLA, C.J. (1978). Angiotensin regulates release and synthesis of serotonin in brain. *Science*, **202**, 1091–1093.

PHILLIPS, M.I. (1987). Functions of angiotensin in the central nervous system. *Annu. Rev. Physiol.*, **49**, 413–435.

RICHARDS, M.L. & SADEE, W. (1985). *In vivo* opiate receptor binding of oripavines to $\mu$, $\delta$ and $\kappa$ sites in rat brain as determined by an *ex vivo* labeling method. *Eur. J. Pharmacol.*, **114**, 343–353.

ROBERTSON, M.J., BARNES, J.C., DREW, G.M., CLARK, K.L., MARSHALL, F.H., MICHEL, A., MIDDLEMISS, D., ROSS, B.C., SCOPES, D. & DOWLE, M.D. (1992). Pharmacological profile of GR117289 *in vitro*: a novel potent and specific non-peptide angiotensin $AT_1$-receptor antagonist. *Br. J. Pharmacol.*, **107**, 1173–1180.

SONG, K., ZHUO, J. & MENDELSOHN, F.A.O. (1991). Access of peripherally administered DuP 753 to rat brain angiotensin receptors. *Br. J. Pharmacol.*, **104**, 771–772.

WONG, P.C., PRICE, J.R., CHIU, A.T., DUNCIA, J.V., CARINI, D.J., WEXLER, R.R., JOHNSON, A.L. & TIMMERMANS, P.B.W.M. (1990). Nonpeptide angiotensin II receptor antagonists IX. Pharmacology of EXP3174: an active metabolite of DuP 753, an orally active antihypertensive agent. *J. Pharmacol. Exp. Ther.*, **255**, 211–217.

ZAHRAN, E.D., YE, X., ADES, A.M., REAGAN, L.P. & FLUHARTY, S.J. (1992). Angiotensin-induced cyclic GMP production is mediated by multiple subtypes and nitric oxide in N1E-115 neuroblastoma cells. *J. Neurochem.*, **58**, 1960–1963.

*(Received December 18, 1992*
*Revised February 22, 1993*
*Accepted February 24, 1993)*

*Br. J. Pharmacol.* (1993), **109**, 765–773 © Macmillan Press Ltd, 1993

# Postjunctional inhibitory effect of the $NK_2$ receptor antagonist, SR 48968, on sensory NANC bronchoconstriction in the guinea-pig

Ya-Ping Lou, [1]Lu-Yuan Lee, [2]Hiroyuki Satoh & [3]Jan M Lundberg

Department of Pharmacology, Karolinska Institute, Box 60400, S-104 01 Stockholm, Sweden

**1** The effects of a selective $NK_2$ receptor antagonist, SR 48968, on non-adrenergic non-cholinergic (NANC) bronchoconstriction in the guinea-pig were investigated in both *in vitro* and *in vivo* studies.

**2** In isolated bronchus, the electrical field stimulation (EFS, 1 Hz for 1 min)-induced NANC bronchoconstriction was inhibited by 83% after preincubation with SR 48968 ($10^{-7}$ M) for 1 h. The selective $NK_1$ receptor antagonist, CP 96,345 ($10^{-6}$ M), together with SR 48968 completely abolished the remaining EFS-evoked NANC bronchial contraction. ST 48968 ($10^{-7}$ M) totally blocked the bronchial contraction caused by neurokinin A (NKA), but reduced only slightly the bronchoconstriction caused by high concentrations of substance P (SP) and did not influence the response to acetylcholine (ACh).

**3** In the guinea-pig isolated perfused lung, SR 48968 ($5 \times 10^{-7}$ M) perfusion for 30 min markedly reduced, by 95% and 68% respectively, the increase in lung resistance ($R_L$) and the decrease in dynamic compliance ($C_{Dyn}$) evoked by vagal stimulation (1 Hz for 1 min). Capsaicin ($10^{-8}$ M)-evoked bronchoconstriction was also significantly inhibited by SR 48968 ($5 \times 10^{-7}$ M). However, the same concentration of SR 48968 did not affect the release of neuropeptide calcitonin gene-related peptide (CGRP)-like immunoreactivity (LI) evoked by either vagal stimulation or capsaicin in the isolated perfused lung, suggesting no prejunctional action. SR 48968 ($5 \times 10^{-7}$ M) caused a parallel shift of the concentration-response curve to the right by a factor of 10 for the bronchoconstriction evoked by NKA ($10^{-9}$–$3 \times 10^{-7}$ M) in the isolated lung, while it abolished the contraction induced by the selective $NK_2$ receptor agonist, $Nle^{10}$ NKA(4-10) ($10^{-9}$–$3 \times 10^{-7}$ M).

**4** In *in vivo* studies, ST 48968 (0.3 mg kg$^{-1}$, i.v.) also greatly inhibited the increase in insufflation pressure evoked by either capsaicin (10 μg kg$^{-1}$, i.v.) or NKA (1 μg kg$^{-1}$, i.v.), without any measurable effect on the accompanying hypotensive responses.

**5** The results suggest: (i) ST 48968 is a selective and potent $NK_2$ postjunctional receptor antagonist both *in vitro* and *in vivo* in the guinea-pig, and (ii) the NANC bronchoconstriction evoked by sensory nerve activation either by antidromic nerve stimulation or by capsaicin is mediated mainly via $NK_2$ receptors and only to a minor extent via $NK_1$ receptors.

**Keywords:** Bronchoconstriction; capsaicin; calcitonin gene-related peptide (CGRP); neurokinin A; $NK_2$ receptor antagonist; substance P; SR 48968; vagal stimulation

## Introduction

Activation of vagal capsaicin-sensitive sensory nerves in guinea-pigs causes prolonged non-adrenergic, non-cholinergic (NANC) bronchoconstriction in both *in vivo* and *in vitro* preparations (Lundberg & Saria, 1982). This effect is caused by tachykinins released from peripheral terminals of sensory nerves within bronchial smooth muscle as revealed by inhibitory effects of the first generation of substance P (SP) antagonists (see Lundberg *et al.*, 1983). These peptide analogues also inhibit the effects of neurokinin A (NKA) (Karlsson *et al.*, 1984). More recently, other peptide antagonists have been developed which showed selectivity for neurokinin 1 ($NK_1$) and neurokinin 2 ($NK_2$) receptors. These include L 668,169, which is $NK_1$-selective, and L 659,877, MEN 10,207, MEN 10,376, R 396 (McKnight *et al.*, 1988; Dion *et al.*, 1990; Maggi *et al.*, 1990; 1991), and dactinomycin (DAC, Lundberg & Lou, 1991; Fujii *et al.*, 1991; Lou *et al.*, 1992), which are $NK_2$-selective. The peptide analogues MEN 10,207, MEN 10,376, DAC and L 659,877 inhibit NANC bronchoconstriction in the guinea-pig. It seems clear, however, that guinea-pig bronchi also have $NK_1$ receptors that mediate broncoconstriction in responses to SP or the selective agonists such as $Sar^9Met(O_2)^{11}$-SP (Lou *et al.*, 1992). Interestingly, CP 96,345, a selective $NK_1$ antagonist of non-peptide nature, had no clear-cut influence on the NANC bronchoconstriction evoked by electrical field stimulation (EFS) in the guinea-pig isolated bronchi (Lou *et al.*, 1992). Therefore, a selective $NK_2$ antagonist of non-peptide nature would allow us to determine the relative roles of $NK_1$ and $NK_2$ receptors in mediating the bronchoconstrictor response to neuronally released tachykinins. We have therefore used the recently developed selective and potent non-peptide $NK_2$ antagonist SR 48968 (Emonds-Alt *et al.*, 1992; Advenier *et al.*, 1992) to characterize the NANC bronchoconstriction in guinea-pig airways *in vitro* and *in vivo*. To reveal possible prejunctional inhibitory effects of SR 48968 on peptide release from the sensory nerves we have also used the guinea-pig isolated perfused lung model, in which the bronchoconstrictor response and peptide release can be studied simultaneously (Kröll *et al.*, 1990; Lou *et al.*, 1991).

## Methods

### *Isolated bronchus preparations*

Adult Dunkin-Hartley guinea-pigs (300–400 g) of either sex were killed by a blow on the head. The hilar bronchi were

[1] Present address: Dept. of Physiology, University of Kentucky Medical Center, Lexington, Kentucky 40536-0084, U.S.A.
[2] Present address: Pharmaceutical Research Laboratories, Kyowa Hakko Kogyo Co., Ltd., Shizuoka-Ken, Japan.
[3] Author for correspondence.

isolated and mounted in a 2 ml Perspex chamber containing Krebs-Ringer solution, with the following composition (mM): NaCl 118, $CaCl_2$ 2.5, $MgSO_4$ 1.2, $NaHCO_3$ 24.9, $KH_2PO_4$ 1.2, KCl 4.7, glucose 5.6 and HEPES 12.6, and aerated with 6.5% $CO_2$ in $O_2$. Two L-shaped holders were used to give a resting bronchial tension of 5 millinewton (mN) maintained by readjusting during a 2 h equilibration period. Tension changes were recorded on a Grass 7D polygraph via a Grass FT03C force displacement transducer connected to one of the L-shaped metal holders. Guanethidine ($5 \times 10^{-6}$ M) was present at all times to block sympathetic mechanisms. Electrical field stimulations (EFS, duration: 1 ms) were delivered at 1 Hz for 1 min at 30 min intervals via two electrodes mounted on either side of the preparation. The contraction induced by EFS could be abolished by tetrodotoxin ($3 \times 10^{-7}$ M). Atropine ($10^{-6}$ M) was added to block the muscarinic contraction component and the remaining NANC broncoconstriction was reproducible. After a control NANC response to EFS, the $NK_2$ receptor antagonist, SR 48968 ($10^{-7}$ M) was introduced into the testing chamber for 1 h and then the study of the response to EFS was repeated. Further, EFS was repeated after preincubation with the $NK_1$ receptor antagonist, CP 96,345 ($10^{-6}$ M, 15 min) in addition to SR 48968 ($10^{-7}$ M, 1 h). In another series of experiments, the reverse order of atropine and SR 48968 was given in order to examine the SR 48968 effect on the EFS stimulation-evoked bronchial contraction first, in absence of atropine. In parallel studies with SR 48968 vehicle, there was no decay in the EFS response upon repeated stimulation in isolated bronchus using the same experimental protocol. In separate groups of preparations, the studies of concentration-responses to NKA and SP were performed. Contraction induced by NKA or SP was expressed as a percentage of that induced by acetylcholine (ACh, $10^{-5}$ M), which was tested first in each preparation to establish an internal standard contraction.

### *Guinea-pig isolated perfused lung preparation*

The experimental protocol for the guinea-pig isolated perfused lung model has been described previously in detail (Lou *et al.*, 1991). Briefly, adult Dunkin-Hartley guinea-pigs (250–350 g) of either sex were anaesthetized with pentobarbitone sodium (Mebumal, 60 mg $kg^{-1}$, i.p.). The lungs were perfused through the pulmonary artery with Krebs-Ringer solution (see above). Then, the lungs together with the intubated trachea, cannulated heart and vagus nerves were dissected free and placed in a thoracic chamber saturated with water vapour at 37°C and alternating negative pressures (−1 to −11 $cmH_2O$) were produced by a respirator (Harvard, mod. 665) and a vacuum source connected to the chamber. The chamber pressure, the respiratory air flow and volume were recorded on a Grass Polygraph, from which the lung resistance ($R_L$) and dynamic compliance ($C_{Dyn}$) were calculated by an on-line computer. When a closure of the air passage occurred as the result of a severe bronchoconstriction, the 'inspired' volume generated by the negative chamber pressure was markedly attenuated and in some cases reduced to zero (e.g., Figure 3). The values of 1000% and 100% were set as for calculation purposes for the change of $R_L$ and $C_{Dyn}$ respectively, under these conditions. The vagus nerves were placed in two platinum electrodes connected to an electrical stimulator (bipolar current generator, Hässle, Sweden). In all experiments the ganglionic blocking agent, chlorisondamine ($10^{-6}$ M) was added to inhibit parasympathetic ganglionic transmission, and terbutaline ($10^{-7}$ M) was present in order to stabilize the basal tone of the airways. Vagal sensory nerve fibres were stimulated either by perfusion with capsaicin ($10^{-8}$ M) for 3 min or vagal stimulation (1 Hz, duration: 5 ms) for 1 min of both vagus nerves. Each preparation was only exposed to capsaicin and vagal stimulation once. In other groups of lungs, increasing concentrations of NKA or $Nle^{10}$NKA(4-10) were added until a bronchoconstriction of similar degree to that produced by capsaicin ($10^{-8}$ M) was induced. Experiments were performed by increasing the NKA or $Nle^{10}$NKA(4-10) concentration in a cumulative manner starting from $10^{-10}$ M or $10^{-9}$ M, respectively. Each concentration of agonist was perfused for about 2.5 min. Since our pilot studies revealed no development of tachyphylaxis, paired data could be obtained in each preparation for both control and SR 48968-treated lungs. Each preparation was exposed only to either NKA or $Nle^{10}$NKA(4-10). SR 48968 ($5 \times 10^{-7}$ M) was given 30 min before and during provocation with various stimulants.

### *CGRP-like immunoreactivity*

Tachykinins and CGRP are co-stored in large dense-cored vesicles (Gulbenkian *et al.*, 1986) in the capsaicin-sensitive nerves. Since it is easier to detect CGRP than NKA, overflow of CGRP-like immunoreactivity (LI) was used as a biochemical marker for pulmonary sensory nerve activation in most experiments (Kröll *et al.*, 1990; Lou *et al.*, 1991). Perfusate fractions (3 min) were collected through a right atrial catheter in a beaker placed on ice. Acetic acid was immediately added to give a final concentration of 0.2 M. The perfusate samples were desalted with SEP-PAK $C_{18}$ cartridges, lyophilized and redissolved in buffer before determination of CGRP-LI by radioimmunoassay with an antiserum raised against human CGRP-alpha (RAS 6009, Peninsula, Belmont, CA, U.S.A.; for details see Franco-Cereceda *et al.*, 1989). The detection sensitivity is 3.9 fmol per sample and intra-assay variation for the CGRP assay was 8%. The CGRP-LI overflow has been expressed as percentual increase over that in the basal fraction just before the application of stimulus.

### *Experiments in anaesthetized guinea-pigs*

Dunkin Hartley guinea-pigs (250–400 g) of either sex were used. They were anaesthetized with pentobarbitone sodium (Menuma 50 mg $kg^{-1}$, i.p.). A tracheal cannula was inserted and artificial ventilation was maintained by means of an Ealing constant volume ventilator (Scientific & Research Instrument Ltd., 50-1718, Kent, UK). The insufflation pressure of the lung was measured on a breath-to-breath basis using a Statham low pressure tranducer (PDCR 75/1) to estimate the bronchial smooth muscle tone (Lundberg *et al.*, 1983). The left jugular vein was cannulated for injection of various compounds (capsaicin, NKA or SR 48968). A catheter was also introduced into the left carotid artery to monitor the systemic arterial blood pressue and heart rate via a pressure transducer (Statham 5930 P23AC, Heto Rey, Puerto Rico). Body temperature of the guinea-pigs was kept at 37–38°C with a heating control device (Elbeco Electronics, Uppsala, Sweden). To maintain blood pressure Dextran 70 (Pharmacia, 5 ml at 60 g $l^{-1}$ in saline) was given 5 min before administration of the ganglionic blocker, chlorisondamine (5 mg $kg^{-1}$, i.v.), which blocks both adrenergic and cholinergic reflex mechanisms. Capsaicin (10 μg $kg^{-1}$) or NKA (1 μg $kg^{-1}$) was then injected intravenously after an additional 5 min.

### *Drugs*

Drugs from the following sources were used: atropine (ACO, Solna, Sweden), capsaicin (Fluka Chemie AG, Buchs, Switzerland), chlorisondamine (Ciba-Geigy, AG, Basel, Switzerland), CP 96,345 ((2S, 3S)-cis-2-(diphenylmethy)-N-[(2-methoxyphenyl)-methyl]-1-azabicyclo (2.2.2) octan-3-amine; Pfizer, Groton, CT, U.S.A.), guanethidine sulphate (Ciba-Geigy AG, Basel, Switzerland), human CGRPα, NKA, $Nle^{10}$NKA(4-10) and SP (Peninsula, Belmont, CA, USA), human [$^{125}$I]-CGRPα (Amersham Int., Amersham, England), pentobarbitone sodium (Mebuma; Nord Vacc, Stockholm, Sweden), SR 48968 ((±)-N-methy-N[4-acetylamino-4-phenyl piperidino-2-(3, 4-dichlorophenyl) butyl] benzamide; Sanofi, Montpellier

Cedex, France) and terbutaline (Bricanyl, DRACO, Lund, Sweden). Capsaicin was dissolved in ethanol to give $2 \times 10^{-2}$ M stock solution and then diluted in Krebs solutions just before the experiments. Chlorisondamine was dissolved in diluted acetic acid and then further diluted in the Krebs solution. SR 48968 was dissolved in ethanol and diluted in saline. Concentrated solutions ($10^{-3}$ M) of peptides were made in distilled water whereas $Nle^{10}$NKA(4-10) was initially dissolved in acetic acid as $10^{-3}$ M and then diluted in Krebs solution. All these concentrated peptide solutions were kept at − 20°C until fresh dilutions were made in Krebs solution. The other drugs were dissolved in saline.

### *Statistical evaluations*

Values are expressed as means ± s.e.mean. For statistical analysis the paired or unpaired Student's *t* test, Mann-Whitney U test and Kruskal Wallis analysis of variance were used. $P<0.05$ was considered significant.

## Results

### *Inhibitory effect of SR 48968 on EFS-, NKA and SP-evoked contraction of guinea-pig isolated bronchi*

Electrical field stimulation (EFS, 1 Hz for 1 min) in the presence of guanethidine caused a biphasic bronchial effect, with an initial rapid contraction followed by a sustained contraction. After atropine, the rapid contraction was abolished, leaving the long lasting NANC contraction intact. When calculated as area under the curve (AUC), only about 14% of the bronchconstriction response to EFS was found to be cholinergic (atropine-sensitive) (Figure 1b). SR 48968 at $10^{-8}$ M had no apparent influence on this NANC response. However, SR 48968 at $10^{-7}$ M abolished 83% ($n=6$, $P<0.001$) of the NANC contraction (Figure 1a,b). A mild bronchoconstriction was still present even after treatment with a higher concentration of SR 48968 ($5 \times 10^{-7}$ M) (not shown). When the selective $NK_1$ receptor antagonist, CP

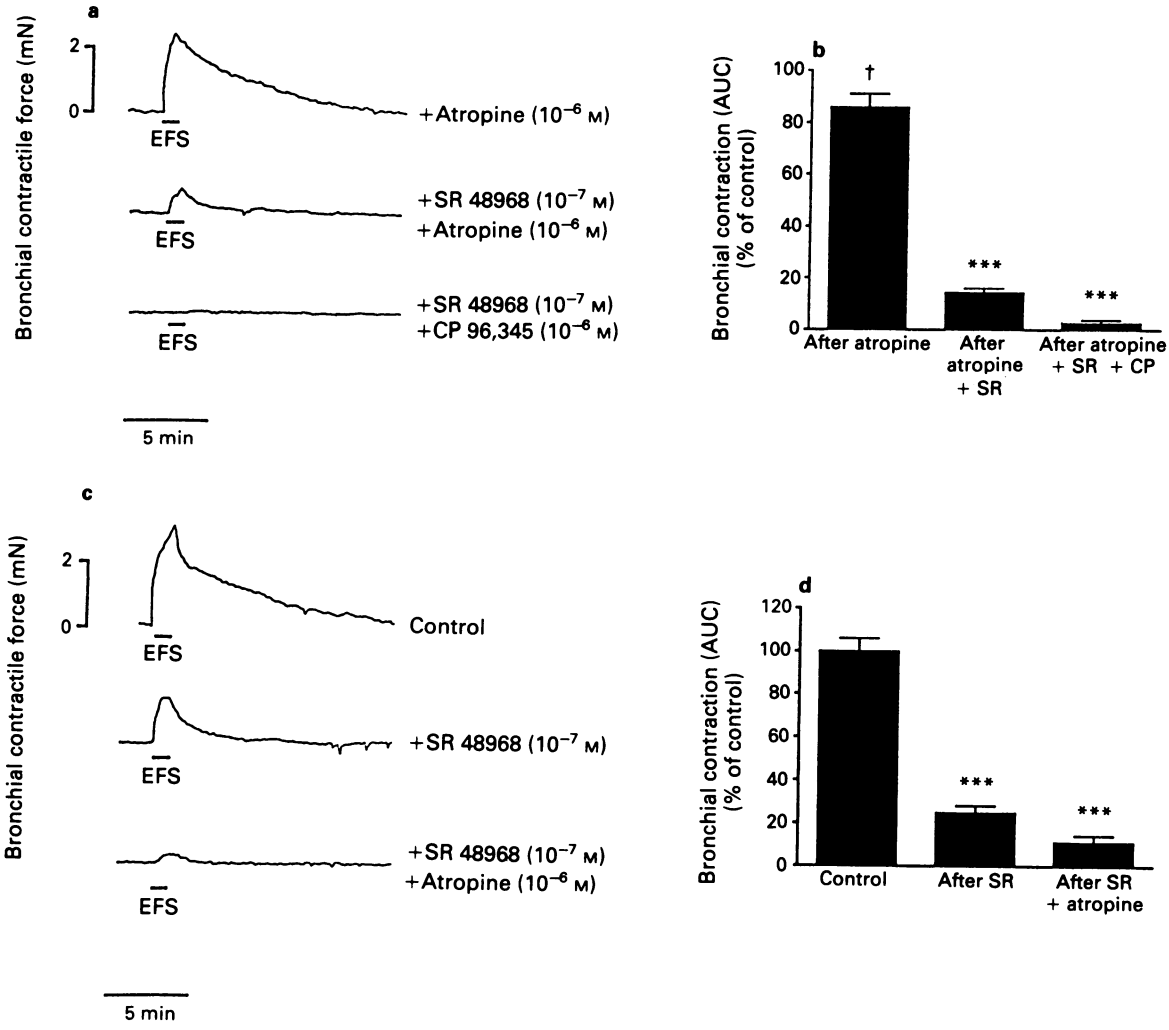



**Figure 1** (a,c) Original tracings showing bronchial contraction of guinea-pig isolated bronchus induced by electrical field stimulation (EFS, 1 Hz for 1 min) as indicated by the bars. Guanethidine ($5 \times 10^{-6}$ M) was present throughout all experiments to abolish adrenergic responses. (a) Top tracing: EFS after the atropine ($10^{-6}$ M) to show non-adrenergic non-cholinergic (NANC) bronchoconstriction. Middle tracing: EFS after incubation of atropine together with SR 48968 ($10^{-7}$ M) for 1 h. Bottom tracing: EFS after pre-exposure to SR 48968 for 1 h and CP 96,345 for 15 min in the presence of atropine ($10^{-6}$ M). (c) Top tracing: control EFS. Middle tracing: EFS after SR 48968 ($10^{-7}$ M) preincubation for 1 h. Bottom tracing: EFS after further addition of atropine ($10^{-6}$ M) in the presence of SR 48968 ($10^{-7}$ M). (b,d) The area under the curve (AUC) generated by EFS was calculated to quantify the contraction. SR: SR 48968. CP: CP 96,345. The AUC obtained from EFS-induced contraction before adding atropine (b) or SR 48968 (d) was used as control (100%). The subsequent stimulations are expressed as % of this control. Each column is the mean (± s.e.mean) of results from 6–8 preparations. For statistical tests the Kruskal Wallis analysis of variance was used. (b): $n=6$, $\dagger P<0.05$ when compared to the response in the absence of atropine; $***P<0.001$ when compared to the response in the presence of atropine without SR 48968 and CP 96,345; (d): $n=8$, $***P<0.001$ when compared to the control.

96,345 ($10^{-6}$ M) was added together with SR 48968 ($10^{-7}$ M), the contraction produced by EFS was totally abolished (Figure 1a,b). In the absence of atropine, SR 48968 ($10^{-7}$ M) greatly (by 75%) inhibited the bronchial contraction induced by EFS (Figure 1c,d). Further addition of atropine ($10^{-6}$ M) then inhibited the first fast contraction which was about 14% of total EFS-evoked contraction (Figure 1c,d).

Both NKA and SP caused bronchial contraction in a concentration-dependent manner. NKA was about 10 fold more potent then SP. NKA at approximately $3 \times 10^{-9}$ M or SP at $3 \times 10^{-8}$ M caused bronchial contraction of a similar magnitude to that induced by EFS. SR 48968 ($10^{-7}$ M) virtually abolished the contraction caused by NKA ($10^{-9}$–$3 \times 10^{-8}$ M) (Figure 2a). The contraction evoked by SP was only slightly reduced at the higher concentrations (Figure 2b). The bronchial contraction induced by acetylcholine ($10^{-7}$–$10^{-5}$ M) was not influenced by SR 48968 ($10^{-7}$ M) (Figure 2c).

### *Effect of SR 48968 on bronchoconstriction and CGRP-LI release in the guinea-pig isolated perfused lung*

After guinea-pig lungs were perfused for 30 min, the basal $R_L$, $C_{Dyn}$ and CGRP-LI release were $0.310 \pm 0.010$ cm$H_2O$/(ml $s^{-1}$) ($n = 15$), $0.356 \pm 0.015$ ml/cm$H_2O$ ($n = 15$), and $12 \pm 2.0$ (fmol/fraction) ($n = 8$), respectively. The basal values were not significantly different between the various groups.

Vagal stimulation (1 Hz for 1 min) caused a very rapid bronchoconstriction, showing decreased tidal volume (Figure 3), increased $R_L$ and decreased $C_{Dyn}$ (Figure 4a), which in some preparations led to total lung closure (Figure 3). Vagal stimulation also caused significant (about two fold of the basal) increase of CGRP-LI overflow (Figure 4b). SR 48968 at $10^{-7}$ M had only a mild inhibitory effect on the bronchoconstriction induced by vagal stimulation ($n = 2$, not shown). In the later experiments, the $5 \times 10^{-7}$ M concentration of SR 48968 was therefore used. SR 48968 ($5 \times 10^{-7}$ M) *per se* had no significant influence on the basal lung function of CGRP overflow. After SR 48968 preincubation for 30 min, the bronchoconstriction evoked by vagal stimulation was greatly inhibited ($R_L$ increase was reduced by 95% and $C_{Dyn}$ decrease was reduced by 68%), though it was not abolished (Figure 3–4a). In contrast, the CGRP-LI release evoked by vagal stimulation was not changed by SR 48968 (Figure 4b).

Capsaicin ($10^{-8}$ M) also caused bronchoconstriction (Figures 3,4a) and CGRP-LI overflow (Figure 4b). This bronchoconstriction developed more slowly than that induced by vagal stimulation (Figure 3), but the peak response was slightly stronger ($R_L$ was increased by >1000%) (Figures 3,4a). The CGRP-LI overflow after capsaicin was higher (about 3 fold) than that produced by vagal stimulation (Figure 4b). SR 48968 ($5 \times 10^{-7}$ M) significantly inhibited the capsaicin-evoked changes in $R_L$ and $C_{Dyn}$ (Figures 3,4a). However, the remaining responses resistant to the SR 48968 pretreatment were larger than those produced by vagal stimulation under the same conditions (Figure 4a). SR 48968 had no influence on the CGRP-LI release by capsaicin (Figure 4b).

Both neurokinin A and the selective $NK_2$ receptor agonist Nle$^{10}$NKA(4-10) caused concentration-dependent bronchoconstriction in isolated perfused lungs, showing decreased tidal volume, increased $R_L$ and decreased $C_{Dyn}$ (Figures 5,6). The threshold concentrations for NKA and Nle$^{10}$NKA(4-10) to induce a bronchoconstriction were about $10^{-9}$ M and $3 \times 10^{-9}$ M, respectively (Figures 5,6). The bronchoconstriction induced by low concentration of NKA ($10^{-9}$ M–$3 \times 10^{-8}$ M) was greatly inhibited by SR 48968 ($5 \times 10^{-7}$ M) leaving the maximal effect uninfluenced, resulting in a parallel, about 10 fold shift to the right of the concentration-response curve (Figures 5,6a,c). In contrast, the bronchoconstriction caused by Nle$^{10}$NKA(4-10) ($10^{-9}$ M–$3 \times 10^{-7}$ M) was almost totally abolished by SR 48968 (Figures 5,6b,d).

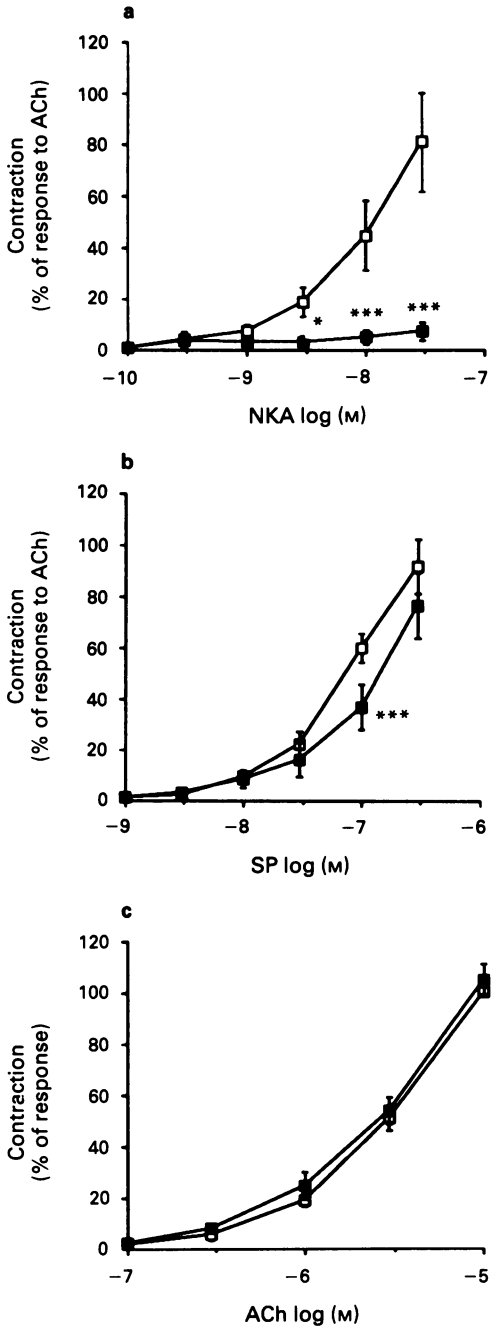



**Figure 2** Concentration-response curve for bronchial contractions in response to neurokinin A (NKA) (a) substance P (SP) (b) and acetylcholine (ACh) (c) in the absence (□, control) or presence (■) of the $NK_2$ receptor antagonist, SR 48968 ($10^{-7}$ M) in guinea-pig isolated bronchi. Contraction was expressed as % of response induced by ACh ($10^{-5}$ M). Data are presented as means ± s.e.mean. $n = 9$, $^*P < 0.05$, $^{***}P < 0.001$, when compared to the control by paired Student's $t$ test.

### *Inhibitory effect of SR 48968 on capsaicin- and NKA-evoked bronchoconstriction in anaesthetized guinea-pigs*

In anaesthetized guinea-pigs the basal insufflation pressure was $16.5 \pm 1.2$ cm$H_2O$ ($n = 10$). Capsaicin (10 μg $kg^{-1}$, i.v.) increased the insufflation pressure by $98 \pm 16\%$ ($n = 6$, $P < 0.01$) (Figure 7) in the presence of the ganglionic blocker, chlorisondamine. The bronchoconstriction peaked within 1 min and returned slowly to baseline after 5 min. In separate groups pretreated with SR 48968 (0.3 mg $kg^{-1}$, i.v.) 5 min before capsaicin injection, the capsaicin-evoked bronchocon-

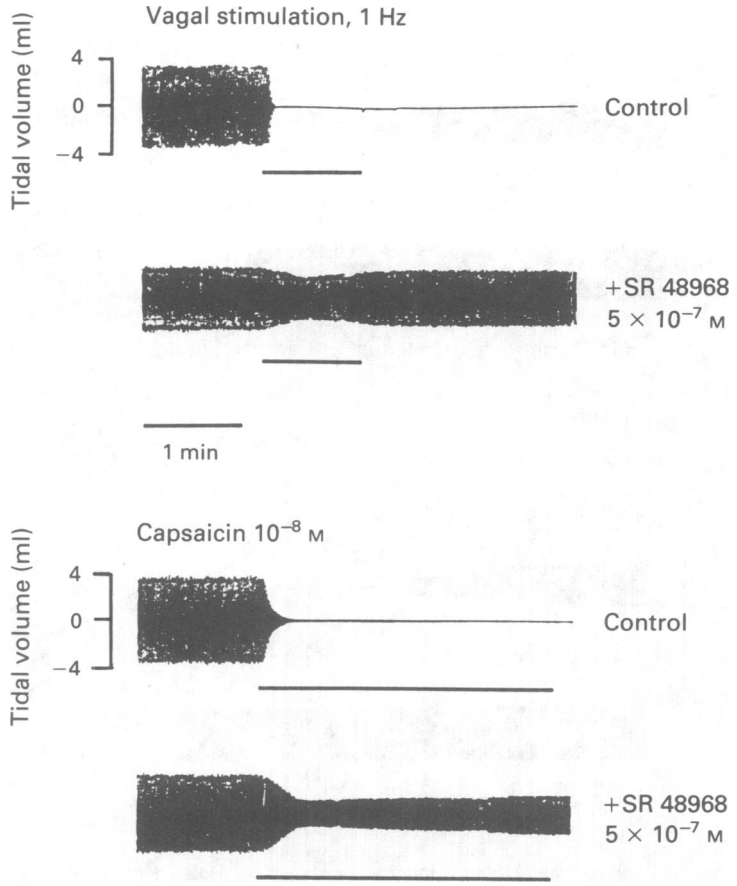



**Figure 3** Original tracings showing the changes in tidal volume induced in guinea-pig isolated perfused lung by vagal stimulation (1 Hz for 1 min) or capsaicin ($10^{-8}$ M for 3 min) without (control) or following preincubation with SR 48968 ($5 \times 10^{-7}$ M) for 30 min. Time scale indicates 1 min. Other bars indicate duration of vagal stimulation or capsaicin perfusion.

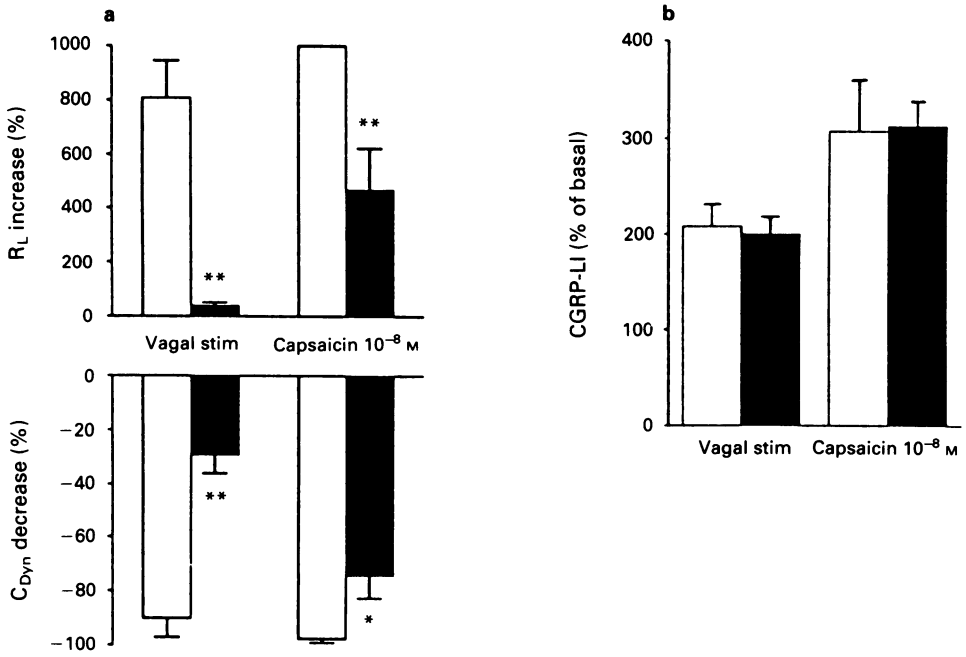



**Figure 4** Effect of SR 48968 on bronchoconstriction (a) and calcitonin gene-related peptide-like immunoreactivity (CGRP-LI) overflow (b) induced by vagal stimulation (1 Hz for 1 min) or capsaicin ($10^{-8}$ M for 3 min) in guinea-pig isolated perfused lung. Experiments were performed without (control, open columns bars) or following preincubation with SR 48968 ($5 \times 10^{-7}$ M for 30 min, solid columns). (a) Bronchoconstriction is expressed as percentage of the increase in lung resistance ($R_L$) or decrease in dynamic compliance ($C_{Dyn}$). 1000% and 100% were taken as the limits for the increase in $R_L$ and decrease in $C_{Dyn}$ respectively, resulting from a complete airway closure (see text for detail explanation). (b) CGRP-LI overflow is expressed as % of basal (the fraction just before stimuli). Data are the mean( ± s.e.mean) results from 4–7 experiments. $*P<0.05$, $**P<0.01$ when compared to the control by Mann-Whitney U test.

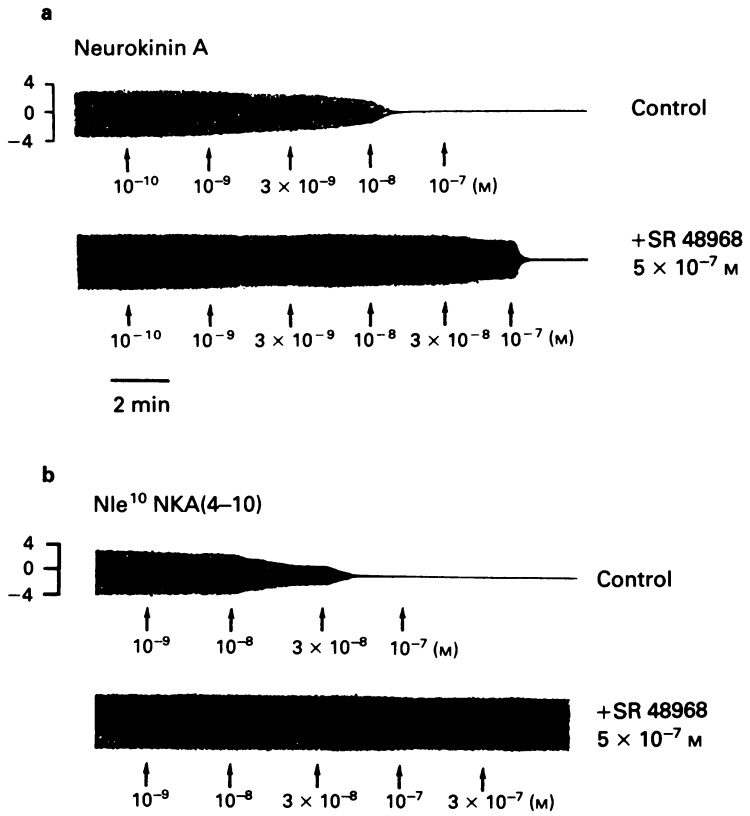



**Figure 5** Original recordings of tidal volume responses induced in guinea-pig isolated perfused lung by neurokinin A (a) or the selective $NK_2$ receptor agonist, $Nle^{10}NKA$ (4–10) (b) added cumulatively. Experiments were performed without (control, above) or following preincubation with SR 48968 ($5 \times 10^{-7}$ M for 30 min, below). Time scale indicates 2 min.

striction was markedly reduced. Thus, SR 48968 reduced the area under the curve (AUC) of bronchoconstriction response by 90% (Figure 7a). In contrast, the capsaicin evoked hypotension was not changed by SR 48968 (Figure 7c).

NKA (1 $\mu g\,kg^{-1}$, i.v.) also caused bronchoconstriction, with an increase of insufflation pressure of 315 ± 34% ($n = 4$, $P < 0.001$). The bronchoconstriction peaked within 1 min and recovered to baseline after 3 min. SR 48968 greatly inhibited this response to NKA, thus it reduced the AUC of the NKA-induced bronchoconstriction by 94% (Figure 7b). The hypotension evoked by NKA was not influenced by SR 48968 (Figure 7d).

## Discussion

The present study further confirms that SR 48968 is a potent selective $NK_2$ receptor antagonist (Advenier *et al.*, 1992; Emond-Alt *et al.*, 1992). Additionally, this non-peptide $NK_2$ antagonist is very effective not only *in vitro* but also *in vivo* in blocking the NANC bronchoconstriction evoked by the activation of sensory nerves in guinea-pig airways. Furthermore, our results showed that SR 48968 had no influence on the release of peptide transmitter from pulmonary sensory neurones, suggesting a selective postjunctional action.

In guinea-pig isolated bronchi, SR 48968 selectively blocked the bronchial contraction induced by NKA while it had little influence on the response induced by acetylcholine or SP. SR 48968 at $10^{-7}$ M had an inhibitory effect similar to that exerted by DAC at $10^{-5}$ M (Lou *et al.*, 1992) and was, therefore, a more potent NKA antagonist than the latter. In the isolated perfused lung, vagal stimulation (1 Hz for 1 min) and capsaicin ($10^{-8}$ M for 3 min) caused bronchoconstriction, which could be totally abolished by capsaicin-pretreatment (Lou & Lundberg, 1992). However, the precise receptor mechanisms involved in the NANC bronchoconstriction had not been characterized earlier, due to the lack of potent selective tachykinin receptor antagonists. Our previous study showed that DAC inhibited the increase in $R_L$ induced by vagal stimulation, while it had no significant influence on the reduction in $C_{Dyn}$ or the bronchoconstriction induced by capsaicin (Lou *et al.*, 1992). In the present study, SR 48968 at a concentration of $5 \times 10^{-7}$ M markedly inhibited both changes in $R_L$ and $C_{Dyn}$ induced by either vagal stimulation or capsaicin. These results indicate the bronchoconstriction was predominantly mediated via $NK_2$ receptors. For further evaluation of these data, we compared the responses to the endogenous ligand, NKA, which has a more dominant effect on $NK_2$ receptors but can also activate other tachykinin receptors ($NK_1$ and $NK_3$) (Drapeau *et al.*, 1987), and the synthetic selective $NK_2$ agonist $Nle^{10}NKA(4\text{-}10)$ (Regoli *et al.*, 1988). The bronchoconstriction induced by $Nle^{10}NKA(4\text{-}10)$ was abolished by SR 48968, while that induced by NKA was reduced but not eliminated. These results suggested that the concentration of $5 \times 10^{-7}$ M SR 48968 was sufficient to block $NK_2$ receptor activation in the isolated lungs. The bronchoconstriction remaining after the SR 48968 pretreatment could be mediated by $NK_1$ receptor stimulated by higher concentrations of NKA or by SP which has a more potent effect on the $NK_1$ receptor. This may also explain why SR 48968 could not completely abolish the bronchoconstriction induced by vagal stimulation and capsaicin, both of which elicit bronchoconstriction via the release of sensory peptides. It is known that capsaicin releases more peptide mediators from sensory nerves than vagal stimulation (Lou *et al.*, 1991). Hence the capsaicin-induced bronchoconstriction was more resistant to SR 48968 or DAC (Lou *et al.*, 1992), than that induced by vagal stimulation. However, we cannot exclude the possibility that SP, which is probably also released by these stimuli (Saria *et al.*, 1988), might contribute

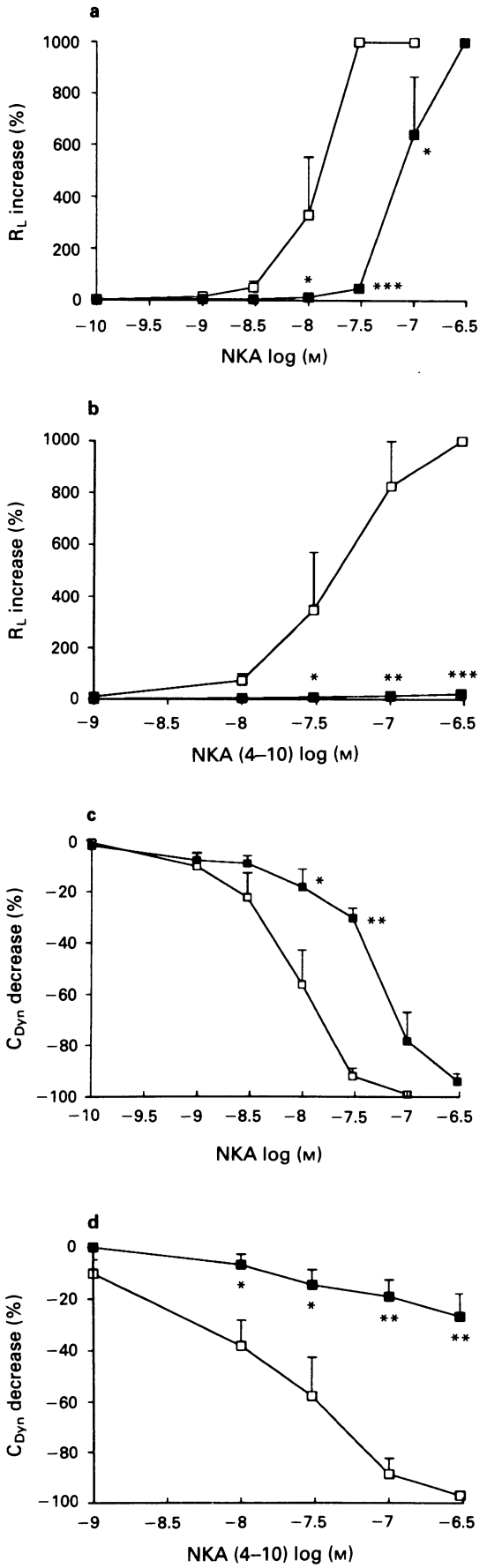



**Figure 6** Concentration-response curves of neurokinin A (NKA)- or the selective $NK_2$ receptor agonist $Nle^{10}$NKA (4–10)-evoked bronchoconstriction in the guinea-pig isolated perfused lung (NKA: a,c; $Nle^{10}$NKA (4–10): b,d). Experiments were performed without (control, □) or following preincubation with SR 48968 ($5 \times 10^{-7}$ M for 30 min, ■). Bronchoconstriction is expressed as percentage of the increase in lung resistance ($R_L$) (a,b) or decrease in dynamic compliance ($C_{Dyn}$) (c,d) when compared to baseline. 1000% and 100% were taken as the limits for the increase in $R_L$ and decrease in $C_{Dyn}$, respectively, resulting from a complete airway closure (see text for detail explanation). Each point is the mean(± s.e.mean) of results from 4 animals. $^*P<0.05$; $^{**}P<0.01$; $^{***}P<0.001$ when compared to control by paired Student's *t* test.

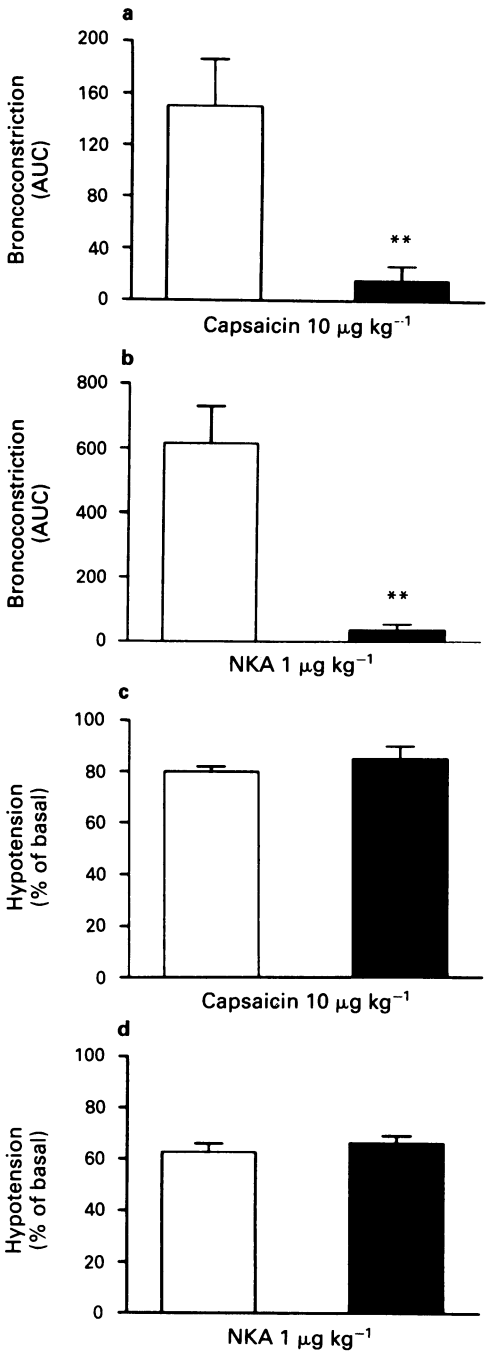



**Figure 7** Effect of ST 48968 (0.3 mg $kg^{-1}$, i.v.) on capsaicin (10 μg $kg^{-1}$, i.v.) and neurokinin A (NKA, 1 μg $kg^{-1}$, i.v.)-induced bronchoconstriction (a,b) or hypotension (c,d) in anaesthetized guinea-pigs. Experiments were performed without (open columns, control) or with SR 48968 (solid columns). Data are calculated as area under the recording curve (AUC) of the bronchoconstrictor or hypotensive effects during 5 min after administration of capsaicin or NKA. Values are the mean(± s.e.mean) of results from 4–6 animals. Significant difference from control is indicated by $^{**}P<0.01$, by the unpaired Student's *t* test.

to the remaining bronchoconstriction via the activation of $NK_1$ receptors, which cannot be blocked by SR 48968. From our results obtained in this and previous studies (Lou *et al.*, 1992) it seems that the $NK_2$ receptor antagonists inhibited the increase in $R_L$ to a greater extent than the decrease in $C_{Dyn}$ in the isolated perfused lung. It has been shown that the contraction of the smooth muscle in the large airways leads primarily to an increase in $R_L$ whereas an increase in flow resistance in the smaller intrapulmonary airways (e.g. mucosal oedema) has a more dominant effect on the reduction in $C_{Dyn}$ (Macklem *et al.*, 1969; Hahn *et al.*, 1976). Moreover, it is known that the $NK_1$ receptors play a major role in sensory nerve evoked-oedema (Delay-Goyet & Lundberg, 1991). Based upon the above experiments, $NK_1$ receptor mechanisms could be involved to some extent in airway obstruction induced by sensory nerve activation in guinea-pig, although $NK_2$ receptors are clearly of greater relative importance.

For further examination of the possible $NK_1$ receptor involvement, we used guinea-pig isolated bronchi, where one can study smooth muscle responses directly without the possible interference of mucosal oedema. In this preparation, we used a lower concentration of SR 48968 ($10^{-7}$ M) but a longer incubation time of 1 h. (In the lung model we used 30 min incubations due to the relatively short duration of the tissue viability). The EFS-evoked NANC bronchial contraction was greatly reduced by SR 48968, suggesting that $NK_2$ receptors were the major targets for endogenously released tachykinins. Thus, these results further support the notion that $NK_2$ receptors may be the primary tachykinin receptors which mediate bronchial smooth muscle contraction upon sensory activation (Lundberg & Lou, 1991). Consistent with our finding in the isolated lung preparation, we cannot exclude $NK_1$ receptor involvement since a small part of the EFS-evoked bronchoconstriction remained, even with the pretreatment of a higher concentration ($5 \times 10^{-7}$ M) of SR 48968. In fact, further addition of the $NK_1$ selective receptor antagonist, CP 96,345 ($10^{-6}$ M) (Snider *et al.*, 1991) completely abolished the remaining EFS-evoked bronchoconstriction. Although it was recently reported that CP 96,345 has non-selective properties and at higher concentrations acts as a $Ca^{2+}$ antagonist in rats (Delay-Goyet *et al.*, 1992), in guinea-pig bronchi with the concentrations and conditions similar to those used in this study, CP 96,345 seems to be a selective $NK_1$ receptor antagonist (Lou *et al.*, 1992).

In anaesthetized guinea-pigs, the marked inhibitory effect of SR 48968 on capsaicin- and NKA-evoked bronchoconstriction became effective very rapidly (within 5 min). Thus, these pharmacological properties of SR 48968 enhance its potential to be used in *in vivo* studies of the role of $NK_2$ receptors in the physiological and pathological changes of airway functions.

Although SR 48968 was reported as a potent and selective $NK_2$ receptor antagonist, based on receptor binding studies and isolated tissue bioassay (Advenier *et al.*, 1992; Emonds-Alt *et al.*, 1992), it was not known whether the substance had any prejunctional effects on sensory nerves or whether there was an autoregulation of peptide release mediated by the $NK_2$ receptor. We studied this issue by using the guinea-pig isolated perfused lung where both function and peptide release can be measured simultaneously in the same preparation. Both vagal stimulation and capsaicin caused significant CGRP release, which was not significantly changed by SR 48968, suggesting the latter had no prejunctional influence on sensory nerve terminals. Therefore, the inhibitory effect of SR 48968 was most likely related to a postjunctional target, i.e. the $NK_2$ receptor on the bronchial smooth muscle.

In conclusion, the present findings indicate that SR 48968 is a potent selective $NK_2$ receptor antagonist, as shown in both *in vitro* and *in vivo* studies in guinea-pigs. Furthermore, the NANC-bronchconstriction induced by activation of vagal sensory nerves is mediated primarily via $NK_2$ receptors, suggesting that NKA has a more dominant influence on the NANC bronchial contraction than SP as an endogenously released mediator.

This study was supported by the Swedish Medical Research Council (14x-6554), the American Council for Tobacco Research, the Swedish Tobacco Company, Swedish National Environmental Protection Board, Svenska Läkaresällskapet and funds from Karolinska Institutet. We thank C. Söderblom and M. Stensdotter for expert technical assistance. We are grateful to Dr X. Emond-Alt, Sanofi Recherche, Montpellier Cedex, France, for the supply of SR 48968 and Dr R.M. Snider, Pfizer, Groton, CT. USA for the supply of CP 96,345. L.-Y. L. was a recipient of the Senior International Fellowship (TW 01734) awarded by the NIH Fogarty Center, U.S.A.

## References

ADVENIER, C., ROUSIIS, N., NGUYEN, Q.T., EMONDS-ALT, X., BRELIERE, J.-C., NELIAT, G., NALINE, E. & REGOLI, D. (1992). Neurokinin A ($NK_2$) receptor revisited with SR 48968, a potent non-peptide antagonist. *Biochem. Biophys. Res. Commun.*, **184**, 1418–1424.

DELAY-GOYET, P., FRANCO-CERECEDA, A., GONSALVES, S.F., CLINGAN, C.A., LOWE III, J.A. & LUNDBERG, J.M. (1992). CP-96,345 antagonism of $NK_1$ receptors and smoke-induced protein extravasation is unrelated to its cardiovascular effects. *Eur. J. Pharmacol.*, **222**, 213–218.

DELAY-GOYET, P. & LUNDBERG, J.M. (1991). Cigarette smoke-induced airway oedema is blocked by the $NK_1$ antagonist, CP-96,345. *Eur. J. Pharmacol.*, **203**, 157–158.

DION, S., ROUISSI, N., NANTEL, F., DRAPEAU, G., REGOLI, D., NALINE, E. & ADVENIER, C. (1990). Receptors for neurokinins in human bronchus and urinary bladder are of the NK-2 type. *Eur. J. Pharmacol.*, **178**, 215–219.

DRAPEAU, G., D'ORLÉANS-JUSTE, P., DION, S., RHALEB, N.-E., ROUISSI, N.-E. & REGOLI, D. (1987). Selective agonists for substance P and neurokinin receptors. *Neuropeptides*, **10**, 43–54.

EMONDS-ALT, X., VILAIN, P., GOULAOUIC, P., PROIETTO, V., VAN-BROECK, D., ADVENIER, C., NALINE, E., NELIAT, G., LE FUR, G. & BRELIÉRE, J.C. (1992). A potent and selective non-peptide antagonist of the neurokinin A ($NK_2$) receptor. *Life Sci.*, **50**, 101–106.

FRANCO-CERECEDA, A., SARIA, A. & LUNDBERG, J.M. (1989). Differential release of calcitonin gene-related peptide and neuropeptide Y from the isolated heart by capsaicin, ischaemia, nicotine, bradykinin and ouabain. *Acta Physiol. Scand.*, **135**, 173–187.

FUJII, T., MURAI, M., MORIMOTO, H., NISHIKAWA, M. & KIYATOH, S. (1991). Effects of actinomycin D on airway constriction induced by tachykinins and capsaicin in guinea-pigs. *Eur. J. Pharmacol.*, **194**, 183–188.

GULBENKIAN, S., MERIGHI, A., WHARTON, J., VARNDELL, J.M. & POLAK, J.M. (1986). Ultrastructural evidence for the coexistence of calcitonin gene related peptide and substance P in the secretory vesicles of peripheral nerves in the guinea-pig. *J. Neurocytol.*, **15**, 535–542.

HAHN, H.L., GRAF, P.D. & NADEL, J.A. (1976). Effect of vagal tone on airway diameters and on lung volume in anesthetized dogs. *J. Appl. Physiol.*, **41**, 581–589.

KARLSSON, J.A., FINNEY, M.J.B., PERSSON, C.G.A. & POST, C. (1984). Substance P antagonists and the role of tachykinins in noncholinergic bronchoconstriction. *Life Sci.*, **35**, 2681–2691.

KRÖLL, F., KARLSSON, J.A., LUNDBERG, J.M. & PERSSON, C.G.A. (1990). Capsaicin-induced bronchoconstriction and neuropeptide release in the guinea-pig perfused lung: evidence for a local axon reflex. *J. Appl. Physiol.*, **68**, 1679–1687.

LOU, Y.-P., DELAY-GOYET, P. & LUNDBERG, J.M. (1992). Selective inhibition by dactinomycin of NANC sensory bronchoconstriction and $^{125}$I-NKA binding due to NK-2 receptor antagonism. *Acta Physiol. Scand.*, **14**, 221–231.

LOU, Y.-P. & LUNDBERG, J.M. (1992). Inhibition of low pH evoked activation of airway sensory nerves by capsazepine, a novel capsaicin-receptor antagonist. *Biochem. Biophys. Res. Commun.*, **189**, 537–544.

LOUS, Y.-P., KARLSSON, J.A., FRANCO-CERECEDA, A. & LUNDBERG, J.M. (1991). Selectivity of ruthenium red in inhibiting bronchoconstriction and CGRP release induced by afferent C-fibre activation in the guinea-pig lung. *Acta Physiol. Scand.*, **142**, 191–199.

LUNDBERG, J.M. & LOU, Y.-P. (1991). Dactinomycin inhibits non-cholinergic bronchoconstriction by capsaicin-sensitive sensory nerves in the guinea-pig by antagonizing neurokinin 2 receptor activation. *Acta Physiol. Scand.*, **141**, 141–142.

LUNDBERG, J.M. & SARIA, A. (1982). Bronchial smooth muscle contraction induced by stimulation of capsaicin sensitive, sensory nerves. *Acta Physiol. Scand.*, **115**, 473–476.

LUNDBERG, J.M., SARIA, A., BRODIN, A., ROSELL, E. & FOLKERS, K. (1983). A substance P antagonist inhibits vagally induced increase in vascular permeability and bronchial smooth muscle contraction in the guinea-pig. *Proc. Natl. Acad. Sci. U.S.A.*, **80**, 1120–1124.

MACKLEM, P.T., WOOLCOCK, A.J., HOGG, J.C., NADEL, J.A. & WILSON, N.J. (1969). Partitioning of pulmonary resistance in the dog. *J. Appl. Physiol.*, **26**, 798–805.

MCKNIGHT, A.T., MAGUIRE, J.J., WILLIAMS, B.J., FOSTER, A.C., TRIDGETT, R. & IVERSEN, L.L. (1988). Pharmacological specificity of synthetic peptides as antagonists at tachykinin receptors. *Regul. Pept.*, **22**, 127.

MAGGI, C.A., PATACHINI, R., GIULIANI, S., ROVERO, P., DION, S. REGOLI, D., GIACHETTI, A. & MELI, A. (1990). Competitive antagonists discriminate between $NK_2$ receptor subtypes. *Br. J. Pharmacol.*, **100**, 558–592.

MAGGI, C.A., PATACCHINI, R., ROVERO, P. & SANTICIOLI, P. (1991). Tachykinin receptor and non-cholinergic bronchoconstriction in the guinea-pig isolated bronchi. *Am. Rev. Resp. Dis.*, **114**, 363–367.

REGOLI, D., DRAPEAU, D., DION, S. & COUTURE, R. (1988). New selective agonists for neurokinin receptors: pharmacological tools for receptor characterization. *Trends Pharmacol. Sci.*, **9**, 290–295.

SARIA, A., MARTLING, C.R., YAN, Z., THEODORSSON-NORHEIM, E. & LUNDBERG, J.M. (1988). Release of multiple tachykinins from sensory nerves in the lung by bradykinin, histamine, nicotine and vagal nerve stimulation. *Am. Rev. Respir. Dis.*, **137**, 1330–1335.

SNIDER, R.M., CONSTANTINE, J.W., LOWE III, J.A., LONGO, K.P., LEBEL, W.S., WOODY, H.A., DROZDA, S.E., DESAI, M.C., VINICK, F.J., SPENCER, R.W. & HESS, H.J. (1991). A potent nonpeptide antagonist of the substance P (NK1) receptor. *Science*, **251**, 435–436.

*(Received December 7, 1992*
*Revised February 8, 1993*
*Accepted February 25, 1993)*

*Br. J. Pharmacol.* (1993), **109**, 774–778 © Macmillan Press Ltd, 1993

# Effects of rolipram and siguazodan on the human isolated bronchus and their interaction with isoprenaline and sodium nitroprusside

Y. Qian, E. Naline, *J.-A. Karlsson, *D. Raeburn & [1]C. Advenier

Faculté de Médecine Paris-Ouest, 15, Rue de l'Ecole de Médecine, F-75270 Paris, Cedex 06, France and *Rhône-Poulenc Rorer, Dagenham Research Centre, Rainham Road South, Dagenham, Essex RM10 7XS

**1** The effects of the selective inhibitors of cyclic AMP phosphodiesterase type IV (rolipram) and type III (siguazodan) and their interactions with isoprenaline and sodium nitroprusside have been studied in the human isolated bronchus.

**2** On bronchi under resting tone rolipram was, in terms of potency ($pD_2 = 7.77 \pm 0.14$, $n = 8$), very similar to isoprenaline ($pD_2 = 7.31 \pm 0.12$, $n = 12$) and salbutamol ($pD_2 = 7.12 \pm 0.17$, $n = 10$) and approximately 10 fold more potent than siguazodan ($pD_2 = 6.80 \pm 0.12$, $n = 6$). In terms of efficacy ($E_{max}$, expressed as percentage of maximal effect induced by theophylline 3 mM), both rolipram and siguazodan were less efficient ($E_{max} = 74 \pm 6.7\%$, $n = 8$ and $66 \pm 7.5\%$, $n = 6$, respectively) than isoprenaline ($E_{max} = 98 \pm 0.4\%$, $n = 12$) and salbutamol ($E_{max} = 83 \pm 2.4\%$, $n = 10$).

**3** During precontraction induced by methacholine ($3 \times 10^{-7}$ M) or acetylcholine ($10^{-3}$ M), concentration-response curves to rolipram and siguazodan were shifted to the right and maximal effects reduced. Rolipram was more potent than siguazodan and, in terms of efficacy, it was less active.

**4** Rolipram $10^{-8}$ and $10^{-7}$ M but not siguazodan potentiated the effects of isoprenaline as shown by the shift to the left of the concentration-response curve to isoprenaline. Sodium nitroprusside-induced relaxation was not modified by either drug.

**5** These results show that rolipram is a potent relaxant of the human isolated bronchus, potentiating the effects of β-adrenoceptor stimulation and suggest that, as previously demonstrated in other species (guinea-pig, cow) (Tomkinson *et al.*, 1993), there may be a connection between the $\beta_2$-adrenoceptor subtype, which predominate in human airway smooth muscle, and the cyclic AMP phosphodiesterase type IV.

**Keywords:** Human airway smooth muscle; phosphodiesterase inhibitors; β-adrenoceptors; rolipram; siguazodan; isoprenaline; salbutamol; sodium nitroprusside

## Introduction

Elevation of tissue adenosine 3':5'-cyclic monophosphate (cyclic AMP) levels leads to relaxation of airway smooth muscle preparations. Amongst the potential mechanisms whereby this effect occurs are reduction in intracellular calcium levels, inhibition of inositol phospholipid hydrolysis, and alteration in the sensitivity of contractile proteins to calcium or activation of potassium channels (Giembycz & Raeburn, 1991). The breakdown of cyclic AMP to 5'AMP in tissues is dependent upon the activity of tissue cyclic nucleotide phosphodiesterases (PDE).

At least five distinct phosphodiesterase isoenzymes are present in mammalian airway smooth muscle, each having different selectivities and $K_m$ values for cyclic AMP and guanosine 3':5'-cyclic monophosphate (cyclic GMP). Among these, type III (low $K_m$, cyclic GMP-inhibited) and type IV (high $K_m$, cyclic AMP-selective) isoenzymes appear to be important for the regulation of cyclic AMP breakdown in intact airway smooth muscle from canine, bovine or human airways (Torphy *et al.*, 1988; Silver *et al.*, 1988; Beavo & Reifsnyder, 1990; Nicholson *et al.*, 1991; Torphy & Undem, 1991; Hall & Hill, 1992; Giembycz *et al.*, 1992).

Since β-adrenoceptor agonists act by increasing the tissue content of cyclic AMP, subsequent to stimulation of adenylyl cyclase, it was of interest to study the relationship between β-adrenoceptor activation and the type of PDE involved in the effects of β-adrenoceptor agonists. Tomkinson *et al.* (1993) have recently hypothesized that there may be a connection between the β-adrenoceptor subtype ($\beta_1$ or $\beta_2$) which predominates in a tissue and the functional importance of the PDE (III or IV) isoenzyme in reducing smooth muscle contractility in various species (including guinea-pig, cow, pig, and mouse) and demonstrated that there was a relationship between $\beta_2$-adrenoceptor and cyclic AMP PDE type IV on the one hand and $\beta_1$-adrenoceptor and cyclic AMP PDE type III on the other hand.

The aim of this study was to extend these investigations to the human airway smooth muscle. We compared the effects of isoprenaline, salbutamol, rolipram, an inhibitor of PDE type IV, and siguazodan (SK&F 94836), an inhibitor of PDE type III, and their interactions on the human isolated bronchus.

## Methods

### *Human bronchus preparation*

Human bronchial tissue (usually with an inner diameter of 1 to 4 mm) was obtained from patients undergoing surgery for lung cancer but taken at a distance from malignancy. Bronchi were dissected free of parenchyma and transported to the laboratory in Krebs solution previously aerated with a mixture of 95% $O_2$ and 5% $CO_2$ (pH 7.40). The tissue was stored overnight at 4°C and the experiment was performed the next day. Previous experience in this laboratory and published data have demonstrated that overnight storage of tissue does not alter its reactivity.

[1] Author for correspondence.

Bronchial rings from a segmental bronchus were prepared and suspended in parallel in Krebs solution under an initial load of 2.0 g. After 1 h of equilibration with washing every 15 min, the resting load was between 1 and 2 g. Under these conditions, the responses obtained were reproducible. Force of contraction was measured isometrically with strain gauges (UF1), amplifiers, and I. O. S.-Moise 3 recorder system (EMKA Technologies, Mitry Mory, France). The composition of the Krebs solution was (mM): NaCl 118, KCl 5.4, $CaCl_2$ 2.5, $KH_2PO_4$ 1.1, $MgSO_4$ 0.6, $NaHCO_3$ 25 and glucose 11.7.

In all experiments, human bronchi were first contracted maximally with acetylcholine $10^{-3}$ M and then relaxed with theophylline $3 \times 10^{-3}$ M. These concentrations did not alter responsiveness of the tissue. A 1 h rest period was observed before the beginning of the experimental procedure.

### *Experimental procedures*

*Concentration-response curves obtained with isoprenaline, salbutamol, siguazodan and rolipram* Following the resting period, the bronchial rings were either left under resting load or were contracted with methacholine $3 \times 10^{-7}$ M or acetylcholine $10^{-3}$ M. After the contraction plateau was reached, concentration-response curves were established by cumulative addition of isoprenaline, salbutamol or the phosphodiesterase inhibitors siguazodan and rolipram at intervals of 5–30 min to obtain a relaxation plateau. After the maximal effect of each drug was obtained, theophylline $3 \times 10^{-3}$ M was added to the bath in order to determine the maximal relaxation. Only one concentration-response curve was recorded in each ring.

*Influence of siguazodan and rolipram on concentration-response curves to isoprenaline and sodium nitroprusside (SNP)* Following the resting period, bronchial rings were pretreated for 30 min with Krebs solution (control) or one concentration of siguazodan ($10^{-8}$, $10^{-7}$, $10^{-6}$, and $10^{-5}$ M) or rolipram ($10^{-9}$, $10^{-8}$, and $10^{-7}$ M). Each concentration-response curve for relaxation by isoprenaline or SNP was obtained with cumulative additions of the drug after the bronchial ring had been brought to a steady level of contraction with acetylcholine $10^{-4}$ M. Finally, theophylline $3 \times 10^{-3}$ M was added in order to determine the maximal relaxation. Only one concentration-response curve was recorded in each ring.

### *Expression and statistical analysis of the results*

The relaxant effects of isoprenaline, salbutamol, siguazodan or rolipram are expressed as a percentage of the relaxation produced by theophylline $3 \times 10^{-3}$ M. $pD_2$ values represent the negative logarithm of the concentration of isoprenaline, salbutamol, siguazodan or rolipram which induces a relaxation equal to 50% of maximal effect induced by itself. $E_{max}$ values represent the maximal relaxation induced by isoprenaline, salbutamol, siguazodan or rolipram and are expressed as percentage of that induced by theophylline $3 \times 10^{-3}$ M.

Statistical analysis of the results was performed by analysis of variance and Student's $t$ test. All values are expressed as mean ± standard error of the mean; $P$ values lower than 0.05 were considered to be significant.

### *Drugs*

The drugs used were: theophylline (Theophylline Bruneau, Paris, France), acetylcholine HCl (Pharmacie Central des Hôpitaux, Paris, France), isoprenaline HCl (Laboratoires Winthrop, Paris, France), methacholine HCl, salbutamol sulphate, sodium nitroprusside (Sigma, St Louis, U.S.A), siguazodan, rolipram (synthesized by Rhône-Poulenc Rorer, Dagenham, Essex).

All drugs were dissolved daily in distilled water and diluted in Krebs solution.

## Results

### *Activity of isoprenaline, salbutamol, siguazodan and rolipram on the human isolated bronchus*

The concentration-response curves to the relaxant effects of isoprenaline, salbutamol and the selective phosphodiesterase inhibitors, rolipram and siguazodan, on human bronchi at resting tone or precontracted with methacholine $3 \times 10^{-7}$ M or acetylcholine $10^{-3}$ M are shown in Figures 1 and 2. The potency and efficacy of these substances were calculated by determining the $pD_2$ values and the maximal effects ($E_{max}$) (Table 1).

Table 1 shows that on bronchi at resting tone, rolipram was, in terms of potency, very similar to isoprenaline and salbutamol and approximately 10 fold more potent than siguazodan. During precontraction induced by methacholine $3 \times 10^{-7}$ M, the order of potency of these substances remained the same but siguazodan was, in terms of efficacy, more effective than rolipram.

In bronchi precontracted with acetylcholine $10^{-3}$ M, the concentration-response curves to rolipram and siguazodan were, as with methacholine, displaced to the right (Figure 2). The maximal effects of rolipram and siguazodan were reduced when compared with the resting tone situation. Rolipram was more potent than siguazodan and, in terms of efficacy, it was less effective.

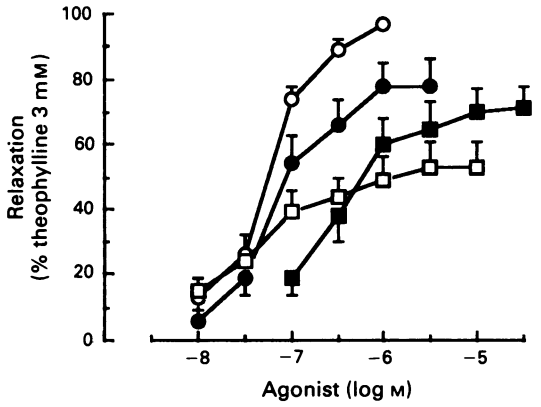



**Figure 1** Concentration-response (relaxation) curves to isoprenaline (○), salbutamol (●), rolipram (□) and siguazodan (■) of human isolated bronchi. Experiments were performed on preparations precontracted with methacholine $3 \times 10^{-7}$ M. The number of experiments is indicated in Table 1. Values are mean ± s.e.mean.

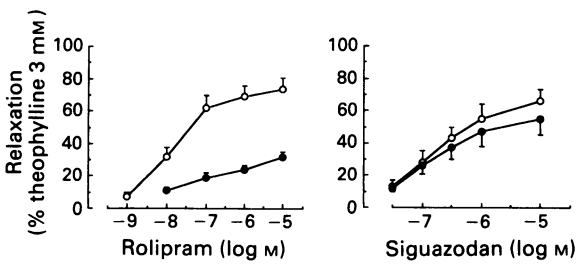



**Figure 2** Concentration-response (relaxation) curves to siguazodan and rolipram of human isolated bronchi. Experiments were performed on preparations at resting tone (○) or precontracted with acetylcholine $10^{-3}$ M (●). The number of experiments is indicated in Table 1. Values are mean ± s.e.mean.

*Influence of rolipram and siguazodan on concentration-response curves to isoprenaline and sodium nitroprusside*

Figure 3 shows that after 30 min incubation of human bronchi with rolipram $10^{-8}$ and $10^{-7}$ M, the concentration-response curves to isoprenaline were significantly shifted to the left and the maximal effect of isoprenaline was increased. In contrast, concentration-response curves to isoprenaline were not modified by siguazodan $10^{-8}$ to $10^{-5}$ M. Finally, concentration-response curves to sodium nitroprusside were not displaced after 30 min incubation with rolipram or siguazodan.

## Discussion

In a previous paper, Tomkinson *et al.* (1993) compared the relaxant properties of a PDE III inhibitor, siguazodan, and a PDE type IV inhibitor, rolipram, on the guinea-pig, bovine, murine and porcine airway smooth muscle. They observed that the potency of rolipram approached those of isoprenaline and salbutamol on the guinea-pig and bovine trachea, where $\beta_2$-adrenoceptors predominate, but rolipram was significantly less active than isoprenaline on the porcine bronchus (1000 fold) and murine trachea (>2000 fold), where $\beta_1$-adrenoceptors predominate. They also demonstrated that siguazodan was 100 fold more active than rolipram on porcine tissues but 15 times less potent on guinea-pig airways. On the basis of these results, Tomkinson *et al.* (1993) suggested that there might be a connection between the $\beta$-adrenoceptor subtype which predominates in a given tissue and the functional importance of the PDE isoenzyme in reducing smooth muscle contractility. They postulated a possible relationship between the $\beta_2$-adrenoceptor subtype and the functional importance of the PDE type IV isoenzyme on the one hand, and between the $\beta_1$-adrenoceptor and the PDE type III isoenzyme on the other. De Boer *et al.* (1992) have

**Table 1** $pD_2$ and $E_{max}$ of isoprenaline, salbutamol and the selective phosphodiesterase inhibitors on the human isolated bronchus at resting tone or contracted with methacholine (MCh) $3 \times 10^{-7}$ M or acetylcholine (ACh) $10^{-3}$ M

| | *Resting tone* | | | *MCh* ($3 \times 10^{-7}$ M) | | | *ACh* ($10^{-3}$ M) | | |
|---|---|---|---|---|---|---|---|---|---|
| | n | $pD_2$ | $E_{max}$ | *n* | $pD_2$ | $E_{max}$ | *n* | $pD_2$ | $E_{max}$ |
| Isoprenaline | 12 | 7.31 ± 0.12 | 98 ± 0.4 | 5 | 7.28 ± 0.06 | 97 ± 1.0 | 11 | 6.56 ± 0.13 | 85 ± 3.7 |
| Salbutamol | 10 | 7.12 ± 0.17 | 83 ± 2.4 | 5 | 7.19 ± 0.04 | 76 ± 7.7 | 11 | 6.62 ± 0.15 | 55 ± 6.5 |
| Rolipram | 8 | 7.77 ± 0.14 | 74 ± 6.7 | 5 | 7.47 ± 0.04 | 53 ± 8.1 | 8 | 7.28 ± 0.21 | 32 ± 3.0 |
| Siguazodan | 6 | 6.80 ± 0.12 | 66 ± 7.5 | 5 | 6.51 ± 0.09 | 71 ± 6.9 | 6 | 6.92 ± 0.09 | 55 ± 9.6 |

*n* = number of experiments.
$pD_2$: the negative logarithm of the concentration of isoprenaline, salbutamol, rolipram or siguazodan which induces a relaxation equal to 50% of maximal effect induced by itself.
$E_{max}$: maximal effect as percentage of maximal effect induced by theophylline $3 \times 10^{-3}$ M.

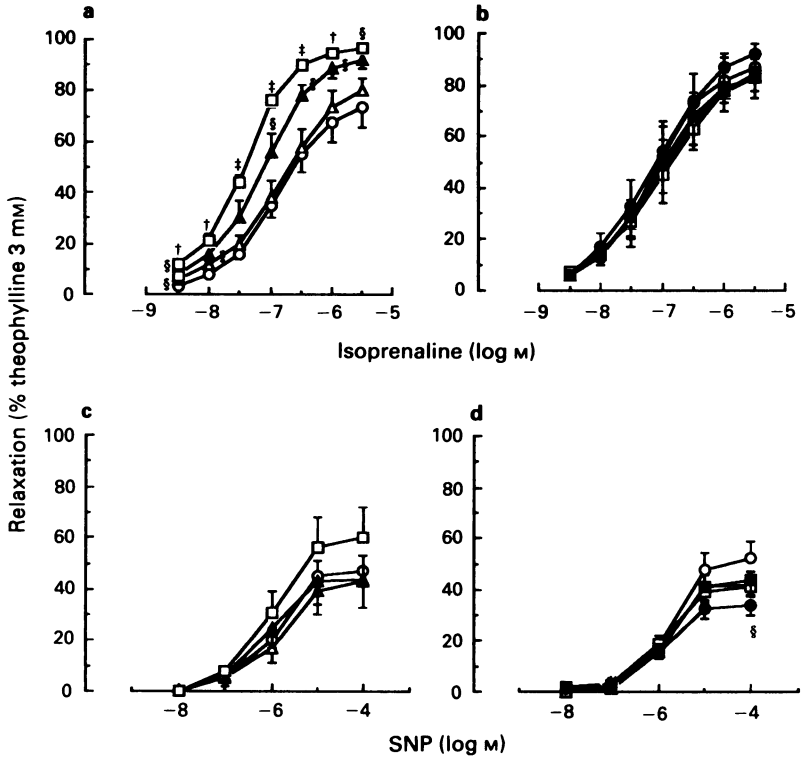



**Figure 3** Influence of rolipram (a,c) or siguazodan (b,d) on the concentration-response curves to isoprenaline (a,b) or sodium nitroprusside (SNP) (c,d) of human isolated bronchi, precontracted with acetylcholine $10^{-4}$ M. Concentration-response curves to isoprenaline or SNP were performed after 30 min incubation with saline (control, ○), rolipram or siguazodan ($10^{-9}$ M: △, $10^{-8}$ M; ▲, $10^{-7}$ M: □, $10^{-6}$ M: ■, $10^{-5}$ M: ●). Values are mean ± s.e.mean of 5 to 7 experiments. Significant differences from control are: §$P<0.05$; †$P<0.01$; ‡$P<0.001$.

reported that PDE types I, II, IV and V can be isolated by ion-exchange chromatography from human, isolated bronchial muscle. PDE IV was the main cyclic AMP hydrolytic activity. A distinct PDE III activity was not obtained but it was suggested that small amounts of PDE III may have co-eluted with the PDE IV.

Our results on the isolated human bronchus precontracted with methacholine $3 \times 10^{-7}$ M, corresponding to 30% of the maximal contraction induced by this substance – i.e. under conditions similar to those described by Tomkinson *et al.* (1993) on the airways of guinea-pig, cow, pig and mouse – tend to support previous observations and suggest that there may be a similar relationship between $\beta_2$-adrenoceptors and PDE type IV in the human bronchus since rolipram seems to be as potent (or slightly more potent) than isoprenaline and salbutamol, and about 10 fold more potent than siguazodan. Since both rolipram and the selective PDE III inhibitor Org 9935 were potently active at concentrations required for selectivity (de Boer *et al.*, 1992), both PDE III and IV may be important in regulating contractility. Indeed de Boer *et al.* (1992) demonstrated that equally potent inhibition of methacholine-induced contractions was seen with selective type IV and type III cyclic AMP PDE inhibitors. This was not the case in our study where rolipram was 10 fold more potent than siguazodan. The reason for this discrepancy is not clear but may be due to different PDE III inhibitory potency between Org 9935 and siguazodan. It is interesting to note (see Table 1) that while rolipram was the more potent cyclic AMP PDE inhibitor, siguazodan produced the greater maximum relaxation in the precontracted (but not basal) tissues. This supports the view of de Boer *et al.* (1992) that the relative amount of a PDE isoenzyme may not reflect the functional importance of its inhibition. It is also possible that the functional importance of PDE III and IV may vary with the contractile state of the tissue.

The observations concerning the relationship between $\beta_2$-adrenoceptors and the functional effects of PDE type IV inhibition in airways smooth muscle preparations are also supported by our finding that in smooth muscle relaxant concentrations, rolipram potentiates the bronchodilator effects of isoprenaline, whereas under the same conditions siguazodan does not. In contrast to zaprinast (Zhang *et al.*, 1992), neither rolipram nor siguazodan potentiate the effects of sodium nitroprusside. These data indicate that these substances do not modulate cyclic GMP hydrolysis. One may argue that we have used isoprenaline which is an agonist of both $\beta_1$-and $\beta_2$-adrenoceptors and, in consequence, the $\beta_1$-adrenoceptor might also be related to PDE type IV. It has however been clearly shown that the stimulation of $\beta_1$-adrenoceptors in the airways is without functional effect either in man (Löfdahl & Svedmyr, 1982; 1984) or in guinea-pig (Iakovidis *et al.*, 1980; Johansson & Waldeck, 1981). Our results are concordant with those of Hall *et al.* (1992) who have demonstrated that rolipram potentiated the increase in [$^3$H]-cyclic AMP induced by isoprenaline in primary cultures of human tracheal smooth muscle cells whereas siguazodan did not . Our results are also in agreement with Zaagsma *et al.* (1992) who showed that rolipram or the PDE III/PDE IV inhibitor Org 30029 potentiated the inhibitory effect of fenoterol on the antigen-induced contraction of the passively sensitized human bronchial isolated smooth muscle, whereas the PDE III selective inhibitor milrinone was inactive. Zaagsma *et al.* (1992) also demonstrated that the $\beta$-adrenergic inhibition of antigen-induced histamine release from guinea-pig peripheral lung was potentiated in the presence of rolipram. Human bronchi seem to differ from the bronchi of dog or guinea-pig on which it has been demonstrated that the effects of isoprenaline were potentiated by either siguazodan (SK&F 94836) or Ro 20-1724, a PDE type IV inhibitor (Torphy *et al.*, 1988; Rhoden & Barnes, 1990).

Thus, in the airways at least, PDE type IV inhibition may result in a potentiation that is specific to the effects of $\beta_2$-adrenoceptor stimulation. This is of interest for substances to be used in the treatment of asthma and goes side by side with other specific and potentially interesting effects of PDE type IV inhibitors, such as inhibition of the microvascular leakage induced by PAF in the guinea-pig (Raeburn & Karlson, 1992; Ortiz *et al.*, 1992), of the N-formylmethionyl-leucyl-phenylalanine (fMLP)-stimulated superoxide release and fMLP/thiomerosal elicited leukotriene biosynthesis by human polymorphonuclear leukocytes (Schudt *et al.*, 1991), as well as inhibition of mediator release from human basophils, mast cells, monocytes or neutrophils (Peachell *et al.*, 1990; Neilson *et al.*, 1990) or of superoxide formation in guinea-pig eosinophils (Dent *et al.*, 1990).

Our results also show that, contrary to those reported by Giembycz *et al.* (1992) on the human trachea, rolipram relaxes the human bronchus at resting tone. This discrepancy might be due to a difference in preparation (trachea *versus* bronchus), but this is unlikely since these authors have shown that PDE type IV is predominant in the human trachea and Hall *et al.* (1992) have demonstrated that rolipram elevated basal [$^3$H]-cyclic AMP levels in primary cultures of human tracheal smooth muscle cells. The discrepancy may also be due to differences in experimental conditions, since the dilatation reserve is perhaps greater distally, but in their experiments Giembycz *et al.* (1992) have shown that SK&F 94120, a PDE III inhibitor, relaxes the trachea irrespective of whether it is at resting tone or contracted with methacholine.

In any case, our results are similar to those of Hall & Hill (1992) who observed a relaxant effect of rolipram on the bovine isolated trachea at resting tone and a shift to the right of rolipram concentration-response curves by functional antagonism under the influence of methacholine. Hall & Hill (1992) also observed a relaxant effect of SK&F 94120 and siguazodan, both PDE type III inhibitors, as we did with siguazodan on the human isolated bronchus and as Giembycz *et al.* (1992) did with SK&F 94120 on the human isolated trachea.

## References


BEAVO, J.A. & REIFSNYDER, D.H. (1990). Primary sequence of cyclic nucleotide phosphodiesterase isozymes and the design of selective inhibitors. *Trends Pharmacol. Sci.*, **11**, 150–155.

DE BOER, J., PHILPOTT, A.J., VAN AMSTERDAM, R.G.M., SHAHID, M., ZAAGSMA, J. & NICHOLSON, C.D. (1992). Human bronchial cyclic nucleotide phosphodiesterase isoenzymes: biochemical and pharmacological analysis using selective inhibitors. *Br. J. Pharmacol.*, **106**, 1028–1034.

DENT, G., RABE, K., GIEMBYCZ, M.A. & BARNES, P.J. (1990). Inhibition of eosinophil respiratory burst activity by type IV-, but not type III-selective cAMP phosphodiesterase inhibitors (abstract). *Am. Rev. Respir. Dis.*, **141**, A878.

GIEMBYCZ, M.A., BELVISI, M.G., MIURA, M., PETES, M.J., YACOUB, M. & BARNES, P.J. (1992). Cyclic nucleotide phosphodiesterases in human trachealis and the mechanical effect of isozyme selective inhibitors (abstract). *Am. Rev. Resp. Dis.*, **145**, A378.

GIEMBYCZ, M.A. & RAEBURN, D. (1991). Putative substrates for cyclic nucleotide dependent protein kinases and the control of airway smooth muscle tone. *J. Auton. Pharmacol.*, **11**, 365–398.

HALL, I.P. & HILL, S.J. (1992). Effects of isozyme selective phosphodiesterase inhibitors on bovine tracheal smooth muscle tone. *Biochem. Pharmacol.*, **43**, 15–17.

HALL, I.P., WIDDOP, S., TOWNSEND, P. & DAYKIN, K. (1992). Control of cyclic AMP levels in primary cultures of human tracheal smooth muscle cells. *Br. J. Pharmacol.*, **107**, 422–428.

IAKOVIDIS, D., MALTA, E., MCPHERSON, G.A. & RAPER, C. (1980). *In vitro* activity of RO363, a $\beta_1$-adrenoceptor selective agonist. *Br. J. Pharmacol.*, **68**, 677–685.

JOHANSSON, U. & WALDECK, B. (1981). Beta$_1$-adrenoceptors mediating relaxation of the guinea-pig trachea: experiments with prenalterol, a $\beta_1$-selective adrenoceptor agonist. *J. Pharm. Pharmacol.*, **33**, 353–356.

LÖFDAHL, C.-G. & SVEDMYR, N. (1982). Effects of prenalterol in asthmatic patients. *Eur. J. Clin. Pharmacol.*, **23**, 297–302.

LÖFDAHL, C.-G. & SVEDMYR, N. (1984). Effects of xamoterol (ICI 118,587) in asthmatic patients. *Br. J. Clin. Pharmacol.*, **18**, 597–601.

NEILSON, C.P., VESTAL, R.E., STURM, R.J. & HEASLIP, R. (1990). Effects of selective phosphodiesterase inhibitors on the polymorphonuclear leukocyte respiratory burst. *J. Allergy Clin. Immunol.*, **86**, 801–808.

NICHOLSON, C.D., CHALLISS, R.A.J. & SHAHID, M. (1991). Differential modulation of tissue function and therapeutic potential of selective inhibitors of cyclic nucleotide phosphodiesterase isoenzymes. *Trends Pharmacol. Sci.*, **12**, 19–27.

ORTIZ, J.L., CORTIJO, J., VALLÉS, J.M., BOU, J. & MORCILLO, E.J. (1992). Rolipram inhibits PAF-induced airway microvascular leakage in guinea-pig: a comparison with milrinone and theophylline. *Fund. Clin. Pharmacol.*, **6**, 247–249.

PEACHELL, P.T., UNDEM, B.J., SCHLEIMER, R.P., LICHTENSTEIN, L.M. & TORPHY, T.J. (1990). Action of isozyme-selective phosphodiesterase (PDE) inhibitors on human basophil (abstract). *FASEB. J.*, **4**, A639.

RAEBURN, D. & KARLSSON, J.A. (1992). Comparison of the effects of isoenzyme-selective phosphodiesterase inhibitors and theophylline on PAF-induced plasma leak in the guinea-pig airways *in vivo* (abstract). *Am. Rev. Respir. Dis.*, **145**, A612.

RHODEN, K.J. & BARNES, P.J. (1990). Potentiation and nonadrenergic neural relaxation in guinea pig airways by a cyclic cAMP phosphodiesterase inhibitor. *J. Pharmacol. Exp. Ther.*, **252**, 396–402.

SCHUDT, C., WINDER, S., FORDERKUNZ, S., HATZELMANN, A. & ULLRICU, V. (1991). Influence of selective phosphodiesterase inhibitors on human neutrophil functions and level of cAMP and Ca$_i$. *Naunyn Schmieds Arch. Pharmacol.*, **344**, 682–690.

SILVER, P.J., HAMEL, L.T., PERRONE, M.H., BENTLEY, R.G., BUSHOVER, C.R. & EVANS, D.B. (1988). Differential pharmacological sensitivity of cyclic nucleotide phosphodiesterase isozymes isolated from cardiac muscle, arterial and airway smooth muscle. *Eur. J. Pharmacol.*, **150**, 85–94.

TOMKINSON, A., KARLSSON, J.A. & RAEBURN, D. (1993). Comparison of the effects of selective inhibitors of phosphodiesterase type III or IV in airway smooth muscle with differing $\beta$-adrenoceptor subtype. *Br. J. Pharmacol.*, **108**, 57–61.

TORPHY, T.J., BURMAN, M., HUANG, L.B.F. & TUCKER, S.S. (1988). Inhibition of the low Km cyclic AMP phosphodiesterase in intact canine trachealis by SK&F 94836: mechanical and biochemical responses. *J. Pharmacol. Exp. Ther.*, **246**, 843–850.

TORPHY, T.J. & UNDEM, B.J. (1991). Phosphodiesterase inhibitors: new opportunities for the treatment of asthma. *Thorax*, **46**, 512–523.

ZAAGSMA, J., VAN AMSTERDAM, R.G.M., TEN BERGE, R.E.J. & ZEILSTRA, L.J.W. (1992). Modulation of allergic and non-allergic contraction of guinea pig lung strips and small bronchi by selective and non selective phosphodiesterase inhibitors (abstract). *Am. Rev. Resp. Dis.*, **145**, A858.

ZHANG, Y., PALETTE-PAYS, C., NALINE, E., VAROQUAUX, O. & ADVENIER, C. (1993). Effect of molsidomine and linsidomine on the human isolated bronchus and the guinea-pig isolated trachea. *J. Pharm. Pharmacol.*, **45**, (in press).

*(Received December 2, 1992*
*Revised February 8, 1993*
*Accepted March 1, 1993)*

*Br. J. Pharmacol.* (1993), **109**, 779–787 © Macmillan Press Ltd, 1993

# Thiocyanate ions selectively antagonize AMPA-evoked responses in *Xenopus laevis* oocytes microinjected with rat brain mRNA

[2]Derek Bowie & [1]Trevor G. Smart

The School of Pharmacy, Department of Pharmacology, 29–39 Brunswick Square, London WC1N 1AX

**1** Responses to kainate (KA), willardiine and α-amino-3-hydroxy-5-methyl-4-isoxazolepropionic acid (AMPA) were recorded from rat brain mRNA-injected *Xenopus laevis* oocytes by use of a two-electrode voltage clamp.

**2** Thiocyanate ($SCN^-$; 50 μM–4 mM) ions reversibly and selectively inhibited the membrane current responses to AMPA in a non-competitive manner without affecting KA or willardiine-induced responses.

**3** The inhibition of AMPA-induced responses by $SCN^-$ was dependent on the $SCN^-$ concentration with an estimated $IC_{50}$ of 1 mM. The antagonism was not dependent on the AMPA concentration.

**4** The response to a high concentration of AMPA (100–200 μM) exhibited a peak inward current which declined to a steady-state. $SCN^-$ inhibited the steady-state current more than the peak response. The inhibition was unaffected by prior incubation with concanavalin-A (Con-A; 10 μM).

**5** Responses to KA were antagonized by AMPA in a competitive manner, suggesting that both agonists may activate a common receptor-channel complex. This interaction between two non-NMDA agonists was not affected by the $SCN^-$-induced inhibition of the AMPA response.

**6** AMPA-induced responses recorded from large cultured cerebellar neurones by whole-cell recording were also inhibited by $SCN^-$ in a non-competitive manner. The AMPA-induced peak current was less affected than the steady-state response.

**7** We conclude that $SCN^-$ can inhibit the response to AMPA in expressed non-NMDA receptors in *Xenopus* oocytes and also in native receptors in cultured cerebellar neurones. One possible mechanism of action for $SCN^-$ inhibition of responses to AMPA may involve a Con-A-insensitive, non-NMDA receptor-mediated desensitization.

**Keywords:** Non-NMDA receptors; AMPA; thiocyanate; *Xenopus laevis*; intracellular recording; mRNA translation; cerebellar neurones; patch clamp

## Introduction

In radioligand binding and electrophysiological studies, a variety of cations have been shown to modulate the properties of excitatory amino acid (EAA) receptors. For example, at N-methyl-D-aspartate (NMDA) receptors, both $Mg^{2+}$ and $Zn^{2+}$ can act as non-competitive antagonists (Mayer *et al.*, 1984; Nowak *et al.*, 1984; Peters *et al.*, 1987; Westbrook & Mayer, 1987; Enomoto *et al.*, 1992) by binding to discrete sites on the NMDA receptor-channel complex (Mayer *et al.*, 1988). In addition, modulation of the external pH by changing the $H^+$ ion concentration also inhibited the activity of NMDA receptors in a non-competitive manner probably by binding to another discrete site (Tang *et al.*, 1990; Vyklicky *et al.*, 1990; Traynelis & Cull-Candy, 1990; 1991). As all these ions are naturally present *in vivo* in the central nervous system (CNS), they may be capable of regulating the activity of one or more members of the NMDA receptor family under physiological or even pathological conditions (cf. Forsythe *et al.*, 1988; McDonald & Johnston, 1990).

In comparison, non-NMDA receptors are not apparently regulated by endogenous substances which are so vital for NMDA receptor modulation, such as glycine (Johnson & Ascher, 1987) and $Mg^{2+}$ (Nowak *et al.*, 1984; Mayer *et al.*, 1984). Nevertheless responses evoked by kainate (KA) can be non-competitively depressed by divalent cations such as $Hg^{2+}$ (Kiskin *et al.*, 1989; Umbach & Gundersen, 1989) or $Ca^{2+}$ (Perouansky & Grantyn, 1989; Gu & Huang, 1991). Moreover, in binding studies, $Ca^{2+}$ is the most potent cation to depress [$^3$H]-KA binding (Honore *et al.*, 1986; Monaghan *et al.*, 1986) and could be used to distinguish selectively between KA and α-amino-3-hydroxy-5-methyl-4-isoxazolepropionic acid (AMPA) binding to non-NMDA receptors.

As with NMDA receptors, lowering the external pH also reduced non-NMDA receptor-mediated function (Randle *et al.*, 1988; Christensen & Hida, 1990; Vyklicky *et al.*, 1990; Traynelis & Cull-Candy, 1991). However, in comparison to NMDA receptors, $Zn^{2+}$ ions could either enhance or inhibit non-NMDA-induced responses, depending on the zinc concentration (Mayer *et al.*, 1988; Rassendren *et al.*, 1990).

In contrast to the various effects exerted by numerous cations, anions have not featured prominently as modulators of EAA receptors, which is not surprising since these ions are unlikely to interfere with essentially cation-permeable ligand-gated ion channels. A notable exception to this general exclusion is the chaotropic anion, thiocyanate ($SCN^-$). In the presence of $SCN^-$, binding of the non-NMDA agonist, AMPA to brain membranes was considerably enhanced, but the binding of KA remained unaffected (Honore & Nielsen, 1985; Murphy *et al.*, 1987). This useful finding resulted in the majority of radioligand binding assays for AMPA employing thiocyanate ions as an experimental tool to increase the affinity of the receptor for this agonist (Honore & Drejer, 1988), allowing differentiation between AMPA and KA binding. The mechanism of action for $SCN^-$ to enhance AMPA binding is unknown and perhaps more important, the functional effects of $SCN^-$ ions on non-NMDA receptors have rarely been addressed.

In the present study we investigated the functional effects

[1] Author for correspondence.
[2] Present address: Laboratoire de Physiologie Generale, Universite Louis Pasteur, 21, rue Rene Descartes, F67084, Strasbourg Cedex, France.

of $SCN^-$ on expressed non-NMDA receptors in rat brain mRNA-injected *Xenopus* oocytes, and also on native non-NMDA receptors maintained in cultured cerebellar neurones. In particular we examine whether an anion-selective binding site exists on the non-NMDA receptor complex which is capable of selectively modulating receptor function following activation by AMPA or KA.

A preliminary report of part of this work has appeared previously (Bowie & Smart, 1991).

## Methods

### *Extraction and injection of* Xenopus laevis *oocytes*

Female *Xenopus laevis* toads (140–200 g) were anaesthetized in a cold solution of ethyl-m-aminobenzoate (Tricaine) prior to the removal of part of an ovary containing 50–100 oocytes. Oocytes were manually separated from the ovary wall and placed in modified Barth's medium (MBM) containing (mM) at pH 7.6: NaCl 110, KCl 1, $NaHCO_3$ 2.4, Tris HCl 7.5, $Ca(NO_3)_2$ 0.33, $CaCl_2$ 0.41, $MgSO_4$ 0.82 and streptomycin, 10 μg $ml^{-1}$. Only oocytes at developmental stages V and VI (Dumont, 1972) were selected for mRNA injection. Each oocyte was injected into the equatorial region with 50 nl of a 1 mg $ml^{-1}$ mRNA solution. Injected oocytes were then incubated at 18°C for 2–3 days to allow the expression of receptor protein. After this period, all oocytes were stored in MBM at 10°C and re-fed with fresh MBM every 2 days. This prolonged the survival of the oocytes for up to 4–5 weeks. Translationally-active mRNA was extracted from 3–6 week-old rat brain (without the cerebellum) by a guanidinium thiocyanate/caesium chloride method and purified by oligo-dT column chromatography (Chirgwin *et al.*, 1976).

### *Dissociated cultures of cerebellar neurones*

Cerebellar cultures were prepared as described previously (Smart, 1992). Briefly, cerebellar cortices were removed from embryonic day 17–18 rats (E17–18) and chopped into slices in ice-cooled plating medium containing: minimum essential medium (MEM) with 10% v/v foetal calf serum, 10% v/v horse serum, 2 mM glutamine, 0.6% w/v glucose and 100 units $ml^{-1}$ penicillin-G and 100 μg $ml^{-1}$ streptomycin. The neurones were mechanically dissociated through nylon mesh (diameter 210 μm) and plated onto poly-L-lysine coated dishes and incubated at 37°C with 95% air/5% $CO_2$. After 4 days the plating medium was removed and replaced with a growth medium which retained the contents of the plating medium except for the foetal calf serum. Large cerebellar neurones were used for electrophysiology after 20 days in culture and were distinguished from granule cells on the basis of soma diameter and dendritic morphology (see Smart, 1992 for discussion).

### *Electrophysiology*
### *Intracellular two-electrode voltage clamp in* Xenopus *oocytes*

Xenopus oocytes were secured to the base of a Perspex bath (volume 0.5–1 ml) coated with Sylgard following placement within a circle of insect pins. Cells were impaled with two microelectrodes manufactured from thin-walled borosilicate glass and filled with 3 M KCl solution providing resistances of 5–10 MΩ for the voltage and 1–2 MΩ for the current microelectrodes. Electrophysiological recordings were made using an Axoclamp 2A amplifier in two-electrode voltage clamp mode and membrane currents were monitored on a Brush-Gould thermal chart recorder (2200). All drugs were applied in frog Ringer via the bath superfusion system (rate 8–10 ml $min^{-1}$) through a gravity fed inlet placed 5 mm away from the oocyte surface. The frog Ringer contained (mM): NaCl 110, KCl 2, HEPES 5, $CaCl_2$ 1.8, pH 7.4. Only oocytes with input resistances of 1–5 MΩ and resting membrane potentials of −40 to −60 mV were accepted for experimentation.

### *Whole-cell recording from cultured neurones*

Experiments were performed with a List EPC7 amplifier by the whole-cell patch clamp recording method. Patch electrodes were fabricated from thin walled borosilicate glass and filled with a pipette solution containing (mM): KCl 150, $CaCl_2$ 0.279, $MgCl_2$ 1, Na-EGTA 0.5, HEPES 10, pH 7.1. Pipettes had resistances ranging from 1–50 MΩ. The neurones were viewed under phase-contrast optics and continually superfused in a 35 mm culture dish (volume 1 ml) with a Krebs solution containing (mM): NaCl 140, KCl 4.7, $MgCl_2$ 1.2, $CaCl_2$ 2, glucose 11, HEPES 5, pH 7.4 at 30°C. Drugs and Krebs solutions were applied to the neurones by a rapid perfusion system consisting of a multibarrelled pipette made from Quad glass (Q-tube, Clarks Electromedical). The concentration-response relation for AMPA was determined with a U-tube perfusion system for drug application (Krishtal & Pidoplichko, 1980; Fenwick *et al.*, 1982). The U- or Q-tubes were placed within 300 μm of the cell under study.

## Results

### *Differential antagonism of non-NMDA induced responses by thiocyanate ions*

In *Xenopus* oocytes injected with rat brain mRNA and voltage clamped at −60 mV holding potential, bath-application of AMPA (4–100 μM) or willardiine (10–320 μM) produced small reproducible inward membrane currents (11 ± 1.4 nA for AMPA, $n = 10$; 10 ± 2 nA for willardiine, $n = 6$) and associated conductance increases when compared to the larger responses induced by 80 μM KA in the same cells (84 ± 8 nA; $n = 9$). The responses evoked by higher concentrations of AMPA (50–100 μM) also differed by exhibiting an apparent desensitization during continued application of the agonist. This contrasted with the apparently maintained amplitudes of the KA- or willardiine-induced currents and with responses induced by low concentrations of AMPA (4–10 μM; Figure 1). Desensitizing AMPA-induced responses were characterized by a discernible peak inward current which decayed to a steady-state during agonist application. Following the removal of AMPA, the membrane current quite often exhibited a rebound inward tail current, prior to decaying back to the holding current (Figure 1a).

The inclusion of 50 μM–4 mM thiocyanate ions ($SCN^-$; sodium salt) in the Ringer solution did not affect the resting membrane potential or input conductance of mRNA-injected or uninjected *Xenopus* oocytes. However, responses induced by AMPA (4–100 μM) were selectively antagonized by $SCN^-$ with the peak and steady-state currents for 100 μM AMPA reduced by 55 ± 4 and 74 ± 3% respectively ($n = 8$). The onset of antagonism and the recovery from inhibition was rapid and showed no evidence of any use-dependence. In contrast to AMPA-induced responses, 2 mM $SCN^-$ did not significantly affect the amplitude of either 80 μM KA-induced (102 ± 5%) or 100 μM willardiine-induced (99 ± 3%) membrane currents ($n = 5$; Figure 1b/c).

### *Thiocyanate ions non-competitively inhibited AMPA-induced currents*

The mechanism of inhibition of AMPA-induced currents by $SCN^-$ was analyzed using concentration-response curves obtained by measuring the steady-state current amplitudes of the responses to AMPA (2.5–200 μM). Bath-application of $SCN^-$ (2 mM) inhibited the AMPA concentration-response curve in a non-competitive manner, simply depressing the

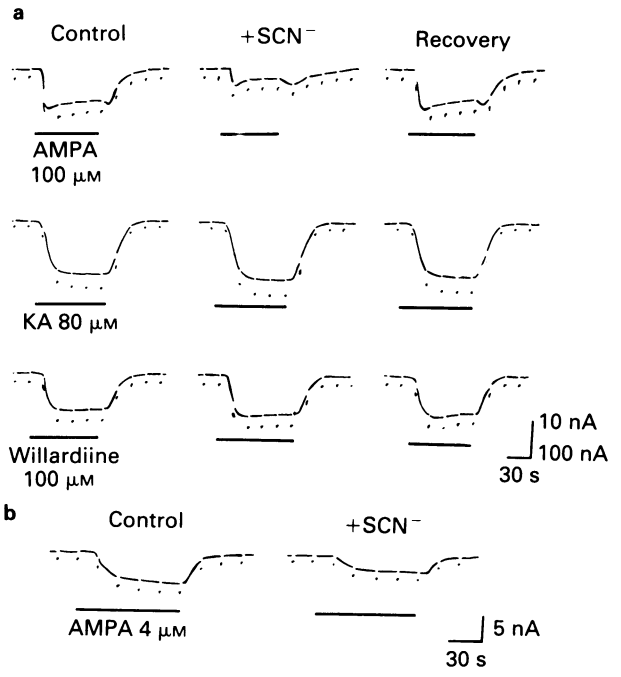



**Figure 1** Thiocyanate ions selectively inhibited α-amino-3-hydroxy-5-methyl-4-isoxazolepropionic acid (AMPA)-induced responses. (a) Inward membrane currents were induced by AMPA (100 μM), kainate (KA, 80 μM) or willardiine 100 μM in rat brain mRNA-injected oocytes voltage clamped at a holding potential of − 60 mV in the presence and absence of 2 mM $SCN^-$. In this and some of the subsequent figures, hyperpolarizing voltage commands (5–10 mV, 1.5 s, 0.05 Hz) were applied to monitor the membrane conductance and the agonists were applied for the duration indicated by the solid lines. Note the decaying responses to AMPA and the lower current amplitudes to AMPA and willardiine compared to KA. The 10 nA calibration only applies to currents induced by AMPA and willardiine. (b) Low concentrations of AMPA exhibited maintained current amplitudes in the presence or absence of 2 mM $SCN^-$.

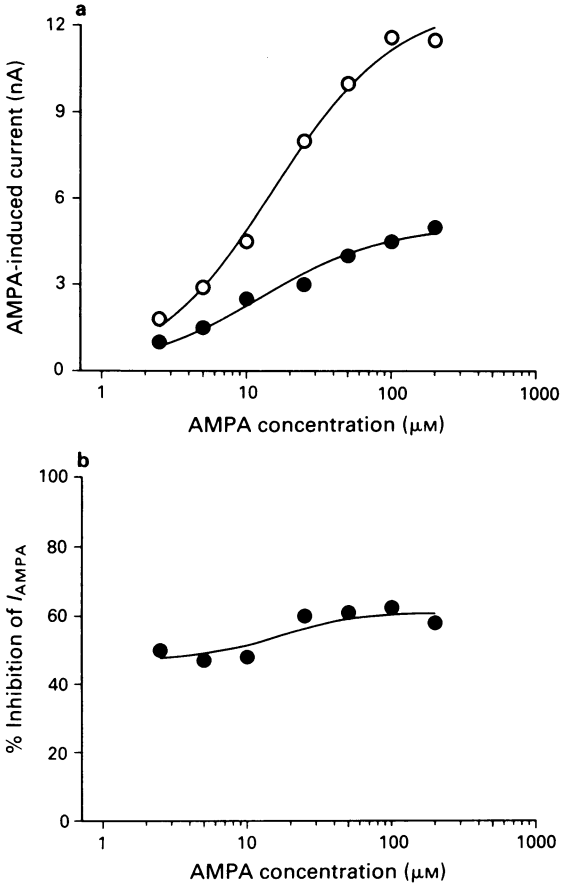



**Figure 2** Thiocyanate ions non-competitively antagonize α-amino-3-hydroxy-5-methyl-4-isoxazolepropionic acid (AMPA)-induced responses. (a) Typical concentration-response curves for responses to AMPA were obtained in the presence (●) and absence (○) of 2 mM $SCN^-$. The curves were fitted using a receptor model state function of the form, $Y/Y_{max} = \{[A]/[A] + K_A\}^n$, where A, $K_A$ and n represent agonist concentration, dissociation constant and the Hill coefficient. The data were fitted according to a Marquadt non-linear least squares routine. $K_A$ and n were estimated in control Ringer to be 12.7 ± 1.2 μM and 1.2 ± 0.33 ($r = 0.9968$); and in 2 mM $SCN^-$, 12.5 ± 1.9 μM and 1.0 ± 0.5 ($r = 0.9902$). (b) The percentage inhibition of the AMPA-induced responses by 2 mM $SCN^-$ are plotted against the AMPA concentration. Data were calculated from (a).

curve without inducing any lateral shifting (Figure 2a). Estimation of the $EC_{50}$s for AMPA in the absence and presence of $SCN^-$ were similar at 19 and 15 μM respectively. The corresponding percentage-inhibition plot for AMPA-induced responses revealed that the antagonism produced by $SCN^-$ was only slightly dependent on the agonist concentration, with 4 μM AMPA-induced responses inhibited by 50 ± 4% and responses to 100 μM AMPA reduced by 63 ± 3% ($n = 8$; Figure 2b). The absence of any noticeable shift by an antagonist in a dose-response curve is often formally interpreted as indicating no change in the apparent affinity of the receptor for an agonist. This may be true for the action of $SCN^-$ on the non-NMDA receptors; however, we cannot discount an effect of $SCN^-$ on other processes preceding ion channel activation.

In Figure 3a, the membrane current induced by AMPA in control Ringer solution displayed a slow decline from the peak response, but did not reveal any evidence of a rebound tail current following removal of the agonist (cf. Figure 1a). In the presence of low concentrations of $SCN^-$ (0.5 mM), the AMPA-induced response was depressed and the slow decline in the current amplitude was also without any rebound tail current (Figure 3a); however, after exposure of the oocyte to higher concentrations of $SCN^-$ (> 1 mM), the AMPA-induced responses were antagonized to a greater extent and following cessation of AMPA application an inward rebound tail current was often revealed. The concentration of $SCN^-$ required to produce a half-maximal inhibition ($IC_{50}$) in the steady-state AMPA-induced response was determined from an inhibition plot constructed for AMPA responses in the presence of 50 μM–4 mM $SCN^-$. In Figure 3b, the response induced by 50 μM AMPA was reduced in a concentration-dependent manner by $SCN^-$ with an $IC_{50}$ of 1 mM.

### *Thiocyanate ions and desensitization of non-NMDA receptors*

The decline in the AMPA-induced peak current was observed on rapidly superfusing the oocyte at 8–10 ml $min^{-1}$ and could represent a component of receptor desensitization since it was also accompanied by a decline in the membrane conductance. This fade in the peak current was assessed by calculating a ratio of the steady-state current ($I_{ss}$), measured after 90 s in AMPA-containing Ringer, to the initial peak current ($I_p$). A clear peak current which exhibited desensitization to a smaller steady-state response was only observed at AMPA concentrations > 50 μM and the corresponding ration, $I_{ss}/I_p$, was reduced with increasing AMPA concentration (Figure 4b). This reduction in the $I_{ss}/I_p$ ratio was accounted for by a reduced $I_{ss}$, suggesting that the measurement of $I_{ss}$ was more susceptible to the effect of desensitization than $I_p$. For example, rapid bath-application of 200 μM AMPA ($I_{ss}/I_p = 0.67 \pm 0.04$, $n = 4$) induced a current which desensitized more so than a response induced by 100 μM AMPA (0.83 ± 0.03, $n = 10$; Figure 4a). Declining AMPA-

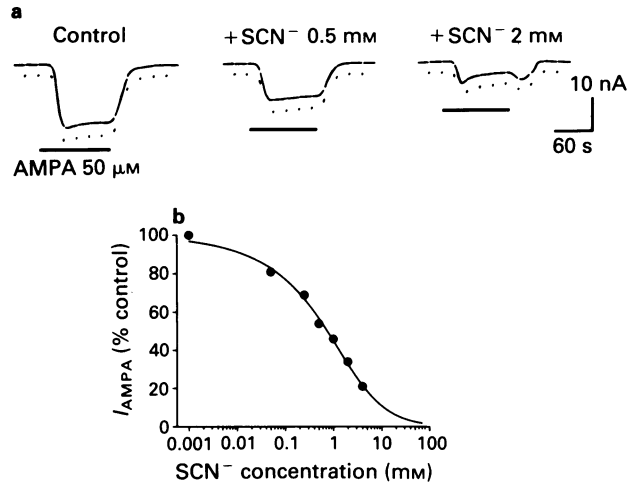



**Figure 3** Dependence of α-amino-3-hydroxy-5-methyl-4-isoxazolepropionic acid (AMPA)-induced response antagonism on $SCN^-$ concentration. (a) Inward currents induced by AMPA (50 μM) were recorded from a single oocyte voltage clamped at − 60 mV holding potential in control Ringer and 0.5 or 2 mM $SCN^-$. Note the initial decay of the AMPA-induced response and the appearance of an inward rebound tail current in the presence of 2 mM $SCN^-$ following the removal of AMPA. (b) Dose-response analysis for the inhibition by 1 μM–4 mM $SCN^-$ of a response to AMPA (50 μM). The data were fitted to the equation, $Y'/Y = 1-\{[B]/([B] + K_B)\}$, whereby Y' represents the AMPA-induced current response in the presence of $SCN^-$ and Y the control response amplitude. B and $K_B$ represent $SCN^-$ concentration and the apparent dissociation constant respectively. $K_B$ was estimated as 3.1 ± 0.56 mM and n = 0.43 ± 0.04.

induced currents were generally not observed if a slower agonist-perfusion rate (< 5 ml $min^{-1}$) was employed (Bowie, 1991).

The rebound inward tail current amplitude was also more clearly resolved in responses to the higher AMPA concentrations (50–200 μM; Figure 4a) and could always be correlated with the onset of desensitization in the peak AMPA-induced current.

By using AMPA concentrations that induced a desensitizing current response (> 50 μM), the peak AMPA-induced current was inhibited to a lesser extent than the steady-state current in the presence of 2 mM $SCN^-$. Accordingly, $I_{ss}/I_p$ for 100 μM AMPA-induced currents was reduced by $SCN^-$ from 0.86 ± 0.06 to 0.52 ± 0.06 ($n = 8$; Figure 4b).

The reduction in the $I_{ss}/I_p$ ratio following treatment with $SCN^-$, raised the possibility that $SCN^-$ might be inhibiting AMPA-induced responses by increasing receptor desensitization. This was investigated using the plant lectin, concanavalin-A (Con-A), which reduces desensitization of glutamate or AMPA-induced responses mediated by neuronal non-NMDA receptors (Mayer & Vyklicky, 1989). Pretreatment of mRNA-injected oocytes for 30–45 min with 10 μM Con-A selectively enhanced the responses elicited by 100 μM AMPA when compared to 80 μM KA-induced responses. Both $I_p$ and $I_{ss}$ for the AMPA responses were enhanced by 25 ± 3% and 40 ± 5% respectively over the control values prior to Con-A treatment ($n = 3$). This differential effect of Con-A resulted in only a small increase in the $I_{ss}/I_p$ ratio for AMPA-induced (100 μM) responses from 0.83 ± 0.03 ($n = 10$) to 0.9 ± 0.04 ($n = 3$; Figure 4b). This enhancement was apparently irreversible and could still be observed up to 60 min following exposure to Con-A.

In the presence of 2 mM $SCN^-$, the residual $I_p$ and $I_{ss}$ responses to 100 μM AMPA in Con-A-treated oocytes were reduced by 54 ± 2% and 67 ± 7% respectively (Figure 4c). In comparison, prior to the treatment with Con-A in the same mRNA-injected oocytes, $SCN^-$ reduced $I_p$ and $I_{ss}$ by 55 ± 4% and 74 ± 3% ($n = 8$). Lower concentrations of Con-A

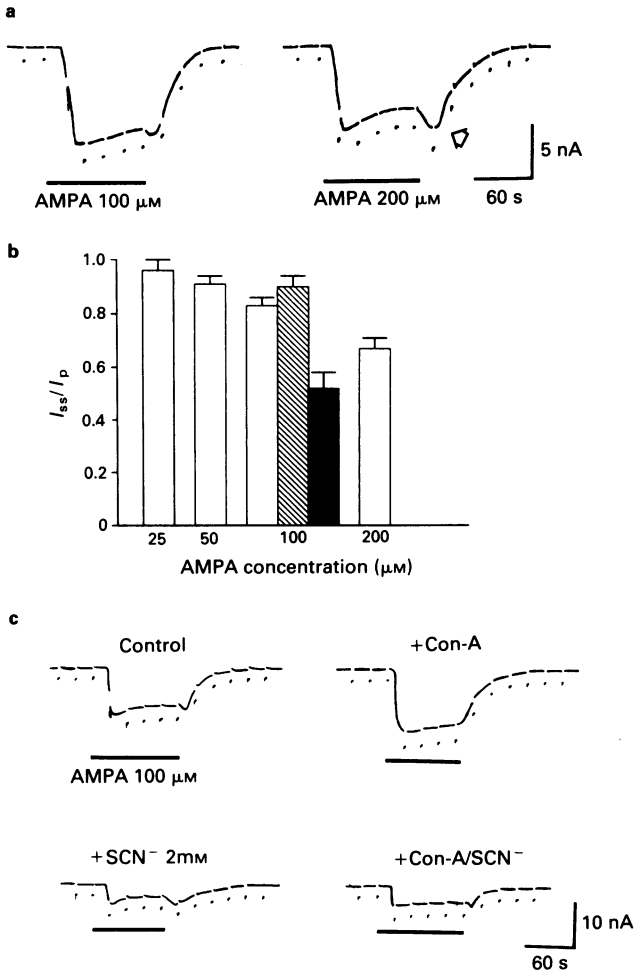



**Figure 4** Desensitization of α-amino-3-hydroxy-5-methyl-4-isoxazolepropionic acid (AMPA)-induced responses. Effect of concanavalin A (Con-A) and $SCN^-$. (a) Saturating concentrations of AMPA (100–200 μM) evoked desensitizing responses with clear peak inward currents and rebound tail currents which appeared after the removal of AMPA. The tail currents (arrow) were more clearly resolved with higher concentrations of AMPA which displayed more overt desensitization. (b) A ratio of the steady-state current ($I_{ss}$), measured after 90 s in the presence of AMPA, to the initial peak inward current ($I_p$), is plotted against the agonist concentration (open columns). Increasing AMPA concentration caused this ratio to decrease, consistent with dose-dependent desensitization. For oocytes exposed to 100 μM AMPA, pretreatment with 10 μM Con-A increased the $I_{ss}/I_p$ ratio (hatched column), whereas in other oocytes, addition of 2 mM $SCN^-$ reduced this ratio (solid column). All values represent means ± s.e.mean from 3–10 mRNA-injected oocytes. (c) Responses evoked by 100 μM AMPA in a single oocyte voltage clamped at − 60 mV were recorded in four different solutions including: control Ringer; + 2 mM $SCN^-$; and following a recovery from $SCN^-$ (not shown), after a 30 min exposure to 10 μM Con-A; and finally after Con-A treatment, in 2 mM $SCN^-$. The AMPA-induced responses in control Ringer exhibited a rebound tail current which was lost in Con-A-treated oocytes.

(1 μM) were less effective in reducing the level of non-NMDA receptor desensitization.

### *Effect of thiocyanate ions on the antagonism of kainate-induced responses by AMPA*

Many studies on native non-NMDA receptors on catfish retinal neurones (O'Dell & Christensen, 1989), and mammalian hippocampal and spinal cord neurones (Zorumski & Yang, 1988; Thio *et al.*, 1991; Patneau & Mayer, 1991; see Gasic & Hollman, 1992, for review) and also on expressed

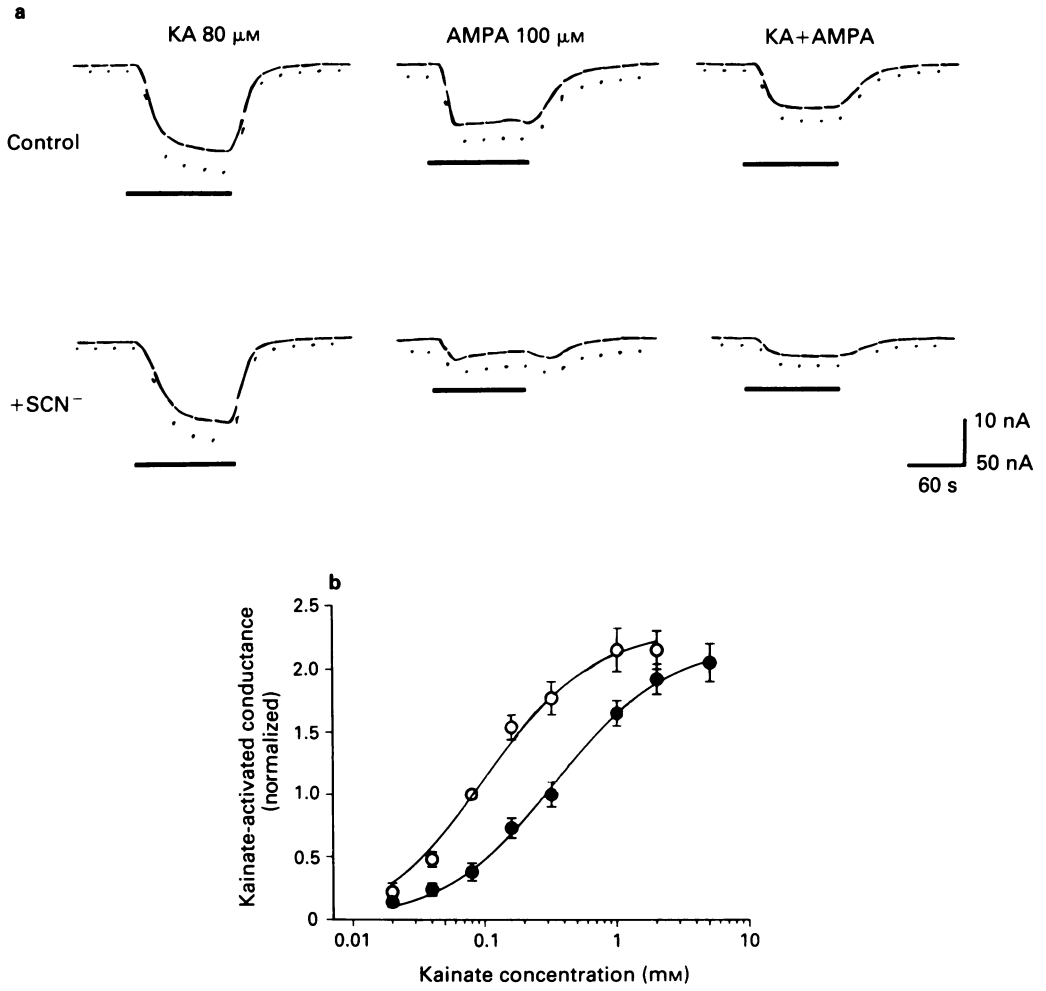



**Figure 5** Antagonism by α-amino-3-hydroxy-5-methyl-4-isoxazolepropionic acid (AMPA) of responses to kainate (KA) are unaffected by $SCN^-$. (a) Sample responses of rat brain mRNA-injected oocytes to bath-applied KA (80 μM), AMPA (100 μM) and combinations of 80 μM KA + 100 μM AMPA in the absence and presence of 2 mM $SCN^-$. Note the smaller amplitude currents induced by AMPA compared to responses evoked by KA. The 10 nA calibration applies only to the AMPA-induced responses. Holding potential − 60 mV. (b) Concentration-response curves for responses to KA in the absence (○) and presence (●) of 100 μM AMPA were fitted with the state function and method described in Figure 2. All values are mean ± s.e.mean and normalized to the response amplitude of 80 μM KA in control Ringer. For control oocytes, the apparent $K_A$ was estimated at 67.6 ± 7 μM and n = 1.4 ± 0.2. In the presence of 100 μM AMPA, $K_A$ = 302.2 ± 17.8 μM and n = 1.1 ± 0.17 ($n$ = 3).

non-NMDA receptors in *Xenopus* oocytes (Verdoorn & Dingledine, 1988), have observed that responses to KA can be inhibited by co-application of either quisqualate or AMPA. These studies have proposed that both AMPA and KA may be acting on the same receptor complexes, since the inhibition of KA responses is of a competitive nature. This conclusion received some support from more recent molecular cloning studies which have demonstrated that particular non-NMDA receptor subunits derived from cDNAs are sensitive to both AMPA and KA (e.g. GluR1-4; although some are relatively insensitive to AMPA, e.g., GluR6; see Gasic & Hollman, 1992, for review). In this study, using rat brain mRNA-injected oocytes, near saturating concentrations of AMPA (100 μM) consistently inhibited the response induced by 80 μm KA by 54 ± 2% ($n$ = 10; Figure 5a). The antagonism was rapid in onset and the recovery was not apparently use-dependent. The KA concentration-response curve was antagonized by AMPA (100 μM) producing a lateral shift in the curve, suggesting a competitive mode of antagonism (Figure 5b). The apparent dissociation constants ($K_A$) for KA, estimated from a two-independent binding site receptor model (Bowie, 1991) applied to the data in the absence and presence of 100 μM AMPA, were calculated as, 67.6 ± 7 μM and 302.2 ± 17.8 μM ($n$ = 3) respectively.

In the presence of $SCN^-$ (2 mM), the KA-induced response was unaffected, but the response to AMPA was reduced by 74 ± 3%; furthermore, AMPA was now more effective in inhibiting the KA response (82 ± 5%; $n$ = 3; Figure 5a). This reduction in the response amplitude to KA plus AMPA in the presence of $SCN^-$ could be mostly accounted for by the $SCN^-$-induced reduction in the AMPA response alone. Thus AMPA may still be equi-effective as an apparent antagonist of responses to KA even in the presence of $SCN^-$. However, in receptor expression studies, we cannot of course discount the possibility that $SCN^-$ may have a selective action on particular non-NMDA receptors expressed from heterogeneous mRNA injected into *Xenopus* oocytes; but, it should be noted, that such a situation also pertains to neuronal studies, which are likely to contain heterogeneous populations of non-NMDA receptors.

### *AMPA-induced responses on cultured cerebellar neurones are inhibited by thiocyanate ions*

Large cultured cerebellar neurones were whole-cell voltage clamped at − 60 mV holding potential and AMPA (10 μM) was rapidly applied from an adjacent four-barrelled flow pipette (Q-tube). The membrane currents induced by AMPA

displayed a characteristic large peak current which rapidly decayed to a much smaller steady-state current (Figure 6a). Application of 2 mM $SCN^-$ via the rapid perfusion pipette did not alter the holding current nor the resting conductance of these neurones. On co-application of $SCN^-$ with AMPA, the peak current responses were slightly reduced by 22 ± 5%, but the steady-state responses were more susceptible to antagonism by $SCN^-$, being reduced by 45 ± 7% ($n = 4$; Figure 6a). To reproduce the responses observed with expressed non-NMDA receptors in *Xenopus* oocytes, the flow rate from the Q-tube was reduced such that the fast peak current to AMPA was not resolved and only the steady-state current remained (Figure 6a). Application of 2 mM $SCN^-$ reduced the steady-state current by 41% and revealed a fast decaying inward peak current in response to 10 μM AMPA. This reduction in the AMPA response by $SCN^-$ was not use-dependent and a comparable level of inhibition could be achieved by co-application of 10 μM AMPA and 2 mM $SCN^-$ without any prior incubation in $SCN^-$-containing Krebs solution.

The type of antagonism exerted by $SCN^-$ on the AMPA-induced responses was assessed from the equilibrium concentration-response curve characteristics. Different concentrations of AMPA were rapidly applied from a U-tube (see Methods) in the absence and presence of $SCN^-$ and the steady-state inward current was measured as a more reliable indicator of agonist efficacy compared to the peak current (Figure 6c). A two-independent binding site receptor model was used to determine the apparent dissociation constant ($K_A$) for AMPA. In control Krebs solution, $K_A$ was 6.91 ± 0.35 μM ($n = 3$) remaining unaffected in 2 mM $SCN^-$ where $K_A$ was estimated as 7.02 ± 0.4 μM. Similar to the dose-response curve for expressed non-NMDA receptors in oocytes, $SCN^-$ depressed the AMPA dose-response curve in cerebellar neurones in a non-competitive manner with little dependence on the agonist concentration.

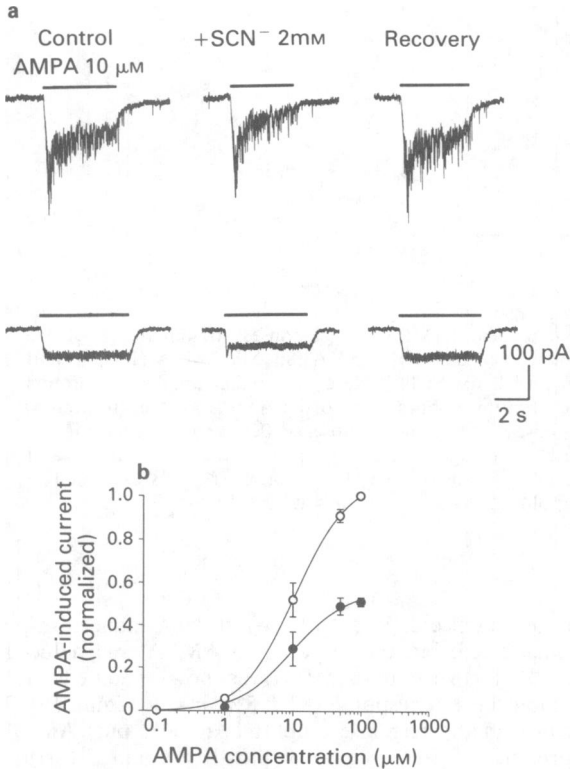



**Figure 6** Responses to α-amino-3-hydroxy-5-methyl-4-isoxazolepropionic acid (AMPA) on cultured cerebellar neurones are antagonised by $SCN^-$. (a) Upper traces, in a large cultured cerebellar neurone voltage clamped at − 60 mV holding potential, rapid-application of 10 μM AMPA in control Krebs from a Q-tube evoked a rapidly decaying current with a steady-state component. $SCN^-$ (2 mM) was also applied from the Q-tube, note the greater reduction in the steady-state current compared to the peak current. Lower traces, by slowing the rate of drug application (10 μM AMPA) the fast peak current was not resolved leaving a predominantly steady-state AMPA-induced current. $SCN^-$ reduced the amplitude of the AMPA current revealing a small initial inward tail current. (b) Concentration-response analysis for responses to AMPA in the absence (○) and presence (●) of 2 mM $SCN^-$. Values are means ± s.e.mean from 5 neurones. The data were fitted with the state function described in Figure 2, providing apparent values of $K_A = 6.91 \pm 0.35$ μM and $n = 1.43 \pm 0.05$ in control Krebs, and $K_A = 7.02 \pm 0.4$ μM and $n = 1.33 \pm 0.13$ in $SCN^-$. Different concentrations of AMPA were delivered from a U-tube in control Krebs or in 2 mM $SCN^-$.

## Discussion

### *SCN ions differentially modulate AMPA binding and AMPA-induced responses*

Thiocyanate ions belong to a group of agents known as chaotropic ions which favour the transfer of apolar groups into the water phase (Hatefi & Hanstein, 1969). Traditionally chaotropic ions have been used as general biochemical reagents to dissociate a variety of particulate proteins and multicomponent enzymes (Sawyer & Puckridge, 1973). In radioligand binding studies of non-NMDA receptors, chaotropic ions increased the specific binding of [$^3$H]-AMPA in rat brain membranes by up to 800% of basal binding at concentrations ranging from 1–100 mM (Honore & Nielsen, 1985; Murphy *et al.*, 1987; Olsen *et al.*, 1987; Honore & Drejer, 1988; Nielsen *et al.*, 1988; Shahi & Baudry, 1992). Honore & Drejer (1988) have proposed that AMPA can bind to a receptor which exists in two interconvertible states of low and high affinity with $SCN^-$ favouring formation of the high affinity state. Interestingly, the binding of other non-NMDA agonists, such as KA, are unaffected by the presence of $SCN^-$ (Murphy *et al.*, 1987; Honore & Nielsen, 1988).

This selective action of $SCN^-$ was also observed in our electrophysiological analyses on non-NMDA receptors expressed in *Xenopus* oocytes, where perhaps surprisingly, $SCN^-$ inhibited responses to AMPA without affecting KA-induced responses. The concentrations of $SCN^-$ used in the present study (2–10 mM) were lower than those routinely employed in binding studies (typically 100 mM); however, even using comparable concentrations of $SCN^-$ in binding studies, [$^3$H]-AMPA binding was still clearly enhanced (Shahi & Baudry, 1992). The AMPA concentration-response curve for expressed non-NMDA receptors was antagonized in a non-competitive manner by $SCN^-$, suggesting that $SCN^-$ is unlikely to be competing for the agonist recognition site. This antagonism is probably not due to an expression artifact of the *Xenopus laevis in vitro* translation system, since a similar mode of antagonism was observed when $SCN^-$ was studied on native non-NMDA receptors in cultured cerebellar neurones.

### *Mechanism of antagonism of AMPA-induced responses by $SCN^-$*

The antagonism of AMPA-induced responses by $SCN^-$ could occur by a variety of mechanisms, including: (i) ion channel block, (ii) enhancing receptor desensitization, (iii) allosteric modulation of ion channel opening by specific agonists, (iv) chelation/inactivation of the agonist in solution.

Non-NMDA agonist-gated ion channels are permeable only to cations and on this basis alone, it appears very unlikely that $SCN^-$ could exert a blockage of the open channel by entering the channel lumen. Moreover, for both expressed receptors in *Xenopus* oocytes and native receptors in cerebellar neurones, the degree of block by $SCN^-$ was only minimally dependent on the agonist concentration, in-

dicating that the blockade is not selective for just the open states of the ion channel.

By enhancing desensitization, $SCN^-$ could conceivably effect a non-competitive depression of the AMPA dose-response curve. At high AMPA concentrations (> 100 μM), where apparent desensitization of the response was maximal, $SCN^-$ antagonized the steady-state AMPA response more than the peak current, thereby decreasing the $I_{ss}/I_p$ ratio. In previous studies on hippocampal neurones, the rapidly desensitizing AMPA-induced current suggests that $I_{ss}$ represents the AMPA response at a greater level of desensitization since it was markedly enhanced by Con-A treatment, whereas $I_p$ was relatively insensitive (Mayer & Vyklicky, 1989). In addition, a study of the single channel currents activated by quisqualate on hippocampal neurones, revealed that $I_p$ may be carried by rapidly-inactivating high conductance channels (single channel conductance ($\gamma$) = 35pS; Tang *et al.*, 1989), whereas the maintained current (approximating to $I_{ss}$) was carried mostly by low conductance channels ($\gamma$ = 8pS; Jahr & Stevens, 1987; Cull-Candy & Usowicz, 1987; Ascher & Nowak, 1988).

In our study, the rapidly-inactivating membrane current evoked by AMPA was clearly not fully resolved due to the inherent limitations associated with rapid drug application onto large cells such as the *Xenopus* oocyte with a cell diameter of approximately 1 mm. Consequently, $I_p$ does not represent AMPA activating a non-NMDA receptor(s) at a minimal level of desensitization and it was therefore not possible to determine absolutely whether $SCN^-$ ions selectively affected $I_{ss}$ or $I_p$. However, using cultured cerebellar neurones, we resolved both the rapidly densensitizing and steady-state currents induced by AMPA, and $SCN^-$ appeared to antagonize the steady-state responses to a greater extent. The apparently greater effect of $SCN^-$ on $I_{ss}$ might suggest that $SCN^-$ is enhancing desensitization perhaps by causing the channel to adopt a low conductance open state conformation (cf. Jahr & Stevens, 1987; Cull-Candy & Usowicz, 1987; Ascher & Nowak, 1988).

One feature of the present results which is apparently inconsistent with this model was the observation that Con-A treatment, which reduces receptor desensitization, did not affect the antagonism of AMPA-induced responses by $SCN^-$. We cannot discount the possibility that $SCN^-$ may enhance desensitization by a Con-A insensitive mechanism. This possibility is supported by the antagonism of KA-induced responses by AMPA where both agonists are thought to bind to the same receptor protein(s). The degree of antagonism was also suggested to be due to the level of desensitization induced by AMPA (Kiskin *et al.*, 1986; Patneau & Mayer, 1991); this interaction was insensitive to Con-A treatment (Mayer & Vyklicky, 1989) and also in our study, to $SCN^-$ ions.

If $SCN^-$ can modulate receptor desensitization, then this might explain the increased binding of [$^3$H]-AMPA by $SCN^-$ and also the reduction in the AMPA-induced membrane current. The nature of radioligand binding studies necessarily requires an incubation of the agonist/antagonist with the receptor preparation for longer periods of time, compared to that routinely used in electrophysiological studies. This suggests that the non-NMDA receptors in binding studies would have entered into one or more desensitized states which is usually associated with high affinity binding sites for ligands. We would then predict that the response amplitude and the $EC_{50}$ for AMPA would both be reduced by $SCN^-$ (cf. Patneau & Mayer, 1990; Barnard & Henley, 1990); however, our data clearly show that the $EC_{50}$ is apparently unaffected.

### *AMPA-induced rebound tail currents*

The rebound tail current observed following washout of AMPA was enhanced in the presence of $SCN^-$. This phenomenon also appeared to be related to receptor desensitization, but in other studies, desensitization of AMPA responses have been clearly demonstrated to occur either in the absence (Kiskin *et al.*, 1986; Trussell *et al.*, 1988; Zorumski & Yang, 1988; Mayer & Vyklicky, 1989; O'Dell & Christensen, 1989), or presence of a rebound current (Vyklicky *et al.*, 1986; Vlachova *et al.*, 1987; Tang *et al.*, 1988; Perouansky & Grantyn, 1989). One explanation for the production of rebound tail currents involves a 'self-block' of the ion channel by the agonist; a concept originally proposed for nicotinic agonists at the frog neuromuscular junction (Adams, 1975). Relief of the block following washout of the agonist might allow re-activation of the receptor by previously 'trapped' agonist molecules resulting in a small tail current. A similar mechanism was also suggested to account for the 'after-current' following the discontinuation of quisqualate application to spinal neurones (Vyklicky *et al.*, 1986; Vlachova *et al.*, 1987). However, the structure of the AMPA molecule with two, presumably dissociated carboxyl groups, suggests that the penetration of AMPA molecules into the cation-selective ion channel would probably be thermodynamically unfavourable. Moreover, a similar rebound current induced by AMPA on expressed non-NMDA receptors in *Xenopus* oocytes, was devoid of any voltage sensitivity (Geoffroy *et al.*, 1991). The rebound current was accounted for by postulating that a decrease in receptor occupancy during washout of the agonist allowed a fast re-activation of the receptor, producing an increase in the membrane current (Geoffroy *et al.*, 1991). The manifestation of the AMPA-induced 'rebound' current in $SCN^-$ containing Ringer solution, may reflect a dissociative effect of $SCN^-$ on non-NMDA receptor protein structure, by binding to a discrete site from the agonist recognition site. The possibility of $SCN^-$ ions allosterically modulating channel gating and possibly also enhancing desensitization, has not yet been discounted.

In the presence of $SCN^-$, the shape of the AMPA dose-response curve, exhibiting a reduced maximum and with no lateral shift, suggests that $SCN^-$ is not chelating or chemically inactivating the agonist molecules (Smart & Constanti, 1982). A recent study by Shahi & Baudry (1992) in hippocampal slices monitored the extracellular excitatory post-synaptic potential (e.p.s.p.). Ionophoresis of $SCN^-$ ions resulted in an enhanced slope to the e.p.s.p. by approximately 25%. This was an unexpected result based on our findings of $SCN^-$ inhibiting non-NMDA receptors. Molecular cloning studies have now revealed a number of different non-NMDA receptor cDNAs (see Gasic & Hollman, 1992) which may have discrete distributions in the CNS and different functional properties (Keinanen *et al.*, 1990; Sommer *et al.*, 1990; Lambolez *et al.*, 1992; Gasic & Hollman, 1992). Therefore, it is possible that various heteromeric combinations of these subunits may be differentially sensitive to $SCN^-$ ions.

### *Discrete binding sites for non-NMDA agonists on the same receptor complex?*

In oocytes injected with rat brain mRNA, the membrane currents evoked by KA and AMPA are thought to be mediated by common receptor complexes (Verdoorn & Dingledine, 1988). This also concurs with the notion of a common binding site for AMPA and KA on some native or expressed non-NMDA receptors (Boulter *et al.*, 1990; Keinanen *et al.*, 1990; Patneau & Mayer, 1991). Patneau & Mayer (1991) proposed that both agonists bind to the same receptor and show mutual competition for the agonist recognition site. For the non-NMDA receptors expressed in our study, discrete binding sites for AMPA and KA is also a possibility, even on the same receptor protein(s), since $SCN^-$ ions selectively antagonized responses to AMPA compared to KA-induced responses. However, expression of non-NMDA receptors in *Xenopus* oocytes from mRNA may yield heterogeneous populations of non-NMDA receptors. Two alternative hypotheses are now possible to explain the effects of $SCN^-$: AMPA and kainate may bind to completely different

receptor populations and $SCN^-$ will bind only to the 'AMPA-sensitive' receptors. This would be compatible with our results of $SCN^-$ selectively inhibiting responses to AMPA, but this concept would not easily explain the competitive shift in the kainate dose-response curve induced by AMPA, nor the extra depression of responses to kainate caused by AMPA in the presence of $SCN^-$; alternatively, there might be a mixture of AMPA/kainate-sensitive receptors and discrete populations of AMPA and kainate-sensitive receptors. Presumably in this scenario, $SCN^-$ will bind to more than one population of receptors. This is a complex situation and the behaviour of the system cannot be easily predicted without constraining assumptions for which, at present, we do not have any experimental justification.

The most parsimonious conclusion that can be drawn from our results is that the non-competitive antagonism produced by $SCN^-$, suggests that this ion does not displace AMPA from the binding site but probably modulates channel gating from a novel allosteric site. Furthermore, as an antagonist in this study, $SCN^-$ has the novel distinction for non-NMDA receptors, of being able to differentiate between AMPA and KA-induced responses.

This work was supported by the MRC, Wellcome Trust and SERC. We are grateful to Mike Webb (Sandoz) for the provision of rat mRNA. We thank our colleagues at The School of Pharmacy for helpful discussions.

## References


ADAMS, P.R. (1975). A study of desensitization using voltage clamp. *Pflügers Arch.*, **360**, 135–144.

ASCHER, P. & NOWAK, L. (1988). Quisqualate and kainate-activated channels in mouse central neurones in culture. *J. Physiol.*, **399**, 227–245.

BARNARD, E.A. & HENLEY, J.M. (1990). The non-NMDA receptors: types, protein structure and molecular biology. *Trends Pharmacol. Sci.*, **11**, 500–507.

BOULTER, J., HOLLMANN, M., O'SHEA-GREENFIELD, A., HARTLEY, M., DENERIS, E., MARON, C. & HEINEMANN, S. (1990). Molecular cloning and functional expression of glutamate receptor subunit genes. *Science*, **249**, 1033–1037.

BOWIE, D. (1991). Functional properties of vertebrate non-NMDA excitatory amino acid receptors expressed in *Xenopus laevis* oocytes. *Ph.D. Thesis, London University.*

BOWIE, D. & SMART, T.G. (1991). Non-NMDA receptors expressed in *Xenopus laevis* oocytes after injection with rat brain mRNA are differentially antagonised by thiocyanate ions. *J. Physiol.*, **434**, 95P.

CHIRGWIN, J.M., PRYZBYLA, A.E., MACDONALD, R.J. & RUTTER, W.J. (1979). Isolation of biologically active ribonucleic acid from sources enriched in ribonuclease. *Biochemistry*, **18**, 5249–5299.

CHRISTENSEN, B.N. & HIDA, E. (1990). Protonation of histidine groups inhibits gating of the quisqualate/kainate channel protein in isolated catfish cone horizontal cells. *Neuron*, **5**, 471–478.

CULL-CANDY, S.G. & USOWICZ, M.M. (1987). Multiple-conductance channels activated by excitatory amino acids in cerebellar neurones. *Nature*, **325**, 525–528.

DUMONT, J.N. (1972). Oogenesis in *Xenopus laevis* (Daudin), 1. Stages of oocyte development in laboratory maintained animals. *J. Morphol.*, **136**, 153–180.

ENOMOTO, R., OGITA, K., HAN, D. & YONEDA, Y. (1992). Differential modulation by divalent cations of [$^3$H]MK-801 binding in brain synaptic membranes. *J. Neurochem.*, **59**, 473–481.

FENWICK, E.M., MARTY, A. & NEHER, E. (1992). A patch-clamp study of bovine chromaffin cells and of their sensitivity to acetylcholine. *J. Physiol.*, **331**, 577–597.

FORSYTHE, I.D., WESTBROOK, G.L. & MAYER, M.L. (1988). Modulation of excitatory synaptic transmission by glycine and zinc in cultures of mouse hippocampal neurons. *J. Neurosci.*, **8**, 3733–3741.

GASIC, G.P. & HOLLMANN, M. (1992). Molecular neurobiology of glutamate receptors. *Annu. Rev. Physiol.*, **54**, 507–536.

GEOFFROY, M., LAMBOLEZ, B., AUDINAT, E., HAMON, B., CREPEL, F., ROSSIER, J. & KADO, R.T. (1991). Reduction of desensitization of a glutamate ionotropic receptor by antagonists. *Mol. Pharmac.*, **39**, 587–591.

GU, Y. & HUANG, L.-Y.M. (1991). Block of kainate receptor channels by $Ca^{2+}$ in isolated trigeminal neurons of rat. *Neuron*, **6**, 777–784.

HATEFI, Y. & HANSTEIN, W.G. (1969). Solubilization of particulate proteins and non-electrolytes by chaotropic agents. *Biochemistry*, **62**, 1129–1136.

HONORE, T. & DREJER, J. (1988). Chaotropic ions affect the conformation of quisqualate receptors in rat cortical membranes. *J. Neurochem.*, **51**, 457–461.

HONORE, T. & NIELSEN, M. (1985). Complex structure of quisqualate-sensitive glutamate receptors in rat cortex. *Neurosci. Lett.*, **54**, 27–32.

HONORE, T., DREJER, J. & NIELSEN, M. (1986). Calcium discriminates two [$^3$H] kainate binding sites with different molecular target sizes in rat cortex. *Neurosci. Lett.*, **65**, 47–52.

JAHR, C.E. & STEVENS, C.F. (1987). Glutamate activates multiple single channel conductances in hippocampal neurons. *Nature*, **325**, 522–525.

JOHNSON, J.W. & ASCHER, P. (1987). Glycine potentiates the NMDA response in cultured mouse brain neurones. *Nature*, **325**, 529–531.

KEINANEN, K., WISDEN, W., SOMMER, B., WERNER, P., HERB, A., VERDOORN, T.A., SAKMANN, B. & SEEBURG, P.H. (1990). A family of AMPA-selective glutamate receptors. *Science*, **249**, 556–560.

KISKIN, N.I., KRISHTAL, O.A., TSYNDRENKO, A.Y. & AKAIKE, N. (1986). Are sulphydryl groups essential for function of the glutamate-operated receptor ionophore complex. *Neurosci. Lett.*, **66**, 305–310.

KRISHTAL, O.A. & PIDOPLICHKO, V.I. (1980). A receptor for protons in the nerve cell membrane. *Neuroscience*, **5**, 2325–2327.

LAMBOLEZ, B., AUDINAT, E., BOCHET, P., CREPEL, F. & ROSSIER, J. (1992). AMPA receptor subunits expressed by single Purkinje cells. *Neuron*, **9**, 247–258.

MAYER, M.L. & VYKLICKY, L. (1989). Concanavalin A selectively reduces desensitization of mammalian neuronal quisqualate receptors. *Proc. Natl. Acad. Sci. U.S.A.*, **86**, 1411–1415.

MAYER, M.L., VYKLICKY, L. & WESTBROOK, G.L. (1989). Modulation of excitatory amino acid receptors by group IIB metal cations in cultured mouse hippocampal neurones. *J. Physiol.*, **415**, 329–350.

MAYER, M.L., WESTBROOK, G.L. & GUTHRIE, P.B. (1984). Voltage dependent block by $Mg^{2+}$ of NMDA responses in spinal cord neurons. *Nature*, **309**, 261–263.

MAYER, M.L., WESTBROOK, G.L. & VYKLICKY, L. (1988). Sites of antagonist action on N-methyl-D-aspartic acid receptors studied using fluctuation analysis and a rapid perfusion technique. *J. Neurophysiol.*, **60**, 645–663.

MCDONALD, J.W. & JOHNSTON, M.V. (1990). Physiological and pathophysiological roles of excitatory amino acids during central nervous system development. *Brain Res. Rev.*, **15**, 41–70.

MONAGHAN, D.T., NGUYEN, L. & COTMAN, C.W. (1986). The distribution of [$^3$H] kainate sites in primate hippocampus is similar to the distribution of both $Ca^{2+}$-sensitive and $Ca^{2+}$-insensitive [$^3$H] kainate binding sites in rat hippocampus. *Neurochem. Res.*, **11**, 1073–1082.

MURPHY, D.E., SNOWHILL, E.W. & WILLIAMS, M. (1987). Characterisation of quisqualate recognition sites in rat brain tissue using DL-[$^3$H]-α-amino-3-hydroxy-5-methyl-4-isoxazolepropionic acid (AMPA) and a filtration assay. *Neurochem. Res.*, **12**, 775–782.

NIELSEN, E.O., CHA, J.-H.J., HONORE, T., PENNEY, J.B. & YOUNG, A.B. (1988). Thiocyanate stabilizes AMPA binding to the quisqualate receptor. *Eur. J. Pharmacol.*, **157**, 197–203.

NOWAK, L., BREGESTOVSKI, P., ASCHER, P., HERBERT, A. & PROCHIANTZ, A. (1984). Magnesium gates glutamate-activated channels in mouse central neurones. *Nature*, **307**, 462–465.

O'DELL, T.J. & CHRISTENSEN, B.N. (1989). Horizontal cells isolated from catfish retina contain two types of excitatory amino acid receptors. *J. Neurophysiol.*, **61**, 1097–1109.

OLSEN, R.W., SZAMRAJ, O. & HOUSER, C.R. (1987). [$^3$H]AMPA binding to glutamate receptor sub-populations in rat brain. *Brain Res.*, **402,** 243–254.

PATNEAU, D.K. & MAYER, M.L. (1990). Structure-activity relationships for amino acid transmitter candidates acting at N-methyl-D-aspartate and quisqualate receptors. *J. Neurosci.*, **10,** 2385–2399.

PATNEAU, D.K. & MAYER, M.L. (1991). Kinetic analysis of interactions between kainate and AMPA: evidence for activation of a single receptor in mouse hippocampal neurons. *Neuron*, **6,** 785–798.

PEROUANSKY, M. & GRANTYN, R. (1989). Separation of quisqualate- and kainate-selective glutamate receptors in cultured neurons from the rat superior colliculus. *J. Neurosci.*, **9,** 70–80.

PETERS, S., KOH, J. & CHOI, D.W. (1987). Zinc selectively blocks the action of N-methyl-D-aspartate on cortical neurons. *Science*, **236,** 589–593.

RANDLE, J.C.R., VERNIER, P., GARRIGUES, A.-M. & BRAULT, E. (1988). Properties of the kainate channel in rat brain mRNA injected Xenopus oocytes: ionic selectivity and blockage. *Mol. Cell. Biochem.*, **80,** 121–132.

RASSENDREN, F.A., LORY, P., PIN, J.P. & NARGEOT, J. (1990). Zinc has opposite effects on NMDA and non-NMDA receptors in Xenopus oocytes. *Neuron*, **4,** 733–740.

SAWYER, W.H. & PUCKERIDGE, J. (1973). The dissociation of proteins by chaotropic salts. *J. Biol. Chem.*, **248,** 8429–8433.

SHAHI, K. & BAUDRY, M. (1992). Increasing binding affinity of agonists to glutamate receptors increases synaptic responses at glutamatergic synapses. *Proc. Natl. Acad. Sci. U.S.A.*, **89,** 6881–6885.

SMART, T.G. (1992). A novel modulatory binding site for zinc on the $GABA_A$ receptor complex in cultured rat neurones. *J. Physiol.*, **447,** 587–625.

SMART, T.G. & CONSTANTI, A. (1982). A novel effect of zinc on the lobster muscle GABA receptor. *Proc. R. Soc. B.*, **215,** 327–341.

SOMMER, B., KEINANEN, K., VERDOORN, T.A., WISDEN, W., BURNASHEV, N., HERB, A., KOHLER, M., TAKAGI, T., SAKMANN, B. & SEEBURG, P.H. (1990). Flip and flop: a cell-specific functional switch in glutamate-operated channels in the CNS. *Science*, **249,** 1580–1585.

TANG, C.M., DICHTER, M. & MORAD, M. (1989). Quisqualate activates a rapidly inactivating high conductance ionic channel in hippocampal neurons. *Science*, **243,** 1474–1477.

TANG, C.M., DICHTER, M. & MORAD, M. (1990). Modulation of the N-methyl-D-aspartate channel by extracellular $H^+$. *Proc. Natl. Acad. Sci. U.S.A.*, **87,** 6445–6449.

THIO, L.L., CLIFFORD, D.B. & ZORUMSKI, C.F. (1991). Characterisation of quisqualate receptor desensitization in cultured rat hippocampal neurons. *J. Neurosci.*, **11,** 3430–3441.

TRAYNELIS, S.F. & CULL-CANDY, S.G. (1990). Proton inhibition of N-methyl-D-aspartate receptors in cerebellar neurons. *Nature*, **345,** 347–350.

TRAYNELIS, S.F. & CULL-CANDY, S.G. (1991). Pharmacological properties and $H^+$ sensitivity of excitatory amino acid channels in rat cerebellar granule neurones. *J. Physiol.*, **433,** 727–763.

TRUSSELL, L.O., THIO, L.L., ZORUMSKI, C.F. & FISCHBACH, G.D. (1988). Rapid desensitization of glutamate receptors in vertebrate central neurons. *Proc. Natl. Acad. Sci. U.S.A.*, **85,** 2834–2838.

UMBACH, J.A. & GUNDERSEN, C.B. (1989). Mercuric ions are potent noncompetitive antagonists of human brain kainate receptors expressed in Xenopus oocytes. *Mol. Pharmacol.*, **36,** 582–588.

VERDOORN, T.A. & DINGLEDINE, R. (1988). Excitatory amino acid receptors expressed in *Xenopus* oocytes: agonist pharmacology. *Mol. Pharmacol.*, **34,** 298–307.

VLACHOVA, V., VYKLICKY, L., VYKLICKY, L.Jr. & VYSKOCIL, F. (1987). The action of excitatory amino acids on chick spinal cord neurons in culture. *J. Physiol.*, **386,** 425–438.

VYKLICKY, L., VLACHOVA, V. & KRUSEK, J. (1990). The effect of external pH changes on responses to excitatory amino acids in mouse hippocampal neurones. *J. Physiol.*, **430,** 497–517.

VYKLICKY, L., VYKLICKY, L.Jr., VYSKOCIL, F., VLACHOVA, V., UJEC, E. & MICHEL, J. (1986). Evidence that excitatory amino acids not only activate the receptor channel complex but also lead to use-dependent block. *Brain Res.*, **363,** 148–151.

WESTBROOK, G.L. & MAYER, M.L. (1987). Micromolar concentrations of $Zn^{2+}$ antagonise NMDA and GABA responses of hippocampal neurons. *Nature*, **328,** 640–643.

ZORUMSKI, C.F. & YANG, J. (1988). AMPA, kainate, and quisqualate activate a common receptor-channel complex on embryonic chick motoneurons. *J. Neurosci.*, **8,** 4277–4286.

*(Received October 13, 1992*
*Revised February 23, 1993*
*Accepted March 1, 1993)*

*Br. J. Pharmacol.* (1993), **109**, 788–792 © Macmillan Press Ltd, 1993

# Inhibition by sumatriptan of central trigeminal neurones only after blood-brain barrier disruption

Holger Kaube, Karen L. Hoskin & [1]Peter J. Goadsby

Department of Neurology, The Prince Henry Hospital, Little Bay Sydney, N.S.W., Australia

**1** The 5-hydroxytryptamine ($5\text{-HT}_1$)-like agonist, sumatriptan, is highly efficient in the relief of migraine headache and its accompanying symptoms.

**2** Experimental evidence has indicated that its site of action may be on the cranial vessels or on the trigeminal innervation of the cranium, or both, since sumatriptan does not pass the blood-brain barrier easily under normal circumstances. It is, however, not clear whether the blood-brain barrier is normal or abnormal during a migraine attack.

**3** In this study, single unit activity and trigeminal somatosensory evoked potentials in central trigeminal neurones were monitored during electrical stimulation of the superior sagittal sinus.

**4** Intravenous administration of sumatriptan ($100\,\mu g\,kg^{-1}$) did not alter trigeminal evoked activity unless the permeability of the blood-brain barrier had been increased by infusion of an hyperosmolar mannitol solution. After blood-brain barrier disruption, sumatriptan decreased the peak-to-peak amplitude of evoked potentials by $40 \pm 6\%$ and the probability of firing of single units by $30 \pm 9\%$. Mannitol infusions alone in control animals caused no changes in evoked potentials or single unit activity.

**5** The data suggest that in normal circumstances sumatriptan does not have sufficient access to trigeminal neurones to alter their function.

**Keywords:** Headache; migraine; 5-HT receptor; sumatriptan, central trigeminal neurones; blood-brain barrier

## Introduction

Migraine is well recognized clinically although its fundamental pathophysiology is unknown. Based on both clinical and experimental data we have proposed a unifying hypothesis integrating both the central nervous system structures, such as the trigeminal nucleus caudalis, and the trigeminal innervation of the meninges and cranial vessels (Goadsby *et al.*, 1991a). The synthesis and clinical trial of the novel 5-hydroxytryptamine ($5\text{-HT}_1$-like) agonist, sumatriptan, has provided both an important addition to clinical practice and a valuable research tool. The site of action of sumatriptan is of particular interest as it may provide a direction for further drug development and an understanding of at least part of the mechanism of migraine.

It has been proposed that the site of action of sumtriptan is at cranial arteries as a highly selective vasoconstrictor (Feniuk *et al.*, 1991), or in the periphery at the trigeminovascular innervation of the cranium (Markowitz *et al.*, 1988). Both hypotheses for a peripheral site of action are consistent with the fact that under normal circumstances sumatriptan cannot penetrate the blood-brain barrier in substantial amounts (Humphrey *et al.*, 1991).

In a series of well conceived experiments it has been shown that whereas intravenous administration of sumatriptan neither effects frontal cortex levels of 5-HT (Sleight *et al.*, 1990) nor pial vessel diameter (Connor *et al.*, 1992), local injection of the drug can alter both 5-HT levels in brain and pial vessel diameter. Since it has been shown that vasodilatation of cranial vessels may not necessarily be a sufficient stimulus to activate trigeminal neurones (Kaube *et al.*, 1992), vasoconstriction may, therefore, not be the only mechanism responsible for the clinical efficacy of the drug in migraine (Goadsby *et al.*, 1991b; Ferrari, 1991). Given that other drugs with similar pharmacological actions that are also useful in migraine, such as dihydroergotamine, have access to central nervous system binding sites (Goadsby & Gundlach, 1991) it is of interest that sumatriptan directly applied by iontophoresis to trigeminal neurones inhibits single unit activity linked to sagittal sinus stimulation in 20% of tested units (Boers, 1989). The prospect of a central locus of action of sumatriptan would then stand as a third alternative to explain its action.

In order to investigate the effects of systemically administered sumatriptan on the central processing of trigeminal noxious stimuli, we combined the electrophysiological model of sagittal sinus stimulation and recording from the dorsolateral cervical spinal cord, that we have previously characterized (Lambert *et al.*, 1988; Goadsby & Zagami, 1991), with hyperosmolar infusions to disrupt the blood-brain barrier. Mannitol was used as an hyperosmolar agent because of its low toxicity and the well-documented time course of its action (Cosolo *et al.*, 1989). As a marker for increased permeability of the blood-brain barrier we chose Evans Blue which can be detected in small quantities by fluorescence microscopy techniques.

## Methods

Eleven female cats weighing $2.7 \pm 0.2$ kg were anaesthetized initially with 1.5% halothane and then α-chloralose (60 mg $kg^{-1}$, i.p.) and prepared for physiological monitoring. The femoral artery and vein were cannulated in order to measure blood pressure and heart rate and provide access for drug administration, respectively. Cardiovascular parameters and pupillary reaction to noxious pinching of the forepaw were used to determine the need for supplementary anaesthesia. The animals were endotracheally intubated, ventilated with 40% oxygen and paralyzed after the surgical procedures with repeated doses of gallamine triethiodide (6 mg $kg^{-1}$, i.v., as required). Body temperature and end-expiratory $CO_2$ were monitored and maintained within physiological limits.

[1] Author for correspondence.

### *Surgery*

After mounting in a stereotactic frame, a circular midline craniotomy (2 cm in diameter) and C1/C2-laminectomy were performed for access to the superior sagittal sinus (SSS) and the recording site in the C2 spinal cord. Possible artefacts from arterial pulsation and respiratory movement were reduced by: bilateral pneumothoraces, suspension of the thoracic spinal processes, clamping of the C1 lateral spinal processes and covering the cervical spinal cord with a layer of agar gel. At the recording site the pia mater was carefully removed to facilitate the insertion of the electrode. The dura mater and falx adjacent to the SSS were dissected over 10 mm and the sinus suspended over bipolar platinum hook electrodes. To prevent dehydration and for electrical insulation against the cortex, a paraffin bath was built with a dam of dental acrylic around the craniotomy and a small polyethylene sheet was inserted under the SSS.

### *Stimulation*

To activate trigeminal primary afferents, the SSS was stimulated with a Grass S88 stimulator driving a stimulus isolation unit (SIU5A; 150 V, 250 μs duration, 0.3 $s^{-1}$). Tungsten-in-glass microelectrodes (tip length/diameter: 50/15 μm, impedance: $<200$ kΩ) were lowered into the dorsolateral spinal cord 4–5 mm caudal to the mid-point of the C2-rootlets between 500 and 1500 mm below the surface with a hydraulic micropositioner (Kopf, Model 650, USA) to record somatosensory evoked potentials and single unit activity.

### *Recording*

Electrical responses were amplified and filtered (NeuroLog, total system gain: 20,000–30,000; bandwidth for field potentials: d.c.-5.5 kHz; for action potentials: 300 Hz–5.5 kHz). For the recording of single unit activity, the signal was first passed through a window discriminator for spike detection while for evoked potentials the amplified signal was directly fed to the analog input of an A/D conversion card (LabMaster, Ohio, U.S.A.) in an IBM-compatible microcomputer (80386/80387 based) and sampled at 20 kHz. Evoked potentials were averaged over 100 repetitive stimulations and linked single unit activity recorded in post-stimulus histograms (sweep length 50 ms) with a custom written programme (Microsoft C) and stored on hard disk. Baseline recordings with 100 averages each were repeated at least three times to ensure that single unit and field potential responses in the spinal cord to SSS stimulation were reproducible over time.

### *Study design*

Animals were randomly assigned to two different experimental interventions. After baseline data had been obtained group one animals (controls, $n = 5$) were given an intravenous infusion with 35 ml $mg^{-1}$ mannitol (12.5%) over 12 min to investigate the effect of increasing the permeability of the blood-brain barrier on electrophysiological responses to trigeminal stimulation in the dorsolateral cervical spinal cord. Responses were recorded during the infusion and after 15, 30, 45 and 60 min. In the second group ($n = 6$), after baseline recordings sumatriptan (Glaxo, Ware UK; 100 μg $kg^{-1}$) was administered intravenously and responses monitored again after 15, 30, 45 and 60 min. The animals were then subjected to the same hyperosmolar infusion and monitoring scheme as group one. Throughout the experiments electrophysiological data, blood pressure and heart rate were pulse code modulated (Vetter, 16 Channel) and stored on video tape to enable later review. After the animals were killed with KCl, 100 responses were elicited to obtain slow potentials that only consisted of the electrical artefact. This component was then subtracted from all previous recordings prior to determining the peak-to-peak amplitudes. Data were compared by the Wilcoxon matched pairs signed ranks test (Siegel, 1956) and assessed for significance at the $P<0.05$ level.

### *Blood-brain barrier integrity*

In preliminary experiments carried out to determine the parameters for the hyperosmolar infusion scheme, animals were injected with 2% Evans Blue (50 mg $kg^{-1}$) followed in some animals by mannitol infusions and perfused with saline and 10% formaldehyde through the thoracic descending aorta. The spinal cords were removed. Spinal cord levels C1 to C3 were sectioned on a cryo-microtome at 50 μm, and inspected under a fluorescent microscope at 365 nm to evaluate the presence of Evans Blue qualitatively as an indicator for an increased permeability of the blood-brain barrier.

## Results

Physiological parameters of the eleven animals included in the analysis were normal (Table 1). The studies with Evans Blue confirmed that the mannitol infusions that were used increased blood-brain barrier permeability in the upper cervical spinal cord. Systemic arterial blood pressure was increased (14 ± 5 mmHg) after the injection of sumatriptan for 5 to 15 min while mannitol infusions also caused a transient elevation of blood pressure (19 ± 3 mmHg) lasting up to 30 min.

### *Electrophysiological data*

Electrical stimulation of the superior sagittal sinus elicited linked electrophysiological responses in the dorsolateral C2 spinal cord. Baseline peak-to-peak amplitudes for trigeminal somatosensory evoked potentials were 438 ± 161 μV in Group 1 animals and 451 ± 188 μV in Group 2. The latencies for the peak of the first component were 9.8 ± 0.4 ms and 9.3 ± 0.4 ms, respectively. The baseline probability of firing for linked single units in the dorsolateral area was 0.44 ± 0.06 with a latency of 6.9 ± 0.6 ms for the fastest component in the post stimulus histogram. Infusions with mannitol alone (group 1) had no effect on the field potentials (3 ± 10%; Figure 1). Sumatriptan alone (group 2) led only to a small transient increase in peak-to-peak amplitudes of trigeminal evoked potentials that was maximal after 30 min. After disruption of the blood-brain barrier with mannitol the evoked responses were significantly reduced by 40 ± 6% ($P = 0.03$, $n = 6$; Figure 2). The effects on single units were similar. Only the combination of intravenous sumatriptan and disruption of the blood-brain barrier led to a significant inhibition (Figure 3) in the probability of firing of single units (30 ± 9%). There was no consistent effect of sumatriptan or mannitol administration alone on the latencies of evoked potentials or single units.

**Table 1** Cardiovascular and blood gas parameters†

| *Blood pressure* (mmHg) | *Heart rate* ($min^{-1}$) | *pH* | $P_{CO_2}$ (mmHg) | $P_{O_2}$ (mmHg) |
|---|---|---|---|---|
| 114 ± 4 | 185 ± 5 | 7.33 ± 0.02 | 35 ± 1 | 212 ± 7‡ |

†$n = 11$
‡On 40–45% inspiratory $O_2$.

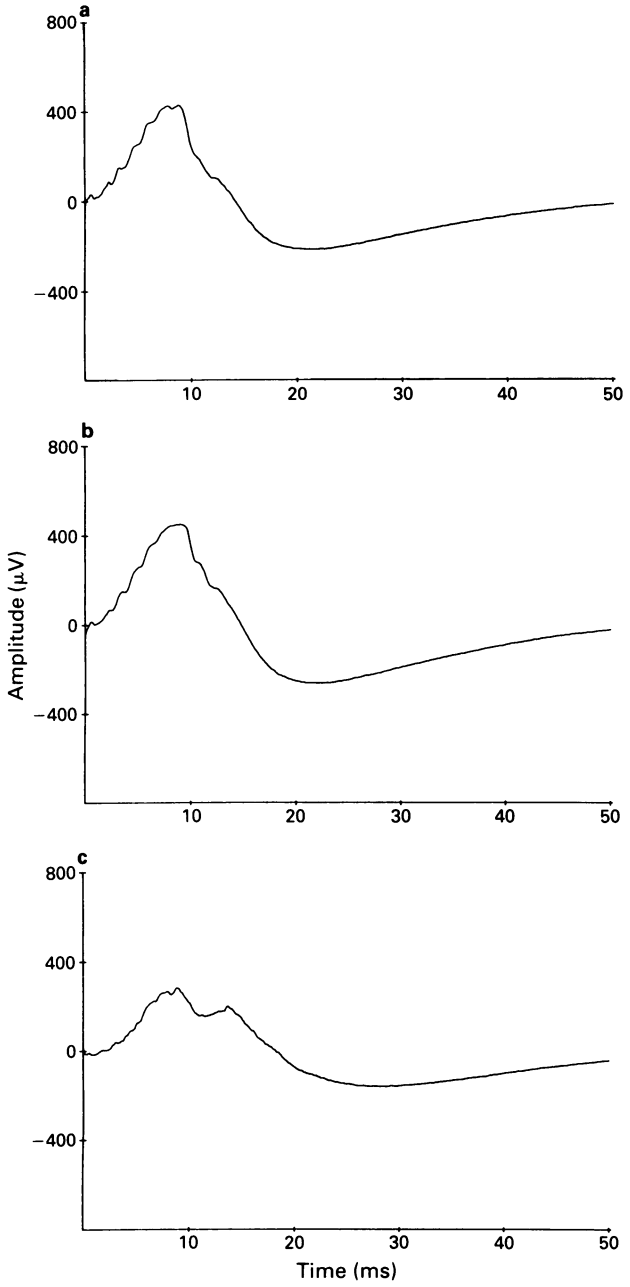



**Figure 1** Trigeminal somatosensory evoked potentials (average of 100 repetitive recordings) after electrical stimulation of the superior sagittal sinus recorded from the dorsolateral C2 spinal cord. (a) Control; (b) recording 30 min after injection of sumatriptan (100 $\mu g\ kg^{-1}$); (c) evoked potentials 30 min after infusion of 12.5% mannitol (90 min after sumatriptan).

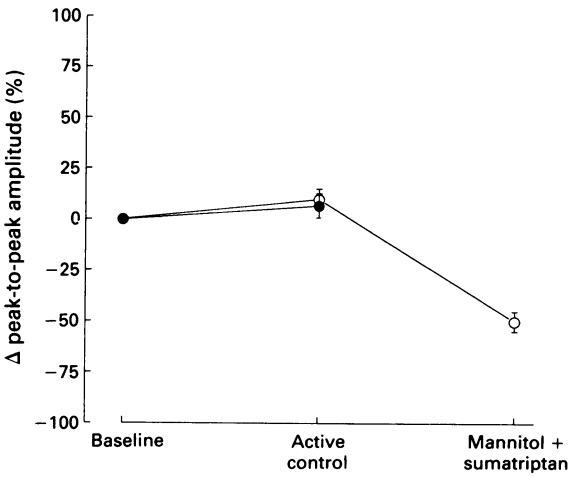



**Figure 2** Group differences of means and standard errors of peak-to-peak amplitudes of trigeminal somato-sensory evoked potentials after superior sagittal sinus stimulation (100 averages) recorded from the C2 spinal cord. Experimental animals (group 2, O) received sumatriptan and mannitol; controls (group 1, ●) received only mannitol infusions.

## Discussion

These data demonstrate that sumatriptan can interact with the transmission of nociceptive input in central trigeminal neurones suggesting inhibitory modulation of synapses at the second order neurone if entry of the drug into the central nervous system has been facilitated. The time interval between the injection of sumatriptan and the hyperosmolar infusion was 60 min and was long enough to allow the temporary changes in blood pressure and field potential amplitudes to recover before the next intervention. Since sumatriptan has a plasma half-life of 2–4 h, enough active compound was still available after 1 h when the mannitol infusion was given.

Essential to the interpretation of these data is that the blood-brain barrier was sufficiently disrupted by the intravenous mannitol infusion. Usually hyperosmolar agents are infused intra-arterially through the carotid arteries to achieve high concentrations in the cerebral circulation (Cosolo *et al.*, 1989). Because of the small calibre and complexity of the arterial supply to the cervical spinal cord and medulla in the cat selective cannulation of spinal arteries to guarantee high arterial mannitol concentrations is impractical. In addition we wished to avoid manipulations of the spinal blood supply to ensure spinal cord viability. In preliminary experiments increasing arterial perfusion pressure or cranial venous pressure rendered the recording site more unstable and led to loss of the recorded cell. Although the total mannitol concentrations in the vascular bed of the target tissue obtained by intravenous infusion are lower than can be expected from arterial infusions, the increased uptake of Evans Blue in the spinal tissue indicates an increased permeability of the blood-brain barrier in the experimental animals as opposed to the controls. It is also possible that the high fluid load during the infusions of 30 ml $kg^{-1}$ over a short period of time may have contributed to the impairment of the blood-brain barrier while a further facilitating factor may have been some superficial neural injury to spinal cord resulting from the removal of the pia at the recording site. All of these considerations apply equally to the control and treated groups and are, therefore, unlikely to be the reason for the results as described.

As the inhibition of the electrophysiological responses only occurred after the administration of both sumatriptan and mannitol, it is most likely that the disruption of the blood-brain barrier is pivotal in facilitating the inhibitory effect of sumatriptan. The decrease in firing after mannitol infusion could have been caused by physico-mechanical changes in the neural tissue induced by the blood pressure changes or the increased intravascular volume resulting in the loss of the monitored single units. This could not explain why this effect would only occur in animals that had been pretreated with sumatriptan. The recording with long tipped, low impedance tungsten-in-glass microelectrodes enabled us to record field potentials and single unit activity together. However, the low spatial discrimination of such electrodes often leads to the recruitment of more than one single unit action potential. In the case of firing clusters our analysis software did not allow us to distinguish between cell body and axonal action potentials. It was also not possible to perform a cluster analysis of

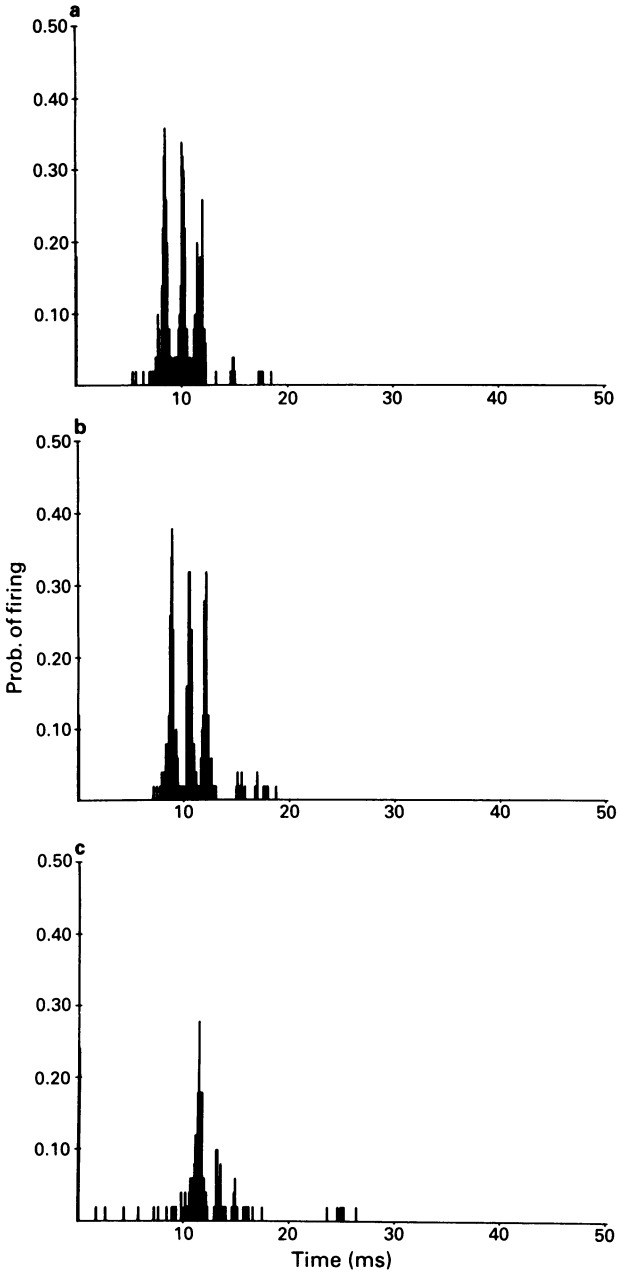



**Figure 3** Poststimulus histograms of single unit activity (average of 100 repetitive recordings) after electrical stimulation of the superior sagittal sinus recorded from the dorsolateral C2 spinal cord. (a) Control recording; (b) recording 30 min after injection of sumatriptan, 100 $\mu g\,kg^{-1}$; (c) single unit activity 30 min after infusion of 12.5% mannitol (90 min after sumatriptan).

multiple single unit firing to identify which or how many units stopped firing after the pharmacological intervention. However, it was a consistent finding that the total probability of firing computed for the whole post-stimulus interval was markedly decreased only after the administration of sumatriptan and mannitol.

Data in the literature support the view that under normal circumstances there is a minimal entry of sumtriptan into the brain. Ten minutes after an intravenous dose of 1 $mg\,kg^{-1}$ of [$^{14}$C]-sumatriptan in the rat only some 0.05% of the dose could be located in the brain (Humphrey *et al.*, 1990). In a study in rat it has been shown that intravenous injection of sumatriptan did not alter brain production of 5-HT while a local injection, that would bypass the blood-brain barrier, reduced brain 5-HT levels (Sleight *et al.*, 1990). Furthermore, sumatriptan has no effect on isolated pial vessels unless it is injected directly around those vessels when it acts as a vasoconstrictor, again suggesting that the blood-brain barrier must be passed for a significant action to be seen (Connor *et al.*, 1992). The data reported here extend this concept more directly into the brain regions likely to be involved in migraine. Neither the frontal cortex nor pial vessels are thought to play a role in the pathogenesis of the disorder nor are they thought to be affected during resolution of an attack. Our data represent a clear demonstration of an effect of sumatriptan in the trigeminal nucleus, after blood-brain barrier disruption.

It was not possible to distinguish in these studies whether the observed modulation of the central trigeminal pathway was based on a direct effect of sumatriptan on inhibitory 5-$HT_1$-like receptors at second order synapses or mediated through descending 5-hydroxytryptaminergic antinociceptive pathways from supraspinal centres but it was certainly not peripheral. Since supramaximal stimulation of afferent C-fibres in the superior sagittal sinus was used in the studies, peripheral transduction mechanisms were bypassed and it is, therefore, very unlikely that the vasoconstrictive properties of sumatriptan on cranial vessels (Feniuk *et al.*, 1991), its inhibitory effect on the release of calcitonin gene-related peptide from trigeminal nerve terminals (Goadsby & Edvinsson, 1993) or its blockade of neurogenic inflammation (Moskowitz & Buzzi, 1991) could have accounted for the results observed. Such peripheral effects would also not depend on the presence of hyperosmolar infusions. It is not known whether the integrity of the blood-brain barrier is impaired during migraine attacks although it is important to note that drowsiness or sedation are recognized as albeit less common side effects of parenteral sumatriptan administration indicating a possible central site of action.

These data are certainly consistent with a peripheral action of sumatriptan on the as yet unproven assumption that the blood-brain barrier is normal in migraine and suggest a further target for future anti-migraine drugs. Future clinical research with better imaging techniques, radiolabelled drugs and tracers will reveal more about the role of supraspinal and spinal structures in the pathophysiology of migraine. These data suggest that the status of the blood-brain barrier in migraine must be studied if the action and site of action of antimigraine compounds is to be understood since these drugs have significant actions in the central nervous system if access to the brain is possible.

These experiments were supported by the National Health and Medical Research Grant and by grants from Warren and Cheryl Anderson, The J.A. Perini Family Trust, The Basser Trust, the Australian Brain Foundation and Glaxo Group Research, England. The authors thank Dr Patrick Humphrey for helpful discussion, Dr Geoffrey Lambert for advice concerning the electrophysiological techniques and Mr Mark Hellier for his excellent technical assistance. H.K. is the recipient of the International Headache Society Research Grant 1992 and is supported by Glaxo GmbH, Hamburg, Germany. P.J.G. is a Wellcome Senior Research Fellow.

## References


BOERS, P.M. (1989). The central projections of craniovascular nerves: modulation by physiological and pharmacological means. *Bachelor of Medical Science Thesis*, University of New South Wales, Sydney, Australia.

CONNORS, H.E., STUBBS, C.M., FENIUK, W. & HUMPHREY, P.P.A. (1992). Effect of sumatriptan, a selective 5-HT1-like receptor agonist, on pial vessel diameter in anaesthetised cats. *J. Cereb. Blood Flow Metab.*, **12,** 514–519.

COSOLO, W.C., MARTINELLO, P., LOUIS, W.J. & CHRISTOPHIDIS, N. (1989). Blood-brain barrier disruption using mannitol: time course and electron microscopy studies. *Am. J. Physiol.*, **256,** R443–R447.

FENIUK, W., HUMPHREY, P.P.A., PERREN, M.J., CONNOR, H.E. & WHALLEY, E.T. (1991). Rationale for the use of 5-HT1-like agonists in the treatment of migraine. *J. Neurol.*, **238,** S57–S61.

FERRARI, M.D. (1991). Treatment of migraine attacks with sumatriptan. *New Eng. J. Med.*, **325,** 316–321.

GOADSBY, P.J. & EDVINSSON, L. (1993). The trigeminovascular system and migraine: studies characterising cerebrovascular and neuropeptide changes seen in man and cat. *Ann. Neurol.*, **33,** (in press).

GOADSBY, P.J. & GUNDLACH, A.L. (1991). Localization of [$^3$H]-dihydroergotamine binding sites in the cat central nervous system: relevance to migraine. *Ann. Neurol.*, **29,** 91–94.

GOADSBY, P.J. & ZAGAMI, A.S. (1991). Stimulation of the superior sagittal sinus increases metabolic activity and blood flow in certain regions of the brainstem and upper cervical spinal cord of the cat. *Brain*, **114,** 1001–1011.

GOADSBY, P.J., ZAGAMI, A.S. & LAMBERT, G.A. (1991a). Neural processing of craniovascular pain: a synthesis of the central structures involved in migraine. *Headache*, **31,** 365–371.

GOADSBY, P.J., ZAGAMI, A.S., DONNAN, G.A., SYMINGTON, G., ANTHONY, M., BLADIN, P.F. & LANCE, J.W. (1991b). A double blind placebo controlled crossover study of sumatriptan in the treatment of acute migraine attacks. *Lancet*, **ii,** 782–783.

HUMPHREY, P.P.A., FENIUK, W., MARRIOTT, A.S., TANNER, R.J.N., JACKSON, M.R. & TUCKER, M.L. (1991). Preclinical studies on the anti-migraine drug, sumatriptan. *Eur. Neurol.*, **31,** 282–290.

HUMPHREY, P.P.A., FENIUK, W., PERREN, M.J., BERESFORD, I.J.M., SKINGLE, M. & WHALLEY, E.T. (1990). Serotonin and migraine. *Ann. New York Acad. Sci.*, **600,** 587–598.

KAUBE, H., HOSKIN, K.L. & GOADSBY, P.J. (1992). Activation of the trigeminovascular system by mechanical distension of the superior sagittal sinus in the cat. *Cephalalgia*, **12,** 133–136.

LAMBERT, G.A., GOADSBY, P.J., ZAGAMI, A.S. & DUCKWORTH, J.W. (1988). Comparative effects of stimulation of the trigeminal ganglion and the superior sagittal sinus in cerebral blood flow and evoked potentials in the cat. *Brain Res.*, **453,** 143–149.

MARKOWITZ, S., SAITO, K. & MOSKOWITZ, M.A. (1988). Neurogenically mediated plasma extravasation in dura mater: effect of ergot alkaloids. A possible mechanism of action in vascular headache. *Cephalalgia*, **8,** 83–91.

MOSKOWITZ, M.A. & BUZZI, M.G. (1991). Neuroeffector functions of sensory fibres: implications for headache mechanisms and drug actions. *J. Neurol.*, **238,** S18–S22.

SIEGEL, S. (1956). *Non-parametric Statistics for the Behavioural Sciences*. Kogakusha, Tokyo: McGraw-Hill.

SLEIGHT, A.J., CERVENKA, A. & PEROUTKA, S.J. (1990). In vivo effects of sumatriptan (GR 43175) on extracellular levels of 5-HT in the guinea pig. *Neuropharmacol.*, **29,** 511–513.


*(Received November 23, 1992*
*Revised February 16, 1993*
*Accepted March 3, 1993)*

*Br. J. Pharmacol.* (1993), **109**, 793–801 © Macmillan Press Ltd, 1993

# Pharmacological characterization of muscarinic receptor-activated cation channels in guinea-pig ileum

Shan Chen, [1]Ryuji Inoue & Yushi Ito

Department of Pharmacology, Faculty of Medicine, Kyushu University, Fukuoka 812, Japan

**1** The pharmacological properties of cationic currents activated by acetylcholine (ACh) ($I_{cat}$) in guinea-pig ileal smooth muscle cells were investigated, with conventional single patch electrode or nystatin-perforated whole-cell recording. Cs-aspartate was used as the internal solution to allow selective measurement of $I_{cat}$.

**2** Well-known K channel blockers, tetraethylammonium (TEA), 4-aminopyridine (4-AP), procaine and quinine as well as a Ca releasing agent, caffeine, all produced concentration-dependent inhibition of $I_{cat}$ with rapid onset (time constant $\sim$100 ms), when applied externally. The recovery from the inhibition on washout also occurred rapidly in the order of 100 ms except in the case of quinine. Approximate values of the half inhibitory concentrations ($IC_{50}$) were 10 mM for TEA and caffeine, 1–5 mM for 4-AP and procaine, and 1 $\mu$M for quinine. The mode of inhibition was voltage-dependent, i.e., depolarization relieved the inhibition with no change in reversal potential.

**3** Externally applied diphenylamine-2-carboxylate (DPC) derivatives, DCDPC and flufenamic acid, produced potent inhibition of $I_{cat}$ at micromolar concentrations ($IC_{50}$s were $<30$ $\mu$M for DCDPC and 32 $\mu$M for flufenamic acid). The onset of and recovery from inhibition occurred slowly and the degree of inhibition depended on the membrane potential only weakly, without any discernible change in the reversal potential.

**4** All of the above-tested drugs exhibited comparable inhibitory actions on the voltage-dependent Ca current in the concentration ranges effective at inhibiting $I_{cat}$. However, amongst them, quinine and flufenamic acid seemed to have several-fold better selectivity for the $I_{cat}$ channel than for the voltage-dependent Ca channel.

**5** Internally dialysed GTPγS (100 $\mu$M) induced inward cationic currents. The effects of drugs on these currents were similar to their effects on the $I_{cat}$ current.

**6** These results clearly indicate that many drugs used as pharmacological tools in smooth muscle research exert considerable nonspecific effects on various types of channels. The mechanism of inhibition and the relevance to use of these drugs as blockers for the $I_{cat}$ channel are discussed.

**Keywords:** Acetylcholine (ACh); nonselective cation channels; blockers; smooth muscle

## Introduction

In mammalian intestinal smooth muscles muscarinic receptor activation leads to at least two major consequences, production of inositol 1,4,5 trisphosphate and membrane depolarization due to increased $Na^+$ permeability. The latter can be ascribed to the opening of cation ($I_{cat}$), channels, which serve as the main route for $Na^+$ as well as $Ca^{2+}$ influx. Although some details of the biophysical nature of the $I_{cat}$ channel have already been published and the involvement of a pertussis toxin-sensitive guanosine 5'-triphosphate (GTP)-binding protein in its activation has been suggested (e.g., Inoue, 1991b), very little effort has been made to characterize the pharmacological properties of this channel, and thus information about selective blockers is lacking.

Recently, it was reported that diphenylamine-2-carboxylate (DPC) derivatives such as 3',5-dichloro-DPC (DCDPC) and flufenamic acid are very potent and relatively selective blockers for $Ca^{2+}$-activated cation channels in colonic epithelial cells (Gögelein & Capek, 1990). Although the $Ca^{2+}$-activated cation channels appear to be very different from the $I_{cat}$ channels in mode of activation and voltage-dependence, some essential properties are similar. For example, single channel conductances of both types of channels range between 20–30 pS and the kinetics are slow in both cases (Inoue *et al.*, 1987; Swandulla & Partridge, 1990; Vogalis *et al.*, 1990) as compared with voltage-dependent Na,K and Ca channels. In addition, some of the $Ca^{2+}$-activated cation channels are reported to be voltage-sensitive and the open probability is increased as the membrane is depolarized (Sturgess *et al.*, 1987; Ehara *et al.*, 1988), as is observed in the case of $I_{cat}$ channel (Inoue & Isenberg, 1990b), and the $I_{cat}$ channel is also sensitive to changes in the intracellular $Ca^{2+}$ concentration (Inoue & Isenberg, 1990c). These observations imply the presence of considerable structural homology between the $Ca^{2+}$-activated cation channels and the $I_{cat}$ channel. It is therefore of great interest to examine how the above-mentioned blockers for the $Ca^{2+}$-activated cation channels act on the $I_{cat}$ channel.

In the present study, we have investigated the effects of DPC-derivatives as well as well-known K channel blockers and some other agents which are frequently used as pharmacological tools in electrophysiological studies on excitable membranes. As a result of this work, we found that quinine and DPC derivatives such as DCDPC and flufenamic acid are very potent inhibitors of $I_{cat}$, and unfavourable nonspecific actions on other types of channels are also evident.

## Methods

### *Cell dispersion and electrical recordings*

The procedures used for dispersion of single ileal smooth muscle cells, the system for recording the membrane currents and the method of rapid application of drugs were the same as described previously (Inoue, 1991a; Inoue & Kuriyama, 1993). Briefly, guinea-pigs of either sex weighing 600–1000 g were stunned and exanguinated. Thin sheets of longitudinal

[1] Author for correspondence.

smooth muscle (1–2 mm × 5–10 mm) were gently stripped off by hand from the terminal part of ileum, then incubated in Ca-free solution containing 0.5–1.0 mg ml$^{-1}$ actinase (Kaken, Tokyo, Japan) and 1 mg ml$^{-1}$ collagenase (type I, Sigma) at 35°C for 15–20 min. The digested sheets of ileal muscle were cut into pieces and triturated in Ca free solution until yielding a sufficient number of cells. Currents were recorded with a commercial patch clamp amplifier (Axopatch 1D, Axon Instruments, Burlingame, CA, U.S.A.) in conjunction with an A/D, D/A converter (Labmaster TL-1 DMA, Axon Instruments), which was run under the control of an IBM compatible personal computer (AMSC-ATC, Alps Electronic, Japan) with 'pClamp v.5.5' programmes (Axon Instruments). All experiments were carried out at room temperature.

### *Nystatin-perforated whole-cell recording*

Patch pipettes (3–5 Mohm) were made from 1.5 mm pyrex glass capillaries. Fresh nystatin stock solution was made every day by dissolving the powder (Sigma) in dimethylsulphoxide (DMSO) to give a concentration of 50 mg ml$^{-1}$. This was ultrasonicated for about 15 min. The stock solution was further diluted 200–500 times with the internal solution (Cs-aspartate complemented with 1 mM EGTA) and ultrasonicated again for 15 min just before use. Whole-cell recording was achieved with a pipette which was first momentarily dipped in a nystatin-free internal solution and then backfilled with one complemented with nystatin. The timing of the dipping was a critical step to determine the success of forming a 'giga-seal' and subsequent chemical perforation. The other procedures of whole-cell recording were the same as described above.

### *Solutions*

The bathing and pipette solutions were the following (mM): modified Krebs solution: $Na^+$ 140, $K^+$ 5, $Mg^{2+}$ 1.2, $Ca^{2+}$ 2, $Cl^-$ 151.4, HEPES/Tris 10 (pH 7.35–7.4); Cs aspartate internal solution: $Cs^+$ 140, $Mg^{2+}$ 2, $Cl^-$ 24, aspartate$^-$ 120, EGTA10/4~5$Ca^{2+}$ and HEPES 10 (titrated to 7.2–7.25 with Tris base). The Ca-free solution was made by simply omitting $Ca^{2+}$.

### *Chemicals*

Flufenamic acid and niflumic acid were purchased from Wako (Osaka, Japan). DPC and DCDPC were generous gifts from Dr R. Greger (University of Freiburg). DPC derivates were freshly dissolved into DMSO and then diluted 1000–10000 times by the bathing solution so as to give a final DMSO concentration of no more than 0.1% for any experiment; 0.1% DMSO did not show any effects on its own. The other chemicals used in the present study were purchased

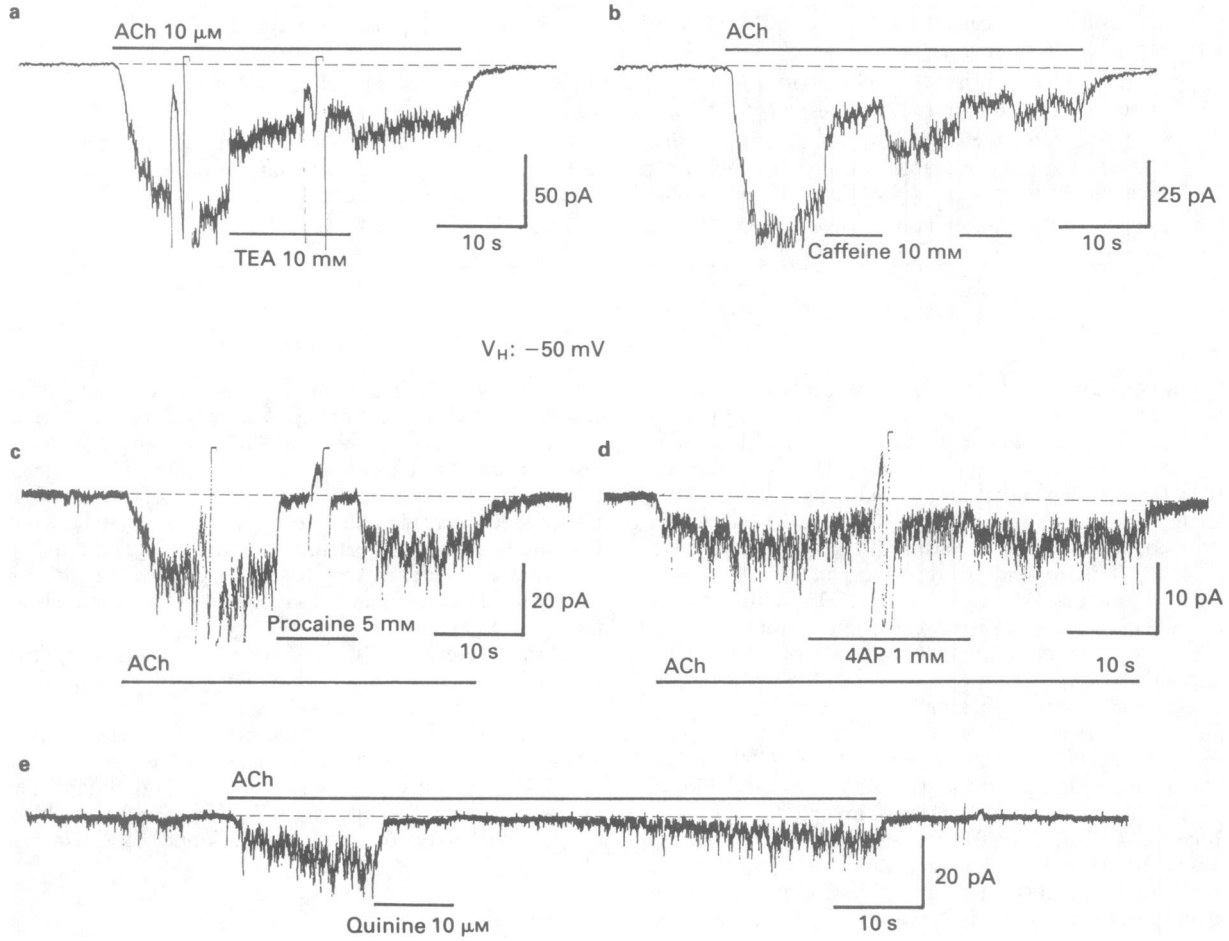



**Figure 1** Rapid reduction in the acetylcholine (ACh)-evoked inward currents by K channel blockers and caffeine. Recordings were made with conventional patch electrode whole-cell recording, in which the cell membrane was disrupted by negative pressure after a 'giga-seal' was formed. Throughout the following figures this recording configuration was used, unless otherwise stated (i.e. Figures 4 and 5). The bath and pipette contained modified Krebs solution and Cs-aspartate internal solution, respectively. In the continued presence of 10 μM ACh (indicated by long bars), clamped cells were swiftly moved from the control bathing solution to one containing either tetraethylammonium (TEA) 10 mM (a), caffeine 10 mM (b), procaine 5 mM (c), 4-aminopyridine (4-AP) 1 mM (d) or quinine 10 μM (e) (indicated by short bars). The onset and offset of solution changes are approximate. The speed and efficacy of the rapid solution change are demonstrated in Figure 2. The membrane was held at − 50 mV. Vertical deflections represent slow ramps as shown in Figure 7.

from the following: TEA, indomethacin and nystatin (Sigma), 4-AP (Nacalai, Kyoto, Japan), procaine and caffeine (Wako, Osaka, Japan), quinine and quinidine (Tokyo Kasei, Tokyo). Changes in pH due to tested drugs were minimized by adjusting the pH of stock solutions with addition of Tris base or HEPES as appropriate before use.

## Results

### *The effect of K channel blockers on* $I_{cat}$

As $I_{cat}$ is very sensitive to changes in the intracellular $Ca^{2+}$ concentration ($[Ca^{2+}]_i$), a mixture of EGTA and $Ca^{2+}$ was included in the internal solution to clamp the $[Ca^{2+}]_i$ to 100–200 nM (see Methods) to minimize any secondary changes in the current amplitude and kinetics due to the altered $[Ca^{2+}]_i$ (Inoue & Isenberg, 1990c). This strategy appeared to work satisfactorily since the potentiating effect of voltage-dependent $Ca^{2+}$ influx on the $I_{cat}$ (Inoue & Isenberg, 1990c) was only brief and marginal. Furthermore, membrane depolarizations to − 30 mV–0 mV, which generate a long-lasting Ca inward current and subsequent contraction of smooth muscle cells when $[Ca^{2+}]_i$ is buffered weakly, did not contract cells examined over 1 min. Under these conditions, however, the inward currents evoked by 10 μM ACh showed a decay to a varying extent, with a time constant of 30–60 s, and underwent a strong rundown on repeated application. Therefore, we first assessed the effects of blockers on $I_{cat}$ with a fast solution exchange device based not on sequential but on a single administration of ACh as performed previously (Inoue, 1991a).

Figure 1 demonstrates the time course of several well-established blockers on $I_{cat}$. K channel blockers such as TEA, 4-AP and procaine all caused clear inhibition. The inhibitions seemed to occur rapidly within about 50–100 ms, the speed of which compares to that of solution exchange as demonstrated by Na removal in Figure 2. The inhibitory action of these agents was reversible because the degree of inhibition evaluated at onset and recovery from blockade was in close agreement. For example, with TEA 10 mM, the percentage inhibition was 37% and 35% respectively at onset and recovery (Figure 1a). Caffeine, a $Ca^{2+}$ releaser from the sarcoplasmic reticulum (SR), also produced inhibition of $I_{cat}$ at a concentration of 10 mM, the nature of which appeared similar to that produced by the K channel blockers (also see below). Figure 3a summarizes the results pooled from many cells with various concentrations of these blockers. The half inhibitory concentrations ($IC_{50}$s) were between 2 and 5 mM for 4-AP, 1 and 5 mM for procaine, and about 10 mM for TEA and caffeine. It should be noted that all the $IC_{50}$ values

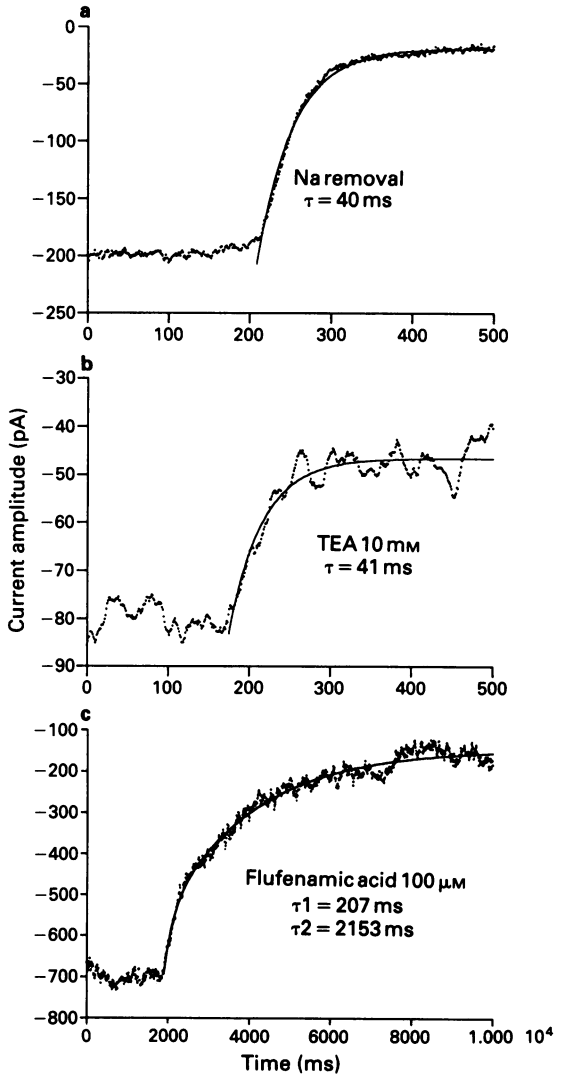



**Figure 2** Efficiency of the rapid solution changing system evaluated by Na removal and the onset of tetraethylammonium (TEA) or flufenamic acid induced inhibition of the acetylcholine (ACh)-evoked inward current. (a) At a holding potential of − 50 mV, $Na^+$ was removed from the bathing solution, by switching from normal Krebs solution to $Na^+$-free Krebs solution (Tris replacement) in the continued presence of 10 μM ACh. The time constant of decrease in the $I_{cat}$ amplitude is 40 ms in this experiment (on average, 39 ± 9 ms, $n = 4$). On reintroduction of $Na^+$, the current recovered with the time constant of 42 ± 5 ms ($n = 4$). The slower time constant of the solution change as compared to a similar method applied to rat and bullfrog sensory neurons (ca. 10 ms; Bean, 1990) may be due to the spindle shape of ileal smooth muscle cells. (b and c) The time course of inhibition of the ACh-evoked current by 10 mM TEA (b) or 100 μM flufenamic acid (c). Note that the time constant for TEA-induced inhibition (41 ms) compares to that for Na removal, while that for flufenamic acid is considerably slower (fast and slow time constants are 207 and 2153 ms, respectively). The fast time constant for flufenamic acid was not always observed.

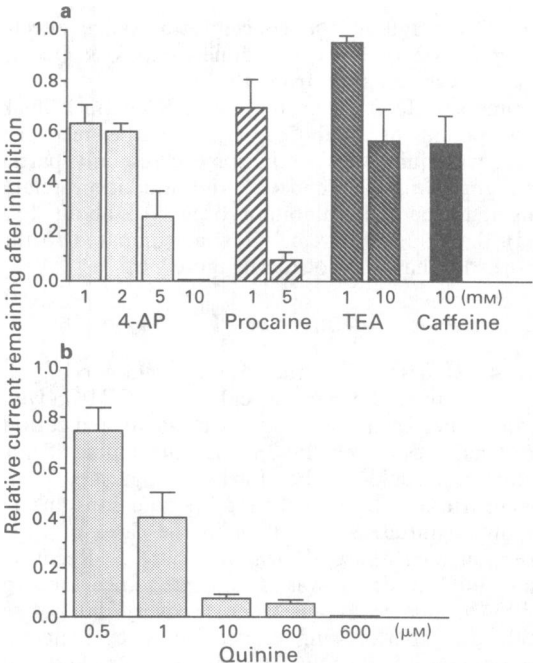



**Figure 3** Concentration-dependence of the inhibition of the acetylcholine (ACh)-evoked inward current by K channel blockers and caffeine. The results obtained from experiments similar to those shown in Figure 1 are summarized. Each column represents mean (and s.e.) calculated from 5–10 experiments by measuring the fraction of the ACh (10 μM)-evoked current which remained in the presence of the tested drug. In the case of quinine (b), the best fit using the equation in Figure 5 gave values of 0.84 μM and 1.94 for K and n, respectively.

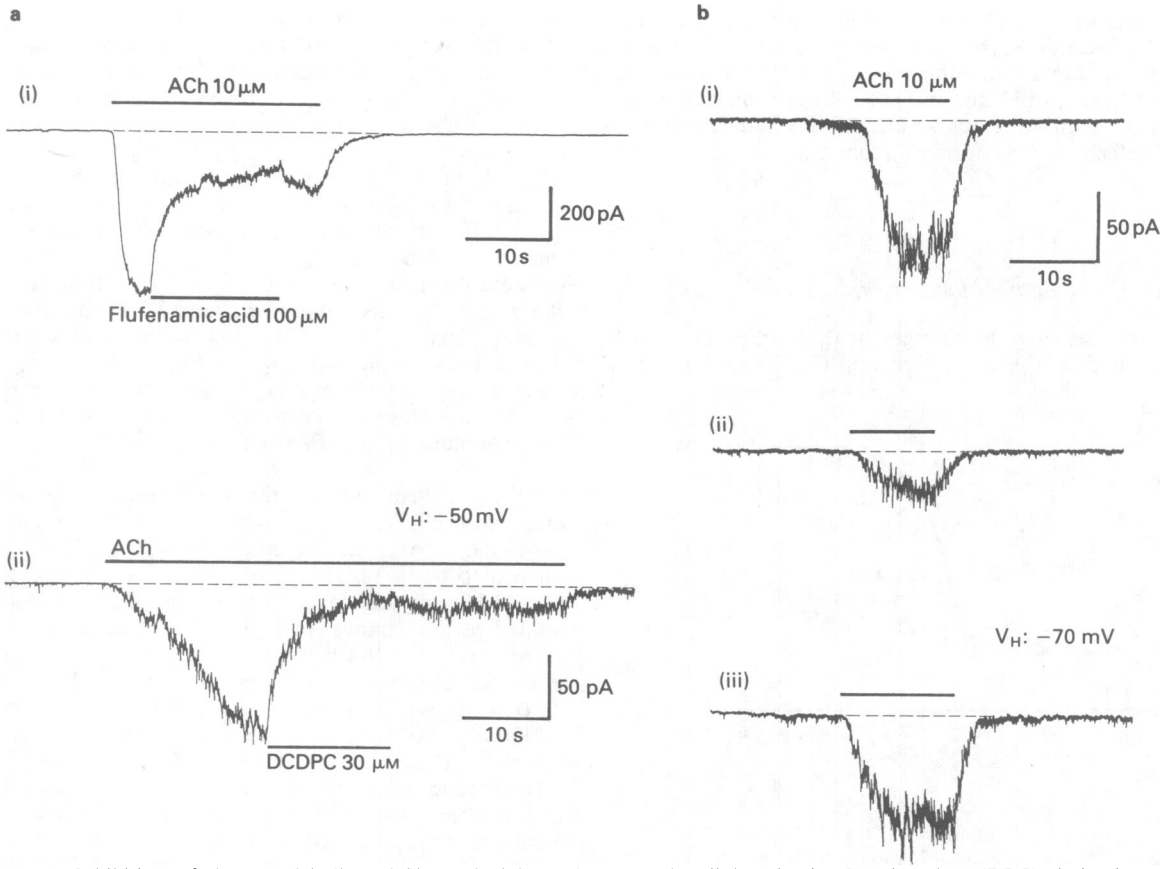



**Figure 4** Inhibition of the acetylcholine (ACh)-evoked inward current by diphenylamine-2-carboxylate (DPC) derivatives. (a) Currents were recorded with conventional whole-cell recording. ACh and DPC derivatives were applied at bars with a fast solution change. Conditions used here are the same as in Figure 1. (b) Currents recorded with the nystatin-perforated whole-cell recording before (b(i)), after 10 min pretreatment with (b(ii)) and 10 min after washout of (b(iii)) 50 μM flufenamic acid. Flufenamic acid was added in the bath with ordinary bath superfusion, while 10 μM ACh was rapidly applied at bars with a fast solution exchange device described in Figure 1 in the continued presence of flufenamic acid. The holding potential was − 70 mV. ACh 10 μM was added during the bars.

obtained here fall in the concentration-range effective for blocking certain types of K channels (Cook & Quast, 1990) or causing $Ca^{2+}$ release from the SR.

Quinine is different from the above K channel blockers. It is very potent at inhibiting $I_{cat}$, but the recovery after washout was quite slow or in some cases only partial over 30 s (Figure 1e). The concentration-inhibition relationship reveals that the half inhibition occurs at about 1 μM (see legend); the value is extremely low as compared to those for the other K channel blockers (Figure 3b).

### *DPC derivatives potently block* $I_{cat}$

Figure 4a shows actual traces of inhibition of $I_{cat}$ by two DPC derivatives, flufenamic acid and DCDPC, which are reported to be potent blockers of $Ca^{2+}$-activated cation channels (Gögelein & Capek, 1990). The time course of inhibition was slow and could not be clearly distinguished from those of desensitization. It seemed that the time constant was one order of magnitude slower than in the cases of K channel blockers such as those shown in Figure 2. Recovery after washing out the drugs was incomplete, since the degree of inhibition evaluated at onset and recovery did not seem to coincide. For this reason, we decided to evaluate the inhibitory potency of the DPC derivatives on repeated application of ACh employing the nystatin-perforated whole-cell recording method (Horn & Marty, 1988; also see Methods).

Figure 4b shows actual current traces before, during and after the application of 50 μM flufenamic acid with nystatin-perforated whole-cell recording. At a holding potential as negative as − 70 mV with $Cs^+$ in the pipete solution, contamination of $I_{cat}$ with another possible inward current, e.g. a $Ca^{2+}$-activated $Cl^-$ current, seemed negligible because the reversal potential of the inward current evoked by 10 μM ACh did not shift significantly on halving the extracellular $Cl^-$ concentration (8.0 ± 5.4 mV for normal Krebs ($n = 11$) vs. 8.6 ± 2.9 mV for 75 mM Cl Krebs ($n = 4$)). Under these conditions, time-dependent reduction in the $I_{cat}$ amplitude was no more than 20% over 30 min on repeated applications of 10 μM ACh with an interval of 5–10 min (also see Figure 1 in Inoue & Kuriyama, 1992), otherwise the data were discarded. This greatly reduced errors of overestimating the effects of blockers, which may arise from rundown. As shown in Figure 4b (ii), administration of 50 μM flufenamic acid for 10 min resulted in reduction in the $I_{cat}$ current by 70%. This inhibitory effect persisted over a few minutes after the washout of flufenamic acid, and was evident when the drug was administered for several minutes and then washed out just before the application of ACh. The latter observation excludes the involvement of open channel blockade mechanism reported for e.g., MK801 which is known as a potent and selective blocker of NMDA-type cation channels (Huetter & Bean, 1988). Figure 5 summarizes the concentration-dependent inhibition caused by various DPC derivatives. The $IC_{50}$s are smaller than 30 μM for DCDPC but larger than 100 μM for DPC and niflumic acid (Figure 5a). The concentration-inhibition curve for flufenamic acid gives an $IC_{50}$ of 32 μM and a cooperativity number of one (open circles in Figure 5b).

### *Effect of blockers of the* $I_{cat}$ *channel on the voltage-dependent Ca channel*

The selectivity of these agents was investigated in a study of their effects on the voltage-dependent Ca channels. Figure 6a illustrates the current-voltage relationship in the presence and

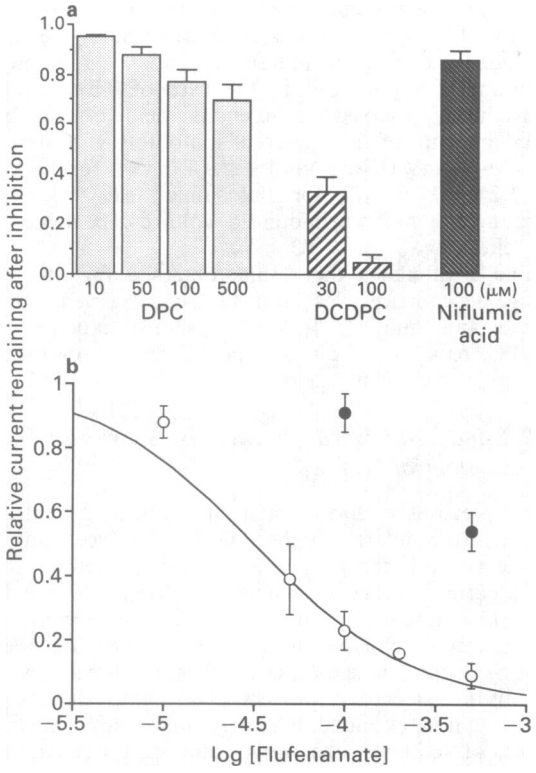



**Figure 5** Concentration-dependence of the inhibition of the acetylcholine (ACh)-evoked inward currents by diphenylamine-2-carboxylate (DPC) derivatives. The results of nystatin-perforated whole-cell recording seen in Figure 4b are summarized. The degree of inhibition was calculated as the ratio of $I_{cat}$ current amplitude in the presence of a drug tested versus that in control response. Control responses were obtained before and after application of DPC derivatives, in order to check the rundown of currents (see text), and the first response was used as the reference. (a) Each column represents mean (+s.d.) calculated from 3–6 cells, respectively. (b) Concentration-inhibition curve of the ACh (10 μM)-evoked inward current for flufenamic acid (○). The curve was fitted by an empirical Hill type equation $(1/(1 + ([\text{flufenamic acid}]/K)^n)$ where [flufenamic acid], K and n denote the concentration of flufenamic acid, the concentration of flufenamic acid to produce 50% inhibition and the cooperatively number. The best fit of the data points (○) gave K = 32 μM and n = 1; (●) represent the fraction of voltage-dependent Ca currents remaining in the presence of flufenamic acid. The currents were measured either with voltage-ramps (see Figure 6a) or by depolarizing pulses. Data points were obtained from 3–7 cells.

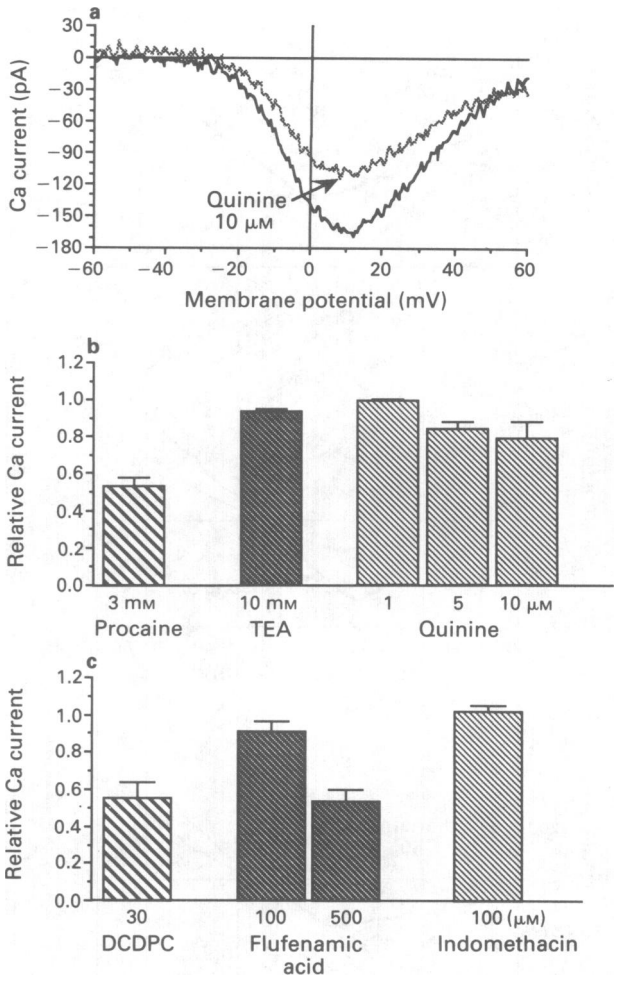



**Figure 6** Inhibition of voltage-dependent Ca channels by various drugs. The bath contained modified Krebs solution and the pipette Cs-aspartate solution in which only 10 mM EGTA, instead of EGTA/Ca mixture, and 2 mM ATP were added. (a) An 800 ms voltage ramp (− 120 to 80 mV) was applied at a rate of 0.25 $V^{-1}$ to activate voltage-dependent Ca currents. Leak currents due to depolarization were obtained in the presence of 5 μM nicardipine and subtracted. The currents were plotted against membrane potential as shown in Figure 7. (b and c) The fraction of Ca current remaining in the presence of the drugs named in the figure.

absence of 10 μM quinine, evaluated by a 800 ms ramp pulse. The presence of quinine resulted in reduction of the voltage-dependent Ca current, the extent of which was virtually voltage-independent. As summarized in Figure 6b, quinine reduced the voltage-dependent Ca current by no more than 20% at a concentration of 10 μM, which inhibited $I_{cat}$ by more than 90% (Figure 3b). In contrast, 3 mM procaine produced inhibition of the voltage-dependent Ca current and $I_{cat}$ to a similar extent.

With DPC derivatives, 30 μM DCDPC, which is the most potent at inhibiting $I_{cat}$, also caused a comparable inhibition of the voltage-dependent Ca current, whereas 100 μM flufenamic acid, which produces ca. 80% reduction in $I_{cat}$, affected the voltage-dependent Ca current only slightly (Figure 6c and filled circles in Figure 5b).

These results indicate that quinine and flufenamic acid are the preferred blockers among the above-tested drugs against $I_{cat}$ channel with regard to selectivity on the voltage-dependent Ca channels. The ratio of the inhibitory effect on $I_{cat}$ versus that on the voltage-dependent Ca current is 4.5 and 7.9 for 10 μM quinine and 100 μM flufenamic acid respectively, while this value is near to 1.0 in the case of 30 μM DCDPC (1.47).

### *Influence of blockers on the ionic selectivity and voltage-dependence of the $I_{cat}$ current*

The mechanisms underlying the inhibitory actions of the above-mentioned agents on $I_{cat}$ may be complicated, e.g., the onset and recovery time course seem to be different among different agents as shown in Figure 2. In order to get further insight, we compared the voltage-dependence and ionic selectivity of the $I_{cat}$ current before and after the applications of blockers with ramp command voltages. This approach is practical because only one ramp instead of a set of step pulses allows not only measurement of the reversal potential but a more complete delineation of the voltage-dependence of the $I_{cat}$ current. As illustrated in Figure 7a (the uppermost trace), the membrane was first held at − 120 mV for 250 ms, to set the $I_{cat}$ current in a steady state (time constant of relaxation at this potential is 40–50 ms, Inoue & Isenberg, 1990b), and then depolarized by a ramp at a rate of 0.1 $V\,s^{-1}$. The net current corresponding to this voltage change in the absence of ACh was nearly ohmic (the middle pale trace), but changed to an inverted bell-shaped curve in the presence of ACh (the bottom thick trace). The current component sensitive to ACh was then defined as a difference of net currents in the presence and absence of ACh (i.e., the

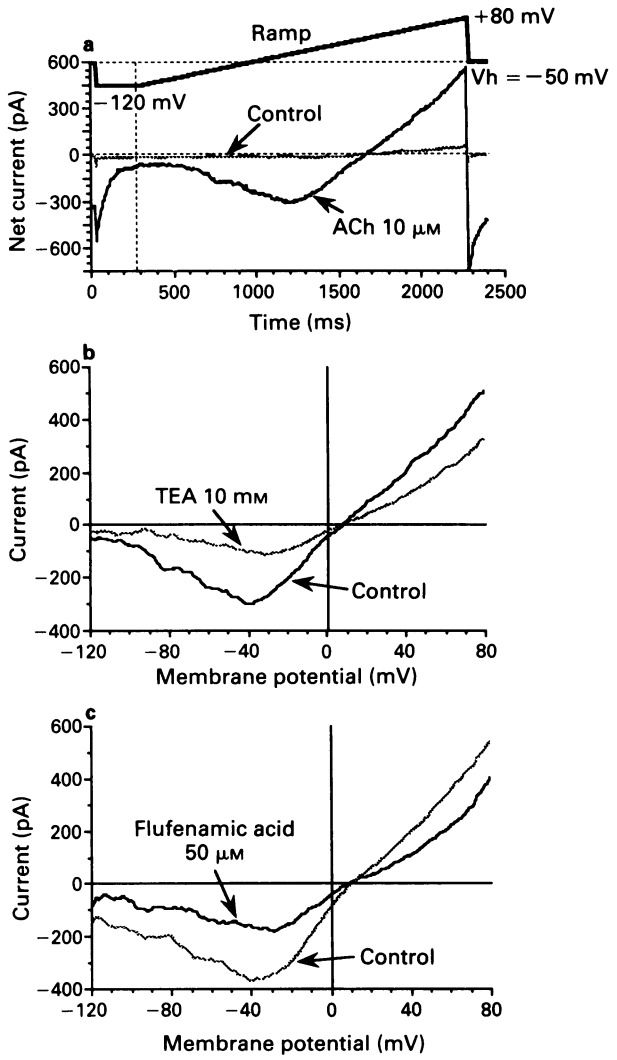



**Figure 7** Changes in the current-voltage relationships of the acetylcholine (ACh)-evoked inward current by addition of tetraethylammonium (TEA) or flufenamic acid. The bath and pipette conditions were the same as in Figure 1. (a) The voltage ramp protocol employed. Three traces represent a voltage change (uppermost bold line), corresponding currents in the absence (middle pale) and the presence (bottom thick) of 10 μM ACh, respectively. In order to block the voltage-dependent Ca current, 5 μM nicardipine was present. (b and c) The difference currents (bottom trace − middle trace in a) were converted into current-voltage curves.

bottom trace − the middle trace). Figure 7b and c plot the ACh-sensitive currents obtained in this way against membrane potential. The validity of this method of assessing the voltage dependency was verified by the close agreement of Boltzmann parameters obtained by the two different voltage protocols under the same ionic conditions: the half maximum activation potential ($V_h$) and the slope factor (k) were $-47.9 \pm 4.9$ mV and $-18.0 \pm 3.7$ mV for the above ramp protocol ($n = 10$) and $-45.9 \pm 4.6$ mV and $-21.4 \pm 2.1$ mV for the multiple step pulse protocol, respectively (see Figure 8 of this paper and Table 1 in Inoue, 1991a).

Both TEA 10 mM and flufenamic acid 50 μM flattened the current-voltage relationship for $I_{cat}$ but the reversal potential was unaffected (Figure 7b and c). As summarized in Table 1, no significant shift of reversal potential was observed in the presence of any blocker listed. This suggests that the blockers do not change the ionic selectivity of the $I_{cat}$ channel.

The steady state activation curves calculated from the current-voltage relationships were shifted to the right in the presence of TEA, while little shift was observed in the presence of flufenamic acid: the shift of $V_h$ value ($\Delta V_h$) was only a few mV for flufenamic acid but amounted to 12 mV for TEA (Figure 8a(ii) and a(i)). Furthermore, the degree of inhibition at a given membrane potential is reduced as the membrane is depolarized in the case of TEA, while only small relief is observed for flufenamic acid (Figure 8b(i) and b(ii)). The ratio of the degree of inhibition at + 80 mV over that at − 80 mV ($I_{80}/I_{-80}$) is $1.9 \pm 0.4$ ($n = 4$) for TEA 10 mM and $1.2 \pm 0.2$ ($n = 3$) for flufenamic acid 50 μM, clearly indicating the more pronounced voltage-dependence of the TEA effect.

Table 1 tabulates the results obtained for other drugs. Voltage-dependence was also clearly observed for 4-AP, caffeine and quinine. In one available experiment with DCDPC, only weak voltage-dependence was observed as in the case of flufenamic acid.

### *GTPγS-induced inward currents also show a similar pharmacological profile*

It was previously reported that in guinea-pig ileal smooth muscle intracellularly applied GTPγS induces an inward cationic current, the properties of which resemble those of the $I_{cat}$ current (Inoue & Isenberg, 1990a; Komori & Bolton, 1990). This curent is thought to be induced through persistent activation of a pertussis toxin-sensitive G-protein that might be coupled to the $I_{cat}$ channel rather directly, where the association-dissociation process of ACh to the muscarinic receptor can be excluded. We therefore tested whether or not the sties of actions of the above-mentioned drugs are located downstream of the receptor, by observing their effects on the GTPγS-induced inward current. After the start of internal dialysis with 100 μM GTPγS, noisy inward currents were observed and reached a level ranging from − 10 to − 75 pA ($-35 \pm 21$ pA, $n = 10$) within 10–20 min. Usually, these currents were maintained for 30–60 min and declined slowly. As shown in Figure 9, addition of 5 mM procaine, 10 μM quinine or 30 μM DCDPC in the bath suppressed the noisy inward current almost completely, while 10 mM TEA and 10 mM caffeine (data not shown) reduced the current to about the half of the original amplitude. After washout of the drugs, recovery from the inhibition occurred in several minutes with quinine and DCDPC. Quinidine (10 μM), which is a stereoisomer of and equipotent with quinine, also markedly diminished the GTPγS-induced inward current. Other classes of K channel blockers such as charybdotoxin and glibenclamide showed no discernible effects on the GTPγS-induced currents.

The inhibitory potencies and time courses of the drugs tested are consistent with those described for the $I_{cat}$ current. This supports the hypothesis that the drugs act somewhere downstream of the receptor, most likely at the level of the $I_{cat}$ channel protein.

## Discussion

The main findings of the present study are: (1) many agents used as pharmacological tools in smooth muscle research including TEA, 4-AP, procaine, quinine and caffeine are all able to inhibit the $I_{cat}$ channel at concentrations in normal use, but micromolar quinine might be useful to block selectively the $I_{cat}$ channel. (2) Potent blockers for the $Ca^{2+}$-activated cation channel, e.g. DPC derivatives, are also effective at inhibiting the $I_{cat}$ channel at micromolar concentrations. The observed effects are likely to be actions on the $I_{cat}$ current itself, since any indirect effects of these agents were minimized with internal dialysis with Cs aspartate and clamping $[Ca^{2+}]_i$ with a $Ca^{2+}$/EGTA mixture. The mode of inhibition of the various agents appears to differ in time course and voltage-dependence and will be discussed below. Such differences apparently divide the agents into two groups, fast (K channel blockers and caffeine) and slow blockers (DPC derivatives).

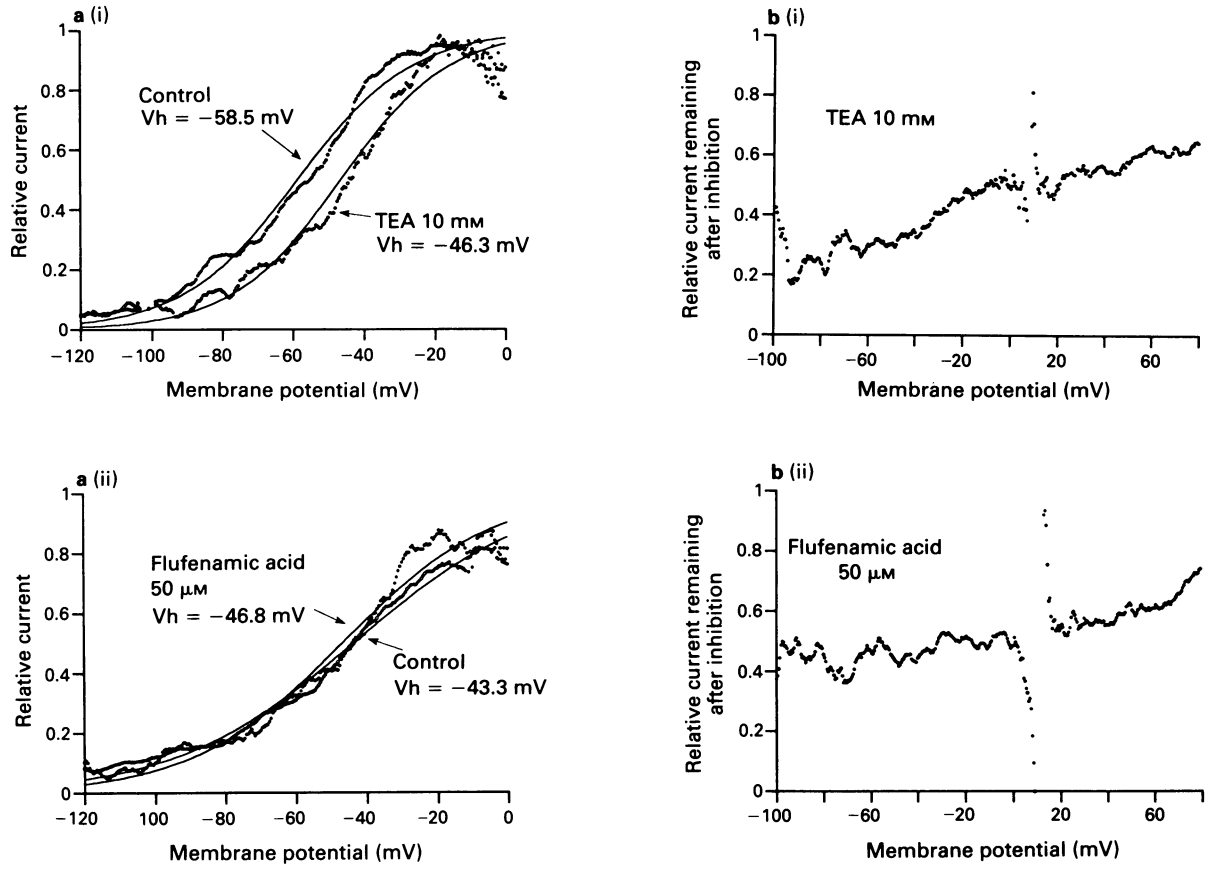



**Figure 8** Steady state activation curve and voltage-dependence of the acetylcholine (ACh)-evoked inward current in the presence of either tetraethylammonium (TEA) or flufenamic acid. (a) Examples of the steady state activation curve of $I_{cat}$ evaluated from Figure 7b and c. The chord conductance, the ratio of the $I_{cat}$ amplitude over the driving force (the membrane potential − the reversal potential), was calculated at a given membrane potential and then normalized to its maximum. At membrane potentials positive to 0 mV, which are near to the reversal potential, serious scatter in calculated values were observed due to the small current amplitudes and driving forces, thus such data were not included in the evaluation. Smooth sigmoid curves represent theoretical ones drawn from using parameters of the best fit according to the Boltzmann equation $1/(1 + \exp((Vm-Vh)/k))$, where Vm, Vh and k denote the membrane potential, the half-maximum activation potential and the slope factor, respectively. (b) Changes in the degree of inhibition by TEA 10 mM (i) or flufenamic acid 50 μM (ii) as a function of the membrane potential.

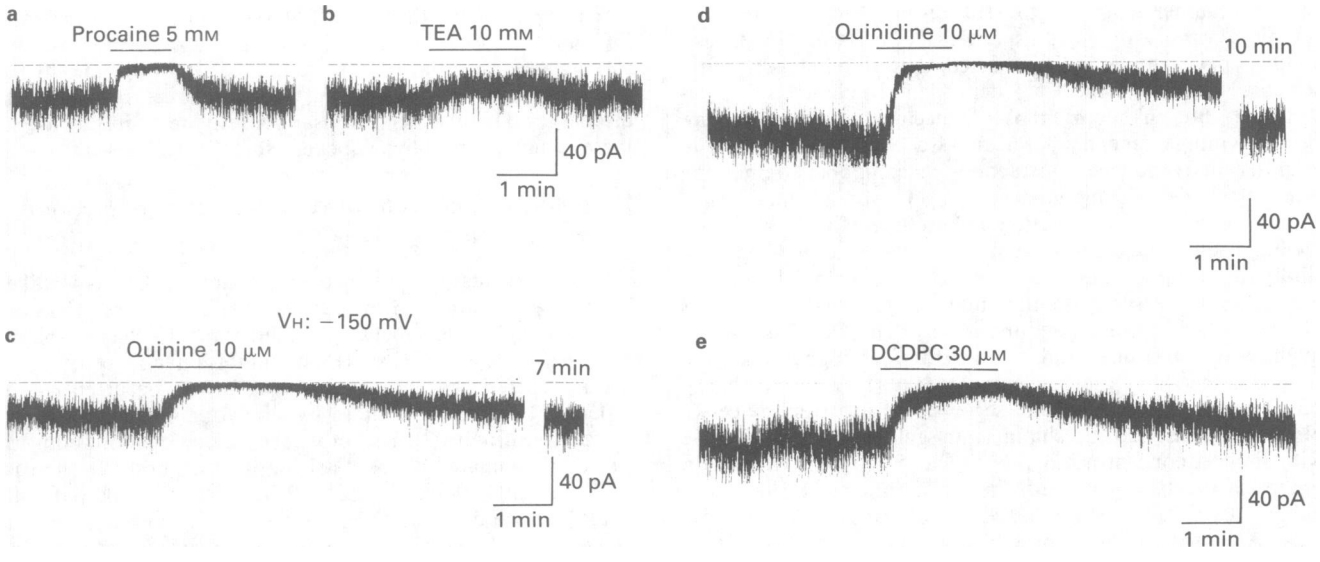



**Figure 9** Effects of various drugs on the GTPγS-induced inward current. The same conditions as in Figure 1 were used except that 100 μM GTPγS was included in the pipette. At a holding potential of − 50 mV, various drugs were superfused into the bath at a rate of 0.07–0.08 ml $s^{-1}$ (the chamber volume is 0.2 ml).

**Table 1** Comparison of the reversal potential, voltage-dependence of the inhibitory effect ($I_{80}/I_{-80}$) and shift in the half-maximum activation potential (Δ Vh) in the presence of various drugs

| | *Erev* (mV) | $I_{80}/I_{-80}$ | Δ *Vh* (mV) |
|---|---|---|---|
| Control | 8.0 ± 5.4 (11) | NA | NA |
| TEA (10 mM) | 6.8 ± 1.6 (4) | 1.9 ± 0.4 (4) | 14.6 ± 2.7 (3) |
| Caffeine (10 mM) | 5.2 ± 1.7 (3) | 1.9 ± 0.5 (3) | 20.7 |
| 4-AP (1 mM) | 10.9 ± 1.6 (4) | 3.1 ± 0.7 (4) | 13.9 ± 2.2 (3) |
| Quinine (1 μM) | 9.8 ± 1.4 (2) | 2.2 ± 0.3 (3) | 10.7 ± 2.9 (2) |
| Flufenamic acid (50 μM) | 6.1 ± 5.6 (3) | 1.2 ± 0.2 (3) | 4.0 ± 2.3 (3) |
| DCDPC (30 μM) | 5.7 | 1.1 | 0.5 |

The numbers in parentheses represent the number of experiments. For the definition of $I_{80}/I_{-80}$ see the text. Control indicates the modified Krebs solution without drugs. NA indicates no available data. For abbreviations, see text.

### *K channel blockers and caffeine as nonspecific blockers*

As generally documented in the literature, TEA in millimolar concentration is able to block several distinct classes of K channels including $Ca^{2+}$-dependent K channels, the delayed rectifier K channel, and the ATP-sensitive K channel (Cook & Quast, 1990). Amongst them, a large conductance K channel (designated as the maxi-K channel) is the most susceptible to TEA applied both externally and internally, the $IC_{50}$ for the external TEA being as low as 0.3 mM in various smooth muscles. Millimolar concentrations of 4-AP are also reported to block the delayed rectifier (e.g. Beech & Bolton, 1990) as well as fast inactivating voltage-dependent K currents (A-like currents; Okabe *et al.*, 1987; Beech & Bolton, 1989; Imaizumi *et al.*, 1990; Smirnov & Aaronson, 1992). Procaine (1–10 mM), together with other local anaesthetics, blocks not only a broad range of voltage-dependent channels (Na and K channels, Cook & Quast, 1990; Ca channels, the present work) but also the $Ca^{2+}$ release process from the internal stores of smooth muscles (Itoh *et al.*, 1981). Caffeine (5–20 μM) is frequently used as an experiment tool to mobilize $Ca^{2+}$ into the cytosol from the SR (Iino, 1989), but also inhibited the $I_{cat}$ channel ($IC_{50}$ is c.a. 10 mM) not due to its $Ca^{2+}$ releasing action since the $[Ca^{2+}]_i$ was clamped in the range of 100–200 nM in the present experiments. These observations clearly indicate that the effective concentration ranges of K channel blockers and caffeine considerably overlap those which inhibit the $I_{cat}$ channel, and thus emphasize the need of special care for designing and interpreting experiments with the aid of such pharmacological agents.

Quinine seems to be one of the most desirable blockers of the $I_{cat}$ channel from the present results, but the literature reveals a variety of its nonspecific actions (Cook & Quast, 1990). For example, it is reported that quinine is a fairly selective blocker of the $Ca^{2+}$-dependent K channels ($IC_{50}$ is $> 10$ μM) but in submillimolar concentrations it also suppresses voltage-dependent Na and Ca channels. Further, in angiotensin II-induced contractions, a component remaining after blockade of voltage-dependent Ca or K channels is found to be further inhibited by quinine (Cook & Quast, 1990). These observations seem to exclude largely the possibilty of using quinine as a selective $I_{cat}$ channel blocker. However, it deserves attention that the reported $IC_{50}$ values against other currents are not lower than 5 μM, most frequently 10 μM–1 mM, and are several fold higher than the $IC_{50}$ obtained for the $I_{cat}$ current (1 μM). This raises the possibility that quinine can serve as a relatively selective blocker for the cation channels in guinea-pig ileal muscle with limited concentration ranges (ca. 5–10 μM). In fact, in preliminary experiments with the intracellular recording technique, 10 μM quinine abolished depolarizations evoked by 1 μM ACh with only modest changes in spike discharge.

### *The effects of DPC derivatives on the $I_{cat}$ channel*

The inhibitory potencies of DPC derivatives on the $I_{cat}$ channel accord approximately with those observed against $Ca^{2+}$-activated cation channels by use of single channel recordings (Gögelein & Pfannmüller, 1989; Gögelein *et al.*, 1990; Siemer & Gögelein, 1992). The sequence of inhibitory efficacy is DCDPC > flufenamic acid >> DPC ⩾ niflumic acid and the $IC_{50}$ for DCDPC or flufenamic acid is about 10 μM, although the tested drugs were administered from the outer side of the cell membrane whilst most of data for the $Ca^{2+}$-activated cation channels were obtained in the inside-out patch configuration. In rat exocrine pancreatic cells, DPC derivatives block Cl conductances with comparable efficacy to $Ca^{2+}$-activated cation channels (Gögelein & Pfannmüller, 1989). However, conflicting evidence has been provided on the inability of 10 μM DCDPC to affect Cl channels in distal colonic epithelial cells of the same species (Gögelein & Capek, 1990). In our experiments, we did not observe the effects of these drugs on the Cl conductance in the guinea-pig ileum, since such a conductance could hardly be detected under the experimental conditions employed. However, the voltage-dependent Ca current showed almost the same sensitivity to 30 μM DCDPC as did the $I_{cat}$ current. Furthermore, 100 μM flufenamic, DPC and DCDPC exerted inhibitory effects on the transient outward currents during depolarizing pulses, the properties of which are similar to those described e.g. by Benham & Bolton (1986) and Ohya *et al.* (1987) (Chen, Inoue & Ito, unpublished data). These observations suggest that internal Ca stores are also a major target of these drugs, since Poronik *et al.* (1992) have recently provided evidence that several synthesized DPC derivatives including flufenamic acid and DPC possess the capability of provoking calcium transients in the absence of external calcium. In addition, we noticed in our preliminary microelectrode experiments that 30 μM–100 μM flufenamic acid and DCDPC abolish slow membrane oscillations (the so-called slow waves, Bolton, 1979), resulting in membrane hyperpolarizations of 10–20 mV and subsequent cessation of spike discharge. These observations obviously restrict the use of these drugs as selective blockers for the $I_{cat}$ current.

### *Possible mechanisms involved in the action of blockers for the $I_{cat}$ current*

From the results of some mechanistic approaches undertaken in the present study, at least two important different features have become evident between caffeine and K channel blockers, and DPC derivatives. First, inhibition and recovery of the $I_{cat}$ current by the former drug group occurred in the order of 100 ms, while those by the latter were considerably slower (see Figure 2). Secondly, the degree of inhibition was strongly attenuated by depolarizing the membrane in the case of K channel blockers and caffeine but was relieved only weakly in the cases of DPC derivatives. In addition, the site of action of blockers is not on the muscarinic receptor but probably on the $I_{cat}$ channel itself from the observations on GTPγS-induced inward currents. One possible explanation may be as follows. In cation-permeable channels, large positively charged molecules such as TEA, in the extracellular space, are believed to be driven into the orifice or

attracted near to a negatively charged binding site located midway down the channel pore along the transmembrane potential gradient, and to interfere with the permeation of cations (e.g. Hille, 1984). Such interference could occur rapidly due to their easy access and be relieved by depolarization of the membrane due to reduction of the potential gradient which might slow the binding process of the drug molecules. On the other hand, DPC derivatives possess high lipophilicity and are highly membrane-permeable, although most of the molecules are negatively charged at a physiological pH (Gögelein & Phannmüller, 1989). This might enable the drugs to pass through the plasma membrane to an internal site. This mechanism seems consistent with slow onset and recovery of their inhibitions. Indeed, the inhibitory effect of flufenamic acid or DCDPC on the $I_{cat}$ currents persisted for several minutes even after washout of the drugs, and their efficacies on the $I_{cat}$ channel are similar to those on the $Ca^{2+}$-activated cation channels, where the drugs are applied at the intracellular side of the plasma membrane. In addition, this view is consistent with the finding that DPC derivatives decrease the open probability of the $Ca^{2+}$-activated cation channels but such an effect is not associated with the appearance of flickering within long opening intervals, which is usually observed for open channel blockade (Gögelein & Capek, 1990).

We are grateful to Dr A.F. Brading (University Department of Pharmacology, Oxford) for her critical reading of our manuscript, and Dr R. Greger (University of Freiburg) for his kind gifts of DPC derivatives.

## References


BEAN, B.P. (1990). ATP-activated channels in rat and bullfrog sensory neurons: concentration-dependence and kinetics. *J. Neurosci.*, **10**, 1–10.

BEECH, D.J. & BOLTON, T.B. (1989). A voltage-dependent outward current with fast kinetics in single smooth muscle cells isolated from rabbit portal vein. *J. Physiol.*, **412**, 397–414.

BEECH, D.J. & BOLTON, T.B. (1990). Two components of potassium current activated by depolarization of single smooth muscle cells from the rabbit portal vein. *J. Physiol.*, **418**, 293–309.

BENHAM, C.D. & BOLTON, T.B. (1986). Spontaneous transient outward currents in single visceral and vascular smooth muscle cells of rabbit jejunum and guinea-pig mesenteric artery. *J. Physiol.*, **371**, 45–67.

BOLTON, T.B. (1979). Mechanisms of action of transmitters and other substances on smooth muscle. *Physiol. Rev.*, **59**, 606–718.

COOK, N.S. & QUAST, U. (1990). Potassium channel pharmacology. In *Potassium channels*. pp. 181–255. ed. Cook, N.S. Chichester: Ellis Horwood Ltd.

EHARA, K., NOMA, A. & ONO, K. (1988). Calcium-activated non-selective cation channel in ventricular cells isolated from adult guinea-pig hearts. *J. Physiol.*, **403**, 117–133.

GÖGELEIN, H. & CAPEK, K. (1990). Quinine inhibits chloride and nonselective cation channels in isolated rat distal colon cells. *Biochim. Biophys. Acta*, **1027**, 191–198.

GÖGELEIN, H., DAHLEM, D., ENGLERT, H.C. & LANG, H.J. (1990). Flufenamic acid, mefenamic acid inhibit single nonselective cation channels in the rat exocrine pancreas. *FEBS Lett.*, **268**, 79–82.

GÖGELEIN, H. & PFANNMÜLLER, B. (1989). The nonselective cation channel in the basolateral membrane of rat exocrine pancreas. *Pflügers Arch.*, **413**, 287–298.

HUETTER, J.E. & BEAN, B.P. (1988). Block of N-methyl-D-aspartate-activated current by the anticonvulsant MK 801: selective binding to open channels. *Proc. Natl. Acad. U.S.A.*, **85**, 1307–1311.

HORN, R. & MARTY, A. (1988). Muscarinic activation of ionic currents measured by a new whole-cell recording method. *J. Gen. Physiol.*, **92**, 145–159.

HILLE, B. (1984). *Ionic Channels of Excitable Membranes*. Sunderland, Massachusetts: Sinauer Associates Inc.

IINO, M. (1989). Calcium-induced calcium release mechanism in guinea pig taenia caeci. *J. Gen. Physiol.*, **94**, 363–383.

IMAIZUMI, Y., MURAKI, K. & WATANABE, M. (1990). Characteristics of transient outward currents in single smooth muscle cells from the ureter of the guinea-pig. *J. Physiol.*, **427**, 301–324.

INOUE, R. (1991a). Effect of external $Cd^{2+}$ and other divalent cations on carbachol-activated nonselective cation channels in guinea-pig ileum. *J. Physiol.*, **442**, 447–463.

INOUE, R. (1991b). Ion channels involved in responses to muscarinic receptor activation in smooth muscle. In *Ion Channels of Vascular Smooth Muscle Cells and Endothelial Cells*. ed. Sperelakis, N. & Kuriyama, H. pp. 81–91. New York: Elsevier Science Publishing Co., Inc.

INOUE, R. & ISENBERG, G. (1990a). ACh activates nonselective cation channels in guinea pig ileum through a G-protein. *Am. J. Physiol.*, **258**, C1173–C1178.

INOUE, R. & ISENBERG, G. (1990b). Effect of membrane potential on ACh-induced inward current in guinea-pig ileum. *J. Physiol.*, **424**, 57–71.

INOUE, R. & ISENBERG, G. (1990c). Intracellular Ca ions modulate ACh-induced inward current in guinea-pig ileum. *J. Physiol.*, **424**, 73–92.

INOUE, R., KITAMURA, K. & KURIYAMA, H. (1987). ACh activates single sodium channels in smooth muscle cells. *Pflügers Arch.*, **410**, 69–74.

INOUE, R. & KURIYAMA, H. (1992). Stabilized recording of ACh activated non-selective cationic conductance in guinea-pig ileal smooth muscle using a nystatin-permeabilized whole-cell recording. *Jpn. J. Pharmacol.*, **58**, suppl. II, 345P.

INOUE, R. & KURIYAMA, H. (1993). Dual regulation of cation-selective channels by muscarinic and $\alpha_1$-adrenergic receptors in the rabbit portal vein. *J. Physiol.*, **465**, 427–448.

ITOH, T., KURIYAMA, H. & SUZUKI, H. (1981). Excitation-coupling in smooth muscle cells of the guinea-pig mesenteric artery. *J. Physiol.*, **321**, 513–535.

KOMORI, S. & BOLTON, T.B. (1990). Role of G-proteins in muscarinic receptor inward and outward currents in rabbit jejunal smooth muscle. *J. Physiol.*, **427**, 395–419.

OHYA, Y., KITAMURA, K. & KURIYAMA, H. (1987). Cellular calcium regulates outward currents in rabbit intestinal smooth muscle cell. *Am. J. Physiol.*, **252**, C401–C410.

OKABE, K., KITAMURA, K. & KURIYAMA, H. (1987). Features of 4-aminopyridine sensitive outward current observed in single smooth muscle cells from the rabbit pulmonary artery. *Pflügers Arch.*, **409**, 561–568.

PORONIK, P., WARD, M.C. & COOK, D.I. (1992). Intracellular $Ca^{2+}$ release by flufenamic acid and other blockers of the non-selective cation channel. *FEBS Lett.*, **296**, 245–248.

SIEMER, C. & GÖGELEIN, H. (1992). Activation of nonselective cation channels in the basolateral membrane of rat distal colon crypt cells by prostaglandin $E_2$. *Pflügers Arch.*, **420**, 319–328.

SMIRNOV, S. & AARONSON, P.I. (1992). $Ca^{2+}$-activated and voltage-gated currents in smooth muscle cells isolated from human mesenteric arteries. *J. Physiol.*, **457**, 431–454.

STURGESS, N.C., HALES, C.N. & ASHFORD, M.L.J. (1987). Calcium and ATP regulate the activity of a non-selective cation channel in a rat insulinoma cell line. *Pflügers Arch.*, **409**, 607–615.

SWANDULLA, D. & PARTRIDGE, L.D. (1990). Non-specific cation channels. In *Potassium Channels*. ed. Cook, N.S. pp. 167–180. Chichester: Ellis Horwood Ltd.

VOGALIS, F. & SANDERS, K.M. (1990). Cholinergic stimulation activates a non-selective cation current in canine pyloric circular muscle cells. *J. Physiol.*, **429**, 223–236.


*(Received February 4, 1993*
*Revised March 5, 1993*
*Accepted March 9, 1993)*

*Br. J. Pharmacol.* (1993), **109**, 802–806 © Macmillan Press Ltd, 1993

# Involvement of nitric oxide synthase in the delayed vasodilator response to ultraviolet light irradiation of rat skin *in vivo*

[1]J.B. Warren, R.K. Loi & M.L. Coughlan

Department of Applied Pharmacology, National Heart & Lung Institute, Dovehouse Street, London SW3 6LY

**1** The role of nitric oxide synthase and cyclo-oxygenase in the skin blood flow response to ultraviolet light B (u.v.B) irradiation was investigated in the rat *in vivo*.

**2** Local skin blood flow changes were measured in the shaved dorsal skin of anaesthetized male Sprague-Dawley rats with a laser Doppler flow probe.

**3** u.v.B irradiation caused delayed onset vasodilatation and by 18 h basal blood flow increased by $125 \pm 25\%$ ($P < 0.05$, $n = 12$ rats, mean ± s.e.mean).

**4** Indomethacin, 3 nmol per site, $N^G$-nitro-L-arginine methyl ester (L-NAME) 100 nmol per site, but not D-NAME 100 nmol per site, injected locally 17.5 h after u.v.B irradiation abolished the 18 h increase in blood flow.

**5** The nitric oxide synthase inhibitor L-NAME, $N^G$-monomethyl-L-arginine (L-NMMA) and canavanine, 10 and 100 nmol per site injected at 17.5 h, suppressed significantly the u.v.B 18 h response in a dose-dependent manner. The order of potency was L-NAME > canavanine = L-NMMA. The effect of L-NAME was reversed partially by the co-injection of an excess of L-arginine.

**6** Topical application of the corticosteroid, clobetasol 17-propionate, immediately after irradiation inhibited the 18 h u.v.B response in a dose-dependent manner.

**7** The delayed onset microcirculatory vasodilatation induced by u.v.B involves both nitric oxide synthase and cyclo-oxygenase in this *in vivo* model. Topical corticosteroids may attenuate the response by inhibiting both prostaglandin and nitric oxide synthesis pathways.

**Keywords:** Nitric oxide; nitric oxide synthase; ultraviolet light; sunburn; inflammation; corticosteroids; vascular smooth muscle; endothelium; vasodilatation; prostaglandins

## Introduction

Vasodilatation of the microcirculation is a key component of the inflammatory reaction and influences both oedema formation and leucocyte accumulation. The skin response to u.v.B irradiation was chosen as an inflammatory model for the present study as changes in blood flow can be assessed readily by a non-invasive laser Doppler flow probe. The sunburn reaction, caused primarily by u.v.B irradiation, causes increased local blood flow. The mechanisms controlling this reaction are not understood, although in man the reaction is attenuated by both non-steroidal anti-inflammatory drugs (NSAIDs) and corticosteroids (Hughes *et al.*, 1992). Exposing multiple small areas of skin to u.v.B allows the comparison, within the same animal, of several test agents injected locally into irradiated sites.

Both cyclo-oxygenase and nitric oxide synthase (NOS) influence microvascular tone and both enzymes contribute to the inflammatory response. Prostaglandins are implicated in several models of inflammation and NSAIDs diminish the vasodilator response to inflammatory stimuli (Williams & Peck, 1977; Warren *et al.*, 1992). Corticosteroids also inhibit this vasodilator response by a prostaglandin dependent mechanism via the suppression of phospholipase $A_2$ (Flower & Blackwell, 1979). Corticosteroids differ from NSAIDs in their additional ability to inhibit the inducible form of nitric oxide synthase, iNOS (Di-Rosa *et al.*, 1990; Radomski *et al.*, 1990; Smith *et al.*, 1991; McCall *et al.*, 1991; Nathan, 1992). This enzyme is induced to release NO by several inflammatory stimuli such as interleukin-1, tumour necrosis factor and endotoxin (Moncada & Higgs, 1991; Nathan, 1992). In rat skin, both nitric oxide and prostaglandins are involved in the response to endotoxin injected locally (Warren *et al.*, 1992). The aim of the present study was to determine if similar mechanisms were involved in the vasodilator response of rat skin to u.v.B.

Two main subtypes of the NOS enzyme have been described. The $Ca^{2+}$-dependent, constitutive enzyme (cNOS) is present in endothelial cells and is involved in the control of vascular tone (Moncada & Higgs, 1991; Nathan, 1992). The second, iNOS, is $Ca^{2+}$-independent and predominates in vascular smooth muscle cells, although present to a lesser extent in endothelial cells (Moncada & Higgs, 1991; Nathan, 1992). It has been proposed that these two subtypes differ in their sensitivity to inhibition by arginine analogues. Thus, L-canavanine, a basic amino acid which resembles L-arginine, inhibits iNOS but not cNOS (McCall *et al.*, 1989; Iyengar *et al.*, 1987). It has been suggested also that $N^G$-nitro-L-arginine methyl ester (L-NAME) is 100 fold more potent than $N^G$-monomethyl-L-arginine (L-NMMA) at inhibiting cNOS in endothelial cells whereas L-NMMA is more potent than L-NAME at inhibiting iNOS in leucocytes (McCall *et al.*, 1989; Gross *et al.*, 1990). Three inhibitors of NOS, L-NAME, canavanine and L-NMMA, were chosen for the present study to determine if their relative potency in inhibiting iNOS was similar to that of previous studies. The potency of a topical corticosteroid, clobetasol 17-propionate, at preventing the vasodilator response to u.v.B irradiation, was also assessed.

## Methods

### *Animals*

Male Sprague-Dawley rats were anaesthetized with Hypnorm (fentanyl citrate/fluanisone) 0.3 ml $kg^{-1}$, i.m. The dorsal skin was shaved with electric clippers and depilated with a commercial depilating cream (Immac) followed by close shaving

[1] Author for correspondence.

with a glass microscope slide. The dorsal skin was then rinsed thoroughly with warm water and the rats left for 1 h before use. Six to eight sites, depending on the protocol, were marked out on the dorsal skin with a black paper stencil. Each of the holes in the stencil was 6 mm diameter. Baseline skin red cell flux, as an index of blood flow, was measured in the marked sites using a laser Doppler flow meter. With the paper stencil in position to shield the remaining skin, the sites were exposed to u.v.B irradiation. Blood flow responses were measured 4 or 18 h later, depending on the protocol, with the rats sedated with Hypnorm. All experiments were performed in a temperature controlled laboratory at 23– 25°C. All injections were given as 100 μl volumes via a 27 wire gauge needle. The lesions induced by u.v.B caused no signs of distress and similar, or more marked, lesions in the skin of human volunteers were not painful (preliminary observations).

### *Blood flow measurements (laser Doppler)*

Blood flow was measured in the dorsal skin with a laser-Doppler flow probe (Perimed II, Stockholm, Sweden). Each reading took 15 s with a 10 s interval between readings and the mean of three readings per site were taken. Results were recorded as red blood cell flux (the number of moving red cells detected by the laser beam × mean cell velocity) and expressed as a percentage of a standardized signal obtained in a particulate control medium. The laser Doppler was set at 4 Hz, gain 10 and a time constant of 1.5 s. The output was recorded on a Maclab and Macintosh Apple Computer (Apple Computer Inc, Cupertino, Ca, U.S.A.) set at an input of 10 V and chart speed of 4 mm $s^{-1}$. Test compounds were injected in a randomized site pattern.

### *Ultraviolet B irradiation*

A high dose u.v.B lamp was used (StaFL 400 W, Starma Ltd., Romford, Essex). A filter was used to prevent heat transmission. The u.v.B intensity at the skin surface was measured with a UVX radiometer (UVX-31, UVP Ltd, Cambridge, GB) with spectral sensitivity in the wavelength range of 280–310 nm. The intensity was 20 mW $cm^{-2}$ with the lamp held 30 cm from the skin. All sites were exposed for 9 min. This dose caused approximately a 100% increase in skin blood flow at 18 h.

### *Experimental protocols*

In a preliminary time course experiment, baseline blood flow was measured in marked sites in 6 rats and this was repeated 4 h and 18 h after irradiation.

A further 12 rats were irradiated in 5 sites after baseline blood flow was measured in each site. At 17.5 h the sites were injected with either phosphate buffered saline as control, indomethacin 3 nmol per site, L-NAME 100 nmol per site, L-arginine 10 μmol per site or L-NAME 100 nmol + L-arginine 10 μmol per site and blood flow re-measured at 18 h. In an additional 3 sites per rat, which were not irradiated, baseline blood flow measurements were followed by the injection of either control, indomethacin 3 nmol per site or L-NAME 100 nmol per site and blood flow re-measured 30 min after injection. To determine if the small change in blood flow in non-exposed skin induced by indomethacin or L-NAME was significant, an additional 16 rats were studied to examine effects on basal blood flow of control, indomethacin and L-NAME as above.

A separate batch of 6 rats received either D-NAME 100 nmol per site or control to duplicate sites 17.5 h after u.v.B irradiation and blood flow was measured at 18 h.

To determine if L-NAME or indomethacin act as non-specific vasoconstrictors, their effect on iloprost-induced vasodilatation was determined. Blood flow response were measured 30 min after the injection of control, iloprost 1 nmol per site, iloprost 1 nmol + L-NAME 100 nmol per site, and iloprost 1 nmol and indomethacin 3 nmol per site in 6 rats.

Three inhibitors of nitric oxide synthase were compared in a further experiment. Baseline blood flow was measured in 8 sites in 6 rats. One site was not irradiated as control and the other 7 irradiated and then injected 17.5 h later with the inhibitors L-NAME, canavanine, L-NMMA (each at 10 and 100 nmol per site), or phosphate buffered saline as control, and blood flow measured again at 18 h.

To test the effect of a topical corticosteroid on the u.v.B response, baseline blood flow readings were measured in 8 marked sites per rat. Two sites on each flank were covered whilst the other two sites on each flank were exposed to u.v.B. After exposure, the 4 sites on the left flank were painted with vehicle solution 0.5 ml and the 4 sites on the right flank with steroid solution 0.5 ml. Blood flow was re-measured in all 8 sites 18 h after irradiation and the animals then overdosed with anaesthetic. Three groups of 9 rats each received either 0.1, 0.01 or 0.001% concentrations of clobetasol 17-propionate.

### *Drugs and chemicals*

Indomethacin was made as a stock solution of $10^{-2}$ M in ethanol and then diluted in phosphate-buffered saline. Clobetasol 17-propionate was dissolved in 20% diethylacetamide, 40% acetone and 40% ethanol and this vehicle was used as the control. Iloprost was the generous gift of Schering AG Pharmaceutical Research, Berlin, Germany. All other drugs were dissolved and diluted in phosphate-buffered saline. Pentobarbitone sodium was from May & Baker. Other drugs and chemicals were from the Sigma Chemical Co., Poole, Dorset.

### *Statistical analysis*

Data are presented as mean ± s.e.mean. Statistical analysis was performed by analysis of variance (ANOVA) and results termed significant if $P<0.05$.

## Results

Ultraviolet B irradiation caused a delayed onset increase in skin blood flow when injected intradermally in rat skin *in vivo*. This was readily detected by laser Doppler flow probe, but was only visible as a slight reddening of the skin between 15 and 24 h after exposure. In a preliminary experiment in six rats the % increase in basal blood flow in irradiated sites was 66 ± 23% at 4 h and 124 ± 20% at 18 h (18 h response significantly greater than the 4 h response, $P<0.05$ ANOVA). In three animals the inhibition of the 18 h u.v.B response was greater if L-NAME was injected at 17.5 h than if injected at 17 h; injection immediately after irradiation had no effect on the 18 h response, D-NAME, 100 nmol per site, injected 17.5 h after u.v.B exposure had no significant effect on the 18 h response; the % change in blood flow was − 8 ± 6%, 146 ± 25% and 113 ± 15% in non-exposed sites injected with phosphate-buffered saline, exposed sites injected with phosphate-buffered saline, and exposed sites injected with D-NAME, respectively ($n = 6$ rats).

Figure 1 shows that L-NAME had a small vasoconstrictor effect in control skin sites when blood flow was re-measured 30 min after injection ($P<0.05$, ANOVA). This could indicate basal release of the endogenous vasodilator nitric oxide, although this response may depend upon the mild irritation of shaving. Exposure of sites to u.v.B irradiation increased basal blood flow significantly at 18 h in control sites which had been injected with phosphate buffered saline at 17.5 h and the effect of u.v.B was abolished by the local injection of either indomethacin or L-NAME ($P<0.05$ in each case, ANOVA).

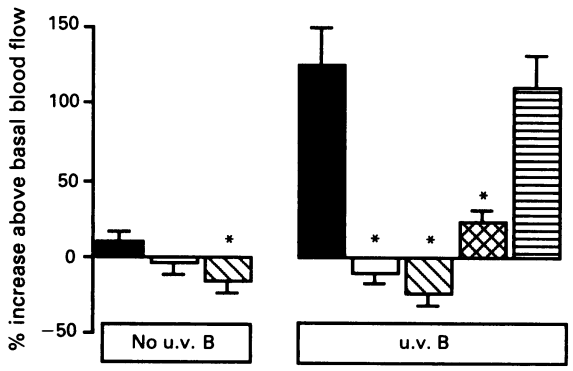



**Figure 1** The inhibition of the vasodilator response to u.v.B irradiation by the nitric oxide synthase inhibitor, $N^G$-nitro-L-arginine methyl ester (L-NAME) and the cyclo-oxygenase inhibitor, indomethacin, in rat skin. Control (solid columns); indomethacin 3 nmol per site (open columns); L-NAME 100 nmol per site (hatched column); L-NAME + L-arginine 10 μmol per site (cross-hatched column); or L-arginine 10 μmol per site (horizontally lined column); were injected 17.5 h after exposure of the shaved dorsal skin to u.v.B. The vasodilator response was measured in both irradiated and non-irradiated skin sites at 18 h. L-NAME significantly reduced blood flow in non-irradiated sites and both L-NAME and indomethacin significantly reversed the effect of u.v.B irradiation (*$P<0.05$ in each case). The effect of L-NAME on u.v.B irradiation was partially reversed by the co-injection of L-arginine (*$P<0.05$). Each column represents the mean ± s.e.mean percentage change in basal blood flow for 12–28 rats.

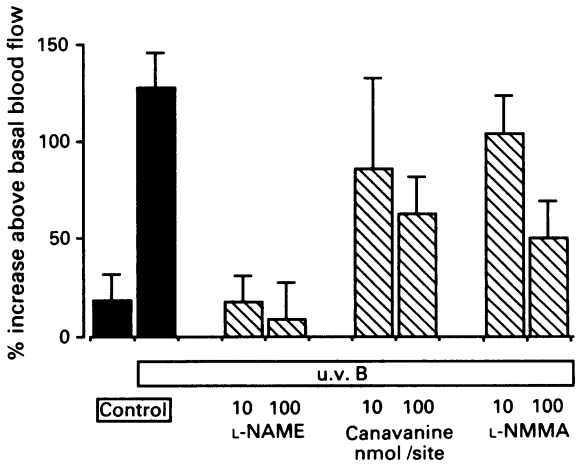



**Figure 2** Comparison of the attenuation of the blood flow response to u.v.B irradiation in rat skin by 3 inhibitors of nitric oxide synthase $N^G$-nitro-L-arginine methyl ester (L-NAME), canavanine and $N^G$-monomethyl-L-arginine (L-NMMA) (hatched columns) were injected at 10 and 100 nmol per site 17.5 h after exposure of the shaved dorsal skin to u.v.B irradiation and the vasodilator response measured at 18 h. The change in blood flow in control injected, non-irradiated sites is shown by the first solid column, and in control injected and irradiated sites by the second solid column. All three agents significantly inhibited the response and this was dose-dependent (*$P<0.05$ in each case). Results are the mean + s.e.mean of 6 rats.

The possibility that L-arginine could reverse the effects of L-NMMA was tested. L-NAME at 100 nmol per site was not reversed completely by an excess of L-arginine; in the experiment depicted in Figure 1, irradiated sites injected with L-arginine 10 μmol per site showed a similar response to those irradiated and injected with control buffer. There was partial reversal of the effects of L-NAME by the co-injection of L-NAME with an excess of L-arginine, $P<0.05$, ANOVA, $n=12$. In a further four rats, a lower dose of L-NAME was reversed to a greater extent, the increase in blood flow at 18 h in irradiated sites was 70 ± 1%, − 55 ± 4 and 45 ± 35% when injected with control, L-NAME 10 nmol per site, and L-NAME 10 nmol + L-arginine 10 μmol per site respectively (all mean ± s.e.mean).

L-NAME and indomethacin did not significantly affect the response to iloprost. Iloprost 1 nmol per site caused a 158 ± 18% increase in blood flow at 30 min compared to 42 ± 15% change in control sites. Co-injection of L-NAME or indomethacin with iloprost caused a 154 ± 19% and 106 ± 20% change in blood flow respectively ($n=6$).

All three inhibitors of nitric oxide synthase suppressed the 18 h blood flow response to u.v.B in a dose-dependent manner when injected locally into sites which were irradiated 17.5 h previously (Figure 2, $P<0.05$ in each case, ANOVA). Canavanine and L-NMMA were equipotent whereas L-NAME was at least ten fold more potent than the other two. In a separate experiment, canavanine 100 nmol per site had no significant effect on basal skin blood flow at 30 min the effect in canavanine injected sites being 38 ± 18% change and 5 ± 12% in control sites ($n=6$ rats).

Figure 3 shows that increased blood flow in u.v.B irradiated skin was attenuated by topical steroid treatment. Clobetasol 17-propionate applied topically immediately after exposure suppressed the response in a dose-dependent manner. It was effective at 0.1, 0.01 and 0.001% concentrations ($P<0.05$ in each case compared with control). With the 0.1% concentration there is the suggestion that the control response is diminished, consistent with some systemic absorption of clobetasol from the treated side acting on the control side. In non-irradiated sites the blood flow changes at 18 h in

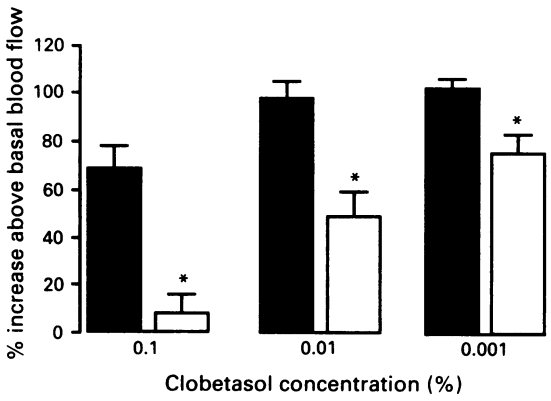



**Figure 3** The inhibition of the vasodilator response to u.v.B in rat skin by the corticosteroid, clobetasol, applied topically immediately after irradiation. The graph shows the increase in blood flow at 18 h in the irradiated sites for those sites treated with vehicle control (solid columns) and those treated with clobetasol (open columns). The results at each concentration are the mean + s.e.mean of 9 rats, *$P<0.05$ in each case.

vehicle- and steroid-treated sites were respectively − 6 ± 6% and − 13 ± 8% in the 0.1% steroid group; 4 ± 2% and 2 ± 4% in the 0.01% steroid group; and 13 ± 7% and 16 ± 5% in the 0.001% group.

## Discussion

The present study shows that exposure to u.v.B irradiation causes a delayed increase in blood flow in shaved rat skin *in vivo*. Three different inhibitors of NOS antagonized the increase in blood flow indicating that endogenous nitric oxide is involved. The inhibition by canavanine implicates the inducible form of NOS, as iNOS from leucocytes is inhibited

by canavanine whereas cNOS is not (Iyengar *et al.*, 1987; McCall *et al.*, 1989). It has been suggested that L-NMMA is at least as effective as L-NAME at inhibiting leucocyte iNOS (McCall *et al.*, 1989; Gross *et al.*, 1990), however, L-NAME was at least ten fold more potent in the present study at inhibiting the u.v.B response. Discrepancies in the relative potency of the arginine analogues may arise from the minor differences in the subclasses of the NOS group of enzymes (Nathan, 1992). The delayed onset of the blood flow response and its inhibition by a corticosteroid makes it most likely that it is the inducible form of the enzyme that is involved.

The effect of L-NAME was reversed by an excess of L-arginine which suggests that NO was formed from L-arginine. The reversal by L-arginine was not complete, particularly when a high dose of L-NAME was used, consistent with L-NAME having some irreversible inhibitory action on NOS (Dwyer *et al.*, 1991). We have shown previously that the D-isomer of NMMA is inactive in rat skin (Warren *et al.*, 1992) and the D- isomer of NAME had no effect on the u.v.B response in the present experiment.

An intermediate in the reaction to u.v.B that can induce iNOS is interleukin-1 (IL-1). Epidermal cells irradiated *in vivo* or *in vitro* increase their synthesis of IL-1 (Schwarz *et al.*, 1987) and this may contribute to the sunburn reaction in man (Murphy *et al.*, 1989). IL-1 is a potent stimulus to iNOS, an action prevented by corticosteroids (Busse & Mulsch, 1990; Schini *et al.*, 1991; Moncada & Higgs, 1991; Nathan, 1992). Future experiments with a specific IL-1 antagonist may elucidate the role of IL-1 further.

The cellular origin of the nitric oxide in the present model is not clear. Vascular smooth muscle is the most likely source as iNOS predominates in this tissue, in contrast to the endothelium where cNOS predominates. Neurones also release nitric oxide, although it is possible to induce an erythema response to u.v.B in denervated skin in man (Lewis *et al.*, 1927), suggesting normal nerve function is not a pre-requisite. Leucocytes are yet another source that has not been excluded. There is evidence to suggest that nitric oxide-mediated vasodilatation contributes to the oedema component of inflammation as several vasodilators potentiate oedema (Williams & Peck, 1977a; Williams, 1982; Warren *et al.*, 1992) and nitric oxide is involved in the oedema response to substance P in rat skin (Hughes *et al.*, 1990).

The inhibition of the u.v.B-induced hyperaemia by indomethacin implicates prostaglandins in the pathogenesis of this response, although prostaglandin production was not measured directly. The response to u.v.B is slow in onset suggesting enzyme induction, possibly of the inducible form of cyclo-oxygenase (Masferrer *et al.*, 1992). Corticosteroids may suppress the u.v.B response by inhibiting the inducible form of cyclo-oxygenase (Masferrer *et al.*, 1992), by inhibiting phospholipase $A_2$ (Axelrod, 1983), as well as by preventing the induction of iNOS. Prostaglandins are potent vasodilators of the microcirculation (Messina *et al.*, 1975; Williams, 1979; Messina & Kaley, 1980), in contrast to their low activity in large blood vessels (Gordon & Martin, 1983; Gryglewski *et al.*, 1986). Prostaglandins and nitric oxide might be synergistic in the microcirculation, analogous to their combined inhibition of platelet aggregation (Moncada & Higgs, 1991), although there is no evidence this is the case in the vasculature.

In conclusion, the pathogenesis of u.v.B-induced vasodilatation of the microcirculation of rat skin *in vivo* involves endogenous nitric oxide. The response was abolished by NOS inhibitors and the effectiveness of canavanine implicates the inducible form of NOS as the enzyme involved. Indomethacin was as effective as the NOS inhibitors suggesting a link between vasodilator prostaglandins and nitric oxide within the microcirculation. The suppression of the reaction by corticosteroids may be explained by the dual inhibition of both phospholipase $A_2$, and hence prostaglandin production, and the inhibition of iNOS.

This work was supported by the British Heart Foundation.

## References


AXELROD, L. (1983). Inhibition of prostacyclin production mediates permissive effect of glucocorticoids on vascular tone. *Lancet*, **ii**, 904–906.

BUSSE, R. & MULSCH, A. (1990). Induction of nitric oxide synthase by cytokines in vascular smooth muscle cells. *FEBS Lett.*, **275**, 87–90.

DI-ROSA, M., RADOMSKI, M., CARNUCCIO, R. & MONCADA, S. (1990). Glucocorticoids inhibit the induction of nitric oxide synthase in macrophages. *Biochem. Biophys. Res. Commun.*, **172**, 1246–1252.

DWYER, M.A., BREDT, D.S. & SNYDER, S.H. (1991). Nitric oxide synthase: irreversible inhibition by L-$N^G$- nitroarginine in brain in vitro and in vivo. *Biochem. Biophys. Res. Commun.*, **176**, 1136–1141.

FLOWER, R.J. & BLACKWELL, G.J. (1979). Anti-inflammatory steroids induce biosynthesis of a phospholipase A2 inhibitor which prevents prostaglandin biosynthesis. *Nature*, **278**, 456–459.

GORDON, J.L. & MARTIN, W. (1983). Stimulation of endothelial prostacyclin production plays no role in endothelium-dependent relaxation of the pig aorta. *Br. J. Pharmacol.*, **80**, 179–186.

GROSS, S.S., STUEHR, D.J., AISAKA, K., JAFFE, E.A., LEVI, R. & GRIFFITH, O.W. (1990). Macrophage and endothelial cell nitric oxide synthesis: cell-type selective inhibition by $N^G$-aminoarginine, $N^G$-nitroarginine and $N^G$-methylarginine. *Biochem. Biophys. Res. Commun.*, **170**, 96–103.

GRYGLEWSKI, R.J., MONCADA, S. & PALMER, R.M.J. (1986). Bioassay of prostacyclin and endothelium-derived relaxing factor (EDRF) from porcine aortic endothelial cells. *Br. J. Pharmacol.*, **87**, 685–694.

HUGHES, G.S., FRANCOM, S.F., MEANS, L.K., BOHAN, D.F., CARUANA, C. & HOLLAND, M. (1992). Synergistic effects of oral nonsteroidal drugs and topical corticosteroids in the therapy of sunburn in humans. *Dermatology*, **184**, 54–58.

HUGHES, S.R., WILLIAMS, T.J. & BRAIN, S.D. (1990). Evidence that endogenous nitric oxide modulates oedema formation induced by substance P. *Eur. J. Pharmacol.*, **191**, 481–484.

IYENGAR, R., STUEHR, D.J. & MARLETTA, M.A. (1987). Macrophage synthesis of nitrite, nitrate, and N-nitrosamines: precursors and role of the respiratory burst. *Proc. Natl. Acad. Sci. U.S.A.*, **84**, 6369–6373.

LEWIS, T., HARRIS, K.E. & GRANT, R.T. (1927). Observations relating to the infuence of the cutaneous nerves on various reactions of the cutaneous vessels. *Heart*, **14**, 1–15.

MASFERRER, J.L., SEIBERT, K., ZWEIFEL, B. & NEEDLEMAN, P. (1992). Endogenous glucocorticoids regulate an inducible cyclooxygenase enzyme. *Proc. Natl. Acad. Sci. U.S.A.*, **89**, 3917–3921.

MCCALL, T.B., BOUGHTON-SMITH, N.K., PALMER, R.M., WHITTLE, B.J. & MONCADA, S. (1989). Synthesis of nitric oxide from L-arginine by neutrophils. Release and interaction with superoxide anion. *Biochem. J.*, **261**, 293–296.

MCCALL, T.B., PALMER, R.M. & MONCADA, S. (1991). Induction of nitric oxide synthase in rat peritoneal neutrophils and its inhibition by dexamethasone. *Eur. J. Immunol.*, **21**, 2523–2527.

MESSINA, E. & KALEY, G. (1980). Microcirculatory response to prostacyclin and PGE2 in the rat cremaster muscle. *Adv. Prostaglandins Thromboxane Res.*, **7**, 719–722.

MESSINA, E.J., WEINER, R. & KALEY, G. (1975). Inhibition of bradykinin vasodilation and potentiation of norepinephrine and angiotensin vasoconstriction by inhibition of prostaglandin synthesis in skeletal muscle of the rat. *Circ. Res.*, **37**, 430–437.

MONCADA, S. & HIGGS, E.A. (1991). Nitric oxide: physiology, pathophysiology and pharmacology. *Pharmacol. Rev.*, **43**, 109–141.

MURPHY, G.M., DOWD, P.M., HUDSPITH, B.N., BROSTOFF, J. & GREAVES, M.W. (1989). Local increase in interleukin-1-like activity following UVB irradiation of human skin in vivo. *Photo-Dermatology*, **6**, 268–274.

NATHAN, C. (1992). Nitric oxide as a secretory product of mammalian cells. *FASEB J.*, **6**, 3051–3064.

RADOMSKI, M.W., PALMER, R.M. & MONCADA, S. (1990). Glucocorticoids inhibit the expression of an inducible, but not the constitutive, nitric oxide synthase in vascular endothelial cells. *Proc. Natl. Acad. Sci. U.S.A.*, **87**, 10043–10047.

SCHINI, V.B., JUNQUERO, D.C., SCOTT-BURDEN, T. & VANHOUTTE, P.M. (1991). Interleukin-1 beta induces the production of an L-arginine-derived relaxing factor from cultured smooth muscle cells from rat aorta. *Biochem. Biophys. Res. Commun.*, **176**, 114–121.

SCHWARZ, T., URBANSKA, A., GSCHNAIT, F. & LUGER, T.A. (1987). UV-irradiated epidermal cells produce a specific inhibitor of interleukin 1 activity. *J. Immunol.*, **138**, 1457–1463.

SMITH, R.E., PALMER, R.M. & MONCADA, S. (1991). Coronary vasodilatation induced by endotoxin in the rabbit isolated perfused heart is nitric oxide-dependent and inhibited by dexamethasone. *Br. J. Pharmacol.*, **104**, 5–6.

WARREN, J.B., COUGHLAN, M.L. & WILLIAMS, T.J. (1992). Endotoxin-induced vasodilation in anesthetized rat skin involves nitric oxide and prostaglandin synthesis. *Br. J. Pharmacol.*, **106**, 953–957.

WILLIAMS, T.J. (1979). Prostaglandin $E_2$, prostaglandin $I_2$ and the vascular changes of inflammation. *Br. J. Pharmacol.*, **65**, 517–524.

WILLIAMS, T.J. (1982). Vasoactive intestinal polypeptide is more potent than prostaglandin $E_2$ as a vasodilator and oedema potentiator in rabbit skin. *Br. J. Pharmacol.*, **77**, 505–509.

WILLIAMS, T.J. & PECK, M.J. (1977). Role of prostaglandin-mediated vasodilatation in inflammation. *Nature*, **270**, 530–532.

*(Received January 4, 1993*
*Revised February 23, 1993*
*Accepted March 10, 1993)*

*Br. J. Pharmacol.* (1993), **109**, 807–813 © Macmillan Press Ltd, 1993

# Effects of intracerebroventricular injection of histamine and related compounds on corticosterone release in rats

Susumu Tsujimoto, Yasushi Okumura, Chiaki Kamei & [1]Kenji Tasaka

Department of Pharmacology, Faculty of Pharmaceutical Sciences, Okayama University, Okayama 700, Japan

**1** The effects of intracerebroventricular (i.c.v.) injection of histamine and related compounds on plasma adrenocorticotrophic hormone (ACTH) and corticosterone concentrations were studied in conscious rats.

**2** Histamine at doses of 5–20 $\mu g\,kg^{-1}$ rapidly increased plasma ACTH and corticosterone concentrations almost simultaneously, and subsequent courses were also similar to each other. However, in the case of CRF-41 (i.v.), the plasma ACTH concentration first increased followed by an increase in plasma corticosterone concentration. Even in hypophysectomized rats, a significant increase in plasma corticosterone concentration was induced by histamine at doses of 20 and 50 $\mu g\,kg^{-1}$.

**3** Histamine at doses of 10 and 20 $\mu g\,kg^{-1}$ elicited an increase in the amplitude of adrenal nerve activity, and electrical stimulation to the adrenal nerves resulted in an increase in plasma corticosterone concentration.

**4** Both $H_1$-agonist (2-methylhistamine) and $H_2$-agonists (4-methylhistamine and impromidine) also induced similar effects to those of histamine. Pretreatment with pyrilamine caused an inhibition of histamine-induced increase in plasma ACTH and corticosterone concentrations, while both cimetidine and ranitidine failed to inhibit this effect. However, both $H_2$-blockers were effective in inhibiting the 4-methylhistamine-induced elevation of plasma ACTH and corticosterone concentrations.

**5** Neither (**R**)-α-methylhistamine nor thioperamide had a significant effect, indicating that the $H_3$-receptor is not involved in the histamine-induced increase in plasma ACTH and corticosterone concentrations.

**6** From these findings, it was concluded that (1) electrical signals transmitted from the brain to the adrenal gland through the neurones may be involved in the rapid corticosterone release induced by histamine, and (2) not only $H_1$- but also $H_2$-receptors are implicated in histamine-induced hormone secretions in rats, though the contribution of the $H_2$-receptor is less important than that of the $H_1$-receptor.

**Keywords:** Histamine; intracerebroventricular injection; ACTH; corticosterone secretion; hypophysectomy; adrenal nerve activity; $H_1$-blocker; $H_2$-blocker

## Introduction

We have shown that the intracerebroventricular (i.c.v.) injection of histamine in dogs caused an elevation of plasma adrenocorticotrophic hormone (ACTH) and cortisol concentrations via the $H_1$-receptor (Tsujimoto *et al.*, 1993). In addition, an increase of plasma cortisol occurred much faster than that of plasma ACTH, and the extent of cortisol release induced by histamine was more remarkable than that of ACTH release. Although it is known that the primary physiological and pharmacological effects of ACTH result from the secretion of adrenocortical steroids (Haynes, 1990), these findings seem to suggest that histamine-induced cortisol release is elicited to some extent without involvement of ACTH. In such circumstances, it is reasonable to assume that signal transfer through the neurones connecting the brain to the adrenal gland may be involved in the rapid corticosterone release due to i.c.v. histamine injection. On the other hand, Bugajski & Gadek (1983) demonstrated that in stressed rats, the corticosterone response to histamine is mediated by both $H_1$- and $H_2$-central receptors. Also, it has been reported that the $H_2$-receptor is responsible for histamine-induced ACTH release in rats and man (Morita & Koyama, 1979; Knigge *et al.*, 1983). From these findings, it seems likely that species differences exist between dogs and rats in histamine-induced corticosteroidgenesis, especially in the participating receptor. The presence of the $H_3$-receptor, which is responsible for the feedback control of histamine synthesis and release, has also been demonstrated (Arrang *et al.*, 1987). However, it is not known whether or not the $H_3$-receptor is involved in histamine-induced steroidgenesis.

Therefore, the present study was undertaken to clarify the mechanism of glucocorticoid release induced by i.c.v. injection of histamine in rats, and especially to elucidate whether or not the signal transfer through the neurones to the adrenal gland is involved in the rapid corticosteroid release.

## Methods

### *Animals*

Male Wistar rats weighing 250–300 g were used. All animals were maintained in an air-conditioned room controlled for temperature (24–25°C) and humidity (50–60%). The animals were given food and water *ad libitum*.

### *Implantation of guide cannula*

Under sodium pentobarbitone anaesthesia (35 mg $kg^{-1}$, i.p.), the rat was placed in the stereotaxic apparatus (Narishige, SR-5), and a stainless steel cannula was implanted into the lateral ventricle (A:5.4, L:1.5, H:3.0) according to the atlas of de Groot (1959). Two weeks after surgery, the animals were used in the experiments.

[1] Author for correspondence.

### Collection of blood samples

After sodium pentobarbitone anaesthesia (35 mg $kg^{-1}$, i.p.), polyethylene tubing (Igarashi, Size 15) was inserted into the left carotid artery. Starting 8 h after surgery (rats were awake and moved freely), blood samples were collected through the implanted tube after drug administration. Blood samples were promptly centrifuged at 4°C, and separated plasma was used for ACTH and corticosterone determinations.

### Assays for plasma ACTH and corticosterone

Plasma ACTH concentration was measured by radioimmunoassay (DPC · ACTH assay kit, Diagnostic Products Corporation, Los Angeles, CA, U.S.A.). The kit employs a double antibody $^{125}$I-radioimmunoassay and allows the quantitative measurement of ACTH in plasma. The lowest detectable concentration is 8 pg $ml^{-1}$ and practically no cross-reactivity was detected between [Met$^5$]enkephalin, [Leu$^5$]enkephalin, neurotensin, β-endorphin, substance P, somatostatin and α-MSH. The coefficient of variance in inter- and intra-assays was 5.7% ($n = 9$) and 8.2% ($n = 9$), respectively. Plasma corticosterone concentration was determined by the microfluorometric method of Glick *et al.* (1964) with some modifications. In short, iso-octane (1.0 ml) was added to a test tube containing a plasma sample (100 μl), mixed thoroughly and centrifuged. After removal of the iso-octane layer, 2.0 ml of chloroform was added. After mixing, aqueous layer was replaced by 0.2 ml of 0.1 N-NaOH solution, and centrifuged after mixing. Chloroform phase (1.0 ml) was transferred to another test tube containing 2.0 ml of ethanol:sulphuric acid (35:65) and mixed well. Under the excitation beam of 470 nm, fluorescence intensity of the acid phase was measured at 520 nm. Appropriate concentrations of standard and blank were processed in parallel. The coefficient of variance in inter- and intra-assays was 10.5% ($n = 5$) and 7.3% ($n = 6$), respectively.

### Hypophysectomy

In some experiments, hypophysectomy was performed in rats with an implanted cannula (in the lateral ventricle). Seven hours after cannulation of the left carotid artery, the hypophysis was removed according to the method of Tanaka (1955) under sodium thiopentone anaesthesia (50 mg $kg^{-1}$, i.v.). Briefly, the injection needle which connected the syringe (admitted 2 ml of saline in 3 ml size) was inserted into the external auricular opening. The needle was pushed to contact the hypophysis after breaking through the tympanic membrane. Thereafter, by drawing up the plunger of the syringe, the hypophysis was removed in the syringe. One hour after hypophysectomy, the experiment was started. At the end of each experiment, the completeness of the hypophysectomy was confirmed.

### Recording of the adrenal nerve activity

Adrenal nerve activity was recorded according to the method of Togashi (1983). The animals with implanted cannulae (to the lateral ventricle) were anaesthetized with urethane, the adrenal nerve was retroperitoneally dissected, and cut close to the adrenal gland. Spontaneous efferent, nerve mass discharge was recorded from the distal end of the nerve by means of bipolar platinum wire electrodes. The nerve activity, recorded in warm liquid paraffin, was amplified and displayed on a memory oscilloscope (VC-10, Nihon Kohden) and photographed directly. The discharge rate of adrenal nerve activity was examined after passing through a window discriminator (Nihon Koden, Type EN-601J) which picked out signal discharge excluding the background noise. Two hours after the operation, the experiment to test the drug effect was initiated.

### Stimulation of adrenal nerves

The left adrenal nerve was retroperitoneally dissected under urethane anaesthesia, 6 h after the cannulation of the left carotid artery had been performed. After 2 h of rest, the adrenal nerve was stimulated electrically through bipolar platinum wire electrodes (100 Hz, 1 ms, 500 μA, for 60 s). Thereafter, a blood sample was taken.

### Chemicals

The drugs used were histamine dihydrochloride (Nacalai Tesque), 2-methylhistamine dihydrochloride (SK&F), 4-methylhistamine dihydrochloride (SK&F), impromidine trihydrochloride (SK&F), pyrilamine maleate (ICN · K&K Labs), cimetidine (Fujisawa), ranitidine hydrochloride (Glaxo), (**R**)-α-methylhistamine oxalate (Research Biochemicals), thioperamide hydrochloride (provided by Eisai) and corticotropin releasing factor-41 (CRF-41, Peptide Institute). In the case of i.c.v. injection, all the drugs were dissolved in saline and adjusted to pH 7.2 and injected in a volume of 5 μl with a constant speed of 30 s through the implanted guide cannula.

### Statistical analysis

The ANOVA and Dunnett's test were used for estimating the differences between the means of the test group and the control group. Numeral indicates the mean ± s.e.mean.

## Results

### Effect of histamine on plasma ACTH and corticosterone concentrations

The i.c.v. injection of histamine at a dose of 2 μg $kg^{-1}$ caused some elevation of plasma ACTH concentration, but not to a significant degree. At doses of 5–20 μg $kg^{-1}$, histamine induced a significant elevation of plasma ACTH concentration in a dose-dependent manner (5 μg $kg^{-1}$, $P<0.05$; 10 and 20 μg $kg^{-1}$, $P<0.01$). At a dose of 20 μg $kg^{-1}$, a significant increase was observed from 5 min which persisted even after 60 min (Figure 1). On the other hand, a moderate increase in plasma corticosterone occurred at a dose of 2 μg $kg^{-1}$ histamine and the increase became more marked as the doses increased. At a dose of 20 μg $kg^{-1}$, plasma corticosterone

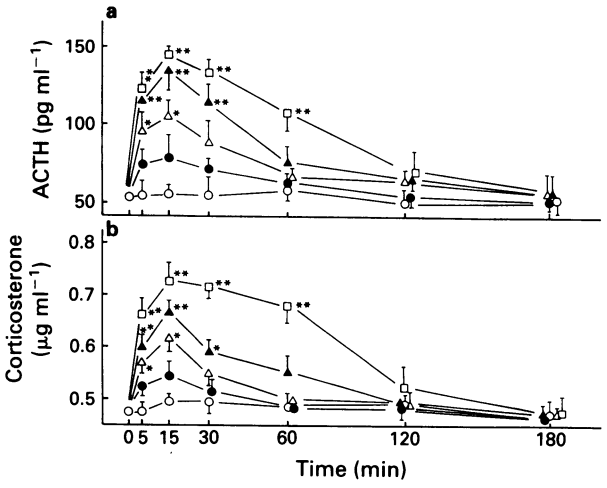



**Figure 1** Changes in plasma ACTH (a) and corticosterone (b) concentrations induced by intracerebroventricular injection of histamine in rats. Each point indicates the mean ± s.e.mean ($n = 5$–6). Control (○); histamine 2 μg $kg^{-1}$ (●); 5 μg $kg^{-1}$ (△); 10 μg $kg^{-1}$ (▲); 20 μg $kg^{-1}$ (□). Significantly different from the control group: $*P<0.05$ and $**P<0.01$.

increased ($P<0.01$) very promptly as in the case of ACTH, and sequential changes in plasma concentrations of both ACTH and corticosterone were quite similar at all dosages of histamine injected (Figure 1).

### *Effect of CRF-41 on plasma ACTH and corticosterone concentrations*

To identify the sequential changes in plasma ACTH and corticosterone concentrations after CRF-41 injection, the effect of CRF-41 was studied. When CRF-41 (10 $\mu g\,kg^{-1}$) was injected intravenously, plasma ACTH concentration rapidly increased and reached a peak 5 min after injection. By contrast, plasma corticosterone concentration increased gradually and reached a peak 30–60 min after CRF-41 injection (Figure 2).

### *Effect of histamine on plasma ACTH and corticosterone concentrations in hypophysectomized rats*

One hour after hypophysectomy, plasma ACTH and corticosterone concentrations decreased by about 40% and 25%, respectively, compared with pre-operational values. When histamine (i.c.v.) was injected 1 h after the operation at a dose of 20 $\mu g\,kg^{-1}$, it caused a significant increase in corticosterone concentration at 5 and 15 min ($P<0.05$), while at a dose of 50 $\mu g\,kg^{-1}$, a remarkable increase in plasma corticosterone concentration was noticed from 5 to 60 min ($P<0.05$ or $P<0.01$). In this case, no change in plasma ACTH was induced by histamine even at a dose of 50 $\mu g\ kg^{-1}$ (Figure 3).

### *Effect of histamine on adrenal nerve activity*

To confirm whether or not i.c.v. injection of histamine is effective in stimulating the adrenal gland through the neuronal pathway, electrical signals were recorded on the adrenal nerve. Discharge rates and the amplitudes of adrenal nerve activity were 104.0 ± 2.5 Hz ($n = 5$) and 18.2 ± 1.0 $\mu V$ ($n = 5$), respectively. I.c.v. injection of histamine at doses of 10 and 20 $\mu g\,kg^{-1}$ immediately increased the amplitude of electrical signals. The increase became significant 5 min ($P<0.05$ or $P<0.01$) after histamine application and lasted for 30 min ($P<0.01$). However, histamine caused no significant effect on the rate of discharge (Table 1). When $C_1$ transection was performed, the adrenal nerve activity disappeared almost instantaneously in all cases ($n = 3$).

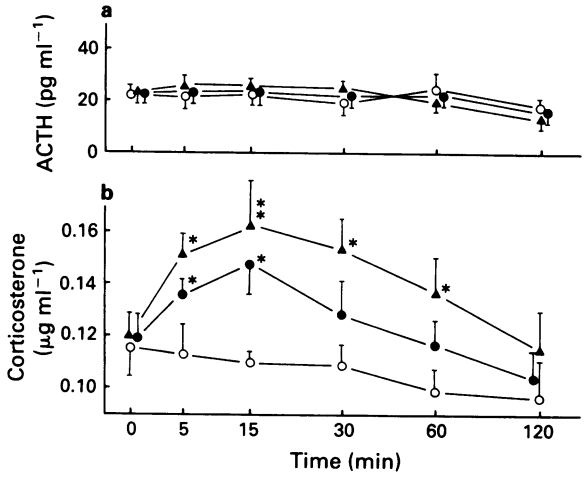



**Figure 3** Changes in plasma ACTH (a) and corticosterone (b) concentrations induced by intracerebroventricular injection of histamine in hypophysectomized rats. Control (○); histamine 20 $\mu g\,kg^{-1}$ (●); 50 $\mu g\,kg^{-1}$ (▲). Histamine was injected 1 h after hypophysectomy. Each point indicates the mean ± s.e.mean ($n = 5$–6). Significantly different from the control group: $*P<0.05$ and $**P<0.01$.

### *Effect of stimulation of the adrenal nerves on plasma ACTH and corticosterone concentrations*

When plasma ACTH and corticosterone concentrations were measured after operation, the values were 61.5 ± 2.8 pg $ml^{-1}$ and 0.54 ± 0.02 $\mu g\,ml^{-1}$, respectively. These values were somewhat higher than those seen before the operation (53.5 ± 4.1 pg $ml^{-1}$ for ACTH and 0.49 ± 0.02 $\mu g\,ml^{-1}$ for corticosterone). Electrical stimulation to the adrenal nerve resulted in an increase in plasma corticosterone concentration. A significant effect was observed from 5 to 30 min ($P<0.01$) after stimulation of the adrenal nerve. However, plasma ACTH concentration was not affected (Table 2).

### *Effects of 2-methylhistamine, 4-methylhistamine and impromidine on plasma ACTH and corticosterone concentrations*

When 2-methylhistamine, a representative $H_1$-agonist, was injected i.c.v. at doses of 10–50 $\mu g\,kg^{-1}$, both plasma ACTH

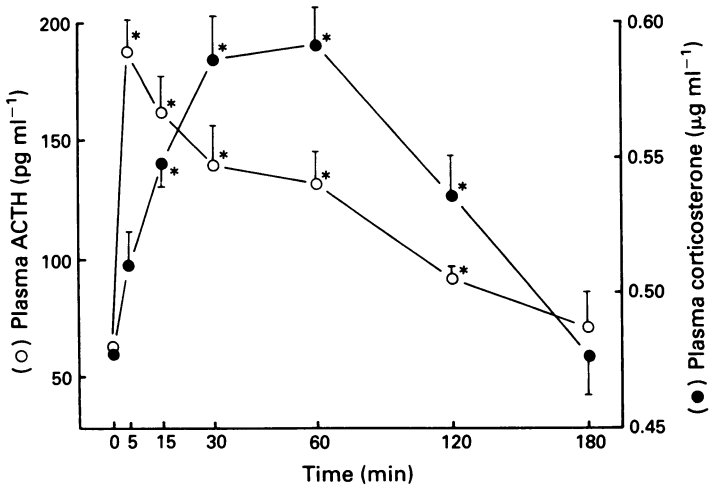



**Figure 2** Changes in plasma ACTH and corticosterone concentrations induced by intravenous injection of CRF-41 in rats. Each point indicates the mean ± s.e.mean ($n = 5$). CRF-41 was injected at a dose of 10 $\mu g\,kg^{-1}$. Plasma ACTH, pg $ml^{-1}$ (○); plasma corticosterone, $\mu g\,ml^{-1}$ (●). Significantly different from pre-drug value: $*P<0.05$.

**Table 1** Effect of intracerebroventricular injection of histamine on the adrenal nerve activity in rats

| Drug | Dose ($\mu g\ kg^{-1}$) | Discharge rates (Hz) Before | 5 | 15 | 30 | 60 | 120 min |
|---|---|---|---|---|---|---|---|
| Control | – | 101.0 ± 2.5 | 102.0 ± 4.1 | 105.0 ± 3.4 | 104.0 ± 3.3 | 104.0 ± 3.3 | 102.0 ± 3.2 |
| Histamine | 10 | 105.0 ± 4.7 | 108.0 ± 3.8 | 111.0 ± 3.5 | 109.5 ± 4.0 | 108.0 ± 3.8 | 106.5 ± 4.0 |
| | 20 | 106.5 ± 4.6 | 106.5 ± 4.6 | 109.5 ± 3.4 | 112.5 ± 2.6 | 111.0 ± 2.7 | 106.5 ± 4.6 |
| Drug | Dose ($\mu g\ kg^{-1}$) | Amplitudes ($\mu V$) Before | 5 | 15 | 30 | 60 | 120 min |
| Control | – | 18.2 ± 1.0 | 18.6 ± 1.0 | 18.3 ± 1.4 | 18.1 ± 1.2 | 18.5 ± 1.9 | 18.2 ± 1.4 |
| Histamine | 10 | 18.4 ± 1.0 | 23.2 ± 1.2* | 30.2 ± 2.0** | 28.5 ± 1.4** | 23.6 ± 0.9 | 18.7 ± 0.9 |
| | 20 | 18.2 ± 1.3 | 30.2 ± 1.8** | 36.6 ± 0.9** | 29.1 ± 1.3** | 26.4 ± 1.5 | 19.7 ± 1.2 |

Control: the same volume of saline was injected.
Each value indicates mean ± s.e.mean ($n = 5$).
Significantly different from the control group: $^*P<0.05$ and $^{**}P<0.01$.

**Table 2** Effect of stimulation of the adrenal nerves on the plasma ACTH and corticosterone concentrations

| Treatment | ACTH concentration ($pg\ ml^{-1}$) Before | 5 | 10 | 15 | 30 | 60 min |
|---|---|---|---|---|---|---|
| Control | 61.5 ± 2.8 | 63.2 ± 3.6 | 61.2 ± 2.6 | 62.5 ± 3.8 | 62.4 ± 2.9 | 62.3 ± 4.7 |
| ES | 61.7 ± 3.7 | 64.9 ± 4.3 | 59.4 ± 4.8 | 63.9 ± 4.2 | 64.7 ± 4.5 | 60.0 ± 6.6 |
| Treatment | Corticosterone concentration ($\mu g\ ml^{-1}$) Before | 5 | 10 | 15 | 30 | 60 min |
| Control | 0.54 ± 0.02 | 0.55 ± 0.02 | 0.55 ± 0.01 | 0.54 ± 0.02 | 0.53 ± 0.02 | 0.55 ± 0.02 |
| ES | 0.55 ± 0.02 | 0.60 ± 0.02 | 0.63 ± 0.01** | 0.65 ± 0.02** | 0.64 ± 0.02** | 0.61 ± 0.02 |

ES: electrical stimulation. Adrenal nerves were stimulated electrically (100 Hz, 1 ms, 500 $\mu A$, for 60 s).
Each value indicates mean ± s.e.mean ($n = 6$).
Significantly different from control group: $^{**}P<0.01$.

and corticosterone concentrations increased. A significant increase was observed at doses of 20 and 50 $\mu g\ kg^{-1}$ ($P<0.05$ or $P<0.01$). When 4-methylhistamine and impromidine, $H_2$-agonists, were similarly injected, an increase in both plasma ACTH and corticosterone concentrations was elicited, but in both cases the potencies were slightly less than those induced by 2-methylhistamine. A significant increase was observed at doses higher than 20 $\mu g\ kg^{-1}$ in both cases ($P<0.05$ or $P<0.01$, Figure 4).

### *Effects of pyrilamine, cimetidine and ranitidine on the elevation of plasma ACTH and corticosterone concentrations induced by histamine*

As shown in Table 3, when pyrilamine, an $H_1$-antagonist, was injected i.c.v. before histamine (10 $\mu g\ kg^{-1}$) at a dose of 26 $\mu g\ kg^{-1}$ (the molar equivalent of 10 $\mu g\ kg^{-1}$ of histamine), it significantly inhibited histamine-induced ACTH and corticosterone elevations ($P<0.05$). On the other hand, when the $H_2$-antagonists, cimetidine and ranitidine, at doses of 22 $\mu g\ kg^{-1}$ and 28 $\mu g\ kg^{-1}$ (each dose equivalent to 10 $\mu g\ kg^{-1}$ of histamine), were given as pretreatment by i.c.v. injections, no visible changes were elicited in histamine-induced (10 $\mu g\ kg^{-1}$) ACTH and corticosterone release. At the doses employed in the experiment, pyrilamine, cimetidine or ranitidine did not induce an effect.

### *Effects of cimetidine and ranitidine on the elevation of plasma ACTH and corticosterone concentrations induced by 4-methylhistamine*

When cimetidine at a dose of 44 $\mu g\ kg^{-1}$ (equivalent to a dose of 20 $\mu g\ kg^{-1}$ of 4-methylhistamine) or ranitidine at a dose of 56 $\mu g\ kg^{-1}$ (equivalent to a dose of 20 $\mu g\ kg^{-1}$ of 4-methylhistamine) was injected i.c.v. in combination with 4-methylhistamine (20 $\mu g\ kg^{-1}$), the elevation of plasma ACTH and corticosterone concentrations induced by 4-methylhistamine was significantly inhibited ($P<0.05$, Table 4). Cimetidine or

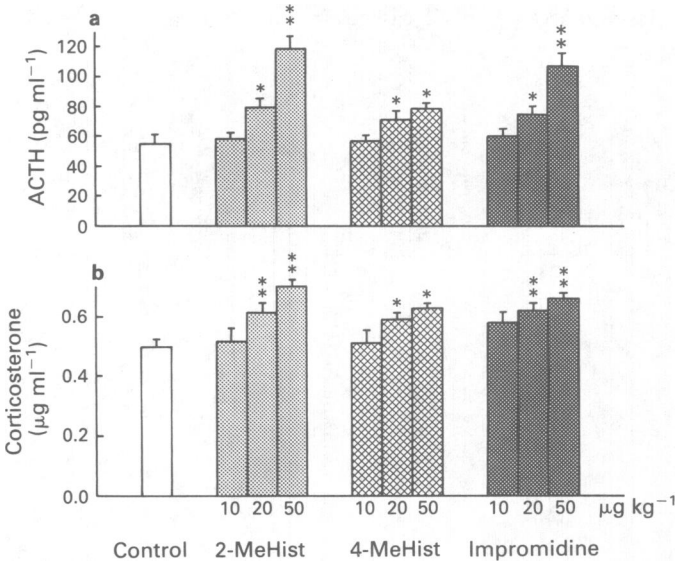



**Figure 4** Changes in plasma ACTH (a) and corticosterone (b) concentrations induced by intracerebroventricular injection of 2-methylhistamine (2-MeHist), 4-methylhistamine (4-MeHist) and impromidine in rats. Each column represents the mean ± s.e.mean ($n = 5$–8). Drugs were injected 15 min before the blood sampling. Significantly different from control group: $^*P<0.05$ and $^{**}P<0.01$.

**Table 3** Effects of pyrilamine, cimetidine and ranitidine on the elevation of plasma ACTH and corticosterone concentrations induced by intracerebroventricular injection of histamine (Hist) in rats

| *Drugs* | *ACTH concentration* (pg ml$^{-1}$) | *Corticosterone concentration* (μg ml$^{-1}$) |
|---|---|---|
| Control | 55.6 ± 4.4 | 0.50 ± 0.02 |
| Hist 10 μg kg$^{-1}$ | 134.8 ± 14.0 | 0.66 ± 0.02 |
| Hist + pyrilamine 26 μg kg$^{-1}$ | 68.6 ± 12.0* | 0.54 ± 0.04* |
| Hist + cimetidine 22 μg kg$^{-1}$ | 140.4 ± 19.3 | 0.66 ± 0.04 |
| Hist + ranitidine 28 μg kg$^{-1}$ | 133.3 ± 12.2 | 0.65 ± 0.08 |
| Pyrilamine 26 μg kg$^{-1}$ | 57.3 ± 8.4 | 0.52 ± 0.05 |
| Cimetidine 22 μg kg$^{-1}$ | 52.3 ± 3.9 | 0.50 ± 0.07 |
| Ranitidine 28 μg kg$^{-1}$ | 55.7 ± 2.9 | 0.49 ± 0.07 |

Each value indicates mean ± s.e.mean ($n = 5-8$).
Pyrilamine, cimetidine and ranitidine were injected 15 min before injection of histamine. Fifteen minutes after histamine injection, blood was collected.
Significantly different from histamine-treated group: *$P < 0.05$.

**Table 4** Effects of cimetidine and ranitidine on the elevation of plasma ACTH and corticosterone concentrations induced by 4-methylhistamine (4-MeHist)

| *Drugs* | *ACTH concentration* (pg ml$^{-1}$) | *Corticosterone concentration* (μg ml$^{-1}$) |
|---|---|---|
| Control | 55.6 ± 4.4 | 0.50 ± 0.02 |
| 4-MeHist 20 μg kg$^{-1}$ | 70.4 ± 4.2 | 0.59 ± 0.02 |
| 4-MeHist + cimetidine 44 μg kg$^{-1}$ | 56.0 ± 3.5* | 0.51 ± 0.03* |
| 4-MeHist + ranitidine 56 μg kg$^{-1}$ | 55.0 ± 2.3* | 0.48 ± 0.03* |
| Cimetidine 44 μg kg$^{-1}$ | 54.8 ± 1.6 | 0.51 ± 0.04 |
| Ranitidine 56 μg kg$^{-1}$ | 54.3 ± 2.6 | 0.50 ± 0.02 |

Each value indicates mean ± s.e.mean ($n = 5-6$).
Cimetidine and ranitidine were injected 15 min before histamine injection. Fifteen minutes after 4-methylhistamine injection, blood was collected.
Significantly different from 4-methylhistamine-treated group: *$P < 0.05$.

ranitidine alone caused no appreciable effect even at doses of 44 μg kg$^{-1}$ and 56 μg kg$^{-1}$, respectively.

### *Effects of (R)-α-methylhistamine and thioperamide on plasma ACTH and corticosterone concentrations*

Neither (R)-α-methylhistamine nor thioperamide, an $H_3$-receptor agonist and antagonist, respectively, caused any change in plasma ACTH concentrations at doses of 20 and 50 μg kg$^{-1}$. Similarly, no changes were observed in plasma corticosterone concentrations (Table 5).

## Discussion

In preliminary experiments, we studied the most appropriate way to collect blood in rats, because the trauma of anaesthesia and surgery themselves may affect ACTH and corticosterone concentrations in the blood. To avoid such artifacts, blood samples were collected in the following conditions and the concentrations of ACTH and corticosterone were compared: by cardiac puncture with and without anaesthesia; via the cannula in the carotid artery under anaesthesia (8 h after surgery) and via the cannula in the carotid artery without anaesthesia and in unrestrained conditions (8 h after

**Table 5** Effects of (R)-α-methylhistamine ((R)-α-MeHist) and thioperamide on plasma ACTH and corticosterone concentrations

| *Drugs* | *Dose* (μg kg$^{-1}$) | Before | 5 | 15 | 30 | 60 | 120 min |
|---|---|---|---|---|---|---|---|
| | | | *ACTH concentration* (pg ml$^{-1}$) | | | | |
| Control | – | 52.0 ± 3.5 | 50.5 ± 3.2 | 49.6 ± 2.9 | 49.8 ± 4.1 | 50.2 ± 2.5 | 50.6 ± 3.9 |
| (R)-α-MeHist | 20 | 52.5 ± 2.7 | 51.0 ± 3.4 | 50.7 ± 2.8 | 53.1 ± 3.8 | 53.5 ± 3.8 | 51.0 ± 4.3 |
| | 50 | 51.0 ± 4.2 | 52.0 ± 2.7 | 51.0 ± 3.6 | 52.8 ± 3.1 | 51.9 ± 2.7 | 51.0 ± 4.4 |
| Thioperamide | 20 | 52.0 ± 4.3 | 51.7 ± 3.6 | 48.6 ± 3.5 | 49.2 ± 4.2 | 48.7 ± 3.4 | 48.7 ± 3.9 |
| | 50 | 51.3 ± 4.0 | 47.6 ± 3.7 | 47.6 ± 3.0 | 50.9 ± 5.5 | 50.4 ± 2.7 | 52.4 ± 4.1 |
| | | | *Corticosterone concentration* (μg ml$^{-1}$) | | | | |
| Control | – | 0.49 ± 0.02 | 0.50 ± 0.02 | 0.52 ± 0.02 | 0.52 ± 0.03 | 0.51 ± 0.03 | 0.51 ± 0.03 |
| (R)-α-MeHist | 20 | 0.50 ± 0.04 | 0.50 ± 0.04 | 0.49 ± 0.03 | 0.53 ± 0.04 | 0.53 ± 0.02 | 0.51 ± 0.02 |
| | 50 | 0.49 ± 0.02 | 0.51 ± 0.01 | 0.50 ± 0.07 | 0.52 ± 0.04 | 0.49 ± 0.03 | 0.51 ± 0.04 |
| Thioperamide | 20 | 0.50 ± 0.04 | 0.48 ± 0.03 | 0.51 ± 0.04 | 0.53 ± 0.04 | 0.48 ± 0.04 | 0.48 ± 0.03 |
| | 50 | 0.49 ± 0.02 | 0.48 ± 0.03 | 0.51 ± 0.03 | 0.50 ± 0.05 | 0.52 ± 0.02 | 0.50 ± 0.02 |

Each value indicates mean ± s.e.mean ($n = 5-7$).

anaesthesia and surgery). As a result, it was found that the most suitable way was via the cannula in the carotid artery without anaesthesia and in unrestrained conditions. Under these conditions, both ACTH and corticosterone concentrations were always stable and were lower than those of animals subjected to the other procedures; hence this protocol was selected for the experiments described.

In the present study, it was found that i.c.v. injection of histamine induced almost simultaneous increase in plasma ACTH and glucocorticoid concentrations in rats. In dogs, the increase in plasma corticosterone concentration was more rapid and more remarkable than that seen in ACTH after i.c.v. injection of histamine (Tsujimoto *et al.*, 1993). A similar result was observed in the present study, although the changes in plasma concentrations were less marked than those seen in dogs. In the case of i.v. injection of CRF-41, a rapid initial increase in plasma ACTH concentration was followed by a gradual increase in plasma corticosterone concentration in rats. These findings seem to indicate that corticosterone release induced by i.c.v. injection of histamine takes place to some extent without involvement of ACTH release. As shown in Figure 3, a significant increase in plasma corticosterone concentration was induced by i.c.v. injection of histamine even in hypophysectomized rats. It may be assumed, therefore, that part of the corticosterone release elicited by histamine was produced without participation of ACTH secretion. Consequently, it was postulated that electrical signals passing through the neurones connecting the brain to the adrenal cortex may be essential to bring about histamine-induced corticosterone secretion.

Halász & Szentágothai (1959) suggested the possible existence of an afferent nervous connection between the adrenal cortex and the opposite nucleus ventromedial hypothalamus. In the present study, the amplitude of the adrenal nerve activity increased after i.c.v. injection of histamine. Therefore, it seems quite certain that i.c.v. injected histamine stimulates the adrenal gland via a neuronal pathway. Unsicker (1971) reported that nerve fibres are regularly found in the fasciculata zone of the rat adrenal cortex, and nerve fibres containing synaptic vesicles and two types of dense-cored vesicles in contact with endocrine cells have been observed by electron microscopy.

The finding that electrical stimulation of the adrenal nerve resulted in an increase in plasma corticosterone concentration may support the assumption that the adrenal cortex is also innervated by the adrenal nerve. Actually, it has been reported that the adrenal cortex contains a complex autonomic innervation, one part of which innervates the cortex independently of the splanchnic nerve, while the other part appears to originate in the adrenal medulla to be regulated by splanchnic nerve activity (Holzwarth *et al.*, 1987). Morphological evidence for adrenal cortical nerves indicates that several peptidergic neuronal systems exist in the adrenal cortex such as vasoactive intestinal peptide (VIP), neuropeptide Y and substance P (Holzwarth *et al.*, 1987). Infusion of VIP to the capsule-glomerulosa system caused a dose-dependent output of corticosterone (Hozwarth *et al.*, 1987). Furthermore, when primary cultured bovine adrenocortical cells were treated with substance P, cortisol output increased in a dose-dependent fashion (Yoshida *et al.*, 1992). As a result of these findings, it can be postulated that i.c.v. injection of histamine stimulates the adrenal nerves, and this may, in turn, result in the release of substance P or VIP in the adrenal cortex which, results in corticosterone release. As shown in Table 2, plasma ACTH concentration was not elevated after electrical stimulation of the adrenal nerves, while corticosterone release was induced. This clearly indicates that corticosterone can be released from the adrenal gland without involvement of the hypophysis-adrenocortical system.

In the present study, $H_2$-agonists, 4-methylhistamine and impromidine also caused an effect similar to that seen after histamine application, though the effects of these drugs were weaker than those of histamine or 2-methylhistamine. In addition, both cimetidine and ranitidine, $H_2$-receptor antagonists, caused an inhibition of plasma ACTH and corticosterone increase induced by 4-methylhistamine. However, neither antagonist was effective in inhibiting the histamine-induced increase in plasma ACTH and corticosterone concentrations. On the contrary, Bugajski & Gadek (1983) reported that cimetidine and metiamide inhibited histamine-induced corticosterone increase. It seems likely that histamine-induced hormone secretion is mediated mainly through $H_1$-receptor, and to a lesser extent through the $H_2$-receptor. Consequently, even if $H_2$-antagonists blocked corticosteroidgenesis due to histamine via the $H_2$-receptor, the effect through the $H_1$-receptor may appear. This postulation seems to coincide with the fact that both cimetidine and ranitidine inhibited the 4-methylhistamine-induced response but not the histamine effect. Neither (**R**)-α-methylhistamine nor thioperamide caused a significant elevation of plasma ACTH and corticosterone concentrations even at a dose of $50\,\mu g\,kg^{-1}$. Arrang *et al.* (1987) reported that (**R**)-α-methylhistamine and thioperamide are highly potent and selective agonist and antagonist respectively for $H_3$-receptors. Therefore, it is likely that the $H_3$-receptor may not be involved in histamine-induced ACTH and corticosterone secretions.

From these findings, it was concluded that (1) a neuronal pathway from the hypothalamus to the adrenal cortex may be essential for the rapid increase in the corticosterone concentration induced by histamine, and that (2) not only the $H_1$- but also the $H_2$-receptor is involved in the histamine-induced adrenocortical response in rats.

## References


ARRANG, J.-M., GARBARG, M., LANCELOT, J.-C., LECOMTE, J.-M., POLLARD, H., ROBBA, M., SCHUNACK, W. & SCHWARTZ, J.-C. (1987). Highly potent and selective ligands for histamine $H_3$-receptors. *Nature*, **327**, 117–123.

BUGAJSKI, J. & GADEK, A. (1983). Central $H_1$- and $H_2$-histaminergic stimulation of pituitary-adrenocortical response under stress in rats. *Neuroendocrinol.*, **36**, 424–430.

GLICK, D., REDLICH, D. VON. & LEVIN, S. (1964). Fluorometric determination of corticosterone and cortisol in 0.02–0.05 milliliters of plasma or submilligram samples of adrenal tissue. *Endocrinol.*, **74**, 653–655.

DE GROOT, J. (1959). The rat forebrain in stereotaxic coordinates. *Verh. K. Ned. Acad. Wet. Natuurkund.*, **52**, 1–40.

HALÁSZ, B. & SZENTÁGOTHAI, J. (1959). Histologischer Beweis einer nervösen Signalübermittlung von der Nebennierenrinde zum Hypothalamus. *Z. Zellforsch.*, **50**, 297–306.

HAYNES, R.C. Jr. (1990). Adrenocorticotropic hormone: adrenocortical steroids and their synthetic analogs; inhibitors of the synthesis and actions of adrenocortical hormones. In *The Pharmacological Basis of Therapeutics*, 8th ed. Gilman, A.G., Rall, T.W., Nies, A.S. & Taylor, P. pp. 1431–1462. New York: Pergamon Press.

HOLZWARTH, M.A., CUNNINGHAM, L.A. & KLEITMAN, N. (1987). The role of adrenal nerves in the regulation of adrenocortical functions. *Ann. N.Y. Acad. Sci.*, **512**, 449–464.

KNIGGE, U., WOLLESEN, F., DEJGAARD, A., LARSEN, K. & CHRISTIANSEN, P.M. (1983). The effect of histamine stimulation and $H_2$-receptor inhibition on the pituitary prolactin and ACTH release and on cortisol secretion in human males. *Horm. Metabol. Res*,. **15**, 89–91.

MORITA, Y. & KOYAMA, K. (1979). Histamine-induced ACTH secretion and inhibitory effect of antihistaminic drugs. *Jpn. J. Pharmacol.*, **29**, 59–65.

TANAKA, A. (1955). A simple method of hypophysectomy on rats. *Annu. Rep. Shionogi. Res. Lab.*, **5**, 678–681.

TOGASHI, H. (1983). Central and peripheral effects of clonidine on the adrenal medullary function in spontaneously hypertensive rats. *J. Pharmacol. Exp. Ther.*, **225**, 191–197.

TSUJIMOTO, S., KAMEI, C., YOSHIDA, T. & TASAKA, K. (1993). Changes in plasma ACTH and cortisol levels induced by intracerebroventricular injection of histamine and its related compounds in dogs. *Pharmacology*, (in press).

UNSICKER, K. (1971). On the innervation of the rat and pig adrenal cortex. *Z. Zellforsch.*, **116**, 151–156.

YOSHIDA, T., MIO, M. & TASAKA, K. (1992). Cortisol secretion induced by substance P from bovine adrenocortical cells and its inhibition by calmodulin inhibitors. *Biochem. Pharmacol.*, **43**, 513–517.

*(Received October 29, 1992*
*Revised February 22, 1993*
*Accepted February 24, 1993)*

*Br. J. Pharmacol.* (1993), **109**, 814–818 © Macmillan Press Ltd, 1993

# *In vivo* release of dopamine from rat striatum, substantia nigra and prefrontal cortex: differential modulation by baclofen

Marti Santiago, Alberto Machado & [1]Josefina Cano

Departamento de Bioquimica, Facultad de Farmacia, E-41012 Sevilla, Spain

**1** The effect of baclofen, a $GABA_B$ receptor agonist, on the release of dopamine from the striatum (ST), substantia nigra (SN) and prefrontal cortex (PFC) of the rat was examined by intracerebral microdialysis.

**2** Perfusion of baclofen 50 μM did not affect the striatal release of dopamine. However, dopamine release was markedly reduced in the SN and PFC.

**3** 3,4-Dihydroxyphenylacetic acid and homovanillic acid output increased in the ST and decreased in the SN and PFC when baclofen was perfused through the microdialysis probe. 5-Hydroxyindoleacetic acid levels were not affected in any experimental condition by baclofen perfusion.

**4** The results suggest that $GABA_B$ receptors modulate the release of dopamine in the SN and PFC, but do not affect the striatal release of dopamine, which indicates that the role of GABA receptor activation is different in the dopaminergic terminals of the ST and PFC.

**Keywords:** Dopamine; microdialysis; (±)-baclofen; $GABA_B$ receptor agonist; striatum; substantia nigra; prefrontal cortex

## Introduction

γ-Aminobutyric acid (GABA) is known to be a major inhibitory neurotransmitter in the central nervous system and is thought to play important roles in various neurological and mental disorders. GABA interacts with two main types of sites referred to as $GABA_A$ and $GABA_B$ receptors (Bowery *et al.*, 1980; 1987; Hill & Bowery, 1981). $GABA_A$ receptors are oligomeric receptor proteins that form an integral $Cl^-$ ion channel (Olsen, 1982; Schofield *et al.*, 1987), thus contributing to the prompt inhibition of cellular excitability. The $GABA_A$ receptor is sensitive to the effects of muscimol (a GABA agonist) and bicuculline (a GABA antagonist). Less is currently known about $GABA_B$ receptors which do not contain an integral ion channel and are thus responsible for slower responses through receptor-G-protein-effector complexes. G-protein may be directly coupled to $K^+$ or $Ca^{2+}$ channels. The $GABA_B$ receptor is sensitive to baclofen (a GABA agonist) and, to some extent to muscimol, but is not sensitive to bicuculline (Hill & Bowery, 1981; Johnston, 1986).

Evidence has accumulated that GABA is involved in the regulation of other neuronal systems, such as dopaminergic (Dray, 1979; O'Neill, 1986) and cholinergic (Ferkany & Enna, 1980; Scatton & Bartholini, 1982; Miller & Richter, 1986) neurones. The major and extensive focus of studies of neurotransmitter interactions has been in the striatum (ST) and substantia nigra (SN) which are connected by the striatonigral GABAergic pathway and nigrostriatal dopaminergic pathway (Ladinsky *et al.*, 1976; Dray, 1979; Ferkany & Enna, 1980). However, little is known concerning dopamine-GABA interactions within the cerebral cortex. While there is no evidence of direct interrelationships or connections between dopamine afferents and intracortical GABA neurones (Verney *et al.*, 1990), current topographical data on the dopamine and GABA innervation of the rat cerebral cortex raise the possibility of such interactions. Immunocytochemical visualization of dopamine terminals by electron microscopy showed that these cortical afferents in rat prefrontal cortex (PFC) form synaptic contacts (Van Eden *et al.*, 1987; Séquéla *et al.*, 1988), preferentially on the dendritic tree of the pyramidal neurones (Verney *et al.*, 1990). Likewise, cortical GABA terminals also form synaptic contact onto pyramidal neurones (Houser *et al.*, 1984; Séguéla *et al.*, 1985). These pyramidal neurones are the dominant afferent to the neostriatum, therefore, the inhibitory effect of dopamine and GABA on the cortical neurones could regulate the output of the PFC.

In the present paper, we have studied the effect of baclofen on the release of dopamine in the PFC by means of an intracerebral microdialysis technique. For comparison and discussion of the results obtained in the PFC, we have carried out parallel experiments in the ST and SN.

## Methods

### *Animals and drug treatment*

Male albino Wistar rats were used for the experiments. The rats were housed in plastic cages (35 × 35 × 40 cm) and allowed free access to food and water.

The following drugs were dissolved in the perfusion fluid: (±)-baclofen and nomifensine maleate (Research Biochemical Inc., Natick, MA, U.S.A.).

### *Surgery and brain dialysis*

Microdialysis in the ST, SN and PFC was performed with an I-shaped cannula (Santiago & Westerink, 1990). The exposed tip of the dialysis membrane was 4, 2 and 3 mm, respectively. The dialysis tube (i.d., 0.22 mm; o.d., 0.31 mm) was prepared from polyacrylonitrile/sodium methalyl sulphonate copolymer (AN 69, Hospal, Bologna, Italy). The *in vitro* recovery of the membrane (4 mm length; $n = 5$) was: 22.7 ± 1.8%, for dopamine; 31.6 ± 2.5%, for 3,4-dihydroxyphenylacetic acid (DOPAC); 28.5 ± 2.2%, for homovanillic acid (HVA); and 29.5 ± 2.6%, for 5-hydroxyindoleacetic acid (5-HIAA). The probes were implanted into the ST [A/P 0.6, L/M 2.8, V/D 6.0, from bregma point and dura], left SN [A/P 3.8, L/M 3.8, V/D 8.7, from interaural line and dura, at an angle of 12°] and left PFC [A/P 3.2, L/M 1.3, V/D 3.0, from bregma point and dura, at an angle of 14°] during general chloral hydrate (400 mg $kg^{-1}$, i.p.) and local lignocaine (10% w/v in water) anaesthesia.

[1] Author for correspondence at: Departamento de Bioquimica, Bromatologia y Toxicologia, Facultad de Farmacia, E-41012 Sevilla, Spain.

The perfusion experiments were carried out 24–48 h after implantation of the probes. Brain dialysis was performed with a fully automated on-line system as has been previously described (Westerink *et al.*, 1987). In brief, two polyethylene tubes (inner diameter = 0.28 mm) were connected to the outlets of the dialysis tube. One tube (45 cm in length) was connected to the perfusion pump, and the other (45 cm in length) to the injection valve of the high performance liquid chromatography (h.p.l.c.) apparatus. From the time baclofen was included in the Ringer solution delivered by the perfusion pump to the time when the first sample with baclofen was injected onto the column, there was a lag time of about 30 min; the data presented are corrected to account for this lag time. With the help of an electronic timer, the injection valve was held in the load position for 15 min, during which the sample loop (40 μl) was filled with dialysate. The valve then switched automatically to the injection position for 15 s. This procedure was repeated every 15 min, which was the time needed to record a complete chromatogram. The ST, SN and PFC were perfused with a Ringer solution at a flow rate of 1.5 μl $min^{-1}$ (perfusor VI, B. Braun, Melsungen, Germany). The composition of the Ringer solution was (in mM): NaCl 140, KCl 4.0, $CaCl_2$ 1.2 and $MgCl_2$ 1.0.

When the experiment was terminated, the rat was given an overdose of chloral hydrate, and the brain was fixed with 4% paraformaldehyde via intracardiac perfusion. Coronal sections (40 μm thick) were made, and dialysis probes placement localized according to the atlas of Paxinos & Watson, 1986.

### *Chemical assays*

Dopamine, DOPAC, HVA and 5-HIAA were quantitated by h.p.l.c. with electrochemical detection. A Kontron 420 pump was used in conjunction with a glassy carbon electrode set at − 780 mV (ANTEC, The Netherlands). A Merck Lichrocart cartridge (125 mm × 4 mm) column filled with Lichrospher reverse-phase $C_{18}$ 5 μM material was used. The mobile phase consisted of a mixture of 0.05 M sodium acetate, 0.4 mM 1-octanesulphonic acid, 0.3 mM $Na_2EDTA$ and 70 ml methanol $l^{-1}$, adjusted to pH 4.1 with acetic acid. The flow rate was 0.8 ml $min^{-1}$ and the detection limit for dopamine, DOPAC, HVA and 5-HIAA was 5, 5, 20 and 15 fmol per injection, respectively.

### *Expression of results and statistics*

The average of the last four stable samples before drug-treatment was considered as the control and was defined as 100%. All values given are expressed as percentages of controls. Difference between the average dialysate concentrations of the control and drugs treatment was compared by Kruskal-Wallis analysis of variance by ranks, and, where appropriate (H value greater than the 95% confidence level), comparison of the means was carried out by the Mann-Whitney U-test.

## Results

Table 1 summarizes the extracellular levels of dopamine, DOPAC, HVA and 5-HIAA in the ST, SN and PFC in the absence (control) and in the presence (+ nomifensine) of the dopamine uptake inhibitor, nomifensine (5 μM). Dopamine release was increased by nomifensine 7.5, 6.8 and 10.0 times in the ST, SN and PFC, respectively.

The PFC is characterized by a HVA output higher than DOPAC output (Abercrombie *et al.*, 1989; Maisonneuve *et al.*, 1990). In the present paper, we found that HVA outflow was twice the DOPAC outflow (Table 1), in agreement with the previous studies.

Baclofen (50 μM) was either perfused alone for 1 h or co-perfused with nomifensine (5 μM) (which was included in the Ringer solution during the whole experiment) for 1 h. Nomifensine was included to stimulate the basal release of dopamine in the PFC, which was near to the detection limit of our equipment. Baclofen (50 μM), did not affect dopamine release in the ST either with or without nomifensine (5 μM) (Figure 1a and b). In contrast, baclofen (50 μM) produced a significant decrease in dopamine release in the SN (Figures 2a and b) and PFC (Figure 3). The strongest effect was seen with baclofen alone perfused into the SN (Figure 1a).

DOPAC and HVA levels were affected differently by baclofen (50 μM) when the ST results are compared to the SN or PFC values. In the first brain structure, baclofen (50 μM) produced a marked increase in the output of DOPAC and HVA (Figures 1a and b). However, in the SN (Figure 2a and b) and PFC (Figure 3), baclofen (50 μM) produced a significant decrease in the output of DOPAC and HVA.

5-HIAA levels were not affected by baclofen (50 μM) in any of the brain structures studied (data not shown).

## Discussion

The present study has demonstrated that, activation of $GABA_B$ receptors by baclofen perfusion into the PFC and SN results in inhibition of dopamine release, but no effect on dopamine release in the ST. These results show that the action of baclofen on dopamine release from terminals is different in the PFC from the ST. These differences could be due to either the different origin of these dopaminergic terminals or different distribution of $GABA_B$ receptors in each structure.

**Table 1** Basal values of dopamine (DA), 3,4-dihydroxyphenylaceticacid (DOPAC), homovanillic acid (HVA) and 5-hydroxyindoleacetic acid (5-HIAA) in the corpus striatum, substantia nigra and prefrontal cortex

| | *DA* | *DOPAC* | *HVA* | *5-HIAA* |
|---|---|---|---|---|
| *Striatum* | | | | |
| Control[1] (7) | 12.6 ± 1.1 | 1657.1 ± 182.2 | 1231.1 ± 143.9 | 1059.9 ± 128.9 |
| + Nomifensine[2] (9) | 94.2 ± 13.6** | 755.7 ± 68.7** | 626.7 ± 39.1** | 931.9 ± 55.7 |
| *Substantia nigra* | | | | |
| Control[1] (9) | 1.0 ± 0.1 | 82.0 ± 16.6 | 74.1 ± 11.0 | 1374.3 ± 78.2 |
| + Nomifensine[2] (6) | 6.8 ± 2.4** | 66.1 ± 15.4 | 62.8 ± 9.9 | 1039.0 ± 73.4** |
| *Prefrontal cortex* | | | | |
| Control[1] (4) | 0.3 ± 0.03 | 13.2 ± 0.9 | 27.0 ± 1.1 | 325.9 ± 32.5 |
| + Nomifensine[2] (7) | 3.0 ± 0.4** | 12.7 ± 0.9 | 28.0 ± 2.7 | 344.0 ± 53.2 |

Data are mean ± s.e.mean values, expressed as fmol $min^{-1}$. Number of animals in parentheses. Nomifensine was infused at 5 μM concentration.

**$P < 0.01$, compared with its corresponding control value (Student's $t$ test).

[1]Experiments carried out 24 h after surgery.

[2]Experiments carried out 48 h after surgery.

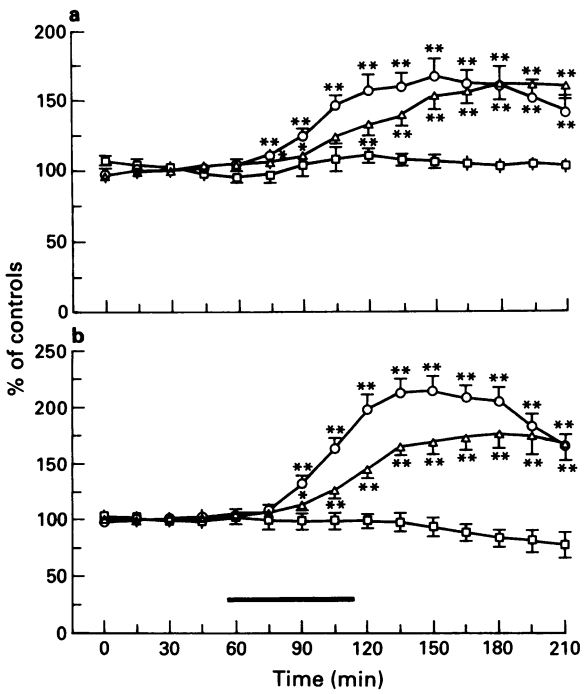



**Figure 1** Effect of the perfusion of (±)-baclofen 50 μM (black bar) on the extracellular output of dopamine (□), 3,4-dihydroxyphenylacetic acid (○) and homovanillic acid (△) in the corpus striatum in the absence (a, $n = 7$) and in the presence (b, $n = 7$) of nomifensine (5 μM). The data are means ± s.e.mean values, expressed as percentages of the controls. Statistical significance (Kruskal-Wallis followed by Mann-Whitney U-test): $*P<0.05$; $**P<0.01$, compared with the control value.

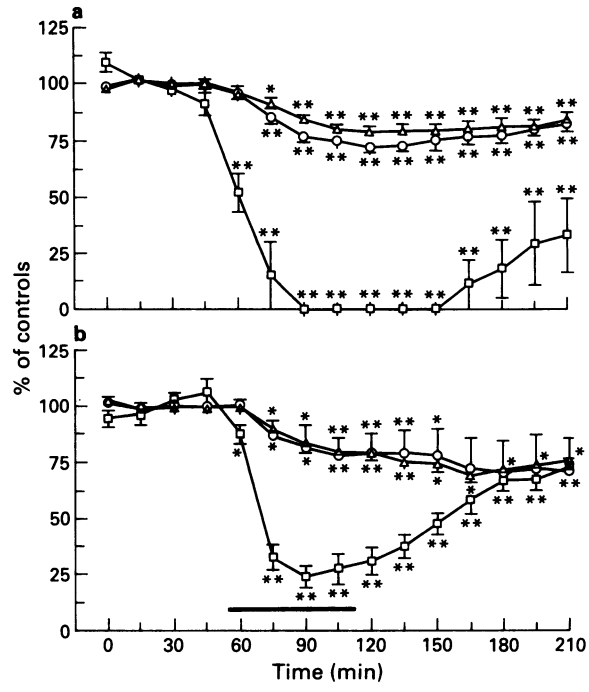



**Figure 2** Effect of the perfusion of (±)-baclofen 50 μM (black bar) on the extracellular output of dopamine (□), 3,4-dihydroxyphenylacetic acid (○) and homovanillic acid (△) in the substantia nigra in the absence (a, $n = 8$) and in the presence (b, $n = 6$) of nomifensine (5 μM). The data are means ± s.e.mean values, expressed as percentages of the controls. Statistical significance (Kruskal-Wallis followed by Mann-Whitney U-test): $*P<0.05$; $**P<0.01$, compared with the control value.

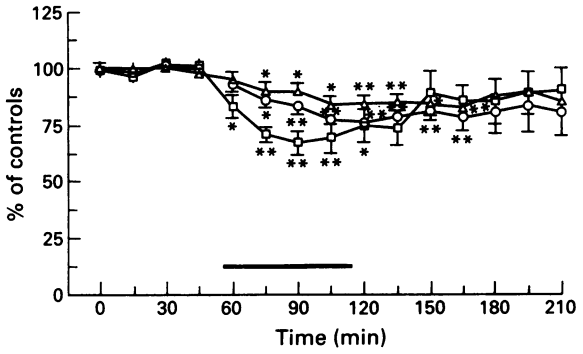



**Figure 3** Effect of the perfusion of (±)-baclofen 50 μM (black bar) on the extracellular output of dopamine (□), 3,4-dihydroxyphenylacetic acid (○) and homovanillic acid (△) in the prefrontal cortex in the presence of nomifensine (5 μM). The data are means ± s.e.mean values ($n = 6$), expressed as percentages of the controls. Statistical significance (Kruskal-Wallis followed by Mann-Whitney U-test): $*P<0.05$; $**P<0.01$, compared with the control value.

It has been reported that GABA stimulates *in vitro* dopamine release in the ST and that GABA receptors are involved in this action (Giorguieff *et al.*, 1978). For example, muscimol and GABA stimulate dopamine release from striatal slices (Giorguieff *et al.*, 1978; Martin & Haubrich, 1978), indicating that $GABA_A$ receptors are implicated in this action. With respect to $GABA_B$ receptors, our results with microdialysis do not suggest a presynaptic location for them on dopaminergic terminals in the ST, as baclofen infusion had no effect on dopamine release. These results are in agreement with those obtained by Bonano & Raiteri (1987) who reported that baclofen was without effect on dopamine release from synaptosomes, while Waldmeier *et al.* (1992) have also indicated by microdialysis that baclofen does not affect striatal GABA release. Arias-Montano *et al.* (1991) suggested that $GABA_B$ receptors on dopaminergic terminals could control the synthesis of dopamine and the increase in DOPAC found in the present study after baclofen perfusion into the ST would support this view, since it has been suggested that DOPAC is formed from newly synthesized dopamine (Zetterström *et al.*, 1988).

In the SN, it is generally observed that $GABA_A$ receptor agonists stimulate dopaminergic neurones, while $GABA_B$ receptor agonists inhibit them (Olpe *et al.*, 1977; Grace & Bunney, 1984; Pinnock, 1984; Lacey *et al.*, 1988; Kalivas *et al.*, 1990). Therefore, it is well established that nigrostriatal dopaminergic neurones are under inhibitory GABAergic control by local circuits (Waldmeier, 1990). Based on these data, it has been proposed that $GABA_B$ receptors may be located directly on the dopamine perikarya where stimulation results in membrane hyperpolarization mediated by an increase in potassium conductance (Grace & Bunney, 1984; Lacey *et al.*, 1988). The present results are in agreement with the inhibition by $GABA_B$ receptors of the nigral dopaminergic activity, since baclofen infusion into the SN decreased the release of dopamine in the SN. It has been reported that intranigral injection of GABA decreases dopamine release in the ipsilateral ST (Reid *et al.*, 1988), while nigral perfusion of baclofen (10 μM) decreases dopamine release in the same SN and in the ipsilateral ST (Westerink *et al.*, 1992). However, Cheramy *et al.* (1978) showed that baclofen perfusion by means of a push-pull cannula into the SN produced an increase in the dopamine release in the SN and in the ipsilateral ST. A different position of the probe in the SN could explain these differences; an idea supported by the results of Floran *et al.* (1988) using slices showing that baclofen inhibits GABA release in the SN pars reticulata but not in the SN pars compacta. Neurones in the SN pars reticulata are much more sensitive to iontophoretic applica-

tion of GABA than are those of the SN pars compacta (Aghajanian & Bunney, 1975; Dray *et al.*, 1976).

Baclofen exerts a depressant action on synaptic transmission in the neocortex (Howe *et al.*, 1987), that is believed to result primarily from the activation of presynaptic $GABA_B$ receptors. Our results suggest that GABA in PFC inhibits the dopamine release by $GABA_B$ receptor activation, since baclofen perfused in the PFC produced a significant decrease in the extracellular output of dopamine and its metabolites, similar to that produced in the SN and completely different from that of the ST. These findings could suggest that the localization and role of the $GABA_B$ receptors in the PFC is similar to that in the SN and support the special characteristics of the dopaminergic terminals in the PFC in comparison to those of ST (Bannon *et al.*, 1981; Chiodo *et al.*, 1984). It is interesting to point out that the effect of baclofen, which is similar on A9 (Westerink *et al.*, 1992, present results) and A10 (Kalivas *et al.*, 1990) dopamine perikarya, contrasts with their terminals (ST and PFC; from present results). These differences between PFC and ST could be due to different local circuits in each structure.

This effect of baclofen seems to be reciprocal since dopamine administration has been found to decrease the release of GABA in cerebral cortex *in vitro* (Flint *et al.*, 1985). Likewise, the activation of $D_2$ receptors induces inhibition of the electrically evoked release of [$^3$H]-GABA from prefrontal cortical slices (Penit-Soria *et al.*, 1989). In addition to these biochemical data, current electrophysiological and pharmacological findings also support the possibility of an interaction between dopamine and GABA in the cerebral cortex (Penit-Soria *et al.*, 1987). Immunocytochemical visualization of dopamine and GABA terminals by electron microscopy showed that these cortical afferents in rat prefrontal cortex form synaptic contact preferentially on the pyramidal neurones (Houser *et al.*, 1984; Séguèla *et al.*, 1985; Verney *et al.*, 1990), therefore the functional output of the PFC could depend on dopamine-GABA local interactions.

One possible explanation for the observed decrease in DOPAC and HVA levels in the ST could be that control experiments were carried out 24 h after surgery and experiments including nomifensine in the Ringer solution were carried out 48 h after surgery. It has been reported previously that basal levels of DOPAC and HVA outflow change in the striatum when 24 and 48 h after surgery were compared (Robinson & Camp, 1991; Zis *et al.*, 1991). However, it is important to point out that the stability of the basal values of DOPAC and HVA in the PFC and SN when 24 h and 48 h levels after surgery are compared (Table 1). These discrepant results found in the PFC and SN with respect to the striatum argue against the possibility of a decline in 'recovery' in the brain, secondary to gliosis-related changes in diffusion (Westerink & Tuinte, 1986; Benveniste & Diemer, 1987).

The baclofen effect was specific for dopaminergic neurones, since 5-HIAA values were not affected by this $GABA_B$ receptor agonist, which could suggest that baclofen does not affect 5-hydroxytryptamine metabolism in any of the structures studied.

Our demonstration of the modulation of dopamine responsiveness by $GABA_B$ receptors leads to the conclusion that the function of dopamine might partially depend on its interaction with GABA systems. Considering the numerous baclofen therapeutic agents that are used clinically, it is important to be aware of the possibility that this drug might exert different effects on dopamine function, depending on the brain structure implicated.

This research was supported by a grant from DGICYT PM91-0097. M.S. thanks Ministerio de Educación y Ciencia, Spain, for a Contrato de Incorporación.

## References

ABERCROMBIE, E.D., KEEFE, K.A., DIFRISIA, D.S. & ZIGMOND, M.J. (1989). Differential effect of stress on in vivo dopamine release in striatum, nucleus accumbens, and medial frontal cortex. *J. Neurochem*, **52**, 1655–1658.

AGHAJANIAN, G.K. & BUNNEY, B.S. (1975). Dopaminergic and non-dopaminergic neurons of the substantia nigra: Differential responses to putative transmitters. In *Neuropsychopharmacology*. ed. Boissier, J.R., Hippius, H. & Pichot, P. pp. 444–452. New York: Excerpta Medica, Amsterdam and American Elsevier Pub. Co. Inc.

ARIAS-MONTANO, J.A., MARTINEZ-FONG, A. & ACEVES, J. (1991). Gamma-aminobutyric acid (GABA-B) receptor-mediated inhibition of tyrosine hydroxylase activity in the striatum of rat. *Neuropharmacol.*, **30**, 1047–1051.

BANNON, M.J., BUNNEY, E.B. & ROTH, R.H. (1981). Mesocortical dopamine neurones: rapid transmitter turnover compared to other brain catecholamine systems. *Brain Res.*, **218**, 376–382.

BENVENISTE, H. & DIEMER, N.H. (1987). Cellular reactions to implantation of a microdialysis tube in the rat hippocampus. *Acta Neuropathol. (Berlin)*, **74**, 234–238.

BONANNO, G. & RAITERI, M. (1987). Coexistence of carries for dopamine and GABA uptake on the same nerve terminal in the rat brain. *Br. J. Pharmacol.*, **91**, 237–243.

BOWERY, N.J., HILL, D.R., HUDSON, A.L., DOBLE, A., MIDDLEMISS, D.N., SHAW, J. & TURNBULL, M. (1980). (−)Baclofen decreases neurotransmitter release in the mammalian CNS by an action at a novel GABA receptor. *Nature*, **283**, 92–94.

BOWERY, N.G., HUDSON, A.L. & PRICE, G.W. (1987). $GABA_A$ and $GABA_B$ receptor site distribution in the rat central nervous system. *Neuroscience*, **20**, 365–383.

CHERAMY, A., NIEOULLON, A. & GLOWINSKI, J. (1987). GABAergic processes involved in the control of dopamine release from nigrostriatal dopaminergic neurons in the cat. *Eur. J. Pharmacol.*, **48**, 281–295.

CHIODO, L.A., BANNON, M.J., GRACE, A.A. & ROTH, R.H. (1984). Evidence for the absence of impulse regulating somatodendritic and synthesis-modulating nerve terminal autoreceptors on subpopulations of mesocortical dopamine neurones. *Neuroscience*, **12**, 1–16.

DRAY, A. (1979). The striatum and substantia nigra: a commentary on their relationships. *Neuroscience*, **4**, 1407–1439.

DRAY, A., GONYE, T.J. & OAKLEY, N.R. (1976). Caudate stimulation and substantia nigra activity in the rat. *J. Physiol*, **259**, 825–829.

FERKANY, J.W. & ENNA, S.J. (1980). Interaction between GABA agonists and the cholinergic muscarinic system in rat corpus striatum. *Life Sci.*, **27**, 143–149.

FLINT, R.S., MURPHY, J.M., CALKINS, P.M. & MCBRIDE, W.J. (1985). Monoamine amino acid and cholinergic interactions in slices of rat cerebral cortex. *Brain Res. Bull.*, **15**, 197–202.

FLORAN, B., SILVA, I., NAVA, C. & ACEVES, J. (1988). Presynaptic modulation of the release of GABA and $GABA_A$ receptors in pars compacta and $GABA_B$ receptors in pars reticulata of the rat substantia nigra. *Eur. J. Pharmacol.*, **150**, 277–286.

GIORGUIEFF, M.-F., KEMEL, M.L., GLOWINSKI, J. & BESSON, M.J. (1978). Stimulation of dopamine release by GABA in rat striatal slices. *Brain Res.*, **139**, 115–121.

GRACE, A.A. & BUNNEY, B.S. (1984). The control of firing pattern in nigral dopamine neurons: burst firing. *J. Neurosci.*, **4**, 2877–2890.

HILL, D.R. & BOWERY, N.G. (1981). $^3$H-baclofen and $^3$H-GABA bind to bicuculline-insensitive $GABA_B$ sites in rat brain. *Nature*, **290**, 149–152.

HOUSER, C.R., VAUGHN, J.E., HENDRY, S.C.H., JONES, E.G. & PETERS, A. (1984). GABA neurons in the cerebral cortex. In *Cerebral Cortex*, Vol. 2: *Functional Properties of Cortical Cells*. ed. Jones, E.G. & Peters, A. pp. 63–90. New York: Plenum Press.

HOWE, J.R., SUTOR, B. & ZEIGLGANSBERGER, W. (1987). Baclofen reduces post-synaptic potentials of rat cortical neurones by an action other than its hyperpolarizing action. *J. Physiol.*, **384**, 539–569.

JOHNSTON, G.A.R. (1986). Multiplicity of GABA receptors. In *Benzodiazepine/GABA Receptors and Chloride Channels*. ed. Olsen, R.W. & Venter, J.G. pp. 55–71. New York: Alan R. Liss.

KALIVAS, P.W., DUFFY, P. & EBERHARDT, H. (1990). Modulation of A10 dopamine neurons by gamma-aminobutyric acid agonists. *J. Pharmacol. Exp. Ther.*, **253**, 858–866.

LACEY, M.G., MERCURI, N.B. & NORTH, R.A. (1988). On the potassium conductance increase activated by GABA-B and dopamine D2 receptors in rat substantia nigra neurons. *J. Physiol.*, **401**, 437–453.

LADINSKY, H., CONSOLO, S., BIANCHI, S. & JORI, A. (1976). Increase in striatal acetylcholine by picrotoxin in the rat: evidence for a gabaergic-dopaminergic-cholinergic link. *Brain Res.*, **108**, 351–361.

MAISONNEUVE, I.M., KELLER, R.W. & GLICK, S.D. (1990). Similar effects of D-amphetamine and cocaine on extracellular dopamine levels in medial prefrontal cortex of rats. *Brain Res.*, **535**, 221–226.

MARTIN, G.E. & HAUBRICH, D.R. (1978). Striatal dopamine release and contraversive rotation elicited by intranigrally applied muscimol. *Nature*, **275**, 230–231.

MILLER, J.A. & RICHTER, J.A. (1986). Effects of GABAergic drugs in vivo on high-affinity choline uptake in vitro in mouse hippocampal synaptosomes. *J. Neurochem.*, **47**, 1916–1918.

OLPE, H.R., SCHELLENBERG, H. & KOELLA, W.P. (1977). Rotational behavior induced in rats by intranigral application by GABA-related drugs and GABA antagonists. *Eur. J. Pharmacol.*, **45**, 291–298.

OLSEN, R.W. (1982). Drug interactions at the GABA receptor-ionophore complex. *Annu. Rev. Pharmacol.*, **22**, 245–277.

O'NEILL, R.D. (1986). Effects of intranigral injection of taurine and GABA on striatal dopamine release monitored voltammetrically in the unanesthetized rat. *Brain Res.*, **382**, 28–32.

PAXINOS, G. & WATSON, C. (1986). *The Rat Brain in Stereotaxic Coordinates* (second edition). San Diego: Academic Press.

PENIT-SORIA, J., AUDINAT, E. & CREPEL, F. (1987). Excitation of rat prefrontal cortical neurons by dopamine: an in vitro electrophysiological study. *Brain Res.*, **425**, 263–274.

PENIT-SORIA, J., RETAUX, S. & MAURIN, Y. (1989). Effects de la stimulation des récepteurs $D_1$ and $D_2$ dopaminergiques sur la libération d'acide gamma-[$^3$H]aminobutyrique induite électriquement dans le cortex préfrontal du rat. *C.R. Acad. Sci.*, [III], **309**, 441–446.

PINNOCK, R.D. (1984). Hyperpolarizing action of baclofen on neurons in the rat substantia nigra slice. *Brain Res.*, **332**, 337–340.

REID, M., HERRERA-MARSCHITZ, M., HÖKFELT, T., TERENIUS, L. & UNGERSTEDT, U. (1988). Differential modulation of striatal dopamine release by intranigral injection of gamma-aminobutyric acid (GABA), dynorphin A and substance P. *Eur. J. Pharmacol.*, **147**, 411–420.

ROBINSON, T.E. & CAMP, D.M. (1991). The effect of four days of continuous striatal microdialysis on indices of dopamine and serotonin neurotransmission in rats. *J. Neurosci. Meth.*, **40**, 211–222.

SANTIAGO, M. & WESTERINK, B.H.C. (1990). Characterization of the in vivo release of dopamine as recorded by different types of intracerebral microdialysis probes. *Naunyn-Schmied. Arch. Pharmacol.*, **342**, 407–414.

SCATTON, B. & BARTHOLINI, G. (1982). γ-Aminobutyric acid (GABA) receptor stimulation. IV effect of progabide (SL 76002) and other GABAergic agents on acetylcholine turnover in rat brain areas. *J. Pharmacol. Exp. Ther.*, **220**, 689–695.

SCHOFIELD, P.R., DARLISON, M.G., FUJITA, N., BURT, D.R., STEPHENSON, F.A., RODRIGUEZ, H., RHEE, L.M., RAMACHANDRAN, J., REALE, V., GLENCORSE, T.A., SEEBURG, P.H. & BARNARD, E.A. (1987). Sequence and functional expression of the $GABA_A$ receptor shows a ligand-gated receptor super-family. *Nature*, **238**, 221–227.

SÉGUÉLA, P., GAMRANI, H., GEFFARD, M., CALSAS, A. & LE MOAL, M. (1985). Ultrastructural immunocytochemistry of γ-aminobutyrate in the cerebral and cerebellar cortex of the adult rat. *Neuroscience*, **16**, 865–874.

SÉGUÉLA, P., WATKINS, K.C. & DESCARRIES, J. (1988). Ultrastructural features of dopamine axon terminals in the antero-medial and suprarhinal cortex of adult rat. *Brain Res.*, **442**, 11–22.

VAN EDEN, C.G., HOORNEMAN, E.M.D., BUIJS, R.M., MATHISSEN, M.A.H., GEFFARD, M. & UYLINGS, H.B.M. (1987). Immunocytochemical localization of dopamine in the prefrontal cortex of the rat at light electron microscopical level. *Neuroscience*, **22**, 849–862.

VERNEY, C., ALVAREZ, C., GEFFARD, M. & BERGER, B. (1990). Ultrastructural double-labelling study of dopamine terminals and GABA-containing neurons in rat anteromedial cerebral cortex. *Eur. J. Neurosci.*, **2**, 960–972.

WALDMEIER, P.C. (1990). Weak impact of GABA uptake inhibition on nigrostriatal dopamine function. *Biogenic Amines*, **7**, 603–611.

WALDMEIER, P.C., STÖCKLIN, K. & FELDTRAUER, J.-J. (1992). Systemic administration of baclofen and the $GABA_B$ antagonist, CGP 35348, does not affect GABA, glutamate or aspartate in microdialysates of the striatum of conscious rats. *Naunyn-Schmiedeb. Arch. Pharmacol.*, **345**, 548–552.

WESTERINK, B.H.C., DAMSMA, G., ROLLEMA, H., DE VRIES, J.B. & HORN, A.S. (1987). Scope and limitations of in vivo brain dialysis: a comparison of its applications to various neurotransmitter systems. *Life Sci.*, **41**, 1763–1776.

WESTERINK, B.H.C., SANTIAGO, M. & DE VRIES, J.B. (1992). In vivo evidence for a concordant response of terminal and dendritic dopamine release during intranigral infusion of drugs. *Naunyn-Schmiedeb. Arch. Pharmacol.*, **346**, 637–643.

WESTERINK, B.H.C. & TUINTE, M.H. (1986). Chronic use of intracellular dialysis for the in vivo measurement of 3,4-dihydroxyphenylethylamine and its metabolite 3,4-dihydrophenylacetic acid. *J. Neurochem.*, **46**, 181–185.

ZETTERSTRÖM, T., SHARP, T., COLLINS, A.K. & UNGERSTEDT, U. (1988). In vivo measurement of extracellular dopamine and DOPAC in rat striatum after various dopamine-releasing drugs. Implications for the origin of extracellular DOPAC. *Eur. J. Pharmacol.*, **148**, 327–334.

ZIS, A.P., NOMIKOS, G.G., DAMSMA, G. & FIBIGER, H.C. (1991). In vivo neurochemical effects of electroconvulsive shock studied by microdialysis in the rat striatum. *Psychopharmacol.*, **103**, 343–350.

*(Received October 19, 1992*
*Revised February 5, 1993*
*Accepted February 23, 1993)*

*Br. J. Pharmacol.* (1993), **109**, 819–825 © Macmillan Press Ltd, 1993

# Differential properties of type I and type II benzodiazepine receptors in mammalian CNS neurones

*Takashi Yakushiji, Tetsuya Shirasaki, Mitsutoshi Munakata, *Akira Hirata & [1]Norio Akaike

Department of Neurophysiology, Tohoku University School of Medicine, Sendai 980 and *Research Laboratories, Yoshitomi Pharmaceutical Industries Ltd., Fukuoka 871, Japan

**1** The effects of benzodiazepine receptor (BZR) partial agonists, Y-23684 and CL218,872, were compared with its full agonist, diazepam, on γ-aminobutyric acid (GABA)-induced $Cl^-$ current ($I_{Cl}$) in acutely dissociated rat cerebral cortex (CTX), cerebellar Purkinje (CPJ) and spinal ventral horn (SVH) neurones, by the whole-cell mode patch-clamp technique.

**2** The GABA-induced responses were essentially the same in both SVH and CPJ neurones, but the $K_D$ value of the GABA response in CTX neurone was lower than those in the other two brain regions.

**3** Enhancement of the GABA response by the two partial agonists was about one-third of that by diazepam in the SVH neurones (where type II subtype of BZR, $BZ_2$, is predominant), whereas these partial agonists potentiated the GABA response as much as diazepam in CPJ neurones (where the type I subtype of BZR, $BZ_1$, is predominant). In CTX neurones where both type I and II variants are expressed, the augmentation ratio of the GABA response by diazepam was between the values in CPJ and SVH neurones.

**4** In concentration-response relationships of BZR partial agonists, the threshold concentrations, $K_D$ values and maximal augmentation ratio of the GABA response were similar in all CTX, CPJ and SVH neurones. Also, in all preparations, the threshold concentration and $K_D$ values of diazepam action were 10 fold less than those induced by partial agonists.

**5** All BZR agonists shifted the concentration-response relationship for GABA to the left without changing the maximum current amplitude, indicating that activation of both $BZ_1$ and $BZ_2$ increase the affinity of the $GABA_A$ receptor for GABA.

**6** The results are important in clarifying the mechanism of anxiety and might explain the anxioselectivity of BZR partial agonists.

**Keywords:** Benzodiazepine; partial agonist; $GABA_A$ receptor; rat cerebral cortex neurone; rat cerebellar Purkinje cell; rat spinal ventral horn neurone; whole-cell of patch-clamp.

## Introduction

Benzodiazepines (BZPs) have been widely used as clinical anxiolytics. Although these drugs have many advantages, they also have a number of undesirable adverse reactions such as muscle relaxation, dizziness, hypnogenesis and reduction of vigilance, amnesia induction and dependency liability. Therefore, recent research has emphasized the search for novel anxiolytics in which these adverse reactions are absent.

The benzodiazepine receptor (BZR) interacts functionally and structurally with $GABA_A$ and barbiturate receptors which are coupled with $Cl^-$ channel (Olsen 1981), and BZPs facilitate the GABA-induced $Cl^-$ current ($I_{Cl}$) (Study & Barker, 1981; Hattori *et al.*, 1986; Yakushiji *et al.*, 1989a). The search for novel anxiolytics is focusing on partial BZR agonists. They have anxiolytic and anticonvulsant properties, but do not induce ataxia and sedation (Klepner *et al.*, 1979; Morimoto *et al.*, 1990). Y-23684 (see Figure 1), is one such drug. Functional differences such as anxioselectivity, between partial and full agonists may be explained by the following: (1) their intrinsic efficacies and (2) the differences between receptor density in various CNS regions (Haefely, 1987).

On the other hand, two subtypes of BZR, type I ($BZ_1$) and II ($BZ_2$), have been classified pharmacologically. The former is sensitive to CL218,872, one of the partial agonists, and the latter is less sensitive to the drug (Squires *et al.*, 1979). A recent gene cloning technique has also revealed the structural variants of $GABA_A$/BZP receptor subtypes. The $GABA_A$ receptor-$Cl^-$ channel complex consists of some subunits such as α, β, γ, δ, and each subunit has some isoforms, $\alpha_{1-6}$, $\beta_{1-4}$, $\gamma_{1-3}$ (Olsen & Tobin, 1990; Burt & Kamatchi, 1991). A recombinant $GABA_A$ receptor-$Cl^-$ channel complex composed of $\alpha_1$, $\beta_1$, and $\gamma_2$ subunits has $BZ_1$-like properties, whereas one from $\alpha_{2,3 \text{ or } 5}$, $\beta_1$, and $\gamma_2$ subunits has $BZ_2$-like properties. The existence of BZR subtypes complicates the situation of the partial agonists, because of the necessity to consider both affinity and intrinsic efficacy of the ligand for a single receptor subtype. Since we know that the recombinant receptors do not always reflect the physiological condition, it is important to clarify the functional difference in receptor subtypes in mammalian CNS neurones to elucidate the significance of 'partial agonistic effects' on anxioselectivity.

The expression of mRNA encoding the $\alpha_1$ subunit and that encoding $\alpha_2$ and $\alpha_3$ subunits are predominant in cerebellar Purkinje (CPJ) and spinal ventral horn (SVH) neurones, respectively (Young *et al.*, 1981; MacLennan *et al.*, 1991; Persohn *et al.*, 1991; Wisden *et al.*, 1991; Doble & Martin, 1992). Therefore, in the present experiment, we first compared the potency of the full agonist (diazepam) with those of partial agonists (Y-23684 and CL218,872) on the enhancement of GABA-induced $I_{Cl}$ in both CPJ and SVH neurones acutely dissociated from the rat brain and spinal cord, and then studied the properties of all three in cerebral cortex (CTX) neurones.

## Methods

### *Preparation*

CTX, CPJ and SVH neurones were acutely dissociated from 13 to 17, 28 to 35, and 7 to 14 day-old Wistar rats, respectively. Transverse slices (400 μm) of the cortex, cerebellum and spinal cord were cut with a microslicer (Dosaka, DTK-

[1] Author for correspondence at: Department of Neurophysiology, Tohoku University School of Medicine, Sendai 980, Japan.

1000) (Kaneda et al., 1990; Murase et al., 1990; Shirasaki et al., 1991). The slices were pre-incubated in a standard external solution well saturated with pure $O_2$ at room temperature for 50 min. Thereafter, slices were treated with 0.05% pronase, followed by 0.05% thermolysin at 31°C, each for 20 to 40 min. In some experiments, the spinal slices were treated with mixture of 0.3% collagenase and 0.2% alkaline protease-nagase at 31°C for 30 to 40 min. Thereafter, the slices were rinsed well with $Ca^{2+}$-free EGTA solution and stored in well-oxygenated standard external solution. The cerebral frontal cortex, cerebellar Purkinje cell layer and Rexed's laminae VIII and IX in the spinal cord were then micropunched from the slices with a round tipped injection needle under the stereoscopic microscope (Nikon, SMZ-1) and transferred to a culture dish filled with well-oxygenated standard external solution. CTX, CPJ and SVH neurones in the pieces punched from the slices were dissociated mechanically with a fire-polished micro-Pasteur pipette. Neurones were used for experiments within 6 h after the cell dissociation.

### *Solutions*

The composition of external and internal solutions was as follows. Standard external solution (in mM): NaCl 150, KCl 5, $MgCl_2$ 1, $CaCl_2$, 2,*N*-2-hydroxyethylpiperazine-*N'*-2-ethanesulphonic acid (HEPES) 10 and glucuse 10. The pH was ajusted to 7.4 with tris(hydroxymethyl)aminomethane (Tris-base). $Ca^{2+}$-free ethylenglycol-*bis*-(β-aminoethyl ether) *N,N,N',N'*-tetraacetic acid (EGTA) solution: NaCl 124, KCl 5, $KH_2PO_4$ 1.2, $MgSO_4$ 1.3, $NaHCO_3$ 26, EGTA 2 and glucose 10. The pH was adjusted to 7.45 with 5% $CO_2$-95% $O_2$ mixture gas. Internal (pipette) solution: NaCl 30, KCl 50, K-glucuronate 70, $CaCl_2$ 0.25, $MgCl_2$ 1, Mg-ATP 5, EGTA 5 and HEPES 10. The pH was adjusted to 7.2 with Tris-base.

### *Rapid application of external solution by the 'Y-tube' technique*

A rapid application of the external solution was carried out with the 'Y-tube' technique (Murase et al., 1990; Shirasaki et al., 1991). The Y-tube was made of polyethylene tubing (2 mm diameter), and the outlet tip (0.1 mm diameter) was set about 1 to 0.5 mm away from the neurone being recorded. One end of the Y-tube was submerged in either the standard solution or one of the test solutions contained in a test tube. The other end was connected to a vacuum pump through an electromagnetic valve controlled by an electrostimulator (Nihon Kohden, SEN-7103). When the electromagnetic valve was opened, the external solution in the Y-tube was changed by a negative pressure of − 40 cmHg. After the valve was closed, the external solution passed through the outlet of the Y-tube by gravity. This system allows complete exchange of external solution surrounding the recording neurone within 10 to 20 ms.

### *Electrical measurements*

Voltage-clamp recording at a holding potential of − 50 mV was carried out in the whole-cell mode of conventional patch-clamp technique at room temperature (20–23°C). Patch electrodes were pulled on a two stage puller (Narishige, PB-7) and fire-polished on a microforge (Narishige, MF-83). In experiments, the patch electrode was handled by the use of a water driven micromanipulator (Narishige, MW-3). The resistance between the recording electrode filled with internal solution and the reference electrode was 6 to 8 MΩ. The currents were measured with a patch-clamp amplifier (Nihon Kohden, CEZ2300), and monitored on both a storage oscilloscope (Toshiba, 10M62) and a thermal-head penrecorder (Nippondenki San-ei, Recti-horiz-8K21) through filtering at 1 kHz (NF electronic instruments, FV-665). Simultaneously, the current was stored on a video cassette recorder (Mitsubishi, VH-F32) after changing the signal to a digital mode, using a PCM processor (Nihon Kohden, PCM-501ESN).

### *Drugs*

Enzymes used were: pronase (Calbiochem), thermolysin (Sigma), alkaline protease-nagase (Nagase biochemical) and collagenase (Yakuruto). All enzymes were dissolved just before use in standard external solution. Diazepam, 3-methyl-6-(3-trifluoromethyl-phenyl)-1,2,4-triazolo(4,3-b)pyridazine (CL218,872) and (±)-2-(4-chlorophenyl)-5,6-dihydro-[1]benzothiepino [5,4-c]pyridazin-3(2H)-one 7-oxide (Y-23684) were synthesized by Yoshitomi Pharmaceutical Industries (Figure 1). They were first dissolved in dimethyl sulphoxide (DMSO) at $10^{-1}$ M, and then diluted to the final concentration in standard external solution. The maximum concentration of DMSO used was 0.2%, at which concentration it did not affect the GABA response.

### *Statistics*

Data were calculated as mean ± standard error of the mean (s.e.mean) and significance was tested by Student's *t* test.

## Results

### *GABA-induced $I_{cl}$ in the CTX, CPJ and SVH neurones*

Figure 2 shows the GABA-induced $Cl^-$ current ($I_{Cl}$) in CTX (a) and SVH (b) neurones at a holding potential ($V_H$) of − 50 mV. Since the $GABA_A$ response recorded by the use of conventional whole-cell mode of patch-clamp technique decreases time-dependently, 5 mM MgATP was added to the internal solution to prevent the sensitivity-loss for the affinity of $GABA_A$ receptor (run-down) (Chen et al., 1990; Shirasaki et al., 1992). When this was done, the GABA responses were maintained for more than 1 h and increased in a sigmoidal fashion with increase in the concentration of GABA. The responses rapidly activated and successively desensitized towards a steady-state level during continuous application of GABA, in both neurones and the CPJ neurone (raw data not shown). The desensitization was more accelerated with increase in the GABA concentration. The concentration-response relationships for GABA in these neurones are shown in Figure 3. When the peak amplitudes of $I_{Cl}$ induced by GABA of various concentrations were normalized for the maximum values in respective concentration-response relationships, the concentration-response relationships in CPJ and SVH neurones were almost the same, but that in the CTX neurones shifted to a lower concentration-range. The

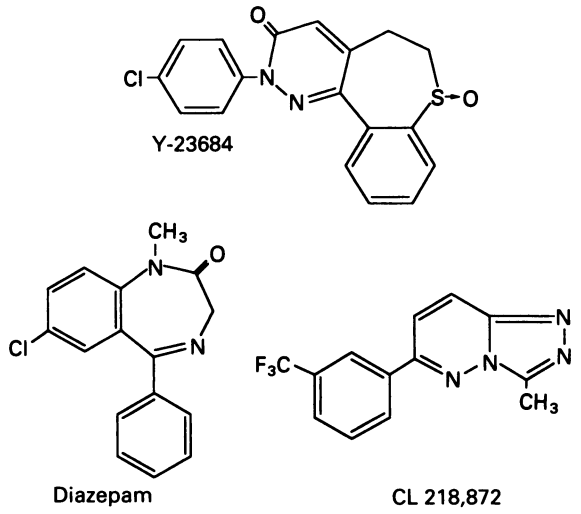



**Figure 1** Chemical structures of diazepam, Y-23684 and CL218,872.

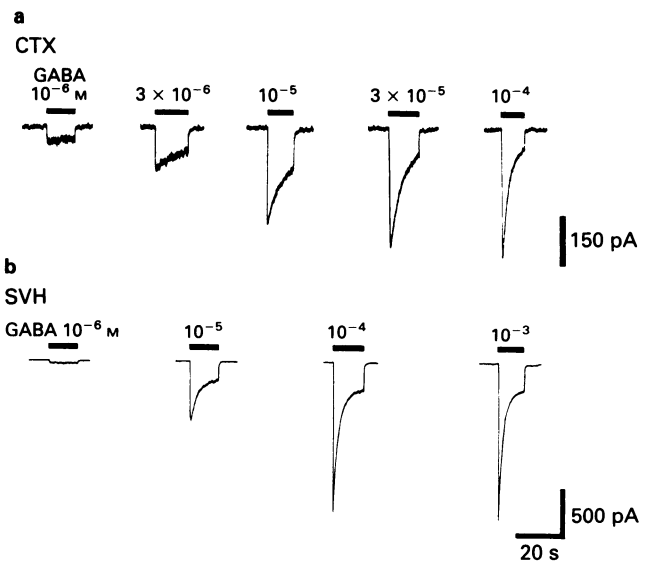



**Figure 2** GABA-induced $I_{Cl}$ in cortical (CTX; a) and spinal ventral horn (SVH; b) neurones at $V_H$ of − 50 mV. GABA was continuously applied by means of the 'Y-tube' technique during the period indicated by the bars above each current trace.

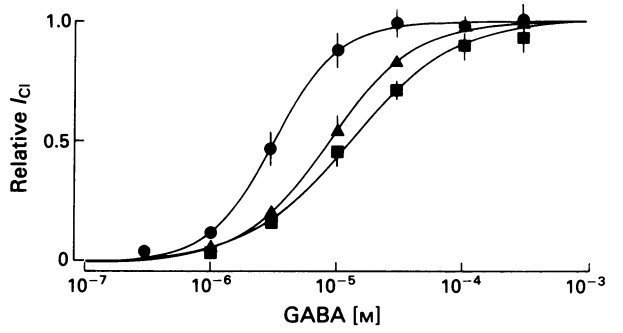



**Figure 3** Concentration-response relationship of GABA response in cortical (●), cerebellar Purkinje (▲) and spinal ventral horn (■) neurones. The peak amplitude as shown in Figure 2 was measured at each concentration and all current amplitudes (Relative $I_{Cl}$) were normalized at the maximum value of individual theoretical concentration-response curve calculated by Eqn (1). $V_H$ − 50 mV. Each point is the average of 3 to 6 neurones with s.e.mean.

concentration-response relationships accorded with the following equation:

$$I = I_{max} \frac{C^n}{C^n + K_D^n} \quad (1)$$

Where, $I$ is the observed GABA-induced $I_{Cl}$, $I_{max}$ the maximum value of current, $C$ the GABA concentration, $K_D$ the apparent dissociation constant, and n the Hill coefficient. The least square fitting of the points gave a $K_D$ value of $3.2 \times 10^{-6}$ M for CTX, $8.8 \times 10^{-6}$ M for CPJ and $1.3 \times 10^{-5}$ M for SVH neurones, and a Hill coefficient of 1.65 for CTX, 1.29 for CPJ and 1.06 for SVH neurones.

### *Effects of BZR agonists on GABA-induced* $I_{Cl}$ *in SVH neurones*

In this experiment we used 7 to 14 day-old rats, because (1) biological binding studies have shown that the percentage of $BZ_2$ in the spinal cord is almost constant (>80%) in every range of aging (Watanabe *et al.*, 1985b), and (2) it is easier to dissociate the motoneurones of young animals than those of adults. None of the BZR agonists themselves evoked any response in dissociated SVH neurones even at the high concentration, but they potentiated that GABA-induced $I_{Cl}$ in a concentration-dependent manner (Figure 4). To examine the difference of their efficacy, $3 \times 10^{-6}$ M GABA was used as a control, at which concentration GABA induced a response equal to almost 10% of its maximum response. Since the action of BZR agonists on GABA-induced $I_{Cl}$ depends on the pretreatment time (Yakushiji *et al.*, 1989b), neurones were pretreated with the agonist for 30 to 60 s which gave the steady-state enhancement. Interestingly, diazepam enhanced the GABA response more strongly in SVH neurones than in CPJ neurones (Figure 4). As shown in Figure 5(a), the enhancement of the GABA response by diazepam was observed from 1 to $3 \times 10^{-9}$ M and increased in a sigmoidal fashion as the diazepam concentration was increased. Finally, potentiation reached 2.24 times that of the control. When the concentration-augmentation relationships accorded with the following equation, the $K_D$ value and the Hill coefficient were $2.3 \times 10^{-8}$ M and 1.36, respectively.

$$I - 1 = (I_{max} - 1) \frac{C^n}{C^n + K_D^n} \quad (2)$$

Where, $I$ is the observed GABA-induced current in the presence of BZR agonist, $I_{max}$ the maximum value of current, $C$ the concentration of BZR agonist, $K_D$ the apparent dissociation constant, and n the Hill coefficient. At concentrations above $3 \times 10^{-6}$ M, the augmentation ratio by diazepam decreased (Yakushiji *et al.*, 1989b). On the other hand, partial agonists, Y-23684 and CL218,872, also potentiated the GABA response in a sigmoidal fashion as their concentration was increased. But, as reported in other preparations such as frog sensory neurones (Yakushiji *et al.*, 1989a), the maximum values in respective concentration-augmentation relationships were significantly smaller than that of diazepam ($P<0.01$). The least square fitting of the points gave a $K_D$ value of $2.3 \times 10^{-7}$ M for Y-23684 and $2.2 \times 10^{-7}$ M for CL218,872, and a Hill coefficient of 1.64 for Y-23684 and 0.97 for CL218,872. The continuous lines in Figure 5(a) were drawn according to equation (2) using $I_{max} = 1.46$ for both Y-23684 and CL218,872. Neither partial agonist produced further augmentation of GABA response at concentrations beyond $3 \times 10^{-5}$ M.

### *Effects of BZR agonists on CPJ neurones*

Expression of BZR subtype in CPJ neurones changes with age, and after 21 days postnatal, $BZ_1$ becomes predominant (>85%) (Lippa *et al.*, 1981; Watanabe *et al.*, 1985a). Therefore, we used 28 to 35 day old rats. In CPJ neurones, no BZR agonists evoked any response. GABA $3 \times 10^{-6}$ M, was chosen as a control to examine the effect of BZR agonists on the GABA response for the reason mentioned above. As shown in Figure 5(b), the facilitatory effect of diazepam on the GABA response was observed from $3 \times 10^{-9}$ M, and the GABA response was potentiated in a sigmoidal fashion as the concentration of diazepam was increased. But, interestingly, the maximum potentiation ratio reached only 1.64 times that of the control of GABA alone. When the concentration-augmentation relationship accorded with equation (2), the $K_D$ value and the Hill coefficient were $2.5 \times 10^{-8}$ M and 1.60, respectively.

In contrast, the maximum augmentation ratios of the GABA response by partial agonists were almost 1.5 times, which were close to those observed in SVH neurones. The least square fitting of the points gave the $K_D$ value of $9.3 \times 10^{-8}$ M for Y-23684 and $1.9 \times 10^{-7}$ M for CL218,872, and a Hill coefficient of 1.37 for Y-23684 and 1.27 for CL218,872. At high concentrations beyond $3 \times 10^{-5}$ M, partial agonists did not produce further augmentation of the GABA response. The continuous lines in Figure 5(b) were drawn according to equation (2) using $I_{max} = 1.55$ for Y-

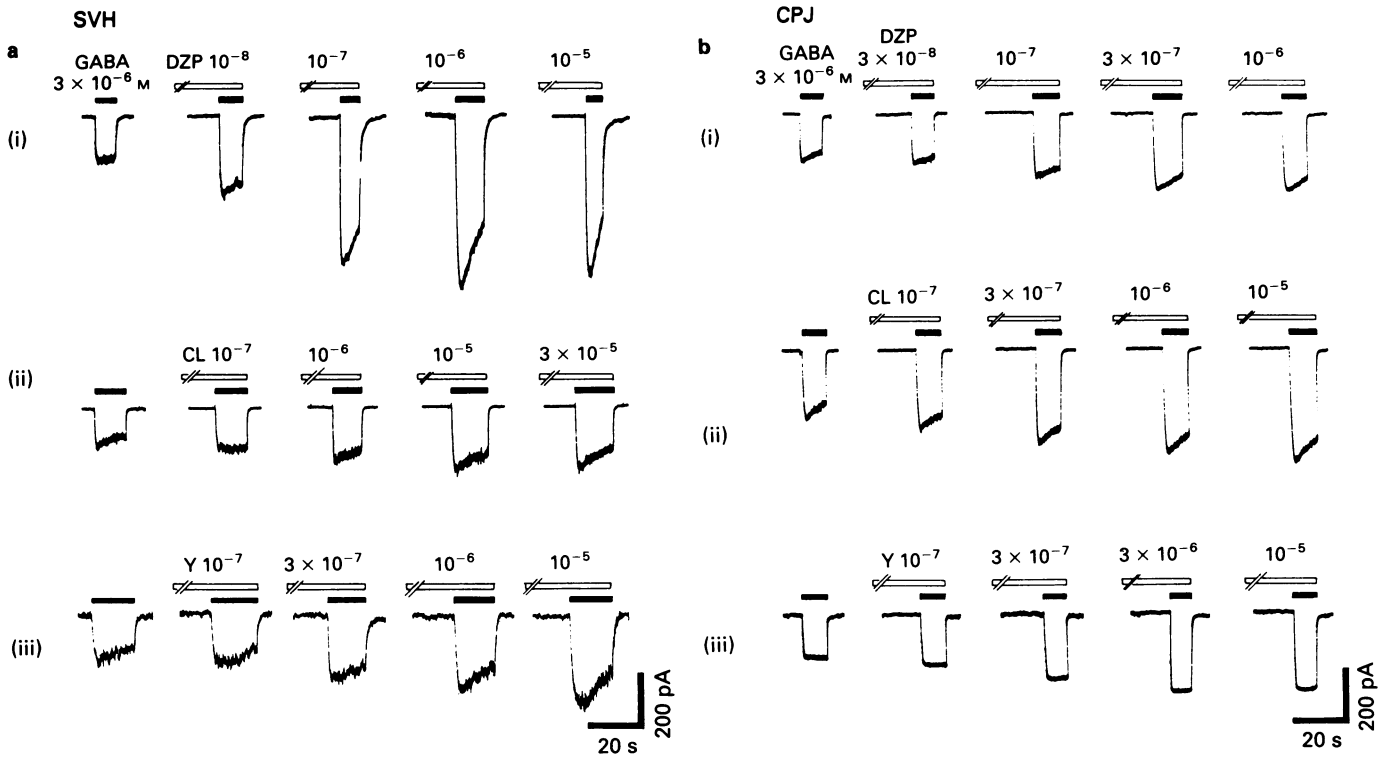



**Figure 4** Augmentation of GABA ($3 \times 10^{-6}$ M) response by BZR agonists in spinal ventral horn (SVH, a) and cerebellar Purkinje (CPJ, b) neurones at $V_H$ of $-50$ mV. Pretreatment with all BZR agonists was for 30 to 60 s. Drugs were applied by means of the 'Y-tube' technique for the period indicated by the bars above each current trace. Note that augmentation ratios of all agonists except diazepam (DZP) in SVH neurones were quite similar. CL: CL 218,872; Y: Y-23684.

23684, and 1.56 for CL218,872. There were no significant differences among the maximum augmentations of the GABA response by three full and partial agonists in dissociated CPJ neurones.

### *Effects of BZR agonists on CTX neurones*

Because the GABA concentration-response relationship in CTX neurones lies in a lower concentration range than those in the other two regions (Figure 3), we chose $10^{-6}$ M GABA as a control. At this concentration, GABA induced a response of almost 10% of the maximum response. The facilitatory characteristics of partial agonists on the GABA response were similar to those in the other two preparations (SVH and CPJ). Threshold concentrations, $K_D$ values and maximum augmentation ratios of the GABA response were $10^{-8}$ M, $1.8 \times 10^{-7}$ M and 1.53 for Y-23684, and $10^{-8}$ M, $3.3 \times 10^{-7}$ M and 1.49 for CL218,872. The Hill coefficients were 1.78 for Y-23684 and 1.36 for CL218,872, respectively. However, the augmentation ratio (1.87) of diazepam lay between the values in CPJ and SVH neurones (Figure 5c). Threshold concentration ($10^{-9}$ M), $K_D$ value ($4.9 \times 10^{-8}$ M) and Hill coefficient (1.42) were similar to those in the CPJ and SVH neurones.

### *Concentration-response relationships for GABA in the presence of BZR agonists*

As described above, the augmentation ratios of the GABA response by diazepam were significantly different in CPJ and SVH neurones. However, the augmentation ratios in CTX neurones which express both $BZ_1$ and $BZ_2$ lay between the values of CPJ and SVH neurones. Therefore, we examined how the BZR agonists change the GABA concentration-response relationships in CPJ and SVH neurones (Figure 6). In both preparations, $3 \times 10^{-7}$ M diazepam and $3 \times 10^{-6}$ M Y-23684 were used, because they induced the maximum augmentation of GABA response in respective concentration-augmentation relationships as shown in Figure 5. In this condition, both diazepam and Y-23684 shifted the GABA-concentration-response curve to the left without changing the maximum response in both SVH and CPJ neurones. However, diazepam shifted the curve more strongly than Y-23684 in SVH neurones (Figure 6a), whereas the effect of diazepam was the same as that of Y-23684 in CPJ neurones (Figure 6b). The maximum response and $K_D$ value of GABA response in SVH neurones were 2.22 and $1.3 \times 10^{-5}$ M for control, 2.17 and $6.4 \times 10^{-6}$ M in the presence of diazepam, and 2.18 and $8.5 \times 10^{-6}$ M in the presence of Y-23684, respectively. The maximum response and $K_D$ value of the GABA response in CPJ neurones were 1.84 and $8.8 \times 10^{-6}$ M for the control, 1.85 and $6.2 \times 10^{-6}$ M in the presence of diazepam, and 1.88 and $6.3 \times 10^{-6}$ M in the presence of Y-23684, respectively. Here, the maximum current amplitudes were shown relative to that induced by $10^{-5}$ M GABA alone, in individual preparations.

## Discussion

GABA-induced $I_{Cl}$ in CPJ and SVH neurones was very similar to those in acutely dissociated frog sensory (Yakushiji *et al.*, 1989b), rat hippocampal (Shirasaki *et al.*, 1991) and nucleus tractus solitarii (NTS) neurones (Shirasaki *et al.*, 1992). However, the $K_D$ value in the concentration-response relationship for GABA in CTX neurones was lower than those in other preparations. Recent purification, molecular cloning, and re-expression studies have revealed that $\beta_1$ and $\gamma_3$ subunits of $GABA_A$ receptor make the recombinant receptor sensitive to GABA (Ymer *et al.*, 1990; Knoflach *et al.*, 1991). However, explaining the different $K_D$ values obtained here by the distribution of $\beta$ or $\gamma$ subunits is unfounded, because no relationship has been shown between their distributions and the difference of the $K_D$ value (Wilson-Shaw *et al.*, 1991; Zhang *et al.*, 1991). The $\alpha_5$ subunit also shifted the

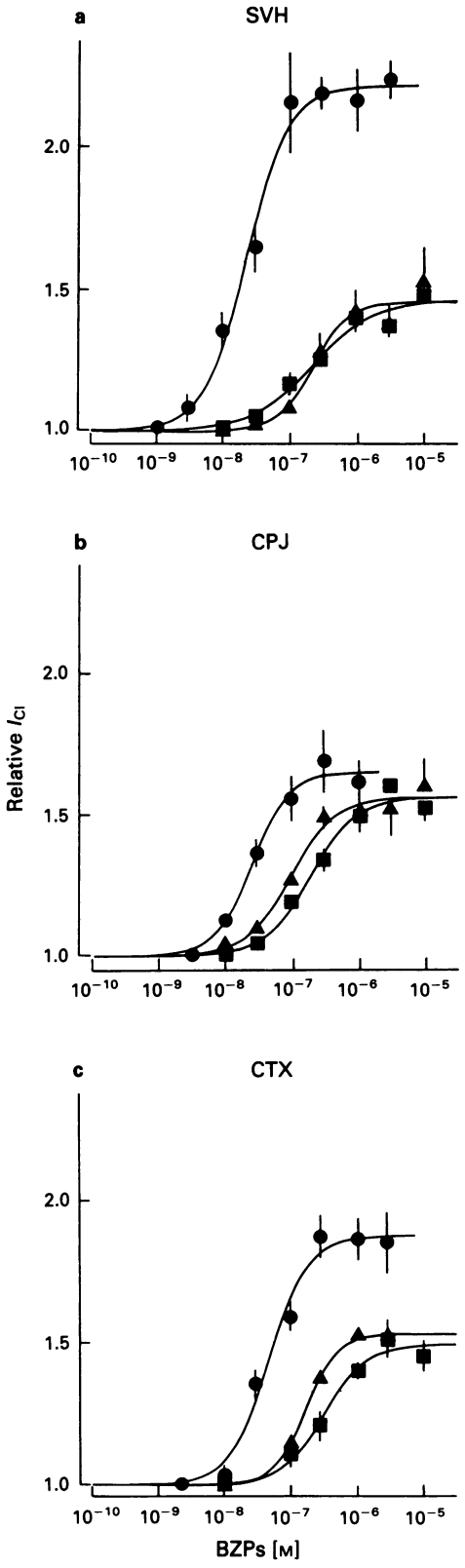



**Figure 5** Concentration-augmentation relationships of BZR agonists for GABA response at $V_H$ of $-50$ mV. The peak current amplitude induced by GABA with one BZR agonist as shown in Figure 4 was measured. All points were normalized for the peak amplitude induced by $10^{-6}$ M (in cortical (CTX) neurone), or $3 \times 10^{-6}$ M (in both cerebellar Purkinje (CPJ) and spinal ventral horn (SVH) neurones) GABA alone. A continuous line was drawn, using Eqn (2). Each point is the average of 4 to 9 neurones with s.e.mean. Note that the concentation-augmentation relationships of CL218,872 (■) and Y-23684 (▲) were very similar in these three different neurones; diazepam (●).

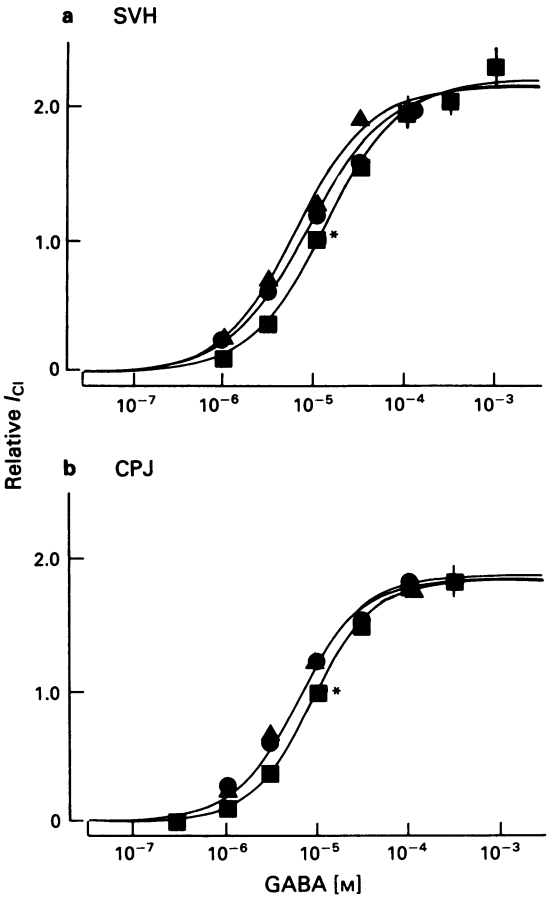



**Figure 6** Effects of diazepam (DZP, $3 \times 10^{-7}$ M, ▲) and Y-23684 ($3 \times 10^{-6}$ M, ●) on GABA-concentration-response relationships in spinal ventral horn (SVH) (a) and cortical Purkinje (CPJ) neurones (b) at $V_H$ of $-50$ mV; (■) control. Pretreatment with BZR agonists was for 30 s and then the mixture of GABA at each concentration and one BZR agonist was applied. All current amplitudes were normalized for the peak amplitude induced by $10^{-5}$ M GABA alone (shown by *). Each point is the average of 4 to 6 neurones. The maximum response was not augmented by either DZP or Y-23684. In spinal ventral horn neurones (a), DZP tended to shift the GABA-concentration-response curve more to the left than did Y-23684.

affinity of recombinant $GABA_A$ receptor to a low concentration range (Malherbe *et al.*, 1990). Moreover, recent *in situ* hybridization studies showed the restricted expression of the $\alpha_5$ subunit in the cerebral cortex, hippocampus and olfactory bulb (Sigel *et al.*, 1990). Therefore, the sensitivity of the $GABA_A$ receptor in CTX neurones is probably based on the presence of $\alpha_5$ subunit.

The main important findings in this study are as follows: (1) Partial and full agonists potentiated the GABA response equally in CPJ neurones ($BZ_1$ predominant). (2) The augmentation ratios of the $GABA_A$ response by two different partial agonists, Y-23684 and CL218,872, were the same, and there were no significant differences for the augmentation pattern among the preparations. (3) The threshold and $K_D$ values of diazepam action were the same in every preparation. For diazepam actions, it seems that the difference of augmentation ratio is not based on the varying numbers of BZR in each preparation, because (a) the maximum current amplitudes of the GABA response were close in both CPJ and SVH neurones, and (b) the Hill coefficients of the diazepam action were not much different in both preparations. Recently, Puia *et al.* (1991) reported that the augmentation ratio of the GABA response by diazepam depends on the variant of the α subunit; that is, the efficacy of diazepam was two or three times greater for the $\alpha_2\beta_1\gamma_2$ and $\alpha_3\beta_1\gamma_2$

assemblages than for the $\alpha_1\beta_1\gamma_2$ assemblage. This finding is compatible with our present findings, because $\alpha_1$ and $\alpha_2$ varients are predominant in CPJ and SVH neurones, respectively.

The subtypes of BZR have been classified by the difference in sensitivity to CL218,872, in which the sensitivity was judged by receptor-binding studies at 0 to 4°C (Squires *et al.*, 1979). According to such an unphysiological binding study, Y-23684 is a non-selective agonist. Present functionally experiments also show the non-selective action of Y-23684 to BZR sensitivity. Judging from (a) this non-selectivity of Y-23684, (b) the result that the maximum augmentation ratios of two partial agonists were the same, and (c) the behavioural data that Y-23684 as well as CL218,872 has good anxioselectivity (Morimoto *et al.*, 1990), the possibility is considerable that BZR partial agonists and *not* $BZ_1$ selective agonists have anxioselectivity. In this case, it seems likely that diazepam acts as a partial agonist at the $BZ_1$ variant (CPJ neurone), but probably not for the reason at first suggested that the pharmacological and physiological properties of $GABA_A$ receptors, such as the sensitivity to GABA, maximum response, Hill coefficient and allosteric modulation, are different for different combinations of subunits. Moreover, $K_D$ values of three agonists used in the present study were close to those obtained from biochemical binding studies (Gee & Yamamura, 1982; Asano *et al.*, 1983; Pritchett *et al.*, 1989; Pritchett & Seeburg, 1990; Takehara, S. personal communication on Y-23684). This suggsts the absence of spare receptors for each receptor subtype. Therefore, the hypothesis described by Haefely (1987) is unlikely, because the presence of spare receptors and difference in the number of receptors are needed to explain the partial agonist action.

Previous classification of BZR subtype has been based on unphysiological binding properties, as mentioned above. Even considering those properties, the difference in affinity of BZR subtype is only close to 10 times. Moreover, the affinity for $BZ_1$ becomes temperature-dependent close to that for $BZ_2$, and at 37°C the difference approaches 3 times (Gee & Yamamura, 1982; Pritchett *et al.*, 1989). Therefore, it may be unwise to classify the selectivity for some ligands such as Y-23684 only by the difference in affinity found in binding assays. In the present experiment, both Y-23684 and CL218,872 are almost 2 times more sensitive to $BZ_1$-predominant CPJ neurones than to the other neurones in the study. However, we could not separate the selectivity by this point. Judging from the present results and anxioselectivity of Y-23684 and CL218,872, we propose here the new classification method based on the functional difference for the maximum enhancement of the GABA response by diazepam and CL218,872, that is, diazepam $\approx$ CL218,872 for $BZ_1$, and diazepam $>$ CL218,872 for $BZ_2$. As shown in Figure 4, all BZR agonists shifted the concentration-response relationship for GABA to the left without changing the maximum current amplitude in each preparation. This indicates that at $BZ_1$ and $BZ_2$, three drugs augment the GABA response by increasing the affinity of the $GABA_A$ receptor for GABA. However, it is not clear at the present stage why the augmentation ratio of the GABA response by diazepam is smaller at $BZ_1$ than at $BZ_2$, although it does depend on the $GABA_A$ receptor composition. To ascertain the validity of our proposition and to explain the different maximum augmentation ratio for diazepam action, further analysis using many other BZR agonists and single channel recordings is necessary.

In conclusion, it has been shown that heterogeneous expression of BZR in CNS neurones and its properties as obtained from re-expression study of $GABA_A$ receptors and *in situ* hybridization are indeed present in native mammalian CNS neurones. In addition, we proposed the possibility that the $BZ_1$ has an important role in the basal mechanism underlying the anxiety. In the present study, we used three distinct cell types. Each of them maintained well the physiological functions of receptors, ionic channels and intracellular signal transduction systems, as well as a different expression pattern for the GABA/BZP receptor subtypes. Thereby, our present findings offer useful data and provide one way to understand the basal mechanism of anxiety. Much experimentation in various CNS neurones contributing to anxiety is needed to support our hypothesis.

We thank Mr D. Bowman for his critical comments. This study was supported by a scholarship to T.S. from the Sumitomo Insurance company and by a Grant-in-Aid for Scientific Research (Nos. 04044029 and 04404023) to N.A. from The Ministry of Education, Science and Culture, Japan.

## References

ASANO, T., YAMADA, Y. & OGASAWARA, N. (1983). Characterization of the solubilized GABA and benzodiazepine receptors from various regions of bovine brain. *J. Neurochem.*, **40**, 209–214.

BURT, D.R. & KAMATCHI, G.L. (1991). $GABA_A$ receptor subtypes: from pharmacology to molecular biology. *FASEB J.*, **5**, 2916–2923.

CHEN, Q.X., STELZER, A., KAY, A.R. & WONG, R.K.S. (1990). $GABA_A$ receptor function is regulated by phosphorylation in acutely dissociated guinea-pig hippocampal neurones. *J. Physiol.*, **420**, 207–221.

DOBLE, A. & MARTIN, I.L. (1992). Multiple benzodiazepine receptors: no reason for anxiety. *Trends Pharmacol. Sci.*, **13**, 76–81.

GEE, K.W. & YAMAMURA, H.I. (1982). Regional heterogeneity of benzodiazepine receptors at 37°C: an *in vitro* study in various regions of the rat brain. *Life Sci.*, **31**, 1939–1945.

HAEFELY, W.E. (1987). Structure and function of the benzodiazepine receptor. *CHIMIA*, **41**, 389–396.

HATTORI, K., OOMURA, Y. & AKAIKE, N. (1986). Diazepam action on γ-amino acid-activated chloride currents in internally perfused frog sensory neurones. *Cell. Mol. Neurobiol.*, **6**, 307–323.

KANEDA, M., WAKAMORI, M., ITO, C. & AKAIKE, N. (1990). Low-threshold calcium current in isolated Purkinje cell bodies of rat cerebellum. *J. Neurophysiol.*, **63**, 1046–1051.

KLEPNER, C.A., LIPPA, A.S., BENSON, D.I., SANO, M.C. & BEER, B. (1979). Resolution of two biochemically and pharmacologically distinct benzodiazepine receptors. *Pharmacol. Biochem. Behav.*, **11**, 457–462.

KNOFLACH, F., RHYNER, T., VILLA, M. KELLENBERGER, S., DRESCHER, U., MALHERBE, P., SIGEL, E. & MÖHLER, H. (1991). The $\gamma_3$-subunit of the $GABA_A$-receptor confers sensitivity to benzodiazepine receptor ligands. *FEBS Lett.*, **293**, 191–194.

LIPPA, A.S., BEER, B., SANO, M.C., VOGEL, R.A. & MEYERSON, L.P. (1981). Differential ontogeny of type I and type II benzodiazepine receptors. *Life Sci.*, **28**, 2343–2347.

MACLENNAN, A.J., BRECHA, N., KHRESTCHATISKY, M., STERNINI, C., TILLAKA-RATNE, N.J.K., CHIANG, M.-Y., ANDERSON, K., LAI, M. & TOBIN, A.J. (1991). Independent cellular and ontogenetic expression of mRNAs encoding three α polypeptides of the rat $GABA_A$ receptor. *Neurosci.*, **43**, 369–380.

MALHERBE, P., SIGEL, E., BAUR, R., PERSOHN, E., RICHARDS, J.G. & MÖHLER, H. (1990). Functional expression and sites of gene transcription of a novel α subunit of the $GABA_a$ receptor in rat brain. *FEBS Lett.*, **260**, 261–265.

MORIMOTO, Y., FUKUDA, T., YAKUSHIJI, T., TAKEHARA, S., ANAMI, K., YAMAMOTO, Y., YASUMATSU, H., NAKAO, T., SETOGUCHI, M. & TAHARA, T. (1990). Anxiolytic properties of Y-23684, a benzodiazepine receptor partial agonist, in comparison with diazepam. *Abstracts 17th Congress of Collegium International Neuro-Psychopharmacologicum*, 169.

MURASE, K., RANDIC, M., SHIRASAKI, T., NAKAGAWA, T. & AKAIKE, N. (1990). Serotonin suppresses N-methyl-D-aspartate responses in acutely isolated spinal dorsal horn neurons of the rat. *Brain Res.*, **525**, 84–91.

OLSEN, R.W. (1981). GABA-benzodiazepine-barbiturate receptor interactions. *J. Neurochem.*, **37**, 1–13.

OLSEN, R.W. & TOBIN, A.J. (1990). Molecular biology of $GABA_A$ receptors. *FASEB J.*, **4**, 1469–1480.

PERSOHN, E., MALHERBE, P. & RICHARDS, J.G. (1991). *In situ* hybridization histochemistry reveals a diversity of $GABA_A$ receptor subunit mRNAs in neurons of the rat spinal cord and dorsal root ganglia. *Neurosci.*, **42**, 497–507.

PRITCHETT, D.B., LÜDDENS, H. & SEEBURG, P.H. (1989). Type I and type II $GABA_A$-benzodiazepine receptors produced in transfected cells. *Science*, **245**, 1389–1392.

PRITCHETT, D.B. & SEEBURG, P.H. (1990). γ-Aminobutyric $acid_A$ receptor $\alpha_5$-subunit creates novel type II benzodiazepine receptor pharmacology. *J. Neurochem.*, **54**, 1802–1804.

PUIA, G., VICINI, S., SEEBURG, P.H. & COSTA, E. (1991). Influence of recombinant γ-aminobutyric acid-$_A$ receptor subunit composition on the action of allosteric modulators of γ-aminobutyric acid-gated $Cl^-$ currents. *Mol. Pharmacol.*, **39**, 691–696.

SHIRASAKI, T., AIBARA, K. & AKAIKE, N. (1992). Direct modulation of $GABA_A$ receptor by intracellular ATP in dissociated rat nucleus tractus solitarii neurones. *J. Physiol.*, **449**, 551–572.

SHIRASAKI, T., KLEE, M.R., NAKAYE, T. & AKAIKE, N. (1991). Differential blockade of bicuculline and strychnine on GABA- and glycine-induced responses in dissociated rat hippocampal pyramidal cells. *Brain Res.*, **561**, 77–83.

SIGEL, E., BAUR, R., TRUBE, G., MÖHLER, H. & MALHERBE, P. (1990). The effect of subunit composition of rat brain $GABA_A$ receptors on channel function. *Neuron*, **5**, 703–711.

SQUIRES, R.F., BENSON, D.I., BRAESTRUP, C., COUPET, J., KLEPNER, C.A., MYERS, V. & BEER, B. (1979). Some properties of brain specific benzodiazepine receptors: new evidence for multiple receptors. *Pharmacol. Biochem. Behav.*, **10**, 825–830.

STUDY, R.E. & BARKER, J.L. (1981). Diazepam and (−)pentobarbital: fluctuation analysis reveal different mechanisms for potentiation of γ-aminobutyric acid response in cultured spinal cord neurons. *Proc. Natl. Acad. Sci. U.S.A.*, **78**, 7180–7184.

WATANABE, Y., HYDE, L., KHATAMI, S., SALAFSKY, B. & SHIBUYA, T. (1985a). The neonatal development of benzodiazepine receptor subtypes in the rat cerebral cortex and cerebellum *Jpn. J. Psychopharmacol.*, **5**, 335–342.

WATANABE, Y., KHATAMI, S., SHIBUYA, T. & SALAFSKY, B. (1985b). Ontogenetic properties of benzodiazepine receptor subtypes in rat spinal cord. *Eur. J. Pharmacol.*, **109**, 307–309.

WILSON-SHAW, D., ROBINSON, M., GAMBARANA, C., SIEGEL, R.E. & SIKELA, J.M. (1991). A novel γ subunit of the $GABA_A$ receptor identified using the polymerase chain reaction. *FEBS Lett.*, **284**, 211–215.

WISDEN, W., GUNDLACH, A.L., BARNARD, E.A., SEEBURG, P.H. & HUNT, S.P. (1991). Distribution of $GABA_A$ receptor subunit mRNA in rat lumbar spinal cord. *Mol. Brain Res.*, **10**, 179–183.

YAKUSHIJI, T., FUKUDA, T., OYAMA, Y. & AKAIKE, N. (1989a). Effects of benzodiazepines and non-benzodiazepine compounds on the GABA-induced responses in frog isolated sensory neurones. *Br. J. Pharmacol.*, **98**, 735–740.

YAKUSHIJI, T., TOKUTOMI, N. & AKAIKE, N. (1989b). Augmentation of GABA-induced chloride current in frog sensory neurons by diazepam. *Neurosci. Res.*, **6**, 309–320.

YMER, S., DRAGUHN, A., WISDEN, W., WERNER, P., KEINÄNEN, K., SHOFIELD, P.R., SPRENGEL, R., PRITCHETT, D.B. & SEEBURG, R.H. (1990). Structural and functional characterization of the $\gamma_1$ subunit of the $GABA_A$/benzodiazepine receptors. *EMBO J.*, **9**, 3261–3267.

YOUNG, W.S., NIEHOFF, D., KUHAR, M.J., BEER, B. & LIPPA, A.S. (1981). Multiple benzodiazepine receptor localization by light microscopic radiohistochemistry. *J. Pharmacol. Exp. Ther.*, **216**, 425–430.

ZHANG, J.-H., SATO, M. & TOHYAMA, M. (1991). Region-specific expression of the mRNAs encoding β subunits ($\beta_1$, $\beta_2$ and $\beta_3$) of $GABA_A$ receptor in the rat brain. *J. Comp. Neurol.*, **303**, 637–657.

*(Received August 6, 1992*
*Revised January 26, 1993*
*Accepted February 24, 1993)*

*Br. J. Pharmacol.* (1993), **109**, 826–830 © Macmillan Press Ltd, 1993

# Endothelin receptors mediating contraction in goat cerebral arteries

*Juan B. Salom, *Germán Torregrosa, *María D. Barberá, *Teresa Jover & [1]*†Enrique Alborch

*Centro de Investigación, Hospital Universitario 'La Fe', and †Departamento de Fisiología, Universidad de Valencia, Spain

**1** The aim of the present study was to identify the subtype of receptor mediating contraction to endothelin-1 and sarafotoxin S6b in goat isolated middle cerebral arteries.

**2** Endothelin-1, endothelin-2 and endothelin-3 contracted cerebral arteries in a concentration-dependent manner. Although the three peptides were full agonists, the order of potency was endothelin-1 = endothelin-2 > endothelin-3, with a relative potency of endothelin-1 and endothelin-2 *versus* endothelin-3 of ~280. Sarafotoxin S6b induced concentration-dependent contractions with lower potency than endothelin-1/endothelin-2, higher potency than endothelin-3 and a higher maximum response than the three endothelins.

**3** The selective $ET_A$-receptor antagonist, BQ-123, did not induce changes in either the resting tension or in the active tone developed by depolarization. In contrast, BQ-123 produced concentration-dependent relaxations of endothelin-1-precontracted cerebral arteries, and to a greater extent of sarafotoxin S6b-precontracted arteries.

**4** Concentration-response curves to endothelin-1 and sarafotoxin S6b were competitively antagonized by BQ-123 ($pA_2$ of $7.43 \pm 0.12$ and $8.41 \pm 0.09$, respectively). In contrast, BQ-123 had no effect on 5-hydroxytryptamine-elicited contractions even at $10^{-6}$ M.

**5** It is concluded that both the order of potency of endothelin isopeptides and the antagonism of BQ-123 point to the existence of $ET_A$ receptors mediating vasoconstriction to endothelin-1 and sarafotoxin S6b in the goat middle cerebral artery. The different antagonistic potency of BQ-123 against endothelin-1 and sarafotoxin S6b suggests the existence of subtypes of $ET_A$ receptors.

**Keywords:** Endothelins; sarafotoxin S6b; BQ-123; cerebral arteries; $ET_A$ receptors

## Introduction

Endothelin-1 is a 21-amino acid endothelium-derived, vasoconstrictor peptide originally isolated from the culture supernatant of porcine aortic endothelial cells (Yanagisawa *et al.*, 1988). After the first report on endothelin-1, the existence of three distinct genes encoding for isopeptides with highly conserved sequence (endothelin-1, endothelin-2 and endothelin-3) was demonstrated (Inoue *et al.*, 1989). Furthermore, the amino acid sequences of sarafotoxins, found in the venom of the burrowing snake *Atractaspis engaddensis*, are very similar to those of endothelins (Kloog & Sokolovsky, 1989). All the endothelins and sarafotoxins are bioactive but differences exist in their pharmacological potencies and profiles (Kitazumi *et al.*, 1990; Cardell *et al.*, 1992).

Two distinct receptor subtypes for endothelins, namely $ET_A$ (Arai *et al.*, 1990) and $ET_B$ (Sakurai *et al.*, 1990) have been cloned and biochemically characterized. Early pharmacological characterization showed that vascular $ET_A$ receptors were endothelin-selective and mediated vasoconstriction (Cardell *et al.*, 1992), while $ET_B$ receptors were non-selective and linked to vasodilatation (Takayanagi *et al.*, 1991). The availability of BQ-123, a selective $ET_A$-receptor antagonist (Ihara *et al.*, 1992a), and of selective $ET_B$-receptor agonists (Williams *et al.*, 1991; Saeki *et al.*, 1991) have led to a reconsideration of early classification as there have been reports of venous $ET_B$ receptors mediating vasoconstriction (Moreland *et al.*, 1992; Sumner *et al.*, 1992) and lung $ET_A$ receptors mediating the release of prostacyclin (D'Orléans-Juste *et al.*, 1992).

Vasoconstrictor responses to endothelin-1 are greater in cerebral arteries than in peripheral arteries (Tanoi *et al.*, 1991), and the pathophysiological significance of endothelin-1 in cerebral vasospasm following subarachnoid hemorrhage is being investigated (Masaki *et al.*, 1992). We have previously reported the vasoconstrictor effects of endothelin-1 on the cerebrovascular bed of the goat (Salom *et al.*, 1991) and compared them with those of sarafotoxin S6b (Salom *et al.*, 1992). In the present study we have examined the agonist potency of endothelin isopeptides (endothelin-1, endothelin-2 and endothelin-3) and used the selective $ET_A$-receptor antagonist, BQ-123, to identify the receptors mediating endothelin-1-and sarafotoxin S6b-induced contraction in goat isolated middle cerebral artery.

## Methods

### *Tissue preparation*

Female goats (30–45 kg) previously sedated with 10 mg $kg^{-1}$ ketamine (Ketalar, Parke Davis, intramuscular) and anaesthetized with 2% sodium thiopentone (Tiobarbital, Palex, intravenous), were killed by intravenous injection of 30 mEq of KCl. The whole brain was rapidly removed, the middle cerebral arteries were dissected free and cut into cylindrical segments measuring 4 mm in length and about 1 mm in outer diameter. Each segment was prepared for isometric tension recording in an organ bath. Two stainless steel L-shaped pins (diameter of 125 μm) were introduced through the arterial lumen. One pin was fixed to the organ bath wall, while the other was connected to a strain gauge (Universal Transducing Cell, UC3, Gould Statham) for isometric tension recording (Omniscribe D 5237-5, Houston Instrument). The organ bath contained 5 ml of Ringer-Locke solution, which was bubbled continuously with 95% $O_2$ and 5% $CO_2$ to give a pH of 7.3–7.4. Temperature was kept at 37°C. A resting tension of 1 g was applied to the arterial segments and they

[1] Author for correspondence at: Centro de Investigación, Hospital Universitario 'La Fe', E-46009, Valencia, Spain.

were allowed to equilibrate for a period of 60–90 min before starting the experiments.

### *Procedure*

The contractile capacity of the arterial segments was examined by exposure to a high-$K^+$ (50 mM) Ringer-Locke solution. The effects of endothelin-1 ($10^{-11}$–$3 \times 10^{-8}$ M), endothelin-2 ($10^{-11}$–$3 \times 10^{-8}$ M), endothelin-3 ($10^{-9}$–$3 \times 10^{-6}$ M) and sarafotoxin S6b ($10^{-11}$–$3 \times 10^{-7}$ M) were studied by cumulative addition of the peptides to the organ bath. The effects of the selective $ET_A$-receptor antagonist BQ-123 ($10^{-10}$–$10^{-6}$ M) itself were examined in arteries at resting tone and in arteries precontracted with either high-$K^+$ (50 mM) medium, endothelin-1 ($10^{-9}$ M) or sarafotoxin S6b ($10^{-8}$ M). To assess the selective antagonistic effects of BQ-123 against endothelin-1 and sarafotoxin S6b, concentration-response curves to endothelin-1 ($10^{-11}$–$3 \times 10^{-7}$ M), sarafotoxin S6b ($10^{-11}$–$3 \times 10^{-6}$ M) and 5-hydroxytryptamine ($10^{-9}$– $3 \times 10^{-5}$ M) were obtained in control conditions and after incubation (30 min) with different concentrations of BQ-123 ($10^{-8}$ M, $10^{-7}$ M, $10^{-6}$ M). Only one concentration-response curve was obtained from one arterial segment. In the experiments with BQ-123 pretreatment control tissues were run in parallel.

### *Statistics*

Contractile responses to endothelin-1, endothelin-2, endothelin-3, sarafotoxin S6b and 5-hydroxytryptamine were expressed as a percentage of a previous contraction induced by 50 mM KCl. Relaxant responses to BQ-123 were expressed as a percentage of previously developed active tone. Concentration-ratios were calculated for the responses at the level of the $EC_{50}$ (half-maximal effective concentration). Maximum effects ($E_{max}$) were expressed as mean ± s.e.mean, and $EC_{50}$ as the geometric mean with its confidence limits (95%) for repeated experiments. Statistical comparisons of $E_{max}$ and $-\log EC_{50}$ ($pD_2$) values between endothelin-1, endothelin-2, endothelin-3 and sarafotoxin S6b, as well as for endothelin-1 and sarafotoxin S6b in the absence and the presence of BQ-123 at different concentrations were obtained by analysis of variance (ANOVA) and Newman-Keuls tests. Relative potencies of endothelin-1 *versus* endothelin-3 and sarafotoxin S6b were calculated. Values of $EC_{50}$ for endothelin-1 and sarafotoxin S6b obtained in the absence and in the presence of BQ-123 at different concentrations were subjected to Schild analysis to obtain $pA_2$ and slope values of antagonism. All the pharmacological and statistical calculations were performed according to Tallarida & Murray (1987). Probability values ($P$) of less than 5% were considered significant.

### *Drugs and solutions*

Endothelin-1 (Peptide Institute Inc.) was dissolved in twice distilled water. Endothelin-2 and endothelin-3 (Peptide Institute Inc.) were dissolved in 0.1% aqueous acetic acid. Sarafotoxin S6b and BQ-123 (cyclo(D-Asp-Pro-D-Val-Leu-D-Trp)) (Nova-Biochem) were dissolved in twice distilled water. All the peptides were diluted in phosphate buffered saline with 0.05% bovine serum albumin (fraction V, Sigma). 5-Hydroxytryptamine (creatinine sulphate complex, Sigma) was dissolved and diluted in 0.9% saline solution. The Ringer-Locke solution had the following composition (mM): NaCl 120, KCl 5.4, $CaCl_2$ 2.2, $MgCl_2$ 1.0, $NaHCO_3$ 25 and glucose 5.6. In KCl-depolarizing solution, NaCl was replaced by an equimolar amount of KCl. The phosphate buffered saline had the following composition (mM): NaCl 150, $NaH_2PO_4$ 10.0.

## Results

Endothelin-1 ($10^{-11}$–$3 \times 10^{-8}$ M), endothelin-2 ($10^{-11}$–$3 \times 10^{-8}$ M) and endothelin-3 ($10^{-9}$–$3 \times 10^{-6}$ M) produced slowly developing, concentration-dependent contractions of the goat middle cerebral artery (Figure 1). As shown in Table 1, maximum responses to the three peptides were not significantly different. Values of $EC_{50}$ for endothelin-1 and endothelin-2 were not significantly different from each other, but both of them were significantly lower ($P<0.01$) than that for endothelin-3. The relative potency of endothelin-1 *versus* endothelin-3 was 280 (range 135–604). Sarafotoxin S6b ($10^{-11}$–$3 \times 10^{-7}$ M) induced concentration-dependent contractions (Figure 3) with an $EC_{50}$ value between those of endothelin-1 and endothelin-3, and a maximum response significantly higher ($P<0.01$) than those of the three endothelins (Table 1). The relative potency of endothelin-1 *versus* sarafotoxin S6b was 3.3 (range 1.5–7.2).

BQ-123 ($10^{-10}$–$10^{-6}$ M) did not induce changes in resting tension or in active tone developed with high-$K^+$ (50 mM) medium. However, BQ-123 induced concentration-dependent relaxations of arteries precontracted with endothelin-1 ($10^{-9}$ M) or sarafotoxin S6b ($10^{-8}$ M). Complete relaxation was induced by BQ-123 in sarafotoxin S6b-precontracted arteries, with a mean $EC_{50}$ of $6.2 \times 10^{-9}$ M. Since concentrations of BQ-123 higher than $10^{-6}$ M could not be used, a true maximum relaxant effect could not be obtained in endothelin-1-precontracted arteries (Figure 2).

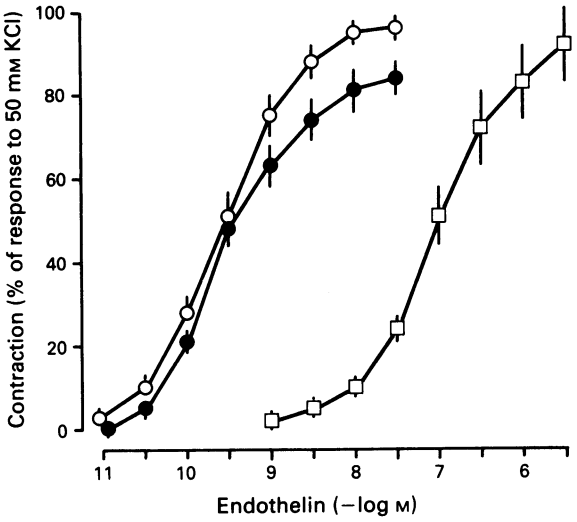



**Figure 1** Concentration-response curves to endothelin-1 (○, $n = 8$), endothelin-2 (●, $n = 8$) and endothelin-3 (□, $n = 8$) in goat isolated middle cerebral arteries. Symbols represent mean values ± s.e.mean.

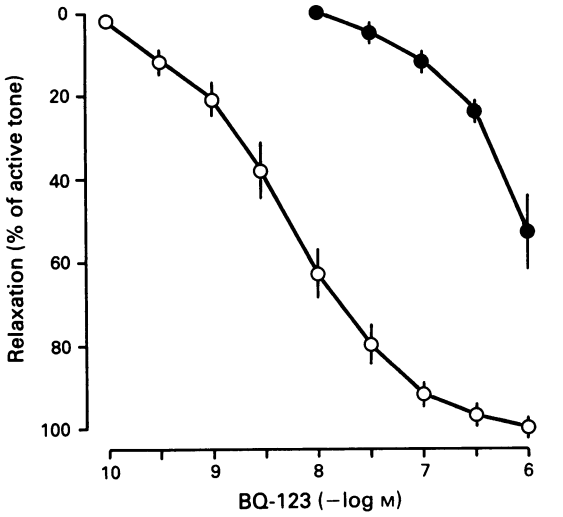



**Figure 2** Concentration-response curves to BQ-123 in goat isolated middle cerebral arteries precontracted with $10^{-9}$ M endothelin-1 (●, $n = 8$) and $10^{-8}$ M sarafotoxin S6b (○, $n = 9$). Symbols represent mean values ± s.e.mean.

BQ-123 ($10^{-8}$–$10^{-6}$ M) produced concentration-dependent, rightward parallel displacement of the concentration-response curves to endothelin-1 and sarafotoxin S6b (Figure 3a and b, respectively). Table 1 summarizes $EC_{50}$ and maximum effect values for endothelin-1 and sarafotoxin S6b in the absence and in the presence of BQ-123. Schild analysis of BQ-123 antagonism yielded a $pA_2$ value of 7.43 ± 0.12 (slope of 1.31 ± 0.17) against endothelin-1, and a $pA_2$ value of 8.41 ± 0.09 (slope of 1.26 ± 0.12) against sarafotoxin S6b. Analysis of the regression lines showed that slope values were not significantly different from unity. In contrast, the concentration-response curve to 5-hydroxytryptamine ($10^{-9}$–$3 \times 10^{-5}$ M) in goat middle cerebral artery was not significantly modified by BQ-123 (Figure 4), even at the highest concentration tested ($10^{-6}$ M).

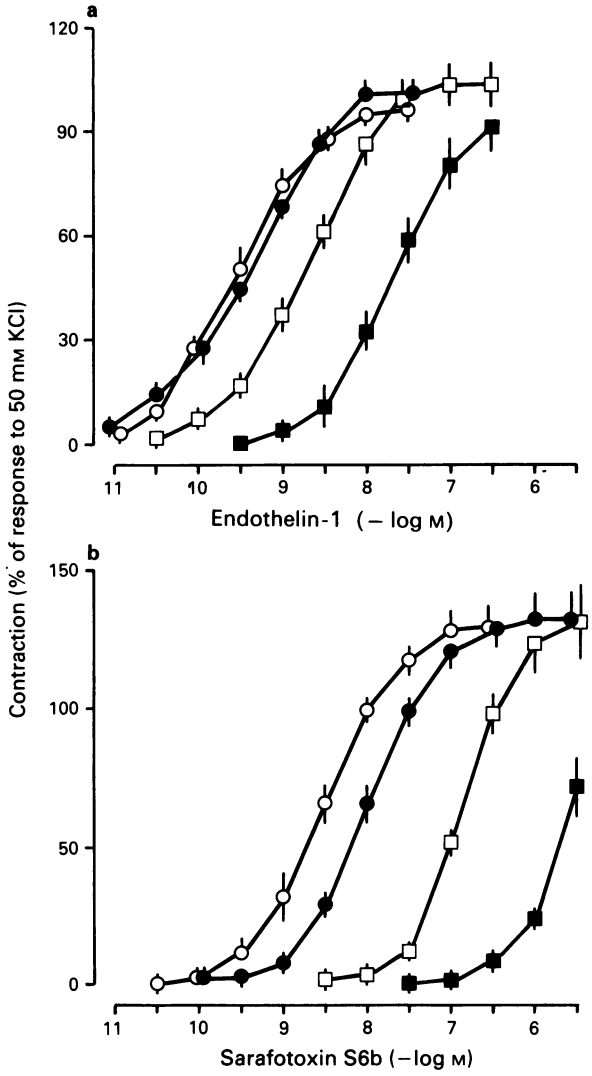



**Figure 3** Concentration-response curves to (a) endothelin-1 and (b) sarafotoxin S6b in goat isolated middle cerebral arteries. (○) Control arteries, $n = 8$ in (a) and $n = 6$ in (b); (●) arteries incubated with $10^{-8}$ M BQ-123, $n = 10$ (a) and $n = 6$ in (b); (□) $10^{-7}$ M BQ-123, $n = 9$ in (a) and $n = 5$ in (b); (■) $10^{-6}$ M BQ-123, $n = 7$ in (a) and $n = 6$ in (b). Symbols represent mean values ± s.e.mean.

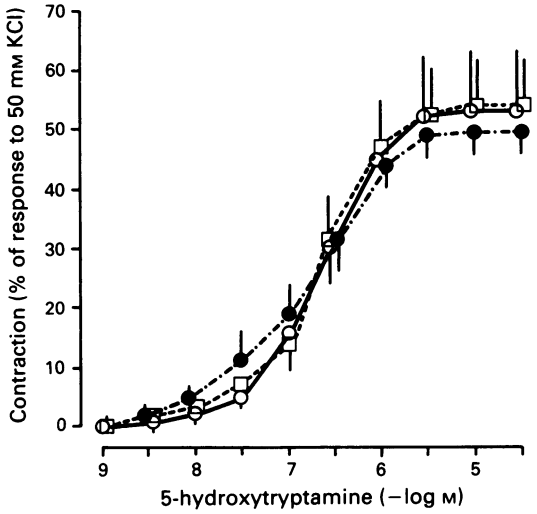



**Figure 4** Concentration-response curves to 5-hydroxytryptamine in goat isolated middle cerebral arteries in control conditions (○, $n = 6$) and after incubation with BQ-123 (●, $10^{-7}$ M, $n = 5$; □ $10^{-6}$ M, $n = 6$). Symbols represent mean values ± s.e.mean.

## Discussion

The cloned receptors for endothelins are classified into two subtypes, $ET_A$ which has a high affinity for endothelin-1 and endothelin-2, but low affinity for endothelin-3 (Arai *et al.*, 1990), and $ET_B$ which has an equal affinity for all three endothelins (Sakurai *et al.*, 1990). Our results show that endothelin-1, endothelin-2 and endothelin-3 were full agonists on goat middle cerebral artery. The order of potency of endothelin isopeptides was endothelin-1 = endothelin-2 > endothelin-3, which is consistent with the existence of $ET_A$

**Table 1** $EC_{50}$ and maximum effect ($E_{max}$) values for endothelin-1 (control and after BQ-123), endothelin-2, endothelin-3 and sarafotoxin S6b (control and after BQ-123) in goat isolated middle cerebral arteries

| *Vasoconstrictor peptide* | *Pretreatment* | *$EC_{50}$ (M)* | *$E_{max}$ (% KCl)* | n |
|---|---|---|---|---|
| Endothelin-1 | None (control) | $2.9\ (1.9–4.4) \times 10^{-10}$ | 96 ± 3 | 8 |
| | BQ-123, $10^{-8}$ M | $3.3\ (1.8–6.0) \times 10^{-10}$ | 102 ± 4 | 10 |
| | BQ-123, $10^{-7}$ M | $2.0\ (1.4–2.8) \times 10^{-9a}$ | 104 ± 6 | 9 |
| | BQ-123, $10^{-6}$ M | $1.8\ (1.1–2.8) \times 10^{-8a}$ | 92 ± 8 | 7 |
| Endothelin-2 | None | $2.5\ (2.0–3.2) \times 10^{-10}$ | 84 ± 4 | 8 |
| Endothelin-3 | None | $8.1\ (5.5–12.0) \times 10^{-8b}$ | 92 ± 9 | 8 |
| Sarafotoxin S6b | None | $2.5\ (1.2–5.1) \times 10^{-9c}$ | 128 ± 7[c] | 6 |
| | BQ-123, $10^{-8}$ M | $1.1\ (0.7–1.6) \times 10^{-8d}$ | 134 ± 6 | 6 |
| | BQ-123, $10^{-7}$ M | $1.5\ (1.1–2.0) \times 10^{-7d}$ | 136 ± 12 | 5 |

$EC_{50}$ values are geometric mean with 95% confidence interval and $E_{max}$ values, expressed as a percentage of previous response to 50 mM KCl, are mean ± s.e.mean from $n$ arterial segments.
[a]Significantly different from control for endothelin-1, $P < 0.01$.
[b]Significantly different from controls for both endothelin-1 and endothelin-2, $P < 0.01$.
[c]Significantly different from controls for endothelin-1, endothelin-2, and endothelin-3, $P < 0.01$.
[d]Significantly different from control for sarafotoxin S6b, $P < 0.01$.

receptors mediating vasoconstriction. Therefore, cerebral arteries resemble other arterial tissues, like rat thoracic aorta (Sumner *et al.*, 1992), guinea-pig pulmonary artery (Cardell *et al.*, 1992), porcine coronary artery (Harrison *et al.*, 1992), and iliac arteries from several species (Moreland *et al.*, 1992), in which the existence of $ET_A$ receptors has been proposed according to endothelin-1/endothelin-2 selectivity. In contrast, endothelin-induced contraction is mediated by non-selective $ET_B$ receptors in venous (Moreland *et al.*, 1992; Sumner *et al.*, 1992), tracheal (Cardell *et al.*, 1992) and intestinal (Yoshinaga *et al.*, 1992) smooth muscles.

With regard to sarafotoxin S6b, this endothelin-related peptide of reptilian origin (Kloog & Sokolovsky, 1989), showed a vasoconstrictor potency lower than endothelin-1 and endothelin-2, but higher than endothelin-3 in goat cerebral arteries. Such an intermediate potency has also been reported for sarafotoxin S6b in pig coronary artery (Harrison *et al.*, 1992). The finding is in agreement with the mediation by $ET_A$ receptors of the sarafotoxin S6b-induced vasoconstriction, since the ability of sarafotoxin S6b to prevent endothelin-1 from binding to the cloned $ET_A$ receptor has been reported to be lower than that of endothelin-1 or endothelin-2, but higher than that of endothelin-3 (Arai *et al.*, 1990).

The synthetic cyclic pentapeptide, BQ-123, is a potent, selective antagonist of $ET_A$ receptors (Ihara *et al.*, 1992a). The use of this antagonist has permitted us to confirm the existence of $ET_A$ receptors mediating vasoconstriction in goat cerebral arteries. First, BQ-123 relaxed cerebral arteries previously contracted with endothelin-1 and sarafotoxin S6b, but did not relax arteries precontracted by depolarization. Second, BQ-123 competitively antagonized the endothelin-1 and sarafotoxin S6b-induced contraction of cerebral arteries. In confirmation of the specificity of BQ-123, 5-hydroxytryptamine-induced contractions remained unchanged. Arterial receptors mediating contraction to endothelins have been usually identified as $ET_A$-type according to endothelin-selectivity (Cardell *et al.*, 1992; Harrison *et al.*, 1992; Moreland *et al.*, 1992) or by using the selective antagonist BQ-123 (Ihara *et al.*, 1992a; Sumner *et al.*, 1992). Since our results demonstrate the presence of $ET_A$ receptors in cerebral arteries, the report that $ET_B$ receptors mediate vasoconstriction in rabbit pulmonary artery (Ihara *et al.*, 1992b) seems to be an exception among arterial tissues.

The antagonistic potency of BQ-123 against endothelin-1-induced contraction of goat cerebral arteries ($pA_2$ of 7.43) is similar to the potency originally reported in porcine coronary artery (Ihara *et al.*, 1992a) and comparable to that found in rat thoracic aorta (Sumner *et al.*, 1992). In contrast, the antagonist potency of BQ-123 against sarafotoxin S6b-induced contraction of cerebral arteries ($pA_2$ of 8.41) was approximately ten times higher than the value generated against endothelin-1-induced contractions. This is consistent with the greater potency of BQ-123 in relaxing sarafotoxin S6b-precontracted arteries than endothelin-1-precontracted arteries, and suggests the existence of a heterogeneous receptor population on goat cerebral arteries (Kenakin, 1987). It is possible that different subtypes of $ET_A$ receptors mediate endothelin-1- and sarafotoxin S6b-elicited responses. A similar differentiation of $ET_A$ receptor subtypes has been proposed for endothelin-1- and endothelin-3-induced contractions in rat thoracic aorta (Sumner *et al.*, 1992). In a previous report (Salom *et al.*, 1992) we have shown that the nature of the extracellular $Ca^{2+}$ source mobilized by endothelin-1 and sarafotoxin S6b in goat cerebral arteries is also different since endothelin-1 depends on free extracellular $Ca^{2+}$ and sarafotoxin S6b depends on externally membrane-bound $Ca^{2+}$. The $Ca^{2+}$ source could be related to the receptor subtype involved in the response to each of the peptides.

In conclusion, both the order of potency of endothelin isopeptides and antagonism of endothelin-1- and sarafotoxin S6b-elicited responses by BQ-123 demonstrate the existence of $ET_A$ receptors mediating vasoconstriction in the goat middle cerebral artery. The difference in the antagonist potency of BQ-123, which is higher against sarafotoxin S6b than against endothelin-1, suggests the existence of subtypes of $ET_A$ receptors.

We thank M.C. Tirados and M.C. Máñez, for technical assistance. M.D.B. holds a F.I.S.S.S. research fellowship, and T.J. holds a research fellowship from Generalitat Valenciana.

## References

ARAI, H., HORI, S., ARAMORI, I., OHKUBO, H. & NAKANISHI, S. (1990). Cloning and expression of a cDNA encoding an endothelin receptor. *Nature*, **348**, 730–732.

CARDELL, L.O., UDDMAN, R. & EDVINSSON, L. (1992). Evidence for multiple endothelin receptors in the guinea-pig pulmonary artery and trachea. *Br. J. Pharmacol.*, **105**, 376–380.

D'ORLEANS-JUSTE, P., TELEMAQUE, S., CLAING, A., IHARA, M. & YANO, M. (1992). Human big-endothelin-1 and endothelin-1 release prostacyclin via the activation of $ET_1$ receptors in the rat perfused lung. *Br. J. Pharmacol.*, **105**, 773–775.

HARRISON, V.J., RANDRIANTSOA, A. & SCHOEFFTER, P. (1992). Heterogeneity of endothelin-sarafotoxin receptors mediating contraction of pig coronary artery. *Br. J. Pharmacol.*, **105**, 511–513.

IHARA, M., NOGUCHI, K., SAEKI, T., FUKURODA, T., TSUCHIDA, S., KIMURA, S., FUKAMI, T., ISHIKAWA, K., NISHIKIBE, M. & YANO, M. (1992a). Biological profiles of higly potent novel endothelin antagonists selective for the $ET_A$ receptor. *Life Sci.*, **50**, 247–255.

IHARA, M., SAEKI, T., FUKURODA, T., KIMURA, S., OZAKI, S., PATEL, A.C. & YANO, M. (1992b). A novel radioligand [$^{125}$I]BQ-3020 selective for endothelin ($ET_B$) receptors. *Life Sci.*, **51**, 47–52.

INOUE, A., YANAGISAWA, M., KIMURA, S., KASUYA, Y., MIYAUCHI, T., GOTO, K. & MASAKI, T. (1989). The human endothelin family: three structurally and pharmacologically distinct isopeptides predicted by three separate genes. *Proc. Natl. Acad. Sci. U.S.A.*, **86**, 2863–2867.

KENAKIN, T.P. (1987). *Pharmacological Analysis of Drug-Receptor Interaction*. New York: Raven Press.

KITAZUMI, K., SHIBA, T., NISHIKI, K., FURUKAWA, Y., TAKASAKI, C. & TASAKA, K. (1990). Structure-activity relationship in vasoconstrictor effects of sarafotoxins and endothelin-1. *FEBS Lett.*, **282**, 103–106.

KLOOG, Y. & SOKOLOVSKY, M. (1989). Similarities in mode and sites of action of sarafotoxins and endothelins. *Trends Pharmacol. Sci.*, **10**, 212–214.

MASAKI, T., YANAGISAWA, M. & GOTO, K. (1992). Physiology and pharmacology of endothelins. *Med. Res. Rev.*, **12**, 391–421.

MORELAND, S., MCMULLEN, D.M., DELANEY, C.L., LEE, V.G. & HUNT, J.T. (1992). Venous smooth muscle contains vasoconstrictor $ET_B$-like receptors. *Biochem. Biophys. Res. Commun.*, **184**, 100–106.

SAEKI, T., IHARA, M., FUKURODA, T., YAMAGIWA, M. & YANO, M. (1991). [Ala$^{1,3,11,15}$]endothelin-1 analogs with $ET_B$ agonistic activity. *Biochem. Biophys. Res. Commun.*, **179**, 286–292.

SAKURAI, T., YANAGISAWA, M., TAKUWA, Y., MIYAZAKI, H., KIMURA, S., GOTO, K. & MASAKI, T. (1990). Cloning of a cDNA encoding a non-isopeptide-selective subtype of the endothelin receptor. *Nature*, **348**, 732–735.

SALOM, J.B., TORREGROSA, G., MIRANDA, F.J., ALABADI, J.A. & ALBORCH, E. (1992). Comparison of the contractile effects of endothelin-1 and sarafotoxin S6b in goat isolated cerebral arteries. *Br. J. Pharmacol.*, **106**, 95–100.

SALOM, J.B., TORREGROSA, G., MIRANDA, F.J., ALABADI, J.A., ALVAREZ, C. & ALBORCH, E. (1991). Effects of endothelin-1 on the cerebrovascular bed of the goat. *Eur. J. Pharmacol.*, **192**, 39–45.

SUMNER, M.J., CANNON, T.R., MUNDIN, J.W., WHITE, D.G. & WATTS, I.S. (1992). Endothelin $ET_A$ and $ET_B$ receptors mediate vascular smooth muscle contraction. *Br. J. Pharmacol.*, **107,** 858–860.

TAKAYANAGI, R., KITAZUMI, K., TAKASAKI, C., OHNAKA, K., AIMOTO, S., TASAKA, K., OHASHI, M. & NAWATA, H. (1991). Presence of non-selective type of endothelin receptor on vascular endothelium and its likage to vasodilation. *FEBS Lett.*, **282,** 103–106.

TALLARIDA, R.J. & MURRAY, R.B. (1987). *Manual of Pharmacological Calculations with Computer Programs.* New York: Springer-Verlag.

TANOI, C., SUZUKI, Y., SHIBUYA, M., SUGITA, K., MASUZAWA, K. & ASANO, M. (1991). Mechanism of enhanced vasoconstrictor responses to endothelin-1 in canine cerebral arteries. *J. Cereb. Blood Flow Metab.*, **11,** 371–379.

WILLIAMS, D.L., JONES, K.L., PETTIBONE, D.J., LIS, E.V. & CLINE-SCHMIDT, B.V. (1991). Sarafotoxin S6c: an agonist which distinguishes between endothelin receptor subtypes. *Biochem. Biophys. Res. Commun.*, **175,** 556–561.

YANAGISAWA, M., KURIHARA, H., KIMURA, S., TOMOBE, Y., KOBAYASHI, M., MITSUI, Y., YAZAKI, Y., GOTO, K. & MASAKI, T. (1988). A novel potent vasoconstrictor peptide produced by vascular endothelial cells. *Nature*, **332,** 411–415.

YOSHINAGA, M., CHIJIIWA, Y, MISAWA, T., HARADA, N. & NAWATA, H. (1992). $Endothelin_B$ receptor on guinea pig small intestinal smooth muscle cells. *Am. J. Physiol.*, **262,** G308–G311.

*(Received February 1, 1993*
*Revised March 5, 1993*
*Accepted March 11, 1993)*

*Br. J. Pharmacol.* (1993), **109**, 831–837 © Macmillan Press Ltd, 1993

# Species-selective binding of [$^3$H]-idazoxan to $\alpha_2$-adrenoceptors and non-adrenoceptor, imidazoline binding sites in the central nervous system

[1]J.F. Hussain, D.A. Kendall & V.G. Wilson

Department of Physiology and Pharmacology, University of Nottingham Medical School, Queen's Medical Centre, Nottingham NG7 2DU

**1** We have used the imidazoline derivative [$^3$H]-idazoxan to define $\alpha_2$-adrenoceptors and non-adrenoceptor, imidazoline binding sites in cerebral cortex membranes of calf, mouse, rat, guinea-pig and man.

**2** Competition experiments using the selective α-adrenoceptor drugs, rauwolscine and corynanthine, indicated that [$^3$H]-idazoxan bound to a single population of sites in the calf and mouse membranes. However, [$^3$H]-idazoxan also labelled non-adrenoceptor, imidazoline binding sites in the rat (15%), guinea-pig (30%) and human (40%) cerebral cortex membranes.

**3** Competition experiments with adrenaline and cirazoline in the guinea-pig cortex, verified [$^3$H]-idazoxan binding to both $\alpha_2$-adrenoceptors and to non-adrenoceptor, imidazoline binding sites.

**4** It has been postulated by several groups that [$^3$H]-idazoxan may possess partial agonist activity. To investigate this further, saturation experiments were performed in the cerebral cortex membranes of all five species in the absence and presence of 300 μM guanosine triphosphate (GTP). GTP had no effect on [$^3$H]-idazoxan binding in guinea-pig cerebral cortex; in both rat and mouse membranes 300 μM GTP increased the dissociation constant for [$^3$H]-idazoxan by 2–3 fold without significantly affecting the $B_{max}$. GTP reduced the $B_{max}$ by approximately 30% and 60% in calf and human cerebral cortex membranes, respectively, without significantly altering the $K_d$.

**5** Saturation experiments were performed in the calf cerebral cortex membranes in the absence and presence of 300 μM GTP with the selective $\alpha_2$-adrenoceptor agonist [$^3$H]-clonidine and the selective muscarinic antagonist [$^3$H]-quinuclidinyl benzilate (QNB). GTP reduced the $B_{max}$ for [$^3$H]-clonidine without altering the $K_d$, but failed to affect either the $B_{max}$ or the $K_d$ for [$^3$H]-QNB.

**6** Saturation experiments were performed in human cerebral cortex membranes in the presence of $\alpha_2$-adrenoceptor blockade with and without GTP. GTP 300 μM reduced the $B_{max}$ for [$^3$H]-idazoxan at the non-adrenoceptor, imidazoline binding sites, without affecting the $K_d$. GTP did not affect [$^3$H]-QNB binding to muscarinic sites.

**7** Thus, there is a need to investigate further the pharmacological actions of [$^3$H]-idazoxan in view of its ability to recognise both $\alpha_2$-adrenoceptors and non-adrenoceptor, imidazoline binding sites and because it might possess agonist activity at some of these sites.

**Keywords:** [$^3$H]-idazoxan; $\alpha_2$-adrenoceptors; guanosine triphosphate; non-adrenoceptor; imidazoline binding sites

## Introduction

The imidazoline derivative, idazoxan, was originally developed as a selective antagonist for $\alpha_2$-adrenoceptors (Doxey *et al.*, 1983), and preliminary radioligand binding results supported this view. Hannah *et al.* (1983) showed that in rabbit cerebral cortex membranes, idazoxan displayed over 1000 fold selectivity for $\alpha_2$-adrenoceptors binding sites labelled by [$^3$H]-clonidine, compared to $\alpha_1$-adrenoceptor binding sites labelled by [$^3$H]-prazosin. Similarly, Pimoule *et al.* (1983) found that [$^3$H]-idazoxan binding in rat cerebral cortical membranes exhibited the characteristics of an $\alpha_2$-adrenoceptor. However, while idazoxan selectively inhibited $\alpha_2$-adrenoceptor-mediated inhibition of twitch responses in the rat isolated vas deferens, $\alpha_2$-adrenoceptor-mediated mydriasis in the rat and $\alpha_2$-adrenoceptor pressor responses in the pithed rat at doses or concentrations that failed to affect $\alpha_1$-adrenoceptor-mediated responses, the degree of selectivity in these functional models was much less than that predicted by the radioligand experiments (Berridge *et al.*, 1983; Doxey *et al.*, 1983).

In a few studies idazoxan has also been reported to display partial agonism at both $\alpha_1$- and $\alpha_2$-adrenoceptors. Paciorek & Shepperson (1983) noted that idazoxan produced prazosin-sensitive pressor responses in the pithed rat. Significantly this 'agonist' activity of idazoxan was not shared by various 2-alkyl analogues of idazoxan (Doxey *et al.*, 1984). In the anaesthetized rabbit, Hannah and coworkers (1983) observed transient pressor responses to a bolus injection of idazoxan which were partially reduced by either the selective $\alpha_1$-adrenoceptor antagonist, prazosin, or the selective $\alpha_2$-adrenoceptor antagonist, yohimbine, but abolished by the non-selective α-adrenoceptor antagonist, phentolamine, suggesting the involvement of both α-adrenoceptor subtypes. Finally, Limberger & Starke (1983) reported that idazoxan inhibited [$^3$H]-noradrenaline release from pre-junctional nerve endings in the rabbit isolated ear artery. Since this effect was sensitive to yohimbine, but resistant to prazosin, idazoxan was assumed to be acting as a partial agonist at pre-junctional $\alpha_2$-adrenoceptors.

More recently it has been recognized that [$^3$H]-idazoxan also binds to non-adrenoceptor, imidazoline binding sites, which have been identified in the rat cerebral cortex (Brown *et al.*, 1990), guinea-pig cerebral cortex (Wikberg & Uhlen, 1990), rabbit kidney (Lachaurd *et al.*, 1986), hamster adipocytes (MacKinnon *et al.*, 1989) and rabbit urethral smooth muscle (Yablonsky *et al.*, 1988). Pharmacologically these sites are characterized by a high affinity for idazoxan and the imidazoline derivative cirazoline, but low affinity for the

[1] Author for correspondence.

endogenous catecholamines, noradrenaline and adrenaline. Although there is limited information concerning the functional response associated with these binding sites, it is noteworthy that idazoxan has been reported to inhibit [$^3$H]-noradrenaline release in the pulmonary artery (Gothert & Molderings, 1991) and to reduce prolactin release in rats (Krulich *et al.*, 1989) by a non-α-adrenoceptor mechanism.

Thus, there is preliminary evidence that, in addition to being an antagonist at some $\alpha_2$-adrenoceptors, idazoxan may also act as a weak agonist in a number of other receptor systems. In the present study we have utilized the property of the guanine nucleotide, guanosine triphosphate (GTP), to reduce agonist binding, but not antagonist binding, to G-protein-coupled receptors (Hoffman *et al.*, 1980) to assess whether idazoxan might be a partial agonist at $\alpha_2$-adrenoceptors and at non-adrenoceptor, imidazoline binding sites in the cerebral cortex from several species. Preliminary observations in calf cerebral cortex membranes have shown that GTP reduces [$^3$H]-idazoxan binding, although the precise nature of the receptor(s) involved was not examined in detail (Hussain *et al.*, 1991). An inhibitory effect of GTP on idazoxan binding to non-adrenoceptor, imidazoline binding sites would also indicate that these sites represent a G-protein-coupled receptor system.

## Methods

### *Membrane preparation*

Calf, rat, guinea-pig, mouse and human cerebral cortex membranes were prepared as described below. The calf brain was obtained from the local abattoir immediately after the slaughter of the animal. The human brain was obtained not more than 8 h *post-mortem* from the Department of Pathology, Queen's Medical Centre. The rat, guinea-pig and mouse cerebral cortices were obtained after killing the animals by decapitation and rapidly removing the brains and dissecting on ice. Cerebral cortices were homogenized in 20 volumes of ice cold Tris buffer (50 mM Tris HCl; pH 7.4) in a Polytron PT disrupter (setting 6; 20–30 s). The homogenate was then centrifuged at 20,000 r.p.m. for 10 min at 4°C. The supernatant was discarded and the pellet resuspended in 20 volumes of Tris buffer and re-centrifuged. The final pellet was resuspended in 4.9 vol of 50 mM Tris buffer for direct use in binding assays or stored at − 20°C. Human and calf cerebral cortex membranes were prepared in a similar manner, except that homogenization of the cortices was achieved with an OMNI-GEN Macro homogenizer to minimize potential hazards associated with aerosol formation. Also, resuspension of the centrifuged pellet was with an Ultra turrax homogenizer sited in a laminar airflow hood.

### *Binding assays*

The affinity of various imidazoline and non-imidazoline compounds for binding sites labelled by [$^3$H]-idazoxan was examined. Competition binding assays were performed by incubating the washed membranes: (200–480 μg protein for the different species) with [$^3$H]-idazoxan (1–2 nM) in the presence or absence of a range of 12–18 concentrations of the competing ligand in a total volume of 500 μl of Tris assay buffer (50 mM Tris HCl; pH 7.4 at 25°C). Non-specific binding was defined as the concentration of bound ligand in the presence of 10 μM cirazoline. After an incubation period of 90 min at 25°C, bound radioactivity was separated from free by vacuum filtration over Whatman GF/B glass fibre filters using a Brandel cell harvester (or Skatron cell harvester for bovine cerebral cortex membranes) and quantified by liquid scintillation spectrometry. Saturation experiments were performed under similar conditions with increasing concentrations of [$^3$H]-idazoxan (0.1 to 10–15 nM). For saturation experiments with [$^3$H]-clonidine and [$^3$H]-quinuclidinyl benzilate (QNB), 100 μM noradrenaline and 10 μM atropine, respectively, were used to determine non-specific binding. The protein content of the tissues was measured by the method of Bradford (1976) with bovine serum albumin as the standard and results expressed as fmol mg$^{-1}$ protein. Kinetic analysis dissociation experiments with [$^3$H]-idazoxan were performed by adding the membranes at time 0 and terminating the incubation at the specific time points by the addition of 10 μM cirazoline.

### *Data analysis*

*Competition and saturation data analysis* The inhibition of the radioligand by competing ligands was analysed to estimate the $IC_{50}$ (concentration of competitor displacing 50% of specifically bound radioligand), with a non-linear least squares programme GraphPad (ISI). The $IC_{50}$ value was converted to an affinity constant ($K_i$) using the expression derived by Cheng & Prusoff (1973):

$$K_i = IC_{50}/(1 + [L]/K_d)$$

In this expression, [L] and $K_d$ represent the radioligand concentration and dissociation constant respectively. All data were initially analysed assuming a one site model of radioligand binding. The data, with Hill coefficients of less than unity were then analysed assuming a two site model. The model which gave a coefficient of correlation closest to one was accepted. GraphPad was also used to perform non-linear regression analysis for fitting data from saturation experiments. The expression used to derive $B_{max}$ and $K_d$ values was:

$$Y = AX/B + X \text{ where } A = B_{max} \text{ and } B = K_d$$

The function fits the data to a rectangular hyperbola graph. GraphPad was also used to analyse the kinetic data to determine the half-lives of the radioligand association and dissociation.

### *Drugs*

Drugs and chemicals were obtained from Sigma or Fisons plc except: [$^3$H]-idazoxan (43 Ci mmol$^{-1}$) Amersham, UK; [$^3$H]-QNB (quinuclidinyl benzilate) (50 Ci mmol$^{-1}$) Amersham, UK; [$^3$H]-clonidine (30 Ci mmol$^{-1}$) Amersham, UK; idazoxan (Reckitt and Colman); cirazoline (Synthelabo Recherche); guanosine-5′ triphosphate disodium salt (Boehringer Mannheim); rauwolscine hydrochloride (Carl Roth, Karlsruhe, Germany); atropine sulphate (BDH Chemicals Ltd).

## Results

### *Pharmacological characterization of [$^3$H]-idazoxan binding in the cerebral cortex from five species*

Figure 1 shows the effect of idazoxan and the yohimbine diastereoisomers rauwolscine and corynanthine at sites labelled by 1–2 nM [$^3$H]-idazoxan in calf, mouse, rat, guinea-pig and human cerebral cortex membranes. Idazoxan was similarly effective in all five species, there being less than a 3 fold difference in the p$K_i$ value between species (Table 1). In each tissue, rauwolscine possessed a high affinity for the sites labelled by [$^3$H]-idazoxan (p$K_i$ around 8) and was between 30–100 fold more potent than corynanthine (Table 1), a finding consistent with labelling of $\alpha_2$-adrenoceptors by [$^3$H]-idazoxan (McGrath, 1982; Daly *et al.*, 1988). However, in the rat, guinea-pig and human cerebral cortex, rauwolscine was clearly able to discriminate between two sites labelled by [$^3$H]-idazoxan (Figure 1c, d, e). The displacement curve for rauwolscine was characterized by a resistant component of [$^3$H]-idazoxan binding between 1 μM and 30 μM rauwolscine. The magnitude of the rauwolscine-resistant component was approximately 15%, 30% and 40% of the total [$^3$H]-idazoxan

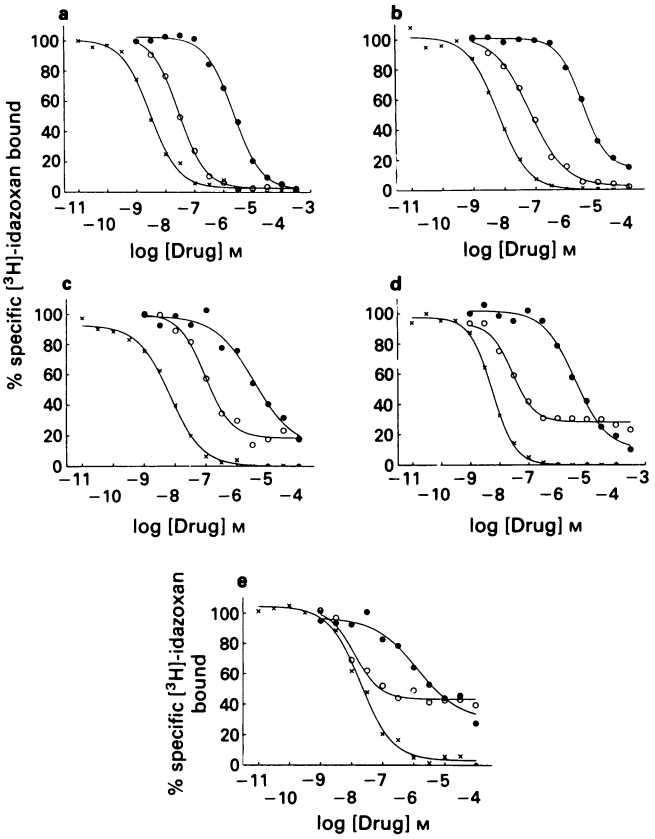



**Figure 1** Inhibition of [³H]-idazoxan binding in the cerebral cortex membranes of the (a) calf, (b) mouse, (c) rat, (d) guinea-pig, and (e) man by rauwolscine (○); corynanthine (●) and idazoxan (×). Non-specific binding was determined in the presence of 10 μM cirazoline and the assay was performed in 50 mM Tris buffer pH 7.4 (final volume 500 μl) for 90 min at 25°C. Non-specific binding was in the range of 10–15% of total binding. The figures are representative of 3 separate experiments.

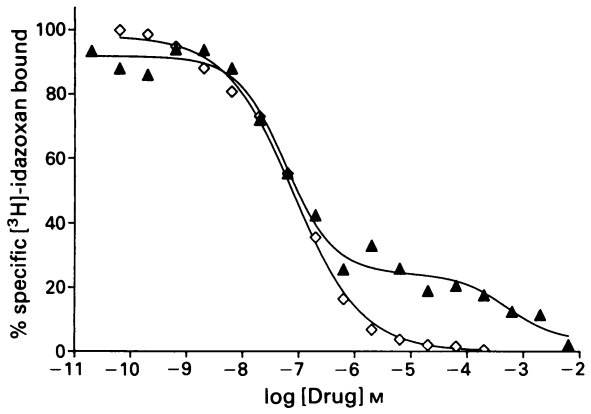



**Figure 2** Inhibition of [³H]-idazoxan binding in the guinea-pig cerebral cortex membranes by adrenaline (▲) and cirazoline (◇). Non-specific binding was determined in the presence of 10 μM cirazoline and the assay was performed in 50 mM Tris buffer pH 7.4 (final volume 500 μl) for 90 min at 25°C. Non-specific binding was in the range of 10–15% of total binding. The figure is representative of 3–5 separate experiments.

binding in the rat, guinea-pig and human cerebral cortex membranes, respectively.

Figure 2 shows the effect of adrenaline and cirazoline against [³H]-idazoxan binding in guinea-pig cerebral cortex membranes. Cirazoline completely displaced [³H]-idazoxan binding with a $pK_i$ of 7.29 and Hill slope (nH) of −0.7 ($n = 2$). The displacement of [³H]-idazoxan by adrenaline (nH of $-0.48 \pm 0.07$, $n = 5$), indicates a low affinity population of sites resistant to adrenaline binding, the $IC_{50}$ of the low affinity component is $> 100$ μM adrenaline; the high affinity component (presumably binding to an adrenoceptor) represents 70% of the specific binding and has a $pK_i$ of $7.62 \pm 0.24$ ($n = 5$). This is essentially in agreement with the observation made with rauwolscine and indicates that the rauwolscine-resistant component of [³H]-idazoxan binding in the guinea-pig cerebral cortex is a non-adrenoceptor, imidazoline binding site (Figure 1d).

### *The effect of 300 μM GTP on saturation binding of [³H]-idazoxan*

Saturation curves were performed with increasing concentrations of [³H]-idazoxan (0.1 to 10–15 nM) in calf, mouse, rat, guinea-pig and human cerebral cortex membranes in the presence and absence of 300 μM GTP (Figure 3). In the absence of 300 μM GTP, the $K_d$ values for [³H]-idazoxan varied from $0.81 \pm 0.17$ nM ($n = 7$) in calf cerebral cortex membranes to $6.67 \pm 0.54$ nM ($n = 4$) in human cerebral cortex membranes. The maximum number of binding sites varied from $119 \pm 5$ fmol mg$^{-1}$ protein ($n = 7$) in calf cerebral cortex membranes to $499 \pm 28.2$ fmol mg$^{-1}$ protein in mouse cerebral cortex membranes ($n = 5$). The dissociation constants and maximum number of binding sites for the other preparations are shown in Table 2.

GTP, 300 μM, had no significant effect on [³H]-idazoxan binding in guinea-pig cerebral cortex (Figure 3d, Table 2). In both rat and mouse cerebral cortex membranes, 300 μM GTP increased the dissociation constant for [³H]-idazoxan by 2–3 fold without significantly affecting $B_{max}$ (Figure 3b,c and Table 2). In marked contrast, 300 μM GTP reduced $B_{max}$ by approximately 30% and 60% in calf and human cerebral cortex membranes, respectively, without significantly altering $K_d$ (Figure 3a,e and Table 2).

Association of [³H]-idazoxan to calf cortex membranes was rapid, equilibrium was reached within 2 min. Figure 4 shows that the half-life for the dissociation of specific [³H]-idazoxan binding from calf cerebral cortex membranes was unaffected by the presence of 300 μM GTP, thereby supporting the complementary saturation experiments which indicate that GTP does not affect the affinity of idazoxan.

**Table 1** Displacement of [³H]-idazoxan (1–2 nM) from calf, human, guinea-pig, rat and mouse cerebral cortex membranes

| *Species* | *Rauwolscine* $pK_i$ (nH) | *Corynanthine* $pK_i$ (nH) | *Idazoxan* $pK_i$ (nH) |
|---|---|---|---|
| Calf | 7.91 ± 0.08; (− 1.09 ± 0.15) | 6.24 ± 0.08; (− 0.79 ± 0.02) | 8.57 ± 0.25; (− 0.97 ± 0.08) |
| Man | 8.26 ± 0.09; (− 0.59 ± 0.07) | 6.55 ± 0.08; (− 0.63 ± 0.07) | 8.19 ± 0.12; (− 0.80 ± 0.10) |
| Guinea-pig | 7.94 ± 0.02; (− 0.77 ± 0.15) | 5.93 ± 0.02; (− 0.97 ± 0.31) | 8.56 ± 0.03; (− 0.92 ± 0.07) |
| Rat | 7.36 ± 0.02; (− 0.72 ± 0.09) | 6.02 ± 0.16; (− 0.78 ± 0.16) | 8.66 ± 0.22; (− 0.79 ± 0.08) |
| Mouse | 7.59 ± 0.07; (− 0.66 ± 0.08) | 5.84 ± 0.04; (− 1.02 ± 0.10) | 8.47 ± 0.09; (− 0.95 ± 0.11) |

The $pK_i$ values were calculated from the displacement of 1–2 nM [³H]-idazoxan from calf, human, guinea-pig, rat and mouse cerebral cortex membranes as described in Methods. Each value represents the mean ± s.e.mean of three separate experiments.

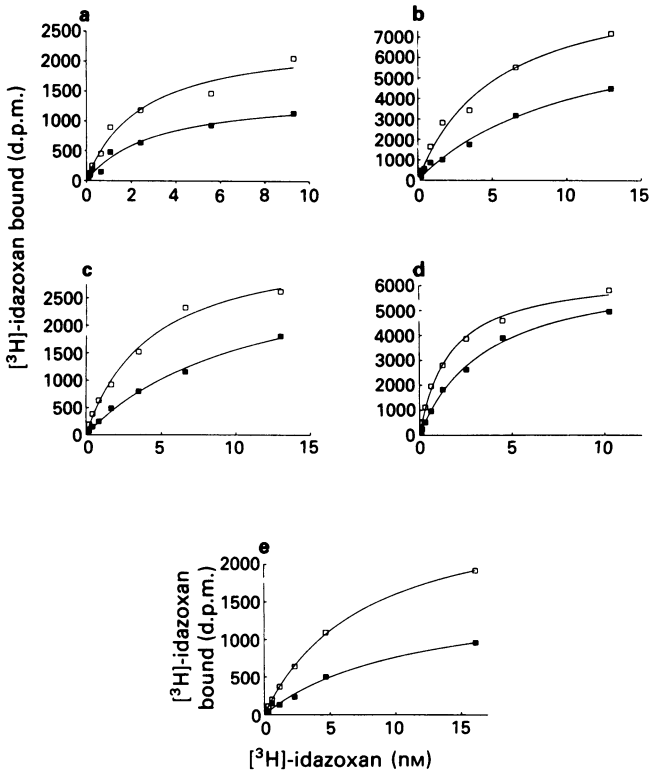



**Figure 3** Saturation curves of [$^3$H]-idazoxan binding to (a) calf, (b) human, (c) guinea-pig, (d) mouse and (e) rat cerebral cortex membranes. The preparations were incubated with increasing concentrations of [$^3$H]-idazoxan in the absence (□) or presence of 300 μM GTP (■). Non-specific binding was determined in the presence of 10 μM cirazoline and the assay was performed in 50 mM Tris buffer pH 7.4 (final volume 500 μl) for 90 min at 25°C. Non-specific binding was in the range of 10–15% of total binding. $B_{max}$ and $K_d$ values were calculated with the computer curve fitting programme GraphPad. The data shown are representative of one experiment with each point determined in duplicate. Similar results were obtained in 3–7 other experiments.

### *Further examination of the effect of GTP in calf and human cerebral cortex membranes*

The finding that 300 μM GTP significantly reduced [$^3$H]-idazoxan binding in calf and human cerebral cortex membranes, without affecting the dissociation constant, prompted further experiments to examine this phenomenon in greater detail. Figure 5 shows the effect of 300 μM GTP on saturation curves for the binding of the selective $\alpha_2$-adrenoceptor agonist, [$^3$H]-clonidine and the selective muscarinic antagonist, [$^3$H]-QNB to calf cerebral cortex membrane. GTP (300 μM) significantly reduced the $B_{max}$ for [$^3$H]-clonidine binding from 51.7 ± 14.7 to 29.0 ± 5.5 fmol mg$^{-1}$ protein ($n = 4$), but the dissociation constant in the presence (4.35 ± 1.39 nM) and absence (3.56 ± 1.27 nM) of 300 μM GTP were not significantly different (Figure 5a). In marked contrast, 300 μM GTP failed to affect either the dissociation constant or the $B_{max}$ value for [$^3$H]-QNB binding (Figure 5b).

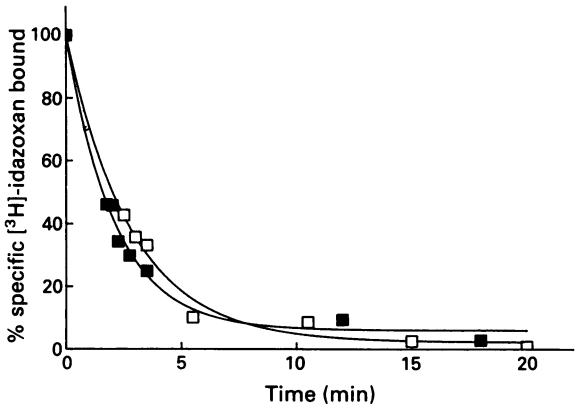



**Figure 4** The effect of 300 μM GTP on the dissociation of [$^3$H]-idazoxan from calf cerebral cortex membranes. Membranes were preincubated for 30 min at 25°C in the presence of 1–2 nM [$^3$H]-idazoxan. Specific binding was determined at various time intervals with the addition of 10 μM cirazoline to the samples starting at time 0 with (■) or without (□) 300 μM GTP. Dissociation of [$^3$H]-idazoxan followed first order kinetics with half-lives of 1.40 ± 0.42 and 1.48 ± 0.48 min, with and without GTP respectively. Half-lives were not significantly different ($P > 0.05$ paired $t$ test).

Figure 6 shows the effect of 300 μM GTP on [$^3$H]-idazoxan binding to human cerebral cortex membranes in the presence of 1 μM rauwolscine (to mask $\alpha_2$-adrenoceptor binding sites). GTP (300 μM) significantly reduced the $B_{max}$ for [$^3$H]-idazoxan at the non-adrenoceptor, imidazoline sites from 86.6 ± 11.7 to 55.7 ± 11.7 ($n = 3$) fmol mg$^{-1}$ protein, without affecting the dissociation constant (9.71 ± 0.86 nM and 9.94 ± 2.29 nM in the absence and presence, respectively, of 300 μM GTP). In contrast, 300 μM GTP failed to affect either the dissociation constant (1.00 ± 0.58 nM and 1.29 ± 0.78 nM ($n = 3$) in the absence and presence, respectively, of GTP) or the $B_{max}$ (567 ± 53 and 562 ± 51 fmol mg$^{-1}$ protein ($n = 3$) in the absence and presence, respectively, of GTP) of [$^3$H]-QNB binding to human cerebral cortex.

## Discussion

In the present study we have shown that the imidazoline derivative [$^3$H]-idazoxan binds to both $\alpha_2$-adrenoceptor and non-adrenoceptor, imidazoline binding sites in cerebral cortex membranes from several species. The $\alpha_2$-adrenoceptor binding sites have been identified by the 100 fold greater potency of rauwolscine compared to its diastereoisomer, corynanthine (see: McGrath, 1982), while the non-adrenoceptor, imidazoline component of [$^3$H]-idazoxan binding has been identified as that portion of the cirazoline-sensitive [$^3$H]-idazoxan binding which is resistant to either adrenaline or

**Table 2** Effect of GTP on the specific binding of [$^3$H]-idazoxan to calf, human, guinea-pig, rat and mouse cerebral cortex membranes

| | $K_d$ (nM) | | $B_{max}$ (fmol mg$^{-1}$) | |
|---|---|---|---|---|
| *Species* | *Control* | *GTP (300 μM)* | *Control* | *GTP (300 μM)* |
| Calf | 0.81 ± 0.17 | 1.03 ± 0.07 | 119.4 ± 4.5 | 82.2 ± 4.2** |
| Man | 6.67 ± 0.54 | 5.39 ± 0.69 | 148.7 ± 9.7 | 56.8 ± 3.0** |
| Guinea-pig | 3.25 ± 0.81 | 4.86 ± 0.87 | 209.7 ± 5.0 | 232.3 ± 7.6 |
| Rat | 5.07 ± 0.74 | 11.17 ± 1.51* | 128.8 ± 10.4 | 127.0 ± 13.1 |
| Mouse | 4.44 ± 0.34 | 13.99 ± 2.20* | 499.0 ± 28.2 | 423.9 ± 34.9 |

Saturation experiments were performed in the absence and presence of 300 μM GTP. Values shown are the mean ± s.e.mean of 3–7 experiments.
*$P < 0.05$; **$P < 0.01$; unpaired $t$ test.

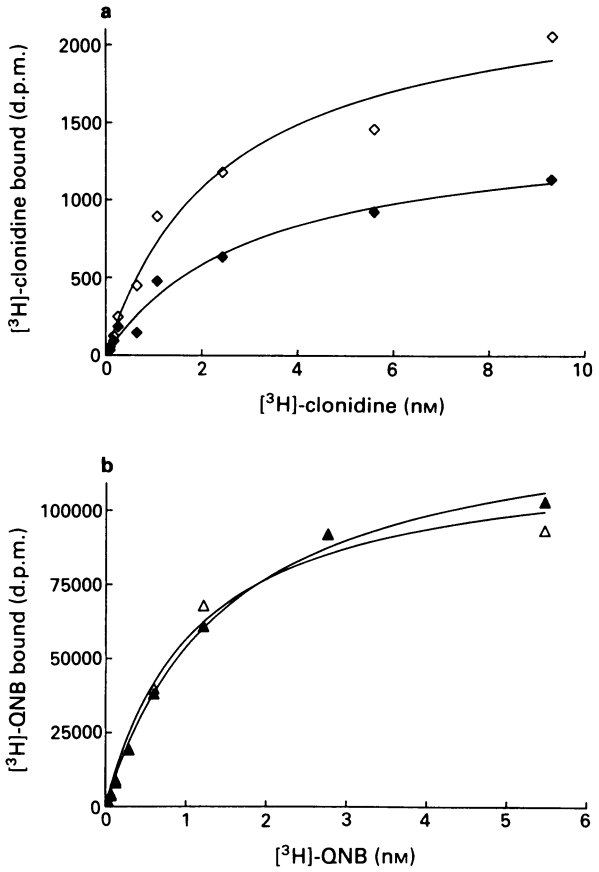



**Figure 5** Saturation curves of (a) [$^3$H]-clonidine and (b) [$^3$H]-quinuclidinylbenzoate ([$^3$H]-QNB) binding to calf cerebral cortex membranes. (a) The preparation was incubated with increasing concentrations of [$^3$H]-clonidine; in the absence (◇) and presence (◆) of 300 μM GTP; non-specific binding was defined in the presence of 10 μM adrenaline. (b) The preparation was incubated with increasing concentrations of [$^3$H]-QNB in the absence (△) and presence (▲) of 300 μM GTP; non-specific binding was defined in the presence of 10 μM atropine. The assay was performed in 50 mM Tris buffer pH 7.4 (final volume 500 μl) for 90 min at 25°C. Non-specific binding was in the range of 10–15% of total binding. $B_{max}$ and $K_d$ values were calculated with the computer curve fitting programme GraphPad. The data shown are representative of one experiment with each point determined in duplicate. Similar results were obtained in 2 other experiments.

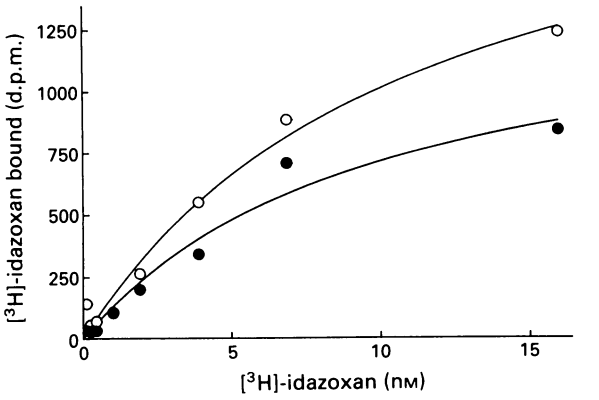



**Figure 6** Saturation curve of [$^3$H]-idazoxan binding to human cerebral cortex membranes. The preparation was incubated with increasing concentrations of [$^3$H]-idazoxan in the presence of 1 μM rauwolscine (○), or in the presence of 1 μM rauwolscine + 300 μM GTP (●). Non-specific binding was determined in the presence of 10 μM cirazoline and the assay was performed in 50 mM Tris buffer pH 7.4 (final volume 500 μl) for 90 min at 25°C. Non-specific binding was in the range of 10–15% of total binding. $B_{max}$ and $K_d$ values were calculated with the computer curve-fitting programme GraphPad. The data shown are representative of one experiment with each point determined in duplicate. Similar results were obtained in 2 other experiments.

rauwolscine. In calf and mouse cerebral cortex membranes, idazoxan labels only $\alpha_2$-adrenoceptors, while in the rat, guinea-pig and human cerebral cortex membranes there is an increasing contribution made by imidazoline binding sites to total [$^3$H]-idazoxan binding. These results are in agreement with earlier reports suggesting the presence of non-adrenoceptor, imidazoline binding sites in the rat (Brown *et al.*, 1990), guinea-pig (Wikberg & Uhlen, 1990) and human cerebral cortex (De Vos *et al.*, 1991).

GTP had no effect on [$^3$H]-idazoxan binding in the guinea-pig cerebral cortex membranes, the $B_{max}$ and $K_d$ values remaining unaltered in the presence of 300 μM GTP. These results suggest that idazoxan might be acting as an antagonist at both $\alpha_2$-adrenoceptors and at non-adrenoceptor, imidazoline binding sites, in this preparation. GTP reduced the affinity of [$^3$H]-idazoxan for $\alpha_2$-adrenoceptors in the mouse cerebral cortex membranes; and also in the rat where 85% of the [$^3$H]-idazoxan binding sites are $\alpha_2$-adrenoceptors. This increase in $K_d$ with no change in $B_{max}$ would be expected of agonist modulation by guanine nucleotides (U'Prichard *et al.*, 1976; Hoffman *et al.*, 1980), suggesting that [$^3$H]-idazoxan may have agonist activity at $\alpha_2$-adrenoceptors.

A decrease in the $B_{max}$ of [$^3$H]-idazoxan binding at $\alpha_2$-adrenoceptors was observed in the calf and human cerebral cortex membranes in the presence of GTP. It has been suggested that the affinity of certain receptors could be reduced by GTP to such a degree that the binding is no longer observable, therefore manifesting itself as a decrease in $B_{max}$ (Ofri *et al.*, 1992). This action of GTP is consistent with its effects on agonist binding to a number of receptor systems e.g. the full $\alpha_2$-adrenoceptor agonist [$^3$H]-UK-14,304 in human platelet membranes (Schloos *et al.*, 1987); the partial $\alpha_2$-adrenoceptor agonist [$^{125}$I]-*p*-iodoclonidine in human platelet membranes (Gerhardt *et al.*, 1990); [$^3$H]-5-hydroxytryptamine (5-HT) in rat hippocampus (Mallat & Hamon, 1982); [$^3$H]-8-OH-DPAT in rat cortical membranes (Harrington & Peroutka, 1990) and the endogenous agonist [$^{125}$I]-neuropeptide Y in human SK-N-MC neuroblastoma cells (Feth *et al.*, 1991). The difference in the effect of GTP on [$^3$H]-idazoxan binding in rat and mouse, and calf and man could be a reflection of $\alpha_2$-adrenoceptor heterogeneity, e.g. the low Hill slopes for rauwolscine in Table 1.

The effect of GTP does not appear to be non-specific because it had no effect on [$^3$H]-QNB binding in the human and calf cortex membranes, and no effect was observed on [$^3$H]-idazoxan binding in the guinea-pig cerebral cortex membranes. The effects of GTP observed in the calf and human cerebral cortex membranes are qualitatively similar to the effects observed with the $\alpha_2$-adrenoceptor partial agonist radioligand [$^3$H]-clonidine in the calf cortex (Figure 5a). The 'agonist' action of idazoxan at $\alpha_2$-adrenoceptors is consistent with the observations of Limberger & Starke (1983); however, idazoxan should still be considered essentially as an antagonist at most $\alpha_2$-adrenoceptors.

The data from the saturation studies in the human cerebral cortex membranes show a reduction in $B_{max}$ by GTP suggesting that idazoxan might be an agonist at non-adrenoceptor binding sites and that these sites could be part of the G-protein receptor superfamily; in support of this there is a similar effect of GTP in the porcine renal cortex (Hussain *et al.*, 1992). A parallel observation has been made for rauwolscine, an $\alpha_2$-adrenoceptor antagonist (De Vos *et al.*, 1991). Rauwolscine binding at 5-$HT_{1A}$ receptors in the human frontal cortex membranes was decreased by GTP (500 μM), indicating an agonist role for rauwolscine at these receptors. Interestingly, GTP has also been reported to influence [$^3$H]-aminoclonidine binding to non-adrenoceptor imidazoline binding sites in the calf ventral lateral medulla (Ernsberger, 1992). Further evidence suggesting agonist activity of idazoxan at non-adrenoceptor, imidazoline binding sites has been reported by Gothert & Molderings (1991) who observed that when $\alpha_2$-adrenoceptors were blocked by either rauwolscine or by exposure to phenoxybenzamine, [$^3$H]-adrenaline

overflow from the rabbit pulmonary artery was inhibited by idazoxan. In addition, a chronic infusion study with idazoxan (1.1 mg $kg^{-1}$ $h^{-1}$ for 5 days) in rabbits showed a down regulation of [$^3$H]-idazoxan binding sites in the kidney membranes, suggesting agonist activity of [$^3$H]-idazoxan at the non-adrenoceptor sites in this preparation (Yakubu *et al.*, 1990).

However, in some systems idazoxan can act as an antagonist at brain non-adrenoceptor, imidazoline binding sites, for example Olmos *et al.* (1991, 1992) reported that chronic treatment with idazoxan (10 mg $kg^{-1}$, i.p. every 12 h, 7 days) consistently increased the density of imidazoline receptors in the brain of Wistar-Kyoto and Sprague-Dawley rats. This up-regulation is consistent with the effect of a chronic treatment with an antagonist on receptor number. There are several reports in the literature of a lack of effect of Gpp(NH)p or GTP on UK-14,304 displacement of [$^3$H]-idazoxan binding at non-$\alpha_2$-adrenoceptor sites (Michel *et al.*, 1989; Langin *et al.*, 1990; Zonnenschein *et al.*, 1990; Lachaud-Pettiti *et al.*, 1991). The apparent contradiction between these previous reports and the current study may derive from different species and tissues used or from methodological differences (e.g. [$^3$H]-idazoxan saturation isotherms were constructed in the present study while the previous studies employed inhibition curves, additionally, it is possible that UK-14,304 is not an agonist at the non-adrenoceptor, imidazoline binding sites).

Thus, there is a need to re-evaluate the actions of idazoxan in light of its ability to recognize both $\alpha_2$-adrenoceptors and non-adrenoceptor, imidazoline binding sites, and because it may possess agonist activity at some of these sites.

We are grateful to the Mason Brothers Abattoir (Nottingham), the Pathology Department (Queen's Medical Centre) and the Smith Kline Foundation. J.F.H. is a SERC/CASE student with Syntex (Edinburgh).

## References


BERRIDGE, T.L., GADIE, B., ROACH, A.G. & TULLOCH, I.F. (1983). $\alpha_2$-Adrenoceptor agonists induce mydriais in the rat by an action within the central nervous system. *Br. J. Pharmacol*, **78,** 507–515.

BRADFORD, M.M. (1976). A rapid and sensitive method for the quantitation of microgram quantities of protein utilizing the principle of protein-dye binding. *Anal. Biochem*, **72,** 248–254.

BROWN, C.M., MACKINNON, A.C., MCGRATH, J.C., SPEDDING, M. & KILPATRICK, A.T. (1990). $\alpha_2$-Adrenoceptor subtypes and imidazoline-like binding sites in the rat brain. *Br. J. Pharmacol.*, **99,** 803–809.

CHENG, Y.-C. & PRUSOFF, W.H. (1973). Relationship between the inhibition constant ($K_i$) and the concentration of inhibitor which causes 50 percent inhibition ($IC_{50}$) of an enzymatic reaction. *Biochem. Pharmacol*, **22,** 3099–3108.

DALY, C.J., MCGRATH, J.C. & WILSON, V.G. (1988). An examination of the post-junctional α-adrenoceptors subtypes for (−)-noradrenaline in several isolated blood vessels form the rabbit. *Br. J. Pharmacol.*, **95,** 473–484.

DEVOS, H., CZERWIEC, E., DEBACKER, J.-P., DEPOTTER, W. & VAUQUELIN, G. (1991). [$^3$H]-Rauwolscine behaves as an agonist for the 5-$HT_{1A}$ receptors in human frontal cortex membranes. *Eur. J. Pharm. (Mol. Pharmacol. Sec.)*, **207,** 1–8.

DOXEY, J.C., ROACH, A.G. & SMITH, C.F.C. (1983). Studies on RX-781094: a selective potent and specific antagonist of $\alpha_2$-adrenoceptors. *Br. J. Pharmacol.*, **78,** 489–505.

DOXEY, J.C., ROACH, A.G., STRACHAN, D.A. & VIRDEE, N.K. (1984). Selectivity and potency of 2-alkyl analogues of the $\alpha_2$-adrenoceptor antagonist (RX 781094) in peripheral systems. *Br. J. Pharmacol,*. **83,** 713–722.

ERNSBERGER, P. (1992). Heterogeneity of imidazoline binding sites: proposal $I_1$ and $I_2$ subtypes. *Fundam. Clin. Pharmacol.*, **6,** P18.

FETH, F., RASCHER, W. & MICHEL, M.C. (1991). G-Protein coupling and signalling of $Y_1$-like neuropeptide Y receptors in SK-N-MC cells. *Naunyn Schmieds Arch. Pharmacol,*. **344,** 1–7.

GERHARDT, M.A., WADE, S.M. & NEUBIG, R.R. (1990). *p*-[$^{125}$I]-Iodoclonidine is a partial agonist at the $\alpha_2$-adrenergic receptor. *Mol. Pharmacol.*, **38,** 214–221.

GOTHERT, M. & MOLDERINGS, G.J. (1991). Involvement of presynaptic imidazoline receptors in the $\alpha_2$-adrenoceptor-independent inhibition of noradrenaline release by imidazoline derivatives. *Naunyn-Schmieds Arch. Pharmacol.*, **343,** 271–282.

HANNAH, J.A.M., HAMILTON, C.A. & REID, J.L. (1983). RX781094, a new potent $\alpha_2$ adrenoceptor antagonist. *In vivo* and *in vitro* studies in the rabbit. *Naunyn Schmieds Arch. Pharmacol.*, **322,** 221–227.

HARRINGTON, M.A. & PEROUTKA, S.J. (1990). Modulation of 5-hydroxytryptamine$_{1A}$ receptor density by nonhydrozyable GTP analogues. *J. Neurochem.*, **54,** 294–299.

HOFFMAN, B.B., MULLIKIN-KILPATRICK, D. & LEFKOWITZ, R.J. (1980). Heterogeneity of radioligand binding to α-adrenergic receptors. Analysis of guanine nucleotide regulation of agonist binding in relation to receptor subtypes. *J. Biol. Chem.*, **255,** 4645–4652.

HUSSAIN, J.F., KENDALL, D.A. & WILSON, V.G. (1992). A possible linkage of non-adrenoceptor, imidazoline binding sites labelled by [$^3$H]-idozoxan to $K^+$ channels and G-proteins. *Br. J. Pharmacol.*, **107,** 323P.

HUSSAIN, J.F., WILSON, V.G. & KENDALL, D.A. (1991). The effect of guanine nucleotides on [$^3$H]-idazoxan binding in the bovine cerebral cortex. *Br. J. Pharmacol.*, **104,** 269P.

KRULICH, L., JURCOVICOVA, J. & LE, T. (1989). Prolactin (PRL) release-inhibiting properties of the $\alpha_2$-adrenergic receptor antagonist idazoxan: comparison with yohimbine. *Life Sci.*, **44,** 809–818.

LACHAUD, V., COUPRY, I., PODEVIN, R.-A., DAUSSE, J.-P., KOENIG, E. & PARINI, A. (1986). Interaction of clonidine and rilmenidine with imidazoline-preferring receptors. *J. Hypertens,*. **6** (Suppl. 4), S511–S518.

LACHAUD-PETTITI, V., PODEVIN, R.-A., CHIETIEN, Y. & PARINI, A. (1991). Imidazoline-guanidinium and $\alpha_2$-adrenergic binding sites in basolateral membranes from human kidney. *Eur. J. Pharmacol. (Mol. Pharmacol. Sec.)*, **206,** 23–31.

LANGIN, D., PARIS, H. & LAFONTAN, M. (1990). Binding of [$^3$H]-idazoxan and its methoxyderivative [$^3$H]-RX821002 in human fat cells: [$^3$H]-idazoxan but not [$^3$H]-RX821002 labels additional non-$\alpha_2$-adrenergic binding sites. *Mol. Pharmacol.*, **37,** 876–885.

LIMBERGER, N. & STARKE, K. (1983). Partial agonist effect of 2-[2-(1,4-benzodioxanyl)]-2-imidazoline (RX781094) at presynaptic $\alpha_2$-adrenoceptors in rabbit ear artery. *Naunyn-Schmieds Arch. Pharmacol.*, **324,** 75–78.

MACKINNON, A.C., BROWN, C.M., SPEDDING, M. & KILPATRICK, A.T. (1989). [$^3$H]-idazoxan binds with high affinity to two sites on hamster adipocytes: an $\alpha_2$-adrenoceptor and a non-adrenoceptor sites. *Br. J. Pharmacol.*, **98,** 1143–1150.

MALLAT, M.C. & HAMON, M. (1982). $Ca^{2+}$-guanine interaction in brain membranes. I. Modulation of central 5-hydroxytryptamine receptors in the rat. *J. Neurochem.*, **38,** 151–161.

MCGRATH, J.C. (1982). Evidence for more than one type of post-junctional α-adrenoceptor. *Biochem. Pharmacol.*, **31,** 467–484.

MICHEL, M.C., BRODDE, O.-E., SCHNEPEL, B., BEHRENDT, J., TSCHAUDA, R., MOTULSKY, H.J. & INSEL, P.A. (1989). Nonadrenergic [$^3$H]-idazoxan binding sites are physically distinct from $\alpha_2$-adrenergic receptors. *Mol. Pharmacol.*, **35,** 324–330.

OFRI, D., RITTER, A.M., LIU, Y., GIOANNINI, T.L., HILLER, J.M. & SIMON, E.J. (1992). Characterization of solubilized opioid receptors: reconstitution and uncoupling of guanine nucleotide-sensitive agonist binding. *J. Neurochem.*, **58,** 628–635.

OLMOS, G., MIRALLES, A., BARTUREN, F. & GARCIA-SEVILLA, J.A. (1991). Repeated idazoxan increases brain imidazoline receptors in normotensive (WKY) but not in hypertensive (SHR) rats. *J. Neurochem.*, **57,** 1811–1813.

OLMOS, G., MIRALLES, A., BARTUREN, F. & GARCIA-SEVILLA, J.A. (1992). Characterization of brain imidazoline receptors in normotensive and hypertensive rats: differential regulation by chronic imidazoline drug treatment. *J. Pharmacol. Exp. Ther.*, **260,** 1000–1007.

PACIOREK, P.M. & SHEPPERSON, N.B. (1983). $\alpha_1$-Adrenoceptor agonist activity of $\alpha_2$-adrenoceptor antagonist in the pithed rat preparation. *Br. J. Pharmacol.*, **79,** 12–14.

PIMOULE, C., SCATTON, B. & LANGER, S.Z. (1983). [$^3$H]-RX781094: a new antagonist ligand labels $\alpha_2$-adrenoceptors in the rat brain cortex. *Eur. J. Pharmacol.*, **95,** 79–85.

SCHLOOS, J., WELLSTEIN, A. & PALM, D. (1987). Agonist binding at $\alpha_2$-adrenoceptors of human platelets using [$^3$H]-UK14,304: regulation by Gpp(NH)p and cations. *Naunyn-Schmieds Arch. Pharmacol.*, **336,** 48–59.

U'PRICHARD, P.C., GREENBERG, D.A. & SNYDER, S.H. (1976). Binding characteristics of a radioligand agonist and antagonist at central nervous system α-noradrenergic receptors. *Mol. Pharmacol.*, **13,** 454–473.

WIKBERG, J.E.S. & UHLEN, S. (1990). Further characterization of the guinea-pig cerebral cortex idazoxan receptor: solubilization, distinction from the imidazoline site, and demonstration of cirazoline as an idazoxan receptor-selective drug. *J. Neurochem.*, **55,** 192–203.

YABLONSKY, F., RIFFAUD, J.P., LACOLLE, J.Y. & DAUSSE, J.P. (1988). Evidence for non-adrenergic binding sites for [$^3$H]-idazoxan in the smooth muscle of rabbit urethra. *Eur. J. Pharmacol.*, **154,** 209–212.

YAKUBU, M.A., DEIGHTON, N.M., HAMILTON, C.A. & REID, J.L. (1990). Differences in the regulation of [$^3$H]-idazoxan and [$^3$H]-yohimbine binding sites in the rabbit. *Eur. J. Pharmacol.*, **176,** 305–311.

ZONNENSCHEIN, R., DIAMANT, S. & ATLAS, D. (1990). Imidazoline receptors in the rat liver cells: a novel receptor or a subtype of $\alpha_2$-adrenoceptors. *Eur. J. Pharmacol.*, **190,** 203–215.

*(Received January 13, 1993*
*Revised February 24, 1993*
*Accepted February 25, 1993)*

*Br. J. Pharmacol.* (1993), **109**, 838–844 © Macmillan Press Ltd, 1993

# Hypercholesterolaemia severely impairs EDRF-dependent collateral perfusion following acute arterial occlusion in rabbit isolated ear

[1]Michael D. Randall, *Jerry A. Smith & Tudor M. Griffith

Departments of Diagnostic Radiology and *Cardiology, University of Wales College of Medicine, Heath Park, Cardiff CF4 4XN

**1** We have used a rabbit isolated buffer-perfused ear as a model of acute arterial occlusion to investigate the effects of dietary-induced hypercholesterolaemia on EDRF-dependent collateral perfusion. The effects of hypercholesterolaemia on endothelium-dependent relaxations to acetylcholine were also investigated in the unligated isolated buffer-perfused ear of the rabbit.

**2** In rabbits receiving a high cholesterol diet (1%) for 4 weeks, blood cholesterol levels were significantly ($P<0.001$) increased ($26.0 \pm 3.6$ vs. $2.6 \pm 0.6$ mmol $l^{-1}$), EDRF-dependent collateral perfusion was similar to that in age-matched controls for the first 15 min after occlusion but then decreased and was significantly ($P<0.01$) less than control during the maintenance phase of collateral perfusion.

**3** Cholesterol feeding for 8 weeks (blood cholesterol = $56.2 \pm 3.8$ vs. $1.3 \pm 0.1$ mmol $l^{-1}$) was associated with almost complete impairment of collateral perfusion, an effect previously observed following inhibition of EDRF synthesis.

**4** Endothelium-dependent relaxations to acetylcholine in isolated perfused ears were impaired in the rabbits fed the diet for 8 weeks but not those fed for 4 weeks. In the 8 week group, the maximum relaxation of tone was $32.6 \pm 11.6\%$ and was significantly ($P<0.01$) less than that in the controls ($77.9 \pm 5.7\%$).

**5** We conclude that EDRF-dependent collateral perfusion is severely impaired in hypercholesterolaemia and that the level of impairment is related to the duration of feeding.

**Keywords:** Rabbit ear, microangiography; collateral flow; hypercholesterolaemia; endothelium-derived relaxing factor (EDRF); nitric oxide

## Introduction

Hypercholesterolaemia is associated with atherogenesis and is therefore a major risk factor for cardiovascular diseases. Since the identification of the endothelium-derived relaxing factor (EDRF; Furchgott & Zawadzki, 1980), now known to be nitric oxide (Palmer *et al.*, 1987), many studies have investigated the effects of hypercholesterolaemia on this important vasoactive factor (see Flavahan, 1992 for review). The first study to investigate fully the effects of dietary-induced hypercholesterolaemia on endothelium-dependent relaxations was by Verbeuren *et al.* (1986), who showed that relatively short-term feeding of rabbits with cholesterol was associated with impaired endothelium-dependent relaxations to agonists and altered vasoconstrictor responses in conduit arteries. This was initially attributed to lipid deposits acting as a barrier to EDRF, as the production of EDRF appeared normal in bioassay experiments, and alterations in vascular smooth muscle responses to nitrovasodilators were only apparent after prolonged cholesterol feeding. However, endothelium-dependent relaxations are also impaired in resistance vessels (Yamamoto *et al.*, 1988; Osborne *et al.*, 1989) and in the microcirculation (Selke *et al.*, 1990; Kuo *et al.*, 1992) where lipid deposition does not occur. This implied that a circulating factor may be responsible for impaired EDRF activity. This notion received support from experiments demonstrating that low-density lipoprotein (LDL), which acts as a cholesterol carrier, inhibited endothelium-dependent relaxations (Andrews *et al.*, 1987). This action, which is greatest for oxidized LDL, is probably due, at least in part, to chemical inactivation of EDRF (Jacobs *et al.*, 1990). A recent study by Mitchell *et al.* (1992) found that native LDL reduced the release of EDRF from cultured bovine aortic endothelial cells through an inhibitory action on the nitric oxide synthase. The significance of this is not clear however, as Minor *et al.* (1990) reported a decrease in dilator activity in bioassay experiments, although the effluent had an increase in nitrogen oxide content measure by chemiluminescence. This implies an increased destruction of EDRF, perhaps by superoxide anions. Supportive evidence for this hypothesis comes from a brief report by Nakamura *et al.* (1990) of increased superoxide anion production beneath atheromatous plaques and a recent report of induction of nitric oxide synthase in the lungs of cholesterol-fed rabbits (Lang *et al.*, 1993). Cooke *et al.* (1991) have ascribed reduced EDRF producton to reduced availability of the L-arginine, the substrate for nitric oxide synthase, because administration of L-arginine reversed the depression of endothelium-dependent relaxation in the rabbit aorta. The ability of L-arginine to restore impaired endothelium-dependent relaxations, in response to both agonist and flow, also extends to the coronary microcirculation in a porcine model of atherosclerosis (Kuo *et al.*, 1992). The mechanism(s) by which hypercholesterolaemia/atherosclerosis impair EDRF activity remain elusive, although it is clear that EDRF activity is impaired throughout the arterial tree.

We have recently demonstrated that EDRF plays a central role in collateral perfusion after acute occlusion (Randall & Griffith, 1992b). In this respect administration of $N^G$-nitro-L-arginine methyl ester (L-NAME), an inhibitor of EDRF synthesis, prior to arterial occlusion was associated with profound reductions in collateral perfusion and this inhibitory effect was reversed by addition of L-arginine, the precursor of EDRF. Arterial occlusion often occurs secondary to a

[1] Author for correspondence.

variety of cardiovascular disorders and so we have now investigated the effects of dietary-induced hypercholesterolaemia on EDRF-dependent collateral perfusion. The model of dietery-induced hypercholesterolaemia that we used is not associated with significant changes in plasma triglycerides (Habib *et al.*, 1986).

## Methods

### *Feeding protocol*

Male New Zealand White rabbits matched by weight (2–2.5 kg) were assigned to either a cholesterol fed group (1% cholesterol in normal chow; Special Diet Services, Essex) or a control group fed the standard diet.

### *Preparation of the rabbit ear vascular bed*

The rabbits were killed by cervical dislocation. An ear was removed and the central artery cannulated and perfused with Holman's solution (composition mM: NaCl 120, KCl 5, $CaCl_2$ 2.5, $NaH_2PO_4$ 1.3, $NaHCO_3$ 25, sucrose 10 and D-glucose 11) at a flow rate of 3.5 ml $min^{-1}$. The physiological buffer also contained 5% (w/v) dextran (mol. wt. 80,000) to increase its viscosity (to ca. 2.3 mPas) and 10 μM indomethacin to eliminate prostanoid activity. The buffer was gassed with 95% $O_2$/5% $CO_2$ and maintained at 35°C.

### *Experimental protocol*

The ear was positioned vertically in front of an X-ray microscope (4 μm focal spot diameter) and loose sutures placed around the central artery at its midpoint and apex as previously described (Randall & Griffith, 1992a,b). Following an equilibration period (1 h), microangiograms were taken of the resting preparations. The exposure time was 15 s at 30 kV. Radiographic contrast was achieved by a 35 s pulse of iohexol diluted 3 fold in the perfusion fluid (final iodine concentration 100 mg $ml^{-1}$). Use of this agent is without significant influence on either vasomotor tone or vascular responses during the X-ray exposure (Griffith *et al.*, 1988). A segment of central ear artery (25.4 ± 0.9 mm; $n = 34$) was then isolated by tightening the sutures and microangiograms were then taken at 2, 5, 10, 15, 30, 60 and 90 min after ligation. Preliminary experiments, in which only the midpoint of the central ear artery was ligated, indicated that there was rapid and complete retrograde filling of the central artery distal to the ligation through the daughter branches of its apical bifurcation. This phenomenon has also been reported in the rabbit ear *in vivo* by other workers (Bellman *et al.*, 1959).

The perfusion pressure of the intact preparation was continuously monitored by means of a pressure transducer placed close to the inflow cannula. The pressure drop across the cannula was determined at the end of each experiment and subtracted from the recorded pressure.

The relaxations to the endothelium-dependent vasodilator acetylcholine were assessed in all groups. Briefly ear preparations were perfused with oxygenated Holman's solution (plus 10 μM indomethacin) at 3.5 ml $min^{-1}$ and after an equilibration period of 1 h perfusion pressure was raised by addition of 1 μM 5-hydroxytryptamine and 1 μM histamine. The vasorelaxant properties of acetylcholine were examined by addition of the agent to perfusion fluid at the desired concentrations in order to construct cumulative concentration-response curves.

### *Quantitation*

The microangiograms were analysed by a semi-interactive image analysis system as previously described (Griffith *et al.*, 1988). A gold calibration grid was placed on the surface of the ear to determine the magnification factor and the radiographs were further magnified by means of an electronic image analysis system. The diameter of each vessel studied was measured 4 times and the results averaged. Filling of the segment isolated between ligatures was assessed as the area of the segment on the angiogram which had filled with radiographic contrast relative to its preocclusion value. Filling of the isolated segment with radiographic contrast media has previously been shown to be dynamic with rapid clearance via low resistance outflow pathways (Randall & Griffith, 1992b) and reflects perfusion via collateral vessels and not time-dependent accumulation of radiographic contrast.

As an estimate of collateral flow, the diameter of a first order branch artery (ca. 200 μm) situated close to but proximal (< 3 mm) to the midpoint ligation was measured as a function of time. This vessel was termed pG1 (i.e. proximal first order generation, see Randall & Griffith, 1992b). These vessels are close to the isolated segment and constitute the main feed vessels to the collateral circulation (Randall & Griffith, 1992b). We have previously shown that the diversion of flow through these vessels to supply a collateral circulation is accompanied by dilatation while the diameter of more proximal (> 3 mm) first order arteries (G1) remains unaltered (see Randall & Griffith, 1992b).

### *Data and statistical analysis*

All data are given as the mean ± s.e.mean and were compared by either paired or unpaired Student's *t* tests or analysis of variance as appropriate. $EC_{50}$ values for vasodilator responses were obtained from individual concentration-response curves as the concentration at which half maximal reduction in established tone occurred.

### *Drugs*

All solutions were prepared on the day of the experiment. Acetylcholine chloride, 5-hydroxytryptamine as creatinine sulphate complex, histamine dihydrochloride (Sigma, Dorset) were all made up in 0.9% (w/v) saline. Iohexol (Omnipaque, Nycomed, U.K.) was diluted in the perfusion fluid. Indomethacin (Sigma) was dissolved in 5% (w/v) $NaHCO_3$. All drugs were then diluted to the required concentrations in the Holman's solution.

## Results

### *Effects of cholesterol supplementation on plasma cholesterol levels*

In the rabbits receiving the cholesterol-enriched diet for 4 weeks, blood cholesterol was 26.0 ± 3.6 mmol $l^{-1}$ ($n = 10$) and was significantly ($P < 0.001$) greater than that found in those fed on the normal diet (2.6 ± 0.6 mmol $l^{-1}$, $n = 10$). In the group receiving the cholesterol-enriched diet for 8 weeks, blood cholesterol levels were 56.2 ± 3.8 mmol $l^{-1}$ ($n = 10$) and was also significantly ($P < 0.01$) higher than in the rabbits fed the control diet for the same duration (1.3 ± 0.1 mmol $l^{-1}$; $n = 12$).

### *Effects of hypercholesterolaemia for 4 weeks on collateral perfusion*

The perfusion pressure in the resting ear preparation from rabbits receiving the control diet for 4 weeks was 31.8 ± 5.3 mmHg ($n = 9$). Figure 1 shows that 2 min after ligation, filling of the isolated segment was 19.5 ± 4.9% of its preocclusion value ($n = 9$). Filling of the segment increased progressively with time and was 30.9 ± 5.4% at 5 min, 31.6 ± 6.2% at 30 min and 34.5 ± 5.6% at 90 min (all $n = 9$) (Figure 1). Figure 2a shows that the diameter of pG1 increased significantly ($P < 0.05$) from a control value of 265 ± 24 μm

($n = 9$) to a value of 326 ± 26 μm ($n = 9$) 2 min after ligation. This increase in diameter persisted throughout the period of the experiment, peaking at 342 ± 30 μm ($n = 9$) 5 min after ligation (Figure 2a). By contrast the diameter of G1 vessels located more proximal to the ligation did not undergo any significant change in diameter throughout the entirety of the experiment (Figure 2a). After ligation the perfusion pressure in the preparations underwent a modest but significant ($P < 0.05$) increase to 40.4 ± 4.4 mmHg at 2 min to a maximum of 52.4 ± 4.5 mmHg at 90 min (Figure 3).

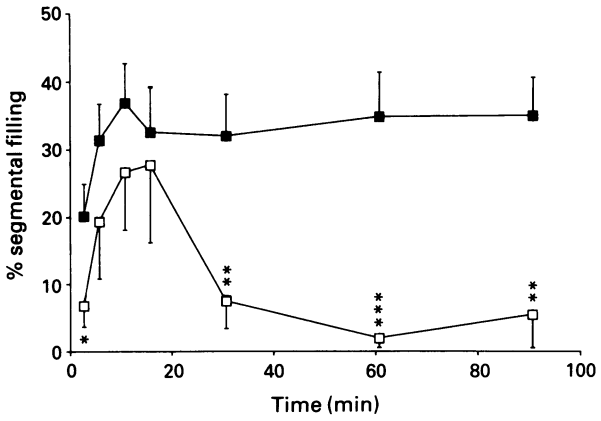



**Figure 1** The level of filling (%) of the isolated segment of the central artery normalized with respect to the preocclusion control value in the control rabbits (■) and those fed the cholesterol-enriched diet for 4 weeks (□). Ligation was performed at 0 min and statistical differences between control and cholesterol fed rabbits are indicated: $*P < 0.05$, $**P < 0.01$ and $***P < 0.001$. Data are given as the mean ± s.e.mean.

In the group of rabbits receiving the cholesterol-supplemented diet for 4 weeks, basal perfusion pressure in the isolated ear preparations was 23.1 ± 5.7 mmHg; 2 min after ligation, filling of the isolated segment was 6.2 ± 3.1% of its preocclusion value and was significantly ($P < 0.05$) less than that seen in the age-matched controls (Figure 1). The degree of filling increased progressively with time being 18.8 ± 8.5% at 5 min, 26.1 ± 8.6% at 10 min reaching a maximum of 27.2 ± 11.5% at 15 min. From 5–15 min the level of filling was similar to that in the control preparations. However, after this time filling decreased such that from 30 min until the end of the experiment it was significantly ($P < 0.01$) less than that found in the controls. Figure 2b shows that prior to ligation the diameter of pG1 was 232 ± 12 μm and after ligation this parameter decreased progressively and was significantly ($P < 0.05$) less than basal, 30 min after ligation (160 ± 34 μm). However, the diameter of more proximal G1 vessels prior to ligation was 268 ± 18 μm and after ligation underwent an increase which was significantly ($P < 0.01$) greater than baseline 10 min ligation (315 ± 32 μm), a change which persisted for the next 50 min (Figure 2b). After ligation and in common with the control group, perfusion pressure also underwent a modest but significant ($P < 0.05$) increase to 44.4 ± 12.4 mmHg at 5 min to a maximum of 54.4 ± 11.3 mmHg at 90 min (Figure 3).

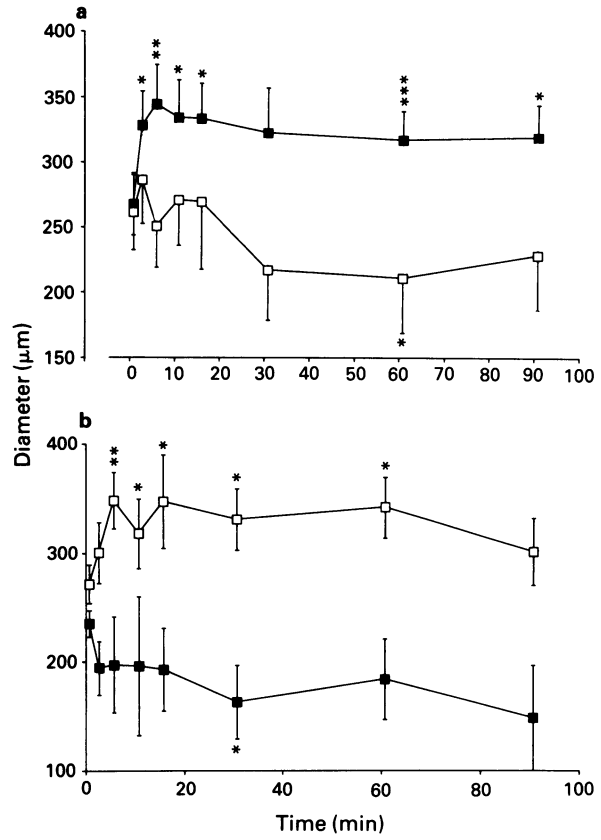



**Figure 2** The diameter changes of the 1st order arterial vessels after arterial occlusion. (a) Shows the time-course of diameter changes in the control rabbits and (b) contains data from the rabbits fed the 1% cholesterol diet for 4 weeks. In both cases the data from pG1 collateral feed vessels are represented by (■) and data from 1st order vessels located some distance from the occlusion (G1) which do not feed the collateral vessels are represented by (□). Ligation was performed at 0 min and statistical differences between resting diameters and diameters after ligation are indicated: $*P < 0.05$, $**P < 0.01$ and $***P < 0.001$. Data are given as the mean ± s.e.mean.

### *Endothelium-dependent relaxations to acetylcholine in the 4 week groups*

In 5 control preparations, resting perfusion pressure was 27.2 ± 13.8 mmHg and following addition of 1 μM 5-hydroxytryptamine and 1 μM histamine, perfusion pressure rose by 104 ± 8 mmHg to 131 ± 19 mmHg. In these preparations acetylcholine (1 nM–10 μM) brought about concentration-related reductions in established tone with an $EC_{50}$ of 143 ± 41 nM and a maximum reduction in established tone of 76.0 ± 7.0% (Figure 4).

In 6 preparations from rabbits treated with the cholesterol-enriched diet, basal perfusion pressure in the ear preparations was 25.2 ± 2.6 mmHg and was increased by 107 ± 28 mmHg to 132 ± 30 mmHg following addition of the combination of vasoconstrictors. In these preparations acetylcholine (1 nM–10 μM) similarly induced concentration-dependent relaxations

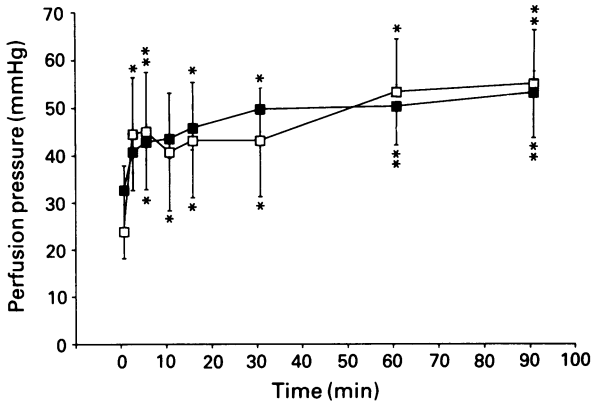



**Figure 3** The changes in perfusion pressure after ligation in the control preparations (■) and those from rabbits receiving the high cholesterol diet for 4 weeks (□). Ligation was performed at 0 min and statistical differences between the basal perfusion pressure and perfusion pressure after ligation are indicated: $*P < 0.05$ and $**P < 0.01$. Data are given as the mean ± s.e.mean.

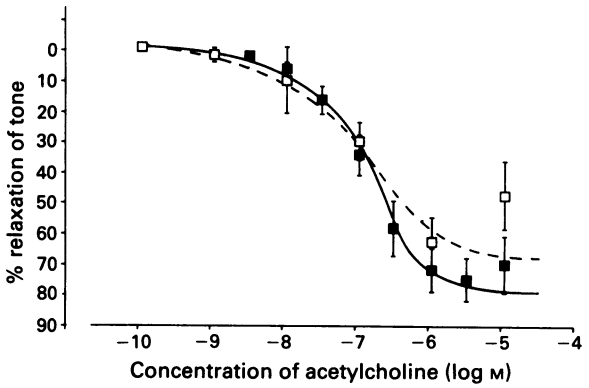



**Figure 4** The concentration-response curves for the relaxation of 5-hydroxytryptamine and histamine-induced tone in the rabbit isolated perfused ear preparations. The data obtained from the control rabbits is indicated by (■) and that from the rabbits fed the high cholesterol diet for 4 weeks is shown by (□). Data are given as the mean ± s.e.mean.

of established tone with an $EC_{50}$ of 82.7 ± 32.0 nM, and a maximum reduction in tone of 63.4 ± 7.8% (Figure 4). These parameters did not differ significantly from those obtained in the control preparations.

### *Effects of hypercholesterolaemia for 8 weeks on collateral perfusion*

In the 11 control preparations, basal perfusion pressure was 46.4 ± 9.5 mmHg; 2 min after ligation, filling of the isolated segment was 23.1 ± 4.8% and this increased to 39.5 ± 4.6% at 10 min and was 35.0 ± 5.1% at 90 min (Figure 5). The level of segmental filling was not significantly different from that in control preparations from animals fed the diet for 4 weeks. (Figures 1 and 5). In preparations from animals receiving the control diet for 8 weeks the diameter of the pG1 vessels increased significantly ($P<0.05$) 2 min after ligation from a baseline value of 251 ± 21 μm to 289 ± 29 μm and this dilatation persisted for the remainder of the occlusion period with a peak value of 334 ± 30 μm at 30 min (Figure 6a). By contrast the diameter of the more proximal G1 vessels did not change from the preligation value of 269 ± 24 μm. In these preparations basal perfusion pressure was 46.4 ± 9.5 mmHg and after ligation underwent a modest but significant increase rising to 63.4 ± 9.2 mmHg ($P<0.01$) at 90 min (Figure 7).

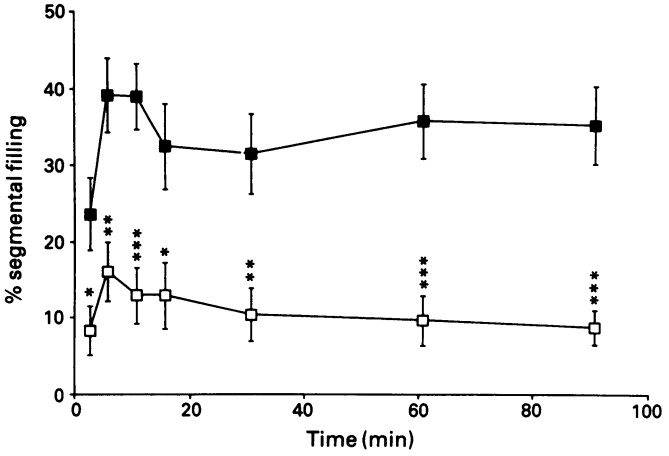



**Figure 5** The level of filling (%) of the isolated segment of the central artery normalized with respect to the preocclusion control value in the control rabbits (■) and those fed the cholesterol-enriched diet for 8 weeks (□). Ligation was performed at 0 min and statistical differences between control and cholesterol fed rabbits are indicated: $*P<0.05$, $**P<0.01$ and $***P<0.001$. Data are given as the mean ± s.e.mean.

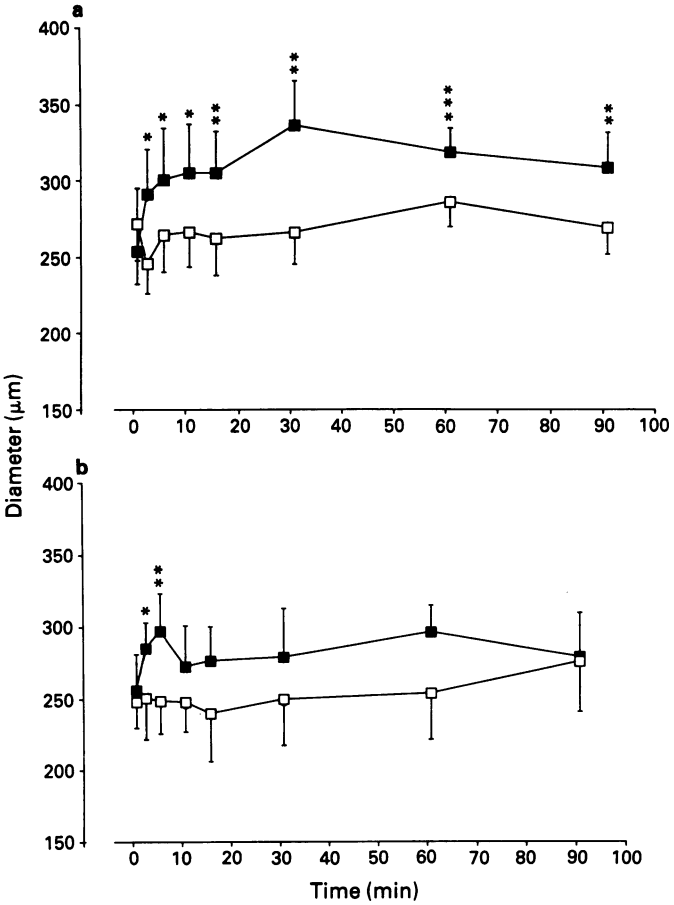



**Figure 6** The diameter changes of the 1st order arterial vessels after arterial occlusion. (a) Shows the time-course of diameter changes in the control rabbits and (b) contains data from the rabbits fed the 1% cholesterol diet for 8 weeks. In both cases the data from pG1 collateral feed vessels are represented by (■) and data from 1st order vessels located some distance from the occlusion which do not feed the collateral vessels are represented by (□). Ligation was performed at 0 min and statistical differences between resting diameters and diameters after ligation are indicated: $*P<0.05$, $**P<0.01$ and $***P<0.001$. Data are given as the mean ± s.e.mean.

In the 9 rabbits receiving the cholesterol-supplemented diet, basal perfusion pressure in the rabbit ear was 31.3 ± 4.2 mmHg and was not statistically different from the corresponding control value reported above. In these preparations segmental filling 2 min after ligation was 7.8 ± 3.2% of the preocclusion value and was therefore significantly less ($P<0.05$) than that in the age-matched controls (Figure 5). The level of filling in these experimental preparations did not change significantly for the entire 90 min and was therefore significantly less than observed in the age-matched controls throughout the period of ligation. The impairment of segmental filling was accompanied by limited vasodilatation of pG1 vessels during the first 5 min after occlusion from a control value of 253 ± 26 μm to a maximum of 295 ± 26 μm at 5 min, after which time the diameter returned to a level not significantly different from preligation (Figure 6b). The diameter of G1 vessels located proximally further away from the ligation did not undergo any significant diameter change after occlusion. After ligation perfusion pressure increased significantly ($P<0.05$) for the first 15 min and then returned to a value not significantly different from pre-ligation (Figure 7).

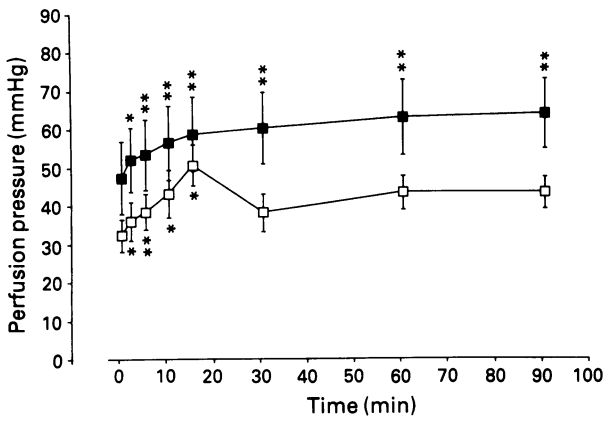



**Figure 7** The changes in perfusion pressure after ligation in the control preparations (■) and those from rabbits receiving the high cholesterol diet for 8 weeks (□). Ligation was performed at 0 min and statistical differences between the basal perfusion pressure and perfusion pressure after ligation are indicated: $*P<0.05$ and $**P<0.01$. Data are given as the mean ± s.e.mean.

### *Endothelium-dependent relaxations to acetylcholine in the 8 week groups*

In 8 control preparations resting perfusion pressure was 23.4 ± 4.2 mmHg and following addition of 1 μM 5-hydroxytryptamine and 1 μM histamine, perfusion pressure rose by 103 ± 15 mmHg to 126 ± 16 mmHg. In these preparations acetylcholine (10 nM–30 μM) brought about concentration-related reductions in established tone with an $EC_{50}$ of 283 ± 56 nM and a maximum reduction in established tone of 77.9 ± 5.7% (Figure 8).

In 4 preparations from rabbits fed the cholesterol-enriched diet for 8 weeks, basal perfusion pressure in the ear preparations was 19.5 ± 2.1 mmHg and was increased by 124 ± 22 mmHg to 143 ± 21 mmHg following addition of the combination of vasoconstrictors. In these preparations acetylcholine (1 nM–10 μM) similarly induced concentration-dependent relaxations of established tone with an $EC_{50}$ of 175 ± 53 nM, and a maximum reduction in tone of 32.6 ± 11.6% (Figure 8). The maximum relaxation was significantly less ($P<0.01$) than that found in the age-matched controls, the $EC_{50}$ value was not significantly different from the controls.

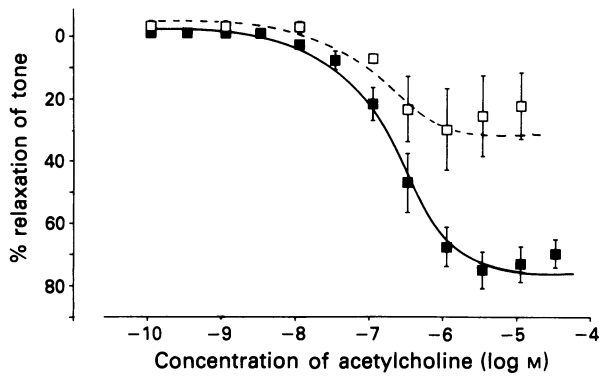



**Figure 8** The concentration-response curves for the relaxation of 5-hydroxytryptamine and histamine-induced tone in the rabbit isolated perfused ear preparations. The data obtained from the control rabbits is indicated by (■) and that from the rabbits fed the high cholesterol diet for 8 weeks is shown by (□). Data are given as the mean ± s.e.mean.

## Discussion

We have previously demonstrated that collateral perfusion after acute arterial occlusion is strictly dependent on the release of EDRF (Randall & Griffith, 1992b). We now report that in hypercholesterolaemia, a condition associated with reduced EDRF activity, there is substantial impairment of collateral perfusion.

The impairment of collateral perfusion was indicated by the reduced filling, compared to controls, of the segment isolated between occlusions which is fed by the collateral circulation in an EDRF-dependent manner (Randall & Griffith, 1992b). In the rabbits receiving the high cholesterol diet for 4 weeks the depression of the segmental filling was only apparent 15 min after occlusion, indicating that the initiation of collateral perfusion was not impaired by this feeding regimen. After 15 min and during the maintenance phase, segmental filling was reduced and therefore collateral perfusion was depressed relative to that in the controls. Moreover, the level of collateral-dependent filling during the maintenance phase in the preparations from the hypercholesterolaemic rabbits had actually decreased when compared to that found immediately after ligation, indicating that collateral-dependent perfusion was impaired. In the rabbits fed the high cholesterol diet for 8 weeks, the profile of collateral perfusion was less complex, in that segmental filling was less than that observed in the controls immediately after ligation and remained at this level for the entirety of the experiment. The level of collateral-dependent perfusion observed in these hypercholesterolaemic rabbits is identical to that found in normal preparations which have been pretreated with the selective inhibitor of the nitric oxide synthase, $N^G$-nitro-L-arginine methyl ester (Randall & Griffith, 1992b). These results would therefore support the notion that hypercholesterolaemia impairs collateral perfusion, which is critically dependent on EDRF, and that the level of impairment is related to duration of cholesterol feeding.

The results obtained with the preparations from the 4 week cholesterol group are complex in that only the maintenance and not the initiation of collateral perfusion was impaired. The time-related impairment of collateral perfusion was accompanied by constriction of the collateral feed vessels (pG1) 30 min after occlusion. Interestingly, the G1 vessels located some distance from the midpoint occlusion underwent dilatation suggesting that there was vascular steal away from the collateral vessels and therefore the occluded zone. This phenomenon was not observed in the preparations from the rabbits fed a normal diet or in previous studies (Randall & Griffith, 1992b). That vascular steal did not occur in the rabbits fed the cholesterol diet for 8 weeks may perhaps suggest that the mechanisms which may be responsible for it are also impaired by longer cholesterol feeding. These observations point to a reduction in collateral conductance occurring several minutes after occlusion leading to poor maintenance of perfusion. The mechanisms for this are not clear from the present experiments, although there may be several possibilities. Firstly, some workers have indicated that there may be a reduction in the availability of L-arginine in hypercholesterolaemia (Cooke *et al.*, 1991). In the present context a reduced availability of the nitric oxide synthase substrate may lead to depletion if the system is under constant stimulation, which would be the case during EDRF-dependent collateral perfusion. However, in three experiments (data not shown) administration of L-arginine to the perfusion fluid 60 min after occlusion did not restore collateral perfusion in the subsequent 30 min, indicating that it is unlikely that a simple depletion of L-arginine may explain the present impairment. An alternative explanation for the impairment of collateral-dependent perfusion may reside in the production or induction of a direct or indirect vasoconstrictor mechanism. Possible examples include the production of superoxide anion (see Moncada *et al.*, 1991), which is known to occur in atherosclerotic lesions in genetically hypercholes-

terolaemic rabbits (Nakamura *et al.*, 1990). Superoxide anion inactivates EDRF (Gryglewski *et al.*, 1986; Rubanyi & Vanhoutte, 1986), has vasoconstrictor activity (Katusic & Vanhoutte, 1989) and stimulates the release of endogenous vasoconstrictors (Shimokawa & Vanhoutte, 1989). The endogenous vasoconstrictor identified by Shimokawa & Vanhoutte (1989) was a prostanoid which cannot account for the changes observed in the present study, for the cyclo-oxygenase inhibitor indomethacin was present throughout the current study. Recent studies have identified an increase in the release of the potent endogenous vasoconstrictor, endothelin-1, from the aorta of cholesterol fed rabbits (Patrignani *et al.*, 1992).

Parallel to the collateral perfusion studies, agonist-evoked endothelium-dependent relaxations to acetylcholine in the unligated isolated ear of the rabbit were also examined. These results indicated that after 4 weeks of feeding, endothelium-dependent relaxations to agonists were not impaired. However, in the rabbits treated for 8 weeks there was severe depression of the relaxations indicating impairment of agonist-dependent EDRF activity. These results should be considered separately from the collateral perfusion studies as there are significant differences between agonist and basal EDRF activity in the rabbit ear (Randall & Griffith, 1991). Furthermore, the responses to acetylcholine were assessed against tone induced by the combination of 5-hydroxytryptamine and histamine which only constrict larger arterial vessels (Griffith *et al.*, 1988) hence the data provides limited information regarding EDRF activity in smaller vessels. Nevertheless, the data from the 8 week group clearly supports there being severe impairment of EDRF activity. The lack of impairment of agonist-dependent EDRF responses in the 4 week group contrasts the severe depression of EDRF-dependent collateral perfusion and may suggest that collateral vessels or basal EDRF release is more susceptible to the deleterious effects of hypercholesterolaemia than agonist-stimulated EDRF activity in the larger arterial vessels.

The present study indicates that even short-term hypercholesterolaemia is associated with impaired endothelial functioning, at least in terms of collateral perfusion. These results correlate with data obtained in rabbits fed a hypercholesterolaemic diet of 2% cholesterol for 2–3 weeks showing potentiated ischaemia-reperfusion injury in the coronary vasculature (Tilton *et al.*, 1987). Potentially, the impairment reported by these authors could be related to a reduction in flow distribution perhaps involving collateral vessels.

In conclusion, the results of the present study show that hypercholesterolaemia impairs EDRF-dependent collateral perfusion after arterial occlusion. Hypercholesterolaemia is known to predispose towards arterial occlusion through promoting vasospasm, therefore the action on collateral perfusion outlined in the current study could potentially exacerbate vessel occlusion.

This work was funded by a grant from the British Heart Foundation. The authors thank Professor G.M. Roberts of the University of Wales College of Medicine for his support and interest.

## References


ANDREWS, H.E., BRUCKDORFER, K.R., DUNN, R.C. & JACOBS, M. (1987). Low-density lipoproteins inhibit endothelium-dependent relaxations in rabbit aorta. *Nature*, **327**, 237–239.

BELLMAN, S., FRANK, H.A., LAMBERT, P.B. & ROY, A.J. (1959). Studies of collateral vascular responses. I Effects of selective occlusions of major trunks within an extensively anastomosing arterial system. *Angiology*, **10**, 214–232.

COOKE, J.P., ANDON, N.A., GIRERD, X.J., HIRSCH, A.T. & CREAGER, M.A. (1991). Arginine restores cholinergic relaxation of hypercholesterolemic rabbit aorta. *Circulation*, **83**, 1057–1062.

FLAVAHAN, N.A. (1992). Atherosclerosis or lipoprotein-induced endothelial dysfunction. Potential mechanisms underlying reduction in EDRF/nitric oxide activity. *Circulation*, **85**, 1927–1938.

FURCHGOTT, R.F. & ZAWADZKI, J.V. (1980). The obligatory role of endothelial cells in the relaxation of vascular smooth muscle by acetylcholine. *Nature*, **288**, 373–376.

GRIFFITH, T.M., EDWARDS, D.H., DAVIES, R.Ll., HARRISON, T.J. & EVANS, K.T. (1988). Endothelium-dependent relaxing factor (EDRF) and resistance vessels in the intact ear vascular bed: a microangiographic study of the rabbit isolated ear. *Br. J. Pharmacol.*, **93**, 654–662.

GRYGLEWSKI, R.J., PALMER, R.M.J. & MONCADA, S. (1986). Superoxide anion is involved in the breakdown of endothelium-derived relaxing factor. *Nature*, **320**, 454–456.

HABIB, J.B., BOSSALLER, C., WELLS, S., WILLIAMS, C., MORRISETT, J.D. & HENRY, P.D. (1986). Preservation of endothelium-dependent vascular relaxation in cholesterol-fed rabbit by treatment with calcium blocker PN 200110. *Circ. Res.*, **58**, 305–309.

JACOBS, M., PLANE, F. & BRUCKDORFER, K.R. (1990). Native and oxidized low-density lipoproteins have different inhibitory effects on endothelium-derived relaxing factor in the rabbit aorta. *Br. J. Pharmacol.*, **100**, 21–26.

KATUSIC, Z.S. & VANHOUTTE, P.M. (1989). Superoxide anion is an endothelium-derived contracting factor. *Am. J. Physiol.*, **257**, H33–H37.

KUO, L., DAVIES, M.J., CANNON, S. & CHILIAN, W.M. (1992). Pathophysiological consequences of atherosclerosis extend into the coronary microcirculation. *Circ. Res.*, **70**, 465–476.

LANG, D., SMITH, J.A. & LEWIS, M.J. (1993). Induction of a calcium-independent NO-synthase by hypercholesterolaemia in the rabbit. *Br. J. Pharmacol.*, **108**, 290–292.

MINOR, R.L., MYERS, P.R., GUERRA, R., BATES, J.N. & HARRISON, D.G. (1990). Diet-induced atherosclerosis increases the release of nitrogen oxides from rabbit aorta. *J. Clin. Invest.*, **86**, 2109–2116.

MITCHELL, J.A., WARNER, T.D., HUANG, Z-J., FÖRSTERMANN, U. & MURAD, F. (1992). Native LDL inhibits the release of endothelial derived relaxing factor by reducing the activity of endothelial nitric oxide synthase. *J. Vasc. Res.*, **29**, 169.

MONCADA, S., PALMER, R.M.J. & HIGGS, E.A. (1991). Nitric oxide: physiology, pathophysiology and pharmacology. *Pharmacol. Rev.*, **43**, 109–142.

NAKAMURA, M., TAGAWA, H. & TOMOIKE, H. (1990). Reduced release of EDRF and significant inactivation of EDRF at tunica media beneath the atheromatous plaque in aortas of WHHL rabbits. *Arch. Int. Pharmacodyn. Ther.*, **205**, 269.

OSBORNE, J.A., SIEGMAN, M.J., SEDAR, A.W., MOOERS, S.U. & LEFER, A.M. (1989). Lack of endothelium-dependent relaxation in coronary resistance arteries of cholesterol-fed rabbits. *Am. J. Physiol.*, **256**, (*Cell Physiol.*, **25**) C591–C597.

PALMER, R.M.J., FERRIGE, A.G. & MONCADA, S. (1987). Nitric oxide release accounts for the biological activity of endothelium-derived relaxing factor. *Nature*, **327**, 524–526.

PATRIGNANI, P., DAFFONCHIO, L., HERNANDEZ, A., DE CATERINA, R. & PATRONO, C. (1992). Release of contracting factors by aortae of normal and atherosclerotic rabbits. *J. Vasc. Res.*, **29**, 178.

RANDALL, M.D. & GRIFFITH, T.M. (1991). Differential effects of L-arginine on the inhibition by $N^G$-nitro-L-arginine methyl ester of basal and agonist-stimulated EDRF activity. *Br. J. Pharmacol.*, **104**, 743–749.

RANDALL, M.D. & GRIFFITH, T.M. (1992a). Effects of BRL 38227, sodium nitroprusside and verapamil on collateral perfusion following acute arterial occlusion in the rabbit isolated ear. *Br. J. Pharmacol.*, **106**, 315–323.

RANDALL, M.D. & GRIFFITH, T.M. (1992b). EDRF plays central role in collateral flow after arterial occlusion in rabbit ear. *Am. J. Physiol.*, **263** (*Heart Circ. Physiol.* **32**) H752–H760.

RUBANYI, G.M. & VANHOUTTE, P.M. (1986). Superoxide anions and hyperoxia inactivate endothelium-derived relaxing factor. *Am. J. Physiol.*, **250**, H822–H827.

SELKE, F.W., ARMSTRONG, M.L. & HARRISON, D.G. (1990). Endothelium-dependent vascular relaxation is abnormal in the coronary microcirculation of atherosclerotic primates. *Circulation*, **81**, 1586–1593.

SHIMOKAWA, H. & VANHOUTTE, P.M. (1989). Impaired endothelium-dependent relaxation to aggregating platelets and related vasoactive substances in porcine coronary arteries in hypercholesterolemia and atherosclerosis. *Circ. Res.*, **64**, 900–914.

TILTON, R.G., COLE, P.A., ZIONS, J.D., DAUGHERTY, A., LARSON, K.B., SUTERA, S.P., KILO, C. & WILLIAMSON, J.R. (1987). Increased ischemia-reperfusion injury to the heart associated with short-term, diet-induced hypercholesterolaemia in rabbits. *Circ. Res.*, **60,** 551–559.

VERBEUREN, T.J., JORDAENS, F.H., ZONNEKEYN, L.L., VAN HOVE, C.E., COENE, M.C. & HERMAN, A.G. (1986). Effect of hypercholesterolemia on vascular reactivity in the rabbit. *Circ. Res.*, **58,** 552–554.

YAMAMOTO, H., BOSSALLER, C., CARTWRIGHT, J. & HENRY, P.D. (1988). Videomicroscopic demonstration of defective cholinergic arteriolar vasodilation in atherosclerotic rabbit. *J. Clin. Invest.*, **81,** 1752–1758.

*(Received December 14, 1992*
*Revised February 9, 1993*
*Accepted February 25, 1993)*

*Br. J. Pharmacol.* (1993), **109**, 845–851 © Macmillan Press Ltd, 1993

# Non-adrenergic, non-cholinergic neural activation in guinea-pig bronchi: powerful and frequency-dependent stabilizing effect on tone

[1]A. Lindén, *A. Ullman, C.-G. Löfdahl & B.-E. Skoogh

Divisions of Pulmonary Medicine, Renströmska Hospital, University of Göteborg, PO Box 17301, S-40264 Gothenburg and *Clinical Pharmacology, Sahlgrenska Hospital, University of Göteborg, S-413 45 Gothenburg, Sweden

**1** We examined non-adrenergic, non-cholinergic (NANC) stimulation for its stabilizing effect on bronchial smooth-muscle tone with respect to its regulatory power and the effect of variations in neural impulse frequency.

**2** The guinea-pig isolated main bronchus ($n = 4-12$) was pretreated with indomethacin (10 μM) and incubated with atropine (1 μM) and guanethidine (10 μM). Electrical field stimulation (EFS: 1200 mA, 0.5 ms, 240 s) was applied at various levels of tone prior to EFS: first without tone, then at a moderate tone induced by histamine (0.3 μM) and, finally, at a high tone induced by histamine (6 μM). Three different stimulation frequencies (1, 3 or 10 Hz) were used in order to produce moderate to near-maximum contractile and relaxant NANC neural responses. Both the contractile and the relaxant NANC responses were tetrodotoxin-sensitive in the guinea-pig isolated main bronchus (3 Hz).

**3** Without tone prior to EFS, NANC activation (1, 3 or 10 Hz) induced a pronounced contractile response. At a moderate level of tone prior to EFS, NANC activation induced a less pronounced contractile response. At the highest level of tone prior to EFS, NANC activation induced a relaxant response. All these NANC responses adjusted the tone towards a similar level and this 'stabilization level' was 56(6)% at 1 Hz, 65(3)% at 3 Hz and 56(5)% at 10 Hz, expressed as a percentage of the maximum histamine-induced (0.1 mM) tone in each airway preparation.

**4** There was a difference of approximately 90% of maximum between the highest and the lowest tone level prior to NANC activation. This difference was reduced by the converging contractile and relaxant NANC responses and the magnitude of this 'convergence effect' was 40(8)% at 1 Hz, 72(4)% at 3 Hz and 90(2)% at 10 Hz.

**5** These findings indicate that NANC neural activation stabilizes bronchial smooth-muscle tone via a contraction when the tone is low prior to activation and via a relaxation when the tone is high prior to activation. The NANC stabilizing effect on tone appears to be powerful and its magnitude can be controlled by the neural impulse frequency. The level of tone towards which the NANC responses converge does not appear to be markedly altered by variations in the impulse frequency. Our findings are consistent with a regulatory role for NANC responses in the control of bronchial smooth-muscle tone.

**Keywords:** Airway smooth muscle; guinea-pig bronchi; *in vitro*; neural regulation; non-adrenergic, non-cholinergic; tone

## Introduction

In human and guinea-pig airways, non-adrenergic, non-cholinergic (NANC) neural activation can produce both a contractile and a relaxant smooth-muscle response *in vitro* and *in vivo* (Coburn & Tomita, 1973; Richardson & Beland, 1976; Yip *et al.*, 1981; Doidge & Satchell, 1982; Scolcsanyi & Bartho, 1982; Andersson & Grundström, 1983; Lundberg *et al.*, 1983; Martling *et al.*, 1984; Taylor *et al.*, 1984; Palmer *et al.*, 1986; Ichinose *et al.*, 1988; Lammers *et al.*, 1988; Lindén *et al.*, 1991a; Venugopalan *et al.*, 1991; Lötvall *et al.*, 1992). The role of these NANC responses in healthy and diseased airways is, however, uncertain.

A recent study demonstrated that, depending on the level of smooth-muscle tone prior to activation, NANC activation evokes either a contraction or a relaxation, converging towards a similar tone level in the guinea-pig isolated trachea (Lindén *et al.*, 1991b). As indicated *in vitro*, NANC responses may thus counteract changes in tone and play a stabilizing role in the control of tone. It is, however, not known whether this type of NANC stabilizing effect is powerful enough to counteract pronounced changes in tone. It is also uncertain how the NANC stabilizing effect on tone can be controlled.

We hypothesized that, because the magnitude of the contractile and relaxant NANC response increases with the neural impulse frequency (Lindén *et al.*, 1991a; Venugopalan *et al.*, 1991), the magnitude of the NANC stabilizing effect on tone could be controlled by variations in the impulse frequency. However, on the basis of previous studies, the possibility cannot be excluded that the contractile and the relaxant NANC response have different impulse frequency optima (Lindén *et al.*, 1991a; Venugopalan *et al.*, 1991). It is therefore unclear how variations in the neural impulse frequency influence the NANC stabilizing effect on tone.

In the present study on the guinea-pig isolated main bronchus, we examined the NANC stabilizing effect on smooth-muscle tone with respect to its regulatory power and the effect of variations in neural impulse frequency.

## Methods

### *Airway preparation*

Sixty female Dunkin-Hartley guinea-pigs (350–500 g) were killed by cervical dislocation and exsanguination. The thoracic contents were removed and placed in a 200 ml oxygenated (94% $O_2$:6% $CO_2$) dissection bath filled with buffered Krebs-Ringer solution (mM: NaCl 118, KCl 5.9,

[1] Author for correspondence.

$CaCl_2$ 2.5, $MgSO_4$ 1.2, $NaH_2PO_4$ 1.2, $NaHCO_3$ 25.5 and glucose 5.6) at room temperature. The distal (intrathoracic) trachea and the main bronchi were dissected free and two airway rings were cut transversely from each airway segment. Each ring contained four to five cartilaginous rings. The airway rings were opened longitudinally along the anterior, cartilaginous part and connected to steel hooks as isolated strips. These preparations were mounted vertically in warmed (37°C) and oxygenated organ baths (8 ml), which were continuously flushed with fresh Krebs-Ringer solution (0.4 ml $min^{-1}$). This handling kept the airways histologically intact (Lindén, 1992).

### *Tension recordings*

The semi-isometric tension was continuously recorded with the preparations tied to Grass force transducers (FT03) via steel hooks. The transducer signals were digitally transformed and registered in a Macintosh II computer using the Lab-VIEW signal-processing software (National Instruments, Austin, Texas, U.S.A.) (Ullman *et al.*, 1990).

### *Electrical field stimulation*

Constant current generators provided electrical field stimulation (EFS) via platinum electrodes mounted on opposite sides of the airway preparation (Lindén *et al.*, 1991b). Square biphasic electrical impulses of 0.5 ms duration were used for both control contractions (1200 mA, 12 Hz for 20 s) and NANC activation (300–1500 mA, 1, 3 and 10 Hz for 240 s). NANC activation was carried out with cholinergic (muscarinic) blockade using atropine and adrenergic depletion with guanethidine (Kamikawa & Shimo, 1976; Andersson & Grundström, 1983; Brock & Cunnane, 1988).

### *Protocols*

*General procedures* The spontaneous airway tone was initially abolished by indomethacin (10 μM) (Lindén *et al.*, 1991c) which was continuously present in the Krebs-Ringer solution throughout the experiments. A passive tension of 1.2 g (1 g = 9.81 mN) was applied to the preparation during 25 min of initial equilibration and a control contraction was induced by EFS. A wash-out followed and the passive tension was re-adjusted to 1.2 g. Atropine (1 μM) and guanethidine (10 μM) were then added to the Krebs-Ringer solution and incubated for 70 min before any additional EFS took place. These drugs were also continuously present throughout the experiments. In the experiments including repeated NANC activation, a wash-out followed each EFS and the tone was allowed to return to the same level as that prior to EFS before the subsequent EFS. All the experiments ended with a flushing period of 25 min followed by a contraction induced by histamine (0.1 mM, more than $EC_{100}$).

*Impulse current and NANC responses* The contractile NANC response was examined without tone prior to activation. This examination was performed on the main bronchus, since the contractile NANC response is more pronounced than the relaxant NANC response in this segment (Lindén *et al.*, 1991a). The relaxant NANC response was examined at an increased tone, established by the addition of histamine (6 μM) 20 min prior to EFS. This latter examination was performed on the distal trachea, since the relaxant NANC response is more pronounced than the contractile NANC response in this segment (Lindén *et al.*, 1991a). A series of EFS (3 Hz) was performed at gradually increasing ($n = 2$) or decreasing ($n = 2$) current levels, using 60 min intervals for both contractile and relaxant responses.

*Reproducibility of NANC responses* In the main bronchus, the contractile NANC response was evoked without tone prior to activation, whereas the relaxant NANC response was evoked at an increased histamine-induced (6 μM) tone prior to activation. For both types of responses, three repeated EFS (1200 mA, 3 Hz) were performed, with 60 min intervals used for contractile responses and 40 min intervals for relaxant responses.

*Decay in applied tension and the contractile NANC response* After the initial adjustment of the applied, passive tension to 1.2 g in the main bronchus, the tension level was continuously recorded for 240 min in order to estimate the time course of its decay.

In additional experiments, the magnitude of the contractile NANC response was examined at various levels of applied, passive tension. Using the main bronchus without tone prior to activation, a series of EFS (1200 mA, 3 Hz) was performed at gradually increasing ($n = 2$) or decreasing ($n = 2$) levels of applied, passive tension with 60 min intervals.

*Sensitivity to tetrodotoxin of the contractile and relaxant NANC response in the main bronchus* The flushing of the organ baths was stopped immediately after the addition of atropine and guanethidine. The neurotoxin tetrodotoxin (10 μM) (Caterall, 1980) or its vehicle alone (0.67% per ml acetic acid) was then added and was continuously present. The contractile NANC response was evoked without tone prior to EFS. The relaxant NANC response was evoked at a histamine-induced (6 μM) tone prior to EFS. EFS (1200 mA, 3 Hz) was then performed followed by a wash-out. It has previously been demonstrated that tetrodotoxin (10 μM) does not significantly reduce smooth-muscle contractility (Lindén *et al.*, 1991a).

*Impulse frequency and NANC stabilizing effect on tone in the main bronchus* The stimulation frequencies 1, 3 or 10 Hz were used in order to evoke moderate to near-maximum, neurally-mediated NANC responses. Higher frequencies were avoided since it has previously been demonstrated that they induce a pronounced tetrodotoxin-resistant NANC contraction which may indicate non-neural transmission (Lindén *et al.*, 1991a). In each airway preparation, only one stimulation frequency was used and it was repeated in three EFS. The first of the three NANC responses was evoked by EFS (1200 mA, 1, 3 or 10 Hz) without tone prior to activation. Wash-out and 20 min of flushing followed. The tone was then increased by histamine (0.3 μM, approximately $EC_{50}$) 20 min prior to the subsequent EFS. The second EFS (1200 mA, 1, 3 or 10 Hz) was then performed followed by another wash-out and 20 min of flushing. The tone was thereafter increased by histamine (6 μM, approximately $EC_{90}$) 20 min prior to the subsequent EFS. The third EFS (1200 mA, 1, 3 or 10 Hz) was performed and was followed by wash-out.

### *Drugs*

Atropine sulphate (Sigma), guanethidine sulphate (Ciba-Geigy) and histamine dichloride (E Merck) were dissolved in Krebs-Ringer solution. Indomethacin (Dumex, Confortid 5 mg $ml^{-1}$) was diluted in Krebs-Ringer solution. Tetrodotoxin (Sigma) was initially dissolved in 50% acetic acid and was then diluted in Krebs-Ringer solution (vehicle, see protocols).

### *Data analysis*

*Tone levels* The data on the NANC stabilizing effects were expressed as tone in relation to the minimum and maximum tone and were calculated as follows: The total (active plus passive) tension (Lindén *et al.*, 1991c) was measured immediately before, at the end of and 25 min after each EFS. The tension level before the first EFS and therefore before the addition of any histamine was regarded as purely passive tension (Lindén *et al.*, 1991c). Within each airway prepara-

tion, the difference in tension between the level prior to the NANC response evoked without induced tone and the peak level during the maximum histamine-induced contraction (0.1 mM) was regarded as the maximum active tension. Within each preparation, all the levels of active tension (tone) were related to and expressed as a percentage of this maximum active tension (% of maximum tone).

*Convergence effect* This term was used as an estimation of the added power of the converging contractile and relaxant NANC responses (Lindén *et al.*, 1991b). The convergence effect was defined on the basis of the difference between the lowest (no histamine) and the highest level of tone (histamine 6 μM) established prior to NANC activation by EFS. The converging contractile and relaxant NANC responses to EFS reduced this difference in tone and this reduction constituted the convergence effect.

*Stabilization level* This term was used to designate the level towards which the contractile and relaxant NANC responses tended to adjust tone and describes the balance between these contractile and relaxant responses (Lindén *et al.*, 1991b). As mentioned above, three EFS were evoked within the same airway preparation, each at a different level of tone prior to stimulation. The tone level at the end of each of these three EFS constituted the basis for calculating a mean value within each airway preparation. This mean value was defined as the stabilization level.

*Relationship between tone prior to and at the end of NANC activation* This analysis was conducted in order to characterize the degree of independence for the tone level at the end of NANC activation in relation to the tone level prior to NANC activation. The analysis was performed by means of linear regression (Colton, 1974).

*Statistical evaluation* The results were generally expressed as the arithmetic mean (s.e.mean) with $n$ representing the number of guinea-pigs (independent observations). Unless otherwise stated, paired or unpaired data were compared by Student's $t$ distribution (two-tailed) determined at 95% confidence intervals (Colton, 1974).

The relationship between the impulse frequency and the convergence effect was analysed by determining the non-parametric correlation coefficient (Colton, 1974) which was then evaluated by Pitman's non-parametric test (Bradley, 1968). When analysing the relationship between the tone prior to and at the end of NANC activation, the linear regression coefficients were determined for each animal by $t$ distribution at 95% confidence intervals (Colton, 1974). These regression coefficients were then compared by Pitman's non-parametric test (Bradley, 1968).

## Results

### *The effect on NANC responses induced by changes in tone prior to EFS*

Without induced tone prior to EFS, and in the presence of indomethacin, atropine and guanethidine, NANC activation by EFS evoked a contractile response in the main bronchus (Figure 1). The contractile NANC response to EFS became smaller when the tone prior to EFS was increased by the addition of histamine (0.3 μM). A further increase in the tone prior to EFS, produced by the addition of more histamine (6 μM), reversed the NANC contraction into a relaxation. This pattern was observed in 6/6 preparations at 1 Hz, in 12/12 preparations at 3 Hz and in 4/4 preparations at 10 Hz.

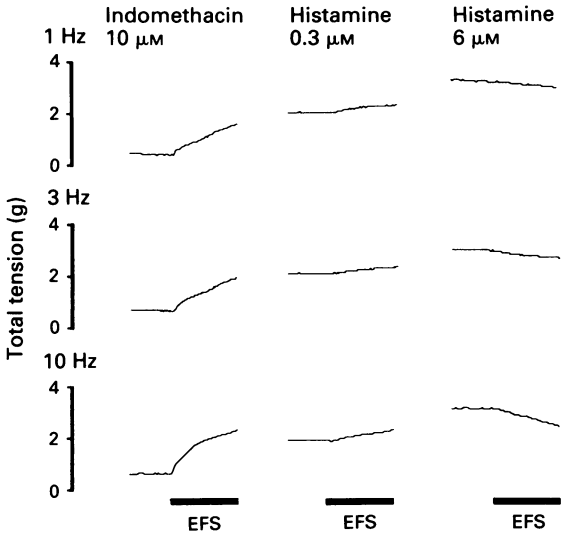



**Figure 1** Original tracings of the response to NANC activation by electrical field stimulation (EFS: 0.5 ms, 1200 mA, 1, 3 or 10 Hz for 240 s) in the guinea-pig isolated main bronchus, at various levels of tone prior to activation. The three bronchial preparations were pretreated by indomethacin (10 μM), atropine (1 μM) and guanethidine (10 μM).

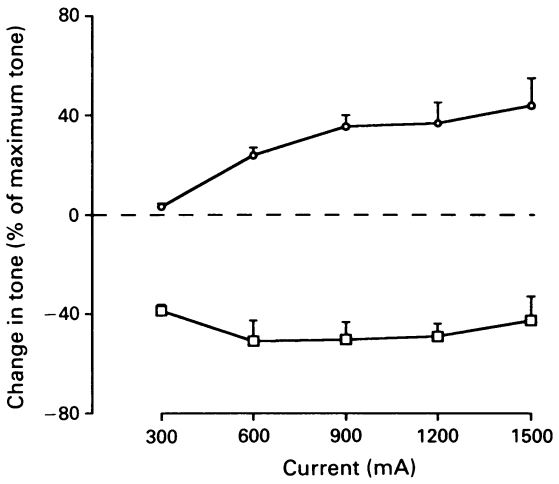



**Figure 2** Current-response characteristics of the contractile (main bronchus, ○) and relaxant (distal trachea, □) NANC response to electrical field stimulation (EFS: 0.5 ms, 3 Hz for 240 s) in guinea-pig isolated airways (pretreatment as in Figure 1). The contractile NANC response ($n = 4$) was evoked without tone prior to EFS whereas the relaxant NANC response ($n = 4$) was evoked at a histamine-induced tone (6 μM) prior to EFS. The data are presented as mean (with s.e.mean) change in tone, expressed as a percentage of the maximum histamine-induced (0.1 mM) tone which was 2.14(0.44) g in the main bronchus and 1.98(0.12) g in the trachea.

### *Impulse current and NANC activation*

Both contractile and relaxant NANC responses were obtained at currents of 300–1500 mA (Figure 2). As both the contractile and the relaxant NANC response displayed a high degree of activation at 1200 mA, this current was used in all subsequent experiments.

### *Reproducibility of NANC responses*

Repeating NANC activation by EFS three times consecutively, we found that the mean (s.e.mean) third contractile NANC response was 101(9)% of the first one. This minor increase was not statistically significant (95% confidence

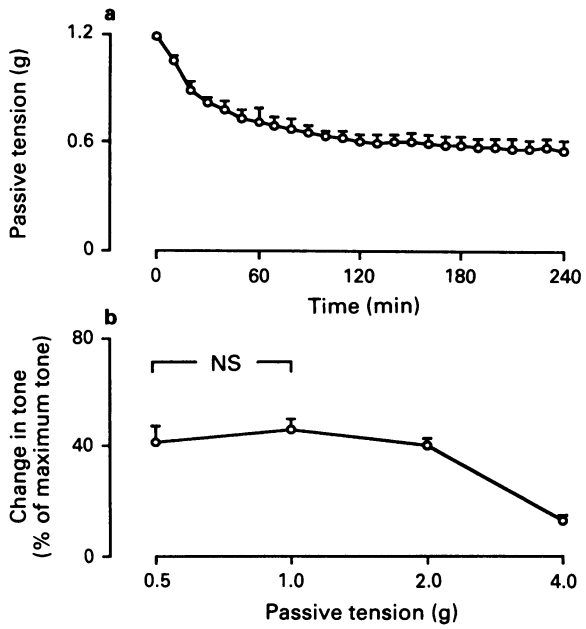



**Figure 3** (a) Decay of the initially applied passive tension (Methods) in the guinea-pig isolated main bronchus (pretreatment as in Figure 1). The data are presented as mean (with s.e.mean) tension in grams (g); $n = 4$. (b) The contractile NANC response to electrical field stimulation (EFS: 0.5 ms, 1200 mA, 3 Hz for 240 s) at various levels of applied tension in the guinea-pig isolated main bronchus (pretreatment as in Figure 1). The data are presented as mean (with s.e.mean) change in tone, expressed as a percentage of the maximum histamine-induced (0.1 mM) tone which was 3.66(0.32) g. $n = 4$. NS = $P > 0.05$, Student's two-tailed $t$ distribution.

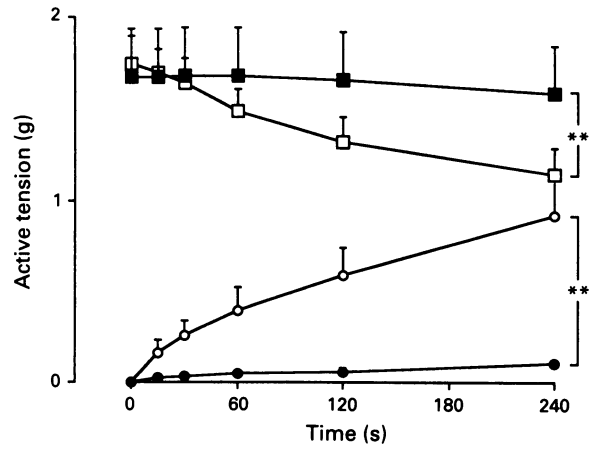



**Figure 4** Time course of the contractile and relaxant non-adrenergic, non-cholinergic (NANC) response to electrical field stimulation (EFS: 0.5 ms, 1200 mA, 3 Hz for 240 s; pretreatment as in Figure 3) with (closed symbols) and without (open symbols) tetrodotoxin (10 μM) in the guinea-pig isolated main bronchus. The contractile NANC response was evoked without induced tone (●, ○) whereas the relaxant NANC response was evoked at a histamine-induced (6 μM) tone (■, □). The data are presented as mean (with s.e.mean) active tension (Methods) in g. **$P < 0.01$, Student's two-tailed $t$ distribution. $n = 6-11$.

interval for difference: − 29–31% of initial response, $n = 4$). Using a corresponding approach, we found that the mean (s.e.mean) third relaxant NANC response was 118(6)% of the first one. Although this increase was modest, it proved to be statistically significant (95% confidence interval for difference: 1–34% of initial response, $n = 6$). As the repeated activation of the relaxant NANC response was conducted, there was also a mean (s.e.mean) reduction in tone prior to activation constituting 12(3)% of maximum tone. This reduction was statistically significant (95% confidence interval for difference: 4–21% of maximum tone). The initial contractile response was 0.98(0.20) g and the initial relaxant response was 1.02(0.05) g.

### *Decay in applied tension and the contractile NANC response*

The decay in applied, passive tension was most pronounced during the first 60 min after the final adjustment of the passive tension (Figure 3a). This time interval corresponded to the drug incubation period in all experiments except these. During the time interval 70 to 160 min, when the influence of the impulse frequency on the NANC stabilizing effect was examined (below), the mean (s.e.mean) decay in passive tension was 0.10(0.01) g only. Although this decay in passive tension was small, it proved to be statistically significant (95% confidence interval for decay: 0.06–0.14 g, $n = 4$). The decay in passive tension did, however, occur within the tension interval from 1.0 to 0.5 g (Figure 3a). As demonstrated by the experiments on the magnitude of the contractile NANC response at various levels of applied, passive tension (Figure 3b), the mean (s.e.mean) difference in contractile NANC response at 0.5 g and at 1.0 g was 4(3)% of maximum tone only. This latter difference in contractile NANC response was not statistically significant (95% confidence interval for difference: − 6–14% of maximum tone, $n = 4$).

### *Sensitivity to tetrodotoxin of the contractile and relaxant NANC response in the main bronchus*

Tetrodotoxin induced a mean (s.e.mean) reduction in the contractile NANC response of 0.82(0.19) g and of 0.52(0.14) g in the relaxant NANC response (Figure 4), at an impulse frequency of 3 Hz. This effect of tetrodotoxin was statistically significant for both the NANC contraction (95% confidence interval for reduction: 0.34–1.30 g, $n = 6$) and the NANC relaxation (95% confidence interval for reduction: 0.20–0.83 g, $n = 11$).

### *Impulse frequency and NANC stabilizing effect on tone in the main bronchus*

Without tone prior to activation (no histamine), the mean (s.e.mean) contractile NANC response increased from 34(8)% at 1 Hz, to 54(4)% at 3 Hz and to 58(4)% at 10 Hz, in % of maximum tone (Figure 5a). No such frequency-dependent increase in contractile NANC response was observed with a moderate tone (histamine 0.3 μM) prior to activation (Figure 5a). However, with a near-maximum tone prior to activation (histamine 6 μM), the relaxant NANC response increased from 6(1)% at 1 Hz, to 18(2)% at 3 Hz and to 33(3)% of maximum tone at 10 Hz (Figure 5a).

*Convergence effect* The difference between the lowest (no histamine) and the highest level of tone (histamine 6 μM) established prior to NANC activation by EFS (PreEFS) was approximately 90% of maximum tone. At the end of NANC activation (EFS), this difference in tone was markedly reduced by the converging contractile and relaxant NANC responses, a NANC convergence effect, which thus tended to stabilize tone (Figure 5a). The magnitude of this NANC convergence effect was 40(8)% at 1 Hz, 72(4)% at 3 Hz and 90(2)% at 10 Hz, as a percentage of maximum tone. The correlation between the magnitude of the NANC convergence effect and the impulse frequency ($r = 0.67$, non-parametric) proved statistically significant ($P < 0.001$, Pitman's non-parametric test, $n = 4-12$).

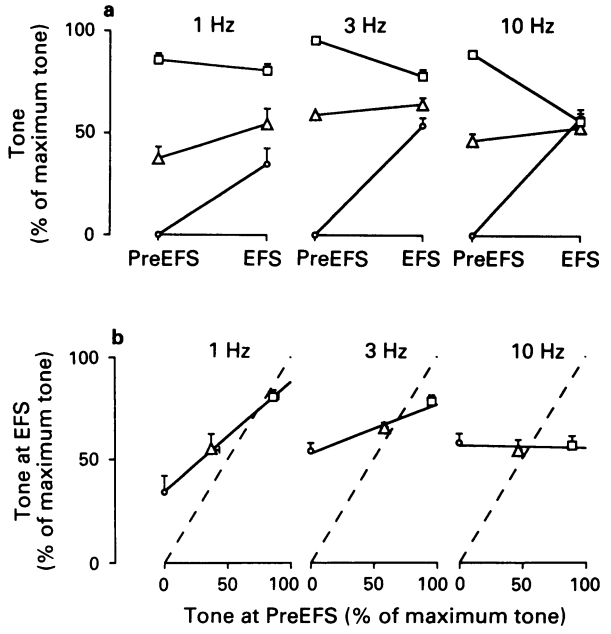



**Figure 5** The effect of variations in impulse frequency on the NANC stabilizing effect on tone in the guinea-pig isolated main bronchus. (a) Tone levels prior to (PreEFS) and at the end of (EFS) NANC activation by electrical field stimulation (EFS: 0.5 ms, 1200 mA for 240 s) at various impulse frequencies. Three tone levels were established prior NANC activation: no tone (pretreatment as in Figure 1 alone, ○), a moderate tone (addition of histamine 0.3 μM, △) and a near-maximum tone (addition of histamine 6 μM, □). (b) The relationship between the level of tone prior to (PreEFS) and at the end of NANC activation (EFS) at various impulse frequencies (continuous lines). For comparison, the line of identity is presented in each figure (dashed line with regression coefficient = 1.0). Based on the same experiments as (a). In both (a) and (b), the data are presented as mean (with s.e.mean) percentage of the maximum histamine-induced (0.1 mM) tone which was 2.56(0.25) g, 2.34(0.20) g and 2.52(0.06) g in the preparations used for 1, 3 and 10 Hz respectively. $n = 4-12$.

*Stabilization level* The NANC convergence effect resulted in an adjustment of tone towards (1 and 3 Hz) or to (10 Hz) a similar level – a stabilization level (Figure 5a). At 1 Hz, the mean (s.e.mean) stabilization level was 56(6)%, at 3 Hz it was 65(3)% and at 10 Hz it was 56(5)% of maximum tone. A comparison of these stabilization levels (mean (s.e.mean) difference: 1 versus 3 Hz: 9(6)%, 1 versus 10 Hz: 0(10)% and 3 versus 10 Hz: 9(8)%), revealed no statistically-significant difference (95% confidence intervals for differences: 1 versus 3 Hz: −5–22%, 1 versus 10 Hz: −22–23%, 3 versus 10 Hz: −9–27%, as a percentage of maximum tone, $n = 4-12$). After the end of NANC activation, the tone returned to a level similar to that prior to activation (data not shown).

*Relationship between tone prior to and at the end of NANC activation* The degree of independence for the tone level at the end of NANC (EFS) activation in relation to the tone level prior to NANC activation (PreEFS) was analysed as the relationship between these tone levels (Figure 5b). The slope of this relationship was indicated by the linear regression coefficient determined for each guinea-pig at 1, 3 and 10 Hz respectively. The regression coefficient became smaller as the stimulation frequency was increased; the mean (s.e.mean) regression coefficient was 0.54(0.07) at 1 Hz (95% confidence interval: 0.35–0.73, $n = 6$) and 0.25(0.04) at 3 Hz (95% confidence interval: 0.17–0.33, $n = 12$) and −0.01(0.02) at 10 Hz (95% confidence interval: −0.09–0.07, $n = 4$). The difference between the regression coefficients at 1 and 3 Hz was statistically significant ($P < 0.001$, Pitman's non-parametric test, $n = 6-12$), as was the difference between the regression coefficients at 3 and 10 Hz ($P < 0.01$, Pitman's non-parametric test, $n = 4-12$).

## Discussion

This study demonstrated that in the guinea-pig isolated main bronchus, NANC neural activation can counteract changes in smooth-muscle tone via a contraction or a relaxation, depending on the level of tone prior to activation. This NANC stabilizing effect on bronchial tone is powerful and its magnitude can be controlled by variations in the impulse-frequency.

The NANC stabilizing effect on tone is a new aspect of the role of NANC mechanisms in the control of bronchial smooth-muscle tone (Lindén *et al.*, 1991b). We therefore performed separate experiments as an attempt to exclude the hypothetical possibility that methodological errors could explain our findings. For instance, since we stimulated each airway preparation repeatedly, a pronounced tachyphylaxis of the contractile NANC response could have contributed to the reversal of the NANC response from a contraction to a relaxation. However, the contractile NANC response demonstrated no pronounced tachyphylaxis. We did find a small increase in the relaxant NANC response during repeated activation but, in these experiments, the increased relaxation could be attributed to a moderate reduction in tone prior to NANC activation. The increase in the relaxant NANC response also appeared to be too small to explain the observed reversal from a contraction to a relaxation. Our experiments on the relationship between the applied, passive tension and the contractile NANC response demonstrated that, during the relevant time course, the decay in the passive tension does not markedly alter the magnitude of the contractile NANC responses. In this respect, the recent demonstration of converging contractile and relaxant NANC responses in the guinea-pig distal trachea (Lindén *et al.*, 1991b) also argues against the importance of any decay in passive tension. This is because we used a parallel experimental design in the referred study instead of the present sequential design (methods). We also performed current response experiments which ascertained that the current level which was used induced a pronounced activation of both the contractile and relaxant NANC response.

Another methodological factor of hypothetical importance is the use of histamine when increasing tone prior to NANC activation. The reason for this is the recent finding that histamine may inhibit the contractile NANC response via a $H_3$-receptor prejunctionally (Ichinose & Barnes, 1989). If this were the case, the exogenously administered histamine could contribute to the reversal from a contractile to a relaxant NANC response. In our model, however, we have previously demonstrated this type of reversed response in the distal trachea of the guinea-pig, without any exogenously administered histamine (Lindén *et al.*, 1991b). In the latter study, we used separate preparations for low, intermediate and high levels of tone prior to NANC activation. These different levels of tone were established by modulating the spontaneous smooth-muscle tone using inhibitors of cyclo-oxygenase and phosphodiesterase (Lindén *et al.*, 1991c). The reversed direction of the NANC response is also unlikely to be caused by endogenously released histamine because of the use of separate preparations, with one electrical field stimulation performed in each preparation at the same time. The present use of histamine is therefore less likely as an explanation of the reversed NANC response. For this and the above mentioned reasons, we believe that we can exclude methodological errors as an explanation of the NANC stabilizing effect on bronchial tone *in vitro*.

The NANC stabilizing effect on bronchial smooth-muscle tone, exerted by converging contractile and relaxant neural

responses, requires that both the direction and the magnitude of these responses are related to the level of tone prior to NANC activation. The previous data on such a relationship are limited. However, one original tracing from one human isolated bronchus has been published by de Jongste *et al.* (1987) and provides some information in this respect. This tracing indicates that the magnitude of the relaxant NANC response increases as the tone (active tension) prior to NANC activation is increased from a low to a moderate level. We add to this the present observation that the level of tone (active tension) prior to activation determines both the direction and magnitude of the NANC neural response in the guinea-pig isolated main bronchus in a similar way to that in the guinea-pig isolated trachea (Lindén *et al.*, 1991b).

The mechanism controlling the direction of the NANC response is probably postganglionic, since we used electrical field stimulation which is thought to activate nerves postganglionically (Coburn & Tomita, 1973; Skoogh, 1986). Based on the present data, however, it is not possible to differentiate between a pre- and a postjunctional site for this mechanism but this mechanism does appear to be independent of the cyclo-oxygenase system, since indomethacin was continuously present in our study. Neither adrenergic nor cholinergic mechanisms should be involved, since our preparations were pretreated with atropine and guanethidine.

In contrast to several other studies on guinea-pig airways, we found a relaxant NANC response in the main bronchus of this species (Grundström *et al.*, 1981; Andersson & Grundström, 1983; Karlsson *et al.*, 1984; Lindén *et al.*, 1991a,b). We ascertained a major neural origin of this relaxant response by abolishing it with tetrodotoxin, using stimulation parameters producing a sub-maximum response. In agreement with our findings, Souhrada *et al.* (1980) have published tracings of a relaxant response in the guinea-pig bronchus of the first generation, but they did not determine whether or not it was adrenergic. The absence of the relaxant NANC response in the main bronchus in most previous studies can probably be explained by the fact that the level of tone prior to NANC activation was not sufficiently high. Our demonstration of the contractile NANC response in the guinea-pig isolated main bronchus is in line with other studies (Andersson & Grundström, 1983; Kamikawa & Shimo, 1989; Lindén *et al.*, 1991a,b). We ascertained a major neural origin of this contractile response as well, by abolishing it with tetrodotoxin, using stimulation parameters producing a sub-maximum response.

In the present study, the balance between the contractile and the relaxant NANC response, the stabilization level, was not markedly different for impulse frequencies producing moderate to near-maximum contractile and relaxant NANC responses in the guinea-pig isolated main bronchus. However, in contrast to our findings, Venugopalan *et al.* (1991) recently suggested that a selective recruitment of the relaxant NANC response can occur through a change in the impulse frequency. This suggestion was based upon frequency-response experiments using different *in vitro* and *in vivo* models for the contractile and the relaxant NANC response. The lung parenchymal strip was used for the contractile NANC response *in vitro* and Venugopalan *et al.* (1991) did not demonstrate that their NANC responses *in vitro* were tetrodotoxin-sensitive at any impulse frequency. The results of Venugopalan *et al.* (1991) might therefore have been confused by non-neural NANC responses as well as by contractions by interstitial cells and vascular smooth-muscle responses (Kapanci *et al.*, 1974).

We used the added magnitude of the contractile and relaxant NANC responses, the convergence effect, to estimate the regulatory power of NANC activation in the guinea-pig isolated main bronchus. This convergence effect correlated to the impulse frequency in the range of 1 to 10 Hz. At 10 Hz, the convergence effect abolished the difference between the highest and lowest level of tone prior to NANC activation. At the end of NANC activation, the tone was thus adjusted to a very similar level, which required a convergence effect of approximately 90% of maximum tone. This strongly indicates that the NANC stabilizing effect on bronchial tone is powerful and that this power can be controlled by the neural impulse frequency.

We also characterized the degree of independence for the tone level at the end of NANC activation in relation to the tone level prior to NANC activation by analysing the relationship between these tone levels. This analysis was performed by means of linear regression in order to estimate its slope at the various stimulation frequencies. The regression coefficient at 1 Hz showed that a low tone prior to NANC activation was moderately increased at the end of NANC activation. On the other hand, a high tone prior to NANC activation was moderately reduced at the end of NANC activation. As the frequency was increased, the regression coefficient became significantly smaller. The tone level at the end of NANC activation thus became less affected by the tone prior to activation. At 10 Hz, the regression coefficient was very close to zero, thereby suggesting that NANC activation can adjust tone to a stabilization level which is almost constant and independent of the tone level prior to activation. This emphasizes the high accuracy of the NANC stabilizing effect and also its considerable regulatory power. As measured in the guinea-pig isolated main bronchus, the NANC stabilizing effect is thus powerful enough to counteract pronounced changes in tone.

In the human isolated segmental bronchus, NANC activation evokes a contractile or a relaxant NANC response and both these responses are tetrodotoxin-sensitive (Richardson & Béland, 1976; Lundberg *et al.*, 1983; Taylor *et al.*, 1984; Palmer *et al.*, 1986). It appears as if the direction of the NANC neural response is also dependent upon the level of tone prior to activation in human airways *in vivo*, since inhalation of the c-fibre stimulant capsaicin produces non-cholinergic bronchoconstriction when no basal tone is induced whereas the same drug produces non-adrenergic bronchodilatation when inhaled at an increased basal tone (Fuller *et al.*, 1985; Lammers *et al.*, 1988). It is therefore possible that NANC neural activation can stabilize tone in human bronchi as well as in guinea-pig bronchi. If this is the case, the stabilizing NANC effect might have both physiological and pathological implications.

It has been suggested that activation of an axon reflex may contribute to bronchoconstriction in asthmatic airways via the release of contractile peptides (Barnes, 1986; 1991; Lundberg *et al.*, 1987; Karlsson *et al.*, 1988). In view of the stabilizing NANC effect on bronchial tone *in vitro*, it is tempting to extend the hypothesis about the axon reflex and to speculate that NANC mechanisms have a regulatory role which involves an axon reflex also in healthy airways. The present and previous (Lindén *et al.*, 1991a,b) demonstrations of powerful contractile and relaxant NANC neural responses are compatible with significant effects on tone if the balance between this contractile and relaxant response is altered. This type of imbalance is also consistent with recent data suggesting an increase in the putative contractile NANC transmitter, substance P, and a decrease in the putative relaxant NANC transmitter, vasoactive intestinal polypeptide, in the airways of severe asthmatics (Ollerenshaw *et al.*, 1989; 1991).

In conclusion, this study indicates that NANC neural activation stabilizes bronchial tone via a contraction when the tone is low prior to activation and via a relaxation when the tone is high prior to activation. This NANC stabilizing effect appears to be powerful and its magnitude can probably be controlled by the neural impulse frequency. The present data are consistent with a regulatory role for NANC contractile and relaxant responses in the control of bronchial smooth-muscle tone.

This study was approved by the Experimental Ethics Committee of the Medical Faculty of the University of Göteborg (Dno 92/89). Financial support was given by the Swedish Medical Research Council, the Swedish Heart-Lung Fund and Hermann Krefting's Foundation. The authors thank Anders Odén, PhD, for performing some of the statistical calculations.

## References


ANDERSSON, R.G.G. & GRUNDSTRÖM, N. (1983). The excitatory non-cholinergic, non-adrenergic nervous system of the guinea pig airways. *Eur. J. Respir. Dis.*, **131**, 141–157.

BARNES, P.J. (1986). Asthma as an axon reflex. *Lancet*, **1**, 242–245.

BARNES, P.J. (1991). Neuropeptides and asthma. *Am. Rev. Respir. Dis.*, **143**, S28–S32.

BRADLEY, J.W. (1968). In *Distribution-free Statistical Tests* pp. 68–86. London: Prentice-Hall

BROCK, J.R. & CUNNANE, T.C. (1988). Studies on the mode of action of bretylium and guanethidine in post-ganglionic sympathetic nerve fibres. *Arch. Pharmacol.*, **338**, 504–509.

CATERALL, W.A. (1980). Neurotoxins that act on voltage-sensitive sodium channels in excitable membranes. *Annu. Rev. Pharmacol. Toxicol.*, **20**, 15–43.

COBURN, R.F. & TOMITA, T. (1973). Evidence for non-adrenergic inhibitory nerves in the guinea pig trachealis muscle. *Am. J. Physiol.*, **224**, 1072–1079.

COLTON, T. (1974). Statistical inference. In *Statistics in Medicine*. 1st ed. pp. 99–252. Boston: Little, Brown and Company.

DE JONGSTE, J.C., MONS, H., BONTA, I.L. & KERREBIJN, K.F. (1987). Cholinergic and non-adrenergic inhibitory nerve-mediated responses of isolated human airways from patients with and without COPD or asthma. In *Human Airway Smooth Muscle* Ch. 16, pp 179–193. Cip-data Den Haag: Koninklijke Bibliotheek.

DOIDGE, J.M. & SATCHELL, D.G.. (1982). Adrenergic and non-adrenergic inhibitory nerves in mammalian airways. *J. Auton. Nerv. System*, **5**, 83–99.

FULLER, R., DIXON, C.M.S. & BARNES, P.J. (1985). Bronchoconstrictor response to inhaled capsaicin in humans. *J. Appl. Physiol.*, **58**, 1080–1084.

GRUNDSTRÖM, N., ANDERSSON, R.G.G. & WIKBERG, J.E.S. (1981). Pharmacological characterization of the autonomous innervation of the guinea pig tracheobronchial smooth muscle. *Acta Pharmacol. Toxicol.*, **49**, 150–157.

ICHINOSE, M. & BARNES, P.J. (1989). Histamine H3-receptors modulate nonadrenergic noncholinergic neural bronchoconstriction in guinea-pig in vivo. *Eur. J. Pharmacol.*, **174**, 49–55.

ICHINOSE, M., INOUE, H., MIURA, M. & TAKASHIMA, T. (1988). Non-adrenergic bronchodilation in normal subjects. *Am. Rev. Respir. Dis.*, **138**, 31–34.

KAMIKAWA, Y. & SHIMO, Y. (1976). Pharmacological differences of non-adrenergic inhibitory response and of ATP-induced relaxation in guinea-pig tracheal strip-chains. *J. Pharmacol. Pharm.*, **28**, 854–855.

KAMIKAWA, Y. & SHIMO, Y. (1989). Adenosine selectively inhibits noncholinergic transmission in guinea pig bronchi. *J. Appl. Physiol.*, **66**, 2084–2091.

KAPANCI, Y., ASSIMACOPOULOS, A., IRLE, C., ZWAHLEN, A. & GABBIANI, G. (1974). 'Contractile interstitial cells' in pulmonary alveolar septa: a possible regulator of ventilation/perfusion ratio? *J. Cell Biol.*, **60**, 375–392.

KARLSSON, J.-A., FINNEY, M.J.B., PERSSON, C.G.A. & POST, C. (1984). Substance P antagonists and the role of tachykinins in non-cholinergic bronchoconstriction. *Life Sci.*, **35**, 2681–2691.

KARLSSON, J.-A., SANT'AMBROGIO, G. & WIDDICOMBE, J. (1988). Afferent neural pathways in cough and reflex bronchoconstriction. *J. Appl. Physiol.*, **65**, 1007–1023.

LAMMER, J.-W.J., MINETTE, P., MCCUSKER, M.T., CHUNG, K.F. & BARNES, P.J. (1988). Nonadrenergic bronchodilator mechanisms in normal human subjects in vivo. *J. Appl. Physiol.*, **64**, 1817–1822.

LINDÉN, A. (1992). A non-adrenergic, non-cholinergic stabilizing mechanism in the neural regulation of airway smooth-muscle tone. *Doctoral dissertation, University of Goteborg, Sweden*, pp. 21–23.

LINDÉN, A., ULLMAN, A., SKOOGH, B.-E. & LÖFDAHL, C.-G. (1991a). Non-adrenergic, non-cholinergic regulation of guinea pig airway smooth-muscle – indomethacin-induced changes and segmental differences. *Pulm. Pharmacol.*, **4**, 170–176.

LINDÉN, A., ULLMAN, A., LÖFDAHL, C.-G. & SKOOGH, B.-E. (1991b). Non-adrenergic, non-cholinergic neural activation stabilizes smooth muscle tone independently of eicosanoid factors in guinea-pig isolated airways. *Br. J. Pharmacol.*, **104**, 509–513.

LINDÉN, A., LÖFDAHL, C.-G., ULLMAN, A. & SKOOGH, B.-E. (1991c). In vitro characteristics of spontaneous airway tone in the guinea pig. *Acta Physiol. Scand.*, **142**, 351–357.

LÖTVALL, J.O., BEN-MENACHEM, E., AUGUSTINSSON, K.E., LUNDE, H., SVEDMYR, N. & HEDNER, T. (1992). Electrical stimulation of the left cervical vagus in one patient with chronic airways obstruction: effect on FEV1. *Am. Rev. Resp. Dis.*, **145**, (S2), A66.

LUNDBERG, J.M., LUNDBLAD, L., ÄNGGÅRD, A., MARTLING, C.-R., THEODORSSON-NORHEIM, E., STJÄRNE, P. & HÖKFELT, T.G. (1987). Bioactive peptides in capsaicin-sensitive C-fiber afferents of the airways. In *The Airways: Neural Control in Health and Disease*. ed. Kaliner, M.A. & Barnes, P.J. pp. 417–445. New York: Marcel Dekker.

LUNDBERG, J.M., MARTLING, C.-R. & SARIA, A. (1983). Substance P and capsaicin-induced contraction of human bronchi. *Acta Physiol. Scand.*, **119**, 49–53.

MARTLING, C.-R., SARIA, A., ANDERSSON, P. & LUNDBERG, J.M. (1984). Capsaicin pretreatment inhibits vagal cholinergic and non-cholinergic control of pulmonary mechanics in the guinea pig. *Naunyn-Schmied. Arch. Pharmacol.*, **325**, 343–348.

OLLERENSHAW, S., JARVIS, D., WOOLCOCK, A., SULLIVAN, C. & SCHEIBNER, T. (1989). Absence of immunoreactive vasoactive intestinal polypeptide in tissue from the lungs of patients with asthma. *N. Engl. J. Med.*, **320**, 1244–1248.

OLLERENSHAW, S., JARVIS, D., WOOLCOCK, A.J. & SULLIVAN, C.E. (1991). Substance P immunoreactive nerves in airways from asthmatics and non-asthmatics. *Eur. Resp. J.*, **4**, 673–682.

PALMER, J.B.D., CUSS, F.M.C. & BARNES, P.J. (1986). VIP and PHM and their role in non-adrenergic inhibitory responses in isolated human airways. *J. Appl. Physiol.*, **61**, 1322–1328.

RICHARDSON, J. & BÉLAND, J. (1976). Non-adrenergic inhibitory nervous system in human airways. *J. Appl. Physiol.*, **41**, 764–770.

SCOLCSANYI, J. & BARTHO, L. (1982). Capsaicin-sensitive non-cholinergic excitatory innervation of the guinea-pig tracheobronchial smooth muscle. *Neurosci. Lett.*, **34**, 247–251.

SKOOGH, B.-E. (1986). Parasympathetic ganglia in the airways. *Bull. Eur. Physiopathol. Respir.*, **22** (S7), 143–147.

SOUHRADA, J.F., MELZER, E. & GRANTHAM, P. (1980). Some characteristics of the purinergic nervous system in normal and sensitized airway smooth muscle. *Resp. Physiol.*, **40**, 199–209.

TAYLOR, S.M., PARÉ, P.D. & SCHELLENBERG, R.R. (1984). Cholinergic and non-adrenergic mechanisms in human and guinea pig airways. *J. Appl. Physiol.*, **56**, 958–965.

ULLMAN, A., CIABATTONI, G., LÖFDAHL, C.-G., LINDÉN, A., SVEDMYR, N. & SKOOGH, B.-E. (1990). Epithelium-derived PGE2 inhibits the contractile response to cholinergic stimulation in isolated ferret trachea. *Pulm. Pharmacol.*, **3**, 155–160.

VENUGOPALAN, C.S., HOLMES, E.P., FUCCI, V. & GUTHRIE, A.J. (1991). Stimulation frequency-dependent nonadrenergic non-cholinergic airway responses of the guinea-pig. *J. Appl. Physiol.*, **70**, 1006–1010.

YIP, P., PALOMBINI, B. & COBURN, R.F. (1981). Inhibitory innervation to the guinea pig trachealis muscle. *J. Appl. Physiol.*, **50**, 374–382.


*(Received April 27, 1992*
*Revised February 22, 1993*
*Accepted February 25, 1993)*

*Br. J. Pharmacol.* (1993), **109**, 852–858 © Macmillan Press Ltd, 1993

# Inhibition by nitric oxide-donors of human polymorphonuclear leucocyte functions

[1]E. Moilanen, P. Vuorinen, H. Kankaanranta, T. Metsä-Ketelä & [2]H. Vapaatalo

Department of Biomedical Sciences, University of Tampere, P.O. Box 607, SF-33101 Tampere, Finland

**1** The study was designed to test the hypothesis that nitric oxide (NO)-releasing compounds increase guanosine 3':5'-cyclic monophosphate (cyclic GMP) production in human polymorphonuclear leucocytes (PMNs) and concomitantly inhibit PMN functions, i.e. leukotriene $B_4$ ($LTB_4$) synthesis, degranulation, chemotaxis and superoxide anion ($O_2^-$) release. The effects of two new NO-releasing compounds, GEA 3162 and GEA 5024 were compared to 3-morpholino-sydnonimine (SIN-1) and S-nitroso-N-acetyl-penicillamine (SNAP).

**2** GEA 3162 and GEA 5024 (1–100 μM) inhibited Ca ionophore A23187-induced $LTB_4$ and β-glucuronidase release, chemotactic peptide FMLP-induced chemotaxis and opsonized zymosan-triggered chemiluminescence dose-dependently in human PMNs. SIN-1 and SNAP were weaker inhibitors.

**3** Cellular cyclic GMP production was increased after exposure to NO-donors concomitantly with the inhibition of PMN functions. No alterations in the levels of adenosine 3':5'-cylic monophosphate (cyclic AMP) were detected.

**4** The results suggest that NO, possibly through increased cyclic GMP, inhibits the activation of human PMNs and may thus act as a local modulator in inflammatory processes.

**Keywords:** PMN functions; nitric oxide; nitric oxide-releasing compounds; SIN-1; guanosine 3':5-cyclic monophosphate; leukotriene $B_4$; β-glucuronidase; chemotaxis; superoxide anion

## Introduction

Cyclic nucleotides are known to modulate neutrophil activation processes. An increase in the intracellular concentrations of adenosine 3':5'-cyclic monophosphate (cyclic AMP) induced for example by β-adrenoceptor agonists, prostaglandin E or histamine or the cell-permeant analogue of cyclic AMP, $N^6$, 2'-O-dibutyryl adenosine 3':5'-cyclic monophosphate ($Bt_2$ cyclic AMP), inhibit several neutrophil functions (Ignarro & George, 1974; Zurier *et al.*, 1974; Burde *et al.*, 1989; Ervens *et al.*, 1991; Wenzel-Seifert *et al.*, 1991). Based on the hypothesis of the opposing actions of cyclic AMP and guanosine 3':5'-cyclic monophosphate (cyclic GMP) (Goldberg *et al.*, 1975), it was suggested that cyclic GMP might stimulate leucocyte activation. More recent studies do, however, indicate that, depending on the stimuli and experimental conditions, cyclic GMP often inhibits neutrophil functions (Ney *et al.*, 1990; Schröder *et al.*, 1990; Ervens *et al.*, 1991; Wenzel-Seifert *et al.*, 1991).

Endothelium-derived relaxing factor (EDRF) is a labile substance produced by vascular endothelium (Furchgott & Zawadzki, 1980). The known biological functions of EDRF include vasodilatation (Furchgott, 1983) and inhibition of platelet aggregation (Furlong *et al.*, 1987; Radomski *et al.*, 1987). These effects are believed to be mediated by the activation of soluble guanylate cyclase and an increase in the intracellular concentrations of cyclic GMP in the target cells (see Moncada *et al.*, 1991).

Pharmacological and chemical evidence indicates that EDRF is identical with or closely related to nitric oxide (NO) and is synthesized from L-arginine (Ignarro *et al.*, 1987; Palmer *et al.*, 1987; 1988; Myers *et al.*, 1990). Recently neutrophils and other leucocytes have been reported to release a factor which functionally and chemically resembles EDRF (Rimele *et al.*, 1988; McCall *et al.*, 1989; Salvemini *et al.*, 1989; Schmidt *et al.*, 1989; Wright *et al.*, 1989). The pathophysiological functions of the endothelium-derived NO in the interactions between leucocytes and endothelial cells, as well as those of the neutrophil-derived NO in the inflammatory response, remain mostly unknown. There are some data indicating that NO or NO-releasing compounds can inhibit neutrophil function (Ney *et al.*, 1990; Schröder *et al.*, 1990; Kubes *et al.*, 1991; Wenzel-Seifert *et al.*, 1991).

In the present study we tested the hypothesis that NO-releasing compounds increase cyclic GMP in human polymorphonuclear leucocytes (PMNs) with concomitant inhibition of PMN functions, i.e. chemotaxis, degranulation, leukotriene (LT) production and superoxide anion ($O_2^-$) release. Two new potent NO-donors, GEA 3162 and GEA 5024, 4-aryl-substituted oxatriazol derivatives were compared to earlier known NO-donors 3-morpholino-sydnonimine (SIN-1) and S-nitroso-*N*-acetyl-penicillamine (SNAP).

## Methods

### *PMN isolation*

Blood samples were collected from healthy volunteers who had abstained from taking any drugs for at least 14 days before sampling. Polymorphonuclear and mononuclear leucocytes were separated by Ficoll-Paque density gradient centrifugation and erythrocytes removed by dextran sedimentation followed by lysis with Tris-buffered 0.15 M ammonium chloride (Bøyum, 1976; Moilanen *et al.*, 1988). After the purification procedure the viability of the cells was >97% as determined by Trypan blue exclusion and the PMN suspension contained less than 2% contaminating mononuclear leucocytes.

To evaluate the direct cytotoxicity of the compounds tested, Trypan blue staining and the measurement of released lactate dehydrogenase (LDH) were included in the protocols. LDH activity was measured in the cell-free supernatants by an enzymatic method (The Committee on Enzymes on the Scandinavian Society for Clinical Chemistry and Clinical

[1] Author for correspondence.
[2] Present address: Department of Pharmacology and Toxicology, University of Helsinki, P.O. Box 8, SF-00014 Helsinki University, Finland.

Physiology, 1976). None of the NO-donors tested decreased PMN viability as measured by these tests in the incubation conditions described in the PMN function assays.

### *Leukotriene $B_4$ synthesis and assay*

PMNs, $5 \times 10^6$ cells suspended in 500 μl of Dulbecco's phosphate buffered saline (DPBS), were preincubated for 10 min at 37°C. Thereafter the NO-donors were added into the incubate. After 3 min the cells were activated by addition of Ca ionophore A23187 (final concentration 1.0 μM). After a 10 min incubation at 37°C the cells were pelleted by centrifugation (10 000 *g* for 30 s). The supernatants were collected and kept at −20°C until assayed for leukotriene $B_4$ ($LTB_4$).

The incubates were deproteinized by addition of three volumes of acetonitrile, evaporated under nitrogen and resolved in the mobile phase of the high performance liquid chromatography (h.p.l.c.) assay. The $LTB_4$ assay was based on that described by Borgeat & Samuelsson (1979). We used a ChromSpher $C_{18}$ column (2 × 10 cm; Chrompack, Middelburg, The Netherlands) and a mixture of methanol:water: acetic acid 70:30:0.1 (v:v:v) as the mobile phase (Moilanen *et al.*, 1988); u.v. absorbance at 280 nm was recorded to detect $LTB_4$. The peak of $LTB_4$ was identified and verified by adding unlabelled or radiolabelled $LTB_4$ into the samples and by radioimmunoassay (Moilanen *et al.*, 1988). The values of $LTB_4$ were corrected for recoveries (which were >90%) by using prostaglandin $B_1$ ($PGB_1$) as an internal standard.

### *β-Glucuronidase release and assay*

PMN suspensions were treated as described above. β-Glucuronidase activity in the cell-free supernatants was assayed spectrophotometrically according to the method described by Stahl & Fishman (1984) by measuring the formation of phenolphthalein from phenolphthalein-b-(D)-glucuronide as the substrate. The enzyme activity released from $10^6$ cells is expressed as nmol phenolphthalein formed from the hydrolysed substrate calculated from a phenolphthalein standard curve.

### *Chemotaxis*

The NO-donors were incubated with PMNs for 10 min. Thereafter the chemotactic movement of the cells towards the chemotactic peptide *N*-formyl-methionyl-leucyl-phenylalanine (FMLP, 10 nM; 90 min; 37°C) was measured using a modified Boyden chamber technique with $^{51}Cr$-labelled PMNs (Gallin *et al.*, 1973; Kankaanranta *et al.*, 1991). The incubation conditions were chosen to be optimal on the basis of our previous data (Kankaanranta *et al.*, 1991). In each batch of cells the counts per minute (c.p.m.) − value of the cells reaching the filter between the chambers in the control experiment (where cells migrated towards FMLP in the absence of the tested compounds) was set as 100%. The PMN migration in the presence of the NO-donors was expressed as a percentage of the control. Original data (in c.p.m.) were used in the statistical analysis.

### *Whole blood chemiluminescence*

The luminol-enhanced chemiluminescence (CL) responses of leucocytes in diluted whole blood activated by opsonized zymosan were studied to evaluate the effects of NO-donors on a burst in oxidative metabolism as decribed earlier (Lilius *et al.*, 1987). The CL emission was measured at 37°C for 60 min in a volume of 500 μl of Hank's balanced salt solution (HBSS) containing 400 μM luminol, 0.1% gelatin, 1 mg opsonized zymosan and 40, 55 or 80 nl blood in the absence or presence of the NO-donor, using an automatic luminometer set-up (LKB Wallac 1251 Luminometer, Turku, Finland connected to an IBM compatible PC computer equipped with a luminometer control and graphics programme, TriStar Enterprise Ltd., Tampere, Finland). The maximum CL was obtained in 15 to 20 min and was plotted against blood volume in the sample. The linear regression line was calculated and the results expressed as mV $\mu l^{-1}$ of blood. The background noise and the CL caused by the reaction mixture in the absence of blood and zymosan was subtracted from the CL response before the calculations.

The spontaneous CL responses of the NO-donors were measured in a volume of 500 μl of HBSS and in the presence of 400 μM luminol in tubes covered with paraffin. HBSS solutions were bubbled either with oxygen or nitrogen immediately before use. The reaction was initiated by adding 50 μl of freshly prepared drug solution made in HBSS. The spontaneous CL emission was monitored for 30 min and the maximal response was recorded. The background current of the photomultiplier tube was less than 1 mV.

### *Cyclic nucleotide assays*

PMN incubations were stopped by adding ice cold trichloroacetic acid (TCA, final concentration 6%) and samples were centrifuged (10 000 *g* for 10 min). The supernatants were washed four times with water-saturated ethyl ether, diluted with an equal volume of 100 mM sodium acetate buffer (pH 6.2) and stored at −20°C until assayed for cyclic AMP and cyclic GMP. For the cyclic GMP determinations the samples were acetylated and measured by radioimmunoassay (RIA) as described earlier (Axelsson *et al.*, 1988). Cyclic AMP levels were measured without acetylation by RIA.

### *Statistics*

The results are expressed as mean ± s.e. mean. The drug concentration that caused 50% inhibition ($IC_{50}$) was estimated in each experiment on the basis of a semi-logarithmic dose-response curve. Statistical analysis was carried out by general linear models analysis of variance (GLM ANOVA) (Solo, BMDP Statistical Software, Los Angeles, Ca., U.S.A.). Differences were considered significant when $P < 0.05$.

### *Drugs and chemicals*

The two 4-aryl-substituted oxatriazol derivatives GEA 3162 and GEA 5024 (Figure 1), SIN-1 and SNAP were kindly provided by GEA Ltd, Copenhagen, Denmark.

Ficoll-Paque (Pharmacia Fine Chemicals AB, Uppsala, Sweden); Ca ionophore A23187, phenolphthalein-b-(D)-glucuronide, phenolphthalein, FMLP, zymosan and luminol (Sigma Chemical Company, St. Louis, M.O., U.S.A.); $LTB_4$ and $PGB_1$ (Cayman Chemical, Ann Arbor, M.I., U.S.A.); $^{51}Cr$-labelled $Na_2CrO_4$ and cyclic AMP RIA (Amersham International, Buckinghamshire, U.K.); $^{125}I$-labelled cyclic GMP (Du Pont, NEN Research Products, Boston, Mass., U.S.A.) were obtained as indicated.

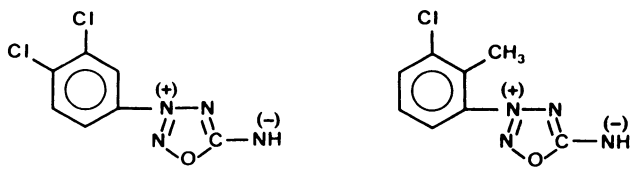



**Figure 1** The chemical structures of GEA 3162 and GEA 5024.

## Results

### *Effects of NO-donors on $LTB_4$ synthesis*

Unstimulated PMNs did not produce detectable amounts of $LTB_4$ (detection limit 3 pmol/$10^6$ cells). When PMNs were stimulated with Ca ionophore A23187 (1.0 μM; 10 min; 37°C), the $LTB_4$ concentrations assayed in the incubates were 27 ± 1 pmol/$10^6$ cells ($n = 20$).

The effects of NO-donors on PMN functions were tested at the following drug concentrations: GEA 3162 and GEA 5024 0.1–100 μM, SIN-1 and SNAP 0.1/1–1000 μM. Each of the NO-releasing compounds inhibited $LTB_4$ release from human PMNs dose-dependently (Figure 2). The new compounds GEA 3162 ($IC_{50}$ 36 ± 12 μM) and GEA 5024 ($IC_{50}$ 30 ± 2 μM) produced their effects at concentrations that were one tenth or less of those needed for SIN-1 ($IC_{50}$ 340 ± 80 μM) and SNAP ($IC_{50}$ 700 ± 200 μM).

### *Effects of NO-donors on β-glucuronidase release*

GEA 3162 and GEA 5024 suppressed β-glucuronidase release from A23187-activated PMNs dose-dependently, GEA 3162 causing its effects at somewhat lower drug concentrations than GEA 5024 ($IC_{50}$s 16 ± 4 μM and 33 ± 7 μM, respectively; $P < 0.05$) (Figure 3). SIN-1 at a concentration of 1 mM was also inhibitory causing a 33 ± 2% decrease whereas SNAP at concentrations up to 1 mM was inactive.

### *Effects of NO-donors on PMN chemotaxis*

The chemotactic peptide FMLP (10 nM; 90 min; 37°C) placed in the lower well of the chemotaxis chamber, caused 51 ± 3% ($n = 20$) of the PMNs ($10^6$ cells) added to the upper well to migrate into the filter system between the upper and lower well during the 90 min incubation time. The random migration without any chemoattractant in these incubation conditions was 17 ± 2%.

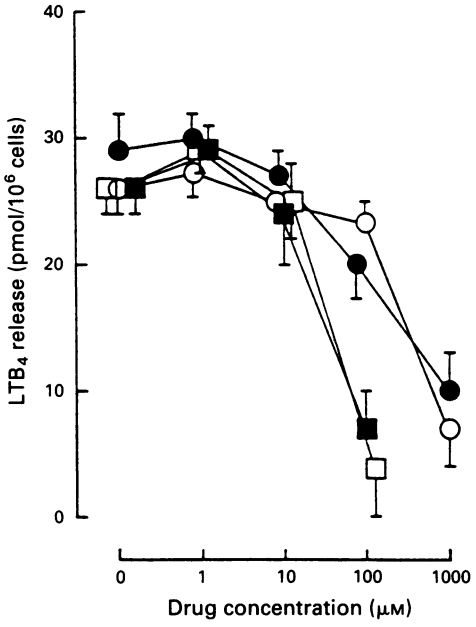



**Figure 2** The dose-response curves of the inhibitory action of GEA 3162 (■), GEA 5024 (□), 3-morpholino-sydnonimine (○) and S-nitroso-*N*-penicillamine (●) on A23187-induced leukotriene $B_4$ ($LTB_4$) release from human PMNs. The cells were incubated for 3 min at 37°C with the NO-donor before stimulation with A23187 (1.0 μM; 10 min; 37°C). Mean ± s.e.mean, duplicate experiments with cells from 5 donors.

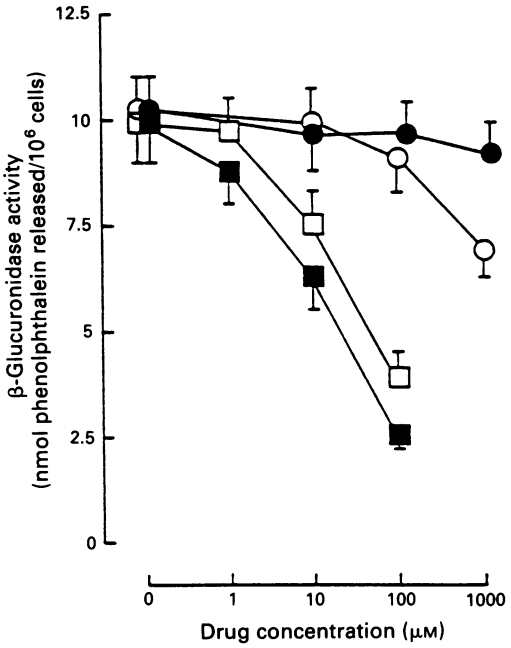



**Figure 3** The dose-response curves of the inhibitory action of GEA 3162 (■), GEA 5024 (□), 3-morpholino-sydnonimine (○) and S-nitroso-*N*-penicillamine (●) on A23187-induced β-glucuronidase release from human PMNs. The cells were incubated for 3 min at 37°C with the NO-donor before stimulation with A23187 (1.0 μM; 10 min; 37°C). Mean ± s.e.mean, duplicate experiments with cells from 6 donors.

GEA 3162 and GEA 5024 were effective inhibitors of FMLP-induced chemotactic movement of human PMNs ($IC_{50}$s 6 ± 1 μM and 14 ± 2 μM, respectively) (Figure 4). SIN-1 decreased chemotaxis slightly (20 ± 10%) at the highest concentration tested (1 mM) but SNAP was inactive up to a 1 mM concentration.

### *Effects of NO-donors on whole blood chemiluminescence*

Figure 5 shows the spontaneous CL caused by GEA 3162, GEA 5024, SIN-1 and SNAP in oxygen and nitrogen atmospheres. In contrast to the other NO-donors tested, SIN-1 at concentrations which were inhibitory in PMN function tests caused a strong spontaneous CL, especially in an oxygen atmosphere. Therefore it was not possible to test the effects of SIN-1 on leucocyte CL at drug concentrations higher than 10 μM.

The control values of zymosan-induced superoxide production in human blood cells as measured by luminol-enhanced CL were 136 ± 8 mV $\mu l^{-1}$ of blood ($n = 30$). GEA 3162 and GEA 5024 suppressed the CL response dose-dependently even at submicromolar drug concentrations, the former being more potent ($IC_{50}$s 0.4 ± 0.03 μM and 1.4 ± 0.1 μM, respectively; $P < 0.001$) (Figure 6). At higher drug concentrations SIN-1 and SNAP were also inhibitory. SIN-1 at 10 μM concentrations (which was the highest drug concentration that did not interfere with spontaneous CL) caused 12 ± 5% inhibition of the CL response. SNAP suppressed the whole blood CL dose-dependently over the concentration range of 10–1000 μM, the highest concentration causing 50 ± 3% inhibition.

### *Effects of NO-donors on cyclic nucleotide production*

Figure 7 shows the effects of GEA 3162 and GEA 5024 (0.1–100 μM) as well as those of SIN-1 and SNAP (0.1–1000 μM) on cyclic GMP production in human PMNs

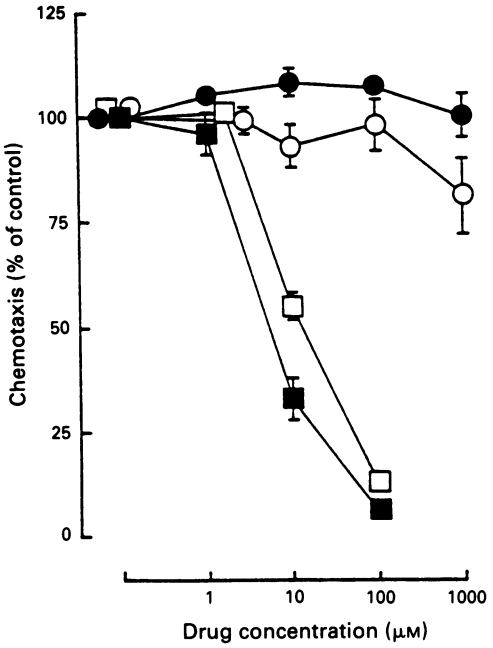



**Figure 4** The dose-response curves of the inhibitory action of GEA 3162 (■), GEA 5024 (□), 3-morpholino-sydnonimine (○) and S-nitroso-*N*-penicillamine (●) on PMN chemotaxis. PMNs were incubated for 10 min at 37°C with the NO-donor before the commencement of chemotaxis assay. FMLP (10 nM; 90 min; 37°C) was used as the chemotactic agent. In each batch of cells the counts per minute (c.p.m.) -value of the $^{51}$Cr-labelled cells reaching the filter between the chambers in the control experiment (where cells migrated towards FMLP in the absence of the tested compounds) was set as 100%. The PMN migration in the presence of the NO-donors was expressed as a percentage of the control. Mean ± s.e.mean, triplicate experiments with cells from 5 donors.

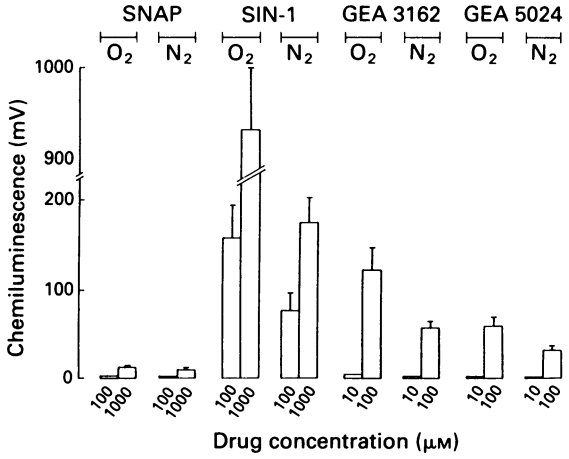



**Figure 5** Spontaneous luminol-enhanced chemiluminescence induced by GEA 3162, GEA 5024, S-morpholino-syndnonimine (SIN-1) and S-nitroso-*N*-penicillamine (SNAP) in oxygen ($O_2$) and nitrogen ($N_2$) atmospheres. The reaction was initiated by the addition of freshly prepared solution of the NO-donor into Hank's balanced salt solution containing 400 μM luminol. The chemiluminescence emission was monitored for 30 min and the maximal response is shown. Mean ± s.e. mean, 5 separate experiments.

during a 10 min incubation. This time was chosen to correspond with the incubation time in the experiments of $LTB_4$ and β-glucuronidase release and whole blood CL as well as the exposure time of the PMNs to the NO-donor before the start of the chemotaxis assay. Each NO-donor enhanced

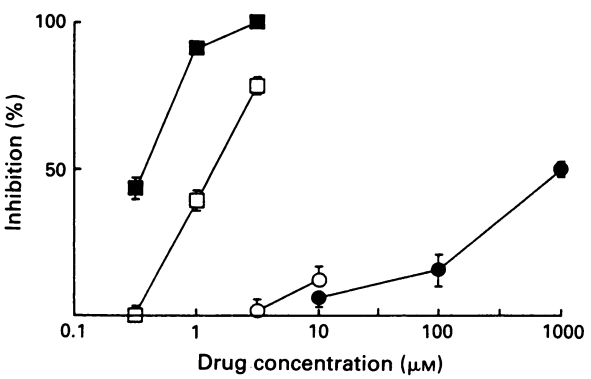



**Figure 6** The dose-response curves of the inhibitory action of GEA 3162 (■), GEA 5024 (□), S-morpholino-sydnonimine (○) and S-nitroso-*N*-penicillamine (●) on opsonized zymosan-induced luminol-enhanced chemiluminescence (CL) in diluted blood. Samples were incubated for 3 min at 37°C with the NO-donor before addition of opsonized zymosan (1 mg/tube). In each experiment, the CL response (mV $\mu l^{-1}$ of blood) in the control experiment (i.e. in the absence of the tested compounds) was set at 100%. The CL response in the presence of the NO-donor was expressed as a percentage of the control values. Mean ± s.e.mean, duplicate experiments with cells from 7–9 donors.

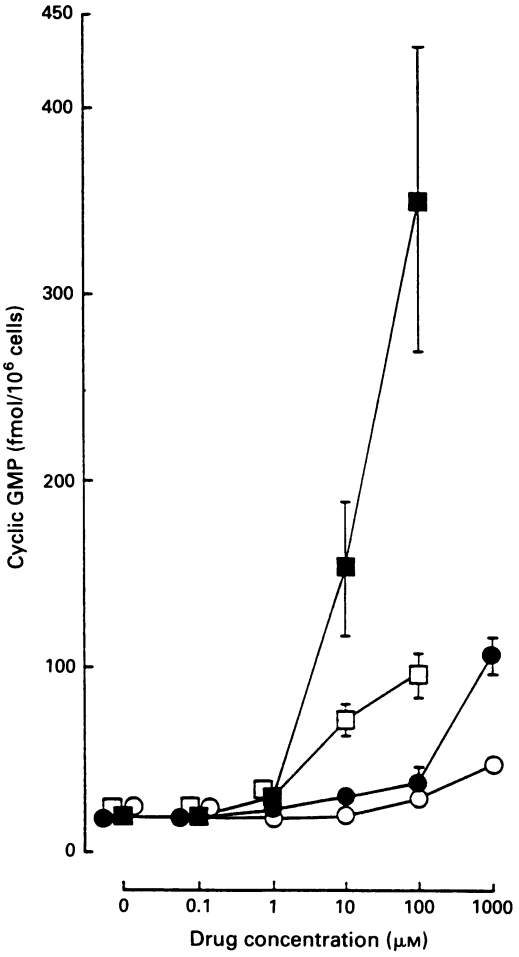



**Figure 7** The effects of GEA 3162 (■), GEA 5024 (□), S-morpholino-sydnonimine (○) and S-nitroso-*N*-penicillamine (●) on cyclic GMP levels in human PMNs. The cells were incubated for 10 min at 37°C with the NO-donor and thereafter the incubations were stopped by the addition of cold trichloroacetic acid. Mean ± s.e.mean, duplicate experiments with cells from 4–7 donors.

cyclic GMP production in PMNs dose-dependently, the order of potency being GEA 3162 > GEA 5024 > SNAP > SIN-1.

The time-response curves of the cyclic GMP-enhancing effects of GEA 3162 (10 and 100 μM), GEA 5024 (10 and 100 μM), SIN-1 (100 and 1000 μM) and SNAP (100 and 1000 μM) show that GEA 3162 and GEA 5024 increased the cyclic GMP levels more rapidly and at lower drug concentrations than SIN-1 and SNAP (Figure 8). The time-response effects of lower drug concentrations (GEA 3162 and GEA 5024 at 0.1 and 1 μM; SIN-1 and SNAP at 1 and 10 μM) were measured in two experiments (data not shown). No increase in the cyclic GMP synthesis in PMNs could be detected except in the case of 1 μM GEA 3162 which caused a mild transient increase (up to 43 fmol/$10^6$ cells) during 10–30 min incubations.

None of the NO-donors tested had any significant effect on cyclic AMP concentrations in human PMNs during a 10 min incubation (data not shown).

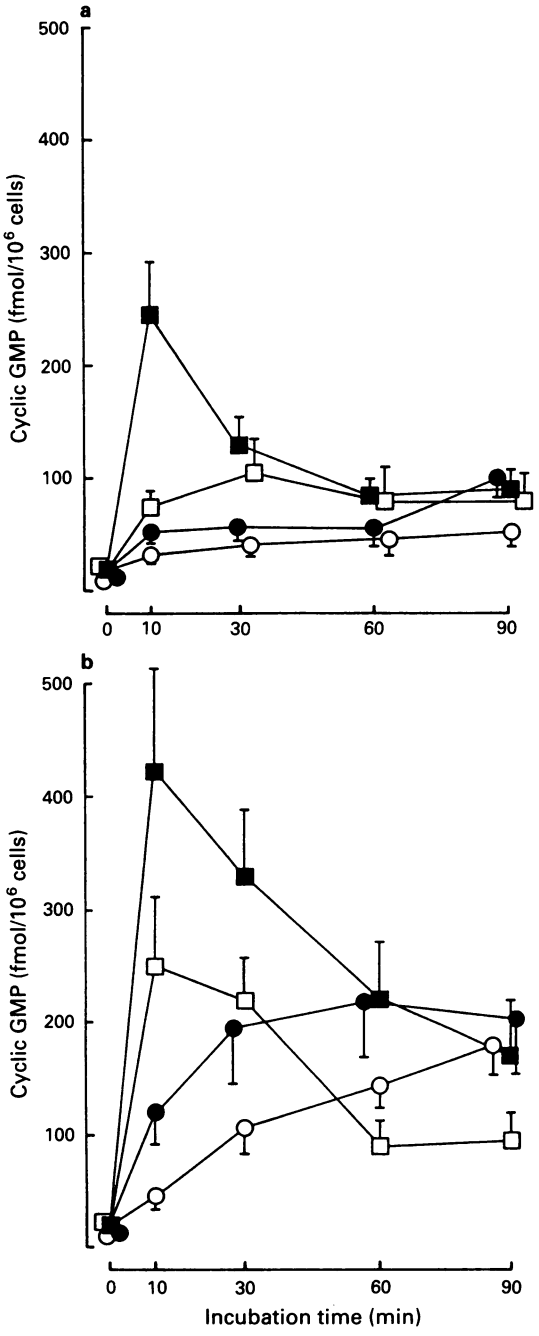



**Figure 8** The time-response curves of the effects of GEA 3162, GEA 5024, S-morpholino-sydnonimine (SIN-1) and S-nitroso-*N*-penicillamine (SNAP) on the production of cyclic GMP in human PMNs. The cells were incubated with the NO-donor for 10–90 min at 37°C and thereafter the incubations were stopped by the addition of cold trichloroacetic acid. In (a), GEA 3162 10 μM (■); GEA 5024 10 μM (□); SIN-1 100 μM (○); SNAP 100 μM (●). In (b) GEA 3162 100 μM (■); GEA 5024 100 μM (□); SIN-1 1000 μM (○); SNAP 1000 μM (●). Mean ± s.e.mean, duplicate experiments with cells from 5 donors.

## Discussion

Two new oxatriazol derivatives, GEA 3162 and GEA 5024, proved to be potent inhibitors of both receptor-mediated (FMLP-induced chemotaxis and opsonized zymosan-induced chemiluminescence) and Ca ionophore-triggered (A23187-induced degranulation and $LTB_4$ release) activation of human PMNs *in vitro*. On a molar basis, the new compounds were more than ten fold as potent as the known NO-donors SIN-1 and SNAP. The inhibitory activity of SIN-1 detected in the present study was similar to that reported recently (Ney *et al.*, 1990; Schröder *et al.*, 1990; Wenzel-Seifert *et al.*, 1991).

Chemical characteristics of sydnonimines (e.g. SIN-1) include their ability to release $O_2^-$ in addition to NO in aqueous solutions (Feelisch *et al.*, 1989; Feelisch, 1991). This could explain the strong spontaneous chemiluminescence induced by SIN-1 in an oxygen-containing buffer. The concomitant release of NO and $O_2^-$ by SIN-1 may also lead to an attenuation in its responses as NO is inactivated by $O_2^-$ (Gryglewski *et al.*, 1986). In addition, such a chemical interaction may result in the formation of peroxynitrite, which is toxic due to its decomposition into potent cytotoxic oxidants (Beckman *et al.*, 1990). Our luminometric data indicate that GEA 3162 and GEA 5024 differ from SIN-1 in that they do not release significant amounts of $O_2^-$ in concentrations up to 100 μM. This accords with the results of Robak *et al.* (personal communication) who measured the ability of these compounds to release NO by the oxyhaemoglobin method (Gryglewski *et al.*, 1989) and to generate $O_2^-$ by a method based on the reduction of nitro blue tetrazolium (Feelisch *et al.*, 1989). The differences in their ability to release $O_2^-$ offers a possible explanation for the differences between the potencies of SIN-1 and the new NO-donors GEA 3162 and GEA 5024 in inhibiting PMN functions.

Cyclic GMP production in PMNs was increased when the cells were exposed to NO-donors, GEA 3162 and GEA 5024 causing their effects at lower drug concentrations and more rapidly than SIN-1 and SNAP. Unlike platelets, where the antiaggregatory activity of NO is mediated by increased intracellular cyclic GMP (see Moncada *et al.*, 1991) the role of cyclic GMP in PMNs is obscure. Cyclic AMP has been reported to inhibit PMN functions, e.g. degranulation and $O_2^-$ production probably through cyclic AMP-dependent protein kinase-mediated prosphorylation of specific proteins (Kramer *et al.*, 1988; Kim *et al.*, 1989; Misaki *et al.*, 1989; Mueller & Sklar, 1989). Recent results show that in certain experimental conditions a cell-permeant analogue of cyclic GMP, $N^2$,2′-O-dibutyryl guanosine 3′:5′-cyclic monophosphate ($Bt_2$cyclic GMP) inhibits PMN functions, e.g. FMLP and platelet-activating factor-induced $O_2^-$ production (Ervens *et al.*, 1991) and FMLP-triggered degranulation (Schröder *et al.*, 1990; Wenzel-Seifert *et al.*, 1991). Neutrophils have a cyclic GMP-dependent protein kinase and the intracellular localization of this enzyme is transiently redistributed when the cells are stimulated by FMLP (Pryzwansky *et al.*, 1990). This suggests that the cyclic GMP-mediated effects could occur through phosphorylation of specific proteins. Moreover, depending on the cyclic nucleotide phosphodiesterase isozymes, cyclic GMP is known to inhibit or stimulate cyclic AMP-specific phosphodiesterases (see Beavo & Reifsnyder, 1990). This effect does not, however, explain the present results since no alterations in the levels of int-

racellular cyclic AMP were detected.

Results from studies using cyclic GMP analogues or cyclic GMP-enhancing compounds suggest that the effects of cyclic GMP on PMN activation are dependent on the type and concentration of the stimulant used (Ney *et al.*, 1990; Schröder *et al.*, 1990; Ervens *et al.*, 1991; Wenzel-Seifert *et al.*, 1991). For instance, $Bt_2$cyclic GMP was reported to inhibit PAF- and FMLP-stimulated $O_2^-$ formation but to potentiate C5a-induced $O_2^-$ formation whereas $Bt_2$cyclic GMP had no effect on $O_2^-$ release induced by Ca ionophore A23187, arachidonic acid, phorbol myristate acetate, sodium fluoride, hexachlorocyclohexane or $LTB_4$ (Ervens *et al.*, 1991). Moreover, $Bt_2$cyclic GMP and another widely used cyclic GMP analogue, 8-bromo-cyclic GMP, were inhibitory only in high concentrations (1 mM). This may reflect the complexity of the regulatory effects of cyclic GMP in PMNs. However, when interpreting the results, the relatively poor selectivity and potency of the cyclic GMP analogues should be kept in mind. For instance, $Bt_2$cyclic GMP has been reported to activate cyclic AMP-dependent protein kinase at lower concentrations than cyclic GMP-dependent protein kinase (Francis *et al.*, 1988). The cellular concentrations of 8-bromo-cyclic GMP remain rather low due to poor penetration into the cells and hydrolysis by phosphodiesterases (Butt *et al.*, 1992). In the present work we found that the new potent NO-donors, GEA 3162 and GEA 5024, inhibited PMN functions concomitantly with a rapid and prompt increase in cyclic GMP synthesis. GEA 3162 and GEA 5024 inhibited PMN activation independently of whether the cells were activated by FMLP, opsonized zymosan or Ca ionophore A23187. When compared to the cyclic GMP analogues or the NO-donor SIN-1 used previously, GEA 3162 and GEA 5024 induced very high transient levels of cellular cyclic GMP, which could explain their potent inhibitory effects on PMN activation.

The $IC_{50}$ values of the NO-donors tested varied from one PMN function to another. GEA 3162 and GEA 5024 inhibited opsonized zymosan-induced $O_2^-$ formation and FMLP-induced chemotaxis at lower drug concentrations than A23187-triggered degranulation and $LTB_4$ synthesis. The inhibitory effects of SIN-1 on PMN chemotaxis and degranulation were weaker than its effects on $LTB_4$ synthesis. SNAP (100–1000 μM) inhibited $LTB_4$ release and $O_2^-$ formation but did not affect chemotaxis or degranulation. These variations could be explained by differences in the experimental conditions, for instance differences in the incubation milieu depending on whether the cells were incubated in diluted blood or in buffer. Also the incubation time during which the cells were exposed to NO was longer in the chemotaxis assay than in the other PMN function tests. Another possibility is that the sensitivity of these cellular events to cyclic GMP-mediated processes is different. Thirdly, the possible cyclic GMP-independent direct effects of NO could mediate some of the detected inhibitory effects on PMNs. For instance, NO has been reported to modify catalytically active non-haem and haem-bound Fe ion in various enzymes and this serves as an OFF signal for the enzyme (Ignarro, 1990; Moncada *et al.*, 1991). The enzyme 5-lipoxygenase that forms $LTB_4$ contains a non-haem iron and iron chelating compounds are known to inhibit this enzyme (McMillan & Walker, 1992; Musser & Kreft, 1992).

Activated neutrophils release NO (Rimele *et al.*, 1988; McCall *et al.*, 1989; Salvemini *et al.*, 1989; Schmidt *et al.*, 1989; Wright *et al.*, 1989). The pathophysiological function of this NO is mostly unknown. The present results support the idea that the PMN-derived NO could act as a negative feedback signal for PMNs and thus restrict the inflammatory process. Furthermore, NO-releasing compounds form a new group of agents with potential anti-inflammatory capacity.

In conclusion, the new NO-releasing compounds GEA 3162 and GEA 5024 were shown to be potent inducers of cyclic GMP production in human PMNs *in vitro*. The compounds inhibited FMLP- and A23187-triggered activation of PMNs concomitantly with the increase in cyclic GMP. The results suggest that NO and/or cyclic GMP inhibit the activation of human PMNs.

The authors thank Dr Søren Bols Pedersen and Dr Tim Corell for reviewing the manuscript. Antisera for cyclic GMP assays were kindly provided by Prof. Rolf Andersson and Dr Krister Axelsson (deceased in September 1991), Institute of Pharmacology, University of Linköping, Linköping, Sweden. The skilful technical assistance of Ms Niina Railo and Mr Seppo Toivonen and the secretarial help of Ms Sinikka Lähdekorpi is gratefully acknowledged. The study was supported by a grant from the Academy of Finland (H.V.).

## References

AXELSSON, K.L., BORNEFELDT, K.E., NORLANDER, B. & WIKBERG, J.E.S. (1988). Attomole sensitive radioimmunossay for cyclic GMP. *Second Messengers Phosphoproteins*, **12**, 145–154.

BEAVO, J.A. & REIFSNYDER, D.H. (1990). Primary sequence of cyclic nucleotide phosphodiesterase isoenzymes and the design of selective inhibitors. *Trends Pharmacol. Sci.*, **11**, 150–155.

BECKMAN, J.S., BECKMAN, T.W., CHIEN, J., MARSHALL, P.A. & FREEMAN, B.A. (1990). Apparent hydroxyl radical production by peroxynitrite: implications for endothelial injury from nitric oxide and superoxide. *Proc. Natl. Acad. Sci. U.S.A.*, **87**, 1620–1624.

BORGEAT, P. & SAMUELSSON, B. (1979). Metabolism of arachidonic acid in polymorphonuclear leukocytes. Structural analysis of novel hydroxylated compounds. *J. Biol. Chem.*, **254**, 7865–7869.

BØYUM, A. (1976). Isolation of lymphocytes, granulocytes and macrophages. *Scand. J. Immunol.* (Suppl.), **5**, 9–15.

BURDE, R., SEIFERT, R., BUSCHAUER, A. & SCHULTZ, G. (1989). Histamine inhibits activation of human neutrophils and HL-60 leukemic cells via $H_2$ receptors. *Naunyn-Schmied. Arch. Pharmacol.*, **340**, 671–678.

BUTT, E., NOLTE, C., SCHULZ, S., BELTMAN, J. BEAVO, J.A., JASTORFF, B. & WALTER, U. (1992). Analysis of functional role of cGMP-dependent protein kinase in intact human platelets using a specific activator 8-parachlorophenylthio-cGMP. *Biochem. Pharmacol.*, **43**, 2591–2600.

THE COMMITTEE ON ENZYMES OF THE SCANDINAVIAN SOCIETY FOR CLINICAL CHEMISTRY AND CLINICAL PHYSIOLOGY (1976). Recommended methods for the determination of four enzymes in blood. *Scand. J. Clin. Lab. Invest.*, **33**, 291–306.

ERVENS, J., SCHULTZ, G. & SEIFERT, R. (1991). Differential inhibition and potentiation of chemoattractant-induced superoxide formation in human neutrophils by the cell-permeant analogue of cyclic GMP, $N^2$,2′-O-dibutyryl guanosine 3′:5′-cyclic monophosphate. *Naunyn-Schmied. Arch. Pharmacol.*, **343**, 370–376.

FEELISCH, M. (1991). The biochemical pathways of nitric oxide formation from nitrovasodilators: appropriate choice of exogenous NO donors and aspects of preparation and handling of aqueous NO solutions. *J. Cardiovasc. Pharmacol.*, **17** (Suppl. 3), S25–S33.

FEELISCH, M., OSTROWSKI, J. & NOACK, E. (1989). On the mechanism of NO release from sydnonimines. *J. Cardiovasc. Pharmacol.*, **14** (Suppl. 11), S13–S22.

FRANCES, S.H., BRADLEY, D.N., TODD, B.W., WELLS, J.N. & CORBIN, J.D. (1988). Relaxation of vascular and tracheal smooth muscle by cyclic nucleotide analogs that preferentially activate purified cGMP-dependent protein kinase. *Mol. Pharmacol.*, **34**, 506–517.

FURCHGOTT, R.F. (1983). Role of endothelium in responses of vascular smooth muscle. *Circ. Res.*, **53**, 557–573.

FURCHGOTT, R.F. & ZAWADZKI, J.V. (1980). The obligatory role of endothelial cells in the relaxation of arterial smooth muscle by acetylcholine. *Nature*, **288**, 373–376.

FURLONG, B., HENDERSON, A.H., LEWIS, M.J. & SMITH, J.A. (1987). Endothelium-derived relaxing factor inhibits *in vitro* platelet aggregation. *Br. J. Pharmacol.*, **90**, 687–692.

GALLIN, J.I., CLARK, R.A. & KIMBALL, H.R. (1973). Granulocyte chemotaxis: an improved in vitro assay employing $^{51}$Cr-labelled granulocytes. *J. Immunol.*, **110,** 233–240.

GOLDBERG, N.D., HADDOX, M.K., NICHOL, S.E., GLASS, D.B., SANFORD, C.H., KUEHL, F.A. & ESTENSEN, R. (1975). Biologic regulation through opposing influences of cyclicGMP and cyclic AMP: the yin-yang hypothesis. *Adv. Cycl. Nucl. Res.*, **5,** 307–330.

GRYGLEWSKI, R.J., KORBUT, R., KALECINSKA, A. & ZEMBOWICZ, A. (1989). Interaction between stimulators of adenylate and guanylate cyclases in human leukocytes, platelets and arteries. *Int. J. Tiss. Reac.*, **11,** 269–274.

GRYGLEWSKI, R.J., PALMER, R.M.J. & MONCADA, S. (1986). Superoxide anion is involved in the breakdown of endothelium-derived vascular relaxing factor. *Nature*, **320,** 454–456.

IGNARRO, L.J. (1990). Haem-dependent activation of guanylate cyclase and cyclicGMP formation by endogenous nitric oxide: a unique transduction mechanism for transcellular signaling. *Pharmacol. Toxicol.*, **67,** 1–7.

IGNARRO, L.J., BUGA, G.M., WOOD, K.S., BYRNS, R.E. & CHAUDHURI, G. (1987). Endothelium-derived relaxing factor produced and released from artery and vein is nitric oxide. *Proc. Natl. Acad. Sci. U.S.A.*, **84,** 9265–9269.

IGNARRO, L.J. & GEORGE, W.J. (1974). Hormonal control of lysosomal enzyme release from human neutrophils: elevation of cyclic nucleotide levels by autonomic neurohormones. *Proc. Natl. Acad. Sci. U.S.A.*, **71,** 2027–2031.

KANKAANRANTA, H., MOILANEN, E. & VAPAATALO, H. (1991). Tolfenamic acid inhibits leukotriene $B_4$-induced chemotaxis of polymorphonuclear leukocytes in vitro. *Inflammation*, **15,** 137–143.

KIM, U.-H., KIM, J.W. & RHEE, S.G. (1989). Phosphorylation of phospholipase C-γ by cAMP-dependent protein kinase. *J. Biol. Chem.*, **264,** 20167–20170.

KRAMER, I.M., VAN DER BEND, R.L., VERHOEVEN, A.J. & ROOS, D. (1988). The 47-kDa protein involved in the NADPH:$0_2$ oxidoreductase activity of human neutrophils is phosphorylated by cyclic AMP-dependent protein kinase without induction of a respiratory burst. *Biochim. Biophys. Acta*, **971,** 189–196.

KUBES, P., SUZUKI, M. & GRANDER, D.N. (1991). Nitric oxide: an endogenous modulator of leukocyte adhesion. *Proc. Natl. Acad. Sci. U.S.A.*, **88,** 4651–4655.

LILIUS, E.-M., MÄKI, A.-L., PROSKIN, J. & RAJAMÄKI, A. (1987). Leukocytes as immunosensors: whole blood chemiluminescence (CL) in human leukemias. In *Bioluminescence and Chemiluminescence. New Perspectives.* ed. Schölmerich, J., Andreesen, R., Kapp, A., Ernst, M. & Woods, W.G. pp. 53–56. Chichester: John Wiley & Sons.

MCCALL, T.B., BOUGHTON-SMITH, N.K., PALMER, R.M.J., WHITTLE, B.J.R. & MONCADA, S. (1989). Synthesis of nitric oxide from L-arginine by neutrophils. *Biochem. J.*, **261,** 293–296.

MCMILLAN, R.M. & WALKER, E.R.H. (1992). Designing therapeutically effective 5-lipoxygenase inhibitors. *Trends Pharmacol. Sci.*, **13,** 323–330.

MISAKI, N., IMAIZUMI, R. & WATANABE, Y. (1989). Cyclic AMP-dependent protein kinase interferes with GTP γ-S stimulated $IP_3$ formation in differentiated HL-60 cell membranes. *Life Sci.*, **45,** 1671–1678.

MOILANEN, E., ALANKO, J., SEPPÄLÄ, E. & VAPAATALO, H. (1988). Effects of antirheumatic drugs on leukotriene $B_4$ and prostanoid synthesis in human polymorphonuclear leukocytes in vitro. *Agents Actions*, **24,** 387–394.

MONCADA, S., PALMER, R.M.J. & HIGGS, E.A. (1991). Nitric oxide: physiology, pathophysiology, and pharmacology. *Pharmacol. Rev.*, **43,** 109–142.

MUELLER, H. & SKLAR, L.A. (1989). Coupling of antagonistic signalling pathways in modulation of neutrophil function. *J. Cell. Biochem.*, **40,** 287–294.

MUSSER, J.H. & KREFT, A.F. (1992). 5-Lipoxygenase: properties, pharmacology, and the quinolinyl(bridged)aryl class of inhibitors. *J. Med. Chem.*, **35,** 2501–2524.

MYERS, P.R., MINOR, R.L., GUERRA, R., BATES, J.N. & HARRISON, D.G. (1990). Vasorelaxant properties of the endothelium-derived relaxing factor more closely resemble s-nitrosocysteine than nitric oxide. *Nature*, **343,** 161–163.

NEY, P., SCHRÖDER, H. & SCHRÖR, K. (1990). Nitrovasodilator-induced inhibition of $LTB_4$ release from human PMN may be mediated by cyclic GMP. *Eicosanoids*, **3,** 243–245.

PALMER, R.M.J., ASHTON, D.S. & MONCADA, S. (1988). Vascular endothelial cells synthetize nitric oxide from L-arginine. *Nature*, **333,** 664–666.

PALMER, R.M.J., FERRIGE, A.G. & MONCADA, S. (1987). Nitric oxide release accounts for the biological activity of endothelium-derived relaxing factor. *Nature*, **327,** 524–526.

PRYZWANSKY, K.B., WYATT, T.A., NICHOLS, H. & LINCOLN, T.M. (1990). Compartmentalization of cyclic GMP-dependent protein kinase in formyl-peptide stimulated neutrophils. *Blood*, **76,** 612–618.

RADOMSKI, M.W., PALMER, R.M.J. & MONCADA, S. (1987). Comparative pharmacology of endothelium-derived relaxing factor, nitric oxide and prostacyclin in platelets, *Br. J. Pharmacol.*, **92,** 181–187.

RIMELE, T.J., STURM, R.J., ADAMS, L.M., HENRY, D.E., HEASLIP, R.J., WEICHMAN, B.M. & GRIMES, D. (1988). Interaction of neutrophils with vascular smooth muscle: identification of a neutrophil-derived relaxing factor. *J. Pharmacol. Exp. Ther.*, **245,** 102–111.

SALVEMINI, D., DE NUCCI, G., GRYGLEWSKI, R.J. & VANE, J.R. (1989). Human neutrophils and mononuclear cells inhibit platelet aggregation by releasing a nitric oxide-like factor. *Proc. Natl. Acad. Sci. U.S.A.*, **86,** 6328–6332.

SCHMIDT, H.H.W., SEIFERT, R. & BÖHME, E. (1989). Formation and release of nitric oxide from human neutrophils and HL-60 cells induced by a chemotactic peptide, platelet activating factor and leukotriene $B_4$. *FEBS Lett.*, **244,** 357–360.

SCHRÖDER, H., NEY, P., WODITSCH, I. & SCHRÖR, K. (1990). Cyclic GMP mediated SIN-1-induced inhibition of human polymorphonuclear leukocytes. *Eur. J. Pharmacol.*, **182,** 211–218.

STAHL, P.D. & FISHMAN, W.H. (1984). b-D-Glucuronidase. In *Methods of Enzymatic Analysis.* ed. Bergmeyer, J. & Grassl, M. vol. IV, pp. 246–256. Weinheim: Verlag Chemie.

WENZEL-SEIFERT, K., ERVENS, J. & SEIFERT, R. (1991). Differential inhibition and potentiation by cell-permeant analogues of cyclic AMP and cyclic GMP and NO-containing compounds of exocytosis in human neutrophils. *Naunyn-Schmied. Arch. Pharmacol.*, **344,** 396–402.

WRIGHT, C.D., MULSCH, A., BUSSE, R. & OSSWALD, H. (1989). Generation of nitric oxide by human neutrophils. *Biochem. Biophys. Res. Commun.*, **160,** 813–819.

ZURIER, R.B., WEISSMANN, G., HOFFSTEIN, S., KAMMERMAN, S. & TAI, H.H. (1974). Mechanisms of lysosomal enzyme release from human leukocytes. *J. Clin. Invest.*, **53,** 297–309.

*(Received July 24, 1992*
*Revised February 24, 1993*
*Accepted March 3, 1993)*

*Br. J. Pharmacol.* (1993), **109**, 859–865 © Macmillan Press Ltd, 1993

# 3,4 Dichlorobenzamil-sensitive, monovalent cation channel induced by palytoxin in cultured aortic myocytes

[1]Catherine Van Renterghem & Christian Frelin

Institut de Pharmacologie Moléculaire et Cellulaire, UPR 411 CNRS, 660 Route des Lucioles, Sophia Antipolis, F-06560 Valbonne, France

**1** Smooth muscle cells were dispersed from rat aorta and then cultured. The action of palytoxin on rat aortic myocytes was analysed by measurement of $^{22}Na^+$ uptake and single channel recording techniques.

**2** Palytoxin induced an increase in $^{22}Na^+$ uptake, with a concentration of 50 nM producing half-maximal activation. The action of palytoxin was inhibited by amiloride derivatives and by ouabain. The concentrations of inhibitor producing half-maximal inhibition were 10 μM for 3,4 dichlorobenzamil, 30 μM for benzamil, 100 μM for phenamil and 1 mM for ouabain.

**3** In outside-out patches, palytoxin induced single channel currents that reversed near 0 mV with NaCl or KCl in the extracellular solution, but were outward with N-methyl-D-glucamine chloride or $CaCl_2$ (110 mM), indicating that palytoxin induced a cation channel permeable to $Na^+$ and $K^+$ ($P_K/P_{Na} = 1.2$) but not to $Ca^{2+}$ ($P_K/P_{Ca} > 30$) or to N-methyl-D-glucamine (NMDG) ($P_K/P_{NMDG} > 11$). The unit channel conductance was 11–14 pS.

**4** A high (>0.1 mM) extracellular concentration of $Ca^{2+}$ was necessary to observe channel activation by palytoxin. A high (150 mM) extracellular concentration of $K^+$ partially prevented and reversed channel activation by palytoxin.

**5** The channel activity was fully blocked by 3,4 dichlorobenzamil (20 μM) and partially blocked by phenamil (50 μM). It was not reduced by ouabain (200 μM).

**Keywords:** Palytoxin; vascular smooth muscle cell; non-selective cation channel; $Na^+$ infux; 3,4 dichlorobenzamil

## Introduction

Palytoxin (PTX) consists of a long aliphatic, partially unsaturated chain with interspersed cyclic ether, hydroxyl and carboxyl groups (Moore *et al.*, 1982). It is one of the most potent toxins known and acts by impairing the function of excitable cells such as neuronal cells (Dubois & Cohen, 1977; Pichon, 1982) and cardiac cells (Sauviat *et al.*, 1987). PTX induces profound vasoconstriction and increases systemic blood pressure (Ito *et al.*, 1977). In different vascular preparations, PTX induces long lasting contractions that are partially sensitive to L-type $Ca^{2+}$ channel antagonists, to indomethacin and to prazosin, an antagonist of $\alpha_1$-adrenoceptors (Karaki *et al.*, 1985). Smaller contractions are observed in the presence of an intact vascular endothelium and these can be increased by methylene blue (Nagase *et al.*, 1987). Taken together these results suggest that the vascular action of PTX involves (i) a direct action on vascular smooth muscle cells, (ii) the release of noradrenaline by nerve terminals (Karaki *et al.*, 1985; Nagase & Karaki, 1987), and (iii) the release of vasoconstrictor prostaglandins (Nagase & Karaki, 1987). These vasoconstrictor responses are partly counteracted by nitric oxide released by vascular endothelial cells (Nagase *et al.*, 1987).

Although it is clear that $Na^+$ plays a central role in the action of PTX (Habermann, 1989; Sauviat, 1992) the exact mechanism by which PTX acts remains to be established. Habermann proposed that PTX binds to the ($Na^+$,$K^+$) ATPase and converts the enzyme into an open channel that allows $Na^+$ influx and $K^+$ efflux (Habermann, 1989). In excitable cells, the depolarization consecutive to the increased membrane permeability to $Na^+$ may trigger $Ca^{2+}$ uptake by L-type voltage-dependent $Ca^{2+}$ channels (Habermann, 1989). In cardiomyocytes (Ikeda *et al.*, 1988; Muramatsu *et al.*, 1988), in frog erythrocytes (Kim *et al.*, 1991) and in neuroblastoma cells (Rouzaire-Dubois & Dubois, 1990), PTX opens a non-selective cation channel that is permeable to $Na^+$ and $K^+$. Recent attention has been given to the action of various amiloride derivatives on PTX actions. In chick cardiomyocytes, PTX increases the permeability to $H^+$, thereby leading to an intracellular acidification, and to a secondary activation of the $Na^+/H^+$ antiporter (Frelin *et al.*, 1990b). As a consequence, part of the PTX-activated $^{22}Na^+$ flux component could be inhibited by ethylisopropylamiloride (Frelin *et al.*, 1990b). The remaining PTX-activated $^{22}Na^+$ flux is blocked by 3,4 dichlorobenzamil, another derivative of amiloride that is well known to block the $Na^+/Ca^{2+}$ exchange activity (Frelin *et al.*, 1990a). Finally, amiloride has been reported to block PTX-induced inward currents in frog skeletal muscles (Ecault & Sauviat, 1991). In this study, we characterize PTX-induced channels in aortic myocytes with a combination of $^{22}Na^+$ uptake measurements and single channel current recordings, and define the properties of interaction of this channel with amiloride derivatives and with ouabain.

## Methods

### *Cell culture*

Wistar AF/Han rats (6–9 week old) were stunned and killed by cervical dislocation. The thoracic aorta was removed, cleared of fat and connective tissues and digested with collagenase and elastase as previously described (Van Renterghem & Lazdunski, 1991). Cells were grown in a M199 culture medium (GIBCO) supplemented with foetal bovine serum (GIBCO; 20%), glutamine (2 mM), penicillin (100 units $ml^{-1}$), and streptomycin (100 μg $ml^{-1}$) in collagen coated dishes (electrophysiological experiments) or regular culture dishes ($^{22}Na^+$ uptake experiments). For $^{22}Na^+$ uptake experiments, stock cultures were trypsinized and passaged

[1] Author for correspondence.

once a week and cells used at passages 2–10. No change in the responses to PTX was observed as cells were passaged *in vitro*. Sparse primary cultures (3–8 day old) or first passage cultures were used for electrophysiological experiments. Only dark cells with the spindle-shape morphology of contractile myocytes were chosen for patch recording.

### *Flux experiments*

Cells, seeded into 24 well tissue culture clusters, were first equilibrated for 15 min at 37°C in a $K^+$-free modified Earle's salt solution containing (in mM): NaCl 145, $CaCl_2$ 1.8, $MgCl_2$ 0.8, N-2-hydroxyethylpiperazine-*N'*-2 enthanesulphonic acid (HEPES)/tris-hydroxymethylaminomethane (Tris) 25. Cells were then switched to a $K^+$-free modified Earle's salt solution supplemented with 4 $\mu$Ci ml$^{-1}$ $^{22}Na^+$ (Amersham; 0.5 Ci mg$^{-1}$) and PTX. A $K^+$-free solution was used to prevent $^{22}Na^+$ efflux by the ($Na^+$, $K^+$)ATPase. After 3 min of incubation at 37°C, the incubation solution was aspirated off and cells washed 4 times with $MgCl_2$ (0.1 M). Cells were then scraped off into NaOH (0.1 M) and the cell-associated radioactivity was counted. When the action of inhibitors was tested, inhibitors were added at the same time as PTX. The sensitivity of the ($Na^+$,$K^+$)ATPase of aortic myocytes to ouabain was determined in $^{86}Rb^+$ uptake experiments. Cells in 24 well tissue culture clusters were loaded with $Na^+$ by equilibrating cells for 15 min in a $K^+$-free Earle's salt solution supplemented with 10 $\mu$M monensin (Calbiochem). Cells were then placed for 3 min in an Earle's salt solution containing 5 mM KCl and supplemented with the desired concentrations of ouabain and 2 $\mu$Ci ml$^{-1}$ $^{86}Rb^+$ (Amersham; 8 mCi mg$^{-1}$). Cells were washed with $MgCl_2$ (0.1 M) and the cell-associated radioactivity was counted.

Protein contents were determined according to Bradford (1976).

### *Electrophysiological recordings and analysis*

Single channel currents were measured (EPC 7, List Electronic, Darmstadt-Eberstadt, Germany) from excised patches in the outside-out configuration, using 12–17 MΩ patch electrodes. Data were recorded on a video tape recorder after digitization (44 kHz; PCM, Biologic, Grenoble, France), transferred to a microcomputer (Plessey systems, model 6220, Irvine, Calif., U.S.A.) after low pass filtering (see figure legends for bandwidth), and plotted with a digitial plotter (Hewlett-Packard, Sunnyvale, Calif., U.S.A.). Single channel current amplitudes were measured from the gaussian fit of current density histograms. Linear fits were calculated by the least square regression method. The open state probability ($P$(O)) was measured from the gaussian fit of current density histograms. Inward currents (from extracellular face to intracellular face) are given negative values and represented downwards. All external solutions contained glucose (5 mM). The 'normal extracellular solution' at pH 7.4 contained (in mM): NaCl 150, KCl 5, $CaCl_2$ 2, $MgCl_2$ 1, HEPES/NaOH 10. Reduced external $Ca^{2+}$ concentration (0.1 mM; Figure 7) was obtained with a mixture of $MgCl_2$ (4.0 mM), $CaCl_2$ (1.30 mM), and ethylene glycol *bis* (β-aminoethyl ether), *N,N,N',N'* tetraacetic acid (EGTA) (1.20 mM). Free calcium concentration was computed as described previously (Fabiato & Fabiato, 1979). Other external solutions at pH 7.4 contained (in mM): $CaCl_2$ 2, $MgCl_2$ 1 plus KCl 150 and HEPES/KOH 10 ('150 mM $K^+$ solution'), or 150 N-methyl D-glucamine (NMDG) chloride and 10 HEPES/Tris ('150 mM NMDG solution'), or 108 $CaCl_2$ and 10 HEPES/$Ca(OH)_2$ ('110 mM $Ca^{2+}$ solution'). The 'pipette solution' at pH 7.2 contained (in mM): KCl 150, $MgCl_2$ 4, HEPES/KOH 10, EGTA 2, and $CaCl_2$ 1.79 or 0.16 (free $Ca^{2+}$ ions concentration: 1 $\mu$M or 10 nM). Changing the internal $Ca^{2+}$ concentration from 10 nM to 1 $\mu$M did not alter the properties of PTX-induced channels. PTX was applied near the patch through a microperfusion system.

Means ± s.e.mean are indicated.

### *Toxin and drugs*

3,4 Dichlorobenzamil (3,4 DCB) was synthesized as previously described (Vigne *et al.*, 1988). Ethylisopropylamiloride (EIPA), benzamil and phenamil were obtained from Dr E.J. Cragoe Jr. Palytoxin, from *Palythoa caribaeorum*, was kindly provided by Dr E. Habermann. It was dissolved in distilled water and kept frozen as 0.1 mM stock solutions. Final dilutions were made immediately before use.

## Results

### *Palytoxin induces $Na^+$ uptake by aortic myocytes*

PTX activated a $^{22}Na^+$ flux component in cultured aortic myocytes. The PTX concentration producing half-maximal activation was 50 nM (Figure 1a). Similar results were obtained with smooth muscle cells of the A7r5 cell line (not shown). The PTX-activated $^{22}Na^+$ influx component was prevented by 3,4 DCB, benzamil and by phenamil. The concentrations that produced half-maximal inhibition ($IC_{50}$) were 10 $\mu$M, 30 $\mu$M and 100 $\mu$M for 3,4 DCB, benzamil and phenamil respectively (Figure 1b). The action of PTX was reduced by less than 10% by amiloride (300 $\mu$M) or EIPA (300 $\mu$M). The PTX-activated $^{22}Na^+$ influx component was also inhibited by ouabain with an $IC_{50}$ value at 1 mM (Figure 2). The dose-response curve for ouabain inhibition of the $^{86}Rb^+$ uptake by the ($Na^+$,$K^+$)ATPase shows an $IC_{50}$ value of 30 $\mu$M (Figure 2). These results indicate a 30 fold

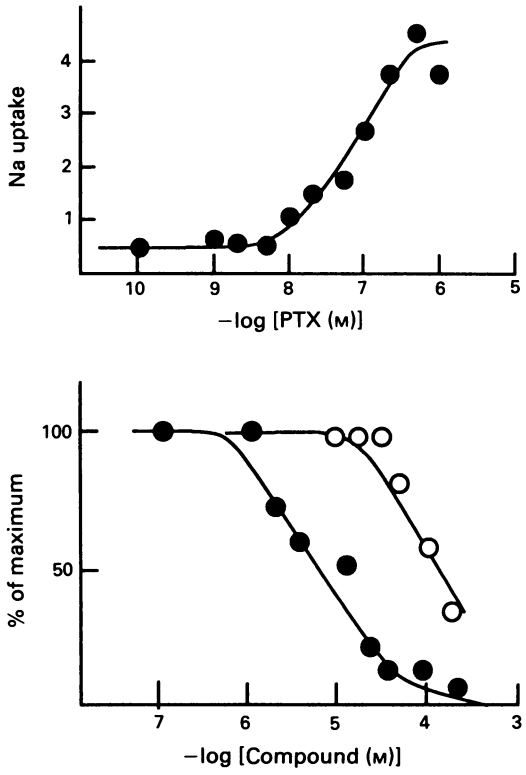



**Figure 1** Palytoxin (PTX) activates $^{22}Na^+$ uptake by aortic myocytes. (a) Dose-response curve for PTX action on $^{22}Na^+$ uptake by aortic myocytes. $^{22}Na^+$ uptake is expressed in d.p.m. × $10^{-5}$ 3 min$^{-1}$ mg$^{-1}$ of protein. (b) Dose-response curves for 3,4 dichlorobenzamil (●) and phenamil (○) inhibition of the PTX (100 nM) activated $^{22}Na^+$ influx component in aortic myocytes.

difference in the actions of ouabain on the PTX-activated $^{22}Na^+$ influx and on the $(Na^+,K^+)$ATPase activity. The difference is probably larger than this value, since the action of ouabain is well known to be competitively antagonized by external $K^+$. The sensitivity of the $(Na^+,K^+)$ATPase to ouabain was measured in the presence of external $K^+$ (5 mM). PTX-activated $^{22}Na^+$ influx was measured in $K^+$-free solutions.

### *Palytoxin induces non selective cation channels in aortic myocytes*

During patch recording from rat aortic smooth muscle cells, application of PTX to the extracellular membrane face commonly induced single channel inward currents (Figure 3). Inward currents following PTX (100 nM) application were observed in 34 out of 37 outside-out patches bathed in the 'normal extracellular solution'. Similar channels were observed following application of PTX to patches excised from aortic cells of the A7r5 cell-line (2 out of 3 patches, not shown). The number of channels activated was dependent on the concentration applied (4 patches), with a threshold concentration near 1 nM (Figure 3). This value is very near the threshold concentration for PTX-induced increase in $^{22}Na^+$ uptake by aortic myocytes (Figure 1a), suggesting that the channels observed in patch clamp experiments are probably responsible for the PTX-activated $^{22}Na^+$ flux component. PTX action was rapidly reversible upon washing (Figure 3c).

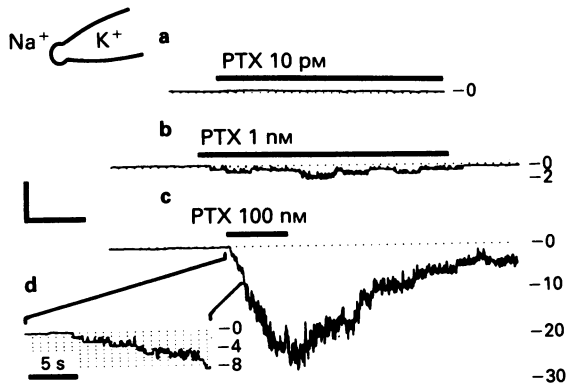



**Figure 3** Concentration-related induction by palytoxin (PTX) of single channel inward currents in outside-out patches. PTX 10 pM (a), 1 nM (b), or 100 nM (c,d) was applied for the time indicated by the bars (a–c). Holding potential, − 30 mV. In (c), the maximal number of channels open in the patch was estimated from the single channel current amplitude to be 29. Opening of the first channels in (c) is shown on an expanded time scale (d). These recordings were obtained from a batch of cells presenting a particularly large response to PTX. Current scale bar: 2 pA, time scale bar: 1 min (a–c), or 5 s (d). Sampling: 10 Hz (a–c) or 500 Hz (d); filtering: 4 Hz (a–c) or 200 Hz (d). 'Normal external solution', and 'pipette solution' with 10 nM free $Ca^{2+}$.

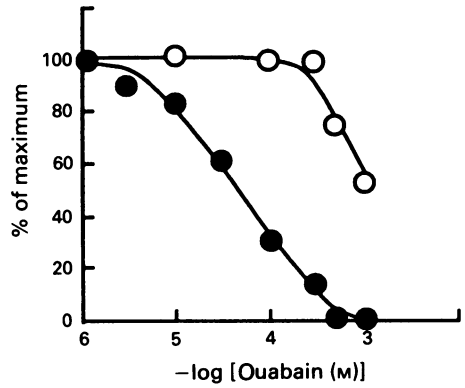



**Figure 2** Dose-response curve for ouabain inhibition of the palytoxin (100 nM)-activated $^{22}Na^+$ influx component (○), and of $^{86}Rb^+$ uptake by the $(Na^+/K^+)$ATPase (●).

The current/voltage relation for PTX-activated channels was linear (Figure 4). The single channel conductance was 10.8 ± 0.8 pS ($n = 9$), and the reversal potential was − 2.7 ± 2.1 mV ($n = 9$). It was possible to observe PTX-induced single channel currents in patches exposed to symmetrical '150 mM $K^+$ solutions' (Figure 5a–b; see also Figure 8). The single channel conductance, measured from the current/voltage relations presented in Figure 5b was 14.3 ± 0.6 pS ($n = 4$). The reversal potential was − 0.2 ± 0.8 mV ($n = 4$). Finally, when NMDG was substituted for inorganic monovalent cations in the extracellular solution, only outward currents were observed (Figure 5c–e). The current/voltage relation (Figure 5e) indicated a single channel conductance of 2.0 ± 0.1 pS ($n = 5$) and a reversal potential more negative than an extrapolated value of − 60 mV.

### *Permeability ratios of the palytoxin-induced channel*

Assuming that the contribution of divalent cations and chloride ions to the currents was negligible in the conditions of Figures 4 and 5, and using the Goldman, Hodgkin, Katz equation and the limit for the reversal potential ($E_{rev}$) value,

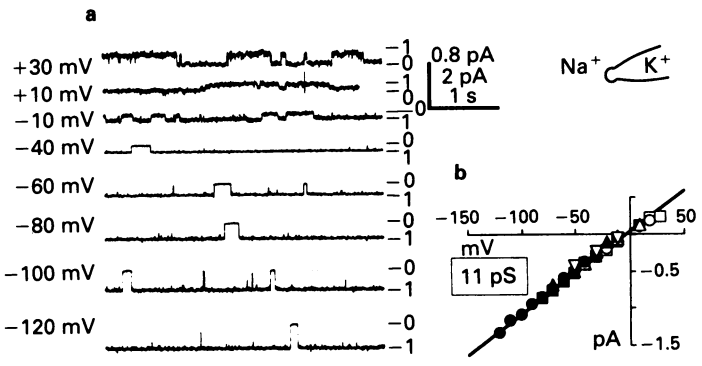



**Figure 4** Current-voltage relation in the 'normal extracellular solution'. (a) Single channel currents recorded in the presence of palytoxin (PTX, 100 nM). Holding potentials: + 30, + 10, − 10, − 40, − 60, − 80, − 100, and − 120 mV. Current scale bar: 0.8 pA (3 upper traces) or 2 pA, time scale bar: 1 s. Sampling: 1 kHz, filtering: 400 Hz. (b) Corresponding current-to-voltage relations obtained from individual outside-out patches. The single channel conductance value measured by linear fit of data between − 120 and − 10 mV (straight line) is 11.1 pS, and the reversal potential − 3 mV.

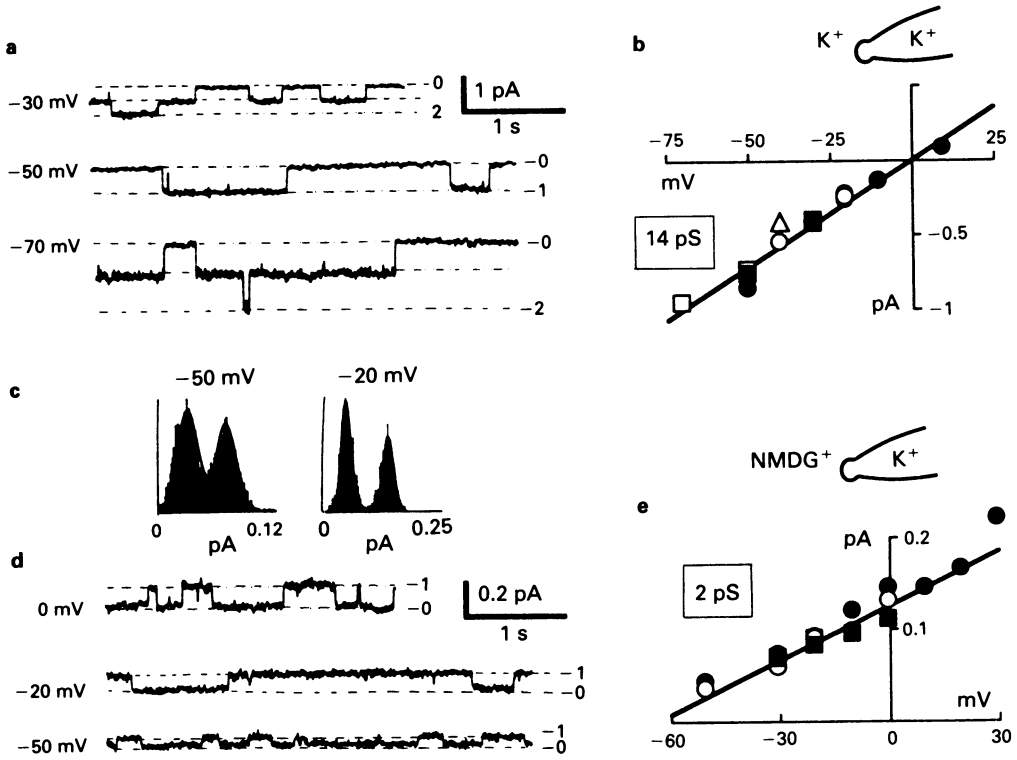



**Figure 5** Ionic selectivity of palytoxin (PTX)-induced channels. (a) Single channel currents recorded in the presence of PTX (100 nM) in the '150 mM $K^+$ solution'. Holding potentials: − 30, − 50, and − 70 mV. (b) Corresponding current-voltage relations obtained from individual outside-out patches. The single channel conductance value measured by linear fit of data (straight line) is 14.2 pS, and the reversal potential 0 mV. (c,d) Single channel currents recorded in the presence of PTX (100 nM) in the '150 mM NMDG solution' (d), and current density histograms for currents recorded at − 50 (left) and − 20 mV (c). Holding potentials: 0, − 20, and − 50 mV. (d) Corresponding current-voltage relations obtained from individual outside-out patches. The single channel conductance value measured by linear fit of data between − 30 and + 20 mV (straight line) is 2.0 pS. Current scale bar: 1 pA (a) or 0.2 pA (d), time scale bar: 1 s. Sampling: 1 kHz, filtering: 400 Hz.

permeability ratios were estimated to $P_K/P_{Na} = 1.2$ and $P_K/P_{NMDG} > 11$. Assuming that the contribution of divalent cations to the currents was negligible, the limit for the reversal potential value ($E_{rev} < -60$ mV) obtained with the '150 NMDG solution' (Figure 5e) leads us to conclude the $P_K/P_{Cl} > 16$.

### *Palytoxin-induced channels are not permeable to $Ca^{2+}$*

The permeability of PTX-induced channels to divalent cations was next examined. When 110 mM $Ca^{2+}$ was substituted for monovalent cations in the extracellular solution, only outward currents were recorded through PTX-induced channels (Figure 6) even for holding potentials as negative as − 60 mV. PTX (100 nM)-induced outward currents were detected in 4 out of 6 patches. The single channel conductance of outward currents with $Ca^{2+}$ as the main extracellular cation was 1.6 ± 0.1 pS ($n = 4$), a value close to the value observed with NMDG (2.0 ± 0.1 pS; Figure 5e). Assuming that the contribution of chloride ions to the currents was negligible and using the limit value for $E_{rev}$ ($E_{rev} < -70$ mV) obtained by linear extrapolation of the data obtained in the '110 $Ca^{2+}$ solution' (Figure 6d), $P_K/P_{Ca}$ was estimated to > 30 (from an extension of the Goldman, Hodgkin, Katz equation; Lakshminarayanaiah, 1984).

### *Extracellular $Ca^{2+}$ is necessary for channel induction by palytoxin*

It is known that PTX requires the presence of external $Ca^{2+}$ for its activity (Habermann, 1989; Ecault & Sauviat, 1991; Rouzaire-Dubois & Dubois, 1990). Figure 7 shows that when the $Ca^{2+}$ concentration in the extracellular solution ($[Ca^{2+}]_o$) was reduced to 0.1 mM, application of PTX did not result in channel activity. Increasing $[Ca^{2+}]_o$ to 1 mM in the continued presence of PTX rapidly induced channel activity, and this effect could be reversed by returning $[Ca^{2+}]_o$ to 0.1 mM (Figure 7). Absence of channel induction by PTX (100 nM) with a low $[Ca^{2+}]_o$ (< 100 μM) was observed in 19 patches. Reversible induction when switching from 100 μM to 1 mM was observed in 3 patches.

### *Extracellular $K^+$ prevents and reverses channel induction by palytoxin*

Figure 8a shows that when $K^+$ was substituted for $Na^+$ in the extracellular solution, cation channel induction by PTX occurred with only a very low efficiency. Such a very low efficiency of channel induction by PTX (100 nM) in the '150 mM $K^+$ solution' was observed in 11 out of 11 patches. Following channel induction in the normal extracellular solution, a sudden replacement of $Na^+$ by $K^+$ resulted in the closure of most channels within a few seconds (Figure 8b,c). This attenuation of the channel activity was observed in 6 out of 6 patches. Return to normal extracellular $Na^+$ was followed by a progressive reactivation of the channels within a few minutes (Figure 8b). The single channel amplitude was slightly increased following replacement of $Na^+$ by $K^+$ (see Figures 4b and 5d). Sudden replacement of $Na^+$ by $Li^+$ resulted in the closure of about two thirds of the channels within 3 min, and switching to $Li^+$ after channel closure by $K^+$ did not induce reactivation of the channels within 4–5 min (2 patches; not illustrated).

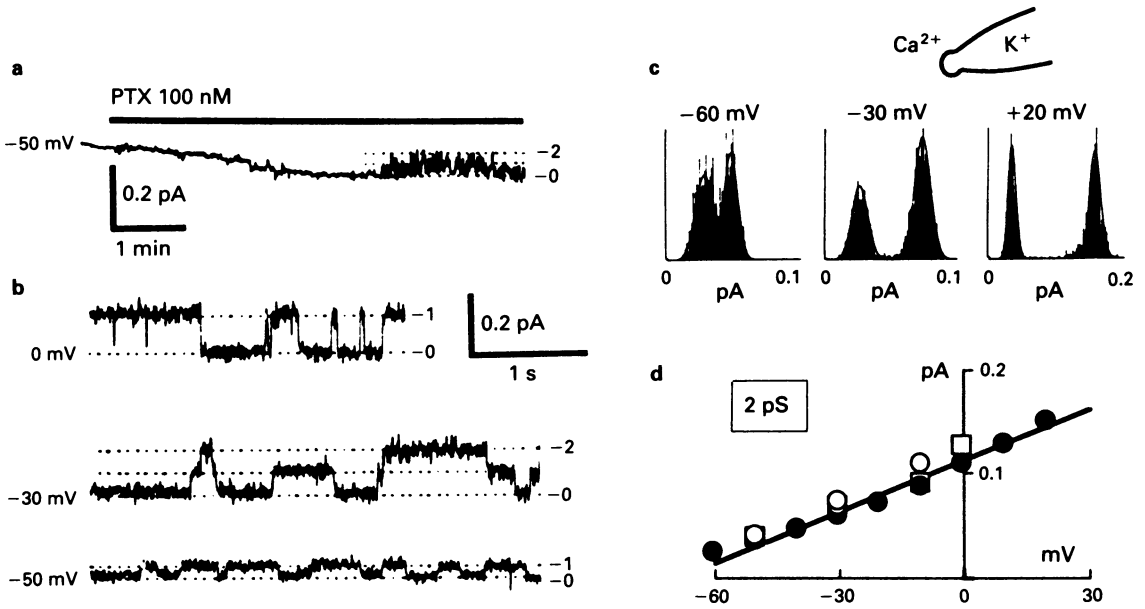



**Figure 6** Non-permeability of palytoxin (PTX)-induced channels to $Ca^{2+}$ ions. (a,b) Single channel currents recorded in the presence of PTX (100 nM) in the '110 mM $Ca^{2+}$ solution'. Holding potentials: − 50 (a), 0, − 30, and − 50 mV (b). Current scale bar: 0.2 pA, time scale bar: 1 min (a), 1 s (b). Sampling: 10 Hz (a), 1 kHz (b); filtering: 4 Hz (a), 400 Hz (b). (c) Current density histograms for currents recorded at − 60 (left), − 30 (middle), and + 20 mV. (d) Corresponding current-to-voltage relations obtained from individual outside-out patches. The single channel conductance value measured by linear fit of data between − 30 and + 20 mV (straight line) is 1.6 pS.

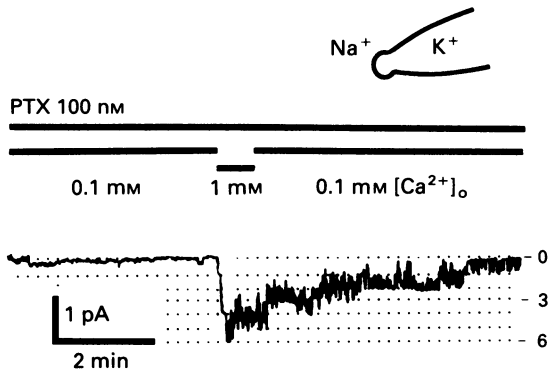



**Figure 7** Influence of extracellular $Ca^{2+}$ on the channel activity. Currents recorded in the presence of palytoxin (PTX, 100 nM). 'Normal external solution', except that the concentration of $Ca^{2+}$ was lowered to 0.1 mM during most of the experiment, as indicated. Holding potential: − 30 mV. Current scale bar: 1 pA, time scale bar: 2 min. Sampling 7 Hz, filtering: 3 Hz.

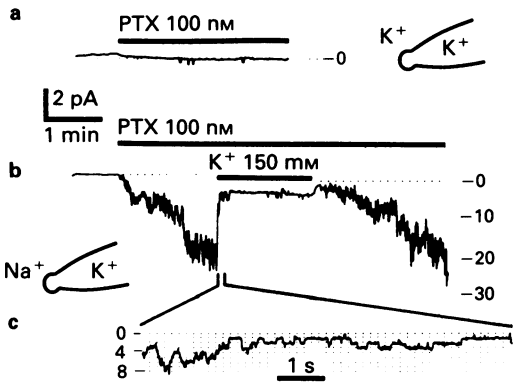



**Figure 8** Influence of extracellular $K^+$ on the channel activity. (a) Palytoxin (PTX, 100 nM) was applied for the time indicated in the '150 mM $K^+$ solution'. (b) PTX (100 nM) was applied for the time indicated. The 'normal extracellular solution' was replaced by the '150 mM $K^+$ solution' for the time indicated. Closure of the last channels following substitution of $K^+$ for $Na^+$ in experiment (b) is shown on an expanded time scale (c). Holding potential: − 30 mV. Current scale bar: 2 pA, time scale bar: 1 min (a,b), or 1 s (c). Sampling: 10 Hz (a,b) or 50 Hz (c); filtering: 4 Hz (a,b) or 20 Hz (c).

### *Amiloride derivatives, but not ouabain, inhibit palytoxin-activated channels*

Exposing outside-out patches to 3,4 DCB (20–50 μM) produced a period of flickering, followed by a quasi full block of PTX-activated channels (Figure 9a). The channel $P(O)$ was reduced by 95 ± 5% ($n = 6$). This observation is consistent with the fact that 3,4 DCB (20 μM) blocked more than 80% of the PTX-activated $^{22}Na^+$ uptake component (see Figure 1b). Phenamil (50 μM) also produced a flickering of the PTX-activated channel current (Figure 9b), but this was not followed by a closure of the channel. The channel $P(O)$ was reduced by 35 ± 6% ($n = 3$) in the presence of phenamil (50 μM). At this concentration, phenamil inhibited 16% of the PTX-activated $^{22}Na^+$ flux component (Figure 1b). Finally, ouabain (200 μM) had no effect on the PTX-activated currents within 5 min (Figure 9c), and the channel $P(O)$ was unchanged (+ 2 ± 2%, $n = 3$). At this concentration, ouabain had no action on the PTX-activated $^{22}Na^+$ flux component (Figure 2).

## Discussion

This paper describes 3,4 DCB-sensitive, voltage-independent, $Na^+$ and $K^+$ permeable channels induced by PTX in aortic myocytes. The following observations indicate that PTX-induced channels were permeable to monovalent cations, with little ion selectivity. (i) Using the 'pipette solution' (KCl

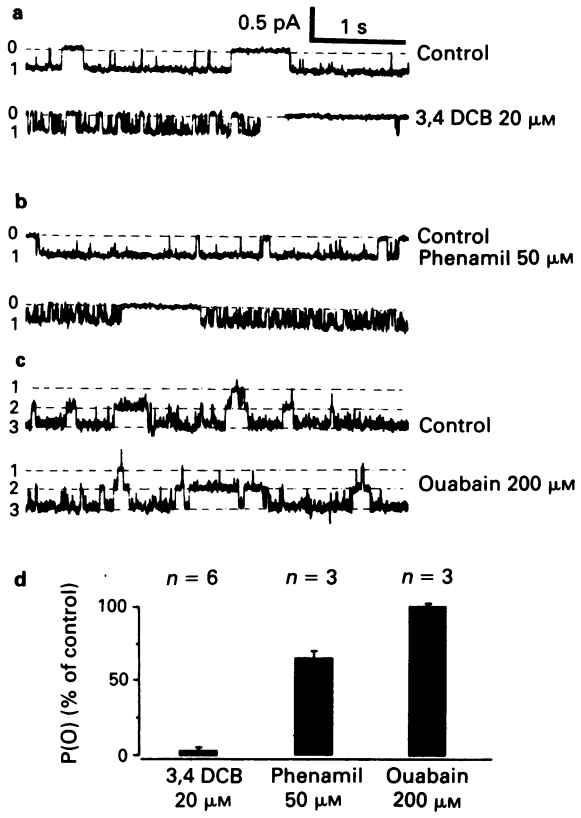



**Figure 9** Sensitivity to amiloride derivatives and not to ouabain of palytoxin (PTX)-induced channels. Single channel currents recorded in the presence of PTX (100 nM) in the 'normal extracellular solution'. Upper traces: control conditions. Lower traces: currents recorded starting 1 min (left) or 2 min after addition of 3,4 dichlorobenzamil (3,4 DCB, 20 μM) (a), or 3 min after addition of phenamil (50 μM) (b), or ouabain (200 μM) (c). Holding potential: − 30 mV. Current scale bar: 0.5 pA, time scale bar: 1 s. Sampling: 1 kHz, filtering: 400 Hz. (d) Mean open state probabilities in the presence of 3,4 DCB, phenamil or ouabain expressed relative to their values before drug addition. Means ± s.e.mean are indicated.

150 mM), the corresponding currents reversed at − 3 mV when recorded in the 'normal extracellular solution' (NaCl 150 mM, KCl 5 mM) (Figure 3b), and at 0 mV when recorded in the '150 mM $K^+$ solution' (Figure 4b). (ii) When NMDG or $Ca^{2+}$ were substituted for inorganic monovalent cations in the extracellular solution, only outward currents were recorded (Figure 4c–e and 5a–d). Taken together these results indicate that in rat aortic myocytes, PTX activates a cation channel that is permeable to $Na^+$ and $K^+$, but not to $NMDG^+$ or to $Ca^{2+}$. These properties are similar to those of the 9 pS channel previously shown to be induced by PTX in ventricular cardiomyocytes (Muramatsu *et al.*, 1988; Ikeda *et al.*, 1988) and in frog erythrocytes (Kim *et al.*, 1991). The channels induced by PTX in both ventricular myocytes (Muramatsu *et al.*, 1988; Ikeda *et al.*, 1988) and aortic myocytes (Figure 5a–d) have no measurable permeability to $Ca^{2+}$. In mouse neuroblastoma cells, PTX also induces a non-selective cation channel, but its unit conductance is larger (26 pS) (Rouzaire-Dubois & Dubois, 1990). The permeability of PTX-induced channels in aortic myocytes to other monovalent cations was not investigated. In other cell types, PTX induces channels that are also permeable to $NH_4^+$, $Li^+$, $Cs^+$ and guanidinium (Sauviat, 1992).

This paper also analyses the interaction of amiloride derivatives with PTX-induced channels. The PTX-activated $^{22}Na^+$ influx component was prevented by amiloride derivatives with the following rank order of potency: 3,4 DCB ($IC_{50}$ = 10 μM) > benzamil ($IC_{50}$ = 30 μM) > phenamil ($IC_{50}$ = 100 μM) >> amiloride, EIPA. Very similar results were obtained in electrophysiological experiments. 3,4 DCB, at a dose that inhibited 80% of the PTX-activated $^{22}Na^+$ flux component (Figure 1b) induced a flickering of the PTX-induced channels followed by their nearly complete blockade (Figure 9). Phenamil at a dose that inhibited 16% of the PTX-activated $^{22}Na^+$ flux component (Figure 1b) produced a flickering of the channel activity and a 35% reduction in the open state probability (Figure 9). 3,4 DCB was shown previously to prevent PTX-activated $^{22}Na^+$ uptake by chick cardiomyocytes with an $IC_{50}$ value (8 μM) similar to the one found in this study (10 μM) (Frelin *et al.*, 1990a). The pharmacological profile of action of amiloride derivatives on the PTX-induced channel differs from that on the epithelium $Na^+$ channel for which phenamil is the more potent inhibitor (Barbry *et al.*, 1986). It is also distinct from that of the $Na^+/H^+$ antiporter for which EIPA is the most potent inhibitor (Vigne *et al.*, 1983).

3,4 DCB is the most potent inhibitor of PTX-induced channels found in this study. 3,4 DCB has been reported to inhibit a variety of membrane ion transport processes such as the $Na^+/Ca^{2+}$ exchanger (Siegl *et al.*, 1984; Kaczorowski *et al.*, 1985; Floreani *et al.*, 1987; Vigne *et al.*, 1988), L-type $Ca^{2+}$ channels (Garcia *et al.*, 1990), and the $(Na^+,K^+)$ ATPase (Floreani *et al.*, 1987). The $IC_{50}$ values for 3,4 DCB inhibition of the PTX-activated $Na^+$ influx in aortic myocytes and in chick cardiomyocytes (8–10 μM) are similar to the $IC_{50}$ values reported for 3,4 DCB inhibition of the $Na^+/Ca^{2+}$ exchanger in neuronal cells (Kaczorowski *et al.*, 1985), in cardiac cells (Siegl *et al.*, 1984; Floreani *et al.*, 1987), and in aortic myocytes (Vigne *et al.*, 1988). Since PTX is known to induce a rise in the intracellular $Ca^{2+}$ concentration ($[Ca^{2+}]_i$) in cardiomyocytes (Frelin *et al.*, 1990a), we previously proposed that the 3,4 DCB sensitive $^{22}Na^+$ uptake activated by PTX could result from an increased activity of the $Na^+/Ca^{2+}$ exchange system consecutive to a primary rise in $[Ca^{2+}]_i$. The observation that 3,4 DCB inhibits PTX-induced channels in excised patches indicates however that the action of 3,4 DCB was unlikely to be a secondary action mediated by the $Na^+/Ca^{2+}$ exchanger. The ion-specificity of the PTX-induced channel differs also from that of the $Na^+/Ca^{2+}$ exchanger. First, $Ca^{2+}$, one of the substrates of the $Na^+/Ca^{2+}$ exchanger hardly permeates through PTX-induced channels (Figure 6a–d). Second, $K^+$, which is not transported by the $Na^+/Ca^{2+}$ exchanger, permeates through PTX-activated channels (Figure 5a,b). Although we cannot exclude the possibility that, in intact cells, a secondary activation of the $Na^+/Ca^{2+}$ exchange system may actually occur, our results suggest that 3,4 DCB has a direct action on PTX-induced channels.

Evidence has been presented that PTX may act through the $(Na^+,K^+)$ATPase in erythrocytes (Habermann, 1989). We show here that ouabain inhibited PTX-activated $^{22}Na^+$ uptake in aortic myocytes (Figure 2). The $IC_{50}$ value for ouabain inhibition (1 mM) is however more than 30 times as great as that for the inhibition of the $(Na^+,K^+)$ATPase activity as measured in $^{86}Rb^+$ flux experiments (30 μM) (Figure 2). We also observed in electrophysiological experiments that, at a concentration (200 μM) that inhibited 80% of the $(Na^+,K^+)$ATPase activity, ouabain had no action on the channel activity (Figure 9). These results suggest that the $(Na^+,K^+)$ATPase was unlikely to be the site of action of PTX in aortic myocytes.

A channel activity identical to that recorded in the presence of PTX has never been observed in aortic myocyte membranes in the absence of the toxin. This observation raises the hypothesis that PTX may act as an ionophore, by itself forming pores in the cell membrane. However PTX-induced channels share several properties with an epithelial-like $Na^+$ channel recently described in aortic myocytes (Van Renterghem & Lazdunski, 1991). (i) The epithelial-like $Na^+$ channel has a single channel conductance of 10 pS close to the value observed for PTX activated channels (11 pS, Figure

4). (ii) It is not voltage-dependent. (iii) It shows slow kinetics with very long openings (s). (iv) It is sensitive to high concentrations of amiloride derivatives (Van Renterghem & Lazdunski, 1991). These observations suggest the alternative hypothesis that PTX might act as an agonist of the epithelial-like $Na^+$ channel. Properties of the PTX-induced channel and the smooth muscle $Na^+$ channel differ however in some respects. First, whereas the epithelial-like channel is selective for $Na^+$ ($P_{Na}/P_K > 11$) (Van Renterghem & Lazdunski, 1991), the PTX-induced channel does not discriminate between $Na^+$ and $K^+$ ($P_{Na}/P_K = 0.9$). The difference in ion-selectivity does not mean necessarily that different structures are involved. It is known that activation of voltage-dependent, tetrodotoxin-sensitive $Na^+$ channels by a variety of neurotoxins is accompanied by a loss in the ion-selectivity (Khodorov & Revenko, 1979; Frelin *et al.*, 1981). Second, whereas epithelial-like $Na^+$ channels were most easily recorded in the cell-attached configuration, suggesting that as yet unidentified intracellular factors are required for their activity (Van Renterghem & Lazdunski, 1991), PTX-induced channels were currently recorded in excised patches with no evidence for a run down. It could be that PTX, like agonists of voltage-dependent channels, stabilizes an open conformation and bypasses the normal regulation of the channel activity.

We are very grateful to Dr E. Habermann for generously providing us with PTX. We thank N. Boyer, V. Friend and V. Dalmasso for expert technical assistance, and Prof. M. Lazdunski for continuous support. This work was supported by the Centre National de la Recherche Scientifique and the Ministère de la Défense Nationale (grant DRET 90/192).

## References

BARBRY, P., FRELIN, C., VIGNE, P., CRAGOE, E.J. & LAZDUNSKI, M. (1986). [$^3$H]Phenamil, a radiolabelled diuretic for the analysis of the amiloride sensitive $Na^+$ channels in kidney membranes. *Biochem. Biophys. Res. Commun.*, **135**, 25–32.

BRADFORD, M.M. (1976). A rapid and sensitive method for the quantification of microgram quantities of protein utilizing the principle of protein-dye coupling. *Anal. Biochem.*, **72**, 248–254.

DUBOIS, J.M. & COHEN, J.B. (1977). Effects of palytoxin on membrane potential and current of frog myelinated fibers. *J. Pharmacol. Exp. Ther.*, **201**, 148–155.

ECAULT, E. & SAUVIAT, M.P. (1991). Characterization of the palytoxin induced sodium conductance in frog skeletal muscle. *Br. J. Pharmacol.*, **102**, 523–529.

FABIATO, A. & FABIATO, F. (1979). Calculator programs for computing the composition of solutions containing multiple metals and ligands used for experiments in skinned muscle cells. *J. Physiol. (Paris)*, **75**, 463–505.

FLOREANI, M., TESSARI, M., DEBETTO, P., LUCIANI, S. & CARPENEDO, F. (1987). Effects of N-chlorobenzyl analogues of amiloride on myocardial contractility, Na-Ca exchange carrier and other cardiac enzymatic activities. *Naunyn-Schmied. Arch. Pharmacol.*, **336**, 661–669.

FRELIN, C., VIGNE, P. & LAZDUNSKI, M. (1981). The specificity of the sodium channel for monovalent cations. *Eur. J. Biochem.*, **119**, 437–442.

FRELIN, C., VIGNE, P. & BREITTMAYER, J.P. (1990a). Mechanism of the cardiotoxic action of palytoxin. *Mol. Pharmacol.*, **38**, 904–909.

FRELIN, C., VIGNE, P. & BREITTMAYER, J.P. (1990b). Palytoxin acidifies chick cardiac cells and activates the $Na^+/H^+$ antiporter. *FEBS Lett.*, **264**, 63–66.

GARCIA, M.L., KING, V.F., SHEVELL, J.L., SLAUGHTER, R.S., SUAREZ-KURTZ, G., WINQUIST, R.J. & KACZOROWSKI, G.J. (1990). Amiloride analogs inhibit L type calcium channels and display calcium entry blocker activity. *J. Biol. Chem.*, **265**, 3763–3771.

HABERMANN, E. (1989). Palytoxin acts through $Na^+,K^+$-ATPase. *Toxicon*, **27**, 1171–1187.

IKEDA, M., MITANI, K. & ITO, K. (1988). Palytoxin induces a nonselective cation channel in single ventricular cells of rat. *Naunyn-Schmied. Arch. Pharmacol.*, **337**, 591–593.

ITO, K., KARAKI, H. & URAKAWA, N. (1977). The mode of contractile action of palytoxin on vascular smooth muscle. *Eur. J. Pharmacol.*, **46**, 9–14.

KACZOROWSKI, G.J., BARROS, F., DETHMERS, J.K. & TRUMBLE, M.J. (1985). Inhibition of $Na^+/Ca^{2+}$ exchange in pituitary plasma membrane vesicles by analogues of amiloride. *Biochemistry*, **24**, 1394–1403.

KARAKI, H., NAGASE, H., OHIZUMI, Y., SATAKE, N. & SHIBATA, S. (1985). Palytoxin-induced contraction and release of endogenous noradrenaline in rat tail artery. *Br. J. Pharmacol.*, **95**, 183–188.

KHODOROV, B.I. & REVENKO, S.V. (1979). Further analysis of the mechanisms of action of batrachotoxin on the membrane of myelinated nerve. *Neurosci.*, **4**, 1315–1330.

KIM, S.Y., WU, C.H. & BERESS, L. (1991). Palytoxin forms ion channels through Na,K ATPase. In *The Sodium Pump: Recent Developments*. pp. 505–508. New York: The Rockefeller University Press.

LAKSHMINARAYANAIAH, N. (1984). *Equations of Membrane Biophysics*. London: Academic Press, Harcourt Brace Jovanovitch Publisher.

MOORE, R.E., BARTOLINI, G., BARCHI, J., BOTHNER-BY, A.A., DADOK, J. & FORD, J. (1982). Absolute stereochemistry of palytoxin. *J. Am. Chem. Soc.*, **104**, 3776–3779.

MURAMATSU, I., NISHIO, M., KIGOSHI, S. & UEMARA, D. (1988). Single ionic channels induced by palytoxin in guinea pig ventricular myocytes. *Br. J. Pharmacol.*, **93**, 811–816.

NAGASE, H. & KARAKI, H. (1987). Palytoxin induced contraction and release of prostaglandins and norepinephrine in the aorta. *J. Pharmacol. Exp. Ther.*, **242**, 1120–1125.

NAGASE, H., KARAKI, H. & URAKAWA, N. (1987). Palytoxin induced endothelium dependent relaxation in the isolated rat aorta. *Naunyn Schmied. Arch. Pharmacol.*, **335**, 575–579.

PICHON, Y. (1982). Effects of palytoxin on sodium and potassium permeabilities in unmyelinated axons. *Toxicon*, **20**, 41–47.

ROUZAIRE-DUBOIS, B. & DUBOIS, J.M. (1990). Characterization of palytoxin induced channels in mouse neuroblastoma cells. *Toxicon*, **28**, 1147–1158.

SAUVIAT, M.P. (1992). Palytoxin: characterization of mode of action in excitable cells. *Methods Neurosci.*, **8**, 332–346.

SAUVIAT, M.P., PATER, C. & BERTON, J. (1987). Does palytoxin open a sodium sensitive channel in cardiac muscle? *Toxicon*, **25**, 695–704.

SIEGL, P.K.S., CRAGOE, E.J., TRUMBLE, M.J. & KACZOROWSKI, G.J. (1984). Inhibition of $Na^+/Ca^{2+}$ exchange in membrane vesicles and papillary muscle preparations from guinea pig heart by analogs of amiloride. *Proc. Natl. Acad. Sci. U.S.A.*, **81**, 3238–3242.

VAN RENTERGHEM, C. & LAZDUNSKI, M. (1991). A new non voltage dependent, epithelial like $Na^+$ channel in vascular smooth muscle cells. *Pflügers Arch.*, **419**, 401–408.

VIGNE, P., BREITTMAYER, J.P., DUVAL, D., FRELIN, C. & LAZDUNSKI, M. (1988). The $Na^+/Ca^{2+}$ antiporter in aortic smooth muscle cells. *J. Biol. Chem.*, **263**, 8078–8083.

VIGNE, P., FRELIN, C., CRAGOE, E. & LAZDUNSKI, M. (1983). Ethylisopropylamiloride: a new and highly potent derivative of amiloride for the inhibition of the $Na^+/H^+$ exchange system in various cell types. *Biochem. Biophys. Res. Commun.*, **116**, 86–90.

*(Received November 6, 1992*
*Revised March 1, 1993*
*Accepted March 8, 1993)*

*Br. J. Pharmacol.* (1993), **109**, 866–872 © Macmillan Press Ltd, 1993

# Antiarrhythmic drugs, clofilium and cibenzoline are potent inhibitors of glibenclamide-sensitive $K^+$ currents in *Xenopus* oocytes

[1]Hidenari Sakuta, Koichi Okamoto & Yasuhiro Watanabe

Department of Pharmacology, National Defense Medical College, 3-2 Namiki, Tokorozawa, Saitama 359, Japan

**1** The novel $K^+$ channel opener, Y-26763 induced outward $K^+$ currents in voltage-clamped follicle-enclosed *Xenopus* oocytes in a concentration-dependent manner with an $EC_{50}$ value of 58 μM.

**2** The Y-26763-induced $K^+$ current was completely and reversibly blocked by glibenclamide (an ATP-sensitive $K^+$ channel blocker) in a concentration-dependent manner ($IC_{50}$ 140 nM). Effects of several antiarrhythmic drugs on Y-26763-induced glibenclamide-sensitive $K^+$ currents were investigated.

**3** (±)-Cibenzoline, RS-2135, pirmenol, lorcainide and KW-3407 (class I antiarrhythmic drugs, $Na^+$ channel blockers) suppressed Y-26763 responses in a concentration-dependent manner with $IC_{50}$ values (in μM) of 6.6, 54, 68, 71 and 370, respectively.

**4** Clofilium, E-4031, MS-551 and bretylium (class III antiarrhythmic drugs which increase the action potential duration) also suppressed Y-26763 responses concentration-dependently, $IC_{50}$ values (in μM) were 3.3, 660, 980 and $\geqslant 2000$, respectively. N-acetylprocainamide (class III antiarrhythmic drug) scarcely suppressed Y-26763 responses.

**5** The glibenclamide-sensitive $K^+$ currents elicted by KRN2391 were also suppressed by all these antiarrhythmic drugs.

**6** The antiarrhythmic drugs, clofilium and (±)-cibenzoline block glibenclamide-sensitive $K^+$ channels in *Xenopus* oocytes at concentrations comparable to their therapeutic plasma levels.

**Keywords:** Antiarrhythmic drug; cibenzoline; clofilium; Y-26763; KRN2391; glibenclamide; $K^+$ channel; *Xenopus laevis* oocyte; calmodulin antagonist

## Introduction

The ATP-sensitive $K^+$ ($K_{ATP}$) channel was first described in mammalian myocardial cells (Noma, 1983), and has also been observed in the pancreatic β-cell (Ashcroft *et al.*, 1984; Cook & Hales, 1984), the smooth muscle (Noack *et al.*, 1992), the skeletal muscle (Spruce *et al.*, 1985) and the brain (Ashford *et al.*, 1988). This $K^+$ channel is activated in the presence of ATP by a new class of $K^+$ channel openers such as cromakalim, pinacidil or diazoxide (Escande *et al.*, 1988), and is inactivated by sulphonylureas such as glibenclamide (Sturgess *et al.*, 1985), by imidazoline derivatives such as phentolamine (Plant & Henquin, 1990; Dunne, 1991), by barbiturates such as pentobarbitone (Kozlowski & Ashford, 1991), by phenothiazines such as chlorpromazine (Müller *et al.*, 1991) and by the inhibitor of $Ca^{2+}$ mobilization, TMB-8 (Szewczyk *et al.*, 1992).

The oocyte of *Xenopus laevis* has an endogenous $K^+$ channel which is activated by $K^+$ channel openers such as cromakalim and pinacidil (Honoré & Lazdunski, 1991) and KRN2391 (Sakuta *et al.*, 1992a). Since this oocyte $K^+$ channel is inactivated by glibenclamide (Honoré & Lazdunski, 1991) but not by charybdotoxin (an inhibitor of $Ca^{2+}$-activated $K^+$ channel) or dendrotoxin (an inhibitor of voltage-dependent $K^+$ channel) (Honoré & Lazdunski, 1991), the $K^+$ channel appears to belong to the family of ATP-sensitive $K^+$ channels, though its sensitivity to ATP is not yet proven by single channel studies.

An agent which acts to suppress the ATP/glibenclamide-sensitive $K^+$ channel has potential as an antiarrhythmic drug (Kantor *et al.*, 1990; Notsu *et al.*, 1992). Among conventional antiarrhythmic drugs, some, such as quinidine and verapamil, do suppress ATP/glibenclamide-sensitive $K^+$ channels in rat cardiac cells (Haworth *et al.*, 1989). Antiarrhythmic drugs, disopyramide, aprindine, bepridil and prenylamine potently block glibenclamide-sensitive $K^+$ channels in *Xenopus* oocytes with $IC_{50}$ values of less than 50 μM (Sakuta *et al.*, 1992a). The suppression of ATP/glibenclamide-sensitive $K^+$ channels may be involved in either favourable or unfavourable clinical effects of some antiarrhythmic drugs (see Discussion).

In the present study, we have examined the effects of five class I antiarrythmic drugs ($Na^+$ channel blockers) and five class III antiarrhythmic drugs (agents prolonging the action potential duration (APD)) on glibenclamide-sensitive $K^+$ channels in *Xenopus* oocytes. As a result, we have found that (±)-cibenzoline (a class I antiarrhythmic drug) and clofilium (a class III antiarrhythmic drug) potently suppress glibenclamide-sensitive $K^+$ channels in *Xenopus* oocytes.

## Methods

### *Voltage-clamped recording*

As described previously (Sakuta *et al.*, 1992a,b), oocytes at stage V–VI were collected from female frogs (*Xenopus laevis*) anaesthetized in ice, each oocyte was placed in a recording well (0.2 ml in capacity) and superfused with frog Ringer solution consisting of (in mM) NaCl 120, KCl 2, $CaCl_2$ 1.8 and HEPES 5 (pH 7.4). The membrane potential of the oocyte was then voltage-clamped at a holding potential of −20 mV with two glass microelectrodes each filled with 3 M KCl (1–2 Mohm) using the voltage-clamp amplifier, CEA-1200 (Nihon Kohden, Tokyo, Japan). This holding potential of −20 mV is close to the predicted $Cl^-$ equilibrium potential of the oocyte and was chosen to minimize the $Ca^{2+}$-activated $Cl^-$ current (Honoré & Lazdunski, 1991; Sakuta *et al.*, 1992a,b). All current responses of the oocyte were recorded at room temperature (19–23°C) with a Thermalarray Recorder, RTA-1100 (Nihon Kohden). Only follicle-

[1] Author for correspondence.

enclosed oocytes (not treated with collagenase) were used for all experiments in the present study.

### *Application of drugs and agents*

Y-26763 or KRN2391 ($K^+$ channel openers) dissolved in frog Ringer solution were applied for 20 s by constant flow superfusion (3 ml $min^{-1}$) to evoke a $K^+$ current. Y-26763 was applied at 50 μM routinely and at 10–2000 μM to obtain a concentration-response curve, and KRN2391 was routinely applied at 100 μM. Each test drug or agent, except for charybdotoxin and dendrotoxin, was applied by superfusion for 2 min, and the oocyte was washed for 15 s by superfusion of frog Ringer solution; then the $K^+$ channel opener was applied again to observe the effect of the test drug. As described previously (Sakuta *et al.*, 1992a), this 15 s washing period did not reduce the suppressive effect of the test drug, indicating little wash-off. TMB-8, W-7, W-13, W-5 or antiarrhythmic drugs were dissolved in frog Ringer solution to appropriate concentrations and applied by superfusion (3 ml $min^{-1}$) as described above. Glibenclamide was dissolved in ethanol to be 2.5 mM, then diluted with frog Ringer solution to a final concentration of 5 nM–10 μM (pH 7.4) and applied to each oocyte by superfusion as described previously (Sakuta *et al.*, 1992a).

### *Drugs and agents used*

The following drugs and agents were used (full name and source): Y-26763 ((+)-(**3S,4R**)-4-(N-acetyl-N-benzyloxyamino)-6-cyano-3,4-dihydro-2,2-dimethyl-2*H*-1-benzopyran-3-ol, an active desbenzoyl form of Y27152, gift from Yoshitomi Pharmaceutical Industry Ltd., Osaka, Japan); KRN2391 (N-cyano-*N'*-(2-nitroxyethyl)-3-pyridinecarboximidamide methanesulphonate, gift from Kirin Brewery Co., Takasaki, Japan); E-4031 (1-[2-(6-methyl-2-pyridyl)ethyl]-(4-methanesulphonamidobenzoyl) piperidine, gift from Eisai Pharmaceutical Co., Tokyo, Japan); RS-2135, (3a**R**,12**R**,12a**R**,12b**S**)-12-amino-2,3,3a,4,11, 12,12a,12b-octahydro-10-hydroxyisoquino [2,1,8-1ma] carbazol-5(1*H*)-one hydrochloride 1.5-hydrate, gift from Sankyo Pharmaceutical Co., Tokyo); MS-551 (1,3-dimethyl-6-{2-[*N*-(hydroxyethyl)-3-(4-nitrophenyl) propylamino]-ethylamino}-2,4 (1*H*,3*H*)-pyrimidinedione hydrochloride, gift from Mitsui Pharmaceutial Co., Osaka, Japan); KW-3407 (5-{[2-(diethylamino)ethyl]amino}-7-methoxy-5,11-dihydro[1]-benzoxepino [3,4-*b*]pyridine 1.5-fumarate, gift from Kyowa Hakko Co., Tokyo, Japan); (±)-cibenzoline succinate (gift from Fujisawa Pharmaceutical Co., Osaka, Japan), pirmenol hydrochloride (gift from Warner-Lambert Inc., Tokyo, Japan); clofilium tosylate, bretylium tosylate, lorcainide hydrochloride, glibenclamide, charybdotoxin and dendrotoxin (purchased from Funakoshi Co., Tokyo, Japan); W-5 (N-(6-aminohexyl)-1-naphthalenesulphonamide), W-7 (N-(6-aminohexyl)-5-chloro-1-naphthalenesulphonamide), W-13 (N-(4-aminobutyl)-5-chloro-2-naphthalenesulphonamide), N-acetylprocainmide hydrochloride, TMB-8 (3,4,5-trimethoxybenzoic acid 8-(diethylamino)octyl ester), H-7 (1-(5-isoquinolinylsulphonyl)-2-methylpiperazine) and staurosporine (purchased from Sigma Chemical Co., St. Louis, USA), and collagenase and TEA (tetraethylammonium chloride, purchased from Wako Pure Chemical Co., Osaka, Japan).

### *Estimation of $IC_{50}$ and $EC_{50}$ values*

The $IC_{50}$ value for the inhibition of Y-26763 responses by each test drug was estimated from the log concentration-inhibition curve drawn by linearly connecting observed mean values (cf. Figures 3–7). The $EC_{50}$ value for Y-26763 was also estimated from the log concentration-response curve in the same manner (cf. Figure 1).

## Results

### *The current response induced by Y-26763 in follicle-enclosed* Xenopus *oocytes*

In all follicle-enclosed occytes, Y-26763 (a novel $K^+$ channel opener, Nakajima *et al.*, 1992) at 10–2000 μM induced a non-oscillating and slowly rising outward current at a voltage-clamped membrane potential of −20 mV (Figure 1a). Y-26763 showed a bell-shaped concentration-response curve, that is, the amplitude of Y-26763 responses increased

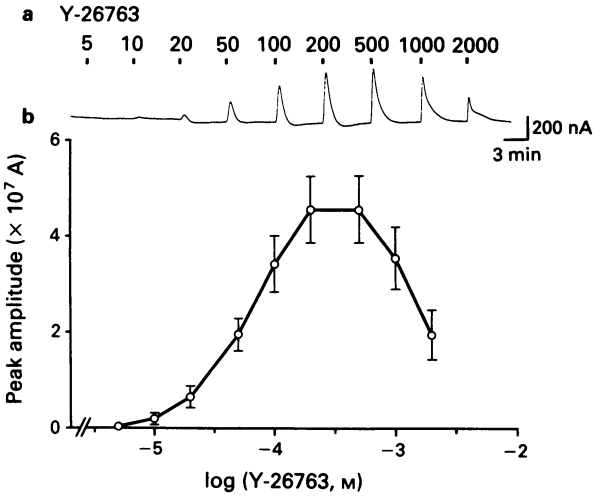



**Figure 1** Y-26763-induced outward currents in follicle-enclosed *Xenopus* oocytes. (a) Responses to 5–2000 μM Y-26763 applied for 20 s (at bars) in one oocyte. (b) A log concentration-response curve for Y-26763 (mean ± s.d., $n = 8$) showing a bell shape. All oocytes used were voltage-clamped at −20 mV.

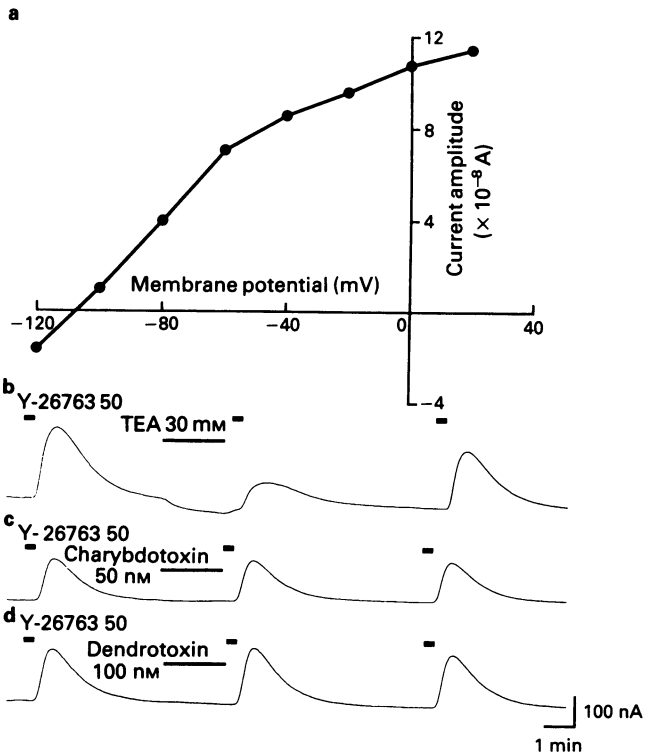



**Figure 2** The reversal potential of Y-26763 responses, and the effects thereon of $K^+$ channel blockers. (a) An *I-V* relation for responses to Y-26763 (50 μM, 20 s) in one oocyte showing the reversal at about −107 mV. (b)–(d) The effect of tetraethylammonium (TEA, 30 mM, 2 min), charybdotoxin (50 nM, 2 min) and dendrotoxin (100 nM, 2 min) on Y-26763 (50 μM) responses in 3 different oocytes voltage clamped at −20 mV.

as the concentration of Y-26763 was raised from 10 μM to 200 μM (apparent $EC_{50}$ = 57.5 μM) and decreased when the concentration was increased from 500 μM to 2 mM as shown in Figure 1a and b. This apparent $EC_{50}$ value of 58 μM was smaller than $EC_{50}$ values for cromakalim (280 μM) and KRN2391 (400 μM) all studied under similar conditions (Sakuta *et al.*, 1992a,b).

The Y-26763-induced current response was carried by the efflux of $K^+$, since it was reversed at a holding potential of about −100 mV (Figure 2a) which is close to the $K^+$ equilibrium potential of the oocyte in frog Ringer solution (Kusano *et al.*, 1982), and was suppressed to 55 ± 6% (mean ± s.d., $n$ = 5) by 30 mM TEA (Figure 2b). In five oocytes tested, Y-26763-induced $K^+$ currents were not affected either by 50 nM charybdotoxin (an inhibitor of $Ca^{2+}$-activated $K^+$ channel) or by 100 nM dendrotoxin (an inhibitor of voltage-dependent $K^+$ channel) (Figure 2c and d).

The relatively selective inhibitor of ATP-sensitive $K^+$ channels, glibenclamide suppressed the $K^+$ currents induced by 50 μM Y-26763 in a concentration-dependent fashion with an $IC_{50}$ of 140 nM (Figure 3a and c). TMB-8 also blocked responses to 50 μM Y-26763 in a concentration-dependent manner with an $IC_{50}$ value of 48 μM (Figure 3b and c). TMB-8 is known to block not only the ATP-sensitive $K^+$ channel in insulin-secreting cells (Szewczyk *et al.*, 1992) but also the voltage-dependent $Na^+$ channel and the voltage-dependent $Ca^{2+}$ channel (Himmel & Raven, 1990).

$K^+$channels which were activated by Y-26763 appear to be present in the follicle cells surrounding the oocyte rather than the plasma membrane of the oocyte itself, because oocytes defolliculated by incubation with collagenase (1 mg $ml^{-1}$ for 4 h) scarcely responded to Y-26763 (data not shown).

### *Effects of class I and class III antiarrhythmic drugs on Y-26763-induced $K^+$ current*

Class I antiarrhythmic drugs, (±)-cibenzoline, RS-2135 (Yorikane *et al.*, 1991), pirmenol, lorcainide and KW-3407

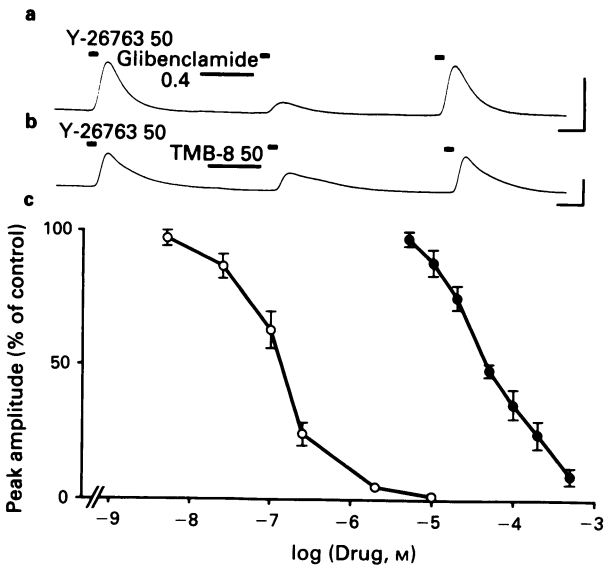



**Figure 3** Effects of ATP-sensitive $K^+$ channel blockers on Y-26763 responses. (a) and (b) Suppression of responses of Y-26763 (50 μM, 20 s, short bars) by glibenclamide (0.4 μM, 2 min, long bar in a) and TMB-8 (50 μM, 2 min, long bar in b) in different oocytes voltage clamped at −20 mV. Calibrations: 200 nA and 1 min. (c) Log concentration-inhibition curves (mean ± s.d., $n$ = 5) for the inhibition of responses to Y-26763 (50 μM, 20 s) by glibenclamide (○) and TMB-8 (●). The ordinate scale shows the peak amplitude of the Y-26763 response (as a % of the control, i.e. in the absence of the test drug), and the abscissa scale is the log molar concentration of test drugs.

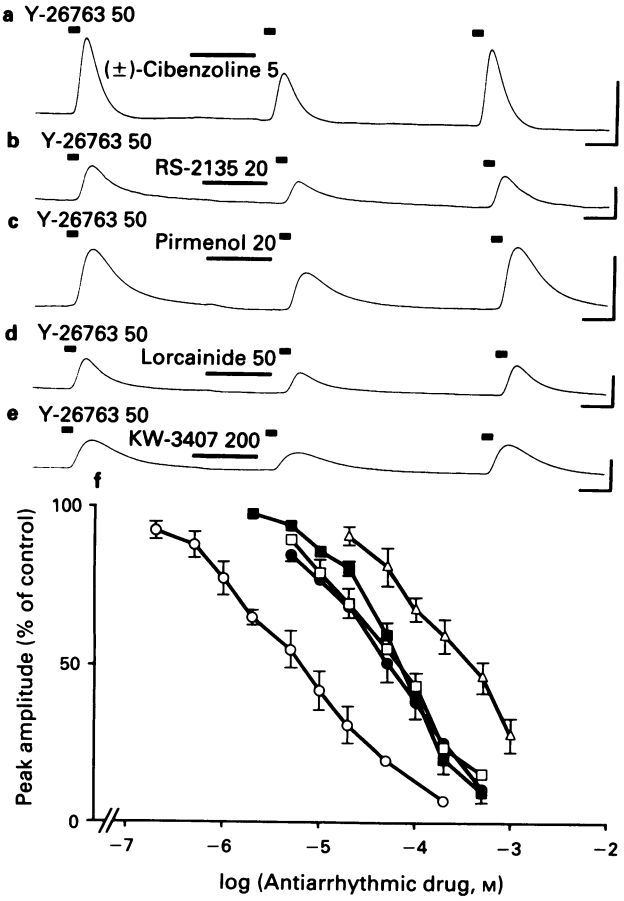



**Figure 4** Effects of class I antiarrhythmic drugs on Y-26763 responses. (a)–(e) Suppression of responses to Y-26763 (50 μM, 20 s, short bars) by the class I drugs indicated (applied for 2 min, (long bars) at concentrations shown in μM) in different oocytes voltage clamped at −20 mV. Calibrations: 200 nA and 1 min. (f) Log concentration-inhibition curves (mean ± s.d., $n$ = 5) for the inhibition of responses to Y-26763 (50 μM, 20 s) by (±)-cibenzoline (○), RS-2135 (●), pirmenol (□), lorcainide (■) and KW-3407 (△). The ordinate scale is the peak amplitude of the Y-26763 response (as a % of the control, i.e. in the absence of an antiarrhythmic drug), and the abscissa scale is the log molar concentration of antiarrhythmic drugs.

(Kumazawa *et al.*, 1990) reversibly suppressed the $K^+$ current induced by 50 μM Y-26763 in a concentration-dependent manner with $IC_{50}$ values (in μM) of 6.6, 54, 68, 71, and 370 as shown in Figure 4a–f. (±)-Cibenzoline was the most potent in this class of drugs tested and its suppressive effect was observed even at concentrations lower than 1 μM.

The class III antiarrhythmic drug, clofilium, also potently blocked Y-26763 responses with an $IC_{50}$ value of 3.3 μM (Figure 5a and f). Other class III antiarrhythmic drugs tested, E-4031 (Adaniya & Hiraoka, 1990), MS-551 (Kamiya *et al.*, 1992) and bretylium, weakly suppressed Y-26763 responses with $IC_{50}$ values (in μM) of 660, 980 and ⩾ 2000, respectively (Figure 5b–d and f), whilst N-acetylprocainamide scarcely suppressed Y-26763 responses (Figure 5e and f).

### *Effects of class I and class III antiarrhythmic drugs on KRN2391-induced $K^+$ current*

Another $K^+$ channel opener, KRN2391 also induces a glibenclamide-sensitive $K^+$ current in *Xenopus* oocytes (Sakuta *et al.*, 1992a). The effect of the above antiarrhythmic drugs on the KRN2391-induced current was examined. As shown in Figure 6a, all class I antiarrhythmic drugs tested, namely (±)-cibenzoline, RS-2135, pirmenol, lorcainide and KW-3407 suppressed current responses to KRN2391 (100 μM) in a concentration-dependent manner with $IC_{50}$ values

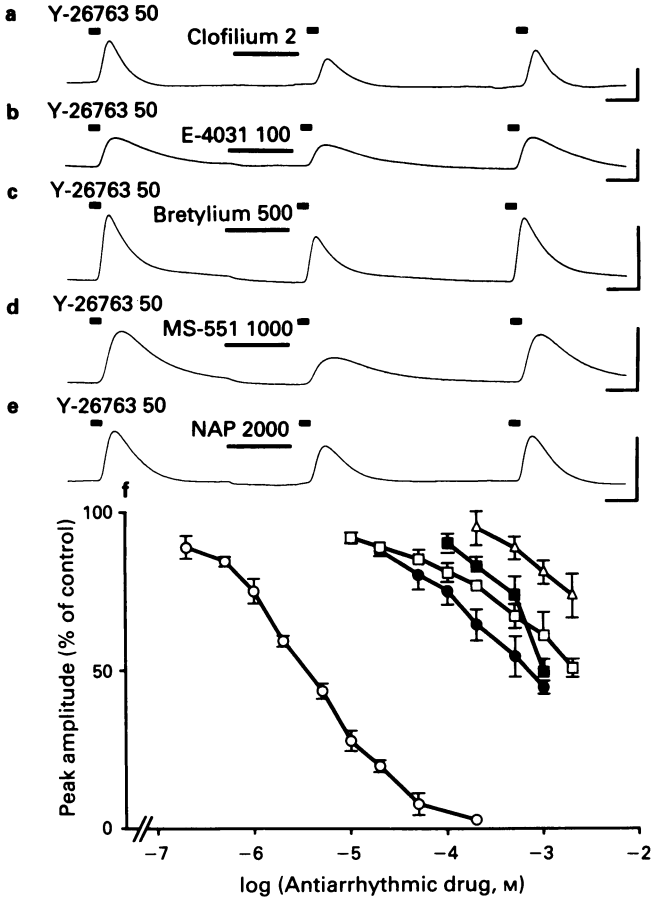



**Figure 5** Effects of class III antiarrhythmic drugs on Y-26763 responses. (a)–(e) Suppression of responses to Y-26763 (50 μM, 20 s, short bars) by the class III drugs indicated (applied for 2 min (long bars) at concentrations shown in μM) in different oocytes voltage clamped at −20 mV. Calibrations: 200 nA and 1 min. (f) Log concentration-inhibition curves (mean ± s.d., $n = 5$) for the inhibition of responses to Y-26763 (50 μM, 20 s) by clofilium (○), E-4031 (●), bretylium (□), MS-551 (■) and N-acetylprocainamide (△). The ordinate scale is the peak amplitude of the Y-26763 response (as a % of the control, i.e. in the absence of an antiarrhythmic drug), and the abscissa scale is the log molar concentration of antiarrhythmic drugs.

(in μM) of 4.5, 71, 96, 120 and 320, respectively). Their relative suppressive potencies on the KRN2391-evoked response were comparable to those on the Y-26763 response.

The $K^+$ current induced by KRN2391 was also suppressed by class III antiarrhythmic drugs, clofilium, MS-551, bretylium and E-4031 with $IC_{50}$ values (in μM) of 5.8, 1200, 1700 and >2000 (Figure 6b), respectively. The $IC_{50}$ values for clofilium and bretylium were comparable to those on Y-26763-induced currents, but the KRN2391-induced $K^+$ current was less sensitive to E-4031 than the Y-26763-induced $K^+$ current either in different oocytes as shown Figure 6b or in a single oocyte (data not shown). N-acetylprocainamide scarcely suppressed KRN2391 responses.

### *Effects of calmodulin antagonists on Y-26763 responses*

Of the antiarrhythmic drugs tested in the present study, clofilium and lorcainide possess calmodulin antagonist activity (Silver *et al.*, 1989; Mannhold *et al.*, 1990). Calmodulin antagonists, W-7, W-13 and W-5 (Hidaka & Tanaka, 1983), suppressed the $K^+$ current induced by 50 μM Y-26763 in a concentration-dependent manner with $IC_{50}$ values (in μM) of 18, 35 and 54, respectively (Figure 7a–d). This rank order of potency agrees with that of their calmodulin antagonist activities (Hidaka & Tanaka, 1983).

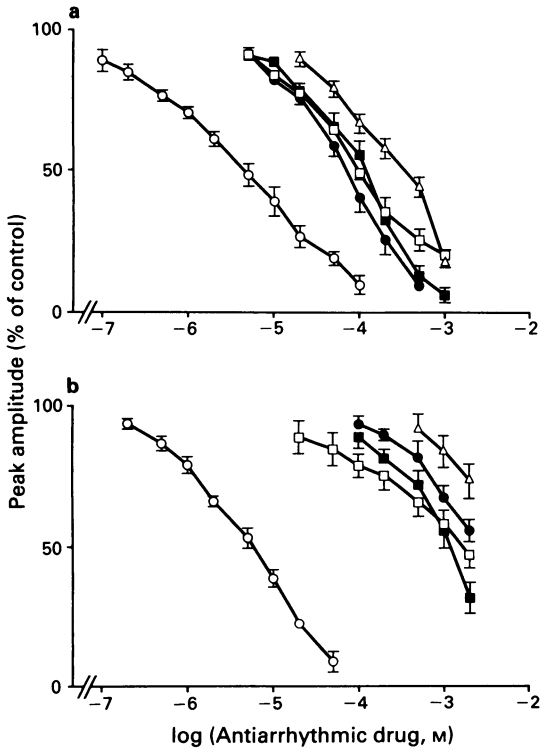



**Figure 6** Log concentration-inhibition curves for the inhibition by class I and III antiarrhythmic drugs of the outward $K^+$ currents induced by KRN2391 (100 μM, 20 s) responses. All values plotted were mean ± s.d. ($n = 5$). (a) The curves for class I drugs, (±)-cibenzoline (○), RS-2135 (●), pirmenol (□), lorcainide (■) and KW-3407 (△); (b) the curves for class III drugs, clofilium (○), E-4031 (●), bretylium (□), MS-551 (■) and N-acetylprocainamide (△). Ordinates are the peak amplitude of the KRN2391 response (as a % of the control, i.e. in the absence of an antiarrhythmic drug), and abscissae are the log molar concentration of antiarrhythmic drugs.

## Discussion

### *Properties of Y-26763-induced outward currents*

It is suggested that Y-26763 activates ATP-sensitive $K^+$ channels in ventricular cardiomyocytes (Ishiguro *et al.*, 1992), and it was demonstrated in the present study that this $K^+$ channel opener evokes glibenclamide-sensitive $K^+$ currents in follicle-enclosed *Xenopus* oocytes (cf. Figures 2 and 3). The Y-26763-induced $K^+$ current was completely blocked by glibenclamide but was insensitive to both charybdotoxin and dendrotoxin (cf. Figure 2). Therefore, Y-26763-induced $K^+$ current may not contain either a $Ca^{2+}$-activated $K^+$ or a voltage-dependent $K^+$ current.

TEA at a very high concentration (30 mM) suppressed Y-26763-induced currents by about 55% (cf. Figure 2). This TEA effect is not necessarily contradictory to the property of ATP-sensitive $K^+$ currents, because the ATP-sensitive $K^+$ current in mouse pancreatic β-cells also shows a weak sensitivity to TEA (Bokvist *et al.*, 1990).

### *Blockade of glibenclamide-sensitive $K^+$ channels by antiarrhythmic drugs and possible mechanism*

Glibenclamide-sensitive $K^+$ channels in *Xenopus* oocytes were potently blocked by clofilium and (±)-cibenzoline in the present study. We have previously reported that various antiarrhythmic drugs block the glibenclamide-sensitive $K^+$ currents induced by KRN2391 in oocytes with potencies in terms of $IC_{50}$ of 6.3 μM for bepridil, 18 μM for disopyramide, 30 μM for aprindine and 38 μM for prenylamine (Sakuta *et*

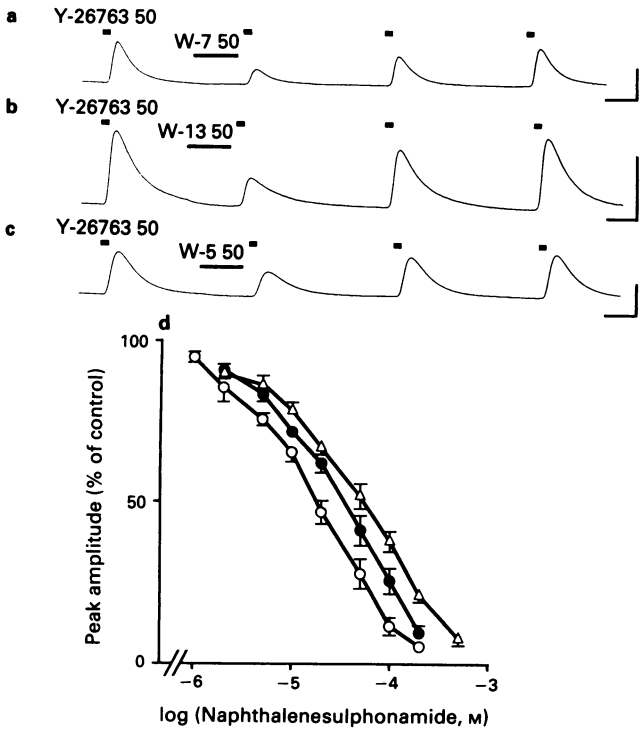



**Figure 7** Effects of calmodulin antagonist naphthalenesulphonamides on Y-26763 responses. (a)–(c) Suppression by W-7 (50 μM, 2 min, long bar in a), W-13 (50 μM, 2 min, long bar in b) and W-5 (50 μM, 2 min, long bar in c) of responses to Y-26763 (50 μM, 20 s, short bars) in 3 different oocytes voltage clamped at −20 mV. Note slow recovery from inhibition by each drug. Calibrations: 200 nA and 90 s. (d) Log concentration-inhibition curves (mean ± s.d., $n = 5$) for the inhibition of responses to Y-26763 (50 μM, 20 s) by W-7 (○), W-13 (●) and W-5 (△). The ordinate scale is the peak amplitude of the Y-26763 response (as a % of the control, i.e., in the absence of a naphthalenesulphonamide), and the abscissa scale is the log molar concentration of naphthalenesulphonamides.

*al.*, 1992a). Thus, the potencies of clofilium ($IC_{50}$ 5.8 μM) and (±)-cibenzoline (4.5 μM) in blocking KRN2391-induced glibenclamide-sensitive $K^+$ currents are comparable to the potency of bepridil.

W-7, W-13 and W5 (calmodulin antagonists), clofilium and lorcanide blocked the $K^+$ currents induced by Y-26763 in oocytes with the rank order of clofilium > W-7 > W-13 > W-5 ≥ lorcainide. This rank order agreed with their reported potencies as calmodulin antagonists (potencies to inhibit $Ca^{2+}$/calmodulin-dependent phosphodiesterase), that is clofilium > W-7 > W-13 > lorcainide ≥ W-5 (Silver *et al.*, 1989; Mannhold *et al.*, 1990; Hidaka & Tanaka, 1983). In addition, several antiarrhythmic drugs and agents having a calmodulin antagonizing activity also block the glibenclamide-sensitive $K^+$ current induced by KRN2391 in *Xenopus* oocytes (Sakuta *et al.*, 1992a). These previous and present findings suggest that the calmodulin antagonist activity of clofilium and lorcainide contributes at least partly to their $K^+$ channel-blocking actions.

The blocking action of KW-3407 and RS-2135 on glibenclamide-sensitive $K^+$ currents appears to be related to phenothiazine-like aromatic rings in their structures. Phenothiazine derivatives such as trifluoperazine and chlorpromazine block ATP/glibenclamide-sensitive $K^+$ channels (Müller *et al.*, 1991). It is suggested that the calmodulin antagonizing activity of phenothiazine derivatives (Weiss & Levin, 1978) contributes to their blocking effect on ATP/glibenclamide-sensitive $K^+$ channels (Sakuta *et al.*, 1992b).

The suppressive effect of (±)-cibenzoline on glibenclamide-sensitive $K^+$ channels in oocytes seems to be related to its imidazoline structure, since several imidazoline derivatives such as phentolamine, tolazoline and antazoline have been reported to block ATP/glibenclamide-sensitive $K^+$ channels in insulin-secreting cells (Plant & Henquin, 1990; Dunne, 1991). For imidazolines, however, a mechanism other than calmodulin antagonism appears to be involved in the blockade of glibenclamide-sensitive $K^+$ channels in *Xenopus* oocytes, because phentolamine and tolazoline are very weak calmodulin antagonists, their $IC_{50}$ values being ≥ 500 μM (Earl *et al.*, 1984).

The glibenclamide-sensitive $K^+$ current in *Xenopus* oocytes is enhanced by activation of adenylate cyclase and is decreased by activation of protein kinase C (Honoré & Lazdunski, 1991). Except for clofilium, however, all drugs tested are known to affect neither the intracellular level of cyclicAMP nor the activity of protein kinase C. Only clofilium was reported to inhibit protein kinase C, but it requires a concentration of 100 μM to do so (Silver *et al.*, 1989), which is about 30 times higher than its $IC_{50}$ value (3.3 μM) for the blockade of Y-26763-induced currents. In addition, protein kinase C inhibitors, staurosporine (1 μM) and H-7 (100 μM) do not affect Y-26763-induced $K^+$ currents (our unpublished observation). Thus, it seems unlikely that the suppressive effect of all 10 antiarrhythmic drugs tested on Y-26763-induced $K^+$ currents is mediated by drug-induced changes in second messengers, cyclicAMP and protein kinase C.

Class I antiarrhythmic drugs, cibenzoline (Matsuoka *et al.*, 1991) and pirmenol (Reder *et al.*, 1980), also possess the class IV action (blockade of the voltage-dependent $Ca^{2+}$ channel). Several $Ca^{2+}$ antagonists are reported to suppress the glibenclamide-sensitive $K^+$ currents in oocytes (Sakuta *et al.*, 1992a). The $Ca^{2+}$ antagonism might change intracellular $Ca^{2+}$ concentration, inhibit $Ca^{2+}$-dependent processes and subsequently affect glibenclamide-sensitive $K^+$ currents. The $Ca^{2+}$ channel blockade by this means, however, is unlikely to be contributing to the suppressive effect of antiarrhythmic drugs on oocyte glibenclamide-sensitive $K^+$ current for the following reasons: (1) the weak $Ca^{2+}$ antagonists, bepridil and prenylamine, block oocyte glibenclamide-sensitive $K^+$ currents much more potently than strong $Ca^{2+}$ antagonists, diltiazem and verapamil (Sakuta *et al.*, 1992a); (2) typical $Ca^{2+}$ antagonists, verapamil and diltiazem, require much higher concentrations to block the $K^+$ current than to block $Ca^{2+}$ channels (Sakuta *et al.*, 1992a); (3) both the active $Ca^{2+}$ antagonist, (−)-verapamil, and the inactive isomer, (+)-verapamil, equipotently block the $K^+$ current (our unpublished observation); and (4) cibenzoline blocked KRN2391-induced $K^+$ currents in oocytes 19 times more potently than (±)-verapamil (cf. Figure 4 and Sakuta *et al.*, 1992a), whilst the potency of cibenzoline in blocking $Ca^{2+}$ channels is only 1/50 of that of (±)-verapamil (Matsuoka *et al.*, 1991).

### *Clinical significance of the blockade of glibenclamide-sensitive $K^+$ channels by antiarrhythmic drugs*

Myocardial ATP/glibenclamide-sensitive $K^+$ channels are opened by an ischaemic condition and are thought to play a major role in the ischaemia-induced shortening of action potential duration and consequent generation of ischaemia-related arrhythmia (Noma, 1983). Therefore, any drug which can block this type of $K^+$ channel theoretically has the potential to suppress ischaemia-induced arrhythmia (Lynch *et al.*, 1992). In support of this idea, ATP-sensitive $K^+$ channel blockers glibenclamide and 5-hydroxydecanoate have been reported to suppress experimental ventricular arrhythmia (Kantor *et al.*, 1990; Notsu *et al.*, 1992). Furthermore, some class I, class II and class IV antiarrhythmic drugs in Vaughan Williams' classification block glibenclamide-sensitive $K^+$ channels (Sakuta *et al.*, 1992a). The present study shows that the class III antiarrhythmic drug, clofilium, and some novel class I antiarrhythmic drugs also block the $K^+$ channels. Thus, it appears that the inhibition of ATP/glibenclamide-sensitive $K^+$ channels may underlie a part of antiarrhythmic effects of some antiarrhythmic drugs.

Disopyramide, quinidine and (±)-cibenzoline are related to rare hypoglycaemic attacks during treatment of arrhythmia (Semel *et al.*, 1983; Phillips *et al.*, 1986; Jeandel *et al.*, 1988). Disopyramide and quinidine suppress glibenclamide-sensitive $K^+$ currents in *Xenopus* oocytes (Sakuta *et al.*, 1992a). (±)-Cibenzoline also potently blocked the $K^+$ currents (cf. Figures 4 and 6). Thus, it is conceivable that these drugs might inactivate ATP/glibenclamide-sensitive $K^+$ channels in pancreatic β-cells, and facilitate the secretion of insulin. In support of this, disopyramide, quinine (an optical isomer of quinidine) and imidazoline derivatives have been reported to stimulate the secretion of insulin from islet cells (Henquin *et al.*, 1975; Nakabayashi *et al.*, 1989; Schulz & Hasselblatt, 1989).

In conclusion, the antiarrhythmic drugs, (±)-cibenzoline and clofilium block the glibenclamide-sensitive $K^+$ channel in *Xenopus* oocytes at concentrations comparable to their therapeutic plasma concentrations. These drugs are as potent as bepridil which is the strongest blocker of glibenclamide-sensitive $K^+$ channels among the antiarrhythmic drugs studied so far.

We would like to express our sincere thanks to Dr Koji Nishikori of Kirin Brewery Co., Ltd., Takasaki, Japan for the kind supply of KRN2391, and to Yoshitomi Pharmaceutical Industry Ltd., Osaka, Japan for Y-26763.

## References


ADANIYA, H. & HIRAOKA, M. (1990). Effects of a novel class III antiarrhythmic agent, E-4031, on reentrant tachycardias in rabbit right atrium. *J. Cardiovasc. Pharmacol.*, **15**, 976–982.

ASHCROFT, F.M., HARRISON, D.E. & ASHCROFT, S.J.H. (1984). Glucose induces closure of single potassium channels in isolated rat pancreatic β-cells. *Nature*, **312**, 446–448.

ASHFORD, M.L.J., STURGESS, N.C., TROUT, N.J., GARDNER, N.J. & HALES, C.N. (1988). Adenosine-5'-triphosphate-sensitive ion channels in neonatal rat cultured central neurones. *Pflügers Arch.*, **412**, 297–304.

BOKVIST, K., RORSMAN, P. & SMITH, P.A. (1990). Block of ATP-regulated and $Ca^{2+}$-activated $K^+$ channels in mouse pancreatic β-cells by external tetraethylammonium and quinine. *J. Physiol.*, **423**, 327–343.

COOK, D.L. & HALES, C.N. (1984). Intracellular ATP directly blocks $K^+$ channels in pancreatic β-cells. *Nature*, **311**, 271–273.

DUNNE, M.J. (1991). Block of ATP-regulated potassium channels by phentolamine and other α-adrenoceptor antagonists. *Br. J. Pharmacol.*, **103**, 1847–1850.

EARL, C.Q., PROZIALECK, W.C. & WEISS, B. (1984). Interaction of alpha adrenergic antagonists with calmodulin. *Life Sci.*, **35**, 525–534.

ESCANDE, D., THURINGER, D., LEGUERN, S. & CAVERO, I. (1988). The potassium channel opener cromakalim (BRL34915) activates ATP-dependent $K^+$ channels in isolated cardiac myocytes. *Biochem. Biophys. Res. Commun.*, **154**, 620–625.

HAWORTH, R.A., GOKNUR, A.B., & BERKOFF, H.A. (1989). Inhibition of ATP-sensitive potassium channels of adult rat heart cells by antiarrhythmic drugs. *Circ. Res.*, **65**, 1157–1160.

HENQUIN, J.C., HOREMANS, B., NENQUIN, M., VERNIERS, J. & LAMBERT, A.E. (1975). Quinine-induced modifications of insulin release and glucose metabolism by isolated pancreatic islets. *FEBS Lett.*, **37**, 280–284.

HIDAKA, H. & TANAKA, T. (1983). Naphthalenesulfonamides as calmodulin antagonists. *Methods Enzymol.*, **17**, 185–194.

HIMMEL, H.M. & RAVEN, U. (1990). TMB-8 as a pharmacological tool in guinea pig myocardial tissues. I. Effects of TMB-8 on force of contraction and on action potential parameters in atrial and papillary muscles. *J. Pharmacol. Exp. Ther.*, **255**, 293–299.

HONORÉ, E. & LAZDUNSKI, M. (1991). Hormone-regulated $K^+$ channels in follicle-enclosed oocytes are activated by vasorelaxing $K^+$ channel openers and blocked by antidiabetic sulfonylureas. *Proc. Natl. Acad. Sci. U.S.A.*, **88**, 5438–5442.

ISHIGURO, M., MIURA, Y. & INUI, J. (1992). Electrophysiological analysis of the effects of Y-26763, an active metabolite of a new K channel opener Y-27152, in the guinea-pig ventricular muscle. *Jpn. J. Pharmacol.*, **58**, 185.

JEANDEL, C., PREISS, M.A., PIERSON, H., PENIN, F., CUNY, G., BANNWARTH, B. & NETTER, P. (1988). Hypoglycemia induced by cibenzoline. *Lancet*, **i**, 1232–1233.

KAMIYA, J., ISHII, M. & KATAKAMI, T. (1992). Antiarrhythmic effects of MS-551, a new class III antiarrhythmic agent, on canine models of ventricular arrhythmia. *Jpn. J. Pharmacol.*, **58**, 107–115.

KANTOR, P.F., COETZEE, W.A., CARMELIET, E.E., DENNIS, S.C. & OPIE, L.H. (1990). Reduction of ischemic $K^+$ loss and arrhythmia in rat hearts. Effects of glibenclamide, a sulfonylurea. *Circ. Res.*, **66**, 478–485.

KOZLOWSKI, R.Z. & ASHFORD, M.L.J. (1991). Barbiturates inhibit ATP-$K^+$ channels and voltage-activated currents in CRI-G1 insulin-secreting cells. *Br. J. Pharmacol.*, **103**, 2021–2029.

KUMAZAWA, T., HARAKAWA, H., OBASE, H., OIJI, Y., NITO, M., KUBO, K., ISHII, A., TOMIOKA, S. & YAMADA, Y. (1990). Synthesis and antiarrhythmic activity of 5,11-dihydro[1]benzoxepino [3,4-b]pyridines. *J. Med. Chem.*, **33**, 3095–3100.

KUSANO, K., MILEDI, R. & STINNAKRE, J. (1982). Cholinergic and catecholaminergic receptors in the *Xenopus* oocyte membrane. *J. Physiol.*, **328**, 143–170.

LYNCH, J.J. Jr., SANGUINETTI, M.C., KIMURA, S. & BASSETT, A.L. (1992). Therapeutic potential of modulating potassium currents in the diseased myocardium. *FASEB J.*, **6**, 2952–2960.

MANNHOLD, R., VOIGT, W., BAST, A. & TIMMERMAN, H. (1990). Interaction of class I compounds with calmodulin. *Arch. Pharmacol. (Weinheim)*, **323**, 487–491.

MATSUOKA, S., NAWADA, T., HISATOME, I., MIYAMOTO, J., HASEGAWA, J., KOTAKE, H. & MASHIBA, H. (1991). Comparison of $Ca^{2+}$ channel inhibitory effects of cibenzoline with verapamil on guinea-pig heart. *Gen. Pharmacol.*, **22**, 87–91.

MÜLLER, M., DE WEILLE, J.R. & LAZDUNSKI, M. (1991). Chlorpromazine and related phenothiazines inhibit the ATP-sensitive $K^+$ channel. *Eur. J. Pharmacol.*, **198**, 101–104.

NAKABAYASHI, N., ITO, T., IGAWA, T., HIRAIWA, Y., IMAMURA, T., SETA, T., KAWATO, M., USUKURA, N. & TAKEDA, R. (1989). Disopyramide induces insulin secretion and plasma glucose diminution: studies using the in situ canine pancreas. *Metabolism*, **38**, 179–183.

NAKAJIMA, T., SHINOHARA, T., YAOKA, O., FUKUNARI, A., SHINAGAWA, K., AOKI, K., KATOH, A., YAMANAKA, T., SETOGUCHI, M. & TAHARA, T. (1992). Y-27152, a long-acting $K^+$ channel opener with less tachycardia: antihypertensive effects in hypertensive rats and dogs in conscious state. *J. Pharmacol. Exp. Ther.*, **261**, 730–736.

NOACK, T., DEITMER, P., EDWARDS, G. & WESTON, A.H. (1992). Characterization of potassium currents modulated by BRL38227 in rat portal vein. *Br. J. Pharmacol.*, **106**, 717–726.

NOMA, A. (1983). ATP-regulated $K^+$ channels in cardiac muscle. *Nature*, **305**, 147–148.

NOTSU, T., TANAKA, I., TAKANO, M. & NOMA, A. (1992). Blockade of the ATP-sensitive $K^+$ channel by 5-hydroxydecanoate in guinea pig ventricular myocytes. *J. Pharmacol. Exp. Ther.*, **260**, 702–708.

PHILLIPS, R.E., LOOAREESUWAN, S., WHITE, N.J., CHANTHAVANICH, P., KARBWANG, J., SUPANARANOND, W., TURNER, R.C. & WARRELL, D.A. (1986). Hypoglycaemia and antimalarial drugs: quinidine and release of insulin. *Br. Med. J.*, **292**, 1319–1321.

PLANT, T.D. & HENQUIN, J.C. (1990). Phentolamine and yohimbine inhibit ATP-sensitive $K^+$ channels in mouse pancreatic β-cells. *Br. J. Pharmacol.*, **101**, 115–120.

REDER, R.F., DANILO, P. Jr. & ROSEN, M.R. (1980). Effects of pirmenol HCl on electrophysiologic properties of cardiac Purkinje fibers. *Eur. J. Pharmacol.*, **61**, 321–333.

SAKUTA, H., OKAMOTO, K. & WATANABE, Y. (1992a). Blockade by antiarrhythmic drugs of glibenclamide-sensitive $K^+$ channels in *Xenopus* oocytes. *Br. J. Pharmacol.*, **107**, 1061–1067.

SAKUTA, H., SEKIGUCHI, M., OKAMOTO, K. & SAKAI, Y. (1992b). Inactivation of glibenclamide-sensitive $K^+$ channels in *Xenopus* oocytes by various calmodulin antagonists. *Eur. J. Pharmacol.*, **226**, 199–207.

SCHULTZ, A. & HASSELBLATT, A. (1989). An insulin-releasing property of imidazoline derivatives is not limited to compounds that block α-adrenoceptors. *Naunyn-Schmied Arch. Pharmacol.*, **340**, 321–327.

SEMEL, J.D., WORTHAM, E. & KARL, D.M. (1983). Fasting hypoglycemia associated with disopyramide. *Am. Heart J.*, **106**, 1160–1161.

SILVER, P.J., CONNELL, M.J., DILLON, K.M., CUMISKEY, W.R., VOLBERG, W.A. & EZRIN, A.M. (1989). Inhibition of calmodulin and protein kinase C by amiodarone and other class III antiarrhythmic agents. *Cardiovasc. Drugs Ther.*, **106**, 675–682.

SPRUCE, A.E., STANDEN, N.B. & STANFIELD, P.R. (1985). Voltage-dependent ATP-sensitive potassium channel of skeletal muscle membrane. *Nature*, **316**, 736–738.

STURGESS, N.C., ASHFORD, M.L.J., COOK, D.L. & HALES, C.N. (1985). The sulphonylurea receptor may be an ATP-sensitive potassium channel. *Lancet*, **ii**, 474–475.

SZEWCZYK, A., DE WEILLE, J.R. & LAZDUNSKI, M. (1992). TMB-8 (8-(N,N-diethylamino)octyl-3,4,5-trimethoxybenzoate) inhibits the ATP-sensitive $K^+$ channel. *Eur. J. Pharmacol.*, **226**, 175–177.

WEISS, B. & LEVIN, R.M. (1978). Mechanism for selectively inhibiting the activation of cyclic nucleotide phosphodiesterase and adenylate cyclase by antipsychotic agents. *Adv. Cycl. Nucleot. Res.*, **9**, 285–303.

YORIKANE, R., MIZUNO, H., ITOH, Y., KOIKE, H., MIYAKE, S., SHIGA, H., KUMAKURA, S., FUKAMI, M., SHIMOJI, Y., HASHIMOTO, T. & TOMITA, K. (1991). Antiarrhythmic and cardiovascular profiles of the fused indole compound (3aR, 12R, 12aR, 12aS)-12-amino-2,3,3a,4,11,12,12a,12b-octahydro-10-hydroxyisoquino[2,1,8-lma]carbazol-5(1H)-one hydrochloride 1,5 hydrate. *Arzneim. Forsch.*, **41**, 1130–1136.

*(Received November 24, 1992*
*Revised March 2, 1993*
*Accepted March 8, 1993)*

*Br. J. Pharmacol.* (1993), **109**, 873–879 © Macmillan Press Ltd, 1993

# Effects of lisinopril on electromechanical properties and membrane currents in guinea-pig cardiac preparations

[1]Carmen Valenzuela, Onésima Pérez, Oscar Casis, Juan Duarte, Francisco Pérez-Vizcaino, Eva Delpón & Juan Tamargo

Department of Pharmacology, School of Medicine, Universidad Complutense, 28040 Madrid, Spain

**1** The effects of the angiotensin-converting enzyme inhibitor, lisinopril, were studied in guinea-pig atria and papillary muscles and in single isolated ventricular cells.

**2** In isolated right atria, lisinopril (0.001–10 μM) decreased the amplitude and rate of the spontaneous contractions. In electrically driven left atria this negative inotropic effect was accompanied by a shortening of the time to peak tension and time for total contraction.

**3** Lisinopril did not modify the electrophysiological characteristics of the ventricular action potentials recorded in papillary muscles perfused with normal Tyrode solution or elicited by isoprenaline in papillary muscles perfused with 27 mM K Tyrode solution.

**4** In single ventricular cells, lisinopril (10 μM) had no effect on the inward L-type $Ca^{2+}$ ($I_{Ca,L}$), the inward rectifier ($I_{K1}$) or the delayed rectifier $K^+$ currents ($I_K$). However, it abolished the stimulation-dependent facilitation of the L-type $Ca^{2+}$ current.

**6** These results indicate that the negative inotropic effect of lisinopril cannot be explained by a decrease in $Ca^{2+}$ entry through L-type channels and suggest that lisinopril may possibly act at an intracellular site to reduce contractile force.

**Keywords:** Lisinopril; atrial and ventricular muscle; action potentials, L-type $Ca^{2+}$ current; $K^+$ currents; ventricular cells of guinea-pig

## Introduction

Since their introduction, the angiotensin-converting enzyme inhibitors have an established role in the treatment of hypertension and congestive heart failure (Braunwald, 1991). Moreover, recent evidence confirmed that chronic angiotensin-converting enzyme inhibition may improve survival in experimental models (Pfeffer *et al.*, 1985; Sweet *et al.*, 1987) and in patients with asymptomatic (SOLVD, 1992) and severe heart failure of various aetiologies (Consensus, 1987; SOLVD, 1991; Pfeffer *et al.*, 1992). Very recently, it has been found that captopril, a sulphydryl angiotensin-converting enzyme inhibitor, reduced contractile force in guinea-pig isolated hearts (Walker *et al.*, 1988), an effect which in isolated ventricular cells has been attributed to an inhibition of $Ca^{2+}$ entry through voltage-dependent L-type channels, $I_{Ca,L}$ (Bryant *et al.*, 1991). However, it is unknown whether this negative inotropic effect is related or not to the chemical structure (-SH group) of captopril.

Lisinopril, is a non sulphydryl, long-acting angiotensin-converting enzyme inhibitor that is the lysine analogue of enalaprilat, the active form of enalapril (Case, 1987; Lancaster & Todd, 1988). In patients with heart failure, lisinopril produced a sustained haemodynamic response and it has proved to be as effective and well-tolerated as enalapril or captopril (Bach & Zardine, 1992; Zannad *et al.*, 1992; Moyses & Higgins, 1992). Thus, the present experiments were undertaken to: (1) characterize the electromechanical effects of lisinopril in guinea-pig atria and ventricular papillary muscles and (2) determine the effects of this drug on $I_{Ca,L}$, the delayed rectifier ($I_K$) and the inward rectifier $K^+$ currents ($I_{K1}$), in single ventricular myocytes isolated from guinea-pig hearts. This would lead to a further insight into the ionic mechanisms responsible for the electrophysiological effects of lisinopril. A preliminary account of some of the results of this study has already been published (Valenzuela *et al.*, 1992a).

[1] Author for correspondence.

## Methods

### *Isolated atria*

Guinea-pigs of either sex weighing 250–350 g were killed by cervical dislocation. The hearts were rapidly excised and right and left atria were dissected and mounted vertically in a 10 ml organ bath containing Tyrode solution of the following composition (mM): NaCl 137, KCl 5.4, $CaCl_2$ 1.8, $MgCl_2$ 1.05, $NaHCO_3$ 24, $NaH_2PO_4$ 0.42, glucose 5.5. The solutions were bubbled with 95% $O_2$ and 5% $CO_2$ and maintained at 34 ± 0.5°C. Under these conditions, right atria beat spontaneously, while left atria were electrically driven at a basal rate of 1 Hz through bipolar platinum electrodes with rectangular pulses (1 ms duration, twice threshold strength) delivered from a programmable stimulator (Cibertec CS 220). Rate and amplitude of contractions were measured isometrically by FT03 force-displacement transducers and recorded on a Grass polygraph (Tamargo, 1980; Díez *et al.*, 1985). Resting tension was adjusted to 1 g and a 30 min equilibration period was allowed to elapse before control measurements were taken. Peak contractile force, maximum rate of rise of force ($df/dt_{max}$), time to peak tension and time for total contractions were obtained from isometric tracings, and averaged from these successive contractions, as previously described (Díez *et al.*, 1985; Pérez-Vizcaino *et al.*, 1991).

After control values for each parameter were obtained, incremental concentrations of lisinopril were added to the bath, to obtain a complete concentration-response curve. The interval between drug concentrations was 30 min, since preliminary time-response studies indicated that at this time the effects have stabilized. The values for the different parameters, obtained in the absence of lisinopril, were used as a control and compared with those obtained after each increment in drug concentration.

### *Electrophysiological recordings*

The experiments were performed in papillary muscles $<1$ mm in diameter isolated from the right ventricle. The

muscles were pinned to the bottom of a Lucite chamber and superfused continuously at a constant rate of 7 ml $min^{-1}$ with Tyrode solution bubbled with 95% $O_2$ and 5% $CO_2$ and maintained at 34 ± 0.5°C. The preparations were initially driven at 1 Hz and a period of 1 h was allowed for equilibration during which a stable impalement was obtained. Electrical stimulation was applied to the surface of the preparation through Teflon-coated bipolar electrodes of silver wire. Driving stimuli, were rectangular pulses (2 ms duration, twice threshold strength) delivered to the preparation from a multipurpose programmable stimulator (Cibertec CS-220).

Transmembrane action potentials (AP) were conventionally recorded through glass microelectrodes filled with 3 M KCl (tip resistance of 8–15 MΩ). The microelectrode was connected via Ag-AgCl half-cell to a high impedance, capacity neutralizing amplifier (WPI model 701). The maximum rate of depolarization ($V_{max}$) of the action potential was obtained by electronic differentiation (Valenzuela *et al.*, 1988; Delpón *et al.*, 1989; 1991b). The differentiator used had an upper limit of linearity of 1000 V $s^{-1}$ and possessed variable input filters (3 Hz–260 Hz). Stimulus intensity and duration of the stimuli were adjusted to obtain a constant latency (1–2 ms) between stimulus and upstroke of the action potential to minimize latency-induced alterations in $V_{max}$ (Valenzuela *et al.*, 1988). Both action potential and $V_{max}$ were displayed on a storage oscilloscope (Tektronix 5104N) and the oscilloscope traces were photographed with a kymographic camera (Grass C4). After a 1 h equilibration period, control measurements were performed. The preparations were then superfused with Tyrode solutions containing increasing concentrations of lisinopril (0.01–10 μM).

Slow responses were elicited in papillary muscles rendered inexcitable by depolarizing with 27 mM K Tyrode solution. Excitability, i.e. slow action potentials, was restored in depolarized muscles driven at 0.12 Hz by adding isoprenaline (1 μM) to the perfusate (Delpón *et al.*, 1989; 1992).

### *Isolation of cardiac myocytes*

Ventricular myocytes were isolated by enzymatic dissociation following the procedure previously described (Valenzuela & Bennett, 1991; Delpón *et al.*, 1991a). Guinea-pigs of either sex (200–300 g) were killed by cervical dislocation. Their hearts were rapidly removed and mounted on a Langendorff perfusion system for retrograde coronary perfusion at a constant rate of 10–15 ml $min^{-1}$. Hearts were initially perfused for 1–2 min with a modified Tyrode solution which contained 1.8 mM $CaCl_2$ and then with a nominally calcium-free solution at 37°C for a further 5 min. Thereafter, the hearts were perfused for another 4 min with the same solution supplemented with 0.12 mg $ml^{-1}$ collagenase (type 1a, Sigma Chemical Co., London) and 0.03 mg $ml^{-1}$ protease (type XIV, Sigma Chemical Co., London). Afterwards the hearts were washed with a high-$K^+$, low $Cl^-$ solution (KB solution) for 4 min and then removed from the Langendorff column and the ventricles dissected and cut into small pieces which were placed in a beaker containing KB solution and gently shaken to disperse the isolated cells. The resulting cell pellet was stored in KB medium for 1–2 h before beginning the experiment. The composition of the Tyrode solution was (mM): NaCl 114, KCl 5.4, $CaCl_2$ 1.8, $MgCl_2$ 1.0, taurine 20, glucose 10, $NaHCO_3$ 24 and $NaH_2PO_4$ 0.42; pH was adjusted to 7.4 by addition of NaOH. The solution was bubbled with 95% $O_2$:5% $CO_2$. Nominally calcium-free Tyrode solution was prepared by simply omitting $CaCl_2$ from the Tyrode solution. The KB solution contained (mM): glutamic acid 70, taurine 10, KCl 20, $KH_2PO_4$ 10, $MgCl_2$ 1.0, succinic acid 5.0, creatine 5.7, dextrose 10.0, EGTA-K 0.2 and HEPES-K 10.0; the pH was adjusted to 7.4 by addition of KOH. All experiments were performed at room temperature (22–23°C) on calcium-tolerant healthy ventricular myocytes (80–100 μm in length) identified by their rod-like and uniformly spaced cross-striated appearance.

A small aliquot of a suspension of dissociated cells was transferred to a 0.5 ml chamber placed on the stage on an inverted microscope (Nikon TMS, Nikon Co., Tokyo). After settling to the bottom of the chamber, cells were superfused with Tyrode solution at 1 ml $min^{-1}$.

The recording pipette (internal) solution contained (mM): K-aspartate 80, KCl 42, $KH_2PO_4$ 10, phosphocreatine 3, HEPES 5.0, MgATP 4, EGTA 5 (pH 7.2 with KOH). When analysing the $K^+$ currents the external solution contained (mM): NaCl 136, KCl 5.4, $CaCl_2$ 1.0, $MgCl_2$ 1.0, $CoCl_2$ 2.0, tetrodotoxin (TTX) 0.03, glucose 10 and HEPES 10; the pH was adjusted to 7.4 by addition of NaOH. To minimize outward $K^+$ currents when analysing the $I_{Ca,L}$, a rich Cs internal solution was used in which K-aspartate and KCl were replaced by Cs-aspartate and CsCl, respectively, and the pH was adjusted to 7.4 by CsOH.

### *Current recording*

Membrane currents were measured by the perforated nystatin patch configuration of the patch-clamp technique (Hamill *et al.*, 1981; Horn & Marty, 1988) using an Axopatch-1C clamp amplifier (Axon Instruments, Foster City, CA, U.S.A.). This method led to permeabilizing cardiac myocytes and recording calcium and potassium currents without a washout of the intracellular media, thus preventing the 'run-down' which these currents exhibit with classical whole-cell recording (Kurachi *et al.*, 1989; Valenzuela *et al.*, 1992b). Micropipettes were constructed from borosilicate glass capillary tubes (Narishige GD-1, Narishige Co., Ltd., Tokyo, Japan) using a programmable patch micropipette puller (Model P-87 Brown-Flaming, Sutter Instruments Co., Novato, CA, U.S.A.). The pipettes had a resistance of 2–4 MΩ when filled with the internal solution and immersed in the Tyrode solution. A liquid junction potential of − 9 mV between the pipette solution and the external solution was corrected for. Series resistance was compensated by an analog circuit. Capacitative and linear leak currents were subtracted by an analogue circuit or digitally by computer. Voltage-clamp command pulses were generated by a 12-bit digital-to-analogue converter. Membrane currents were filtered at 1 kHz (− 3 dB) by a four-pole Bessel filter before sampling was done at 2 kHz by a 12-bit analogue-to-digital converter. During the experiments, membrane potential and current data were displayed on a storage oscilloscope (Tektronix model 7854, Beaverton, OR, U.S.A.) and stored on the hard disk of a Hewlett Packard Vectra QS/16S computer using an analogue-to-digital converter (Interface TL-1, Axon Instruments Inc., Burlingame, CA, U.S.A.) controlled by acquisition and display software (pClamp 5.5. Axon Instruments Inc.) (Valenzuela & Bennett, 1991; Delpón *et al.*, 1991a; Valenzuela *et al.*, 1992b).

The $I_{Ca,L}$ was elicited by applying depolarizing clamp steps of 500 ms from a holding potential of − 40 mV at a rate of 0.3 Hz. Peak inward $I_{Ca,L}$ was measured relative to the zero current level (bath ground). Steady-state membrane currents were monitored by applying hyperpolarizing and depolarizing clamp steps of 5 s duration from a holding potential of − 40 mV at a rate of 0.05 Hz. The steady-state membrane current was measured as the net current at the end of the 5 s clamp step referred to the zero current level. The delayed rectifier $K^+$ current ($I_K$) was monitored by measuring the outward tail currents elicited at the end of 5 s depolarizing clamp steps and return to − 30 mV. The amplitude of tail currents was measured as the difference between the peak outward tail current and the steady current level after decay of the tail current. A holding potential of − 40 mV was used to inactivate the $I_{Na}$ and the T-type $Ca^{2+}$ channels.

After a 15 min period for control measurements, the perfusate was changed to one containing 10 μM lisinopril and data were collected again after 10 min.

### *Drugs*

Lisinopril (ICI Pharma, S.A.) as a powder was initially dissolved in distilled deionized water to make 1 mM stock solutions. Further dilutions were carried out in Tyrode solution to obtain final concentrations between 0.01 and 10 μM.

### *Data analysis and curve fitting*

All data are given as mean ± s.e.mean and Student's *t* test was used to estimate the significance of differences from control values. To analyse block at different voltages or drug concentrations, two-way analysis of variance and Scheffe's test for critical difference were used (Wallenstein *et al.*, 1980). A *P* value of less than 0.05 was considered to be significant.

$I_K$ activation curves were fitted by a Boltzmann distribution using a least-squares fitting routine described by Marquardt (1963)

$$I_K/I_{Kmax} = 1/(1 + \exp[(V_h - V_m)/k])$$

where $V_h$ is the half-point of activation (in mV), $V_m$ is the test potential and k the slope factor for the activation curve (in mV).

## Results

### *Effects on atrial rate and contractile force*

The effects of lisinopril, 0.001–10 μM were studied on rate and amplitude of spontaneous contractions in 9 right atria. Control values for rate and contractile force averaged 160.0 ± 6.8 beats $min^{-1}$ and 510 ± 30.0 mg, respectively. As is shown in Figure 1a, lisinopril (0.01–10 μM) produced a concentration-dependent decrease in the amplitude of atrial contractions which reached statistically significant values at concentrations ⩾ than 0.1 μM. However, at the range of concentrations studied, lisinopril has no effect on atrial rate and sinus node recovery time (not shown).

In 9 left atria driven at a basal rate of 1 Hz the averaged control values of the isometric contractile parameters were: peak contractile force = 631.5 ± 29.8 mg, $df/dt_{max}$ = 14.3 ± 1.2 mg $ms^{-1}$, time to peak tension = 65.3 ± 3.9 ms and the time for total contraction = 211.1 ± 9.1 ms. Figure 1b shows that lisinopril (0.01–10 μM) also decreased the peak contractile force in a concentration-dependent manner, an effect which reached significant values at all concentrations tested. This negative inotropic effect was accompanied by a parallel decrease in $df/dt_{max}$ and by a significant shortening of the time to peak tension and time for total contraction.

### *Effects on action potential characteristics*

The effects of lisinopril in a range of concentrations between 0.01 μM and 10 μM were studied in 8 ventricular papillary muscles stimulated at a basal frequency of 1 Hz. Results obtained under control conditions and 30 min after each increment in drug concentration are shown in Table 1. It can be observed that lisinopril did not produce significant effects on the resting membrane potential, phase 0 characteristics (amplitude and $V_{max}$) and duration of the ventricular action potentials at 50% ($APD_{50}$) and 90% ($APD_{90}$) repolarization at any of the concentrations tested. No changes were also observed in the duration of the ventricular effective refractory period.

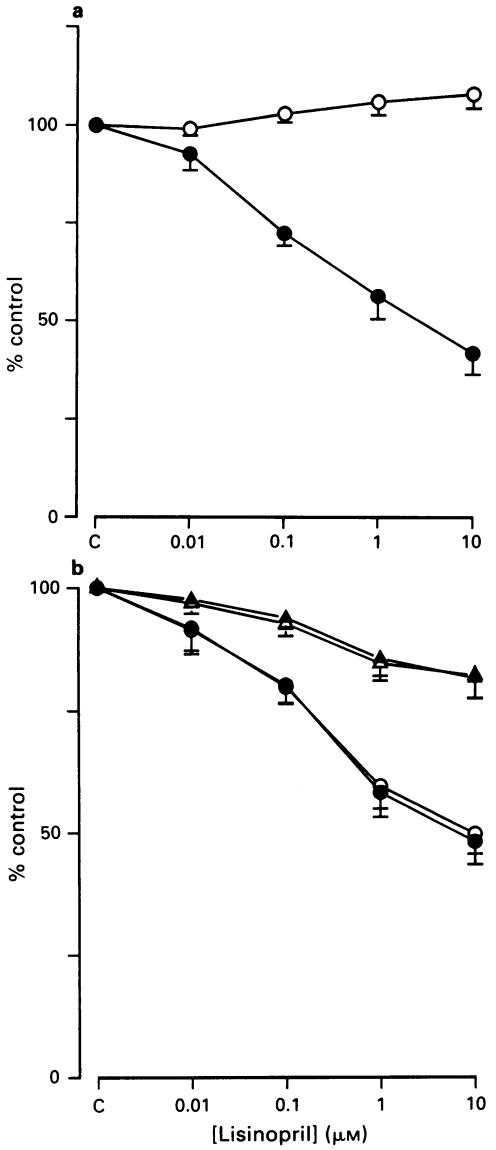



**Figure 1** (a) The effect of lisinopril on rate (○) and amplitude (●) of spontaneous contractions in guinea-pig right atria; (b) the effect of lisinopril on peak contractile force (●), maximum rate of rise of force (○), time to peak tension (▲) and time for total contraction (△) in left atria driven at a basal rate of 1 Hz. Ordinate scale: percentage of control values. Abscissa scale: lisinopril expressed as micromolar concentration. Each point represents the mean of 8 experiments ± s.e.mean.

**Table 1** Electrophysiological effects of lisinopril on transmembrane action potentials in guinea-pig papillary muscles driven at 1 Hz

| *Drug concentration* (μM) | *RMP* (mV) | *APA* (mV) | $V_{max}$ (V $s^{-1}$) | $APD_{50}$ (ms) | $APD_{90}$ (ms) |
|---|---|---|---|---|---|
| 0 | 82.0 ± 0.8 | 118.0 ± 1.6 | 185.4 ± 8.3 | 161.3 ± 10.9 | 191.3 ± 10.9 |
| 0.01 | 82.6 ± 0.7 | 117.0 ± 2.2 | 184.9 ± 8.2 | 148.2 ± 10.6 | 180.4 ± 10.8 |
| 0.1 | 82.0 ± 0.8 | 117.6 ± 1.7 | 183.6 ± 7.8 | 150.3 ± 8.7 | 181.9 ± 10.2 |
| 1 | 82.0 ± 0.7 | 117.6 ± 1.9 | 189.0 ± 8.7 | 145.3 ± 10.5 | 177.6 ± 11.0 |
| 10 | 82.0 ± 1.2 | 117.8 ± 1.9 | 194.6 ± 8.6 | 141.4 ± 11.1 | 171.8 ± 11.6 |

Values are given ± s.e.mean. $n = 8$.

The effects of lisinopril were also studied on the characteristics of the slow action potentials induced by 1 μM isoprenaline in papillary muscles perfused with 27 mM K Tyrode solution and driven at a basal rate of 0.12 Hz. Table 2 summarizes the results obtained in 8 muscles. Lisinopril over the range of concentrations tested (0.01–10 μM) did not modify the resting membrane potential, amplitude, $V_{max}$ and $APD_{50}$ and $APD_{90}$ values of the slow action potentials. These results suggest that the drug did not exhibit class IV antiarrhythmic ($Ca^{2+}$ channel blocking) actions.

### *Effect on* $I_{Ca,L}$

To determine the effects of lisinopril (10 μM) on the L-type $Ca^{2+}$ current ($I_{Ca,L}$), ventricular cells were clamped to a holding potential of − 40 mV, and 500 ms depolarizing pulses were applied every 40 s to membrane potentials between − 30 and + 70 mV. Figure 2a shows typical recording of $I_{Ca,L}$ elicited when 500 ms depolarizing pulses were applied from − 40 mV to + 10 mV in control conditions and in the presence of 10 μM lisinopril. Under control conditions, depolarizing pulses were applied first, evoking the activation of an inward current, which was then followed by the inactivation process. As is shown, 10 μM lisinopril did not modify the maximum amplitude or the inactivation time course of the $I_{Ca,L}$.

Figure 2b shows the current-voltage relationship when a family of 500 ms depolarizing pulses were applied from − 40 to membrane potentials between − 30 and + 70 mV in the absence and in the presence of 10 μM lisinopril. In the absence of lisinopril, the current-voltage relation started at a threshold of − 30 mV, reached a maximum at + 10 mV and the apparent reversal potential at + 50 mV. In 6 cells the averaged peak amplitude of $I_{Ca,L}$ at + 10 mV was 193.9 ± 35.0 pA. This current was abolished within 2–3 min after perfusion with 2 mM Co-containing solution, an inorganic $I_{Ca,L}$ blocker (Isenberg & Klöckner, 1982), but it was insensitive to 10 μM tetrodotoxin (TTX) a specific blocker of $I_{Na}$. Therefore, the recorded inward current was identified as the $I_{Ca,L}$. Lisinopril did not modify either the threshold potential, the potential at which the current reached its maximum or its apparent reversal potential. These findings indicate that lisinopril does not inhibit the $I_{Ca,L}$.

### *Effects of lisinopril on facilitation of* $I_{Ca,L}$

An increase (facilitation) of L-type $Ca^{2+}$ current has been observed when increasing the rate of repetitive depolarization in guinea-pig ventricular myocytes (Mitra & Morad, 1986; Lee, 1987; Zygmunt & Maylie, 1990). Figure 3 shows the effect of stimulation upon $I_{Ca,L}$. Under control conditions, following the application of a train of 16 depolarizing pulses of 200 ms duration from a holding potential of − 40 mV to + 10 mV, at a rate of 0.5 Hz, there was a progressive increase in the $I_{Ca,L}$ amplitude, which is maximal within five pulses. In 5 cells, the facilitation of the $I_{Ca,L}$ measured as the increase in the amplitude of the current, at the fifth pulse of the train, averaged 20.1 ± 11.1%. The figure also shows that the initial rate of increase of the current was unchanged by repetitive depolarization and that the facilitation of $I_{Ca,L}$ was associated with a reduction in the rate of inactivation. However, in the presence of 10 μM lisinopril this phenomenom was abolished (− 0.05 ± 0.005% with respect to the first pulse of the train; $P<0.001$).

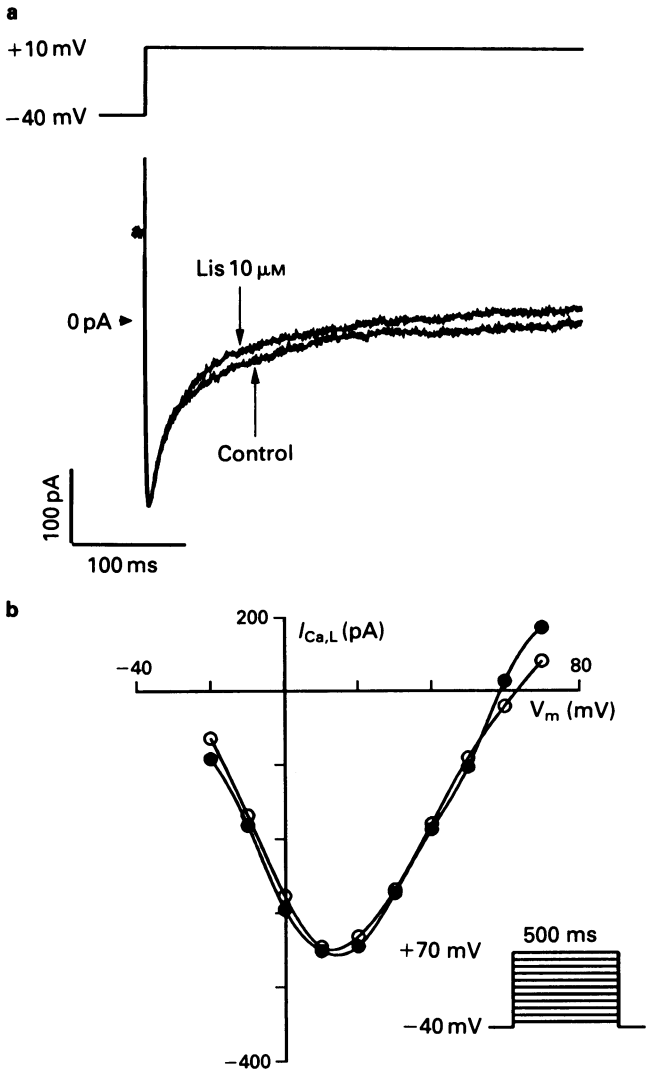



**Figure 2** Effect of 10 μM lisinopril on L-type $Ca^{2+}$ current ($I_{Ca,L}$): (a) examples of current records after depolarizing clamp pulses of 500 ms duration to + 10 mV from a holding potential of − 40 mV before (Control) and after 10 min exposure to lisinopril (Lis); (b) effects of lisinopril on the current-voltage relationship of peak $I_{Ca,L}$ when applying 500 ms depolarizing pulses from − 40 mV to + 70 mV in 10 mV steps as shown in the inset. Each point represents the mean value obtained in 6 cells before (●) and after exposure to lisinopril (○). Standard error bars were omitted for clarity.

**Table 2** Electrophysiological effects of lisinopril on slow action potentials induced by isoprenaline in guinea-pig papillary muscles driven at 0.1 Hz

| *Drug concentration* (μM) | *RMP* (mV) | *APA* (mV) | $V_{max}$ (V $s^{-1}$) | $APD_{50}$ (ms) | $APD_{90}$ (ms) |
|---|---|---|---|---|---|
| 0 | 45.4 ± 1.6 | 83.8 ± 1.0 | 14.8 ± 0.3 | 220.0 ± 10.8 | 240.0 ± 10.9 |
| 0.01 | 45.0 ± 2.5 | 83.0 ± 1.2 | 14.6 ± 0.1 | 215.8 ± 12.3 | 236.6 ± 14.4 |
| 0.1 | 45.2 ± 1.5 | 84.3 ± 1.2 | 14.6 ± 0.4 | 230.5 ± 12.4 | 248.5 ± 13.4 |
| 1 | 45.6 ± 1.7 | 82.4 ± 1.6 | 14.3 ± 0.2 | 211.0 ± 17.6 | 231.5 ± 18.9 |
| 10 | 46.0 ± 2.0 | 83.2 ± 0.8 | 14.3 ± 0.3 | 226.5 ± 10.3 | 245.5 ± 10.5 |

Values are given ± s.e.mean. $n = 8$.

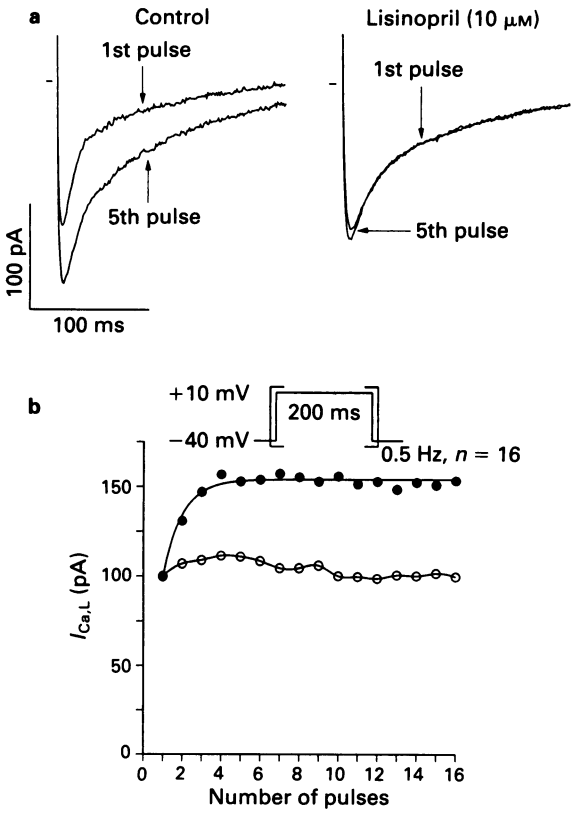



**Figure 3** Effects of 10 μM lisinopril on facilitation of $I_{Ca,L}$. The cells were repetitively depolarized from a holding potential of − 40 mV to a test potential of + 10 mV with a train of 16 pulses of 200 ms duration at a frequency of 0.5 Hz. In (a), current traces obtained during the first (labelled 1) and fifth (labelled 5) pulse are superimposed before (Control) and after 10 min exposure to lisinopril; (b) the facilitation of $I_{Ca,L}$ during the application of a train of pulses in 5 cells in the absence (●) and presence (○) of lisinopril. Standard error bars were omitted for clarity.

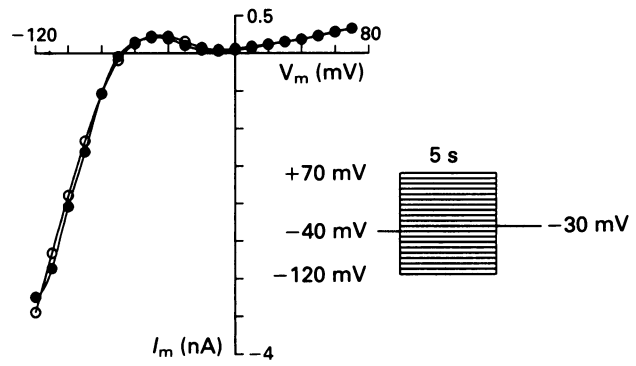



**Figure 4** Effects of lisinopril on the mean steady-state relationship measured in 6 cells when applying 5 s depolarizing or hyperpolarizing pulses in 10 mV steps from a holding potential of − 40 mV. Values were obtained during control perfusion (●) and following 10 min exposure to 10 μM lisinopril (○). Cells were superfused with 2 $mM^{-1}$ Co containing solution.

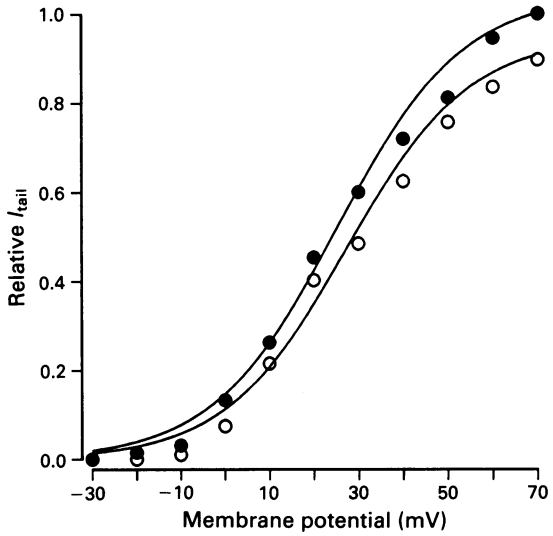



**Figure 5** Effects of lisinopril on the voltage-dependance of $I_K$ was assessed in 5 cells by measuring the amplitude of the tail currents ($I_{tail}$) elicited on return to − 30 mV after 5 s depolarizing pulses from a holding potential of − 40 mV to different test potentials (from − 30 to + 70 mV in 10 mV steps) applied every 30 s. Values were obtained during control perfusion (●) and following 10 min exposure to 10 μM lisinopril (○). The continuous line is the best fit obtained using a Boltzmann equation: $I_K/I_{Kmax} = 1/(1 + \exp[(V_h - V_m)/k])$, where $V_h$ is the half-point of activation (in mV), $V_m$ is the test potential and k the slope factor for the activation curve (in mV).

### *Effect on outward K currents*

The effect of lisinopril on the delayed outward ($I_K$) and the inward rectifying potassium currents ($I_{K1}$) were also studied in 6 cells. In these experiments the holding potential was maintained at − 40 mV to inactivate inward $Na^+$ and T-type $Ca^{2+}$ currents. In addition, the external solution contained 30 mM TTX and 2 mM $CoCl_2$ to block the $Na^+$ and L-type $Ca^{2+}$ currents, respectively. $I_K$ was activated by 5 s depolarizing pulses to potentials from − 30 to + 70 mV (Matsuura *et al.*, 1987) and $I_{K1}$ by hyperpolarizing pulses ranging from − 50 to − 120 mV. Figure 4 shows the effects of lisinopril on the current-voltage relationship. It can be observed that neither the current amplitude of the current induced by depolarizing pulses ($I_K$) nor the current evoked by hyperpolarizing pulses negative to − 40 mV ($I_{K1}$) was affected by 10 μM lisinopril.

The effects of 10 μM lisinopril on the voltage-dependence of $I_K$ was assessed by measuring the amplitude of the tail currents ($I_{tail}$) observed on return to − 30 mV after 5 s-depolarizing pulses to different test potentials (from − 30 to + 70 mV in 10 mV steps) applied every 30 s from a holding potential of − 40 mV. In Figure 5, the currents were normalized relative to the maximum control $I_{tail}$ amplitude for each experiment (value of 1.0) and the resulting values were plotted as a function of membrane potential. Under control conditions the amplitude of $I_{tail}$ recorded at − 30 mV after a depolarizing pulse to + 50 mV averaged 149.4 ± 7.7 pA ($n = 5$). Lisinopril, 10 μM, did not modify the maximum amplitude of the $I_{tail}$ measured at − 30 mV (140.2 ± 10.5 pA, $n = 5$, $P > 0.05$). Under these experimental conditions, $I_K$ was activated at potentials positive to − 30 mV and its amplitude increased at more depolarized levels. In the absence of lisinopril, the half-point ($V_h$) and the slope factor (k) of the steady-state $I_K$ activation curves were 22.3 ± 2.4 mV and 14.2 ± 0.2 mV ($n = 6$) and in the presence of lisinopril 21.5 ± 2.9 mV ($P > 0.05$) and 14.6 ± 0.8 mV ($P > 0.05$), respectively.

## Discussion

The main findings of this study are two fold. First, lisinopril produced a concentration-dependent decrease in peak contractile force in guinea-pig isolated atria. Second, this negative inotropic effect was produced by a range of concentrations of lisinopril that did not modify atrial rate, nor the characteristics of fast ($Na^+$-dependent) and slow ($Ca^{2+}$-

dependent) ventricular action potentials, nor the inward $Ca^{2+}$ current ($I_{Ca,L}$), the delayed rectifier ($I_K$) and the inward rectifier $K^+$ currents ($I_{K1}$).

Both in spontaneously beating right atria and in electrically driven left atria lisinopril produced a concentration-dependent decrease in atrial contractile force. This negative inotropic effect was accompanied by a parallel decrease in the $d\,f/d\,t_{max}$ and by a concentration-dependent shortening of the time to peak tension and the time for total contraction. However, lisinopril had no effect on atrial rate and sinus node recovery time, which suggested that it does not exert a direct inhibition of the sinus node function. Captopril also produced a negative inotropic effect in guinea-pig isolated hearts (Walker *et al.*, 1988) and this effect was attributed to an inhibition of $I_{Ca,L}$ (Bryant *et al.*, 1991). However, in the present experiments the decrease in contractile force appeared at concentrations at which lisinopril had no effect on the duration of the cardiac action potentials. Consequently, it seemed unlikely that its negative inotropic effect was related to a decrease of $Ca^{2+}$ entry through L-type channels. Moreover, lisinopril had no effect on the amplitude of $V_{max}$ of the slow upstroke action potentials induced in $K^+$-depolarized ventricular fibres where the $I_{Na}$ has been voltage-inactivated. Under these conditions, excitability (i.e. slow action potentials) was restored by isoprenaline which increases the open probability of the L-type $Ca^{2+}$ channels (Tsien *et al.*, 1986). Since the $V_{max}$ of the slow action potentials can be considered as a valid index of the $I_{Ca,L}$ (Malecot *et al.*, 1988), these results suggest that lisinopril has no inhibitory effect on this ionic current. To determine whether lisinopril directly inhibits the $I_{Ca,L}$, its effects were analysed on single isolated guinea-pig ventricular cells. Under these conditions a concentration of lisinopril (10 $\mu$M), which reduced the developed contractile force by almost 50%, had no effect on the amplitude or the voltage-dependent properties of the $I_{Ca,L}$. Therefore, and in contrast to what has been previously described with captopril (Bryant *et al.*, 1991), the present experiments demonstrated that the negative inotropic effect of lisinopril cannot be explained through a decrease in $Ca^{2+}$ entry via L-type channels.

Another possible explanation for the decrease in contractility is that lisinopril may possibly act at an intracellular site to reduce contractile force. Two experimental observations support this hypothesis. First, the negative inotropic effect was accompanied by a shortening in the time to peak tension and time for total contraction. These results suggested that lisinopril may decrease the release of $Ca^{2+}$ from the sarcoplasmic reticulum and/or increase the re-uptake of $Ca^{2+}$ in the sarcoplasmic reticulum, but this cannot be determined on the basis of the present results. Second, lisinopril suppressed the increase (facilitation) of the $I_{Ca,L}$ observed during repetitive depolarization in guinea-pig ventricular myocytes (Mitra & Morad, 1986; Lee, 1987; Zygmunt & Maylie, 1990). Facilitation of $I_{Ca,L}$ seems to be mediated by a transient rise in $Ca^{2+}$ near to the inner pore of $Ca^{2+}$ channels, resulting in a reduction in the rate of $Ca^{2+}$-dependent inactivation of $I_{Ca,L}$ and facilitation of $Ca^{2+}$ current during subsequent depolarizations (Zygmunt & Maylie, 1990). Facilitation is also abolished by high concentrations of isoprenaline or caffeine (Tseng, 1988; Zygmunt & Maylie, 1990) which suggest that facilitiation of $I_{Ca,L}$ reflects a change in $Ca^{2+}$ channel phosphorylation (Fedida *et al.*, 1988). Whether lisinopril exerts a similar effect at these levels deserves further investigation.

Lisinopril had no effect on resting membrane potential, amplitude and $V_{max}$ of the action potentials recorded in papillary muscles perfused with Tyrode solution. The lack of effect on phase 0 characteristics strongly suggested that lisinopril did not exert an inhibitory effect on the fast inward sodium current ($I_{Na}$) or the late $Na^+$ current flowing during the plateau in guinea-pig ventricular myocytes (Kiyosue & Arita, 1989). In addition, it explains why lisinopril did not modify intra-atrial and intraventricular excitability and conduction in experimental animals and in man (Lancaster & Todd, 1988). In guinea-pig ventricular cells the repolarization process is mainly due to the interplay between inward ($I_{Ca,L}$ and slowly inactivating or late $Na^+$ current) and outward currents ($I_K$ and $I_{K1}$) (Carmeliet & Vereecke, 1979; Kiyosue & Arita, 1989). The present study demonstrated that lisinopril did not modify any of these ionic currents underlying the maintenance of the action potential plateau, which can explain why no effect was observed on the duration of the action potentials recorded either in normally polarized or in depolarized papillary muscles. Furthermore, the lack of effect on ionic currents evoked by clamp pulses negative to $-30$ mV, which are mainly due to the $I_{K1}$, can explain why it did not modify the resting membrane potential in papillary muscles.

The possible clinical relevance of the present results in patients with congestive heart failure remains to be assessed. The beat dependence of facilitation of $I_{Ca,L}$ is similar to that of the positive staircase (Lee, 1987) and the decay of the inotropic state following postextrasystolic potentiation (Morad & Goldman, 1973). Thus, this phenomenon may play a physiological role in the generation of the force staircase of the heart (Lee, 1987; Zygmunt & Maylie, 1990). However, the net haemodynamic effects of lisinopril result from a complex interplay among direct and indirect cardiac and vascular actions each having the potential to influence the major determinants of cardiac performance (Case, 1987; Lancaster & Todd, 1988). *In vivo*, its most marked effect is a decrease in peripheral vascular resistances which explains the decrease in systemic blood pressure and improved left ventricular systolic performance due to afterload reduction. Thus, it is possible that the direct negative inotropic effect of lisinopril can be counterbalanced *in vivo* by its potent arterial vasodilator action which reduced left ventricular afterload, overriding the expected direct cardiodepressant effects of the drug.

We thank Dr M. Martin (ICI Farma, S.A.) for the generous gift of lisinopril. Financial support was provided by a CICYT Grant (SAF-92-0157) and by ICI Farma, S.A.

## References

BACH, R. & ZARDINI, P. (1992). Long-acting angiotensin-converting enzyme inhibition: once-daily lisinopril versus twice-daily captopril in mild-to-moderate heart failure. *Am. J. Cardiol.*, **70**, 70C–77C.

BRAUNWALD, E. (1991). ACE inhibition- a cornerstone of the treatment of congestive heart failure. *N. Engl. J. Med.*, **325**, 351–353.

BRYANT, S.M., RYDER, K.O. & HART, G. (1991). Effects of captopril on membrane current and contraction in single ventricular myocytes from guinea-pig. *Br. J. Pharmacol.*, **102**, 462–466.

CARMELIET, E. & VEREECKE, J. (1979). Electrogenesis of the action potential and automaticity. In *The Handbook of Physiology. The Cardiovascular System*, Vol. 1. ed. Berne, R., Speralakis, N. & Geiger, S. pp. 269–334. Bethesda: American Physiological Society.

CASE, D.E. (1989). The clinical pharmacology of lisinopril. *J. Human Hypertens.*, **3** (suppl. 1), 127–132.

THE CONSENSUS TRIAL STUDY GROUP (1987). Effects of enalapril on mortality in severe congestive heart failure: results of the Cooperative North Scandinavian Enalapril Survival study (CONSENSUS). *N. Engl. J. Med.*, **316**, 1429–1435.

DELPON, E., VALENZUELA, C. & TAMARGO, J. (1989). Electrophysiological effects of E-3753, a new antiarrhythmic drug, in guinea-pig ventricular muscles. *Br. J. Pharmacol.*, **96**, 970–976.

DELPON, E., SANCHEZ-CHAPULA, J. & TAMARGO, J. (1991a). Further characterization of the effects of imipramine on plateau membrane currents in guinea-pig ventricular myocytes. *Naunyn Schmied. Arch. Pharmacol.*, **344**, 645–652.

DELPON, E., VALENZUELA, C. & TAMARGO, J. (1991b). Electrophysiological effects of the combination of mexiletine and flecainide in guinea-pig ventricular fibres. *Br. J. Pharmacol.*, **103**, 1411–1416.

DELPON, E., VALENZUELA, C., PEREZ, O. & TAMARGO, J. (1992). Electrophysiological effects of CRE-1087 in guinea-pig ventricular fibres. *Br. J. Pharmacol.*, **107**, 515–520.

DIEZ, J., TAMARGO, J. & VALENZUELA, C. (1985). Negative inotropic effect of somatostatin in guinea-pig atrial fibres. *Br. J. Pharmacol.*, **86**, 547–555.

FEDIDA, D., NOBLE, D. & SPINDLER, A. (1988). Mechanism of the use dependence of $Ca^{2+}$ current in guinea-pig myocytes. *J. Physiol.*, **405**, 461–475.

HAMILL, O., MARTY, A., NEHER, E., SACKMANN, B. & SIGWORTH, F. (1981). Improved patch-clamp techniques for high resolution current recording from cells and cell-free membrane patches. *Pflügers Arch.*, **391**, 85–100.

HORN, R. & MARTY, A. (1988). Muscarinic activation of ionic currents measured by a new whole-cell recording method. *J. Gen. Physiol.*, **92**, 145–159.

ISENBERG, G. & KLOCKNER, U. (1982). Calcium currents of isolated bovine ventricular myocytes are fast and of large amplitude. *Pflügers Arch.*, **395**, 30–41.

KIYOSUE, T. & ARITA, M. (1989). Late sodium current and its contribution to action potential configuration in guinea-pig ventricular myocytes. *Circ. Res.*, **64**, 389–397.

KURACHI, Y., ASANO, Y., TAKIKAWA, R. & SUGIMOTO, T. (1989). Cardiac Ca current does not run down and is very sensitive to isoprenaline in the nystatin-method of whole cell recording. *Naunyn-Schmied. Arch. Pharmacol.*, **340**, 219–222.

LANCASTER, S. & TODD, P. (1988). Lisinopril: a preliminary review of its pharmacodynamic and pharmacockinetic properties, and therapeutic use in hypertension and congestive heart failure. *Drugs*, **35**, 646–669.

LEE, K.S. (1987). Potentiation of the calcium-channel currents of internally perfused mammalian heart cells by repetitive depolarization. *Proc. Natl. Acad. Sci. U.S.A.*, **84**, 3941–3945.

MALECOT, C.O. & TRAUTWEIN, W. (1987). On the relationship between $V_{max}$ of slow responses and Ca-current availability in whole-cell clamped guinea pig heart cells. *Pflügers Arch.*, **410**, 15–22.

MARQUARDT, D.W. (1963). An algorithm for least-squares estimation of nonlinear parameters. *J. Soc. Ind. Appl. Math.*, **11**, 431–441.

MATSUURA, H., EHARA, T. & IMOTO, Y. (1987). An analysis of the delayed outward current in single ventricular cells of the guinea-pig. *Pflügers Arch.*, **410**, 596–603.

MITRA, R. & MORAD, M. (1986). Two types of calcium channels in guinea-pig ventricular myocytes. *Proc. Natl. Acad. Sci. U.S.A.*, **83**, 5340–5344.

MORAD, M. & GOLDMAN, Y. (1973). Excitation-cntraction coupling in heart muscle: membrane control for development of tension. *Prog. Biophys. Mol. Biol.*, **27**, 257–313.

MORAD, M. & GOLDMAN, Y. (1973). Excitation-contraction coupling in heart muscle: membrane control for development of tension. *Prog. Biophys. Mol. Biol.*, **27**, 257–313.

PEREZ-VIZCAINO, F., CARRON, R, DELPON, E. & TAMARGO, J. (1991). Effects of (S)-nafenodone, a new antidepressant, in isolated guinea-pig atrial and ventricular muscles fibres. *Eur. J. Pharmacol.*, **199**, 43–50.

PFEFFER, J.M., PFEFFER, M.A. & BRAUNWALD. E. (1985). Influence of chronic captopril therapy on the infarcted left ventricle of the rat. *Circ. Res.*, **57**, 84–95.

PFEFFER, M.A., BRAUNWALD, E., MOYE, L., BASTA, L., BROWN, E.J., CUDDY, T.E., DAVIS, B.R., GELTAN, E.M., GOLDMAN, S., FLACKER, G.G., KLEIN, M., LAMAS, G., PACKER, M., ROULEAU, G.C., ROULEAU, J.L., RUTHERFORD, J., WERTHEIMER, J.H. & HAWKINS, C.M. on behalf of the SAVE investigators (1992). Effect of captopril on mortality and morbidity in patients with left ventricular dysfunction after myocardial infarction. Results of the Survival and Ventricular Enlargement Trial. *N. Engl. J. Med.*, **327**, 669–677.

THE SOLVD INVESTIGATORS (1991). Effects of angiotensin converting enzyme inhibition with enalapril on survival in patients with reduced left ventricular ejection fractions and congestive heart failure: Results of the Treatment Trial of the Studies of Left Ventricular Dysfunction (SOLVD): a randomized double blind trial. *N. Engl. J. Med.*, **325**, 293–302.

THE SOLVD INVESTIGATORS (1992). Effect of enalapril on mortality and the development of heart failure in asymptomatic patients with reduced left ventricular ejection fractions. *N. Engl. J. Med.*, **327**, 685–691.

SWEET, C.S., EMMERT, S.E., STABILITO, I. & RIBEIRO, L.G. (1987). Increased survival in rats with congestive heart failure. *J. Cardiovasc. Pharmacol.*, **10**, 636–642.

TAMARGO, J. (1980). Electrophysiological effects of bunaphtine on isolated rat atria. *Eur. J. Pharmacol.*, **62**, 10–19.

TSENG, G. (1988). Calcium current restitution in mammalian ventricular myocytes is modulated by intracellular calcium. *Circ. Res.*, **63**, 468–482.

TSIEN, R., BEAN, B.P., HESS, H., LANSMAN, L., NILIUS, B. & NOWYCKY, M. (1986). Mechanisms of calcium channel modulation by β-adrenergic agents and dihydropyridine calcium agonists. *J. Mol. Cell. Cardiol.*, **18**, 691–710.

VALENZUELA, C. & BENNETT, P. (1991). Voltage- and use-dependent modulation of calcium channel current in guinea-pig ventricular cells by amiodarone and des-oxo-amiodarone. *J. Cardiovasc. Pharmacol.*, **17**, 894–902.

VALENZUELA, C., DELPON, E. & TAMARGO, J. (1988). Tonic and frequency-dependent Vmax block induced by 5-hydroxypropafenone in guinea-pig ventricular muscles. *J. Cardiovasc. Pharmacol.*, **12**, 423–431.

VALENZUELA, C., PEREZ, O., CASIS, O., DUARTE, J., DELPON, E., PEREZ-VIZCAINO, F. & TAMARGO, J. (1992a). Effects of lisinopril on contractility and electrophysiological properties in guinea-pig cardiac preparations. *Br. J. Pharmacol.*, **107**, 135P.

VALENZUELA, C., SANCHEZ-CHAPULA, J., DELPON, E., PEREZ, O., ELIZALDE, A. & TAMARGO, J. (1992b). Imipramine (IMI) blocks $I_{k,r}$ and delays $I_{k,s}$ activation in guinea-pig ventricular myocytes. *Biophys. J.*, **61**, A253.

WALKER, J.M., BRYANT, S.M. & WESTABY, S. (1988). Captopril has a direct negative inotropic effect on isolated myocardium. *Br. Heart J.*, **59**, 611–612.

WALLENSTEIN, S., ZUCKER, C. & FLEISS, J. (1980). Some statistical methods useful in circulation research. *Circ. Res.*, **47**, 1–9.

ZANNAD, F., VAN DER BROEK, S.A. & BORY, M. (1992). Comparative treatment with lisinopril versus enalapril for congestive heart failure. *Am. J. Cardiol.*, **70**, 78C–83C.

ZYGMUNT, A.C. & MAYLIE, J. (1990). Stimulation-dependent facilitation of the high threshold calcium current in guinea-pig ventricular myocytes. *J. Physiol.*, **428**, 653–671.

*(Received January 27, 1993*
*Accepted March 3, 1993)*

*Br. J. Pharmacol.* (1993), **109**, 880–886 © Macmillan Press Ltd, 1993

# Enhancement by endothelin-1 of microvascular permeability via the activation of $ET_A$ receptors

[1]János G. Filep, Martin G. Sirois, Éva Földes-Filep, Anne Rousseau, Gérard E. Plante, *Alain Fournier, †Mitsuo Yano & Pierre Sirois

Department of Pharmacology, Faculty of Medicine, University of Sherbrooke, Sherbrooke, P.Q., Canada J1H 5N4; *Institut National de la Recherche Scientifique-Santé, Montréal, P.Q., Canada H9R 1G6 and †Central Research Laboratories, Banyu Pharmaceuticals Co., Tsukuba, Japan

**1** The objective of the present experiments was to assess the involvement of endothelin-A ($ET_A$) receptors in mediating the effects of endothelin-1 on microvascular permeability in conscious rats.

**2** Bolus injection of endothelin-1 (0.1 and 1 nmol $kg^{-1}$, i.v.) resulted in a dose-dependent prolonged pressor effect preceded by a transient depressor response. These changes were accompanied by a dose-dependent loss of plasma volume. Endothelin-1 (1 nmol $kg^{-1}$) enhanced the vascular permeability of the upper and lower bronchi, kidney, stomach, duodenum and spleen (up to 270%) as measured by the extravasation of Evans blue dye.

**3** Pretreatment of the animals with the selective $ET_A$ receptor antagonist, BQ-123 (1 mg $kg^{-1}$, i.v.) significantly blunted the pressor response to endothelin-1 without affecting the depressor response. BQ-123 inhibited by 87% the endothelin-1 (1 nmol $kg^{-1}$)-induced plasma volume loss. BQ-123 markedly attenuated protein extravasation elicited by endothelin-1 in the upper and lower bronchi and kidney, whereas it completely inhibited the permeability effect of endothelin-1 in the stomach and duodenum. BQ-123 by itself had no significant effect on the parameters studied.

**4** The endothelin-1 analogue, [Trp(For)$^{21}$]-endothelin-1, in which $Trp^{21}$ is formylated, was as potent a pressor agent as endothelin-1, but had no depressor action. Bolus injection of [Trp(For)$^{21}$]-endothelin-1 (0.1 and 1 nmol $kg^{-1}$, i.v.) evoked similar plasma volume losses to those observed following administration of equimolar doses of endothelin-1. Furthermore, 1 nmol $kg^{-1}$ [Trp(For)$^{21}$]-endothelin-1 evoked increases in protein extravasation similar to endothelin-1, 1 nmol $kg^{-1}$.

**5** The present findings suggest that endothelin-1 enhances microvascular permeability, in part, via the activation of $ET_A$ receptors.

**Keywords:** Endothelin-1; $ET_A$ receptor; protein extravasation; haemoconcentration; airways; gastrointestinal tract; kidney; BQ-123

## Introduction

An increasing body of evidence suggests that, in addition to modulation of vascular tone, endothelin-1 may also play a role in the regulation of vascular permeability. Endothelin-1 causes an increase in haematocrit not fully accounted for by urinary fluid loss (Goetz *et al.*, 1988; Miller *et al.*, 1989; López-Farré *et al.*, 1989), suggesting that this haemoconcentration could result from vascular leakage. Subsequent studies have shown endothelin-1-induced oedema formation in the forearm in man (Dahlöf *et al.*, 1990) and enhanced protein extravasation in selected vascular beds including the airways, heart, gastrointestinal tract and kidney in the rat (Filep *et al.*, 1991; 1992a; Zimmerman *et al.*, 1992). In other studies, endothelin-1 was found to attenuate oedema formation elicited by chemotactic agents in rat and rabbit skin (Brain *et al.*, 1989; Chander *et al.*, 1989) and in the mouse paw (Henriques *et al.*, 1992).

Kinetic analysis of endothelin-1 binding to various tissues, functional data and cross-desensitization experiments implied the possible existence of multiple endothelin receptor subtypes (Sakurai *et al.*, 1992; Sokolovsky, 1992). Recently, the existence of at least two distinct types of endothelin receptors has been demonstrated by cloning cDNAs encoding those subtypes (Arai *et al.*, 1990; Sakurai *et al.*, 1990). The $ET_A$ receptor is highly selective for endothelin-1 (Arai *et al.*, 1990), whereas the $ET_B$ receptor is non-isopeptide-selective (Sakurai *et al.*, 1990). Endothelin receptors mediating vasoconstriction are thought to be of the $ET_A$ receptor subtype; $ET_B$ receptors have been suggested to mediate the depressor and vasodilator responses to endothelin-1 (Ihara *et al.*, 1991; Sakurai *et al.*, 1992). No information is available on the receptors mediating the permeability effect of endothelin-1.

The present study was attempted to identify the receptors responsible for the microvascular permeability effects of endothelin-1 in the conscious rat. In these experiments we have studied the effects of the selective $ET_A$ receptor antagonist, BQ-123 (Ihara *et al.*, 1992) on protein extravasation elicited by endothelin-1 in selected vascular beds and compared the permeability effects of endothelin-1 and its analogue, [Trp(For)$^{21}$]-endothelin-1, which possesses the pressor but not the depressor activity of endothelin-1 (Filep *et al.*, 1992b).

## Methods

The experiments were performed on conscious, chronically catheterized male Wistar rats weighing 225–290 g. The animals were kept in individual metabolic cages and were prepared as described previously (Filep *et al.*, 1987). Briefly, under anaesthesia (ketamine, 75 mg $kg^{-1}$ and sodium pentobarbitone, 15 mg $kg^{-1}$) catheters were implanted into the abdominal aorta and vena cava through the central tail artery and left femoral vein, respectively. The venous catheter

[1] Author for correspondence at present address: Research Center, Maisonneuve-Rosemont Hospital, University of Montréal, 5415 boul. de l'Assomption, Montréal, P.Q., Canada H1T 2M4.

was led subcutaneously to the root of the tail. The catheters emerging from the tail were protected by an acrylic cuff glued to the tail. The cuff was connected to a stainless steel spiral and was fed through the top of the metabolic cage. The animals were allowed to recover completely for at least 4 days following the surgical procedures. During the experiments the animals could move freely and had free access to food and water. Mean arterial blood pressure (MABP) was monitored continuously with a Statham P23 dB pressure transducer. Protein extravasation was estimated by measuring the extravasation of Evans blue dye, which binds to plasma albumin (Rawson, 1943).

### *Experimental protocols*

On the day of the experiment, following an equilibrium period of 1 h, basal cardiovascular parameters were measured for 20 min before drug administration. To measure protein extravasation, Evans blue dye (20 mg $kg^{-1}$, 25 mg $ml^{-1}$ in 0.9% NaCl) was injected i.v. together with either endothelin-1 (1 nmol $kg^{-1}$), the endothelin-1 analogue, [Trp(For)$^{21}$] endothelin-1, in which $Trp^{21}$ was formylated (1 nmol $kg^{-1}$) or their vehicle. Previous experiments showed that at a dose of 1 nmol $kg^{-1}$, endothelin-1 enhances protein extravasation in the rat pulmonary, renal and mesenteric circulation (Filep *et al.*, 1991). The endothelin-1 analogue, [Trp(For)$^{21}$]endothelin-1 is as potent a pressor agent as the mother compound, but it is devoid of the depressor activity in conscious rats (Filep *et al.*, 1992b). Some animals were pretreated with 1 mg $kg^{-1}$ of the selective $ET_A$ receptor antagonist, BQ-123 (Ihara *et al.*, 1992), for 5 min before injection of endothelin-1. Twenty min before, and 10 min after, injection of endothelin-1, blood (approximately 15 µl) was collected through the arterial catheter into heparinized glass capillaries to determine the haematocrit. Ten min after injection of Evans blue dye, the animals were anaesthetized (sodium pentobarbitone, 50 mg $kg^{-1}$) and were perfused with 40 ml 0.9% NaCl through a catheter inserted into the abdominal aorta. Then the thorax was cut open, the trachea, upper bronchi (airways extending from the bifurcation of trachea to its entry into the parenchyma), lower bronchi (defined as major airways surrounded by parenchyma that can be easily dissected without magnification) and portions of pulmonary parenchyma were prepared. Portions of liver, spleen, pancreas, kidney, stomach and duodenum were excised and weighed. Tissue Evans blue dye content was measured by spectrophotometry following extraction with formamide (4 ml per g wet tissue weight) as described previously (Filep *et al.*, 1991). The Evans blue content of each sample was expressed as µg dye per g dry weight of tissue to avoid underestimation of changes due to plasma fluid extravasation.

### *Drugs and chemicals*

Endothelin-1 and [Trp(For)$^{21}$]endothelin-1 were synthesized in our laboratories by solid phase methodology. The purity of the preparations were greater than 97% as measured by high performance liquid chromatography. Endothelin-1 and its analogue were dissolved in distilled water and stored under $N_2$ at − 20°C for up to 4 weeks. On the day of the experiments, an aliquot was removed and diluted further with 0.9% NaCl. BQ-123(-cyclo-(D-Asp-L-Pro-D-Val-L-Leu-D-Trp-)sodium (Banyu Pharmaceuticals Co., Tsukuba, Japan) was dissolved in 0.9% NaCl immediately before use. Evans blue dye was from Sigma Chemical Co. (St Louis, MO, U.S.A.).

### *Data analysis*

Results are expressed as means ± s.e.mean. Changes in plasma volume were calculated according to the formula: Δplasma volume (%) = (100/100-$Hct_i$) × (($Hct_i$-$Hct_f$)/$Hct_f$) × 100, where $Hct_i$ and $Hct_f$ are the haematocrit values obtained 20 min before (initial or control) and 10 min after (final Hct) injection of endothelin-1, respectively.

Statistical evaluation of the data was performed by two-way analysis of variance using ranks (Friedman's test) followed by a Wilcoxon-Wilcox test (Wilcoxon & Wilcox, 1964), to identify differences between control and repeated measurements on the same animals; by Dunn's multiple contrast hypothesis test (Dunn, 1964), when various treatments were compared to the same control; or by Wilcoxon signed rank test and Mann-Whitney U test, for paired and unpaired observations, respectively. A level of $P<0.05$ was considered significant for all tests.

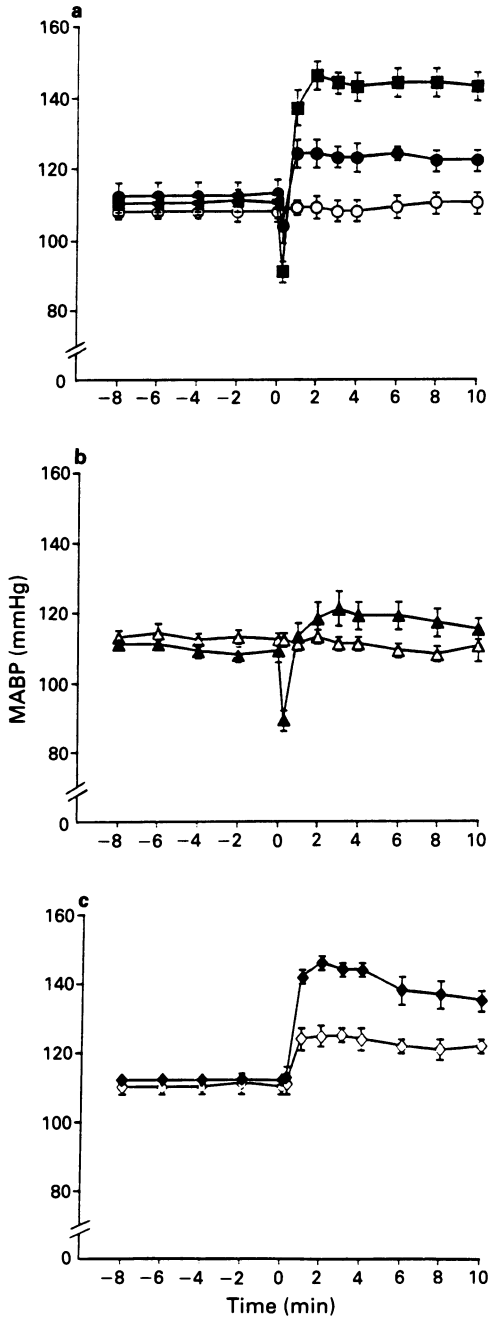



**Figure 1** Blood pressure responses to endothelin-1 and [Trp(For)$^{21}$]-endothelin-1 in the absence and presence of BQ-123 in the conscious rat. Various doses of endothelin-1 or its analogue were injected i.v. at 0 min and BQ-123 was injected at − 5 min as follows: (a) 0.9% NaCl (○) ($n = 6$); endothelin-1, 0.1 nmol $kg^{-1}$ (●) ($n = 5$) or 1 nmol $kg^{-1}$ (■) ($n = 6$); (b) BQ-123, 1 mg $kg^{-1}$ plus 0.9% NaCl (△) ($n = 5$); BQ-123, 1 mg $kg^{-1}$ plus endothelin-1, 1 nmol $kg^{-1}$ (▲) ($n = 6$) and (c) [Trp(For)$^{21}$]-endothelin-1, 0.1 nmol $kg^{-1}$ (◇) ($n = 5$) or 1 nmol $kg^{-1}$ (◆) ($n = 5$). Values are means ± s.e.mean.

## Results

### *Effects on arterial blood pressure and plasma volume*

Bolus i.v. injections of endothelin-1 (0.1 and 1 nmol $kg^{-1}$) evoked prolonged dose-dependent increase in MABP preceded by a transient hypotension (Figure 1a). Administration of BQ-123 (1 mg $kg^{-1}$) by itself did not produce significant changes in MABP, whereas it markedly inhibited the pressor action of endothelin-1 (maximum increases in MABP were $37 \pm 1$ and $11 \pm 3$ mmHg in the absence and presence of BQ-123 following 1 nmol $kg^{-1}$ endothelin-1, respectively, $n = 6$, $P < 0.01$) without affecting the depressor response to endothelin-1 (Figure 1b). Increasing the dose of BQ-123 did not cause further inhibition of the pressor effect of endothelin-1. The endothelin-1 analogue, [Trp(For)$^{21}$]-endothelin-1 appeared to be as effective as a pressor agent as the parent peptide, but, unlike endothelin-1, it did not induce a depressor response (Figure 1c).

Endothelin-1 and [Trp(For)$^{21}$]-endothelin-1-induced changes in MABP were accompanied by a dose-dependent haemoconcentration. At the dose of 0.1 nmol $kg^{-1}$, neither endothelin-1 nor [Trp(For)$^{21}$]-endothelin-1 affected the haematocrit significantly. Following administration of 1 nmol $kg^{-1}$ endothelin-1 or its analogues, the haematocrit increased on average by 11 and 8%, corresponding to about 17 and 12% plasma volume loss, respectively (Table 1). Pretreatment of the animals with BQ-123, 1 mg $kg^{-1}$ resulted in 87% reduction in endothelin-1-induced plasma volume loss. BQ-123 by itself had no significant effect on haematocrit (Table 1).

### *Effects on protein extravasation*

To study the effects of BQ-123 on endothelin-1-induced protein extravasation, the animals received 1 mg $kg^{-1}$ BQ-123 5 min before the combined injection of endothelin-1, 1 nmol $kg^{-1}$ and Evans blue dye (20 mg $kg^{-1}$). BQ-123 reduced the extravasation of Evans blue dye by 42, 66, 100, 100 and 79% in the upper and lower bronchi, stomach, duodenum and kidney, respectively (Figures 2 and 3). Although the mean increase in protein extravasation in the spleen was lower after pretreatment with BQ-123, the effect of endothelin-1 on tissue Evans blue content did not differ significantly from that seen after endothelin-1 alone (Figure 3). BQ-123 by itself did not affect extravasation of Evans blue in the vascular beds studied (Figures 2 and 3).

Injection of 1 nmol $kg^{-1}$ [Trp(For)$^{21}$]-endothelin-1 increased tissue Evans blue content in the upper and lower bronchi on average by 80 and 133%, respectively (Figure 2). Although Evans blue content tended to be higher in the trachea and pulmonary parenchyma, these changes did not reach statistical significance (Figure 2). [Trp(For)$^{21}$]-endothelin-1 injection produced increases of 68, 102, 105, 62 and 125% in Evans blue content in the liver, stomach, duodenum, spleen and kidney, respectively (Figure 2). The endothelin-1 analogue induced changes in protein extravasation did not differ significantly from those observed following endothelin-1 (Figures 2 and 3). Like endothelin-1, [Trp(For)$^{21}$]-endothelin-1 did not enhance protein extravasation in the pancreas, skeletal muscle and skin (Figures 3 and 4).

## Discussion

The results of the present study confirm that the effects of intravenously injected endothelin-1 increase haematocrit (Goetz *et al.*, 1988; Miller *et al.*, 1989, Filep *et al.*, 1991) and protein extravasation in various organs (Filep *et al.*, 1991; Zimmerman *et al.*, 1992) and provide evidence for the involvement of $ET_A$ receptors in mediating the permeability effect of endothelin-1.

Bolus injection of endothelin-1 i.v. resulted in haemoconcentration as evidenced by an increase of about 10% in haematocrit, reflecting a reduction of about 17% in plasma volume. This plasma volume loss was almost completely prevented by pretreatment of the animals with BQ-123. BQ-123 has been reported to be 2500 times more potent in inhibiting the binding of endothelin-1 to $ET_A$ than $ET_B$ receptors *in vitro* (Ihara *et al.*, 1992). Furthermore, BQ-123 significantly attenuated the pressor response to endothelin-1 without affecting its depressor action (Ihara *et al.*, 1992 and the present study). Since $ET_B$ receptors located on the vascular endothelium have been implicated in the mediation of the transient depressor action of endothelin-1 (Saeki *et al.*, 1991; Douglas & Hiley, 1991a), it might be assumed that BQ-123 does not interfere with $ET_B$ receptors *in vivo*. It should be noted, however, that the degree of inhibition of the pressor effect of endothelin-1 by BQ-123 did not exceed 70%. A previous study showed that increasing the dose of BQ-123 (up to 10 mg $kg^{-1}$) did not reduce further the maximum increase in MABP elicited by endothelin-1, rather it shortened the duration of the pressor response to endothelin-1 (Ihara *et al.*, 1992). Furthermore, [Ala$^{1,3,11,15}$]endothelin-1, a selective $ET_B$ receptor agonist (Saeki *et al.*, 1991) has been reported to evoke pressor responses in anaesthetized rats (Douglas & Hiley, 1991a). These observations lend further support to the notion that more than one type of endothelin receptor is involved in the generation of the pressor effect, as

**Table 1** Endothelin-1-induced haemoconcentration and its inhibition by BQ-123 in the conscious rat

| | n | *Haematocrit (vol %)* *Before endothelin-1* | *10 min after injection* | $P^a$ | *Δ Plasma volume (%)* | $P^b$ |
|---|---|---|---|---|---|---|
| Vehicle | 6 | 40.5 ± 0.5 | 40.6 ± 0.3 | NS | − 0.6 ± 1.4 | – |
| Endothelin-1 (0.1 nmol $kg^{-1}$) | 5 | 39.9 ± 0.6 | 40.4 ± 0.4 | NS | − 2.1 ± 2.0 | NS |
| Endothelin-1 (1 nmol $kg^{-1}$) | 6 | 40.1 ± 0.6 | 44.6 ± 0.5 | 0.05 | − 16.6 ± 2.8 | 0.05 |
| BQ-123 (1 mg $kg^{-1}$) | 5 | 41.1 ± 0.9 | 41.1 ± 0.9 | NS | − 0.1 ± 2.7 | NS |
| BQ-123 (1 mg $kg^{-1}$) + endothelin-1 (1 nmol $kg^{-1}$) | 6 | 40.8 ± 1.1 | 41.6 ± 0.6 | NS | − 2.2 ± 3.2 | NS |
| [Trp(For)$^{21}$]-endothelin-1 (0.1 nmol $kg^{-1}$) | 5 | 41.6 ± 0.5 | 42.2 ± 0.7 | NS | − 2.6 ± 2.4 | NS |
| [Trp(For)$^{21}$]-endothelin-1 (1 nmol $kg^{-1}$) | 5 | 41.6 ± 0.9 | 44.8 ± 0.5 | 0.05 | − 12.1 ± 2.4 | 0.05 |

Values are means ± s.e.mean

[a]*P* values were obtained by the Wilcoxon's signed rank test; [b]compared to vehicle by the Dunn's multiple contrast hypothesis test.

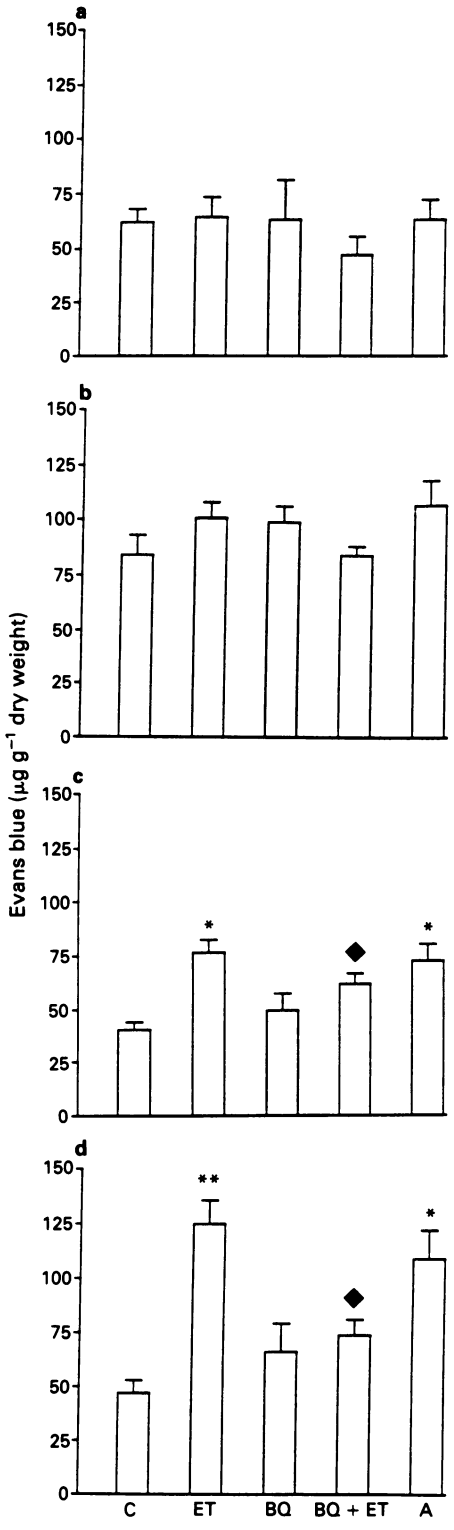



**Figure 2** Effects of endothelin-1, BQ-123 and [Trp(For)$^{21}$]-endothelin-1 on protein extravasation in rat airways: (a) trachea, (b) parenchyma, (c) upper bronchi and (d) lower bronchi. The animals were injected i.v. with 0.9% NaCl (C), endothelin-1 (ET, 1 nmol $kg^{-1}$), BQ-123 (BQ, 1 mg $kg^{-1}$), BQ-123 (1 mg $kg^{-1}$, 5 min prior to endothelin-1) plus endothelin-1, (1 nmol $kg^{-1}$) or [Trp(For)$^{21}$]-endothelin-1 (A, 1 nmol $kg^{-1}$) together with Evans blue dye (20 mg $kg^{-1}$). The rats were killed 10 min after injection of the dye. Values are means with s.e.mean. $n = 5$ for BQ-123 and [Trp(For)$^{21}$]-endothelin-1, $n = 6$ for the other groups. $^*P < 0.05$; $^{**}P < 0.01$ (compared to control); ◆$P < 0.05$ (compared to endothelin-1).

has been demonstrated for endothelin-1-induced vasoconstriction in the pig coronary artery (Harrison *et al.*, 1992).

Although immunoreactive endothelin-1 can be detected in normal rat plasma (Shirakami *et al.*, 1991; Valentin *et al.*, 1991), little is known about the physiological importance of circulating endothelin-1. Administration of BQ-123 neither produced changes in MABP nor affected haematocrit and protein extravasation. Thus, it seems unlikely that circulating endothelin-1 could support blood pressure, or modulate microvascular permeability through the $ET_A$ receptor under physiological conditions, or both. On the other hand, BQ-123 significantly attenuated the accumulation of Evans blue dye, which is bound by plasma albumin, in various organs after injection of endothelin-1. However, BQ-123 appeared to be a more effective inhibitor in the stomach, duodenum and kidney than in the upper and lower bronchi and spleen. In the stomach and duodenum, BQ-123 completely inhibited endothelin-1-induced protein extravasation, whereas only 40% inhibition was observed in the spleen. These findings suggest that different endothelin receptors or mechanisms might mediate the permeability effect of endothelin-1 in different vascular beds. Indeed, endothelin-3 has been reported to promote extravasation of Evans blue dye in skeletal muscle (Valentin *et al.*, 1991), where endothelin-1 failed to alter vascular permeability. It is also possible that the bioavailability of BQ-123 might be different in various organs.

Additional evidence supporting the involvement of $ET_A$ receptors in mediating the permeability effect of endothelin-1 is derived from the experiments with [Trp(For)$^{21}$]-endothelin-1. We have previously reported that formylation of the terminal Trp in endothelin-1 leads to an analogue which retains the pressor activity of endothelin-1, but is devoid of the depressor action (Filep *et al.*, 1992b). The lack of depressor activity may suggest that [Trp(For)$^{21}$]-endothelin-1 does not act on $ET_B$ receptors. In addition to being as potent a pressor agent as the parent peptide, [Trp(For)$^{21}$]-endothelin-1 evoked similar increases in haematocrit as equimolar doses of endothelin-1. Furthermore, [Trp(For)$^{21}$]-endothelin-1 mimicked the effect of endothelin-1 on accumulation of Evans blue dye in the upper and lower bronchi, stomach, duodenum, kidney and spleen, whereas it appeared somewhat more effective than endothelin-1 in the liver. The reason for this latter finding is not clear. However, no other difference in the actions of endothelin-1 and its analogue was observed in the present study. Thus, like endothelin-1, [Trp(For)$^{21}$]-endothelin-1 did not affect microvascular permeability in the trachea, pulmonary parenchyma, pancreas, skin and skeletal muscle.

In the present study parallel changes were observed in vascular permeability and MABP. Thus, enhanced protein extravasation was detected when MABP was elevated following administration of endothelin-1 or [Trp(For)$^{21}$]-endothelin-1, and protein extravasation was inhibited when the pressor response to endothelin-1 was attenuated. However, the increase in blood pressure, *per se*, could not be the basis for the observed protein extravasation. Endothelin-1 was found to be a considerably more potent constrictor of venous than arterial vessels (Yang *et al.*, 1989) and it has a longer duration of action in the venous than arterial vasculature (Warner, 1990). An increase in both pre-, and post-capillary resistance could lead to an increase in capillary hydrostatic pressure. This might explain an enhanced transcapillary fluid transfer, but not an increased protein leakage. Mediator-stimulated increase in protein extravasation is primarily attributable to an increase in the hydraulic conductivity of the microvascular membrane secondary to interendothelial cell gap formation in the venules (Grega *et al.*, 1986). Vasoactive mediators which can elevate microvascular pressure, but do not elicit gap formation could not promote protein efflux and oedema formation (Grega *et al.*, 1986). Accordingly, it has been suggested that endothelin-1 induces gap formation directly or through release of secondary mediators such as platelet-activating factor (Filep *et al.*, 1991) or thromboxane

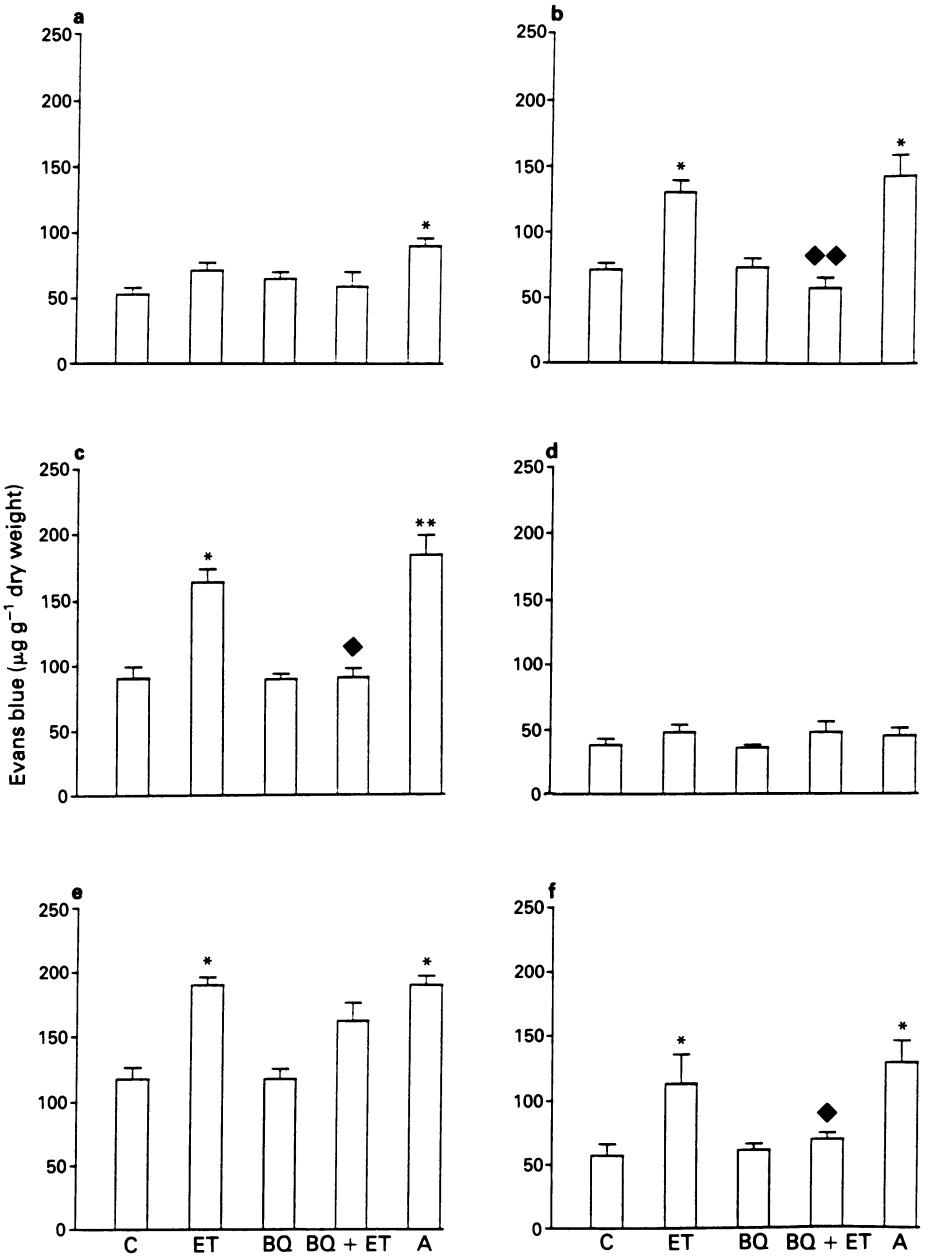



**Figure 3** Effects of endothelin-1, BQ-123 and [Trp(For)$^{21}$]-endothelin-1 on protein extravasation in the rat liver (a), stomach (b), duodenum (c), pancreas (d), spleen (e) and kidney (f). The animals were given i.v. 0.9% NaCl (C), endothelin-1 (ET, 1 nmol kg$^{-1}$), BQ-123 (BQ, 1 mg kg$^{-1}$), BQ-123 (1 mg kg$^{-1}$, 5 min prior to endothelin-1) plus endothelin-1 (1 nmol kg$^{-1}$) or [Trp(For)$^{21}$]-endothelin-1 (A, 1 nmol kg$^{-1}$) together with Evans blue dye (20 mg kg$^{-1}$). The rats were killed 10 min after injection of the dye. Values are means with s.e.mean. $n = 5$ for BQ-123 and [Trp(For)$^{21}$]-endothelin-1, $n = 6$ for the other groups. *$P<0.05$; **$P<0.01$ (compared to control); ◆$P<0.05$; ◆◆$P<0.01$ (compared to endothelin-1).

$A_2$ (Sirois *et al.*, 1992). Changes in capillary pressure are not primary determinants of macromolecular permeability (Amelang *et al.*, 1981; Grega *et al.*, 1986). Indeed, endothelin-1-induced protein extravasation was markedly attenuated by receptor antagonists to platelet-activating factor and thromboxane $A_2$, which did not alter blood pressure responses to endothelin-1 (Filep *et al.*, 1991; Sirois *et al.*, 1992). Moreover, an increase in haematocrit has also been observed after the infusion of a non-pressor dose of endothelin-1 (López-Farré *et al.*, 1989). Although the permeability effect of endothelin-1 appears to be independent of changes in arterial blood pressure, dramatic increases in microvascular pressure might lead to disruption of endothelial junctions, resulting in extravasation of erythrocytes as it has been observed following intra-arterial injections of large doses of endothelin-1 into the rat mesenteric vascular bed (Douglas & Hiley, 1991b).

The potent arteriolar constrictor effect of endothelin-1 could mask any oedema-inducing effect of the peptide as has been suggested for the skin (Brain *et al.*, 1988). Furthermore, topical application of endothelin-1 reduced oedema formation elicited by chemotactic agents in the rat and rabbit skin (Brain *et al.*, 1989; Chander *et al.*, 1989). However, $ET_A$ receptor blockade with BQ-123 did not lead to an increase in protein accumulation in the skin. These findings suggest that either the constrictor action of endothelin-1 is not mediated through $ET_A$ receptors in the skin or endothelin-1 does not

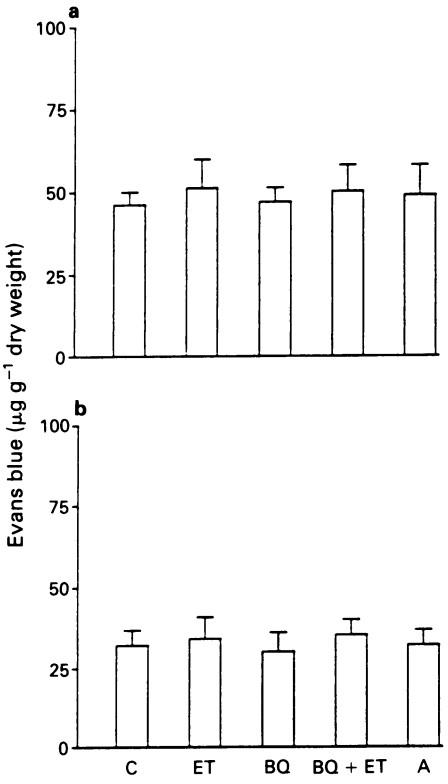



**Figure 4** Evans blue content in the rat skeletal muscle (right quadriceps) (a) and dorsal skin (b) following endothelin-1, BQ-123 and [Trp(For)$^{21}$]-endothelin-1. The animals were given i.v. 0.9% NaCl (C), endothelin-1 (ET, 1 nmol kg$^{-1}$), BQ-123 (BQ, 1 mg kg$^{-1}$), BQ-123 plus endothelin-1 or [Trp(For)$^{21}$]-endothelin-1 (A, 1 nmol kg$^{-1}$) together with Evans blue dye. The rats were killed 10 min after the injection of the dye. Values are means with s.e.mean. $n = 5$ for BQ-123 and [Trp(For)$^{21}$]-endothelin-1, $n = 6$ for the other groups.

enhance permeability in this tissue. The different susceptibility of different vascular beds to endothelin-1 and the differences in the inhibitory effect of BQ-123 on protein accumulation evoked by endothelin-1 may reflect differential sensitivity of the vasculature to endothelin-1 or differences in distribution of endothelin receptor subtypes.

In conclusion, the present data show that endothelin-1-induced haemoconcentration and increase in protein extravasation is mediated, in part, through activation of the $ET_A$ receptor. The different susceptibility of various vascular beds to the inhibitory action of BQ-123, however, suggest that in certain vascular beds this might not be the sole mechanism by which endothelin-1 enhances vascular permeability.

This study was supported by a grant from the Medical Research Council of Canada. J.G.F. and E.F.F. are in receipt of Fellowships from the Medical Research Council of Canada. A.F. is a Scholar of the Fonds de la Recherche en Santé du Québec and P.S. is in receipt of a Medical Research Council of Canada Scientist Award.

## References

AMELANG, E., PRASAD, G.M., RAYMOND, R.M. & GREGA, G.J. (1981). Interactions among inflammatory mediators on edema formation in the canine forelimb. *Circ. Res.*, **49**, 298–306.

ARAI, H., HORI, S., ARAMORI, I., OHKUBO, H. & NAKANISHI, S. (1990). Cloning and expression of a cDNA encoding an endothelin receptor. *Nature*, **348**, 730–732.

BRAIN, S.D., CROSSMAN, D.C., BUCKLEY, T.L. & WILLIAMS, T.J. (1989). Endothelin-1: demonstration of potent effects on the microcirculation of humans and other species. *J. Cardiovasc. Pharmacol.*, **13** (Suppl. 5), S147–S149.

BRAIN, S.D., TIPPINS, J.R. & WILLIAMS, T.J. (1988). Endothelin induces potent microvascular constriction. *Br. J. Pharmacol.*, **95**, 1005–1007.

CHANDER, C.L., MOORE, A.R., DESA, F.M. HOWAT, D.W. & WILLOUGHBY, D.A. (1989). Anti-inflammatory effects of endothelin-1. *J. Cardiovasc. Pharmacol.*, **13** (Suppl. 5), S218–S219.

DAHLÖF, B., GUSTAFSSON, D., HEDNER, T., JERN, S. & HANSSON, L. (1990). Regional hemodynamic effects of endothelin-1 in rat and man: unexpected adverse reactions. *J. Hypertension*, **8**, 811–817.

DOUGLAS, S.A. & HILEY, C.R. (1991a). Endothelium-dependent mesenteric vasorelaxant effects and systemic actions of endothelin(16-21) and other endothelin-related peptides in the rat. *Br. J. Pharmacol.*, **104**, 311–320.

DOUGLAS, S.A. & HILEY, C.R. (1991b). Responses to endothelin-1, human proendothelin(1-38) and porcine proendothelin(1-39) in the rat on intravenous administration and in the blood perfused mesentery. *Neurochem. Int.*, **18**, 445–454.

DUNN, O.J. (1964). Multiple comparisons using rank sums. *Technometrics*, **6**, 241–252.

FILEP, J., FÖLDES-FILEP, E. & FRÖLICH, J.C. (1987). Vascular responses to leukotrienes $B_4$, $C_4$ and $D_4$ following FPL 55712, indomethacin, saralasin, phentolamine and verapamil in the conscious rat. *Br. J. Pharmacol.*, **90**, 431–439.

FILEP, J.G., FÖLDES-FILEP, E., ROUSSEAU, A., FOURNIER, A., SIROIS, P. & YANO, M. (1992a). Endothelin-1 enhances vascular permeability in the rat heart through the $ET_A$ receptor. *Eur. J. Pharmacol.*, **219**, 343–344.

FILEP, J.G., ROUSSEAU, A., FOURNIER, A. & SIROIS, P. (1992b). Structure-activity relationship of analogues of endothelin-1: dissociation of hypotensive and pressor actions. *Eur. J. Pharmacol.*, **220**, 263–266.

FILEP, J.G., SIROIS, M.G., ROUSSEAU, A., FOURNIER, A. & SIROIS, P. (1991). Effects of endothelin-1 on vascular permeability in the conscious rat: interactions with platelet-activating factor. *Br. J. Pharmacol.*, **104**, 797–804.

GOETZ, K.L., WANG, B.C., MADWED, J.B., ZHU, J.L. & LEADLY, Jr. R.J. (1988). Cardiovascular, renal and endocrine responses to intravenous endothelin in the conscious dog. *Am. J. Physiol.*, **255**, R1064–R1068.

GREGA, G.J., ADAMSKI, S.W. & DOBBINS, D.E. (1986). Physiological and pharmacological evidence for the regulation of permeability. *Fed. Proc.*, **45**, 96–100.

HARRISON, V.J., RANDRIANTSOA, A. & SCHOEFFTER, P. (1992). Heterogeneity of endothelin-sarafotoxin receptors mediating contraction of pig coronary artery. *Br. J. Pharmacol.*, **105**, 511–513.

HENRIQUES, M.G.M.O., RAE, G.A., CORDEIRO, R.S.B. & WILLIAMS, T.J. (1992). Endothelin-1 inhibits PAF-induced paw oedema and pleurisy in the mouse. *Br. J. Pharmacol.*, **106**, 579–582.

IHARA, M., FUKURODA, T., SAEKI, T., NISHIKIBE, M., KOJIRI, K., SUDA, H. & YANO, M. (1991). An endothelin ($ET_A$) antagonist isolated from Streptomyces misakiensis. *Biochem. Biophys. Res. Commun.*, **178**, 132–137.

IHARA, M., NOGUCHI, K., SAEKI, T., FUKURODA, T., TSUCHIDA, S., KIMURA, S., FUKAMI, T., ISHIKAWA, K., NISHIKIBE, M. & YANO, M. (1992). Biological profiles of highly potent novel endothelin antagonists selective for the $ET_A$ receptor. *Life Sci.*, **50**, 247–255.

LÓPEZ-FARRÉ, A., MOÑTANES, I., MILLÂS, I. & LÓPEZ-NOVOA, J.M. (1989). Effect of endothelin on renal function in rats. *Eur. J. Pharmacol.*, **163**, 187–189.

MILLER, W.L., REDFIELD, M.M. & BURNETT, J.C. (1989). Integrated cardiac, renal, and endocrine actions of endothelin. *J. Clin. Invest.*, **83**, 317–320.

RAWSON, R.A. (1943). The binding of T-1824 and structurally related diazo dyes by the plasma proteins. *Am. J. Physiol.*, **138**, 708–717.

SAEKI, T., IHARA, M., FUKURODA, T., YAMAGIWA, M. & YANO, M. (1991). [Ala$^{1,3,11,15}$]endothelin-1 analogs with $ET_B$ agonistic activity. *Biochem. Biophys. Res. Commun.*, **179**, 286–292.

SAKURAI, T., YANAGISAWA, M. & MASAKI, T. (1992). Molecular characterization of endothelin receptors. *Trends Pharmacol. Sci.*, **13**, 103–108.

SAKURAI, T., YANAGISAWA, M., TAKUWA, Y., MIYAZAKI, H., KIMURA, S., GOTO, K. & MASAKI, T. (1990). Cloning of a cDNA encoding a non-isopeptide selective subtype of the endothelin receptor. *Nature*, **348**, 732–735.

SHIRAKAMI, G., NAKAO, K., SAITO, Y., MAGARIBUCHI, T., JOUGASAKI, M., MUKOYAMA, M., ARAI, H., HOSODA, K., SUGA, S., OGAWA, Y., YAMADA, T., MORI, K. & IMURA, H. (1991). Acute pulmonary alveolar hypoxia increases lung and plasma endothelin-1 levels in conscious rats. *Life Sci.*, **48**, 969–976.

SIROIS, M.G., FILEP, J.G., ROUSSEAU, A., FOURNIER, A., PLANTE, G.E. & SIROIS, P. (1992). Endothelin-1 enhances vascular permeability in the conscious rat: role of thromboxane $A_2$. *Eur. J. Pharmacol.*, **214**, 119–125.

SOKOLOVSKY, M. (1992). Structure-function relationships of endothelins, sarafotoxins, and their receptor subtypes. *J. Neurochem.*, **59**, 809–821.

VALENTIN, J.P., GARDNER, D.G., WIEDEMANN, E. & HUMPHREYS, H. (1991). Modulation of endothelin effects on blood pressure and hematocrit by atrial natriuretic peptide. *Hypertension*, **17**, 864–869.

WARNER, T.D. (1990). Simultaneous perfusion of rat isolated superior mesenteric arterial and venous beds: comparison of their vasoconstrictor and vasodilator responses to agonists. *Br. J. Pharmacol.*, **99**, 427–433.

WILCOXON, F. & WILCOX, R.A. (1964). *Some Rapid Approximate Statistical Procedures*. pp. 36–38. Pearl River, NY: Lederle Laboratories.

YANG, Z.H., BÜHLER, F.R., DIEDERICH, D. & LÜSCHER, T.F. (1989). Different effects of endothelin-1 on cAMP- and cGMP-mediated vascular relaxation in human arteries and veins: comparison with norepinephrine. *J. Cardiovasc. Pharmacol.*, **13** (Suppl. 5), S129–S131.

ZIMMERMAN, R.S., MARTINEZ, A.J., MAYMIND, M. & BARBEE, R.W. (1992). Effect of endothelin on plasma volume and albumin escape. *Circ. Res.*, **70**, 1027–1034.

*(Received November 30, 1992*
*Revised February 22, 1993*
*Accepted March 10, 1993)*

*Br. J. Pharmacol.* (1993), **109**, 887–891 © Macmillan Press Ltd, 1993

# Attenuation of contractions to acetylcholine in canine bronchi by an endogenous nitric oxide-like substance

Yuansheng Gao & [1]Paul M. Vanhoutte

Department of Physiology and Biophysics, Mayo Clinic and Mayo Foundation, Rochester, MN 55905 and Center for Experimental Therapeutics, Baylor College of Medicine Houston, TX 77030, U.S.A.

**1** The involvement was assessed of an endogenous nitric oxide-like substance in contractions of canine bronchi to acetylcholine.

**2** Canine third order bronchial rings, in some of which the epithelium was removed mechanically, were suspended in organ chambers and isometric tension was recorded. In some experiments, the content of guanosine 3',5'-cyclic monophosphate (cyclic GMP) of the bronchi was also measured.

**3** Acetylcholine induced concentration-dependent contractions. The contractions were potentiated by nitro-L-arginine (an inhibitor of the synthesis of nitric oxide), oxyhaemoglobin (a scavenger of nitric oxide), and methylene blue (an inhibitor of soluble guanylate cyclase). The magnitude of the potentiation to acetylcholine-induced contractions by these inhibitors were not significantly different between tissues with and without epithelium.

**4** Acetylcholine induced a concentration-dependent increase in intracellular content of cyclic GMP, which was similar in bronchi with and without epithelium. These increases were abolished by nitro-L-arginine and methylene blue.

**5** During contractions to acetylcholine, exogenous nitric oxide relaxed the canine bronchi. The relaxations were not affeced by nitro-L-arginine, but were augmented by superoxide dismutase plus catalase, and were abolished by methylene blue.

**6** These observations suggest that, during contraction evoked by acetylcholine, the production of an endogenous nitric oxide-like substance increases and in turn attenuates the response of the airways to the muscarinic agonist. However, the endogenous nitric oxide-like substance does not play a major role in the epithelium-dependent attenuation of the contraction to acetylcholine in canine bronchi.

**Keywords:** Airway smooth muscle; epithelium; nitric oxide; cyclic GMP

## Introduction

In 1980, Furchgott and Zawadzki discovered that endothelium-derived relaxing factor is released by blood vessels in response to acetylcholine. This factor was later identified as nitric oxide or a nitric oxide-like substance (Palmer *et al.*, 1987). It can be produced not only by endothelial cells (Furchgott & Vanhoutte, 1989; Moncada *et al.*, 1991) but also by vascular smooth muscle cells (Gold *et al.*, 1989; Schini & Vanhoutte, 1991), nerve cells (Gillespie *et al.*, 1989; Li & Rand, 1989; Bredt *et al.*, 1990; Tucker *et al.*, 1990), macrophages (Stuehr & Marletta, 1987), and neutrophils (McCall *et al.*, 1989). Nitric oxide (or a nitric oxide-like substance) has an important role in the modulation of the reactivity of blood vessels (Furchgott & Vanhoutte, 1989; Moncada *et al.*, 1991), neuronal communications (Gillespie *et al.*, 1989; Knowles *et al.*, 1989; Li & Rand, 1989; Bredt *et al.*, 1990; Schuman & Madison, 1991), and immunological reactions (Stuehr & Marletta, 1987; McCall *et al.*, 1989).

Most functions exerted by nitric oxide or nitric oxide-like substances are mediated by activation of the soluble guanylate cyclase, and the resulting augmentation of the production of guanosine 3':5'-cyclic monophosphate (cyclic GMP) (Furchgott & Vanhoutte, 1989; Moncada *et al.*, 1991). In bovine tracheal smooth muscle, acetylcholine increases the content of intracellular cyclic GMP (Katsuki & Murad, 1977; Sheng *et al.*, 1991). This increase is abolished by selective inhibitors of nitric oxide synthase and by an inhibitor of guanylate cyclase (methylene blue), suggesting that a nitric oxide-like substance is produced in bovine airways (Sheng *et al.*, 1991). The present study was designed to determine whether or not an endogenous nitric oxide-like substance modulates the responsiveness of canine airways to acetylcholine.

[1] Author for correspondence at Houston address.

## Methods

Experiments were performed on bronchi taken from mongrel dogs of either sex (15–25 kg), anaesthetized with pentobarbitone sodium (30 mg $kg^{-1}$, intravenously) and killed by exsanguination. Third order bronchial segments (outside diameter: 4–6 mm; length: 8–10 mm) were dissected free from the lung and paired rings (length: 4–5 mm) were prepared from each segment. In one ring of each pair, care was taken not to damage the epithelium; in the other ring, the tips of a watchmaker's forceps were inserted into the lumen, and the epithelial layer was removed by gently rolling the tissue back and forth on saline-loaded filter paper. The successful removal of the epithelium was confirmed histologically (Gao & Vanhoutte, 1988).

The rings were suspended in organ chambers filled with 25 ml of modified Krebs-Ringer bicarbonate solution (composition, mM: NaCl 118.3, KCl 4.7, $CaCl_2$ 2.5, $MgSO_4$ 1.2, $KH_2PO_4$ 1.2, $NaHCO_3$ 25.0, calcium disodium edetate 0.026, glucose 11.1; control solution) maintained at 37 ± 0.5°C and aerated with 95% $O_2$:5% $CO_2$ (pH = 7.4). Each ring was suspended between two stirrups passed through its lumen. One stirrup was anchored to the bottom of the organ chamber; the other was connected to a strain gauge (Statham Gould UC2) for the measurement of isometric force.

At the beginning of each experiment the bronchial rings were brought to their optimal resting tension. This was achieved by progressive stretches (0.5 g increments imposed at 15 min intervals) until the contractile response to electrical field stimulation [0.5 ms, 32 Hz, 15 V, 30 s (Gao & Vanhoutte, 1988)] was maximal. The field stimulation was applied by means of two rectangular platinum electrodes placed parallel to the bronchial ring. Electrical stimulation consisted of square waves delivered by a stimulator (Grass SD9) and a d.c. amplifier (Mayo Clinic, Section of Engineering). The optimal resting tensions averaged 0.9 ± 0.1 g for bronchi with

and without epithelium. One hour of equilibration was allowed after reaching the optimal point of the length-active tension relationship.

To reduce degradation of acetylcholine by acetylcholinesterase, the experiments were performed following blockade of the enzyme with the irreversible inhibitor echothiophate ($10^{-7}$ M; 15 min of incubation, followed by a 30-min washout; Brimijoin *et al.*, 1978).

### *Measurements of cyclic GMP*

The tissues were incubated in either control solution (37°C, 95% $O_2$ and 5% $CO_2$) or in the presence of either nitro-L-arginine ($3 \times 10^{-5}$ M) or methylene blue ($10^{-5}$ M). After 45 min of equilibration, acetylcholine was added. The preparations were freeze-clamped rapidly 2 min after the addition of the cholinergic transmitter. Later, they were thawed in trichloroacetic acid (6%), homogenized in a glass potter homogenizer, sonicated for 5 s, and centrifuged (2000 *g* for 15 min). The supernatant was extracted with four volumes of water-saturated dimethyl ether and lyophilized; the pellets were weighed. The lyophilized samples were resuspended in 0.5 ml of sodium acetate buffer (0.05 M, pH 6.2) and the content of cyclic GMP was determined with a cyclic GMP kit (Biomedical Technologies Inc., Stoughton, MA, U.S.A.). The cross-reactivity of cyclic GMP antiserum with other compounds was: cyclic AMP, 0.1%; GMP, <0.0001%; GDP, <0.00001%; GTP, 0.00001%; ATP, <0.00001%. The content of cyclic nucleotide is expressed as pmol $mg^{-1}$ tissue (Gao & Vanhoutte, 1992).

### *Oxyhaemoglobin*

Bovine haemoglobin type 1, supplied by Sigma Chemical (St. Louis, MO, U.S.A.), contains a mixture of oxyhaemogoblin and the oxidized derivative methaemoglobin. The content of oxyhaemogoblin was raised by adding to a 1 mM solution of commercial haemoglobin in distilled water a 10 fold molar excess of the reducing agent sodium dithionite ($Na_2S_2O_4$). Sodium dithionite was then removed by dialysis in 15 l of distilled water (containing 0.001% EDTA) for 2 h at room temperature. The percentage of oxyhaemogoblin was determined spectrophotometrically (Komori *et al.*, 1988).

### *Preparation of nitric oxide*

A gas bulb sealed with a silicon rubber injection septum was filled with nitric oxide from a cylinder (Union Carbide, Chicago, IL, U.S.A.). An appropriate volume (1 and 3 ml) was removed with a syringe and injected into another gas bulb filled with 100 ml of distilled water, which had been gassed with helium for about 3 h, giving stock solutions of nitric oxide of $3.7 \times 10^{-4}$ M and $1.1 \times 10^{-3}$ M (Komori *et al.*, 1988).

### *Drugs*

Acetylcholine chloride, methylene blue, nitro-L-arginine (Sigma Chemicals, St. Louis, MO, U.S.A.), echothiophate iodide (Ayerst Laboratories). These drugs were prepared in distilled water. Except where stated otherwise, inhibitory drugs were added to the organ chambers at least 30 min before a concentration-response curve to acetylcholine was obtained, and kept in contact with the tissues throughout the experiment.

### *Statistical analysis*

The results are expressed as means ± s.e.mean. Statistical evaluation of the data was by Student's *t* test for unpaired observations. When *P* was less than 0.05, the difference was considered to be statistically significant. When data of more than two groups were compared, ANOVA was used. In all experiments, *n* equals the number of dogs from which tissues were studied.

## Results

### *Isometric tension*

Acetylcholine ($10^{-9}$ to $10^{-4}$ M) caused concentration-dependent contractions of canine bronchial rings. Tissues with epithelium were significantly less sensitive to acetylcholine than those without (determined by $-\log EC_{50}$). The maximal contractile responses to the agonist were similar in tissues with and without epithelium (Figure 1 and Table 1). Nitro-L-arginine ($3 \times 10^{-5}$ M), oxyhaemogoblin ($10^{-5}$ M) and methylene blue ($10^{-5}$ M) caused leftward displacements in the concentration-effect curve to acetylcholine both in bronchi with and without epithelium (Figure 1 and Table 1). Those inhibitors did not affect significantly the maximal contractions of the tissues to acetylcholine, the difference between preparations with and without epithelium (Figure 1 and Table 1), or the resting tension of the tissues (data not shown).

Following contractions to the $EC_{50}$ of acetylcholine ($4 \times 10^{-7}$ M; tensions developed: 7.5 ± 1.4 g, $n = 5$), nitric oxide induced concentration-dependent relaxations in preparations without epithelium. The relaxations were augmented significantly by superoxide dismutase (SOD; 150 u $ml^{-1}$) plus catalase (1200 u $ml^{-1}$) (Figure 2) but not by inactivated (by 30 min boiling) SOD plus catalase (data not shown). The nitric oxide-induced relaxations were not affected significantly by nitro-L-arginine ($3 \times 10^{-5}$ M) but were abolished by methylene blue ($10^{-5}$ M) (Figure 2).

### *Cyclic GMP*

Acetylcholine induced similar concentration-dependent increases in the content of cyclic GMP of tissues with and without epithelium (Figure 3). The increases were abolished by nitro-L-arginine ($3 \times 10^{-5}$ M) and methylene blue ($10^{-5}$ M) (Figure 4).

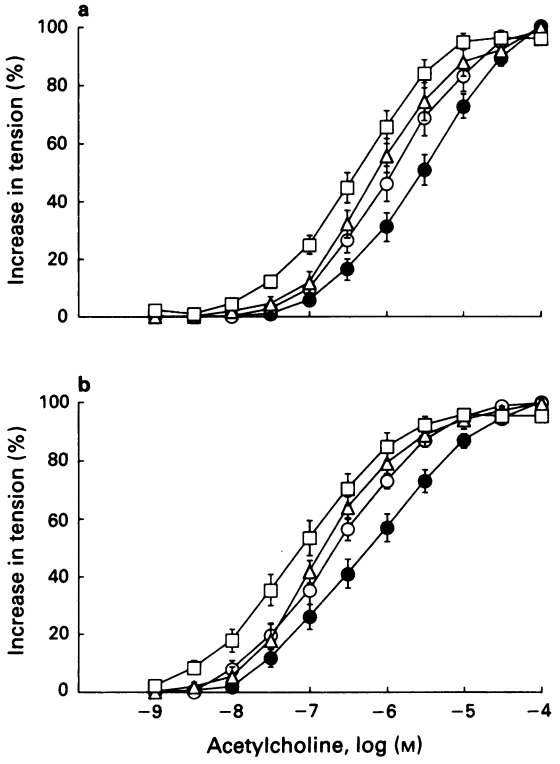



**Figure 1** Effects of nitro-L-arginine ($3 \times 10^{-5}$ M) (○), oxyhaemoglobin ($10^{-5}$ M) (△), and methylene blue ($10^{-5}$ M) (□) on contractions of canine bronchi with (a) and without (b) epithelium to acetylcholine; control (●). Values are means ± s.e.mean ($n = 6-15$), and are expressed as a percentage of the maximal contraction to acetylcholine.

**Table 1** Pharmacological agents and contractile responses of canine bronchi with and without epithelium to acetylcholine

| | $-log\ EC_{50}$ | | | *Maximal response* (g) | |
|---|---|---|---|---|---|
| | *with epithelium* | *without epithelium* | *Concentration ratio* | *with epithelium* | *without epithelium* |
| Control | 5.56 ± 0.12 | 6.26 ± 0.14* | 4.90 ± 1.32 | 11.03 ± 0.79 | 10.75 ± 0.81 |
| Nitro-L-arginine ($3 \times 10^{-5}$ M) | 5.90 ± 0.16† | 6.67 ± 0.10*† | 5.99 ± 1.28 | 12.46 ± 0.67 | 13.46 ± 1.00 |
| Oxyhaemoglobin ($10^{-5}$ M) | 6.07 ± 0.15† | 6.82 ± 0.10*† | 5.67 ± 1.33 | 12.33 ± 0.94 | 10.75 ± 2.04 |
| Methylene blue ($10^{-5}$ M) | 6.37 ± 0.13†‡ | 7.09 ± 0.16*†‡ | 5.64 ± 1.49 | 10.26 ± 1.10 | 9.71 ± 0.78 |

Data are expressed as means ± s.e.mean ($n = 6$ to 15). *Significantly different from rings with epithelium; †Significantly different from response in the respective control group; ‡Significantly different rings treated with N-L-arginine ($P < 0.05$).

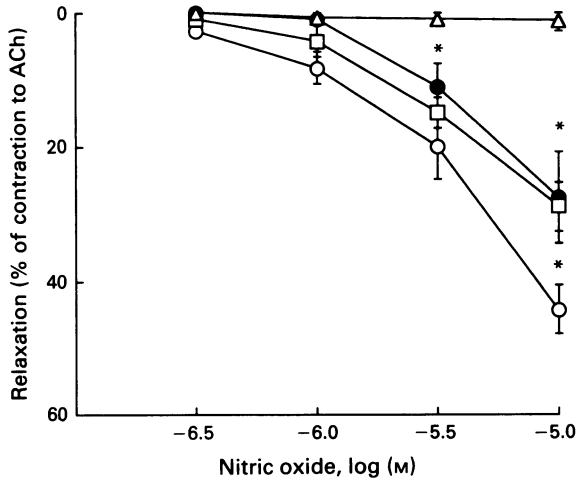



**Figure 2** Effects of superoxide dismustase (SOD; 150 u ml$^{-1}$) plus catalase (1200 u ml$^{-1}$) (○)); nitro-L-arginine ($3 \times 10^{-5}$ M) (□) and methylene blue ($10^{-5}$ M) (△) on relaxations of canine bronchi without epithelium to nitric oxide during contractions to acetylcholine ($4 \times 10^{-7}$ M). Value are means ± s.e.mean ($n = 5$) and are expressed as a percentage of contraction to acetylcholine ($4 \times 10^{-7}$ M). *Significant difference from control ($P < 0.05$).

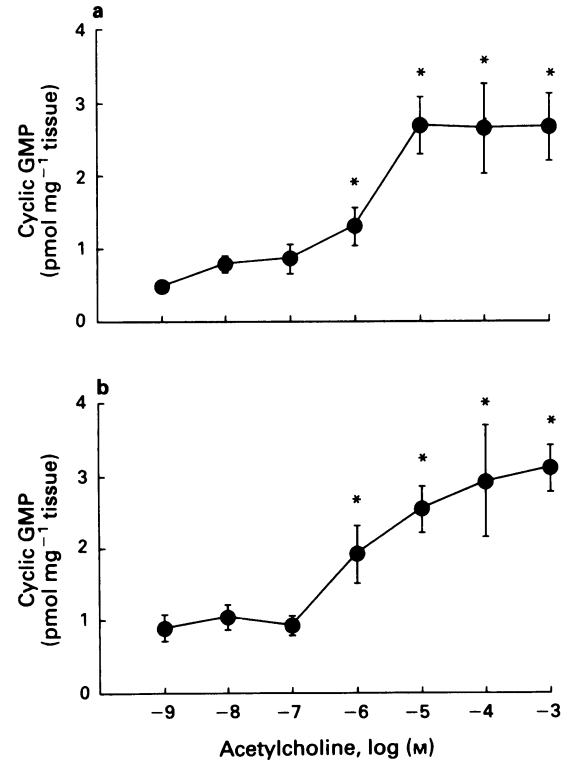



**Figure 3** Effects of acetylcholine on the content of intracellular cyclic GMP of canine bronchi with (a) and without (b) epithelium. Values are means ± s.e.mean, $n = 5$–8. *Significant difference from control.

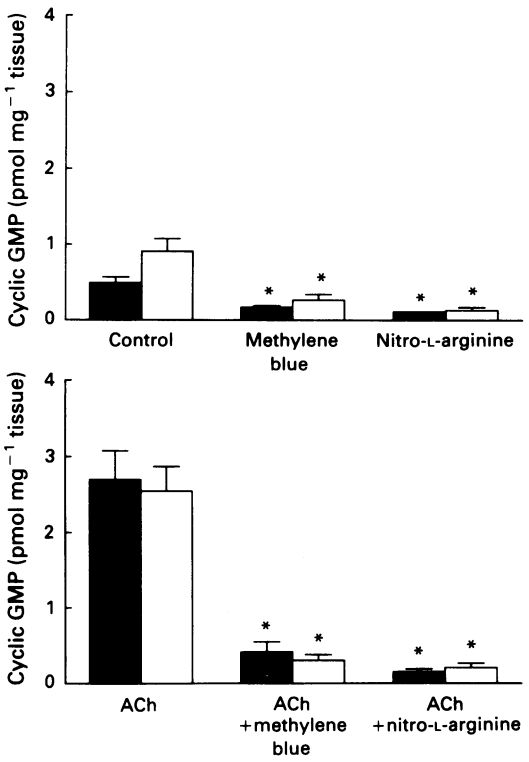



**Figure 4** Effects of methylene blue ($10^{-5}$ M) or nitro-L-arginine ($3 \times 10^{-5}$ M) on the increases in content of cyclic GMP induced by acetylcholine ($10^{-5}$ M) in canine bronchi with (solid columns) and without (open columns) epithelium. Values are means ± s.e.mean. $n = 4$–8. *Significant difference from control ($P < 0.05$).

## Discussion

In the present study, the contractions of canine bronchi to acetylcholine were potentiated by nitro-L-arginine (an inhibitor of the synthesis of nitric oxide: Mülsch & Busse, 1990) oxyhaemoglobin (a scavenger of nitric oxide: Doyle & Hoekstra, 1981; Martin *et al.*, 1984) and methylene blue (a scavenger of nitric oxide: Marshall *et al.*, 1988; Wolin *et al.*, 1990 and an inhibitor of soluble guanylate cyclase: Martin *et al.*, 1984). Thus, it is likely that an endogenous nitric oxide-like substance attenuates the responses of airways to the muscarinic agonists. The present study shows that nitro-L-arginine was less potent in potentiating contractions to acetylcholine than methylene blue. This may be partially due to the fact that methylene blue not only blocks the effect of nitric oxide by scavenging this radical and by inhibiting guanylate cyclase, but also has other pharmacological effects. In porcine aortic endothelial cells methylene blocks the production of prostacyclin ($PGI_2$) by a mechanism independent of inhibition of soluble guanylate cyclase (Martin *et al.*, 1989).

In canine bronchi, methylene blue inhibits the basal release of $PGI_2$ and acetylcholine-induced release of both prostaglandin $E_2$ ($PGE_2$) and $PGI_2$ (Gao & Vanhoutte, 1992). These prostaglandins relax canine bronchi (Stuart-Smith & Vanhoutte, 1988). Thus methylene blue may potentiate contraction induced by acetylcholine in part by inhibiting the release of relaxing prostanoids.

In the canine bronchi studied, during stimulation with acetylcholine the intracellular content of cyclic GMP increased. A similar phenomenon has been reported for the bovine trachea (Katsuki & Murad, 1977; Sheng *et al.*, 1991). Since the increase in the level of cyclic nucleotide was abolished by nitro-L-arginine, it appears to be induced by an endogenous nitric oxide-like substance. Comparing changes in the content of cyclic GMP and those in contractions of the tissues, the attenuation of the contraction of the tissue occurred at low concentrations of acetylcholine while no significant increase in the intracellular content of cyclic GMP is observed. It is possible that small increases in cyclic GMP content, probably limited to certain cell compartments, which cannot be detected with the methods employed, may be sufficient to modify the responses of the smooth muscle. Furthermore, the rate of cyclic GMP turnover, not necessarily accompanied by a detectable change in intracellular cyclic GMP, may also determine changes in the functions of the cells which are controlled by the nucleotide (Triner *et al.*, 1977). Thus, it is possible that attenuations of contractions to acetylcholine at low concentrations of the muscarinic agonist are also mediated by an endogenous nitric oxide-like substance.

The possible role of nitric oxide (or a nitric oxide-like substance) in the modulation of the responses of airways is also supported by the findings that nitric oxide caused relaxations of canine bronchi (without epithelium) during contractions to acetylcholine. The relaxations induced by exogenous nitric oxide were not affected by nitro-L-arginine, although they were abolished by methylene blue and potentiated by superoxide dismutase plus catalase, which protect nitric oxide from scavenging by oxygen-derived free radicals (Rubanyi & Vanhoutte, 1986). The ability of nitric oxide to relax airway smooth muscle has been reported in the bovine trachea (without epithelium) (Buga *et al.*, 1989) and the guinea-pig trachea (with and without epithelium) (Munakata *et al.*, 1990). In the guinea-pig trachea, nitric oxide induces larger relaxations in tissues with than in those without epithelium. This may be because the epithelium acts as a barrier to exogenous nitric oxide (Munakata *et al.*, 1990).

The respiratory epithelium not only acts as a physical barrier, it may release a factor(s) to inhibit the responses of the underlying smooth muscle to a variety of bronchoconstrictors including acetylcholine (Flavahan *et al.*, 1985; Barnes *et al.*, 1985; Vanhoutte, 1988; Morrison *et al.*, 1990). In the present study, the difference in contractions to acetylcholine between tissues with and without epithelium was not affected by nitro-L-arginine, oxyhaemoglobin, or methylene blue. Furthermore, acetylcholine induced similar increases in the content of intracellular cyclic GMP in tissues with and without epithelium. Thus, the epithelium may not be a major source for endogenous nitric oxide-like substance (Munakata *et al.*, 1990; Spina & Page, 1991).

In the guinea-pig trachea, nitric oxide is one of the transmitters which mediate non-adrenergic, non-cholinergic (NANC) relaxations (Tucker *et al.*, 1990; Belvisi *et al.*, 1991; Li & Rand, 1991). Although NANC innervation exists in the airways of many species such as rats, rabbits, cats, cows, horses, monkeys and man, it has not been described in the airways of the dog (Diamond & Altiere, 1988). Thus, it is unlikely that the attenuation of contractions to acetylcholine in canine airways is mediated by nitric oxide released from NANC nerves. The endothelial cells of blood vessels, macrophages, and neutrophils in the bronchial wall are all capable of producing nitric oxide (Stuehr & Marletta, 1987; O'Rourke & Vanhoutte, 1990; McCall *et al.*, 1991). Whether or not these cells can release sufficient nitric oxide to affect airway reactivity, and furthermore, whether or not airway smooth muscle may also produce nitric oxide remains to be clarified.

The authors thank Mr Robert R. Lorenz, Mr Barnabas Desta, and Mr Dewayne O. Coney for their excellent technical assistance. This study was supported in part by the National Heart, Lung and Blood Institute Grant HL 39423, and by an unrestricted Research Award of Toyobo Co., Ltd., Japan.

## References

BARNES, P.J., CUSS, F.M. & PALMER, J.M. (1985). The effect of airway epithelium on smooth muscle contractility in bovine trachea. *Br. J. Pharmacol.*, **86**, 685–691.

BELVISI, M.G., STRETTON, D. & BARNES, P.J. (1991). Nitric oxide as an endogenous modulator of cholinergic neurotransmission in guinea-pig airways. *Eur. J. Pharmacol.*, **198**, 219–221.

BREDT, D.S., HWANG, P.M. & SNYDER, S.H. (1990). Localization of nitric oxide synthase indicating a neural role for nitric oxide. *Nature*, **347**, 768–770.

BRIMIJOIN, S., SKAU, K. & WIERMAA, M.J. (1978). On the origin and fate of external acetylcholinesterase in peripheral nerve. *J. Physiol.*, **285**, 143–158.

BUGA, G.M., GOLD, M.E., WOOD, K.S., CHAUDHURI, G. & IGNARRO, L.J. (1989). Endothelium-derived nitric oxide relaxes nonvascular smooth muscle. *Eur. J. Pharmacol.*, **161**, 61–72.

DIAMOND, L. & ALTIERE, R.J. (1988). Airway nonadrenergic noncholinergic inhibitory nervous system. In *Lung Biology in Health and Disease. The Airways, Neural Control in Health and Disease*, vol. 33. ed Kaliner, M.A. & Barnes, P.J. pp. 343–394. New York: Marcel Dekker, Inc.

DOYLE, M.P. & HOEKSTRA, J.W. (1981). Oxidation of nitric oxides by bound dioxygen on hemoproteins. *J. Inorg. Biochem.*, **14**, 351–354.

FLAVAHAN, N.A., AARHUS, L.L., RIMELE, T.J. & VANHOUTTE, P.M. (1985). Respiratory epithelium inhibits bronchial smooth muscle tone. *J. Appl. Physiol.*, **58**, 834–838.

FURCHGOTT, R.F. & VANHOUTTE, P.M. (1989). Endothelium-derived relaxing and contracting factors. *FASEB J.*, **3**, 2007–2018.

FURCHGOTT, R.F. & ZAWADZKI, J.V. (1980). The obligatory role of endothelial cells in the relaxation of arterial smooth muscle by acetylcholine. *Nature*, **288**, 373–376.

GAO, Y. & VANHOUTTE, P.M. (1988). Removal of the epithelium potentiates acetylcholine in depolarizing canine bronchial smooth muscle. *J. Appl. Physiol.*, **65**, 2400–2405.

GAO, Y. & VANHOUTTE, P.M. (1992). Effects of hydrogen peroxide on the responsiveness of isolated canine bronchi: role of prostaglandin $E_2$ and $I_2$. *Am. J. Physiol.*, **263**, L402–L408.

GILLESPIE, J.S., LIU, X. & MARTIN, W. (1989). The effect of L-arginine and $N^G$-monomethyl-L-arginine on the response of the rat anoccoccygeus to NANC nerve stimulation. *Br. J. Pharmacol.*, **98**, 1080–1082.

GOLD, M.E., BUSH, P.A. & IGNARRO, L.J. (1989). Depletion of arterial L-arginine causes reversible tolerance to endothelium-dependent relaxation. *Biochem. Biophys. Res. Commun.*, **164**, 714–721.

KATSUKI, S. & MURAD, F. (1977). Regulation of adenosine cyclic 3',5'-monophosphate and guanosine cyclic 3',5'-monophosphate levels and contractility in bovine tracheal smooth muscle. *Mol. Pharmacol.*, **13**, 330–341.

KNOWLES, R.G., PALACIOS, M., PALMER, R.M.J. & MONCADA, S. (1989). Formation of nitric oxide from L-arginine in the central nervous system: a transduction mechanism for stimulation of soluble guanylate cyclase. *Proc. Natl. Acad. Sci. U.S.A.*, **86**, 5159–5162.

KOMORI, K., LORENZ, R.R. & VANHOUTTE, P.M. (1988). Nitric oxide, ACh, and electrical and mechanical properties of canine arterial smooth muscle. *Am. J. Physiol.*, **255**, H207–H212.

LI, C.G. & RAND, M.J. (1989). Evidence for a role of nitric oxide in the NANC-mediated relaxations in the rat anoccoccygeus muscle. *Clin. Exp. Physiol. Pharmacol.*, **16**, 933–938.

LI, C.G. & RAND, M.J. (1991). Evidence for the NANC relaxant response of guinea-pig trachea to electrical field stimulation is mediated by nitric oxide. *Br. J. Pharmacol.*, **104**, 91–94.

MARSHALL, J.J., WEI, E.P. & KONTOS, H.A. (1988). Independent blockade of cerebral vasodilatation from acetylcholine and nitric oxide. *Am. J. Physiol.*, **255,** H847–H854.

MARTIN, W., DRAZAN, K.M. & NEWBY, A.C. (1989). Methylene blue but not changes in cyclic GMP inhibits resting and bradykinin stimulated production of prostacyclin by pig aortic endothelial cells. *Br. J. Pharmacol.*, **97,** 51–56.

MARTIN, W., VILLANI, G.M., JOTHIANANDAN, D. & FURCHGOTT, R.F. (1984). Selective blockade of endothelium-dependent and glyceryl trinitrate-induced relaxation by hemoglobin and by methylene blue in the rabbit aorta. *J. Pharmacol. Exp. Ther.*, **232,** 708–716.

MCCALL, T.B., BOUGHTON-SMITH, N.K., PALMER, R.M.J., WHITTLE, B.J.R. & MONCADA, S. (1989). Synthesis of nitric oxide from L-arginine by neutrophils. Release and interaction with superoxide anion. *Biochem. J.*, **261,** 293–296.

MONCADA, S., PALMER, R.M.J. & HIGGS, E.A. (1991). Nitric oxide: physiology, pathology and pharmacology. *Pharmacol. Rev.*, **43,** 109–142.

MORRISON, K.J., GAO, Y. & VANHOUTTE, P.M. (1990). Epithelial modulation of airway smooth muscle. *Am. J. Physiol.*, **258,** L254–L262.

MÜLSCH, A. & BUSSE, R. (1990). $N^G$-nitro-L-arginine ($N^5$-[imini (nitroamine)methyl]-L-ornithine) impairs endothelium-dependent dilations by inhibiting cytosolic nitric oxide synthesis from L-arginine. *Naunyn-Schmied Arch Pharmacol.*, **341,** 143–147.

MUNAKATA, M., MASAKI, Y., SAKUMA, I., UKITA, H., OTSUKA, Y., HOMMA, Y. & KAWAKAMI, Y. (1990). Pharmacological differentiation of epithelium-derived relaxing factor from nitric oxide. *J. Appl. Physiol.*, **69,** 665–670.

O'ROURKE, S.T. & VANHOUTTE, P.M. (1990). Adrenergic responsiveness of isolated canine bronchial arteries. *Am. J. Physiol.*, **259,** H156–H161.

PALMER, R.M.J., FERRIGE, A.G. & MONCADA, S. (1987). Nitric oxide release accounts for the biological activity of endothelium-derived relaxing factor. *Nature*, **327,** 524–526.

RUBANYI, G.M. & VANHOUTTE, P.M. (1986). Superoxide anions and hyperoxia inactive endothelium-derived relaxing factor. *Am. J. Physiol.*, **250,** H822–H827.

SCHINI, V.B. & VANHOUTTE, P.M. (1991). L-arginine evokes both endothelium-dependent and -independent relaxations in L-arginine-depleted aortas of the rat. *Circ. Res.*, **68,** 209–216.

SCHUMAN, E.M. & MADISON, D.V. (1991). A requirement for the intracellular messenger nitric oxide in long-term potentiation. *Science*, **254,** 1503–1506.

SHENG, H., ISHII, K. & MURAD, F. (1991). Generation of an endothelium-derived relaxing factor-like substance in bovine tracheal smooth muscle. *Am. J. Physiol.*, **260,** L489–L493.

SPINA, D. & PAGE, C.P. (1991). The release of a non-prostanoid inhibitory factor from rabbit bronchus detected by co-axial bioassay. *Br. J. Pharmacol.*, **102,** 896–903.

STUART-SMITH, K. & VANHOUTTE, P.M. (1988). Arachidonic acid evokes epithelium-dependent relaxations in canine airways. *J. Appl. Physiol.*, **65,** 2170–2180.

STUEHR, D.J. & MARLETTA, M.A. (1987). Induction of nitrite/nitrate synthesis in murine macrophages by BCG infection, lymphokines or interferon-γ. *J. Immunol.*, **139,** 518–525.

TRINER, L., VULLIEMOZ, Y. & VEROSKY, M. (1977). Cyclic 3',5'-adenosine monophosphate and bronchial tone. *Eur. J. Pharmacol.*, **41,** 37–46.

TUCKER, J.F., BRAVE, S.R., CHARALAMBOUS, L., HOBBS, A.J. & GIBSON, A. (1990). L-$N^G$-nitro arginine inhibits non-adrenergic, non-cholinergic relaxation of guinea-pig isolated tracheal smooth muscle. *Br. J. Pharmacol.*, **100,** 663–664.

VANHOUTTE, P.M. (1988). Epithelium-derived relaxing factor(s) and bronchial reactivity. *Am. Rev. Respir. Dis.*, **138,** S24–S30.

WOLIN, M.S., CHERRY, P.D., RODENBURY, J.M., MESSINA, E.J. & KALEY, G. (1990). Methylene blue inhibits vasodilatation of skeletal muscle arterioles to acetylcholine and nitric oxide via the extracellular generation of superoxide anion. *J. Pharmacol. Exp. Ther.*, **254,** 872–876.

*(Received November 19, 1992*
*Revised March 1, 1993*
*Accepted March 4, 1993)*

# British Journal of Pharmacology

VOLUME 109 (3) JULY 1993

SPECIAL REPORTS

**N. Marczin, A. Papapetropoulos, T. Jilling & J.D. Catravas.** Prevention of nitric oxide synthase induction in vascular smooth muscle cells by microtubule depolymerizing agents 603

**A.L. Brizzolara, R. Crowe & G. Burnstock.** Evidence for the involvement of both ATP and nitric oxide in non-adrenergic, non-cholinergic inhibitory neurotransmission in the rabbit portal vein 606

**D.A. Craig & G.R. Martin.** 5-$HT_{1B}$ receptors mediate potent contractile responses to 5-HT in rat caudal artery 609

PAPERS

**R. Vargas, B. Wroblewska, A. Rego, J. Hatch & P.W. Ramwell.** Oestradiol inhibits smooth muscle cell proliferation of pig coronary artery 612

**C.J. Grossman, G.J. Kilpatrick & K.T. Bunce.** Development of a radioligand binding assay for 5-$HT_4$ receptors in guinea-pig and rat brain 618

**A. Renouard, P.S. Widdowson & A. Cordi.** [$^3$H]-idazoxan binding to rabbit cerebral cortex recognises multiple imidazoline $I_2$-type receptors: pharmacological characterization and relationship to monoamine oxidase 625

**A. Miwa, S. Kaneta, K. Motoki, Y. Jinno, H. Kasai, Y. Okada, H. Fukushima & N. Ogawa.** Vasorelaxant mechanism of KRN2391 and nicorandil in porcine coronary arteries of different sizes 632

**J.G. Filep, B. Battistini & P. Sirois.** Induction by endothelin-1 of epithelium-dependent relaxation of guinea-pig trachea *in vitro*: role for nitric oxide 637

**S. Guarini, C. Bazzani, & A. Bertolini.** Role of neuronal and vascular $Ca^{2+}$-channels in the ACTH-induced reversal of haemorrhagic shock 645

**B.Y. Muhammad & I. Kitchen.** Effect of delayed weaning on opioid receptor control of swim stress-induced antinociception in the developing rat 651

**M.J.A. van Veldhuizen, M.G.P. Feenstra, R.P.W. Heinsbroek & G.J. Boer.** *In vivo* microdialysis of noradrenaline overflow: effects of α-adrenoceptor agonists and antagonists measured by cumulative concentration-response curves 655

**K. Suzuki, K.M. Ito, Y. Minayoshi, H. Suzuki, M. Asano & K. Ito.** Modification by charybdotoxin and apamin of spontaneous electrical and mechanical activity of the circular smooth muscle of the guinea-pig stomach 661

**D.G. Hurrell, C.L. Perreault, L. Miao, B.J. Ransil & J.P. Morgan.** Cellular mechanism of the positive inotropic effect of hydralazine in mammalian myocardium 667

**S. Muto, M. Imai & Y. Asano.** Effect of nafamostat mesilate on $Na^+$ and $K^+$ transport properties in the rabbit cortical collecting duct 673

**K. Harada, A. Miwa, S. Kaneto, T. Izawa, H. Fukushima & N. Ogawa.** Effects of KRN2391, nicorandil and diltiazem on the changes in the electrocardiogram caused by endothelin-1 in anaesthetized rats 679

**Y. Habara & T. Kanno.** Dual effects of chlorobutanol on secretory response and intracellular $Ca^{2+}$ dynamics in isolated pancreatic acini of the rat 685

**M.F. Gurden, J. Coates, F. Ellis, B. Evans, M. Foster, E. Hornby, I Kennedy, D.P. Martin, P. Strong, C.J. Vardey & A. Wheeldon.** Functional characterization of three adenosine receptor types 693

**T. Sharp, R. McQuade, J.R. Fozard & D. Hoyer.** The novel 5-$HT_{1A}$ receptor antagonist, SDZ 216-525, decreases 5-HT release in rat hippocampus *in vivo* 699

**A. Suzuki & T. Itoh.** Effects of calyculin A on tension and myosin phosphorylation in skinned smooth muscle of the rabbit mesenteric artery 703

**J.M.A. Laird, R.J. Hargreaves &. R.G. Hill.** Effect of RP 67580, a non-peptide neurokinin$_1$ receptor antagonist, on facilitation of a nociceptive spinal flexion reflex in the rat 713

**J.M. Dickenson & S.J. Hill.** Intracellular cross-talk between receptors coupled to phospholipase C via pertussis toxin-sensitive and insensitive G-proteins in $DDT_1MF$-2 cells 719

**B. Robertson & D.G. Owen.** Pharmacology of a cloned potassium channel from mouse brain (MK-1) expressed in CHO cells: effects of blockers and an 'inactivation peptide' 725

**A. Eglezos, P. Cucchi, R. Patacchini, L. Quartara, C.A. Maggi & J. Mizrahi.** Differential effects of BQ-123 against endothelin-1 and endothelin-3 on the rat vas deferens: evidence for an atypical endothelin receptor 736

**C.W. Shuttleworth, K.M. Sanders & K.D. Keef.** Inhibition of nitric oxide synthesis reveals non-cholinergic excitatory neurotransmission in the canine proximal colon 739

**B. Clarke, M. Spedding, L. Patmore & J.G. McCormack.** Protective effects of ranolazine in guinea-pig hearts during low-flow ischaemia and their association with increases in active pyruvate dehydrogenase 748

**N. Watson, J. Maclagan & P.J. Barnes.** Endogenous tachykinins facilitate transmission through parasympathetic ganglia in guinea-pig trachea 751

**F.H. Marshall, S.A. Clark, A.D. Michel & J.C. Barnes.** Binding of angiotensin antagonists to rat liver and brain membranes measured *ex vivo* 760

**Y.-P. Lou, L.-Y. Lee, H. Satoh & J.M. Lundberg.** Postjunctional inhibitory effect of the $NK_2$ receptor antagonist, SR 48968, on sensory NANC bronchoconstriction in the guinea-pig 765

**Y. Qian, E. Naline, J.-A. Karlsson, D. Raeburn & C. Advenier.** Effects of rolipram and siguazodan on the human isolated bronchus and their interaction with isoprenaline and sodium nitroprusside 774

**D. Bowie & T.G. Smart.** Thiocyanate ions selectively antagonize AMPA-evoked responses in *Xenopus laevis* occytes microinjected with rat brain mRNA 779

**H. Kaube, K.L. Hoskin & P.J. Goadsby.** Inhibition by sumatriptan of central trigeminal neurones only after blood-brain barrier disruption 788

**S. Chen, R. Inoue & Y. Ito.** Pharmacological characterization of muscarinic receptor-activated cation channels in guinea-pig ileum **793**

**J.B. Warren, R.K. Loi & M.L. Coughlan.** Involvement of nitric oxide synthase in the delayed vasodilator response to ultraviolet light irradiation of rat skin *in vivo* **802**

**S. Tsujimoto, Y. Okumura, C. Kamei & K. Tasaka.** Effects of intracerebroventricular injection of histamine and related compounds on corticosterone release in rats **807**

**M. Santiago, A. Machado & J. Cano.** *In vivo* release of dopamine from rat striatum, substantia nigra and prefrontal cortex: differential modulation by baclofen **814**

**T. Yakushiji, T. Shirasaki, M. Munakata, A. Hirata & Norio Akaike.** Differential properties of type I and type II benzodiazepine receptors in mammalian CNS neurones **819**

**J.B. Salom, G. Torregrosa, M.D. Barberá, T. Jover & E. Alborch.** Endothelial receptors mediating contraction in goal cerebral arteries **826**

**J.F. Hussain, D.A. Kendall & V.G. Wilson.** Species-selective binding of [$^3$H]-idazoxan to $\alpha_2$-adrenoceptors and non-adrenoceptor, imidazoline binding sites in the central nervous system **831**

**M.D. Randall, J.A. Smith & T.M. Griffith.** Hypercholesterolaemia severely impairs EDRF-dependent collateral perfusion following acute arterial occlusion in rabbit isolated ear **838**

**A. Lindén, A. Ullman, C.-G. Löfdahl & B.-E. Skoogh.** Non-adrenergic, non-cholinergic neural activation in guinea-pig bronchi: powerful and frequency-dependent stabilizing effect on tone **845**

**E. Moilanen, P. Vuroinen, H. Kankaanranta, T. Metsä-Ketelä & H. Vapaatalo.** Inhibition by nitric oxide-donors of human polymorphonuclear leucocyte functions **852**

**C. Van Renterghem & C. Frelin.** 3,4 Dichlorobenzamil-sensitive, monovalent cation channel induced by palytoxin in cultured aortic myocytes **859**

**H. Sakuta, K. Okamoto & Y. Watanabe.** Antiarrhythmic drugs, clofilium and cibenzoline are potent inhibitors of glibenclamide-sensitive $K^+$ currents in *Xenopus* oocytes **866**

**C. Valenzuela, O. Pérez, O. Casis, J. Duarte, F. Pérez-Vizcaino, E. Delpón & J. Tamargo.** Effects of lisinopril on electromechanical properties and membrane currents in guinea-pig cardiac preparations **873**

**J.G. Filep, M.G. Sirois, É. Földes-Filep, A. Rousseau, G.E. Plante, A. Fournier, M. Yano & P. Sirois.** Enhancement by endothelin-1 of microvascular permeability via the activation of $ET_A$ receptors **880**

**Y. Gao & P.M. Vanhoutte.** Attenuation of contractions to acetylcholine in canine bronchi by an endogenous nitric oxide-like substance **887**

## SPECIAL REPORTS

The purpose of *Special Reports* is to provide rapid publication for **new** and **important** results which the Editorial Board considers are likely to be of special pharmacological significance. *Special Reports* will have publication priority over all other material and so authors are asked to consider carefully the status of their work before submission.

In order to speed publication there is normally no revision allowed beyond very minor typographical or grammatical corrections. If significant revision is required, the Board may either invite rapid re-submission or, more probably, propose that it be re-written as a Full Paper and be re-submitted for consideration. In order to reduce delays, proofs of *Special Reports* will be sent to authors but **essential corrections must reach the Production Office within 48 hours of receipt.** Authors should ensure that their submitted material conforms exactly to the following requirements.

*Special Reports* should normally occupy no more than two printed pages of the Journal; two illustrations (Figures or Tables, with legends) are permitted. As a guideline, with type face of 12 pitch and double-line spacing, a page of A4 paper could contain about 400 words. The absolute maximum length of the *Special Report* is 1700 words. For each Figure or Table, please deduct 200 words. The manuscript should comprise a Title page with key words (maximum of 10), a Summary consisting of a single short paragraph, followed by Introduction, Methods, Results, Discussion and References (maximum of 10). In all other respects, the requirements are the same as for Full Papers (see current 'Instructions to Authors').

**Edited for the British Pharmacological Society by**

**A.T. Birmingham** *(Chairman)*
**R.W. Horton** *(Secretary)*
**W.A. Large** *(Secretary)*

EDITORIAL BOARD

**J.A. Angus** Victoria, Australia
**M.L.J. Ashford** Cambridge
**G.W. Bennett** Nottingham
**W.C. Bowman** Glasgow
**N.G. Bowery** London
**Alison F. Brading** Oxford
**S.D. Brain** London
**K.T. Bunce** Ware
**K.D. Butler** Horsham
**M. Caulfield** London
**M.K. Church** Southampton
**S.J. Coker** Liverpool
**R.A. Coleman** Ware
**A.J. Cross** London
**V. Crunelli** Cardiff
**T.C. Cunnane** Oxford
**F. Cunningham** London
**A. Dray** London
**J.R. Docherty** Dublin
**J.M. Edwardson** Cambridge
**W. Feniuk** Cambridge
**J.R. Fozard** Basle, Switzerland
**Allison D. Fryer** Baltimore, USA
**Sheila M. Gardiner** Nottingham
**C.J. Garland** Southampton
**L.G. Garland** Beckenham
**A. Gibson** London
**R. Gristwood** Barcelona, Spain
**T. Hedner** Gothenburg, Sweden
**P.E. Hicks** Leuville-sur-Orge, France
**S.J. Hill** Nottingham
**J.C. Hunter** Cambridge
**C.C. Jordan** Ware
**K.A. Kane** Glasgow
**D.A. Kendall** Nottingham
**P. Leff** Loughborough
**H.D. Lux** Planegg, Germany
**R. McMillan** Macclesfield
**J. Maclagan** London
**G. Martin** Beckenham
**W. Martin** Glasgow
**A. Mathie** London
**D.N. Middlemiss** Harlow
**R.C. Miller** Strasbourg, France
**P.K. Moore** London
**R.J. Naylor** Bradford
**C.D. Nicholson** Oss, The Netherlands
**C.P. Page** London
**B.K. Park** Liverpool
**A.N. Payne** Beckenham
**F.L. Pearce** London
**J.D. Pearson** London
**M.H.T. Roberts** Cardiff
**P.J. Roberts** Bristol
**C. Robinson** London
**G.J. Sanger** Harlow
**M.A. Simmonds** London
**J.M. Sneddon** Sunderland
**P. Sneddon** Glasgow
**K. Starke** Freiburg, Germany
**P.V. Taberner** Bristol
**C. Thiemermann** London
**M.D. Tricklebank** Harlow
**M.B. Tyers** Ware
**S.P. Watson** Oxford
**K.J. Watling** Cambridge
**A.H. Weston** Manchester
**B.J.R. Whittle** Beckenham
**Eileen Winslow** Riom, France

CORRESPONDING EDITORS

**P.R. Adams** Stony Brook, U.S.A.
**C. Bell** Melbourne, Australia
**F.E. Bloom** La Jolla, U.S.A.
**A.L.A. Boura** Clayton, Australia
**N.J. Dun** Toledo, U.S.A.
**R.F. Furchgott** New York, U.S.A.
**T. Godfraind** Brussels, Belgium
**S.Z. Langer** Paris, France
**R.J. Miller** Chicago, U.S.A.
**R.C. Murphy** Denver, U.S.A.
**E. Muscholl** Mainz, Germany
**R.A. North** Portland, U.S.A.
**M. Otsuka** Tokyo, Japan
**M.J. Rand** Melbourne, Australia
**S. Rosell** Södertalje, Sweden
**P. Seeman** Toronto, Canada
**L. Szekeres** Szeged, Hungary
**B. Uvnas** Stockholm, Sweden
**P.A. Van Zwieten** Amsterdam, Netherlands
**V.M. Varagič** Belgrade, Yugoslavia
**G. Velo** Verona, Italy
**Wang Zhen Gang** Beijing, China
**M.B.H. Youdim** Haifa, Israel

**Papers will be considered for publication on all aspects of pharmacology, including chemotherapy.**

**Manuscripts (two copies) should be sent to Editorial Office, British Journal of Pharmacology, St. George's Hospital Medical School, Cranmer Terrace, London SW17 0RE. Authors should consult the Instructions to Authors and the Nomenclature Guidelines for Authors in Vol. 108, 275–284. These Instructions and Guidelines also appear with the journal Index for volumes 105–107, 1992.**

The *British Journal of Pharmacology* is published monthly by the Scientific & Medical Division, Macmillan Press Ltd. The journal is covered by *Current Contents*, *Excerpta Medica* and *Index Medicus*.

All business correspondence and reprint requests should be addressed to the Scientific & Medical Division, Macmillan Press Ltd., Houndmills, Basingstoke, Hampshire RG21 2XS, UK. Telephone: (0256) 29242; Fax: (0256) 810526.

Enquiries concerning advertising space or rates should be addressed to: Michael Rowley, Advertisement Manager, Macmillan Press Ltd., 4 Little Essex Street, London WC2R 3LF. Telephone: 071 836 6633; Fax: 071 379 0820.

Annual subscription prices for 1993 EC £455, elsewhere £499/US$923 (sterling rate is definitive). Orders must be accompanied by remittance. Cheques should be made payable to Macmillan Press, and sent to: Macmillan Press Ltd., Subscription Department, Brunel Road, Houndmills, Basingstoke, Hampshire RG21 2XS, UK.
Overseas subscribers may make payments into UK Post Office Giro Account No. 5192455. Full details must accompany the payment.

*British Journal of Pharmacology* (ISSN 0007–1188) is published monthly by Macmillan Publishers Ltd, c/o Mercury Airfreight International Ltd, 2323 Randolph Avenue, Avenel, NJ 07001, USA. Subscription price is $923.00 per annum. 2nd class postage is paid at Rahway NJ. *Postmaster*: send address corrections to Macmillan Publishers, c/o Mercury Airfreight International Ltd, 2323 Randolph Avenue, Avenel NJ 07001.

All rights of reproduction are reserved in respect of all papers, articles, illustrations, etc., published in this journal in all countries of the world.

All material published in this journal is protected by copyright, which covers exclusive rights to reproduce and distribute the material. No material published in this journal may be reproduced or stored on microfilm or in electronic, optical or magnetic form without the written authorisation of the Publisher.

Authorization to photocopy items for internal or personal use, or the internal or personal use of specific clients, is granted by Macmillan Press Ltd for libraries and other users registered with the Copyright Clearance Center (CCC) Transactional Reporting Service, provided that the base fee of $9.00 per copy is paid directly to CCC, 21 Congress St., Salem, MA 01970, USA.

Apart from any fair dealing for the purposes of research or private study, or criticism or review, as permitted under the Copyright, Designs and Patent Act 1988, this publication may be reproduced, stored or transmitted, in any form or by any means, only with the prior permission in writing of the publishers, or in the case of reprographic reproduction, in accordance with the terms of licences issued by the Copyright Licensing Agency.

© The British Pharmacological Society & Macmillan Press Ltd, 1993.
ISSN 0007–1188

0007–1188/93 $9.00 + $0.00

**S. Chen, R. Inoue & Y. Ito.** Pharmacological characterization of muscarinic receptor-activated cation channels in guinea-pig ileum **793**

**J.B. Warren, R.K. Loi & M.L. Coughlan.** Involvement of nitric oxide synthase in the delayed vasodilator response to ultraviolet light irradiation of rat skin *in vivo* **802**

**S. Tsujimoto, Y. Okumura, C. Kamei & K. Tasaka.** Effects of intracerebroventricular injection of histamine and related compounds on corticosterone release in rats **807**

**M. Santiago, A. Machado & J. Cano.** *In vivo* release of dopamine from rat striatum, substantia nigra and prefrontal cortex: differential modulation by baclofen **814**

**T. Yakushiji, T. Shirasaki, M. Munakata, A. Hirata & Norio Akaike.** Differential properties of type I and type II benzodiazepine receptors in mammalian CNS neurones **819**

**J.B. Salom, G. Torregrosa, M.D. Barberá, T. Jover & E. Alborch.** Endothelial receptors mediating contraction in goal cerebral arteries **826**

**J.F. Hussain, D.A. Kendall & V.G. Wilson.** Species-selective binding of [$^3$H]-idazoxan to $\alpha_2$-adrenoceptors and non-adrenoceptor, imidazoline binding sites in the central nervous system **831**

**M.D. Randall, J.A. Smith & T.M. Griffith.** Hypercholesterolaemia severely impairs EDRF-dependent collateral perfusion following acute arterial occlusion in rabbit isolated ear **838**

**A. Lindén, A. Ullman, C.-G. Löfdahl & B.-E. Skoogh.** Non-adrenergic, non-cholinergic neural activation in guinea-pig bronchi: powerful and frequency-dependent stabilizing effect on tone **845**

**E. Moilanen, P. Vuroinen, H. Kankaanranta, T. Metsä-Ketelä & H. Vapaatalo.** Inhibition by nitric oxide-donors of human polymorphonuclear leucocyte functions **852**

**C. Van Renterghem & C. Frelin.** 3,4 Dichlorobenzamil-sensitive, monovalent cation channel induced by palytoxin in cultured aortic myocytes **859**

**H. Sakuta, K. Okamoto & Y. Watanabe.** Antiarrhythmic drugs, clofilium and cibenzoline are potent inhibitors of glibenclamide-sensitive $K^+$ currents in *Xenopus* oocytes **866**

**C. Valenzuela, O. Pérez, O. Casis, J. Duarte, F. Pérez-Vizcaino, E. Delpón & J. Tamargo.** Effects of lisinopril on electromechanical properties and membrane currents in guinea-pig cardiac preparations **873**

**J.G. Filep, M.G. Sirois, É. Földes-Filep, A. Rousseau, G.E. Plante, A. Fournier, M. Yano & P. Sirois.** Enhancement by endothelin-1 of microvascular permeability via the activation of $ET_A$ receptors **880**

**Y. Gao & P.M. Vanhoutte.** Attenuation of contractions to acetylcholine in canine bronchi by an endogenous nitric oxide-like substance **887**

## SPECIAL REPORTS

The purpose of *Special Reports* is to provide rapid publication for **new** and **important** results which the Editorial Board considers are likely to be of special pharmacological significance. *Special Reports* will have publication priority over all other material and so authors are asked to consider carefully the status of their work before submission.

In order to speed publication there is normally no revision allowed beyond very minor typographical or grammatical corrections. If significant revision is required, the Board may either invite rapid re-submission or, more probably, propose that it be re-written as a Full Paper and be re-submitted for consideration. In order to reduce delays, proofs of *Special Reports* will be sent to authors but **essential corrections must reach the Production Office within 48 hours of receipt.** Authors should ensure that their submitted material conforms exactly to the following requirements.

*Special Reports* should normally occupy no more than two printed pages of the Journal; two illustrations (Figures or Tables, with legends) are permitted. As a guideline, with type face of 12 pitch and double-line spacing, a page of A4 paper could contain about 400 words. The absolute maximum length of the *Special Report* is 1700 words. For each Figure or Table, please deduct 200 words. The manuscript should comprise a Title page with key words (maximum of 10), a Summary consisting of a single short paragraph, followed by Introduction, Methods, Results, Discussion and References (maximum of 10). In all other respects, the requirements are the same as for Full Papers (see current 'Instructions to Authors').

BRITISH JOURNAL OF PHARMACOLOGY VOLUME 109 (3) 1993

SPECIAL REPORTS

**N. Marczin, A. Papapetropoulos, T. Jilling & J.D. Catravas.** Prevention of nitric oxide synthase induction in vascular smooth muscle cells by microtubule depolymerizing agents 603

**A.L. Brizzolara, R. Crowe & G. Burnstock.** Evidence for the involvement of both ATP and nitric oxide in non-adrenergic, non-cholinergic inhibitory neurotransmission in the rabbit portal vein 606

**D.A. Craig & G.R. Martin.** 5-$HT_{1B}$ receptors mediate potent contractile responses to 5-HT in rat caudal artery 609

PAPERS

**R. Vargas, B. Wroblewska, A. Rego, J. Hatch & P.W. Ramwell.** Oestradiol inhibits smooth muscle cell proliferation of pig coronary artery 612

**C.J. Grossman, G.J. Kilpatrick & K.T. Bunce.** Development of a radioligand binding assay for 5-$HT_4$ receptors in guinea-pig and rat brain 618

**A. Renouard, P.S. Widdowson & A. Cordi.** [$^3$H]-idazoxan binding to rabbit cerebral cortex recognises multiple imidazoline $I_2$-type receptors: pharmacological characterization and relationship to monoamine oxidase 625

**A. Miwa, S. Kaneta, K. Motoki, Y. Jinno, H. Kasai, Y. Okada, H. Fukushima & N. Ogawa.** Vasorelaxant mechanism of KRN2391 and nicorandil in porcine coronary arteries of different sizes 632

**J.G. Filep, B. Battistini & P. Sirois.** Induction by endothelin-1 of epithelium-dependent relaxation of guinea-pig trachea *in vitro*: role for nitric oxide 637

**S. Guarini, C. Bazzani, & A. Bertolini.** Role of neuronal and vascular $Ca^{2+}$-channels in the ACTH-induced reversal of haemorrhagic shock 645

**B.Y. Muhammad & I. Kitchen.** Effect of delayed weaning on opioid receptor control of swim stress-induced antinociception in the developing rat 651

**M.J.A. van Veldhuizen, M.G.P. Feenstra, R.P.W. Heinsbroek & G.J. Boer.** *In vivo* microdialysis of noradrenaline overflow: effects of α-adrenoceptor agonists and antagonists measured by cumulative concentration-response curves 655

**K. Suzuki, K.M. Ito, Y. Minayoshi, H. Suzuki, M. Asano & K. Ito.** Modification by charybdotoxin and apamin of spontaneous electrical and mechanical activity of the circular smooth muscle of the guinea-pig stomach 661

**D.G. Hurrell, C.L. Perreault, L. Miao, B.J. Ransil & J.P. Morgan.** Cellular mechanism of the positive inotropic effect of hydralazine in mammalian myocardium 667

**S. Muto, M. Imai & Y. Asano.** Effect of nafamostat mesilate on $Na^+$ and $K^+$ transport properties in the rabbit cortical collecting duct 673

**K. Harada, A. Miwa, S. Kaneto, T. Izawa, H. Fukushima & N. Ogawa.** Effects of KRN2391, nicorandil and diltiazem on the changes in the electrocardiogram caused by endothelin-1 in anaesthetized rats 679

**Y. Habara & T. Kanno.** Dual effects of chlorobutanol on secretory response and intracellular $Ca^{2+}$ dynamics in isolated pancreatic acini of the rat 685

**M.F. Gurden, J. Coates, F. Ellis, B. Evans, M. Foster, E. Hornby, I Kennedy, D.P. Martin, P. Strong, C.J. Vardey & A. Wheeldon.** Functional characterization of three adenosine receptor types 693

**T. Sharp, R. McQuade, J.R. Fozard & D. Hoyer.** The novel 5-$HT_{1A}$ receptor antagonist, SDZ 216-525, decreases 5-HT release in rat hippocampus *in vivo* 699

**A. Suzuki & T. Itoh.** Effects of calyculin A on tension and myosin phosphorylation in skinned smooth muscle of the rabbit mesenteric artery 703

**J.M.A. Laird, R.J. Hargreaves &. R.G. Hill.** Effect of RP 67580, a non-peptide neurokinin$_1$ receptor antagonist, on facilitation of a nociceptive spinal flexion reflex in the rat 713

**J.M. Dickenson & S.J. Hill.** Intracellular cross-talk between receptors coupled to phospholipase C via pertussis toxin-sensitive and insensitive G-proteins in $DDT_1MF$-2 cells 719

**B. Robertson & D.G. Owen.** Pharmacology of a cloned potassium channel from mouse brain (MK-1) expressed in CHO cells: effects of blockers and an 'inactivation peptide' 725

**A. Eglezos, P. Cucchi, R. Patacchini, L. Quartara, C.A. Maggi & J. Mizrahi.** Differential effects of BQ-123 against endothelin-1 and endothelin-3 on the rat vas deferens: evidence for an atypical endothelin receptor 736

**C.W. Shuttleworth, K.M. Sanders & K.D. Keef.** Inhibition of nitric oxide synthesis reveals non-cholinergic excitatory neurotransmission in the canine proximal colon 739

**B. Clarke, M. Spedding, L. Patmore & J.G. McCormack.** Protective effects of ranolazine in guinea-pig hearts during low-flow ischaemia and their association with increases in active pyruvate dehydrogenase 748

**N. Watson, J. Maclagan & P.J. Barnes.** Endogenous tachykinins facilitate transmission through parasympathetic ganglia in guinea-pig trachea 751

**F.H. Marshall, S.A. Clark, A.D. Michel & J.C. Barnes.** Binding of angiotensin antagonists to rat liver and brain membranes measured *ex vivo* 760

**Y.-P. Lou, L.-Y. Lee, H. Satoh & J.M. Lundberg.** Postjunctional inhibitory effect of the $NK_2$ receptor antagonist, SR 48968, on sensory NANC bronchoconstriction in the guinea-pig 765

**Y. Qian, E. Naline, J.-A. Karlsson, D. Raeburn & C. Advenier.** Effects of rolipram and siguazodan on the human isolated bronchus and their interaction with isoprenaline and sodium nitroprusside 774

**D. Bowie & T.G. Smart.** Thiocyanate ions selectively antagonize AMPA-evoked responses in *Xenopus laevis* occytes microinjected with rat brain mRNA 779

**H. Kaube, K.L. Hoskin & P.J. Goadsby.** Inhibition by sumatriptan of central trigeminal neurones only after blood-brain barrier disruption 788

**S. Chen, R. Inoue & Y. Ito.** Pharmacological characterization of muscarinic receptor-activated cation channels in guinea-pig ileum 793

**J.B. Warren, R.K. Loi & M.L. Coughlan.** Involvement of nitric oxide synthase in the delayed vasodilator response to ultraviolet light irradiation of rat skin *in vivo* 802

**S. Tsujimoto, Y. Okumura, C. Kamei & K. Tasaka.** Effects of intracerebroventricular injection of histamine and related compounds on corticosterone release in rats 807

**M. Santiago, A. Machado & J. Cano.** *In vivo* release of dopamine from rat striatum, substantia nigra and prefrontal cortex: differential modulation by baclofen 814

**T. Yakushiji, T. Shirasaki, M. Munakata, A. Hirata & Norio Akaike.** Differential properties of type I and type II benzodiazepine receptors in mammalian CNS neurones 819

**J.B. Salom, G. Torregrosa, M.D. Barberá, T. Jover & E. Alborch.** Endothelial receptors mediating contraction in goal cerebral arteries 826

**J.F. Hussain, D.A. Kendall & V.G. Wilson.** Species-selective binding of [$^3$H]-idazoxan to $\alpha_2$-adrenoceptors and non-adrenoceptor, imidazoline binding sites in the central nervous system 831

**M.D. Randall, J.A. Smith & T.M. Griffith.** Hypercholesterolaemia severely impairs EDRF-dependent collateral perfusion following acute arterial occlusion in rabbit isolated ear 838

**A. Lindén, A. Ullman, C.-G. Löfdahl & B.-E. Skoogh.** Non-adrenergic, non-cholinergic neural activation in guinea-pig bronchi: powerful and frequency-dependent stabilizing effect on tone 845

**E. Moilanen, P. Vuroinen, H. Kankaanranta, T. Metsä-Ketelä & H. Vapaatalo.** Inhibition by nitric oxide-donors of human polymorphonuclear leucocyte functions 852

**C. Van Renterghem & C. Frelin.** 3,4 Dichlorobenzamil-sensitive, monovalent cation channel induced by palytoxin in cultured aortic myocytes 859

**H. Sakuta, K. Okamoto & Y. Watanabe.** Antiarrhythmic drugs, clofilium and cibenzoline are potent inhibitors of glibenclamide-sensitive $K^+$ currents in *Xenopus* oocytes 866

**C. Valenzuela, O. Pérez, O. Casis, J. Duarte, F. Pérez-Vizcaino, E. Delpón & J. Tamargo.** Effects of lisinopril on electromechanical properties and membrane currents in guinea-pig cardiac preparations 873

**J.G. Filep, M.G. Sirois, É. Földes-Filep, A. Rousseau, G.E. Plante, A. Fournier, M. Yano & P. Sirois.** Enhancement by endothelin-1 of microvascular permeability via the activation of $ET_A$ receptors 880

**Y. Gao & P.M. Vanhoutte.** Attenuation of contractions to acetylcholine in canine bronchi by an endogenous nitric oxide-like substance 887

Typeset by Elite Typesetting Techniques, Southampton, Hampshire
and printed in Great Britain by Unwin Brothers Ltd., The Gresham Press, Old Woking, Surrey

## PREPARATION OF MANUSCRIPTS

Authors are strongly recommended to read the full *Instructions to Authors* and *Nomenclature Guidelines for Authors* (*Br. J. Pharmacol.* 1993, **108,** 275–284) before submitting a manuscript for publication in the *British Journal of Pharmacology*. The manuscript and cover letter should be checked against the following list before mailing.

The original and one copy of the manuscript must be supplied. Manuscripts must be typed in double-line spacing on one side of A4 paper, in type not smaller than 12 characters per inch or 10 point. Both copies to include Tables and a set of labelled Figures. One set of Figures without numbers or letters is also to be included. The text to be arranged in the following subsections:

1. **Title**—To have no more than 150 characters on a separate page, which should also include a Short Title (50 characters maximum) and the name and address of the author for correspondence.

2. **Summary**—To be arranged in numbered paragraphs (Full Papers) or a single paragraph (Special Reports).
   —to include aims, principal results and conclusions.
   —to include Key words (10 maximum) at end of summary.

3. **Introduction**—To contain concise statements of the problem and the aims of the investigation.

4. **Methods**—To have brief but adequate account of the procedures; *full names of drugs* (*including those referred to by manufacturer's code*), sources of drugs and statistical tests to be stated.

5. **Results**—To have no repetition of data in Figures, Tables and text.

6. **Discussion**—Findings and conclusions to be placed in context of other relevant work.
   *NB* Simple repetition of results and unwarranted speculation are not acceptable.

7. **Acknowledgments**—Sources of support. Sources of drugs not widely available commercially.

8. **References**—All references in the text to be included in the Reference List and *vice versa*. References in alphabetical order with complete citations; Journals publishing 'in press' papers identified.
   *References to manuscripts submitted to other journals but not yet accepted are not allowed.*

9. **Tables**—Each on a separate page and prepared in accordance with current requirements of the Journal.

10. **Figures**—Both labelled and non-labelled Figures to be prepared in accordance with current requirements of the Journal (see *Instructions to Authors*, 1993, **108,** 275–281) and provided with Figure Number and Authors' names on back (*in pencil*).
    —each legend to be typed on a separate page and carrying keys to symbols.
    —keys to symbols and histograms must not appear on the figures themselves, but in the respective legends.
    —'box style' figures are not in keeping with the Journal style; line drawings etc must have only left-hand and bottom axes.

11. **Manuscripts**—To be accompanied by a declaration signed by each author that
    (a) results are original
    (b) approval of all persons concerned has been given to submit manuscripts for consideration (see also 12b)
    (c) the same material is neither 'in press' (i.e. is in proof or has definitely been accepted for publication) nor under consideration elsewhere. Furthermore it will not be submitted or published elsewhere before a decision has been reached by the Editorial Board of the *British Journal of Pharmacology* and will not be submitted elsewhere if accepted by the *British Journal of Pharmacology*.
    (d) Copyright assignment is included.

12. **Cover letter**—To state clearly
    (a) Corresponding author's full postal address, telephone, telex or Fax number
    (b) where appropriate, that *either* ethical approval has been given for investigation *or* Company or Institutional permission to publish work has been received.

13. **Reminder**—Packaging to be sufficiently robust to protect Figures and to withstand mailing.

Failure to comply with *Instructions to Authors* may lead to substantial delays in processing, review and publication and may even jeopardize acceptance of the manuscript.

### NOMENCLATURE

Authors are reminded that accepted receptor and associated terminology is laid out in *Nomenclature Guidelines for Authors*, as published in the *British Journal of Pharmacology, Br. J. Pharmacol.*, 1993, **108,** 282–284.